

October 3, 2012

Elmo E. Collins, Regional Administrator, Region IV
U.S. Nuclear Regulatory Commission
1600 East Lamar Blvd.
Arlington, Texas 76011-4511

Subject: **Docket No. 50-361**
Confirmatory Action Letter - Actions to Address Steam Generator Tube Degradation
San Onofre Nuclear Generating Station, Unit 2

- References:
1. Letter from Mr. Peter T. Dietrich (SCE) to Mr. Elmo E. Collins (USNRC), dated March 23, 2012, Steam Generator Return-to-Service Action Plan, San Onofre Nuclear Generating Station
 2. Letter from Mr. Elmo E. Collins (USNRC) to Mr. Peter T. Dietrich (SCE), dated March 27, 2012, Confirmatory Action Letter 4-12-001, San Onofre Nuclear Generating Station, Units 2 and 3, Commitments to Address Steam Generator Tube Degradation

Dear Mr. Collins:

On March 23, 2012, Southern California Edison (SCE) submitted a letter (Reference 1) to the NRC describing actions it planned to take with respect to issues identified in the steam generator (SG) tubes of San Onofre Nuclear Generating Station (SONGS) Units 2 and 3. On March 27, 2012, the NRC responded by issuing a Confirmatory Action Letter (CAL) (Reference 2), describing the actions that the NRC and SCE agreed would be completed to address those issues and ensure safe operations. The purpose of this letter is to report the completion of the Unit 2 CAL actions, which are to be completed prior to entry of Unit 2 into Mode 2 (as defined in the SONGS technical specifications).

Completion of the Unit 2 CAL actions is summarized below. Detailed information demonstrating fulfillment of Actions 1 and 2 of the CAL is provided in SCE's Unit 2 Return to Service Report which is included as [Enclosure 2](#) of this letter. [Enclosure 1](#) provides a list of new commitments identified in this letter.

CAL ACTION 1:

“Southern California Edison Company (SCE) will determine the causes of the tube-to-tube interactions that resulted in steam generator tube wear in Unit 3, and will implement actions to prevent loss of integrity due to these causes in the Unit 2 steam generator tubes. SCE will establish a protocol of inspections and/or operational limits for Unit 2, including plans for a mid-cycle shutdown for further inspections.”

COMPLETION OF CAL ACTION 1:

SCE has determined the causes of tube-to-tube interactions that resulted in SG tube wear in Unit 3, as summarized below. In addition, SCE implemented actions to prevent loss of tube integrity due to these causes in the Unit 2 SGs and established a protocol of inspections and operational limits, including plans for a mid-cycle shutdown. These are summarized under CAL Action 2.

Causes of Tube-to-Tube Interactions in Unit 3

As noted in Reference 1, the SG tube wear that caused a Unit 3 SG tube to leak was the result of tube-to-tube interaction. This type of wear was confirmed to exist in a number of other tubes in the same region in both Unit 3 SGs. Subsequent inspections of the Unit 2 SGs found this type of wear also existed in a single pair of tubes (one contact location) in one of the two Unit 2 SGs (SG 2E-089).

To determine the cause of the tube-to-tube wear (TTW), SCE performed extensive inspections and analyses, and commissioned the assistance of experts in the fields of thermal-hydraulics and in SG design, manufacturing, operation, and maintenance. Based on the results of these inspections and analyses, SCE determined the cause of the TTW in the two Unit 3 SGs was fluid elastic instability (FEI), resulting from the combination of localized high steam velocity, high steam void fraction, and insufficient contact forces between the tubes and the anti-vibration bars (AVBs). The FEI caused vibration of SG tubes in the in-plane direction that resulted in TTW in a localized area of the SGs. Details of SCE’s investigation and cause evaluation are provided in Section 6 of [Enclosure 2](#).

Corrective and Compensatory Actions, Inspections, and Operational Limits

To prevent loss of integrity due to FEI and TTW in Unit 2, SCE implemented corrective and compensatory actions and established a protocol of inspections and operational limits, including plans for a mid-cycle shutdown. These are described in CAL Action 2 below.

CAL ACTION 2:

“Prior to entry of Unit 2 into Mode 2, SCE will submit to the NRC in writing the results of your assessment of Unit 2 steam generators, the protocol of inspections and/or operational limits, including schedule dates for a mid-cycle shutdown for further inspections, and the basis for SCE’s conclusion that there is reasonable assurance, as required by NRC regulations, that the unit will operate safely.”

COMPLETION OF CAL ACTION 2:

Assessment of Unit 2 Steam Generators

SCE evaluated the causes of TTW in the Unit 3 SGs and the applicability of those causes to Unit 2 and inspected the Unit 2 SGs for evidence of similar wear. SCE determined the TTW effects were much less pronounced in Unit 2 where two adjacent tubes were identified with TTW indications. The wear depth was less than 15% through-wall wear, which is below the threshold of 35% through-wall at which tube plugging is required. These two tubes are located in the same region of the SG as those with TTW in Unit 3. Given that the thermal hydraulic conditions are essentially the same in both units, the significantly lower level of TTW in Unit 2 has been attributed to manufacturing differences that resulted in greater contact between the tubes and AVBs in Unit 2, providing greater tube support. Details of SCE's investigation and cause evaluation are provided in Section 6 of [Enclosure 2](#).

Actions to Prevent Loss of Integrity due to TTW in Unit 2 SG Tubes Including Protocol of Inspections and Operational Limits

SCE has taken actions to prevent loss of Unit 2 SG tube integrity due to TTW including establishing a protocol of inspections and operational limits to provide assurance that Unit 2 will operate safely. These actions are summarized below, with details provided in Section 8 of [Enclosure 2](#). The operational assessments performed to confirm the adequacy of these operational limits are described in Section 10 of [Enclosure 2](#).

1. SCE will administratively limit Unit 2 to 70% reactor power prior to a mid-cycle shutdown (Commitment 1). Limiting Unit 2 power to 70% eliminates the thermal hydraulic conditions that cause FEI from the SONGS Unit 2 SGs by reducing the steam velocity and void fraction. Further, at 70% power, the SONGS Unit 2 SGs will operate within an envelope of steam velocity and void fraction that has proven successful in the operation of other SGs of similar design. Thus, limiting power to 70% ensures that loss of tube integrity due to FEI will not occur.
2. SCE plugged the two tubes with TTW in Unit 2. As a preventive measure, additional tubes were plugged in the Unit 2 SGs. Tubes were selected for preventive plugging using correlations between wear characteristics in Unit 3 tubes and actual wear patterns found in Unit 2 tubes. Removing these tubes from service will prevent any further wear of these tubes from challenging tube integrity.
3. SCE will shut down Unit 2 for a mid-cycle SG inspection outage within 150 cumulative days of operation at or above 15% power (Commitment 2). This shortened inspection interval will ensure that any potential tube wear will not challenge the structural integrity of the in-service tubes. The protocol for mid-cycle inspections is provided in Section 8.3 of [Enclosure 2](#).

To ensure that these actions are effective in preventing a loss of tube integrity due to FEI, SCE retained the experience and expertise of AREVA NP, Westinghouse Electric Company LLC, and Intertek/APTECH. These companies routinely perform operational assessments (OAs) of SGs for the U.S. nuclear industry. AREVA and Westinghouse also have extensive steam generator design experience. SCE retained these companies to develop independent OAs using different methodologies to evaluate whether, under the operational limits imposed by SCE, SG tube

integrity will be maintained until the next SG inspection. Each of these independent OAs demonstrates that operating at 70% power will prevent loss of tube integrity beyond the 150 cumulative day inspection interval.

The actions to operate at reduced power and shut down for a mid-cycle inspection within 150 cumulative days of operation are interim compensatory actions. SCE will reevaluate these actions during the mid-cycle inspection based on the data obtained during the inspections. In addition, SCE has established a project team to develop and implement a long term plan for repairing the SGs.

Defense-in-depth measures were developed to provide increased safety margin in the unlikely event of tube-to-tube degradation in the Unit 2 SGs during operation at 70% power. These actions, identified in Section 9 of [Enclosure 2](#), will facilitate early detection of a SG tube leak and ensure immediate and appropriate plant operator and management response.

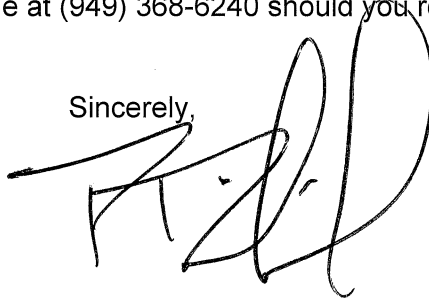
Basis for Conclusion of Reasonable Assurance

SCE has evaluated the causes of TTW in the Unit 3 SGs and, as described in response to CAL Action 2 above, has completed corrective and compensatory actions in Unit 2 to prevent loss of tube integrity due to these causes. Tubes within regions of the Unit 2 SGs that might be susceptible to FEI have been plugged. In addition, as described in response to CAL Action 2 above, SCE has established operational limits that eliminate the thermal-hydraulic conditions associated with FEI from the SONGS Unit 2 SGs. Specifically, operation of Unit 2 will be administratively limited to 70% power. Within 150 cumulative days of operation at or above 15% power, Unit 2 will be shut down for inspection to confirm the condition of the SG tubes. The analyses and OAs performed by SCE and independent industry experts demonstrate that under these conditions, tube integrity will be maintained. On this basis, SCE concludes that Unit 2 will operate safely.

We understand that the NRC will conduct inspections at SONGS to confirm the bases for the above information.

Please call me or Mr. Richard St. Onge at (949) 368-6240 should you require any further information.

Sincerely,



Enclosures: 1. List of Commitments
2. Unit 2 Return to Service Report

cc: NRC Document Control Desk
R. Hall, NRC Project Manager, San Onofre Units 2 and 3
G. G. Warnick, NRC Senior Resident Inspector, San Onofre Units 2 and 3
R. E. Lantz, Branch Chief, Division of Reactor Projects, Region IV

ENCLOSURE 1

List of Commitments

**Enclosure 1
List of Commitments**

This table identifies actions discussed in this letter that Southern California Edison commits to perform. Any other actions discussed in this submittal are described for the NRC's information and are not commitments.

	Description of Commitment	Scheduled Completion Date
1	Prior to a mid-cycle shutdown of Unit 2, SCE will administratively limit operation of Unit 2 to 70% power (refer to cover letter, Completion of CAL Action 2).	mid-cycle shutdown of Unit 2
2	SCE will shut down Unit 2 for a mid-cycle steam generator (SG) inspection outage. During this outage, inspections of Unit 2 SG tubes will be performed to confirm the effectiveness of the corrective and compensatory actions taken to address tube-to-tube wear in the Unit 2 SGs. (refer to cover letter, Completion of CAL Action 2).	within 150 cumulative days of operation at or above 15% power
3	SCE will install a temporary N-16 radiation detection system (refer to Enclosure 2, Section 9.2). The temporary N-16 detectors will be located on the Unit 2 main steam lines and be capable of detecting an increase in steam line activity.	prior to Unit 2 entry into Mode 2
4	SCE Plant Operators will receive training on use of the new detection tools for early tube leak identification and on lessons learned from response to the January 31, 2012, Unit 3 shutdown due to a steam generator (SG) tube leak (refer to Enclosure 2, Section 9.4.2).	prior to Unit 2 entry into Mode 2
5	SCE will upgrade the Unit 2 Vibration and Loose Part Monitor System (refer to Enclosure 2, Section 11.1). The new system will provide additional monitoring capabilities for steam generator secondary side noise.	prior to Unit 2 entry into Mode 2
6	SCE will install analytic and diagnostic software (GE Smart Signal) utilizing existing instrumentation (refer to Enclosure 2, Section 11.2).	prior to Unit 2 entry into Mode 2

ENCLOSURE 2

San Onofre Nuclear Generating Station

Unit 2 Return to Service Report

[Proprietary Information Redacted]



SOUTHERN CALIFORNIA
EDISON[®]

An *EDISON INTERNATIONAL*[®] Company

Enclosure 2

SOUTHERN CALIFORNIA EDISON
An *EDISON INTERNATIONAL* Company

**SAN ONOFRE NUCLEAR GENERATING STATION
UNIT 2 RETURN TO SERVICE REPORT
October 3, 2012**

Table of Contents

	Page
RECORD OF REVISION	2
LIST OF TABLES	6
LIST OF FIGURES	7
ABBREVIATIONS AND ACRONYMS.....	8
1.0 EXECUTIVE SUMMARY	10
1.1 Occurrence and Detection of the Unit 3 Tube Leak	10
1.2 Inspections of the Steam Generator Tubes and Cause Evaluations of Tube Wear	11
1.3 Compensatory, Corrective, and Defense-in-Depth Actions.....	11
1.4 Operational Assessments	11
1.5 Conclusion.....	12
2.0 INTRODUCTION.....	13
3.0 BACKGROUND	14
3.1 Steam Generator Tube Safety Functions.....	14
3.2 SG Regulatory/Program Requirements.....	15
3.3 The SONGS Steam Generator Program.....	16
4.0 UNIT 2 AND 3 REPLACEMENT STEAM GENERATORS.....	17
5.0 UNIT 3 EVENT – LOSS OF TUBE INTEGRITY	18
5.1 Summary of Event.....	18
5.2 Safety Consequences of Event.....	19
5.2.1 Deterministic Risk Analyses.....	19
5.2.2 Probabilistic Risk Assessment (PRA)	20
6.0 UNIT 3 EVENT INVESTIGATION AND CAUSE EVALUATION	21
6.1 Summary of Inspections Performed	21
6.2 Summary of Inspection Results.....	22
6.3 Cause Analyses of Tube-to-Tube Wear in Unit 3.....	30
6.3.1 Mechanistic Cause.....	30
6.3.2 Potential Applicability of Unit 3 TTW Causes to Unit 2	30
6.4 Industry Expert Involvement.....	31
6.5 Cause Analysis Summary	31

Table of Contents
(continued)

		Page
7.0	UNIT 2 CYCLE 17 INSPECTIONS AND REPAIRS	32
7.1	Unit 2 Cycle 17 Routine Inspections and Repairs	32
7.2	Unit 2 Cycle 17 Inspection in Response to TTW in Unit 3.....	33
7.3	Differences between Units 2 and 3	36
8.0	UNIT 2 CORRECTIVE AND COMPENSATORY ACTIONS TO ENSURE TUBE INTEGRITY ..	37
8.1	Limit Operation of Unit 2 to 70% Power	37
8.2	Preventive Tube Plugging for TTW	45
	8.2.1 Screening Criteria for Selecting Tubes for Plugging	45
	8.2.2 Plant Operations with Tubes Plugged in Unit 2.....	48
8.3	Inspection Interval and Protocol of Mid-cycle Inspections.....	48
	8.3.1 Inspection of Inservice Tubes (Unplugged)	48
	8.3.2 Inspection of Plugged Tubes	48
9.0	UNIT 2 DEFENSE-IN-DEPTH ACTIONS.....	50
9.1	Injection of Argon into the Reactor Coolant System (RCS).....	50
9.2	Installation of Nitrogen (N-16) Radiation Detection System on the Main Steam Lines ...	50
9.3	Reduction of Administrative Limit for RCS Activity Level	50
9.4	Enhanced Operator Response to Early Indication of SG Tube Leakage	50
	9.4.1 Operations Procedure Changes	50
	9.4.2 Operator Training.....	50
10.0	UNIT 2 OPERATIONAL ASSESSMENT.....	51
11.0	ADDITIONAL ACTIONS.....	52
11.1	Vibration Monitoring Instrumentation.....	52
11.2	GE Smart Signal™	52
12.0	CONCLUSIONS.....	53
13.0	REFERENCES.....	54

Table of Contents
(continued)

Page

ATTACHMENTS

- 1 SONGS Unit 2 Relevant Technical Specifications
- 2 AREVA Document 51-9182368-003, SONGS 2C17 Steam Generator Condition Monitoring Report*
- 3 AREVA Document 51-9180143-001, SONGS Unit 3 February 2012 Leaker Outage – Steam Generator Condition Monitoring Report*
- 4 MHI Document L5-04GA564, Tube Wear of Unit-3 RSG - Technical Evaluation Report*
- 5 MHI Document L5-04GA571, Screening Criteria for Susceptibility to In-Plane Tube Motion*
- 6 SONGS U2C17 Steam Generator Operational Assessment*

* [Proprietary Information Redacted]

List of Tables

	Page
TABLE 5-1: SONGS UNIT 3 SG 3E-088 IN-SITU PRESSURE TESTS WITH TUBE LEAKAGE	19
TABLE 6-1: STEAM GENERATOR WEAR DEPTH SUMMARY	29
TABLE 7-1: TTW COMPARISON BETWEEN UNIT 2 AND UNIT 3 SGS	36
TABLE 8-1: INDEPENDENT ATHOS COMPARISON RESULTS – STEAM QUALITY	38
TABLE 8-2: COMPARISON OF MAXIMUM VOID FRACTION	40
TABLE 8-3: COMPARISON OF MAXIMUM INTERSTITIAL VELOCITY (FT/S)	42
TABLE 8-4: UNIT 2 STEAM GENERATOR TUBE PLUGGING SUMMARY	45

List of Figures

	Page
FIGURE 3-1: REPLACEMENT STEAM GENERATOR SECTION VIEW	14
FIGURE 6-1: STEAM GENERATOR SECTION VIEW SKETCH	23
FIGURE 6-2: UNIT 2 DISTRIBUTION OF WEAR AT AVB SUPPORTS	24
FIGURE 6-3: UNIT 3 DISTRIBUTION OF WEAR AT AVB SUPPORTS	24
FIGURE 6-4: UNIT 2 DISTRIBUTION OF WEAR AT TSP SUPPORTS	25
FIGURE 6-5: UNIT 3 DISTRIBUTION OF WEAR AT TSP SUPPORTS	25
FIGURE 6-6: PROBABILITY OF DETECTION FOR TUBE WEAR	26
FIGURE 6-7: 3E-088 ROTATING COIL INSPECTION REGION	27
FIGURE 6-8: 3E-089 ROTATING COIL INSPECTION REGION	28
FIGURE 7-1: 2E-088 ROTATING COIL INSPECTION REGION	34
FIGURE 7-2: 2E-089 ROTATING COIL INSPECTION REGION	35
FIGURE 8-1: STEAM QUALITY CONTOUR PLOTS FOR 100% POWER AND 70% POWER.....	39
FIGURE 8-2: MAXIMUM VOID FRACTION VERSUS POWER LEVEL AND	41
FIGURE 8-3: INTERSTITIAL VELOCITY CONTOUR PLOTS FOR 100% POWER AND 70% POWER	43
FIGURE 8-4: GAP VELOCITY AT 100% POWER AND 70% POWER FOR 2E-088 R141C89.....	44
FIGURE 8-5: GAP VELOCITY AT 100% POWER AND 70% POWER FOR 2E-089 R141C89.....	44
FIGURE 8-6: 2E-088 PLUGGING AND STABILIZING MAP	46
FIGURE 8-7: 2E-089 PLUGGING AND STABILIZING MAP	47

ABBREVIATIONS AND ACRONYMS

2E-088	Unit 2 Steam Generator E-088
2E-089	Unit 2 Steam Generator E-089
3E-088	Unit 3 Steam Generator E-088
3E-089	Unit 3 Steam Generator E-089
AILPC	Accident Induced Leakage Performance Criterion
Ar	Argon
ATHOS	Analysis of Thermal-Hydraulics of Steam Generators
AVB	Anti-Vibration Bar
CDP	Core Damage Probability
CM	Condition Monitoring
DA	Degradation Assessment
DID	Defense in Depth
ECT	Eddy Current Testing
EFPD	Effective Full Power Days
EPRI	Electric Power Research Institute
ETSS	Examination Technique Specification Sheet
FEI	Fluid Elastic Instability
FIV	Flow Induced Vibration
FO	Foreign Object
FOSAR	Foreign Object Search and Retrieval
gpd	Gallons Per Day
INPO	Institute of Nuclear Power Operations
LERP	Large Early Release Probability
MHI	Mitsubishi Heavy Industries, Ltd.
MSLB	Main Steam Line Break
MWt	Megawatt Thermal
N-16	Nitrogen – 16
NEI	Nuclear Energy Institute
NODP	Normal Operating Differential Pressure
OA	Operational Assessment
OSG	Original Steam Generator
post-trip SLB	Steam Line Break Post-Trip Return-To-Power Event
PRA	Probabilistic Risk Assessment
RB	Retainer Bar
RCPB	Reactor Coolant Pressure Boundary
RCE	Root Cause Evaluation
RCS	Reactor Coolant System
Ref.	Reference
RSG	Replacement Steam Generator
SCE	Southern California Edison
SG	Steam Generator
SGTR	Steam Generator Tube Rupture
SIPC	Structural Integrity Performance Criterion
SLB	Steam Line Break
SGP	Steam Generator Program
SONGS	San Onofre Nuclear Generating Station
SR	Stability Ratio
T/H	Thermal-Hydraulics
TEDE	Total Effective Dose Equivalent
TS	Technical Specification
TSP	Tube Support Plate

TTW	Tube-to-Tube Wear
TW	Through Wall
TWD	Through Wall Depth
U2C17	Unit 2 Cycle 17
UFSAR	Updated Final Safety Analysis Report
UT	Ultrasonic Testing
WEC	Westinghouse Electric Company

1.0 EXECUTIVE SUMMARY

On January 31, 2012, a leak was detected in a steam generator (SG) in Unit 3 of the San Onofre Nuclear Generating Station (SONGS). Southern California Edison (SCE) operators promptly shut down the unit in accordance with plant operating procedures. The leak resulted in a small radioactive release to the environment that was well below the allowable federal limits. Subsequently, on March 27, 2012, the Nuclear Regulatory Commission (NRC) issued a Confirmatory Action Letter (CAL) (Ref. 1) to SCE describing actions that the NRC and SCE agreed must be completed prior to returning Units 2 and 3 to service.

To address the tube leak and its causes, SCE assembled a technical team including experts in the fields of thermal hydraulics (T/H) and in SG design, manufacture, operation, and maintenance. The team performed extensive investigations into the causes of the tube leak and developed compensatory and corrective actions that SCE has implemented to prevent recurrence of the tube-to-tube wear (TTW) that caused the leak. SCE also implemented defense-in-depth (DID) measures to provide additional safety margin. SCE has planned SG inspections following a shortened operating interval to confirm the effectiveness of its compensatory and corrective actions.

As required by the SONGS technical specifications (TSs), the SONGS Steam Generator Program (SGP), and industry guidelines, an Operational Assessment (OA) must be performed to ensure that SG tubing will meet established performance criteria for structural and leakage integrity during the operating period prior to the next planned inspection. Because of the unusual and unexpected nature of the SG TTW, SCE commissioned three independent OAs by experienced vendors. These vendors applied different methodologies to ensure a comprehensive and diverse evaluation. An additional OA was performed to evaluate SG tube wear other than TTW. Each of these OAs independently concluded that the compensatory and corrective actions implemented by SCE are sufficient to address tube wear issues so that the Unit 2 SGs will operate safely.

The purpose of this report is to provide detailed information demonstrating completion of CAL actions required prior to entry of Unit 2 into Mode 2. The report also describes in detail the basis for the conclusion that Unit 2 will continue to operate safely after restart.

This report describes:

- Results of inspections of the SG tubes
- Causes of the tube wear in the Unit 2 and Unit 3 SGs
- Compensatory and corrective actions that SCE has taken to address tube wear in Unit 2
- OAs that have been performed to demonstrate that those compensatory and corrective actions ensure that TTW will be prevented until the next SG inspections
- Additional controls and DID actions that SCE is implementing to ensure health and safety of the public in the unlikely event of a loss of SG tube integrity

1.1 Occurrence and Detection of the Unit 3 Tube Leak

New SGs were placed into service at SONGS Units 2 and 3 in 2010 and 2011, respectively. The replacement steam generators (RSGs) were installed to resolve corrosion and other degradation issues present in the original steam generators (OSGs). The RSGs were designed and manufactured by Mitsubishi Heavy Industries (MHI). On January 9, 2012, after 22 months of operation, Unit 2 was shut down for a routine refueling and SG inspection outage. This was the first inspection of the Unit 2 SG tubes performed following SG replacement. The condition monitoring (CM) assessment performed to evaluate the results of this inspection confirmed that the SG performance criteria were satisfied during the operating interval.

On January 31, 2012, while the Unit 2 outage was in progress, SONGS Unit 3 was operating at 100 percent power when a condenser air ejector radiation monitor alarm indicated a primary-to-secondary leak. Unit 3 was

promptly shut down in accordance with plant operating procedures and placed in a stable cold shutdown condition. The TS limit for operational leakage (150 gallons per day (gpd)) was not exceeded during the event. A small, monitored radioactive release to the environment occurred, resulting in an estimated 0.0000452 mrem dose to the public. This estimated dose was well below the allowable federal limit specified in 10 CFR 20 of 100 mrem per year to a member of the public.

1.2 Inspections of the Steam Generator Tubes and Cause Evaluations of Tube Wear

Subsequent to the reactor cooldown, extensive inspection, testing, and analysis of SG tubes was performed in both Unit 3 SGs. This was the first inspection of the Unit 3 SG tubes performed following SG replacement after approximately 11 months of operation. The leak was identified in SG 3E-088 and was caused by TTW in the U-bend portion of the tube in Row 106 Column 78. Additional inspections revealed significant TTW in many tubes in Unit 3.

In accordance with SGP requirements for unexpected degradation, SCE initiated a cause evaluation of the TTW phenomenon. The Root Cause Evaluation (RCE) Team used significant input from the SG Recovery Team which included the services of MHI and industry experts in the fields of T/H and in SG design, manufacturing, operation, and repair. The mechanistic cause of the TTW in Unit 3 was identified as fluid elastic instability (FEI), caused by a combination of localized high steam velocity (tube vibration excitation forces), high steam void fraction (loss of ability to dampen vibration), and insufficient tube to anti-vibration bar (AVB) contact to overcome the excitation forces. The FEI resulted in a vibration mode of the SG tubes in which the tubes moved in the in-plane direction parallel to the AVBs in the U-bend region. This resulted in TTW in a localized region of the Unit 3 SGs.

Although no TTW had been detected during the routine inspections of all tubes in Unit 2, the unit was not returned to service pending an evaluation of the susceptibility of the Unit 2 SGs to the TTW found in Unit 3. In March 2012, as part of this evaluation, additional inspections using a more sensitive inspection method were performed on the Unit 2 tubes. Shallow TTW was identified between two adjacent tubes in SG 2E-089.

1.3 Compensatory, Corrective, and Defense-in-Depth Actions

SCE has implemented compensatory and corrective actions that will prevent loss of integrity due to TTW in Unit 2, including:

1. Limiting Unit 2 to 70% power prior to a mid-cycle SG inspection outage
2. Preventively plugging tubes in both SGs
3. Shutting down Unit 2 for a mid-cycle SG inspection outage within 150 cumulative days of operation at or above 15% power

SCE has also implemented conservative DID measures to provide an increased safety margin in the unlikely event of tube-to-tube degradation in the Unit 2 SGs during operation at 70% reactor power. Additionally, SCE has provided enhanced plant monitoring capability to assist in evaluating the condition of the SGs.

1.4 Operational Assessments

As required by the CAL (Ref. 1), SCE has prepared an assessment of the Unit 2 SGs that addresses the causes of TTW wear found in the Unit 3 SGs, prior to entry of Unit 2 into MODE 2.

Due to the significant levels of TTW found in Unit 3 SGs, SCE assessed the likelihood of additional TTW in Unit 2 from several different perspectives, utilizing the experience and expertise of AREVA NP, Westinghouse Electric Company, LLC (WEC), and Intertek/APTECH. Each of these companies routinely prepare OAs to assess the safety of operation of SGs at U.S. nuclear power plants. These companies developed independent OAs to

evaluate the TTW found at SONGS and the compensatory and corrective actions being implemented to address TTW in the Unit 2 SGs. These OAs apply different methodologies to ensure a comprehensive and diverse evaluation. Each of these OAs concluded that the compensatory and corrective actions implemented by SCE are sufficient to address tube wear issues so that the Unit 2 SGs will operate safely. The results of these analyses fulfill the TS requirement to demonstrate that SG tube integrity will be maintained over the reduced operating cycle until the next SG inspection.

1.5 Conclusion

On the basis of the compensatory and corrective actions, DID actions, and the results of the OAs, SCE concludes that Unit 2 will operate safely at 70% power for 150 cumulative days of operation with substantial safety margin and without loss of tube integrity. Reducing power to 70% eliminates the thermal hydraulic conditions that cause FEI and associated TTW from the SONGS Unit 2 SGs. After this period of operation, Unit 2 will be shut down for inspection of the steam generator tubes to confirm the effectiveness of the compensatory and corrective actions that have been taken. SCE will continue to closely monitor steam generator tube integrity and take corrective actions as appropriate to ensure the health and safety of the public is maintained.

2.0 INTRODUCTION

On March 27, 2012, the NRC issued a CAL (Ref. 1) to SCE describing actions that the NRC and SCE agreed would be completed prior to returning Units 2 and 3 to service. The purpose of this report is to provide detailed information to demonstrate fulfillment of Actions 1 and 2 of the CAL, which are required to be completed prior to entry of Unit 2 into Mode 2. The actions as stated in the CAL are as follows:

CAL ACTION 1: "Southern California Edison Company (SCE) will determine the causes of the tube-to-tube interactions that resulted in steam generator tube wear in Unit 3, and will implement actions to prevent loss of integrity due to these causes in the Unit 2 steam generator tubes. SCE will establish a protocol of inspections and/or operational limits for Unit 2, including plans for a mid-cycle shutdown for further inspections."

CAL ACTION 2: "Prior to entry of Unit 2 into Mode 2, SCE will submit to the NRC in writing the results of your assessment of Unit 2 steam generators, the protocol of inspections and/or operational limits, including schedule dates for a mid-cycle shutdown for further inspections, and the basis for SCE's conclusion that there is reasonable assurance, as required by NRC regulations, that the unit will operate safely."

This report describes the actions SCE has taken to return Unit 2 to service while ensuring that the unit will operate safely. Because the SGs in Units 2 and 3 have the same design, the causes of the tube leak in Unit 3 and the potential susceptibility of Unit 2 SGs to the same mechanism are also addressed. This report will demonstrate that actions have been completed to prevent loss of integrity in the Unit 2 SG tubes due to these causes.

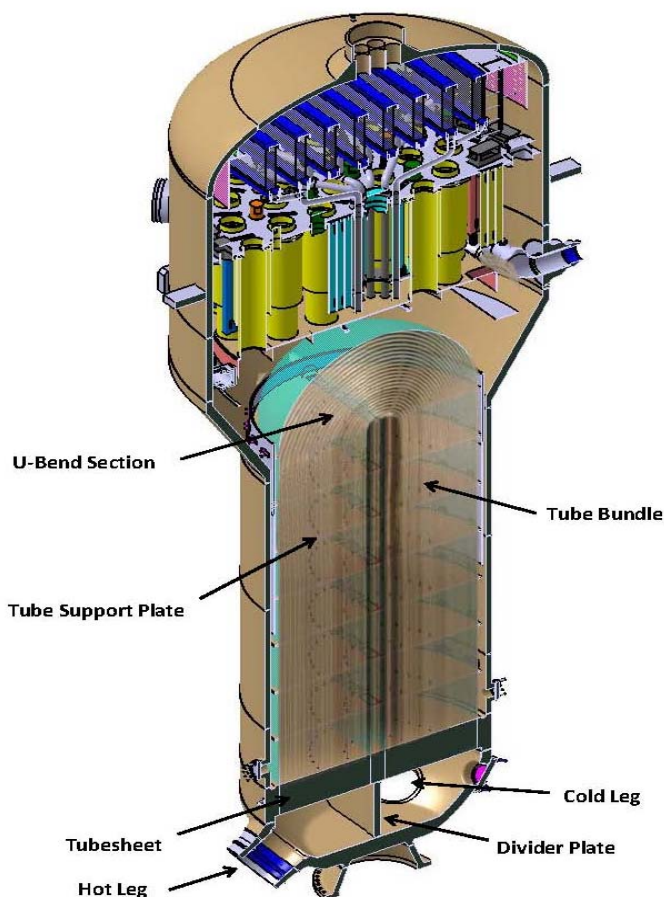
3.0 BACKGROUND

3.1 Steam Generator Tube Safety Functions

The Reactor Coolant System (RCS) circulates primary system water in a closed cycle, removing heat from the reactor core and internals and transferring it to the secondary side main steam system. The SGs provide the interface between the RCS and the main steam system. Reactor coolant is separated from the secondary system fluid by the SG tubes and tube sheet, making the RCS a closed system and forming a barrier to the release of radioactive materials from the core. The secondary side systems also circulate water in a closed cycle transferring the waste heat from the condenser to the circulating water system. However, the secondary side is not a totally closed system and presents several potential release paths to the environment in the event of a primary-to-secondary leak.

The SG tubes have a number of important safety functions. As noted above, the SG tubes are an integral part of the Reactor Coolant Pressure Boundary (RCPB) and, as such, are relied on to maintain primary system pressure and inventory. The SG tubes isolate the radioactive fission products in the primary coolant from the secondary system. In addition, as part of the RCPB, the SG tubes act as the heat transfer surface that transfers heat from the primary system to the secondary system. Figure 3-1 provides a section view of a SONGS SG.

Figure 3-1: Replacement Steam Generator Section View



3.2 SG Regulatory/Program Requirements

The nuclear industry and the NRC have instituted rigorous requirements and guidelines to ensure that SG tube integrity is maintained such that the tubes are capable of performing their intended safety functions. Title 10 of the Code of Federal Regulations (10 CFR) establishes the fundamental regulatory requirements with respect to integrity of the SG tubes. The SONGS TSs include several requirements relating to the SGs including the requirement that SG tube integrity is maintained and all SG tubes reaching the tube repair criteria are plugged in accordance with the SGP (TS 3.4.17), that a SGP is established and implemented to ensure that SG tube integrity is maintained (TS 5.5.2.11), that a report of the inspection and CM results be provided to the NRC following each SG inspection outage (TS 5.7.2.c), and that the primary-to-secondary leakage through any one SG is limited to 150 gpd (TS 3.4.13). These TSs are provided in their entirety in Attachment 1.

TS 5.5.2.11, Steam Generator Program, requires the establishment and implementation of a SGP to ensure that SG tube integrity is maintained. The SGP ensures the tubes are repaired, or removed from service by plugging the tube ends, before the structural or leakage integrity of the tubes is impaired. TS 3.4.13 includes a limit on operational primary-to-secondary leakage, beyond which the plant must be promptly shutdown. Should a flaw exceeding the tube repair limit not be detected during the periodic tube inspections, the leakage limit provides added assurance of timely plant shutdown before tube structural and leakage integrity are impaired.

TS 5.5.2.11 requires the SGP to include five provisions, which are summarized below

- a. CM assessments shall be conducted during each SG inspection outage to evaluate the “as found” condition of the tubing with respect to the performance criteria for structural integrity and accident induced leakage. The purpose of the CM assessment is to ensure that the SG performance criteria have been met for the previous operating period.
- b. SG tube integrity shall be maintained by meeting the specified performance criteria for tube structural integrity, accident induced leakage, and operational leakage.
- c. Tubes found by in-service inspection to contain flaws with a depth equal to or exceeding 35% of the nominal tube wall thickness shall be plugged.
- d. Periodic SG tube inspections shall be performed as specified in the TS. The inspection scope, inspection methods, and inspection intervals shall be such as to ensure that SG tube integrity is maintained until the next SG inspection.
- e. Provisions shall be made for monitoring operational primary-to-secondary leakage.

TS 3.4.13, RCS Operational Leakage, limits primary-to-secondary leakage through any one SG to 150 gpd. The limit of 150 gpd per SG is based on the operational leakage performance criterion in the Nuclear Energy Institute (NEI) 97-06, Steam Generator Program Guidelines (Ref. 2). The limit is based on operating experience with SG tube degradation mechanisms that result in tube leakage.

3.3 The SONGS Steam Generator Program

The purpose of the SGP is to ensure tube integrity and compliance with SG regulatory requirements. The program contains a balance of prevention, inspection, evaluation and repair, and leakage monitoring measures. The SONGS SGP (Ref. 10), which implements the requirements specified in TS 5.5.2.11, is based on the NEI 97-06, Steam Generator Program Guidelines (Ref. 2) and its referenced Electric Power Research Institute (EPRI) guidelines. Use of the SGP ensures that SGs are inspected and repaired consistent with accepted industry practices.

The SGP requires assessments of SG integrity. This assessment applies to SG components which are part of the primary pressure boundary (e.g., tubing, tube plugs, sleeves and other repairs). It also applies to foreign objects (FOs) and secondary side structural supports (e.g., tube support plates (TSPs)) that may, if severely degraded, compromise pressure-retaining components of the SG. Three types of assessments are performed to provide assurance that the SG tubes will continue to satisfy the appropriate performance criteria: (1) Degradation Assessment (DA); (2) CM Assessment; and (3) OA.

The DA is the planning process that identifies and documents information about plant-specific SG degradation. The overall purpose of the DA is to prepare for an upcoming SG inspection through the identification of the appropriate examinations and techniques, and ensuring that the requisite information for integrity assessment is obtained. The DA performed for Unit 2 Cycle 17 (U2C17) SG Inspection Outage is discussed in Section 7.1 of this report.

The CM is backward looking, in that its purpose is to confirm that adequate SG tube integrity has been maintained during the previous inspection interval. The CM involves an evaluation of the as-found condition of the tubing relative to the integrity performance criteria specified in the TS. The tubes are inspected according to the EPRI Pressurized Water Reactor SG Examination Guidelines (Ref. 3). Structural and leakage integrity assessments are performed and results compared to their respective performance criteria. If satisfactory results are not achieved, a RCE is performed and appropriate corrective action taken. The results of this analysis are factored into future DAs, inspection plans, and OAs of the plant. The CM results for U2C17 are presented in Section 7 of this report.

The OA differs from the CM assessment in that it is forward looking rather than backward looking. Its purpose is to demonstrate that the tube integrity performance criteria will be met throughout the next inspection interval. During the CM assessments, inspection results are evaluated with respect to the appropriate performance criteria. If this evaluation is successful, an OA is performed to show that integrity will be maintained throughout the next interval between inspections. If any performance criterion is not met during performance of CM, a RCE is required to be performed and the results are to be factored into the OA strategy. The results of the OA determine the allowable operating time for the upcoming inspection interval. The OA addressing all degradation mechanisms found during U2C17 is discussed in Section 10 of this report.

4.0 UNIT 2 AND 3 REPLACEMENT STEAM GENERATORS

New SGs were placed into service at SONGS Units 2 and 3 in 2010 and 2011, respectively. The RSGs were intended to resolve corrosion and other degradation issues present in the OSGs. The RSGs were designed and manufactured by MHI.

The steam generator is a recirculating, vertical U-tube type heat exchanger converting feedwater into saturated steam. The steam generator vessel pressure boundary is comprised of the channel head, lower shell, middle shell, transition cone, upper shell and upper head. The steam generator internals include the divider plate, tubesheet, tube bundle, feedwater distribution system, moisture separators, steam dryers and integral steam flow limiter installed in the steam nozzle. The channel head is equipped with one reactor coolant inlet nozzle and two outlet nozzles. The upper vessel is equipped with the feedwater nozzle, steam nozzle and blowdown nozzle. In the channel head, there are two 18 inch access manways. In the upper shell, there are two 16 inch access manways. The steam generator is equipped with six handholes and 12 inspection ports providing access for inspection and maintenance. In addition, the steam generators are equipped with several instrumentation and minor nozzles for layup and chemical recirculation intended for chemical cleaning.

5.0 UNIT 3 EVENT – LOSS OF TUBE INTEGRITY

5.1 Summary of Event

On January 31, 2012, while the Unit 2 refueling and SG inspection outage was in progress, SONGS Unit 3 was in Mode 1 operating at 100 percent power, when a condenser air ejector radiation monitor alarm indicated a primary-to-secondary leak. A rapid power reduction was commenced when the primary-to-secondary leak rate was determined to be greater than 75 gpd with an increasing rate of leakage exceeding 30 gpd per hour. The reactor was manually tripped from 35 percent power, and placed in a stable cold shutdown condition in Mode 5. The TS 3.4.13 limit for RCS operational leakage (150 gpd) was not exceeded. A small, monitored radioactive release to the environment occurred, resulting in an estimated 0.0000452 mrem dose to the public, which was well below the allowable federal limit specified in 10 CFR 20 of 100 mrem per year to a member of the public.

Subsequent to the reactor cooldown, extensive inspection, testing, and analysis of SG tube integrity commenced in both Unit 3 SGs. This was the first inspection of the Unit 3 SG tubes performed following SG replacement after approximately eleven months of operation. The work scope included the following activities: bobbin probe and rotating probe examinations using eddy current testing (ECT), secondary and primary side visual examinations, and in-situ pressure testing. The location of the leak in SG 3E-088, which resulted in the Unit 3 shutdown, was determined to be in the U-bend portion of the tube in Row 106 Column 78. ECT was subsequently performed on 100% of the tubes in both Unit 3 SGs. During these inspections, unexpected wear was discovered in both SGs including wear at AVBs, TSPs, RBs, and significant TTW in the U-bend area of the tubes. The TTW in Unit 3 was found to be much more extensive than in Unit 2, where only two tubes in one SG were determined to be affected.

The EPRI guidelines (Ref. 4) allow assessment of the structural and accident induced leakage integrity to be performed either analytically or through in-situ pressure testing. In accordance with EPRI guidelines and the SGP, in-situ pressure testing was performed on a total of 129 tubes in Unit 3, (73 in SG 3E-088 and 56 in SG 3E-089) in March 2012. The pressure tests were performed to determine if the tubes met the performance criteria in the TS (Attachment 1). The testing resulted in detected leaks in eight tubes in SG 3E-088 at the pressures indicated in Table 5-1. The failure location for all eight tubes was in the U-bend portion of the tube bundle in the tube freespan area. The locations of the tubes that were pressure tested and the tubes that failed the pressure tests are shown in Figure 6-7 and Figure 6-8. The first tube listed in the table (location 106-78) was the tube with the through-wall leak which resulted in the Unit 3 shutdown on January 31, 2012. No leaks were detected in the remaining 121 tubes tested in Unit 3. For the eight tubes indicating leakage, three tubes failed both the accident induced leakage performance criterion (AILPC) and the structural integrity performance criterion (SIPC); and 5 tubes passed the AILPC but failed the SIPC. All tubes met the operational leakage performance criterion of TS Limiting Condition for Operation 3.4.13. Details of the Unit 3 inspections and in-situ testing results are documented in the Unit 3 CM Report included as Attachment 3.

Additional testing performed to identify the extent and cause of the abnormal wear is presented in Section 6. Required reports in response to the reactor shut down and in-situ test failures were made to the NRC in accordance with 10 CFR 50.72 and 50.73 (Refs. 5-8).

Table 5-1: SONGS Unit 3 SG 3E-088 In-Situ Pressure Tests with Tube Leakage

Test Date, Time	Tube Location (row-column)	Maximum Test Pressure Achieved (see Note 1)	Performance Criteria Not Met (see Note 2)
03/14/12, 1120PDT	106-78	2874 psig	Accident Induced Leakage
03/14/12, 1249PDT	102-78	3268 psig	Accident Induced Leakage
03/14/12, 1425PDT	104-78	3180 psig	Accident Induced Leakage
03/15/12, 1109PDT	100-80	4732 psig	Structural Integrity
03/15/12, 1437PDT	107-77	5160 psig	Structural Integrity
03/15/12, 1604PDT	101-81	4889 psig	Structural Integrity
03/15/12, 1734PDT	98-80	4886 psig	Structural Integrity
03/16/12, 1216PDT	99-81	5026 psig	Structural Integrity

Note 1

Test Pressures:
(Calculated)

Normal Operating Differential Pressure (NODP) Test Pressure = 1850 psig
Accident Induced Leakage DP (Main Steam Line Break) Test Pressure = 3200 psig
Structural Integrity Limit (3 x NODP) Test Pressure = 5250 psig

Note 2

Performance Criteria:

Structural Integrity – No burst at 3 x NODP test pressure
Accident Induced Leakage - leak rate < 0.5 gpm at MSLB test pressure
Operational Leakage - TS Limiting Condition for Operation 3.4.13

5.2 Safety Consequences of Event

As discussed above, the Unit 3 shutdown on January 31, 2012, due to a SG tube leak, resulted in a small, monitored radioactive release to the environment, well below allowable limits. The potential safety significance of the degraded condition of the Unit 3 SG tubes is discussed below.

5.2.1 Deterministic Risk Analyses

The SONGS Updated Final Safety Analysis Report (UFSAR) Section 15.10.1.3.1.2 presents the current licensing basis steam line break (SLB) post-trip return-to-power event (post-trip SLB). Based on the actual plant RCS chemistry data, the accident-induced iodine spiking factor of 500, and the estimated SG tube rupture leakage rate, the calculated dose would have been at least 32 percent lower than the dose consequences reported in the UFSAR for the post-trip SLB event with a concurrent iodine spike. The postulated post-trip SLB with tube rupture and concurrent iodine spike Exclusion Area Boundary, Low Population Zone, and Control Room doses would be less than 0.068 Rem Total Effective Dose Equivalent (TEDE), which is well below the post-trip SLB Control Room limit of 5 Rem TEDE, and the Exclusion Area Boundary and Low Population Zone limit of 2.5 Rem TEDE.

The potential for a seismically-induced tube rupture was also evaluated. The analysis determined the equivalent flaw characteristics of the most limiting degraded tube in Unit 3 SG 3E-088 from its in-situ pressure test result. This tube, Row 106 Column 78 (the leaking tube), sustained an in-situ test pressure of 2,874 psi before exceeding leakage limits. This in-situ test pressure, which is slightly more than twice the operating differential pressure on the tube, corresponds to the limiting stress for crack penetration or plastic collapse with large deformation. The combined stresses due to operating differential pressure and seismic forces corresponding to SONGS Design Basis Earthquake (DBE) are lower than this limiting stress and are also less than the allowable stress for the faulted condition (i.e., including DBE) according to the American Society of Mechanical Engineers Code. Therefore, the degraded tube would not have burst under this worst case loading.

5.2.2 Probabilistic Risk Assessment

A Probabilistic Risk Assessment (PRA) was performed to analyze the risk impact of the degraded SG tubes on SONGS Unit 3 SG 3E-088 with respect to two cases: (1) any increased likelihood of an independent SG tube rupture (SGTR) at normal operating differential pressure (NODP), or (2) due to a SGTR induced by an excess steam demand event, also referred to as a main steam line break (MSLB). The SONGS PRA model was used to calculate the increases in Core Damage Probability (CDP) and Large Early Release Probability (LERP) associated with each case. In both cases, all postulated core damage sequences are assumed to result in a large early release since the containment will be bypassed due to the SGTR; therefore, the calculated CDP and LERP are equal. The total Incremental LERP (ILERP) due to the degraded SG tubes (i.e., the sum of the two analyzed cases) was determined to be less than 2×10^{-7} . This small increase in risk is attributed to two factors. First, the exposure time for the postulated increased independent SGTR initiating event frequency case was very short (0.1 Effective Full Power Month (EFPM)). Second, a MSLB alone does not generate sufficient differential pressure to cause tube rupture in Case 2. The differential pressure across the SG tubes necessary to cause a rupture will not occur if operators prevent RCS re-pressurization in accordance with Emergency Operating Instructions.

6.0 UNIT 3 EVENT INVESTIGATION AND CAUSE EVALUATION

6.1 Summary of Inspections Performed

Following the identification of SG tube leakage in the Unit 3 SG 3E-088, extensive inspections were performed to determine the location and cause of the leak. The location of the leak was identified by filling the SG secondary side with nitrogen and pressurizing to 80 psig. The test identified the tube located at Row 106, Column 78 (R106 C78) as the source of the leakage. Using eddy current bobbin and rotating probes, the tube at R106 C78 and those immediately adjacent to it were inspected and the leakage location was confirmed. The leak location was in the U-bend portion of the tube in the “freespan” area between AVB support locations (refer to Figure 6-1).

To determine the extent of the wear that had resulted in a leak, an eddy current bobbin probe examination of the full-length of all tubes in both Unit 3 SGs was performed. The locations of tubes with TTW are shown on Figures 6-7 and 6-8. Based on the results of the bobbin probe examinations, TTW indications were then examined using a more sensitive +Point™ rotating probe. Figure 6-6 illustrates a comparison of the sensitivity of the two types of examinations. The more sensitive rotating probe examinations were also performed on a region of tubes adjacent to the tubes with detected TTW. This region is also shown on Figures 6-7 and 6-8. TTW indications were identified in 161 tubes in 3E-088 and 165 tubes in 3E-089. All of the TTW flaws were located in the U-bend portion of the tubes between TSPs 7H and 7C (shown on Figure 6-1).

The more sensitive eddy current rotating probe provided an estimated depth and overall length of TTW flaws on each tube examined. The examination technique (EPRI Examination Technique Specification Sheet, ETSS 27902.2) was site validated by building a test specimen with flaws similar to the TTW flaws observed in Unit 3. Comparison of estimated wear depths with actual wear depths of the specimen supported the conclusion that ETSS 27902.2 conservatively estimated the depths across the entire range of depths tested (from 5% through-wall to 81% through-wall).

The tubes with flaws identified by ECT were analyzed to determine if they were capable of meeting the SONGS TS tube integrity performance criteria (Attachment 1). Tubes that did not meet the performance criteria based on analysis were tested via in-situ pressure testing. As described in detail in Section 5 and in the CM report (Attachment 3), a total of 129 tubes in the Unit 3 SGs were selected for in-situ pressure testing. Three tubes failed both the AILPC and the SIPC, and 5 tubes passed the AILPC but failed the SIPC as defined in TS 5.5.2.11. These eight tubes are listed in Table 5-1. Figure 6-7 and Figure 6-8 show the locations of the tubes that were in-situ tested and the eight tubes that did not meet the performance criteria.

Secondary side remote visual inspections were performed to supplement the eddy current results and provide additional information in support of the cause evaluation. The inspections included the 7th TSP and inner bundle passes at AVBs B04 and B09 (shown on Figure 6-1). The 7th TSP inspection revealed no unexpected or unusual conditions. The inner bundle passes included several inspections between columns 73 and 87 and showed instances of wear indications that extended outside the AVB intersection. This was confirmed by eddy current data. Additional passes were made between columns 50 and 60. These inspections did not show any AVB wear outside the AVB intersections.

6.2 Summary of Inspection Results

This section provides a summary of the different types of tube wear found in the SONGS Unit 2 and 3 SGs. Wear is characterized as a loss of metal on the surface of one or both metallic objects that are in contact during movement.

The following types of wear were identified in the SONGS Units 2 and 3 SG tubes:

- AVB wear - wear of the tubing at the tube-to-AVB intersections
- TSP wear - wear of the tubing at the tube-to-TSP intersections
- TTW - wear in the tube free-span sections between the AVBs located in the U-bend region.
- RB wear - wear of the tubing at a location adjacent to a RB (RBs are not designed as tube supports for normal operation)
- FO wear - wear of the tubing at a location adjacent to a FO.

Most of the tube wear identified in the SGs is adjacent to a tube support. Figure 6-1 is a side view of an SG, showing the relationship of the tubes to the two types of tube supports: TSPs in the straight portions and AVBs in the U-bend portions of the tubes. All tubes are adjacent to many of these two types of tube supports. The RB supports are not shown because a very small number of tubes are adjacent to them.

TTW indications occurred in the free span sections of the tubes. The “free span” is that section of the tube between support structures (AVBs and TSPs shown in Figure 6-1). TTW occurred almost exclusively in Unit 3 and is located on both the hot and cold leg side of the U-tube. In many cases, the region of the tube with TTW has two separate indications on the extrados and intrados of the tube. The wear indications on neighboring tubes have similar depth and position (ranging from 1.0 to 41 inches long and 4% to 100% throughwall) along the U-bend, confirming the tube-to-tube contact.

Table 6-1 provides the Wear Depth Summary for each of the four SGs based on eddy current examination results. Detailed results of the examinations performed are provided in the Units 2 and 3 CM reports included as Attachments 2 and 3. Figures 6-2 through 6-5 provide distributions of wear at AVB and TSP supports for all four SGs.

Figure 6-1: Steam Generator Section View Sketch

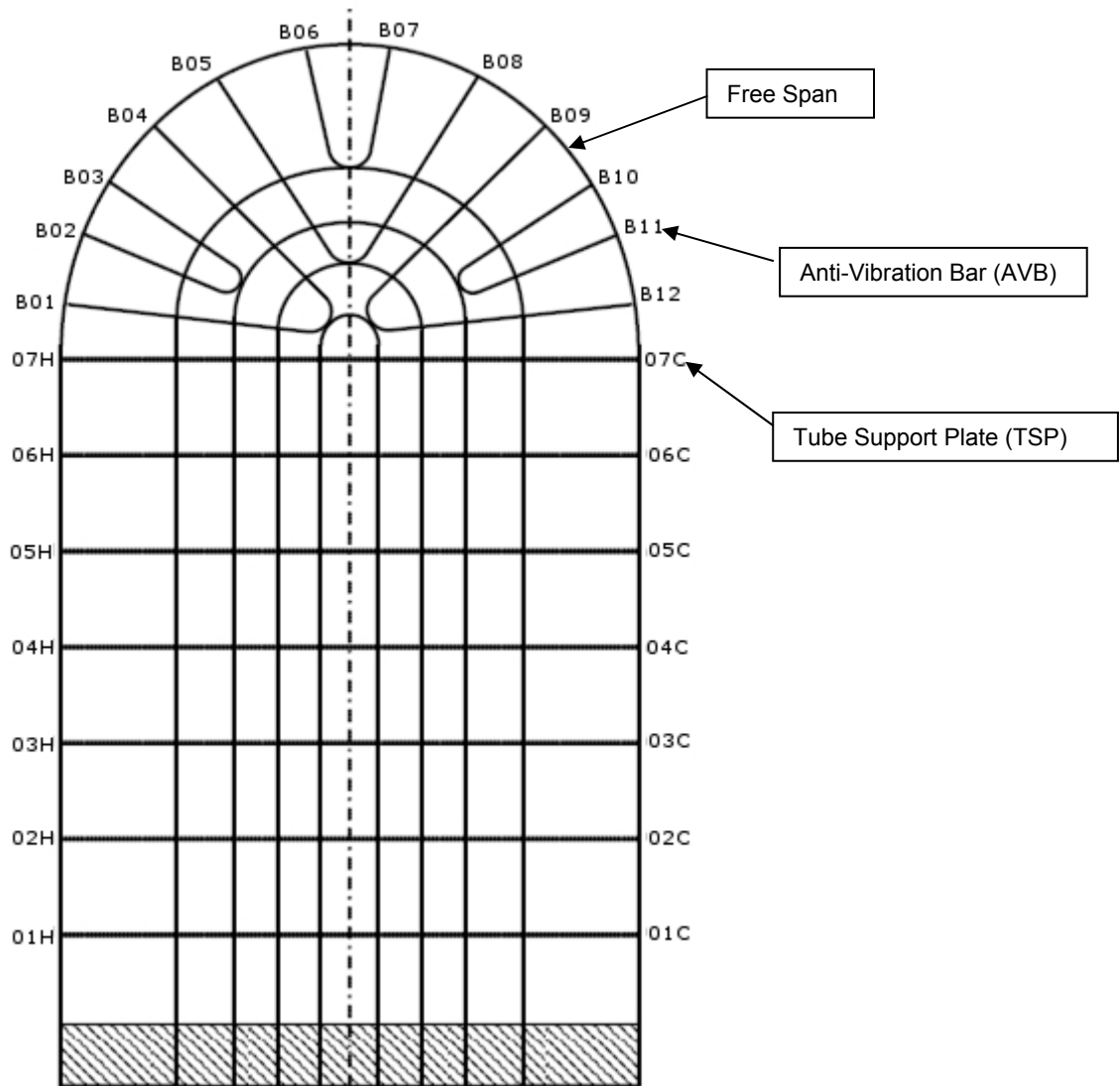


Figure 6-2: Unit 2 Distribution of Wear at AVB Supports

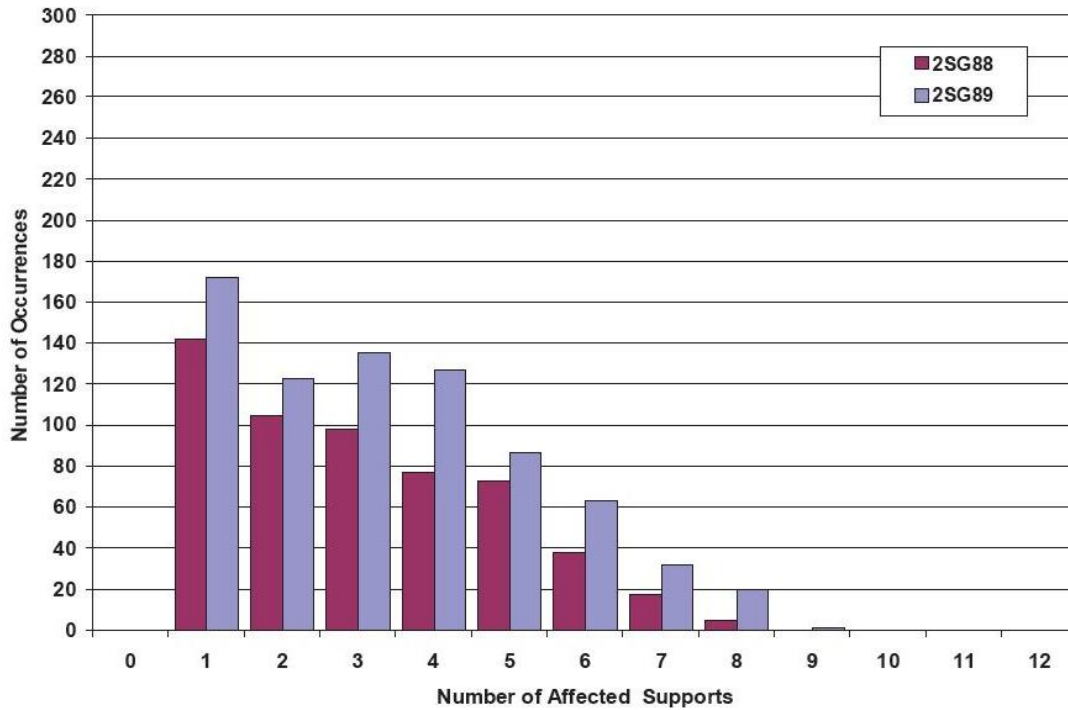


Figure 6-3: Unit 3 Distribution of Wear at AVB Supports

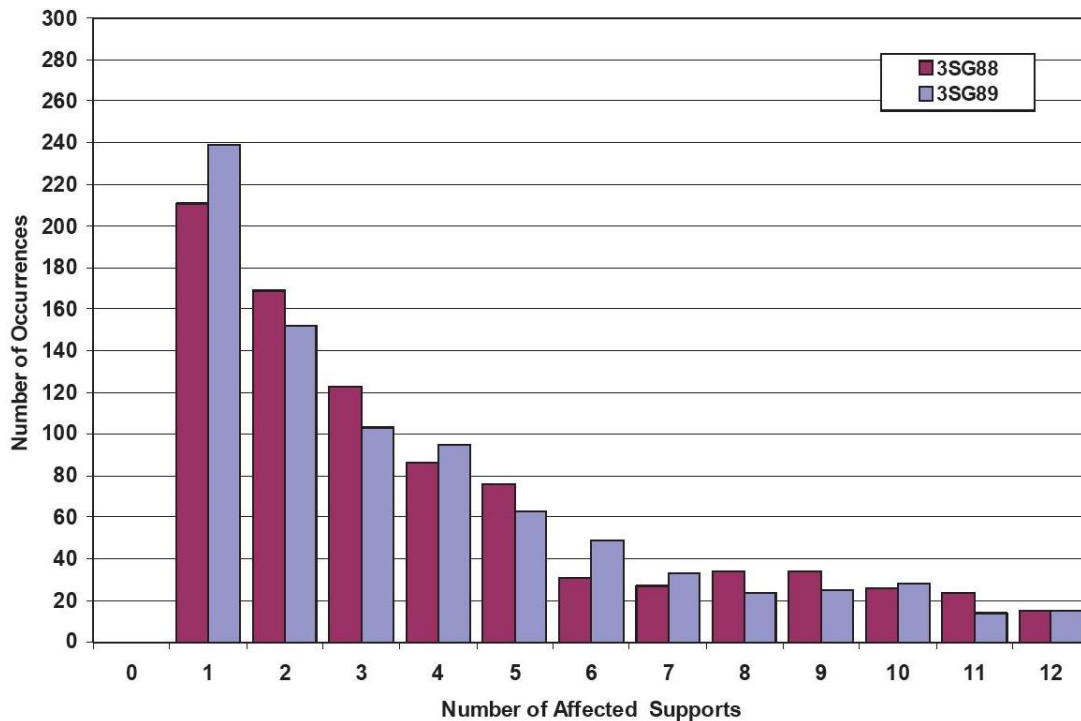


Figure 6-4: Unit 2 Distribution of Wear at TSP Supports

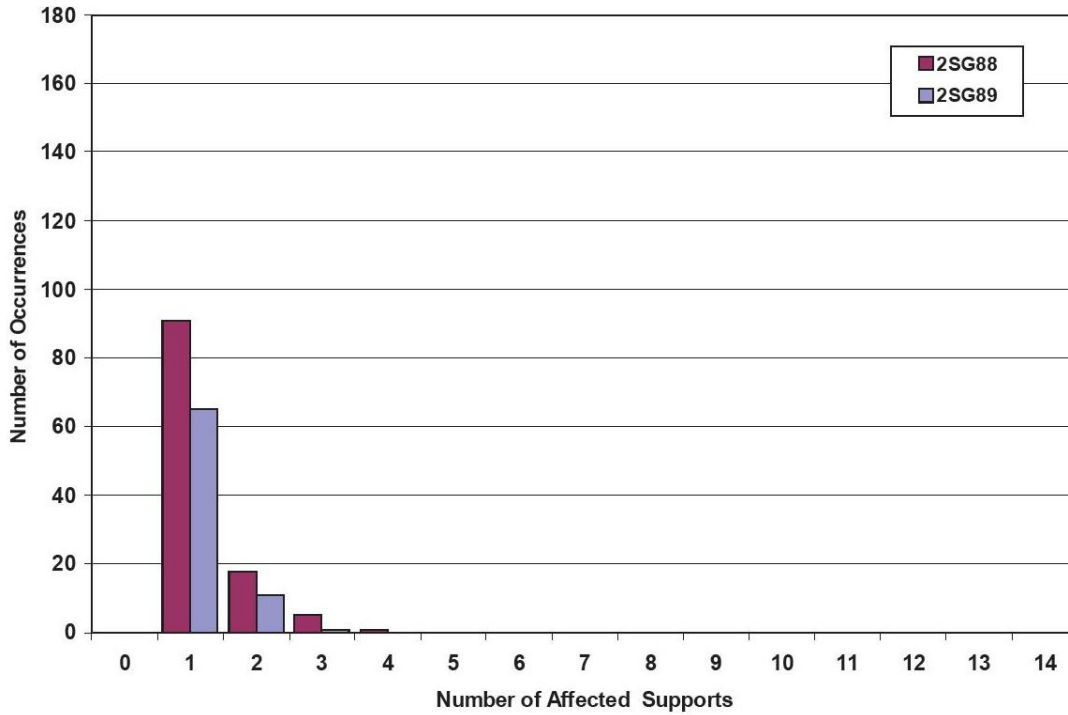


Figure 6-5: Unit 3 Distribution of Wear at TSP Supports

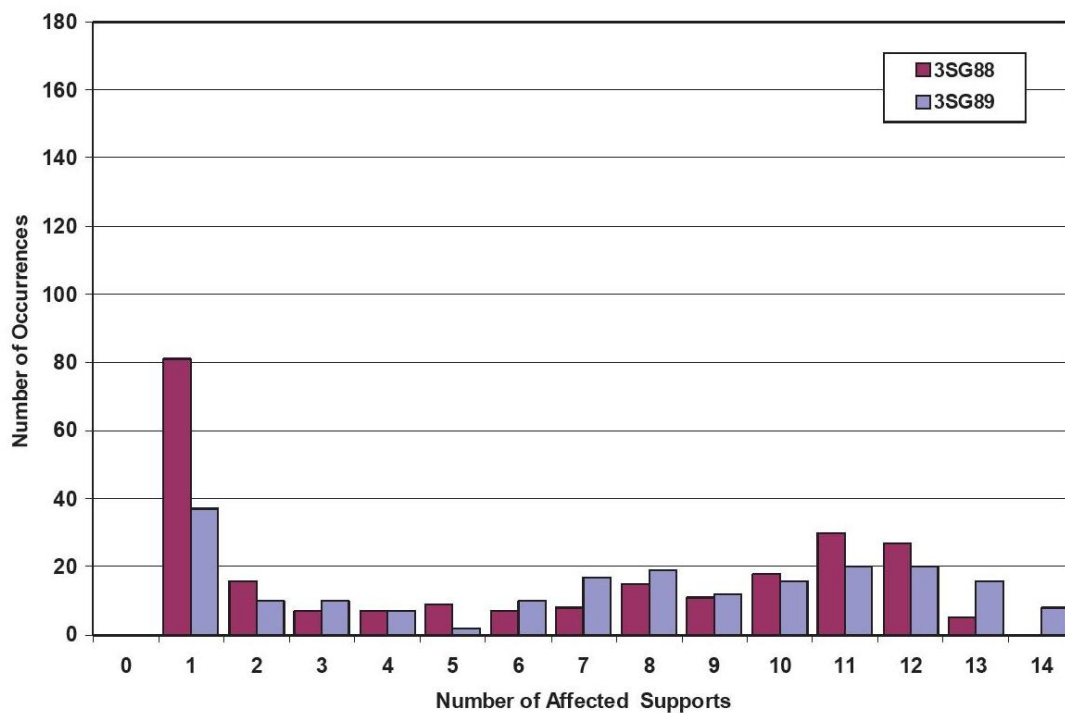


Figure 6-6: Probability of Detection for Tube Wear

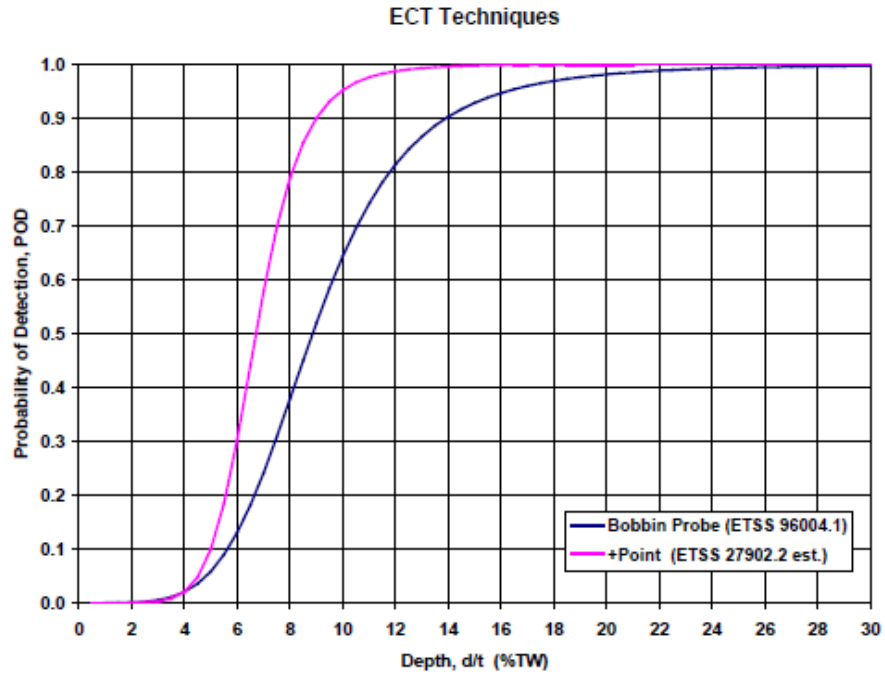


Figure 6-7: 3E-088 Rotating Coil Inspection Region

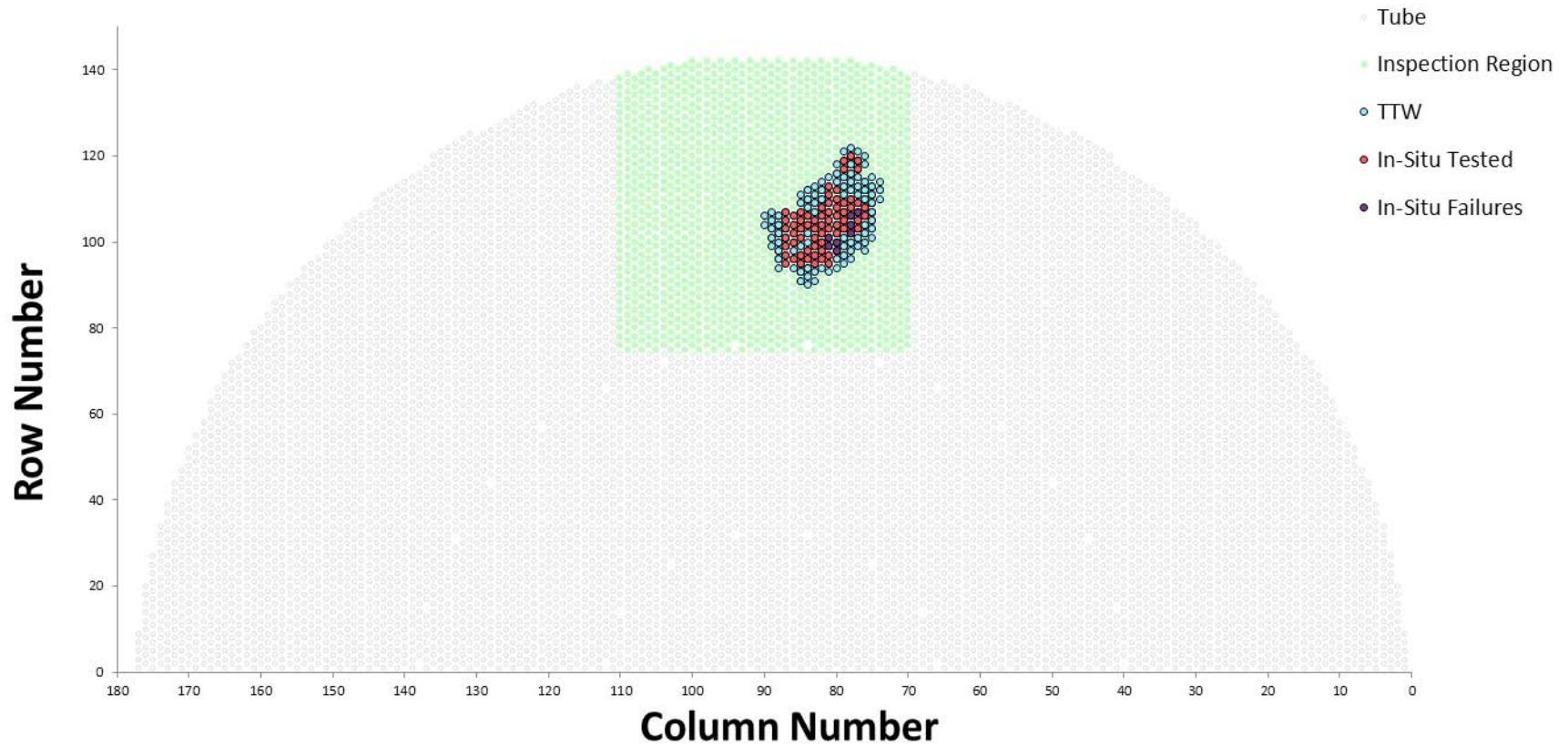
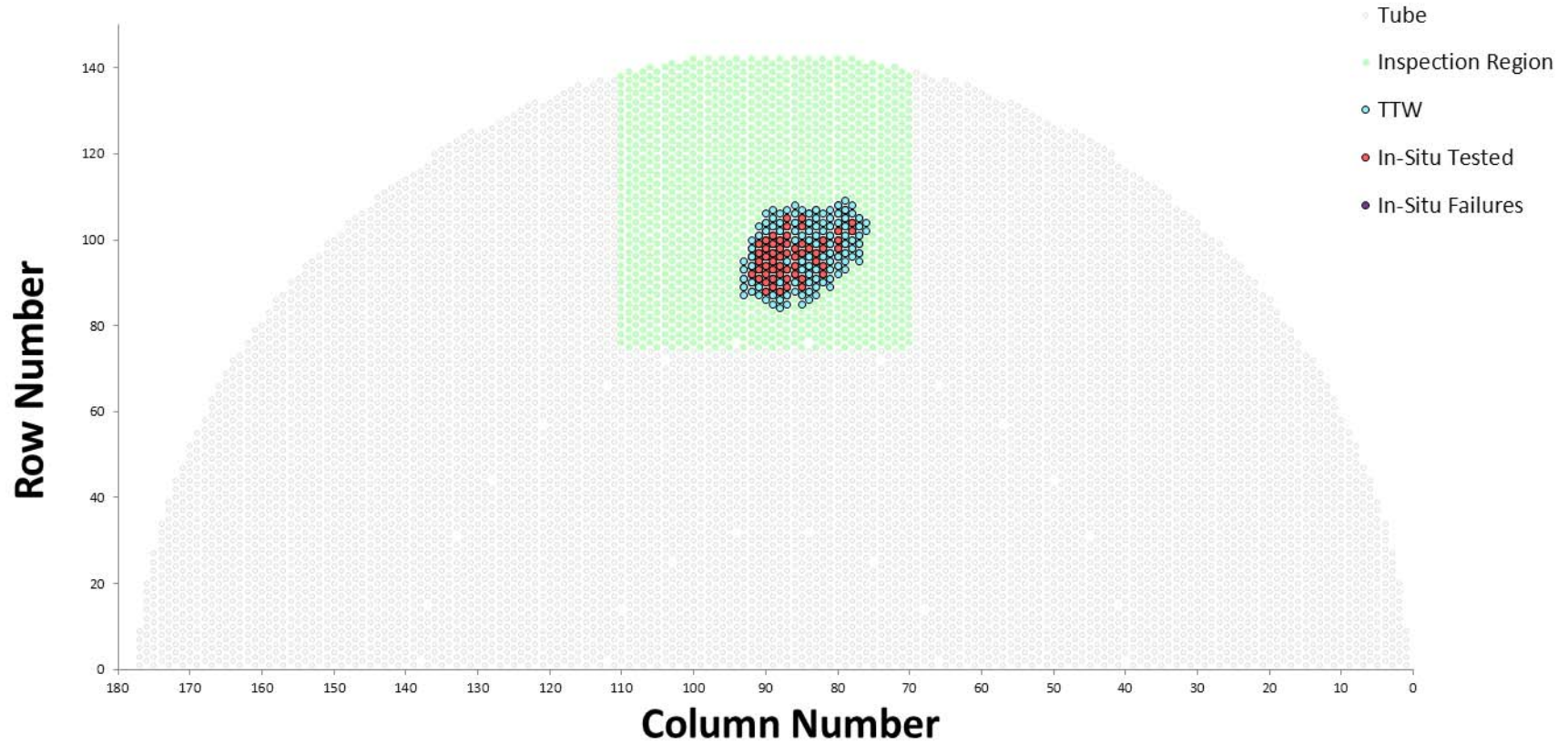


Figure 6-8: 3E-089 Rotating Coil Inspection Region



SONGS Unit 2 Return to Service Report

Table 6-1: Steam Generator Wear Depth Summary

SG 2E-088							
TW Depth	AVB Wear Indications	TSP Indications	TTW Indications	Retainer Bar Indications	Foreign Object Indications	Total Indications	Tubes with Indications
TW ≥ 50%	0	0	0	1	0	1	1
35 - 49%	2	0	0	1	0	3	3
20 - 34%	86	0	0	0	2	88	74
10 - 19%	705	108	0	0	0	813	406
TW < 10%	964	117	0	0	0	1081	600
Total	1757	225	0	2	2	1986	734*
SG 2E-089							
TW Depth	AVB Wear Indications	TSP Indications	TTW Indications	Retainer Bar Indications	Foreign Object Indications	Total Indications	Tubes with Indications
TW ≥ 50%	0	0	0	1	0	1	1
35 - 49%	0	0	0	1	0	1	1
20 - 34%	78	1	0	3	0	82	67
10 - 19%	1014	85	2	0	0	1101	496
TW < 10%	1499	53	0	0	0	1552	768
Total	2591	139	2	5	0	2737	861*
SG 3E-088							
TW Depth	AVB Wear Indications	TSP Indications	TTW Indications	Retainer Bar Indications	Foreign Object Indications	Total Indications	Tubes with Indications
TW ≥ 50%	0	117**	48	0	0	165	74
35 - 49%	3	217	116	2	0	338	119
20 - 34%	156	506	134	1	0	797	197
10 - 19%	1380	542	98	0	0	2020	554
TW < 10%	1818	55	11	0	0	1884	817
Total	3357	1437	407	3	0	5204	919*
SG 3E-089							
TW Depth	AVB Wear Indications	TSP Indications	TTW Indications	Retainer Bar Indications	Foreign Object Indications	Total Indications	Tubes with Indications
TW ≥ 50%	0	91**	26	0	0	117	60
35 - 49%	0	252	102	1	0	355	128
20 - 34%	45	487	215	0	0	747	175
10 - 19%	940	590	72	0	0	1602	450
TW < 10%	2164	94	1	0	0	2259	838
Total	3149	1514	416	1	0	5080	887*

* This value is the number of tubes with a wear indication of any depth at any location. Since many tubes have indications in more than one depth category, the total number of tubes with wear indications is not the additive sum of the counts for the individual depth categories.

** All TSP indications ≥50% TW were in tubes with TTW indications.

6.3 Cause Analyses of Tube-to-Tube Wear in Unit 3

6.3.1 Mechanistic Cause

SCE established a RCE team to investigate the condition, extent of condition, and cause of the event in Unit 3 and to determine corrective actions. The RCE was conducted, documented, and reviewed in accordance with the SONGS Corrective Action Program (CAP). The RCE Team used systematic approaches to identify the mechanistic cause of the TTW, including failure modes analysis (Kepner-Tregoe). The RCE team had access to and used significant input from the SG Recovery Team, which included the services of MHI and industry experts in the fields of T/H and in SG design, manufacturing, operation, and repair.

The failure modes analysis identified a list of 21 possible causes. The list was narrowed down, using facts, analysis, and expert input, to a list of eight potential causes that warranted further technical evaluation. The potential causes included manufacturing/fabrication, shipping, primary side flow induced vibration, divider plate weld failure and repair, additional rotations following divider plate repair, TSP distortion, tube bundle distortion during operation (flowering), and T/H conditions/modeling.

The eight potential causes underwent rigorous analysis using both empirical and theoretical data, and support-refute methodology. This approach identified likely causes and eliminated non-causes. Each of the potential causes was evaluated by engineering analysis of the supporting and refuting data. The mechanistic cause of the TTW in Unit 3 was identified as FEI, involving the combination of localized high steam velocity (tube vibration excitation forces), high steam void fraction (loss of ability to dampen vibration), and insufficient tube to AVB contact to overcome the excitation forces. A more detailed discussion of the cause of FEI in the Unit 3 SGs is provided in MHI's Technical Evaluation Report, which is included as Attachment 4.

6.3.2 Potential Applicability of Unit 3 TTW Causes to Unit 2

At the time of the Unit 3 SG tube leak, Unit 2 was in the first refueling outage after SG replacement and undergoing ECT inspections per the SGP. Following the discovery of TTW in Unit 3, additional Unit 2 inspections identified two tubes with TTW indications in SG 2E-089. The location of TTW in the Unit 2 SG was in the same region of the bundle as in the Unit 3 SGs indicating causal factors might be similar to those resulting in TTW in the Unit 3 SGs. Because of the similarities in design between the Unit 2 and 3 RSGs, it was concluded that FEI in the in-plane direction was also the cause of the TTW in Unit 2.

After the RCE for TTW was prepared, WEC performed analysis of Unit 2 ECT data and concluded TTW was caused by the close proximity of these two tubes during initial operation of the RSGs. With close proximity, normal vibration of the tubes produced the wear at the point of contact. With proximity as the cause, during operation the tubes wear until they are no longer in contact, a condition known as 'wear arrest'. This wear mechanism is addressed in Section 10 and Attachment 6.

As described in Section 8, the compensatory and corrective actions implemented to prevent loss of tube integrity caused by TTW in Unit 2 are sufficient to conservatively address both identified causes.

6.4 Industry Expert Involvement

Upon discovery of TTW in Unit 3, SCE commissioned the services of industry experts to assist in assessing the cause of this phenomenon. SCE selected experts based upon their previous experience in design, evaluation, tube vibration, testing and causal determinations related to SGs. Members included experts in T/H and SGPs from MPR Associates, AREVA, Babcock & Wilcox Canada, Palo Verde Nuclear Generating Station, EPRI, Institute of Nuclear Power Operations (INPO), and MHI, as well as experienced consultants including former NRC executives and a research scientist. A series of panel meetings were conducted during which testing and analysis results were presented. The panel members assessed whether the current work by SCE and its partners was sufficient in understanding the TTW phenomenon and whether the corrective actions developed were sufficient to ensure tube integrity in the future.

6.5 Cause Analysis Summary

SCE has determined the mechanistic cause of the TTW in Unit 3 was FEI, resulting from the combination of localized high steam velocity, high steam void fraction, and insufficient contact forces between the tubes and the AVBs. The FEI resulted in a vibration mode of the SG tubes in which the tubes moved in the in-plane direction, parallel to the AVBs, in the U-bend region. This resulted in TTW in a localized area of the SGs. As discussed in the following sections, SCE has identified actions to prevent loss of integrity due to FEI in the Unit 2 SG tubes. The extent of condition inspections performed in Unit 2 and differences identified between Units 2 and 3 are discussed in Section 7. The compensatory and corrective actions to prevent loss of integrity due to these causes in the Unit 2 SG tubes are discussed in Section 8.

7.0 UNIT 2 CYCLE 17 INSPECTIONS AND REPAIRS

On January 9, 2012, Unit 2 was shut down for a routine refueling and steam generator inspection outage after approximately 22 months of operation. As discussed in Section 3.3, the SGP requires a CM assessment to confirm that SG tube integrity has been maintained during the previous inspection interval. SCE conducted a number of inspections on each of the two Unit 2 SGs (2E-088 and 2E-089) in accordance with the SGP. Based on the inspection results, the Unit 2 CM assessment (included as Attachment 2) concluded that the TS SG performance criteria were satisfied by the Unit 2 SGs during the operating period prior to the current U2C17 outage. The TS performance criteria for tube integrity for all indications were satisfied through a combination of ECT examination, analytical evaluation, and in-situ pressure testing. The operational leakage criterion was satisfied because the Unit 2 SGs experienced no measurable primary-to-secondary leakage during the operating period preceding the Cycle 17 outage.

The Unit 2 outage was in progress on January 31, 2012, when Unit 3 was shut down in response to a tube leak. Although the SG performance criteria had been met by the Unit 2 SGs, the unit was not returned to service pending an evaluation of the tube leak in Unit 3. Subsequent to the discovery of TTW conditions in the U-bend region of the Unit 3 SGs, additional inspections were performed on the Unit 2 tubes and shallow TTW was identified in two adjacent tubes in SG 2E-089.

Section 7.1 provides a summary of results from the routine inspections performed in Unit 2 and Section 7.2 provides a summary of results from the additional Unit 2 inspections performed in response to the discovery of TTW in Unit 3. Details of all the inspections are provided in the Unit 2 CM report (Attachment 2). Section 7.3 summarizes the differences observed between Units 2 and 3.

7.1 Unit 2 Cycle 17 Routine Inspections and Repairs

The SGP requires that a DA be performed prior to a SG inspection outage to develop an inspection plan based on the type and location of flaws to which the tubes may be susceptible. This assessment was performed prior to the inspection and was updated when unexpected degradation mechanisms were found during the inspection. These unexpected degradation mechanisms included (1) RB wear and (2) the TTW observed in Unit 3.

Initially, eddy current bobbin probe examinations of the full length of each tube was performed on 100% of the tubes in both Unit 2 SGs. Selected areas were then inspected using a more sensitive rotating +Point™ examination. During the ECT examinations, wear was detected at AVBs, TSPs and RB locations. Six tubes with high wear indications (equal to or exceeding 35% of the tube wall thickness) were found. Four of those indications occurred in the vicinity of the RBs and two were associated with AVB locations as shown in Table 6-1. One in-situ pressure test was performed on a tube with RB wear, with satisfactory results. No other indications required in-situ pressure testing. Numerous smaller depth wear indications were also reported at other AVB and TSP locations. The ECT results are summarized in Table 6-1.

In accordance with TS 5.5.2.11.c, tubes that are found to have indications of degradation equal to or exceeding 35% through wall (TW) are removed from service by the installation of a plug in both ends of the tube. Once plugs are installed in both ends of a tube, they prevent primary system water from entering the tube. Plugs may also be used to preventively remove tubes from service. Use of preventive plugging is discussed in Section 8.2.

An RCE was completed for the unexpected RB wear. The RCE concluded that the RB size (diameter and length) was inadequate to prevent the RB from vibrating and contacting adjacent tubes during normal plant operation. The vibration source was a turbulent two phase flow (water and steam) across the RBs. As a corrective action, the 94 tubes adjacent to the RBs in each Unit 2 SG were plugged, including two tubes with RB wear in SG 2E-088 and four tubes with RB wear in SG 2E-089.

Four additional tubes were plugged due to wear at AVB locations. Two of these were plugged as required for wear depths equal to or exceeding 35% TW; the other two with through wall depths (TWDs) of approximately 32% were plugged as a preventive measure. A significant number of tubes were preventively plugged and removed from service using screening criteria based on TTW indications in Unit 3. Table 6-1 provides the total numbers of tubes and indications due to all types of wear in the Unit 2 SGs. The tubes and criteria used to select tubes to be removed from service by preventive plugging due to their susceptibility to TTW are discussed in Section 8.2 and Attachment 5.

During the eddy current inspection of SG 2E-088, FO indications and FO wear indications were reported in two adjacent tubes at the 4th TSP. A secondary side foreign object search and retrieval (FOSAR) effort was performed and the object was located and removed. A follow-up analysis identified the object as weld metal debris. The two adjacent tubes were left in service because the indications were below the TS plugging limit and the cause of the degradation had been removed.

Remote visual inspections were performed to confirm the integrity of the RBs. The results of these visual inspections are summarized below:

- No cracking or degradation of RBs or RB-to-retaining bar welds was observed
- No cracking or degradation of AVB end caps or end cap-to-RB welds was observed
- No FOs or loose parts were found in the RB locations

Post sludge lancing FOSAR examination at the top-of-tubesheet (periphery and the no-tube lane) found no evidence of degradation and no FOs.

7.2 Unit 2 Cycle 17 Inspection in Response to TTW in Unit 3

Subsequent to the discovery of TTW conditions in the U-bend region of Unit 3 SGs, an additional review of the U-bend region bobbin probe data was performed for the Unit 2 SGs. The tubes selected for review encompassed the suspected TTW zone as observed in Unit 3 and tubes surrounding that zone. Over 1,000 tubes in each Unit 2 SG were reviewed. The review included a two-party manual analysis (primary/secondary) of the complete U-bend with emphasis on the detection of low level freespan indications, which may not have been reported during the original analysis of the U2C17 bobbin coil data. No new indications were identified during this review.

Additional examinations of the U-bends were performed using rotating probe (+Point™) technology. The scope of this examination is identified on the tubesheet maps provided in Figure 7-1 and Figure 7-2. During this examination, two adjacent tubes with TTW indications were detected. The indications were approximately 6 inches long, located between AVBs B09 and B10 in tubes R111 C81 and R113 C81 in SG 2E-089. Figure 7-2 shows the location of the two tubes with TTW in 2E-089. The maps in Figure 6-7 and Figure 6-8 show the inspection region overlaying the locations of the TTW found in the Unit 3 SGs.

SCE notified the NRC of the discovery of the two tubes with TTW in a letter dated April 20, 2012. (Ref. 9)

Remote visual inspections of the secondary side upper tube bundle were conducted in the Unit 2 SGs. These inspections were similar to those performed in Unit 3 SGs to assist in the development of the mechanistic root cause of TTW and tube wear at RB locations. No indications of TTW or other conditions associated with the FEI in Unit 3 (i.e., AVB wear extending outside the supports) were observed.

Rotating Pancake Coil ECT and Ultrasonic Testing (UT) were performed to measure the tube-to-AVB gap sizes in the Unit 2 SGs. Tube-to-AVB gap data was used to validate the contact force distribution model used in the TTW OA, (Attachment 6, Appendix B).

Figure 7-1: 2E-088 Rotating Coil Inspection Region

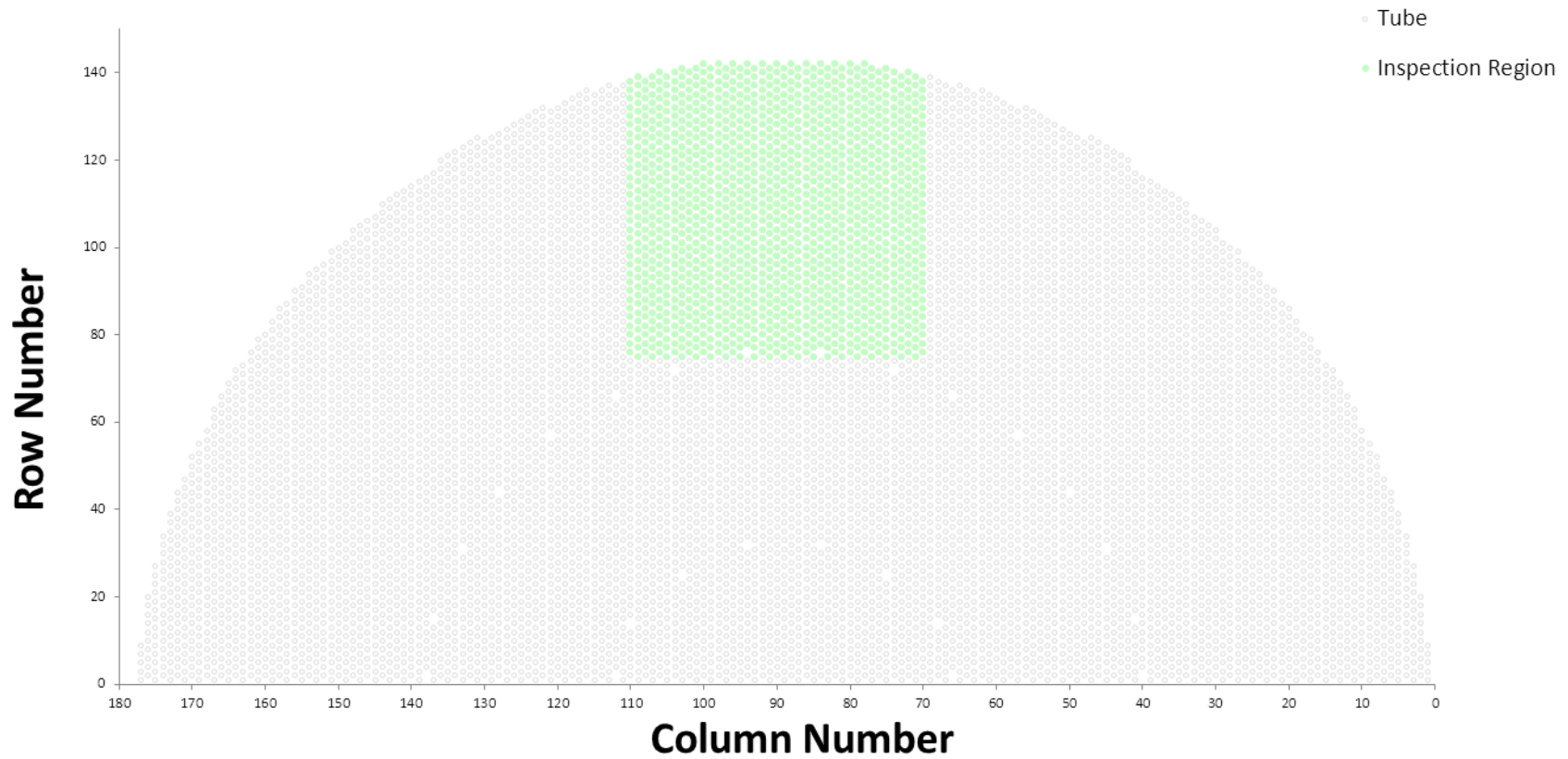
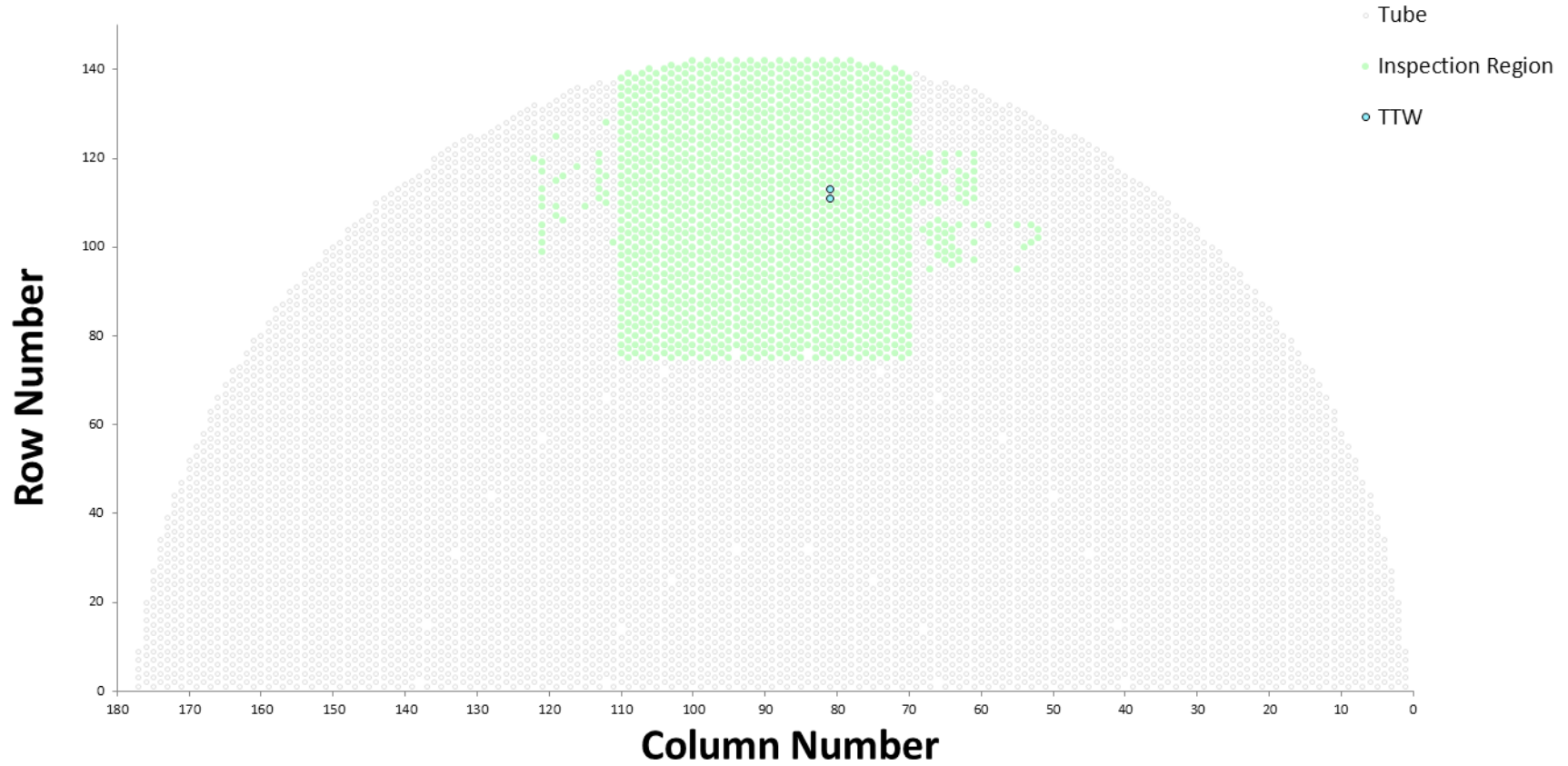


Figure 7-2: 2E-089 Rotating Coil Inspection Region



7.3 Differences between Units 2 and 3

As discussed in Section 6, inspections of the Unit 3 SG's found significant levels of TTW while Unit 2 SGs were limited to two shallow indications at one area of contact between two tubes.

A comparison of TTW and of factors associated with TTW between Unit 2 and Unit 3 SGs is provided below:

Table 7-1: TTW Comparison between Unit 2 and Unit 3 SGs

Description	Unit 2	Unit 3
TTW Indications	2	823
TTW Tubes	2	326
Max Depth (ECT %TW)	14%	99%
Max Length (inches)	~6	~41
TTW In-Situ Pressure Tests	0	129
TTW In-Situ Pressure Tests (Unsatisfactory)	0	8
Operating Period (EFPD)	627	338

In addition to the above parameters, differences in manufacturing dimensional tolerance dispersion (distribution of dimensional values for manufacturing parameters that remain within acceptable tolerances) exist between the Units 2 and 3 SGs. Manufacturing process improvements implemented during the fabrication of the Unit 3 SGs resulted in lower manufacturing dispersion than in the Unit 2 SGs. MHI concluded that the reduced manufacturing dispersion in the Unit 3 SGs resulted in smaller average tube-to-AVB contact force than in the Unit 2 SGs. Due to the smaller average tube-to-AVB contact force, Unit-3 was more susceptible to in-plane vibration.

8.0 UNIT 2 CORRECTIVE AND COMPENSATORY ACTIONS TO ENSURE TUBE INTEGRITY

SCE has implemented the following corrective and compensatory actions to prevent the loss of SG tube integrity due to TTW in Unit 2:

1. Limiting Unit 2 to 70% power prior to a mid-cycle SG inspection outage (CAL Response Commitment 1)
2. Preventively plugging tubes in both SGs (complete)
3. Shutting down Unit 2 for a mid-cycle SG inspection outage within 150 cumulative days of operation at or above 15% power (CAL Response Commitment 2)

The actions to operate at reduced power and perform a mid-cycle inspection within 150 cumulative days of operation are interim compensatory actions. SCE will reevaluate these actions during the mid-cycle inspection using data obtained during the inspections. In addition, SCE has established a project team to develop and implement a long term plan for repairing the SGs. SCE will keep the NRC informed of any findings or developments in the future.

SCE has performed an OA to assess the adequacy of the compensatory actions taken in Unit 2. The OA results demonstrate that operating at 70% power level will prevent loss of tube integrity due to TTW. In particular, reducing power to 70% eliminates the T/H conditions that cause FEI and associated TTW from the SONGS Unit 2 SGs. The OA and supporting analyses are summarized in Section 10 and provided in Attachment 6.

8.1 Limit Operation of Unit 2 to 70% Power

SCE will administratively limit Unit 2 to 70% reactor power prior to a mid-cycle SG inspection outage. The cause of the TTW in the Unit 3 SGs was in-plane tube vibration due to FEI, resulting in tube-to-tube contact and wear. An indication of whether a tube is susceptible to FEI is a calculated term defined as the stability ratio (SR). The SR calculation takes into account T/H conditions (including fluid flow and damping) and tube support conditions and provides a measure of the margin to a critical velocity value at which the tubes may experience the onset of instability due to FEI. The OA and its supporting analyses provided in Section 10 and Attachment 6 demonstrate that operating at 70% power will result in acceptable SRs in Unit 2.

Three independent comparisons were performed of the T/H parameters of SONGS RSGs operating at 100% and 70% power. SONGS RSG's were compared with five operating plants with recirculating SGs of similar design that have not observed TTW. The SONGS RSG's were also compared with the SONGS OSGs. The comparisons were conducted as follows:

- (1) SCE Engineering conducted a study of average T/H parameters
- (2) WEC performed an Analysis of Thermal-Hydraulics of Steam Generators (ATHOS) study of SONGS RSGs to OSGs
- (3) An industry expert in SG design performed an independent ATHOS comparison of T/H parameters that can influence FEI

Based on these comparisons, Plant A was selected for detailed analysis due to similarity of design characteristics and thermal power rating. Both SONGS and Plant A SGs use a U-bend design with the same tube diameter and pitch. Plant A operates at 1355 megawatts thermal per SG (MWt/SG) bounding the SONGS RSGs at 70% power (1210 MWt/SG). Plant A RSGs and SONGS RSGs utilize out-of-plane AVBs in the U-bend. Plant A RSGs have operated for two fuel cycles without indications of TTW.

Results of the comparisons of three T/H parameters (steam quality, void fraction, and fluid velocity) are presented in the following subsections. These results demonstrate that operating SONGS SGs at 70% power improves the T/H parameters to values lower than those in Plant A at 100% power.

Steam Quality

Steam quality, defined as mass fraction of vapor in a two-phase mixture, is an important factor used in determining SRs. Steam quality is directly related to void fraction for a specified saturation state. This description is important when considering effects on damping. Damping is the result of energy dissipation and delays the onset of FEI. Damping is greater for a tube surrounded by liquid compared to a tube surrounded by gas. Since quality describes the mass fraction of vapor in a two-phase mixture, it provides insight into the fluid condition surrounding the tube. A higher steam quality correlates with dryer conditions and provides less damping. Conversely, lower steam quality correlates with wetter conditions resulting in more damping, which decreases the potential for FEI.

Steam quality also directly affects the fluid density outside the tube, affecting the level of hydrodynamic pressure that provides the motive force for tube vibration. When the energy imparted to the tube from hydrodynamic pressure (density times velocity squared or ρv^2) is greater than the energy dissipated through damping, FEI will occur. When steam quality decreases, the density of the two-phase mixture increases, decreasing velocity. Since the hydrodynamic pressure is a function of velocity squared, the velocity term decreases faster than the density increases. Small decreases in steam quality significantly decrease hydrodynamic pressure and the potential for FEI.

Steam quality in the SONGS RSGs was calculated for 100% and 70% power using the industry expert's independent ATHOS model and compared to Plant A at 100% power. The results of the calculations are summarized in Table 8-1 and graphically presented in Figure 8-1.

Limiting SONGS power to 70% reduces steam quality and hydrodynamic pressure to values less than Plant A. Plant A has not experienced TTW.

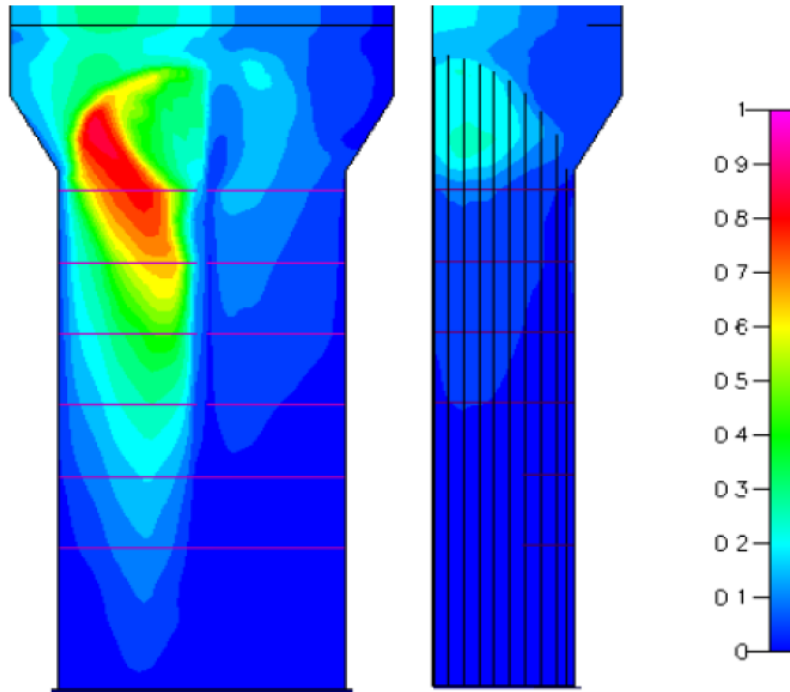
Table 8-1: Independent ATHOS Comparison Results – Steam Quality

	SONGS 100%	SONGS 70%	Plant A 100%
Thermal Power (MWt)	1715	1199	1368
Primary Inlet Temp (°F)	597.8	589.1	596.0
Maximum Mixture Density (kg/m3)	782	772	782
Minimum Mixture Density (kg/m3)	34	97	43
Maximum Dynamic Pressure (N/m2)	4140	2430	4220
Maximum Steam Quality	0.876	0.312	0.734

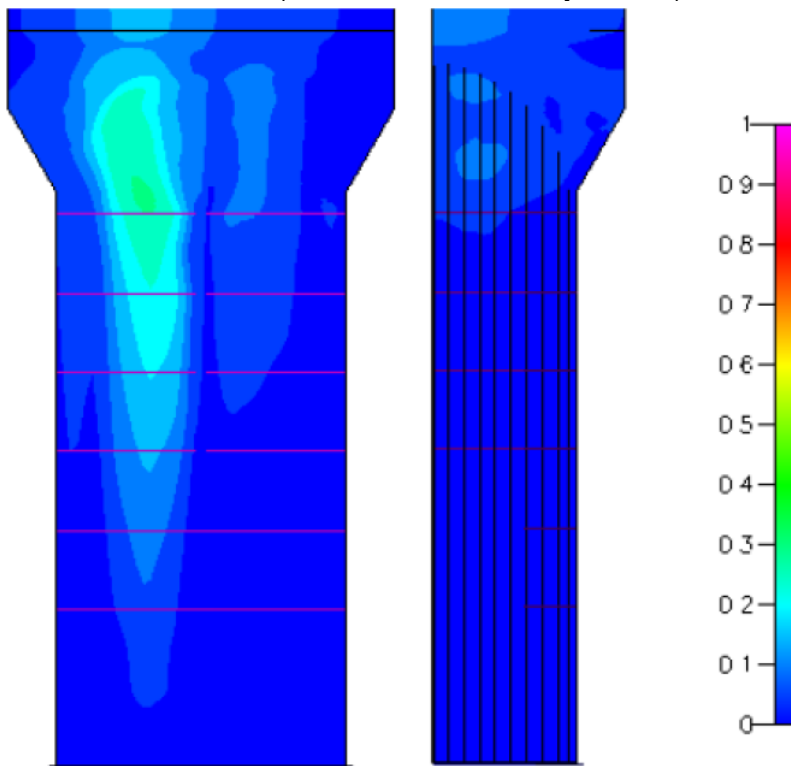
Note: The thermal power levels were calculated in the independent ATHOS comparison.

Figure 8-1: Steam Quality Contour Plots for 100% Power and 70% Power

100% Power (Maximum Steam Quality = 0.876 from Independent ATHOS T/H Comparison)



70% Power (Maximum Steam Quality = 0.312)



Void Fraction

Void fraction, defined as volume fraction of vapor in a two-phase mixture, is a factor used in determining SRs. A higher void fraction represents a lower percentage of liquid in the steam. Liquid in the steam dampens the movement of tubes. Higher void fractions result in less damping. Decreasing the void fraction in the upper bundle region during power operation increases damping and reduces the potential for FEI.

The void fraction in the SONGS RSGs was calculated at 100% and 70% power using ATHOS models from MHI, an independent industry expert, and WEC. The results are summarized in Table 8-2.

A significant effect of limiting power to 70% is the elimination of void fractions greater than Plant A. Plant A has not experienced TTW.

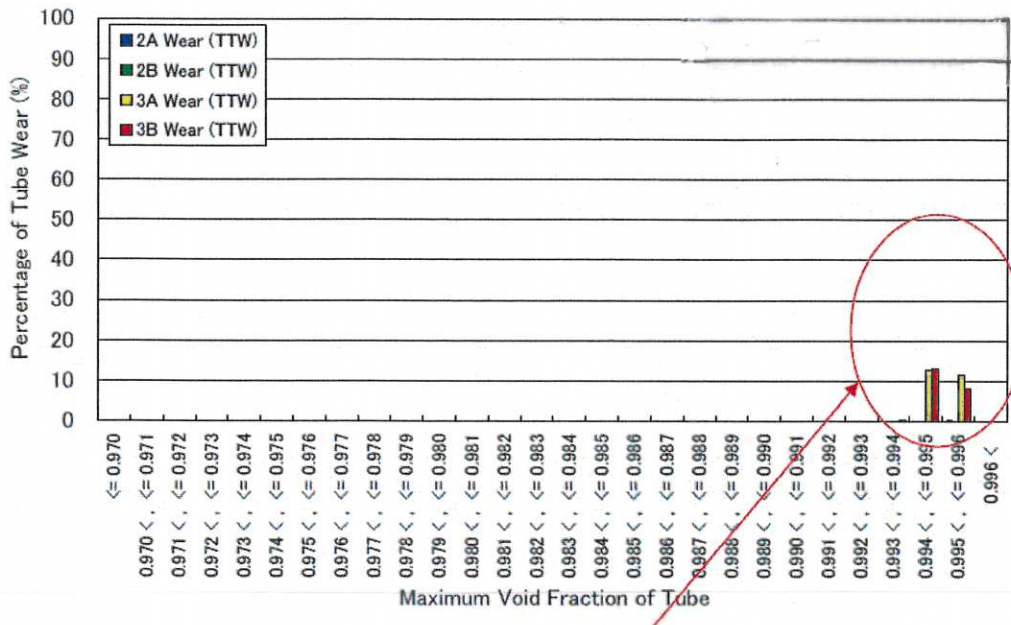
Table 8-2: Comparison of Maximum Void Fraction

	SONGS 100%	SONGS 70%	Plant A 100%	SONGS OSGs 100%
Thermal Power (MWt)	1729	1210	1355	1709
Bend Type	U-Bend	U-Bend	U-Bend	Square Bend
MHI ATHOS T/H Results	0.996	0.927	-	-
Independent ATHOS T/H Comparison	0.994	0.911	0.985	-
WEC ATHOS T/H Comparison	0.9955	0.9258	-	0.9612

Note: Not all sources had access rights to the ATHOS models of some of the comparison plants, resulting in blank cells in this table.

Void fractions at the locations of tubes with TTW in the RSGs are shown in Figure 8-2. The figure demonstrates that the occurrence of TTW was limited to tubes operating with maximum void fractions of greater than 0.993.

Figure 8-2: Maximum Void Fraction versus Power Level and Ratio of Tube Wear versus Maximum Void Fraction



Wear indication on tubes which are located in the region where max void fraction exceeds 0.993

By limiting power to 70% as presented in Table 8-2, void fractions are reduced to levels well below those associated with the TTW experienced at 100% power in the SONGS RSGs.

Fluid Velocity

The fluid velocity in a steam generator’s secondary side is a factor in SR calculations. Hydrodynamic pressure is the fluid velocity squared multiplied by the fluid density (ρv^2) and is described in the “Steam Quality” section above.

The results of the velocity calculations are summarized in Table 8-3 and a graphical presentation of the results throughout a SG is shown in Figure 8-3. Interstitial velocity is a representative average velocity of flow through a porous media, which accounts for the structures and flow obstructions in the flow path.

Table 8-3: Comparison of Maximum Interstitial Velocity (ft/s)

	SONGS 100%	SONGS 70%	Plant A 100%	SONGS OSGs 100%
Thermal Power (MWt)	1729	1210	1355	1709
Bend Type	U-Bend	U-Bend	U-Bend	Square Bend
MHI ATHOS T/H Results	23.60	13.38	-	-
Independent ATHOS T/H Comparison	22.08	11.91	17.91	-
WEC ATHOS T/H Comparison	28.30	13.28	-	22.90

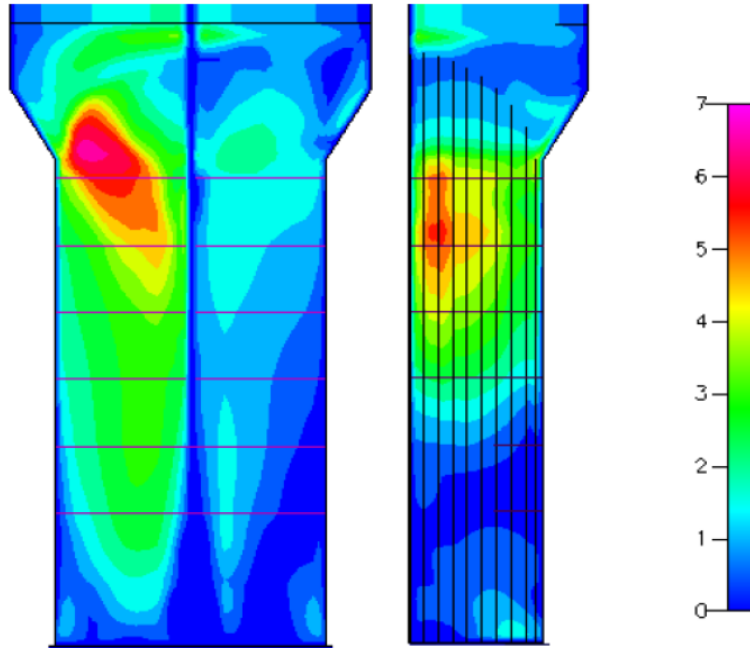
Note: Not all sources had access rights to the ATHOS models of some of the comparison plants, resulting in blank cells in this table.

An additional analysis of velocity at different locations along a tube at 100% and 70% power was performed by WEC. This analysis used gap velocity, which relates to interstitial velocity through the geometric arrangement of the tube bundle and the angle of incidence between the fluid flow and tube (interstitial velocity multiplied by a surface porosity based on the tube bundle geometry). Tube R141 C89 has the longest bend radius in the bundle and relatively high gap velocities. A significant reduction in gap velocity for this tube occurs in the U-bend (mainly the hot leg side) when power is limited to 70%. The results for 2E-088 are shown in Figure 8-4, and results for 2E-089 are shown in Figure 8-5. The slight differences in the plots for the two SGs are caused by differences in numbers and locations of plugged tubes.

Limiting power to 70% significantly reduces fluid velocity. The reduction in fluid velocity significantly reduces the potential for FEI.

Figure 8-3: Interstitial Velocity Contour Plots for 100% Power and 70% Power

100% Power (Maximum Interstitial Velocity = 6.73 m/s = 22.08 ft/s
from Independent ATHOS T/H Comparison)



70% Power (Maximum Interstitial Velocity = 3.63 m/s = 11.91 ft/s)

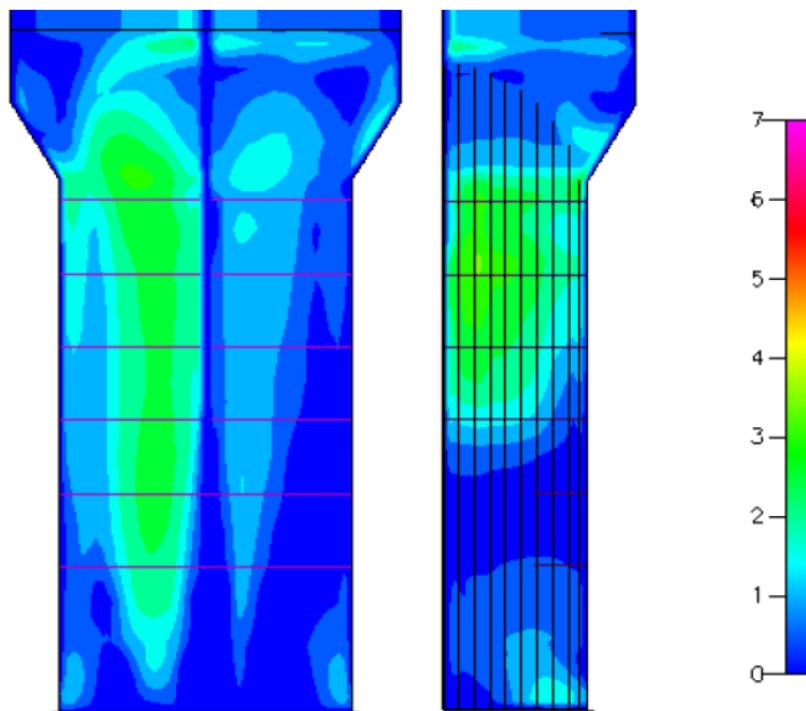
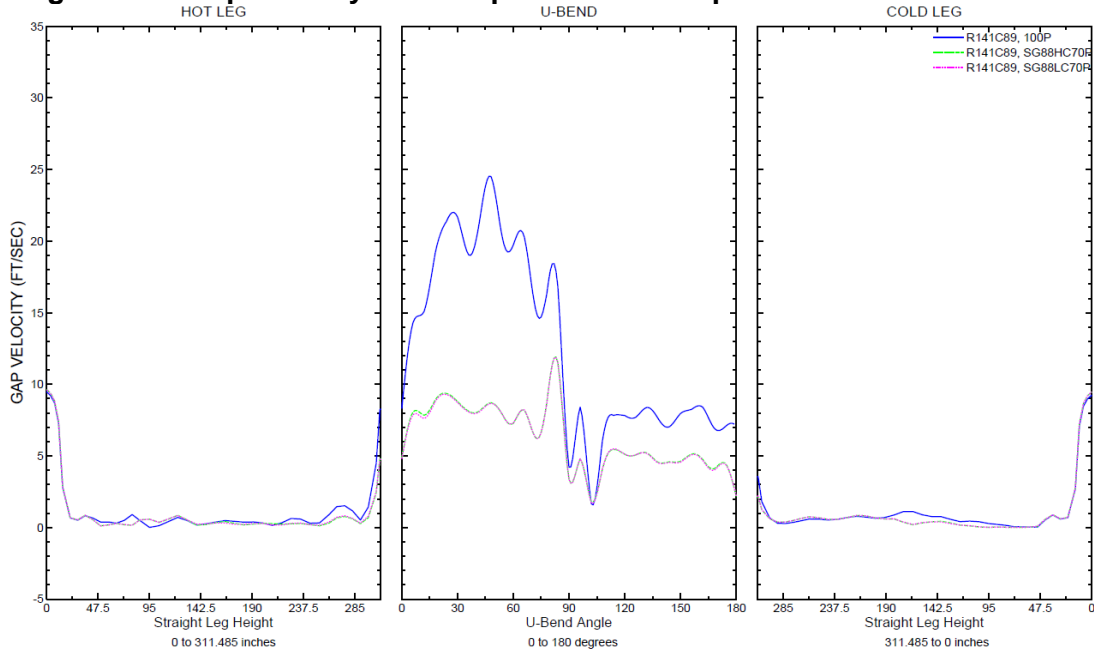
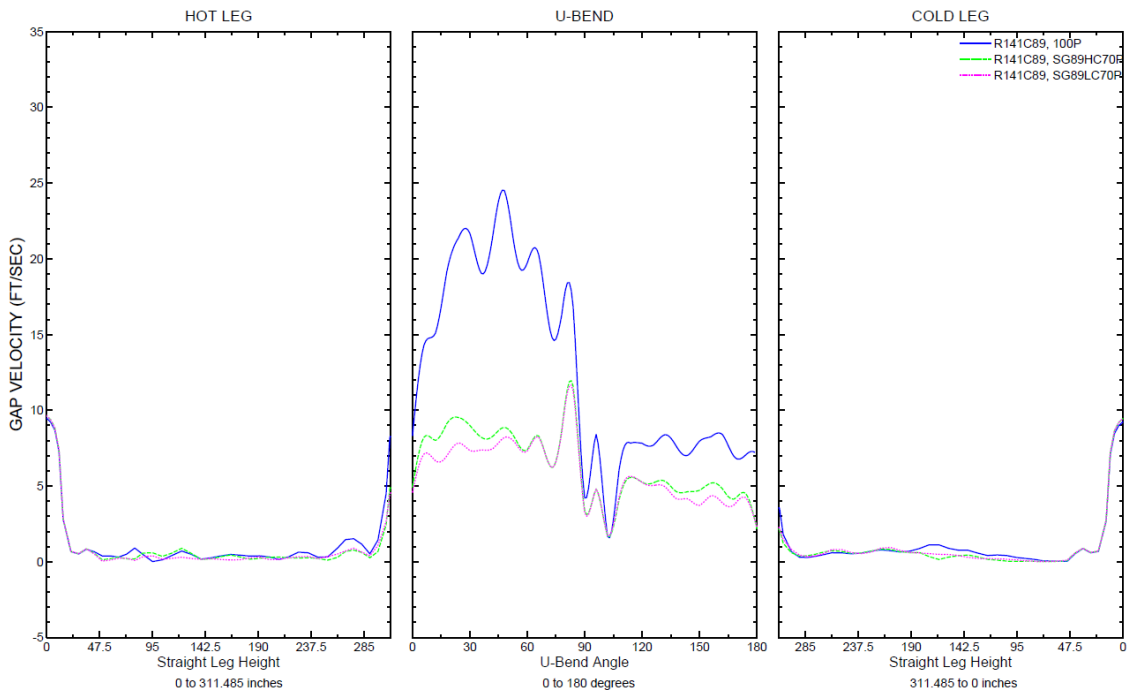


Figure 8-4: Gap Velocity at 100% power and 70% power for 2E-088 R141C89



* Note: Two lines are shown for 70% power because separate ATHOS simulations were run for each half of the tube bundle due to the asymmetrical plugging in the SG

Figure 8-5: Gap Velocity at 100% power and 70% power for 2E-089 R141C89



* Note: Two lines are shown for 70% power because separate ATHOS simulations were run for each half of the tube bundle due to the asymmetrical plugging in the SG.

MHI's ATHOS model was used to calculate the T/H input parameters for the SR calculations. ATHOS is an EPRI computer program used by SG design companies in North America. SCE commissioned two independent T/H analyses to verify the MHI ATHOS analysis. These independent verifications were performed by WEC using ATHOS and AREVA using their T/H computer code CAFCA4. MPR Associates compared the three T/H analyses (MHI ATHOS, WEC ATHOS, and AREVA CAFCA4) and concluded the models predicted similar void fraction, quality, and velocity results.

8.2 Preventive Tube Plugging for TTW

Tubes were identified for preventive plugging using correlations between wear characteristics in Unit 3 tubes and wear patterns at AVBs and TSPs in Unit 2. The screening criteria used to select these tubes is discussed in Section 8.2.1. Removing these tubes from service prevents future wear from challenging SG performance criteria for structural and leakage integrity. These tubes were plugged in addition to the 4 tubes plugged for AVB wear and the 182 tubes plugged as a preventive measure against potential RB wear (described in Section 7.1). A summary of all tubes selected for plugging in Unit 2 is provided in Table 8-4. The impact on operations of the plugged tubes is discussed in Section 8.2.2.

8.2.1 Screening Criteria for Selecting Tubes for Plugging

After identification of the TTW in Unit 3, additional examinations of the susceptible region in Unit 2 identified shallow TTW on two adjacent tubes. Although the 14% TW depth of these indications was below the TS plugging threshold of 35%, the tubes were stabilized and plugged to reduce the risk of tube failure due to continued wear. Using screening criteria developed by MHI from TTW indications in Unit 3, SCE selected 101 tubes in 2E-088 and 203 tubes in 2E-089 for preventive plugging. Nine screening criteria were identified using the quantity and location of AVB and TSP wear indications, length of AVB wear indications, average void fraction over the length of the tube, location of the tube within the tube bundle, and coupling between adjacent susceptible tubes. These criteria are provided in Attachment 5.

Table 8-4 provides a summary of all the tubes selected for plugging in Unit 2. The locations of the Unit 2 tubes selected for plugging and stabilization using the preventive plugging criteria are shown in Figure 8-6 and Figure 8-7. Additional screening criteria was provided by industry expert review (wear at 6 Consecutive AVBs) and WEC (TSP wear).

Table 8-4: Unit 2 Steam Generator Tube Plugging Summary

Steam Generator	TWD \geq 35% at AVB	TWD 30-35% at AVB	Wear at RB	TTW	Preventive Retainer Bar	TTW Preventive			Total Tubes Selected
						MHI Screening Criteria	Wear at 6 Consecutive AVBs	WEC Screening Additions	
2E-088	2	2	2	0	92	101	6	2	207
2E-089	0	0	4	2	90	203	6	3	308

Figure 8-6: 2E-088 Plugging and Stabilizing Map

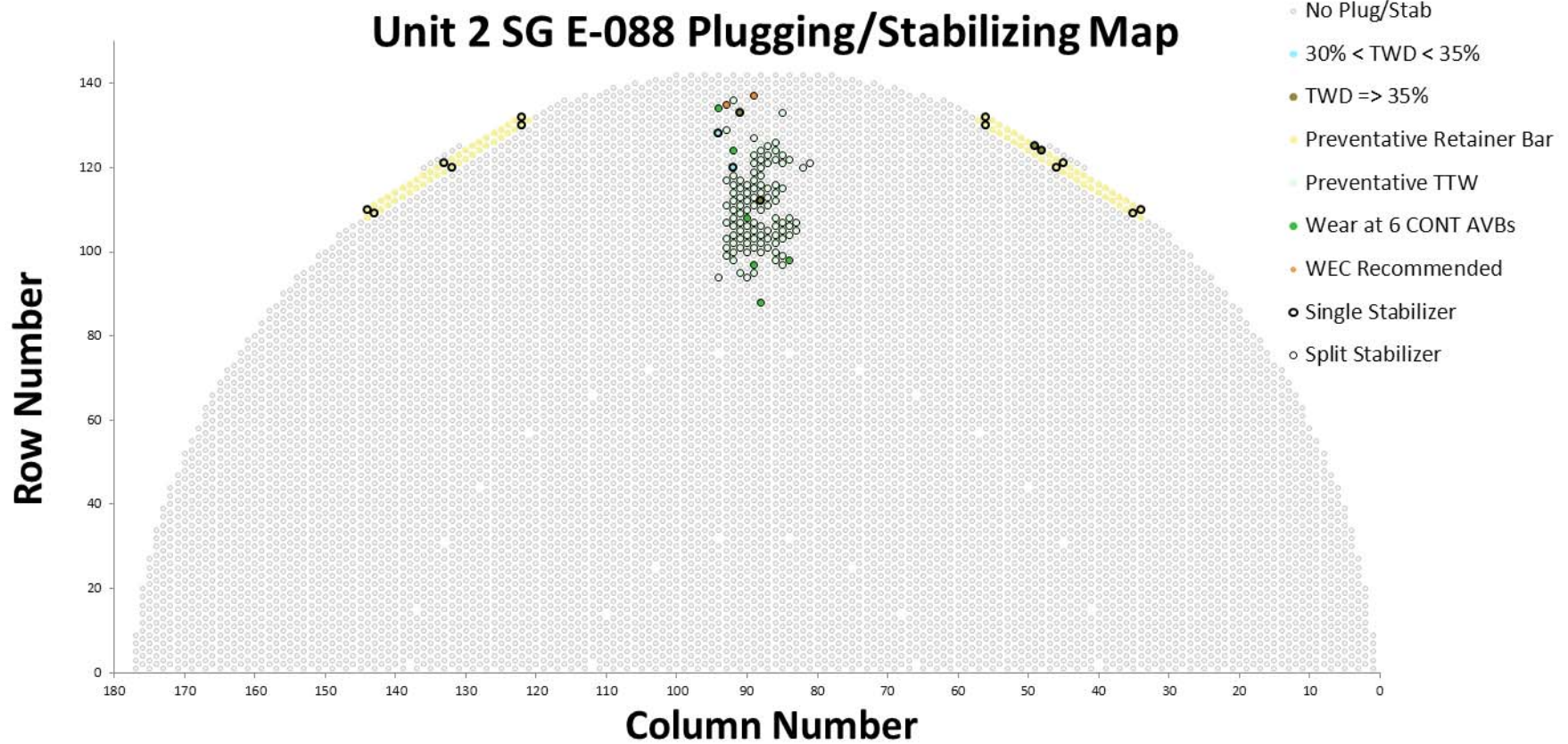
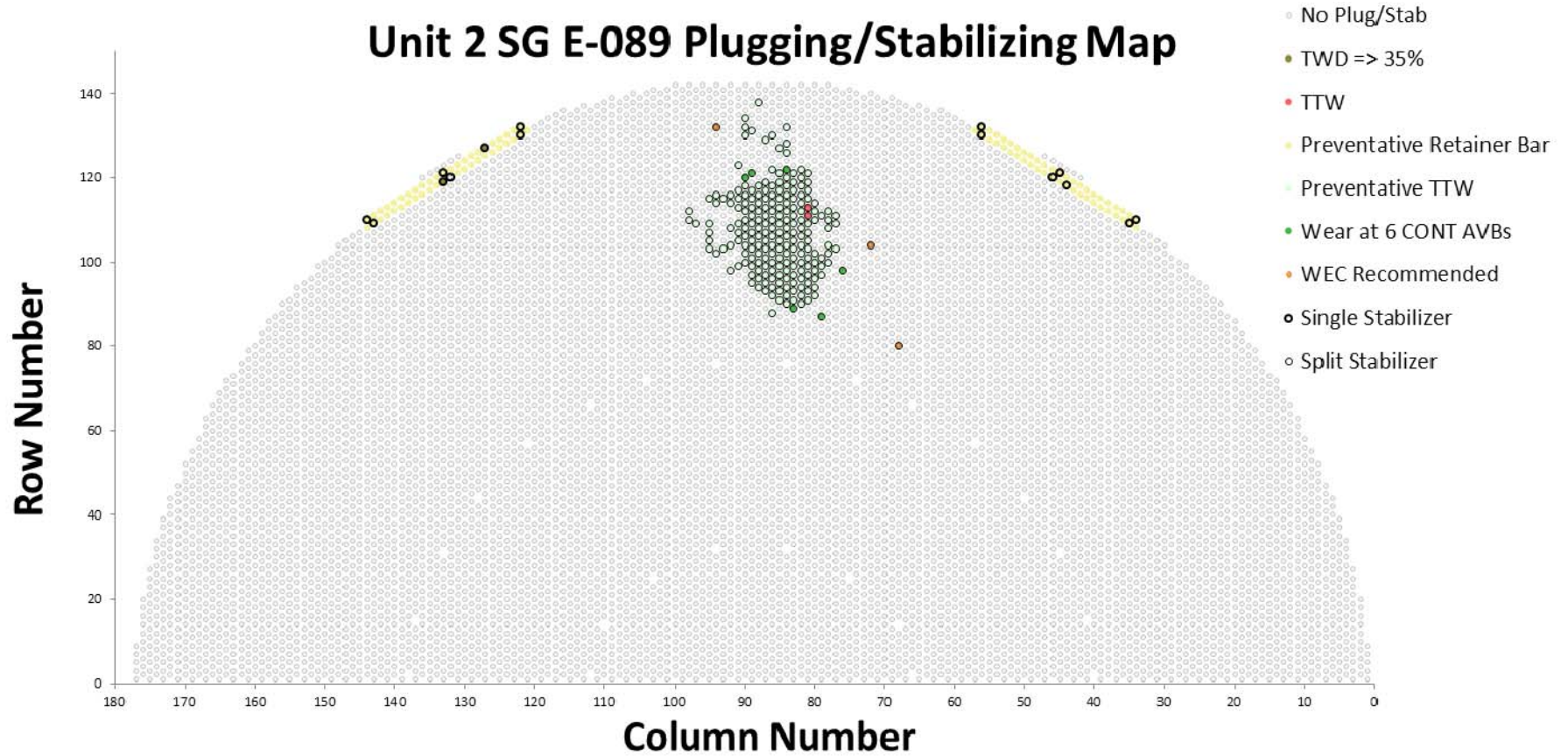


Figure 8-7: 2E-089 Plugging and Stabilizing Map



8.2.2 Plant Operations with Tubes Plugged in Unit 2

Results from MHI's ATHOS calculations were used to analyze the effect of the plugged region on tubes remaining in service. The T/H parameters evaluated were:

- Maximum void fraction, velocity, and hydrodynamic pressure along the U-bend
- Average void fraction, velocity, and hydrodynamic pressure along the hot leg portion of the U-bend
- Average void fraction, velocity, and hydrodynamic pressure along the U-bend

The effect of 4% tube plugging on the remaining in-service tubes was evaluated and determined to be insignificant.

With power limited to 70%, there is no adverse impact on surrounding tubes of the preventive plugging in the Unit 2 SGs.

8.3 Inspection Interval and Protocol of Mid-cycle Inspections

As demonstrated in Section 8.1, limiting operations to 70% power significantly reduces the potential for FEI and improves tube stability margins. To provide additional safety margin, the Unit 2 inspection interval has been limited to 150 days of operation at or above 15% power. The protocol for the inspections to be performed during the mid-cycle outage is described below. (CAL Response Commitment 2)

8.3.1 Inspection of Inservice Tubes (Unplugged)

The following inspections will be performed during the mid-cycle SG inspection outage:

- Eddy Current Bobbin Coil Examinations of the full length of all in-service tubes
- Rotating Coil Examinations of the following areas:
 - a. U-bend region – inspection scope will repeat the pattern used during the refueling outage. (~1300 tubes/SG)
 - b. TSP and AVB wear bobbin coil indications $\geq 20\%$
- Visual inspection of small diameter RBs and welds

8.3.2 Inspection of Plugged Tubes

Plugged tubes will be inspected to determine if the compensatory and corrective actions (plugging and operating at reduced power) have been effective. The following inspections and evaluations are planned:

- Visual examination will be performed on all installed tube plugs
- 12 tubes in each SG will be unplugged and the stabilizer(s) removed to assess the effectiveness of the TTW compensatory and corrective actions. Following these inspections, all tubes will be re-plugged and stabilizers installed. The tubes will be selected as follows:
 - The 2 tubes with previous TTW indications
 - 5 tubes adjacent to tubes with TTW wear
 - 5 tubes selected from representative locations that were preventively plugged as part of the compensatory and corrective actions for TTW

Unit 2 Return to Service Report

- Any new TTW and TSP ECT indications will be assessed to determine if they are the result of FEI during the prior operating period or are cases of previously undetected wear (less than the probability of detection for the ECT probes used during the prior inspection).
- Confirmed new TTW or increases in TTW indication size beyond ECT uncertainty will require a review of the corrective actions implemented during the current inspection.

9.0 UNIT 2 DEFENSE-IN-DEPTH ACTIONS

As described in Section 8, Section 10, and Attachment 6, the compensatory and corrective actions taken by SCE eliminate the T/H conditions that cause FEI and associated TTW from the SONGS SGs. Nonetheless, SCE has developed DID measures to provide an increased safety margin even if tube-to-tube degradation in the Unit 2 SGs were to occur. The following actions have been taken to improve the capability for early detection of a SG tube leak and ensure immediate plant operator response.

9.1 Injection of Argon into the Reactor Coolant System (RCS)

Plant design has been modified to allow periodic injection of Argon (Ar-40) into the RCS. Ar-40 is activated over a short period of time to become Ar-41. The increased RCS activity makes it easier to detect primary-to-secondary tube leaks.

9.2 Installation of Nitrogen (N-16) Radiation Detection System on the Main Steam Lines

Plant design will be modified prior to Unit 2 startup (entry into Mode 2) by installing a temporary N-16 radiation detection system (CAL Response Commitment 3). This system is in addition to existing radiation monitoring systems and includes temporary N-16 detectors located on the main steam lines. This system provides earlier detection of a tube leak and initiation of operator actions.

9.3 Reduction of Administrative Limit for RCS Activity Level

The plant procedure for chemical control of primary plant and related systems has been modified to require action if the specific activity of the reactor coolant Dose Equivalent (DE) Iodine (I-131) exceeds the normal range of 0.5 $\mu\text{Ci/gm}$, which is one-half of the TS Limit of 1.0 $\mu\text{Ci/gm}$. In the event that the normal range is exceeded, Operations is required to initiate the Operational Decision Making process to evaluate continued plant operation.

9.4 Enhanced Operator Response to Early Indication of SG Tube Leakage

9.4.1 Operations Procedure Changes

The plant operating procedure for responding to a reactor coolant leak has been modified to require plant Operators to commence a reactor shutdown upon a valid indication of a primary-to-secondary SG tube leak at a level less than allowed by the plant's TSs. This procedure change requires earlier initiation of operator actions in response to a potential SG tube leak.

9.4.2 Operator Training

Plant Operators will receive training on use of the new detection tools for early tube leak identification (e.g., plant design changes described above), and lessons learned in responding to the January 31, 2012, Unit 3 shutdown due to a SG tube leak (CAL Response Commitment 4). This training will enhance operator decision making and performance in responding to an indication of a SG tube leak and will be completed prior to plant startup.

10.0 UNIT 2 OPERATIONAL ASSESSMENT

As defined in NEI 97-06 (Ref. 2), the OA is a “Forward looking evaluation of the SG tube conditions that is used to ensure that the structural integrity and accident leakage performance will not be exceeded during the next inspection interval.” The OA projects the condition of SG tubes to the time of the next scheduled inspection outage and determines their acceptability relative to the TS tube integrity performance criteria (Attachment 1).

As required by the CAL (Ref. 1), SCE has prepared an assessment of the Unit 2 SGs that addresses the causes of TTW wear found in the Unit 3 SGs, prior to entry of Unit 2 into MODE 2. The OA provided in Attachment 6 provides that assessment.

Due to the significant levels of TTW found in Unit 3 SGs, SCE has assessed the likelihood of additional TTW in Unit 2 from several different perspectives involving the experience and expertise of AREVA, WEC, and Intertek/APTECH. These companies developed independent OAs to address the TTW found at SONGS. These OAs apply different methodologies to ensure a comprehensive and diverse evaluation. The results of these analyses fulfill the TS requirement to demonstrate that SG tube integrity will be maintained until the next SG inspection. The OAs demonstrate that limiting operation to 70% power will prevent loss of tube integrity due to TTW. In particular, reducing power to 70% eliminates the T/H conditions that cause FEI and associated TTW from the SONGS Unit 2 SGs. The reduced 150 cumulative day inspection interval provides additional safety margin beyond the longer allowable inspection intervals identified in the OAs.

11.0 ADDITIONAL ACTIONS

As previously discussed, the OAs performed by AREVA, WEC, and Intertek/APTECH confirm that the compensatory and corrective actions implemented by SCE will result in continued safe operation of Unit 2 and that SG tube integrity will be maintained. SCE also implemented conservative DID measures to minimize the impact on public and environmental health and safety even if tube integrity were compromised. Additionally, SCE is establishing enhanced plant monitoring capability as described below.

11.1 Vibration Monitoring Instrumentation

The Vibration and Loose Parts Monitoring System (VLPMS) is designed in accordance with NRC Regulatory Guide 1.133, "Loose-Part Detection Program for the Primary System of Light-Water-Cooled Reactors" to detect loose metallic parts in the primary system. VLPMS includes accelerometers mounted externally to the SGs. The VLPMS sensors detect acoustic signals generated by loose parts and flow. The signals from these sensors are compared with preset alarm setpoints. Validated alarms are annunciated on a panel in the control room.

To improve sensitivity of the VLPMS, the system is being upgraded to WEC's Digital Metal Impact Monitoring System (DMIMS-DX) during U2C17 refueling outage (CAL Response Commitment 5). The following improvements will be implemented by the upgrade:

- Relocation of existing VLPMS accelerometers (2 per SG) from the support skirt to locations above and below the tubesheet. These will remain as VLPMS sensors to meet Regulatory Guide 1.133.
- Increased sensitivity accelerometers (2 per SG) will be installed at locations above and below the tubesheet.
- Increased sensitivity accelerometers (2 per SG) will be installed on an 8 inch hand hole high on the side of the SGs to monitor for secondary side noises at the upper tube bundle.

The upgraded system will provide SCE with additional monitoring capabilities for secondary side acoustic signals.

11.2 GE Smart Signal™

SCE will utilize GE Smart Signal™, which is an analytic tool that aids in diagnosis of equipment conditions (CAL Response Commitment 6). The tool will be used to analyze historical plant process data from the Unit 2 SGs following the inspection interval.

12.0 CONCLUSIONS

As noted in Reference 1, the SG tube wear that caused a Unit 3 SG tube to leak on January 31, 2012, was the result of tube-to-tube interaction. This type of wear was confirmed to exist in a number of other tubes in the same region in both Unit 3 SGs. Subsequent inspections of the Unit 2 SGs identified this type of wear also existed in two adjacent tubes in Unit 2 SG E-089.

To determine the cause of the TTW, SCE performed extensive inspections and analyses. SCE commissioned experts in the fields of T/H and in SG design, manufacturing, operation, and repair to assist with these efforts. Using the results of these inspections and analyses, SCE determined the cause of the TTW in the two Unit 3 SGs was FEI, caused by a combination of localized high steam velocity, high steam void fraction, and insufficient contact forces between the tubes and the AVBs. FEI caused in-plane tube vibration that resulted in TTW in a localized region of the SGs. The TTW in Unit 2 SG E-089 may have been caused by FEI, or alternatively, close proximity of the two tubes may have led to TTW from normal vibration.

SCE determined the TTW effects were much less severe in Unit 2 where two tubes were identified with TTW indications of less than 15% TW wear. These two tubes are located in the same region of the SGs as those with TTW in Unit 3. Given that the T/H conditions are essentially the same in both units, the less severe TTW in Unit 2 is attributed to manufacturing differences. Those differences increased tube-to-AVB contact forces in Unit 2, providing greater tube support.

To prevent loss of SG tube integrity due to TTW in Unit 2, SCE has implemented interim compensatory and corrective actions and established a protocol of inspections and operating limits. These include:

1. Limiting Unit 2 to 70% power prior to a mid-cycle SG inspection outage (CAL Response Commitment 1)
2. Preventively plugging tubes in both SGs (complete)
3. Shutting down Unit 2 for a mid-cycle SG inspection outage within 150 cumulative days of operation at or above 15% power (CAL Response Commitment 2)

On the basis of the compensatory and corrective actions discussed in Section 8, the DID actions presented in Section 9, and the results of the OAs presented in Section 10 and Attachment 6, SCE concludes that Unit 2 will operate safely at 70% power for 150 cumulative days of operation. Reducing power to 70% eliminates the T/H conditions that cause FEI and associated TTW from the SONGS Unit 2 SGs. SCE will continue to closely monitor SG tube integrity, perform SG inspections during the mid-cycle outage, and take compensatory and corrective actions to ensure the health and safety of the public.

13.0 REFERENCES

- 1 Confirmatory Action Letter (CAL) – Letter from Elmo E. Collins (NRC) to Peter T. Dietrich (SCE), dated March 27, 2012, Confirmatory Action Letter 4-12-001, San Onofre Nuclear Generating Station, Units 2 and 3, Commitments to Address Steam Generator Tube Degradation
- 2 Nuclear Energy Institute NEI 97-06, Steam Generator Program Guidelines, Revision 3, January 2011
- 3 Electric Power Research Institute (EPRI), Pressurized Water Reactor Steam Generator Examination Guidelines
- 4 EPRI 1019038, 1019038 Steam Generator Management Program: Steam Generator Integrity Assessment Guidelines, Revision 3, November 2009
- 5 Event Notification Number 47628 - Telephone notification, Manual Trip Due to a Primary to Secondary Leak, made to the NRC Emergency Notification System (ENS) as required by 10 CFR 50.72(b)(2)(iv)(B)
- 6 Event Notification Number 47744 (including 2 followups) - Telephone notifications, Unit 3 Steam Generator Tubes Failed In-Situ Pressure Testing, made to the NRC ENS as required by 10 CFR 50.72(b)(3)(ii)(A)
- 7 Unit 3 LER 2012-001, dated March 29, 2012, Manual Reactor Trip Due to the SG Tube Leak as required by 10 CFR 50.73(a)(2)(iv)(A), actuation of the Reactor Protection System
- 8 Unit 3 LER 2012-002, dated May 10, 2012, SG Tube Degradation Indicated by Failed In-situ Pressure Testing as required by 10 CFR 50.73(a)(2)(ii)(A), a condition which resulted in a principal safety barrier being seriously degraded (i.e., serious SG tube degradation)
- 9 Letter from Peter T. Dietrich (SCE) to Elmo Collins (USNRC), dated April 20, 2012, Update of Unit 2 SG Tube Inspection Results
- 10 SONGS Steam Generator Program (SO23-SG-1)

ATTACHMENT 1

SONGS Unit 2 Relevant Technical Specifications

3.4 REACTOR COOLANT SYSTEM (RCS)

3.4.17 Steam Generator (SG) Tube Integrity

LCO 3.4.17 SG tube integrity shall be maintained.

AND

All SG tubes satisfying the tube repair criteria shall be plugged in accordance with the Steam Generator Program.

APPLICABILITY: MODES 1, 2, 3, and 4.

ACTIONS

-----NOTE-----

Separate Condition entry is allowed for each SG tube.

CONDITION	REQUIRED ACTION	COMPLETION TIME
A. One or more SG tubes satisfying the tube repair criteria and not plugged in accordance with the Steam Generator Program.	A.1 Verify tube integrity of the affected tube(s) is maintained until the next refueling outage or SG tube inspection.	7 days
	<u>AND</u> A.2 Plug the affected tube(s) in accordance with the Steam Generator Program.	Prior to entering MODE 4 following the next refueling outage or SG tube inspection
B. Required Action and associated Completion Time of Condition A not met. <u>OR</u> SG tube integrity not maintained.	B.1 Be in MODE 3.	6 hours
	<u>AND</u> B.2 Be in MODE 5.	36 hours

SURVEILLANCE REQUIREMENTS

SURVEILLANCE	FREQUENCY
SR 3.4.17.1 Verify SG tube integrity in accordance with the Steam Generator Program.	In accordance with the Steam Generator Program
SR 3.4.17.2 Verify that each inspected SG tube that satisfies the tube repair criteria is plugged in accordance with the Steam Generator Program.	Prior to entering MODE 4 following a SG tube inspection

5.5 Procedures, Programs, and Manuals (continued)

5.5.2.8 Primary Coolant Sources Outside Containment Program (continued)

system (post-accident sampling return piping only until such time as a modification eliminates the post-accident piping as a potential leakage path). The program shall include the following:

- a. Preventive maintenance and periodic visual inspection requirements; and
- b. Integrated leak test requirements for each system at refueling cycle intervals or less.

5.5.2.9 Pre-Stressed Concrete Containment Tendon Surveillance Program

This program provides controls for monitoring any tendon degradation in pre-stressed concrete containment, including effectiveness of its corrosion protection medium, to ensure containment structural integrity. Program itself is relocated to the LCS.

5.5.2.10 Inservice Inspection and Testing Program

This program provides controls for inservice inspection of ASME Code Class 1, 2, and 3 components and Code Class CC and MC components including applicable supports. The program provides controls for inservice testing of ASME Code Class 1, 2, and 3 components. The program itself is located in the LCS.

5.5.2.11 Steam Generator (SG) Program

A Steam Generator Program shall be established and implemented to ensure that SG tube integrity is maintained. In addition, the Steam Generator Program shall include the following provisions:

- a. Provisions for condition monitoring assessments. Condition monitoring assessment means an evaluation of the "as found" condition of the tubing with respect to the performance criteria for structural integrity and accident induced leakage. The "as found" condition refers to the condition of the tubing during an SG inspection outage, as determined from the inservice inspection results or by other means, prior to the plugging of tubes. Condition monitoring assessments shall be conducted during each outage during which the SG tubes are inspected or plugged, to confirm that the performance criteria are being met.

(continued)

5.5 Procedures, Programs, and Manuals (continued)

5.5.2.11 Steam Generator (SG) Program (continued)

- b. Performance criteria for SG tube integrity. SG tube integrity shall be maintained by meeting the performance criteria for tube structural integrity, accident induced leakage, and operational LEAKAGE.
1. Structural integrity performance criterion: All in-service steam generator tubes shall retain structural integrity over the full range of normal operating conditions (including startup, operation in the power range, hot standby, and cool down and all anticipated transients included in the design specification) and design basis accidents. This includes retaining a safety factor of 3.0 against burst under normal steady state full power operation primary-to-secondary pressure differential and a safety factor of 1.4 against burst applied to the design basis accident primary-to-secondary pressure differentials. Apart from the above requirements, additional loading conditions associated with the design basis accidents, or combination of accidents in accordance with the design and licensing basis, shall also be evaluated to determine if the associated loads contribute significantly to burst or collapse. In the assessment of tube integrity, those loads that do significantly affect burst or collapse shall be determined and assessed in combination with the loads due to pressure with a safety factor of 1.2 on the combined primary loads and 1.0 on axial secondary loads.
 2. Accident induced leakage performance criterion: The primary to secondary accident induced leakage rate for any design basis accident, other than a SG tube rupture, shall not exceed the leakage rate assumed in the accident analysis in terms of total leakage rate for all SGs and leakage rate for an individual SG. Leakage is not to exceed 0.5 gpm per SG and 1 gpm through both SGs.
 3. The operational LEAKAGE performance criterion is specified in LCO 3.4.13, "RCS Operational LEAKAGE."

(continued)

5.5 Procedures, Programs, and Manuals (continued)

5.5.2.11 Steam Generator (SG) Program (continued)

c. Provisions for SG tube repair criteria.

1. Tubes found by inservice inspection to contain flaws with a depth equal to or exceeding 35% of the nominal tube wall thickness shall be plugged.

- d. Provisions for SG tube inspections. Periodic SG tube inspections shall be performed. The number and portions of the tubes inspected and methods of inspection shall be performed with the objective of detecting flaws of any type (e.g., volumetric flaws, axial and circumferential cracks) that may be present along the length of the tube, from the tube-to-tubesheet weld at the tube inlet to the tube-to-tubesheet weld at the tube outlet, and that may satisfy the applicable tube repair criteria. The tube-to-tubesheet weld is not part of the tube.

In addition to meeting the requirements of d.1, d.2, and d.3 below, the inspection scope, inspection methods, and inspection intervals shall be such as to ensure that SG tube integrity is maintained until the next SG inspection. An assessment of degradation shall be performed to determine the type and location of flaws to which the tubes may be susceptible and, based on this assessment, to determine which inspection methods need to be employed and at what locations.

1. Inspect 100% of the tubes in each SG during the first refueling outage following SG replacement.
2. Inspect 100% of the tubes at sequential periods of 144, 108, 72, and thereafter, 60 effective full power months. The first sequential period shall be considered to begin after the first inservice inspection of the SGs. In addition, inspect 50% of the tubes by the refueling outage nearest the midpoint of the period and the remaining 50% by the refueling outage nearest the end of the period. No SG shall operate for more than 72 effective full power months or three refueling outages (whichever is less) without being inspected.
3. If crack indications are found in any SG tube, then the next inspection for each SG for the degradation mechanism that caused the crack indication shall not exceed 24 effective full power months or one refueling outage (whichever is less). If definitive information, such as from examination of a pulled tube, diagnostic non-destructive testing, or engineering evaluation indicates that a crack-like indication is not associated with a crack(s), then the indication need not be treated as a crack.

- e. Provisions for monitoring operational primary to secondary LEAKAGE.

5.7 Reporting Requirements (continued)5.7.2 Special Reports

Special Reports may be required covering inspection, test, and maintenance activities. These special reports are determined on an individual basis for each unit and their preparation and submittal are designated in the Technical Specifications.

Special Reports shall be submitted to the U. S. Nuclear Regulatory Commission, Attention: Document Control Desk, Washington, D. C. 20555, with a copy to the Regional Administrator of the Regional Office of the NRC, in accordance with 10 CFR 50.4 within the time period specified for each report.

The following Special Reports shall be submitted:

- a. When a pre-planned alternate method of monitoring post-accident instrumentation functions is required by Condition B or Condition G of LCO 3.3.11, a report shall be submitted within 30 days from the time the action is required. The report shall outline the action taken, the cause of the inoperability, and the plans and schedule for restoring the instrumentation channels of the function to OPERABLE status.
- b. Any abnormal degradation of the containment structure detected during the tests required by the Pre-Stressed Concrete Containment Tendon Surveillance Program shall be reported to the NRC within 30 days. The report shall include a description of the tendon condition, the condition of the concrete (especially at tendon anchorages), the inspection procedures, the tolerances on cracking, and the corrective action taken.
- c. A report shall be submitted within 180 days after the initial entry into MODE 4 following completion of an inspection performed in accordance with the Specification 5.5.2.11, Steam Generator (SG) Program. The report shall include:

(continued)

5.7 Reporting Requirements (continued)

5.7.2 Special Reports (continued)

1. The scope of inspections performed on each SG,
 2. Active degradation mechanisms found,
 3. Nondestructive examination techniques utilized for each degradation mechanism,
 4. Location, orientation (if linear), and measured sizes (if available) of service induced indications,
 5. Number of tubes plugged during the inspection outage for each active degradation mechanism,
 6. Total number and percentage of tubes plugged to date,
 7. The results of condition monitoring, including the results of tube pulls and in-situ testing.
-
-

3.4 REACTOR COOLANT SYSTEM (RCS)

3.4.13 RCS Operational LEAKAGE

LCO 3.4.13 RCS operational LEAKAGE shall be limited to:

- a. No pressure boundary LEAKAGE;
- b. 1 gpm unidentified LEAKAGE;
- c. 10 gpm identified LEAKAGE; and
- d. 150 gallons per day primary to secondary LEAKAGE through any one Steam Generator (SG).

APPLICABILITY: MODES 1, 2, 3, and 4.

ACTIONS

CONDITION	REQUIRED ACTION	COMPLETION TIME
A. RCS Operational LEAKAGE not within limits for reasons other than pressure boundary LEAKAGE or primary to secondary LEAKAGE.	A.1 Reduce LEAKAGE to within limits.	4 hours
B. Required Action and associated Completion Time of Condition A not met. <u>OR</u> Pressure boundary LEAKAGE exists. <u>OR</u> Primary to secondary LEAKAGE not within limit.	B.1 Be in MODE 3. <u>AND</u> B.2 Be in MODE 5.	6 hours 36 hours

SURVEILLANCE REQUIREMENTS

SURVEILLANCE	FREQUENCY
<p>SR 3.4.13.1 -----NOTES-----</p> <ol style="list-style-type: none"> 1. Not required to be performed in MODE 3 or 4 until 12 hours of steady state operation. 2. Not applicable to primary to secondary LEAKAGE. <p>-----</p> <p>Perform RCS water inventory balance.</p>	<p>-----NOTE-----</p> <p>Only required to be performed during steady state operation. If a transient evolution is occurring 72 hours from the last water inventory balance, then a water inventory balance shall be performed within 120 hours of the last water inventory balance</p> <p>-----</p> <p>72 hours</p>
<p>-----NOTE-----</p> <p>Not required to be performed until 12 hours after establishment of steady state operation.</p> <p>-----</p> <p>SR 3.4.13.2 Verify primary to secondary LEAKAGE is ≤ 150 gallons per day through any one SG.</p>	<p>72 hours</p>

ATTACHMENT 2

AREVA Document 51-9182368-003, SONGS 2C17 Steam Generator Condition Monitoring Report

[Proprietary Information Redacted]



AREVA NP Inc.

Engineering Information Record

Document No.: 51 - 9182368 - 003 (NP)

SONGS 2C17 Steam Generator Condition Monitoring Report

Supplier Status Stamp

VPL No:	1814-AU651-M0156	Rev No:	1	QC:	N/A
<input type="checkbox"/> DESIGN DOCUMENT ORDER NO. <u>800918458</u>		<input checked="" type="checkbox"/> REFERENCE DOCUMENT - INFORMATION ONLY <input type="checkbox"/> VIRP IOM MANUAL			
MFG MAY PROCEED: <input type="checkbox"/> YES <input type="checkbox"/> NO <input checked="" type="checkbox"/> N/A					
<small>STATUS - A status is required for design documents and is optional for reference documents. Drawings are reviewed and approved for arrangements and conformance to specification only. Approval does not relieve the submitter from the responsibility of adequacy and suitability of design, materials, and/or equipment represented.</small>					
<input type="checkbox"/> 1. APPROVED <input type="checkbox"/> 2. APPROVED EXCEPT AS NOTED - Make changes and resubmit. <input type="checkbox"/> 3. NOT APPROVED - Correct and resubmit for review. NOT for field use.					
APPROVAL: (PRINT / SIGN / DATE)					
RE: <u>E. GRIBBLE</u>			<u>10/2/12</u>		
FLS:					
Other:					

SCE DE(123) 5 REV. 3 07/11

REFERENCE: SO123-XXIV-37.8.26



SONGS 2C17 Steam Generator Condition Monitoring Report

Safety Related? YES NO

Does this document contain assumptions requiring verification? YES NO

Does this document contain Customer Required Format? YES NO

Signature Block

Name and Title/Discipline	Signature	P/LP, R/LR, A/A-CRF, A/A-CRI	Date	Pages/Sections Prepared/Reviewed/ Approved or Comments

Note: P/LP designates Preparer (P), Lead Preparer (LP)
 R/LR designates Reviewer (R), Lead Reviewer (LR)
 A/A-CRF designates Approver (A), Approver of Customer Requested Format (A-CRF)
 A/A-CRI designates Approver (A), Approver - Confirming Reviewer Independence (A-CRI)

SONGS 2C17 Steam Generator Condition Monitoring Report

Record of Revision

Revision No.	Pages/Sections/ Paragraphs Changed	Brief Description / Change Authorization
000	All	Original Release
001	Table 5-4	Edited title
	Table 5-7	Revised line 2 entry to max depth of 54%, line 6 entry to 29%
	Table 5-8	Revised second entry to max depth of 30%
	Sect. 6.2.4	Added missing callout to figure 6-6
002	All	Added Sections 2.0, 4.1, 4.2, 4.3, 6.3 and 6.4. Incorporated a significant number of editorial corrections and modifications throughout the document.
003	Section 4.3 Section 6.1 Section 6.2 Table 6-4 Table 6-5 Appendix A and B	Corrected Pre-Service examination statement from “Hot Leg (HL) and Cold Leg (CL) Top of Tubesheet (TTS)” to “Hot Leg (HL) and Cold Leg (CL) Tubesheet (TS)” to reflect that examination covered entire TS instead of just the Top of Tubesheet. Corrected Table number 5-2 to Table 6-2 in Section 6.1 Revised discussion of plugging Corrected Table 6-4 Total Indication Count Values Removed TTW wear and TTW Preventative counts from Table 6-5 Removed Appendix A and B Plugging lists

SONGS 2C17 Steam Generator Condition Monitoring Report

Table of Contents

	Page
SIGNATURE BLOCK.....	2
RECORD OF REVISION	3
LIST OF TABLES	6
LIST OF FIGURES	7
1.0 PURPOSE.....	8
2.0 ABBREVIATIONS AND ACRONYMS.....	9
3.0 SCOPE.....	12
4.0 BACKGROUND	12
4.1 Previous Operating Experience (OE) Related to Tube-to-Tube Wear	16
4.2 Previous Operating Experience Related to Tube-to-AVB Wear	17
4.3 Pre-Service Examination Results.....	18
5.0 PERFORMANCE CRITERIA	19
6.0 INSPECTION SUMMARY.....	20
6.1 Eddy Current Inspections Performed	21
6.2 Degradation Identified	23
6.3 Tube-to-Tube Wear Detection.....	24
6.4 Tube-to-Tube Wear Sizing	25
6.5 Secondary Side Visual Examination Results	26
7.0 CONDITION MONITORING ASSESSMENT	47
7.1 Input Parameters.....	47
7.2 Evaluation of Structural Integrity	49
7.2.1 AVB wear and TSP wear	49
7.2.2 Retainer Bar Wear	49
7.2.3 Foreign Object Wear.....	50
7.2.4 Tube-to-Tube Wear.....	51
7.3 Evaluation of Accident-induced Leakage Integrity	52
7.3.1 AVB wear and TSP wear	52
7.3.2 Retainer Bar Wear	52
7.3.3 Foreign Object Wear.....	52
7.3.4 Tube-to-Tube Wear.....	52
7.4 Evaluation of Operational Leakage Integrity	53
8.0 CONDITION MONITORING CONCLUSION.....	60



SONGS 2C17 Steam Generator Condition Monitoring Report

Table of Contents
(continued)

Page

9.0 REFERENCES.....61

SONGS 2C17 Steam Generator Condition Monitoring Report

List of Tables

Page

TABLE 2-1: ABBREVIATIONS AND ACRONYMS	9
TABLE 4-1: SUMMARY OF PRE-SERVICE INSPECTION RESULTS	18
TABLE 6-1: STEAM GENERATOR TUBE INSPECTION SCOPE SUMMARY (FIRST PHASE).....	27
TABLE 6-2: APRIL 2012 RTS INSPECTION SG TUBE INSPECTION SUMMARY	28
TABLE 6-3: JULY 2012 RTS INSPECTION SG TUBE INSPECTION SUMMARY	28
TABLE 6-4: WEAR INDICATION SUMMARY	29
TABLE 6-5: PLUGGING SUMMARY	30
TABLE 6-6: REPORTED AVB WEAR DEPTHS (%TW).....	30
TABLE 6-7: REPORTED TSP WEAR DEPTHS (%TW).....	30
TABLE 6-8: RETAINER BAR WEAR	31
TABLE 6-9: FOREIGN OBJECT WEAR	31
TABLE 6-10: TUBE-TO-TUBE WEAR	31
TABLE 7-1: SONGS-2 STEAM GENERATOR INPUT VALUES	48
TABLE 7-2: EDDY CURRENT ETSS INPUT VALUES (REFERENCE 5).....	48

SONGS 2C17 Steam Generator Condition Monitoring Report

List of Figures

	Page
FIGURE 4-1: SONGS STEAM GENERATOR SUPPORT STRUCTURE LAYOUT	13
FIGURE 4-2: VIEW FROM ABOVE BUNDLE SHOWING RETAINER BAR LOCATIONS	14
FIGURE 4-3: SKETCH SHOWING RETAINER/RETAINING BAR CONFIGURATION.....	15
FIGURE 6-1: SG 2E-088 AVB WEAR	32
FIGURE 6-2: SG 2E-089 AVB WEAR	33
FIGURE 6-3: SG 2E-088 TSP WEAR – HOT LEG.....	34
FIGURE 6-4: SG 2E-088 TSP WEAR – COLD LEG	35
FIGURE 6-5: SG 2E-089 TSP WEAR – HOT LEG.....	36
FIGURE 6-6: SG 2E-089 TSP WEAR – COLD LEG	37
FIGURE 6-7: SG 2E-088 RETAINER BAR WEAR.....	38
FIGURE 6-8: SG 2E-089 RETAINER BAR WEAR.....	39
FIGURE 6-9: SG 2E-088 FOREIGN OBJECT WEAR.....	40
FIGURE 6-10: TUBE-TO-TUBE WEAR (DETECTED IN SG 2E-089 ONLY).....	41
FIGURE 6-11: SG 2E-088 AVB WEAR DEPTH DISTRIBUTION.....	42
FIGURE 6-12: SG 2E-089 AVB WEAR DEPTH DISTRIBUTION.....	43
FIGURE 6-13: SG 2E-088 TSP WEAR DEPTH DISTRIBUTION.....	44
FIGURE 6-14: SG 2E-089 TSP WEAR DEPTH DISTRIBUTION.....	45
FIGURE 6-15: FOREIGN OBJECT RETRIEVED FROM SG 2E-088.....	46
FIGURE 7-1: CM LIMIT FOR AVB WEAR, ETSS 96004.1	54
FIGURE 7-2: CM LIMIT FOR TSP WEAR, ETSS 96004.1.....	55
FIGURE 7-3: CM LIMIT FOR RB WEAR, ETSS 27903.1.....	56
FIGURE 7-4: CM LIMIT FOR FO WEAR, ETSS 27901.1.....	57
FIGURE 7-5: FOREIGN OBJECT POP-THROUGH AT 2560 PSI, UNIFORM 360° THINNING, ETSS 27901.1	58
FIGURE 7-6: CM LIMIT FOR TUBE-TO-TUBE WEAR, ETSS 27902.2	59

SONGS 2C17 Steam Generator Condition Monitoring Report

1.0 PURPOSE

In accordance with the EPRI Steam Generator Integrity Assessment Guidelines [2], a Condition Monitoring (CM) assessment must be performed at the conclusion of each steam generator eddy current examination. This process is described as “backward-looking,” since its purpose is to confirm that adequate Steam Generator (SG) integrity was maintained during the most recent operating period. It involves an evaluation of the as-found conditions of the steam generator relative to established performance criteria for structural and leakage integrity. The performance criteria are defined in plant Technical Specifications [17] [18]. The performance criteria are based on NEI (Nuclear Energy Institute) 97-06 [1] (see Section 5.0 below).

This report concludes that the SONGS (San Onofre Nuclear Generating Station) steam generator performance criteria were satisfied by Unit 2 during the operating period prior to 2C17.

SONGS 2C17 Steam Generator Condition Monitoring Report

2.0 ABBREVIATIONS AND ACRONYMS

The following table provides a listing of abbreviations and acronyms used throughout this report.

Table 2-1: Abbreviations and Acronyms

Abbreviation or Acronym	Definition
01C to 07C	Tube Support Plate Designations for Cold Leg (7 Locations)
01H to 07H	Tube Support Plate Designations for Hot Leg (7 Locations)
2E-088	Unit 2 Steam Generator 88
2E-089	Unit 2 Steam Generator 89
3E-088	Unit 3 Steam Generator 88
3E-089	Unit 3 Steam Generator 89
3 NOPD	3 Times Normal Operating Pressure Differential
3ΔP	3 Times Normal Operating Pressure Differential
ADI	Absolute Drift Indication
AILPC	Accident Induced Leakage Performance Criterion
ANO	Arkansas Nuclear One
ASME	American Society of Mechanical Engineers
AVB	Anti-Vibration Bar
B01 to B12	AVB Designations (12 Locations)
BLG	Bulge
C	Column
CE	Combustion Engineering
CL or C/L	Cold Leg
CM	Condition Monitoring
DA	Degradation Assessment
DBE	Design Basis Earthquake
DNG	Ding
DNT	Dent
ECT	Eddy Current Testing
EFPD	Effective Full Power Days
EOC	End of Operating Cycle
EPRI	Electric Power Research Institute
ETSS	Examination Technique Specification Sheet
FOSAR	Foreign Object Search and Retrieval
GMD	Geometric Distortion
GPD	Gallons per Day
GPM	Gallons per Minute

SONGS 2C17 Steam Generator Condition Monitoring Report

Table 2-1: Abbreviations and Acronyms

Abbreviation or Acronym	Definition
HL or H/L	Hot Leg
INPO	Institute of Nuclear Power Operators
kHz	Kilohertz
KSI	Thousand Pounds per Square Inch
LER	Licensee Event Report
MBM	Manufacturing Burnish Mark
MHI	Mitsubishi Heavy Industries
MSLB	Main Steam Line Break
NDE	Non Destructive Examination
NEI	Nuclear Energy Institute
NN	Nuclear Notification
NOPD	Normal Operating Pressure Differential
NQI	Non-Quantifiable Indication
NRC	Nuclear Regulatory Commission
NSAL	Nuclear Safety Advisory Letter
OA	Operational Assessment
OE	Operating Experience
OTSG	Once Through Steam Generator
PDA	Percent Degraded Area
PLP	Possible Loose Part
POD	Probability of Detection
PRX	Proximity Indication
PSI	Pounds per Square Inch
PSIG	Pounds per Square Inch Gage
PST	Pacific Standard Time
PVN	Permeability Variation
PWR	Pressurized Water Reactor
QA	Quality Assurance
R	Row
RB	Retainer Bar
RCS	Reactor Coolant System
REPL	Replacement
ROLLED	Rolled Plug Designation
ROLLSTAB	Rolled Plug with a Stabilizer
RPC	Rotating Probe Coil
RSG	Recirculating Steam Generator
SCE	Southern California Edison

SONGS 2C17 Steam Generator Condition Monitoring Report

Table 2-1: Abbreviations and Acronyms

Abbreviation or Acronym	Definition
SG	Steam Generator
SIPC	Structural Integrity Performance Criteria
SL2	St. Lucie Unit 2
SLB	Steam Line Break
SONGS	San Onofre Nuclear Generating Station
SSA	Secondary Side Anomaly
SSI	Secondary Side Inspection
SVI	Single Volumetric Indication
TMI	Three Mile Island
TSP	Tube Support Plate
TTW	Tube to Tube Wear
TW	Through Wall
U3F16B	Unit 3 Outage Designation
UB	U-bend

SONGS 2C17 Steam Generator Condition Monitoring Report

3.0 SCOPE

This evaluation pertains to the SONGS Unit 2 replacement steam generators, which are reactor coolant system components. The CM assessment documented in this report is required to be completed prior to plant entry into Mode 4 during start up after a SG inspection. The Unit 2 SGs passed CM, thus an OA (Operational Assessment) shall be completed for the next inspection interval within 90 days after Mode 4.

This document was originally a portion of AREVA document 51-9177491-001, "SONGS 2C17 Steam Generator Condition Monitoring and Preliminary Operational Assessment" [14]. The decision was made to separate the Condition Monitoring and Operational Assessment portions of the document.

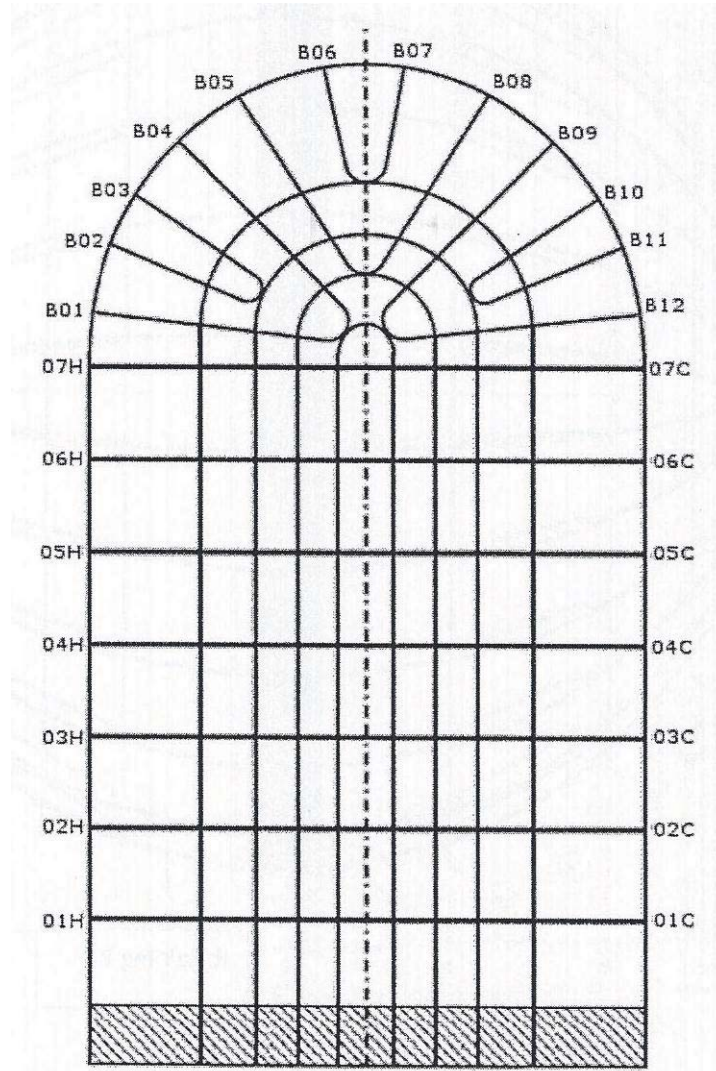
4.0 BACKGROUND



MHI Proprietary

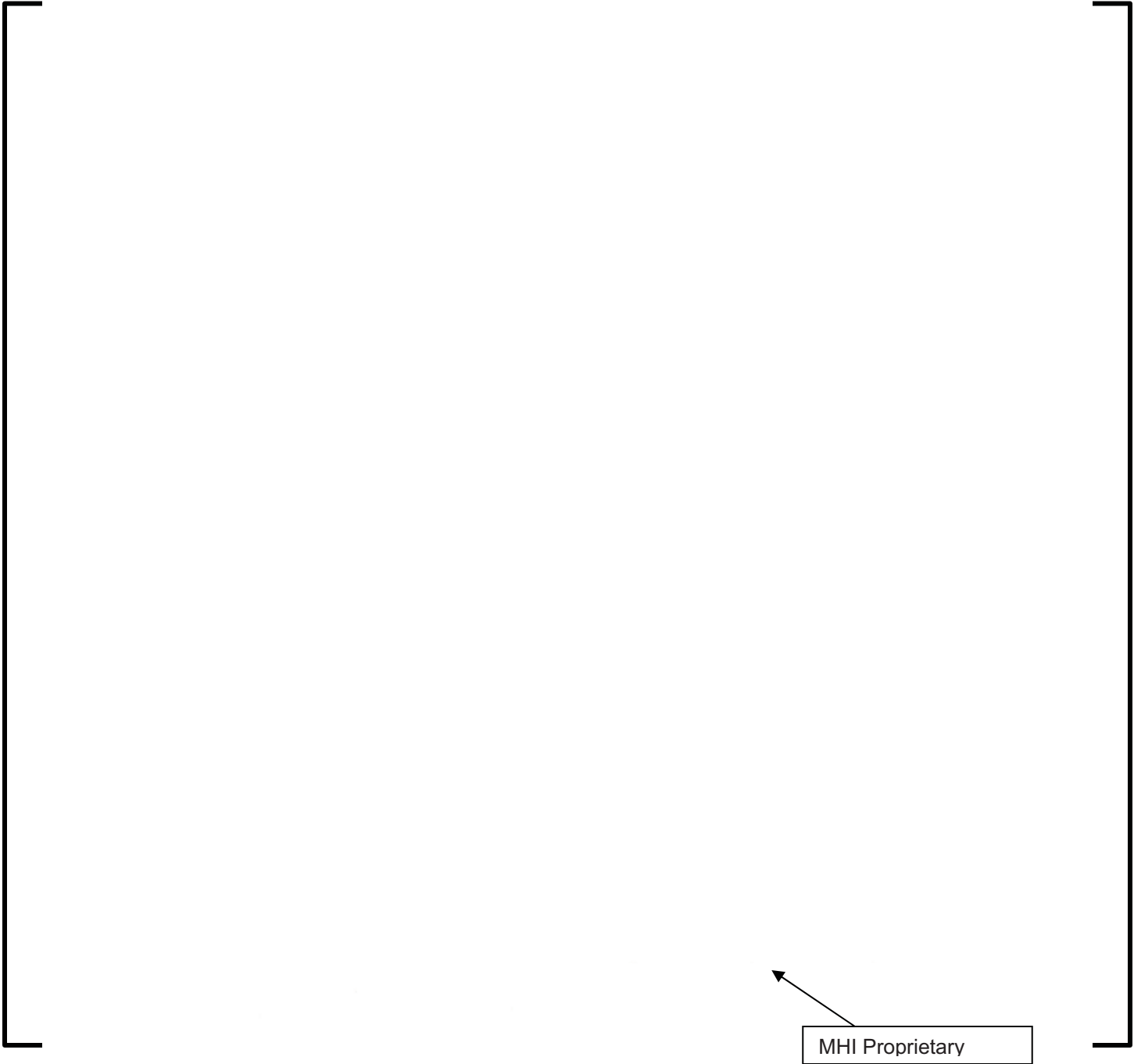
SONGS 2C17 Steam Generator Condition Monitoring Report

Figure 4-1: SONGS Steam Generator Support Structure Layout



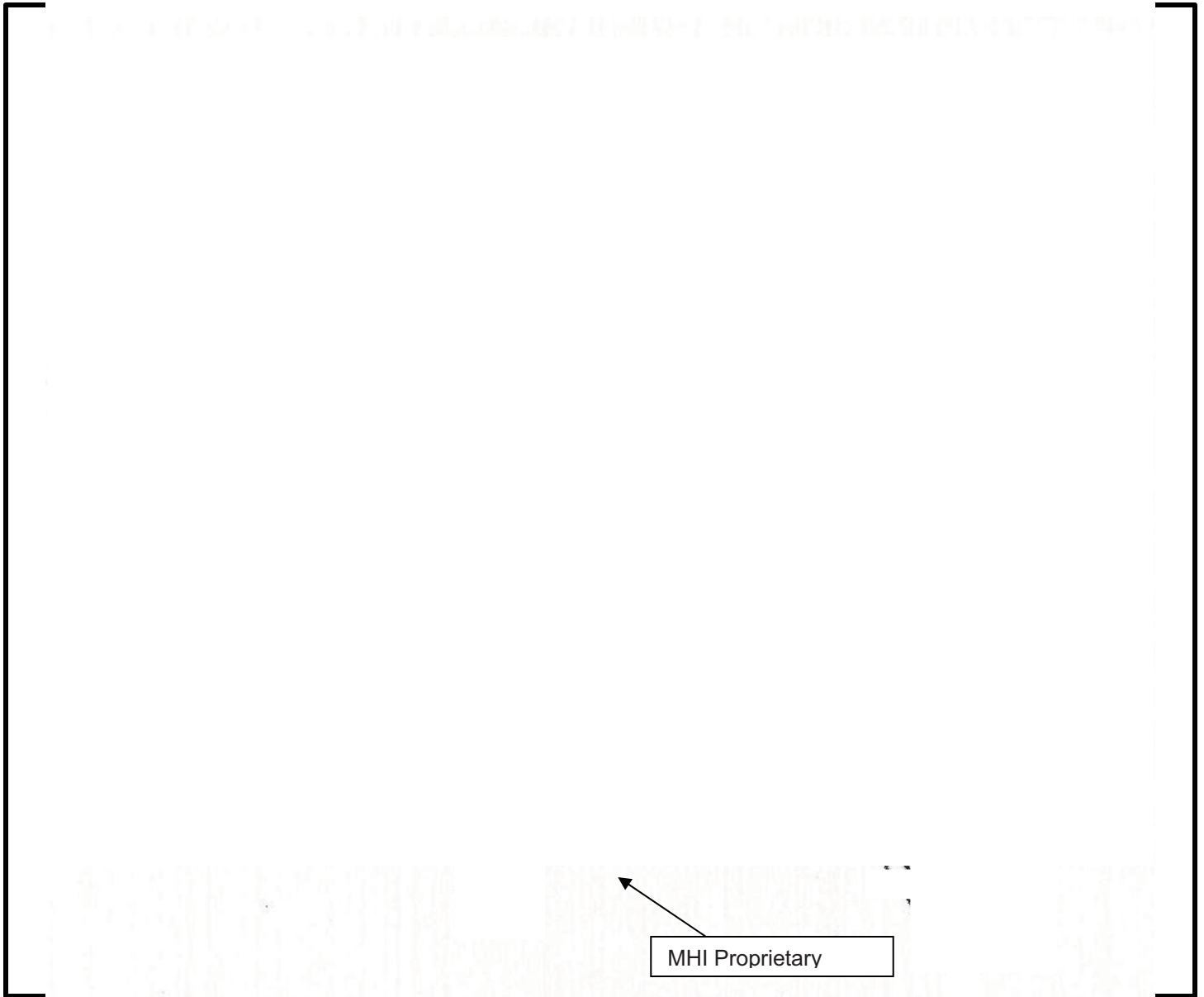
SONGS 2C17 Steam Generator Condition Monitoring Report

Figure 4-2: View From Above Bundle Showing Retainer Bar Locations



SONGS 2C17 Steam Generator Condition Monitoring Report

Figure 4-3: Sketch Showing Retainer/Retaining Bar Configuration



SONGS 2C17 Steam Generator Condition Monitoring Report

4.1 Previous Operating Experience (OE) Related to Tube-to-Tube Wear

Prior to the Songs Unit 3 shutdown in January of 2012, the recent operating experience related to tube-to-tube wear was limited to once-through steam generators. In December 2011, INPO (Institute of Nuclear Power Operators) OE 34946 [19] was released. This Operating Experience Report discusses experience at Three Mile Island Unit 1 (TMI-1). In July 2012, the NRC (Nuclear Regulatory Commission) released Information Notice 2012-07 [20]. This Information Notice contains information on the experience at TMI-1 as well as Oconee and ANO-1 (Arkansas Nuclear One – Unit 1). This section summarizes the experiences at these plants with once-through steam generators.

TMI-1 completed replacement of its original Once Through Steam Generators (OTSGs) in 2010. The design of the OTSG differs from the recirculating steam generator design in that the tubes are straight. The tubes are supported by 15 tube support plates. The first inspection of the TMI-1 replacement steam generators took place in the fall of 2011. During this examination, indications were detected on the absolute channel with no discernible response on the differential channel. The indications were designated as Absolute Drift Indications (ADIs). A comprehensive review of all of the ADIs identified tubes with long shallow wear signals between the eighth and ninth tube support plates. The indications were in adjacent tube combinations of either 2 or 3 tubes (the tube pattern is a triangular pitch). A more detailed investigation led to the conclusion that these wear indications were the result of tube-to-tube contact wear. The lengths ranged from 2 to 8 inches and from 1 to 21 percent through-wall.

As a result of the TMI-1 findings, and because TMI and ANO both have AREVA replacement steam generators, the licensee for Arkansas Nuclear One, Unit 1 (ANO-1) was notified. Upon a review of previously recorded eddy current examination data, it was determined that ANO-1 also had similar indications of tube-to-tube wear. The depth and length of the ANO-1 indications were similar to those recorded at TMI-1

In the spring of 2012, the licensee for Oconee, Unit 3 also detected wear attributed to tube-to-tube contact in their replacement steam generators. Since the design of the Oconee OTSGs, which were built by BWI, is not the same as the TMI or ANO generators, the location of the tube-to-tube wear was different, but the characteristics were similar. The lengths ranged from 1 to 9 inches and the depths ranged up to 20 percent through-wall.

The severity of the replacement OTSG tube-to-tube wear was evaluated and was not found to compromise tube integrity.

The combined experience from the above discussion demonstrated several significant points:

- New or unexpected forms of degradation may be difficult to identify. Robust inspection planning is an important part of identifying new degradation as well as properly characterizing known degradation.
- A comprehensive review of examination data from different perspectives is valuable. By considering the change in indications over time, responses to different channels or techniques, or the spatial distribution of the indications, important information may be found.

SONGS 2C17 Steam Generator Condition Monitoring Report

- The reporting criteria is critical to proper identification of new or existing damage mechanisms.
- Comprehensive examination of new or replacement steam generators is necessary to ensure that performance is as expected.

4.2 Previous Operating Experience Related to Tube-to-AVB Wear

INPO OE 35359 [21] discusses the results of the first two inspections at St. Lucie Unit 2. The recirculating steam generators at St. Lucie Unit 2 were replaced during 2007. During the Cycle 18 Refueling Outage (SL2-18, April 2009), eddy current testing of the replacement steam generators reported over 5800 AVB wear indications in more than 2000 tubes. Fourteen tubes were plugged as a result of the wear indications. None of the indications challenged the Condition Monitoring limits.

Based on the high number of wear indications reported during the SL2-18 inspection, and to further establish growth rates, the St. Lucie Unit 2 SGs were examined again during the next refueling outage at SL2-19 in January 2011. Approximately 3000 new AVB wear indications were reported during the SL2-19 examination. As a result of the SL2-19 inspection, an additional twenty-one (21) tubes were plugged, only one of which exceeded the Plant Technical Specification limit of > 40 %TW (throughwall).

The OE reinforces the importance of inspecting replacement SGs with the bobbin coil at the end of the first cycle of operation, post-replacement. The diagnostic examinations performed with the +Point™ rotating coil concluded that the AVB wear indications could be flat or tapered, single or double sided. These wear characteristics are important to consider when selecting the proper depth-sizing technique(s).

SONGS 2C17 Steam Generator Condition Monitoring Report

4.3 Pre-Service Examination Results

During May and June of 2009, an on-site pre-service examination was performed in the Songs Unit 2 replacement SGs. The examination consisted of 100 % bobbin coil inspection of all tubes (9727 tubes), 100 % inspection of the Hot Leg (HL) and Cold Leg (CL) Tubesheet (TS) region with the +Point™ probe (9727 tubes), and a 100 % inspection of the row 1-15 U-bend regions with the +Point™ probe (1314 tubes).

No significant degradation was detected during this examination. There were a number of geometric type indications reported in each SG (dings, geometric distortions, proximity, bulge). The following table provides a count of the number of tubes and total number of indications for each Unit 2 SG.

Table 4-1: Summary of Pre-Service Inspection Results

Indication Code	SG 2E-088		SG 2E-089	
	Tube Count	Indication Count	Tube Count	Indication Count
BLG (Bulge)	0	0	1	1
DNG (Ding)	1089	2180	1033	2084
GMD (Geometric Distortion)	15	19	21	31
MBM (Manufacturing Burnish Mark)	0	0	2	2
NQI (Non-Quantifiable Indication)	0	0	1	1
PLP (Potential Loose Part)	1	1	0	0
PRX (Proximity)	66	66	42	42
PVN (Permeability Variation)	0	0	1	1

SONGS 2C17 Steam Generator Condition Monitoring Report

5.0 PERFORMANCE CRITERIA

The SONGS-2 performance criteria, based on NEI 97-06 [1] are shown below. The structural integrity and accident-induced leakage criteria were taken from Section 5.5.2.11 [17] from the SONGS-2 Technical Specifications. The operational leakage criterion was taken from Section 3.4.13 [18] of the SONGS Technical Specifications.

- Structural Integrity Performance Criterion: “All inservice steam generator tubes shall retain structural integrity over the full range of normal operating conditions (including startup, operation in the power range, hot standby, and cooldown and all anticipated transients included in the design specification) and design basis accidents. This includes retaining a safety factor of 3.0 against burst under normal steady state full power operation primary-to-secondary pressure differential and a safety factor of 1.4 against burst applied to the design basis accident primary-to-secondary pressure differentials. Apart from the above requirements, additional loading conditions associated with the design basis accidents, or combination of accidents in accordance with the design and licensing basis, shall also be evaluated to determine if the associated loads contribute significantly to burst or collapse. In the assessment of tube integrity, those loads that do significantly affect burst or collapse shall be determined and assessed in combination with the loads due to pressure with a safety factor of 1.2 on the combined primary loads and 1.0 on axial secondary loads.
- Accident-induced Leakage Performance Criterion: “The primary to secondary accident-induced leakage rate for any design basis accident, other than a SG tube rupture, shall not exceed the leakage rate assumed in the accident analysis in terms of total leakage rate for all SGs and leakage rate for an individual SG. Leakage is not to exceed 0.5 gpm per SG and 1 gpm through both SGs.”
- Operational Leakage Performance Criterion: “RCS operational leakage shall be limited to 150 gallons per day primary to secondary leakage through any one steam generator.”

SONGS 2C17 Steam Generator Condition Monitoring Report

6.0 INSPECTION SUMMARY

The SONGS Unit 2, 2C17 inspection scope occurred in three distinct phases. The first phase followed the planned shutdown for the 2C17 refueling outage and first SG ISI.

The next two inspection phases, performed in April and July 2012, were a direct result of a SG tube leak in Unit 3. The tube leak resulted from tube-to-tube wear (TTW) that was caused by fluid-elastic instability. These subsequent inspections are referred to as 2C17 RTS (Return-to-Service) inspections. The second-phase inspection (April 2012) was a full-length U-bend inspection of tubes deemed most susceptible to tube-to-tube wear based on the degradation identified in Unit 3. The third-phase inspection (July 2012) consisted of eddy current testing to measure the gaps between the AVBs and the tubes. Based on the gap measurements, an additional 104 tubes were examined in the U-bend region with the +Point™ coil.

Inspections included the following inspection activities for each of the two replacement steam generators (SG 2E-088 and SG 2E-089) using site validated ECT techniques [7]:

- Bobbin Coil Examinations
 - All in-service tubes, full length tube-end to tube-end
- Rotating Coil Examinations
 - Tubesheet periphery and divider lane tubes (from 3" above to 1" below the top of the tubesheet), both legs, approximately 3 tubes in from the periphery and 2 tubes in from the divider lane
 - Full-length U-bend Exam of Tubes Adjacent to Retainer Bars
 - Specific locations based on results of bobbin inspections (e.g., I-codes, selected wear indications, etc.)
 - Full-length U-bend +Point™ examination of tubes with potential for tube-to-tube wear (2C17 RTS inspection)
 - Full-length U-bend pancake coil examination of selected tubes for measurement of gaps between the AVBs and the tubes (2C17 RTS inspection)
- Secondary Side Visual Examinations
 - Foreign object search and retrieval (FOSAR) as required based on ECT
 - Post sludge lancing FOSAR examination at the top-of-tubesheet (periphery and the divider lane)
 - Visual inspections of the upper tube bundle at the 7th TSP and AVB / retainer bar regions

The subsections below discuss each aspect of the inspection and describe findings that are relevant to Condition Monitoring and operational assessment.

SONGS 2C17 Steam Generator Condition Monitoring Report

6.1 Eddy Current Inspections Performed

A summary of the total number of bobbin probe and rotating probe examinations performed during 2C17 is provided in Table 6-1 and Table 6-2. The Unit 2 examination was in progress when a tube leak developed in Unit 3 SG 2E-088. As a result of finding tube-to-tube wear in Unit 3, additional analysis and examinations were performed in Unit 2.

The original inspection scope included examination of the tubing in SG's 2E-088 and 2E-089 as follows:

- 100% bobbin coil probe (610 mil diameter) examination of the complete tube length in both Steam Generators.
- 100% of all previous (Pre-service exam) and newly reported bobbin coil "I" codes, Possible Loose Part (PLP), Manufacturing Burnish Mark (MBM), Non-Quantifiable Indication (NQI), Bulge (BLG) and Permeability Variation (PVN) locations with at rotating +Point™ / pancake coil probe.
- 100% of all reported bobbin coil Ding (DNG) and Dent (DNT) locations measuring ≥ 2.0 volts with a rotating +Point™ / pancake coil probe.
- A sample of AVB %TW wear indications as defined by SCE and/or tube integrity engineering.

Due to detection of a foreign object and the detection of wear at a retainer bar, scope expansions were performed in SG's 2E-088 and 2E-089 as follows:

- H/L and C/L Tubesheet Periphery exam (TSH/TSC +3/-1 inches with a rotating +Point™ / pancake coil probe.
- H/L and C/L Retainer Bar exam (07H-B06 & 07C-B07) with a single coil rotating +Point™ probe. This exam included all tubes adjacent to retainer bar locations.

SONGS 2C17 Steam Generator Condition Monitoring Report

Due to the detection of tube-to-tube wear (TTW) in Unit 3, additional inspections were performed in Unit 2 after the initial pre-planned scope was completed. These additional inspections were performed in two separate phases in April and July 2012. These inspections are referred to as RTS (Return-to-Service) inspections. These inspections included the following inspections in both steam generators.

- April 2012 RTS inspection: Full-length U-bend +Point™ inspections of tubes believed to be susceptible to TTW based on the affected tube population in Unit 3.
- July 2012 RTS inspection: Full-length U-bend pancake coil inspection of selected tubes for measurements of tube-to-AVB gaps.
- July 2012 RTS inspection: Full-length U-bend +Point™ inspections of 104 tubes in the 2E-089 SG based on the gap measurements.

The full-length U-bend +Point™ inspections performed in April 2012 included 1371 tubes in SG 2E-088 and 1375 tubes in SG 2E-089. Since these inspections were performed for detection of tube-to-tube wear (TTW), the tubes were selected based on the location of the affected tubes in Unit 3. The defined inspection scope bounded the affected tubes in Unit 3 by a minimum of four tubes on all sides. In July 2012, an additional 104 tubes were inspected in the 2E-089 SG over the full length of the U-bend with +Point™. The tubes for these additional inspections were selected based on the tube-to-AVB gap measurements.

A summary of the initial examination and subsequent expansions is provided in 51-9181604-000 [23].

SONGS 2C17 Steam Generator Condition Monitoring Report

6.2 Degradation Identified

The following tube degradation mechanisms were identified during the initial 2C17 inspections and the subsequent 2C17 RTS steam generator eddy current inspections:

- Anti-Vibration Bar (AVB) wear
- Tube Support Plate (TSP) wear
- Retainer Bar (RB) wear
- Foreign Object (FO) wear
- Tube-to-tube wear (TTW)

Table 6-4 summarizes the number of degradation indications and the number of affected tubes for each of the five wear categories. A complete accounting of the number of tubes plugged and stabilized for damage other than TTW during the 2C17 outage is provided in Table 6-5. The plugging information provided in this table is current for non-TTW. Due to the ongoing SG recovery efforts, the plugging strategy and, hence, the plugging and stabilization information for tubes with TTW wear and for tubes plugged as preventative measures for TTW may change prior to startup.

Table 6-6 through Table 6-9 summarize reported AVB wear, TSP wear, RB wear, FO and tube-to-tube wear depths, respectively. Table 6-8, Table 6-9, and Table 6-10 provide detailed information on all of the RB wear, FO wear, and tube-to-tube wear flaws identified. Within Table 6-8, Table 6-9, and Table 6-10, the structurally equivalent length and depth, as well as the overall length and maximum depth of the wear are provided. These structurally equivalent dimensions correspond to a rectangular flaw which would burst at the same pressure as the measured flaw. The structurally equivalent dimensions were determined using the methods described in Section 5.1.5 of Reference 4.

Figure 6-1 through Figure 6-10 provide tubesheet maps illustrating the locations of degradation reported in each steam generator. The AVB wear is most prevalent in the central region of the tubesheet matrix, in longer tube rows (Figure 6-1, Figure 6-2). Two other regions within each SG are also affected to a lesser degree. These regions are located near the periphery in slightly lower rows. TSP wear has affected fewer tubes than has AVB wear. TSP wear was identified at nearly every support elevation, with a greater tendency to occur on the hot leg than on the cold leg (Figure 6-3, Figure 6-4, Figure 6-5, Figure 6-6). RB wear was identified in only six tubes (Figure 6-7, Figure 6-8). Foreign object wear was identified in two tubes in SG 2E-088 (Figure 6-9). Tube-to-tube wear was detected in two tubes in SG 2E-089.

Figure 6-11 and Figure 6-12 provide histograms of the reported depths of AVB wear which demonstrate that the vast majority of AVB wear was less than 25 %TW. Four AVB wear flaws were sized >30%TW and the affected tubes were stabilized and plugged. Figure 6-13 and Figure 6-14 provide histograms of TSP wear depths and illustrate that the growth rate of TSP wear during the first operating cycle was less aggressive than that the growth rate of AVB wear. The maximum reported TSP wear flaw was 20%TW.

SONGS 2C17 Steam Generator Condition Monitoring Report

The retainer bar wear indications were not expected as they have not been reported in other MHI steam generators with the retainer bar design. As a result of the finding of retainer bar wear, the Degradation Assessment was revised during the outage to include this new mechanism.

After the completion of the initial scope of 2C17 inspections, additional inspections were performed as a result of the detection of tube-to-tube wear in Unit 3. Tube-to-tube wear was detected in two adjacent tubes in SG 2E-089. Both flaws measured 14% TWD with +Point™. The Degradation Assessment was also revised to include tube-to-tube wear.

6.3 Tube-to-Tube Wear Detection

Subsequent to finding tube-to-tube wear conditions in the U-bends of the Unit 3 tubing, SCE requested an additional review of the U-bend area bobbin coil data in Unit 2. The tubes selected for review encompassed the suspected tube-to-tube wear zone as defined in Unit 3 and included over 1000 tubes in each steam generator. This review included a two-party manual analysis (primary/secondary) of the complete U-bend (07H to 07C) with emphasis on the detection of low level freespan indications which may not have been reported during the original analysis of the U2C17 bobbin coil data. The analysts were instructed to report any indication detected on the differential channels and all indications measuring ≥ 0.40 volts on channel 6 absolute which would be a primary channel for detection of tube-to-tube wear. All indications identified during the analysis process were reviewed and dispositioned by the primary and secondary resolution analysis team with concurrence from the IQDA (Independent Qualified Data Analyst). None of the indications reviewed by the resolution team were deemed reportable and therefore, no new NQI indications were entered into the database based on this review.

The Unit 2 Return-to-Service inspection performed in April 2012 was comprised of a U-bend +Point™ examination which included 1371 tubes in SG 2E-088 and 1375 tubes in SG 2E089. The number for SG 2E-088 is less than SG 2E-089 because plugging of 4 tubes for AVB wear had already been performed in SG 2E-088 when these inspections were performed. Since these inspections were performed for detection of tube-to-tube wear (TTW), the tubes were selected based on the location of the affected tubes in Unit 3. The defined inspection scope bounded the combined population of affected tubes in both Unit 3 SGs by a minimum of four tubes on all sides. During this inspection, two tubes with indications indicative of tube-to-tube wear (TTW) were reported in SG 2E-089. The indications were approximately 6" long, located between AVBs B09 and B10, on one side of the tube (intrados for one tube and extrados for the other) and measured a maximum depth of 14%TW. The lower voltage amplitude curve defined in EPRI ETSS 27902.2 was used for sizing the indications. The SONGS Unit 2 & 3 site validation for sizing TTW can be found in AREVA document 51-9177744-000 "Site Validation of EPRI Sizing ETSS for Tube-Tube Wear in SONGS Steam Generators" [15].

SONGS 2C17 Steam Generator Condition Monitoring Report

The bobbin coil data for these two tubes was reviewed by the Lead Level III to determine if there were reportable bobbin coil indications associated with the TTW indications. The review revealed a very small amplitude absolute signal in the same vicinity as the TTW indications in both tubes. The Channel 6 amplitude for these two indications was 0.19 volts and 0.26 volts. Based on the amplitude, signal characteristics, and voltage criteria used for the initial bobbin coil review, it was determined that the bobbin indications were not reportable and are in a depth/size range where reliable detectability is a challenge.

A review of the detection performance of the bobbin coil versus the +Point™ coil was performed using the EPRI data for ETSS 27902.2 and the actual Unit 3 tube-to-tube wear data. The review is documented in AREVA Document 51-9179946-001 [16]. The EPRI technique was not specifically developed for tube-to-tube wear, but was the closest technique available. The review showed that the +Point™ probe had a slightly improved Probability of Detection (POD) over the bobbin coil and that the detection level for both techniques was above the minimum level of 0.80 POD at a 90 % LCL. The results of the Unit 3 specific tube-to-tube detection comparison produced similar results.

While the initial bobbin coil examination and subsequent review of bobbin data produced an acceptable detection performance for the depth of the two Unit 2 indications confirmed as tube-to-tube wear, it is likely that the Unit 2 flaw signal amplitudes were below the analysis detection threshold. The supplemental +Point™ examination was performed to provide the best possible detection performance.

During the July 2012 RTS inspection, an additional 104 tubes were inspected with +Point™ over the full length of the U-bend. These tubes were selected based on the tube-to-AVB gap measurements with emphasis placed on tubes having AVB intersections with gaps (as measured by eddy current) on both sides of the tube. No indications of TTW were reported in any of these tubes.

6.4 Tube-to-Tube Wear Sizing

Upon detection of tube-to-tube wear in the Unit 3 SG's, a determination was made that the most appropriate technique for sizing the wear was EPRI ETSS 27902.2 or 27902.5. However, with some initial review, it was apparent that the techniques produced very conservative depth estimates. The depth estimates reported for the deepest flaws were near 100% throughwall, however the tubes had maintained structural integrity at normal operating differential pressure. Using the actual operational conditions the throughwall depth values should have been at around 80 %TW in order to withstand pop-through. Based on the best understanding of the tube-to-tube wear degradation morphology, a standard was designed with two long, gradually-tapered machined wear flaws. Although the sample had only two separate flaws, the length of the flaws made it possible to measure multiple discrete depth sizing grading units. On the basis of these multiple points, a polynomial function was developed to adjust the depth estimates. The revised technique was documented in Reference 15.

The actual flaw sizing was performed using the 27902.2 technique. Screening for selection of in situ pressure test candidates was based on the 27902.2 sizing data without the polynomial correction in Reference 15. This produced a conservative population for in situ pressure testing.

SONGS 2C17 Steam Generator Condition Monitoring Report

6.5 Secondary Side Visual Examination Results

Secondary side visual inspections were performed in accordance with the plan outlined in Reference 8.

During the eddy current inspection of SG 2E-088, foreign object indications and foreign object wear indications were reported in two adjacent tubes at the 4th TSP (see Table 6-9 and Figure 6-9). Consequently, a secondary side foreign object search and retrieval effort was initiated, and the team successfully located and removed the object from the steam generator. Photographs of the object taken during retrieval are provided in Figure 6-15. Note that the FO wear indication identified in tube SG 2E-088 R137 C77 is visible in the upper photo in Figure 6-15. A follow-up analysis performed by SCE identified the object as weld metal debris [13]. These two adjacent tubes are being left in service because the indications are below the Technical Specification plugging limit and the cause of the degradation has been removed.

Due to the eddy current wear indications at the retainer bars, secondary side visual inspections of the retainer bars were performed in both steam generators. These inspections were performed on the retainer bars at B01, B02, B03, B10, B11, and B12. These retainer bars were selected for visual inspection since they are smaller in diameter and all retainer bar wear occurred at one of these locations. The visual inspections were focused on verifying the integrity of the retainer bar and the associated welds. All retainer bars and welds inspected were determined to be in the as-designed configuration. No cracking or degradation of the welds or retainer bars was observed.

The other secondary side examination activities (i.e., post-lancing visual exam at the top-of-tubesheet, visual exams performed in the upper bundle region) identified no foreign objects and no evidence of internal structure degradation. No conditions which could generate foreign objects or threaten tube integrity were identified during these examinations. In response to the detection of tube-to-tube wear in Unit 3, additional secondary side inspections were performed in Unit 2, similar to those done in Unit 3. The Unit 2 inspections in response to the Unit 3 condition included the following:

- Inspection of all small-diameter retainer bars (12).
- Inspection of retaining bars in the regions correlated to AVB/TSP damage in Unit 3 (Hot and Cold leg of bars B04 and B09 from columns 56 to 119).
- Inspection of AVB end caps on the retainer bar in the same area as identified above.
- Inspection through the transition cone handhole from column 73 to 87 through all rows to periphery of the following:
 - 7th Tube Support Plate
 - AVB B04 Hot Leg side column 73 to 87
 - AVB B04 in Columns 50-60
 - AVB B09 in Column 80 to 78

SONGS 2C17 Steam Generator Condition Monitoring Report

These inspections did not detect tube-to-tube wear or any other conditions that may be precursor signals to tube-to-tube wear, such as AVB wear indications extending outside of the intersection between the tube and the AVB.

Table 6-1: Steam Generator Tube Inspection Scope Summary (first phase)

SCOPE DESCRIPTION			S/G 2E-088			S/G 2E-089		
<i>Leg</i>	<i>Exam Description</i>	<i>Extents</i>	<i>Analyzed</i>	<i>Scope</i>	<i>% Completed</i>	<i>Analyzed</i>	<i>Scope</i>	<i>% Completed</i>
Hot / Cold	100 % Bobbin F/L	TEH-TEC	9,727	9,727	100.00%	9,727	9,727	100.00%
Hot	HL Special Interest	Various	33	33	100.00%	15	15	100.00%
Cold	CL Special Interest	Various	45	45	100.00%	16	16	100.00%
Hot / Cold	UB Special Interest	Various	125	125	100.00%	131	131	100.00%
Expansion								
Hot	HL Tubesheet Periphery	TSH+3/-1	1,030	1,030	100.00%	1,030	1,030	100.00%
Cold	CL Tubesheet Periphery	TSC+3/-1	1,030	1,030	100.00%	1,030	1,030	100.00%
Hot	HL Retainer Bar Tube RPC	07H-B06	96	96	100.00%	96	96	100.00%
Cold	CL Retainer Bar Tube RPC	07C-B07	96	96	100.00%	96	96	100.00%
	Total Plan		12,182	12,182	100.00%	12,141	12,141	100.00%

SONGS 2C17 Steam Generator Condition Monitoring Report

Table 6-2: April 2012 RTS Inspection SG Tube Inspection Summary

SCOPE DESCRIPTION			S/G 2E-088			S/G 2E-089		
<i>Leg</i>	<i>Exam Description</i>	<i>Extents</i>	<i>Analyzed</i>	<i>Scope</i>	<i>% Completed</i>	<i>Analyzed</i>	<i>Scope</i>	<i>% Completed</i>
Hot	H/L U-Bend RPC	07H-B07	1,371	1,371	100.00%	1,375	1,375	100.00%
Cold	C/L U-Bend RPC	07C-B07	1,371	1,371	100.00%	1,375	1,375	100.00%
Hot/Cold	U-Bend 2-Coil Special Interest	Various	3	3	100.00%	6	6	100.00%
Hot	H/L U-Bend MagBias RPC	07H-B07	1	1	100.00%	N/A	N/A	N/A
Cold	C/L U-Bend MagBias RPC	07C-B07	1	1	100.00%	N/A	N/A	N/A
	Total Plan		2,745	2,745	100.00%	2,756	2,756	100.00%

Table 6-3: July 2012 RTS Inspection SG Tube Inspection Summary

SCOPE DESCRIPTION			S/G 2E-088			S/G 2E-089		
<i>Leg</i>	<i>Exam Description</i>	<i>Extents</i>	<i>Analyzed</i>	<i>Scope</i>	<i>% Completed</i>	<i>Analyzed</i>	<i>Scope</i>	<i>% Completed</i>
Hot	H/L U-Bend RPC	07H-B07	N/A	N/A	N/A	104	104	100.00%
Cold	C/L U-Bend RPC	07C-B07	N/A	N/A	N/A	104	104	100.00%
	Total Plan		N/A	N/A	N/A	208	208	100.00%

SONGS 2C17 Steam Generator Condition Monitoring Report

Table 6-4: Wear Indication Summary

Steam Generator SG2E88 (Through-Wall Wear)	Anti-Vibration Bar	Tube Support Plat	Tube-to-Tube Wear	Retainer Bar	Foreign Object	Total Indications	Tubes with Indications (out of 9727 total per SG)
≥ 50%	0	0	0	1	0	1	1
35 - 49%	2	0	0	1	0	3	3
20 - 34%	86	0	0	0	2	88	74
10 - 19%	705	108	0	0	0	813	406
< 10%	964	117	0	0	0	1081	600
TOTAL	1757	225	0	2	2	1986	734*

* This value is the number of tubes with wear indications of any depth and at any location. Since many tubes have indications in more than one depth and location, the total number of tubes is less than the total number of indications.

Steam Generator SG2E89 (Through-Wall Wear)	Anti-Vibration Bar	Tube Support Plat	Tube-to-Tube Wear	Retainer Bar	Foreign Object	Total Indications	Tubes with Indications (out of 9727 total per SG)
≥ 50%	0	0	0	1	0	1	1
35 - 49%	0	0	0	1	0	1	1
20 - 34%	78	1	0	3	0	82	67
10 - 19%	1014	85	2	0	0	1101	496
< 10%	1499	53	0	0	0	1552	768
TOTAL	2591	139	2	5	0	2737	861*

* This value is the number of tubes with wear indications of any depth and at any location. Since many tubes have indications in more than one depth and location, the total number of tubes is less than the total number of indications.

SONGS 2C17 Steam Generator Condition Monitoring Report

Table 6-5: Plugging Summary

Reason for Plugging	Steam Generator		Total*
	2E-088	2E-089	
Retainer Bar Wear	2	4	6
AVB Wear >=35%	2		2
AVB Wear <35% for OA Margin	2		2
Preventative - Retainer Bar **	92	90	182
Total	98	94	192

* The plugging status shown in this table is current for non-TTW degradation. Due to the ongoing SG recovery efforts, the plugging strategy related to tubes with TTW and for preventative plugging for TTW may change prior to startup.

** Although 96 tubes were included in the retainer bar inspection scope (see Table 6-1), only 94 tubes were removed from service due to their proximity to the retainer bars. Two tubes were removed from the list of potentially affected tubes after closer review of the design drawings and consultation with MHI.

Table 6-6: Reported AVB Wear Depths (%TW)

SG	Average	Upper 95 th	Maximum
2E-088	10.1	19.2	35
2E-089	9.8	18.0	29
Both SGs	9.9	19.0	35

Table 6-7: Reported TSP Wear Depths (%TW)

SG	Average	Upper 95 th	Maximum
2E-088	9.7	14.0	17
2E-089	10.7	16.0	20
Both SGs	10.1	15.0	20

SONGS 2C17 Steam Generator Condition Monitoring Report

Table 6-8: Retainer Bar Wear

SG	Row	Col	Location	Sizing ETSS	Circ Extent (in)	Axial Extent (in)	Structural Depth (%TW)	Structural Length (in)
2E-088	124	48	B03+0.57"	27903.1	0.35	0.31	43.4	0.27
2E-088	125	49	B03+0.46"	27903.1	0.30	0.28	52.4	0.22
2E-089	118	44	B11-0.50"	27903.1	0.16	0.26	26.5	0.21
2E-089	119	133	B02+0.54"	27903.1	0.46	0.43	83.8	0.29
2E-089	120	132	B10-0.50"	27903.1	0.16	0.23	25.3	0.18
2E-089	120	132	B11-0.42"	27903.1	0.21	0.35	27.0	0.30
2E-089	127	127	B03+0.50"	27903.1	0.31	0.45	34.7	0.30

Table 6-9: Foreign Object Wear

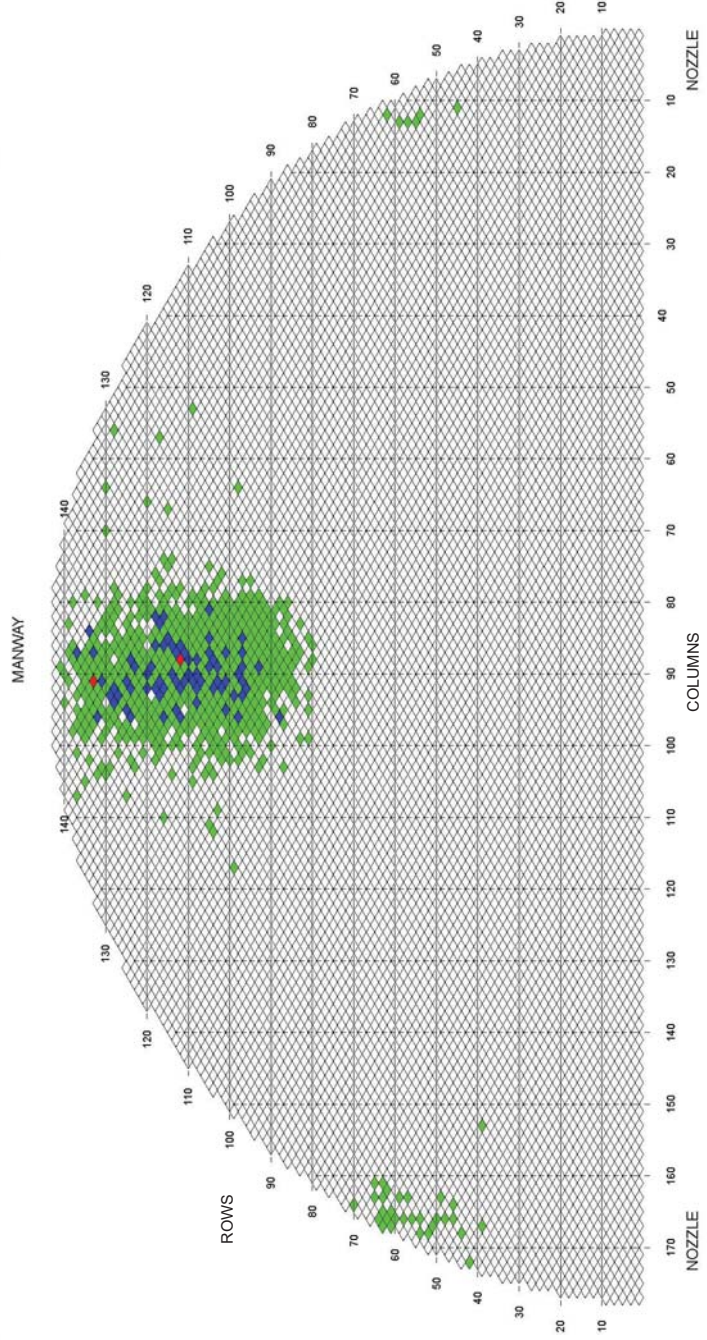
SG	Row	Col	Location	Sizing ETSS	Circ Extent (in)	Axial Extent (in)	Structural Depth (%TW)	Structural Length (in)
2E-088	136	76	04H+0.56"	27901.1	0.31	0.25	25.7	0.21
2E-088	137	77	04H+0.76"	27901.1	0.31	0.20	30.2	0.15

Table 6-10: Tube-to-Tube Wear

SG	Row	Col	Location	Length (in.)	Structural Depth (%TW)	Structural Length (in)
2E-089	111	81	B09 +1.63 to +7.95	6.32	14.0	2.28
2E-089	113	81	B09 +2.03 to +8.22	6.19	13.7	1.67

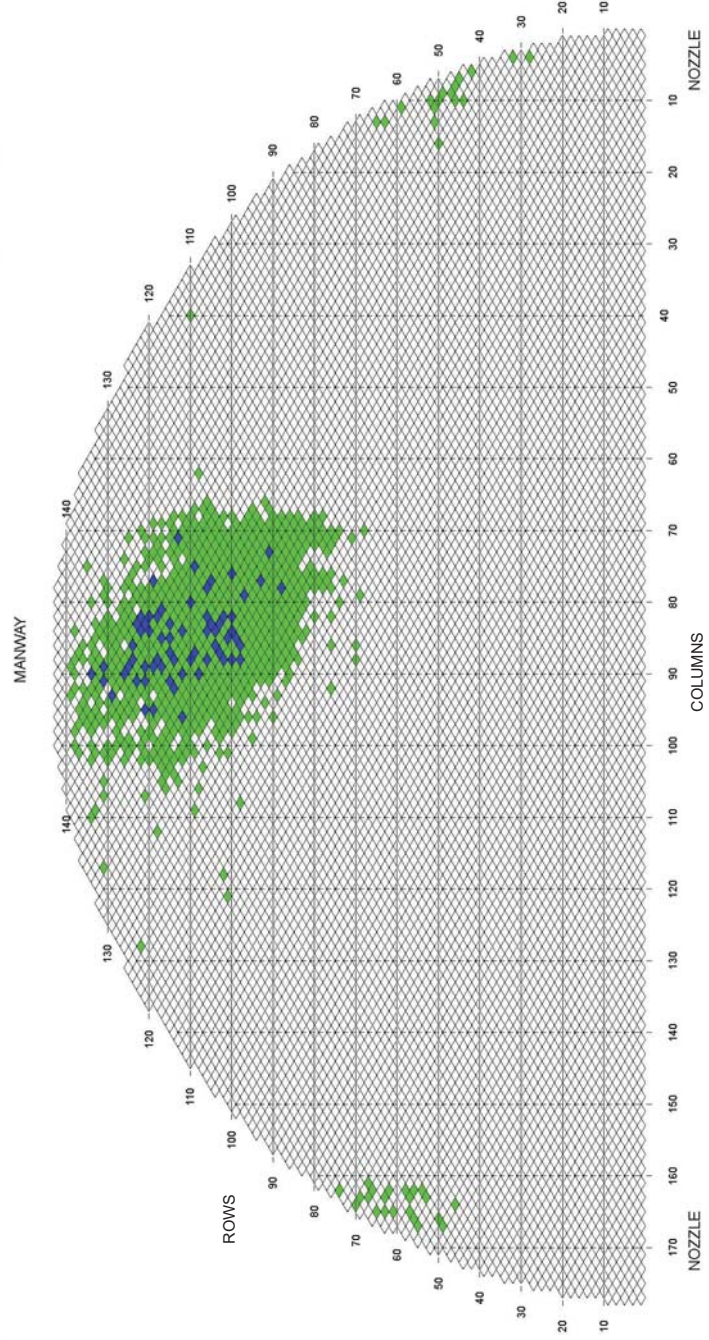
SONGS 2C17 Steam Generator Condition Monitoring Report

Figure 6-1: SG 2E-088 AVB Wear



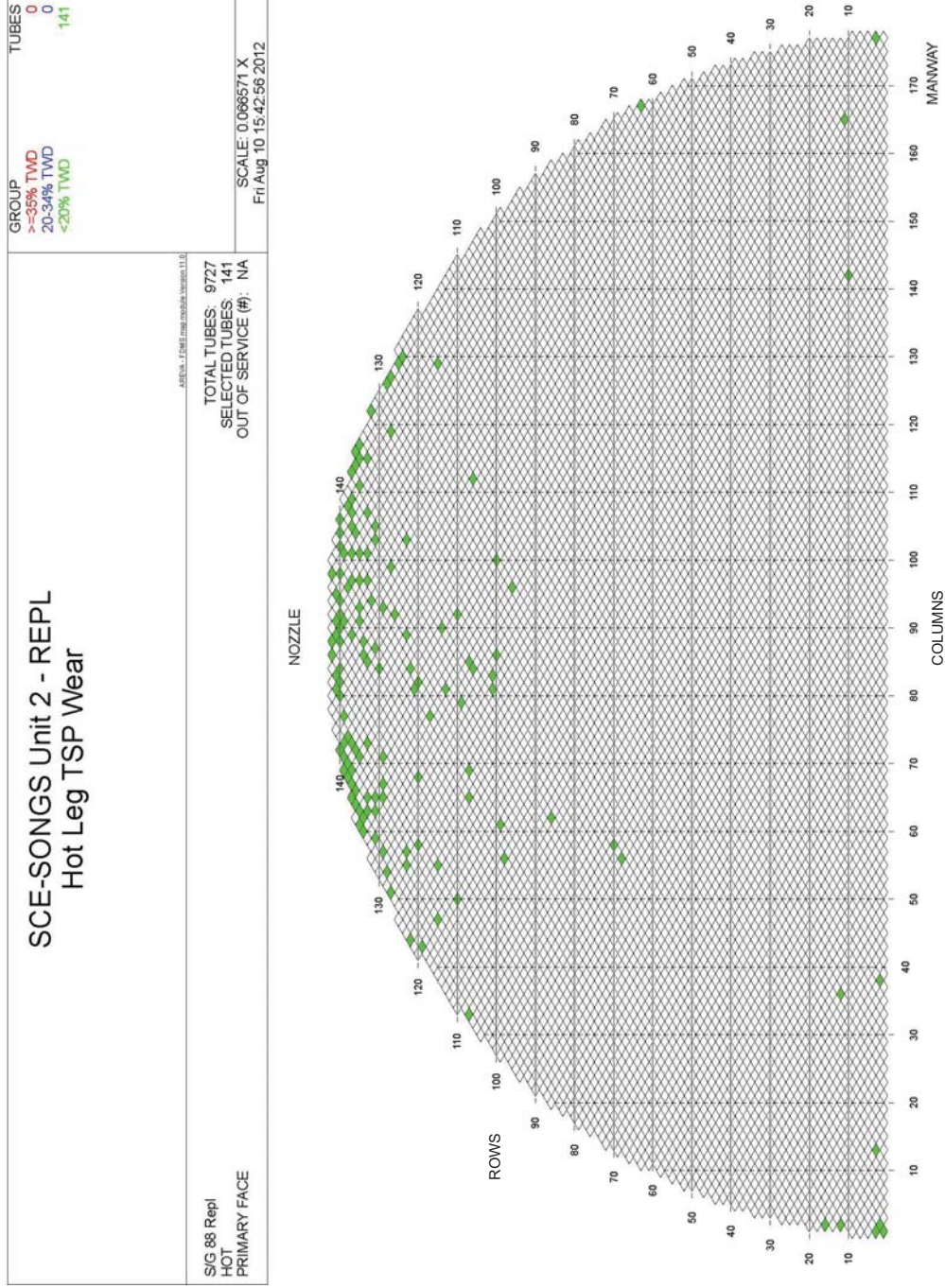
SONGS 2C17 Steam Generator Condition Monitoring Report

Figure 6-2: SG 2E-089 AVB Wear



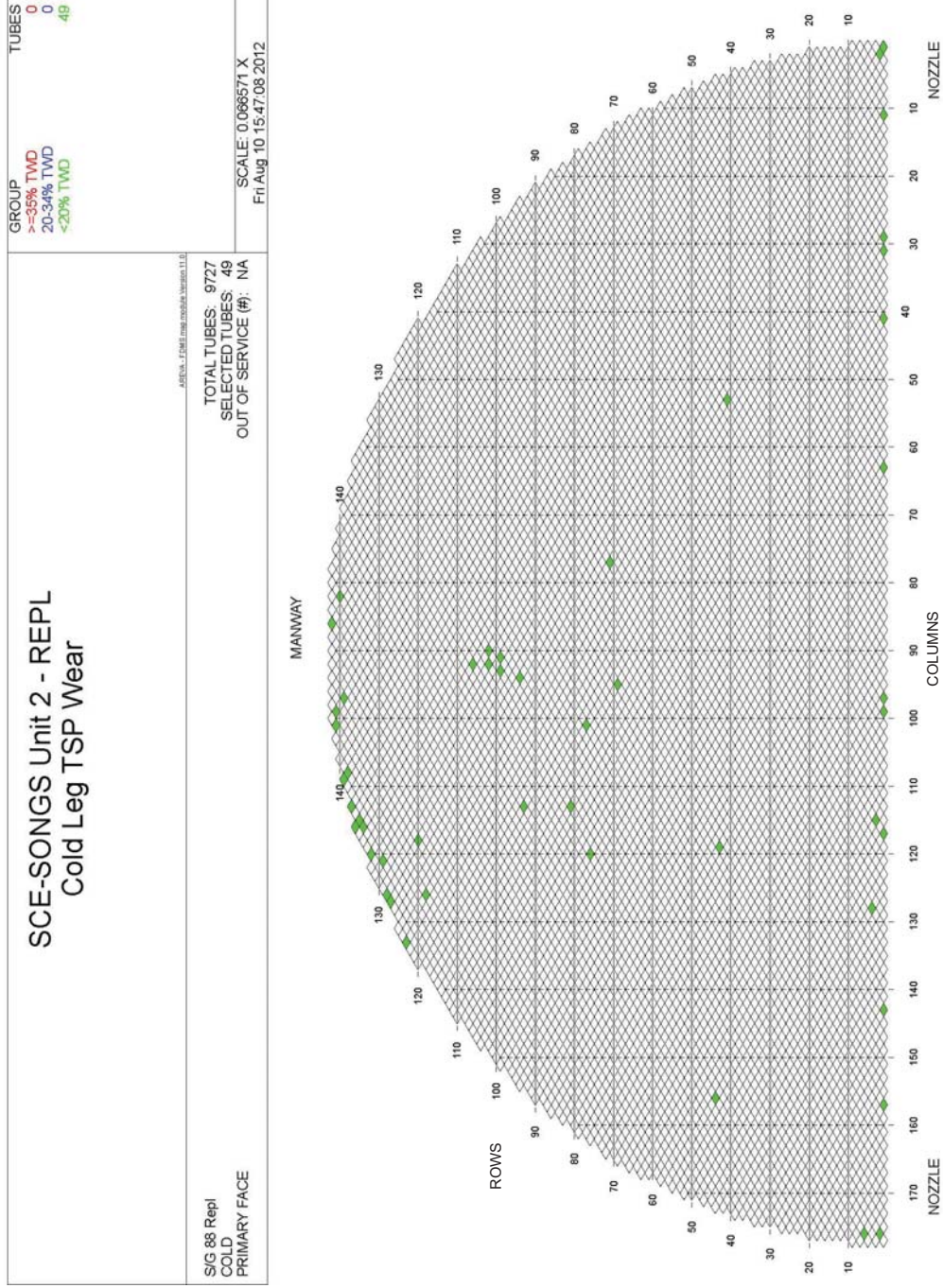
SONGS 2C17 Steam Generator Condition Monitoring Report

Figure 6-3: SG 2E-088 TSP Wear – Hot Leg



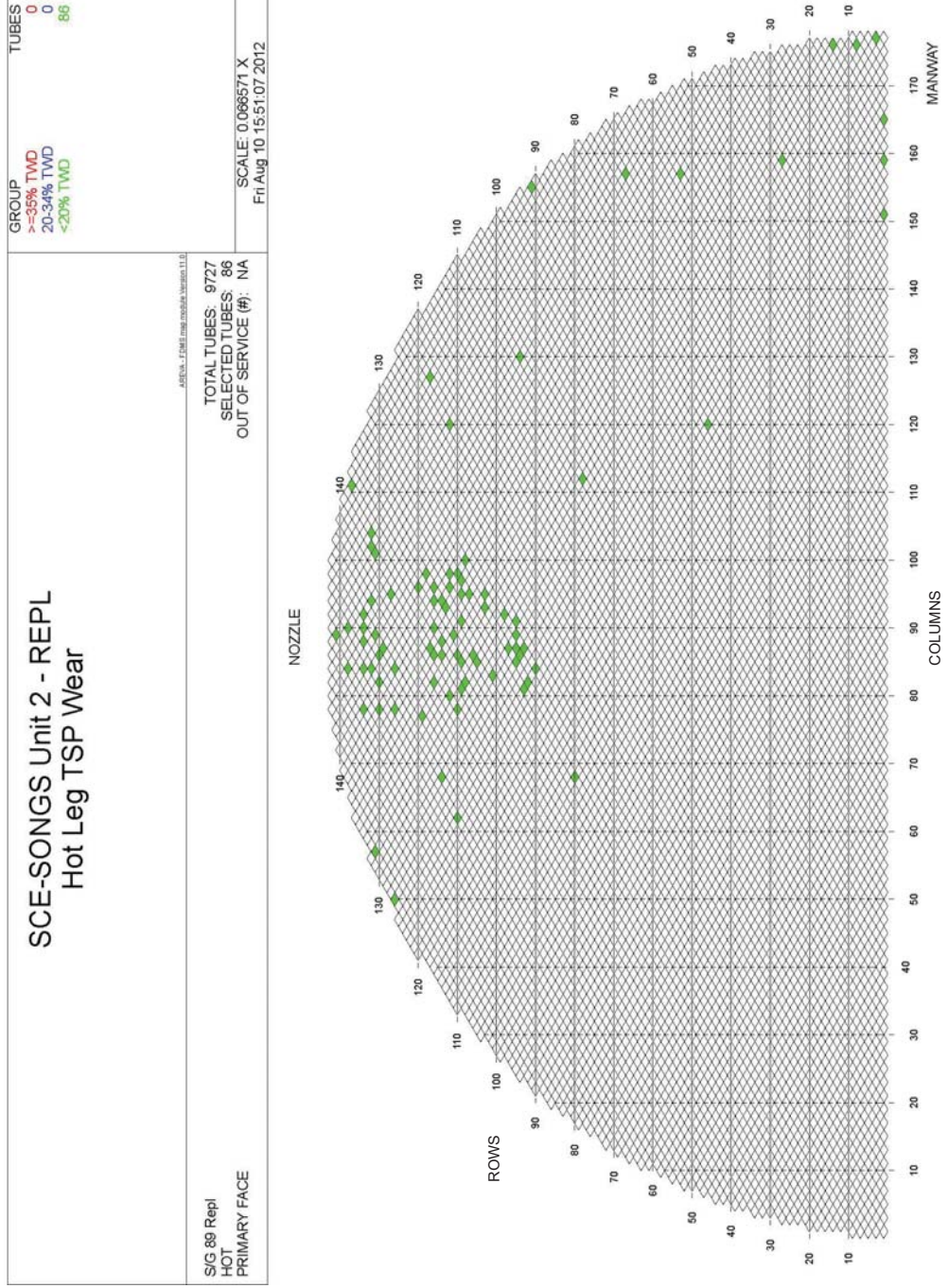
SONGS 2C17 Steam Generator Condition Monitoring Report

Figure 6-4: SG 2E-088 TSP Wear – Cold Leg



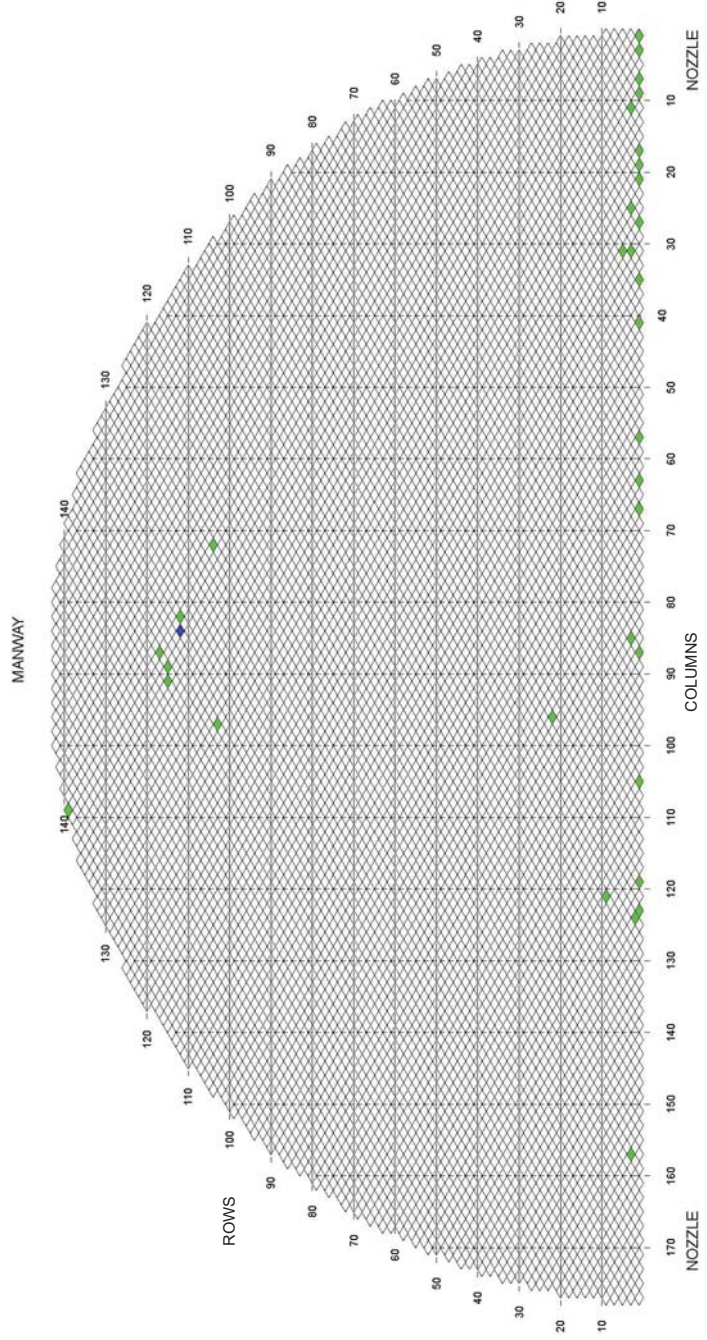
SONGS 2C17 Steam Generator Condition Monitoring Report

Figure 6-5: SG 2E-089 TSP Wear – Hot Leg



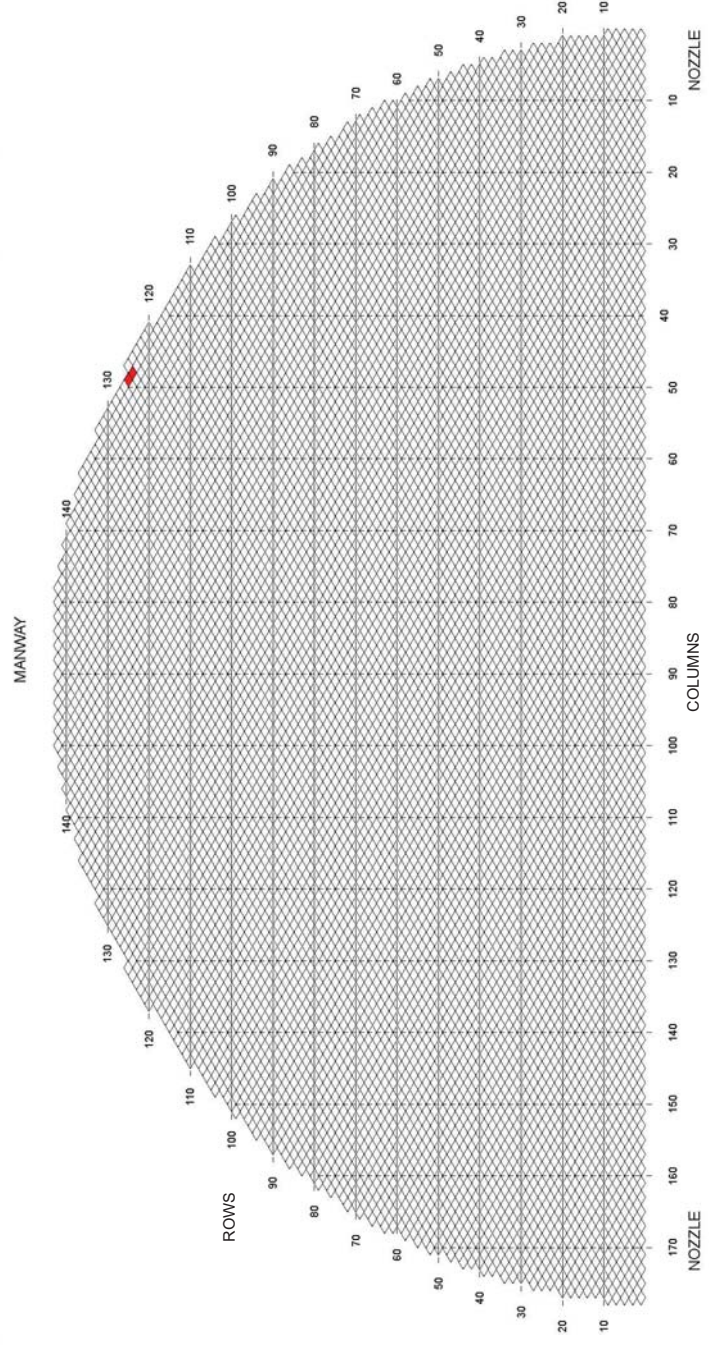
SONGS 2C17 Steam Generator Condition Monitoring Report

Figure 6-6: SG 2E-089 TSP Wear – Cold Leg



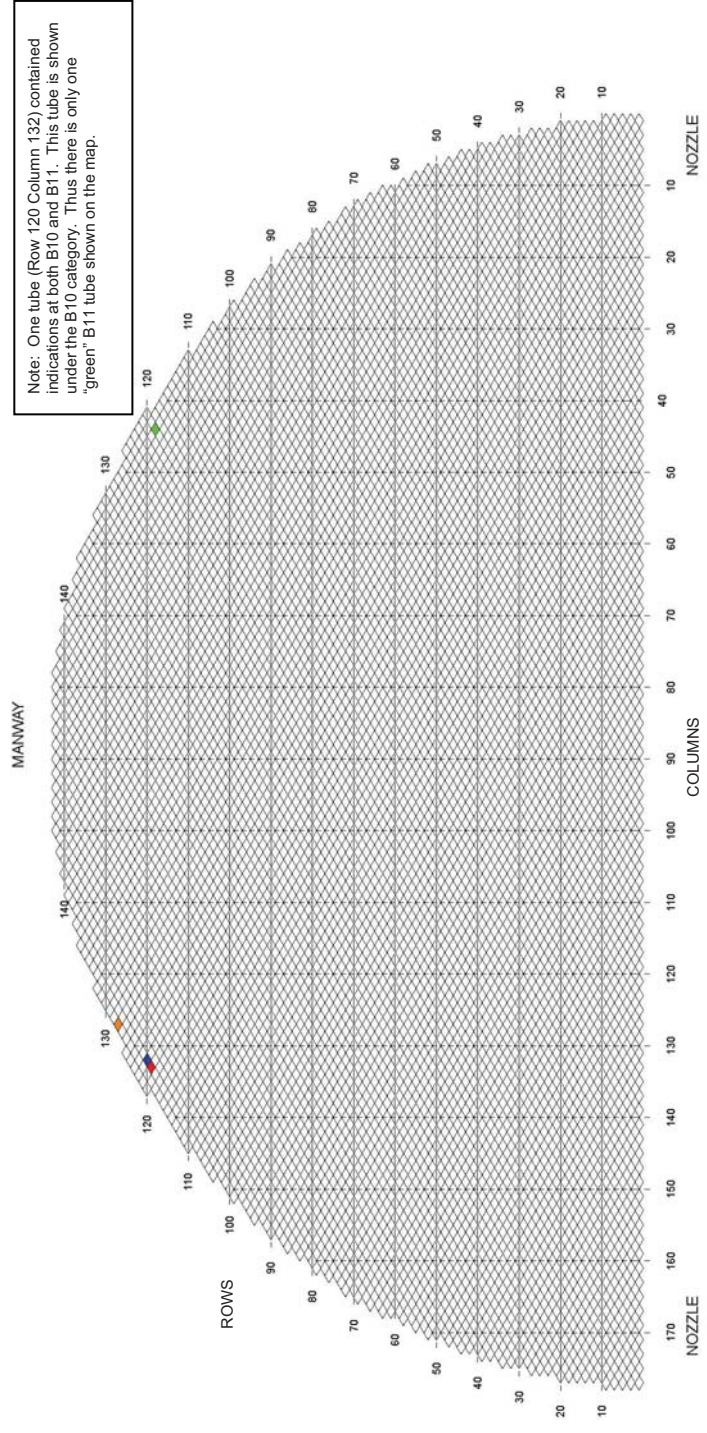
SONGS 2C17 Steam Generator Condition Monitoring Report

Figure 6-7: SG 2E-088 Retainer Bar Wear



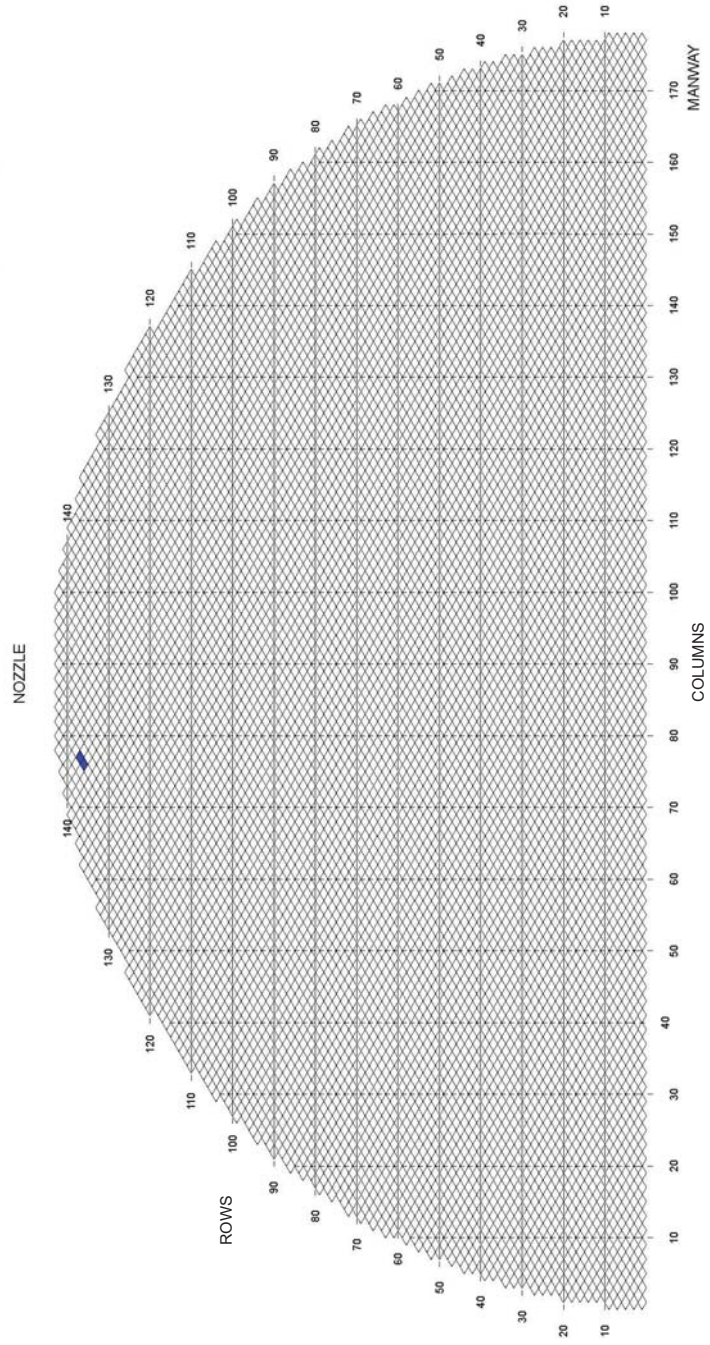
SONGS 2C17 Steam Generator Condition Monitoring Report

Figure 6-8: SG 2E-089 Retainer Bar Wear



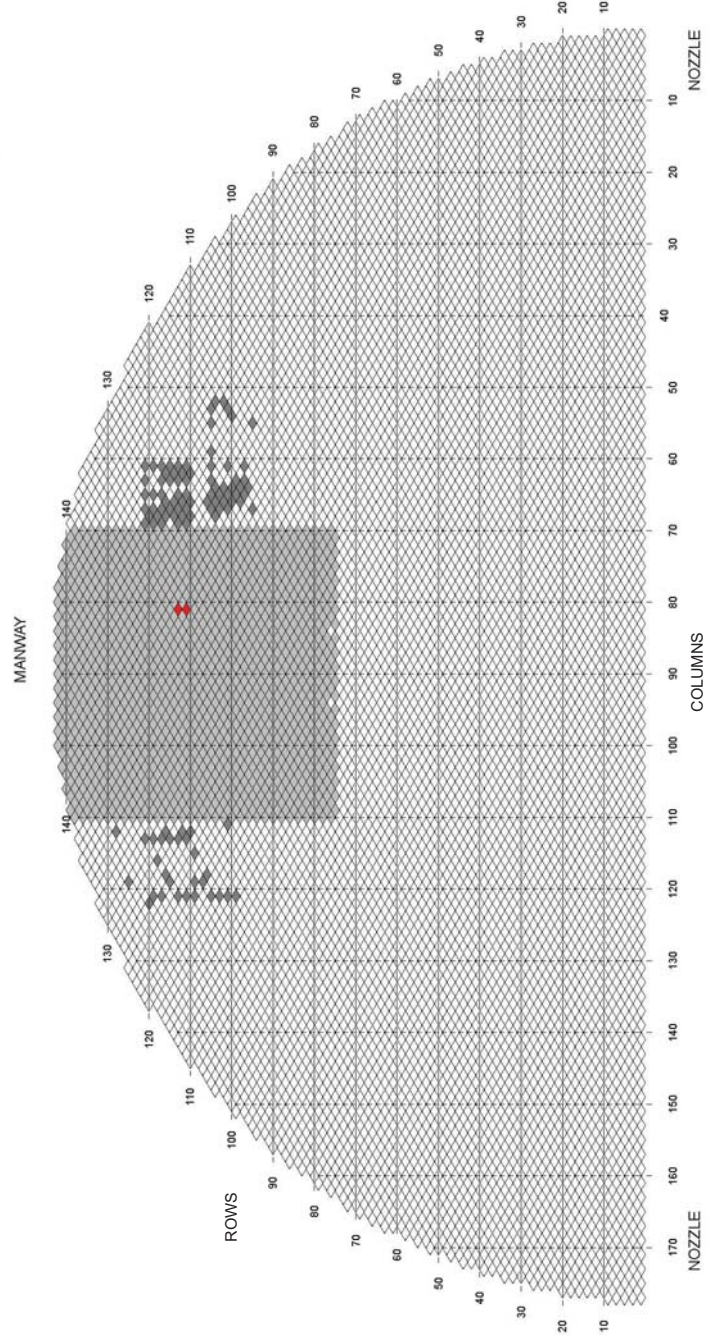
SONGS 2C17 Steam Generator Condition Monitoring Report

Figure 6-9: SG 2E-088 Foreign Object Wear



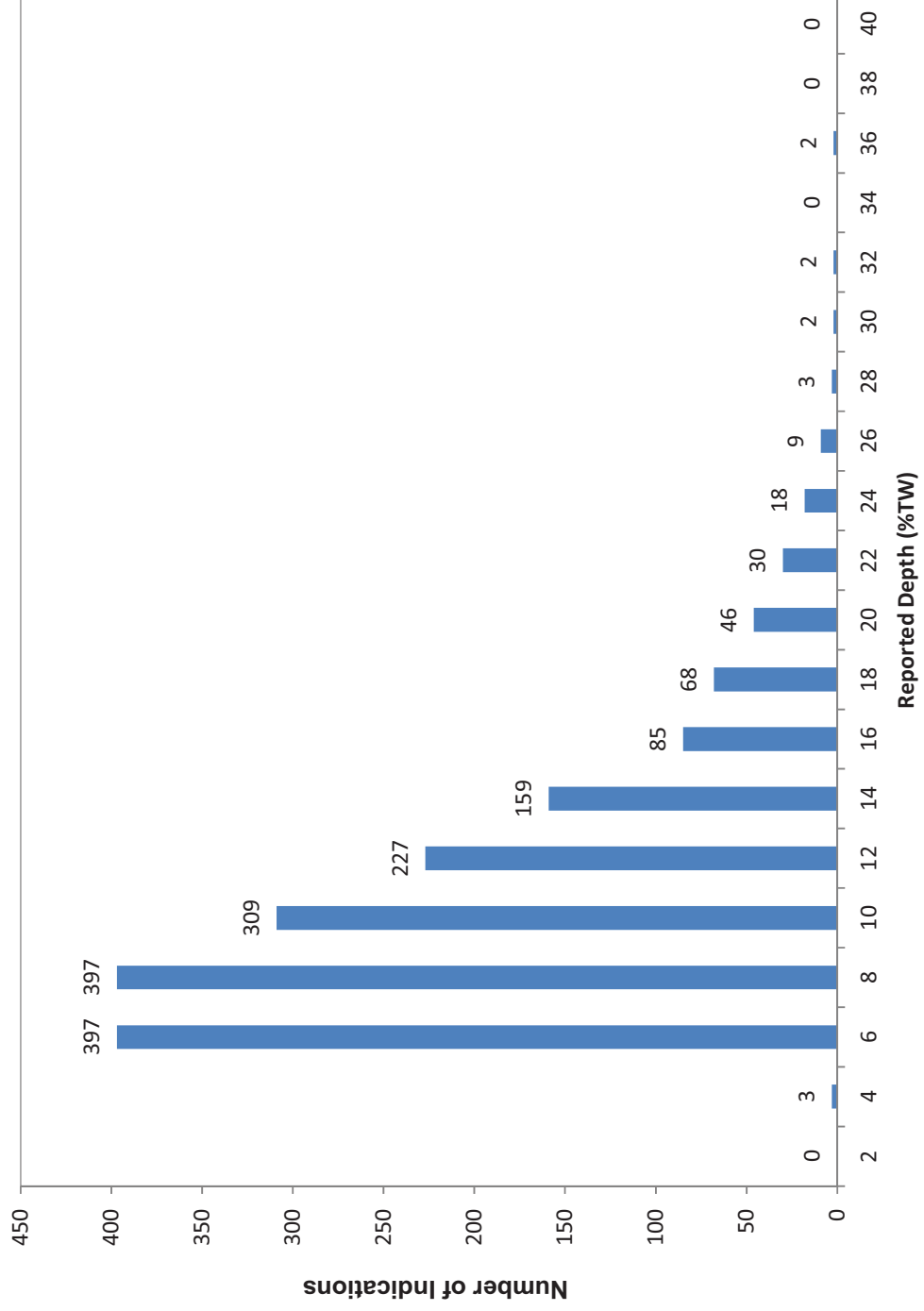
SONGS 2C17 Steam Generator Condition Monitoring Report

Figure 6-10: Tube-to-Tube Wear (Detected in SG 2E-089 Only)



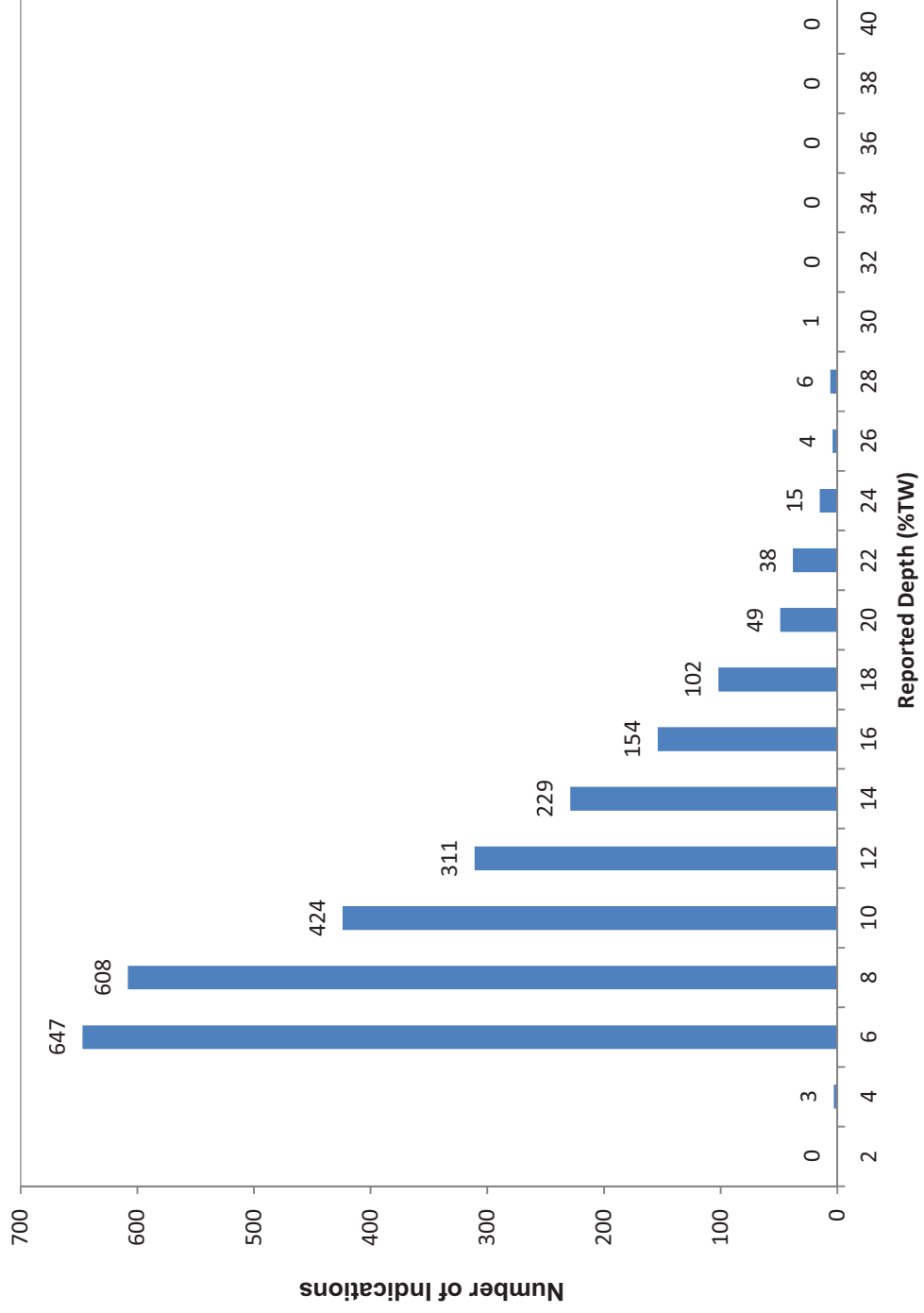
SONGS 2C17 Steam Generator Condition Monitoring Report

Figure 6-11: SG 2E-088 AVB Wear Depth Distribution



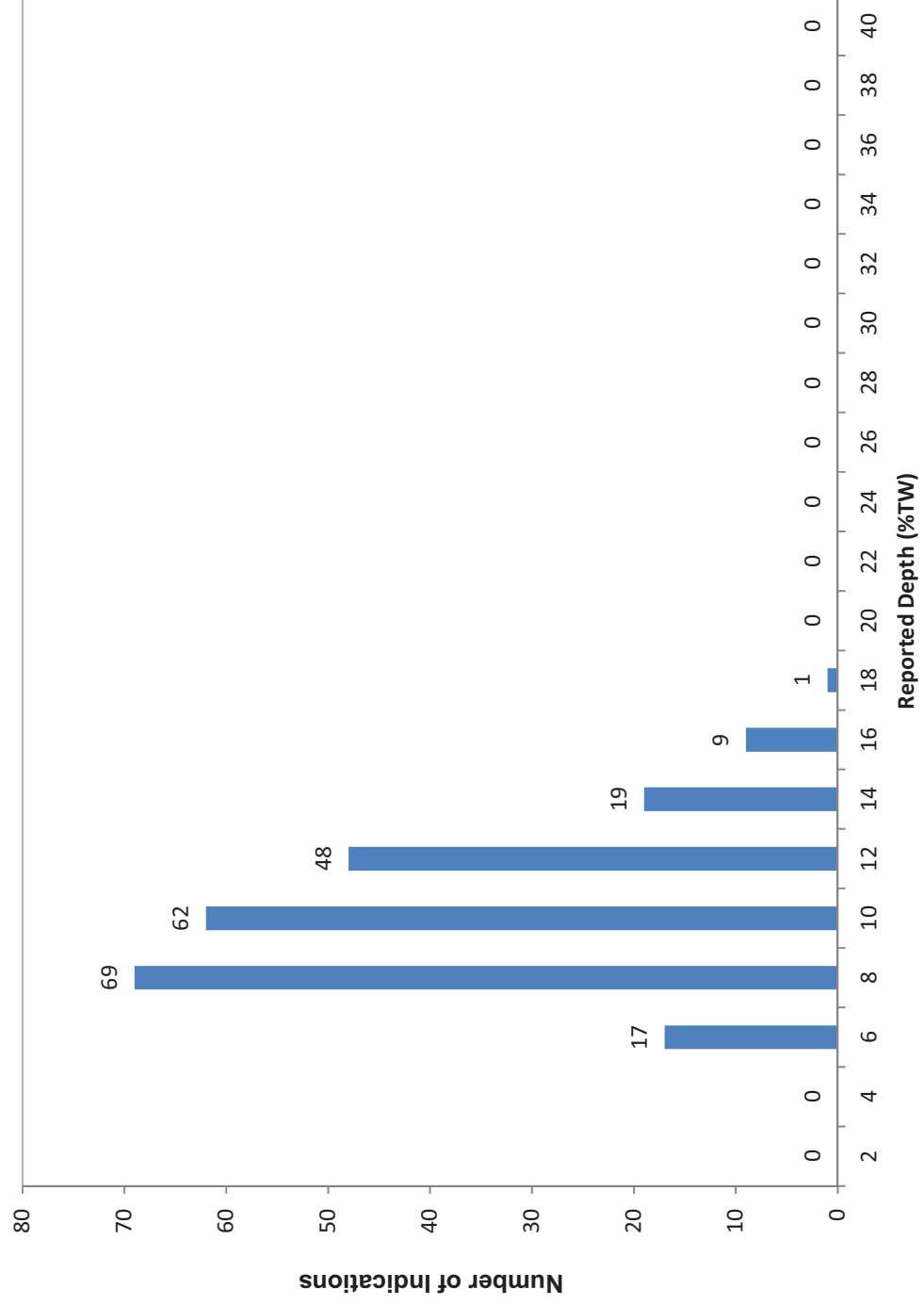
SONGS 2C17 Steam Generator Condition Monitoring Report

Figure 6-12: SG 2E-089 AVB Wear Depth Distribution



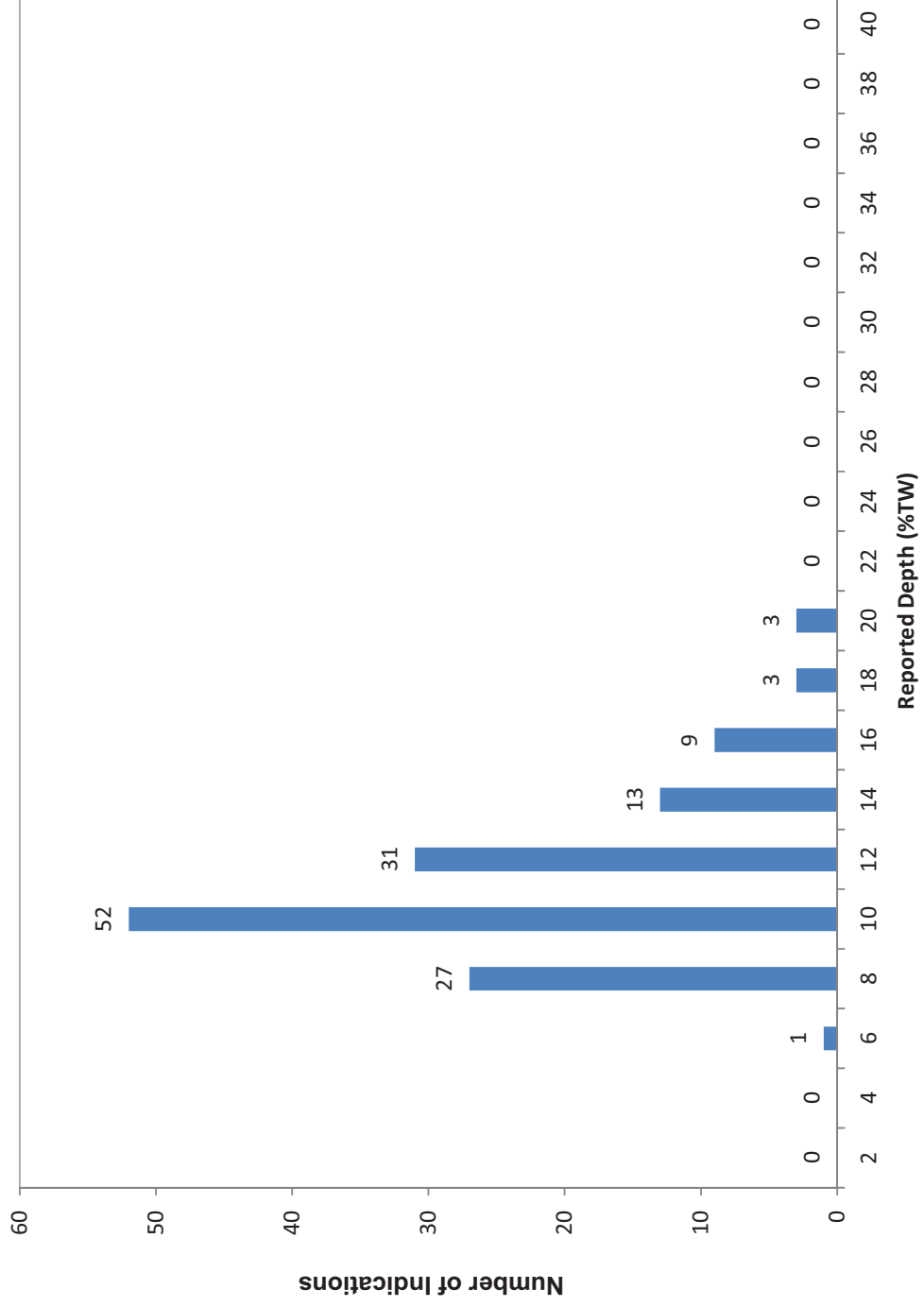
SONGS 2C17 Steam Generator Condition Monitoring Report

Figure 6-13: SG 2E-088 TSP Wear Depth Distribution



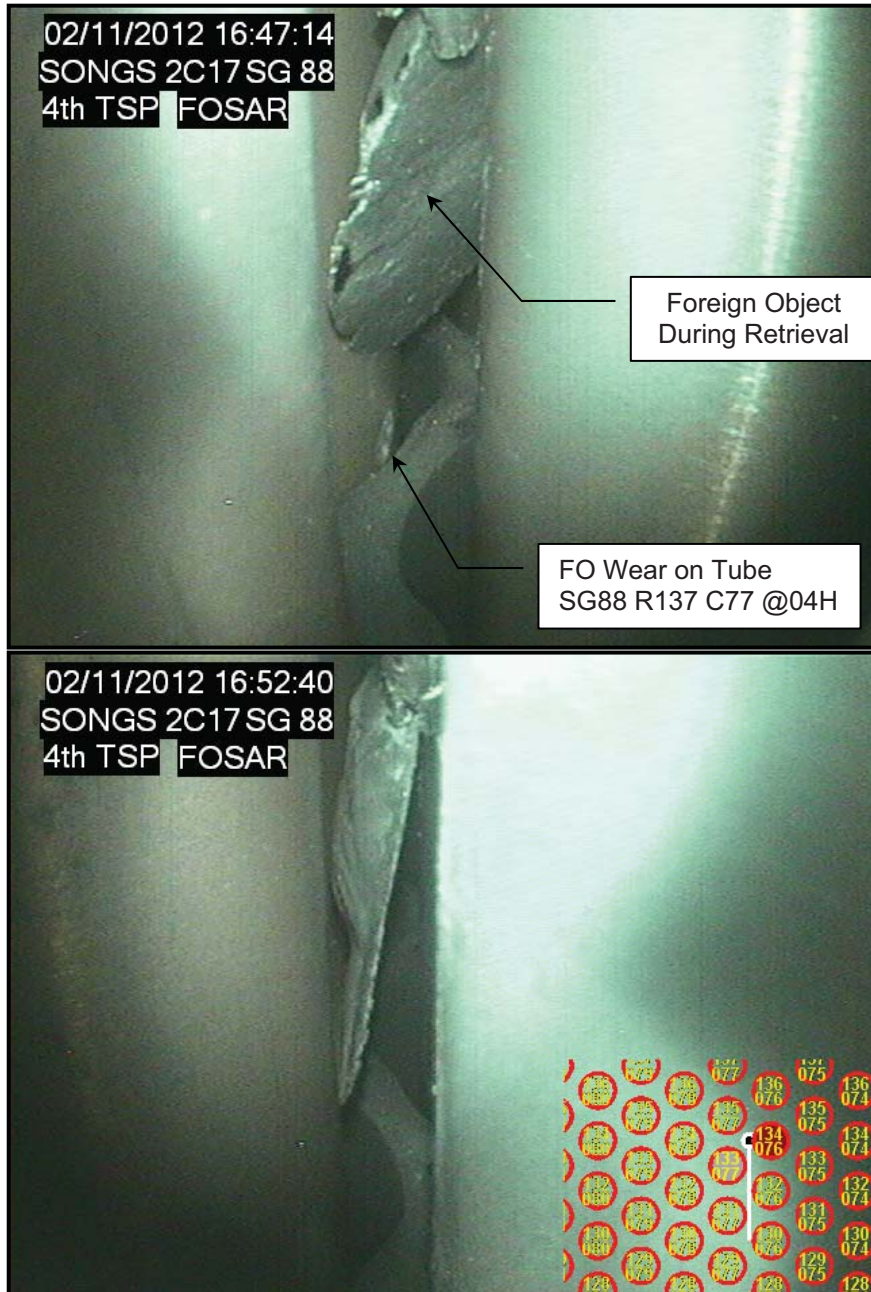
SONGS 2C17 Steam Generator Condition Monitoring Report

Figure 6-14: SG 2E-089 TSP Wear Depth Distribution



SONGS 2C17 Steam Generator Condition Monitoring Report

Figure 6-15: Foreign Object Retrieved from SG 2E-088



SONGS 2C17 Steam Generator Condition Monitoring Report

7.0 CONDITION MONITORING ASSESSMENT

In order to satisfy Condition Monitoring requirements, all degradation mechanisms detected during the 2C17 outage must meet the structural and leakage performance criteria described in Section 5.0. Satisfaction of the CM criteria can be demonstrated either analytically or through in situ pressure testing. Structural and accident-induced leakage integrity are evaluated analytically based on the degradation mechanism's characteristics, including circumferential extent, axial length, and through-wall depth. Operational leakage integrity is monitored via leakage detection systems and procedures during plant operation.

Consistent with the structural integrity criteria described in Section 5.0, the limiting pressure loading occurs at a value of three times the normal operating differential pressure. For SONGS-2 this value is 4290 psi [6]. In addition to pressure loads, the CM must also consider the impact of non-pressure accident loads if they could have a significant effect on the burst pressure of the degraded tubes. A review of the screening guidance of Section 3.7.2 of Reference 2 provides the basis for concluding that non-pressure accident loads are not limiting for the identified tube wear in SONGS-2 SG tubes. Reference 2 indicates that the burst pressure of flat bar wear in U-bend flanks of re-circulating SG tubes (i.e., AVB wear), wear less than 270° in circumferential extent at supports below the top TSP, and degradation with circumferential involvement less than 25 PDA (Percent Degraded Area) anywhere in the tube bundle; will not be significantly affected by non-pressure loads. The accident-induced leakage performance criteria must also be assessed, and in addition to the SLB pressure (2560 psi [6]), must also consider non-pressure loads where appropriate. This is discussed in more detail within this section.

In order for a degraded tube to be returned to service, the degradation must be measured using a qualified ECT sizing technique, and the degradation must be evaluated as acceptable for continued operation. The sizing techniques qualified for use at SONGS-2 are identified in the Degradation Assessment [6] and are detailed in the ECT technique site validation documents [7] and [15]. If a degradation mechanism cannot be sized with appropriate sizing confidence, it is plugged on detection. All degradation identified during the current outage was measured with a qualified ECT technique.

This was the first inservice inspection of the SONGS Unit 2 SG tubes; performed after one cycle of operation following SG replacement. The potential for mechanical wear to develop at various locations within the SGs was recognized prior to the examination, but the identification of significant wear at retainer bars was not specifically anticipated. Although the examination program as planned was well capable of detecting this mechanism, the Degradation Assessment [6] was revised during the outage to include this new mechanism. The identification of tube-to-tube wear was not anticipated and not detected in the initial inspection scope. After the identification of tube-to-tube wear in Unit 3, additional inspections were performed, wherein two tubes in SG 2E-089 with tube-to-tube wear were identified.

7.1 Input Parameters

Table 7-1 and Table 7-2 identify the input parameters used to perform the Condition Monitoring assessment. In particular, these inputs were used within the AREVA Mathcad tool which implements the SG Flaw Handbook equations [10], in order to generate the limit curves discussed in Section 7.2. The flaw model for axial thinning with limited circumferential extent was used for the analyses (Section 5.3.3 of Reference 4). The 4290 psi $3\Delta P$ value is based on a conservative assessment of Unit 2 secondary side steam pressure as measured during cycle 16.

SONGS 2C17 Steam Generator Condition Monitoring Report

Table 7-1: SONGS-2 Steam Generator Input Values

<i>Parameter</i>	<i>Value</i>
Desired probability of meeting burst pressure limit	0.95
Tubing wall thickness	0.043 inch, [7]
Tubing outer diameter	0.750 inch, [7]
Mean of the sum of yield and ultimate strengths at temperature	116000 psi, [11]
Standard deviation of the sum of yield and ultimate strengths	2360 psi, [11]
3 X Normal Operating Pressure Differential (3 NOPD)	4290 psid, [6]
EFPD from SG Replacement through 2C17	627.11, [10]

Table 7-2: Eddy Current ETSS Input Values (Reference 5)

<i>Parameter</i>	<i>ETSS 96004.1</i>	<i>ETSS 27903.1</i>	<i>ETSS 27902.2</i>	<i>ETSS 96910.1</i>	<i>ETSS 27901.1</i>
Probe Type	Bobbin Coil	+Point™	+Point™	+Point™	+Point™
NDE depth sizing regression parameters	Slope = 0.98 Intercept = 2.89 %TW	Slope = 0.97 Intercept = 2.80 %TW	Slope = 1.02 Intercept = 0.94 %TW	Slope = 1.01 Intercept = 4.30 %TW	Slope = 1.05 Intercept = -1.97 %TW
NDE depth sizing technique uncertainty (standard deviation)	4.19 %TW	2.11 %TW	2.87 %TW	6.68 %TW	2.30 %TW
NDE depth sizing analysis uncertainty (standard deviation)	2.10 %TW	1.06 %TW	1.44 %TW	3.34 %TW	1.15 %TW
Total NDE (Sizing and Technique) (standard deviation)*	4.69 %TW	2.36 %TW	3.22 %TW	7.48 %TW	2.60 %TW

* Total uncertainty is the technique and analysis uncertainties combined via the square root of the sum of the squares.

SONGS 2C17 Steam Generator Condition Monitoring Report

7.2 Evaluation of Structural Integrity

7.2.1 AVB wear and TSP wear

AVB wear and TSP wear were evaluated with the flaw model described in Reference 4 as “axial part-throughwall degradation < 135° in circumferential extent.” The maximum circumferential extent of a single 100%TW wear scar formed by a long flat bar positioned tangentially to the tube surface (e.g., an AVB) is 55.4°. For double-sided AVB wear the total circumferential extent for this limiting case would be well below the 135° limit established by this model; hence, this flaw model is appropriate for AVB wear. For double-sided AVB wear and double- or triple-sided TSP wear this model also remains bounding because the AVB and TSP geometries provide sufficient circumferential separation between the wear scars to permit each indication to be treated separately. The separation between centerline contact points for AVB wear and TSP wear is 180° and 120°, respectively, and results in negligible circumferential interaction between separate wear locations in the same axial plane of the tube.

The topic of external loads must be addressed. The maximum reported AVB wear depth (35 %TW), adjusted upward to conservatively account for sizing uncertainty (ETSS 96004.1), is 45%TW. If it assumed that this flaw is double-sided; and it is further conservatively assumed that the total circumferential extent is 111° (see above), the resulting Percent Degraded Area (PDA) would be 14. Similarly, the maximum reported TSP wear depth (20%TW) adjusted to account for NDE uncertainty is 30%TW. If it assumed that this wear depth occurs at all three TSP land contacts, each with the limiting circumferential extent of 55.4°, the resulting PDA would be 14. Because the circumferential involvement of these flaws is less than 25 PDA, external loads need not be considered in the evaluation of burst integrity.

The bobbin probe was used to measure the depth of AVB wear and TSP wear through the application of ETSS 96004.1. CM limit curves for AVB wear and TSP wear based upon ETSS 96004.1 and the parameters provided in Table 7-1 and Table 7-2, are provided in Figure 7-1 and Figure 7-2, respectively. These figures also include the throughwall depth of each indication reported, plotted at the assumed axial flaw length. The assumed flaw length for AVB wear indications was derived from the flaw profiles (using line-by-line sizing). Twenty-two AVB wear indications were profiled with emphasis placed on the deeper indications for profiling. Of the AVB wear scars profiled (using line by line sizing) the maximum structural length was determined to be slightly less than 0.6 inches. A bounding length of 0.7 inches was chosen for the AVB wear as shown on Figure 7-1. This is slightly longer than the 0.59 inch width of the AVBs.

The TSP wear flaws are plotted at a length of 1.4 inches, slightly longer than the thickness of the TSPs (1.38 inches). Since all AVB wear and TSP wear flaws lie below their respective CM limit curves, it is concluded that the structural integrity performance criterion was satisfied with respect to these degradation mechanisms during the operating period preceding the 2C17 outage.

7.2.2 Retainer Bar Wear

Retainer bar wear was also evaluated with the “axial part-throughwall degradation < 135° in circumferential extent” degradation model as described in Reference 4. The maximum measured circumferential extent of RB wear was 0.46 inches (Table 6-8) which corresponds with an angular extent at the mid tube wall of 75°; well within the 135° requirement for this flaw model. Because of the rather short axial extent of the RB wear indications, it is prudent to also consider the potential for rupture in the circumferential direction. For the indication with the largest circumferential extent (0.46

SONGS 2C17 Steam Generator Condition Monitoring Report

inch, SG 2E-089 R119 C133 B02), and a limiting assumption that the wear is 100%TW over the entire circumferential extent, the PDA is found to be 21 PDA (i.e., $(0.46)/(\pi(\text{mid-wall diameter}))$). This limiting flaw was evaluated with the degradation model for circumferential cracking under pressure loading as described in Reference 2. Based on this model the lower bound burst pressure in the circumferential direction was determined to be 6470 psi; much less limiting than the results from the axial part-throughwall model (discussed below). This provides the basis for concluding that the axial part-throughwall degradation model is appropriate for the evaluation of RB wear.

External loads which are assumed to exist concurrently with the SLB accident do not significantly affect burst pressure in tubes with flaws located in the U-bend region on the tube flanks ($\pm 45^\circ$) [2]. +Point™ probe examinations were performed with another eddy current probe placed in an adjacent tube in order to estimate the position of the limiting flaw (SG 2E-089 R119 C133 B02) relative to the tube flank. This testing showed that the flaw lies approximately 40 to 50 degrees from the flank position; consequently, the RB wear may not lie entirely within the flank region. However, it is also known that external loads do not significantly affect burst pressure in tubes with flaws whose circumferential involvement is less than 25 PDA [2]. The upper bound circumferential involvement of the limiting RB wear flaw is only 21 PDA. It is therefore concluded that the limiting Condition Monitoring structural criteria is 3x normal operating pressure differential, rather than 1.2x the combined loading of SLB pressure and external loads. In short, it is appropriate to consider pressure loading-only for the structural integrity evaluation of RB wear flaws.

The axial depth profile of each RB wear flaw was measured using ETSS 27903.1, and this data was used to determine the structurally significant dimensions of the flaws using the methods described in Section 5.1.5 of Reference 4. The results are provided in Table 6-8 and are plotted on the CM curve provided in Figure 7-3. Since the RB wear in tube SG 2E-089 R119 C133 B02 lies above the CM curve in Figure 7-3, it could not be demonstrated on the basis of NDE measurements and analytical evaluation that this tube met the structural integrity performance criteria. Consequently, this tube was subjected to in situ pressure testing. All other RB wear indications lie below the CM curve and, hence, are shown to meet the structural integrity performance criteria analytically.

In situ accident leakage and structural proof testing was performed on tube SG 2E-089 R119 C133 B02 in accordance with the guidance provided in Reference 3. The normal operating, accident level, and proof test hold pressures were adjusted to account for temperature effects on material strength, and other factors related to the test process. All testing was accomplished using full tube pressurization. The tube was held pressurized at the required hold times without any difficulties. No leakage or rupture occurred at any time during the test, thereby successfully demonstrating that the tube met the SONGS accident leakage performance criteria and structural integrity performance criteria during the operating period preceding the 2C17 outage. This result also demonstrates the generous level of conservatism inherent in the flaw sizing and analytical methods used to evaluate SONGS SG tube volumetric degradation. The in situ test results are documented in Reference 12.

7.2.3 Foreign Object Wear

Foreign object wear was evaluated with the “axial part-throughwall degradation $< 135^\circ$ in circumferential extent” flaw model as described in Reference 4. The measured circumferential extent of both reported FO wear flaws was 0.31 inches or 50° , which is well within the 135° constraint of this model. Although these flaws are short axially, the circumferential involvement is only 14 PDA. Thus these tubes would not preferentially burst in the circumferential mode prior to axial burst, and the use of the axial part-throughwall flaw model remains appropriate (see Section 7.2.2). In addition, because these flaws are located well below the top TSP (i.e., they are at the 4th TSP), and because the

SONGS 2C17 Steam Generator Condition Monitoring Report

circumferential involvement is less than 25 PDA, external loads need not be considered in the evaluation of burst integrity.

The +Point™ probe was used to measure the axial depth profile of the flaws through the application of ETSS 27901.1. This data was used to determine the structurally significant dimensions of the flaws (Table 6-9) by applying the methods described in Section 5.1.5 of Reference 4. The applicable CM limit curve, based upon ETSS 27901.1 and the parameters provided in Table 7-1 and Table 7-2, is shown in Figure 7-4 along with the structurally equivalent dimensions of each FO wear flaw. Since both flaws lie well below the CM limit curve, it is concluded that the structural integrity performance criteria was satisfied with respect to foreign object wear during the operating period preceding the 2C17 outage.

7.2.4 Tube-to-Tube Wear

Tube-to-tube wear (TTW) was evaluated with the flaw model described in Reference 4 as “axial part-throughwall degradation < 135° in circumferential extent.” The circumferential extent of a TTW flaw is limited by the geometry of the interacting tubes such that it can be modeled as a single 100%TW wear scar formed by a flat bar positioned tangentially to the tube surface. In this configuration the maximum circumferential extent of the degradation will be 55.4°. For double-sided TTW this model is bounding because the wear geometry provides sufficient circumferential separation between the wear scars to permit each indication to be treated separately. The separation between centerline contact points for double-sided TTW is 180°, and results in negligible circumferential interaction between separate wear locations in the same axial plane of the tube. With respect to external loads, each wear flaw at the same axial location may be treated individually. An individual TTW flaw with a depth of 100%TW and a circumferential extent of 55.4° would be less than 16 PDA. Because the circumferential involvement of this limiting flaw is less than 25 PDA, external loads need not be considered in the evaluation of burst integrity for TTW.

The +Point™ probe was used to estimate the depth and the overall length of TTW through the application of ETSS 27902.2. The flaws had estimated maximum depths of 15% and 14%TW. The maximum indicated length of TTW was 6.32 inches. These lengths and depths are well below the CM limit curve for TTW using ETSS 27902.2 (see Figure 6-6). Despite the fact that both of these flaws clearly meet the structural integrity criterion based on the maximum measured lengths and depths, both flaws were line-by-line sized to obtain structural depths and lengths as well as to obtain information on the shapes of the flaws. Figure 6-6 depicts the structurally-equivalent dimensions of both flaws relative to the CM limit curve.

Based on the shallow depths of the TTW flaws detected, in situ pressure testing of these flaws was not required nor was it performed.

7.3 Evaluation of Accident-induced Leakage Integrity

7.3.1 AVB wear and TSP wear

Volumetric degradation that is predominantly axial in orientation and is greater than 0.25 inch long will leak and burst at essentially the same pressure [2]. The SONGS-2 AVB wear and TSP wear flaws meet this description. The evaluation in Section 7.2.1 demonstrated that the AVB wear and TSP wear identified during the 2C17 outage satisfied the burst integrity criteria at a pressure of 4290 psi. Consequently, the leakage integrity of AVB wear and TSP wear at the much lower SLB pressure differential of 2560 psi is also demonstrated by that evaluation. All of the tubes with AVB wear and TSP wear flaws satisfied the SONGS accident-induced leakage performance criteria during the operating period prior to the 2C17 outage.

7.3.2 Retainer Bar Wear

The accident-induced leakage integrity of tubes with RB wear is bounded by tube SG 2E-089 R119 C133 which had the largest measured RB wear flaw identified during the 2C17 outage. The leakage integrity of this tube was confirmed by in situ pressure testing, during which the tube did not leak or rupture at any pressure level. Based upon the in situ test results it is concluded that all of the tubes with RB wear flaws satisfied the SONGS accident-induced leakage performance criteria during the operating period prior to the 2C17 outage. The in situ test is discussed in more detail in Section 7.2.2 and in Reference 12.

7.3.3 Foreign Object Wear

Since the axial length of the FO wear flaws is less than 0.25 inch it is theoretically possible that pop-through and leakage could occur prior to tube rupture. Per Reference 2, a conservative evaluation of this potential may be performed through the use of the Reference 4 flaw model for uniform depth, 360° volumetric degradation. The limit curve of Figure 7-5 identifies the throughwall limit for uniform 360° thinning at 2560 psi. As with a CM limit, this curve includes the effects of relational, material strength, and NDE sizing uncertainties. The relational uncertainty is the uncertainty between the actual burst pressure and the calculated burst pressure based on known structural lengths and depths. The reported maximum depth and overall axial length for the two FO wear flaws are also shown in Figure 7-5. Because both flaws lie well below the curve it is concluded that the foreign object wear identified did not violate the accident-induced leakage performance criteria during the operating period prior to the 2C17 outage.

7.3.4 Tube-to-Tube Wear

Volumetric degradation that is predominantly axial in orientation and is greater than 0.25 inch long will leak and burst at essentially the same pressure [2]. The tube-to-tube wear flaws meet this description. The evaluation in Section 7.2.4 demonstrated that the tube-to-tube wear identified during the 2C17 outage satisfied the burst integrity criteria at a differential pressure of 4290 psi. Consequently, the leakage integrity of tube-to-tube wear at the much lower SLB pressure differential of 2560 psi is also demonstrated by that evaluation. All of the tubes with tube-to-tube wear flaws satisfied the SONGS accident-induced leakage performance criteria during the operating period prior to the 2C17 outage.

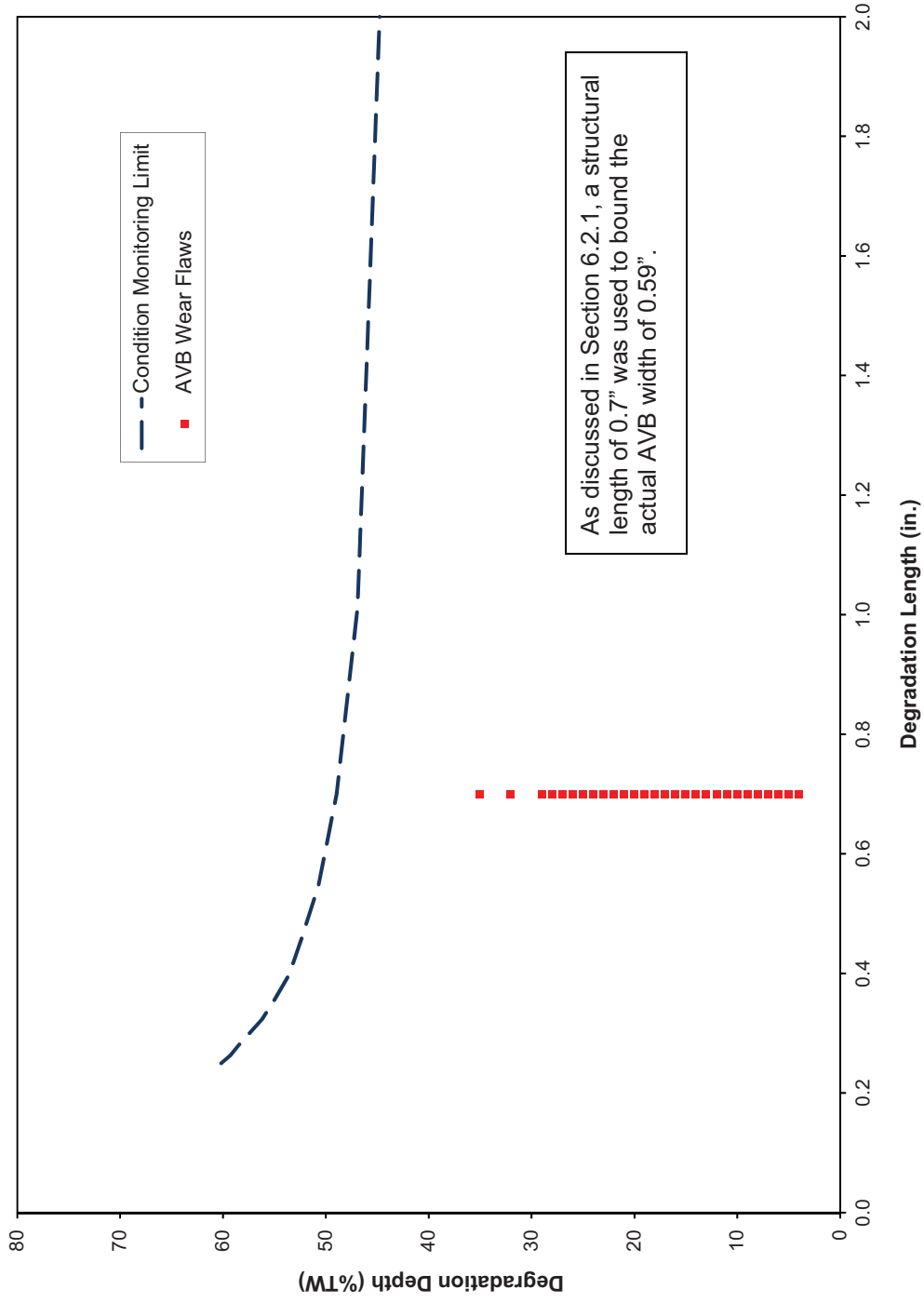
SONGS 2C17 Steam Generator Condition Monitoring Report

7.4 Evaluation of Operational Leakage Integrity

Throughout the operating period preceding the 2C17 outage, SONGS Unit 2 experienced no measurable primary to secondary leakage. Therefore, the operational leakage performance criterion was satisfied during this period.

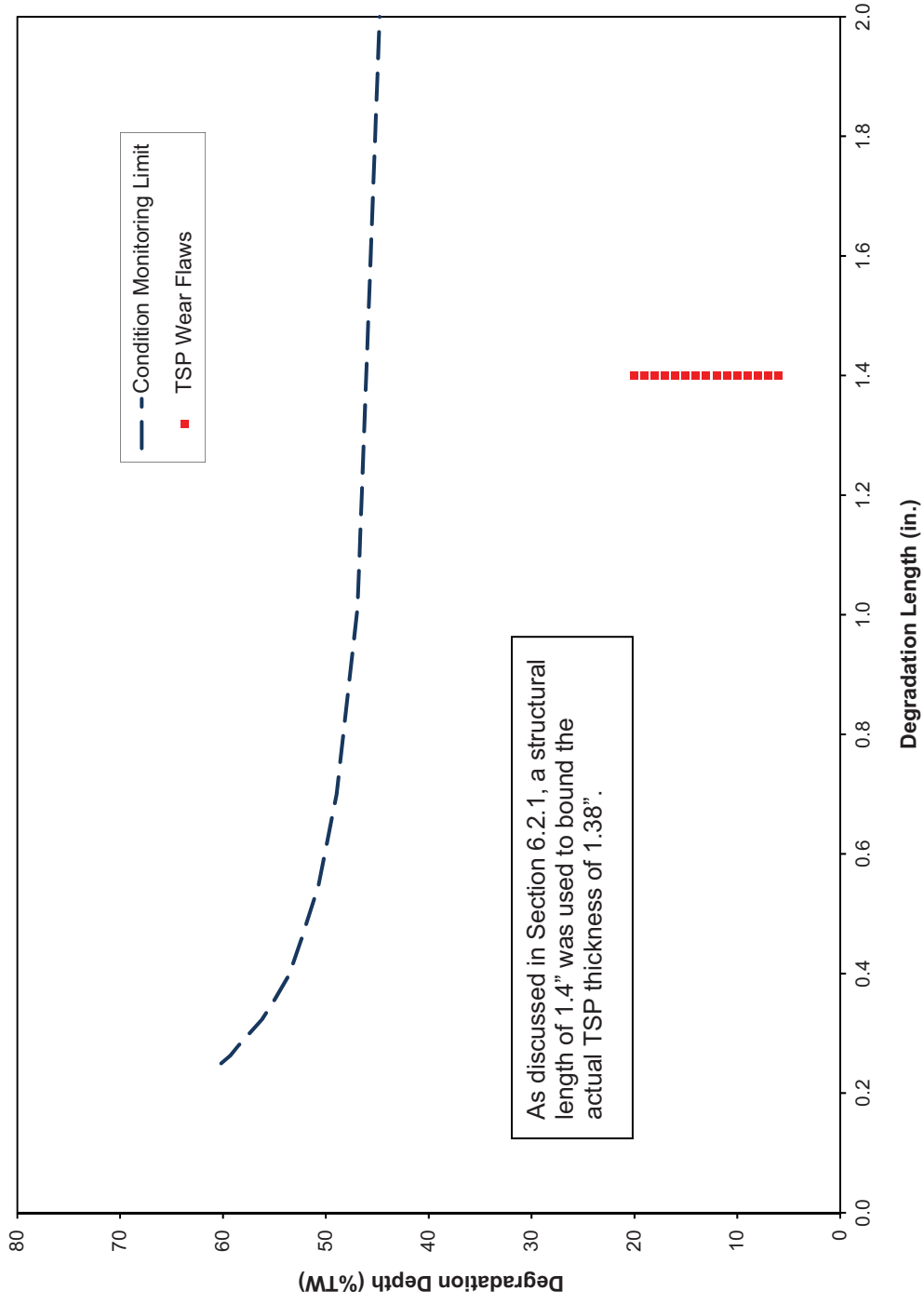
SONGS 2C17 Steam Generator Condition Monitoring Report

Figure 7-1: CM Limit for AVB Wear, ETSS 96004.1



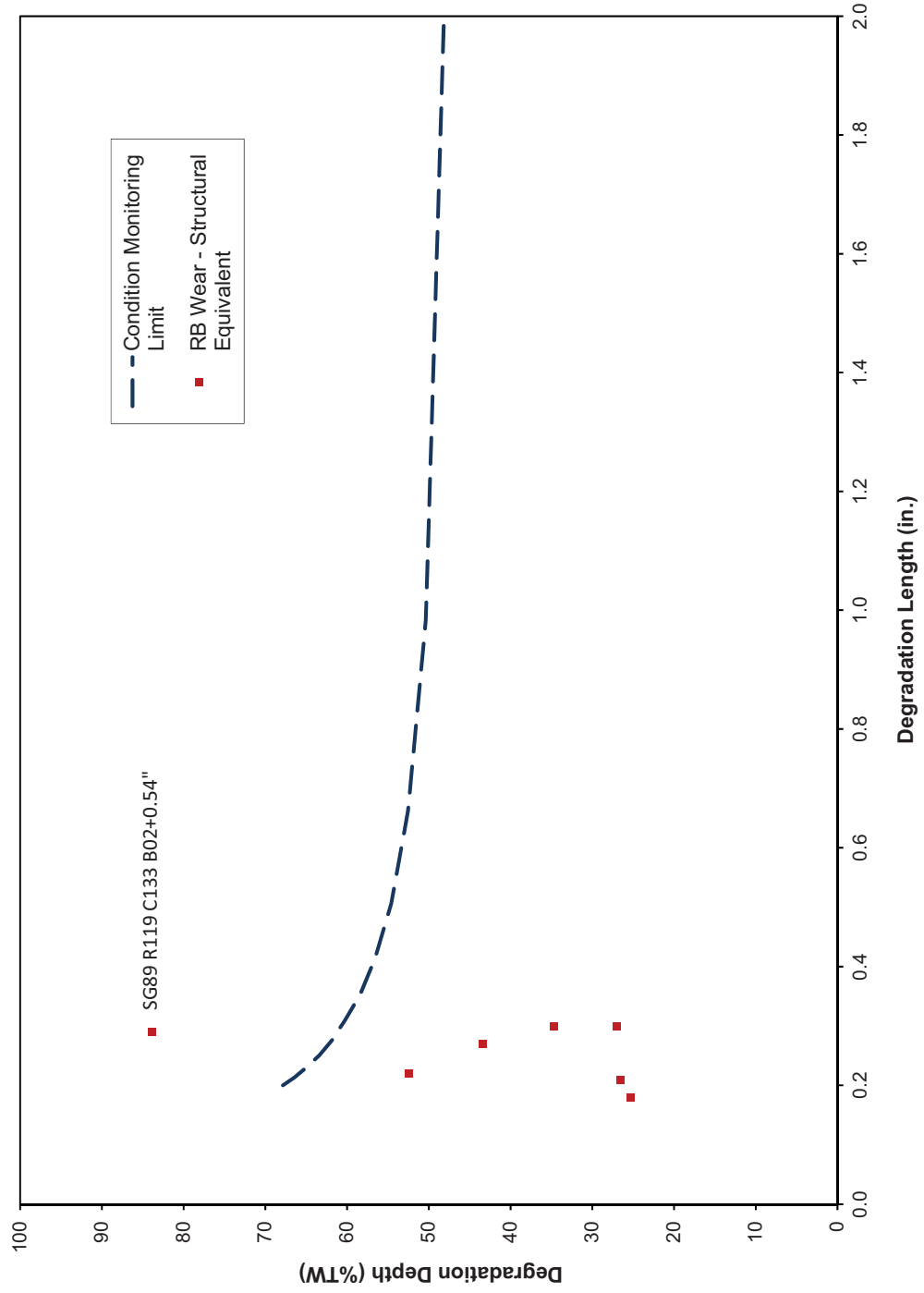
SONGS 2C17 Steam Generator Condition Monitoring Report

Figure 7-2: CM Limit for TSP Wear, ETSS 96004.1



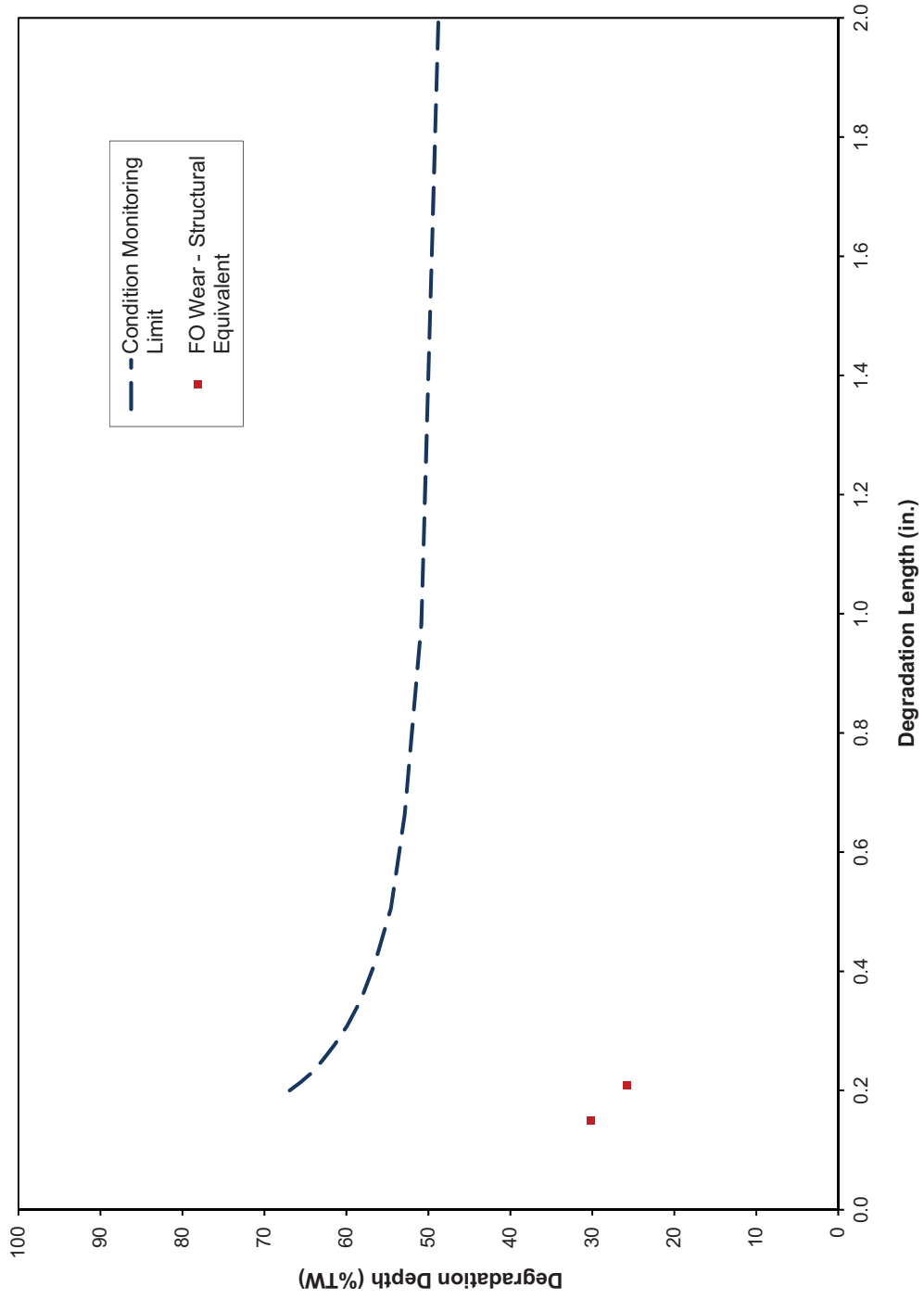
SONGS 2C17 Steam Generator Condition Monitoring Report

Figure 7-3: CM Limit for RB Wear, ETSS 27903.1



SONGS 2C17 Steam Generator Condition Monitoring Report

Figure 7-4: CM Limit for FO Wear, ETSS 27901.1



SONGS 2C17 Steam Generator Condition Monitoring Report

Figure 7-5: Foreign Object Pop-Through at 2560 psi, Uniform 360° Thinning, ETSS 27901.1

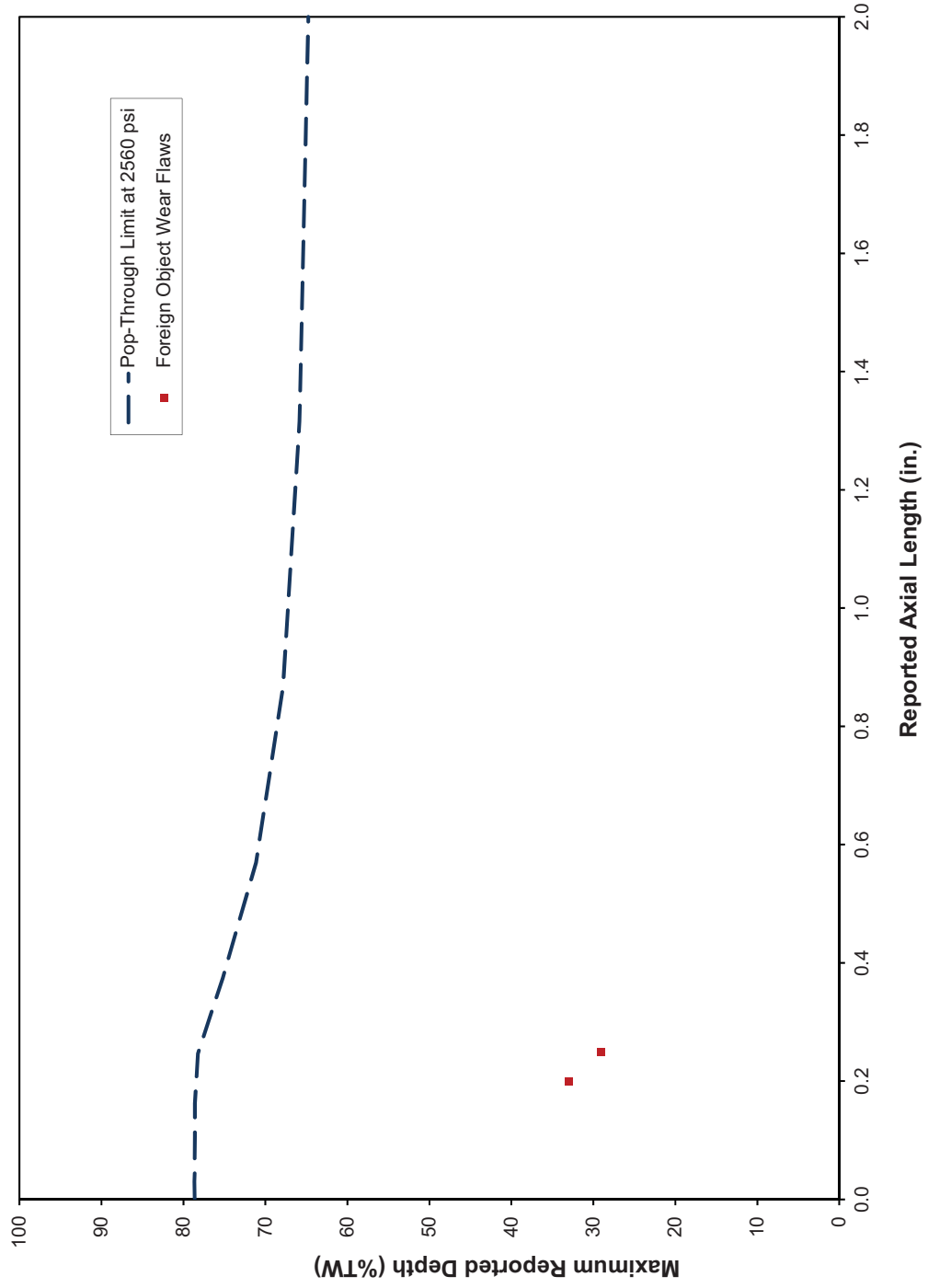
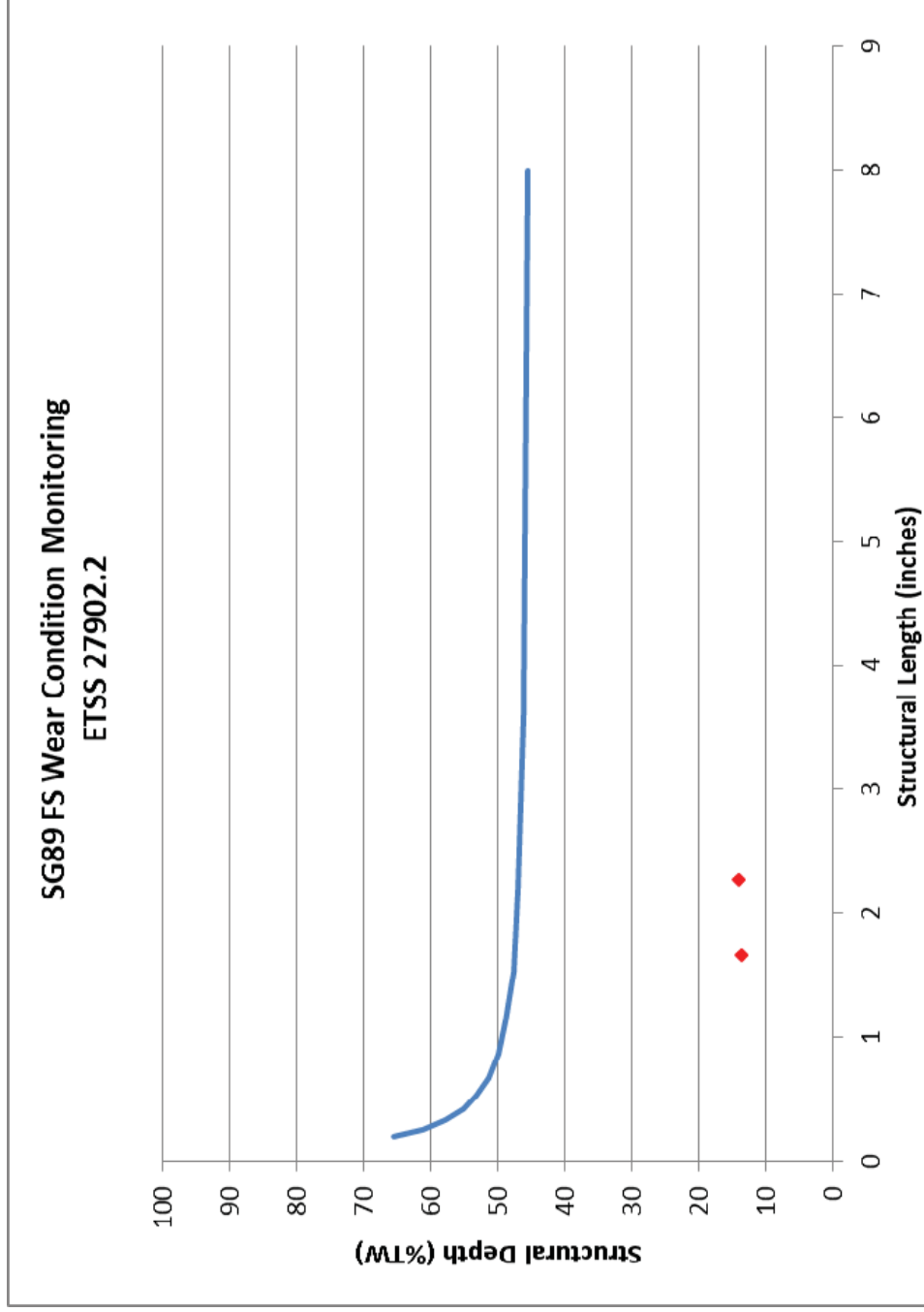


Figure 7-6: CM Limit for Tube-to-Tube Wear, ETSS 27902.2



SONGS 2C17 Steam Generator Condition Monitoring Report

8.0 CONDITION MONITORING CONCLUSION

This Condition Monitoring assessment has evaluated all SG tube degradation detected during the 2C17 outage against the three SONGS technical specification performance criteria. Through a combination of eddy current inspection, analytical evaluation, in situ pressure testing, and operational leakage monitoring it has been determined that the three performance criteria: 1) structural integrity, 2) accident-induced leakage integrity, and 3) operational leakage integrity; were satisfied during the operating period prior to the 2C17 outage.

SONGS 2C17 Steam Generator Condition Monitoring Report

9.0 REFERENCES

1. NEI 97-06, "SG Program Guidelines," Rev. 3, January 2011.
2. EPRI Report 1019038, "SG Integrity Assessment Guidelines: Revision 3", November 2009.
3. EPRI Report 1014983, "Steam Generator In situ Pressure Test Guidelines, Revision 3", August 2007.
4. EPRI Report 1019037 "Steam Generator Degradation Specific Management Flaw Handbook, Revision 1", December 2009.
5. EPRI, SG Management Project, "sgmp.epri.com."
6. AREVA Document 51-9176667-001, "SONGS 2C17 & 3C17 Steam Generator Degradation Assessment"
7. AREVA Document 51-9104383-002, "SONGS Units 2 & 3 Replacement Steam Generators Eddy Current Technique Validation"
8. AREVA Document 03-9170186-003, "Secondary Side Visual Inspection Plan and Procedure for SONGS 2C17" (SONGS Procedure Number SO23-XXVII-25.36)
9. AREVA Document 32-5033045-002, "Mathcad Implementation of SG Flaw Handbook Equations for Integrity Assessment"
10. *Matheny, Southern California Edison, "Numerical Values for the SG DA, SONGS Unit 2, Southern California Edison," January 18, 2012
11. *SONGS Unit 2 Replacement Steam Generator Receipt Inspection QA Document Review Package, (statistics evaluated in Excel file "CMTR Final with Stats.xlsx")
12. AREVA Document 51-9177395-000, "In-Situ Pressure Test Summary for SONGS Unit 2 (Feb 2012)"
13. *SONGS Nuclear Notification 201854749, Created February 13, 2012
14. AREVA Document 51-9177491-001, "SONGS 2C17 Steam Generator Condition Monitoring and Preliminary Operational Assessment"
15. AREVA Document 51-9177744-000, "Site Validation of EPRI Sizing ETSS for Tube-Tube Wear in SONGS Steam Generators"
16. AREVA Document 51-9179946-001, "Comparison of Bobbin and +Point POD for Tube-Tube Wear in SONGS Steam Generators"
17. SONGS Technical Specifications Section 5.5.2.11, "Steam Generator (SG) Program", Amendment 204
18. SONGS Technical Specifications Section 3.4.13, "RCS Operational Leakage", Amendment 204
19. INPO Operating Experience Report OE 34946, "Tube-to-Tube Contact Wear Identified in TMI-1 Steam Generators (TMI-1)"
20. NRC Information Notice 2012-07, "Tube-to-Tube Contact Resulting in Wear in Once-Through Steam Generators"
21. INPO Operating Experience Report OE 35359, "Large Number of Anti-Vibration Bar Wear Indications Reported in the Unit 2 Replacement Steam Generators (St. Lucie)



SONGS 2C17 Steam Generator Condition Monitoring Report

22. MHI Document L5-04GA111, "San Onofre Generating Station, Units 2 & 3 Replacement Steam Generators Vendor Manual", Rev 6 (SONGS Document SO23-617-1-M1273, Rev 6)
23. AREVA Document 51-9181604-000, "SONGS Unit 2 Cycle 17 and U2 Return to Service Eddy Current Inspection Technical Summary"

* These references are not available from the AREVA records center; however, they are available from the SCE document control system. Therefore, these are acceptable references for use on this contract per AREVA NP Procedure 0402-01, Attachment 8 as authorized by the PM signature on page 2.

ATTACHMENT 3

**AREVA Document 51-9180143-001
SONGS Unit 3 February 2012 Leaker Outage
Steam Generator Condition Monitoring Report**

[Proprietary Information Redacted]



AREVA NP Inc.

Engineering Information Record

Document No.: 51 - 9180143 - 001

SONGS Unit 3 February 2012 Leaker Outage - Steam Generator Condition Monitoring Report

Supplier Status Stamp

VPL No:	1814-AU651-M0158	Rev No:	0	QC:	N/A
<input type="checkbox"/> DESIGN DOCUMENT		ORDER NO.	800918458		
<input checked="" type="checkbox"/> REFERENCE DOCUMENT - INFORMATION ONLY		<input type="checkbox"/> VIRP IOM MANUAL			
MFG MAY PROCEED: <input type="checkbox"/> YES <input type="checkbox"/> NO <input checked="" type="checkbox"/> N/A					
<small>STATUS - A status is required for design documents and is optional for reference documents. Drawings are reviewed and approved for arrangements and conformance to specification only. Approval does not relieve the submitter from the responsibility of adequacy and suitability of design, materials, and/or equipment represented.</small>					
<input type="checkbox"/> 1. APPROVED <input type="checkbox"/> 2. APPROVED EXCEPT AS NOTED - Make changes and resubmit. <input type="checkbox"/> 3. NOT APPROVED - Correct and resubmit for review. NOT for field use.					
APPROVAL: (PRINT / SIGN / DATE)					
RE:	E. GRIBBLE		10/01/12		
FLS:					
Other:					

SCE DE(123) 5 REV. 3 07/11

REFERENCE: SO123-XXIV-37.8.26



SONGS Unit 3 February 2012 Leaker Outage - Steam Generator Condition Monitoring Report

Safety Related? YES NO

Does this document contain assumptions requiring verification? YES NO

Does this document contain Customer Required Format? YES NO

Signature Block

Name and Title/Discipline	Signature	P/LP, R/LR, A/A-CRF, A/A-CRI	Date	Pages/Sections Prepared/Reviewed/ Approved or Comments

Note: P/LP designates Preparer (P), Lead Preparer (LP)
R/LR designates Reviewer (R), Lead Reviewer (LR)
A/A-CRF designates Approver (A), Approver of Customer Requested Format (A-CRF)
A/A-CRI designates Approver (A), Approver - Confirming Reviewer Independence (A-CRI)

Table of Contents

	Page
SIGNATURE BLOCK.....	2
RECORD OF REVISION	3
LIST OF TABLES	6
LIST OF FIGURES	7
1.0 PURPOSE.....	9
2.0 ABBREVIATIONS AND ACRONYMS.....	10
3.0 SCOPE.....	13
4.0 BACKGROUND	13
4.1 Previous Operating Experience (OE) Related to Tube-to-Tube Wear	17
4.2 Previous Operating Experience Related to Tube-to-AVB Wear	18
4.3 Pre-Service Examination Results.....	19
5.0 PERFORMANCE CRITERIA	20
6.0 MID-CYCLE 16 OPERATIONAL LEAKAGE	21
7.0 INSPECTION SUMMARY.....	22
7.1 Eddy Current Inspections Performed	23
7.2 Tube-to-Tube Wear Detection.....	23
7.3 Tube-to-Tube Wear Sizing	24
7.4 Degradation Identified	25
7.5 Secondary Side Visual Examination Results	26
8.0 CONDITION MONITORING ASSESSMENT	50
8.1 Input Parameters.....	51
8.2 Evaluation of Structural and Leakage Integrity.....	52
8.2.1 AVB Wear	52
8.2.2 TSP wear	55
8.2.3 Retainer Bar Wear	65
8.2.4 Tube-To-Tube Wear	68
9.0 CONDITION MONITORING CONCLUSION.....	75
10.0 REFERENCES.....	76



SONGS Unit 3 February 2012 Leaker Outage - Steam Generator Condition Monitoring Report

Table of Contents
(continued)

	Page
Appendix A.....	78
Appendix B.....	89

List of Tables

Page

TABLE 2-1: ABBREVIATIONS AND ACRONYMS	10
TABLE 4-1: SUMMARY OF PRE-SERVICE INSPECTION RESULTS	19
TABLE 7-1: STEAM GENERATOR TUBE INSPECTION SCOPE SUMMARY	27
TABLE 7-2: WEAR INDICATION SUMMARY	30
TABLE 7-3: PLUGGING SUMMARY	31
TABLE 7-4: AVB WEAR DEPTHS (%TW) (BOBBIN ETSS 96004.1)	31
TABLE 7-5: TSP WEAR DEPTHS (%TW) (BOBBIN ETSS 96004.1)	31
TABLE 7-6: RETAINER BAR WEAR (+POINT™ ETSS 27903.1)	32
TABLE 7-7: TUBE-TO-TUBE WEAR (%TW) (+POINT™ ETSS 27902.2)	32
TABLE 8-1: SONGS UNIT-3 STEAM GENERATOR INPUT VALUES	51
TABLE 8-2: EDDY CURRENT ETSS INPUT VALUES [5]	52
TABLE 8-3: INCOMPLETE PROOF TESTS OF TSP WEAR EXCEEDING CM LIMIT CURVE	57
TABLE 8-4: IN-SITU TEST RESULT SUMMARY FOR TTW FLAWS	70

List of Figures

	Page
FIGURE 4-1: SONGS STEAM GENERATOR SUPPORT STRUCTURE LAYOUT	14
FIGURE 4-2: VIEW FROM ABOVE BUNDLE SHOWING RETAINER BAR LOCATIONS	15
FIGURE 4-3: SKETCH SHOWING RETAINER/RETAINING BAR CONFIGURATION.....	16
FIGURE 7-1: UNIT 3 AVB WEAR DEPTH DISTRIBUTION (INDICATION COUNT)	33
FIGURE 7-2: COMPARISON OF UNIT 2 AND UNIT 3 AVB WEAR DEPTH DISTRIBUTION (INDICATION COUNT)	34
FIGURE 7-3: UNIT 3 TSP WEAR DEPTH DISTRIBUTION (INDICATION COUNT)	35
FIGURE 7-4: COMPARISON OF UNIT 2 AND UNIT 3 TSP WEAR DEPTH DISTRIBUTION (INDICATION COUNT)	36
FIGURE 7-5: UNIT 3 TTW DEPTH DISTRIBUTION (INDICATION COUNT)	37
FIGURE 7-6: SG 3E-088 AVB WEAR	38
FIGURE 7-7: SG 3E-089 AVB WEAR	39
FIGURE 7-8: SG 3E-088 TSP WEAR – HOT LEG.....	40
FIGURE 7-9: SG 3E-088 TSP WEAR – COLD LEG	41
FIGURE 7-10: SG 3E-089 TSP WEAR – HOT LEG.....	42
FIGURE 7-11: SG 3E-089 TSP WEAR – COLD LEG	43
FIGURE 7-12: SG 3E-088 RETAINER BAR WEAR.....	44
FIGURE 7-13: SG 3E-089 RETAINER BAR WEAR.....	45
FIGURE 7-14: SG 3E-088 TUBE-TO-TUBE WEAR.....	46
FIGURE 7-15: SG 3E-089 TUBE-TO-TUBE WEAR.....	47
FIGURE 7-16: SG 3E-088 TTW INDICATIONS WITH IN-SITU RESULTS.....	48
FIGURE 7-17: SG 3E-089 TTW INDICATIONS WITH IN-SITU RESULTS.....	49
FIGURE 8-1: CM LIMIT FOR AVB WEAR, BOTH SGS, ETSS 96004.1	54
FIGURE 8-2: CM LIMIT FOR TSP WEAR, BOTH SGS, ETSS 96004.1	58
FIGURE 8-3: CM LIMIT FOR SG 3E-088 TSP WEAR, ETSS 96910.1, STRUCTURAL DIMENSIONS	59
FIGURE 8-4: CM LIMIT FOR SG 3E-089 TSP WEAR, ETSS 96910.1, STRUCTURAL DIMENSIONS	60
FIGURE 8-5: IN-SITU TEST RESULTS FOR SG 3E-088 TSP WEAR, ETSS 96910.1, STRUCTURAL DIMENSIONS	61
FIGURE 8-6: IN-SITU TEST RESULTS FOR SG 3E-089 TSP WEAR, ETSS 96910.1, STRUCTURAL DIMENSIONS	62
FIGURE 8-7: AXIAL DEPTH PROFILE – SG 3E-088 R106 C78 07H-1.....	63
FIGURE 8-8: AXIAL POP-THROUGH LIMIT FOR TSP WEAR	64

List of Figures (continued)

Page

FIGURE 8-9: CM LIMIT FOR RB WEAR, ETSS 27903.1.....	67
FIGURE 8-10: CM LIMIT FOR SG 3E-088 TTW, ETSS 27902.2, STRUCTURAL DIMENSIONS.....	71
FIGURE 8-11: CM LIMIT FOR SG 3E-089 TTW, ETSS 27902.2, STRUCTURAL DIMENSIONS.....	72
FIGURE 8-12: IN-SITU TEST RESULTS FOR SG 3E-088 TTW, ETSS 27902.2, STRUCTURAL DIMENSIONS	73
FIGURE 8-13: IN-SITU TEST RESULTS FOR SG 3E-089 TTW, ETSS 27902.2, STRUCTURAL DIMENSIONS	74

SONGS Unit 3 February 2012 Leaker Outage - Steam Generator Condition Monitoring Report

1.0 PURPOSE

In accordance with the EPRI Steam Generator Integrity Assessment Guidelines [2], a Condition Monitoring (CM) assessment must be performed at the conclusion of each steam generator eddy current examination. This process is described as “backward-looking,” since its purpose is to determine whether Steam Generator (SG) integrity was maintained during the most recent operating period. It involves an evaluation of the as-found conditions of the SGs relative to established performance criteria for structural and leakage integrity. The performance criteria are defined in plant Technical Specifications [16] [17] and are based on NEI (Nuclear Energy Institute) 97-06 [1] (see Section 5.0 below).

In late January 2012 during Cycle 16, SONGS (San Onofre Nuclear Generating Station) Unit 3 entered a forced outage due to a SG tube leak, prompting a comprehensive examination of the SGs. This report documents the required SG CM assessment following that examination, and concludes that the tube structural and leakage integrity performance criteria were not satisfied by Unit 3 during Cycle 16 operation.

SONGS Unit 3 February 2012 Leaker Outage - Steam Generator Condition Monitoring Report

2.0 ABBREVIATIONS AND ACRONYMS

The following table provides a listing of abbreviations and acronyms used throughout this report.

Table 2-1: Abbreviations and Acronyms

Abbreviation or Acronym	Definition
01C to 07C	Tube Support Plate Designations for Cold Leg (7 Locations)
01H to 07H	Tube Support Plate Designations for Hot Leg (7 Locations)
2E-088	Unit 2 Steam Generator 88
2E-089	Unit 2 Steam Generator 89
3E-088	Unit 3 Steam Generator 88
3E-089	Unit 3 Steam Generator 89
3 NOPD	3 Times Normal Operating Pressure Differential
3ΔP	3 Times Normal Operating Pressure Differential
ADI	Absolute Drift Indication
AILPC	Accident Induced Leakage Performance Criterion
ANO	Arkansas Nuclear One
ASME	American Society of Mechanical Engineers
AVB	Anti-Vibration Bar
B01 to B12	AVB Designations (12 Locations)
BLG	Bulge
C	Column
CE	Combustion Engineering
CL or C/L	Cold Leg
CM	Condition Monitoring
DA	Degradation Assessment
DBE	Design Basis Earthquake
DNG	Ding
DNT	Dent
ECT	Eddy Current Testing
FFPD	Effective Full Power Days
EOC	End of Operating Cycle
EPRI	Electric Power Research Institute
ETSS	Examination Technique Specification Sheet
FOSAR	Foreign Object Search and Retrieval
GMD	Geometric Distortion
GPD	Gallons per Day
GPM	Gallons per Minute

SONGS Unit 3 February 2012 Leaker Outage - Steam Generator Condition Monitoring Report

Table 2-1: Abbreviations and Acronyms

Abbreviation or Acronym	Definition
HL or H/L	Hot Leg
INPO	Institute of Nuclear Power Operators
kHz	Kilohertz
KSI	Thousand Pounds per Square Inch
LER	Licensee Event Report
MBM	Manufacturing Burnish Mark
MHI	Mitsubishi Heavy Industries
MSLB	Main Steam Line Break
NDE	Non Destructive Examination
NEI	Nuclear Energy Institute
NN	Nuclear Notification
NOPD	Normal Operating Pressure Differential
NQI	Non-Quantifiable Indication
NRC	Nuclear Regulatory Commission
NSAL	Nuclear Safety Advisory Letter
OA	Operational Assessment
OE	Operating Experience
OTSG	Once Through Steam Generator
PDA	Percent Degraded Area
PLP	Possible Loose Part
POD	Probability of Detection
PRX	Proximity Indication
PSI	Pounds per Square Inch
PSIG	Pounds per Square Inch Gage
PST	Pacific Standard Time
PVN	Permeability Variation
PWR	Pressurized Water Reactor
QA	Quality Assurance
R	Row
RB	Retainer Bar
RCS	Reactor Coolant System
REPL	Replacement
ROLLED	Rolled Plug Designation
ROLLSTAB	Rolled Plug with a Stabilizer
RPC	Rotating Probe Coil
RSG	Recirculating Steam Generator

SONGS Unit 3 February 2012 Leaker Outage - Steam Generator Condition Monitoring Report

Table 2-1: Abbreviations and Acronyms

Abbreviation or Acronym	Definition
SCE	Southern California Edison
SG	Steam Generator
SIPC	Structural Integrity Performance Criteria
SL2	St. Lucie Unit 2
SLB	Steam Line Break
SONGS	San Onofre Nuclear Generating Station
SSA	Secondary Side Anomaly
SSI	Secondary Side Inspection
SVI	Single Volumetric Indication
TMI	Three Mile Island
TSP	Tube Support Plate
TTW	Tube to Tube Wear
TW	Through Wall
U3F16B	Unit 3 Outage Designation
UB	U-bend

SONGS Unit 3 February 2012 Leaker Outage - Steam Generator Condition Monitoring Report

3.0 SCOPE

This evaluation pertains to the SONGS Unit 3 replacement SGs, which are reactor coolant system components. The CM assessment is required to be completed prior to plant entry into Mode 4 during start up after a SG inspection. The operational assessment (OA) will be documented separately.

4.0 BACKGROUND

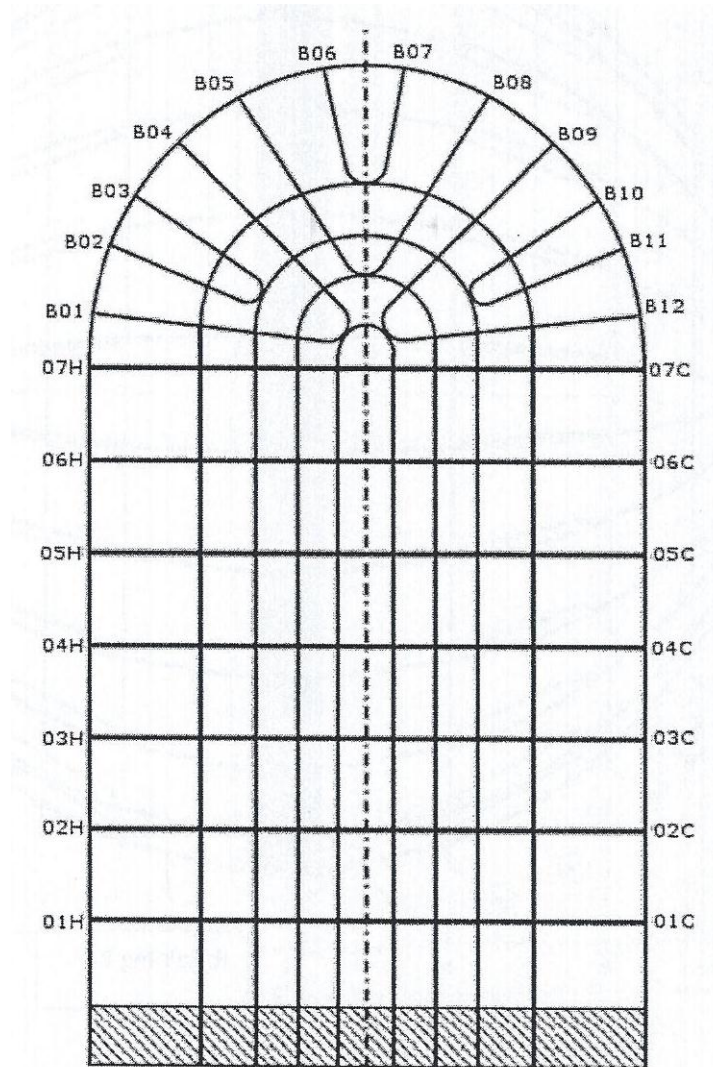
SONGS Unit 3 is a two loop Combustion Engineering (CE) PWR (Pressurized Water Reactor) plant which began commercial operation in 1984. The original CE steam generators were replaced in 2010-2011 with new SGs designed and manufactured by Mitsubishi Heavy Industries (MHI) [21]. The replacements, referred to by MHI as model 116TT-1, incorporate thermally treated Inconel Alloy 690 (I-690TT) tubing which has demonstrated, through laboratory testing and industry experience, superior resistance to stress corrosion cracking as compared with the I-600 tubing used in the original SGs. Other design features include full tubesheet depth hydraulic tube expansion and seven stainless steel trefoil broach Tube Support Plates (TSPs); features chosen primarily to minimize the potential for tube corrosion.

There are 9727 tubes in each SG, in 142 rows and 177 columns, in a triangular pitch arrangement. The tubes in rows 1-13 are thermally stress-relieved to further minimize the potential for in-service stress corrosion cracking in the U-bends.

The tube bundle U-bend region is supported by a floating Anti-Vibration Bar (AVB) structure consisting of six V-shaped AVBs between each tube column. The AVBs were fabricated from ASME (American Society of Mechanical Engineers) SA-479, Type 405 ferritic stainless steel and are equipped with two Alloy 690 (ASME SB-168 UNS N06690) end caps. Each AVB end cap is welded to an Alloy 690 retaining bar. The retaining bars with AVBs attached are supported by twenty four chrome-plated Alloy 690 retainer bars that anchor the assembly to the tubes. Thirteen Alloy 690 bridges run perpendicular to the retaining bars, and hold the entire assembly together. The AVB structure is not attached to any steam generator component. Figure 4-1 illustrates the general layout of the tube support structures. Figure 4-2 and Figure 4-3 illustrate the arrangements of the retainer bars and retaining bars.

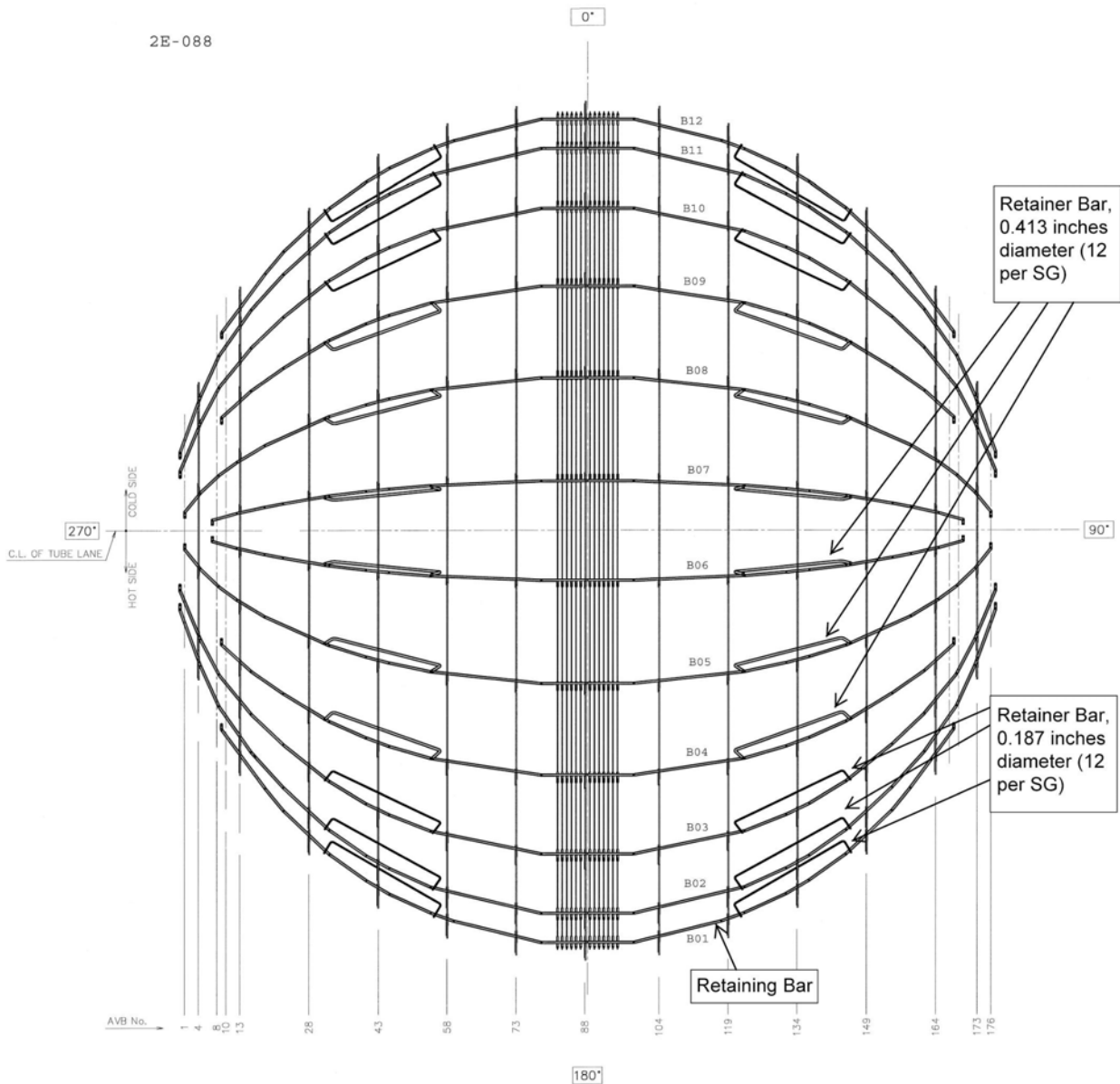
SONGS Unit 3 February 2012 Leaker Outage - Steam Generator Condition Monitoring Report

Figure 4-1: SONGS Steam Generator Support Structure Layout

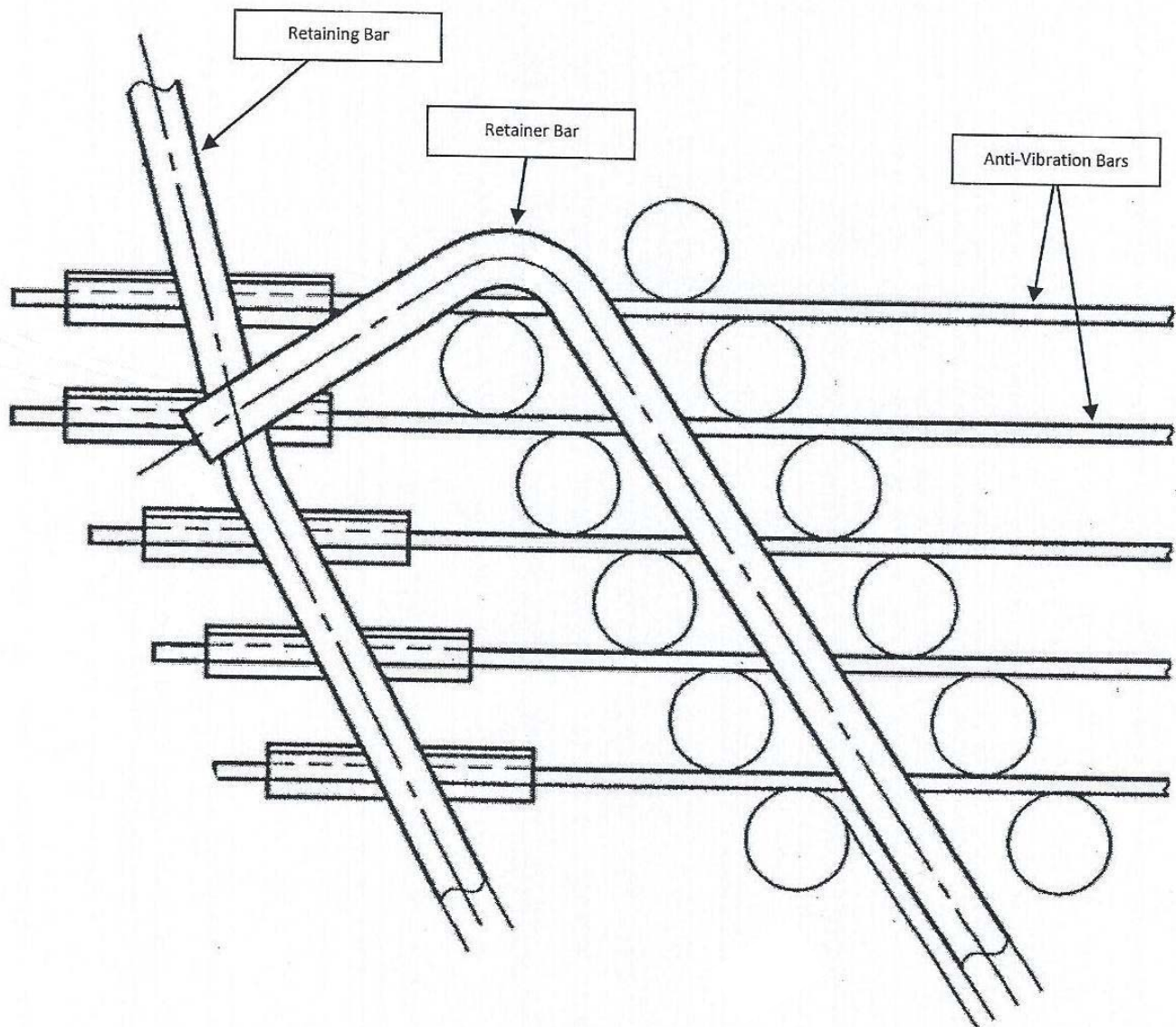


SONGS Unit 3 February 2012 Leaker Outage - Steam Generator Condition Monitoring Report

Figure 4-2: View From Above Bundle Showing Retainer Bar Locations



3: Sketch Showing Retainer/Retaining Bar Configuration



SONGS Unit 3 February 2012 Leaker Outage - Steam Generator Condition Monitoring Report

4.1 Previous Operating Experience (OE) Related to Tube-to-Tube Wear

Prior to the SONGS Unit 3 shutdown in January of 2012, the recent operating experience related to tube-to-tube wear was limited to once-through steam generators (OTSGs). In December 2011, INPO (Institute of Nuclear Power Operators) OE 34946 [18] was released. This Operating Experience Report discusses experience at Three Mile Island Unit 1 (TMI-1). In July 2012, the NRC (Nuclear Regulatory Commission) released Information Notice 2012-07 [19]. This Information Notice contains information on the experience at TMI-1 as well as Oconee as well as ANO-1 (Arkansas Nuclear One – Unit 1). This section summarizes the experiences at these plants with OTSGs.

TMI-1 completed replacement of its original OTSGs in 2010. The design of the OTSG differs from the recirculating SG design in that the tubes are straight. The tubes are supported by 15 tube support plates. The first inspection of the TMI-1 replacement SGs took place in the fall of 2011. During this examination, indications were detected on the absolute channel with no discernible response on the differential channel. The indications were designated as Absolute Drift Indications (ADIs). A comprehensive review of all of the ADIs identified tubes with long shallow wear signals between the eighth and ninth tube support plates. The indications were in adjacent tube combinations of either 2 or 3 tubes (the tube pattern is a triangular pitch). A more detailed investigation led to the conclusion that these wear indications were the result of tube-to-tube contact wear. The lengths ranged from 2 to 8 inches and from 1 to 21 percent through-wall.

As a result of the TMI-1 findings, and because TMI and ANO both have AREVA replacement steam generators, the licensee for Arkansas Nuclear One, Unit 1 (ANO-1) was notified. Upon a review of previously recorded eddy current examination data, it was determined that ANO-1 also had similar indications of tube-to-tube wear. The depth and length of the ANO-1 indications were similar to those recorded at TMI-1

In the spring of 2012, the licensee for Oconee, also detected wear attributed to tube-to-tube contact in their Unit 3 replacement SGs. Because the design of the Oconee OTSG are built by BWI and are not the same as the TMI or ANO generators, the location of the tube-to-tube wear was different, but the characteristics were similar. The lengths ranged from 1 to 9 inches and the depths ranged up to 20 percent through-wall.

The severity of the replacement OTSG tube-to-tube wear was evaluated and was not found to compromise tube integrity.

SONGS Unit 3 February 2012 Leaker Outage - Steam Generator Condition Monitoring Report

The combined experience from the above discussion demonstrated several significant points:

- New or unexpected forms of degradation may be difficult to identify. Robust inspection planning is an important part of identifying new degradation as well as properly characterizing known degradation.
- A comprehensive review of examination data from different perspectives is valuable. By considering the change in indications over time, responses to different channels or techniques, or the spatial distribution of the indications, important information may be found.
- The reporting criteria are critical to proper identification of new or existing damage mechanisms.
- Comprehensive examination of new or replacement steam generators is necessary to ensure that performance is as expected.

4.2 Previous Operating Experience Related to Tube-to-AVB Wear

INPO OE 35359 [20] discusses the results of the first two inspections at St. Lucie Unit 2. The recirculating SGs at St. Lucie Unit 2 were replaced during 2007. During the Cycle 18 Refueling Outage (SL2-18, April 2009), eddy current testing of the replacement SGs reported over 5800 AVB wear indications in more than 2000 tubes. Fourteen tubes were plugged as a result of the wear indications. None of the indications challenged the condition monitoring limits.

Based on the high number of wear indications reported during the SL2-18 inspection, and to further establish growth rates, the St. Lucie Unit 2 SGs were examined again during the next refueling outage at SL2-19 in January 2011. Approximately 3000 new AVB wear indications were reported during the SL2-19 examination. As a result of the SL2-19 inspection, an additional twenty-one (21) tubes were plugged, only one of which exceeded the Plant Technical Specification limit of > 40 %TW (throughwall). None of the indications detected in SL2-19 challenged the condition monitoring limits.

The OE reinforces the importance of inspecting replacement SGs with the bobbin coil at the end of the first cycle of operation, post-replacement. The diagnostic examinations performed with the +Point™ rotating coil concluded that the AVB wear indications could be flat or tapered, single or double sided. These wear characteristics are important to consider when selecting the proper depth-sizing technique(s).

SONGS Unit 3 February 2012 Leaker Outage - Steam Generator Condition Monitoring Report

4.3 Pre-Service Examination Results

The pre-service inspection of the Unit 3 replacement SGs was performed during June of 2010 at the MHI manufacturing facility in Kobe Japan. The examination consisted of 100 % bobbin coil inspection of all tubes (9727 tubes), 100 % inspection of the Hot Leg (HL) and Cold Leg (CL) Tubesheet region with the +Point™ probe (9727 tubes), and a 100 % inspection of the row 1-15 U-bend regions with the +Point™ probe (1314 tubes).

No significant degradation was detected during this examination. There were a number of geometric type indications reported in each SG (dings, geometric distortions, proximity, bulge). The following table provides a count of the number of tubes and total number of indications for each Unit 3 SG.

Table 4-1: Summary of Pre-Service Inspection Results

Indication Code	SG 3E-088		SG 3E-089	
	Tube Count	Indication Count	Tube Count	Indication Count
BLG (Bulge)	10	11	3	3
DNG (Ding)	364	395	706	831
GMD (Geometric Distortion)	3	3	5	5
MBM (Manufacturing Burnish Mark)	0	0	0	0
NQI (Non-Quantifiable Indication)	0	0	0	0
PLP (Possible Loose Part)	6	6	3	3
PRX (Proximity)	106	106	128	128
PVN (Permeability Variation)	0	0	0	0

SONGS Unit 3 February 2012 Leaker Outage - Steam Generator Condition Monitoring Report

5.0 PERFORMANCE CRITERIA

The SONGS Unit-3 performance criteria, based on NEI 97-06 [1], are shown below. The structural integrity and accident-induced leakage criteria were taken from Section 5.5.2.11 [16] from the SONGS Unit-3 Technical Specifications. The operational leakage criterion was taken from Section 3.4.13 [17] of the SONGS Technical Specifications.

- *Structural Integrity Performance Criterion:* All in-service steam generator tubes shall retain structural integrity over the full range of normal operating conditions (including startup, operation in the power range, hot standby, and cooldown, and all anticipated transients included in the design specification) and design basis accidents. This includes retaining a safety factor of 3.0 against burst under normal steady state full power operation primary-to-secondary pressure differential and a safety factor of 1.4 against burst applied to the design basis accident primary-to-secondary pressure differentials. Apart from the above requirements, additional loading conditions associated with the design basis accidents, or combination of accidents in accordance with the design and licensing basis, shall also be evaluated to determine if the associated loads contribute significantly to burst or collapse. In the assessment of tube integrity, those loads that do significantly affect burst or collapse shall be determined and assessed in combination with the loads due to pressure with a safety factor of 1.2 on the combined primary loads and 1.0 on axial secondary loads.
- *Accident-Induced Leakage Performance Criterion:* The primary to secondary accident-induced leakage rate for any design basis accident, other than a SG tube rupture, shall not exceed the leakage rate assumed in the accident analysis in terms of total leakage rate for all SGs and leakage rate for an individual SG. Leakage is not to exceed 0.5 gpm per SG and 1 gpm through both SGs.
- *Operational Leakage Performance Criterion:* "RCS operational leakage shall be limited to 150 gallons per day primary to secondary leakage through any one steam generator."

6.0 MID-CYCLE 16 OPERATIONAL LEAKAGE

On January 31, 2012 while operating under nominal conditions and at full power, a high radiation alarm from the condenser air ejector monitor indicated a tube leak in one of the two SGs. Following is a verbatim excerpt from the abstract section of the Licensee Event Report [15] describing the leakage and subsequent shutdown.

“On 01/31/2012 at 1505 PST, SONGS Unit 3 was in Mode 1 operating at 100 percent power, when a high radiation alarm from the condenser air ejector monitor indicated a tube leak in one of the two steam generators (SGs). A rapid power reduction was commenced in accordance with plant procedures when the primary to secondary leak rate was determined to be greater than 75 gallons per day (gpd) with an increasing rate of leakage exceeding 30 gpd per hour. At 1731 PST, the operators manually tripped the reactor at 35 percent power as directed by procedure, resulting in actuation of the Reactor Protection System which is reportable.”

After cooling to Mode 5 and draining the primary coolant system to midloop, the leaking SG tube (SG 3E-088 R106 C78) was located by filling the secondary side of the SG and pressurizing to 80 psig with nitrogen. The leak location was confirmed by eddy current testing to be within the U-bend portion of the tube bundle, in the tube freespan. The tube degradation which resulted in the leak was tube-to-tube wear (TTW) caused by tube movement caused by fluid-elastic instability (FEI).

Prior to the forced shutdown, the replaced Unit 3 SGs had been operated for approximately 338 EFPD (Effective Full Power Days) in fuel Cycle 16. The tube leak occurred in Unit 3 while Unit 2 was in the midst of a refueling outage. The utility designated the shutdown as U3F16B.

SONGS Unit 3 February 2012 Leaker Outage - Steam Generator Condition Monitoring Report

7.0 INSPECTION SUMMARY

The SONGS Unit 3 leaker outage work scope included the following inspection and testing activities in each of the two replacement SGs (SG 3E-088 and SG 3E-089):

- Bobbin probe and rotating probe examinations using site validated ECT techniques [7] [13]
- Secondary side visual examinations [22]
- In-situ pressure testing [11]

The initial examination following shutdown was a visual examination of the tubesheets of both SG 3E-088 and SG 3E-089 with the goal of identifying the tube(s) exhibiting signs of leakage. The leaking tube was visually identified as SG 3E-088 R-106 C-78. This tube and a two tube bounding pattern surrounding this tube (19 tubes total) were examined full length with the bobbin coil probe to determine the location of the leak and to define the type of degradation associated with the leak. Once this was determined, SCE decided on the initial inspection scope which included the following:

- 100% bobbin coil probe (610 mil diameter) examination of the complete tube length in both Steam Generators.
- 100% of all newly reported bobbin “I” codes, PLP, MBM, NQI, SSA, PRX and PVN locations with a rotating +Point™/pancake coil probe.
- 100% of all reported bobbin coil ding (DNG) and dent (DNT) locations measuring ≥ 2.0 volts with a rotating +Point™/pancake coil probe.
- All reported bobbin AVB %TW wear measuring ≥ 25 %TW and all TSP %TW measuring ≥ 30 %TW.

Based on the examination results, a series of seven (7) examination expansions were performed to better characterize and bound the tube-to-tube wear damage.

The subsections below describe findings that are relevant to the condition monitoring assessment.

7.1 Eddy Current Inspections Performed

A summary of the total number of bobbin probe and rotating probe examinations performed during the current outage is provided in Table 7-1. As indicated in Table 7-1, the examination scope was expanded subsequent to completion of the initial plan. These expansions were implemented in some cases to further characterize identified degradation, and in other cases to further bound regions of potential degradation with the more sensitive +Point™ probe.

7.2 Tube-to-Tube Wear Detection

At the start of the U3F16B inspection, the suspected leaking tube (SG 3E-088 R-106 C-78) along with 18 surrounding tubes were inspected with the bobbin coil probe to determine the axial location of the flaw responsible for the leak and to get an understanding as to what type of degradation was associated with the area of the tube with the through wall indication. The degradation observed in the first nineteen tubes examined included AVB wear, deep wear at the TSP's (both hot and cold leg) and long wear type indications in the U-bend region which were eventually classified as Tube-to-Tube Wear (TTW). It was ultimately determined that the Tube-to-Tube Wear was the type of degradation responsible for the tube leak.

The SONGS eddy current inspection procedure was updated to include enhanced screening of the U-bend area of the tube using the 100 kHz absolute channel with no voltage criteria for the reporting of small amplitude signals in the U-bend area of the tube. All analysts assigned to the SONGS inspection were made aware of the revised procedure and screening process and bobbin coil data was screened according to the new requirements set forth in the bobbin coil technique Examination Technique Specification Sheet (ETSS).

The TTW indications were initially identified as NQI during the bobbin coil analysis with the "from-to" fields of the report line entry defining the overall length. No depth was assigned to the NQI bobbin coil entries. Over 300 NQI's were reported in the U-bend area of each SG. All of the tubes with reported U-bend NQI's were examined with the rotating 1-coil +Point™ probe through the complete region of the U-bend (07H to 07C). Most of the NQI's were confirmed to be degradation categorized as TTW and were reported as Single Volumetric Indications (SVI's).

The TTW indications were very long and ranged in length from approximately 1.0" to 41.0" and in depth from 4% to 100% through wall. In many cases, the region of the tube with the TTW present would have two separate indications, one on the intrados of the tube and one on the extrados of the tube. In this case, two separate SVI's would be reported with measured depth and length. In addition to the tubes with reported bobbin coil NQI's, additional tubes surrounding the TTW region were also examined with the 1-coil rotating +Point™ probe. With these supplemental inspections, a total of 1375 contiguous tubes in each SG were examined the full length of the U-bend (07H-07C) specific to the detection of TTW. As a result of these inspections, 407 TTW SVI indications (161 tubes) were reported in SG 3E-088 and 416 TTW SVI indications (165 tubes) were reported in SG 3E-089.

SONGS Unit 3 February 2012 Leaker Outage - Steam Generator Condition Monitoring Report

The TTW indications were depth sized using EPRI ETSS 27902.2 even though it was known to be very conservative. Selected TTW SVI indications based on depth were line by line sized using the ETSS 27902.2 technique.

The Unit 3 experience in the detection and sizing of the TTW damage mechanism was reflected back into the Unit 2 examination which had just been completed.

7.3 Tube-to-Tube Wear Sizing

Upon detection of tube-to-tube wear in the Unit 3 SG's, a determination was made that the most appropriate technique for sizing the wear was EPRI ETSS 27902.2 or 27902.5. However, with some initial review, it was apparent that the techniques produced very conservative depth estimates. The depth estimates reported for the deepest indications were near throughwall, however the tubes had maintained structural integrity at normal operating differential pressure (NODP). Using the actual tube operational performance, the throughwall depth values should have been around 80 %TW or smaller. Based on the best understanding of the tube-to-tube wear degradation morphology, a wear standard was designed with two machined wear flaws. Although the sample had only two separate flaws, the flaws were fabricated to a maximum depth of 81 % TWD. The length of the flaws made it possible to measure multiple discrete depth sizing grading units. On the basis of these multiple points, a polynomial function was developed to adjust the depth estimates. The revised technique was documented in Reference 13.

The actual flaw sizing was performed using the 27902.2 technique. Screening for selection of In-Situ pressure test candidates was based on the 27902.2 sizing data without the polynomial correction in Reference 13. This produced a conservative population for the In-Situ pressure testing.

 SONGS Unit 3 February 2012 Leaker Outage - Steam Generator Condition Monitoring Report

7.4 Degradation Identified

The following tube wear categories (types) were identified during the current outage inspections:

- Anti-vibration bar (AVB) wear
- Tube support plate (TSP) wear
- Retainer bar (RB) wear
- Tube-to-tube wear (TTW)

Table 7-2 summarizes the number of identified degradation indications for each of the wear categories identified (AVB wear, TSP wear, RB wear, and TTW). A complete accounting of the number of tubes plugged and stabilized is provided in Table 7-3, and the plugging/stabilization lists for both SGs are provided in Appendices A and B. The plugging and stabilization information provided in this table and the appendices is current as of June 2012. Due to the ongoing SG recovery efforts, the plugging strategy and, hence, the plugging and stabilization information shown in this report may change prior to startup.

Table 7-4 through Table 7-7 summarize the reported throughwall depths for each category. Because only four RB wear indications were identified, Table 7-6 lists these indications by tube number and provides the structurally equivalent length and depth, as well as the overall length and maximum depth of the wear. The structurally equivalent dimensions correspond to a rectangular flaw which would burst at the same pressure as the measured flaw; determined using the methods described in Section 5.1.5 of Reference 4.

While AVB wear accounts for the largest number of indications and affected tubes, it is the least structurally challenging damage mechanism among those identified.

Figure 7-1 provides histograms of reported AVB wear depths for both SGs which demonstrate that the vast majority of AVB wear was less than 25 %TW. Approximately 50% more AVB wear indications were identified in Unit 3 than in Unit 2; however, the depth distributions at both units were very similar (Figure 7-2). However, since Unit 3 operated for only part of a cycle, it must be concluded that AVB wear is progressing more aggressively at Unit 3 than at Unit 2.

Figure 7-3 provides histograms of reported TSP wear depths for both SGs. This data illustrates that a significant number of tubes experienced TSP wear with throughwall depths in excess of the criteria for plugging. This contrasts sharply with the relatively minor TSP wear identified at Unit 2 after a full cycle of operation (Figure 7-4).

Only four tubes experienced RB wear but three of the four indications exceeded the 35 %TW plugging criteria.

Figure 7-6 through Figure 7-17 provide tubesheet maps illustrating the locations of degradation reported in each SG. The AVB wear is most prevalent in the central region of the tubesheet matrix, in longer tube rows. The most severe TSP wear occurred in the same region as the TTW: a discrete centralized region of the bundle in higher row tubes (Figure 7-14 through Figure 7-17).

SONGS Unit 3 February 2012 Leaker Outage - Steam Generator Condition Monitoring Report

7.5 Secondary Side Visual Examination Results

Due to the wear degradation detected, significant secondary side inspections (SSI) were performed. The main purposes of these inspections were to provide confirmation of the eddy current results and obtain additional information to help with the root cause evaluation. These visual inspections included the following:

1. All small diameter retainer bars.
2. Retaining bars and AVB end caps associated with B04 and B09.
3. 7th tube support plate
4. Inner bundle passes at B01, B04, and B09.

The retainer bars, retaining bars, and AVB end caps appeared to be structurally sound with no evidence of corrosion, broken welds, etc. The 7th TSP inspection revealed no unexpected or unusual conditions.

The inner bundle passes in the U-bend were performed by going through the transition cone handhole above the 7th TSP and entering the tube bundle at either 90 degree or 30 degree angles. The 90-degree inspections included many passes between Columns 73 and 87. These inspections showed some wear indications that extended slightly outside of the AVB intersection. This phenomenon was confirmed with eddy current. Additional passes were made between Columns 50 and 60. These inspections did not show any AVB wear outside the AVB intersections.

During the secondary side examination activities described above, no foreign objects were identified. In addition, during the eddy current inspection, no potential loose parts were identified. Therefore, no unscheduled secondary side FOSAR (Foreign Object Search and Retrieval) activities were required.

SONGS Unit 3 February 2012 Leaker Outage - Steam Generator Condition Monitoring Report

Table 7-1: Steam Generator Tube Inspection Scope Summary

SCOPE DESCRIPTION			S/G 3E-088			S/G 3E-089		
<i>Leg</i>	<i>Exam Description</i>	<i>Extents</i>	<i>Analyzed</i>	<i>Scope</i>	<i>%Completed</i>	<i>Analyzed</i>	<i>Scope</i>	<i>%Completed</i>
Hot / Cold	100 % Bobbin F/L	TEH-TEC	9,727	9,727	100.00%	9,727	9,727	100.00%
Hot	HL Special Interest	Various	283	283	100.00%	309	309	100.00%
Cold	CL Special Interest	Various	218	218	100.00%	242	242	100.00%
Hot	UB Special Interest	Various	16	16	100.00%	3	3	100.00%
Cold	UB Special Interest	Various	5	5	100.00%	0	0	N/A
Hot/Cold	UB NQI Rows<70	07H-07C	19	19	100.00%	1	1	100.00%
Hot	HL UB NQI Rows>=70	07H-B07	150	150	100.00%	168	168	100.00%
Cold	CL UB NQI Rows>=70	07C-B07	150	150	100.00%	168	168	100.00%

Expansion 1 – Retainer Bar Region

SCOPE DESCRIPTION			S/G 3E-088			S/G 3E-089		
Hot	HL U-Bend Retainer Bar Tubes	07H-B07	90	90	100.00%	93	93	100.00%
Cold	C/L U-Bend Retainer Bar Tubes	07C-B07	90	90	100.00%	93	93	100.00%

Expansion 2 – Bound Tube-to-Tube Wear (TTW) Region

SCOPE DESCRIPTION			S/G 3E-088			S/G 3E-089		
Hot	H/L U-Bend Bounding Region #1	07H-B07	72	72	100.00%	63	63	100.00%
Cold	C/L U-Bend Bounding Region #1	07C-B07	72	72	100.00%	63	63	100.00%

SONGS Unit 3 February 2012 Leaker Outage - Steam Generator Condition Monitoring Report

Expansion 3 – Additional Characterization of Wear

SCOPE DESCRIPTION			S/G 3E-088			S/G 3E-089		
Hot	H/L Straight TWD>20% Not Already RPC'd	Various	N/A	N/A	N/A	3	3	100.00%
Hot	H/L U-Bend TWD>20% Not Already RPC'd	Various	23	23	100.00%	11	11	100.00%
Cold	C/L U-Bend TWD>20% Not Already RPC'd	Various	2	2	100.00%	N/A	N/A	N/A

Expansion 4 – Additional Bounding of TTW Region

SCOPE DESCRIPTION			S/G 3E-088			S/G 3E-089		
Hot	HL U-Bend Freespan Wear Zone Bounding #1	07H-B07	146	146	100.00%	183	183	100.00%
Cold	C/L U-Bend Freespan Wear Zone Bounding #1	07C-B07	146	146	100.00%	183	183	100.00%

Expansion 5 - Additional Characterization of Wear

SCOPE DESCRIPTION			S/G 3E-088			S/G 3E-089		
Hot	H/L TSP +Point	TSP +/-3	133	133	100.00%	N/A	N/A	N/A
Cold	C/L TSP +Point	TSP +/-3	133	133	100.00%	N/A	N/A	N/A
Hot	H/L U-Bend +Point	07H-B07	19	19	100.00%	N/A	N/A	N/A
Cold	C/L U-Bend +Point	07C-B07	19	19	100.00%	N/A	N/A	N/A
Total Plan			11,513	11,513	100.00%	11,310	11,310	100.00%

SONGS Unit 3 February 2012 Leaker Outage - Steam Generator Condition Monitoring Report

Expansion 6 – Post In-Situ Pressure Testing

SCOPE DESCRIPTION			S/G 3E-088			S/G 3E-089		
Hot/Cold	Bobbin F/L	TEH-TEC	73	73	100.00%	56	56	100.00%
Hot	H/L U-Bend RPC	07H-B07	73	73	100.00%	56	56	100.00%
Cold	C/L U-Bend RPC	07C-B07	73	73	100.00%	56	56	100.00%
Hot	H/L Straight TSP Wear	Various	232	232	100.00%	179	179	100.00%
Cold	C/L Straight TSP Wear	Various	180	180	100.00%	172	172	100.00%
Total Plan			631	631	100.00%	519	519	100.00%

Expansion 7 – U-Bend RPC

SCOPE DESCRIPTION			S/G 3E-088			S/G 3E-089		
Hot	H/L U-Bend RPC	07H-B07	993	993	100.00%	964	964	100.00%
Cold	C/L U-Bend RPC	07C-B07	993	993	100.00%	964	964	100.00%
Total Plan			1,986	1,986	100.00%	1,928	1,928	100.00%

SONGS Unit 3 February 2012 Leaker Outage - Steam Generator Condition Monitoring Report

Table 7-2: Wear Indication Summary

Steam Generator SG3E88 (Through-Wall Wear)	Anti-Vibration Bar	Tube Support Plate	Tube-to-Tube Wear	Retainer Bar	Foreign Object	Total Indications	Tubes with Indications (out of 9727 total per SG)
≥ 50%	0	117	48	0	0	165	74
35 - 49%	3	217	116	2	0	338	119
20 - 34%	156	506	134	1	0	797	197
10 - 19%	1380	542	98	0	0	2020	554
< 10%	1818	55	11	0	0	1884	817
TOTAL	3357	1437	407	3	0	5204	919*

* This value is the number of tubes with wear indications at any depth and at any location. Since many tubes have indications in more than one depth and locations, the total number of tubes is less than the total number of indications.

Steam Generator SG3E89 (Through-Wall Wear)	Anti-Vibration Bar	Tube Support Plate	Tube-to-Tube Wear	Retainer Bar	Foreign Object	Total Indications	Tubes with Indications (out of 9727 total per SG)
≥ 50%	0	91	26	0	0	117	60
35 - 49%	0	252	102	1	0	355	128
20 - 34%	45	487	215	0	0	747	175
10 - 19%	940	590	72	0	0	1602	450
< 10%	2164	94	1	0	0	2259	838
TOTAL	3149	1514	416	1	0	5080	887*

* This value is the number of tubes with wear indications at any depth and at any location. Since many tubes have indications in more than one depth and locations, the total number of tubes is less than the total number of indications.

SONGS Unit 3 February 2012 Leaker Outage - Steam Generator Condition Monitoring Report

Table 7-3: Plugging Summary

Reason for Plugging	Steam Generator		Total*
	3E-088	3E-089	
U-bend TTW**	161	165	326
Retainer Bar Wear	3	1	4
AVB Wear >=35%	1		1
Preventative (TTW - MHI Screening)	151	112	263
Preventative (TTW Fence)***	11	14	25
Preventative (Six Consecutive AVB Wear Inds)	2	2	4
Preventative - Retainer Bar	91	93	184
Total	420	387	807

* The plugging status shown in this table is current as of June 2012. Due to the ongoing SG recovery efforts, the plugging strategy and, hence, the numbers shown in this table may change prior to startup.

** Many tubes with TTW also have support wear >=35%. These tubes are only included in the TTW category.

*** "TTW Fence" refers to the plugging and stabilization of tubes to bound tubes with TTW.

Table 7-4: AVB Wear Depths (%TW) (Bobbin ETSS 96004.1)

SG	Average	Upper 95 th	Maximum
3E-088	10.2	19	37
3E-089	8.8	16	30
Both SGs	9.5	18	37

Table 7-5: TSP Wear Depths (%TW) (Bobbin ETSS 96004.1)

SG	Average	Upper 95 th	Maximum
3E-088	25.8	55	72
3E-089	24.7	52	79
Both SGs	25.2	53	79

SONGS Unit 3 February 2012 Leaker Outage - Steam Generator Condition Monitoring Report

Table 7-6: Retainer Bar Wear (+Point™ ETSS 27903.1)

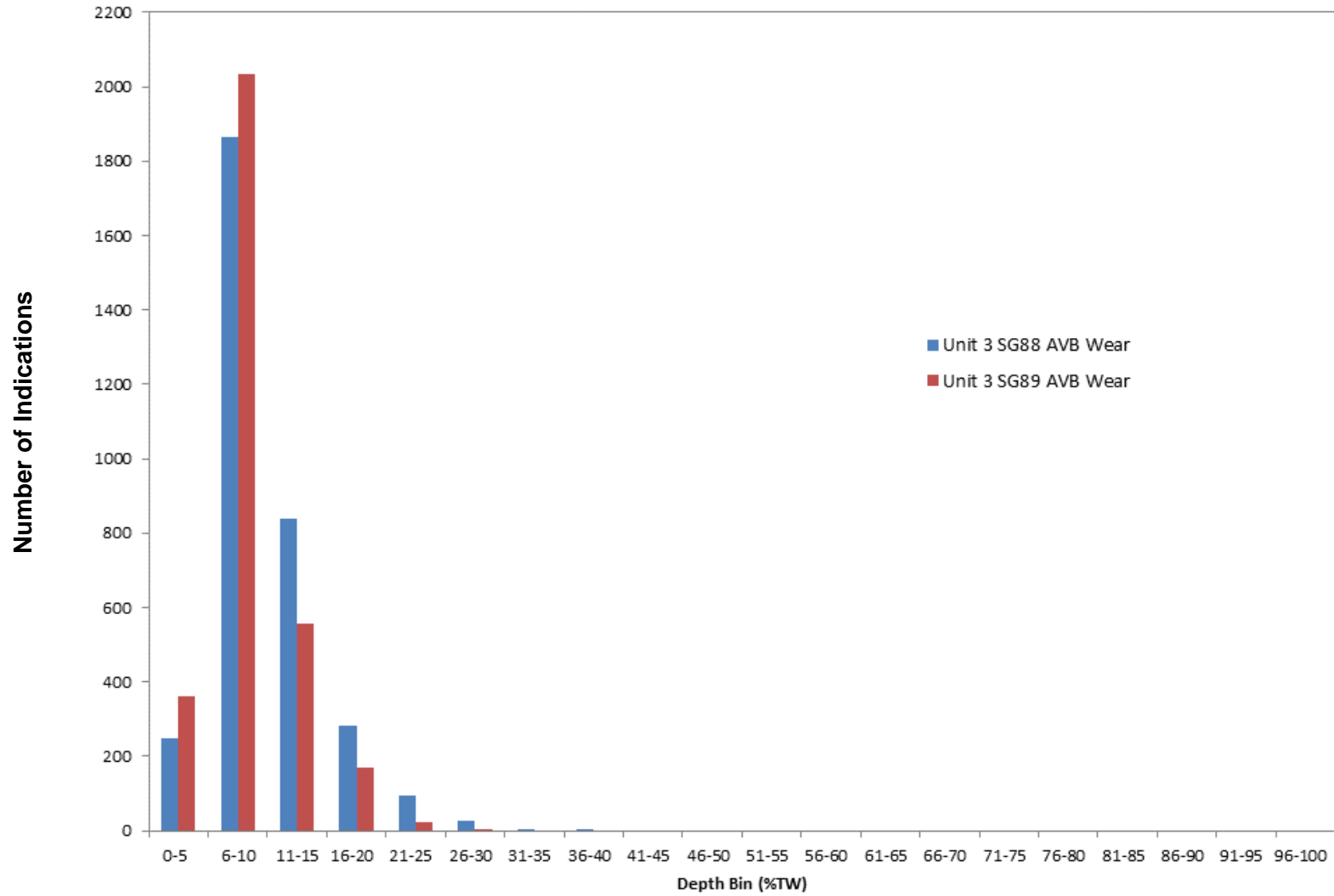
SG	Row	Col	Location	Circ Extent (in)	Axial Extent (in)	Structural Depth (%TW)	Structural Length (in)
3E-088	117	137	B10-0.42"	0.36	0.32	44	0.26
3E-088	125	49	B11-0.50"	0.26	0.31	29	0.27
3E-088	128	126	B10-0.44"	0.26	0.29	39	0.24
3E-089	124	130	B11-0.47"	0.31	0.32	45	0.27

Table 7-7: Tube-to-Tube Wear (%TW) (+Point™ ETSS 27902.2)

SG	Average	Upper 95 th	Maximum
3E-088	32.5	60	99
3E-089	30.4	51	66
Both SGs	31.4	57	99

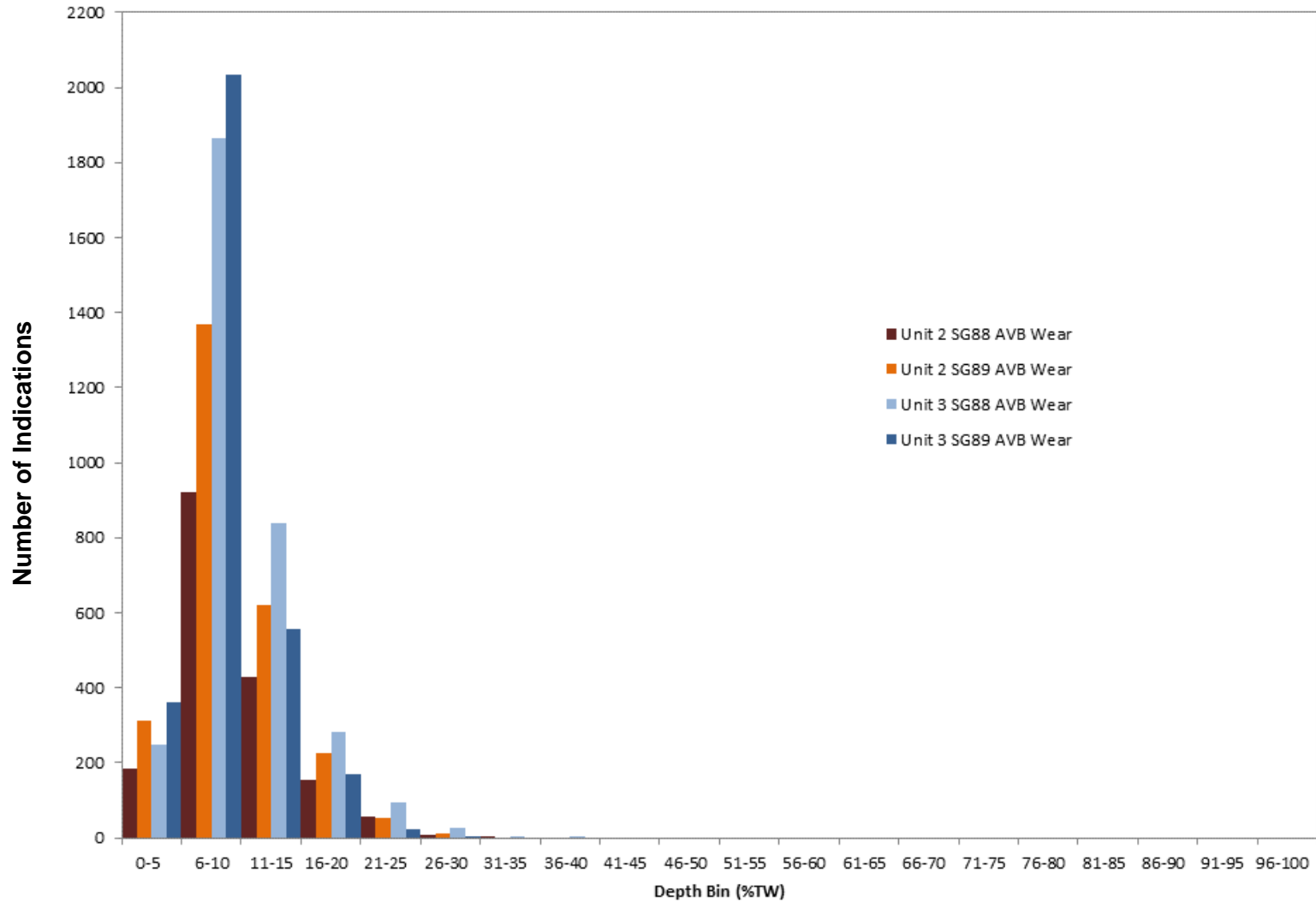
SONGS Unit 3 February 2012 Leaker Outage - Steam Generator Condition Monitoring Report

Figure 7-1: Unit 3 AVB Wear Depth Distribution (Indication Count)



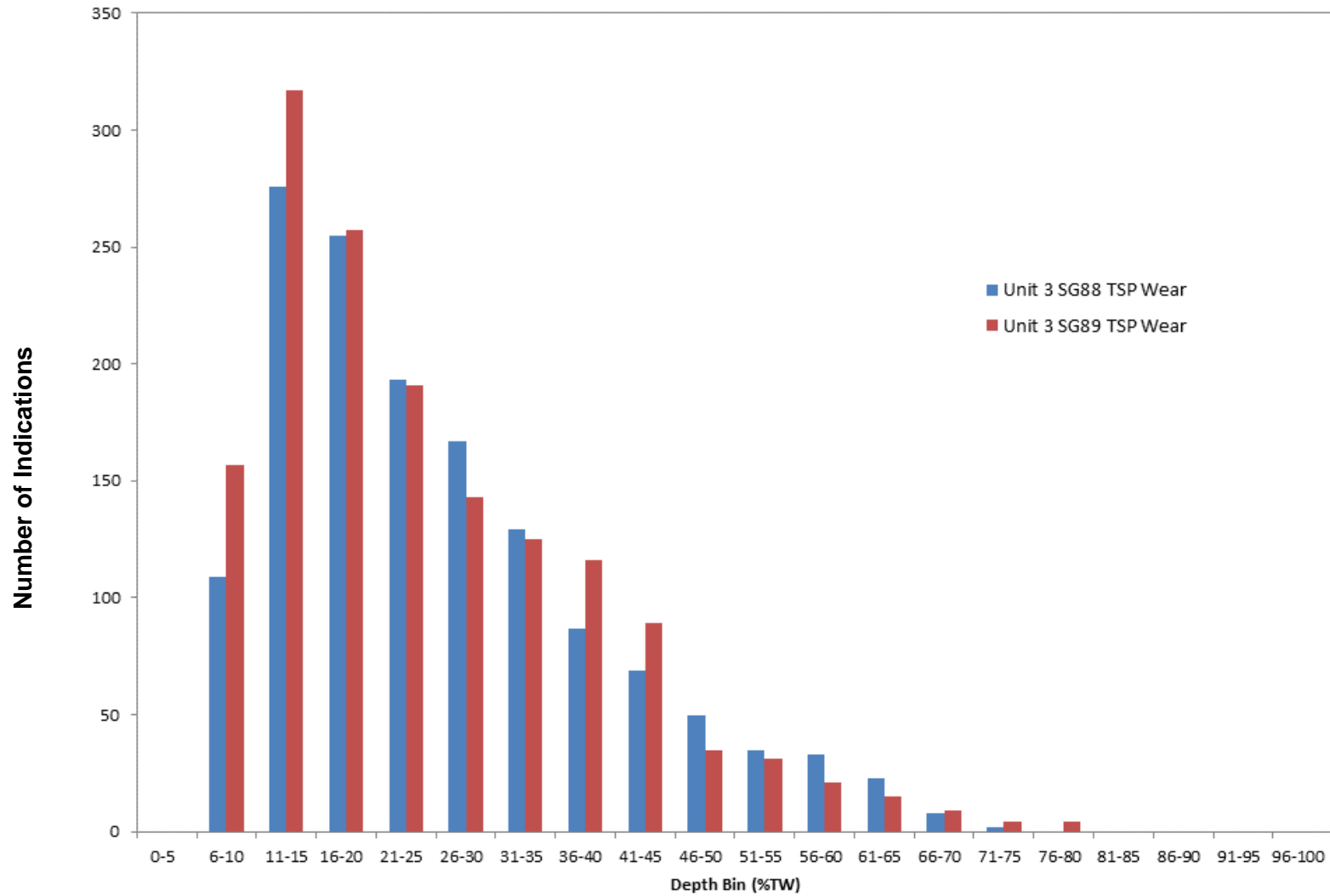
SONGS Unit 3 February 2012 Leaker Outage - Steam Generator Condition Monitoring Report

Figure 7-2: Comparison of Unit 2 and Unit 3 AVB Wear Depth Distribution (Indication Count)



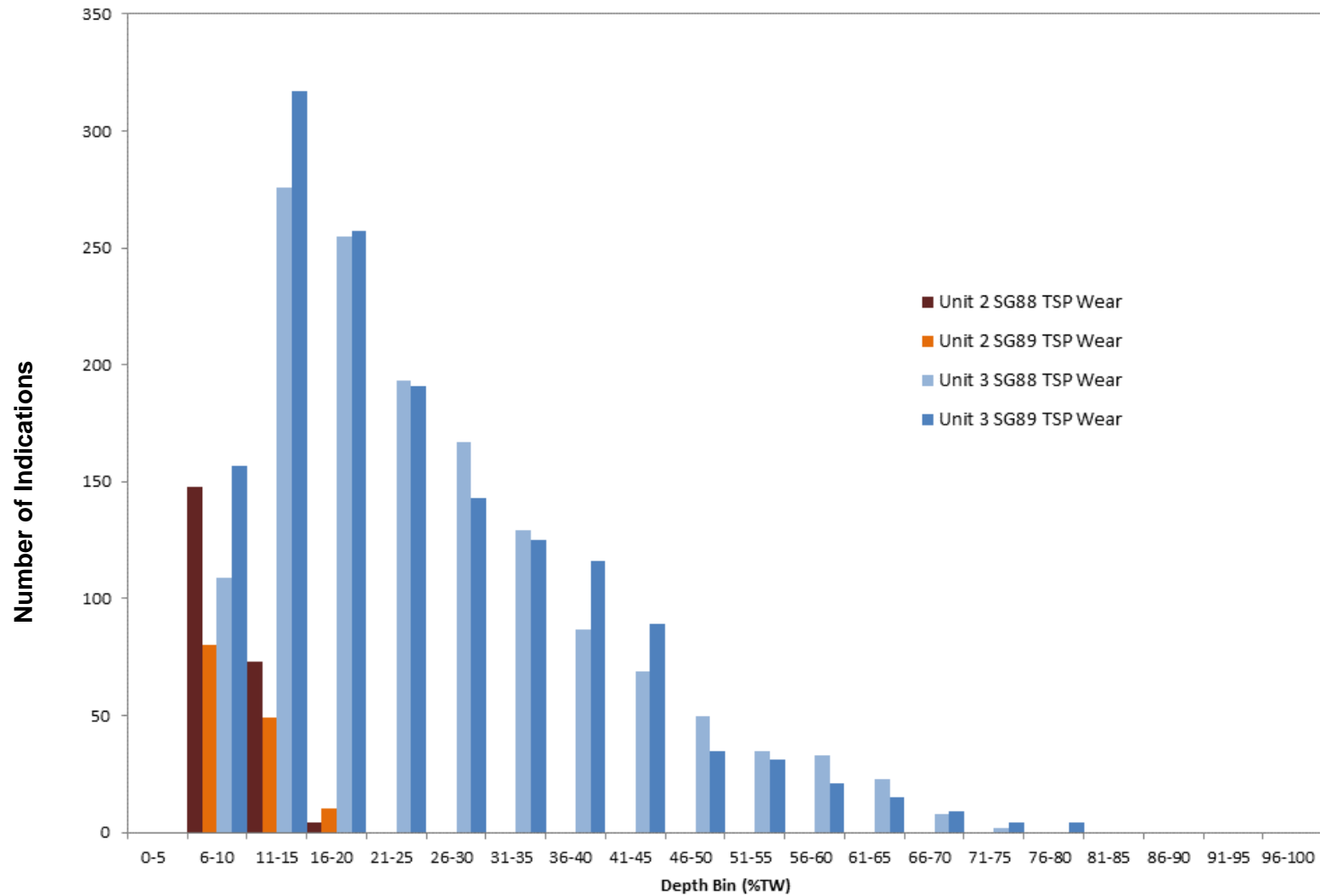
SONGS Unit 3 February 2012 Leaker Outage - Steam Generator Condition Monitoring Report

Figure 7-3: Unit 3 TSP Wear Depth Distribution (Indication Count)



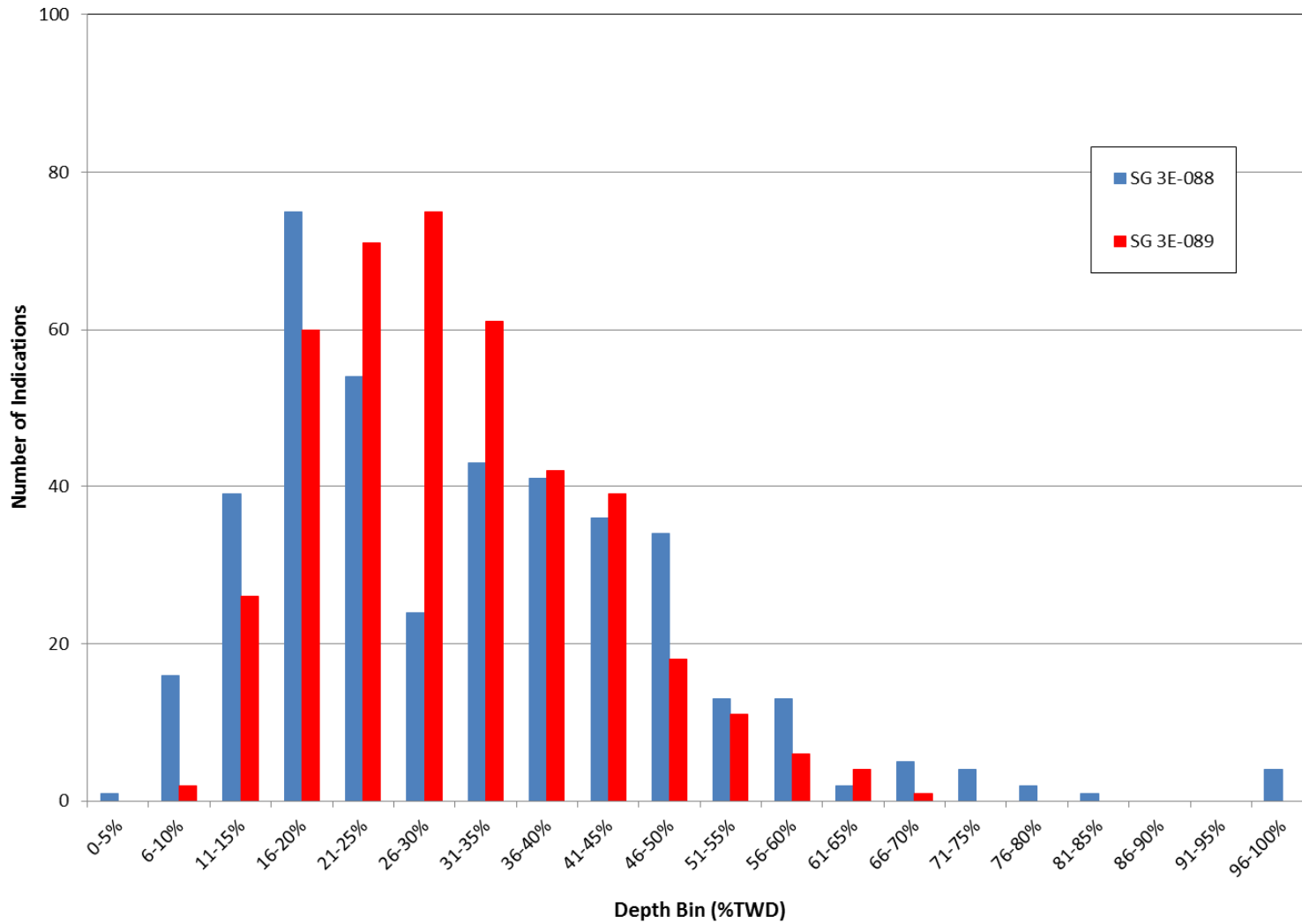
SONGS Unit 3 February 2012 Leaker Outage - Steam Generator Condition Monitoring Report

Figure 7-4: Comparison of Unit 2 and Unit 3 TSP Wear Depth Distribution (Indication Count)



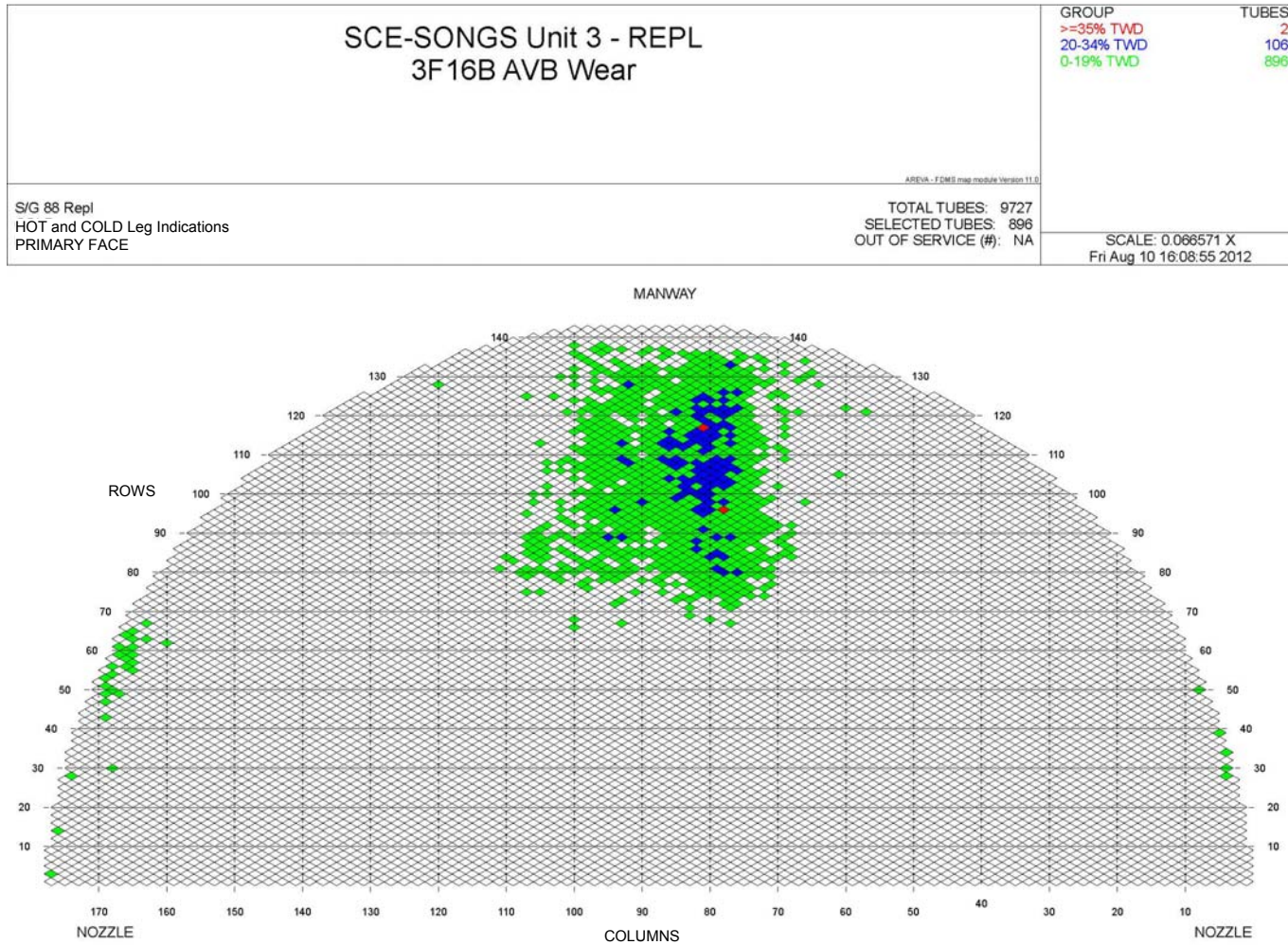
SONGS Unit 3 February 2012 Leaker Outage - Steam Generator Condition Monitoring Report

Figure 7-5: Unit 3 TTW Depth Distribution (Indication Count)



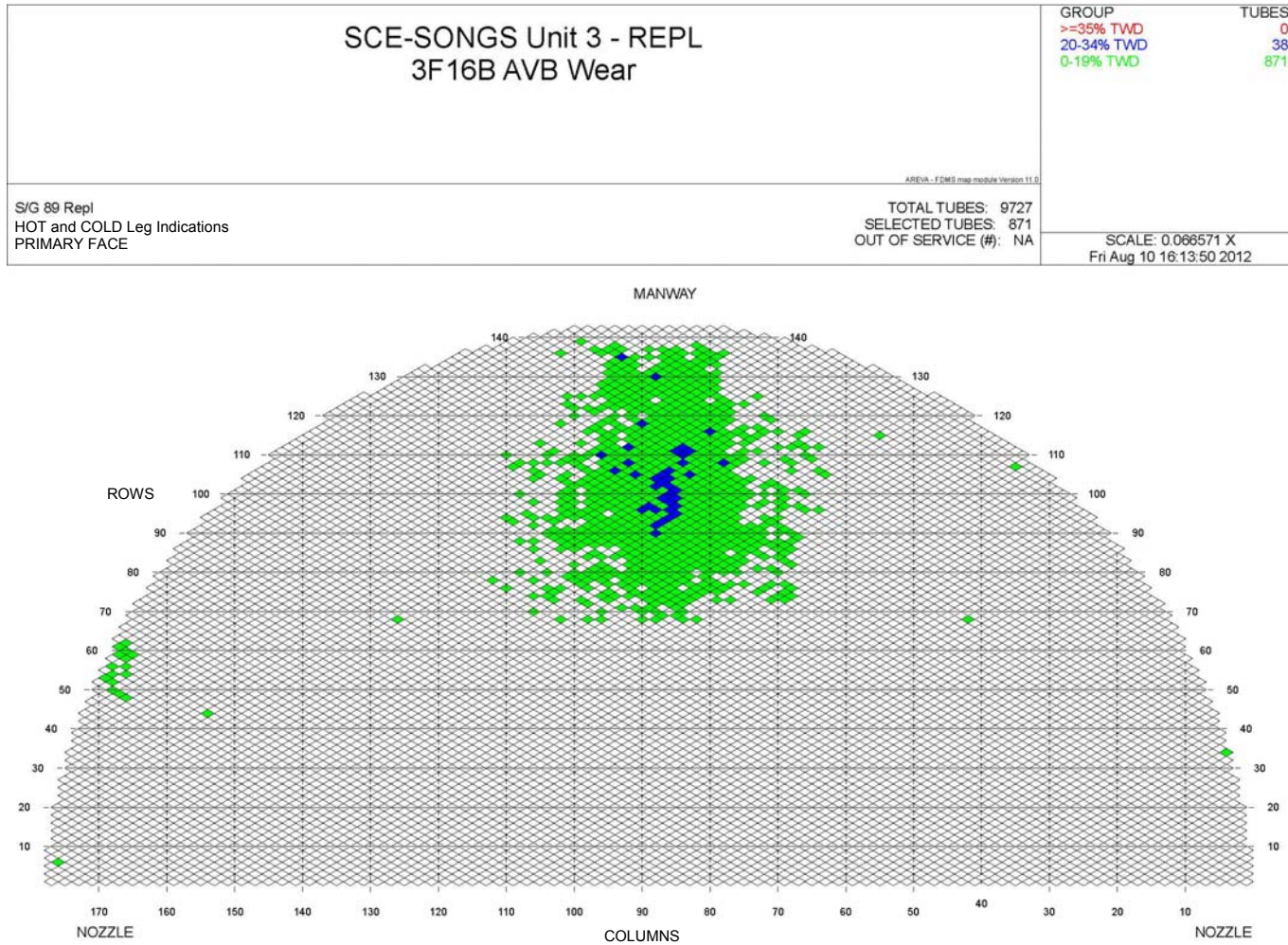
SONGS Unit 3 February 2012 Leaker Outage - Steam Generator Condition Monitoring Report

Figure 7-6: SG 3E-088 AVB Wear



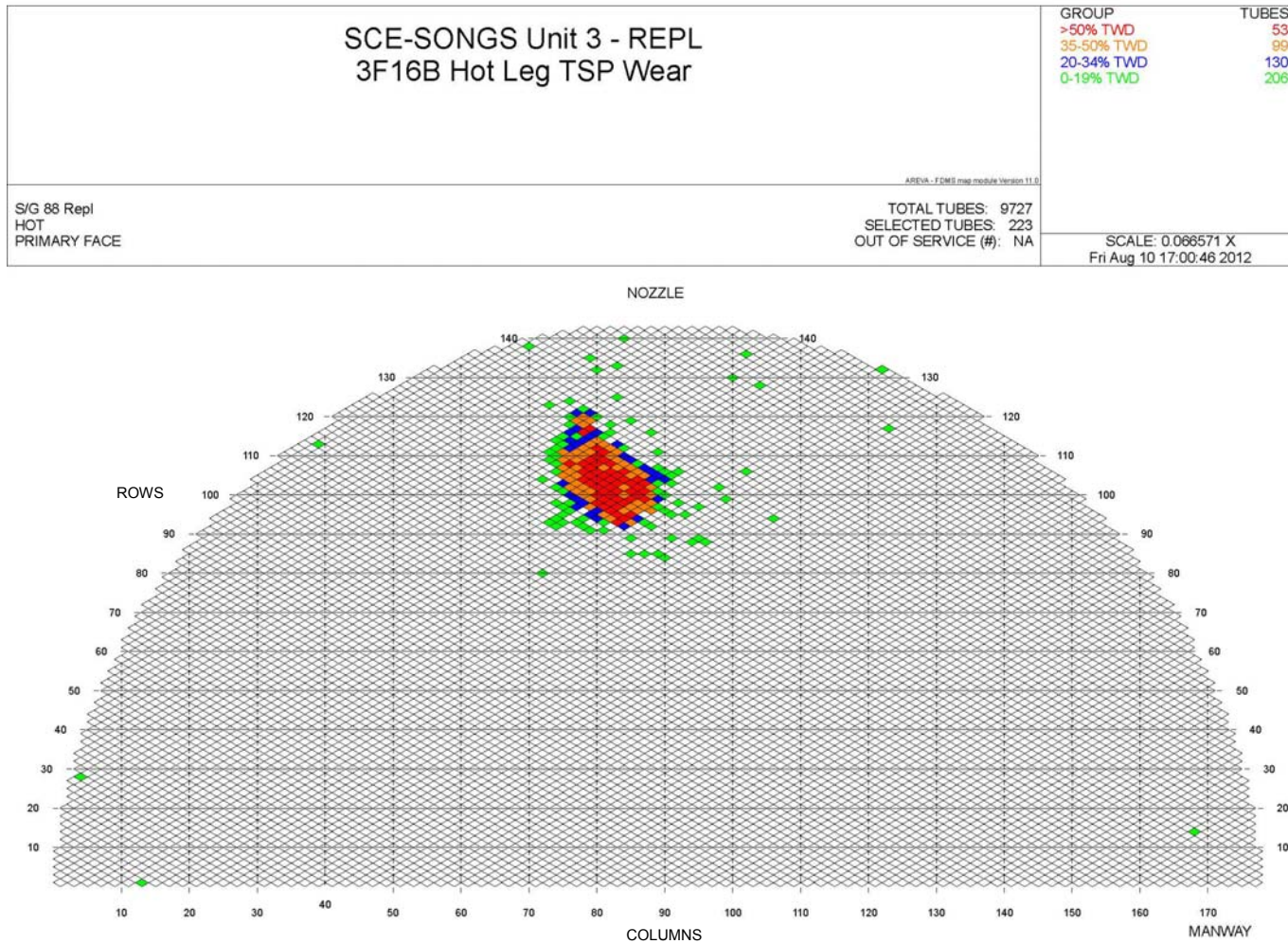
SONGS Unit 3 February 2012 Leaker Outage - Steam Generator Condition Monitoring Report

Figure 7-7: SG 3E-089 AVB Wear



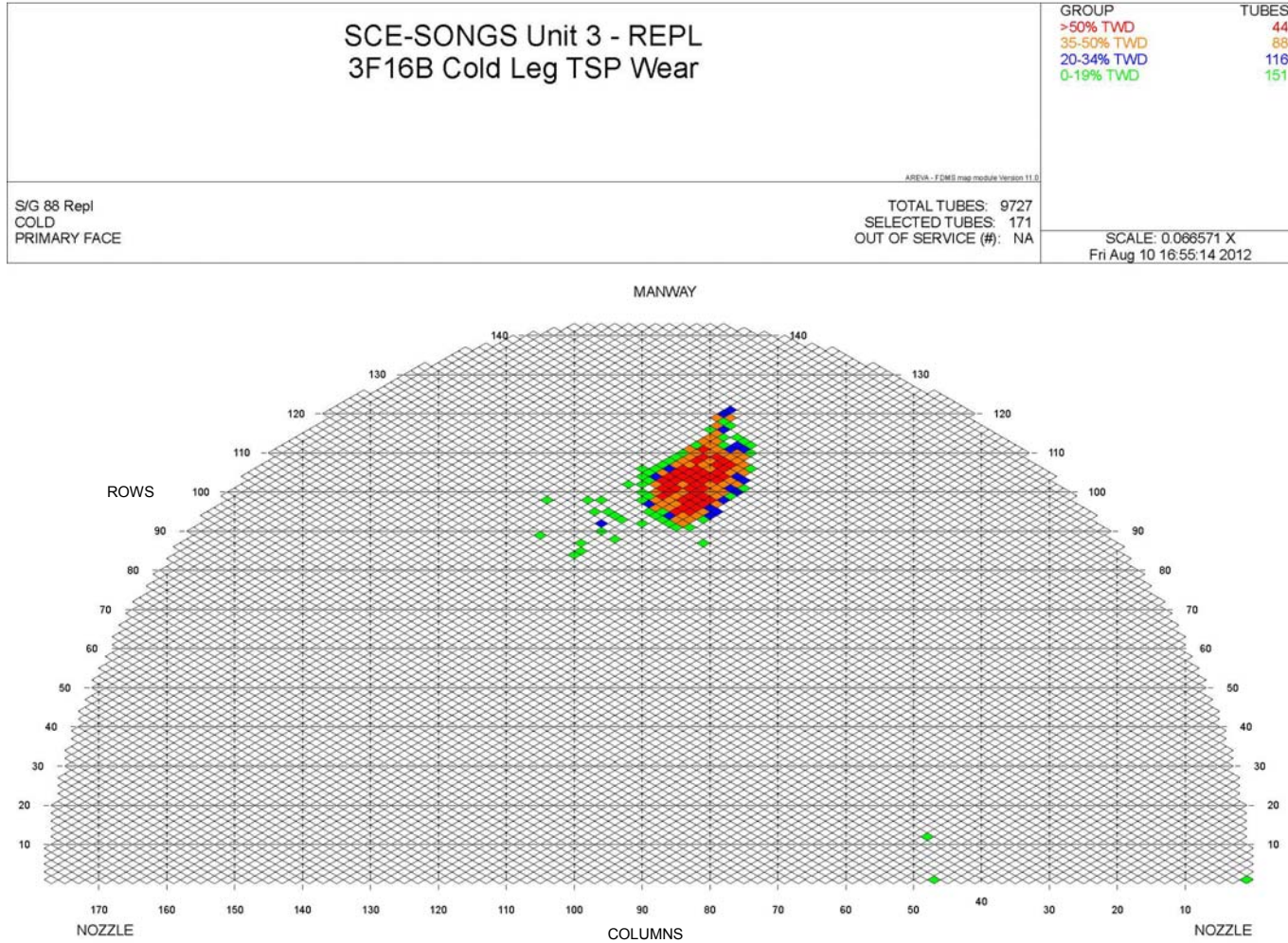
SONGS Unit 3 February 2012 Leaker Outage - Steam Generator Condition Monitoring Report

Figure 7-8: SG 3E-088 TSP Wear – Hot Leg



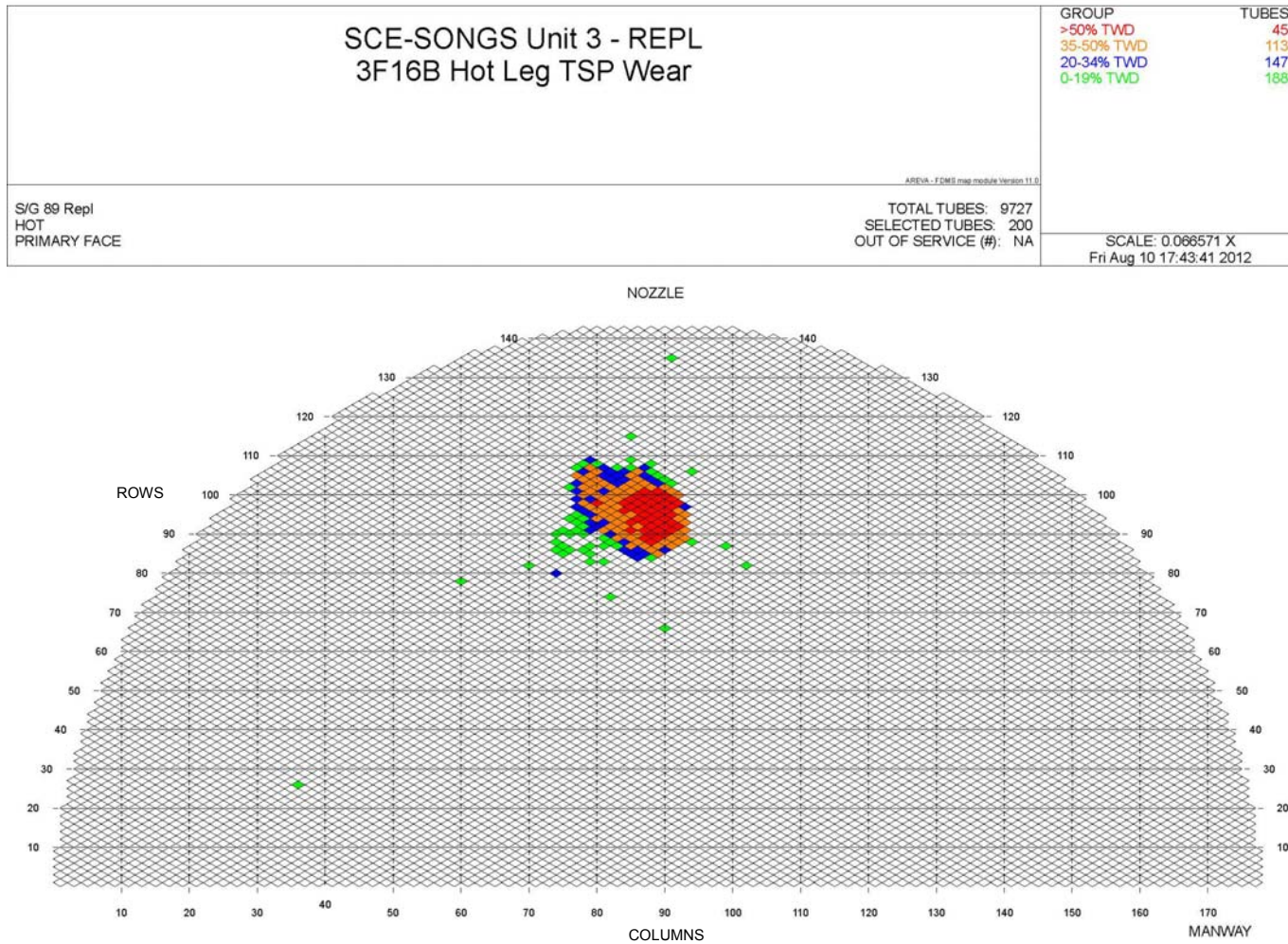
SONGS Unit 3 February 2012 Leaker Outage - Steam Generator Condition Monitoring Report

Figure 7-9: SG 3E-088 TSP Wear – Cold Leg



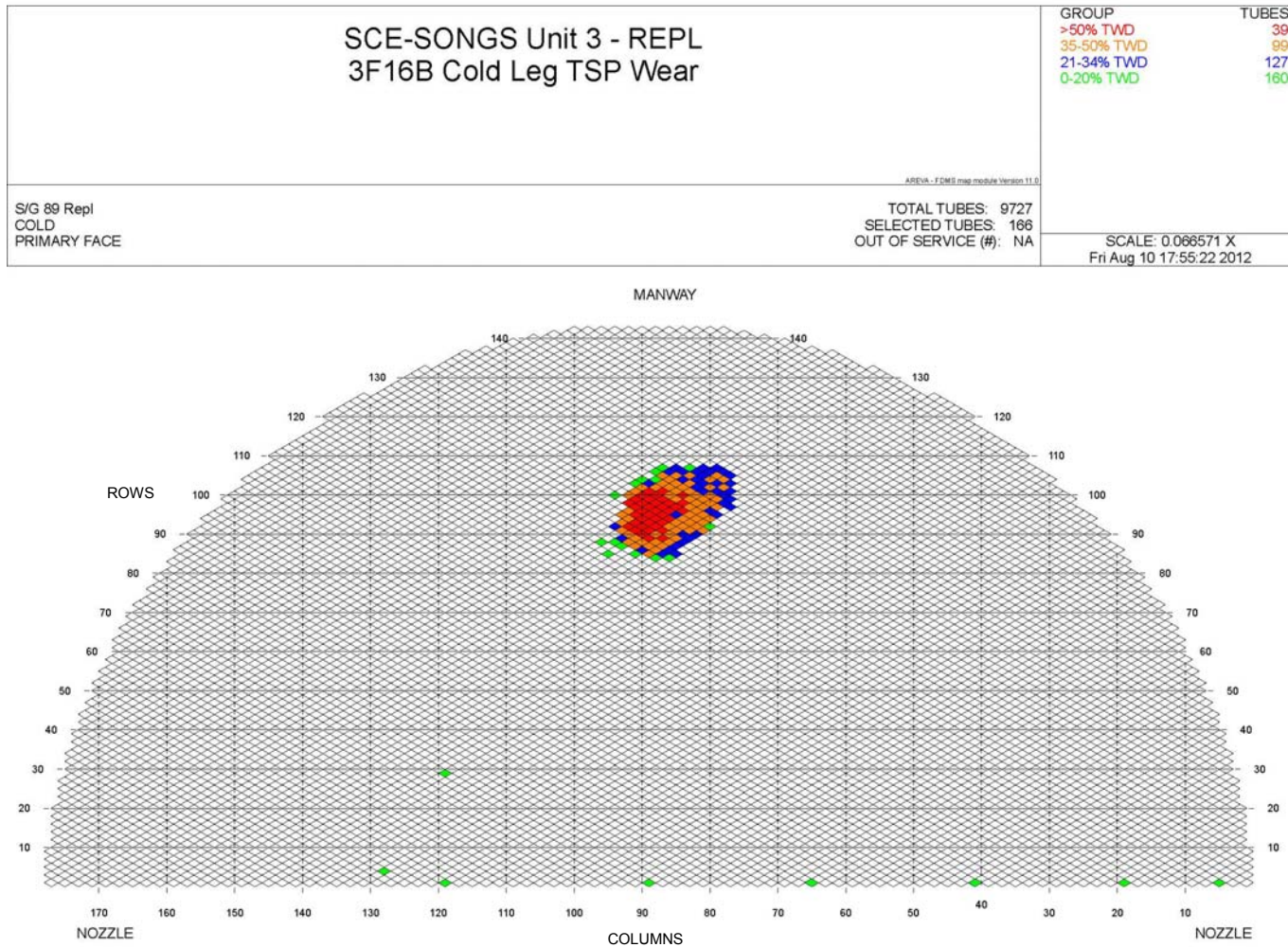
SONGS Unit 3 February 2012 Leaker Outage - Steam Generator Condition Monitoring Report

Figure 7-10: SG 3E-089 TSP Wear – Hot Leg



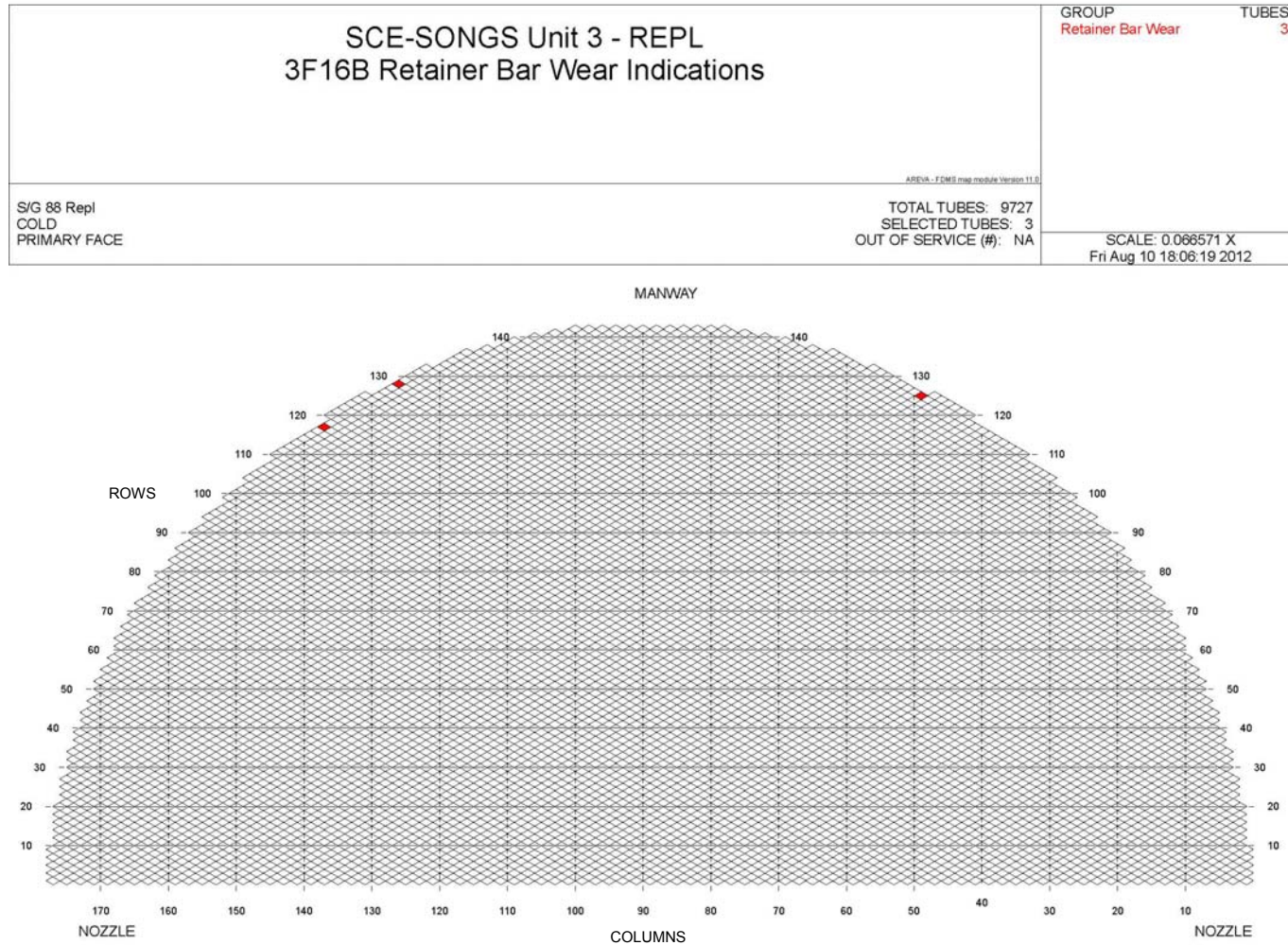
SONGS Unit 3 February 2012 Leaker Outage - Steam Generator Condition Monitoring Report

Figure 7-11: SG 3E-089 TSP Wear – Cold Leg



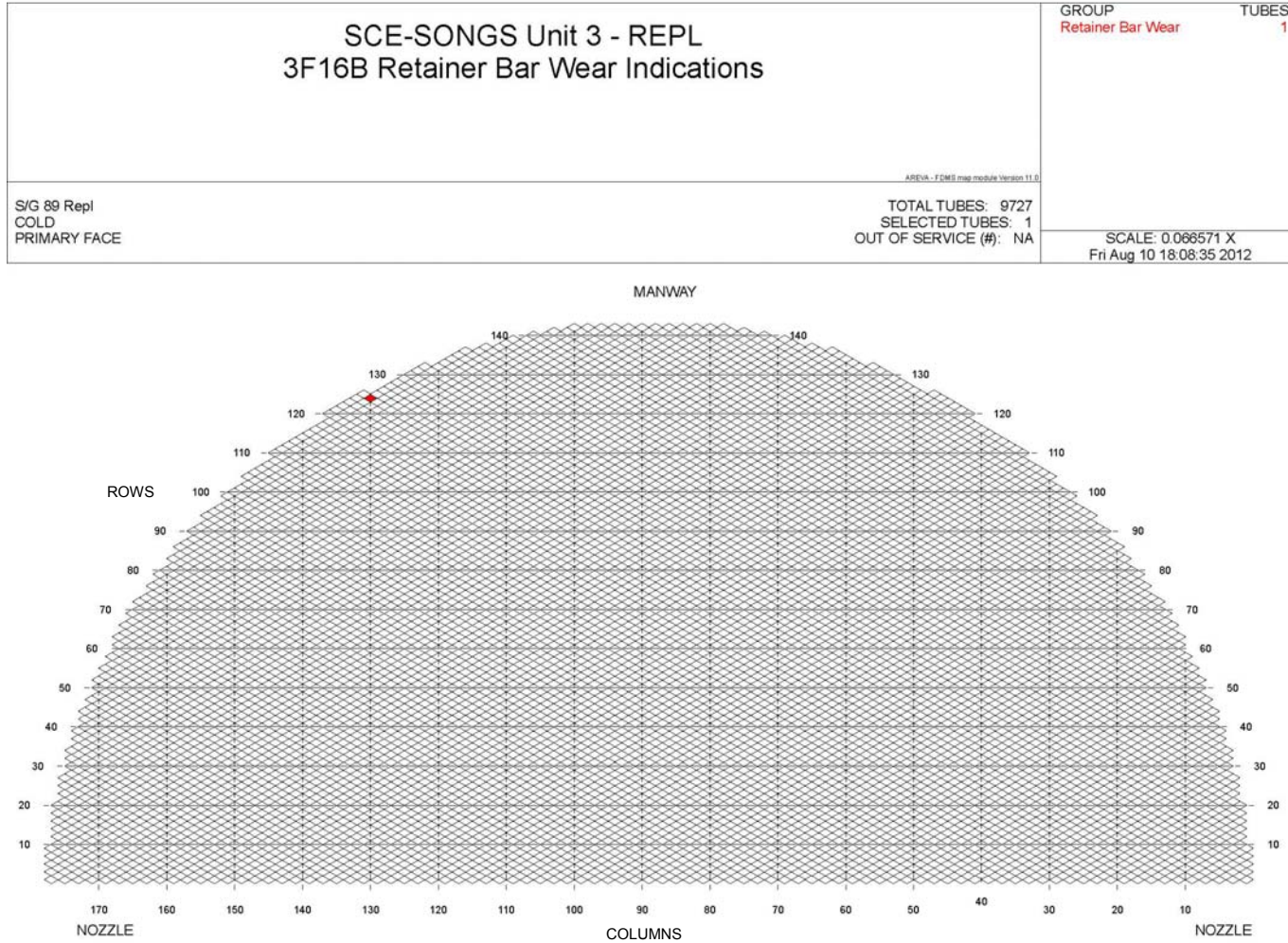
SONGS Unit 3 February 2012 Leaker Outage - Steam Generator Condition Monitoring Report

Figure 7-12: SG 3E-088 Retainer Bar Wear



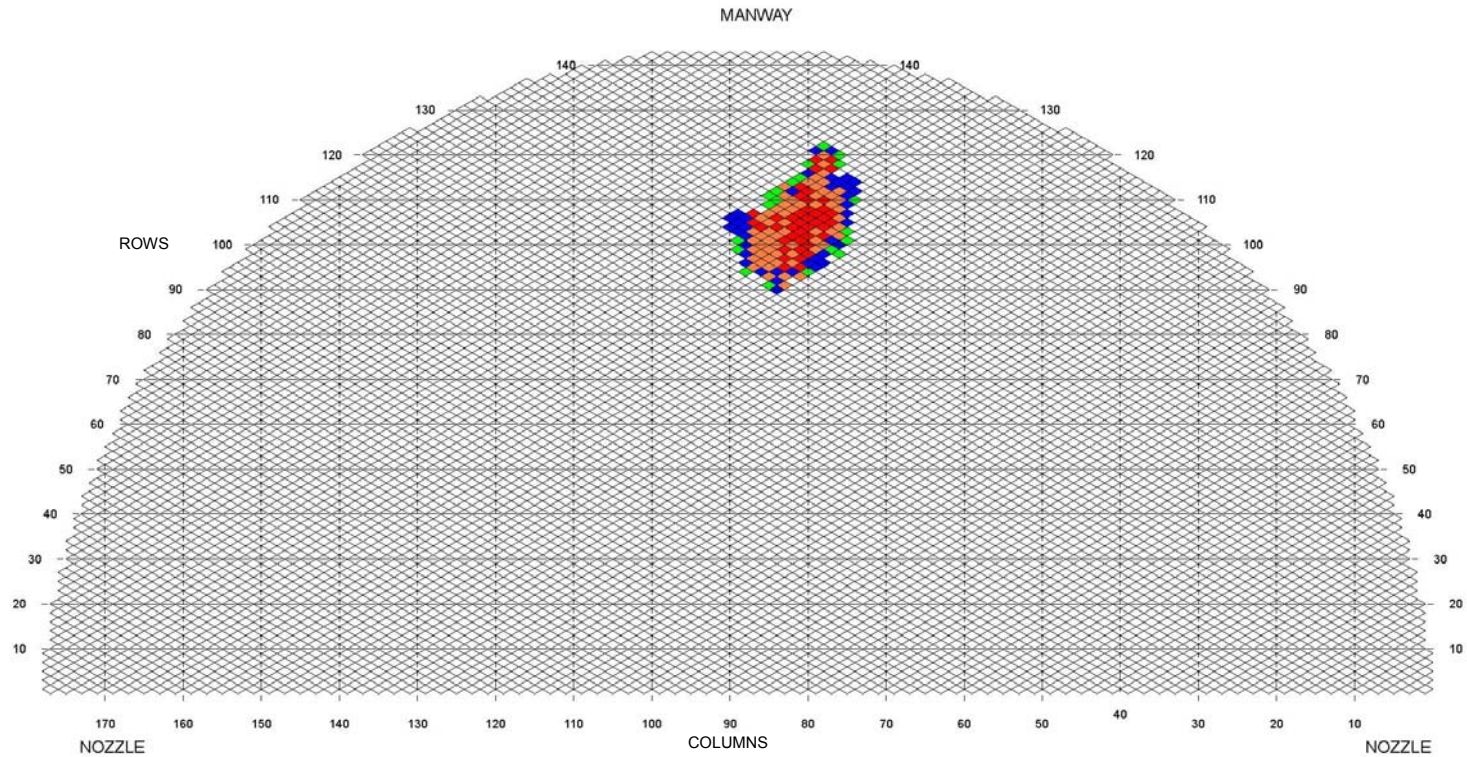
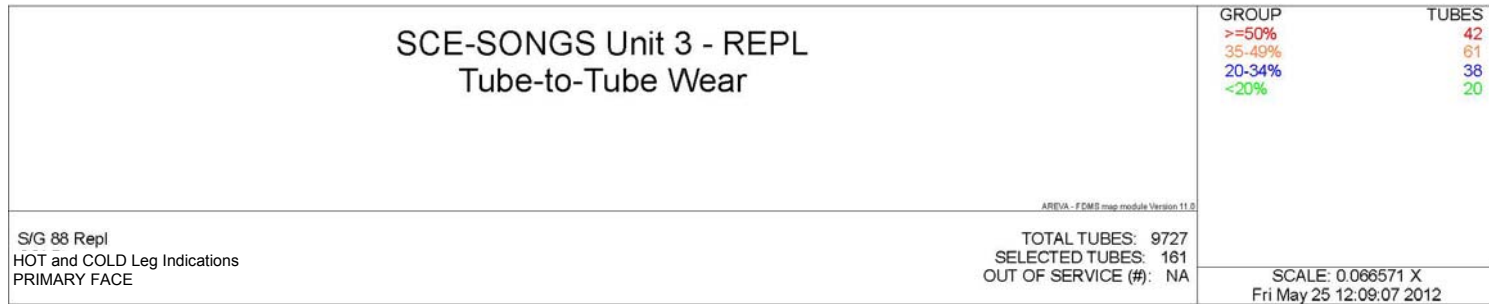
SONGS Unit 3 February 2012 Leaker Outage - Steam Generator Condition Monitoring Report

Figure 7-13: SG 3E-089 Retainer Bar Wear



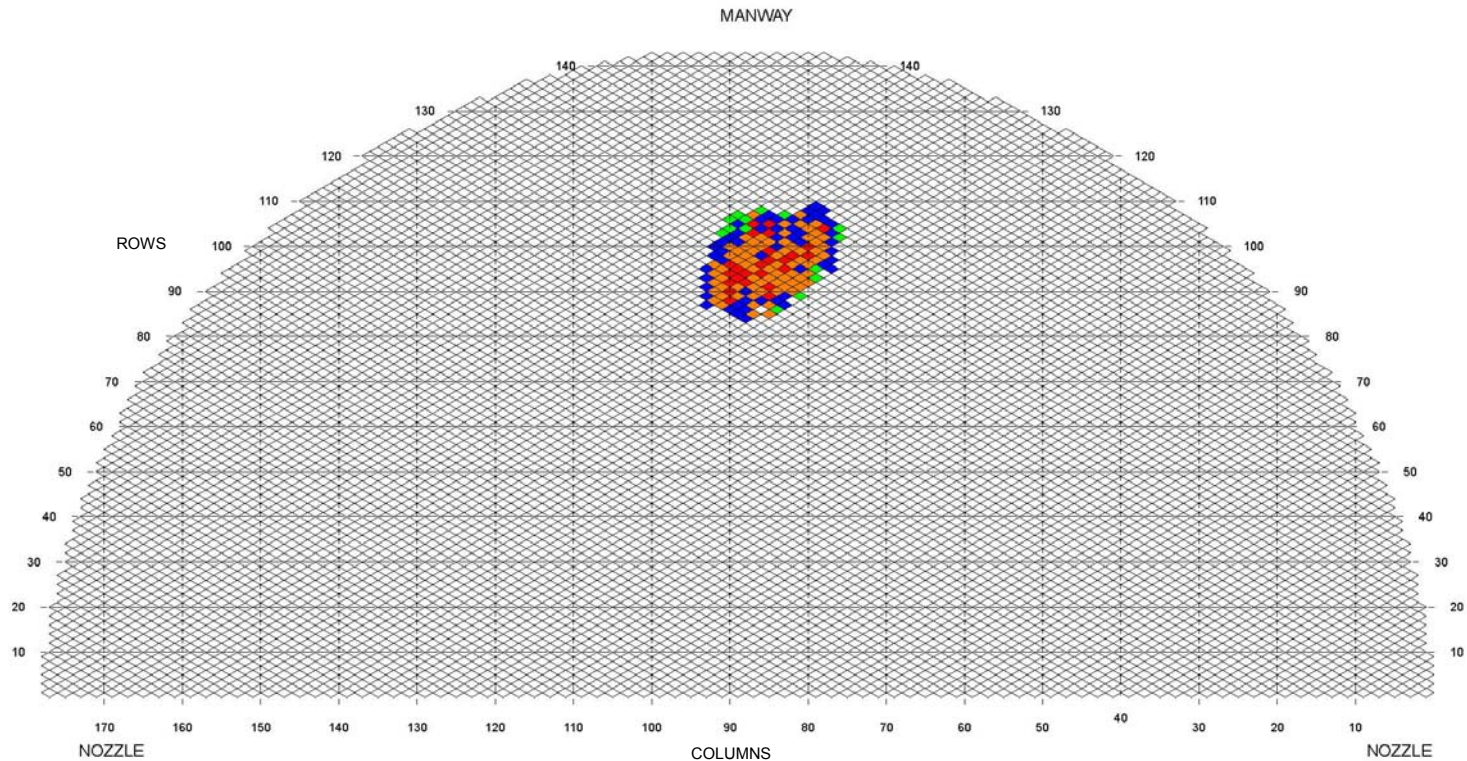
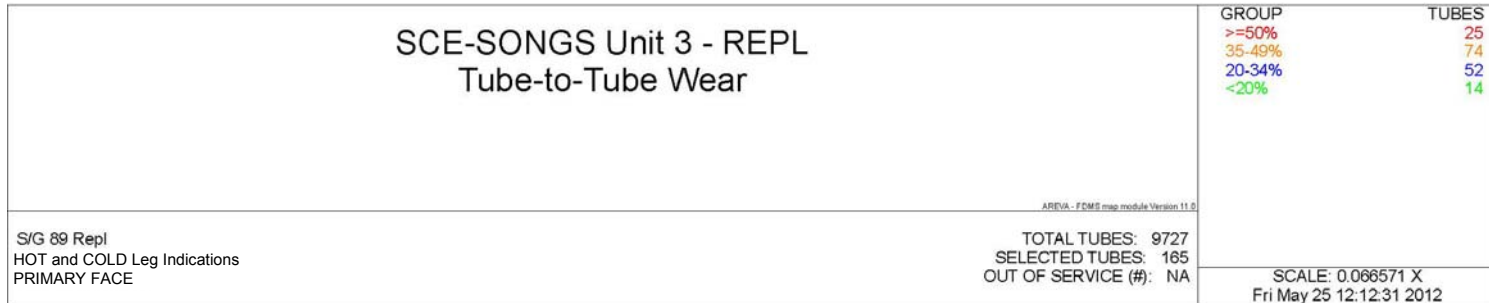
SONGS Unit 3 February 2012 Leaker Outage - Steam Generator Condition Monitoring Report

Figure 7-14: SG 3E-088 Tube-To-Tube Wear



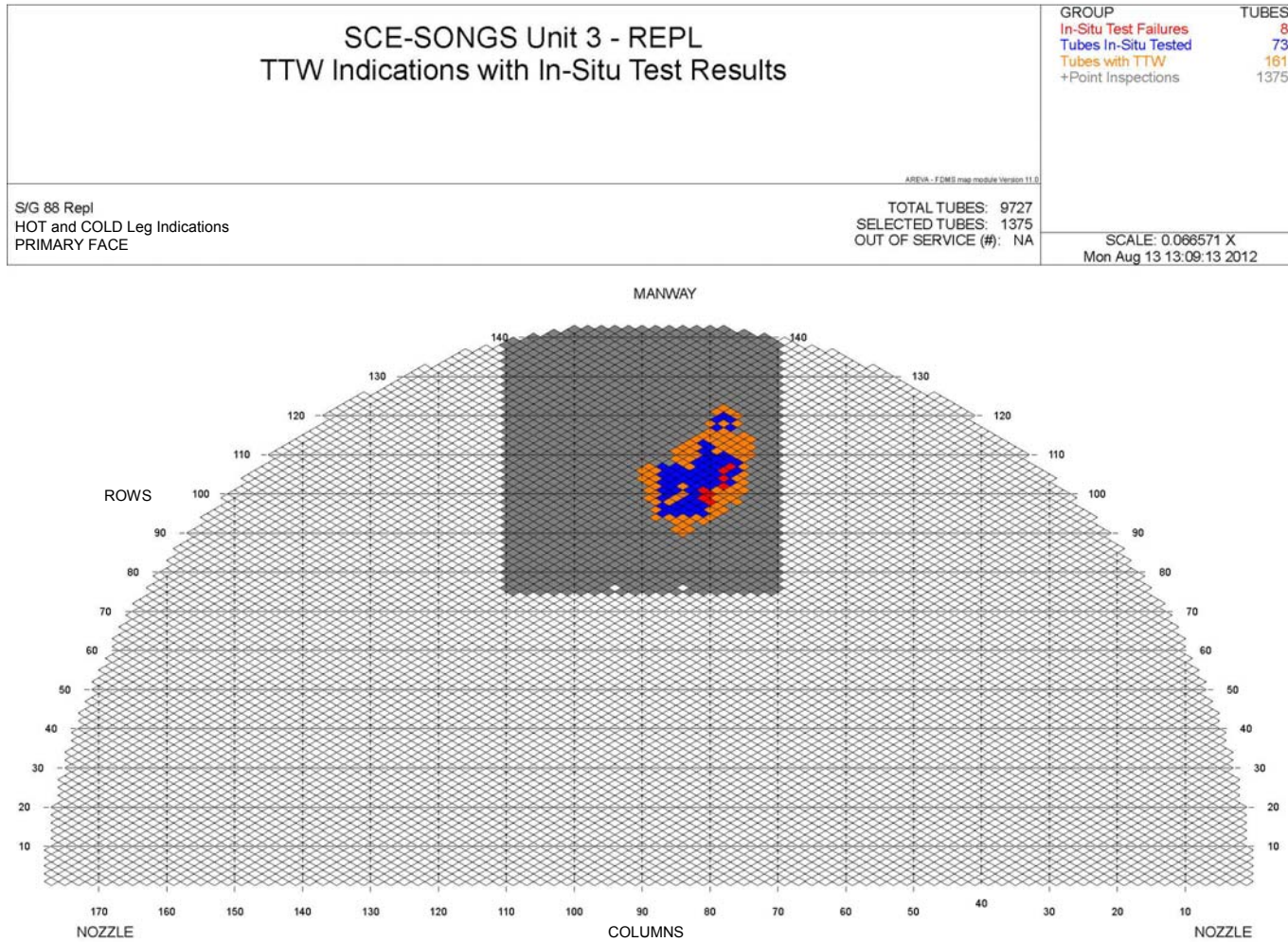
SONGS Unit 3 February 2012 Leaker Outage - Steam Generator Condition Monitoring Report

Figure 7-15: SG 3E-089 Tube-To-Tube Wear



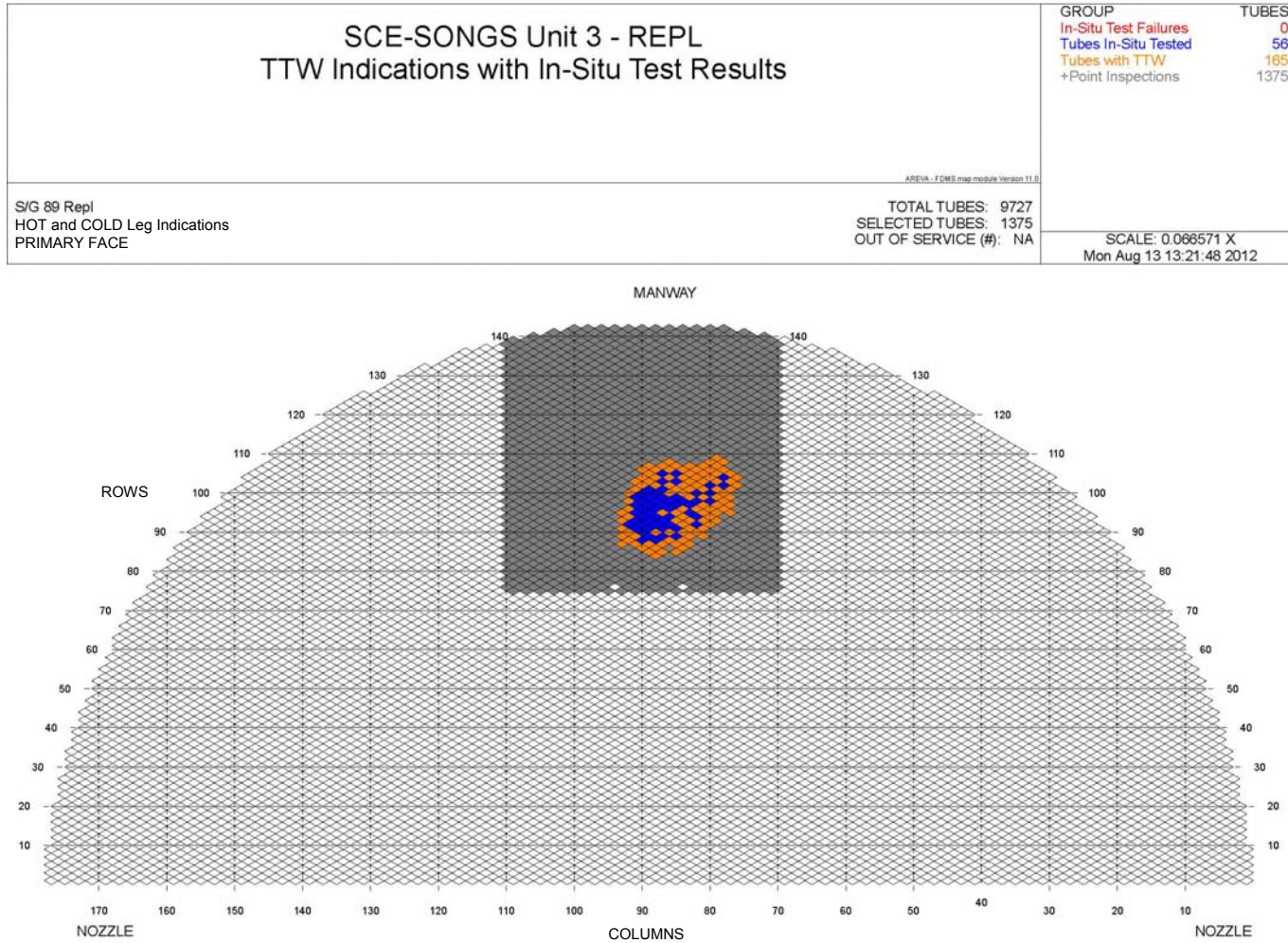
SONGS Unit 3 February 2012 Leaker Outage - Steam Generator Condition Monitoring Report

Figure 7-16: SG 3E-088 TTW Indications with In-Situ Results



SONGS Unit 3 February 2012 Leaker Outage - Steam Generator Condition Monitoring Report

Figure 7-17: SG 3E-089 TTW Indications with In-Situ Results



8.0 CONDITION MONITORING ASSESSMENT

In order to satisfy condition monitoring requirements, all degradation mechanisms detected during the Unit 3 leaker outage must meet the structural and leakage performance criteria described in Section 5.0. Assessment of operational leak integrity is based entirely on whether the operating leakage performance criterion (150 GPD) was exceeded during operation. Because the operating leak rate prior to the forced outage remained below the performance criteria, the operational leakage integrity criterion was met.

Assessment of the structural and accident-induced leakage integrity CM criteria can be performed either analytically or through in-situ pressure testing [3]. An analytical assessment is based upon the degradation mechanism's characteristics, including circumferential extent, axial length, and through-wall depth. In-situ pressure testing provides a means of physically determining whether a tube has met the structural integrity and accident-induced leakage performance criteria. It involves pressurizing a tube, or a locally degraded region within a tube, such that the applied loads are prototypical of the required performance criteria loads. The response of the tube during the test is a direct indicator of whether the tube satisfied the performance criteria. Because the required loading is imposed directly onto the tube under test, some of the uncertainties which must be conservatively represented in an analytical evaluation may be eliminated (in particular, NDE sizing, material strength, and burst equation uncertainties). This improves the likelihood of demonstrating compliance with the CM criteria.

Consistent with the structural integrity criteria described in Section 5.0, the limiting pressure loading occurs at a value of three times the normal operating differential pressure. For Unit 3 this value is 4260 psi [9]. In addition to pressure loads, the CM must also consider the impact of non-pressure accident loads if they could have a significant effect on the burst pressure of the degraded tubes. A review of the screening guidance of Section 3.7.2 of Reference 2 provides the basis for concluding that design-basis, non-pressure accident loads are not limiting for the identified tube wear in the Unit 3 SG tubes. Reference 2 indicates that the burst pressure of degradation less than 270° in circumferential extent at supports below the top TSP, and degradation with circumferential involvement less than 25 PDA (Percent Degraded Area) anywhere in the tube bundle; will not be significantly affected by non-pressure loads. Although significant tube degradation was identified during the forced outage, the circumferential involvement of all degradation was less than 25 PDA. Consequently, the limiting loading scenario for the evaluation of structural integrity is that involving pressure loads only (i.e., three times the normal operating differential pressure). The accident-induced leakage performance criteria must also be assessed, and in addition to the Steam Line Break (SLB) pressure (2560 psi), must also consider non-pressure loads where appropriate. This is discussed in more detail within this section.

In order for a degraded tube to be returned to service, the degradation must be measured using a qualified ECT sizing technique, and the degradation must be evaluated as acceptable for continued operation. The sizing techniques qualified for use at SONGS Unit-3 are identified in the degradation assessment [6] and are detailed in the ECT technique site validation documents [7][13]. If a degradation mechanism cannot be sized with appropriate sizing confidence, it is plugged upon detection. All degradation identified during the current outage was measured with a qualified ECT technique.

This was the first in-service inspection of the SONGS Unit 3 SG tubes; performed after 338 EFPD of operation following SG replacement. The potential for AVB, TSP, and retainer bar wear to develop was recognized prior to the examination. However, the occurrence and severity of tube-to-tube wear was

SONGS Unit 3 February 2012 Leaker Outage - Steam Generator Condition Monitoring Report

not expected. Although the examination program as planned was fully capable of detecting this mechanism, the Degradation Assessment [6] was revised during the outage to include this new mechanism.

8.1 Input Parameters

Table 8-1 and Table 8-2 identify the input parameters used to perform the condition monitoring assessment. In particular, these inputs were used within the AREVA Mathcad tool which implements the SG Flaw Handbook equations [8], in order to generate the limit curves discussed in the following sections. The 4260 psid 3 NOPD value is based on a conservative assessment of Unit 3 secondary side steam pressure as measured during cycle 16.

Table 8-1: SONGS Unit-3 Steam Generator Input Values

<i>Parameter</i>	<i>Value</i>
Desired probability of meeting burst pressure limit	0.95
Tubing wall thickness	0.043 inch, [7]
Tubing outer diameter	0.750 inch, [7]
Mean of the sum of yield and ultimate strengths at temperature	116440 psi, [10]
Standard deviation of the sum of yield and ultimate strengths	2460 psi, [10]
3 X Normal Operating Pressure Differential (3 NOPD)	4260 psid, [9]
MSLB Pressure Differential	2560 psid, [18]
EFPD from SG Replacement through U3 2/12 Leaker Outage	338 EFPD, [9]
Expected EFPD from U3 2/12 Leaker Outage to EOC16	252 EFPD, [9]]

SONGS Unit 3 February 2012 Leaker Outage - Steam Generator Condition Monitoring Report

Table 8-2: Eddy Current ETSS Input Values [5]

<i>Parameter</i>	<i>ETSS 96004.1</i>	<i>ETSS 27903.1</i>	<i>ETSS 27902.2</i>	<i>ETSS 96910.1</i>
Probe Type	Bobbin Coil	+Point™	+Point™	+Point™
NDE depth sizing regression parameters	Slope = 0.98 Intercept = 2.89 %TW	Slope = 0.97 Intercept = 2.80 %TW	Slope = 1.02 Intercept = 0.94 %TW	Slope = 1.01 Intercept = 4.30 %TW
NDE depth sizing technique uncertainty (standard deviation)	4.19 %TW	2.11 %TW	2.87 %TW	6.68 %TW
NDE depth sizing analysis uncertainty (standard deviation)	2.10 %TW	1.06 %TW	1.44 %TW	3.34 %TW
Total NDE (Sizing and Technique) (standard deviation)*	4.69 %TW	2.36 %TW	3.22 %TW	7.48 %TW

* Total uncertainty is the technique and analysis uncertainties combined via the square root of the sum of the squares.

8.2 Evaluation of Structural and Leakage Integrity

8.2.1 AVB Wear

AVB wear was evaluated with the flaw model described in Reference 4 as “axial part-throughwall degradation < 135° in circumferential extent.” The maximum circumferential extent of a single 100%TW wear scar formed by a long flat bar positioned tangentially to the tube surface (e.g., an AVB) is 55.4°. For double-sided AVB wear the total circumferential extent for this limiting case would be well below the 135° limit established by this model; hence, this flaw model is appropriate for AVB wear. In addition, the AVB geometries provide sufficient circumferential separation between the wear scars to permit each indication to be treated separately. The separation between centerline contact points for AVB wear is 180° and results in negligible circumferential interaction between separate wear locations in the same axial plane of the tube.

The topic of external loads must be addressed. As discussed earlier it has been established that due to the limited circumferential involvement of the AVB wear (i.e., <25 PDA), external loads present during design basis accidents, with required margins of safety, are less limiting than normal operating pressure loads evaluated with a safety factor of three. Hence external loads need not be included in the evaluation of AVB wear burst integrity.

 SONGS Unit 3 February 2012 Leaker Outage - Steam Generator Condition Monitoring Report

The bobbin probe was used to measure the depth of AVB wear through the application of ETSS 96004.1. A CM limit curve for AVB wear based upon ETSS 96004.1 and the parameters provided in Table 8-1 and Table 8-2 is provided in Figure 8-1. This figure also includes the throughwall depth of each indication reported. The five largest indications are plotted at their measured axial length, while the rest are plotted at the assumed axial length of 1.8 inches. The assumed flaw length for AVB wear indications was derived from measurements taken on over 350 AVB wear indications in the Unit 3 SGs, wherein the maximum indicated length was 1.59 inches. The field of the eddy current probe extends beyond the dimensions of the coil and thus the probe will sense a flaw before the coil is physically over the flaw. This effect occurs on both ends of the flaw, and the effect becomes more significant as the flaw depth increases. This phenomenon is known as “probe look-ahead” and the net effect is that the axial length reported for a wear flaw will normally be longer than the actual flaw length. Because the above AVB wear measurements were not adjusted downward to reflect the impact of ECT probe look-ahead, these measurements are considered to be appropriately conservative.

Because all AVB wear lies below the CM limit curve, it is concluded that the structural integrity performance criterion was satisfied with respect to AVB wear during the operating period preceding the forced outage.

AVB wear must also be evaluated against the accident-induced leakage performance criterion (AILPC). Under accident conditions, pressure and/or mechanical loading can lead to mechanical tearing of partial depth degradation to create a 100% throughwall leak path. This mechanical tearing is referred to as “pop-through”. Pop-through does not constitute a tube burst in regards to tube integrity but is important when determining leakage integrity.

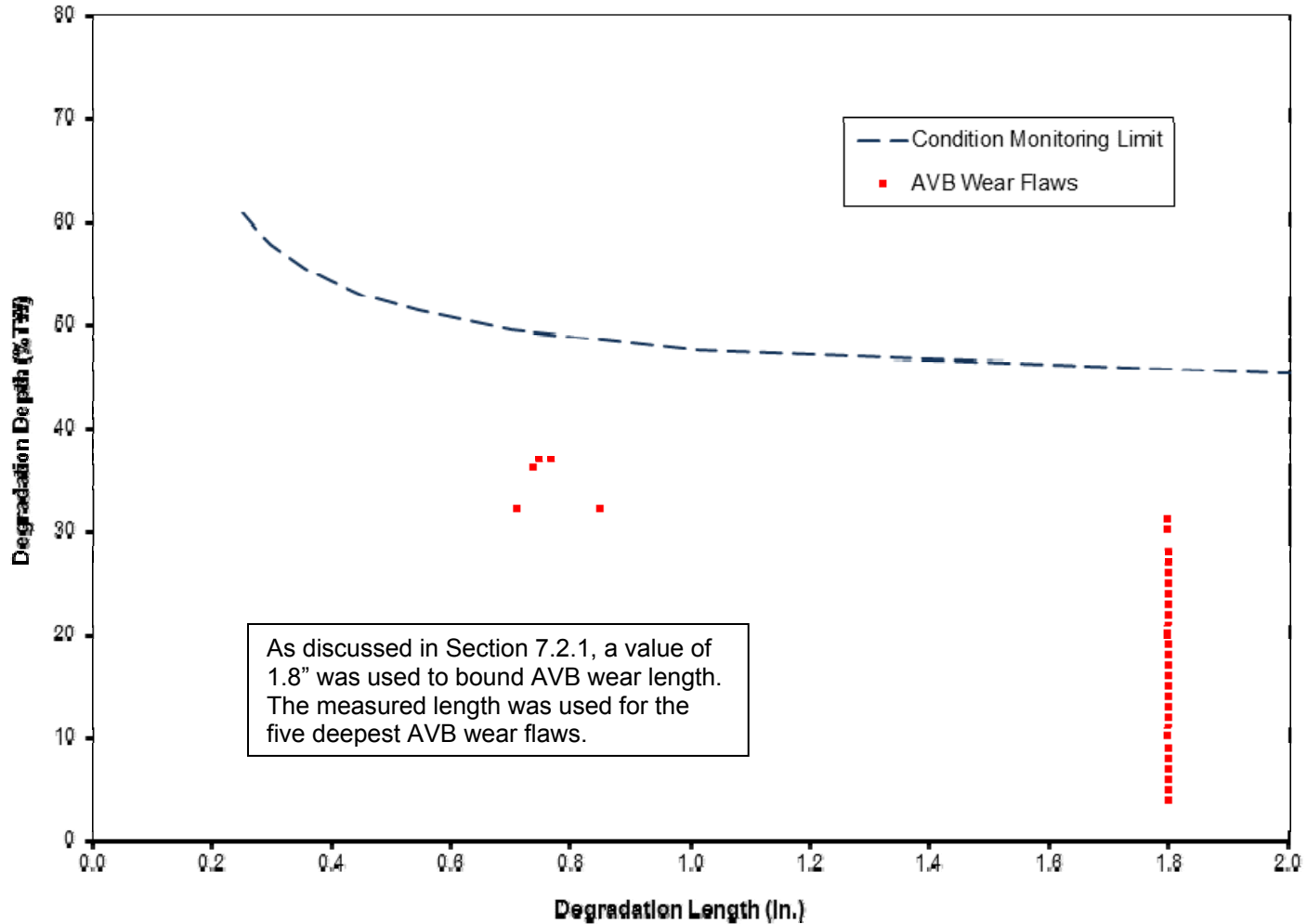
AVB wear resides on the tube flanks (sides facing adjacent columns - not intrados or extrados) where bending stresses resulting from in-plane motion during analyzed events are negligible. In a typical RSG design, limited out-of-plane motion also produces negligible bending stress at the flanks. For the SONGS U-bend support design, moderate out-of-plane bending moments are anticipated during a design basis earthquake (DBE) [12], which would produce bending stress in the limiting tube flanks of approximately 8,500 psi.

The pressure at which circumferential pop-through and leakage will occur in the presence of pressure and external loads may be evaluated using the methods described in Section 9.6.1 of Reference 2. The maximum depth of identified AVB wear was 37%TW. Adjusting upwards to conservatively account for ETSS 96004.1 sizing uncertainty yields an upper bound estimate of 47%TW. Assuming that this limiting AVB wear flaw has a circumferential extent of 55.4° (see earlier discussion), and is subjected to a 20 ksi bending stress, circumferential pop-through would not occur at or below MSLB pressure. Consequently, it is concluded that external loads do not lead to failure to satisfy the AILPC in the circumferential orientation.

Volumetric degradation that is predominantly axial in orientation and is greater than 0.25 inch long will leak and burst at essentially the same pressure per section 9.6.3 of Reference 2. The Unit 3 AVB wear indications meet this description. Since the earlier evaluation demonstrated that the AVB wear identified during the current outage satisfied the burst integrity criteria at a pressure of 4260 psid, the leakage integrity of AVB wear at the much lower MSLB pressure differential of 2560 psid is also demonstrated by that evaluation. Hence, all of the AVB wear indications satisfied the SONGS AILPC during the operating period prior to the leaker outage.

SONGS Unit 3 February 2012 Leaker Outage - Steam Generator Condition Monitoring Report

Figure 8-1: CM Limit for AVB Wear, Both SGs, ETSS 96004.1



8.2.2 TSP wear

TSP wear was evaluated with the flaw model described in Reference 4 as “axial part-throughwall degradation < 135° in circumferential extent.” The maximum circumferential extent of a single 100%TW wear scar formed by a long flat bar positioned tangentially to the tube surface (e.g., a TSP land contact) is 55.4°. For double- or triple-sided TSP wear this model is bounding because the TSP geometry provides sufficient circumferential separation between the wear scars to permit each indication to be treated separately. The separation between centerline contact points for TSP wear is 120°, and results in negligible circumferential interaction between separate wear locations in the same axial plane of the tube. With respect to external loads, each wear flaw at the same support elevation may be treated individually. An individual TSP wear flaw with a depth of 100%TW and a circumferential extent of 55.4° would be less than 16 PDA. Because the circumferential involvement of this limiting flaw is less than 25 PDA, external loads need not be considered in the evaluation of burst integrity for TSP wear.

The bobbin probe was used to estimate the depth of TSP wear through the application of ETSS 96004.1. A CM limit curve for TSP wear based upon ETSS 96004.1 and the parameters provided in Table 8-1 and Table 8-2, is provided in Figure 8-2. This figure also includes the throughwall depth of each indication reported. Indications for which axial length measurements were available are plotted using the bobbin-measured lengths. The rest of the indications are plotted at an assumed axial length of 1.8 inches. This value was derived from measurements taken on over 400 TSP wear indications in the Unit 3 SGs, wherein the maximum indicated length was 1.6 inches. Because these measurements were not adjusted downward to reflect the impact of ECT probe look-ahead, and because the actual flaw length is expected to be limited to the TSP thickness (1.38”), this assumption is considered to be appropriately conservative.

Figure 8-2 illustrates that a substantial number of TSP wear indications exceeded the CM limit. However, this result is based upon bobbin probe estimates of maximum indication depth, assumed to occur over the entire bounding indication length. This is a very conservative approach.

All TSP wear indications with bobbin depths $\geq 20\%$ TW were inspected with +Point™. All +Point™ indications measuring $\geq 38\%$ TW had axial depth profiles performed. The depth profiles were used to calculate each indication’s structurally equivalent depth and length. The structural depth and length correspond to a rectangular flaw which would burst at the same pressure as would a flaw having the measured depth profile. The measurements were performed using +Point™ probe ETSS 96910.1, and the structurally equivalent dimensions were determined using the methods described in Section 5.1.5 of Reference 4.

CM limit curves for TSP wear based upon ETSS 96910.1 are provided for SG 3E-088 and SG 3E-089 in Figure 8-3 and Figure 8-4, respectively. This figure also depicts the structural dimensions of all indications for which axial depth profiling was performed, including those that exceeded the CM curve in Figure 8-2. Note that any given TSP elevation may have multiple wear flaws (i.e., at more than one land contact) and one of the flaws is typically deeper than the others. Since, in some cases, depth profiling was performed on all of the flaws at a given TSP elevation, the figures include many TSP wear indications of lesser significance than those that exceeded the CM curve in Figure 8-2.

The use of structurally equivalent dimensions provides the highest likelihood of analytically demonstrating compliance with the CM structural performance criteria. However, as illustrated in

 SONGS Unit 3 February 2012 Leaker Outage - Steam Generator Condition Monitoring Report

Figure 8-3 and Figure 8-4, many TSP wear indications exceeded the CM curve thus; satisfaction of the CM criteria could not be analytically demonstrated. Consequently, all of the TSP wear flaws that exceeded the CM limit were subjected to in-situ pressure testing in an attempt to demonstrate CM criteria compliance.

Figure 8-5 and Figure 8-6 summarize the results of in-situ testing of TSP wear flaws in each SG. All tested TSP wear in SG 3E-089 satisfied the structural integrity and accident leakage performance criteria. In SG 3E-088 a number of indications could not be tested to the required pressure levels because more limiting TTW in the same tube failed below the target pressure thus terminating the test. These indications are depicted in Figure 8-5 as “Incomplete.” In the absence of a successful in-situ pressure test, those indications identified as incomplete which lie above the CM curve must be considered to be CM structural integrity performance criteria (SIPC) failures. These indications are listed in Table 8-3.

All but four of the TSP wear indications listed in Table 8-3 were successfully tested at the MSLB hold point without leakage, thereby satisfying the AILPC. Compliance with the AILPC could not be demonstrated through in-situ testing for the four indications identified as “In Situ Test Indeterminate” due to the failure of a TTW flaw in the same tube.

Of the four, the indication at location SG 3E-088 R106 C78 07H-1 is the most limiting from a pop-through and leakage perspective. Figure 8-7 provides the axial depth profile for this indication which is predominantly axial in orientation with an overall measured length of 1.79 inches (based on line-by-line sizing), a measured maximum depth of 75%TW (ETSS 96910.1), and a conservatively assumed circumferential extent of 55.4°. Adjusting upwards to account for ETSS 96910.1 depth sizing uncertainty yields an upper bound depth estimate of 92.4%TW.

The pressure at which circumferential pop-through and leakage will occur in the presence of pressure and external loads may be evaluated using the methods described in Section 9.6.1 of Reference 2. For the top TSP, the limiting in-plane and out-of plane bending moment anticipated to occur during a DBE is approximately 209 in-lb [12], which would produce bending stress of approximately 13,100 psi. Under this loading condition and using the above methodology, a 55.4° circumferential flaw with maximum depth 88.9%TW would pop-through at slightly above 2560 psi. For the TSP wear indication in SG 3E-088 R106 C78 07H-1, circumferential pop-through and leakage is projected to occur at 1120 psi, well below the MSLB pressure. Axial pop-through is calculated to occur at less than 1000 psi using the methodology described in Section 9.6.2 of Reference 2. This tube was pressurized to 2874 psi at room temperature without pop-through of the subject wear location, which for comparison with the analytical results, equates to approximately 2400 psi at operating temperature. Clearly the analytical estimation of pop-through pressure is conservative; however, in the absence of a successful in-situ test result, it must be concluded that the TSP wear at location SG 3E-088 R106 C78 07H-1 did not satisfy the AILPC. The upper bound depths of the three remaining indications are below the depth required to pop-through at MSLB pressure; however, all three are projected to pop-through axially (see Figure 8-8).

In summary, 13 TSP wear flaws in seven tubes failed to satisfy the structural integrity performance criteria, and four of the flaws (in two tubes) failed to satisfy the accident-induced leakage performance criteria.

SONGS Unit 3 February 2012 Leaker Outage - Steam Generator Condition Monitoring Report

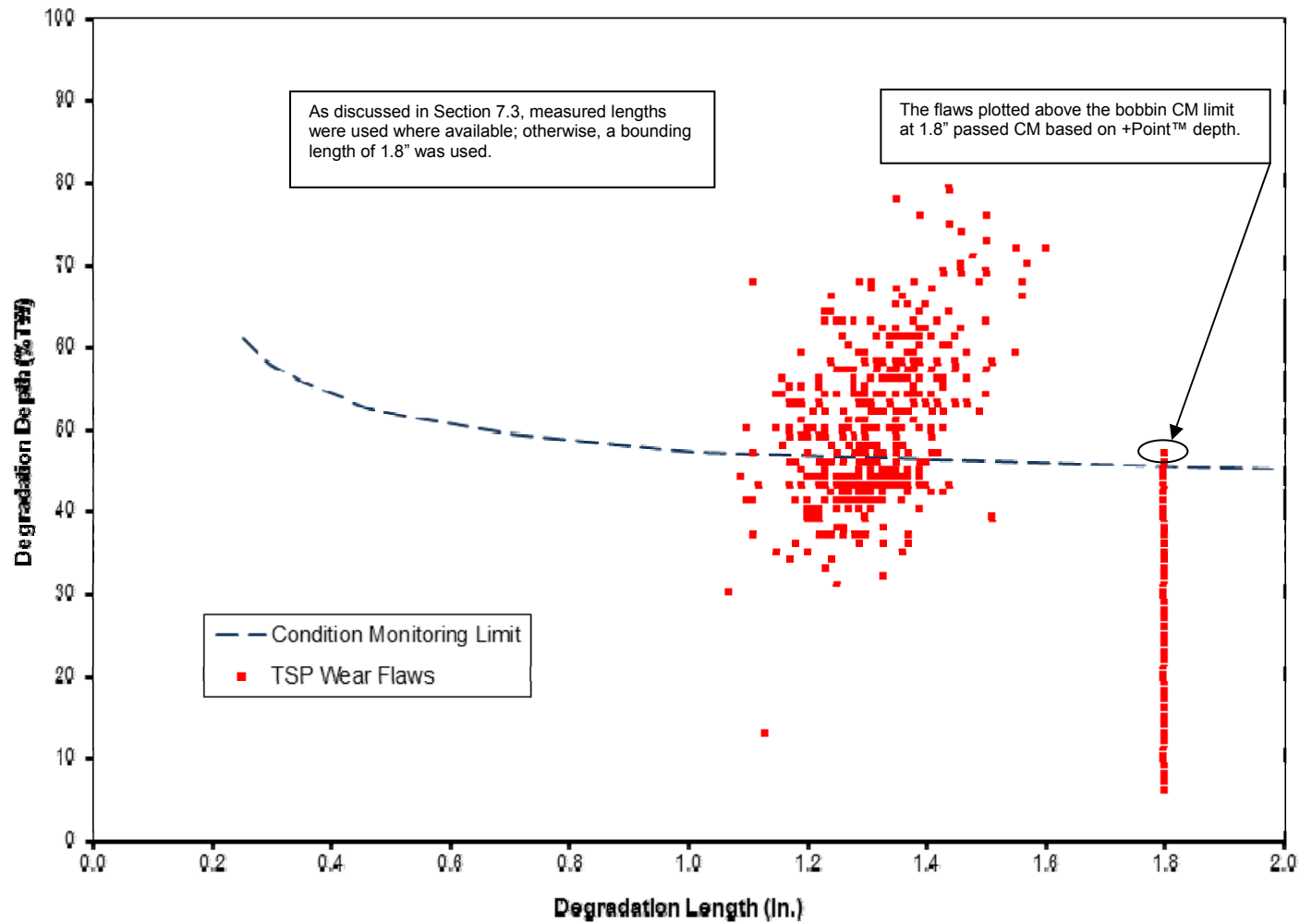
Table 8-3: Incomplete Proof Tests of TSP Wear Exceeding CM Limit Curve

SG	Row	Col	Structural Depth (%TW)	Structural Length (in.)	Location	Test Pressure at Termination (psi)	SIPC Success During In-Situ Test?	AILPC Success During In-Situ Test?	Maximum Measured Depth (%TW)	Overall Length (in.)	Upper Bound Depth (%TW)	Analytical Pop-Through Evaluation		
												Project Circ Pop-Thru Below MSLB?	Project Axial Pop-Thru Below MSLB?	AILPC Success Analytically?
88	98	80	53.3	0.52	07H	4886	No	Yes	NA	NA	NA	NA	NA	NA
88	98	80	46.0	1.00	07C	4886	No	Yes	NA	NA	NA	NA	NA	NA
88	99	81	49.1	1.18	07C	5026	No	Yes	NA	NA	NA	NA	NA	NA
88	99	81	50.8	0.94	07H	5026	No	Yes	NA	NA	NA	NA	NA	NA
88	100	80	44.3	0.61	07H	4732	No	Yes	NA	NA	NA	NA	NA	NA
88	100	80	42.8	1.10	07C	4732	No	Yes	NA	NA	NA	NA	NA	NA
88	101	81	53.1	1.20	07C	4889	No	Yes	NA	NA	NA	NA	NA	NA
88	101	81	50.1	0.88	07H	4889	No	Yes	NA	NA	NA	NA	NA	NA
88	104	78	49.7	0.84	07C	3180	No	In-Situ Test Indeterminate‡	57	1.57	74.2	No	Yes	No
88	104	78	48.6	0.73	07H	3180	No	In-Situ Test Indeterminate‡	58	1.59	75.2	No	Yes	No
88	106	78	64.6	0.96	07H	2874	No	In-Situ Test Indeterminate‡	75	1.79	92.4	Yes	Yes	No
88	106	78	55.3	0.69	07C	2874	No	In-Situ Test Indeterminate‡	65	1.02	82.3	No	Yes	No
88	107	77	47.2	1.56	07C	5160	No	Yes	NA	NA	NA	NA	NA	NA

‡ AILPC failed at a TTW flaw. Test inconclusive for this TSP wear flaw.

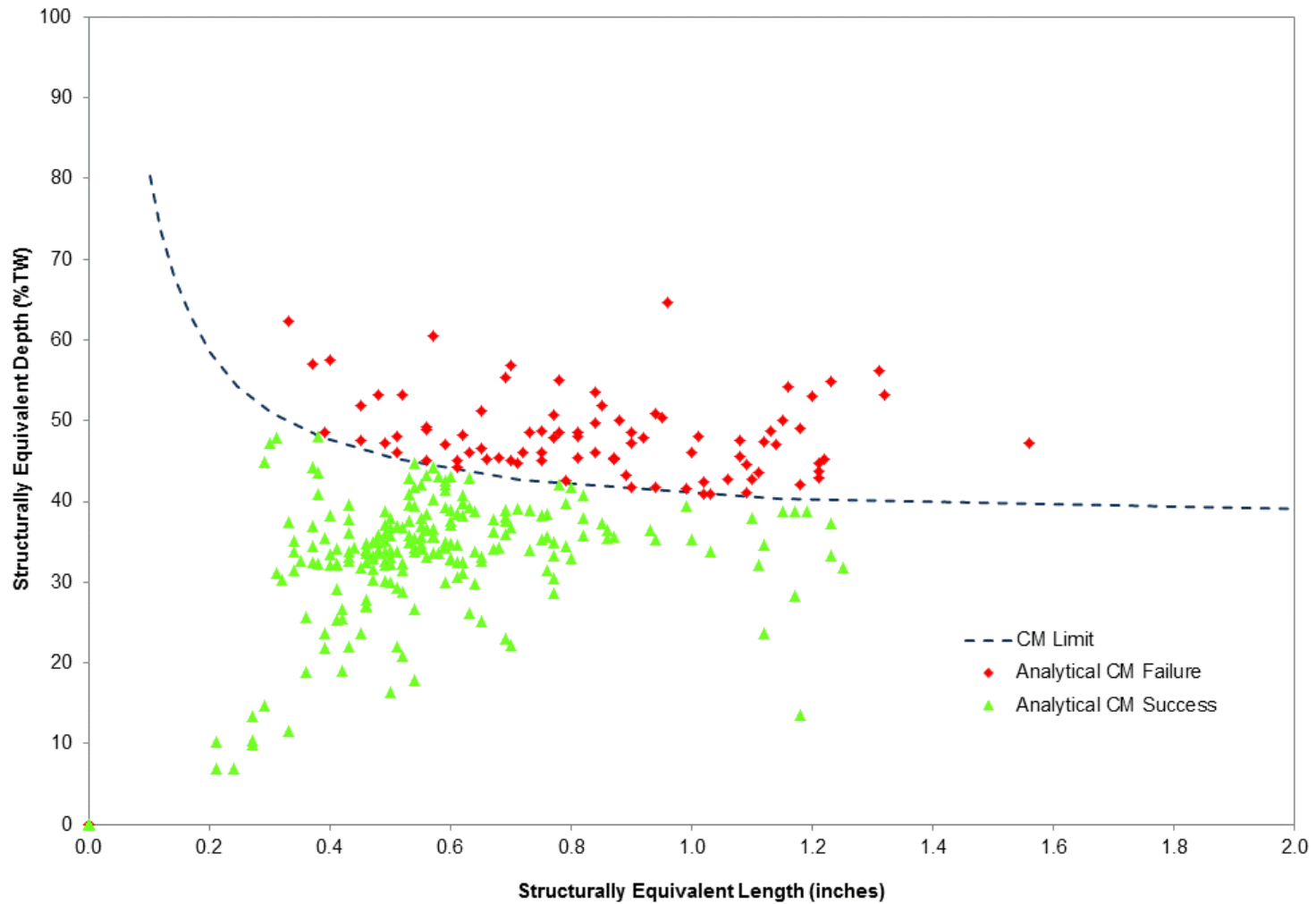
SONGS Unit 3 February 2012 Leaker Outage - Steam Generator Condition Monitoring Report

Figure 8-2: CM Limit for TSP Wear, Both SGs, ETSS 96004.1



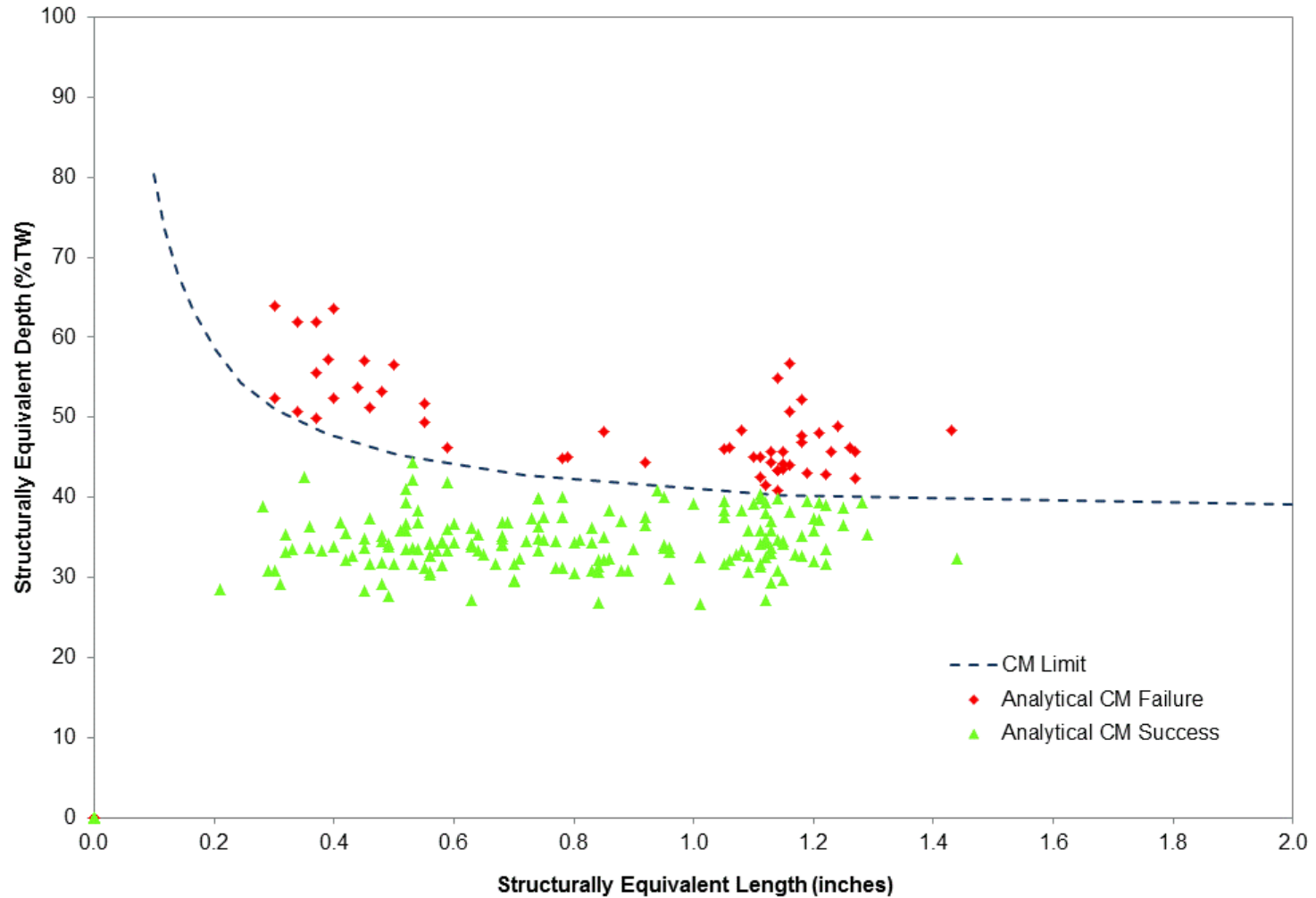
SONGS Unit 3 February 2012 Leaker Outage - Steam Generator Condition Monitoring Report

Figure 8-3: CM Limit for SG 3E-088 TSP Wear, ETSS 96910.1, Structural Dimensions



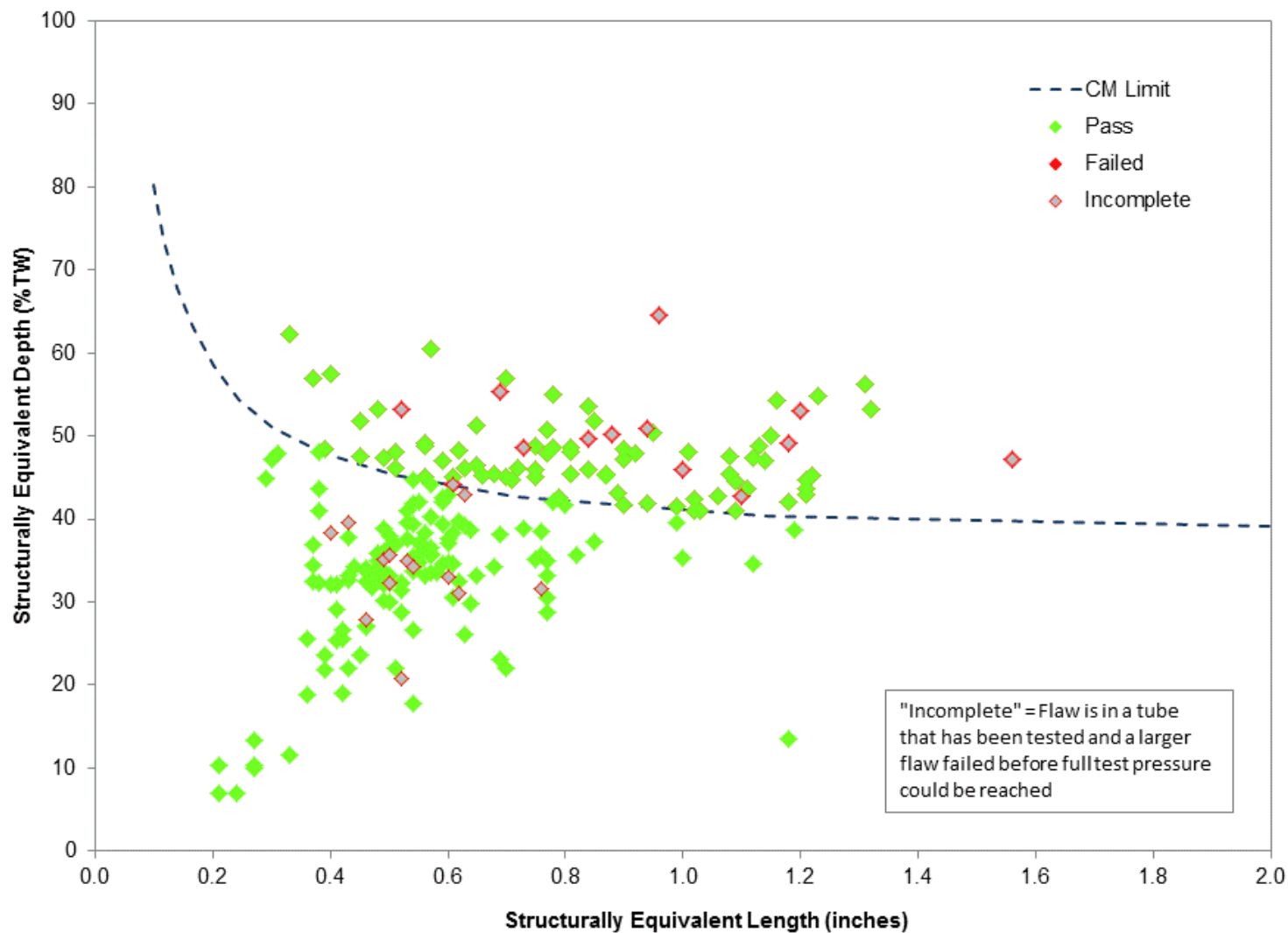
SONGS Unit 3 February 2012 Leaker Outage - Steam Generator Condition Monitoring Report

Figure 8-4: CM Limit for SG 3E-089 TSP Wear, ETSS 96910.1, Structural Dimensions



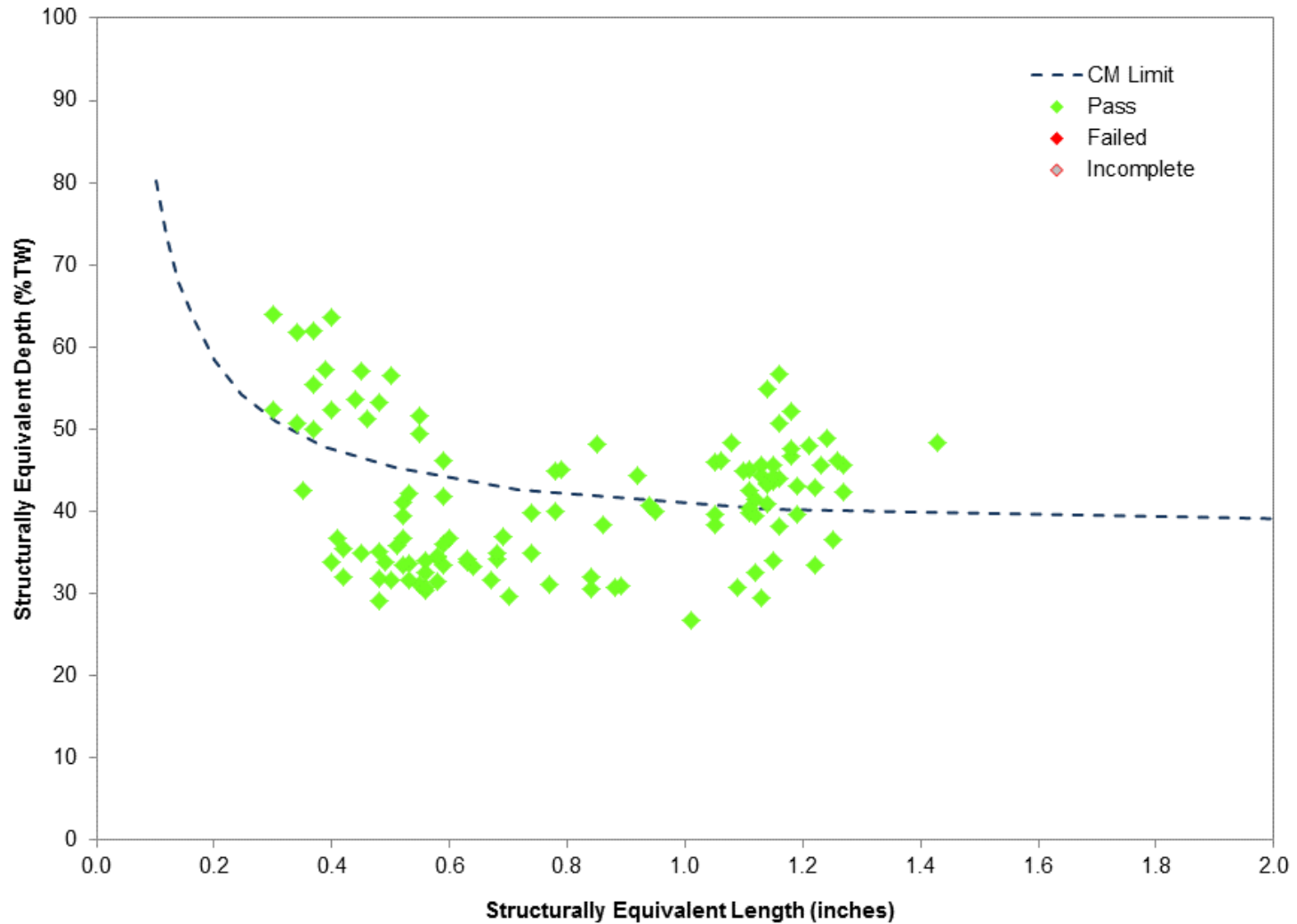
SONGS Unit 3 February 2012 Leaker Outage - Steam Generator Condition Monitoring Report

Figure 8-5: In-Situ Test Results for SG 3E-088 TSP Wear, ETSS 96910.1, Structural Dimensions



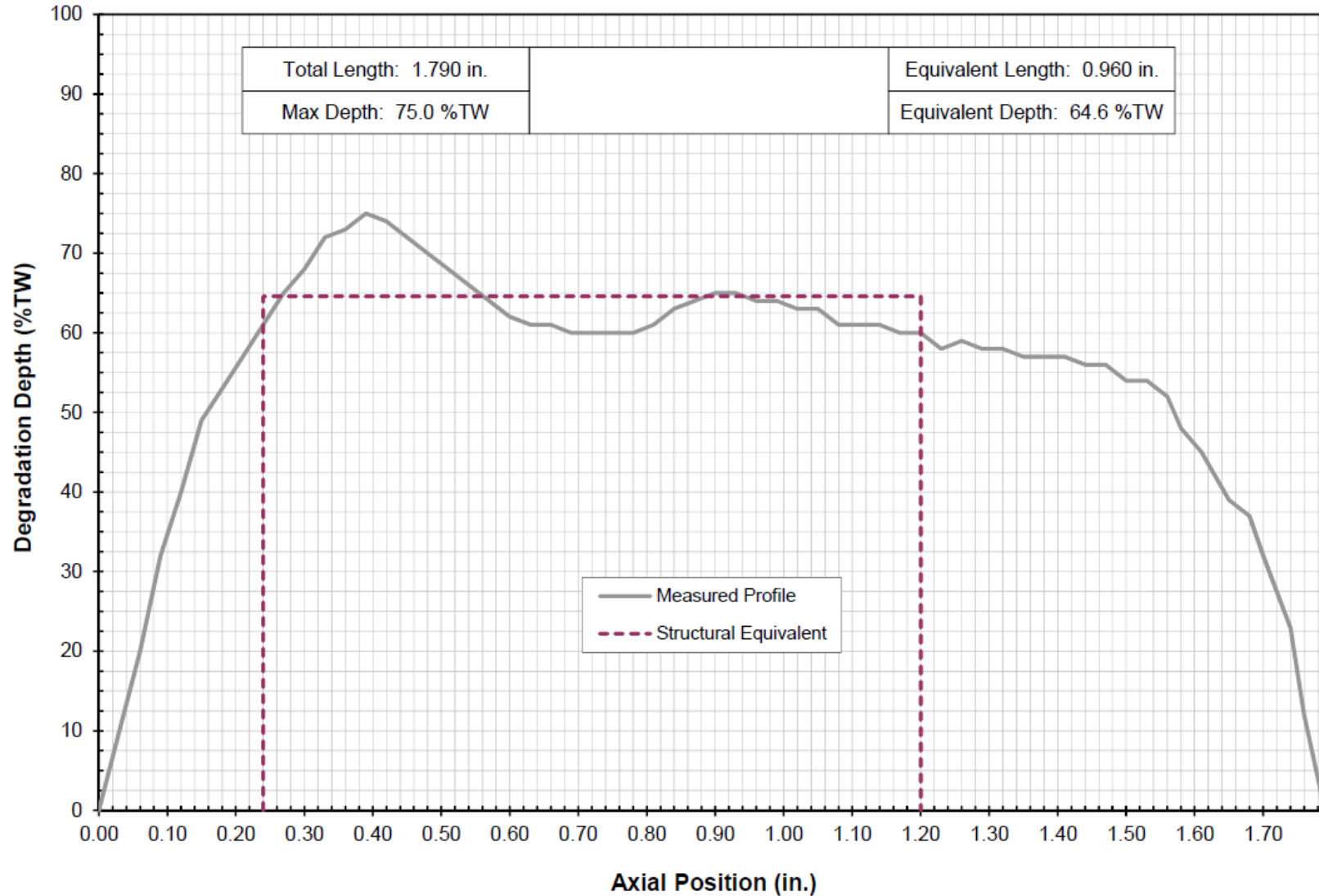
SONGS Unit 3 February 2012 Leaker Outage - Steam Generator Condition Monitoring Report

Figure 8-6: In-Situ Test Results for SG 3E-089 TSP Wear, ETSS 96910.1, Structural Dimensions



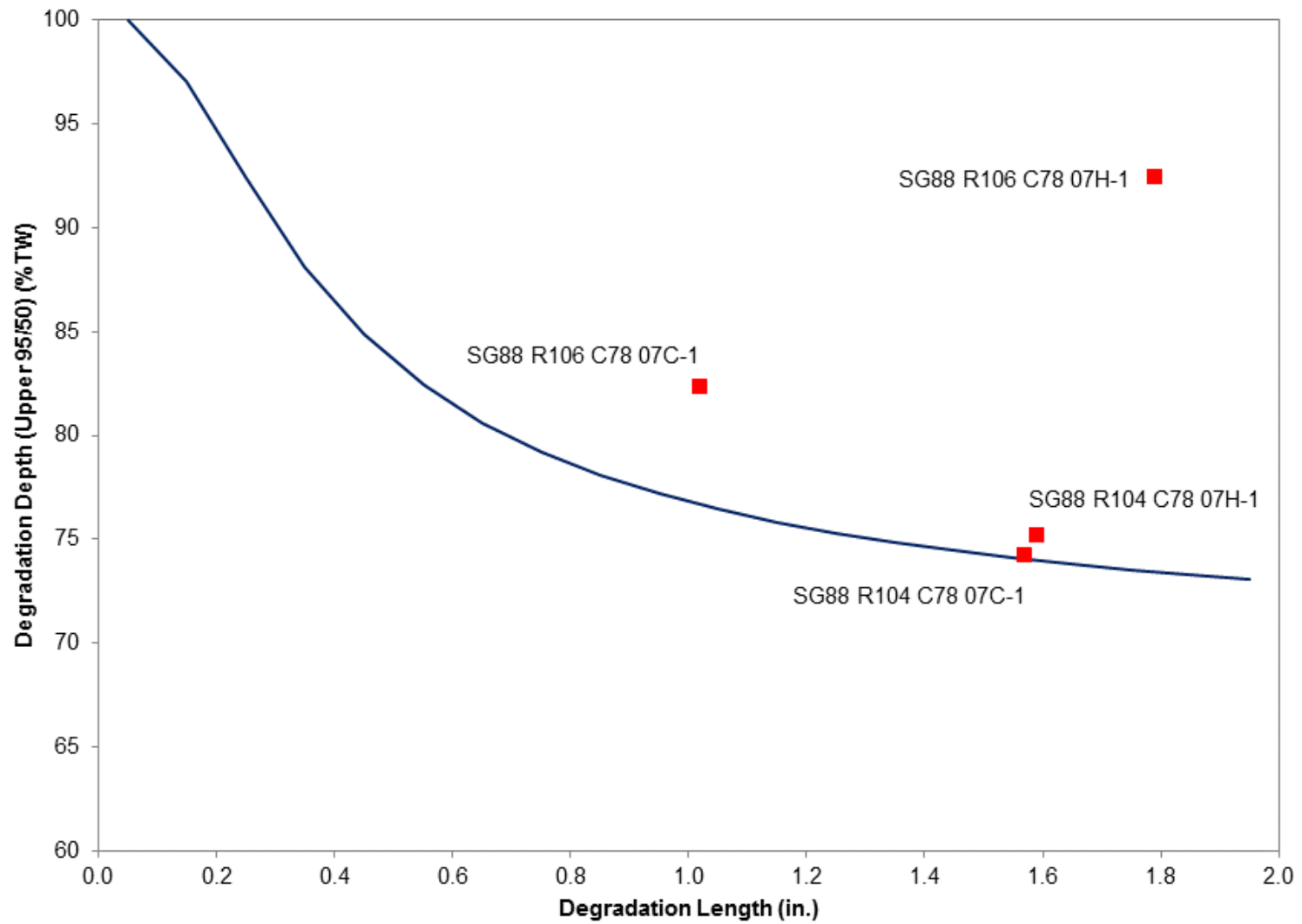
SONGS Unit 3 February 2012 Leaker Outage - Steam Generator Condition Monitoring Report

Figure 8-7: Axial Depth Profile – SG 3E-088 R106 C78 07H-1



SONGS Unit 3 February 2012 Leaker Outage - Steam Generator Condition Monitoring Report

Figure 8-8: Axial Pop-Through Limit for TSP Wear



8.2.3 Retainer Bar Wear

Retainer bar wear was also evaluated with the “axial part-throughwall degradation < 135° in circumferential extent” degradation model as described in Reference 4. The maximum measured circumferential extent of RB wear was 0.36 inches (Table 7-6) which corresponds with an angular extent at the mid tube wall of 58°; well within the 135° requirement for this flaw model. Because of the rather short axial extent of the RB wear indications, it is prudent to also consider the potential for rupture in the circumferential direction. For the indication with the largest circumferential extent (0.36 inch, SG 3E-088 R117 C137 B10), and a limiting assumption that the wear is 100%TW over the entire circumferential extent, the percent degraded area (PDA) is found to be 16 PDA (i.e., $(0.36)/(\pi(\text{mid-wall diameter}))$). This limiting flaw was evaluated with the degradation model for circumferential cracking under pressure loading as described in Reference 2. Based on this model the lower bound burst pressure in the circumferential direction was determined to be 7000 psi; much less limiting than the results from the axial part-throughwall model (discussed below). This provides the basis for concluding that the axial part-throughwall degradation model is appropriate for the evaluation of RB wear.

External loads which are assumed to exist concurrently with the SLB accident do not significantly affect burst pressure in tubes with flaws located in the U-bend region on the tube flanks ($\pm 45^\circ$) [2]. On Unit 2, +Point™ probe examinations were performed with another eddy current probe placed in an adjacent tube in order to estimate the position of the limiting flaw (Unit 2 SG 2E-089 R119 C133 B02) relative to the tube flank. This testing showed that the indication lies approximately 40 to 50 degrees from the flank position; consequently, the RB wear may not lie entirely within the flank region. However, it is also known that external loads do not significantly affect burst pressure in tubes with flaws whose circumferential involvement is less than 25 PDA [2]. The upper bound circumferential involvement of the limiting Unit 3 RB wear indication is only 16 PDA. It is therefore concluded that the limiting condition monitoring structural criteria is 3x normal operating pressure differential, rather than 1.2x the combined loading of SLB pressure and external loads. In short, it is appropriate to consider pressure loading-only for the structural integrity evaluation of RB wear indications.

The axial depth profile of each RB wear indication was measured using ETSS 27903.1, and this data was used to determine the structurally significant dimensions of the indications using the methods described in Section 5.1.5 of Reference 4. The results are provided in Table 7-6 and are plotted on the CM curve provided in Figure 8-9. Since all four RB wear indications lie well below CM curve it is concluded that all Unit 3 RB wear satisfied the structural integrity performance criteria.

RB wear must also be evaluated against the AILPC. For the purpose of this evaluation it is assumed that RB wear resides on the tube intrados or extrados where in-plane motion produces consequential bending stress during analyzed events. For the SONGS SGs, bending moments anticipated in the vicinity of B10 and B11 during a DBE [12], would produce in-plane bending stress of approximately 8,800 psi.

The pressure at which circumferential pop-through and leakage will occur in the presence of pressure and external loads may be evaluated using the methods described in Section 9.6.1 of Reference 2. The maximum depth of identified RB wear was 51%TW. Adjusting upwards to conservatively account for ETSS 27903.1 sizing uncertainty yields an upper bound estimate of 56%TW. Assuming that this limiting RB wear flaw has a circumferential extent of 58° (see earlier discussion), and is subjected to a 20 ksi bending stress, circumferential pop-through would not occur at or below MSLB pressure. Consequently, it is concluded that external loads do not lead to failure to satisfy the AILPC in the

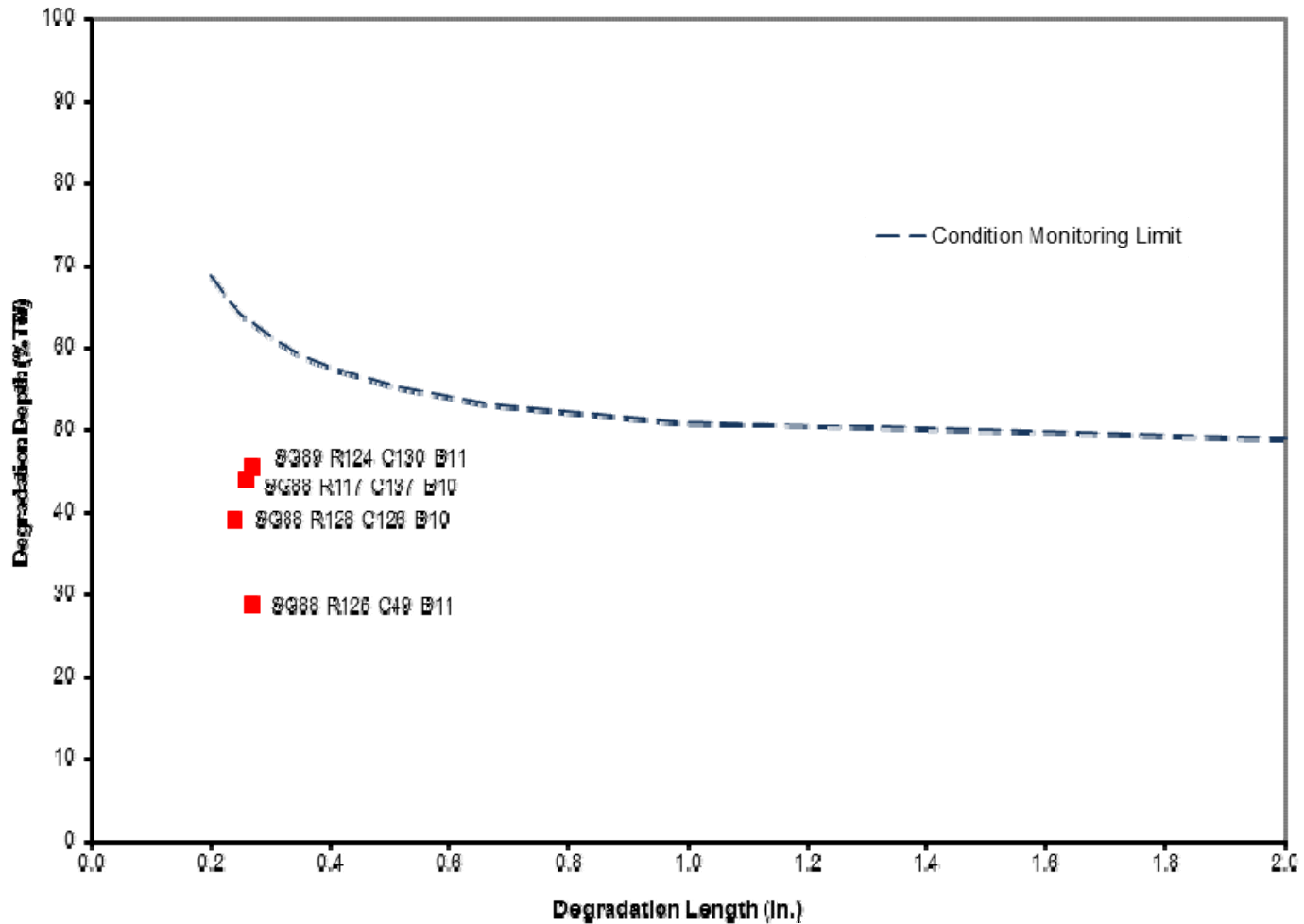
SONGS Unit 3 February 2012 Leaker Outage - Steam Generator Condition Monitoring Report

circumferential orientation. The axial pop-through evaluation performed for TSP wear and summarized in Figure 8-8 is applicable for RB wear and provides the basis for concluding that the limiting RB wear satisfied the AILPC in the axial direction. Hence, all four of the RB wear indications satisfied the SONGS AILPC during the operating period prior to the leaker outage.

It should be noted that multiple eddy current examination techniques and multiple phases of eddy current analysis are applied when characterizing tube degradation to provide as much information and accuracy as practical. Certain indications, such as retainer bar wear, which are detected by the bobbin coil examination are subsequently tested by a rotating coil probe to provide a better and more detailed characterization of the degradation. An initial single-point evaluation of the depth of an indication is performed from the rotating +Point™ data by a resolution analyst. Subsequent analysis of any significant indications is performed to assign a depth evaluation to each scan line of the rotating coil data. This process is called line-by-line sizing and produces a detailed profile of the subject indication. It is not unusual to have some variation between the single-point analysis result and the subsequent line-by-line sizing evaluation. In the case of the SG 3E-089 retainer bar wear, the initial depth report was 46% TW based on EPRI ETSS sizing technique 27903.1 for the Single Volumetric Indication (SVI) report. The line-by-line sizing produced a maximum depth of 51% TW at one position within the indication. As a conservative approach, this maximum depth value of 51% TW was used in the CM analysis of the retainer bar wear degradation.

SONGS Unit 3 February 2012 Leaker Outage - Steam Generator Condition Monitoring Report

Figure 8-9: CM Limit for RB Wear, ETSS 27903.1



8.2.4 Tube-To-Tube Wear

Tube-to-Tube wear was evaluated with the flaw model described in Reference 4 as “axial part-throughwall degradation < 135° in circumferential extent.” The circumferential extent of a TTW flaw is limited by the geometry of the interacting tubes such that it can be modeled as a single 100%TW wear scar formed by a flat bar positioned tangentially to the tube surface. In this configuration the maximum circumferential extent of the degradation will be 55.4°. For double-sided TTW, this model is bounding because the wear geometry provides sufficient circumferential separation between the wear scars to permit each indication to be treated separately. The separation between centerline contact points for double-side TTW is 180°, and results in negligible circumferential interaction between separate wear locations in the same axial plane of the tube. With respect to external loads, each wear indication at the same axial location may be treated individually. An individual TTW indication with a depth of 100%TW and a circumferential extent of 55.4° would be less than 16 PDA. Because the circumferential involvement of this limiting indication is less than 25 PDA, external loads need not be considered in the evaluation of burst integrity for TTW.

The +Point™ probe was used to measure the depth and the overall length of TTW through the application of ETSS 27902.2. The maximum measured length of any TTW indication was 41 inches. Using the flaw model discussed above it was determined that a rectangular flaw 41 inches long and 45%TW would meet the SIPC. Hence, it was concluded that all TTW sized less than 45%TW satisfied the SIPC. Although only TTW exceeding 45%TW required the more detailed flaw profiling analysis, all TTW indications with maximum depth $\geq 40\%$ TW were profiled and analyzed to determine the structurally equivalent dimensions.

CM limit curves for TTW based upon ETSS 27902.2 are provided for SG 3E-088 and SG 3E-089 in Figure 8-10 and Figure 8-11, respectively. The figures also depict the structural dimensions of all indications for which axial depth profiling was performed. The use of structurally equivalent dimensions provides the highest likelihood of analytically demonstrating compliance with the CM structural performance criteria. However, as illustrated in Figure 8-10 and Figure 8-11, many TTW flaws exceeded the CM curve thus; satisfaction of the CM criteria could not be analytically demonstrated. Consequently, all of the TTW that exceeded the CM limit was subjected to in-situ pressure testing in an attempt to demonstrate CM criteria compliance.

8.2.4.1 In-Situ Test Results

Figure 8-12 and Figure 8-13 summarize the results of in-situ testing of TTW indications in each SG. All tested TTW wear in SG 3E-089 satisfied the structural integrity and accident leakage performance criteria. In SG 3E-088 three TTW indications failed both the AILPC and SIPC, and five flaws passed the AILPC but failed the SIPC. These results are summarized in Table 8-4.

In addition, four TTW indications predicted analytically to fail the SIPC, could not be tested to the required pressure levels because more limiting TTW in the same tube failed below the target pressure, terminating the test. These indications are depicted in Figure 8-12 as “Incomplete” (above the CM curve). In the absence of a successful in-situ pressure test, these must be considered to be SIPC failures (see Table 8-4).

SONGS Unit 3 February 2012 Leaker Outage - Steam Generator Condition Monitoring Report

For one TTW flaw a determination could not be made based upon in-situ test result as to whether the AILPC was satisfied. This flaw is labeled in Table 8-4 as “In Situ Test Indeterminate” due to the failure of a TTW flaw in the same tube at a pressure below the target AILPC pressure. The maximum measured throughwall depth of this flaw was 99%TW and the structural length exceeded 2 inches. From Figure 8-8 it must be concluded that this flaw does not satisfy the AILPC.

In summary, 12 TTW flaws in eight tubes failed to satisfy the structural integrity performance criteria, and four of the flaws (in three tubes) failed to satisfy the accident-induced leakage performance criteria.

8.2.4.2 Eddy Current Sizing

Following the detection of TTW, application of ETSS 27902.2 was site validated [13]. This was done by building a test specimen with flaws similar to the TTW flaws observed at SONGS. Many depth estimates were made with +Point™ using ETSS 27902.2. These results were compared with the actual depths of the wear flaws. This comparison showed that ETSS 27902.2 conservatively overestimated the depths across the entire range of depths tested (from 5%TW to 81%TW). The flaws in the test specimen that measured $\geq 70\%$ TW were overestimated by an average of 17%TW.

The conservatism in the sizing technique as discussed above is supported by the in-situ test results. A cursory review of the best estimate burst pressures for the tubes that were in-situ pressure tested shows that approximately 45 failures would have been expected if the NDE sizing was accurate. Because there were only eight tubes that failed in-situ pressure testing, the measured depths are assumed to be overestimated using ETSS 27902.2. Again, this is consistent with the site validation work which showed that ETSS 27902.2 consistently overestimated the depths.

SONGS Unit 3 February 2012 Leaker Outage - Steam Generator Condition Monitoring Report

Table 8-4: In-Situ Test Result Summary for TTW Flaws

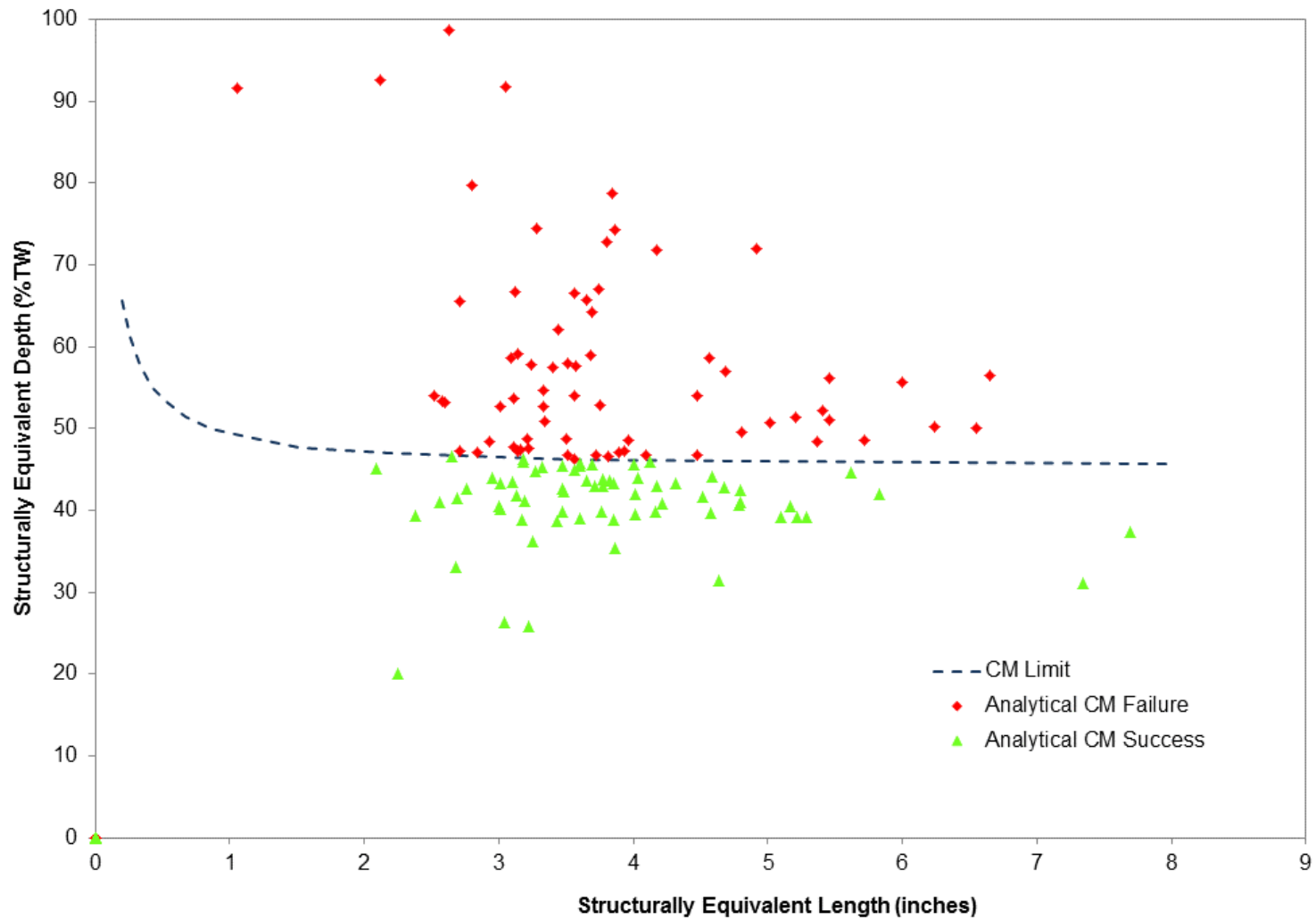
SG	Row	Col	Structural Depth (%TW)	Structural Length (in.)	Location	Test Pressure at Termination (psi)	SIPC Success During In-Situ Test?	AILPC Success During In-Situ Test?	Maximum Measured Depth (%TW)	AILPC Success Analytically?
SG 3E-088	98	80	74.4	3.28	B02	4886	No	Yes	NA	NA
SG 3E-088	99	81	71.8	4.17	B02	5026	No	Yes	NA	NA
SG 3E-088	100	80	79.7	2.8	B02-1	4732	No	Yes	NA	NA
			52.6	3.33	B02-2		No‡	Yes	NA	NA
SG 3E-088	101	81	74.3	3.86	B02-1	4889	No	Yes	NA	NA
			50.7	5.02	B02-2		No‡	Yes	NA	NA
SG 3E-088	102	78	98.7	2.63	B02	3268	No	No	NA	NA
SG 3E-088	104	78	91.7	1.06	B03	3180	No	No	NA	NA
			92.6	2.12	B02		No‡	In-Situ Test Indeterminate‡	99	No
SG 3E-088	106	78	91.7	3.05	B03	2874	No	No	NA	NA
SG 3E-088	107	77	78.8	3.84	B02	5160	No	Yes	NA	NA
			47.5	3.22	B08		No‡	Yes	NA	NA

‡ Failure of SIPC predicted analytically, not proven otherwise by in-situ test. Failure assumed.

‡ AILPC failed at the B03 TTW flaw. Test inconclusive for this flaw.

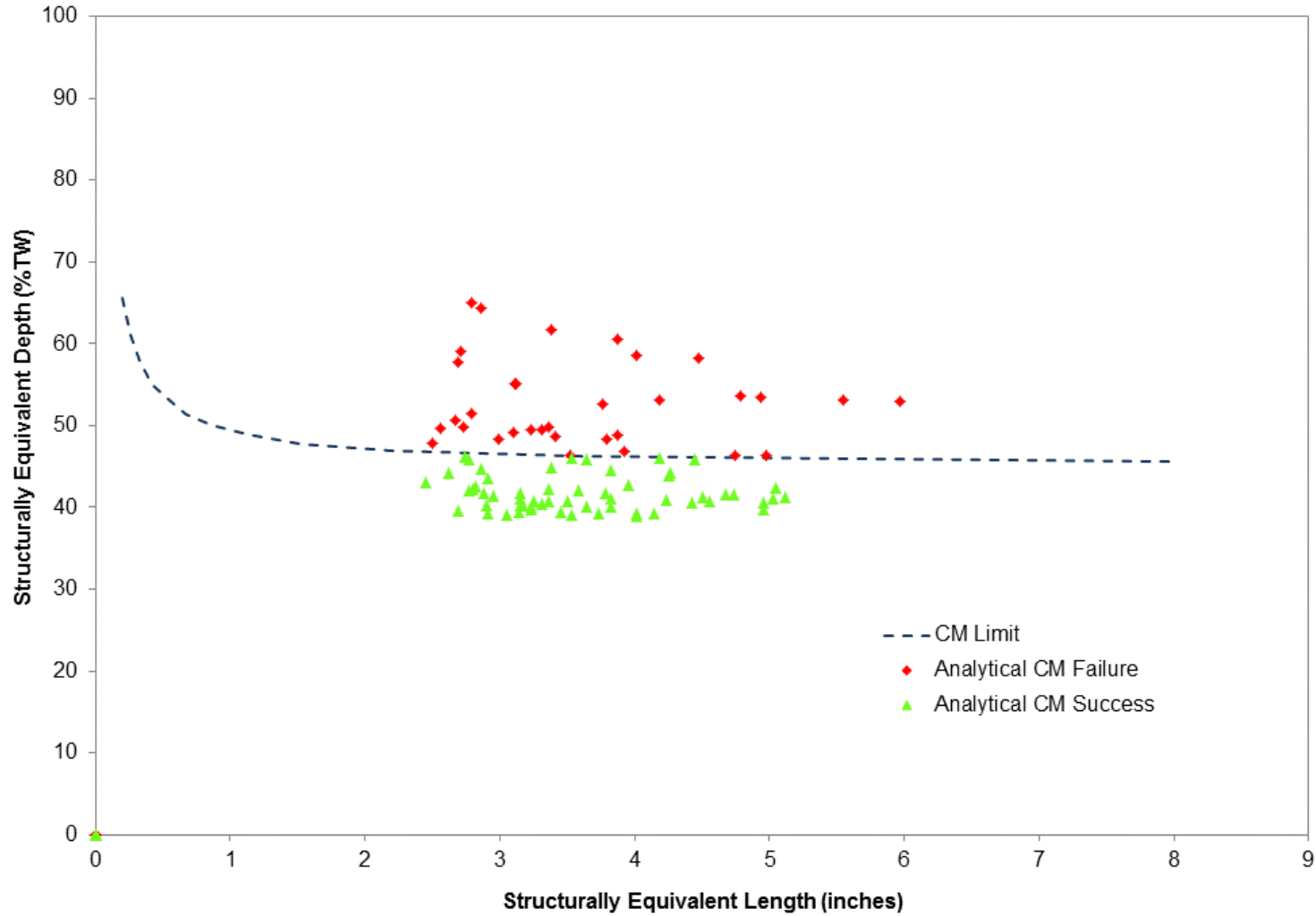
SONGS Unit 3 February 2012 Leaker Outage - Steam Generator Condition Monitoring Report

Figure 8-10: CM Limit for SG 3E-088 TTW, ETSS 27902.2, Structural Dimensions



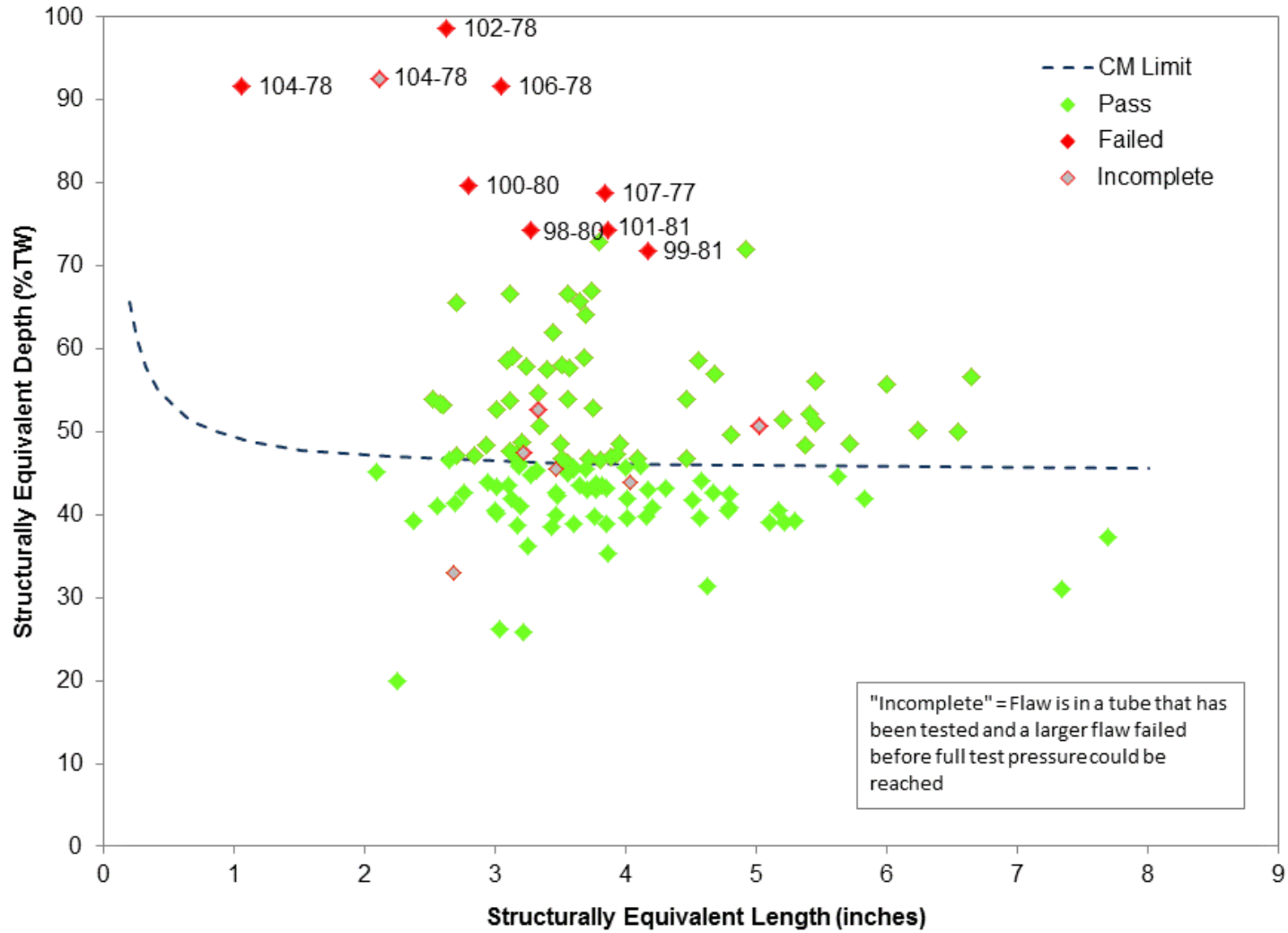
SONGS Unit 3 February 2012 Leaker Outage - Steam Generator Condition Monitoring Report

Figure 8-11: CM Limit for SG 3E-089 TTW, ETSS 27902.2, Structural Dimensions



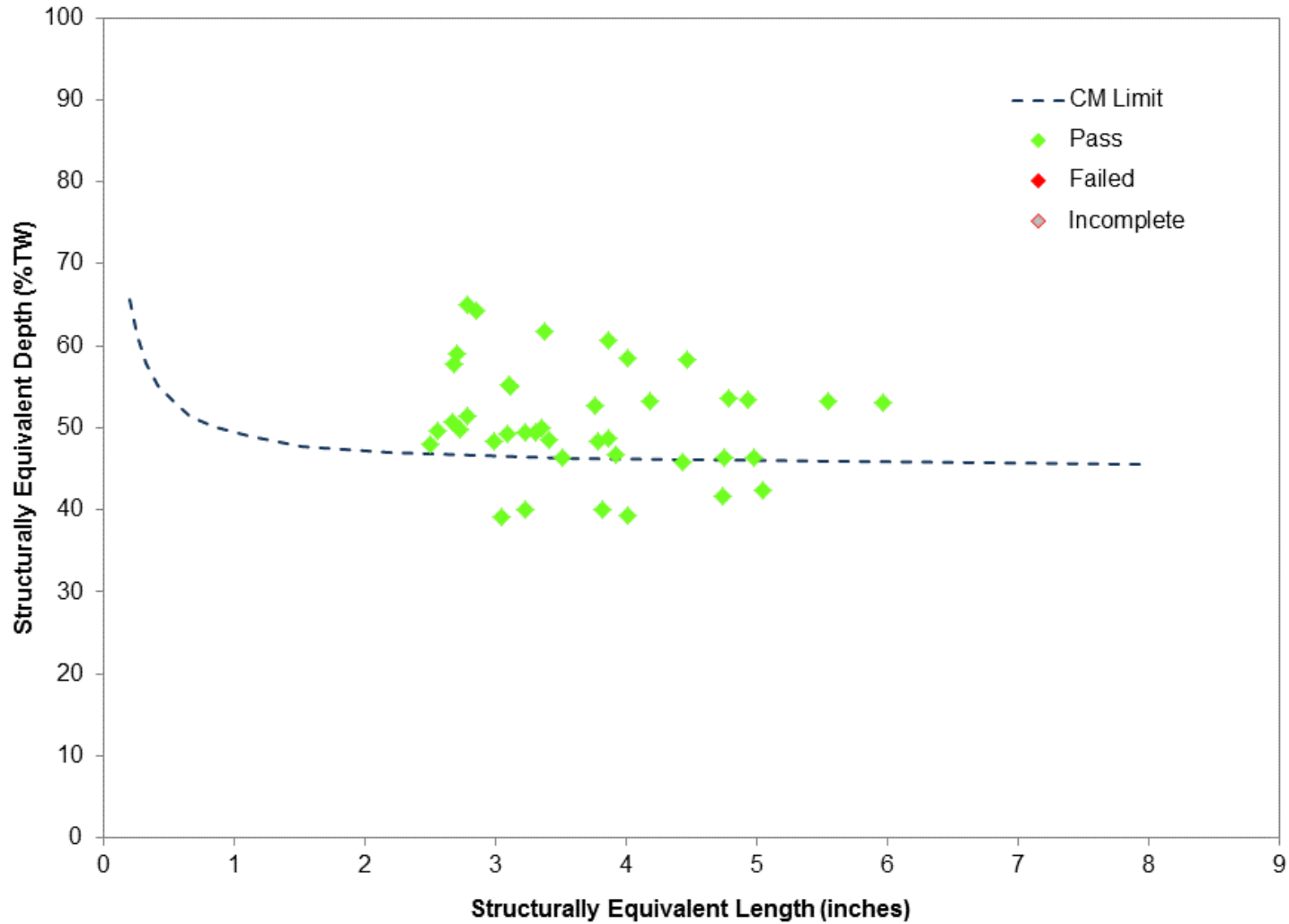
SONGS Unit 3 February 2012 Leaker Outage - Steam Generator Condition Monitoring Report

Figure 8-12: In-Situ Test Results for SG 3E-088 TTW, ETSS 27902.2, Structural Dimensions



SONGS Unit 3 February 2012 Leaker Outage - Steam Generator Condition Monitoring Report

Figure 8-13: In-Situ Test Results for SG 3E-089 TTW, ETSS 27902.2, Structural Dimensions



9.0 CONDITION MONITORING CONCLUSION

This condition monitoring assessment has evaluated all SG tube degradation detected during the Unit 3 2012 leaker outage against the three SONGS Technical Specification performance criteria. Through a combination of eddy current inspection, analytical evaluation, in-situ pressure testing, and operational leakage monitoring, the following conclusions are drawn:

- 1) Despite the fact that operational SG tube leakage resulted in a forced outage, the leak rate remained below the Technical Specification limit (150 GPD); therefore the operational leakage integrity performance criterion was met.
- 2) A total of eight tubes failed to meet the structural integrity performance criterion due to tube-to-tube wear and tube support plate wear.
- 3) A total of three tubes failed to meet the accident-induced leakage performance criterion due to tube-to-tube wear and tube support plate wear.

SONGS Unit 3 February 2012 Leaker Outage - Steam Generator Condition Monitoring Report

10.0 REFERENCES

1. NEI 97-06, "SG Program Guidelines," Rev. 3, January 2011.
2. EPRI Report 1019038, "SG Integrity Assessment Guidelines: Revision 3", November 2009.
3. EPRI Report 1014983, "Steam Generator In Situ Pressure Test Guidelines, Revision 3", August 2007.
4. EPRI Report 1019037 "Steam Generator Degradation Specific Management Flaw Handbook", Revision 1, with error correction in J. Benson email dated 3/30/2012, December 2009.
5. EPRI, SG Management Project, "sgmp.epri.com."
6. AREVA Document 51-9176667-001, "SONGS 2C17 & 3C17 Steam Generator Degradation Assessment."
7. AREVA Document 51-9104383-002, "SONGS Units 2 & 3 Replacement Steam Generator Eddy Current Technique Validation."
8. AREVA Document 32-5033045-002, "Mathcad Implementation of SG Flaw Handbook Equations for Integrity Assessment".
9. *Matheny, Southern California Edison, "Numerical Values for the SG OAs, SONGS Units 2 and 3", February 8, 2012
10. *SONGS Unit 3 Replacement Steam Generator Receipt Inspection QA Document Review Package
11. AREVA Document 51-9179808-000, "In-Situ Pressure Test Results for SONGS U3F16B Outage."
12. *MHI, "SONGS Unit 2 & 3 RSGs, Regulatory Guide 1.121 Analysis," SO23-617-1-C1262, Rev. 4
13. AREVA Document 51-9177744-000 "Site Validation of EPRI Sizing ETSS for Tube-Tube Wear in SONGS Steam Generators".
14. AREVA Document 51-9179946-001, "Comparison of Bobbin and +Point POD for Tube-Tube Wear in SONGS Steam Generators".
15. SCE Licensee Event Report 2012-001-00, "Unit 3 Manual Reactor Trip due to Steam Generator Tube Leak", March 29 2012.
16. SONGS Technical Specifications Section 5.5.2.11, "Steam Generator (SG) Program".
17. SONGS Technical Specifications Section 3.4.13, "RCS Operational Leakage".

SONGS Unit 3 February 2012 Leaker Outage - Steam Generator Condition Monitoring Report

18. INPO Operating Experience Report OE 34946, "Tube –to-Tube Contact Wear Identified in TMI-1 Steam Generators (TMI-1)".
19. NRC Information Notice 2012-7, "Tube-to-Tube Contact Resulting in Wear in Once Through Steam Generators".
20. INPO Operating Experience Report OE 35359, "Large Number of Anti-Vibration Bar Wear Indications Reported in the Unit 2 Replacement Steam Generators (St. Lucie)."
21. *MHI Document L5-04GA111, "San Onofre Generating Station, Units 2 & 3 Replacement Steam Generators Vendor Manual", Rev 6 (SONGS Document SO23-617-1-M1273, Rev 6).
22. AREVA Document 03-9180130-000, "SONGS 3F16B SSI Final Report".

* These references are not available from the AREVA NP records center. However, they are available from the SCE document control system. Therefore, this is an acceptable reference for use on this contract per AREVA NP Procedure 0402-01, Attachment 8 as authorized by the PM signature on page 2

Appendix A

SG 3E-088 Plugging List

SONGS Unit 3 February 2012 Leaker Outage - Steam Generator Condition Monitoring Report

S/G	Row	Col	Hot Leg	Cold Leg	Reason for Tube Repair	Rev
3E088	117	81	ROLLSTAB (750")	ROLLED	AVB Wear >=35%	Rev3
3E088	108	34	ROLLED	ROLLED	Preventative - Retainer Bar	Rev1
3E088	110	34	ROLLSTAB (668")	ROLLED	Preventative - Retainer Bar	Rev1
3E088	109	35	ROLLSTAB (668")	ROLLED	Preventative - Retainer Bar	Rev1
3E088	111	35	ROLLED	ROLLED	Preventative - Retainer Bar	Rev1
3E088	110	36	ROLLED	ROLLED	Preventative - Retainer Bar	Rev1
3E088	112	36	ROLLED	ROLLED	Preventative - Retainer Bar	Rev1
3E088	111	37	ROLLED	ROLLED	Preventative - Retainer Bar	Rev1
3E088	113	37	ROLLED	ROLLED	Preventative - Retainer Bar	Rev1
3E088	112	38	ROLLED	ROLLED	Preventative - Retainer Bar	Rev1
3E088	114	38	ROLLED	ROLLED	Preventative - Retainer Bar	Rev1
3E088	113	39	ROLLED	ROLLED	Preventative - Retainer Bar	Rev1
3E088	115	39	ROLLED	ROLLED	Preventative - Retainer Bar	Rev1
3E088	114	40	ROLLED	ROLLED	Preventative - Retainer Bar	Rev1
3E088	116	40	ROLLED	ROLLED	Preventative - Retainer Bar	Rev1
3E088	115	41	ROLLED	ROLLED	Preventative - Retainer Bar	Rev1
3E088	117	41	ROLLED	ROLLED	Preventative - Retainer Bar	Rev1
3E088	116	42	ROLLED	ROLLED	Preventative - Retainer Bar	Rev1
3E088	118	42	ROLLED	ROLLED	Preventative - Retainer Bar	Rev1
3E088	117	43	ROLLED	ROLLED	Preventative - Retainer Bar	Rev1
3E088	119	43	ROLLED	ROLLED	Preventative - Retainer Bar	Rev1
3E088	118	44	ROLLED	ROLLED	Preventative - Retainer Bar	Rev1
3E088	120	44	ROLLED	ROLLED	Preventative - Retainer Bar	Rev1
3E088	119	45	ROLLED	ROLLED	Preventative - Retainer Bar	Rev1
3E088	121	45	ROLLSTAB (668")	ROLLED	Preventative - Retainer Bar	Rev1
3E088	120	46	ROLLSTAB (668")	ROLLED	Preventative - Retainer Bar	Rev1
3E088	122	46	ROLLED	ROLLED	Preventative - Retainer Bar	Rev1
3E088	121	47	ROLLED	ROLLED	Preventative - Retainer Bar	Rev1
3E088	123	47	ROLLED	ROLLED	Preventative - Retainer Bar	Rev1
3E088	122	48	ROLLED	ROLLED	Preventative - Retainer Bar	Rev1
3E088	124	48	ROLLED	ROLLED	Preventative - Retainer Bar	Rev1
3E088	123	49	ROLLED	ROLLED	Preventative - Retainer Bar	Rev1
3E088	124	50	ROLLED	ROLLED	Preventative - Retainer Bar	Rev1
3E088	126	50	ROLLED	ROLLED	Preventative - Retainer Bar	Rev1
3E088	125	51	ROLLED	ROLLED	Preventative - Retainer Bar	Rev1
3E088	127	51	ROLLED	ROLLED	Preventative - Retainer Bar	Rev1
3E088	126	52	ROLLED	ROLLED	Preventative - Retainer Bar	Rev1
3E088	128	52	ROLLED	ROLLED	Preventative - Retainer Bar	Rev1
3E088	127	53	ROLLED	ROLLED	Preventative - Retainer Bar	Rev1
3E088	129	53	ROLLED	ROLLED	Preventative - Retainer Bar	Rev1
3E088	128	54	ROLLED	ROLLED	Preventative - Retainer Bar	Rev1
3E088	130	54	ROLLED	ROLLED	Preventative - Retainer Bar	Rev1
3E088	129	55	ROLLED	ROLLED	Preventative - Retainer Bar	Rev1
3E088	131	55	ROLLED	ROLLED	Preventative - Retainer Bar	Rev1

SONGS Unit 3 February 2012 Leaker Outage - Steam Generator Condition Monitoring Report

S/G	Row	Col	Hot Leg	Cold Leg	Reason for Tube Repair	Rev
3E088	130	56	ROLLSTAB (668")	ROLLED	Preventative - Retainer Bar	Rev1
3E088	132	56	ROLLSTAB (668")	ROLLED	Preventative - Retainer Bar	Rev1
3E088	131	57	ROLLED	ROLLED	Preventative - Retainer Bar	Rev1
3E088	131	121	ROLLED	ROLLED	Preventative - Retainer Bar	Rev1
3E088	130	122	ROLLSTAB (668")	ROLLED	Preventative - Retainer Bar	Rev1
3E088	132	122	ROLLSTAB (668")	ROLLED	Preventative - Retainer Bar	Rev1
3E088	129	123	ROLLED	ROLLED	Preventative - Retainer Bar	Rev1
3E088	131	123	ROLLED	ROLLED	Preventative - Retainer Bar	Rev1
3E088	128	124	ROLLED	ROLLED	Preventative - Retainer Bar	Rev1
3E088	130	124	ROLLED	ROLLED	Preventative - Retainer Bar	Rev1
3E088	127	125	ROLLED	ROLLED	Preventative - Retainer Bar	Rev1
3E088	129	125	ROLLED	ROLLED	Preventative - Retainer Bar	Rev1
3E088	126	126	ROLLED	ROLLED	Preventative - Retainer Bar	Rev1
3E088	125	127	ROLLED	ROLLED	Preventative - Retainer Bar	Rev1
3E088	127	127	ROLLED	ROLLED	Preventative - Retainer Bar	Rev1
3E088	124	128	ROLLED	ROLLED	Preventative - Retainer Bar	Rev1
3E088	126	128	ROLLED	ROLLED	Preventative - Retainer Bar	Rev1
3E088	123	129	ROLLED	ROLLED	Preventative - Retainer Bar	Rev1
3E088	125	129	ROLLED	ROLLED	Preventative - Retainer Bar	Rev1
3E088	122	130	ROLLED	ROLLED	Preventative - Retainer Bar	Rev1
3E088	124	130	ROLLED	ROLLED	Preventative - Retainer Bar	Rev1
3E088	121	131	ROLLED	ROLLED	Preventative - Retainer Bar	Rev1
3E088	123	131	ROLLED	ROLLED	Preventative - Retainer Bar	Rev1
3E088	120	132	ROLLSTAB (668")	ROLLED	Preventative - Retainer Bar	Rev1
3E088	122	132	ROLLED	ROLLED	Preventative - Retainer Bar	Rev1
3E088	119	133	ROLLED	ROLLED	Preventative - Retainer Bar	Rev1
3E088	121	133	ROLLSTAB (668")	ROLLED	Preventative - Retainer Bar	Rev1
3E088	118	134	ROLLED	ROLLED	Preventative - Retainer Bar	Rev1
3E088	120	134	ROLLED	ROLLED	Preventative - Retainer Bar	Rev1
3E088	117	135	ROLLED	ROLLED	Preventative - Retainer Bar	Rev1
3E088	119	135	ROLLED	ROLLED	Preventative - Retainer Bar	Rev1
3E088	116	136	ROLLED	ROLLED	Preventative - Retainer Bar	Rev1
3E088	118	136	ROLLED	ROLLED	Preventative - Retainer Bar	Rev1
3E088	115	137	ROLLED	ROLLED	Preventative - Retainer Bar	Rev1
3E088	114	138	ROLLED	ROLLED	Preventative - Retainer Bar	Rev1
3E088	116	138	ROLLED	ROLLED	Preventative - Retainer Bar	Rev1
3E088	113	139	ROLLED	ROLLED	Preventative - Retainer Bar	Rev1
3E088	115	139	ROLLED	ROLLED	Preventative - Retainer Bar	Rev1
3E088	112	140	ROLLED	ROLLED	Preventative - Retainer Bar	Rev1
3E088	114	140	ROLLED	ROLLED	Preventative - Retainer Bar	Rev1
3E088	111	141	ROLLED	ROLLED	Preventative - Retainer Bar	Rev1
3E088	113	141	ROLLED	ROLLED	Preventative - Retainer Bar	Rev1
3E088	110	142	ROLLED	ROLLED	Preventative - Retainer Bar	Rev1
3E088	112	142	ROLLED	ROLLED	Preventative - Retainer Bar	Rev1
3E088	109	143	ROLLSTAB (668")	ROLLED	Preventative - Retainer Bar	Rev1



SONGS Unit 3 February 2012 Leaker Outage - Steam Generator Condition Monitoring Report

S/G	Row	Col	Hot Leg	Cold Leg	Reason for Tube Repair	Rev
3E088	111	143	ROLLED	ROLLED	Preventative - Retainer Bar	Rev1
3E088	108	144	ROLLED	ROLLED	Preventative - Retainer Bar	Rev1
3E088	110	144	ROLLSTAB (668")	ROLLED	Preventative - Retainer Bar	Rev1
3E088	92	74	ROLLSTAB (750")	ROLLED	Preventative (MHI for TTW)	Rev4
3E088	94	74	ROLLSTAB (750")	ROLLED	Preventative (MHI for TTW)	Rev4
3E088	102	74	ROLLSTAB (750")	ROLLED	Preventative (MHI for TTW)	Rev4
3E088	106	74	ROLLSTAB (750")	ROLLED	Preventative (MHI for TTW)	Rev4
3E088	108	74	ROLLSTAB (780")	ROLLED	Preventative (MHI for TTW)	Rev4
3E088	93	75	ROLLSTAB (750")	ROLLED	Preventative (MHI for TTW)	Rev4
3E088	95	75	ROLLSTAB (750")	ROLLED	Preventative (MHI for TTW)	Rev4
3E088	121	75	ROLLSTAB (780")	ROLLED	Preventative (MHI for TTW)	Rev4
3E088	92	76	ROLLSTAB (750")	ROLLED	Preventative (MHI for TTW)	Rev4
3E088	94	76	ROLLSTAB (750")	ROLLED	Preventative (MHI for TTW)	Rev4
3E088	96	76	ROLLSTAB (750")	ROLLED	Preventative (MHI for TTW)	Rev4
3E088	116	76	ROLLSTAB (780")	ROLLED	Preventative (MHI for TTW)	Rev4
3E088	122	76	ROLLSTAB (780")	ROLLED	Preventative (MHI for TTW)	Rev4
3E088	124	76	ROLLSTAB (780")	ROLLED	Preventative (MHI for TTW)	Rev4
3E088	81	77	ROLLSTAB (668")	ROLLED	Preventative (MHI for TTW)	Rev4
3E088	87	77	ROLLSTAB (750")	ROLLED	Preventative (MHI for TTW)	Rev4
3E088	89	77	ROLLSTAB (750")	ROLLED	Preventative (MHI for TTW)	Rev4
3E088	93	77	ROLLSTAB (750")	ROLLED	Preventative (MHI for TTW)	Rev4
3E088	95	77	ROLLSTAB (750")	ROLLED	Preventative (MHI for TTW)	Rev4
3E088	97	77	ROLLSTAB (750")	ROLLED	Preventative (MHI for TTW)	Rev4
3E088	123	77	ROLLSTAB (780")	ROLLED	Preventative (MHI for TTW)	Rev4
3E088	125	77	ROLLSTAB (780")	ROLLED	Preventative (MHI for TTW)	Rev4
3E088	80	78	ROLLSTAB (668")	ROLLED	Preventative (MHI for TTW)	Rev4
3E088	82	78	ROLLSTAB (668")	ROLLED	Preventative (MHI for TTW)	Rev4
3E088	84	78	ROLLSTAB (668")	ROLLED	Preventative (MHI for TTW)	Rev4
3E088	86	78	ROLLSTAB (668")	ROLLED	Preventative (MHI for TTW)	Rev4
3E088	88	78	ROLLSTAB (750")	ROLLED	Preventative (MHI for TTW)	Rev4
3E088	90	78	ROLLSTAB (750")	ROLLED	Preventative (MHI for TTW)	Rev4
3E088	92	78	ROLLSTAB (750")	ROLLED	Preventative (MHI for TTW)	Rev4
3E088	94	78	ROLLSTAB (750")	ROLLED	Preventative (MHI for TTW)	Rev4
3E088	124	78	ROLLSTAB (780")	ROLLED	Preventative (MHI for TTW)	Rev4
3E088	130	78	ROLLSTAB (780")	ROLLED	Preventative (MHI for TTW)	Rev4
3E088	81	79	ROLLSTAB (668")	ROLLED	Preventative (MHI for TTW)	Rev4
3E088	83	79	ROLLSTAB (668")	ROLLED	Preventative (MHI for TTW)	Rev4
3E088	85	79	ROLLSTAB (668")	ROLLED	Preventative (MHI for TTW)	Rev4
3E088	87	79	ROLLSTAB (750")	ROLLED	Preventative (MHI for TTW)	Rev4
3E088	89	79	ROLLSTAB (750")	ROLLED	Preventative (MHI for TTW)	Rev4
3E088	91	79	ROLLSTAB (750")	ROLLED	Preventative (MHI for TTW)	Rev4
3E088	93	79	ROLLSTAB (750")	ROLLED	Preventative (MHI for TTW)	Rev4
3E088	123	79	ROLLSTAB (780")	ROLLED	Preventative (MHI for TTW)	Rev4
3E088	80	80	ROLLSTAB (668")	ROLLED	Preventative (MHI for TTW)	Rev4
3E088	82	80	ROLLSTAB (668")	ROLLED	Preventative (MHI for TTW)	Rev4



SONGS Unit 3 February 2012 Leaker Outage - Steam Generator Condition Monitoring Report

S/G	Row	Col	Hot Leg	Cold Leg	Reason for Tube Repair	Rev
3E088	84	80	ROLLSTAB (668")	ROLLED	Preventative (MHI for TTW)	Rev4
3E088	88	80	ROLLSTAB (750")	ROLLED	Preventative (MHI for TTW)	Rev4
3E088	90	80	ROLLSTAB (750")	ROLLED	Preventative (MHI for TTW)	Rev4
3E088	92	80	ROLLSTAB (750")	ROLLED	Preventative (MHI for TTW)	Rev4
3E088	120	80	ROLLSTAB (780")	ROLLED	Preventative (MHI for TTW)	Rev4
3E088	122	80	ROLLSTAB (780")	ROLLED	Preventative (MHI for TTW)	Rev4
3E088	124	80	ROLLSTAB (780")	ROLLED	Preventative (MHI for TTW)	Rev4
3E088	79	81	ROLLSTAB (668")	ROLLED	Preventative (MHI for TTW)	Rev4
3E088	81	81	ROLLSTAB (668")	ROLLED	Preventative (MHI for TTW)	Rev4
3E088	83	81	ROLLSTAB (668")	ROLLED	Preventative (MHI for TTW)	Rev4
3E088	85	81	ROLLSTAB (668")	ROLLED	Preventative (MHI for TTW)	Rev4
3E088	87	81	ROLLSTAB (750")	ROLLED	Preventative (MHI for TTW)	Rev4
3E088	89	81	ROLLSTAB (750")	ROLLED	Preventative (MHI for TTW)	Rev4
3E088	91	81	ROLLSTAB (750")	ROLLED	Preventative (MHI for TTW)	Rev4
3E088	119	81	ROLLSTAB (780")	ROLLED	Preventative (MHI for TTW)	Rev4
3E088	121	81	ROLLSTAB (780")	ROLLED	Preventative (MHI for TTW)	Rev4
3E088	80	82	ROLLSTAB (668")	ROLLED	Preventative (MHI for TTW)	Rev4
3E088	82	82	ROLLSTAB (668")	ROLLED	Preventative (MHI for TTW)	Rev4
3E088	84	82	ROLLSTAB (668")	ROLLED	Preventative (MHI for TTW)	Rev4
3E088	86	82	ROLLSTAB (668")	ROLLED	Preventative (MHI for TTW)	Rev4
3E088	88	82	ROLLSTAB (750")	ROLLED	Preventative (MHI for TTW)	Rev4
3E088	90	82	ROLLSTAB (750")	ROLLED	Preventative (MHI for TTW)	Rev4
3E088	92	82	ROLLSTAB (750")	ROLLED	Preventative (MHI for TTW)	Rev4
3E088	116	82	ROLLSTAB (780")	ROLLED	Preventative (MHI for TTW)	Rev4
3E088	118	82	ROLLSTAB (780")	ROLLED	Preventative (MHI for TTW)	Rev4
3E088	124	82	ROLLSTAB (780")	ROLLED	Preventative (MHI for TTW)	Rev4
3E088	85	83	ROLLSTAB (668")	ROLLED	Preventative (MHI for TTW)	Rev4
3E088	87	83	ROLLSTAB (750")	ROLLED	Preventative (MHI for TTW)	Rev4
3E088	89	83	ROLLSTAB (750")	ROLLED	Preventative (MHI for TTW)	Rev4
3E088	115	83	ROLLSTAB (780")	ROLLED	Preventative (MHI for TTW)	Rev4
3E088	117	83	ROLLSTAB (780")	ROLLED	Preventative (MHI for TTW)	Rev4
3E088	125	83	ROLLSTAB (780")	ROLLED	Preventative (MHI for TTW)	Rev4
3E088	84	84	ROLLSTAB (668")	ROLLED	Preventative (MHI for TTW)	Rev4
3E088	88	84	ROLLSTAB (750")	ROLLED	Preventative (MHI for TTW)	Rev4
3E088	114	84	ROLLSTAB (780")	ROLLED	Preventative (MHI for TTW)	Rev4
3E088	118	84	ROLLSTAB (780")	ROLLED	Preventative (MHI for TTW)	Rev4
3E088	83	85	ROLLSTAB (668")	ROLLED	Preventative (MHI for TTW)	Rev4
3E088	85	85	ROLLSTAB (668")	ROLLED	Preventative (MHI for TTW)	Rev4
3E088	87	85	ROLLSTAB (750")	ROLLED	Preventative (MHI for TTW)	Rev4
3E088	89	85	ROLLSTAB (750")	ROLLED	Preventative (MHI for TTW)	Rev4
3E088	113	85	ROLLSTAB (780")	ROLLED	Preventative (MHI for TTW)	Rev4
3E088	117	85	ROLLSTAB (780")	ROLLED	Preventative (MHI for TTW)	Rev4
3E088	119	85	ROLLSTAB (780")	ROLLED	Preventative (MHI for TTW)	Rev4
3E088	121	85	ROLLSTAB (780")	ROLLED	Preventative (MHI for TTW)	Rev4
3E088	84	86	ROLLSTAB (668")	ROLLED	Preventative (MHI for TTW)	Rev4



SONGS Unit 3 February 2012 Leaker Outage - Steam Generator Condition Monitoring Report

S/G	Row	Col	Hot Leg	Cold Leg	Reason for Tube Repair	Rev
3E088	86	86	ROLLSTAB (668")	ROLLED	Preventative (MHI for TTW)	Rev4
3E088	88	86	ROLLSTAB (750")	ROLLED	Preventative (MHI for TTW)	Rev4
3E088	90	86	ROLLSTAB (750")	ROLLED	Preventative (MHI for TTW)	Rev4
3E088	92	86	ROLLSTAB (750")	ROLLED	Preventative (MHI for TTW)	Rev4
3E088	108	86	ROLLSTAB (780")	ROLLED	Preventative (MHI for TTW)	Rev4
3E088	110	86	ROLLSTAB (780")	ROLLED	Preventative (MHI for TTW)	Rev4
3E088	112	86	ROLLSTAB (780")	ROLLED	Preventative (MHI for TTW)	Rev4
3E088	85	87	ROLLSTAB (668")	ROLLED	Preventative (MHI for TTW)	Rev4
3E088	89	87	ROLLSTAB (750")	ROLLED	Preventative (MHI for TTW)	Rev4
3E088	91	87	ROLLSTAB (750")	ROLLED	Preventative (MHI for TTW)	Rev4
3E088	93	87	ROLLSTAB (750")	ROLLED	Preventative (MHI for TTW)	Rev4
3E088	109	87	ROLLSTAB (780")	ROLLED	Preventative (MHI for TTW)	Rev4
3E088	111	87	ROLLSTAB (780")	ROLLED	Preventative (MHI for TTW)	Rev4
3E088	113	87	ROLLSTAB (780")	ROLLED	Preventative (MHI for TTW)	Rev4
3E088	92	88	ROLLSTAB (750")	ROLLED	Preventative (MHI for TTW)	Rev4
3E088	108	88	ROLLSTAB (780")	ROLLED	Preventative (MHI for TTW)	Rev4
3E088	110	88	ROLLSTAB (780")	ROLLED	Preventative (MHI for TTW)	Rev4
3E088	112	88	ROLLSTAB (780")	ROLLED	Preventative (MHI for TTW)	Rev4
3E088	116	88	ROLLSTAB (780")	ROLLED	Preventative (MHI for TTW)	Rev4
3E088	118	88	ROLLSTAB (780")	ROLLED	Preventative (MHI for TTW)	Rev4
3E088	93	89	ROLLSTAB (750")	ROLLED	Preventative (MHI for TTW)	Rev4
3E088	95	89	ROLLSTAB (750")	ROLLED	Preventative (MHI for TTW)	Rev4
3E088	97	89	ROLLSTAB (750")	ROLLED	Preventative (MHI for TTW)	Rev4
3E088	109	89	ROLLSTAB (780")	ROLLED	Preventative (MHI for TTW)	Rev4
3E088	111	89	ROLLSTAB (780")	ROLLED	Preventative (MHI for TTW)	Rev4
3E088	94	90	ROLLSTAB (750")	ROLLED	Preventative (MHI for TTW)	Rev4
3E088	96	90	ROLLSTAB (750")	ROLLED	Preventative (MHI for TTW)	Rev4
3E088	98	90	ROLLSTAB (750")	ROLLED	Preventative (MHI for TTW)	Rev4
3E088	100	90	ROLLSTAB (750")	ROLLED	Preventative (MHI for TTW)	Rev4
3E088	102	90	ROLLSTAB (750")	ROLLED	Preventative (MHI for TTW)	Rev4
3E088	108	90	ROLLSTAB (780")	ROLLED	Preventative (MHI for TTW)	Rev4
3E088	112	90	ROLLSTAB (780")	ROLLED	Preventative (MHI for TTW)	Rev4
3E088	89	91	ROLLSTAB (750")	ROLLED	Preventative (MHI for TTW)	Rev4
3E088	95	91	ROLLSTAB (750")	ROLLED	Preventative (MHI for TTW)	Rev4
3E088	97	91	ROLLSTAB (750")	ROLLED	Preventative (MHI for TTW)	Rev4
3E088	99	91	ROLLSTAB (750")	ROLLED	Preventative (MHI for TTW)	Rev4
3E088	101	91	ROLLSTAB (750")	ROLLED	Preventative (MHI for TTW)	Rev4
3E088	103	91	ROLLSTAB (750")	ROLLED	Preventative (MHI for TTW)	Rev4
3E088	105	91	ROLLSTAB (750")	ROLLED	Preventative (MHI for TTW)	Rev4
3E088	107	91	ROLLSTAB (750")	ROLLED	Preventative (MHI for TTW)	Rev4
3E088	94	92	ROLLSTAB (750")	ROLLED	Preventative (MHI for TTW)	Rev4
3E088	96	92	ROLLSTAB (750")	ROLLED	Preventative (MHI for TTW)	Rev4
3E088	98	92	ROLLSTAB (750")	ROLLED	Preventative (MHI for TTW)	Rev4
3E088	100	92	ROLLSTAB (750")	ROLLED	Preventative (MHI for TTW)	Rev4
3E088	102	92	ROLLSTAB (750")	ROLLED	Preventative (MHI for TTW)	Rev4



SONGS Unit 3 February 2012 Leaker Outage - Steam Generator Condition Monitoring Report

S/G	Row	Col	Hot Leg	Cold Leg	Reason for Tube Repair	Rev
3E088	104	92	ROLLSTAB (750")	ROLLED	Preventative (MHI for TTW)	Rev4
3E088	106	92	ROLLSTAB (750")	ROLLED	Preventative (MHI for TTW)	Rev4
3E088	108	92	ROLLSTAB (780")	ROLLED	Preventative (MHI for TTW)	Rev4
3E088	89	93	ROLLSTAB (750")	ROLLED	Preventative (MHI for TTW)	Rev4
3E088	93	93	ROLLSTAB (750")	ROLLED	Preventative (MHI for TTW)	Rev4
3E088	95	93	ROLLSTAB (750")	ROLLED	Preventative (MHI for TTW)	Rev4
3E088	97	93	ROLLSTAB (750")	ROLLED	Preventative (MHI for TTW)	Rev4
3E088	99	93	ROLLSTAB (750")	ROLLED	Preventative (MHI for TTW)	Rev4
3E088	101	93	ROLLSTAB (750")	ROLLED	Preventative (MHI for TTW)	Rev4
3E088	105	93	ROLLSTAB (750")	ROLLED	Preventative (MHI for TTW)	Rev4
3E088	107	93	ROLLSTAB (750")	ROLLED	Preventative (MHI for TTW)	Rev4
3E088	88	94	ROLLSTAB (750")	ROLLED	Preventative (MHI for TTW)	Rev4
3E088	94	94	ROLLSTAB (750")	ROLLED	Preventative (MHI for TTW)	Rev4
3E088	89	95	ROLLSTAB (750")	ROLLED	Preventative (MHI for TTW)	Rev4
3E088	88	96	ROLLSTAB (750")	ROLLED	Preventative (MHI for TTW)	Rev4
3E088	90	96	ROLLSTAB (750")	ROLLED	Preventative (MHI for TTW)	Rev4
3E088	92	96	ROLLSTAB (750")	ROLLED	Preventative (MHI for TTW)	Rev4
3E088	89	97	ROLLSTAB (750")	ROLLED	Preventative (MHI for TTW)	Rev4
3E088	91	97	ROLLSTAB (750")	ROLLED	Preventative (MHI for TTW)	Rev4
3E088	87	75	ROLLSTAB (750")	ROLLED	Preventative (Six Consecutive AVB Wear)	Rev5
3E088	78	80	ROLLSTAB (750")	ROLLED	Preventative (Six Consecutive AVB Wear)	Rev5
3E088	109	73	ROLLSTAB (780")	ROLLED	Preventative (TTW Fence)	Rev4
3E088	111	73	ROLLSTAB (780")	ROLLED	Preventative (TTW Fence)	Rev4
3E088	113	73	ROLLSTAB (780")	ROLLED	Preventative (TTW Fence)	Rev4
3E088	115	73	ROLLSTAB (780")	ROLLED	Preventative (TTW Fence)	Rev4
3E088	100	74	ROLLSTAB (750")	ROLLED	Preventative (TTW Fence)	Rev4
3E088	104	74	ROLLSTAB (750")	ROLLED	Preventative (TTW Fence)	Rev4
3E088	116	74	ROLLSTAB (780")	ROLLED	Preventative (TTW Fence)	Rev4
3E088	97	75	ROLLSTAB (750")	ROLLED	Preventative (TTW Fence)	Rev4
3E088	99	75	ROLLSTAB (750")	ROLLED	Preventative (TTW Fence)	Rev4
3E088	117	75	ROLLSTAB (780")	ROLLED	Preventative (TTW Fence)	Rev4
3E088	119	75	ROLLSTAB (780")	ROLLED	Preventative (TTW Fence)	Rev4
3E088	125	49	ROLLSTAB (668")	ROLLED	Retainer Bar Wear	Rev1
3E088	128	126	ROLLSTAB (668")	ROLLED	Retainer Bar Wear	Rev1
3E088	117	137	ROLLSTAB (668")	ROLLED	Retainer Bar Wear	Rev1
3E088	110	74	ROLLSTAB (750")	ROLLED	U-bend TTW	Rev3
3E088	112	74	ROLLSTAB (750")	ROLLED	U-bend TTW	Rev3
3E088	114	74	ROLLSTAB (750")	ROLLED	U-bend TTW	Rev3
3E088	101	75	ROLLSTAB (750")	ROLLED	U-bend TTW	Rev3
3E088	103	75	ROLLSTAB (750")	ROLLED	U-bend TTW	Rev3
3E088	105	75	ROLLSTAB (750")	ROLLED	U-bend TTW	Rev3
3E088	107	75	ROLLSTAB (750")	ROLLED	U-bend TTW	Rev3
3E088	109	75	ROLLSTAB (750")	ROLLED	U-bend TTW	Rev3
3E088	111	75	ROLLSTAB (750")	ROLLED	U-bend TTW	Rev3
3E088	113	75	ROLLSTAB (750")	ROLLED	U-bend TTW	Rev3

SONGS Unit 3 February 2012 Leaker Outage - Steam Generator Condition Monitoring Report

S/G	Row	Col	Hot Leg	Cold Leg	Reason for Tube Repair	Rev
3E088	115	75	ROLLSTAB (750")	ROLLED	U-bend TTW	Rev3
3E088	98	76	ROLLSTAB (750")	ROLLED	U-bend TTW	Rev3
3E088	100	76	ROLLSTAB (750")	ROLLED	U-bend TTW	Rev3
3E088	102	76	ROLLSTAB (750")	ROLLED	U-bend TTW	Rev3
3E088	104	76	ROLLSTAB (750")	ROLLED	U-bend TTW	Rev2
3E088	106	76	ROLLSTAB (750")	ROLLED	U-bend TTW	Rev2
3E088	108	76	ROLLSTAB (750")	ROLLED	U-bend TTW	Rev3
3E088	110	76	ROLLSTAB (750")	ROLLED	U-bend TTW	Rev2
3E088	112	76	ROLLSTAB (750")	ROLLED	U-bend TTW	Rev3
3E088	114	76	ROLLSTAB (750")	ROLLED	U-bend TTW	Rev3
3E088	118	76	ROLLSTAB (750")	ROLLED	U-bend TTW	Rev3
3E088	120	76	ROLLSTAB (750")	ROLLED	U-bend TTW	Rev3
3E088	99	77	ROLLSTAB (750")	ROLLED	U-bend TTW	Rev3
3E088	101	77	ROLLSTAB (750")	ROLLED	U-bend TTW	Rev3
3E088	103	77	ROLLSTAB (750")	ROLLED	U-bend TTW	Rev3
3E088	105	77	ROLLSTAB (750")	ROLLED	U-bend TTW	Rev2
3E088	107	77	ROLLSTAB (780")	ROLLED	U-bend TTW	Rev0
3E088	109	77	ROLLSTAB (750")	ROLLED	U-bend TTW	Rev2
3E088	111	77	ROLLSTAB (750")	ROLLED	U-bend TTW	Rev3
3E088	113	77	ROLLSTAB (750")	ROLLED	U-bend TTW	Rev3
3E088	115	77	ROLLSTAB (750")	ROLLED	U-bend TTW	Rev3
3E088	117	77	ROLLSTAB (750")	ROLLED	U-bend TTW	Rev3
3E088	119	77	ROLLSTAB (750")	ROLLED	U-bend TTW	Rev3
3E088	121	77	ROLLSTAB (750")	ROLLED	U-bend TTW	Rev3
3E088	96	78	ROLLSTAB (750")	ROLLED	U-bend TTW	Rev3
3E088	98	78	ROLLSTAB (750")	ROLLED	U-bend TTW	Rev3
3E088	100	78	ROLLSTAB (750")	ROLLED	U-bend TTW	Rev3
3E088	102	78	ROLLSTAB (780")	ROLLED	U-bend TTW	Rev0
3E088	104	78	ROLLSTAB (780")	ROLLED	U-bend TTW	Rev0
3E088	106	78	ROLLSTAB (780")	ROLLED	U-bend TTW	Rev0
3E088	108	78	ROLLSTAB (750")	ROLLED	U-bend TTW	Rev2
3E088	110	78	ROLLSTAB (750")	ROLLED	U-bend TTW	Rev2
3E088	112	78	ROLLSTAB (750")	ROLLED	U-bend TTW	Rev3
3E088	114	78	ROLLSTAB (750")	ROLLED	U-bend TTW	Rev3
3E088	116	78	ROLLSTAB (750")	ROLLED	U-bend TTW	Rev3
3E088	118	78	ROLLSTAB (750")	ROLLED	U-bend TTW	Rev2
3E088	120	78	ROLLSTAB (750")	ROLLED	U-bend TTW	Rev2
3E088	122	78	ROLLSTAB (750")	ROLLED	U-bend TTW	Rev3
3E088	95	79	ROLLSTAB (750")	ROLLED	U-bend TTW	Rev3
3E088	97	79	ROLLSTAB (750")	ROLLED	U-bend TTW	Rev3
3E088	99	79	ROLLSTAB (750")	ROLLED	U-bend TTW	Rev3
3E088	101	79	ROLLSTAB (750")	ROLLED	U-bend TTW	Rev2
3E088	103	79	ROLLSTAB (750")	ROLLED	U-bend TTW	Rev2
3E088	105	79	ROLLSTAB (750")	ROLLED	U-bend TTW	Rev2
3E088	107	79	ROLLSTAB (750")	ROLLED	U-bend TTW	Rev2



SONGS Unit 3 February 2012 Leaker Outage - Steam Generator Condition Monitoring Report

S/G	Row	Col	Hot Leg	Cold Leg	Reason for Tube Repair	Rev
3E088	109	79	ROLLSTAB (750")	ROLLED	U-bend TTW	Rev2
3E088	111	79	ROLLSTAB (750")	ROLLED	U-bend TTW	Rev3
3E088	113	79	ROLLSTAB (750")	ROLLED	U-bend TTW	Rev2
3E088	115	79	ROLLSTAB (750")	ROLLED	U-bend TTW	Rev2
3E088	117	79	ROLLSTAB (750")	ROLLED	U-bend TTW	Rev2
3E088	119	79	ROLLSTAB (750")	ROLLED	U-bend TTW	Rev3
3E088	121	79	ROLLSTAB (750")	ROLLED	U-bend TTW	Rev3
3E088	94	80	ROLLSTAB (750")	ROLLED	U-bend TTW	Rev3
3E088	96	80	ROLLSTAB (750")	ROLLED	U-bend TTW	Rev3
3E088	98	80	ROLLSTAB (780")	ROLLED	U-bend TTW	Rev0
3E088	100	80	ROLLSTAB (780")	ROLLED	U-bend TTW	Rev0
3E088	102	80	ROLLSTAB (750")	ROLLED	U-bend TTW	Rev2
3E088	104	80	ROLLSTAB (750")	ROLLED	U-bend TTW	Rev2
3E088	106	80	ROLLSTAB (750")	ROLLED	U-bend TTW	Rev2
3E088	108	80	ROLLSTAB (750")	ROLLED	U-bend TTW	Rev2
3E088	110	80	ROLLSTAB (750")	ROLLED	U-bend TTW	Rev2
3E088	112	80	ROLLSTAB (750")	ROLLED	U-bend TTW	Rev2
3E088	114	80	ROLLSTAB (750")	ROLLED	U-bend TTW	Rev3
3E088	116	80	ROLLSTAB (750")	ROLLED	U-bend TTW	Rev3
3E088	118	80	ROLLSTAB (750")	ROLLED	U-bend TTW	Rev3
3E088	93	81	ROLLSTAB (750")	ROLLED	U-bend TTW	Rev3
3E088	95	81	ROLLSTAB (750")	ROLLED	U-bend TTW	Rev2
3E088	97	81	ROLLSTAB (750")	ROLLED	U-bend TTW	Rev2
3E088	99	81	ROLLSTAB (780")	ROLLED	U-bend TTW	Rev0
3E088	101	81	ROLLSTAB (780")	ROLLED	U-bend TTW	Rev0
3E088	103	81	ROLLSTAB (750")	ROLLED	U-bend TTW	Rev2
3E088	105	81	ROLLSTAB (750")	ROLLED	U-bend TTW	Rev2
3E088	107	81	ROLLSTAB (750")	ROLLED	U-bend TTW	Rev2
3E088	109	81	ROLLSTAB (750")	ROLLED	U-bend TTW	Rev2
3E088	111	81	ROLLSTAB (750")	ROLLED	U-bend TTW	Rev2
3E088	113	81	ROLLSTAB (750")	ROLLED	U-bend TTW	Rev2
3E088	115	81	ROLLSTAB (750")	ROLLED	U-bend TTW	Rev3
3E088	94	82	ROLLSTAB (750")	ROLLED	U-bend TTW	Rev3
3E088	96	82	ROLLSTAB (750")	ROLLED	U-bend TTW	Rev2
3E088	98	82	ROLLSTAB (750")	ROLLED	U-bend TTW	Rev2
3E088	100	82	ROLLSTAB (750")	ROLLED	U-bend TTW	Rev2
3E088	102	82	ROLLSTAB (750")	ROLLED	U-bend TTW	Rev2
3E088	104	82	ROLLSTAB (750")	ROLLED	U-bend TTW	Rev2
3E088	106	82	ROLLSTAB (750")	ROLLED	U-bend TTW	Rev2
3E088	108	82	ROLLSTAB (750")	ROLLED	U-bend TTW	Rev2
3E088	110	82	ROLLSTAB (750")	ROLLED	U-bend TTW	Rev2
3E088	112	82	ROLLSTAB (750")	ROLLED	U-bend TTW	Rev3
3E088	114	82	ROLLSTAB (750")	ROLLED	U-bend TTW	Rev3
3E088	91	83	ROLLSTAB (750")	ROLLED	U-bend TTW	Rev3
3E088	93	83	ROLLSTAB (750")	ROLLED	U-bend TTW	Rev2

SONGS Unit 3 February 2012 Leaker Outage - Steam Generator Condition Monitoring Report

S/G	Row	Col	Hot Leg	Cold Leg	Reason for Tube Repair	Rev
3E088	95	83	ROLLSTAB (750")	ROLLED	U-bend TTW	Rev2
3E088	97	83	ROLLSTAB (750")	ROLLED	U-bend TTW	Rev2
3E088	99	83	ROLLSTAB (750")	ROLLED	U-bend TTW	Rev2
3E088	101	83	ROLLSTAB (750")	ROLLED	U-bend TTW	Rev2
3E088	103	83	ROLLSTAB (750")	ROLLED	U-bend TTW	Rev2
3E088	105	83	ROLLSTAB (750")	ROLLED	U-bend TTW	Rev2
3E088	107	83	ROLLSTAB (750")	ROLLED	U-bend TTW	Rev3
3E088	109	83	ROLLSTAB (750")	ROLLED	U-bend TTW	Rev3
3E088	111	83	ROLLSTAB (750")	ROLLED	U-bend TTW	Rev2
3E088	113	83	ROLLSTAB (750")	ROLLED	U-bend TTW	Rev3
3E088	90	84	ROLLSTAB (750")	ROLLED	U-bend TTW	Rev3
3E088	92	84	ROLLSTAB (750")	ROLLED	U-bend TTW	Rev3
3E088	94	84	ROLLSTAB (750")	ROLLED	U-bend TTW	Rev2
3E088	96	84	ROLLSTAB (750")	ROLLED	U-bend TTW	Rev2
3E088	98	84	ROLLSTAB (750")	ROLLED	U-bend TTW	Rev2
3E088	100	84	ROLLSTAB (750")	ROLLED	U-bend TTW	Rev2
3E088	102	84	ROLLSTAB (750")	ROLLED	U-bend TTW	Rev2
3E088	104	84	ROLLSTAB (750")	ROLLED	U-bend TTW	Rev2
3E088	106	84	ROLLSTAB (750")	ROLLED	U-bend TTW	Rev3
3E088	108	84	ROLLSTAB (750")	ROLLED	U-bend TTW	Rev2
3E088	110	84	ROLLSTAB (750")	ROLLED	U-bend TTW	Rev3
3E088	112	84	ROLLSTAB (750")	ROLLED	U-bend TTW	Rev3
3E088	91	85	ROLLSTAB (750")	ROLLED	U-bend TTW	Rev3
3E088	93	85	ROLLSTAB (750")	ROLLED	U-bend TTW	Rev2
3E088	95	85	ROLLSTAB (750")	ROLLED	U-bend TTW	Rev2
3E088	97	85	ROLLSTAB (750")	ROLLED	U-bend TTW	Rev2
3E088	99	85	ROLLSTAB (750")	ROLLED	U-bend TTW	Rev2
3E088	101	85	ROLLSTAB (750")	ROLLED	U-bend TTW	Rev2
3E088	103	85	ROLLSTAB (750")	ROLLED	U-bend TTW	Rev2
3E088	105	85	ROLLSTAB (750")	ROLLED	U-bend TTW	Rev2
3E088	107	85	ROLLSTAB (750")	ROLLED	U-bend TTW	Rev3
3E088	109	85	ROLLSTAB (750")	ROLLED	U-bend TTW	Rev3
3E088	111	85	ROLLSTAB (750")	ROLLED	U-bend TTW	Rev3
3E088	94	86	ROLLSTAB (750")	ROLLED	U-bend TTW	Rev3
3E088	96	86	ROLLSTAB (750")	ROLLED	U-bend TTW	Rev2
3E088	98	86	ROLLSTAB (750")	ROLLED	U-bend TTW	Rev2
3E088	100	86	ROLLSTAB (750")	ROLLED	U-bend TTW	Rev2
3E088	102	86	ROLLSTAB (750")	ROLLED	U-bend TTW	Rev2
3E088	104	86	ROLLSTAB (750")	ROLLED	U-bend TTW	Rev2
3E088	106	86	ROLLSTAB (750")	ROLLED	U-bend TTW	Rev3
3E088	95	87	ROLLSTAB (750")	ROLLED	U-bend TTW	Rev3
3E088	97	87	ROLLSTAB (750")	ROLLED	U-bend TTW	Rev3
3E088	99	87	ROLLSTAB (750")	ROLLED	U-bend TTW	Rev2
3E088	101	87	ROLLSTAB (750")	ROLLED	U-bend TTW	Rev2
3E088	103	87	ROLLSTAB (750")	ROLLED	U-bend TTW	Rev2

SONGS Unit 3 February 2012 Leaker Outage - Steam Generator Condition Monitoring Report

S/G	Row	Col	Hot Leg	Cold Leg	Reason for Tube Repair	Rev
3E088	105	87	ROLLSTAB (750")	ROLLED	U-bend TTW	Rev3
3E088	107	87	ROLLSTAB (750")	ROLLED	U-bend TTW	Rev3
3E088	94	88	ROLLSTAB (750")	ROLLED	U-bend TTW	Rev3
3E088	96	88	ROLLSTAB (750")	ROLLED	U-bend TTW	Rev2
3E088	98	88	ROLLSTAB (750")	ROLLED	U-bend TTW	Rev2
3E088	100	88	ROLLSTAB (750")	ROLLED	U-bend TTW	Rev2
3E088	102	88	ROLLSTAB (750")	ROLLED	U-bend TTW	Rev2
3E088	104	88	ROLLSTAB (750")	ROLLED	U-bend TTW	Rev2
3E088	106	88	ROLLSTAB (750")	ROLLED	U-bend TTW	Rev3
3E088	99	89	ROLLSTAB (750")	ROLLED	U-bend TTW	Rev3
3E088	101	89	ROLLSTAB (750")	ROLLED	U-bend TTW	Rev3
3E088	103	89	ROLLSTAB (750")	ROLLED	U-bend TTW	Rev3
3E088	105	89	ROLLSTAB (750")	ROLLED	U-bend TTW	Rev3
3E088	107	89	ROLLSTAB (750")	ROLLED	U-bend TTW	Rev3
3E088	104	90	ROLLSTAB (750")	ROLLED	U-bend TTW	Rev3
3E088	106	90	ROLLSTAB (750")	ROLLED	U-bend TTW	Rev3

Appendix B

SG 3E-089 Plugging List



SONGS Unit 3 February 2012 Leaker Outage - Steam Generator Condition Monitoring Report

S/G	Row	Col	Hot Leg	Cold Leg	Reason for Tube Repair	Rev
3E089	108	34	ROLLED	ROLLED	Preventative - Retainer Bar	Rev0
3E089	110	34	ROLLSTAB (668")	ROLLED	Preventative - Retainer Bar	Rev0
3E089	109	35	ROLLSTAB (668")	ROLLED	Preventative - Retainer Bar	Rev0
3E089	111	35	ROLLED	ROLLED	Preventative - Retainer Bar	Rev0
3E089	110	36	ROLLED	ROLLED	Preventative - Retainer Bar	Rev0
3E089	112	36	ROLLED	ROLLED	Preventative - Retainer Bar	Rev0
3E089	111	37	ROLLED	ROLLED	Preventative - Retainer Bar	Rev0
3E089	113	37	ROLLED	ROLLED	Preventative - Retainer Bar	Rev0
3E089	112	38	ROLLED	ROLLED	Preventative - Retainer Bar	Rev0
3E089	114	38	ROLLED	ROLLED	Preventative - Retainer Bar	Rev0
3E089	113	39	ROLLED	ROLLED	Preventative - Retainer Bar	Rev0
3E089	115	39	ROLLED	ROLLED	Preventative - Retainer Bar	Rev0
3E089	114	40	ROLLED	ROLLED	Preventative - Retainer Bar	Rev0
3E089	116	40	ROLLED	ROLLED	Preventative - Retainer Bar	Rev0
3E089	115	41	ROLLED	ROLLED	Preventative - Retainer Bar	Rev0
3E089	117	41	ROLLED	ROLLED	Preventative - Retainer Bar	Rev0
3E089	116	42	ROLLED	ROLLED	Preventative - Retainer Bar	Rev0
3E089	118	42	ROLLED	ROLLED	Preventative - Retainer Bar	Rev0
3E089	117	43	ROLLED	ROLLED	Preventative - Retainer Bar	Rev0
3E089	119	43	ROLLED	ROLLED	Preventative - Retainer Bar	Rev0
3E089	118	44	ROLLED	ROLLED	Preventative - Retainer Bar	Rev0
3E089	120	44	ROLLED	ROLLED	Preventative - Retainer Bar	Rev0
3E089	119	45	ROLLED	ROLLED	Preventative - Retainer Bar	Rev0
3E089	121	45	ROLLSTAB (668")	ROLLED	Preventative - Retainer Bar	Rev0
3E089	120	46	ROLLSTAB (668")	ROLLED	Preventative - Retainer Bar	Rev0
3E089	122	46	ROLLED	ROLLED	Preventative - Retainer Bar	Rev0
3E089	121	47	ROLLED	ROLLED	Preventative - Retainer Bar	Rev0
3E089	123	47	ROLLED	ROLLED	Preventative - Retainer Bar	Rev0
3E089	122	48	ROLLED	ROLLED	Preventative - Retainer Bar	Rev0
3E089	124	48	ROLLED	ROLLED	Preventative - Retainer Bar	Rev0
3E089	123	49	ROLLED	ROLLED	Preventative - Retainer Bar	Rev0
3E089	125	49	ROLLED	ROLLED	Preventative - Retainer Bar	Rev0
3E089	124	50	ROLLED	ROLLED	Preventative - Retainer Bar	Rev0
3E089	126	50	ROLLED	ROLLED	Preventative - Retainer Bar	Rev0
3E089	125	51	ROLLED	ROLLED	Preventative - Retainer Bar	Rev0
3E089	127	51	ROLLED	ROLLED	Preventative - Retainer Bar	Rev0
3E089	126	52	ROLLED	ROLLED	Preventative - Retainer Bar	Rev0
3E089	128	52	ROLLED	ROLLED	Preventative - Retainer Bar	Rev0
3E089	127	53	ROLLED	ROLLED	Preventative - Retainer Bar	Rev0
3E089	129	53	ROLLED	ROLLED	Preventative - Retainer Bar	Rev0
3E089	128	54	ROLLED	ROLLED	Preventative - Retainer Bar	Rev0
3E089	130	54	ROLLED	ROLLED	Preventative - Retainer Bar	Rev0
3E089	129	55	ROLLED	ROLLED	Preventative - Retainer Bar	Rev0
3E089	131	55	ROLLED	ROLLED	Preventative - Retainer Bar	Rev0



SONGS Unit 3 February 2012 Leaker Outage - Steam Generator Condition Monitoring Report

S/G	Row	Col	Hot Leg	Cold Leg	Reason for Tube Repair	Rev
3E089	130	56	ROLLSTAB (668")	ROLLED	Preventative - Retainer Bar	Rev0
3E089	132	56	ROLLSTAB (668")	ROLLED	Preventative - Retainer Bar	Rev0
3E089	131	57	ROLLED	ROLLED	Preventative - Retainer Bar	Rev0
3E089	131	121	ROLLED	ROLLED	Preventative - Retainer Bar	Rev0
3E089	130	122	ROLLSTAB (668")	ROLLED	Preventative - Retainer Bar	Rev0
3E089	132	122	ROLLSTAB (668")	ROLLED	Preventative - Retainer Bar	Rev0
3E089	129	123	ROLLED	ROLLED	Preventative - Retainer Bar	Rev0
3E089	131	123	ROLLED	ROLLED	Preventative - Retainer Bar	Rev0
3E089	128	124	ROLLED	ROLLED	Preventative - Retainer Bar	Rev0
3E089	130	124	ROLLED	ROLLED	Preventative - Retainer Bar	Rev0
3E089	127	125	ROLLED	ROLLED	Preventative - Retainer Bar	Rev0
3E089	129	125	ROLLED	ROLLED	Preventative - Retainer Bar	Rev0
3E089	126	126	ROLLED	ROLLED	Preventative - Retainer Bar	Rev0
3E089	128	126	ROLLED	ROLLED	Preventative - Retainer Bar	Rev0
3E089	125	127	ROLLED	ROLLED	Preventative - Retainer Bar	Rev0
3E089	127	127	ROLLED	ROLLED	Preventative - Retainer Bar	Rev0
3E089	124	128	ROLLED	ROLLED	Preventative - Retainer Bar	Rev0
3E089	126	128	ROLLED	ROLLED	Preventative - Retainer Bar	Rev0
3E089	123	129	ROLLED	ROLLED	Preventative - Retainer Bar	Rev0
3E089	125	129	ROLLED	ROLLED	Preventative - Retainer Bar	Rev0
3E089	122	130	ROLLED	ROLLED	Preventative - Retainer Bar	Rev0
3E089	121	131	ROLLED	ROLLED	Preventative - Retainer Bar	Rev0
3E089	123	131	ROLLED	ROLLED	Preventative - Retainer Bar	Rev0
3E089	120	132	ROLLSTAB (668")	ROLLED	Preventative - Retainer Bar	Rev0
3E089	122	132	ROLLED	ROLLED	Preventative - Retainer Bar	Rev0
3E089	119	133	ROLLED	ROLLED	Preventative - Retainer Bar	Rev0
3E089	121	133	ROLLSTAB (668")	ROLLED	Preventative - Retainer Bar	Rev0
3E089	118	134	ROLLED	ROLLED	Preventative - Retainer Bar	Rev0
3E089	120	134	ROLLED	ROLLED	Preventative - Retainer Bar	Rev0
3E089	117	135	ROLLED	ROLLED	Preventative - Retainer Bar	Rev0
3E089	119	135	ROLLED	ROLLED	Preventative - Retainer Bar	Rev0
3E089	116	136	ROLLED	ROLLED	Preventative - Retainer Bar	Rev0
3E089	118	136	ROLLED	ROLLED	Preventative - Retainer Bar	Rev0
3E089	115	137	ROLLED	ROLLED	Preventative - Retainer Bar	Rev0
3E089	117	137	ROLLED	ROLLED	Preventative - Retainer Bar	Rev0
3E089	114	138	ROLLED	ROLLED	Preventative - Retainer Bar	Rev0
3E089	116	138	ROLLED	ROLLED	Preventative - Retainer Bar	Rev0
3E089	113	139	ROLLED	ROLLED	Preventative - Retainer Bar	Rev0
3E089	115	139	ROLLED	ROLLED	Preventative - Retainer Bar	Rev0
3E089	112	140	ROLLED	ROLLED	Preventative - Retainer Bar	Rev0
3E089	114	140	ROLLED	ROLLED	Preventative - Retainer Bar	Rev0
3E089	111	141	ROLLED	ROLLED	Preventative - Retainer Bar	Rev0
3E089	113	141	ROLLED	ROLLED	Preventative - Retainer Bar	Rev0
3E089	110	142	ROLLED	ROLLED	Preventative - Retainer Bar	Rev0
3E089	112	142	ROLLED	ROLLED	Preventative - Retainer Bar	Rev0

SONGS Unit 3 February 2012 Leaker Outage - Steam Generator Condition Monitoring Report

S/G	Row	Col	Hot Leg	Cold Leg	Reason for Tube Repair	Rev
3E089	109	143	ROLLSTAB (668")	ROLLED	Preventative - Retainer Bar	Rev0
3E089	111	143	ROLLED	ROLLED	Preventative - Retainer Bar	Rev0
3E089	108	144	ROLLED	ROLLED	Preventative - Retainer Bar	Rev0
3E089	110	144	ROLLSTAB (668")	ROLLED	Preventative - Retainer Bar	Rev0
3E089	85	75	ROLLSTAB (668")	ROLLED	Preventative (MHI for TTW)	Rev3
3E089	97	75	ROLLSTAB (750")	ROLLED	Preventative (MHI for TTW)	Rev3
3E089	86	76	ROLLSTAB (668")	ROLLED	Preventative (MHI for TTW)	Rev3
3E089	94	76	ROLLSTAB (750")	ROLLED	Preventative (MHI for TTW)	Rev3
3E089	96	76	ROLLSTAB (750")	ROLLED	Preventative (MHI for TTW)	Rev3
3E089	98	76	ROLLSTAB (750")	ROLLED	Preventative (MHI for TTW)	Rev3
3E089	100	76	ROLLSTAB (750")	ROLLED	Preventative (MHI for TTW)	Rev3
3E089	83	77	ROLLSTAB (668")	ROLLED	Preventative (MHI for TTW)	Rev3
3E089	87	77	ROLLSTAB (750")	ROLLED	Preventative (MHI for TTW)	Rev3
3E089	93	77	ROLLSTAB (750")	ROLLED	Preventative (MHI for TTW)	Rev3
3E089	107	77	ROLLSTAB (750")	ROLLED	Preventative (MHI for TTW)	Rev3
3E089	86	78	ROLLSTAB (668")	ROLLED	Preventative (MHI for TTW)	Rev3
3E089	88	78	ROLLSTAB (750")	ROLLED	Preventative (MHI for TTW)	Rev3
3E089	92	78	ROLLSTAB (750")	ROLLED	Preventative (MHI for TTW)	Rev3
3E089	94	78	ROLLSTAB (750")	ROLLED	Preventative (MHI for TTW)	Rev3
3E089	83	79	ROLLSTAB (668")	ROLLED	Preventative (MHI for TTW)	Rev3
3E089	85	79	ROLLSTAB (668")	ROLLED	Preventative (MHI for TTW)	Rev3
3E089	87	79	ROLLSTAB (750")	ROLLED	Preventative (MHI for TTW)	Rev3
3E089	89	79	ROLLSTAB (750")	ROLLED	Preventative (MHI for TTW)	Rev3
3E089	91	79	ROLLSTAB (750")	ROLLED	Preventative (MHI for TTW)	Rev3
3E089	115	79	ROLLSTAB (780")	ROLLED	Preventative (MHI for TTW)	Rev3
3E089	86	80	ROLLSTAB (668")	ROLLED	Preventative (MHI for TTW)	Rev3
3E089	88	80	ROLLSTAB (750")	ROLLED	Preventative (MHI for TTW)	Rev3
3E089	90	80	ROLLSTAB (750")	ROLLED	Preventative (MHI for TTW)	Rev3
3E089	110	80	ROLLSTAB (780")	ROLLED	Preventative (MHI for TTW)	Rev3
3E089	114	80	ROLLSTAB (780")	ROLLED	Preventative (MHI for TTW)	Rev3
3E089	87	81	ROLLSTAB (750")	ROLLED	Preventative (MHI for TTW)	Rev3
3E089	109	81	ROLLSTAB (750")	ROLLED	Preventative (MHI for TTW)	Rev3
3E089	84	82	ROLLSTAB (668")	ROLLED	Preventative (MHI for TTW)	Rev3
3E089	86	82	ROLLSTAB (750")	ROLLED	Preventative (MHI for TTW)	Rev3
3E089	88	82	ROLLSTAB (750")	ROLLED	Preventative (MHI for TTW)	Rev3
3E089	108	82	ROLLSTAB (750")	ROLLED	Preventative (MHI for TTW)	Rev3
3E089	112	82	ROLLSTAB (780")	ROLLED	Preventative (MHI for TTW)	Rev3
3E089	118	82	ROLLSTAB (780")	ROLLED	Preventative (MHI for TTW)	Rev3
3E089	120	82	ROLLSTAB (780")	ROLLED	Preventative (MHI for TTW)	Rev3
3E089	83	83	ROLLSTAB (668")	ROLLED	Preventative (MHI for TTW)	Rev3
3E089	85	83	ROLLSTAB (750")	ROLLED	Preventative (MHI for TTW)	Rev3
3E089	109	83	ROLLSTAB (750")	ROLLED	Preventative (MHI for TTW)	Rev3
3E089	111	83	ROLLSTAB (780")	ROLLED	Preventative (MHI for TTW)	Rev3
3E089	113	83	ROLLSTAB (780")	ROLLED	Preventative (MHI for TTW)	Rev3
3E089	117	83	ROLLSTAB (780")	ROLLED	Preventative (MHI for TTW)	Rev3



SONGS Unit 3 February 2012 Leaker Outage - Steam Generator Condition Monitoring Report

S/G	Row	Col	Hot Leg	Cold Leg	Reason for Tube Repair	Rev
3E089	119	83	ROLLSTAB (780")	ROLLED	Preventative (MHI for TTW)	Rev3
3E089	82	84	ROLLSTAB (668")	ROLLED	Preventative (MHI for TTW)	Rev3
3E089	84	84	ROLLSTAB (750")	ROLLED	Preventative (MHI for TTW)	Rev3
3E089	108	84	ROLLSTAB (750")	ROLLED	Preventative (MHI for TTW)	Rev3
3E089	110	84	ROLLSTAB (780")	ROLLED	Preventative (MHI for TTW)	Rev3
3E089	112	84	ROLLSTAB (780")	ROLLED	Preventative (MHI for TTW)	Rev3
3E089	114	84	ROLLSTAB (780")	ROLLED	Preventative (MHI for TTW)	Rev3
3E089	81	85	ROLLSTAB (668")	ROLLED	Preventative (MHI for TTW)	Rev3
3E089	83	85	ROLLSTAB (750")	ROLLED	Preventative (MHI for TTW)	Rev3
3E089	109	85	ROLLSTAB (750")	ROLLED	Preventative (MHI for TTW)	Rev3
3E089	111	85	ROLLSTAB (780")	ROLLED	Preventative (MHI for TTW)	Rev3
3E089	113	85	ROLLSTAB (780")	ROLLED	Preventative (MHI for TTW)	Rev3
3E089	115	85	ROLLSTAB (780")	ROLLED	Preventative (MHI for TTW)	Rev3
3E089	117	85	ROLLSTAB (780")	ROLLED	Preventative (MHI for TTW)	Rev3
3E089	84	86	ROLLSTAB (750")	ROLLED	Preventative (MHI for TTW)	Rev3
3E089	86	86	ROLLSTAB (750")	ROLLED	Preventative (MHI for TTW)	Rev3
3E089	110	86	ROLLSTAB (780")	ROLLED	Preventative (MHI for TTW)	Rev3
3E089	112	86	ROLLSTAB (780")	ROLLED	Preventative (MHI for TTW)	Rev3
3E089	114	86	ROLLSTAB (780")	ROLLED	Preventative (MHI for TTW)	Rev3
3E089	116	86	ROLLSTAB (780")	ROLLED	Preventative (MHI for TTW)	Rev3
3E089	109	87	ROLLSTAB (750")	ROLLED	Preventative (MHI for TTW)	Rev3
3E089	111	87	ROLLSTAB (780")	ROLLED	Preventative (MHI for TTW)	Rev3
3E089	113	87	ROLLSTAB (780")	ROLLED	Preventative (MHI for TTW)	Rev3
3E089	115	87	ROLLSTAB (780")	ROLLED	Preventative (MHI for TTW)	Rev3
3E089	108	88	ROLLSTAB (750")	ROLLED	Preventative (MHI for TTW)	Rev3
3E089	110	88	ROLLSTAB (780")	ROLLED	Preventative (MHI for TTW)	Rev3
3E089	112	88	ROLLSTAB (780")	ROLLED	Preventative (MHI for TTW)	Rev3
3E089	114	88	ROLLSTAB (780")	ROLLED	Preventative (MHI for TTW)	Rev3
3E089	116	88	ROLLSTAB (780")	ROLLED	Preventative (MHI for TTW)	Rev3
3E089	83	89	ROLLSTAB (750")	ROLLED	Preventative (MHI for TTW)	Rev3
3E089	109	89	ROLLSTAB (750")	ROLLED	Preventative (MHI for TTW)	Rev3
3E089	111	89	ROLLSTAB (780")	ROLLED	Preventative (MHI for TTW)	Rev3
3E089	113	89	ROLLSTAB (780")	ROLLED	Preventative (MHI for TTW)	Rev3
3E089	115	89	ROLLSTAB (780")	ROLLED	Preventative (MHI for TTW)	Rev3
3E089	108	90	ROLLSTAB (750")	ROLLED	Preventative (MHI for TTW)	Rev3
3E089	110	90	ROLLSTAB (780")	ROLLED	Preventative (MHI for TTW)	Rev3
3E089	114	90	ROLLSTAB (780")	ROLLED	Preventative (MHI for TTW)	Rev3
3E089	85	91	ROLLSTAB (750")	ROLLED	Preventative (MHI for TTW)	Rev3
3E089	105	91	ROLLSTAB (750")	ROLLED	Preventative (MHI for TTW)	Rev3
3E089	107	91	ROLLSTAB (750")	ROLLED	Preventative (MHI for TTW)	Rev3
3E089	109	91	ROLLSTAB (750")	ROLLED	Preventative (MHI for TTW)	Rev3
3E089	111	91	ROLLSTAB (780")	ROLLED	Preventative (MHI for TTW)	Rev3
3E089	113	91	ROLLSTAB (780")	ROLLED	Preventative (MHI for TTW)	Rev3
3E089	102	92	ROLLSTAB (750")	ROLLED	Preventative (MHI for TTW)	Rev3
3E089	104	92	ROLLSTAB (750")	ROLLED	Preventative (MHI for TTW)	Rev3

SONGS Unit 3 February 2012 Leaker Outage - Steam Generator Condition Monitoring Report

S/G	Row	Col	Hot Leg	Cold Leg	Reason for Tube Repair	Rev
3E089	106	92	ROLLSTAB (750")	ROLLED	Preventative (MHI for TTW)	Rev3
3E089	108	92	ROLLSTAB (750")	ROLLED	Preventative (MHI for TTW)	Rev3
3E089	110	92	ROLLSTAB (780")	ROLLED	Preventative (MHI for TTW)	Rev3
3E089	112	92	ROLLSTAB (780")	ROLLED	Preventative (MHI for TTW)	Rev3
3E089	97	93	ROLLSTAB (750")	ROLLED	Preventative (MHI for TTW)	Rev3
3E089	99	93	ROLLSTAB (750")	ROLLED	Preventative (MHI for TTW)	Rev3
3E089	101	93	ROLLSTAB (750")	ROLLED	Preventative (MHI for TTW)	Rev3
3E089	105	93	ROLLSTAB (750")	ROLLED	Preventative (MHI for TTW)	Rev3
3E089	107	93	ROLLSTAB (750")	ROLLED	Preventative (MHI for TTW)	Rev3
3E089	109	93	ROLLSTAB (750")	ROLLED	Preventative (MHI for TTW)	Rev3
3E089	111	93	ROLLSTAB (780")	ROLLED	Preventative (MHI for TTW)	Rev3
3E089	88	94	ROLLSTAB (750")	ROLLED	Preventative (MHI for TTW)	Rev3
3E089	92	94	ROLLSTAB (750")	ROLLED	Preventative (MHI for TTW)	Rev3
3E089	94	94	ROLLSTAB (750")	ROLLED	Preventative (MHI for TTW)	Rev3
3E089	96	94	ROLLSTAB (750")	ROLLED	Preventative (MHI for TTW)	Rev3
3E089	98	94	ROLLSTAB (750")	ROLLED	Preventative (MHI for TTW)	Rev3
3E089	100	94	ROLLSTAB (750")	ROLLED	Preventative (MHI for TTW)	Rev3
3E089	102	94	ROLLSTAB (750")	ROLLED	Preventative (MHI for TTW)	Rev3
3E089	106	94	ROLLSTAB (750")	ROLLED	Preventative (MHI for TTW)	Rev3
3E089	108	94	ROLLSTAB (750")	ROLLED	Preventative (MHI for TTW)	Rev3
3E089	110	94	ROLLSTAB (780")	ROLLED	Preventative (MHI for TTW)	Rev3
3E089	91	95	ROLLSTAB (750")	ROLLED	Preventative (MHI for TTW)	Rev3
3E089	93	95	ROLLSTAB (750")	ROLLED	Preventative (MHI for TTW)	Rev3
3E089	99	95	ROLLSTAB (750")	ROLLED	Preventative (MHI for TTW)	Rev3
3E089	101	95	ROLLSTAB (750")	ROLLED	Preventative (MHI for TTW)	Rev3
3E089	107	95	ROLLSTAB (750")	ROLLED	Preventative (MHI for TTW)	Rev3
3E089	85	81	ROLLSTAB (750")	ROLLED	Preventative (Six Consecutive AVB Wear)	Rev4
3E089	122	88	ROLLSTAB (750")	ROLLED	Preventative (Six Consecutive AVB Wear)	Rev4
3E089	101	75	ROLLSTAB (750")	ROLLED	Preventative (TTW Fence)	Rev3
3E089	103	75	ROLLSTAB (750")	ROLLED	Preventative (TTW Fence)	Rev3
3E089	105	75	ROLLSTAB (750")	ROLLED	Preventative (TTW Fence)	Rev3
3E089	106	76	ROLLSTAB (750")	ROLLED	Preventative (TTW Fence)	Rev3
3E089	109	77	ROLLSTAB (750")	ROLLED	Preventative (TTW Fence)	Rev3
3E089	110	78	ROLLSTAB (780")	ROLLED	Preventative (TTW Fence)	Rev3
3E089	111	79	ROLLSTAB (780")	ROLLED	Preventative (TTW Fence)	Rev3
3E089	83	87	ROLLSTAB (750")	ROLLED	Preventative (TTW Fence)	Rev3
3E089	82	88	ROLLSTAB (750")	ROLLED	Preventative (TTW Fence)	Rev3
3E089	84	90	ROLLSTAB (750")	ROLLED	Preventative (TTW Fence)	Rev3
3E089	86	92	ROLLSTAB (750")	ROLLED	Preventative (TTW Fence)	Rev3
3E089	85	93	ROLLSTAB (750")	ROLLED	Preventative (TTW Fence)	Rev3
3E089	86	94	ROLLSTAB (750")	ROLLED	Preventative (TTW Fence)	Rev3
3E089	90	94	ROLLSTAB (750")	ROLLED	Preventative (TTW Fence)	Rev3
3E089	124	130	ROLLSTAB (668")	ROLLED	Retainer Bar Wear	Rev0
3E089	102	76	ROLLSTAB (750")	ROLLED	U-bend TTW	Rev2
3E089	104	76	ROLLSTAB (750")	ROLLED	U-bend TTW	Rev2

SONGS Unit 3 February 2012 Leaker Outage - Steam Generator Condition Monitoring Report

S/G	Row	Col	Hot Leg	Cold Leg	Reason for Tube Repair	Rev
3E089	95	77	ROLLSTAB (750")	ROLLED	U-bend TTW	Rev2
3E089	97	77	ROLLSTAB (750")	ROLLED	U-bend TTW	Rev2
3E089	99	77	ROLLSTAB (750")	ROLLED	U-bend TTW	Rev2
3E089	101	77	ROLLSTAB (750")	ROLLED	U-bend TTW	Rev2
3E089	103	77	ROLLSTAB (750")	ROLLED	U-bend TTW	Rev2
3E089	105	77	ROLLSTAB (750")	ROLLED	U-bend TTW	Rev2
3E089	96	78	ROLLSTAB (750")	ROLLED	U-bend TTW	Rev2
3E089	98	78	ROLLSTAB (750")	ROLLED	U-bend TTW	Rev1
3E089	100	78	ROLLSTAB (750")	ROLLED	U-bend TTW	Rev2
3E089	102	78	ROLLSTAB (750")	ROLLED	U-bend TTW	Rev2
3E089	104	78	ROLLSTAB (750")	ROLLED	U-bend TTW	Rev2
3E089	106	78	ROLLSTAB (750")	ROLLED	U-bend TTW	Rev2
3E089	108	78	ROLLSTAB (750")	ROLLED	U-bend TTW	Rev2
3E089	93	79	ROLLSTAB (750")	ROLLED	U-bend TTW	Rev2
3E089	95	79	ROLLSTAB (750")	ROLLED	U-bend TTW	Rev2
3E089	97	79	ROLLSTAB (750")	ROLLED	U-bend TTW	Rev2
3E089	99	79	ROLLSTAB (750")	ROLLED	U-bend TTW	Rev2
3E089	101	79	ROLLSTAB (750")	ROLLED	U-bend TTW	Rev2
3E089	103	79	ROLLSTAB (750")	ROLLED	U-bend TTW	Rev2
3E089	105	79	ROLLSTAB (750")	ROLLED	U-bend TTW	Rev1
3E089	107	79	ROLLSTAB (750")	ROLLED	U-bend TTW	Rev2
3E089	109	79	ROLLSTAB (750")	ROLLED	U-bend TTW	Rev2
3E089	92	80	ROLLSTAB (750")	ROLLED	U-bend TTW	Rev2
3E089	94	80	ROLLSTAB (750")	ROLLED	U-bend TTW	Rev2
3E089	96	80	ROLLSTAB (750")	ROLLED	U-bend TTW	Rev2
3E089	98	80	ROLLSTAB (750")	ROLLED	U-bend TTW	Rev1
3E089	100	80	ROLLSTAB (750")	ROLLED	U-bend TTW	Rev1
3E089	102	80	ROLLSTAB (750")	ROLLED	U-bend TTW	Rev1
3E089	104	80	ROLLSTAB (750")	ROLLED	U-bend TTW	Rev2
3E089	106	80	ROLLSTAB (750")	ROLLED	U-bend TTW	Rev1
3E089	108	80	ROLLSTAB (750")	ROLLED	U-bend TTW	Rev2
3E089	89	81	ROLLSTAB (750")	ROLLED	U-bend TTW	Rev2
3E089	91	81	ROLLSTAB (750")	ROLLED	U-bend TTW	Rev2
3E089	93	81	ROLLSTAB (750")	ROLLED	U-bend TTW	Rev2
3E089	95	81	ROLLSTAB (750")	ROLLED	U-bend TTW	Rev2
3E089	97	81	ROLLSTAB (750")	ROLLED	U-bend TTW	Rev1
3E089	99	81	ROLLSTAB (750")	ROLLED	U-bend TTW	Rev2
3E089	101	81	ROLLSTAB (750")	ROLLED	U-bend TTW	Rev2
3E089	103	81	ROLLSTAB (750")	ROLLED	U-bend TTW	Rev2
3E089	105	81	ROLLSTAB (750")	ROLLED	U-bend TTW	Rev2
3E089	107	81	ROLLSTAB (750")	ROLLED	U-bend TTW	Rev2
3E089	90	82	ROLLSTAB (750")	ROLLED	U-bend TTW	Rev2
3E089	92	82	ROLLSTAB (750")	ROLLED	U-bend TTW	Rev1
3E089	94	82	ROLLSTAB (780")	ROLLED	U-bend TTW	Rev2
3E089	96	82	ROLLSTAB (750")	ROLLED	U-bend TTW	Rev2

SONGS Unit 3 February 2012 Leaker Outage - Steam Generator Condition Monitoring Report

S/G	Row	Col	Hot Leg	Cold Leg	Reason for Tube Repair	Rev
3E089	98	82	ROLLSTAB (750")	ROLLED	U-bend TTW	Rev1
3E089	100	82	ROLLSTAB (750")	ROLLED	U-bend TTW	Rev2
3E089	102	82	ROLLSTAB (750")	ROLLED	U-bend TTW	Rev2
3E089	104	82	ROLLSTAB (750")	ROLLED	U-bend TTW	Rev2
3E089	106	82	ROLLSTAB (750")	ROLLED	U-bend TTW	Rev2
3E089	87	83	ROLLSTAB (750")	ROLLED	U-bend TTW	Rev2
3E089	89	83	ROLLSTAB (750")	ROLLED	U-bend TTW	Rev2
3E089	91	83	ROLLSTAB (750")	ROLLED	U-bend TTW	Rev1
3E089	93	83	ROLLSTAB (750")	ROLLED	U-bend TTW	Rev1
3E089	95	83	ROLLSTAB (750")	ROLLED	U-bend TTW	Rev2
3E089	97	83	ROLLSTAB (780")	ROLLED	U-bend TTW	Rev2
3E089	99	83	ROLLSTAB (750")	ROLLED	U-bend TTW	Rev1
3E089	101	83	ROLLSTAB (750")	ROLLED	U-bend TTW	Rev1
3E089	103	83	ROLLSTAB (750")	ROLLED	U-bend TTW	Rev1
3E089	105	83	ROLLSTAB (750")	ROLLED	U-bend TTW	Rev2
3E089	107	83	ROLLSTAB (750")	ROLLED	U-bend TTW	Rev2
3E089	86	84	ROLLSTAB (750")	ROLLED	U-bend TTW	Rev2
3E089	88	84	ROLLSTAB (750")	ROLLED	U-bend TTW	Rev2
3E089	90	84	ROLLSTAB (750")	ROLLED	U-bend TTW	Rev2
3E089	92	84	ROLLSTAB (750")	ROLLED	U-bend TTW	Rev1
3E089	94	84	ROLLSTAB (780")	ROLLED	U-bend TTW	Rev2
3E089	96	84	ROLLSTAB (750")	ROLLED	U-bend TTW	Rev1
3E089	98	84	ROLLSTAB (750")	ROLLED	U-bend TTW	Rev1
3E089	100	84	ROLLSTAB (750")	ROLLED	U-bend TTW	Rev1
3E089	102	84	ROLLSTAB (750")	ROLLED	U-bend TTW	Rev1
3E089	104	84	ROLLSTAB (750")	ROLLED	U-bend TTW	Rev2
3E089	106	84	ROLLSTAB (750")	ROLLED	U-bend TTW	Rev2
3E089	85	85	ROLLSTAB (750")	ROLLED	U-bend TTW	Rev2
3E089	87	85	ROLLSTAB (750")	ROLLED	U-bend TTW	Rev2
3E089	89	85	ROLLSTAB (750")	ROLLED	U-bend TTW	Rev2
3E089	91	85	ROLLSTAB (750")	ROLLED	U-bend TTW	Rev2
3E089	93	85	ROLLSTAB (750")	ROLLED	U-bend TTW	Rev1
3E089	95	85	ROLLSTAB (750")	ROLLED	U-bend TTW	Rev1
3E089	97	85	ROLLSTAB (750")	ROLLED	U-bend TTW	Rev1
3E089	99	85	ROLLSTAB (750")	ROLLED	U-bend TTW	Rev1
3E089	101	85	ROLLSTAB (750")	ROLLED	U-bend TTW	Rev1
3E089	103	85	ROLLSTAB (750")	ROLLED	U-bend TTW	Rev2
3E089	105	85	ROLLSTAB (750")	ROLLED	U-bend TTW	Rev2
3E089	107	85	ROLLSTAB (750")	ROLLED	U-bend TTW	Rev2
3E089	88	86	ROLLSTAB (750")	ROLLED	U-bend TTW	Rev2
3E089	90	86	ROLLSTAB (780")	ROLLED	U-bend TTW	Rev2
3E089	92	86	ROLLSTAB (780")	ROLLED	U-bend TTW	Rev2
3E089	94	86	ROLLSTAB (750")	ROLLED	U-bend TTW	Rev1
3E089	96	86	ROLLSTAB (750")	ROLLED	U-bend TTW	Rev1
3E089	98	86	ROLLSTAB (780")	ROLLED	U-bend TTW	Rev2



SONGS Unit 3 February 2012 Leaker Outage - Steam Generator Condition Monitoring Report

S/G	Row	Col	Hot Leg	Cold Leg	Reason for Tube Repair	Rev
3E089	100	86	ROLLSTAB (750")	ROLLED	U-bend TTW	Rev1
3E089	102	86	ROLLSTAB (750")	ROLLED	U-bend TTW	Rev1
3E089	104	86	ROLLSTAB (750")	ROLLED	U-bend TTW	Rev1
3E089	106	86	ROLLSTAB (750")	ROLLED	U-bend TTW	Rev1
3E089	108	86	ROLLSTAB (750")	ROLLED	U-bend TTW	Rev2
3E089	85	87	ROLLSTAB (750")	ROLLED	U-bend TTW	Rev2
3E089	87	87	ROLLSTAB (750")	ROLLED	U-bend TTW	Rev1
3E089	89	87	ROLLSTAB (780")	ROLLED	U-bend TTW	Rev2
3E089	91	87	ROLLSTAB (780")	ROLLED	U-bend TTW	Rev2
3E089	93	87	ROLLSTAB (780")	ROLLED	U-bend TTW	Rev2
3E089	95	87	ROLLSTAB (780")	ROLLED	U-bend TTW	Rev2
3E089	97	87	ROLLSTAB (750")	ROLLED	U-bend TTW	Rev1
3E089	99	87	ROLLSTAB (750")	ROLLED	U-bend TTW	Rev1
3E089	101	87	ROLLSTAB (750")	ROLLED	U-bend TTW	Rev1
3E089	103	87	ROLLSTAB (750")	ROLLED	U-bend TTW	Rev1
3E089	105	87	ROLLSTAB (750")	ROLLED	U-bend TTW	Rev2
3E089	107	87	ROLLSTAB (750")	ROLLED	U-bend TTW	Rev2
3E089	84	88	ROLLSTAB (750")	ROLLED	U-bend TTW	Rev2
3E089	86	88	ROLLSTAB (750")	ROLLED	U-bend TTW	Rev2
3E089	88	88	ROLLSTAB (750")	ROLLED	U-bend TTW	Rev1
3E089	90	88	ROLLSTAB (750")	ROLLED	U-bend TTW	Rev2
3E089	92	88	ROLLSTAB (750")	ROLLED	U-bend TTW	Rev1
3E089	94	88	ROLLSTAB (750")	ROLLED	U-bend TTW	Rev1
3E089	96	88	ROLLSTAB (780")	ROLLED	U-bend TTW	Rev2
3E089	98	88	ROLLSTAB (780")	ROLLED	U-bend TTW	Rev2
3E089	100	88	ROLLSTAB (750")	ROLLED	U-bend TTW	Rev1
3E089	102	88	ROLLSTAB (750")	ROLLED	U-bend TTW	Rev1
3E089	104	88	ROLLSTAB (750")	ROLLED	U-bend TTW	Rev2
3E089	106	88	ROLLSTAB (750")	ROLLED	U-bend TTW	Rev2
3E089	85	89	ROLLSTAB (750")	ROLLED	U-bend TTW	Rev2
3E089	87	89	ROLLSTAB (780")	ROLLED	U-bend TTW	Rev2
3E089	89	89	ROLLSTAB (780")	ROLLED	U-bend TTW	Rev2
3E089	91	89	ROLLSTAB (780")	ROLLED	U-bend TTW	Rev2
3E089	93	89	ROLLSTAB (780")	ROLLED	U-bend TTW	Rev2
3E089	95	89	ROLLSTAB (780")	ROLLED	U-bend TTW	Rev2
3E089	97	89	ROLLSTAB (780")	ROLLED	U-bend TTW	Rev2
3E089	99	89	ROLLSTAB (780")	ROLLED	U-bend TTW	Rev2
3E089	101	89	ROLLSTAB (780")	ROLLED	U-bend TTW	Rev2
3E089	103	89	ROLLSTAB (750")	ROLLED	U-bend TTW	Rev2
3E089	105	89	ROLLSTAB (750")	ROLLED	U-bend TTW	Rev2
3E089	107	89	ROLLSTAB (750")	ROLLED	U-bend TTW	Rev2
3E089	86	90	ROLLSTAB (750")	ROLLED	U-bend TTW	Rev2
3E089	88	90	ROLLSTAB (780")	ROLLED	U-bend TTW	Rev2
3E089	90	90	ROLLSTAB (780")	ROLLED	U-bend TTW	Rev2
3E089	92	90	ROLLSTAB (780")	ROLLED	U-bend TTW	Rev2

SONGS Unit 3 February 2012 Leaker Outage - Steam Generator Condition Monitoring Report

S/G	Row	Col	Hot Leg	Cold Leg	Reason for Tube Repair	Rev
3E089	94	90	ROLLSTAB (780")	ROLLED	U-bend TTW	Rev2
3E089	96	90	ROLLSTAB (780")	ROLLED	U-bend TTW	Rev2
3E089	98	90	ROLLSTAB (750")	ROLLED	U-bend TTW	Rev1
3E089	100	90	ROLLSTAB (750")	ROLLED	U-bend TTW	Rev1
3E089	102	90	ROLLSTAB (750")	ROLLED	U-bend TTW	Rev2
3E089	104	90	ROLLSTAB (750")	ROLLED	U-bend TTW	Rev2
3E089	106	90	ROLLSTAB (750")	ROLLED	U-bend TTW	Rev2
3E089	87	91	ROLLSTAB (750")	ROLLED	U-bend TTW	Rev1
3E089	89	91	ROLLSTAB (780")	ROLLED	U-bend TTW	Rev2
3E089	91	91	ROLLSTAB (780")	ROLLED	U-bend TTW	Rev2
3E089	93	91	ROLLSTAB (780")	ROLLED	U-bend TTW	Rev2
3E089	95	91	ROLLSTAB (780")	ROLLED	U-bend TTW	Rev2
3E089	97	91	ROLLSTAB (750")	ROLLED	U-bend TTW	Rev1
3E089	99	91	ROLLSTAB (780")	ROLLED	U-bend TTW	Rev2
3E089	101	91	ROLLSTAB (750")	ROLLED	U-bend TTW	Rev2
3E089	103	91	ROLLSTAB (750")	ROLLED	U-bend TTW	Rev2
3E089	88	92	ROLLSTAB (750")	ROLLED	U-bend TTW	Rev2
3E089	90	92	ROLLSTAB (750")	ROLLED	U-bend TTW	Rev1
3E089	92	92	ROLLSTAB (780")	ROLLED	U-bend TTW	Rev2
3E089	94	92	ROLLSTAB (780")	ROLLED	U-bend TTW	Rev2
3E089	96	92	ROLLSTAB (750")	ROLLED	U-bend TTW	Rev1
3E089	98	92	ROLLSTAB (750")	ROLLED	U-bend TTW	Rev2
3E089	100	92	ROLLSTAB (750")	ROLLED	U-bend TTW	Rev2
3E089	87	93	ROLLSTAB (750")	ROLLED	U-bend TTW	Rev2
3E089	89	93	ROLLSTAB (750")	ROLLED	U-bend TTW	Rev2
3E089	91	93	ROLLSTAB (750")	ROLLED	U-bend TTW	Rev2
3E089	93	93	ROLLSTAB (750")	ROLLED	U-bend TTW	Rev1
3E089	95	93	ROLLSTAB (750")	ROLLED	U-bend TTW	Rev2

ATTACHMENT 4

MHI Document L5-04GA564 Tube Wear of Unit-3 RSG Technical Evaluation Report

[Proprietary Information Redacted]



Revision History

No.	Revision	Date	Approved	Checked	Prepared
0	Initial issue	See cover sheet			
1	Revised in accordance with RSG-SCE/MHI-12-5698 (Since this report has been wholly revised, the revision bar is omitted)				
2	-Revised in accordance with RSG-SCE/MHI-12-5714 -Revised Appendix-10 by using the latest ATHOS outputs -Added Appendix-16				
3	-Revised in accordance with RSG-SCE/MHI-12-5728 -Revised Appendix-8 and 9 in accordance with Expert Panel's comments				
4	-Revised the main report wholly				
5	-Revised Executive Summary and Section 5.2.2				
6	-Revised in accordance with RSG-SCE/MHI-12-5745				
7	- Revised in accordance with RSG-SCE/MHI-12-5757 and RSG-SCE/MHI-12-5762				
8	- Revised in accordance with RSG-SCE/MHI-12-5775 - Revised Appendix-9 to be consistent with the current full bundle model analysis cases				



No.	Revision	Date	Approved	Checked	Prepared
9	<ul style="list-style-type: none"> - Revised in accordance with RSG-SCE/MHI-12-5786 - Revised Section 4.1.2 and 4.1.3 - Added Fault Tree Evaluation in Section 6 - Undeleted Appendix-16 				



Table of Contents

1. Introduction.....	10
2. Summary of RSG Design for SONGS	10
2.1 Overall RSG Design.....	10
2.2 Tube Bundle Design.....	11
3. Description of Events.....	13
3.1 Unit-2	13
3.1.1. Abstract	13
3.1.2. Sequence of Events	13
3.2 Unit-3	14
3.2.1. Abstract	14
3.2.2. Sequence of Events	14
4. Investigation of Wear Condition.....	15
4.1 ECT Inspection Results.....	15
4.1.1. Types of Tube Wear	18
4.1.2. Tube Wear in Unit-2 (for reference only)	50
4.1.3. Tube Wear in Unit-3	52
4.2 Visual Inspection Results of the Tube Bundle.....	54
4.2.1. Observations Common to Unit-2 and Unit-3	54
4.2.2. Observations in Unit-3.....	54
4.2.3. Observations in Unit-2.....	54
5. Mechanistic Cause Analysis.....	57
5.1 Thermal Hydraulic Condition in the Secondary Side	57
5.2 Evaluation of U-bend Supports Condition.....	64
5.2.1. Out-of-Plane Direction Support	64
5.2.2. In-Plane Direction Support	64
5.2.3. Differences between Unit-2 and Unit-3	65
6. Tube Wear Causes.....	70
6.1 Type 1 Wear (TTW)	71
6.2 Type 2 Wear (AVB wear).....	71
6.3 Type 3 Wear (TSP wear).....	73
6.4 Type 4 Wear (RB wear)	73
7. Conclusions.....	81
8. Countermeasures for Return to Service	82
8.1 Tube Plugging	82
8.1.1. Type 1 Wear	82
8.1.2. Type 2 Wear and Type 3 Wear.....	82



8.1.3.	Type 4 Wear.....	82
8.2	Operating at a Lower Thermal Power	84
9.	References	86

Appendices

Appendix-1	ECT Data Evaluation of tubes with wear around Retainer Bar	1-1
Appendix-2	FEI Evaluation of Tube Straight Portion for Unit-2/3	2-1
Appendix-3	FEI Evaluation of Tube U-bend Portion for Unit-2/3.....	3-1
Appendix-4	Investigation of Unit-2/3 Manufacturing and Inspection Records.....	4-1
Appendix-5	Analytical Simulation of Tube Bundle Rotation and Hydro Static Test.....	5-1
Appendix-6	Investigation of ISI ECT Data for AVB Support Condition for Unit-2/3.....	6-1
Appendix-7	Visual Inspection Results for U-Bend Region for Unit-2/3.....	7-1
Appendix-8	SG Tube Flowering Analysis for Unit-2/3.....	8-1
Appendix-9	Simulation of Manufacturing Dispersion for Unit-2/3.....	9-1
Appendix-10	SG Tube Wear Analysis for Unit-2/3.....	10-1
Appendix-11	(Deleted)	11-1
Appendix-12	Thermal Hydraulic Evaluation of Area Plugging.....	12-1
Appendix-13	(Deleted)	13-1
Appendix-14	Analytical evaluation of the impact on the Tube Support Plate and Tube Bundle due to Tubesheet deflection during Divider Plate detachment....	14-1
Appendix-15	(Deleted)	15-1
Appendix-16	Fatigue Evaluation of the Tube due to In-Plane Vibration.....	16-1





Acronyms and Definitions

2A, 2B, 3A, 3B:	Unit 2 SGs A (E089) & B (E088) and Unit 3 SGs A (E089) & B (E088)
3D:	Three-dimensional
Active support:	Tube support at AVB or TSP, which prevents tube motion in the in-plane and out-of-plane directions
ATHOS:	An EPRI sponsored thermal hydraulic computer program for steam generator flow analysis
AVB:	Anti-Vibration Bar
B01-B12 / AVB01-AVB12:	AVB designations with B01 the first above TSP #7 on the hot leg side
B05 and B06:	Cross-section through the U-bend parallel to AVB B05 and B06
Col:	Tube column number
CDS:	Certified Design Specification of SONGS Unit 2&3 RSGs (SO23-617-01, Revision 3)
ECT:	Eddy Current Testing
FEI:	Fluid Elastic Instability
FIV:	Flow Induced Vibration
Free-span:	Tube section between supports
G-value:	Tube diameter in the U-bend region aligned with tube-to-AVB intersections



Thermal-hydraulic conditions:

The term “thermal-hydraulic conditions” refers to flow velocity, void fraction (steam quality) and hydro-dynamic pressure

Inactive support:

Tube support at AVB or TSP, which does not prevent tube motion in both in-plane and out-of-plane directions

ISI:

In-service Inspection

IVHET:

MHI tube wear analysis program

MHI:

Mitsubishi Heavy Industries

N:

Newton, force (1N equals 0.225lbf)

P/D ratio:

Tube pitch-to-diameter ratio

PSI:

Pre-service Inspection

RB

Retainer Bar

R100C88:

Tube address (Row 100, Column 88)

RSG:

Replacement Steam Generator

SCE:

Southern California Edison

SONGS:

San Onofre Nuclear Generating Station

TSP:

Tube Support Plate

TTW:

Tube-to-Tube Wear

T/H

Thermal and Hydraulic

TSP #1-TSP #7:

Tube support plate numbers from the lower most to the upper most



Executive Summary

On January 31, 2012, during the first cycle after steam generator replacement, San Onofre Nuclear Generating Station (SONGS) Unit 3 was shut down due to indications of a steam generator tube leak. Steam generator tube inspections confirmed one small leak on one tube in one of the two steam generators. Further inspections of 100% of the steam generator tubes in both Unit-3 steam generators discovered unexpected wear, including tube-to-tube as well as tube-to-tube-support structural wear.

Tube wear was found in the tube free span sections, at anti-vibration bars (AVBs), at Tube Support Plates (TSPs) and at retainer bars, and was labeled as follows:

- (i) Type 1 (Tube-to-Tube Wear)
- (ii) Type 2 (AVB wear)
- (iii) Type 3 (TSP wear)
- (iv) Type 4 (Retainer bar wear)

The cause of the first 3 types of tube wear is tube vibration. The causes of tube vibration are the thermal-hydraulic conditions in the SG secondary side and the condition of the tube bundle supports. Type 4 tube wear is due to vibration of the selected retainer bars, rather than the tubes.

Structures in a two-phase flow field have lower resistance to vibration when the fluid void fraction (and hence steam quality) is high. High void fraction (high steam quality) results in the two-phase flow mixture having low density, which in turn results in a high velocity of the two-phase flow and in a low damping factor. Consequently, the dynamic pressure, which is a function of the flow velocity squared, increases. As the dynamic pressure is a major factor causing the structures in the flow field to vibrate, it is more likely for the structures to vibrate when the void fraction (steam quality) is high (as it affects both the flow velocity and the damping factors).

Based on the investigation of the correlation between the void fraction (steam quality) and the number of tubes with wear in a given void fraction region, a strong correlation between the void fraction (steam quality) and the percentage of tubes with wear was identified. Consequently, it is concluded that the thermal-hydraulic conditions in the SG secondary side, namely high void fraction (steam quality) and high flow velocity, along with lack of sufficient in-plane tube support, discussed next, are the main causes of the excessive tube vibration and unexpected wear in the SONGS Unit 2 and Unit 3 SGs. The higher than typical void fraction is a result of a very large and tightly packed tube bundle, particularly in the U-bend,

9

9



with high heat flux in the hot leg side.

Contemporary experience shows that out-of-plane vibration of the SG U-tube is more likely to occur than in-plane vibration, because tube U-bend natural frequency in the out-of-plane direction is lower than natural frequency in the in-plane direction. In the design stage, MHI assumed that the tube support in the out-of-plane direction with “zero” tube-to-AVB gap in hot condition was sufficient to prevent tube from becoming fluid-elastic unstable during operation. But, the recent SONGS experience shows that the flat bar AVBs does not provide friction forces required to prevent tubes from vibrating in the in-plane direction and eventually becoming fluid-elastic unstable under high local secondary thermal-hydraulic conditions such as in the SONGS RSGs. In addition, MHI concludes that in the Unit-3 RSGs low tube and AVB fabrication dimensional dispersion causes that the tube-to-AVB contact forces are not sufficient to prevent the in-plane motion of tubes.

In order to ensure the structural integrity of the tubes after restarting the plant, all tubes which have a potential for losing their integrity during the next operating period should be plugged and thermal power output of the plant should be decreased. Plugging for the Type 1 wear should include not only the tubes with the Type 1 wear but also tubes which are susceptible to the Type 1 wear, for preventative reasons. Plugging for the Type 2 and 3 wear should include the tubes with wear equal to, or greater than, 35% in accordance with Technical Specifications. Plugging for the Type 4 wear should include 94 tubes which are adjacent to the retainer bars. Decreasing the thermal power output will improve thermal-hydraulic conditions (will lower flow velocities and void fractions in the critical tube bundle U-bend region) and thus will reduce the possibility of the occurrence of tube fluid-elastic instability (FEI) leading to unacceptable tube wear.



1. Introduction

After approximately 11 months of power operation following the steam generator replacement, SONGS Unit-3 underwent an unplanned shut down on Jan. 31, 2012 as a result of leakage of primary coolant to the secondary side from a tube in the 3B (3E-088) steam generator (SG). The maximum leakage rate was at approximately 82 gallon/day (~13 liters/hour). Subsequent investigation revealed that the direct cause of the leakage was tube-to-tube wear.

At the time of the Unit-3 leak, SONGS Unit-2 had already completed one cycle of power operation (~22 months) after the steam generator was replaced in the refueling outage since Jan. 9, 2012. Eddy-Current Testing (ECT) inspections were performed on all tubes in both Unit-3 SGs and wear indications on many of the tubes were found. This report presents the evaluation of the mechanistic cause of tube wear and the countermeasures required for Unit-3 return to service.

2. Summary of RSG Design for SONGS

2.1 Overall RSG Design

The SONGS RSGs were specified, designed and fabricated as replacements on a like-for-like basis for the original steam generators in terms of fit, form and function with limited exceptions, and were replaced under the 10CFR50.59 rule. The CDS for the design and fabrication of the RSGs (SO23-617-01, Revision 3) specified the limiting design parameters and materials. Thus, replacement steam generator design with 3/4" tube diameter arranged in 1" triangular pitch, which was the same as in the original steam generators, and the larger heat transfer area than in the original steam generators, was optimal. The other parameters/materials not specified by CDS were established/ selected in the design process. The SONGS RSGs were designed and fabricated to achieve an "effective zero gap" as required by CDS Rev. 3 in order to minimize its potential for tube wear. The CDS also states that the tube support/tube bundle assembly shall be fabricated such as to ensure no damage to the tubes and subsequent operation of the RSG with minimal vibration.



2.2 Tube Bundle Design

The major concern with the large U-tube SGs is their propensity for tube wear in the tube bundle U-bend region. Consequently, minimizing tube wear was given the first priority in the SONGS RSG specification, design and fabrication, and the tube support design and fabrication was discussed by MHI and SCE in numerous design review meetings. As a result, the tube bundle U-bend support design and fabrication was as follows:

- 1) Six (6) V-shaped AVBs (three sets of two) were provided between each tube column.
- 2) The AVB thickness was set such as to provide an effective “zero” tube-to-AVB gap under operating (hot) conditions.
- 3) The AVB end-caps were welded to the retaining bars with the U-bend in the gravity neutral position to achieve uniformity of the gap size and AVB parallelism, using spacers between the AVBs sized based on a mockup test.

The tube bundle and AVB structure configuration and components (AVBs, retaining bars, bridges and retainer bars) are shown in Fig.2-1. MHI investigated field experience with U-bend tube degradation using INPO, NRC and NPE data bases, and concluded that tube wear in the operating U-tube SGs was mostly being caused by out-of-plane tube motion. Consistent with this and Reference 7, only out-of-plane vibration of the SG U-tubes was evaluated because tube U-bend natural frequency in the out-of-plane direction is lower than natural frequency in the in-plane direction and out-of-plane vibration is more likely to occur than in-plane vibration. No SG problems stemming from in-plane tube motion were identified by MHI and thus MHI concluded that the design and fabrication processes described above were sufficient for minimizing tube wear in the SONGS RSGs.

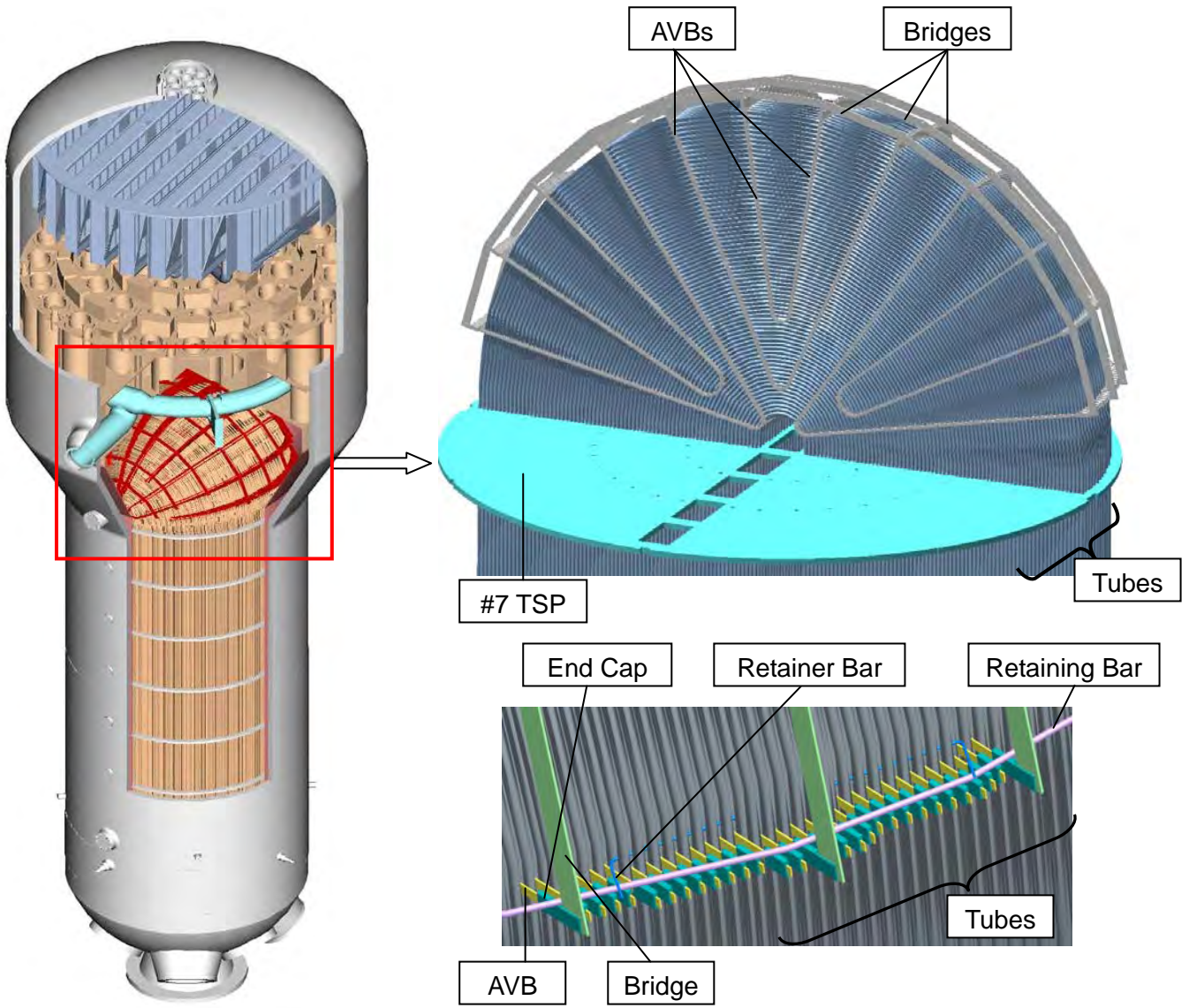


Fig.2-1 Tube Bundle and AVB Structure Configuration



3. Description of Events

3.1 Unit-2

3.1.1. Abstract

During the first refueling outage following steam generator replacement, ECT inspection of the unit 2 steam generator tubes identified a total of 10 tubes with wear depths of 28 to 90% of the tube wall thickness. Six of the affected tubes were located adjacent to the retainer bars. The retainer bars are part of the floating anti-vibration bar (AVB) structure that supports the U-bend region of the tubes. The remaining tubes had detectable wear associated with AVB support points elsewhere in the AVB structure.

3.1.2. Sequence of Events

Fall of 2009

The original Combustion Engineering (CE) SGs were replaced with MHI SGs during the Cycle 16 Refueling Outage.



May, 2010

Unit 2 completed the Cycle 16 Refueling and Steam Generator Replacement outage and returned to service at nominal 100% reactor power.

January 9, 2012

Unit 2 started the Cycle 17 Refueling Outage.

February 5, 2012

Routine ECT inspections of the SGs identified wear indications greater than 35% at two tube locations adjacent to the retainer bars.



3.2 Unit-3

3.2.1. Abstract

During the first cycle after steam generator replacement, on Jan.31, 2012, Unit 3 was shut down due to indication of a steam generator tube leak. Steam generator tube inspections confirmed one small leak on one tube in one of the two steam generators. Continuing inspections of 100% of the steam generator tubes in both Unit-3 steam generators discovered unexpected wear, including tube-to-tube as well as tube-to-tube-support wear.

3.2.2. Sequence of Events

Fall, 2010

The original CE SGs were replaced with MHI SGs during the Cycle 16 Refueling Outage.

February, 2011

Unit 3 completed the Cycle 16 Refueling and Steam Generator Replacement Outage and returned to service at nominal 100% reactor power.

January 31, 2012

During 100% power operation, a high radiation alarm from the condenser air ejector line revealed a primary-to-secondary leak in a SG. SONGS operators responded by rapidly reducing power and then shutting down the plant.



4. Investigation of Wear Condition

4.1 ECT Inspection Results

The basis of ECT data evaluations in this report (except Table 4.1.2-1 and Table 4.1.3-1) is described in Appendix-3 of Reference 8.

Table 4.1.2-1 and Table 4.1.3-1 are based on the information provided by SCE (Reference 9 and 11).



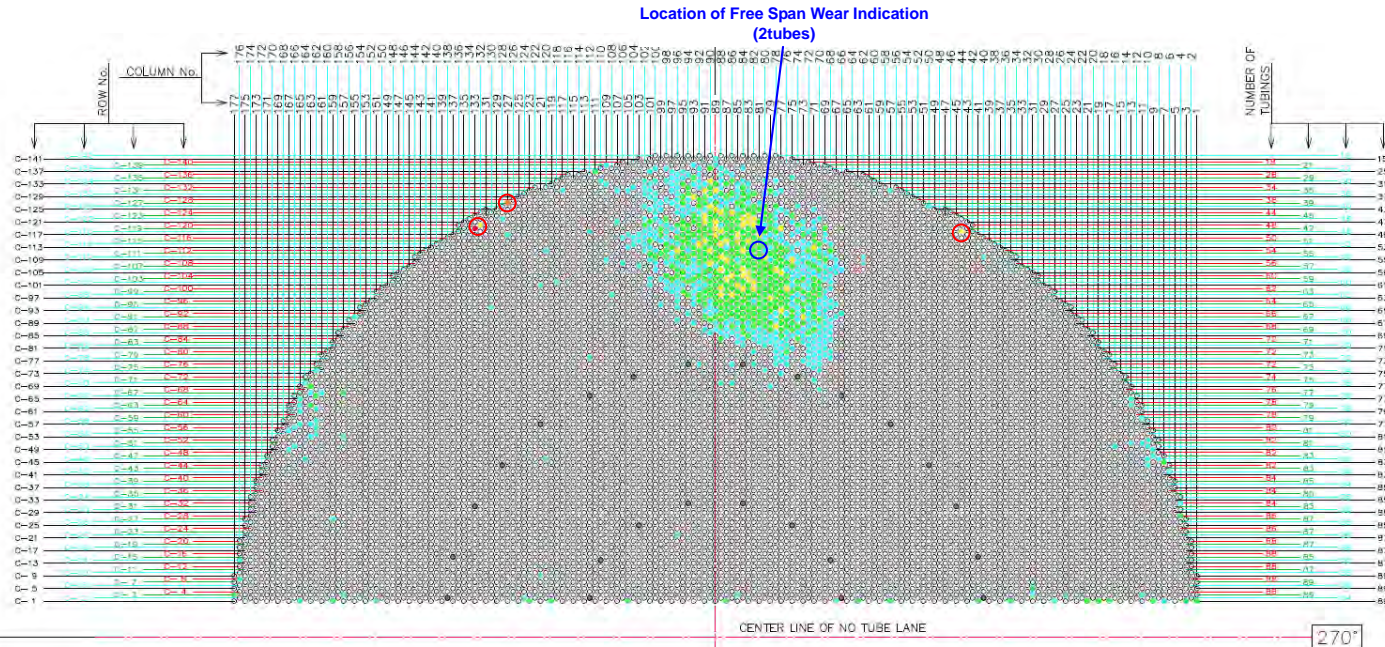
Wear indications obtained from ECT inspection are shown in Fig.4.1-1 and 4.1-2.

ECT Result of SG2A

Legend

- : No Indication
- (light blue) : Between 5-10%
- (green) : Between 11-20%
- (yellow) : Between 21-30%
- (orange) : Between 31-40%
- (red) : Above 41%

○ Location of Retainer Bar Wear Indication (4tubes)



ECT Result of SG2B

Legend

- : No Indication
- (light blue) : Between 5-10%
- (green) : Between 11-20%
- (yellow) : Between 21-30%
- (orange) : Between 31-40%
- (red) : Above 41%

○ Location of Retainer Bar Wear Indication (2tubes)

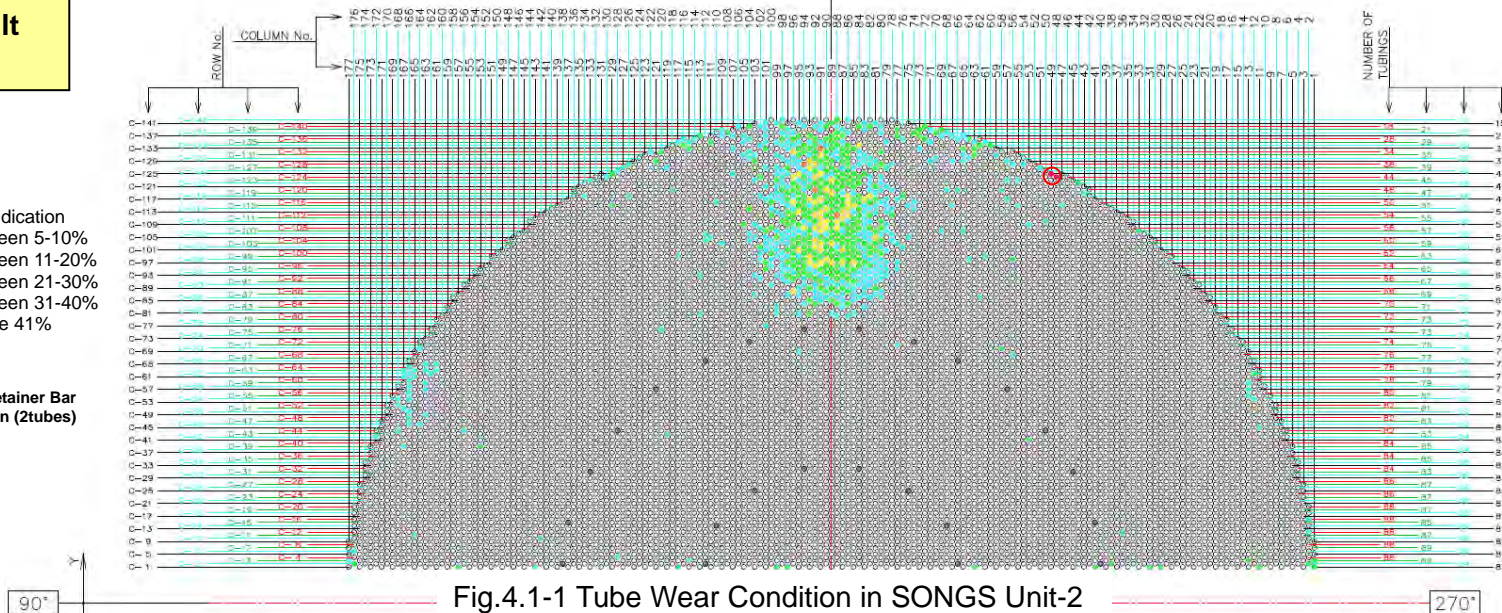


Fig.4.1-1 Tube Wear Condition in SONGS Unit-2

Non-proprietary Version

Document No. L5-04GA564(9)

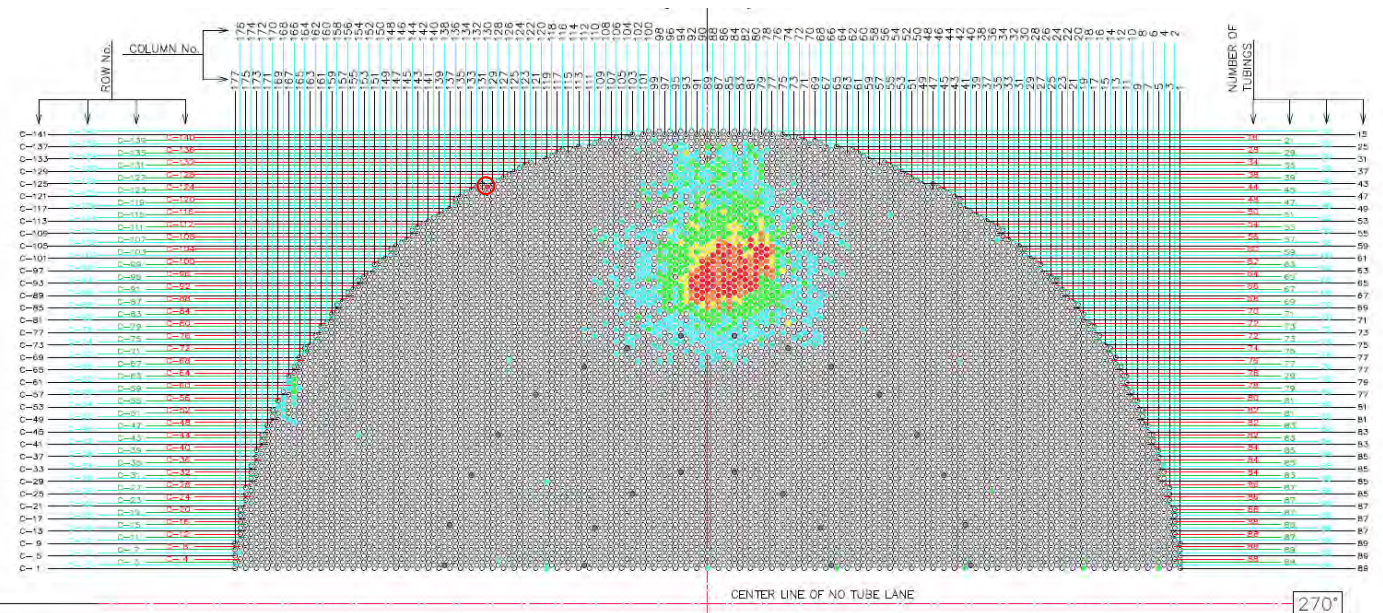


(P.16)

**ECT Result
of SG3A**

- Legend**
- : No Indication
 - (Cyan) : Between 5-10%
 - (Green) : Between 11-20%
 - (Yellow) : Between 21-30%
 - (Orange) : Between 31-40%
 - (Red) : Above 41%

○ Location of Retainer Bar
Wear Indication (1tube)



**ECT Result
of SG3B**

- Legend**
- : No Indication
 - (Cyan) : Between 5-10%
 - (Green) : Between 11-20%
 - (Yellow) : Between 21-30%
 - (Orange) : Between 31-40%
 - (Red) : Above 41%

○ Location of Retainer Bar
Wear Indication (3tubes)

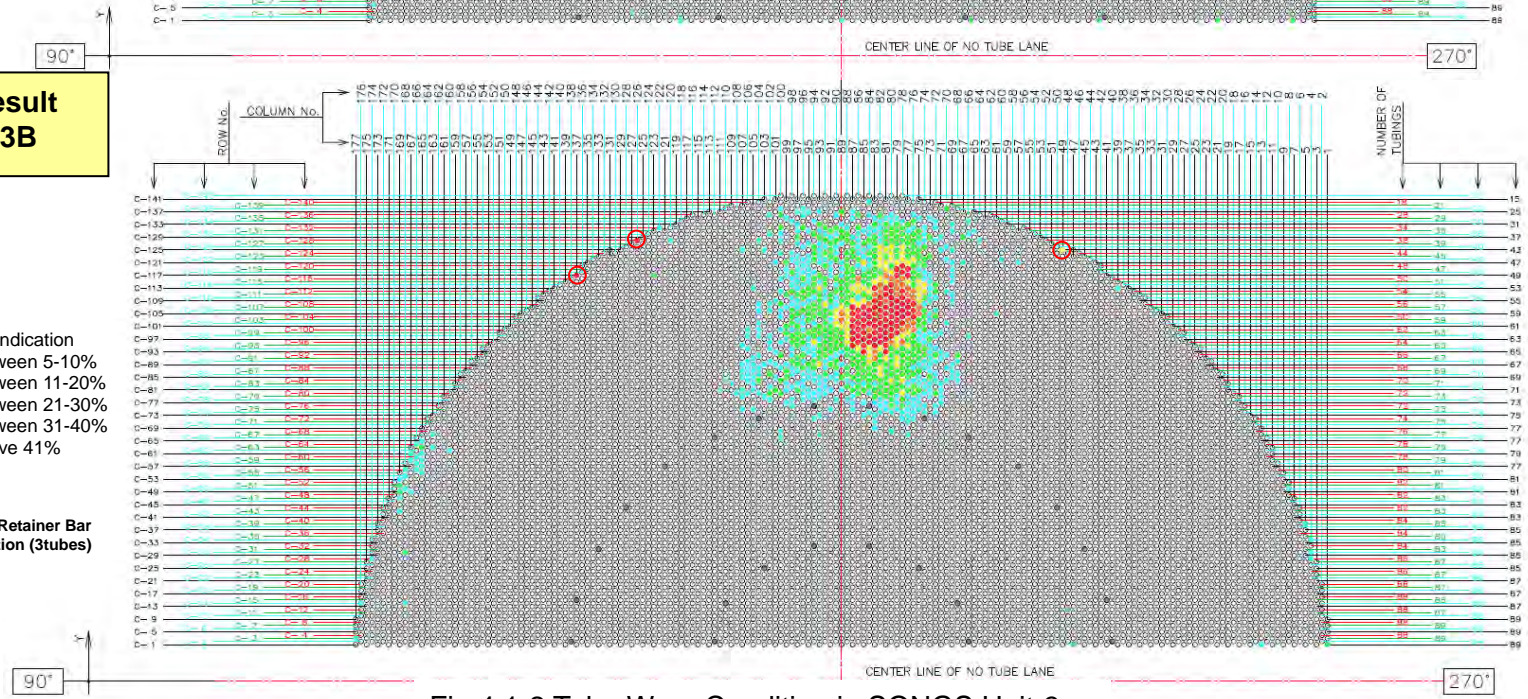


Fig.4.1-2 Tube Wear Condition in SONGS Unit-3





4.1.1. Types of Tube Wear

Tube wear indications were found in the tube free span sections, AVB region and TSP region and were grouped into 4 types as follows:

(i) Type 1 (TTW)

Wear in the tube free-span sections between the AVBs located in the U-bend region. Most of the tubes with this type of wear have also wear indications at AVBs and TSPs. In this case, it is considered that the entire tube, including the straight leg, was vibrating excessively. These tubes are shown in Fig.4.1.1-1.

(ii) Type 2 (AVB wear)

Wear at the tube-to-AVB intersections only with no wear indications in the tube free-span sections. Some of these tubes have wear indications at the TSPs as well. In this case, it is considered that mainly the U-bend section of the tube was vibrating. These tubes are shown in Fig.4.1.1-2.

(iii) Type 3 (TSP wear)

Wear at the tube-to-TSP intersections only in the straight section of the tubes. In this case, it is considered that only the straight section of the tube was vibrating. The tubes with wear at TSPs without wear in the U-bend section are shown in Fig. 4.1.1-3; the tubes with wear at TSPs and with wear in the U-bend section are shown in Fig. 4.1.1-4).

(iv) Type 4 (RB wear)

Wear at the AVB structure retainer bars in the tube U-bend section. These tubes have no wear indications in the free span, at AVBs or at TSPs. In this case, it is considered that the retainer bar itself was vibrating and the tube was not vibrating. These tubes are shown in Fig.4.1.1-2 and in Appendix-1.

Table.4.1.1-1 Wear Type Locations

Wear Pattern	Wear Location			
	Free Span	AVB	TSP	Retainer Bar
Type 1 (TTW)	Yes	Yes	(Yes)	No
Type 2 (AVB wear)	No	Yes	(Yes)	No
Type 3 (TSP wear)	No	No	Yes	No
Type 4 (RB wear)	No	No	No	Yes

Yes : Wear indication was found

(Yes): Wear indication may be present since some tubes with AVB wear indications have no indications at TSP locations

No : No wear indication

Tube wear indications at each AVB and TSP elevation for all wear categories are shown in



Fig.4.1.1-5, 4.1.1-6, 4.1.1-7 and 4.1.1-8.

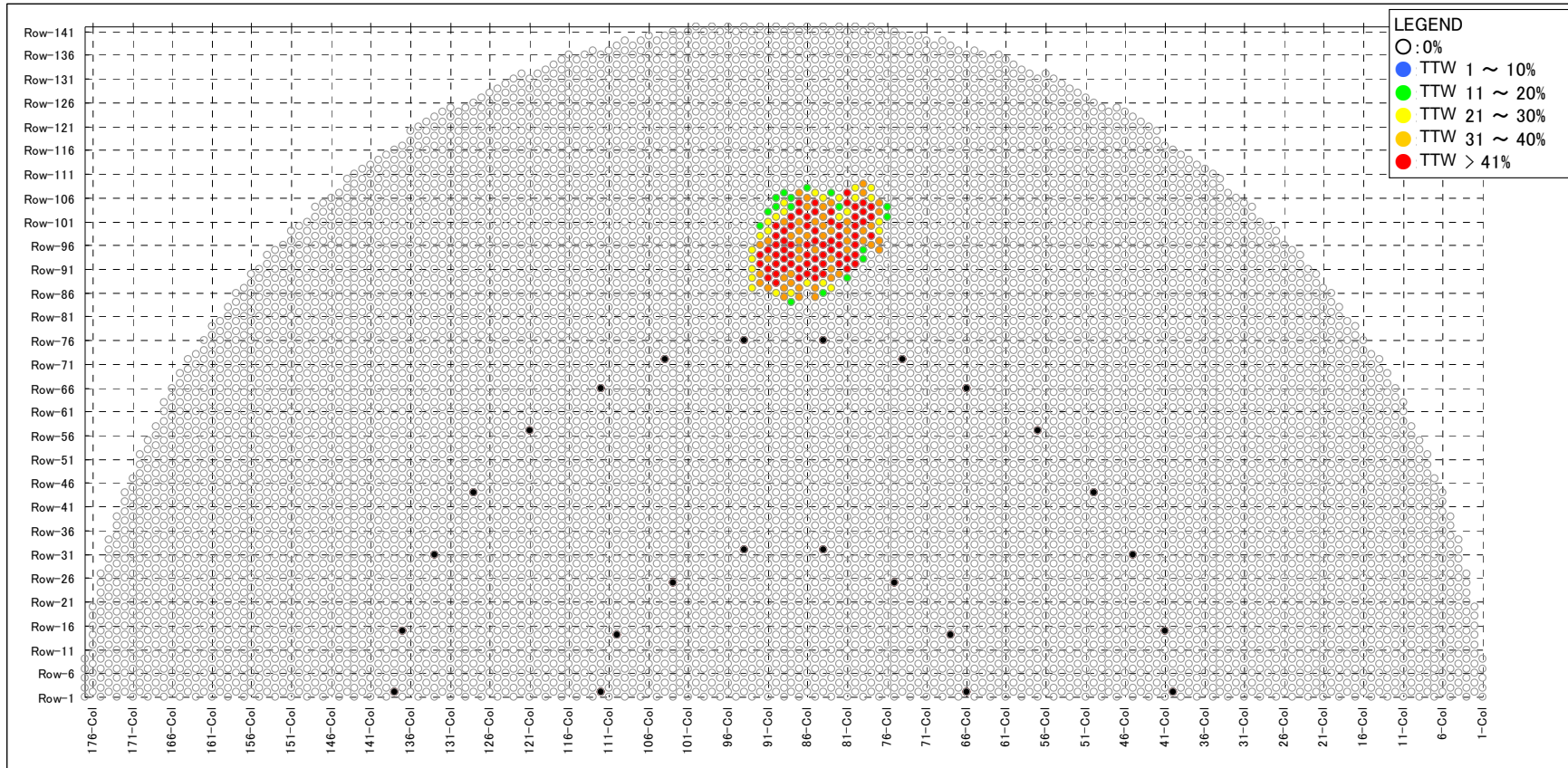


Fig 4.1.1-1(1/2) Tubes with TTW indications in U-bend region

Non-proprietary Version



3B-SG

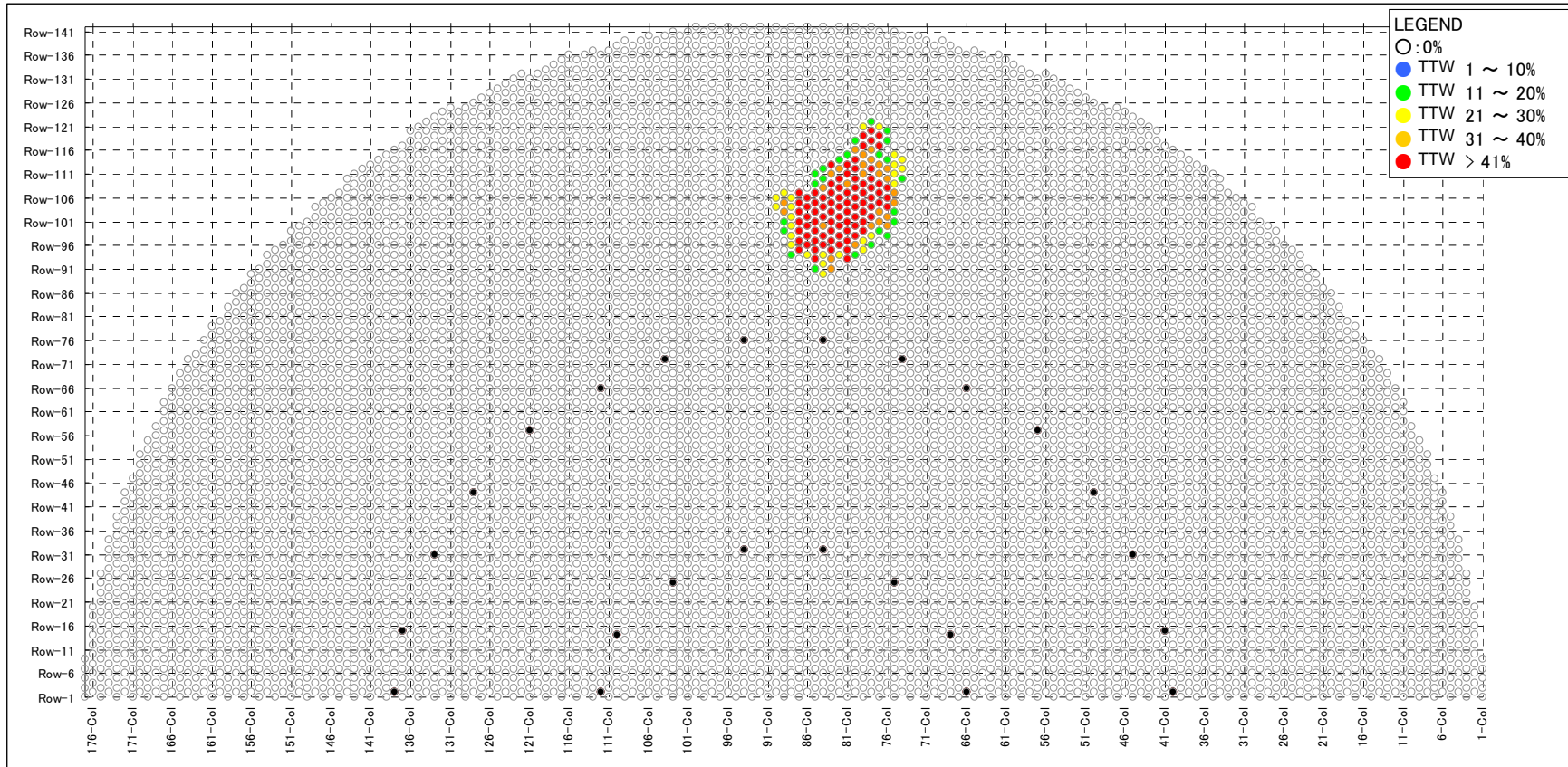


Fig 4.1.1-1(2/2) Tubes with TTW indications in U-bend region

Non-proprietary Version [



Document No. L5-04GA564(9)] (P.21)

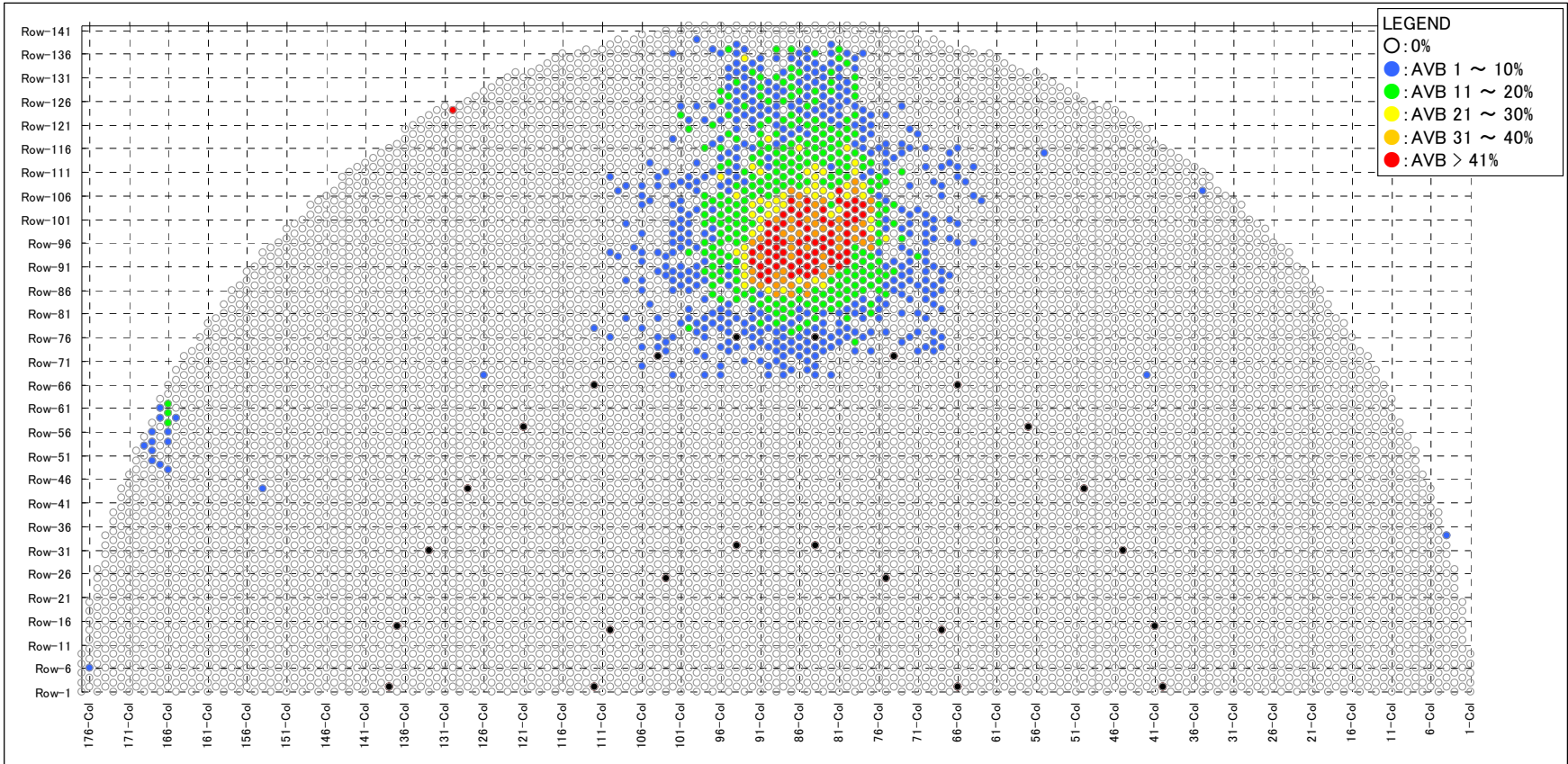


Fig 4.1.1-2(1/2) Tubes with wear indications at AVBs and at retainer bars

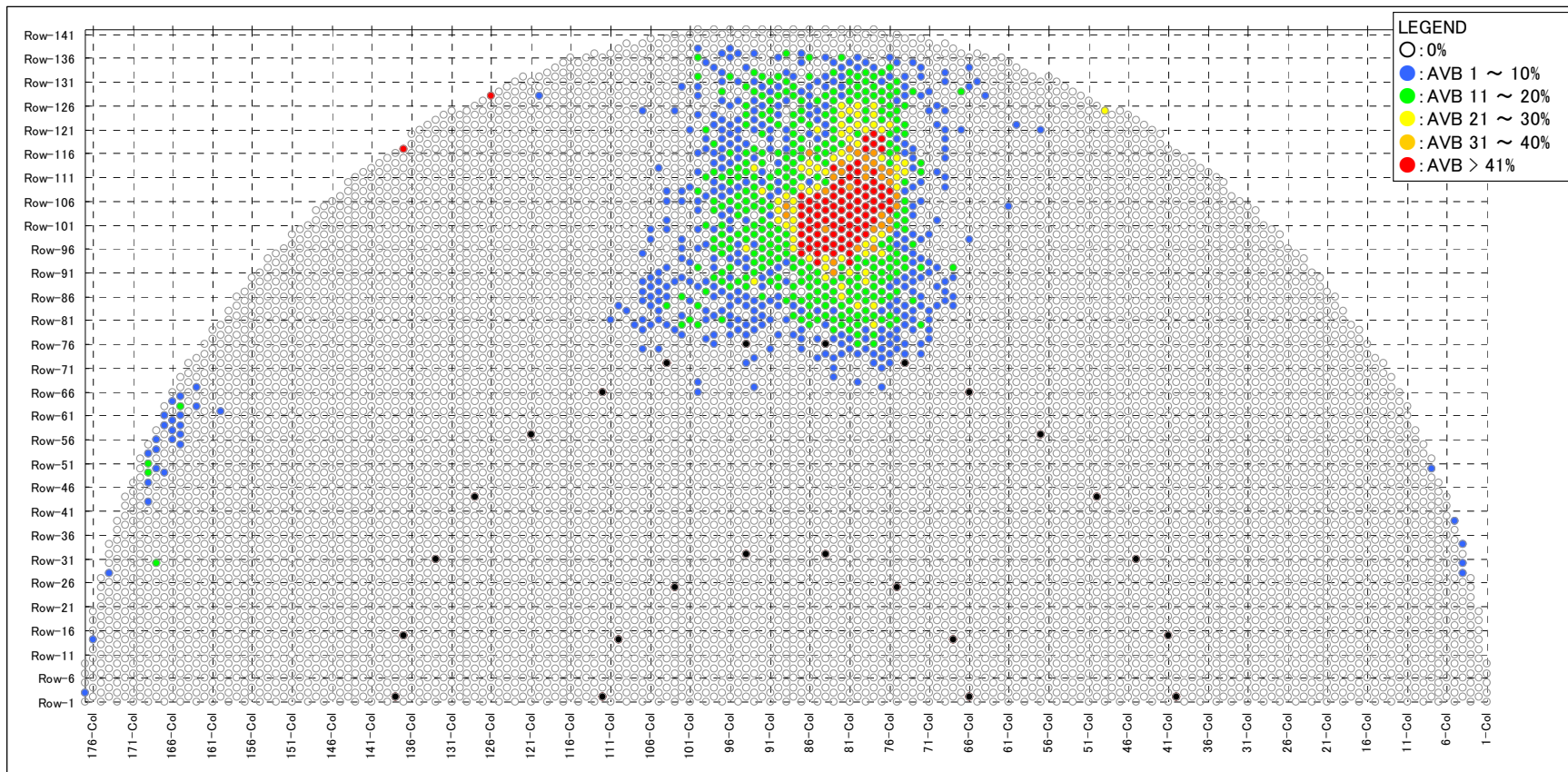


Fig 4.1.1-2(2/2) Tubes with wear indications at AVBs and at retainer bars

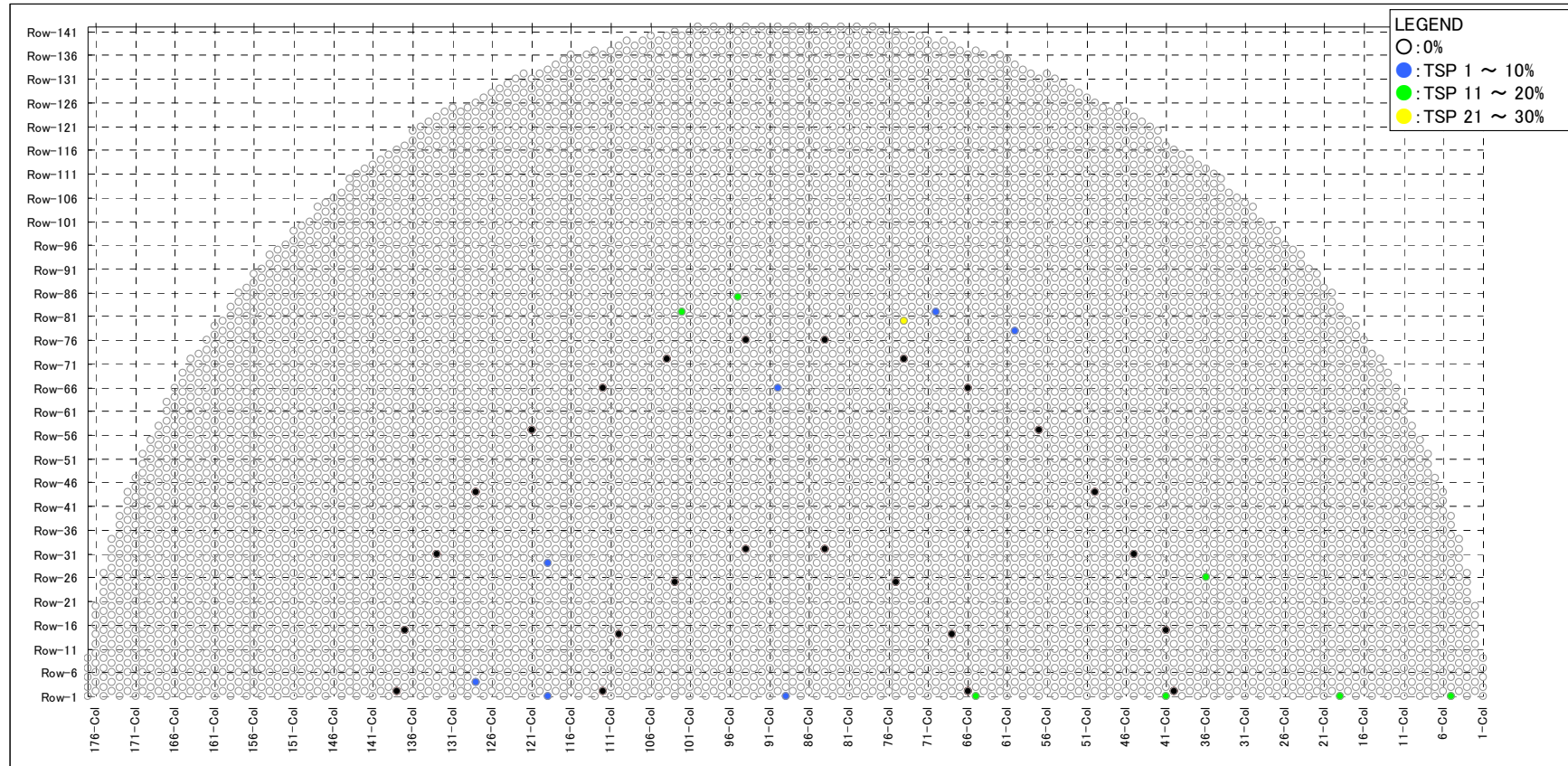


Fig 4.1.1-3(1/2) Tubes with wear indications at TSPs only

Non-proprietary Version



Document No. L5-04GA564(9)
(P.24)

3B-SG

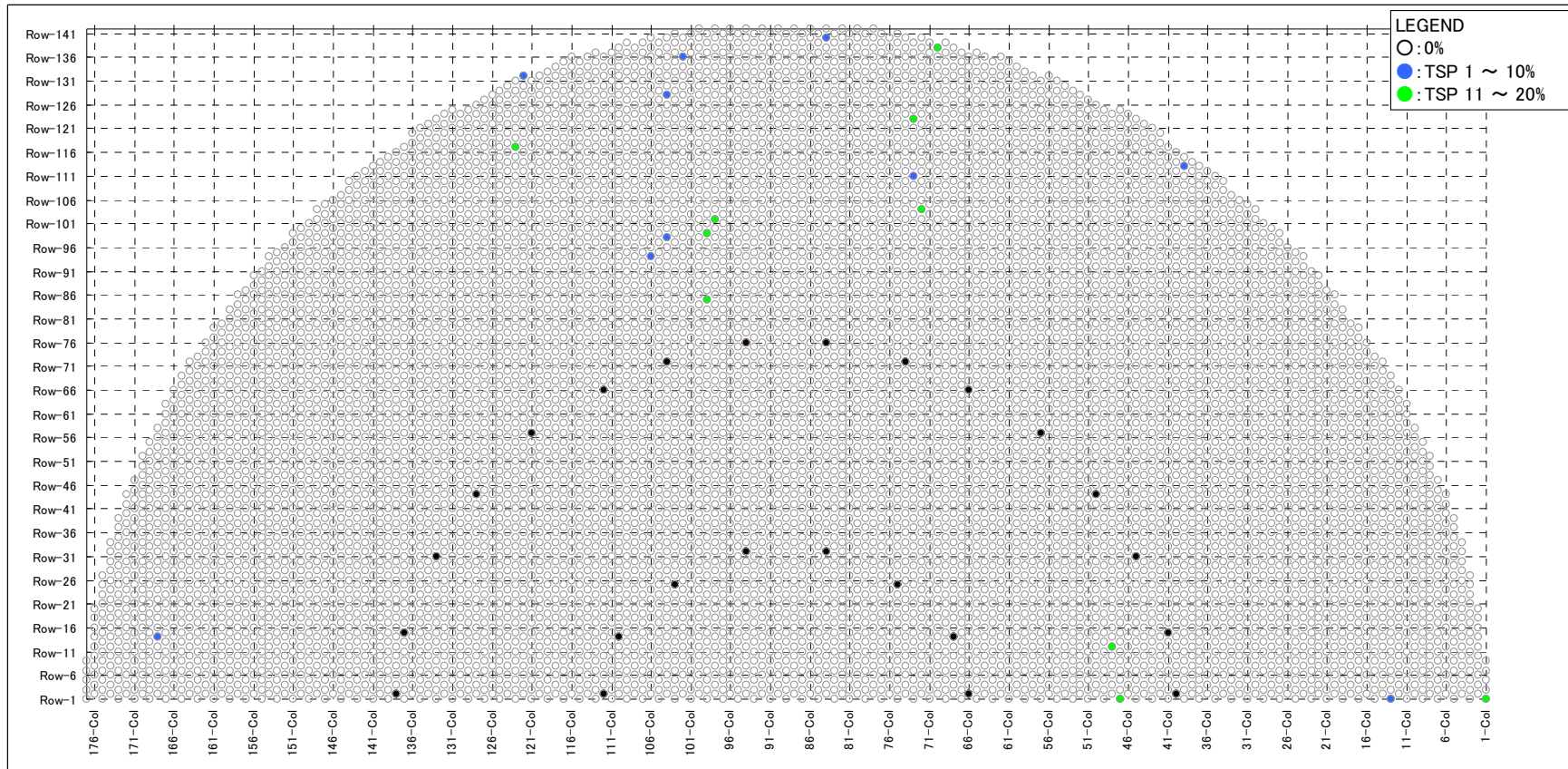


Fig 4.1.1-3(2/2) Tubes with wear indications at TSPs only

Non-proprietary Version [

Document No.L5-04GA564(9)] (P.25)



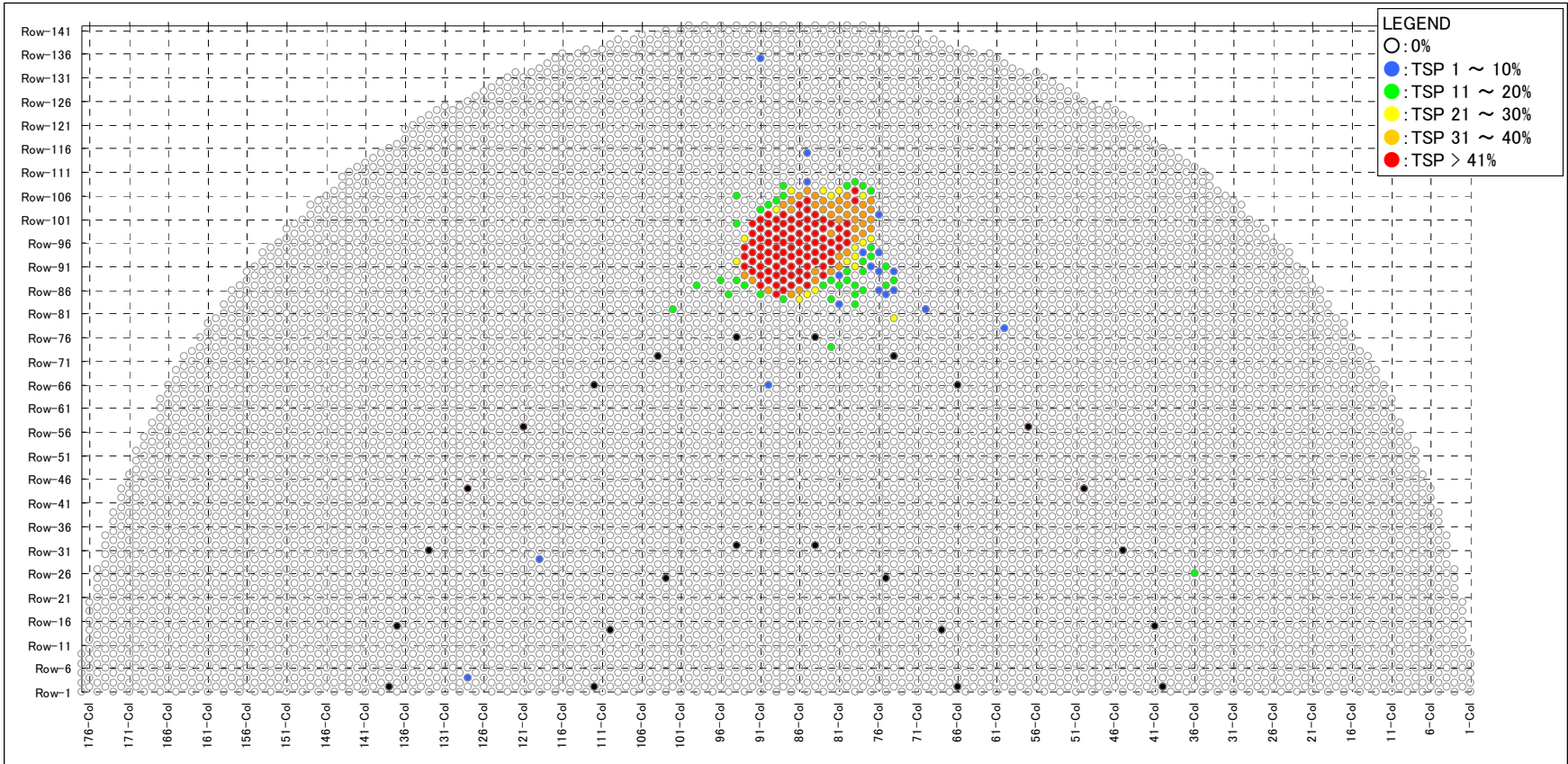


Fig 4.1.1-4(1/2) Tubes with wear indications at TSPs and TTW indications

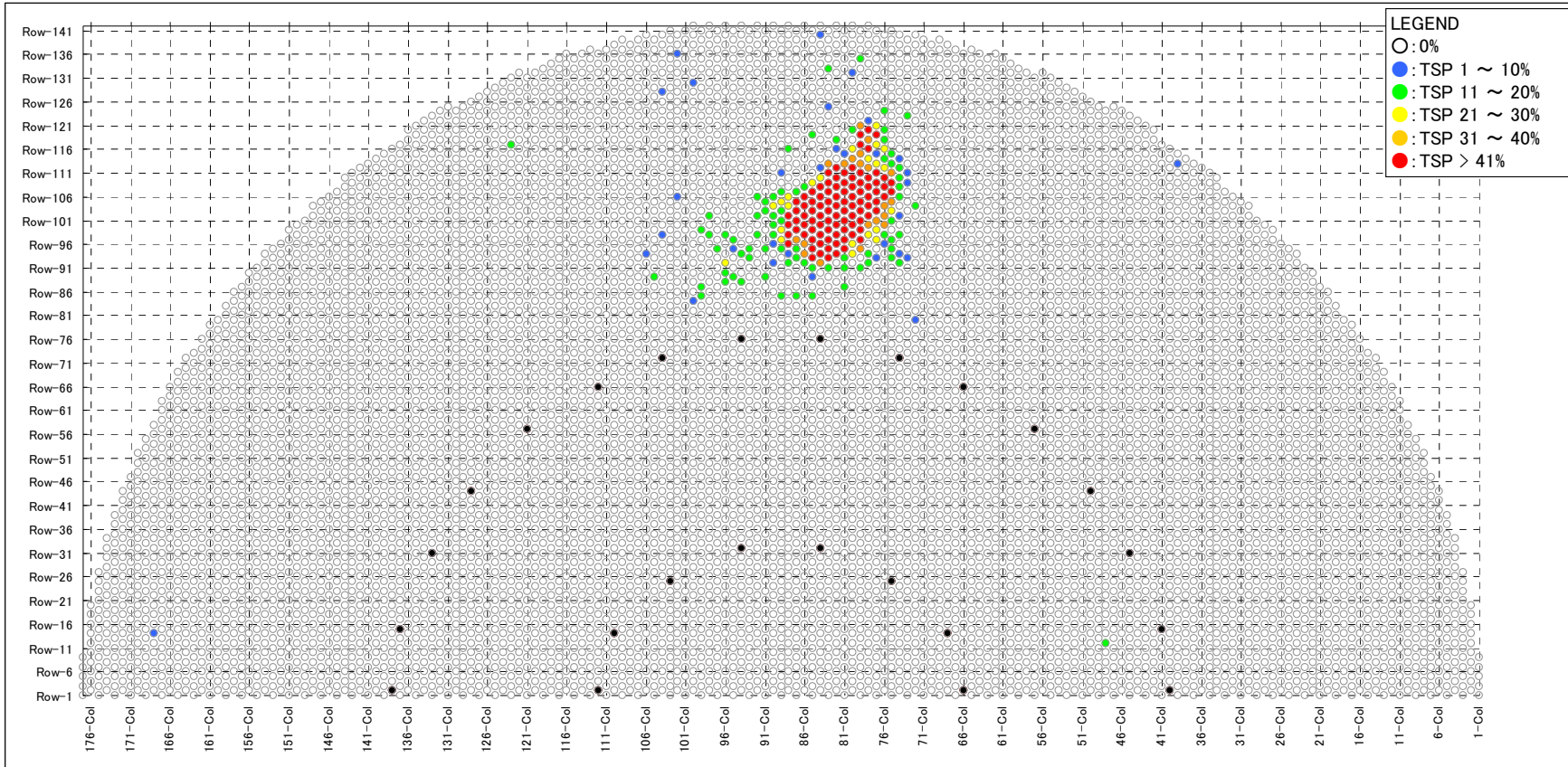
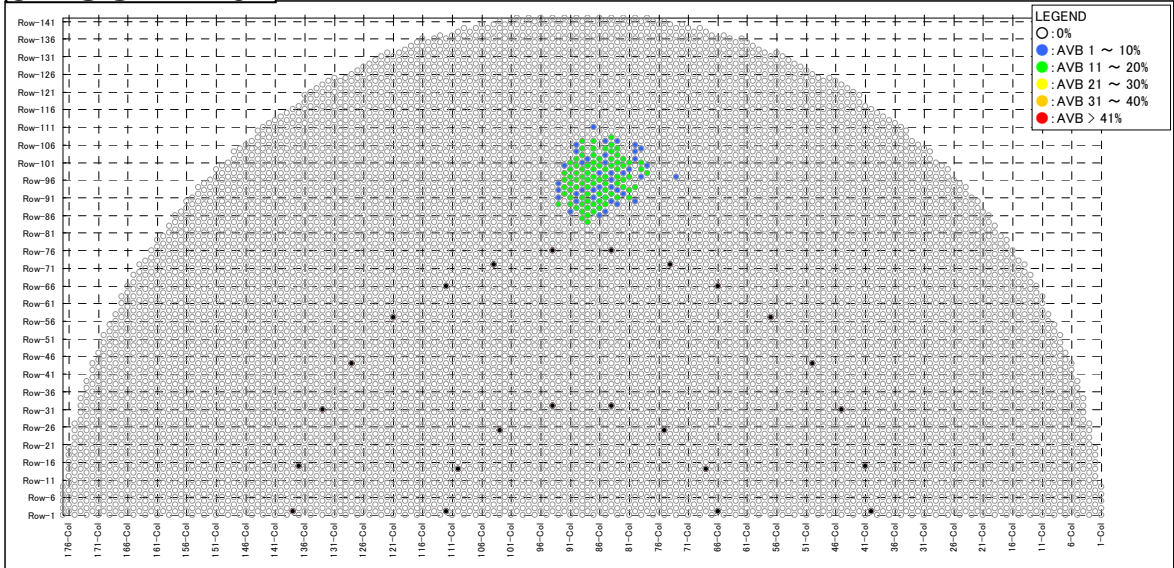


Fig 4.1.1-4(2/2) Tubes with wear indications at TSPs and TTW indications

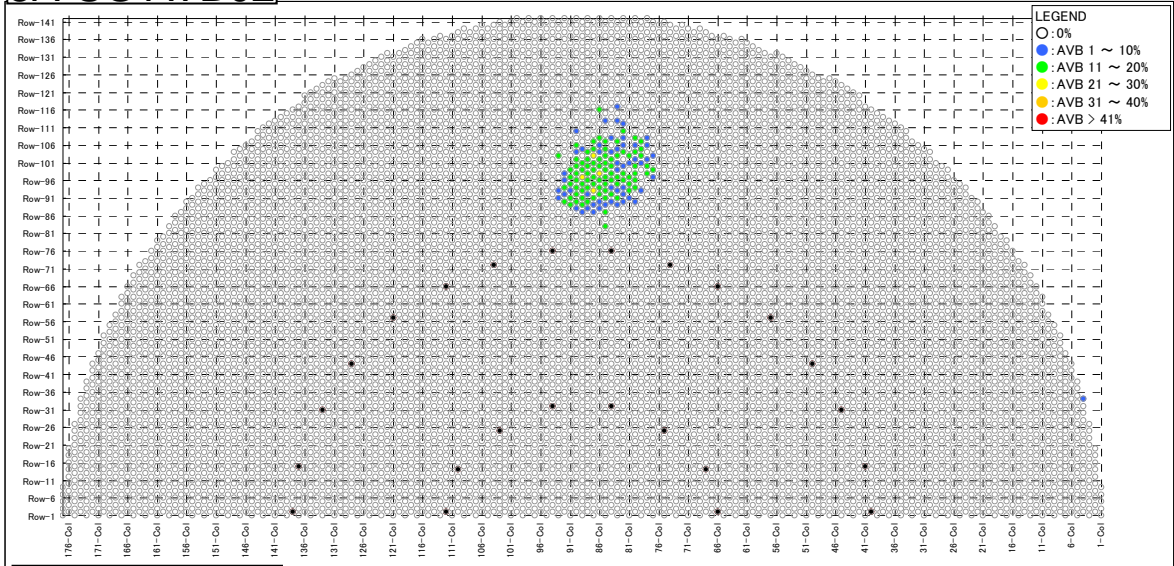




3A-SG AVB01



3A-SG AVB02



3A-SG AVB03

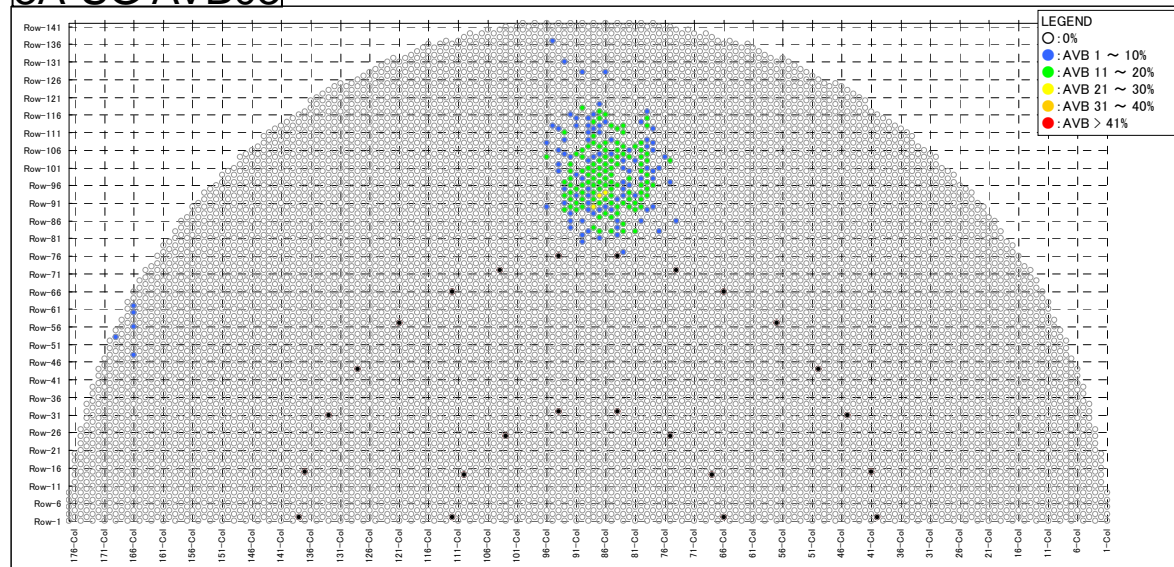
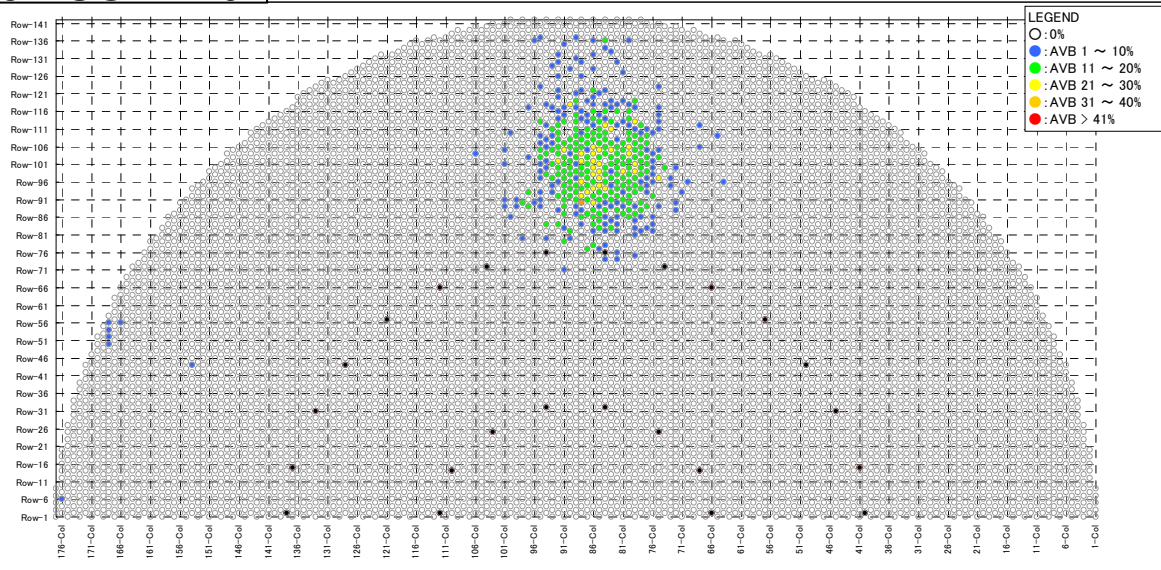


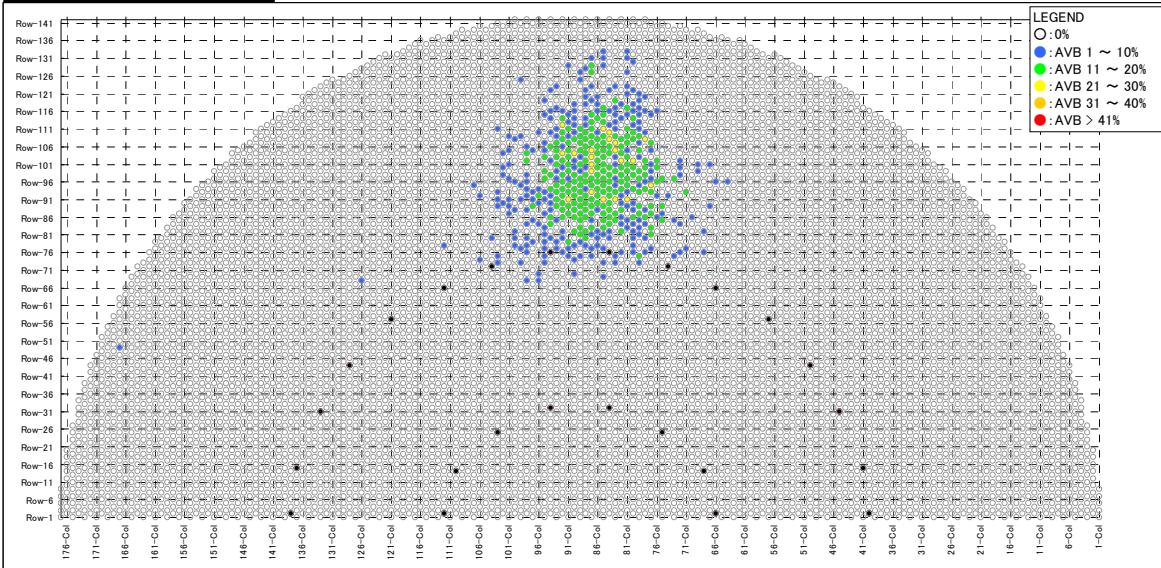
Fig 4.1.1-5 (1/4) Tubes with wear indication (at AVBs)



3A-SG AVB04



3A-SG AVB05



3A-SG AVB06

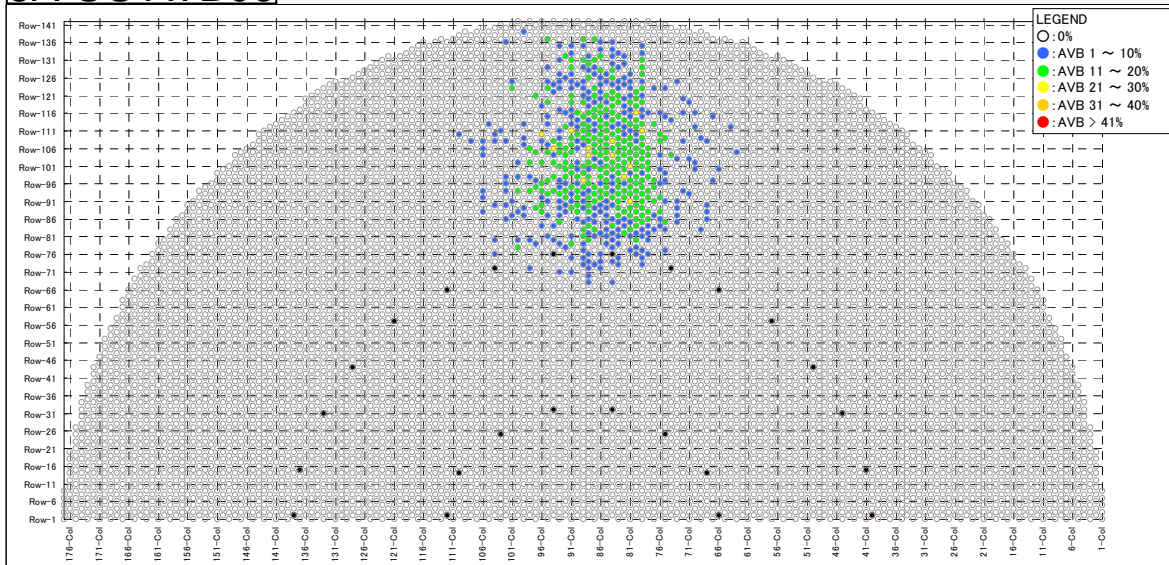
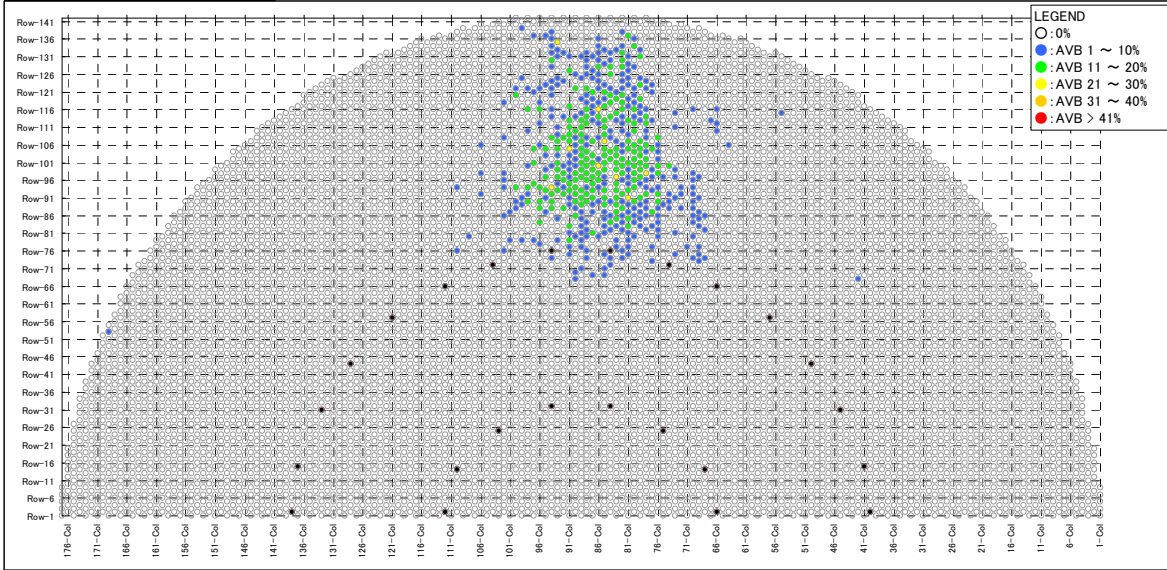


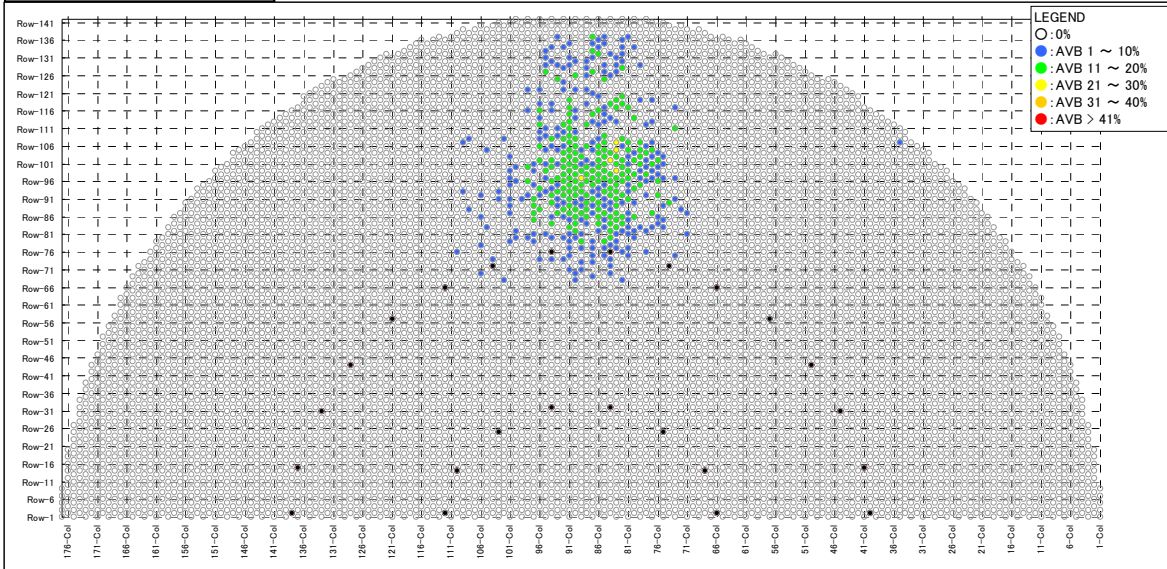
Fig 4.1.1-5 (2/4) Tubes with wear indication (at AVBs)



3A-SG AVB07



3A-SG AVB08



3A-SG AVB09

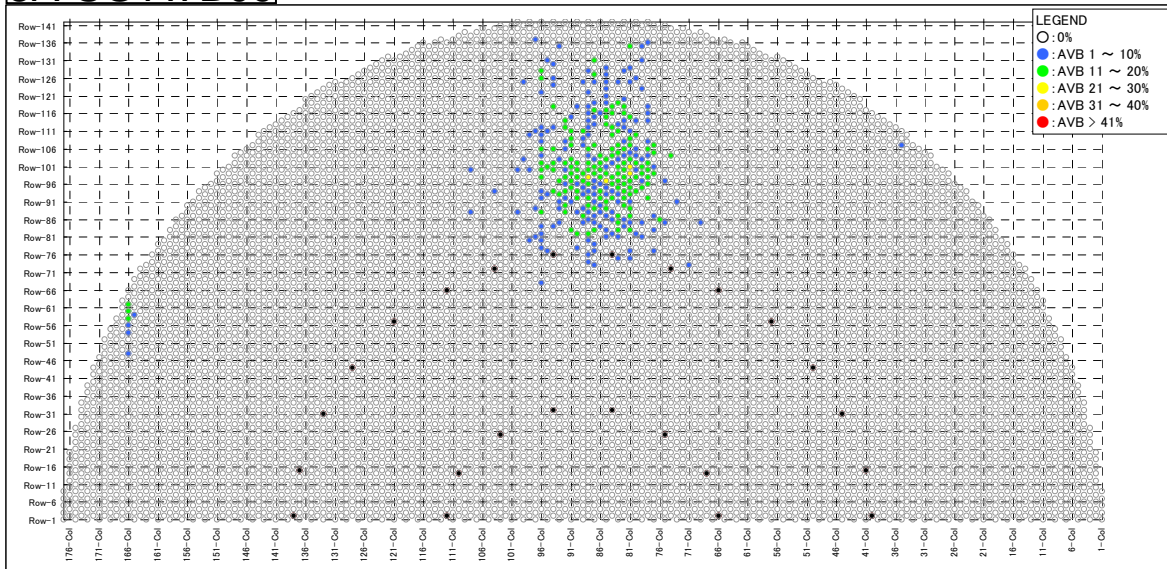
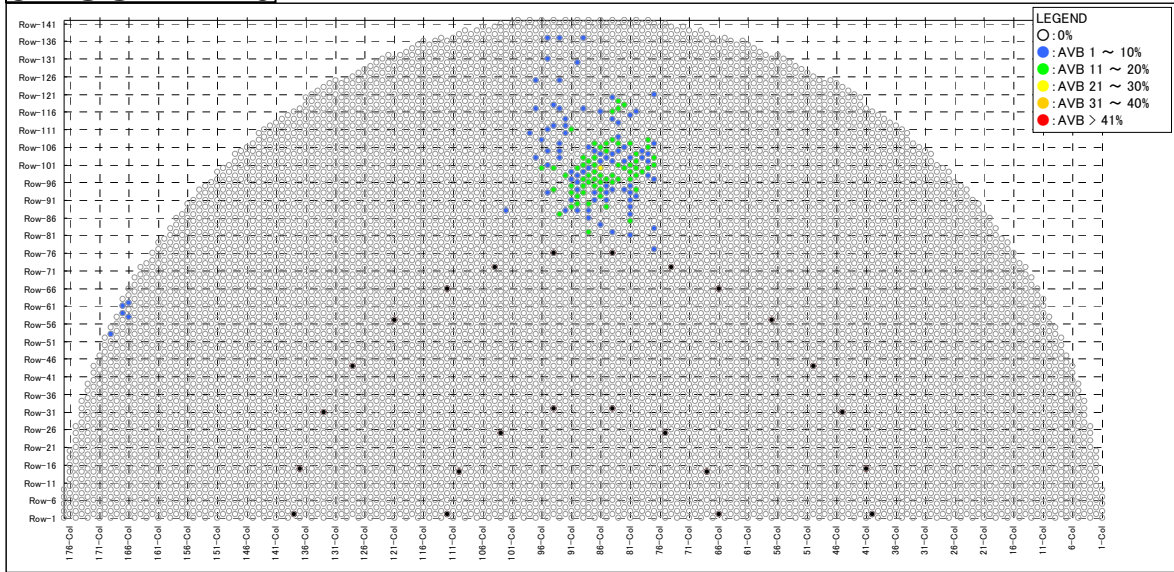


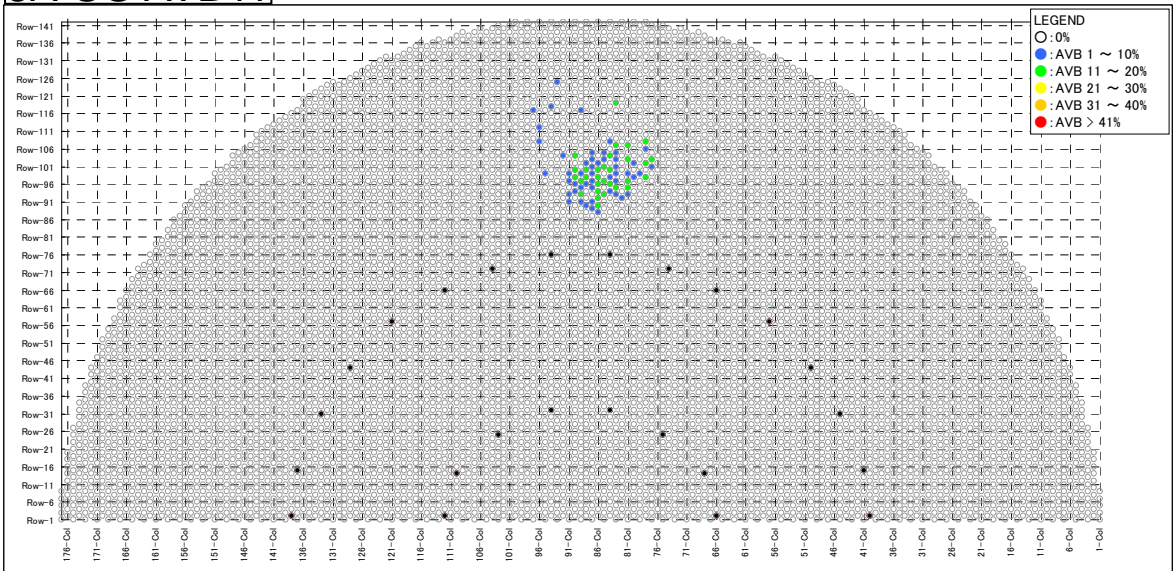
Fig 4.1.1-5 (3/4) Tubes with wear indication (at AVBs)



3A-SG AVB10



3A-SG AVB11



3A-SG AVB12

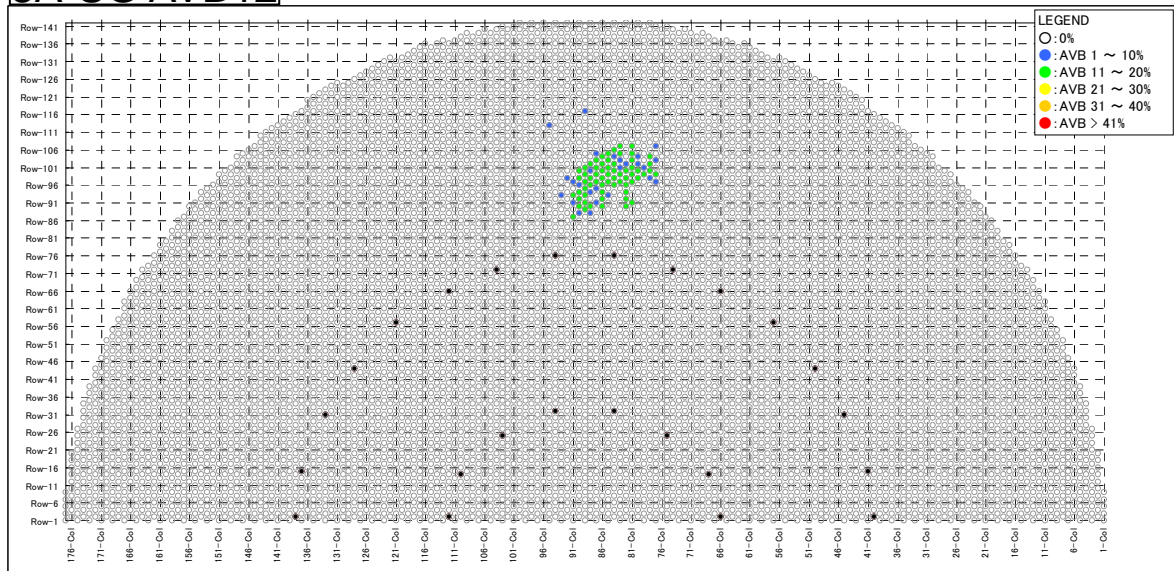


Fig 4.1.1-5 (4/4) Tubes with wear indication (at AVBs)



3A-SG #1TSP

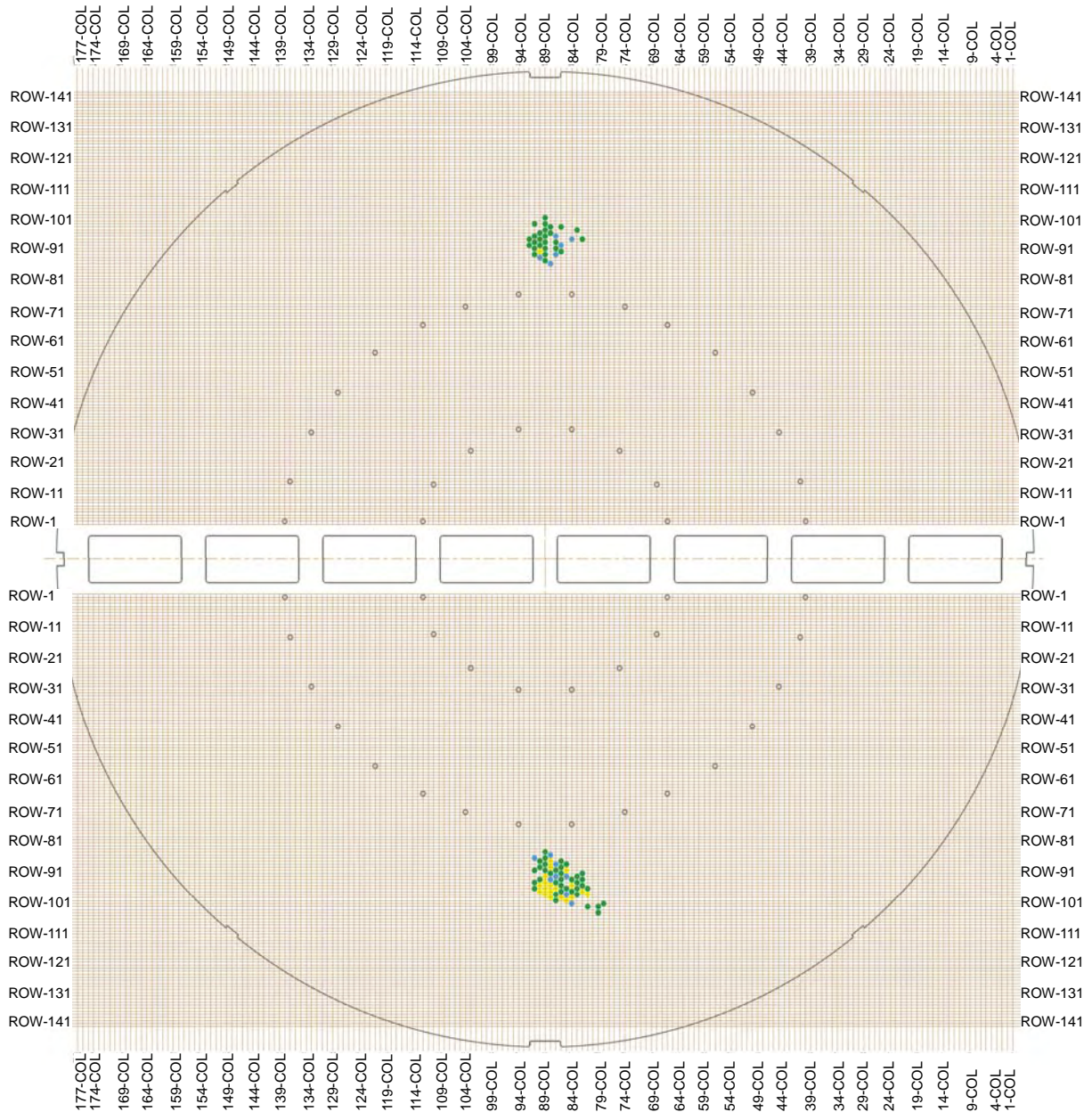


Fig 4.1.1-6 (1/7) Tubes with wear indications at TSPs



3A-SG #2TSP

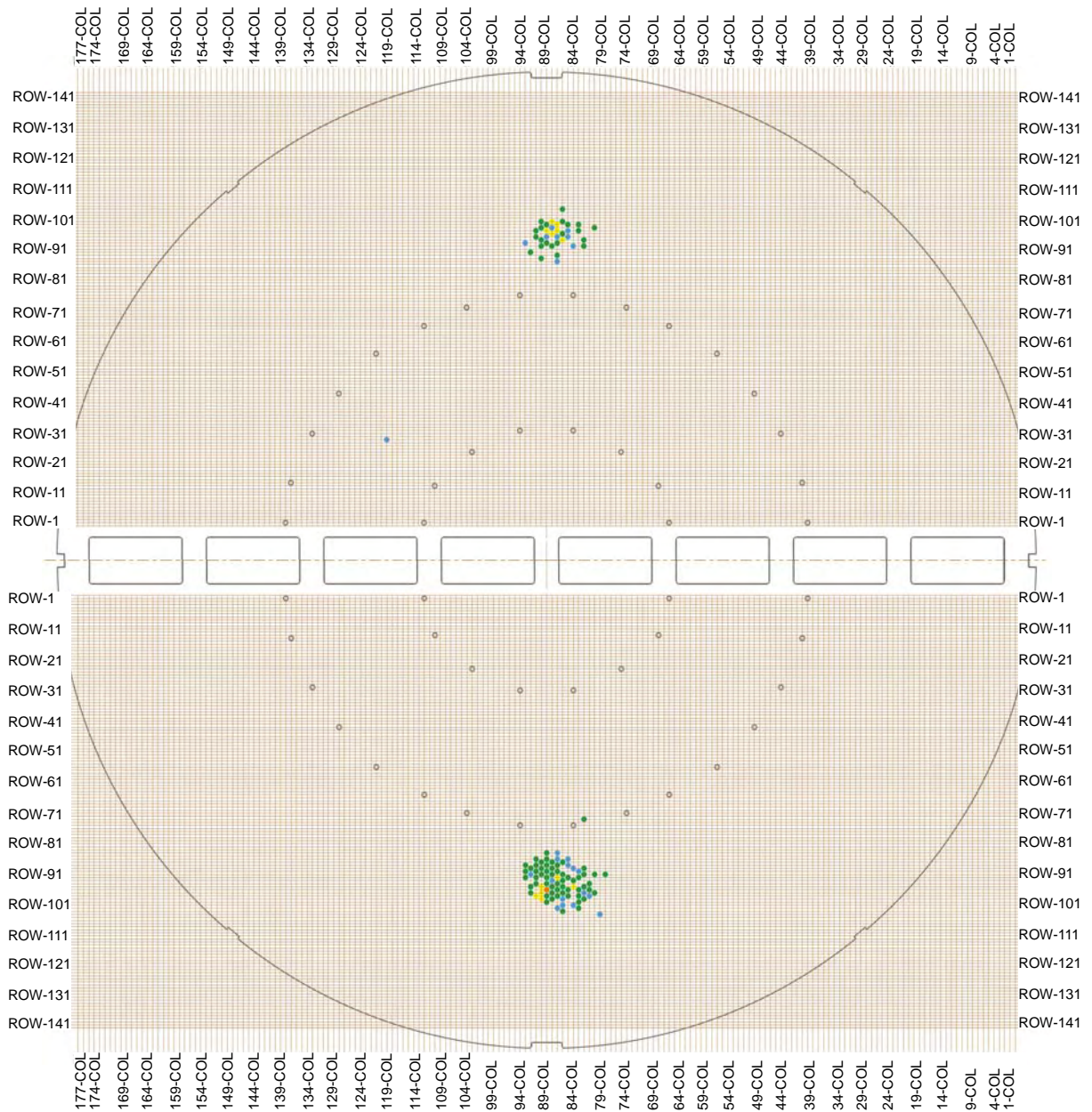


Fig 4.1.1-6 (2/7) Tubes with wear indications at TSPs



3A-SG #3TSP

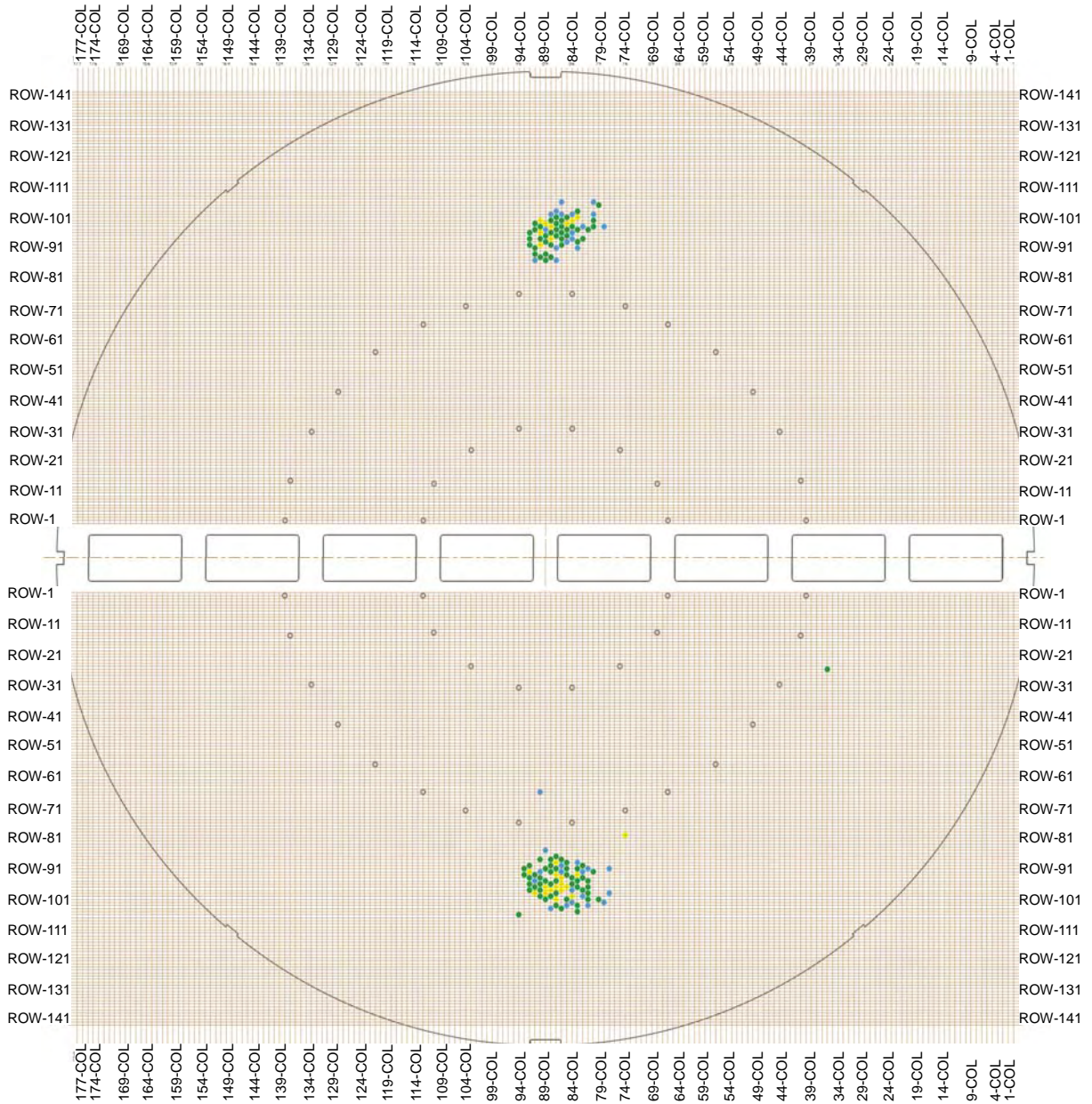


Fig 4.1.1-6 (3/7) Tubes with wear indications at TSPs



3A-SG #4TSP

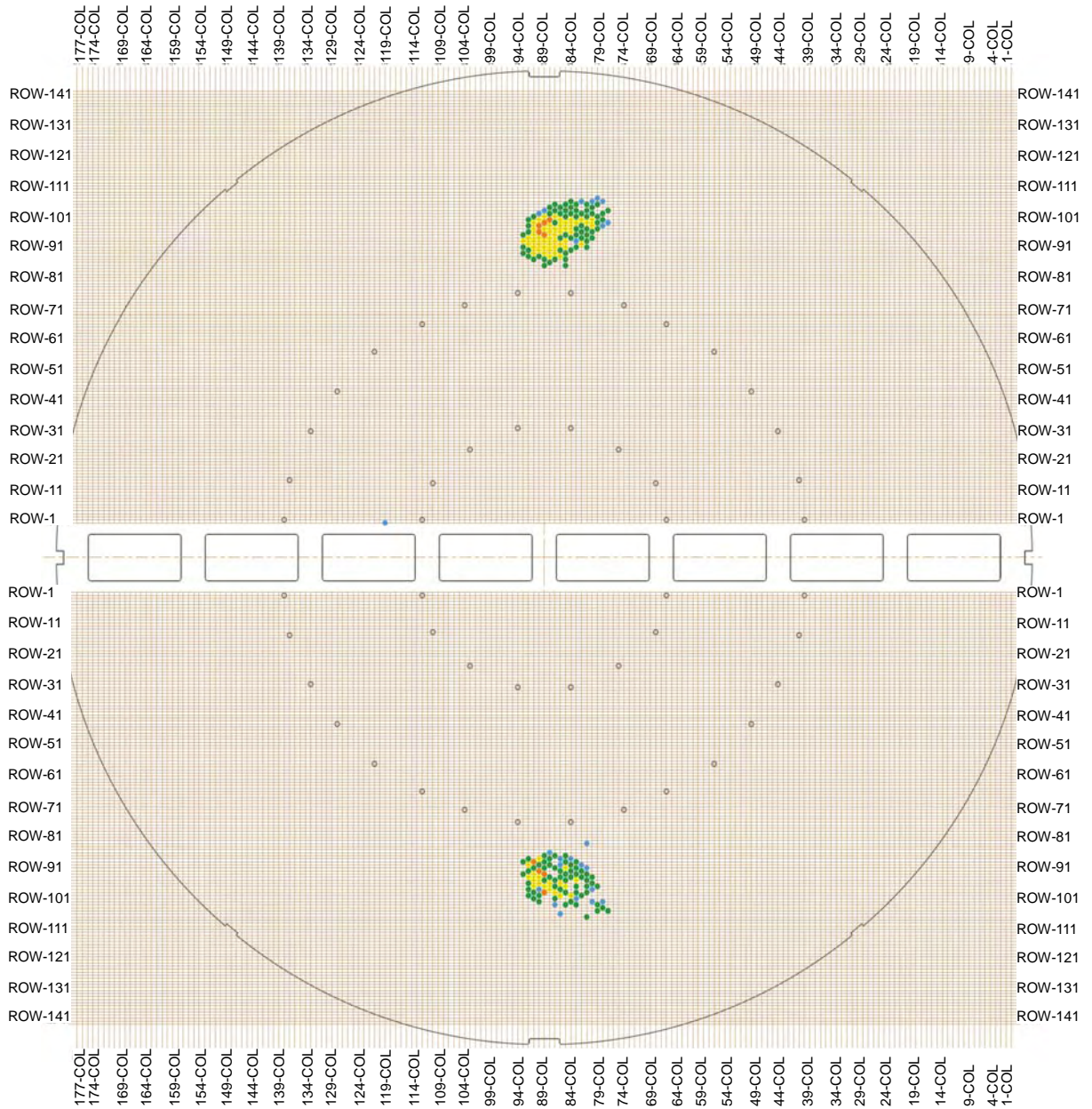


Fig 4.1.1-6 (4/7) Tubes with wear indications at TSPs



3A-SG #5TSP

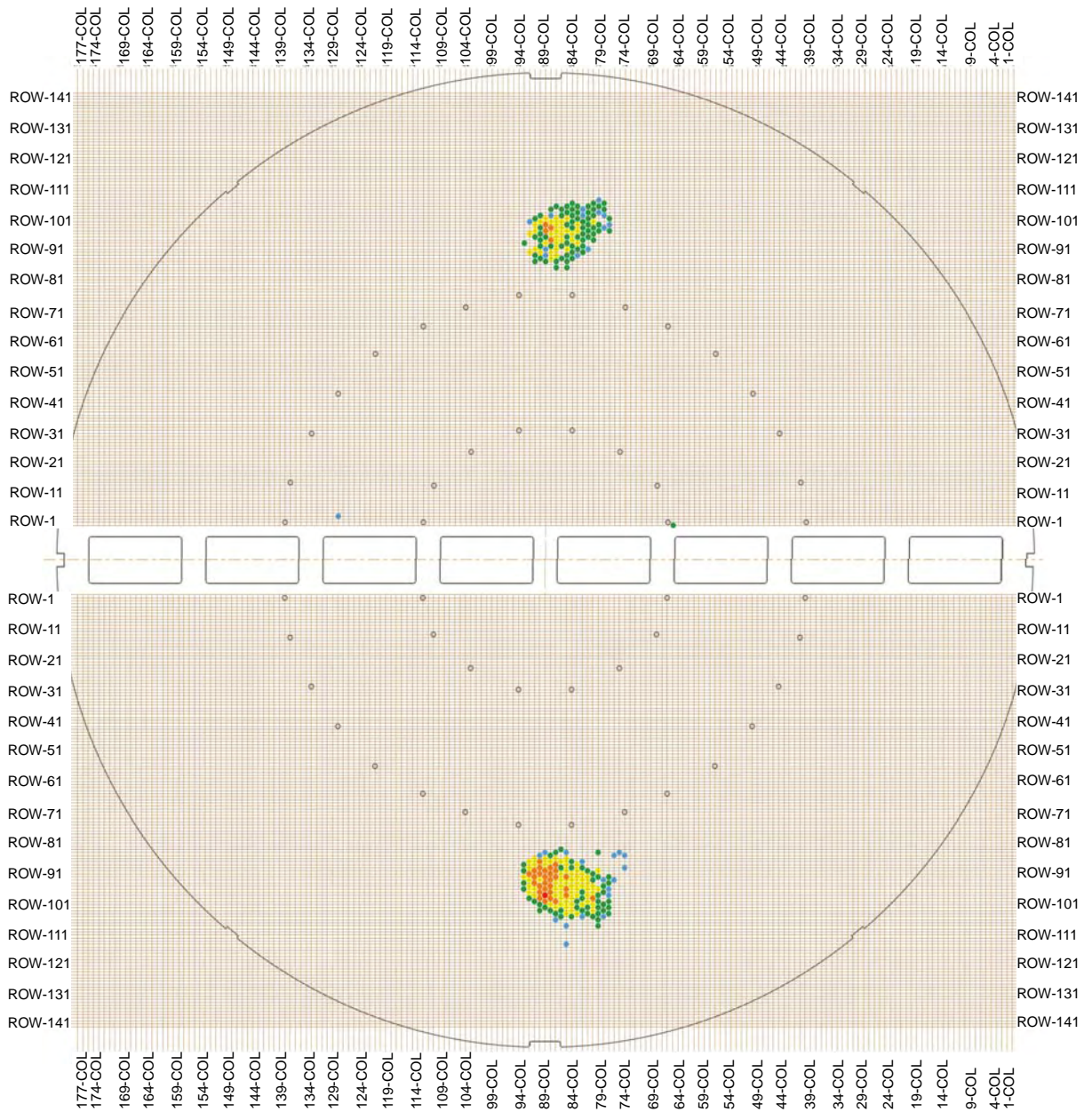


Fig 4.1.1-6 (5/7) Tubes with wear indications at TSPs



3A-SG #6TSP

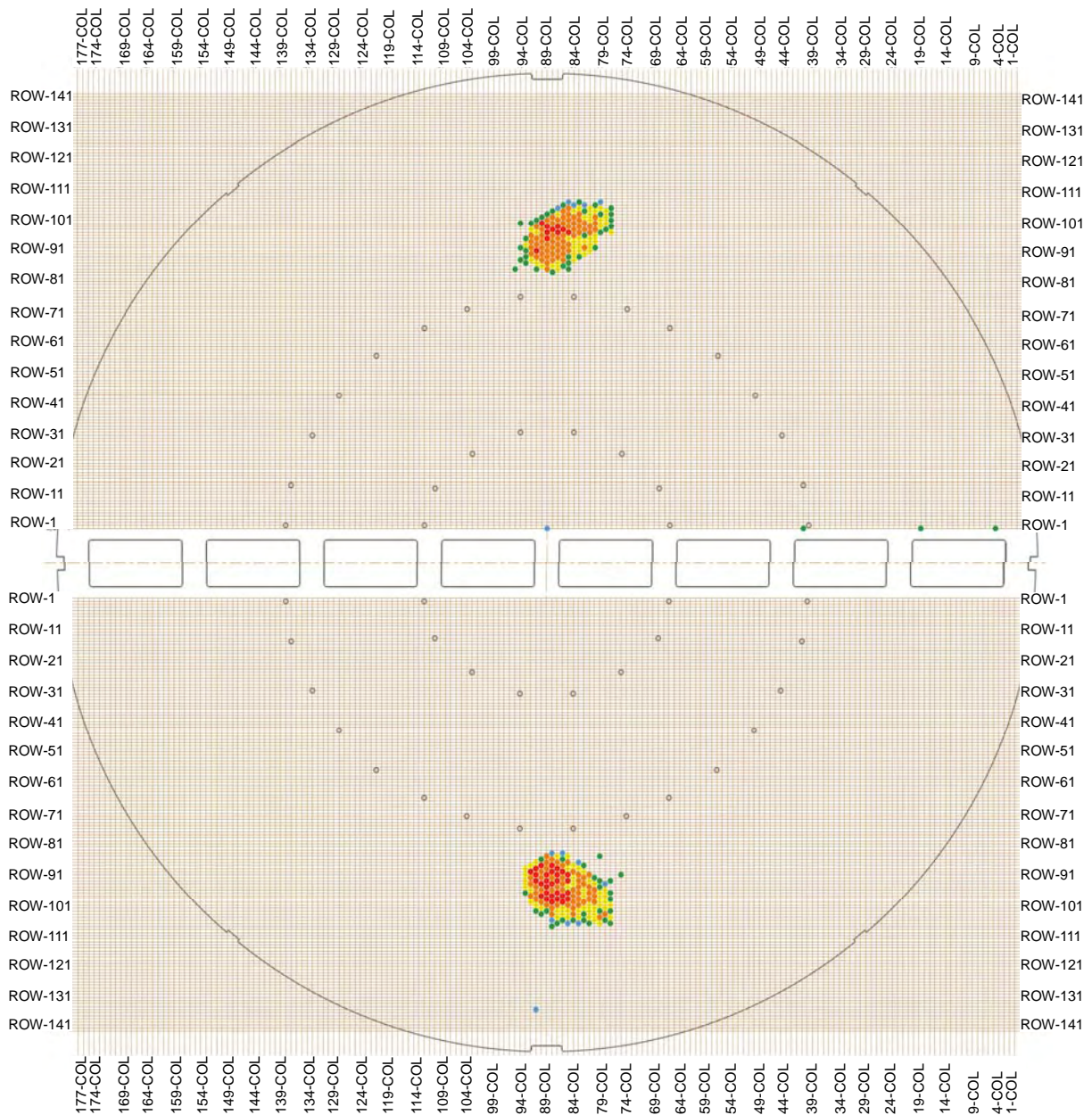


Fig 4.1.1-6 (6/7) Tubes with wear indications at TSPs



3A-SG #7TSP

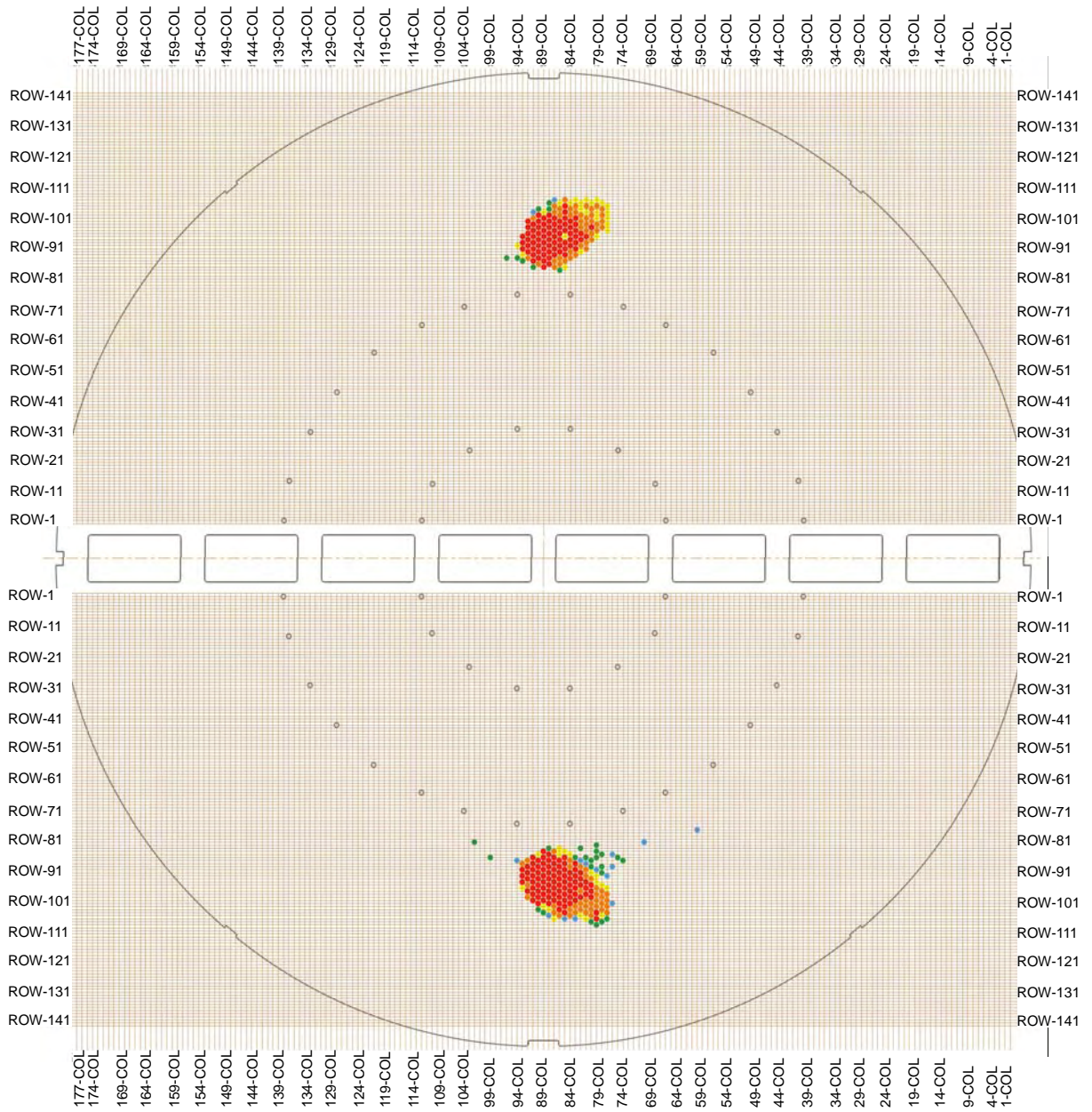
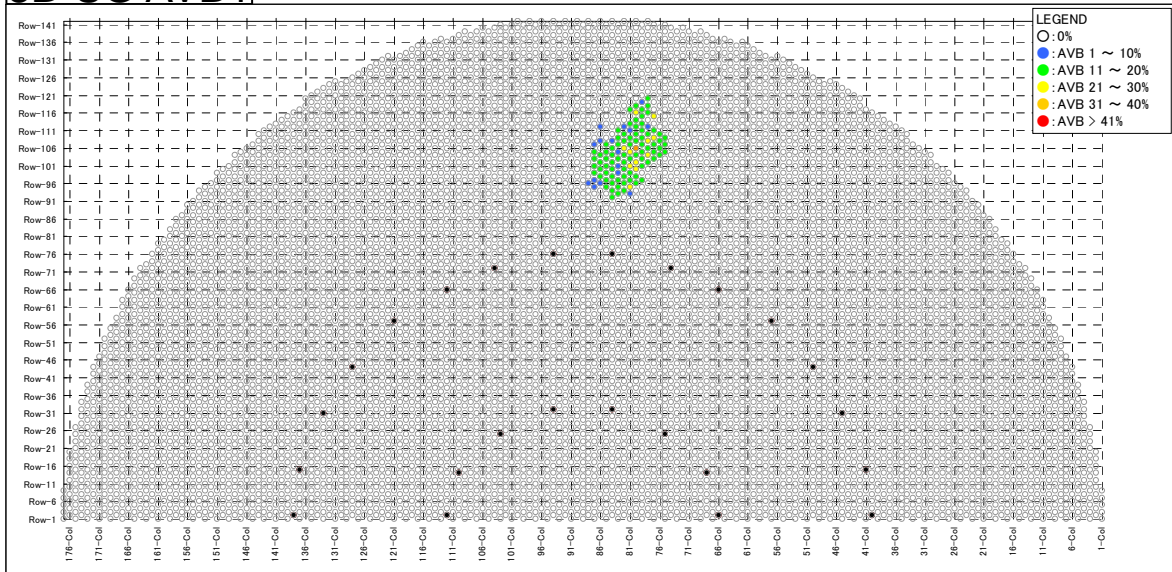


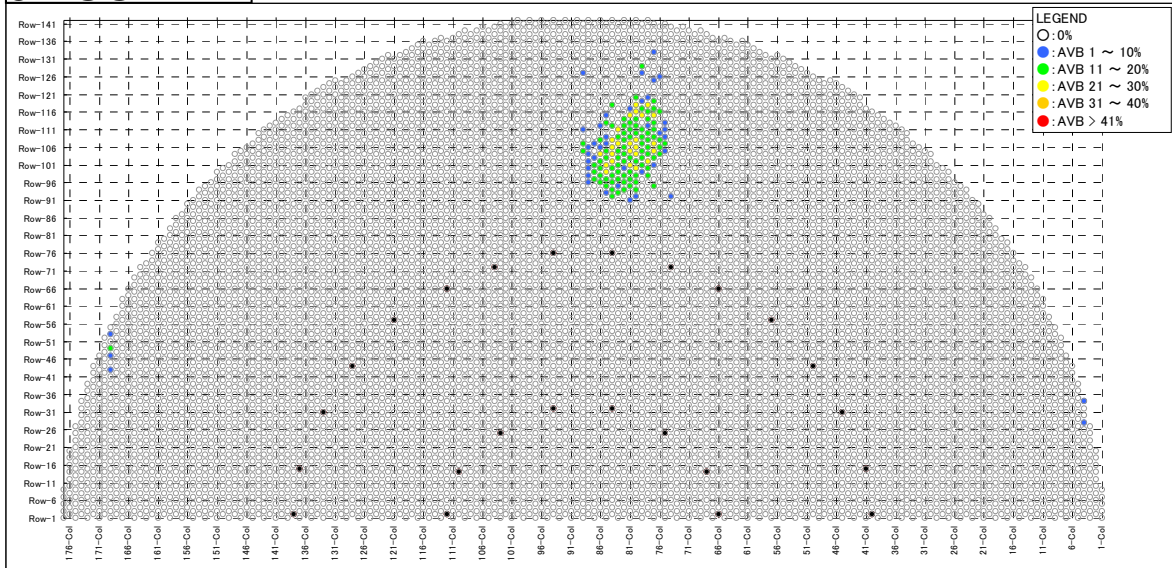
Fig 4.1.1-6 (7/7) Tubes with wear indications at TSPs



3B-SG AVB1



3B-SG AVB2



3B-SG AVB3

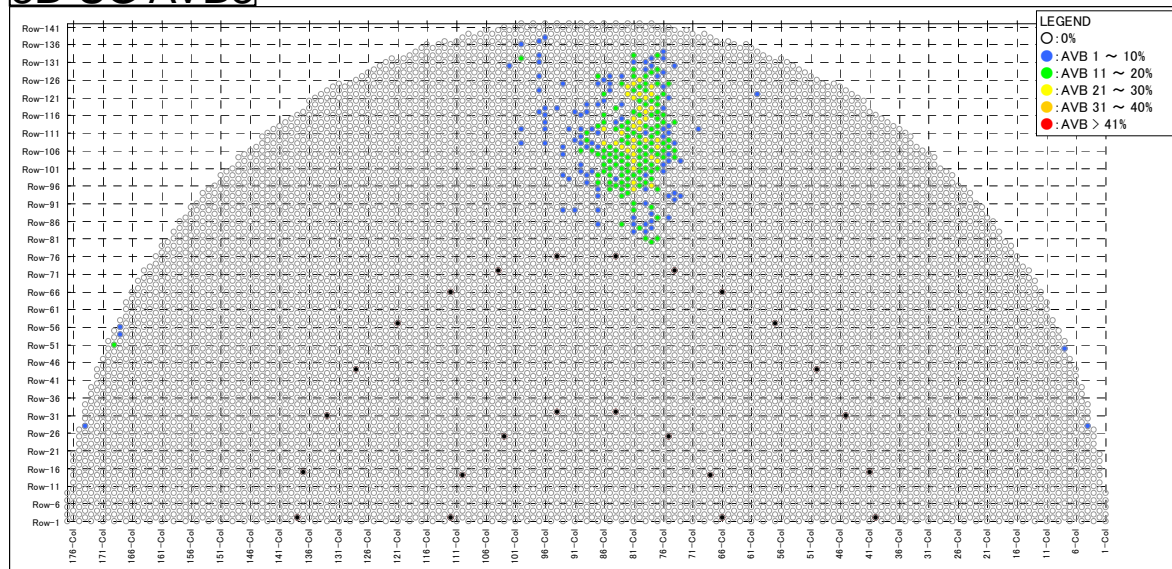
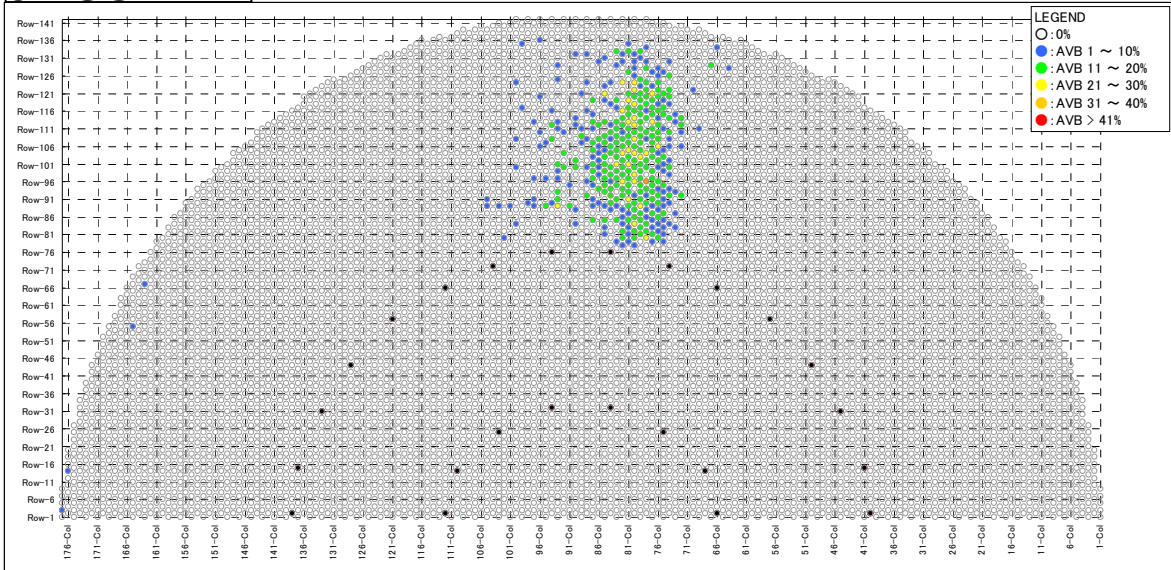


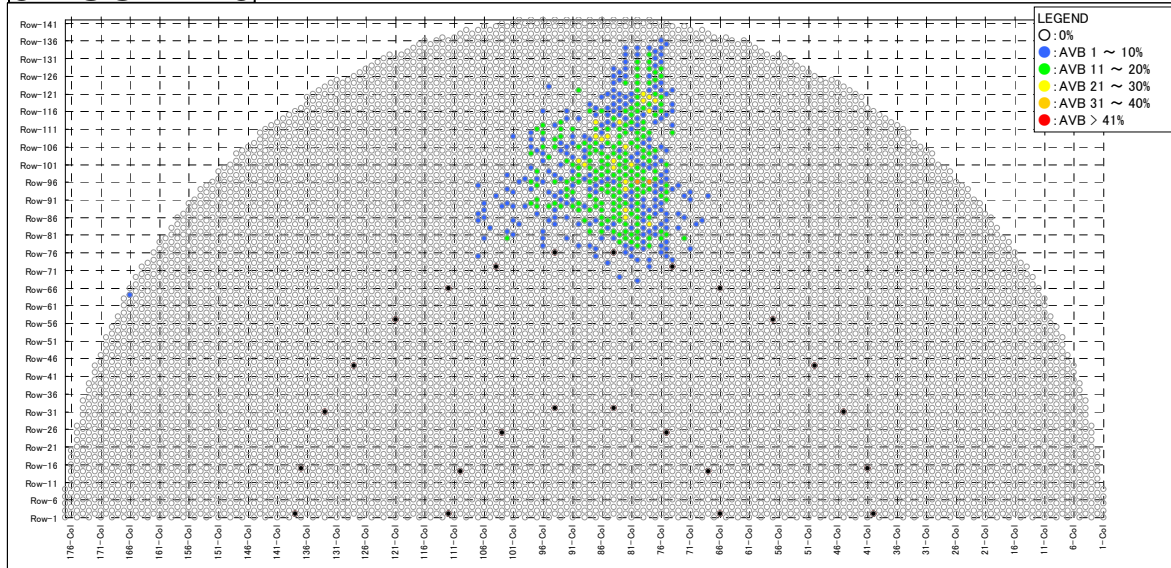
Fig 4.1.1-7 (1/4) Tubes with wear indication (at AVBs)



3B-SG AVB4



3B-SG AVB5



3B-SG AVB6

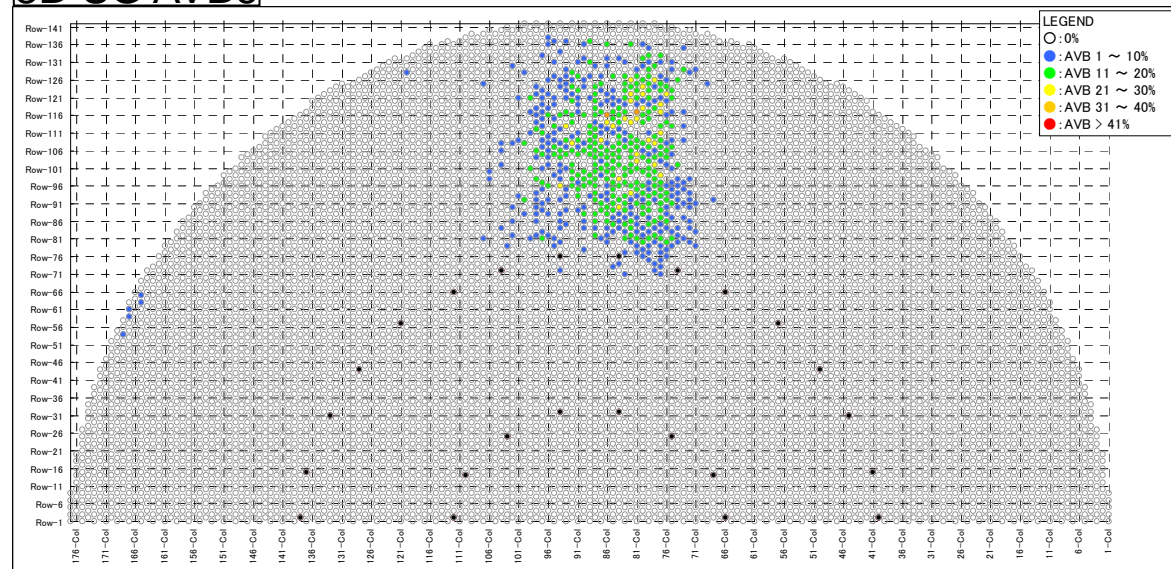
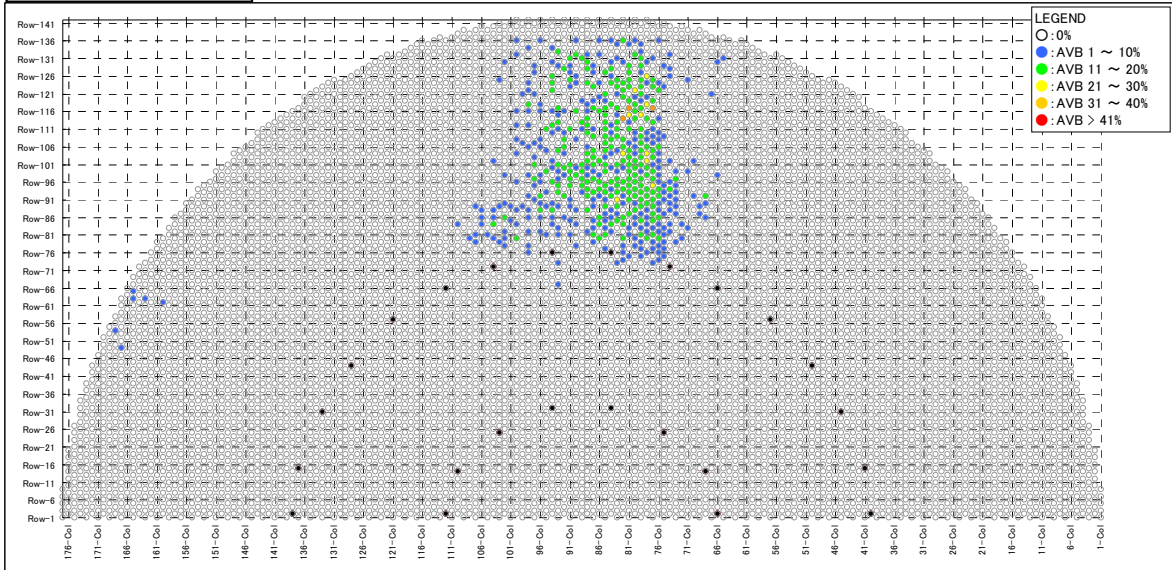


Fig 4.1.1-7 (2/4) Tubes with wear indication (at AVBs)

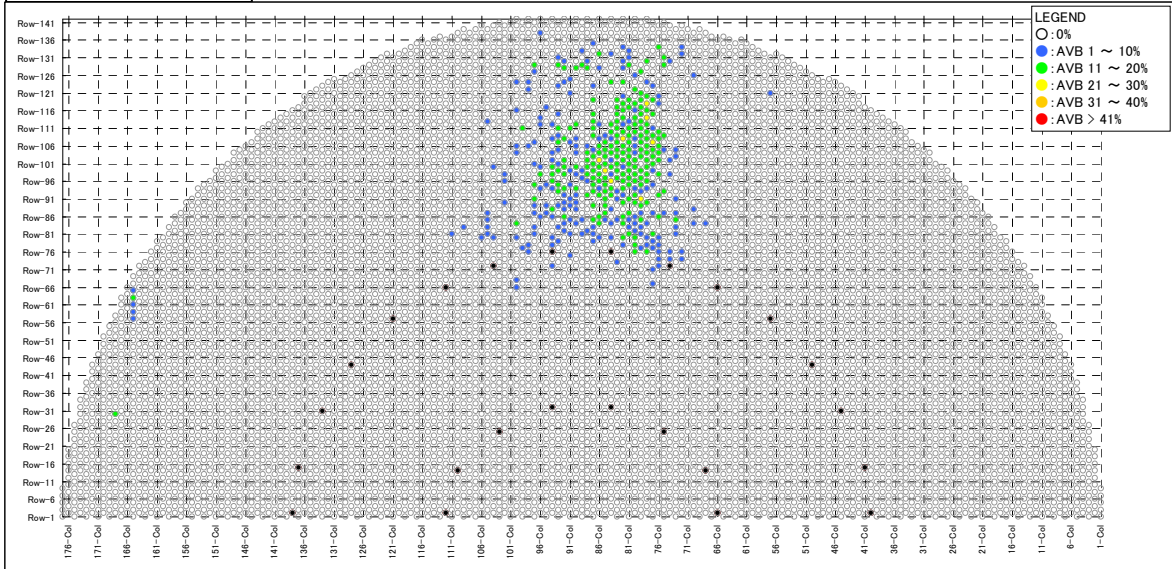
MITSUBISHI HEAVY INDUSTRIES, LTD.



3B-SG AVB7



3B-SG AVB8



3B-SG AVB9

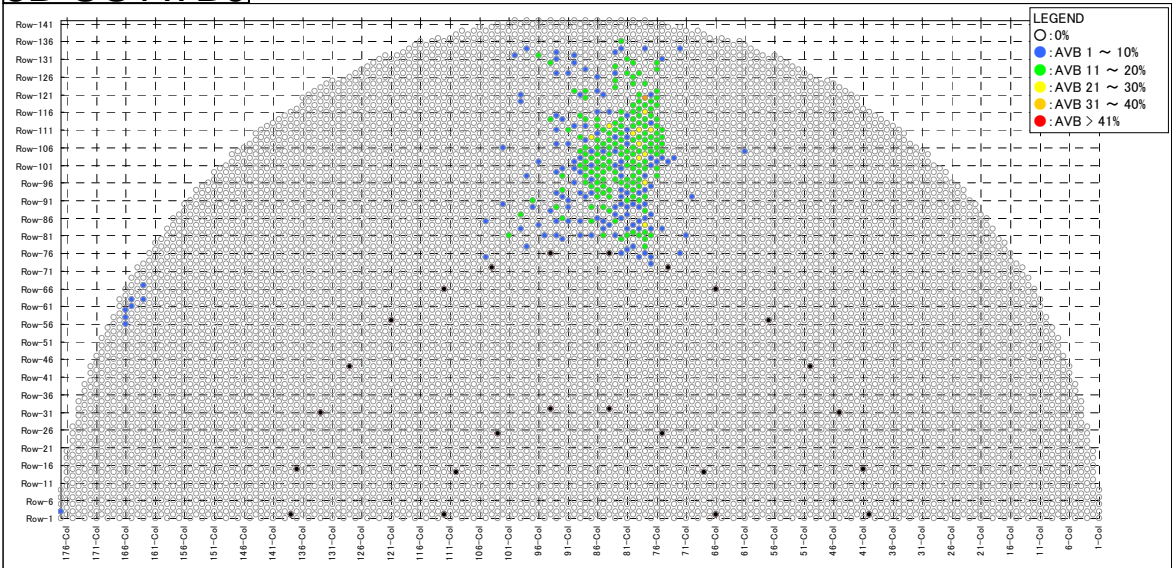
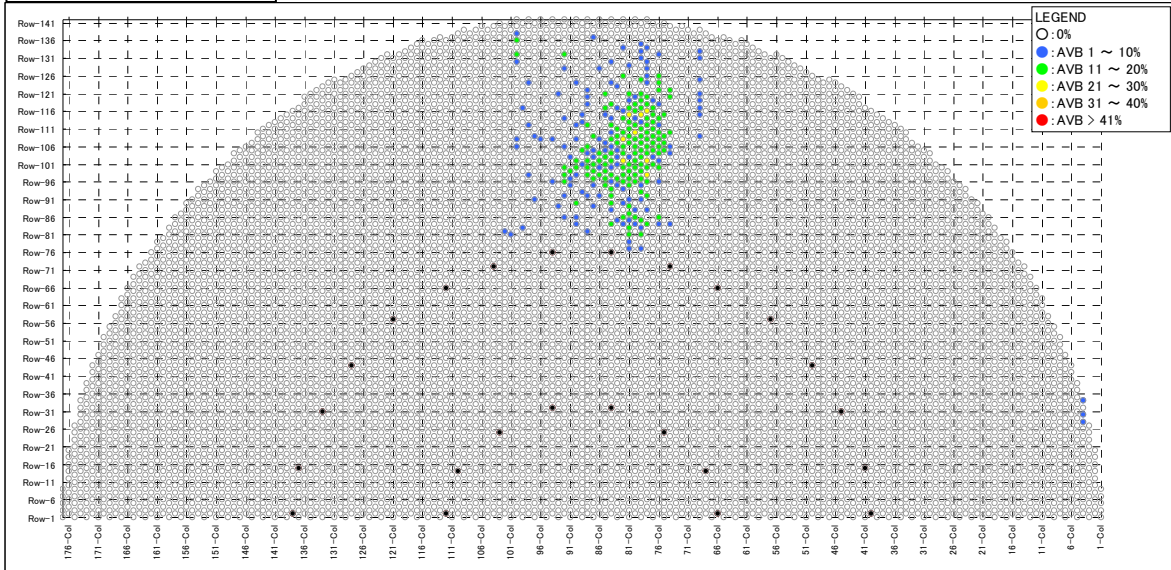


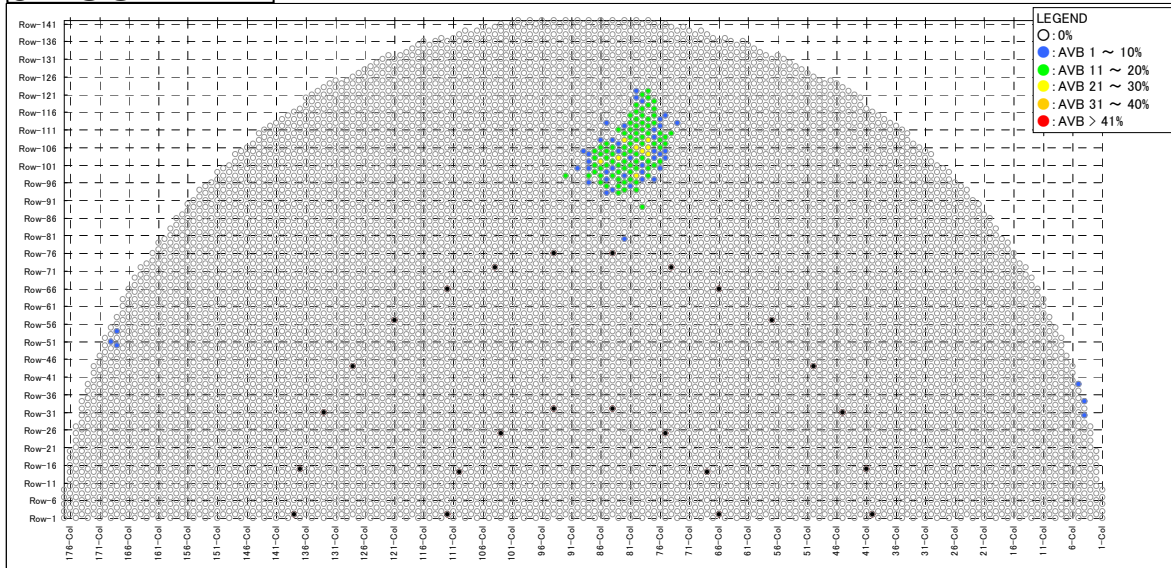
Fig 4.1.1-7 (3/4) Tubes with wear indication (at AVBs)



3B-SG AVB10



3B-SG AVB11



3B-SG AVB12

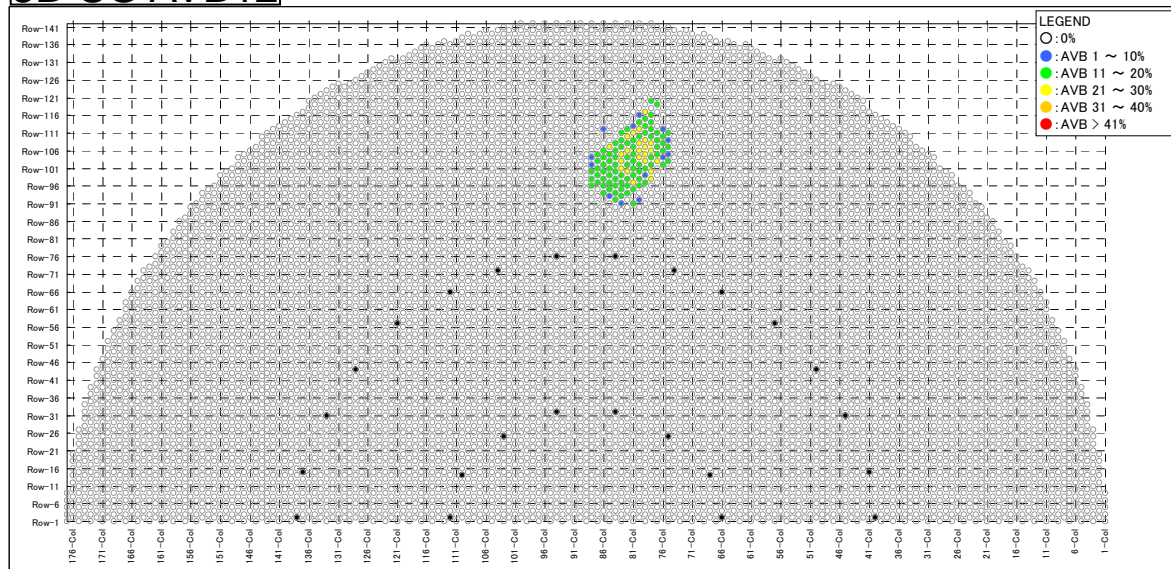


Fig 4.1.1-7 (4/4) Tubes with wear indication (at AVBs)

MITSUBISHI HEAVY INDUSTRIES, LTD.



3B-SG #1TSP

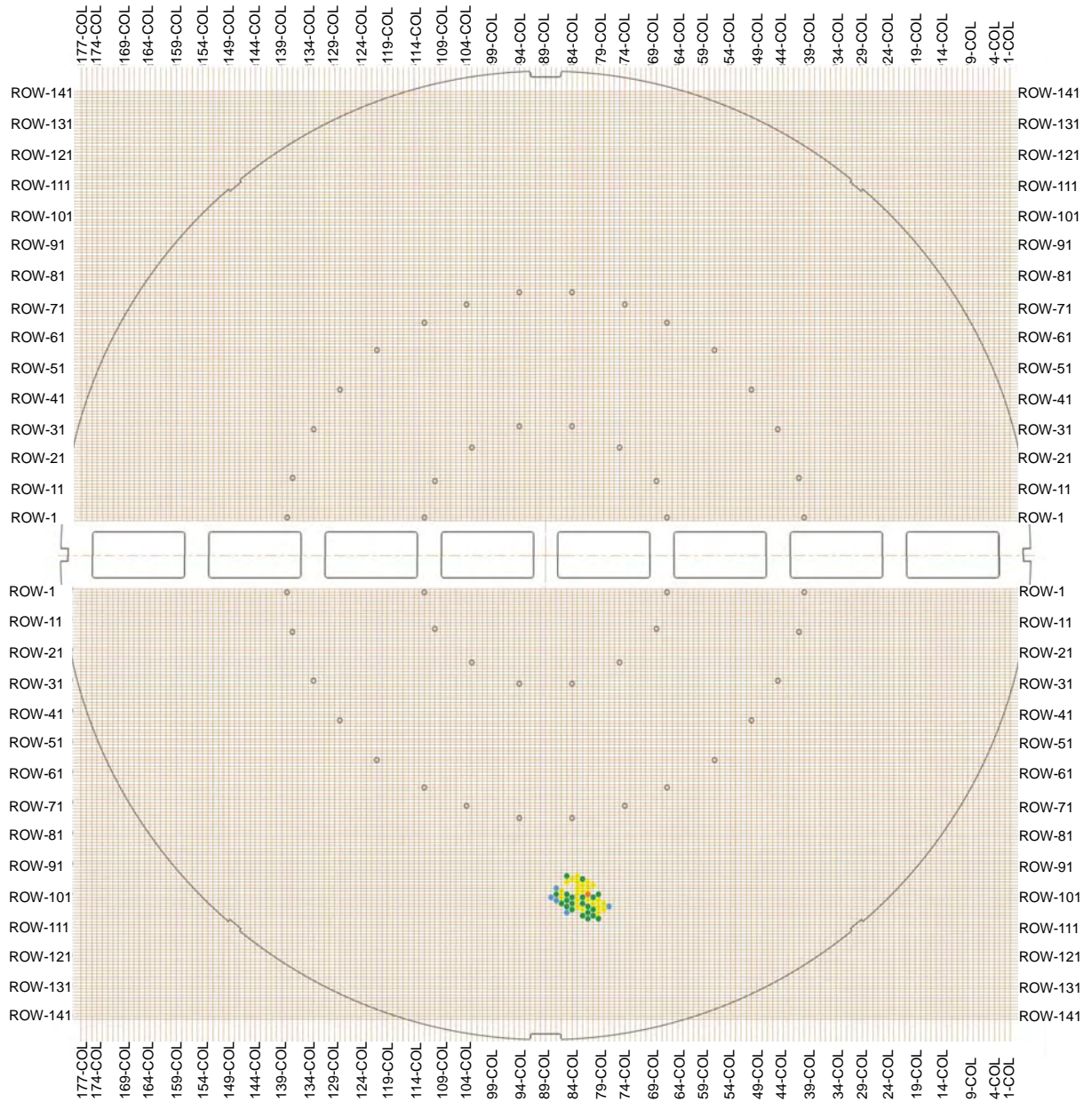


Fig 4.1.1-8 (1/7) Tubes with wear indications at TSPs



3B-SG #2TSP

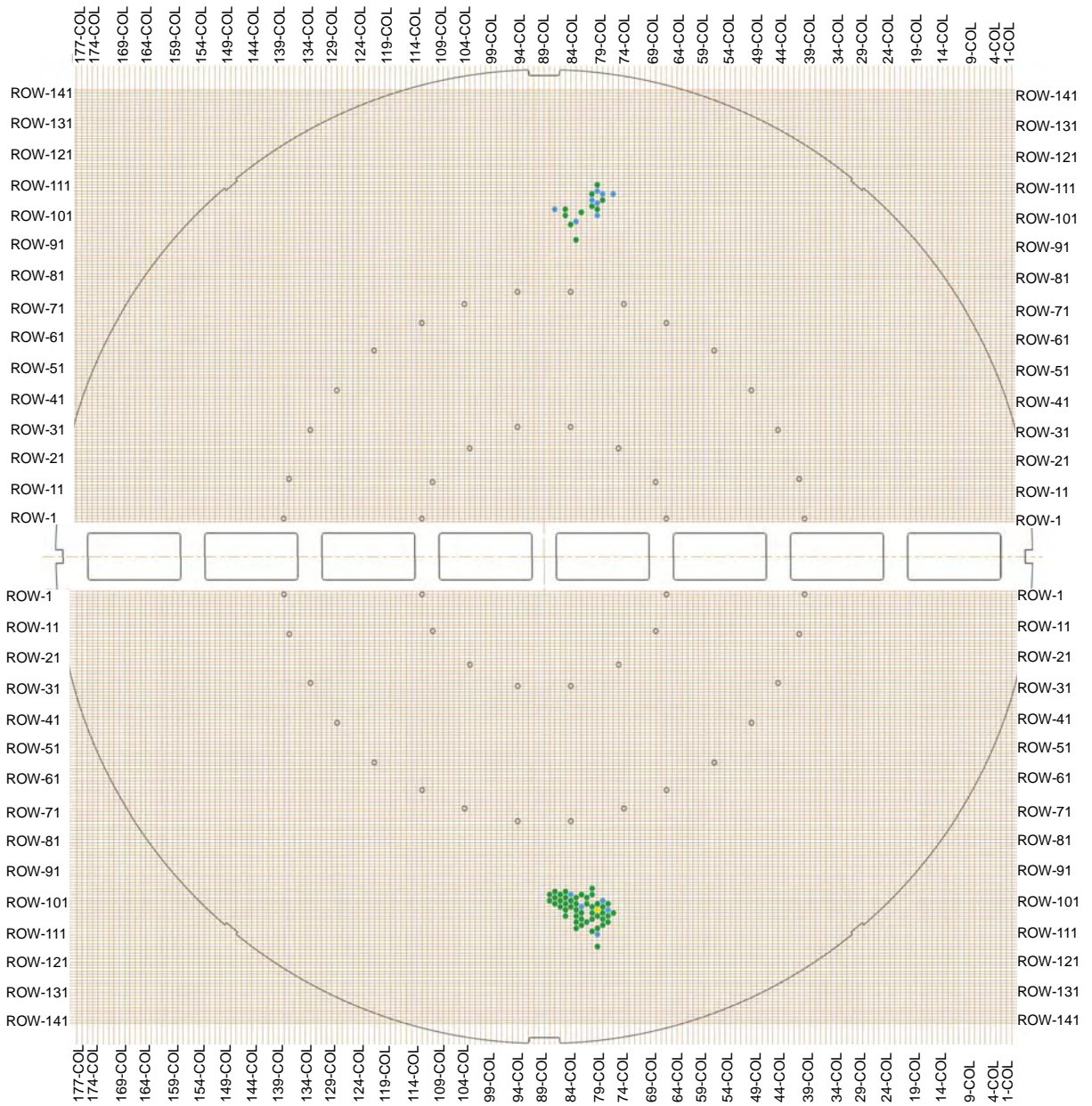


Fig 4.1.1-8 (2/7) Tubes with wear indications at TSPs



3B-SG #3TSP

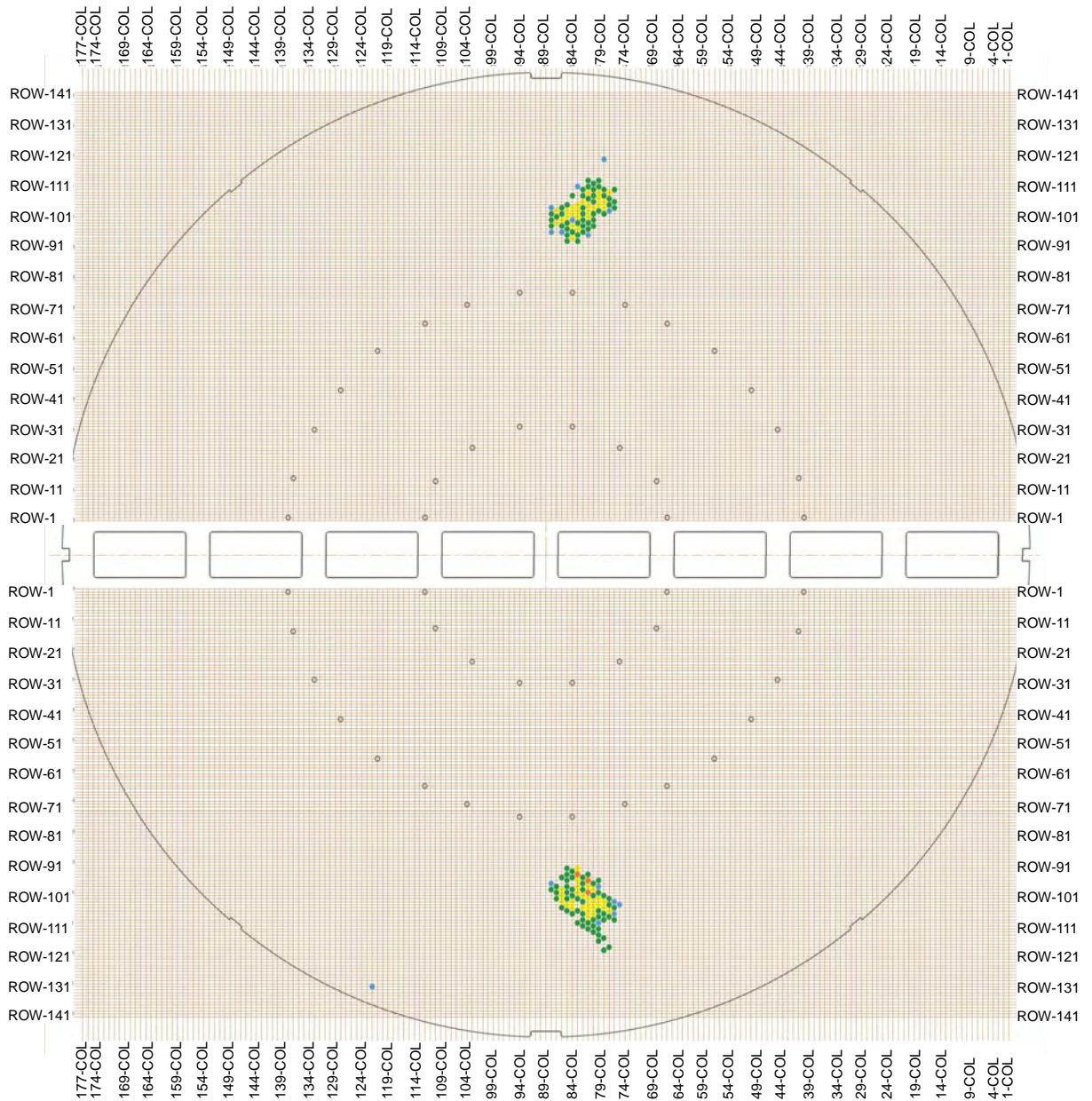


Fig 4.1.1-8 (3/7) Tubes with wear indications at TSPs



3B-SG #4TSP

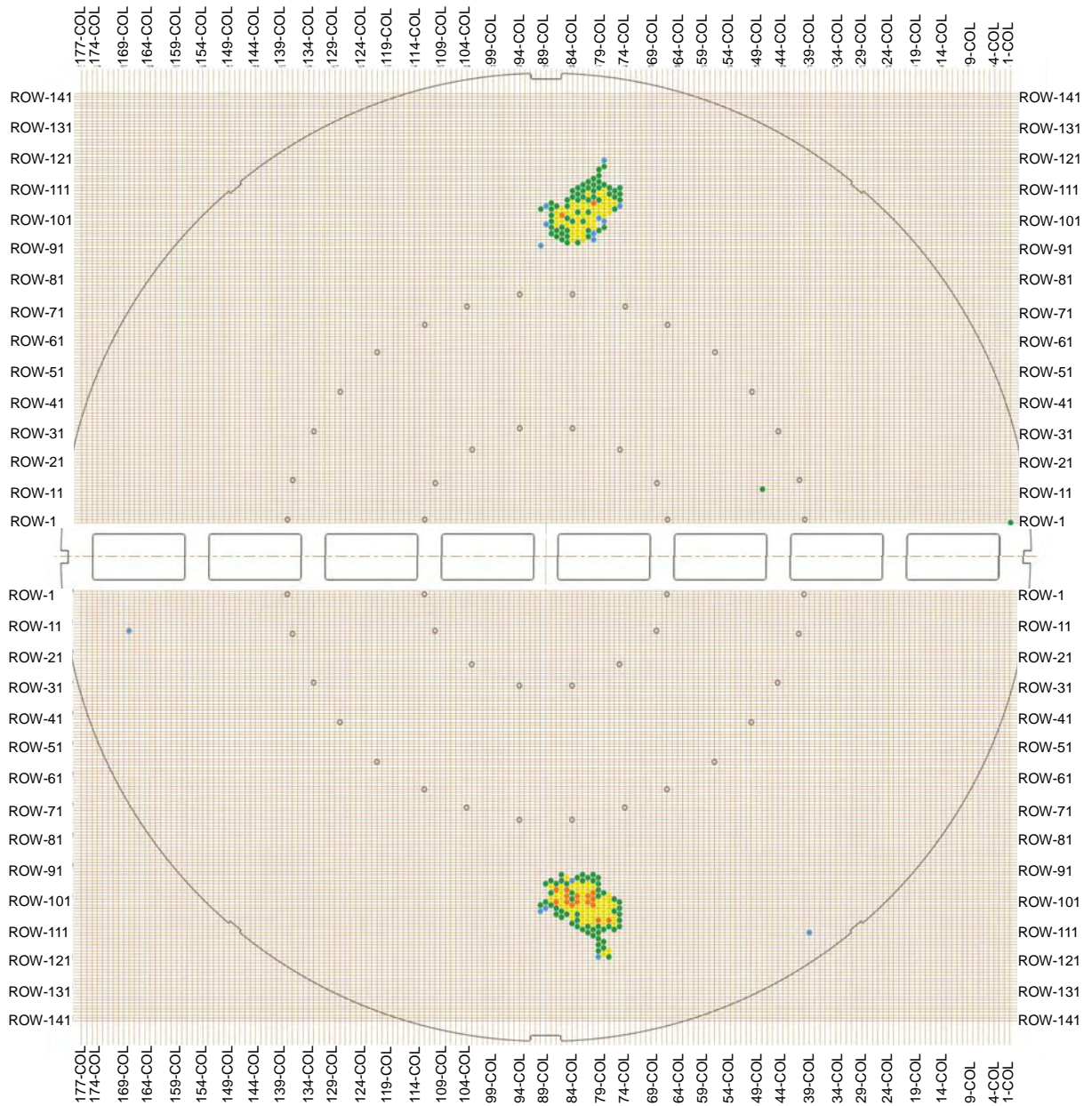


Fig 4.1.1-8 (4/7) Tubes with wear indications at TSPs



3B-SG #5TSP

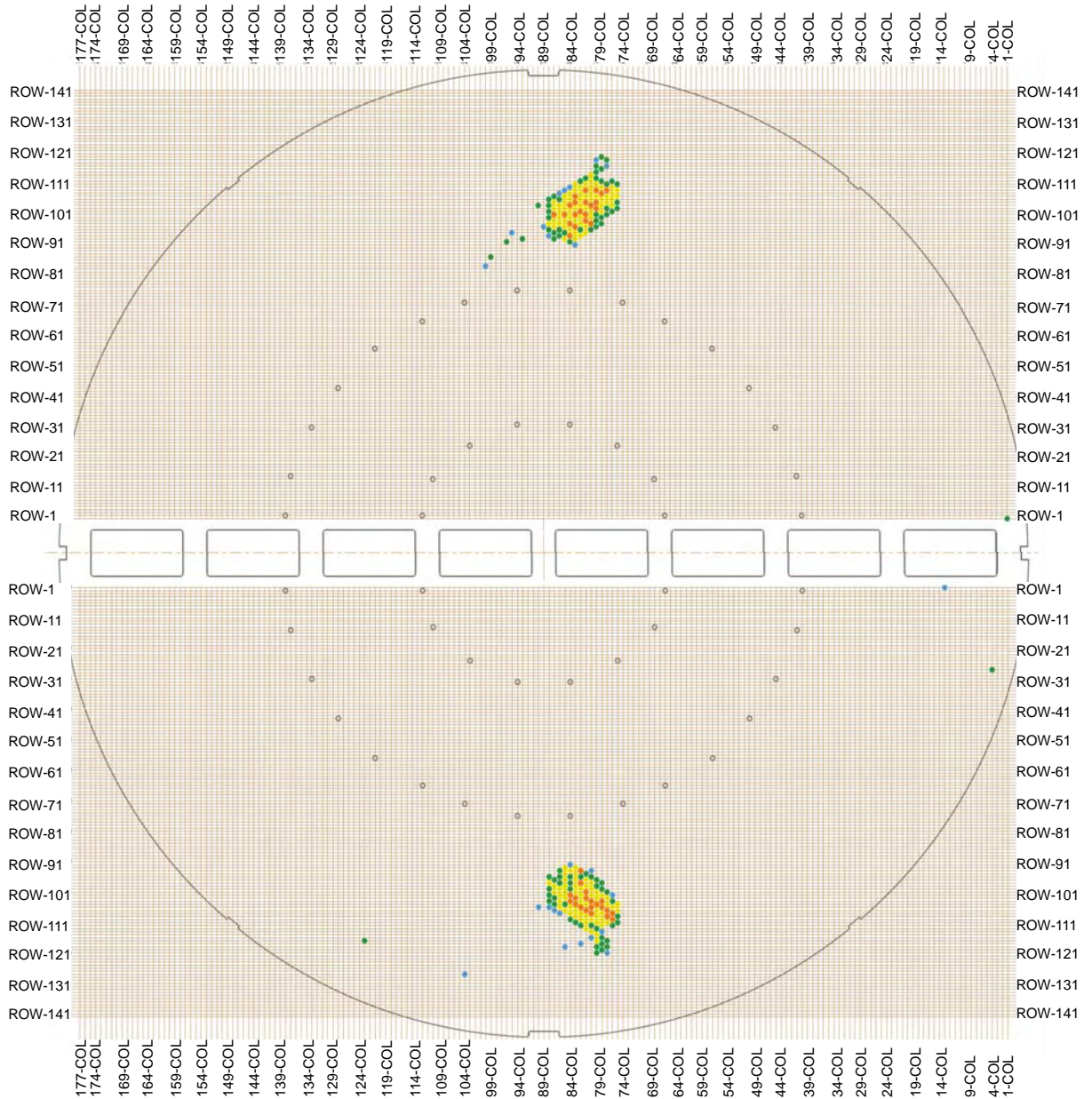


Fig 4.1.1-8 (5/7) Tubes with wear indications at TSPs



3B-SG #6TSP

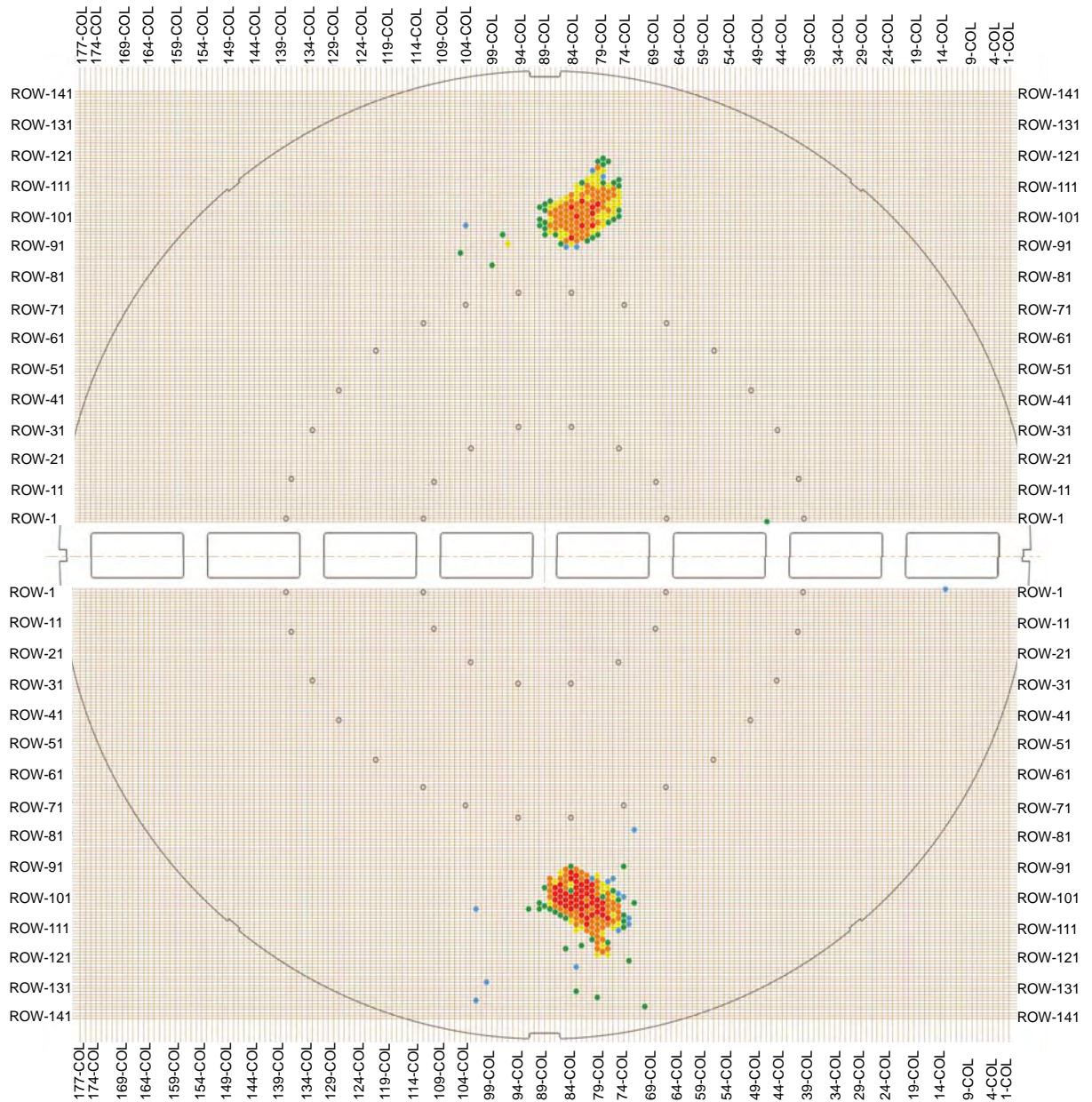


Fig 4.1.1-8 (6/7) Tubes with wear indications at TSPs



3B-SG #7TSP

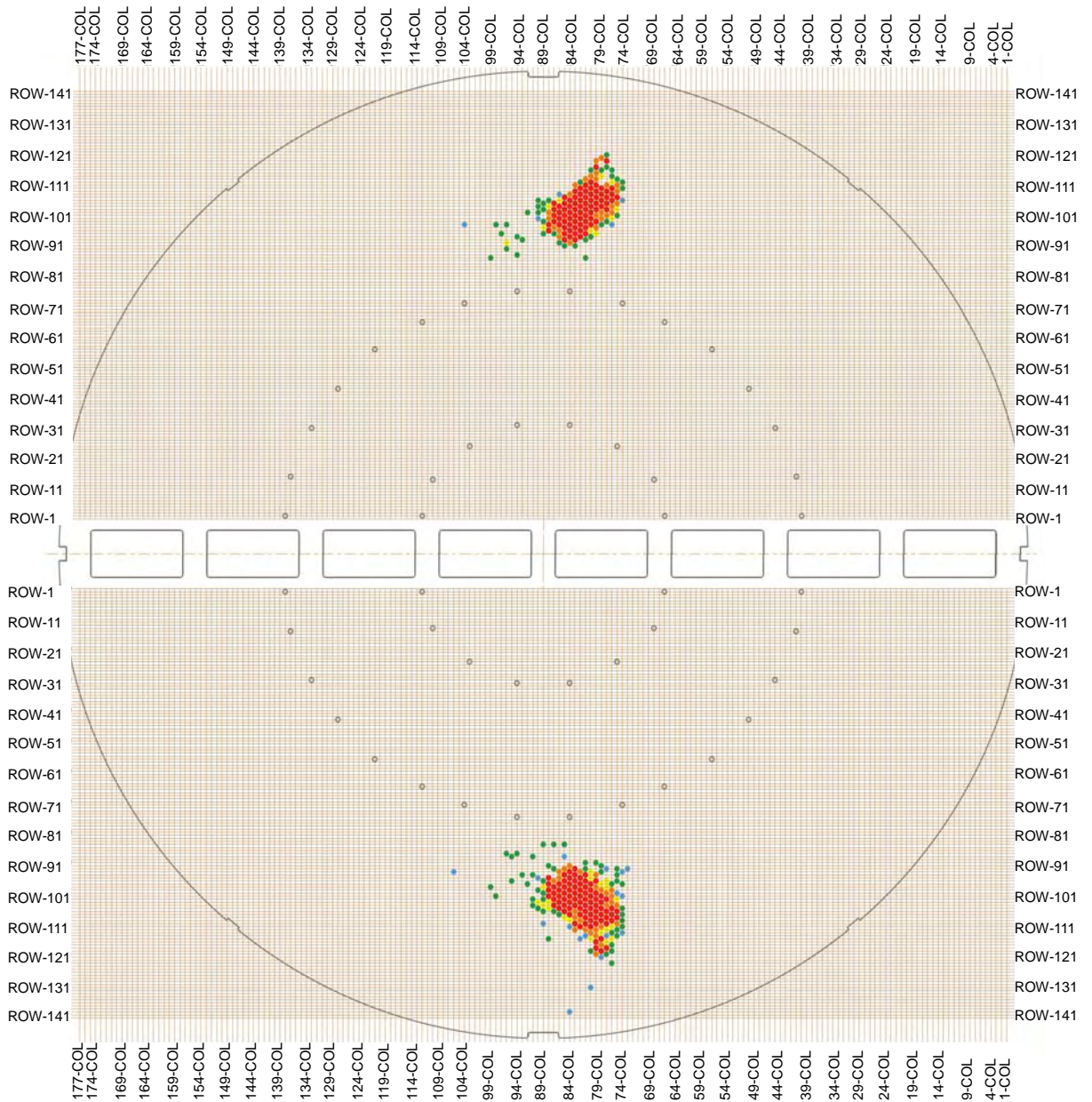


Fig 4.1.1-8 (7/7) Tubes with wear indications at TSPs



4.1.2. Tube Wear in Unit-2 (for reference only)

The tubes in Unit 2 have experienced wear at 4 locations, i.e. wear in the free span area, wear at the AVB bars, wear at the TSPs and wear at retainer bars, as well as wear due to a foreign object. Table 4.1.2-1 shows the number of tubes that have shown wear at these four different locations as well as foreign object wear and is provided by SCE (Reference 9 and 11).

Table 4.1.2-1 Number of Tubes with Wear in SONGS Unit-2

Wear Type	SG 2A (2E-089)	SG 2B (2E-088)	Total
Tube-to-Tube Wear	2	0	2*
AVB Wear	804	595	1399*
TSP Wear	119	180	299*
Retainer Bar Wear	4	2	6*
Foreign Object	0	2	2*
Total	861**	734**	1595**

Notes:

*) The total number of tubes with wear at a given location

***) The total number of tubes with wear at any location

For purposes of analysis in this report, MHI has categorized the tube wear into the four types of wear as defined in Section 4.1.1 (Types of Tube Wear). Table 4.1.2-2 shows the number of tubes in the Unit 2 RSGs that fall into each of these types of wear.

Table 4.1.2-2 Number of Tubes with Type of Wear in SONGS Unit-2

Wear Type	SG 2A (2E-089)	SG 2B (2E-088)	Total
Type 1 (TTW)	2	0	2
Type 2 (AVB wear)	802	595	1397
Type 3 (TSP wear)	53	137	190
Type 4 (RB wear)	4	2	6
Foreign Object	0	2	2
Total	861	736	1597



In this table each of the tubes is only counted once with priority given to Type 1 followed by Type 2, Type-3, Type 4 and Foreign Object. The data in this table is based on the ECT data evaluations described in Appendix-3 of Reference 8 which includes both bobbin ECT and rotated ECT data. The total number of tubes differs from that in table 4.1.2-1 because, as explained in Appendix 3, Reference 8, the data in Table 4.1.2-1 for wear at AVBs and TSPs is based solely on bobbin ECT data.

9



4.1.3. Tube Wear in Unit-3

The number of tubes for each type of tube wear in Unit-3 is listed in Table.4.1.3-1.

The tubes in Unit 3 have experienced wear at 4 locations, i.e. wear in the free span area, wear at the AVB bars, wear at the TSPs and wear at retainer bars. Table 4.1.3-1 shows the number of tubes that have shown wear at these four different locations and is provided by SCE (Reference 9 and 11).

Table.4.1.3-1 Numbers of Tubes with Wear in SONGS Unit-3

Wear Type	SG 3A (3E-089)	SG 3B (3E-088)	Total
Tube-to-Tube Wear	165	161	326*
AVB Wear	871	896	1767*
TSP Wear	214	250	464*
Retainer Bar Wear	1	3	4*
Total	887**	919**	1806**

Notes:

*) The total number of tubes with wear at a given location

***) The total number of tubes with wear at any location

For purposes of analysis in this report, MHI has categorized the tube wear into the four types of wear as defined in Section 4.1.1 (Types of Tube Wear). Table 4.1.3-2 shows the number of tubes in the Unit 3 RSGs that fall into each of these types of wear. 9

Table 4.1.3-2 Number of Tubes with Type of Wear in SONGS Unit-3

Wear Type	SG 3A (3E-089)	SG3B (3E-088)	Total
Type 1 (TTW)	165	161	326
Type 2 (AVB wear)	714	737	1451
Type 3 (TSP wear)	15	20	35
Type 4 (RB wear)	1	3	4
Total	895	921	1816

In this table each of the tubes is only counted once with priority given to Type 1 followed by Type 2, Type-3, and Type 4. This data in this table is based on the ECT data evaluations



described in Appendix-3 of Reference 8 which includes both bobbin ECT and rotated ECT data. The total number of tubes differs from that in Table 4.1.3-1 because as explained in Appendix 3, Reference 8 the data in Table 4.1.3-1 for wear at AVBs and TSPs is based solely on bobbin ECT data.





4.2 Visual Inspection Results of the Tube Bundle

Based on the visual inspection performed along AVBs No.B04 and B09, the following observations were made (see to Appendix-7 for details).

4.2.1. Observations Common to Unit-2 and Unit-3

The AVBs, end caps, and retainer bars were manufactured according to the design. It was confirmed that there were no significant gaps between the AVBs and tubes which might have contributed to excessive tube vibration because the AVBs appear to be virtually in contact with tubes as shown in Fig.4.2-1, Fig.4.2-2 and Fig.4.2-3. ECT wear indications are identified as the Type 1 and Type 2 wear.



4.2.2. Observations in Unit-3

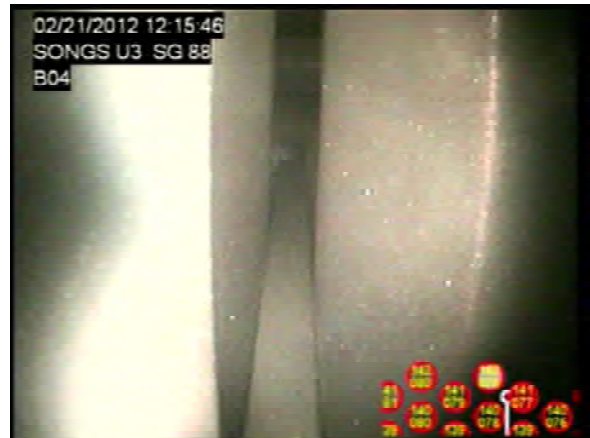
Pattern 1 wear indicating high amplitude in-plane motion of the tube, as shown in Fig 4.2-2, was seen on the tubes with Type 1 wear. Pattern 2 wear, as shown in Fig 4.2-3, was seen on the tubes with the Type 2 wear.

4.2.3. Observations in Unit-2

Pattern 2 wear seen in Unit-3 was also seen on the tubes with the Type 2 wear tubes.



Sample from SG-2A



Sample from SG-3B

Fig.4.2-1 Condition of Tube Wear in SONGS Unit-2 and Unit-3

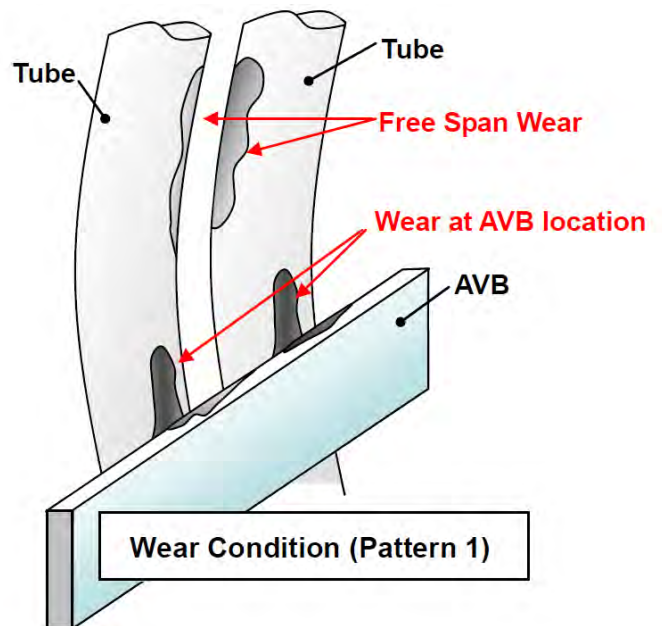
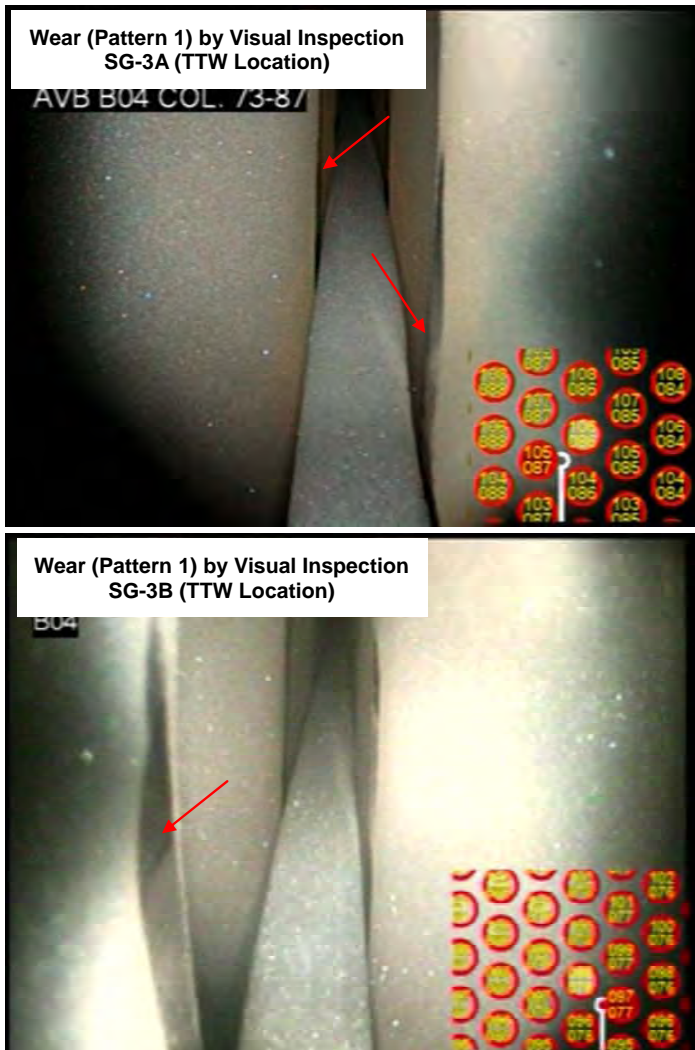


Fig.4.2-2 Illustration of Tube Wear Pattern 1

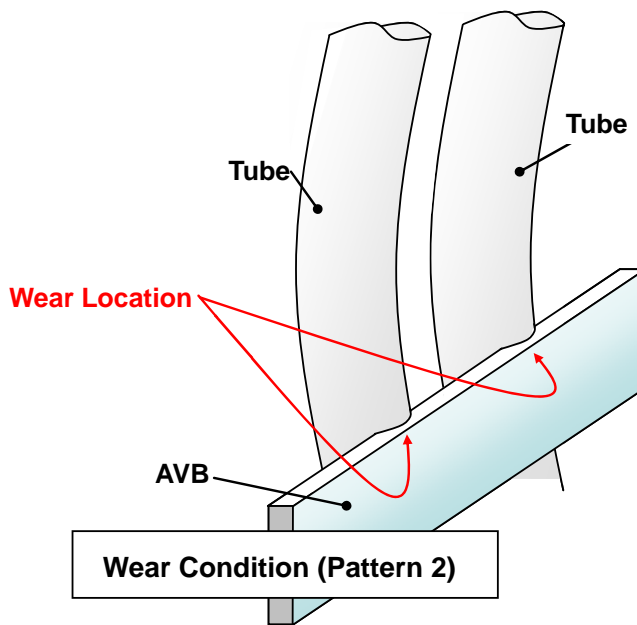


Fig.4.2-3 Illustration of Tube Wear Pattern 2



5. Mechanistic Cause Analysis

The cause of the first 3 types of tube wear (i.e. TTW, AVB wear, TSP wear) is excessive tube vibration. Generally, the causes of tube excessive vibration are the thermal-hydraulic operating conditions of the SG secondary side and lack of sufficient in-plane tube support for the tubes (condition of the tube supports in terms of their effectiveness; active versus inactive tube supports). The cause of the Type 4 tube wear (RB wear) is vibration of the retainer bar itself which is described in Section 6.

5.1 Thermal Hydraulic Condition in the Secondary Side

In general, structures in a two-phase flow field have lower resistance to vibration when a void fraction (percentage of vapor volume in a saturated mixture) or steam quality (percentage of vapor mass in a saturated mixture) is high. The high void fraction (steam quality) results in the two-phase fluid having a low density, which in turn results in an increase of the flow velocity of the two-phase fluid, and in a low damping factor. The increase of the flow velocity (v) causes the increase of the hydrodynamic pressure (ρv^2) which causes structures to vibrate in the flow field. The hydrodynamic pressure is a measure of energy imparted on the structure by the flow field, and damping is a measure of how easily the structure can dissipate this energy. If the amount of energy imparted on the structure is higher than the amount of energy dissipated, the structure (in this case the tubes) will vibrate with progressively increasing amplitudes, which eventually may lead to the tubes becoming fluid-elastic unstable. Also, the unstable tubes will excite the surrounding tubes via two-way coupling with the fluid. Therefore, it is more likely for the tubes to vibrate when the void fraction (steam quality) is high.

Fig.5.1-1 shows the results of the three-dimensional thermal hydraulic analysis of SONGS Unit-2 and 3 SGs (see Reference 5 for detail). This analysis was performed recently using the ATHOS computer code developed by EPRI. As can be seen from the void fraction profile, the highest void fraction is estimated to be [] (and the steam quality is []), which is high compared to the [] void fraction (when steam quality is less than []) for the other SGs designed by MHI based on ATHOS computer code. The higher than typical void fraction is a result of a very large and tightly packed tube bundle, particularly in the U-bend, with high heat flux in the hot leg side. Because this high void fraction is a potentially major cause of the tube FEI, and consequently unexpected tube wear (as it affects both the flow velocity and the damping factors), the correlation between the void fraction (steam quality) and the number of tubes with wear in a given void fraction region was investigated. From this investigation, a strong correlation between the void fraction (steam quality) and the percentage of tubes with the Type 1 and Type 2 wear was identified (see Fig.5.1-2 and Fig.5.1-4). The correlation





between flow velocity and the number of tubes with wear was also investigated. The results show that when the flow velocity is high, the percentage of tubes with wear increases, even though this correlation is not as strong as that between the void fraction (steam quality) and the percentage of tubes with wear (see Fig.5.1-3 and Fig.5.1-5).

Consequently, it is concluded that the thermal-hydraulic conditions in the SG secondary side, namely high void fraction (steam quality) and high flow velocity along with lack of sufficient in-plane tube support, are the main causes of the excessive tube vibration and unexpected wear in the SONGS Unit 2 and Unit 3 RSGs.

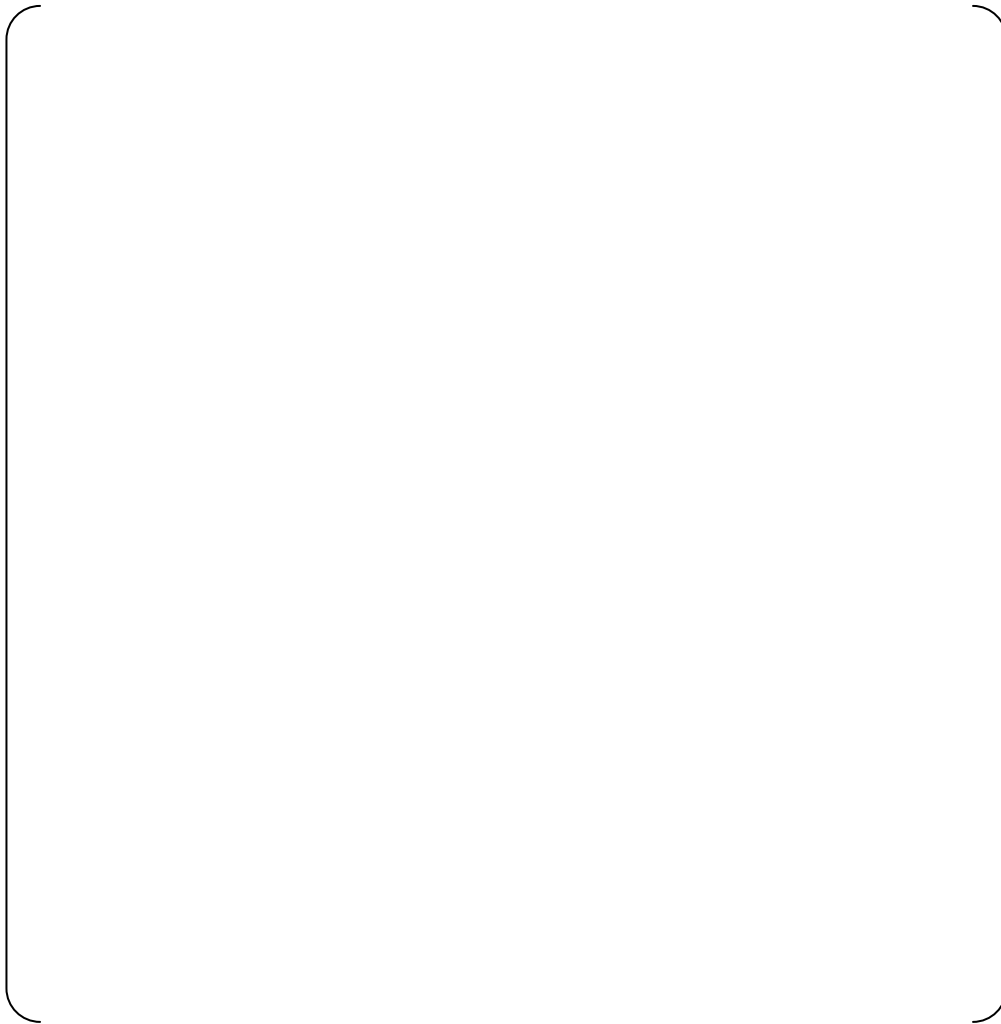


Fig.5.1-1 Thermal Hydraulic Analysis for the Unit-2 and Unit-3 SGs

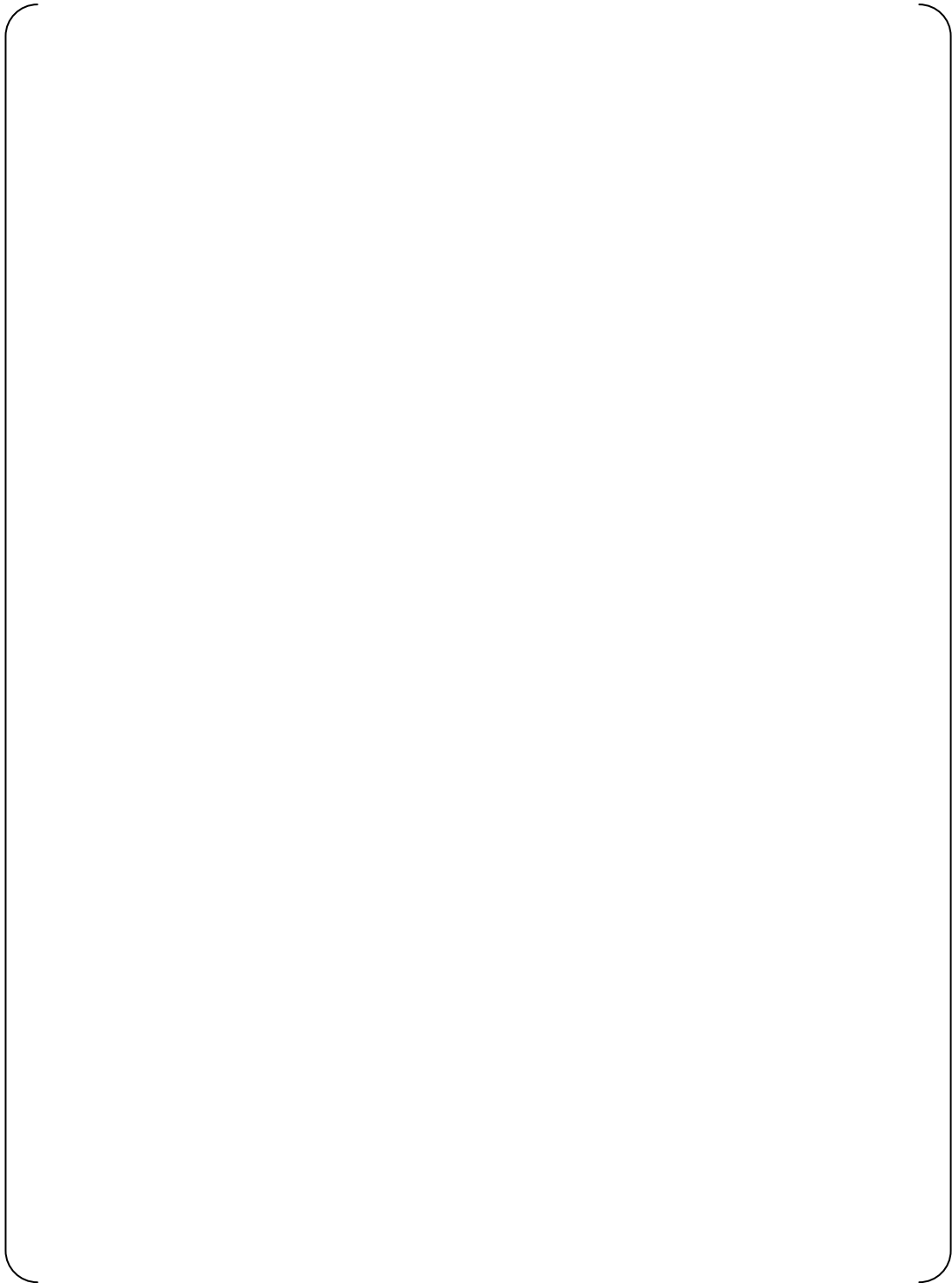


Fig.5.1-2 Correlation between Type 1 Wear (TTW) and Void Fraction (Steam Quality)



Fig.5.1-3 Correlation between Type 1 Wear (TTW) and Flow Velocity

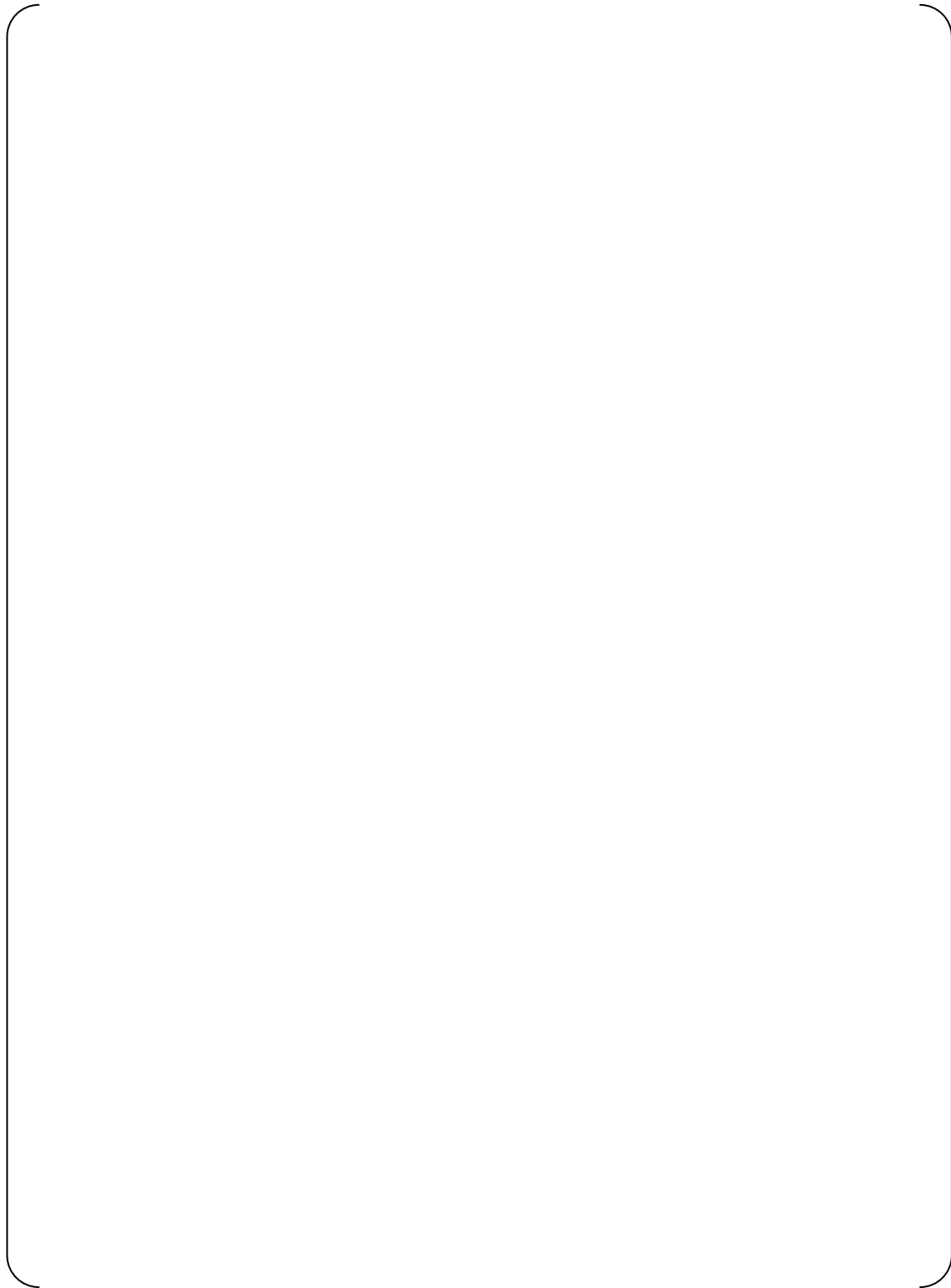


Fig.5.1-4 Correlation between Type 2 Wear (AVB wear) and Void Fraction (Steam Quality)



Fig.5.1-5 Correlation between Type 2 Wear (AVB Wear) and Flow Velocity



5.2 Evaluation of U-bend Supports Condition

5.2.1. Out-of-Plane Direction Support

The SONGS SG tube bundles were designed for out-of-plane U-bend support only with “zero” gaps in the hot condition. Based on visual inspections, the tube-to-AVB gaps in cold condition were as could be expected, i.e., most likely meeting the design premise of “zero gap” in the hot condition.

The recent tube bundle deformation analysis (refer to Appendix-8), which takes into account the tube and AVB dimensional fabrication tolerance dispersion, indicates that the contact forces between the tubes and AVBs produce the friction forces which prevent the distortion of the AVB structure assembly and the dynamic pressure during operation does not increase the tube-to-AVB gaps (see Fig.5.7-3 and Fig.5.7-4 of Appendix-8 for details).

Therefore, MHI has concluded that U-bend support in the out-of-plane direction is adequate.

5.2.2. In-Plane Direction Support

By design, U-bend support in the in-plane direction was not provided for the SONGS SGs. In the design stage, MHI considered that the tube U-bend support in the out-of-plane direction designed for “zero” tube-to-AVB gap in hot condition was sufficient to prevent the tube from becoming fluid-elastic unstable during operation based on the MHI experiences and contemporary practice as described in Section 2.2.

Secondary side thermal-hydraulic conditions in the SONGS SGs during operation appear to be such that the effective fluid flow velocities are higher than the critical velocities in the U-bend in-plane direction for several tubes in a particular region of the tube bundle where the void fraction is very high as described in Section 5.1.

MHI concludes that under the secondary thermal-hydraulic conditions such as in the SONGS SGs, certain tube-to-AVB minimum contact force is required to prevent tubes from vibrating in the in-plane direction and eventually becoming fluid-elastic unstable. Furthermore, MHI concludes that the tube and AVB fabrication dimensional tolerance dispersion results in contact forces between the tubes and AVBs, however, these forces are not sufficient to provide friction forces ample to prevent in-plane motion of the tubes (See reference 10 for details).



5.2.3. Differences between Unit-2 and Unit-3

According to the manufacturing dimensional tolerance analysis (refer to Appendix-4 and Appendix-9 for details), the average contact force in the Unit-3 SGs was found to be smaller than the average contact force in the Unit-2 SGs. Consequently, the contact forces caused by the manufacturing dimensional variations in the Unit-2 SGs are more than two times larger than in the Unit-3 SGs, which is consistent with the tolerance analysis results shown in Fig. 5.2.1. Therefore, it is concluded that the contact forces of Unit-3 were more likely to be insufficient to prevent the in-plane motion of tubes and the Unit-3 SGs were more susceptible to in-plane tube vibration.

9

9

The difference in the contact forces between the Unit-2 and Unit-3 SGs was caused by the manufacturing dimensional tolerance variations, mainly due to improvement of AVB dimensional control. For the Unit-3 AVBs, a [] pressing force was used for the AVB nose portion after bending in order to control the twist and flatness of the AVB more precisely, while [] pressing force was used for the Unit-2 AVBs. Because the manufacturing dimensional variations of the Unit-2 SGs are larger than those of the Unit-3 SGs (AVB twist at AVB nose portion of Unit-2 is larger than that of Unit-3), the tube-to-AVB contact forces of the Unit-2 SGs are greater than those in the Unit-3 SGs, especially at the AVB nose locations, which is evidenced by more ding signals in the Unit-2 SGs than in the Unit-3 SGs.

9

9

A comparison of the Unit-2 and Unit-3 materials, fabrication processes and inspections that might have had an impact on the condition of the U-bend supports is summarized in Table 5.2-1 (refer to Appendix-4 for details) and the evaluations for the factors other than the difference in the AVB pressing forces are summarized below.

(i) Number of Rotations due to Divider Plate Repair

The Unit-3 SGs underwent [] more rotations than the Unit-2 SGs due to the divider plate repair. However, the change in the tube support condition between the Unit-3 and Unit-2 SGs due to the difference in number of rotations was found to be negligibly small (refer to Appendix-5 for details).

(ii) Number of Hydrostatic Tests

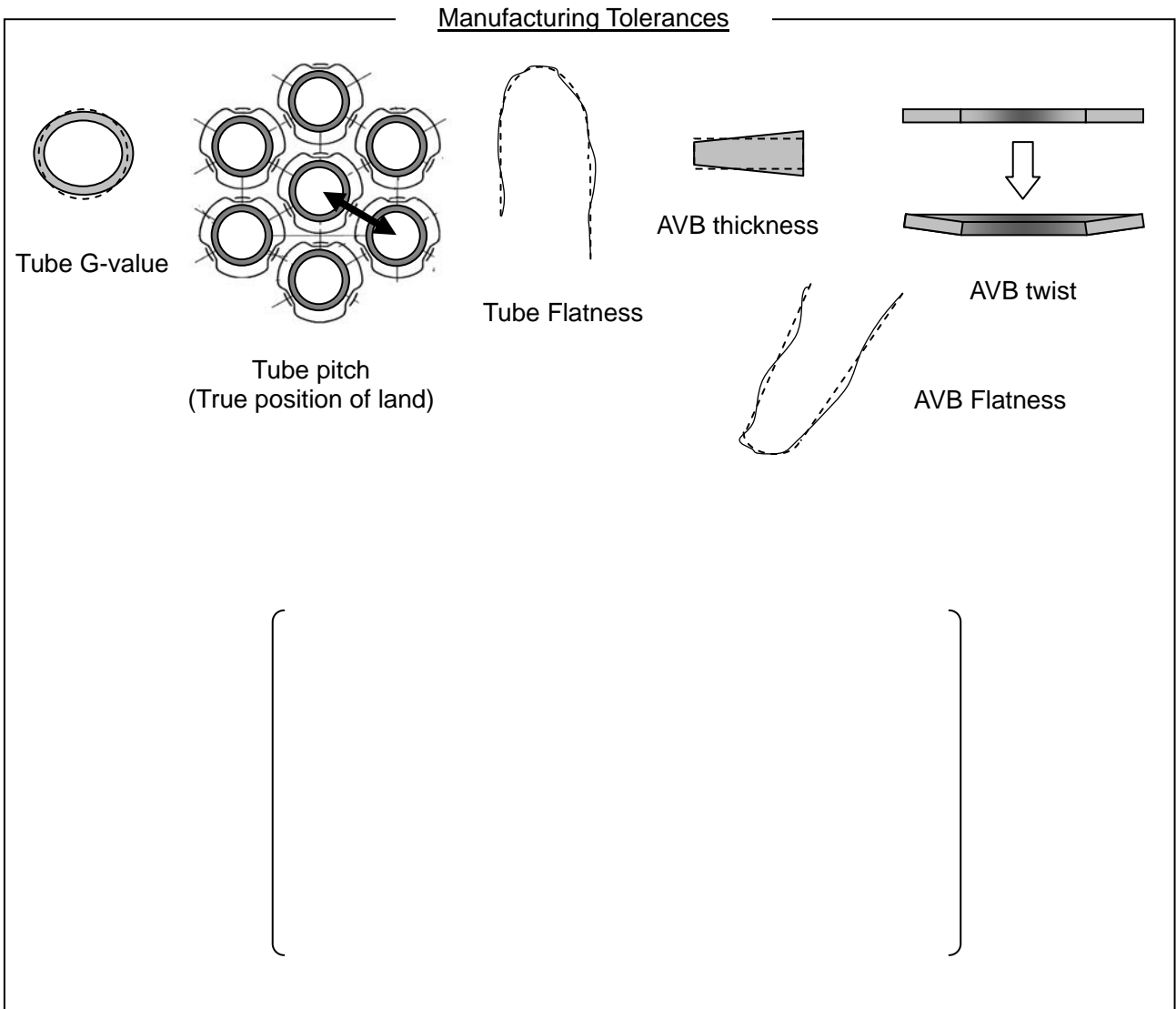
Primary side hydrostatic tests were performed three times for the 3A SG and two times for the 3B SG, compared to only one time for both 2A and 2B SGs. However, the change in the tube support condition between the Unit-3 and Unit-2 SGs due to the number of hydrostatic tests was found to be negligibly small (refer to Appendix-5 and 14 for details).



(iii) Dimensional Control of Tubes and AVBs

The standard deviation of the AVB thickness, the tube outer diameter (G-value), and the number of adjustments to the tube bending radius was smaller in the Unit-3 SGs than in the Unit-2 SGs. Furthermore, the gaps between the outermost tubes and the AVBs are more uniform in the Unit-3 SGs than in the Unit-2 SGs. These findings indicate that the tube and AVB dimensions of the Unit-3 SGs are more uniform, and hence the reaction forces from tubes and AVBs are smaller than the Unit-2 SGs. Consequently, the contact forces caused by the manufacturing dimensional variations in the Unit-3 SGs are smaller than in the Unit-2 SGs, which is consistent with the tolerance analysis results shown in Fig.5.2-1.

The average of all gaps between the tubes in the outermost rows and AVBs along the retaining bars is smaller in the Unit-3 SGs than in the Unit-2 SGs. However, the gaps between the outer-most tubes and AVBs in the center columns do not have significant effect on the contact forces in the inside of the tube bundle and the main reason for this difference is the fact that the gaps in the outer-most rows of the peripheral columns in the Unit-2 SGs were larger than those in the Unit-3 SGs. The average of the gaps between the outermost tubes and AVBs in the center 60 columns (Column 59 to 119), where the wear indications were found, were essentially the same in the Unit-2 and Unit-3 SGs as shown in Fig.5.2-2. Therefore, the difference of the contact forces between Unit-2 and Unit-3 is caused by the difference of the manufacturing dimensional tolerances other than the outer-most tube-to-AVB gaps.



Contact forces of Unit-2 are more than 2 times larger than those of Unit-3.



Fig.5.2-1 Contact Force Simulation with Manufacturing Tolerances



Table 5.2-1 Manufacturing Differences Between Unit-2 and Unit-3 SGs

Item	Unit-2	Unit-3	Reason / Effect
Rotations			Due to divider plate repair
Hydrostatic Test			Due to seal-weld leakage and divider plate repair
AVB pressing force			AVB twist and flatness of Unit-3 SGs are controlled more precisely
Standard Deviation of Tube Outer Diameter (G-value ^{*1}) mils (mm)			Unit-3 has smaller standard deviation
Adjustment of Tube Bending Radius			Unit-3 had fewer adjustments of tube bending radii
Average Gap between Outermost Tube and AVB ^{*2} mils (mm)			Unit-3 has smaller gaps. Most of the difference is in the peripheral columns not the central columns (where the wear indications are found).

Note)

*1: G-values were measured by micrometer.

*2: Outermost peripheral gaps near the retaining bar-to-AVB welds were measured by feeler gages.



Fig.5.2-2 Comparison of the outer-most tube-to-AVB gaps in the center 60 columns



6. Tube Wear Causes

In general, there are 3 types of tube bundle vibration phenomena occurring in fluid environment (see Fig.6-1):

(1) Vortex Shedding Vibration (vibration due to Karman vortex)

In a single-phase flow when fluid is flowing perpendicularly to a tube, a pair of vortices, known as Karman vortices, will form periodically on the right and left side, and downstream of the tube. When the vortices move away from the tube surface periodically, the reaction forces created by them will cause the tube to vibrate. This phenomenon is called vortex shedding vibration.

The fluid flow across the SG tubes in the region of interest (U-bend region) is a two-phase flow with high void fraction (> 0.1). Therefore, no Karman vortices are expected to form periodically downstream of the tube and no vortex shedding induced tube vibration is expected to occur. Empirical data confirms that vortex shedding vibration typically does not occur in two-phase flow environments where the void fraction is greater than 15% (see Reference 1).

(2) Random Vibration

Random vibration is a phenomenon where the tubes vibrate due to forces created by turbulent flow as a result of fluid velocity and density fluctuations. Vibration amplitudes due to random vibration are generally small (smaller than those due to tube fluid-elastic instability).

(3) Fluid Elastic Instability (FEI)

FEI is a phenomenon where the tubes vibrate with increasingly larger amplitudes due to the fluid effective flow velocity exceeding its specific limit (critical velocity) for a given tube and its supporting conditions and a given thermal hydraulic environment. This occurs when the amount of energy imparted on the tube by the fluid is greater than the amount of energy that the tube can dissipate back to the fluid and to the supports.

In the case when vibration occurs in a two-phase flow such as in the SG tube U-bend region, there is a possibility that it is either due to random vibration or FEI. Based upon the abovementioned study of vibration phenomena, the mechanism of each tube wear type is evaluated next based on the fault tree evaluations shown in Fig.6-2 and Fig.6-3.





6.1 Type 1 Wear (TTW)

Based on the results from the rotating pancake coil ECT inspections and visual inspections, MHI concluded that the Type 1 wear (TTW) occurred due to tube in-plane motion (vibration) with a displacement (amplitude) greater than the distance between the tubes in the adjacent rows, resulting in tube-to-tube contact. Tube in-plane motion might have been caused by tube random vibration or FEI. Because the amplitude of random vibration is generally very small, the mechanistic cause of this type of wear is typically tube FEI (refer to Fig.6-1 for the difference between random vibration and FEI).

U-tube out-of-plane direction is more susceptible to flow-induced excitation than the in-plane direction due to lower U-bend natural frequency in the out-of-plane direction. U-tube FEI in the in-plane direction has never been observed in the U-tube SGs before its occurrence in the SONGS SGs. However, recent academic studies (Reference 2 and 3) report that FEI may also occur in the in-plane direction, if tube motion in the in-plane direction is possible (no tube in-plane supports or low tube contact forces with the out-of-plane supports, as concluded by MHI).

9

As described in Section 5.1, the void fraction (steam quality) and the flow velocity are high in the SONGS SGs which means that their tubes are generally more susceptible to vibration. Furthermore, the average tube-to-AVB contact force in the Unit-3 SGs is concluded to be smaller than in the Unit-2 SGs, as described in Section 5.2, which makes the Unit-3 tubes to be even more susceptible to vibration and likely to FEI. Therefore, MHI concludes that in-plane tube motion which caused the Type 1 wear was due to tube FEI. The wear at the AVBs and at TSPs on some of the tubes with the Type 1 wear is an additional effect of these tubes being unstable (refer to Fig.6.1-1).

9

6.2 Type 2 Wear (AVB wear)

Based on the visual inspections, MHI concluded that the Type 2 wear occurred due to tube vibration which caused the tubes to wear against the AVBs at the tube-to-AVB intersections. Tube wear at AVB intersections might have been caused by tube random vibration or FEI. However, because most likely there were no significant gaps between the tubes and AVBs during operation (see Section 5.2.1), the occurrence of tube motion due to FEI is very unlikely (refer to Appendix-3). As described in Section 5.1, the SONGS SG tubes are susceptible to vibration (high void fractions and high flow velocities). Therefore, MHI concludes that the tube

9

9



wear at AVB intersections, which caused the Type 2 wear, was due to the random vibration (refer to Fig.6.2-1).



The Type 1 and Type 2 wear are simulated in the tube wear analysis as shown in Appendix-10.



6.3 Type 3 Wear (TSP wear)

The tubes with the Type 3 wear are located mostly near the TSP flow slots and at the periphery of the tube bundle where the velocities of cross-flow are high (refer Fig.6.3-1). Tube vibration in cross-flow may be caused by tube random vibration or FEI. However, the size of the gap between the TSP tube hole land surface and the tube is limited (design size is []). Thus, the occurrence of tube FEI is unlikely. Therefore, MHI concludes that the Type 3 wear is caused by cross-flow induced random vibration in the region where secondary fluid cross-flow velocities are high (refer Fig.6.3-2). The results of the FEI and random vibration analysis are shown in Appendix-2.

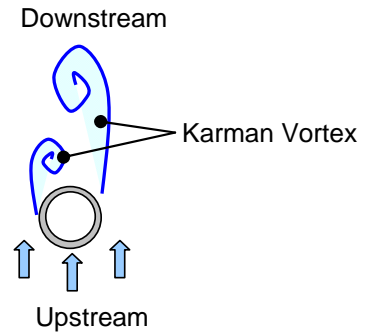
6.4 Type 4 Wear (RB wear)

The tubes with the Type 4 wear have no indications of TTW or AVB wear, or TSP wear, which suggests that it is caused by only the retainer bars vibrating. SONGS SGs have two types of retainer bars, []mm ([]) in diameter and []mm ([]) in diameter. Tube wear was found on the tubes adjacent to the retainer bars, but only at the smaller diameter retainer bars. The retainer bars with the smaller diameter have also a relatively long span as compared with the other SGs fabricated by MHI, which means that the natural frequency of these retainer bars is lower and thus they are more likely to vibrate. Therefore, MHI concludes that the Type 4 wear is caused by random vibration of the retainer bars induced by the secondary fluid exiting the tube bundle (see Reference 4 for details).



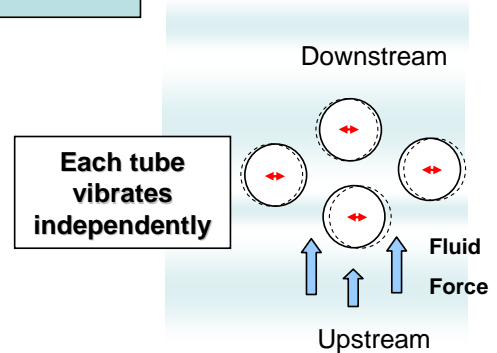
✓ Vortex Shedding Vibration (Vibration due to Karman vortex)

➤ In a single-phase flow when fluid is flowing perpendicularly to a tube, a pair of vortices, known as Karman vortices, will form periodically on the right and left side, and downstream of the tube. When the vortices move away from the tube surface periodically, the reaction forces created by them will cause the tube to vibrate. This phenomenon is called vortex shedding vibration.



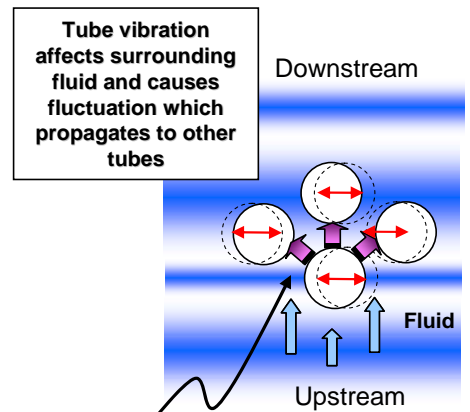
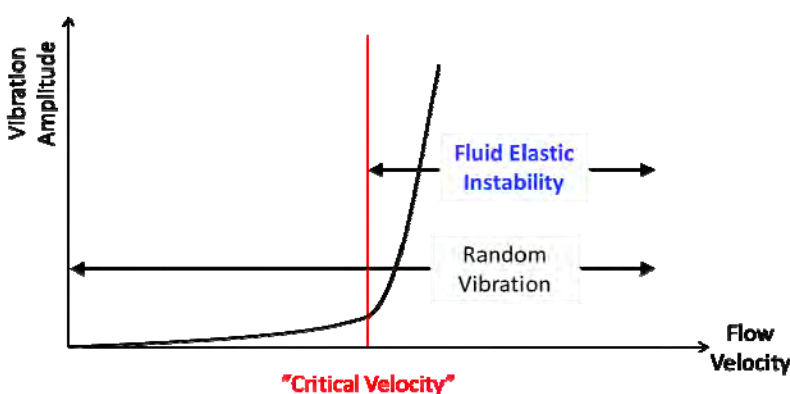
✓ Random Vibration

➤ Random vibration is a phenomenon where the tubes vibrate due to forces created by turbulent flow as a result of fluid velocity and density fluctuations. Vibration amplitudes due to random vibration are generally small (smaller than those due to tube fluid-elastic instability).



✓ Fluid Elastic Instability (FEI)

➤ FEI is a phenomenon where the tubes vibrate with increasingly larger amplitudes due to the fluid effective flow velocity exceeding its specific limit



Coupled Vibration due to tube motion (tube motion affects surrounding fluid flow and leads to flow fluctuation. When tube motion and fluid force fluctuate at the right time, tubes vibrate vigorously)

Fig.6-1 Flow Induced Tube Bundle Vibration



Event	Part	Assumed cause	Evaluation	Conclusion
Wear of tubes for Unit-3	U-bend region	Fluid Elastic Instability (FEI)	Progress of wear in very short period can be caused by FEI.	Yes
		Random vibration	Vibration amplitudes due to random vibration are generally small and not case tube-to-tube wear.	No
		Karman vortex shedding	Karman vortex shedding does not occur in two-phase flow environments.	No
		FEI	Because most likely there were no significant tube-to-AVB gaps during operation, the occurrence of tube out-of-plane FEI is very unlikely.	No
		Random vibration	SONGS SG tubes are susceptible to random vibration due to high void fractions and high flow velocities.	Yes
		Karman vortex shedding	(same as tube-to-tube wear)	No
		vibration of tube	The tubes with retainner bar wear haveNo indications of TTW or AVB wear, or TSP wear, which suggests that it is caused by only the retainner bars vibrating.	No
		vibration of retainner bar	Retainner bars have a relatively small diameter and long span as compared with the other SGs fabricated by MHI, which means that the natural frequency of these retainner bars is lower and thus they are more likely to vibrate.	Yes
		FEI	The size of the gap between the TSP tube hole land surface and the tube is limited. Thus, the occurrence of tube FEI is unlikely.	No
		Random vibration	TSP wear can be caused by the cross-flow induced random vibration in the region where secondary fluid cross-flow velocities are high.	Yes
		Karman vortex shedding	(same as tube-to-tube wear)	No

Fig.6-2 Fault Tree Evaluation for the Causes of Wear



Event	Factor	Investigation	Evaluation	Conclusion	
FEI and Random Vibration	Thermal hydraulic condition	Higher void fraction at U-bend region	Thermal hydraulic analyses	Structures in a two-phase flow field have lower resistance to vibration when a void fraction or steam quality is high. (See Section 5.1 for details.)	Yes
	Structural condition	AVB insertion depth	Confirmation of AVB insertion depth by bobbin ECT signals	It is confirmed that AVB insertion depth is not changed from the design condition for the representative columns (center and edge). (See Section Appendix-4 for details.)	No
		Contact force of AVB to tube	Tube diameter ovality (G value)	Tubes used for Unit-2 have larger variation (standard deviation) of tube G value than those for Unit-3. It is assumed that the contact force of AVB to tube for Unit-2 is relatively large compared with Unit-3. (See Section 5.2.3 and Appendix-9 for details.)	Yes
	Increase of potential of tube vibration	Rotation, handling, etc. of RSGs during manufacturing	AVB twist and thickness	AVB twist and thickness of Unit-2 are larger than those of Unit-3 because of the difference of AVB pressing load. (See Section 5.2.3 and Appendix-9 for details.)	Yes
			ECT data (Ding signals)	The tube-to-AVB contact forces of the Unit-2 SGs are greater than those in the Unit-3 SGs, especially at the AVB nose locations, which is evidenced by more ding signals in the Unit-2 SGs than in the Unit-3 SGs. (See Section 5.2.3 and Appendix-9 for details.)	Yes
			Research of history and records of manufacturing at Kobe shop and deformation analyses of tube bundle	The Unit-3 SGs underwent [more rotations than the Unit-2 SGs due to the divider plate repair. However, the change in the tube support condition between the Unit-3 and Unit-2 SGs due to the difference in number of rotations was found to be negligibly small. (See Section 5.2.3 and Appendix-5 for details.)	No
	Tube-to-AVB gap	Rotation, handling, etc. of RSGs during manufacturing	Research of history and records of manufacturing at Kobe shop and deformation analyses of tube bundle	The Unit-3 SGs underwent [more rotations than the Unit-2 SGs due to the divider plate repair. However, the change in the tube support condition between the Unit-3 and Unit-2 SGs due to the difference in number of rotations was found to be negligibly small. (See Section 5.2.3 and Appendix-5 for details.)	No
			Visual inspection of inside of U-bend region	There were no significant gaps between the AVBs and tubes which might have contributed to excessive tube vibration because the AVBs appears to be virtually in contact with tubes. (See Section 4.2 for details.)	No
	Deformation of U-bend region during operation	Dynamic pressure of secondary fluid and difference of thermal expansion	Deformation analyses of tube bundles by taking into account of > Dynamic pressure of secondary fluid > Difference of thermal expansion	The tube bundle deformation analysis indicates that the contact forces between the tubes and AVBs produce the friction forces which prevent the distortion of the AVB structure assembly and the dynamic pressure during operation does not increase the tube-to-AVB gaps. (See Section 5.2.1 and Appendix-8 for details.)	No

Fig.6-3 Fault Tree Evaluation for the Causes of FEI and Random Vibration





Characteristics of SONGS RSG

【Thermal Hydraulics】

- ✓ Design with High Steam Quality in U-Bend(max [])

【AVB Structure】

- ✓ Tube between 2 flat AVBs
 - AVB Design Assumes Out-of Plane Vibration
 - Since out-of-plane FEI is more likely to happen compared to in-plane FEI, AVBs are placed at the sides of tube to preven out-of-plane vibration
- ✓ 6 V-Shaped AVBs (12support points)
 - Number of AVB Support Points are designed by FEI Evaluation based on ASME Sec.III
 - (Out-of-Plane FEI will not occur even if one of supports is inactive as design basis)
- ✓ Designed and fabricated for "Zero" Gap between Tube and AVB in hot condition

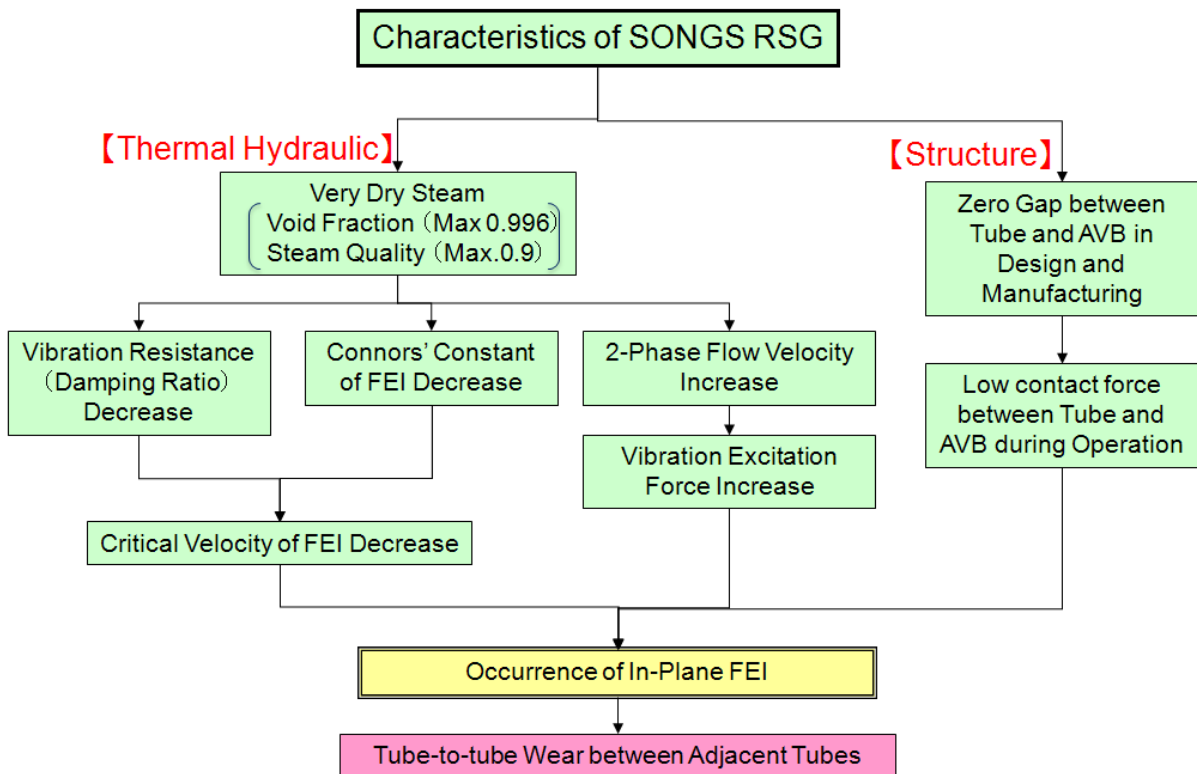
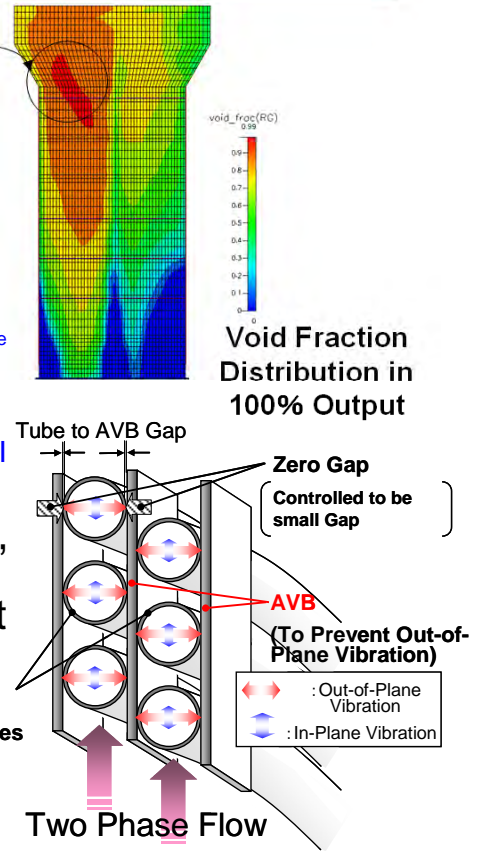


Fig.6.1-1 Type 1 Wear (TTW) Mechanism

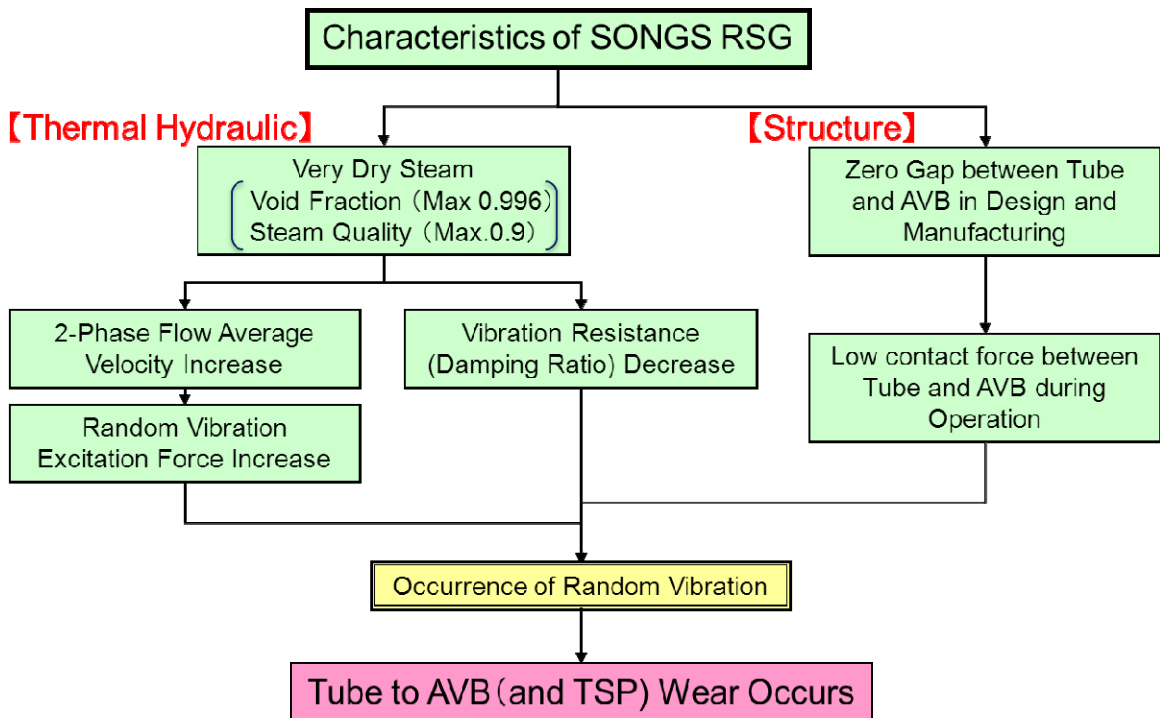
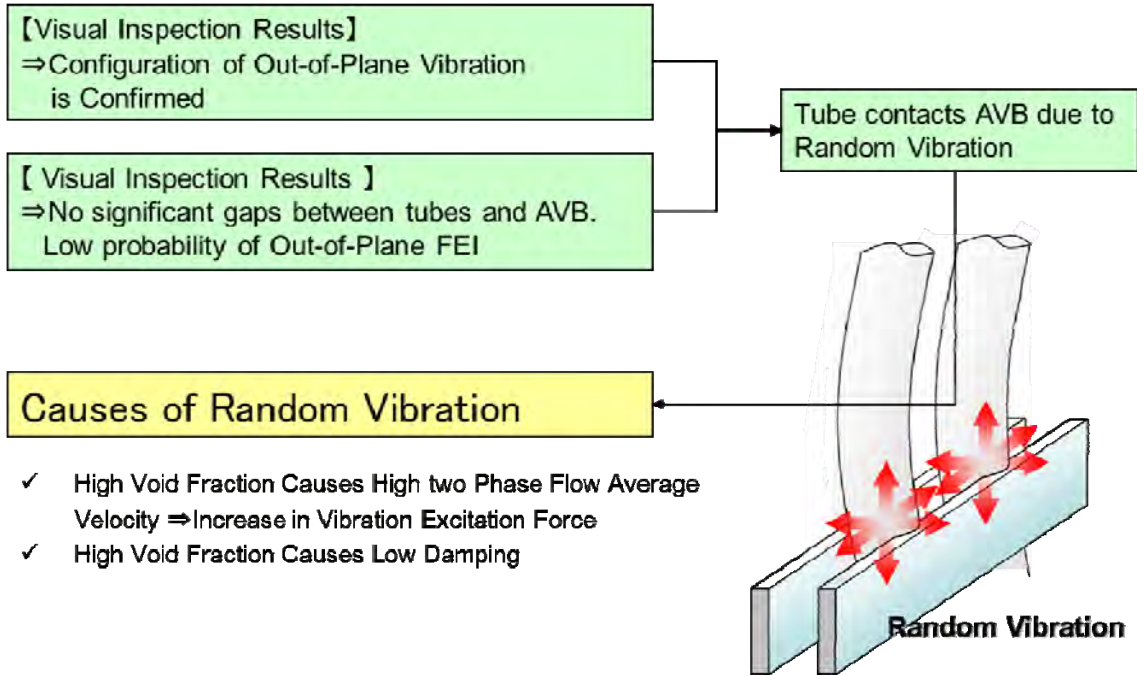


Fig.6.2-1 Type 2 Wear (AVB wear) Mechanism

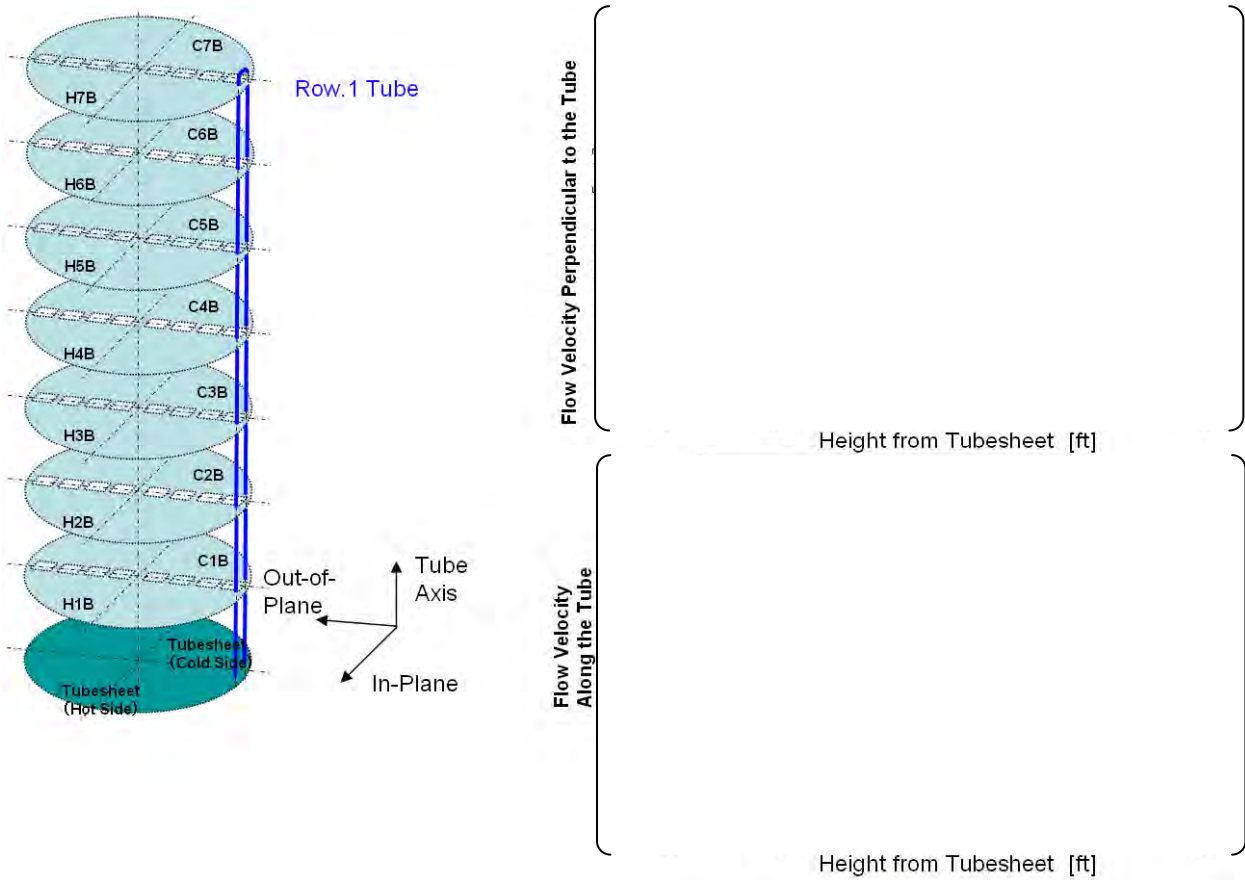


Fig.6.3-1 Flow Velocity Distribution at TSPs

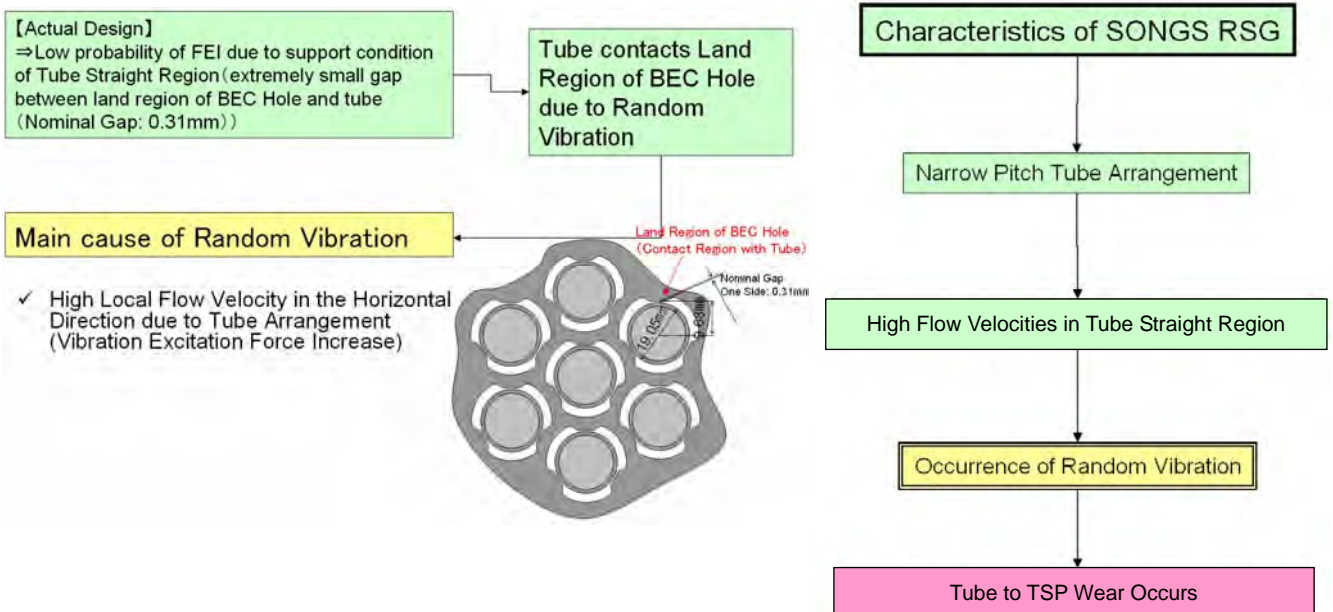


Fig.6.3-2 Type 3 Wear (TSP wear) Mechanism

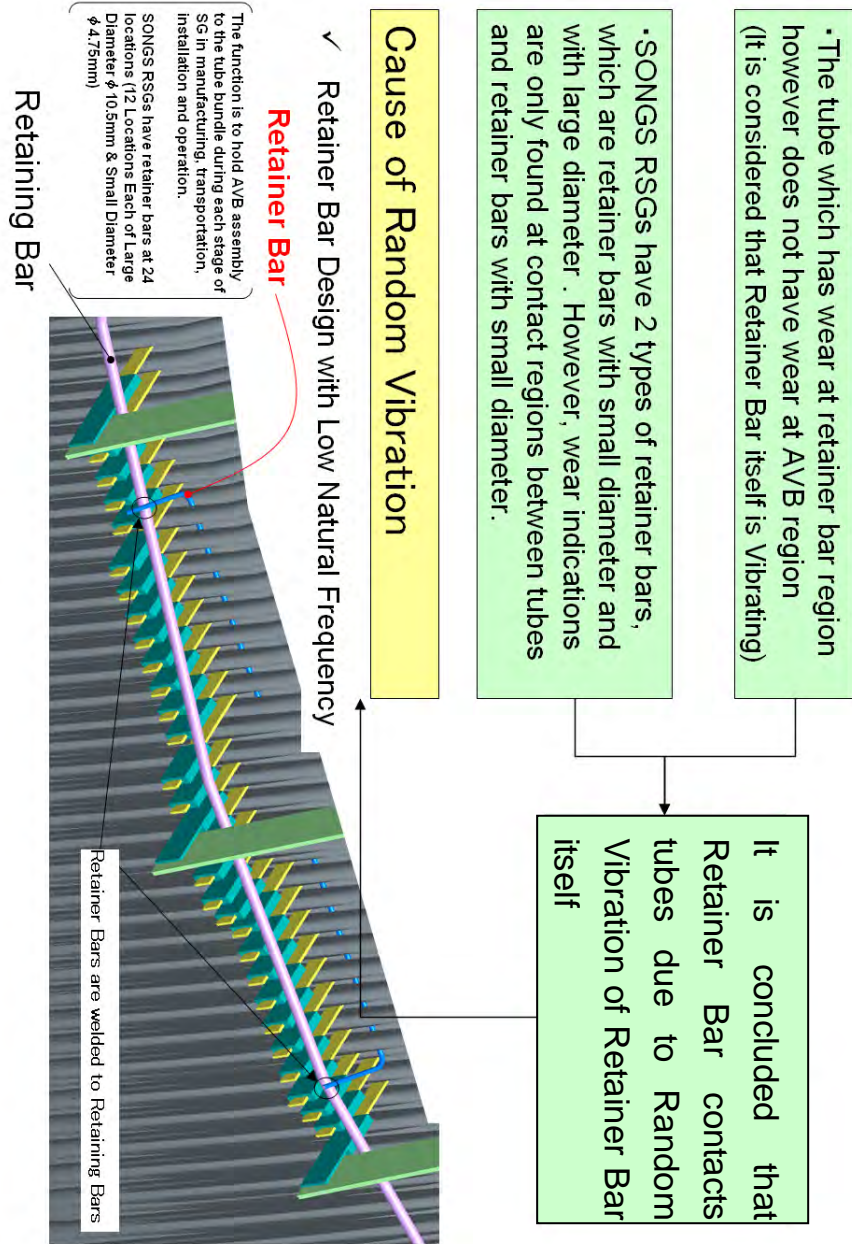


Fig.6.4-1 Type 4 Wear (RB wear) Mechanism



7. Conclusions

In the Unit-3 SGs, the following types of wear were identified:

- (i) Type 1 (TTW)
- (ii) Type 2 (AVB wear)
- (iii) Type 3 (TSP wear)
- (iv) Type 4 (RB wear)

The conclusions regarding mechanistic causes of tube wear are as follows:

- The concluded mechanistic cause of the Type 1 wear is tube FEI in the tube bundle U-bend region, which is caused by a combination of the SG secondary side thermal-hydraulic conditions (high fluid velocity and high void fraction) and inactive AVB support conditions in the in-plane direction.
- The concluded mechanistic cause of the Type 2 and 3 wear is random vibration of the tubes. The Type 2 wear is caused by the tube motion due to high void fractions and high flow velocities. The Type 3 wear is caused by high velocity flow across the straight leg sections of the tubes.
- The concluded mechanistic cause of the Type 4 wear type is vibration of the retainer bar, which is the same as in the Unit-2 SGs and is addressed in Reference 4.

The tube-to-AVB contact forces of Unit-3 were more likely to be insufficient to prevent the in-plane motion of tubes and the Unit-3 SGs were more susceptible to in-plane tube vibration than Unit-2 SGs because the average contact force in the Unit-3 SGs was found to be smaller than the average contact force in the Unit-2 SGs. The difference in the contact forces between the Unit-2 and Unit-3 SGs was caused by the manufacturing dimensional tolerance variations, mainly due to improvement of AVB dimensional control.



8. Countermeasures for Return to Service

The following short term actions should be taken in support of Unit 3 return to service for a limited period of time (if possible). In order to restore SONGS SGs' conformance to the CDS and make them capable of operating without time or reactor power level restrictions, more complex and involving actions (repairs) will be mandatory.

8.1 Tube Plugging

Tubes which exhibit a potential for losing their integrity during the next operating period due to progressive through-wall wear and/or susceptibility to FEI should be plugged. The number of tubes plugged for each type of tube wear is listed in Table 8.1-1.

8.1.1. Type 1 Wear

All tubes with ECT tube wear indications in the free span section should be plugged regardless of the wear depth. Furthermore, tubes with wear indications at the AVB and TSP locations, which are similar to those on the tubes with the wear indication in the free span section, should be preventatively plugged.

8.1.2. Type 2 Wear and Type 3 Wear

Tubes with wear equal to, or greater than, 35% should be plugged in accordance with Technical Specifications.

8.1.3. Type 4 Wear

Tubes with wear indications adjacent to the retainer bars should be plugged regardless of the wear depth. Furthermore, all tubes that have a possibility to come in contact with the retainer bars should be preventatively plugged.



NOTE:

As of this writing, tube plugging has already been performed in the Unit-2 and Unit-3 SGs, and the number of the tubes for each plugging type is listed in Table 8.1-1 below.

Table 8.1-1 Plugged Tubes

Wear Type/Plugging Type	Steam Generator				Total
	2E088	2E089	3E088	3E089	
Type 1 Wear (with wear indication)		2	161	165	328
Type 1 Wear (preventative plugging)	109	212	164	128	613
Type 2 Wear and Type 3 Wear	4		1		5
Type 4 Wear (with wear indication)	2	4	3	1	10
Type 4 Wear (preventative plugging)	92	90	91	93	366
Total	207	308	420	387	1322
% Tubes Plugged	2.2%	3.2%	4.4%	4.0%	

9

9



8.2 Operating at a Lower Thermal Power

As described in Section 6, the major contributor to the tube wear phenomenon in the SONGS SGs is the secondary side thermal-hydraulic conditions in the tube bundle U-bend region of interest at 100% reactor power. The major parameters making these conditions unfavorable from the tube wear perspective are high secondary fluid flow velocities and high void fractions (steam quality).

In general, decreasing the reactor power level will result in the fluid flow velocities and void fractions being lower, and hence tube margins to FEI being larger. Lowering the plant reactor power level to 70% is sufficient to decrease the fluid flow velocities and void fractions in the tube bundle region where tube wear, especially TTW, occurred during the previous operating period to the point at which the tubes remaining in service are not expected to become fluid elastic unstable, as shown in Fig. 8.2-1 (Details of the secondary side thermal-hydraulic conditions are described in Reference 5).

9

The effects of area plugging and power level reduction were investigated in the case study for their impact on tube stability (Reference 6). The results of this study indicate that the changes in the bundle thermal-hydraulic parameters reduce the stability ratios (increase margins to FEI) of the analyzed tubes slightly, but the ratios are still greater than 1.0 at 100% reactor power and the number of consecutive inactive AVB support points being 6 or more. Because no credit can be taken for a change in the tube support condition, as no modifications to the AVB support structure are possible in the short term, only reduction in power level can produce a beneficial reduction of the stability ratio (increase of margin to FEI) for the tubes remaining in service (not plugged).



Fig.8.2-1 Void Fraction or Steam Quality Distribution of Thermal Power Reduction



9. References

- (1) Journal of Fluids and Structures, "Vibration analysis of shell-and-tube heat exchangers: an overview – Part 1:flow, damping , fluid elastic instability", M.J. Pettigrew, C.E. Taylor., March 2003
- (2) ASME, "Fluidelastic Instability and Work-Rate Measurements of Steam-Generator U-Tubes in Air-Water Cross-Flow", V.P.Janzen, E.G.Hagberg, M.J.Pettigrew, C.E.Taylor. February 2005
- (3) Flow-Induced Vibration,Meskell & Bennett (eds) ISBN 978-0-9548583-4-6, "Study on In-flow Fluid-elastic Instability of Circular Cylinder Arrays"], T.Nakamura, Y.Fujita, T.Oyakawa, Y.NI. July 2012
- (4) MHI report, "Retainer Bar Tube Wear Report", L5-04GA561 the latest revision
- (5) MHI report, "Case study of the input parameters and tube plugging impact on internal SG thermal hydraulic parameters", L5-04GA566 the latest revision
- (6) MHI report, "Evaluation of Stability Ratio for Return to Service", L5-04GA567 the latest revision
- (7) JSME, S016-2002, Guideline for Fluid-elastic Vibration Evaluation of U-bend Tube in SG, March 2002
- (8) MHI report, "Screening Criteria for Susceptibility to In-Plane Tube Motion", L5-04GA571 the latest revision
- (9) SCE project letter, "L5-04GA564, REV. 6, TUBE WEAR OF UNIT-3 RSG TECHNICAL EVALUATION REPORT", RSG-SCE/MHI-12-5757, August 2012
- (10) MHI report, "Analytical Evaluations for Operating Assessment", L5-04GA585 the latest revision
- (11) SCE project letter, "Updated ECT Data for Input to Return to Service and Repair Design Documents", RSG-SCE/MHI-12-5749, August 2012



Appendix-1
ECT Data Evaluation of tubes with wear around Retainer Bar



1. Purpose

This appendix provides the ECT data evaluation of tubes with wear around the retainer bars in the two Unit-3 SGs.

2. Result

Table 2-1 shows tube wear identified at the intersections with AVB assembly retainer bars for Unit-3.

Table 2-1. Retainer Bar Tube Wear

SG	Row	Col	Location	Side	+Point depth	Circ extent	Axial extent
3B	117	137	B10 -0.42"	Out	44%	0.47"	0.35"
3B	125	49	B11 -0.50"	Out	28%	0.29"	0.27"
3B	128	126	B10 -0.44"	Out	41%	0.44"	0.32"
3A	124	130	B11 -0.47"	Out	46%	0.45"	0.27"

Note: The retainer bar is captured between two tube rows in each column. "Out" describes the tube with the larger bend radius.

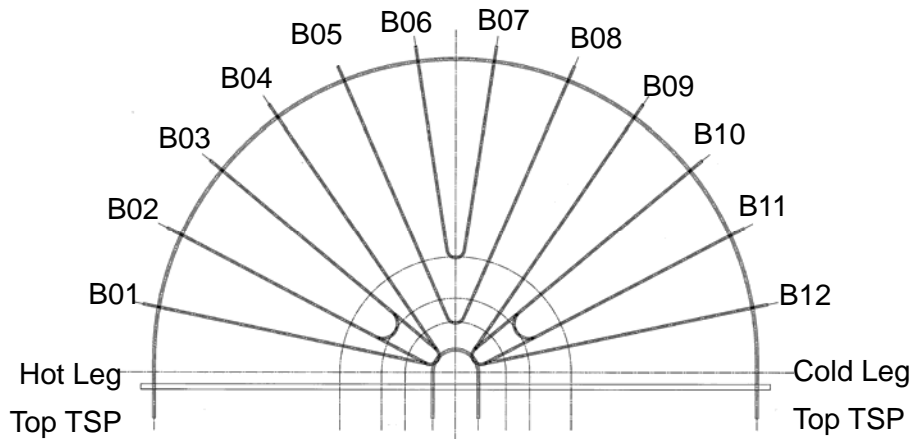


Fig.2-1 Retaining Bar and Retainer Bar Locations



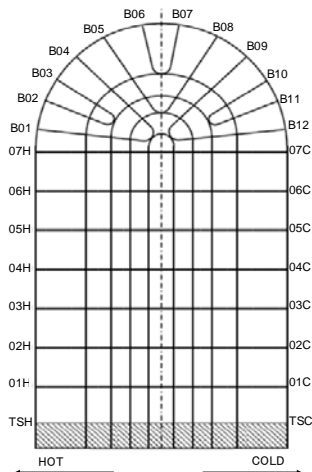
Figures 2-2 and 2-3 provide an overview of the indication locations. Figure 2-4 shows a close-up view of the location with the deepest wear mark.

For these four tubes, it is confirmed by bobbin ECT data that no indication is detected at AVB and TSP contact points except the intersections with retainer bars, as shown in Table 2-2. This shows that the tube wear was not caused by the vibration of the tube but by the vibration of the retainer bar.

Table 2-2 Bobbin ECT results for tubes with retainer bar wear

SG	Row	Column	B01	B02	B03	B04	B05	B06	B07	B08	B09	B10	B11	B12
3B	117	137	-	-	-	-	-	-	-	-	-	W	-	-
	125	49	-	-	-	-	-	-	-	-	-	-	W	-
	128	126	-	-	-	-	-	-	-	-	-	W	-	-
3A	124	130	-	-	-	-	-	-	-	-	-	-	W	-

SG	Row	Column	TSH	01H	02H	03H	04H	05H	06H	07H	07C	06C	05C	04C	03C	02C	01C	TSC
3B	117	137	-	-	-	-	-	-	-	-	-	-	-	-	-	-	-	-
	125	49	-	-	-	-	-	-	-	-	-	-	-	-	-	-	-	-
	128	126	-	-	-	-	-	-	-	-	-	-	-	-	-	-	-	-
3A	124	130	-	-	-	-	-	-	-	-	-	-	-	-	-	-	-	-



- : No wear
W : Wear at retainer bar location

3. Reference

- ECT Data for Input to Return to Service and Repair Design Documents (RSG-SCE/MHI-12-5688), e-mail from SCEs Mr. Calhoun on March 23, 2012 (JST)

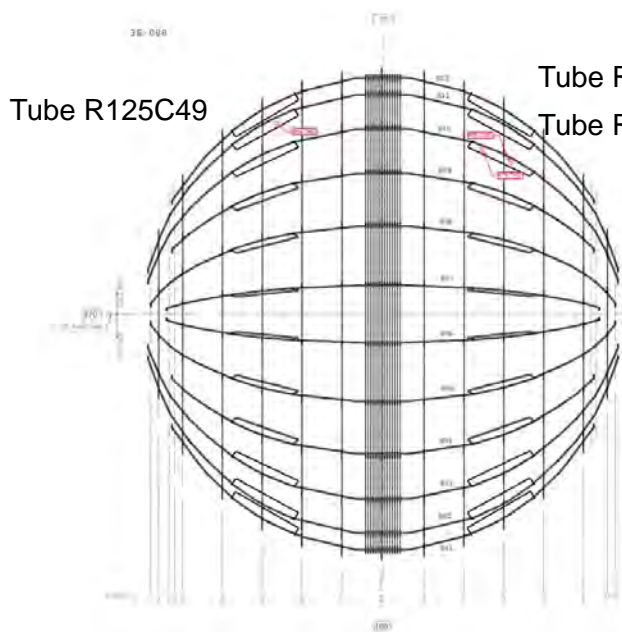


Fig.2-2 Indication locations for Unit-3B

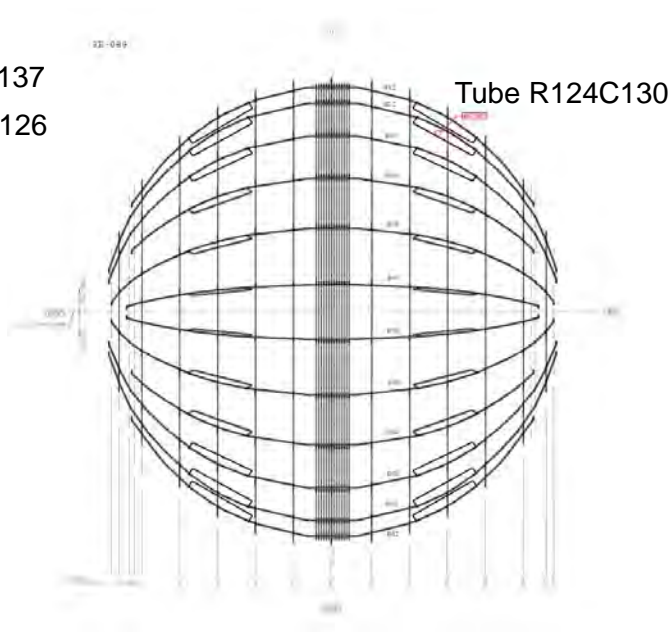


Fig.2-3 Indication location for Unit-3A

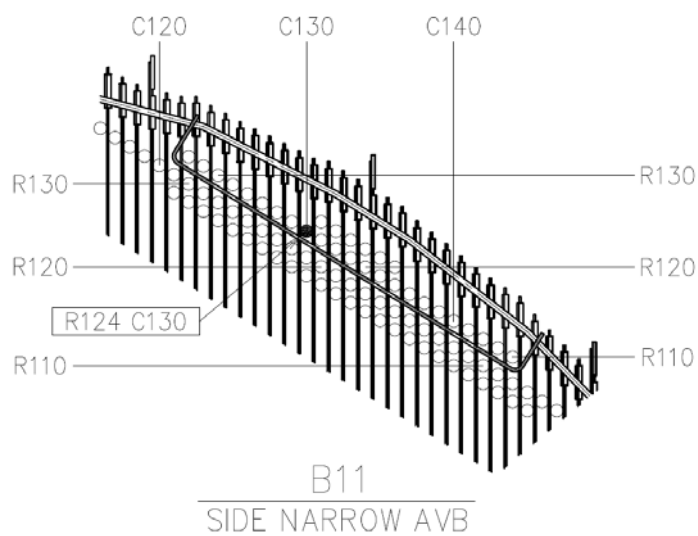


Fig.2-4 Location of 46% Wear (for Unit-3A, R124C130, AVB11 Retainer Bar)



Appendix-2
FEI Evaluation of Tube Straight Portion for Unit-2/3



1. Purpose

Tube-to-tube support plate (TSP) wears at tube straight portions are detected in SONGS-2/3 RSGs. It is possible that the cause of the wears is the fluid elastic instability (FEI) mechanism. The purpose of study provided in appendix-2 is to evaluate the possibility of FEI of the tube straight portion, through the thermal and hydraulic calculations by ATHOS/SGAP computer code and vibration calculations by FIVATS computer code (The evaluation of random excitation mechanism is provided in Appendix-2A).

2. Conclusion

In order to evaluate the possibility of FEI in the tube straight region the stability ratios defined in Section 6 for representative tubes are calculated with assuming TSPs effective supports because the gap between the tube and TSP is enough small. The analysis predicts that FEI of tube straight portions is not possible in case that all TSPs supports are effective. Thus, MHI concludes that the cause of tube-to-TSP wears in SONGS-2/3 RSGs is not due to FEI in the straight portion of tube due to the cross flow.

Table 2-1 Stability ratio calculations summary

Tube address	Stability ratio ^(*)			
	Conservative case ^(**)		Best estimated case ^(***)	
Row 1 Column 1	()	Hot side	()	Hot side
Row 1 Column 13	()	Hot side	()	Hot side
Row 1 Column 89	()	Hot side	()	Hot side
Row 53 Column 57	()	Hot side	()	Hot side
Row 80 Column 74	()	Cold side	()	Hot side
Row 101 Column 29	()	Hot side	()	Hot side
Row 137 Column 77	()	Cold side	()	Hot side

(*) Stability ratio over 1.0 implies a probability of FEI

(**) Critical factor (K=2.4) and damping ratio (h=1.5%) values are used.

(***) The critical factor depending on the volume flow rate quality (β) is used. The total damping which consist of the structural damping, two-phase damping, and squeeze film damping is used.



3. Assumption



- (1) Nominal tube thickness and nominal tube length are used in the evaluation model because the effect of the tolerances of these dimensions on the natural frequency is negligible.
- (2) Contact condition between tube and tube support plate is pin-supported. Fixed supported condition at No. 1 TSP is added.
- (3) Contact condition between tube and active support points by the anti-vibration bar (AVB) is pin-supported. And all points are active.
- (4) Modulus of elasticity of tube is interpolated based on the tube average temperature of $\frac{T_{av} + T_s}{2}$ from table of ASME Boiler and Pressure Vessel Code, Sec II, Materials, 1998 Edition, 2000 addenda (Ref.23).

Where,

- T_{av} : Primary side average temperature (°F)
- T_s : Secondary side temperature (°F)

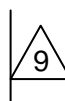
- (5) Tube has the virtual added mass supposing the fluid-structure interaction (FSI) effect as shown in the following formula (Ref.24).

$$m_v = \frac{\pi D_o^2 \rho_o}{4} \left\{ \frac{(D_e/D_o)^2 + 1}{(D_e/D_o)^2 - 1} \right\} \text{ (lbm/ft)} \dots\dots\dots (1)$$

$$D_e/D_o = \left(1 + \frac{1}{2} P/D_o \right) P/D_o \dots\dots\dots (2)$$

Where,

- m_v : Virtual added mass per unit length due to FSI effect;
- ρ_o : Average density of water outside the tube;
- D_o : Tube outside diameter
- P : Tube pitch.





4. Acceptance criteria

Through the tube vibration analysis of the tube straight portion, the stability ratio to FEI is calculated. A stability ratio over 1.0 implies probability of FEI.



5. Design input

The nominal dimensions are obtained from the design drawings (Ref.3 to 20) and the manufacturing tolerances are not considered.

Flow characteristics are obtained from 3 dimensional thermal and hydraulic analysis (see Appendix 12) .Flow velocity, density, void fraction and hydrodynamic pressure are evaluated for representative 7 tubes (Table 5-1). The reason of selection of these tubes is provided in section 6.2.1.

The velocity, density distribution and volume flow rate quality for tube straight portion are provided in Fig.5-0 through 5-21.

The void fraction and velocity on the center vertical plane is provided in Fig.5-22.

The void fraction and velocity above each TSP are provided in Fig.5-24 through 5-31.

Table 5-1 Evaluated Tubes

Row	Column
1	1
1	13
1	89
53	57
80	74
101	29
137	77

(See Fig. 5-23)

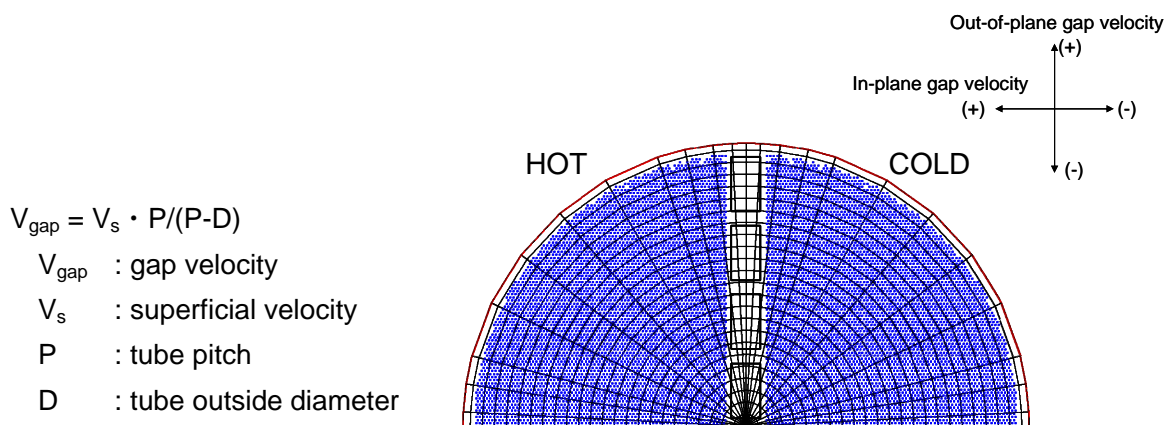


Fig.5-0 Definition of velocity direction



Fig.5-1 Cross flow velocity of tube straight portion (R1C1 tube)



Fig.5-2 Density of tube straight portion (R1C1 tube)



Fig.5-3 Volume flow rate quality (R1C1 tube)



Fig.5-4 Cross flow velocity of tube straight portion (R1C13 tube)



Fig.5-5 Density of tube straight portion (R1C13 tube)



Fig.5-6 Volume flow rate quality (R1C13 tube)



Fig.5-7 Cross flow velocity of tube straight portion (R1C89 tube)



Fig.5-8 Density of tube straight portion (R1C89 tube)



Fig.5-9 Volume flow rate quality (R1C89 tube)



Fig.5-10 Cross flow velocity of tube straight portion (R53C57 tube)



Fig.5-11 Density of tube straight portion (R53C57 tube)



Fig.5-12 Volume flow rate quality (R53C57 tube)



Fig.5-13 Cross flow velocity of tube straight portion (R80C74 tube)



Fig.5-14 Density of tube straight portion (R80C74 tube)



Fig.5-15 Volume flow rate quality (R80C74 tube)



Fig.5-16 Cross flow velocity of tube straight portion (R101C29 tube)



Fig.5-17 Density of tube straight portion (R101C29 tube)



Fig.5-18 Volume flow rate quality (R101C29tube)



Fig.5-19 Cross flow velocity of tube straight portion (R137C77 tube)



Fig.5-20 Density of tube straight portion (R137C77 tube)



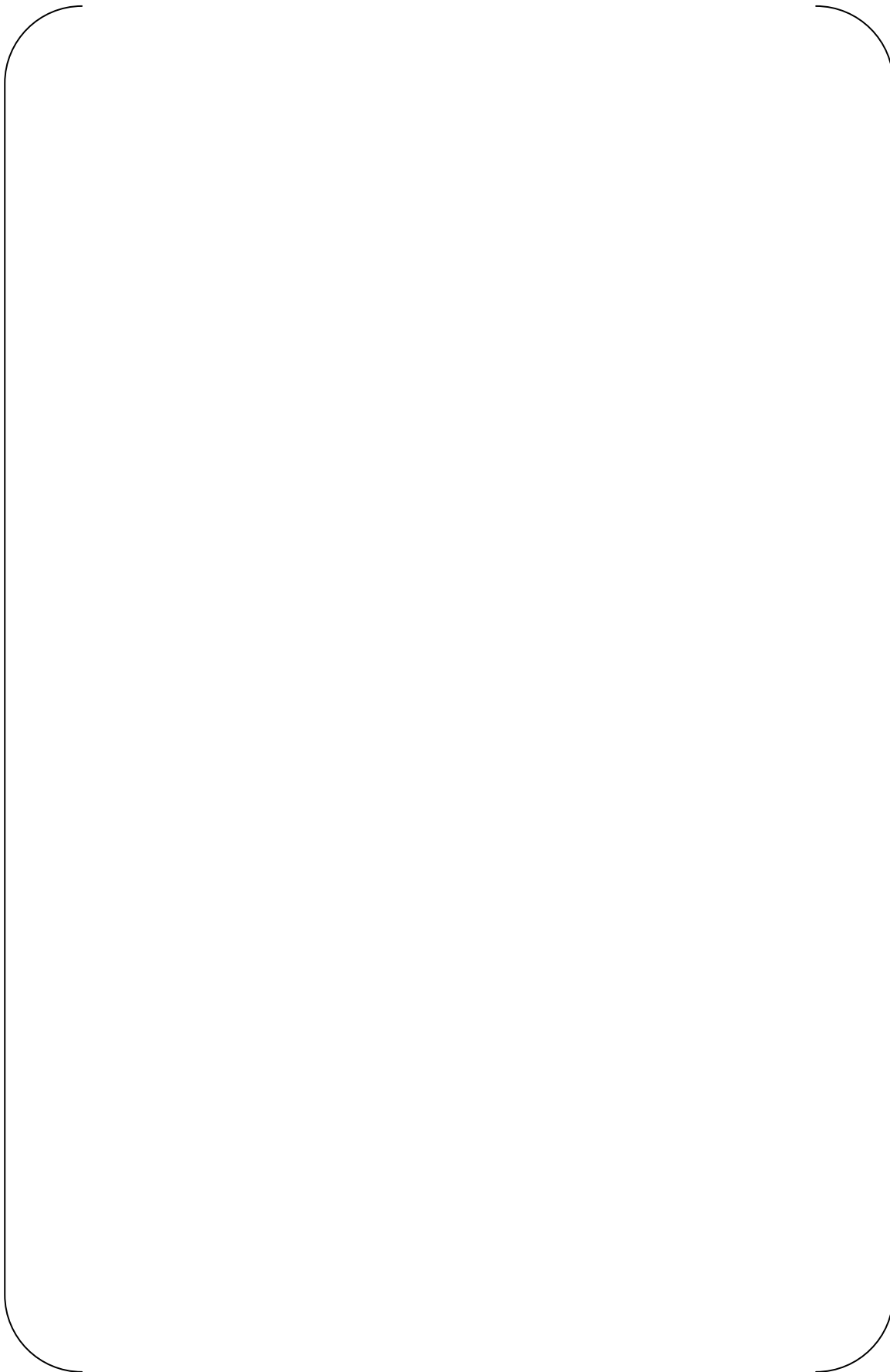
Fig.5-21 Volume flow rate quality (R137C77 tube)



Fig.5-22 Distribution of void fraction and velocity



Fig.5-23 Evaluated tubes



9

Fig.5-24 Distribution of void fraction and velocity above tube sheet



(Note 1)

Note that velocity of contour may mislead, because the velocity of outer circumference of the tube bundle is shown in lower velocity compared to that calculated by ATHOS/SGAP. The accurate values are provided in Appendix-2 Attachment-2.

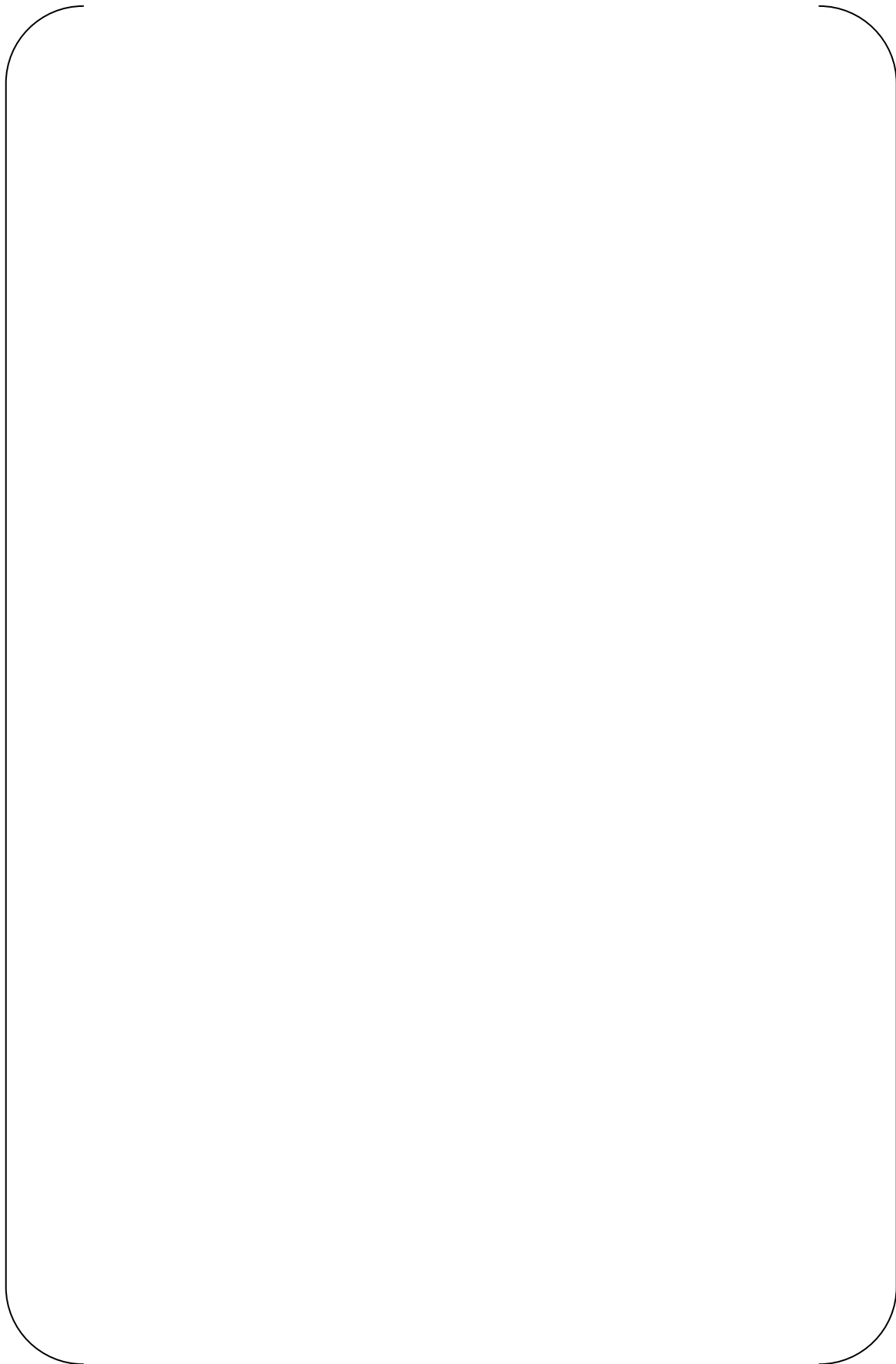


Fig.5-25 Distribution of void fraction and velocity at #1TSP

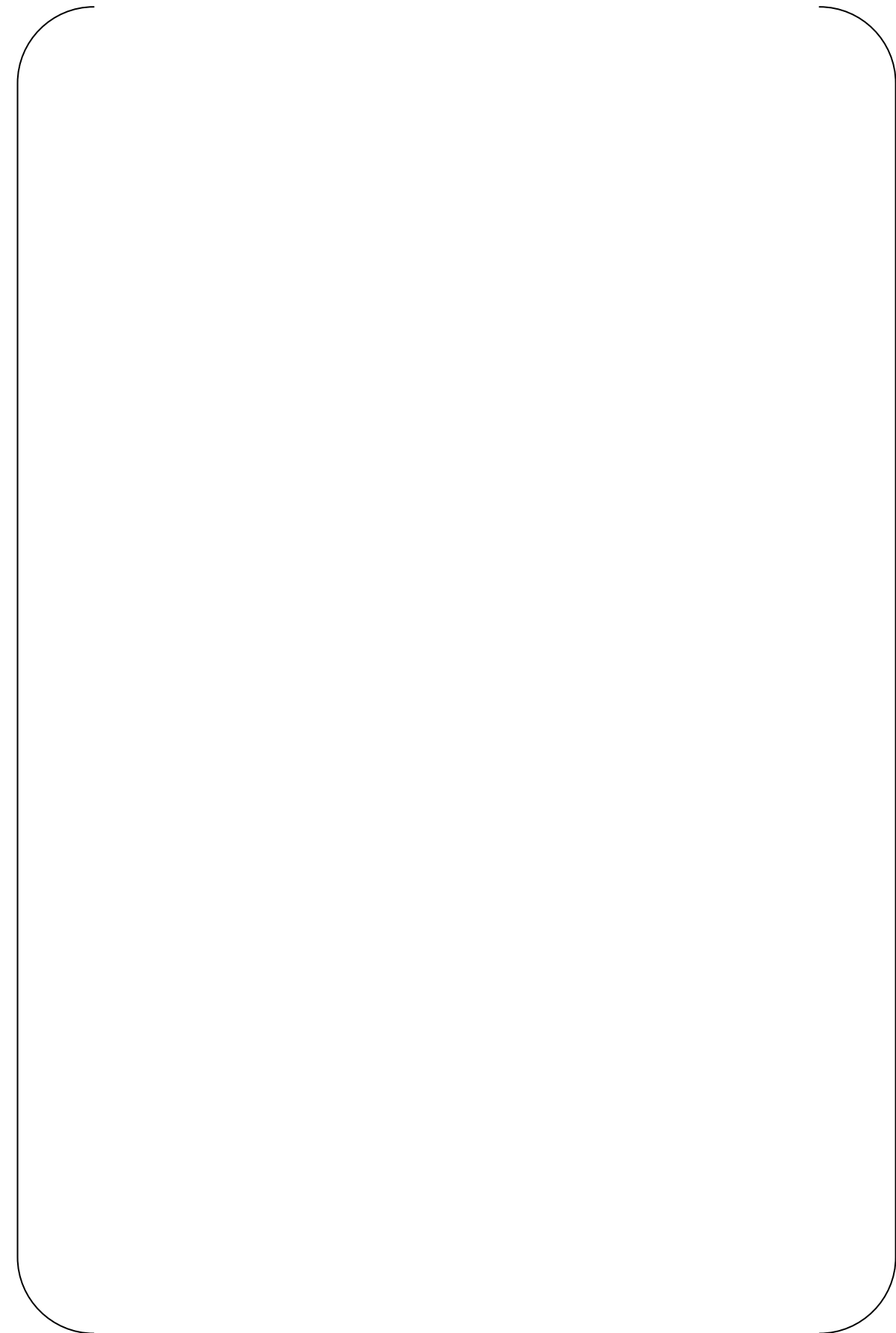
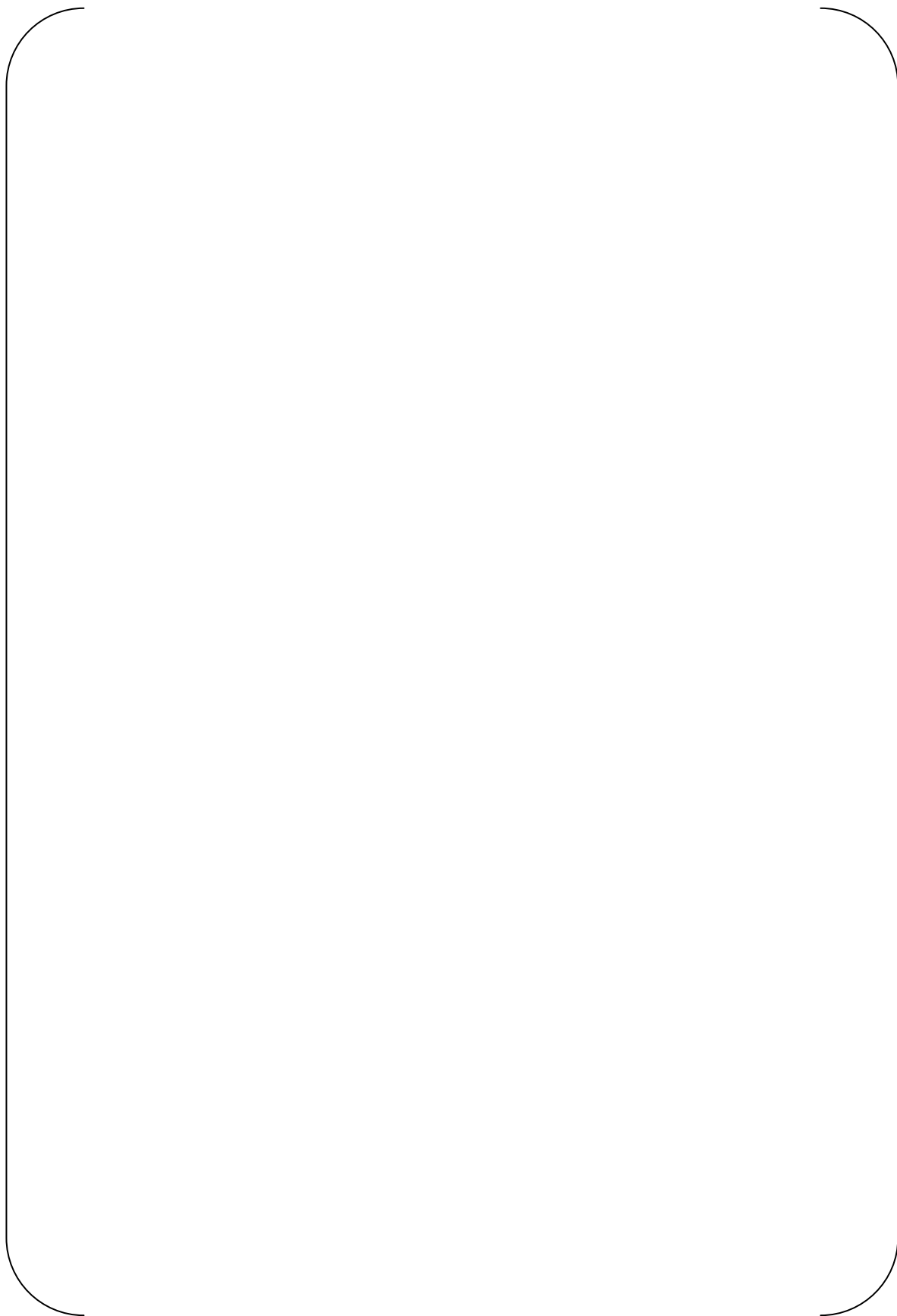


Fig.5-26 Distribution of void fraction and velocity at #2TSP



9

Fig.5-27 Distribution of void fraction and velocity at #3TSP

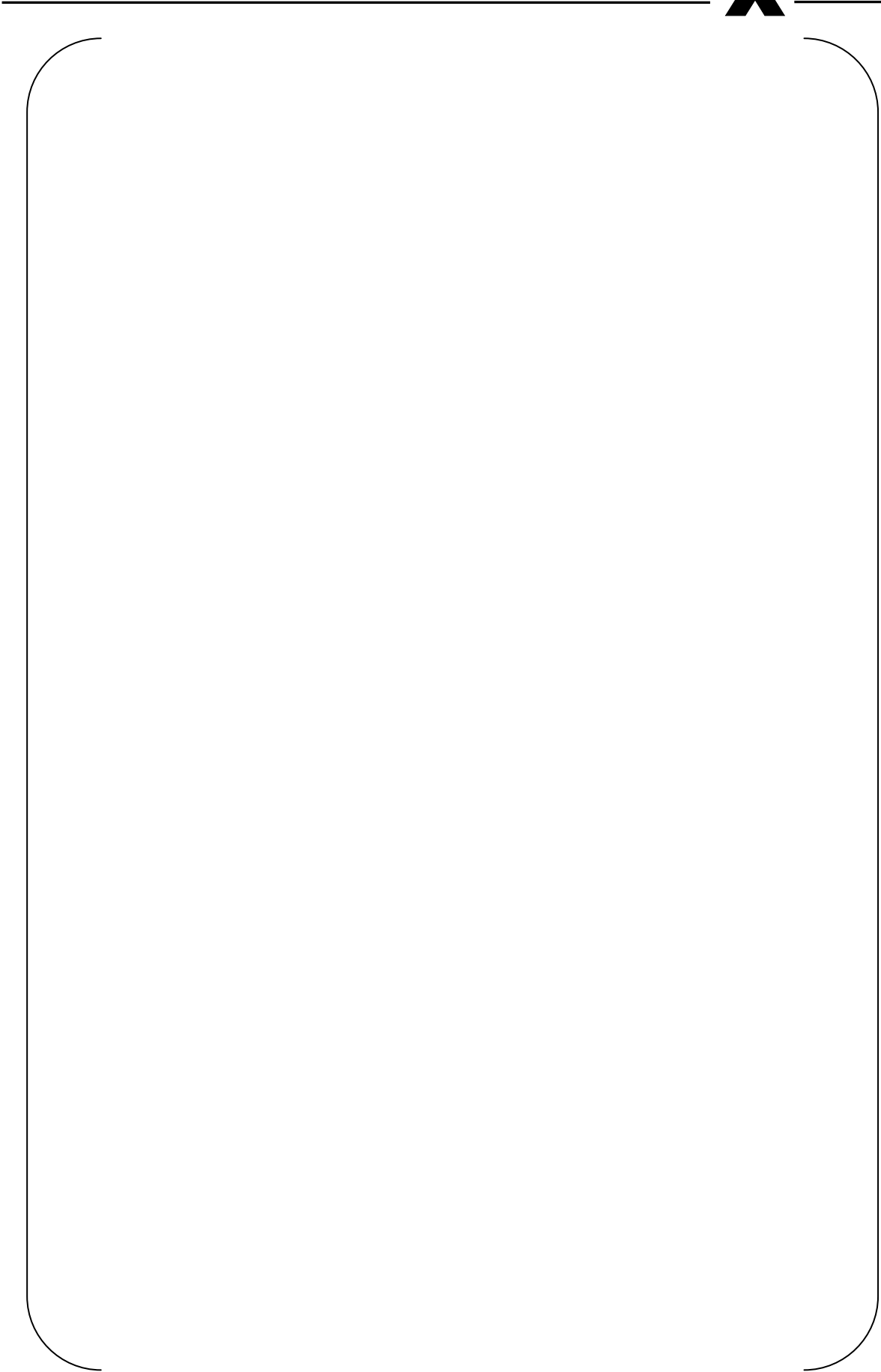


Fig.5-28 Distribution of void fraction and velocity at #4TSP

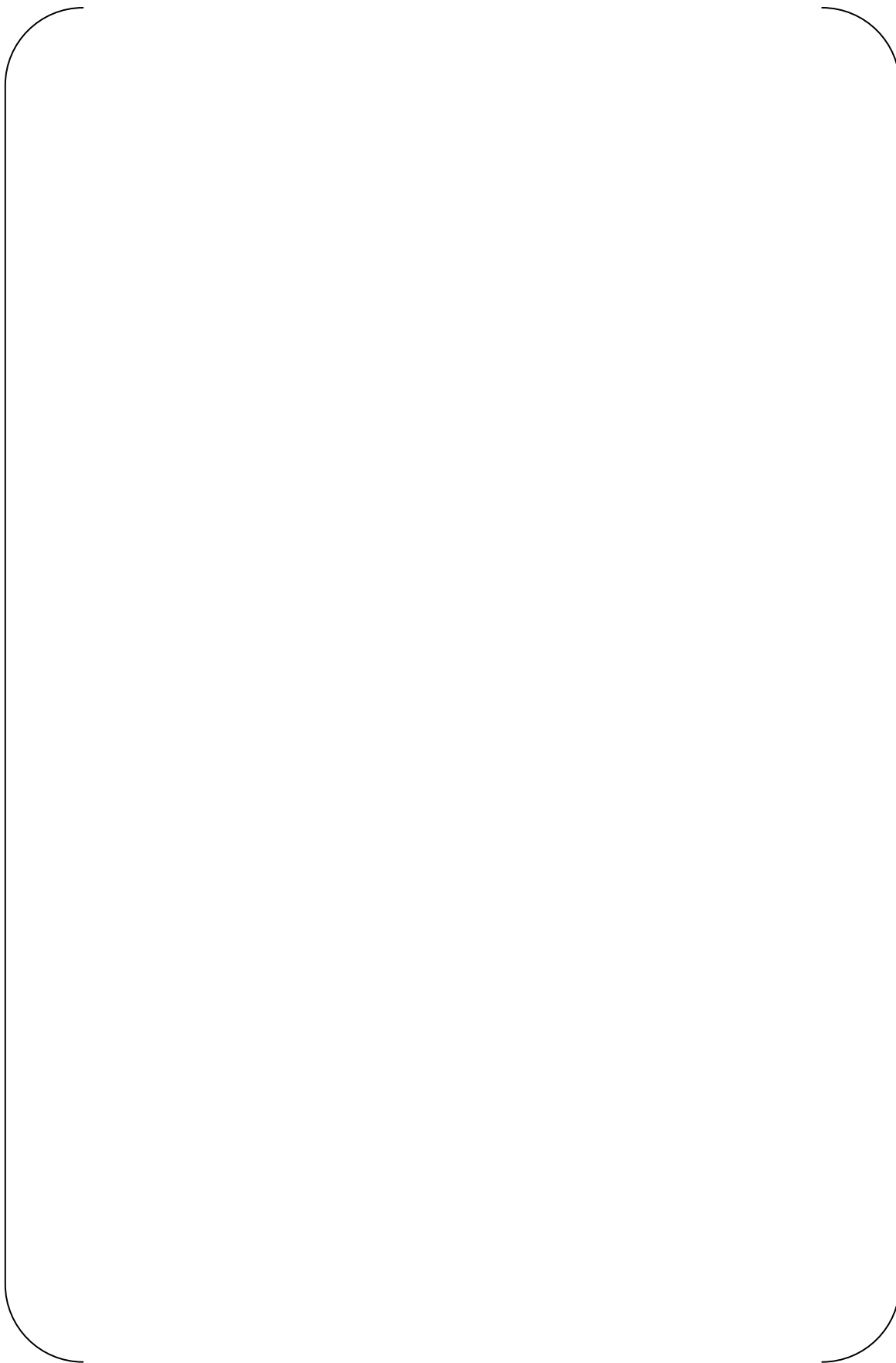


Fig.5-29 Distribution of void fraction and velocity at #5TSP

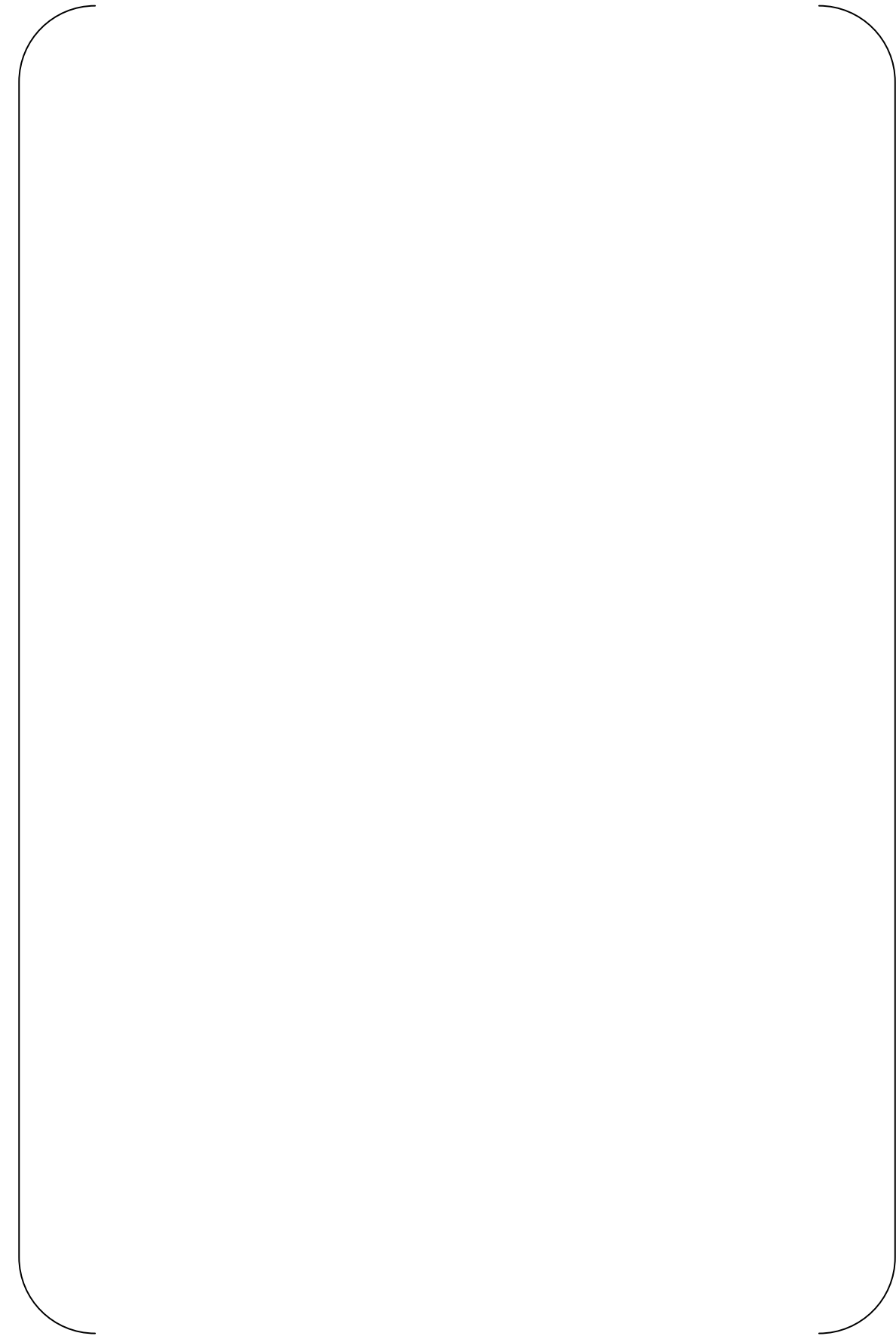


Fig.5-30 Distribution of void fraction and velocity at #6TSP

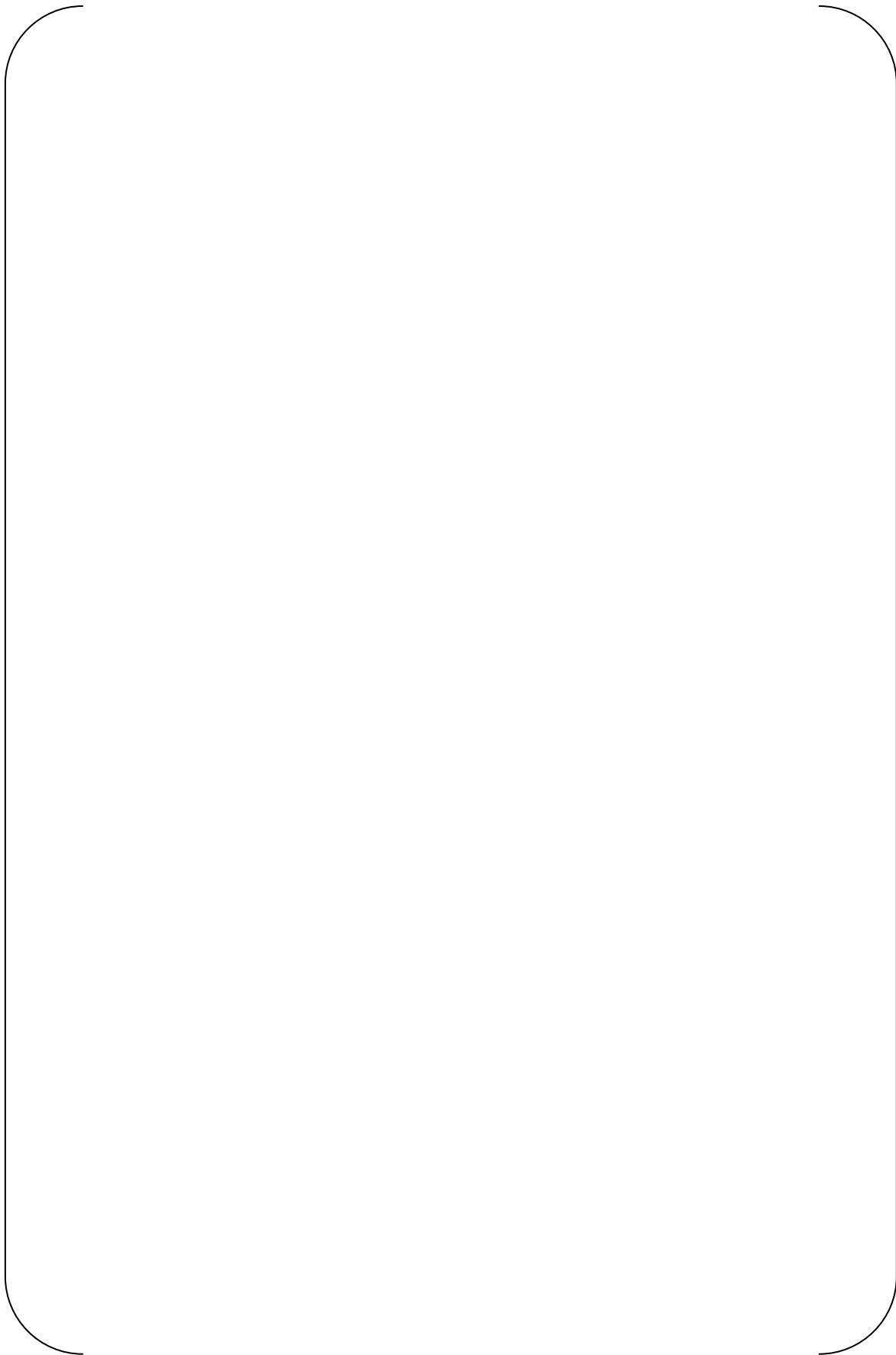


Fig.5-31 Distribution of void fraction and velocity at #7TSP



6. Methodology

6.1 Fluid elastic instability

6.1.1 Basic equation of tube vibration analysis

The term “fluid elastic instability” is generally used to refer to self-excited vibration of tube bundles due to cross flow. In 1969, Connors disclosed the presence of this phenomenon for the first time (Ref.24).

Causes of fluid elastic instability are considered to be the absorption of flow energy due to the interaction of fluid and structure. This phenomenon occurs on tube bundles, and is subjected to effects of tube bundle array. Thus, it is experimentally attempted to determine the criticality of occurrence in various tube bundle arrays.

The critical flow velocity U_c for generating fluid elastic instability is obtained in the following Connors’ formula (Ref.24). This formula is employed in the TEMA (Standards of the Tubular Exchanger Manufactures Association), which is the industrial design standard in the United States.

$$\frac{U_c}{fD_o} = K \left[\frac{m_0 \delta}{\rho_o D_o^2} \right]^{1/2} \dots\dots\dots (3)$$

Where,

- U_c : Critical flow velocity
- f : Tube natural frequency
- D_o : Tube outside diameter
- K : Critical factor
- m_0 : Average tube mass per unit length
- δ : Tube logarithmic decrement(= $2\pi h$)
- h : Damping ratio
- ρ_o : Density of water outside the tube

The critical flow velocity U_c in eq. (3) is evaluated in case of tube vibration of single degree of freedom system with uniform cross flow along the tube axis. In actual tube, however, the vibration of the tube supported by the tube support plate is multi degrees of freedom system with beam type of vibration modes. Therefore, considering the vibration mode and fluid distribution, the effective flow velocity U_{en} is evaluated in the following formula.

$$U_{en} = \left[\frac{\int_0^L \frac{\rho(x)}{\rho_o} \cdot U(x)^2 \cdot \phi_n(x)^2 dx}{\int_0^L \frac{m(x)}{m_o} \cdot \phi_n(x)^2 dx} \right]^{1/2} \dots\dots\dots (4)$$



Where,

- U_{en} : Nth mode effective flow velocity
- $\varphi_n(x)$: Nth vibration mode
- $\rho(x)$: Fluid density distribution of water outside the tube in tube axis direction
- $m(x)$: Tube mass distribution per unit length in tube axis direction
- $U(x)$: Flow velocity distribution orthogonal to tube axis in tube axis direction
- x : Coordinate component along tube axis
- ρ_o : Average density of water outside the tube
- m_o : Average tube mass per unit length
- L : Tube length

The stability ratio is determined as follows in each vibration mode by calculating the ratio of eq. (3) and eq. (4).

$$SR_n = \frac{U_{en}}{U_{cn}} \dots\dots\dots (5)$$

where,

$$\frac{U_{cn}}{f_n \cdot D_o} = K \left[\frac{m_o \delta}{\rho_o D_o^2} \right]^{1/2} \dots\dots\dots (6)$$

This value is called the n-th mode stability ratio SR_n , and if $SR_n > 1$, fluid elastic instability occurs. Generally, the maximum stability ratio in each mode is called the stability ratio of the tube, which is simply expressed as SR.



6.2. Critical factor and damping ratio

It is considered that the ASME code provides the conservative critical factor and damping ratio for the low void fraction region such as the tube straight region (Conservative case). In order to calculate the more realistic stability ratio, we can use the best estimated critical factor and the damping factor.

6.2.1 Conservative case

K=2.4 of the critical factor and h=1.5 % of damping ratio are used as recommended in ASME Sec.III Appendix N-1330 as a code calculation.

6.2.2 Best estimated case

Best estimated values based on recent experiential data are used in this case as follow.

6.2.2.1 Damping ratio

The damping ratio is calculated as the sum of the structural damping (1.0%), two phase damping, and squeeze film damping.

h = h_{ST} + h_{TP}+ h_{SF} (7)

where

h : Total damping ratio

h_{ST} : Structural damping ratio

h_{TP} : Two phase damping ratio

h_{SF} : Squeeze film damping ratio



(1) Structural damping

Since MHI test result (Figure 6.2-1, Ref.26) show the average structural damping value is 1.0% (0.2% in minimum), 1.0% is used for the evaluation.

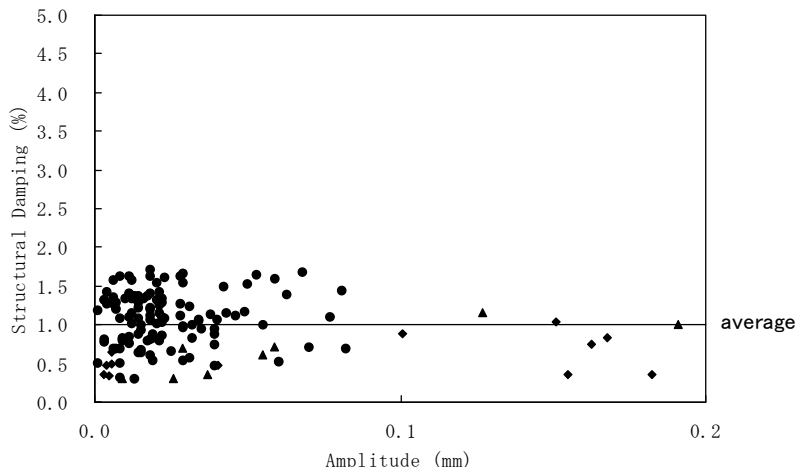


Fig.6.2-1 Structural Damping



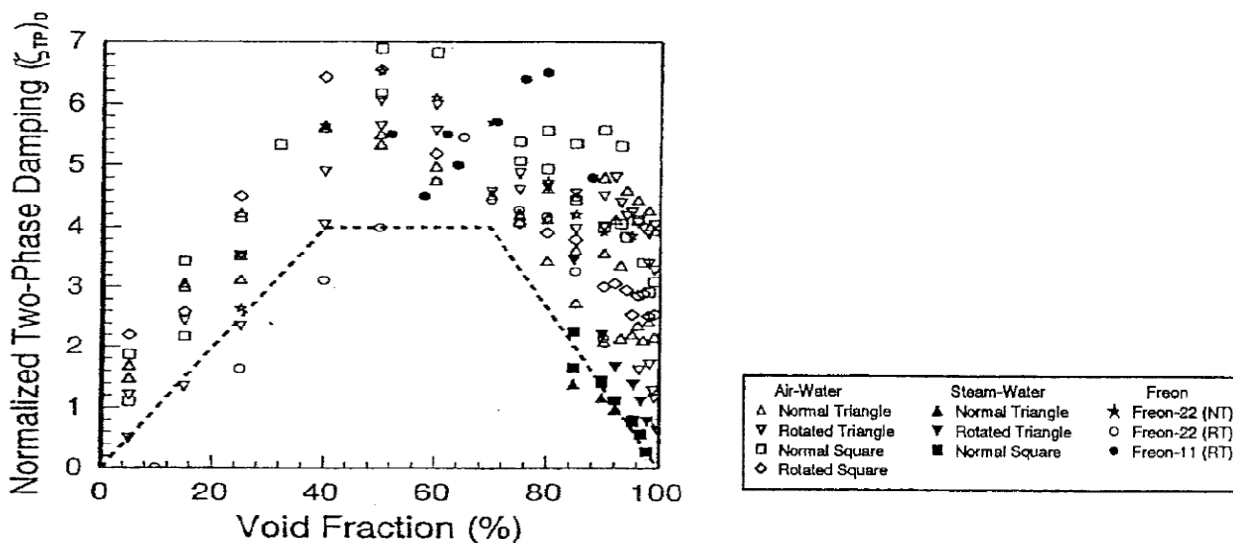
(2) Two-phase damping

Pettigrew's test result of the two phase damping (Figure 6.2-2, Ref.27), which is the function of superficial void fraction, is used to calculate the effective two-phase damping along the tube length by considering vibration mode using the following equation.

$$\frac{\int h_{TP}(\beta(x))\phi^2 dx}{\int \phi^2 dx} \dots\dots\dots (8)$$

Where,

- h_{TP} : Two-phase damping
- β : Superficial void fraction
- Φ : Vibration mode
- x : Tube axis



$$(\zeta_{TP})_D = \zeta_{TP}(\rho_t D^2 / m)^{-1} \{ [1 + (D/D_c)^3] / [1 - (D/D_c)^2]^2 \}^{-1}$$

Fig 6.2-2 Effect of void fraction on two-phase damping



(3) Viscous damping

Since the viscous damping is negligible in high void fraction (Ref.28), it is neglected in this analysis.

(4) Squeeze film damping

Squeeze film damping takes place at the supports and the following equation is based on the available experimental data. (Ref.27)

$$h_{SF} = \left(\frac{N-1}{N} \right) \left[\frac{(1460)}{f} \left(\frac{\rho D^2}{m} \right) \left(\frac{L}{\ell_m} \right)^{\frac{1}{2}} \right] \dots\dots\dots (9)$$

Where,

- h_{SF} : Squeeze film damping
- ρ : Homogeneous density
- D : Tube outside diameter
- N : Number of the support
- f : Natural frequency
- L : Support thickness
- ℓ_m : Characteristic tube length



6.2.2.2 Critical Factor

(1) Effect of the void fraction

Based on MHI experimental data (Ref.30), the critical factor K is evaluated using the equation shown in Figure 6.2-3 which indicates the relation between the superficial void fraction and the critical factor. This experiment was performed under two-phase flow condition using the straight tube bundle of the triangular pitch as shown in Table 6.2-1 and Fig.6.2-4.

The effective superficial void fraction along the tube length is calculated by considering vibration mode and using the following equation in the same manner as the two-phase damping. The obtained critical factor obtained is K, when the value of P/D is 1.33.

$$\bar{\beta} = \frac{\int \beta(x)\phi^2 dx}{\int \phi^2 dx} \dots\dots\dots (10)$$

$$K=f(\bar{\beta}) \dots\dots\dots (11)$$

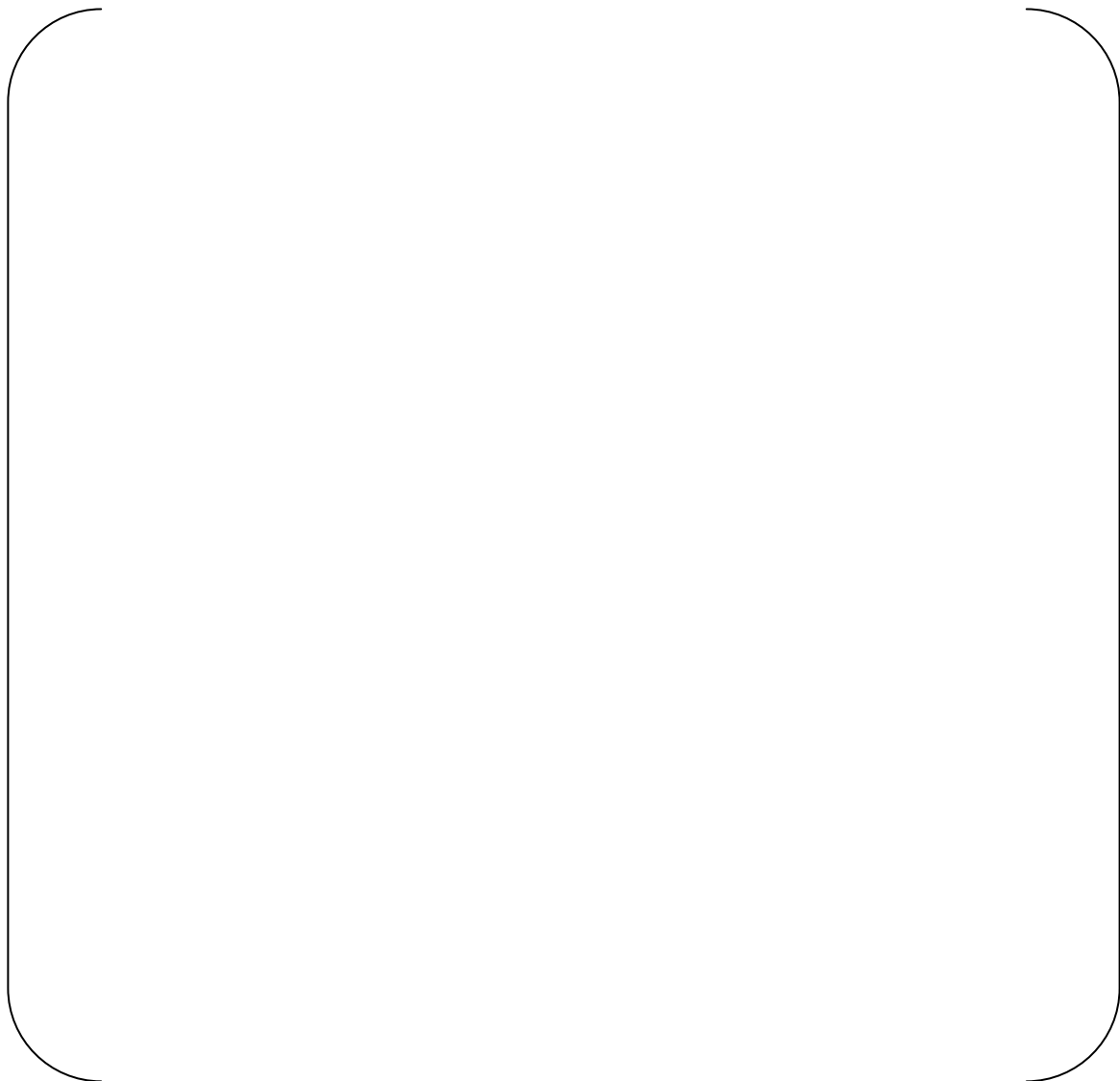


Fig.6.2-3 MHI Experimental Test Result (Relation between Critical Factor and Superficial Void Fraction)



Table 6.2-1 MHI Test Condition

Tube diameter	
Tube pitch	
Number of tubes	
Flow condition	
Pressure	
Temperature	
Superficial void fraction	

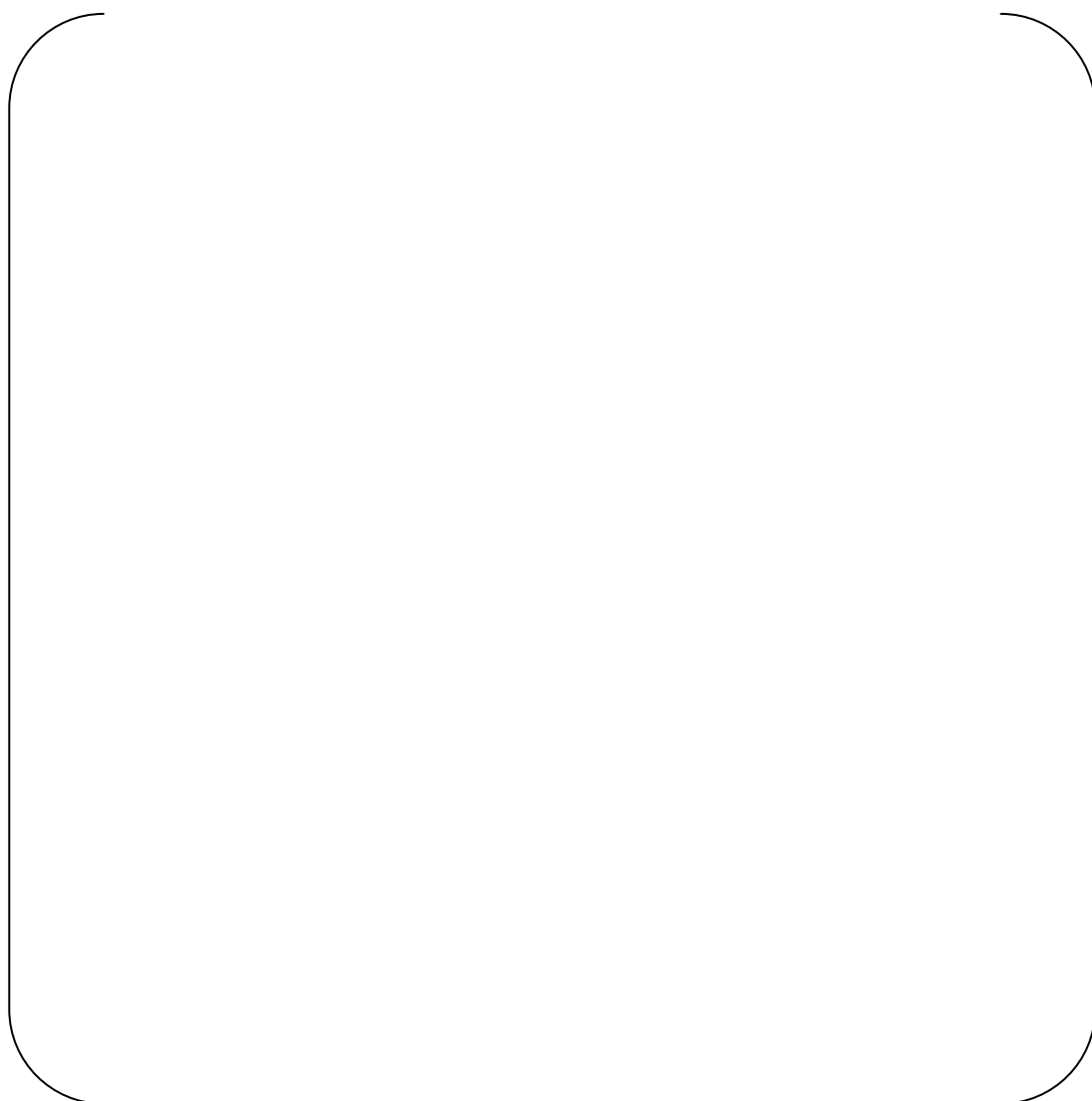


Fig.6.2-4 MHI Test Equipment



6.3. Flow of the evaluation

Evaluation of occurrence of fluid elastic instability in U-tubes is carried out in the following steps :

- ① Using a 1-dimensional Thermal and Hydraulic parameter code (SSPC), determine the tube bundle circulation ratio and other secondary side operating conditions for the normal operating condition (Ref.21).
- ② Using the flow analysis code (ATHOS/SGAP), determine the distributions of flow velocity $U(x)$ and density of the fluid $\rho(x)$ along the tube axis.
- ③ For the damping ratio h and critical factor K , the suggested values based on ASME Sec III Appendix N-1330 are used in conservative case, or eqs. (7), (11) are used in the best estimated case. And from eqs. (3) ~ (5) stability ratio is evaluated (Ref.25)

Figure 6.3-1 describes this process.

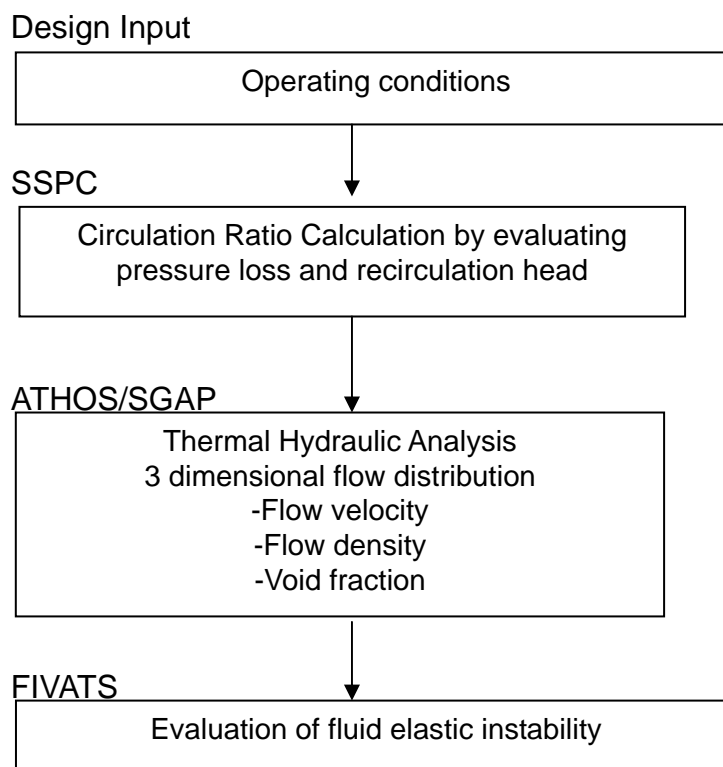


Fig.6.3-1 Flow of the evaluation



6.4 Evaluation Parameters

In general, larger thermal power is more severe for vibration, because the steam flow rate increases. At constant thermal power, lower steam pressure is more severe for vibration than higher pressure, because ρU^2 increases - (the lower ρ causes the higher U).

Basic parameters required for calculations are shown in Table 6.4-1.

Table 6.4-1 Basic parameters for calculation

	Condition of Cycle 16
Plugging	()
T_{cold} (°F)	
T_{hot} (Tsg-in) (°F)	
T_{sg-out} (°F)	
$T_{feedwater}$ (°F)	
Saturation Steam Pressure (psia)	
Steam Mass Flow (lb/hr)	
Circulation ratio	
Thermal power (MWt/SG)	()



6.5 Evaluation of fluid elastic instability

6.5.1 Selection of tubes to be evaluated

The locations of Tube-to-TSP wear at tube straight portions detected in SONGS-2/3 RSGs are shown in Fig. 6.5-1 through 6.5-4. In all SGs, tube-to-TSP wear is present in many Row 1 tubes that border on the tube-free-lane. In addition many of the tubes on the bundle periphery with large bend radii (i.e. Rows 131-142) of 2B-SG exhibit tube-to-TSP wear.

Table 6.5-1 through Table 6.5-3 provides the maximum 10 tube wear depth in each SG. The tube-to-TSP wear distributions at each TSP elevation in each RSGs are provided in Appendix-2 Attachment-1.

Among Row1 tubes, the tube on the bundle periphery (Row 1 Column 1), the tube in column center region (R1C89), and the tube outside of the column region (R1C13) are selected for evaluation. Note that R1C1 tube has the second deepest wear indication at the TSP.

Among bundle periphery tubes, the tube which has the largest wear depth in peripheral tubes (R137C77) and the tube in the middle (R101C29) are selected for evaluation.

In the tube bundles, the tube which has the largest wear depth in all tubes (R80C74) and the tube in the middle of column (R53C57) are selected for evaluation.

As shown in Fig. 5-23, it is considered that the selected tubes cover wide range of tube bundle.

In general, the tube is supported by AVBs so that the tube vibration in U-bend region does not have much effect on the tube vibration of the tube straight part. Thus, the tube vibration model simulating only tube straight part is used for the evaluation.



Table 6.5-1 Max.10 Tube-to-TSP wear depth in 2A-SG

--

Table 6.5-2 Max.10 Tube-to-TSP wear depth in 2B-SG

--

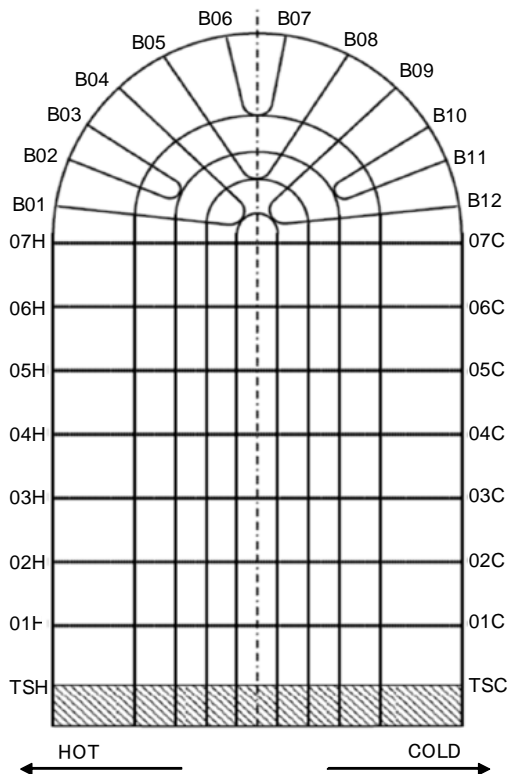


Table 6.5-3 Max.10 Tube-to-TSP wear depth in 3A-SG

--

Table 6.5-4 Max.10 Tube-to-TSP wear depth in 3B-SG

--



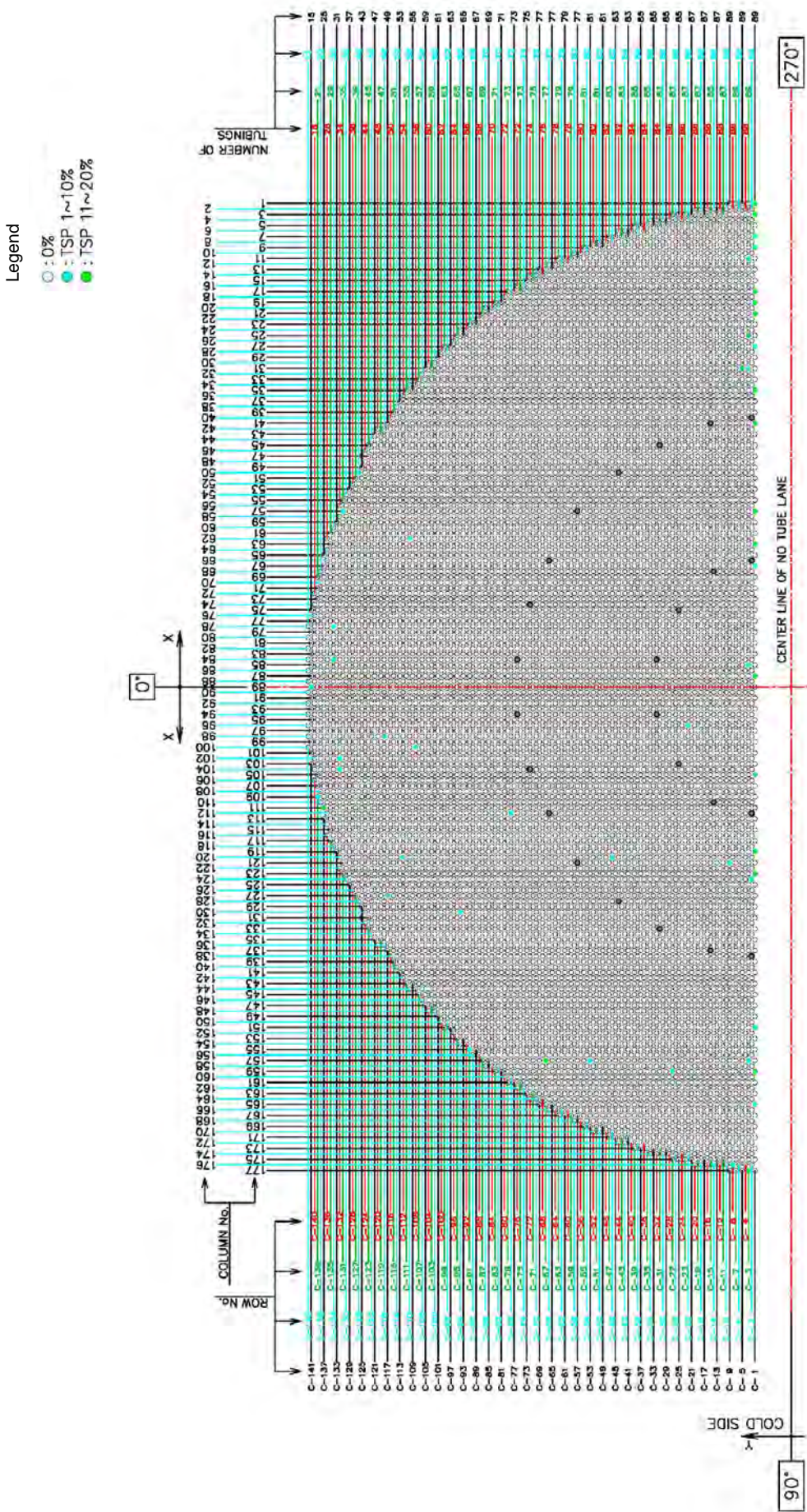


Fig. 6.5-1 Tube-to-TSP wear in 2A-SG



Legend

- : 0%
- : TSP 1~10%
- : TSP 11~20%

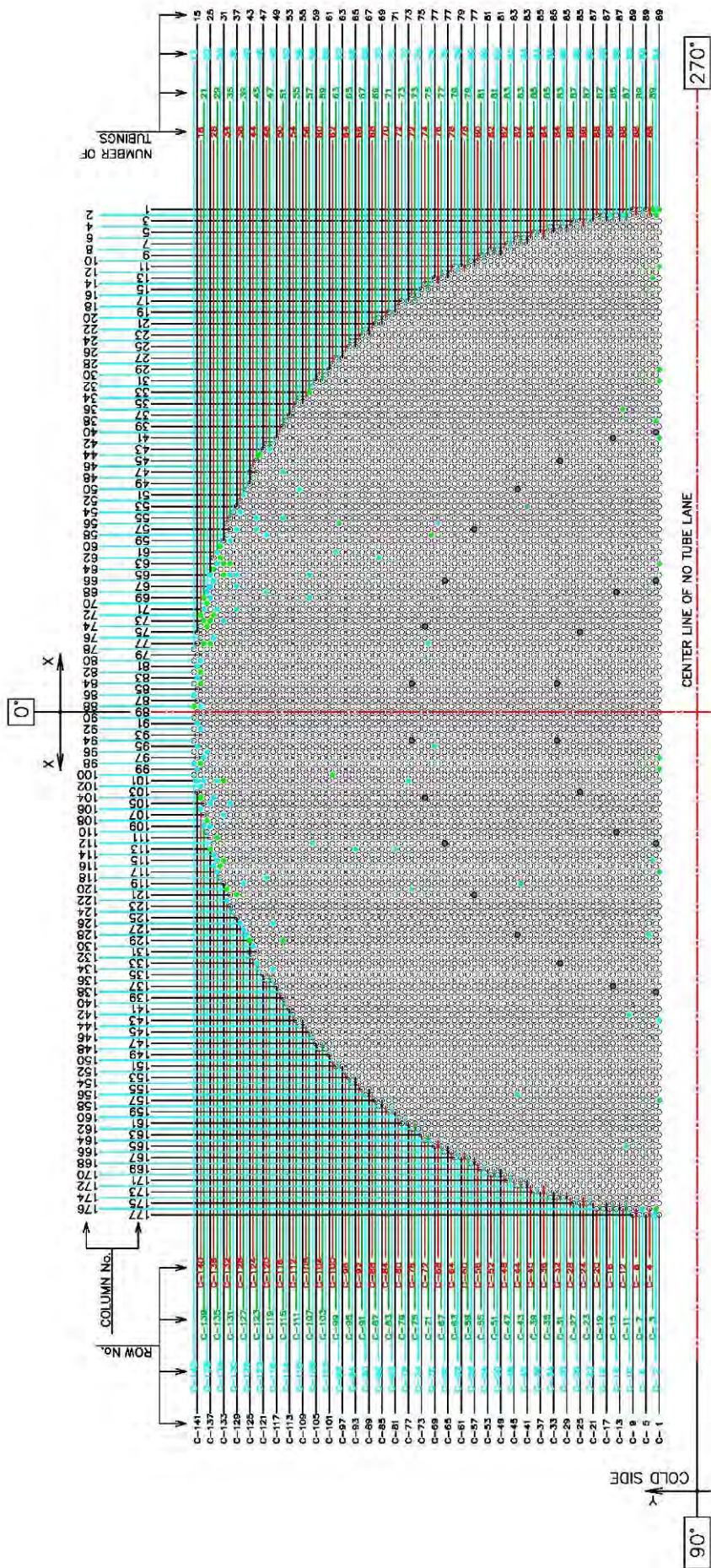


Fig. 6.5-2 Tube-to-TSP wear in 2B-SG

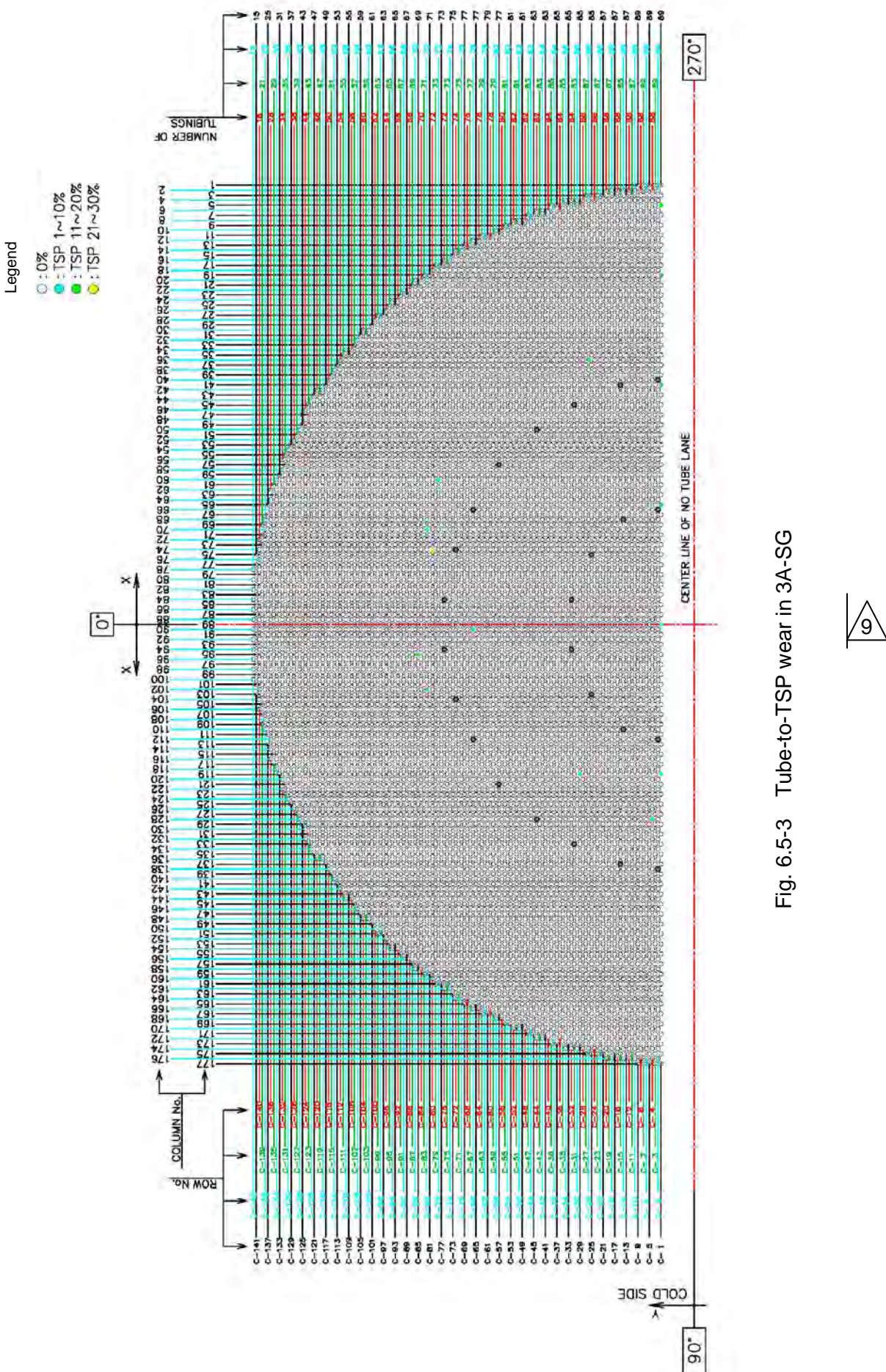


Fig. 6.5-3 Tube-to-TSP wear in 3A-SG



Legend

- : 0%
- : TSP 1~10%
- : TSP 11~20%

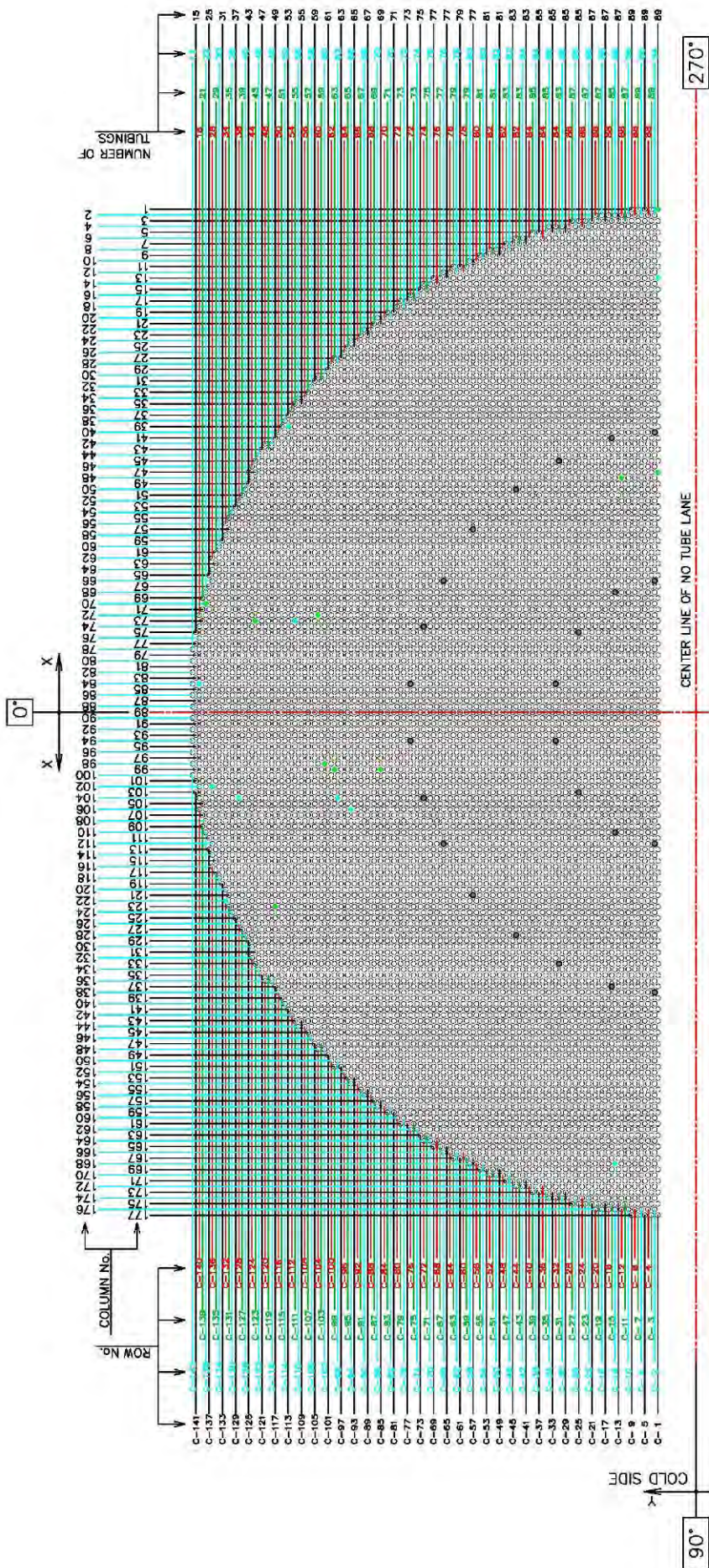


Fig. 6.5-4 Tube-to-TSP wear in 3B-SG





7. Results

(1) Conservative case

The vibration analysis results in case of conservative case (K=2.4, h=1.5%) are shown in Table 7-1 and Fig. 7-1 through 7-3. The maximum stability ratio is 0.67 for R1C1 tube in hot leg. Since the stability ratios are less than 1.0, the analyses imply no FEI occurrence of tube straight portion.

Table 7-1 Stability ratio (conservative case)

Tube		Leg	Mode	Frequency (Hz)	Critical velocity (ft/s)	Effective velocity (ft/s)	Stability ratio
Row	Column						
1	1	COLD					
		HOT					
1	13	COLD					
		HOT					
1	89	COLD					
		HOT					
53	57	COLD					
		HOT					
80	74	COLD					
		HOT					
101	29	COLD					
		HOT					
137	77	COLD					
		HOT					

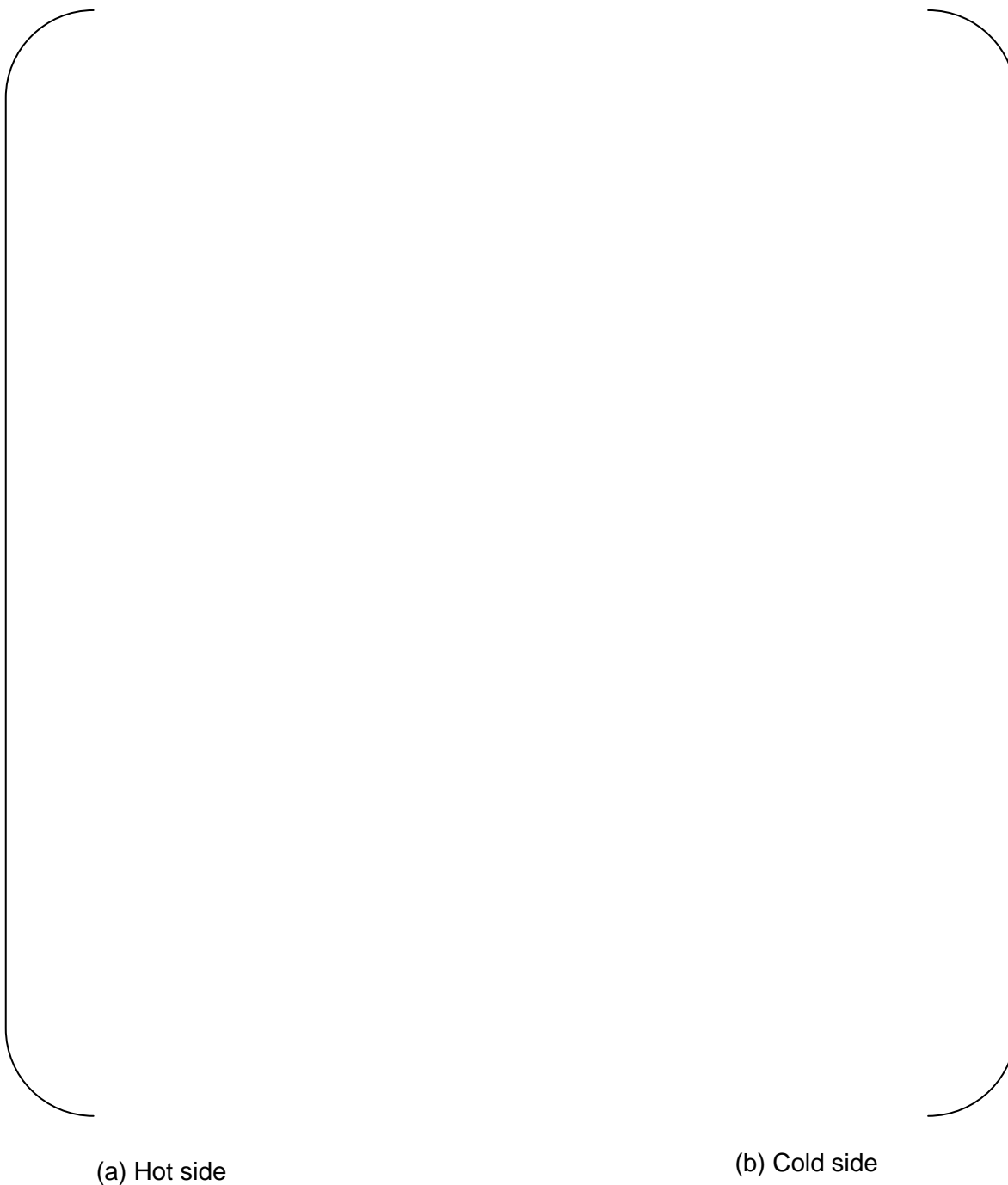


Fig.7-1 Vibration mode diagram for R1C1 tube

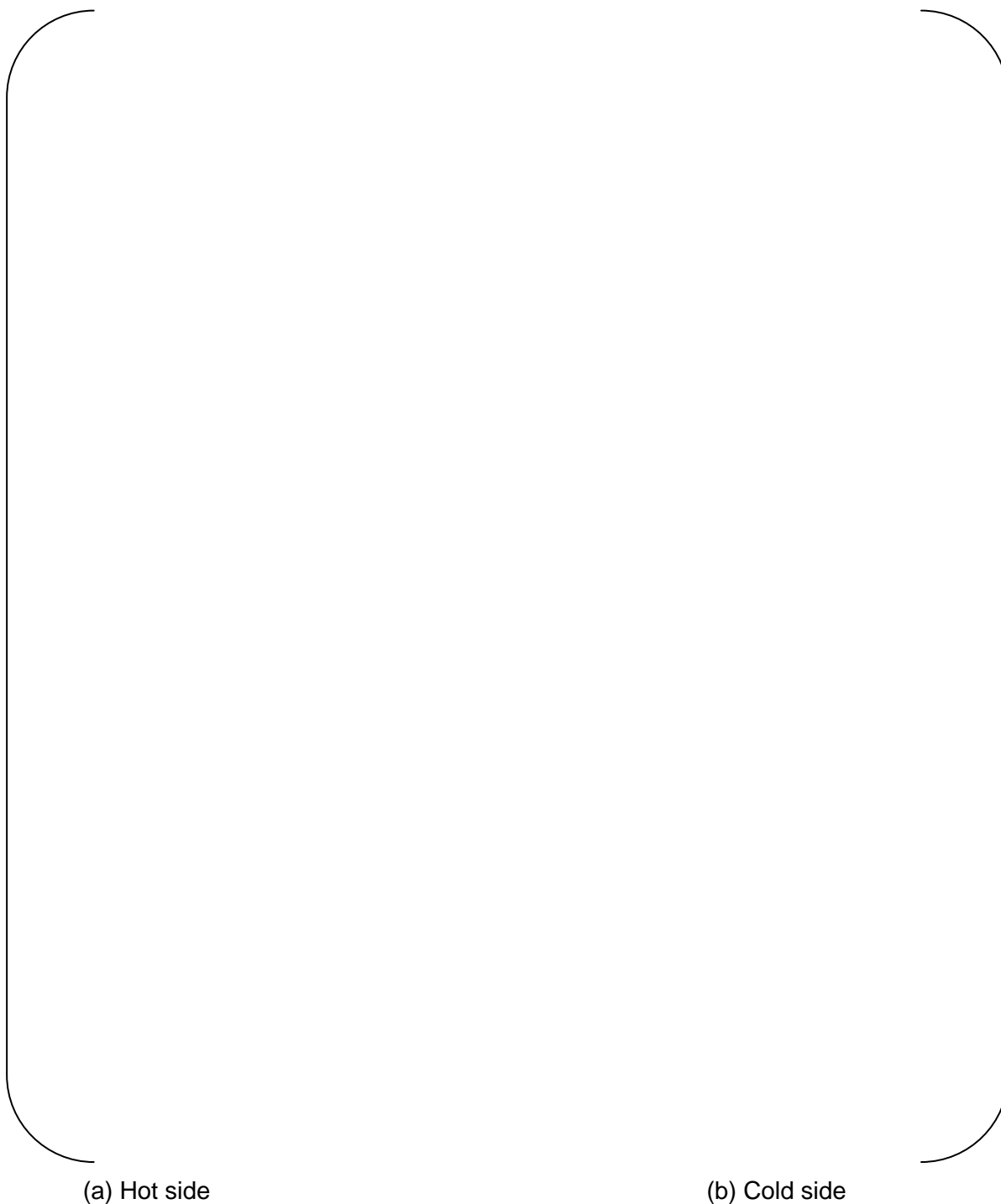


Fig.7-2 Vibration mode diagram for R80C74 tube



(a) Hot side

(b) Cold side

Fig.7-3 Vibration mode diagram for R137C77 tube



(2) Best estimated case

In this case, the best estimated critical factors and damping ratios are calculated based on the recent experimental data. The critical factor and damping ratio are provided in Table 7-2.

Table 7-2 Critical factor and damping ratio(refined case)

Tube		Leg	Mode	Frequency (Hz)	Critical factor	Two phase damping (%)	Squeeze film damping (%)	Total damping (%)(^{*1})
Row	Column							
1	1	COLD))
		HOT						
1	13	COLD						
		HOT						
1	89	COLD						
		HOT						
53	57	COLD						
		HOT						
80	74	COLD						
		HOT						
101	29	COLD						
		HOT						
137	77	COLD))
		HOT						

(*1) Total damping = (Structural damping [1.0%]) + (two phase damping) + (squeeze film damping).

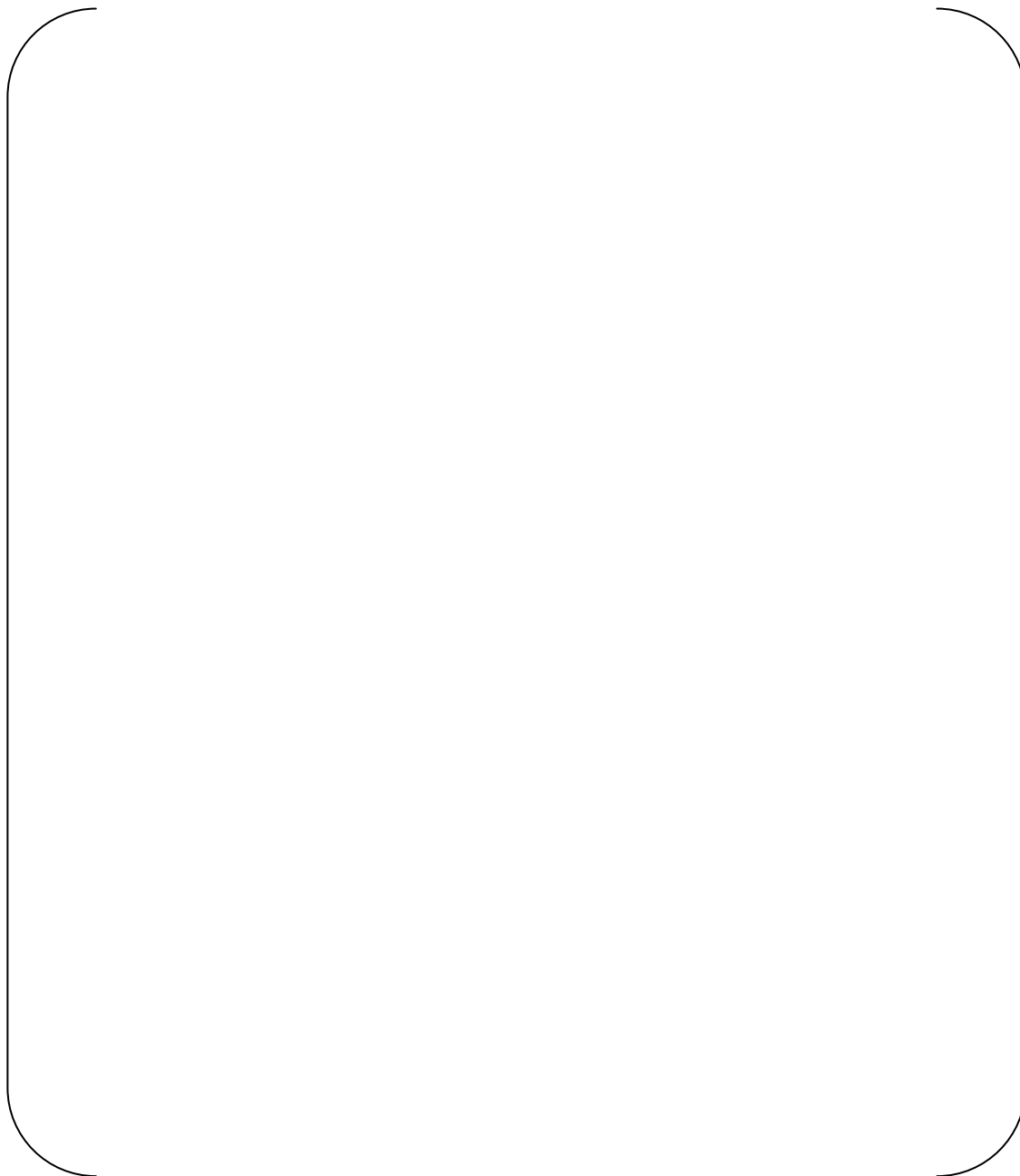


The vibration analysis results in case of refined case (K and h are calculated in detail) are shown in Table 7-3 and Fig. 7-4 through 7-6. The maximum stability ratio is [] for R1C89 tube in hot leg. Since the stability ratios are less than 1.0, the analyses imply no FEI occurrence of tube straight region.

The tube inspection identified the largest tube-to-TSP wear at R80C74 at hot #3-TSP. On the other hand, the calculated stability ratio for R80C74 is [], which is not so large compared to the other tubes. In addition, the tube inspection identified the relatively large tube wear in Row1 tubes in cold leg. However, the stability ratios of Row1 tubes in cold side are smaller than those in hot side. It is evaluated that the stability ratio evaluation does not match the tube wear inspection results. Thus, MHI concludes that the cause of tube-to-TSP wears in SONGS-2/3 RSGs is not due to FEI in the straight portion of tube due to the cross flow.

Table 7-3 Stability ratio (refined case)

Tube		Leg	Mode	Frequency (Hz)	Critical velocity (ft/s)	Effective velocity (ft/s)	Stability ratio
Row	Column						
1	1	COLD					
		HOT					
1	13	COLD					
		HOT					
1	89	COLD					
		HOT					
53	57	COLD					
		HOT					
80	74	COLD					
		HOT					
101	29	COLD					
		HOT					
137	77	COLD					
		HOT					



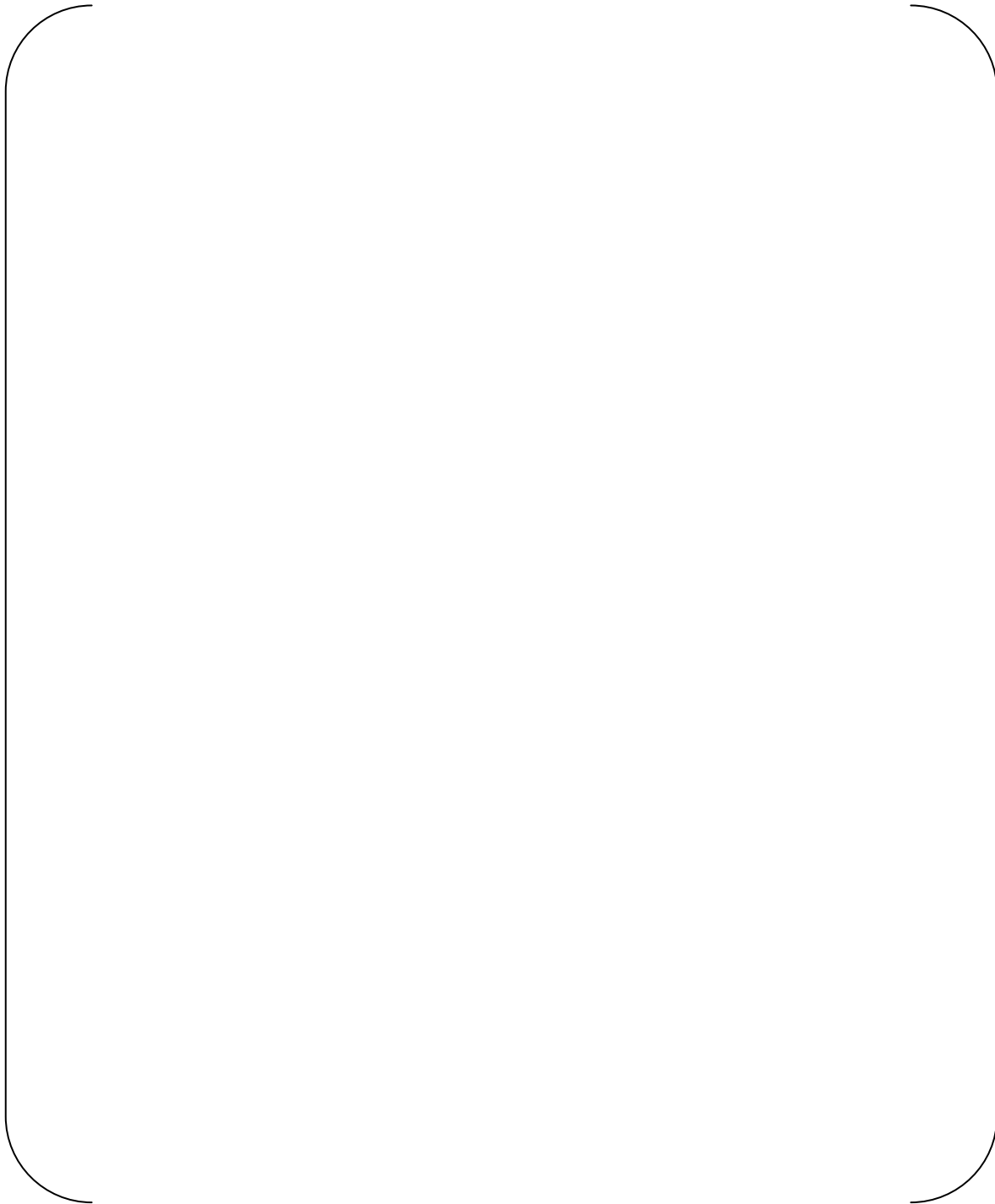
(a) Hot side

(b) Cold side

Fig.7-4 Vibration mode diagram for R1C1 tube



Fig.7-5 Vibration mode diagram for R80C74 tube



(a) Hot side

(b) Cold side

Fig.7-6 Vibration mode diagram for R137C77 tube



8. References

- 1) Deleted
- 2) Deleted
- 3) L5-04FU001 the latest revision, Component and Outline Drawing 1/3
- 4) L5-04FU002 the latest revision, Component and Outline Drawing 2/3
- 5) L5-04FU003 the latest revision, Component and Outline Drawing 3/3
- 6) L5-04FU021 the latest revision, Tube Sheet and Extension Ring 1/3
- 7) L5-04FU022 the latest revision, Tube Sheet and Extension Ring 2/3
- 8) L5-04FU023 the latest revision, Tube Sheet and Extension Ring 3/3
- 9) L5-04FU051 the latest revision, Tube Bundle 1/3
- 10) L5-04FU052 the latest revision, Tube Bundle 2/3
- 11) L5-04FU053 the latest revision, Tube Bundle 3/3
- 12) L5-04FU111 the latest revision, AVB assembly 1/9
- 13) L5-04FU112 the latest revision, AVB assembly 2/9
- 14) L5-04FU113 the latest revision, AVB assembly 3/9
- 15) L5-04FU114 the latest revision, AVB assembly 4/9
- 16) L5-04FU115 the latest revision, AVB assembly 5/9
- 17) L5-04FU116 the latest revision, AVB assembly 6/9
- 18) L5-04FU117 the latest revision, AVB assembly 7/9
- 19) L5-04FU118 the latest revision, AVB assembly 8/9
- 20) L5-04FU119 the latest revision, AVB assembly 9/9
- 21) L5-04GA510 the latest revision, Thermal and Hydraulic Parametric Calculations
- 22) Vibration analysis of shell-and-tube heat exchanger : an overview – Part 1 : flow, damping, fluidelastic instability, M.J. Pettigrew, C.E. Taylor, Journal of fluids and structural 18 (2003) 469-483
- 23) ASME Boiler and Pressure Vessel Code, Sec II, Materials, 1998 Edition through 2000 addenda.
- 24) Connors, H.J., Fluid Elastic Vibration of Tube Arrays Excited by Cross Flow, ASME Annual Meeting, 1970.
- 25) Blevins, R. D., "Flow-induced Vibration", Krieger Publishing Company.
- 26) T. Nakamura, et al., "An advanced method to estimate fluid elastic instability of steam generator U-bend tube bundle.", ASME PVP 2001
- 27) M.J. Pettigrew.,et.al.,2003,"Vibration analysis of shell-and-tube heat exchangers" Journal of Fluids and Structures 18 (2003) 469-483
- 28) S. M. Fluit and M. J. Pettigrew, "Simplified method for predicting vibration and fretting-wear in nuclear steam generator U-bend tube bundle", ASME PVP 2001
- 29) M.J. Pettigrew.,et.al.,2000, "The effects of tube bundle geometry on vibration in two-phase cross-flow"
- 30) WJS16263, MHI Test Report of Fluid Elastic Vibration



Appendix-2 Attachment-1
Tube-to-TSP wear depth diagram for Unit-2/3

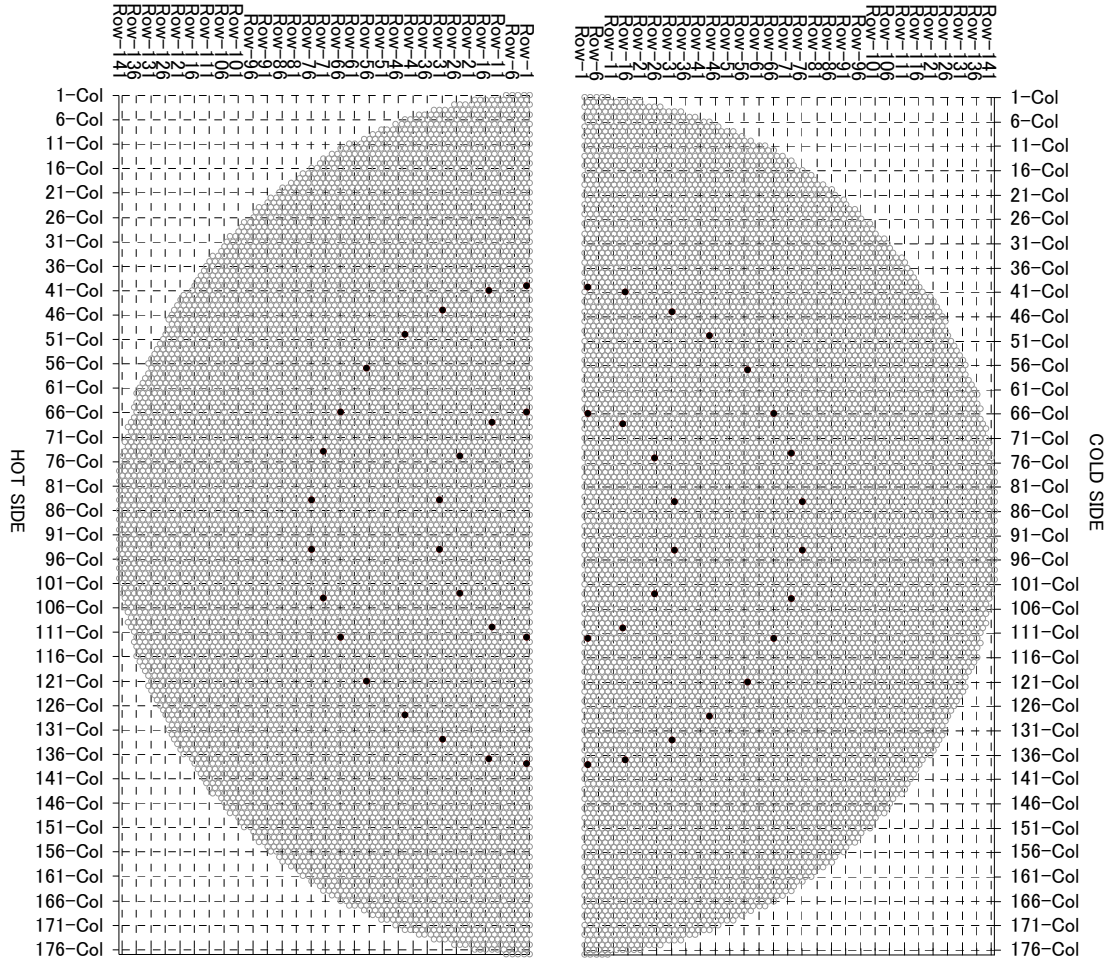
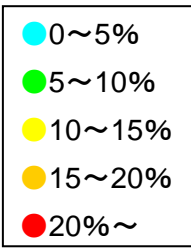


1. Introduction

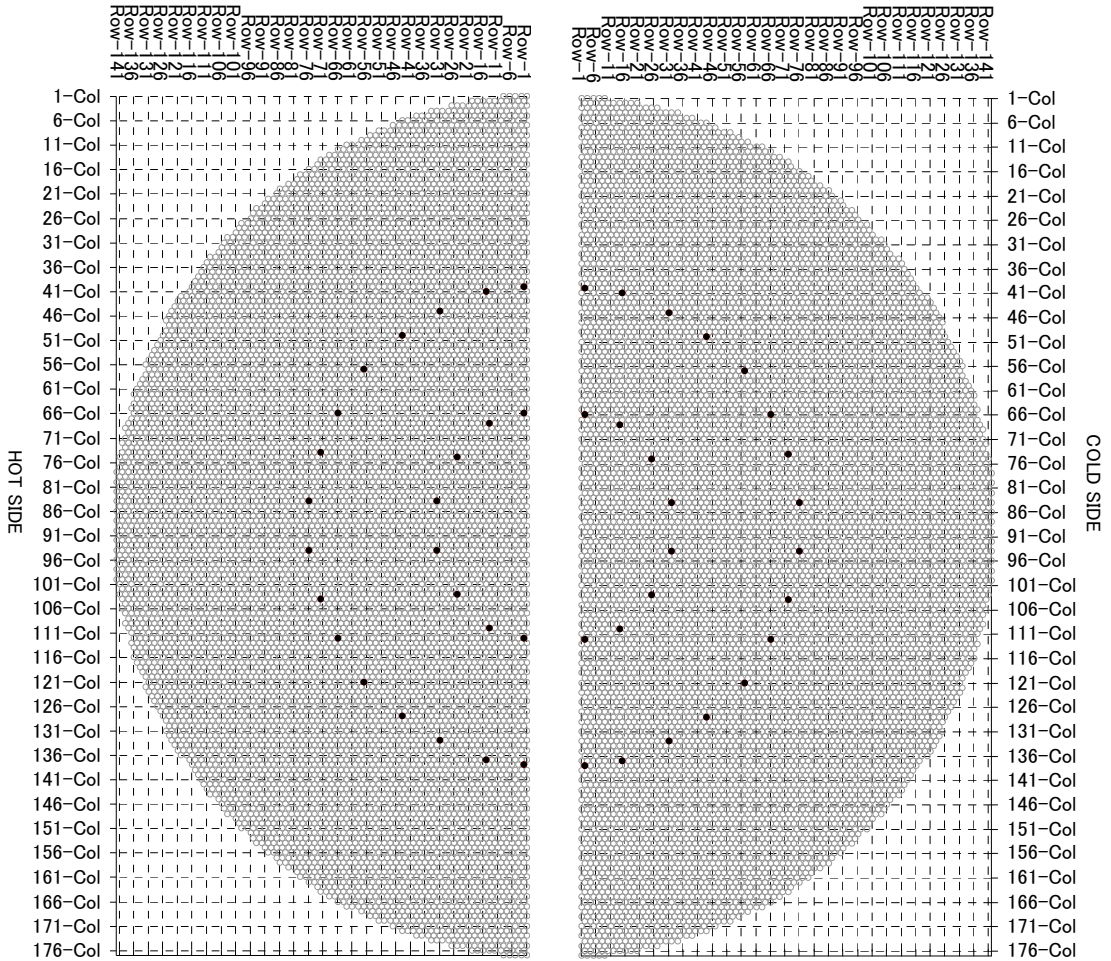
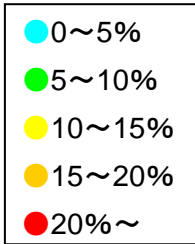
This attachment provides the tube-to-TSP wear depth at each TSP elevation for SONGS-2/3 RSGs.

2. Tube-to-TSP wear depth

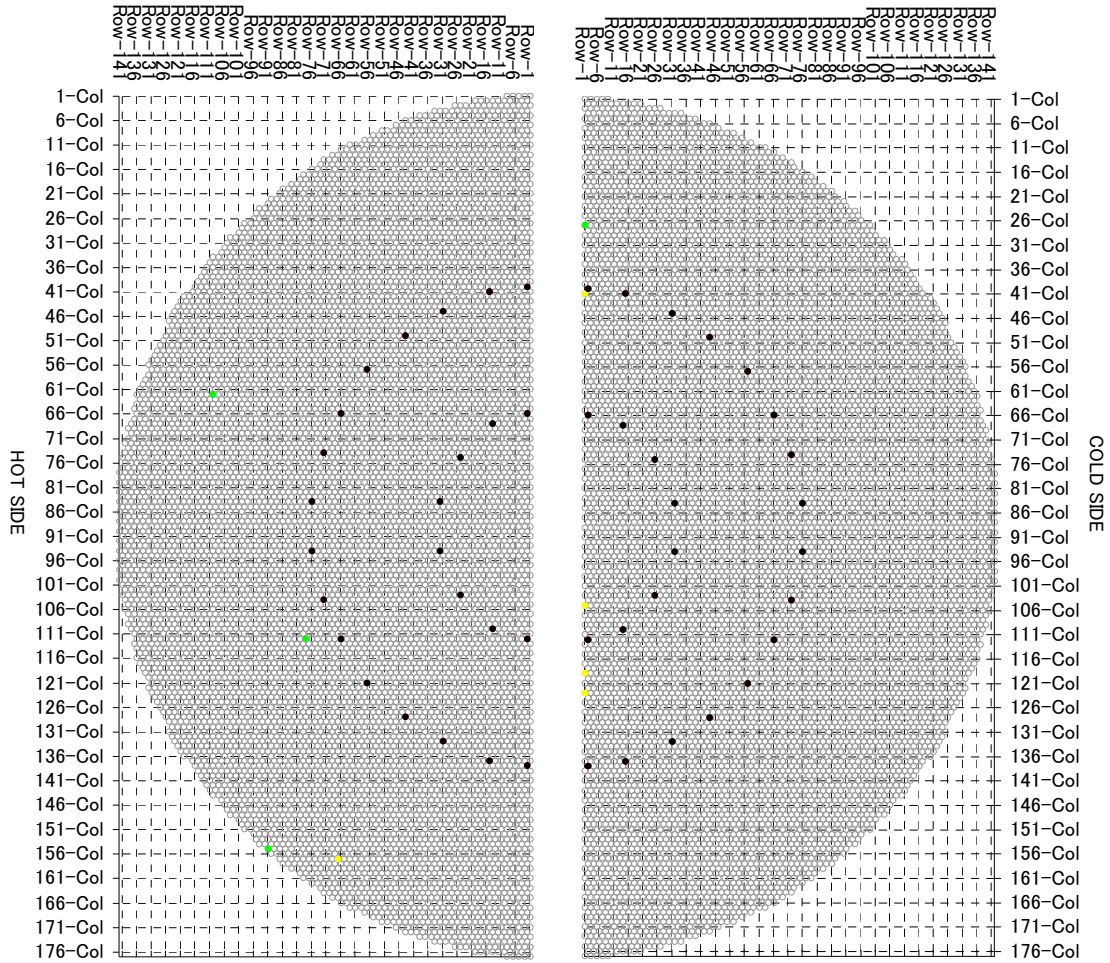
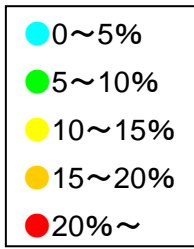
The following figures provide the tube-to-TSP wear depth in %. Note that the figures do not include the tubes with the wear in U-bend region.



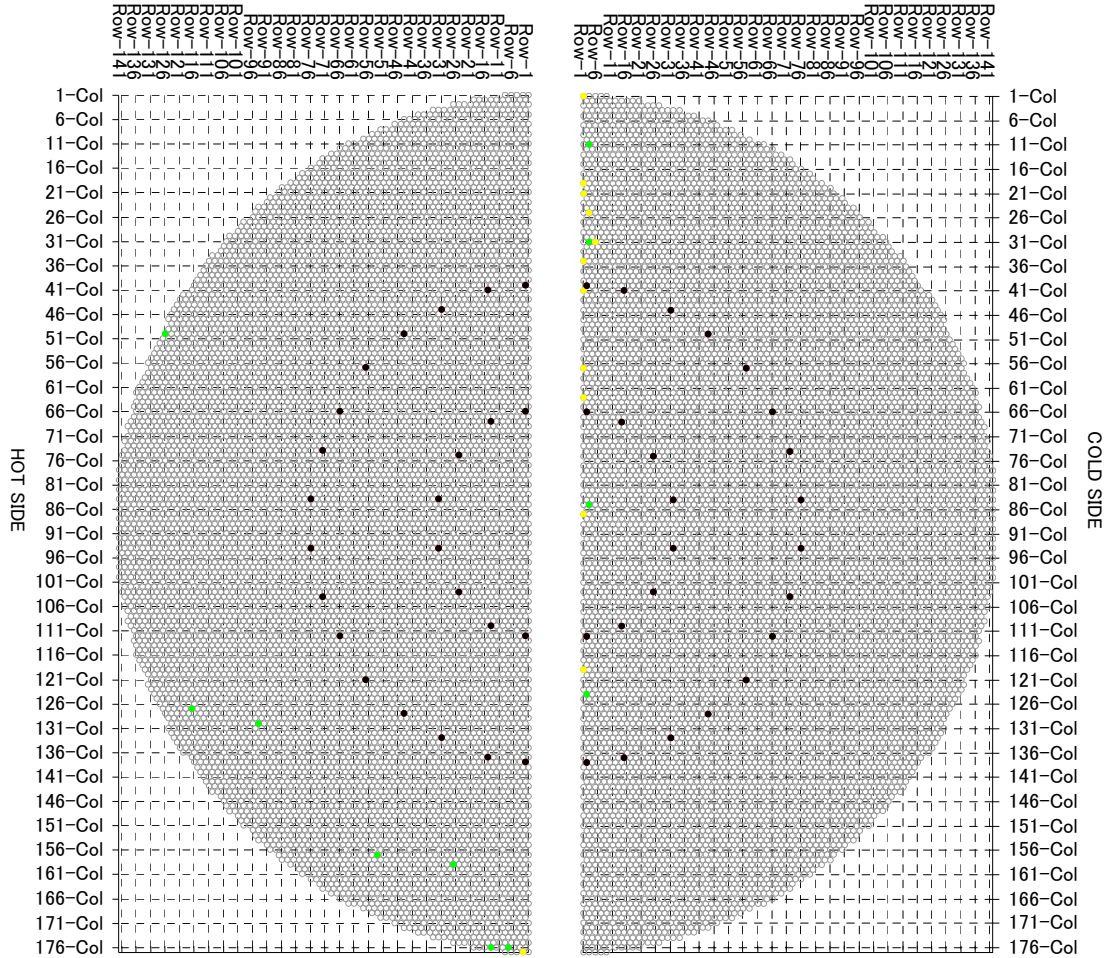
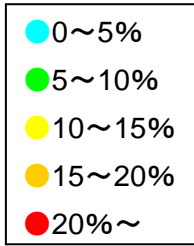
2A_#1TSP



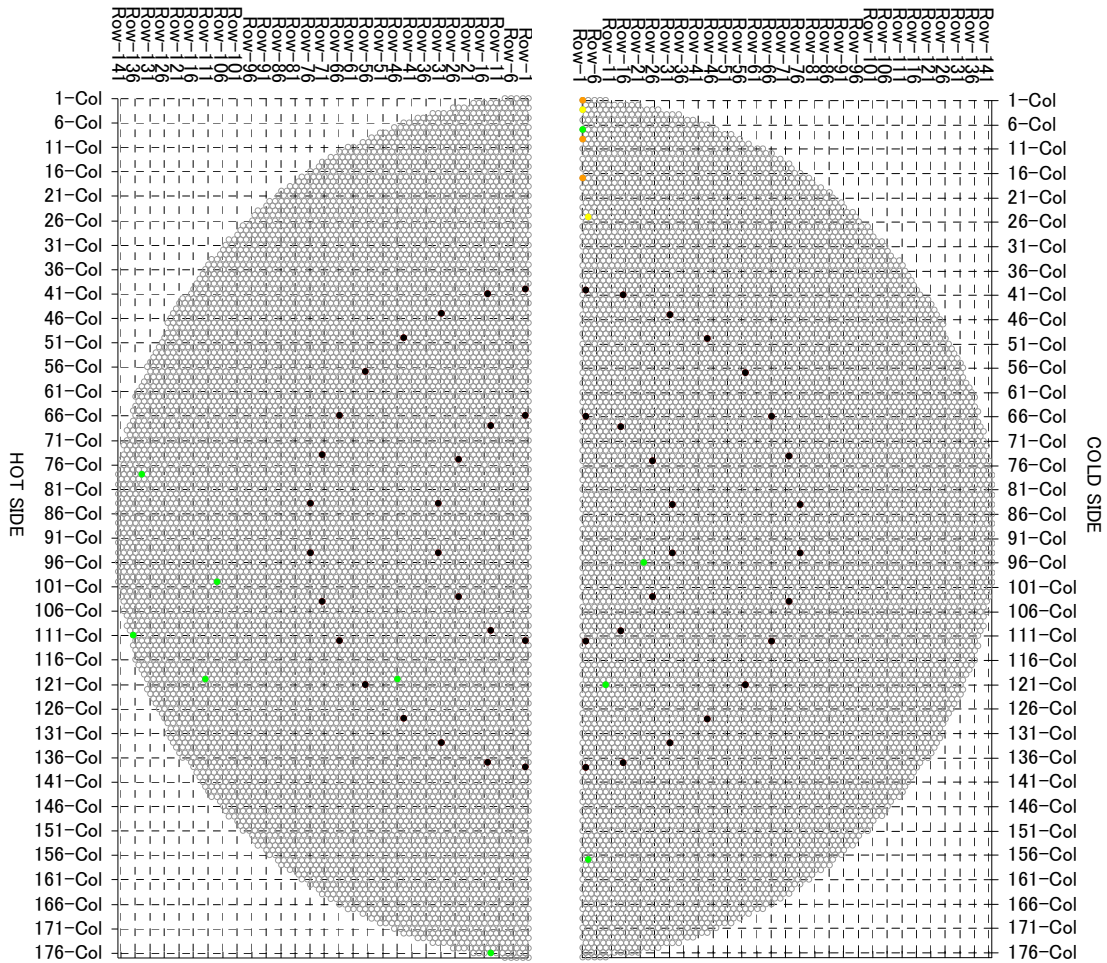
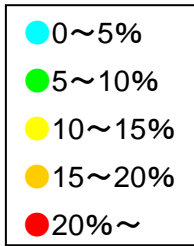
2A_#2TSP



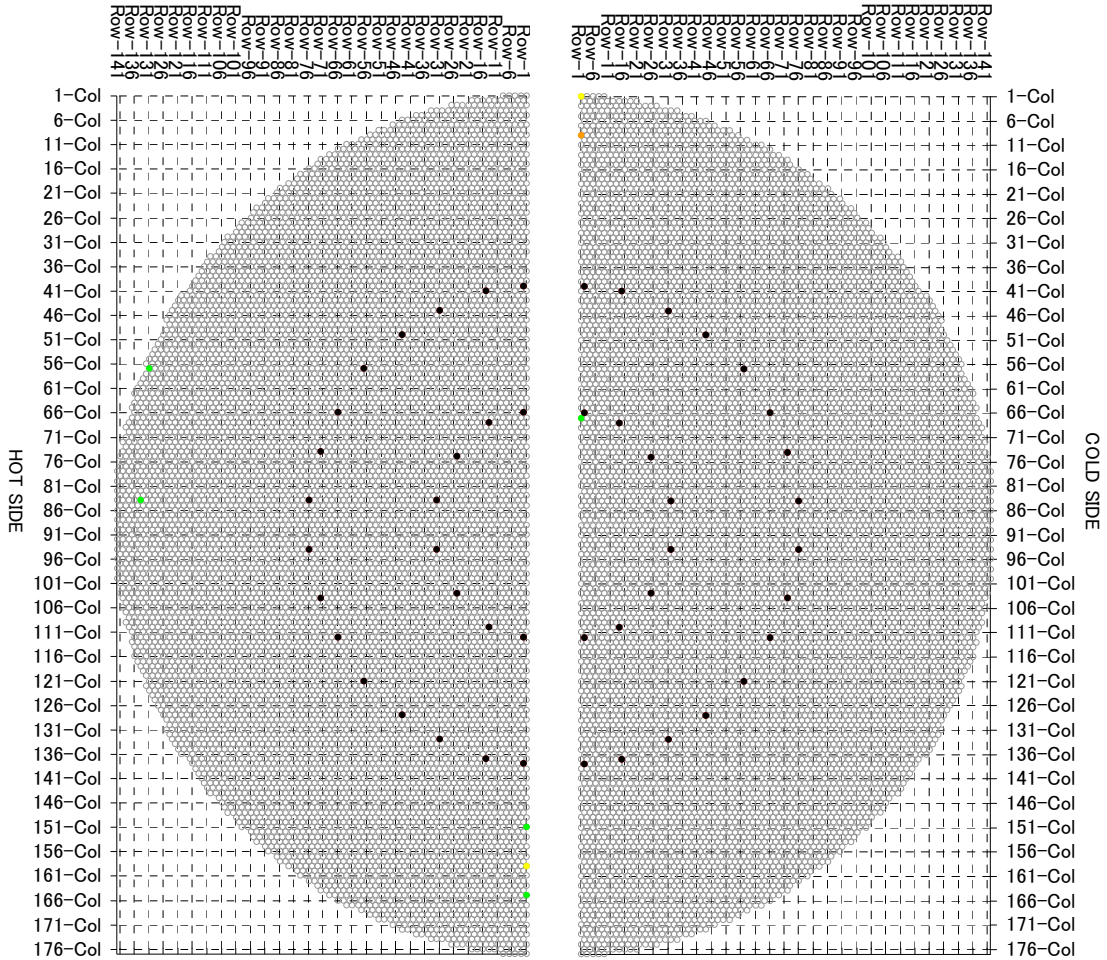
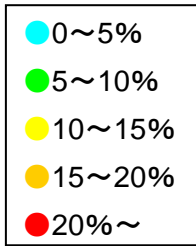
2A_#3TSP



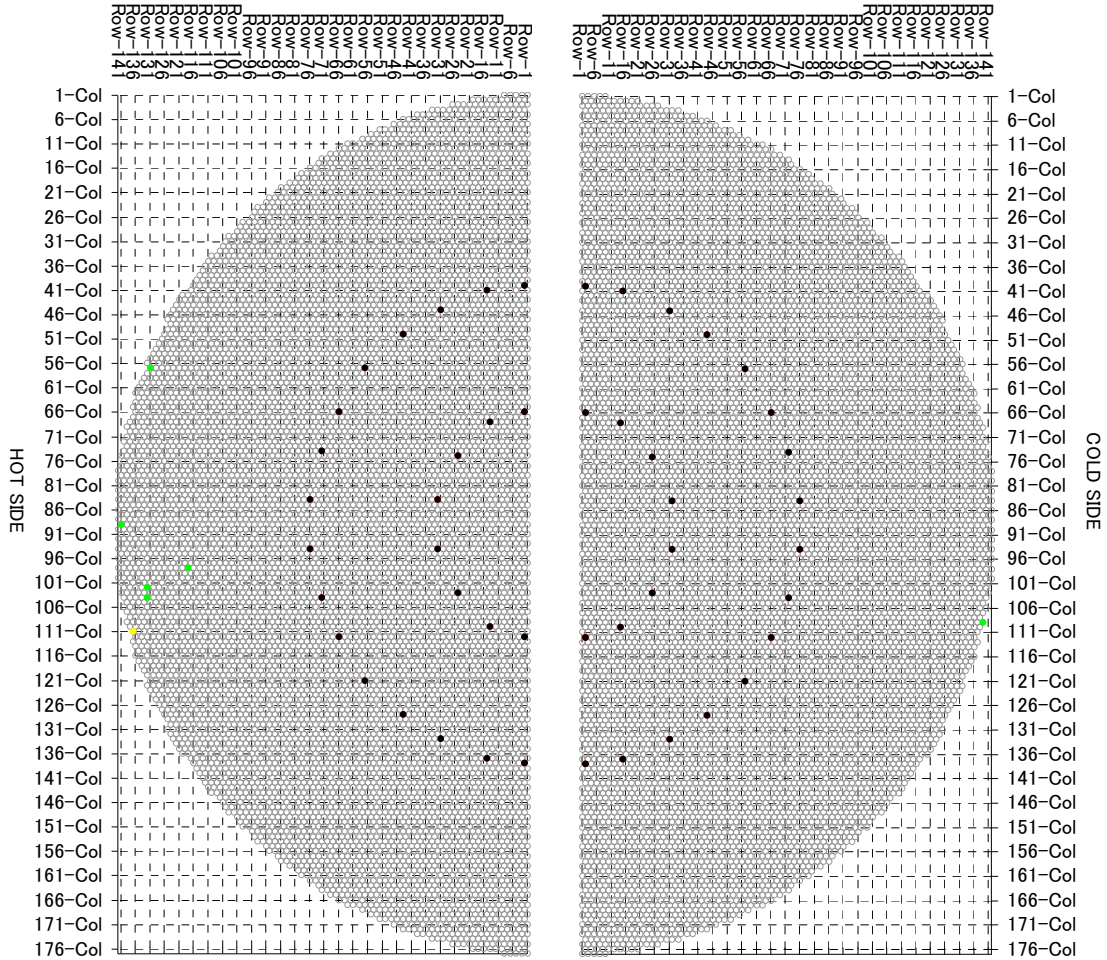
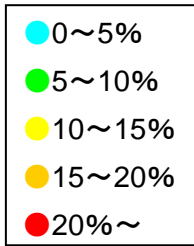
2A_#4TSP



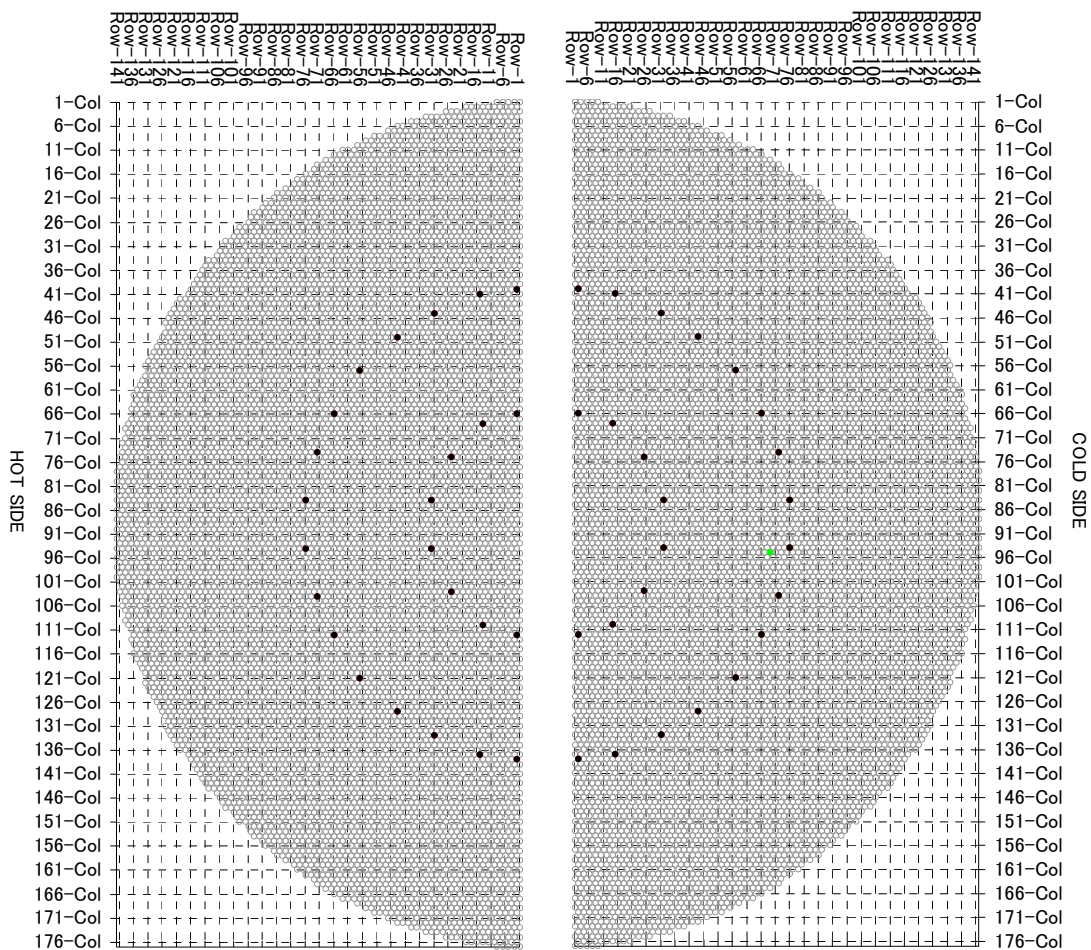
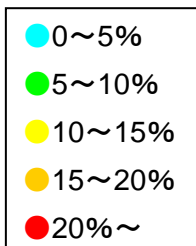
2A_#5TSP



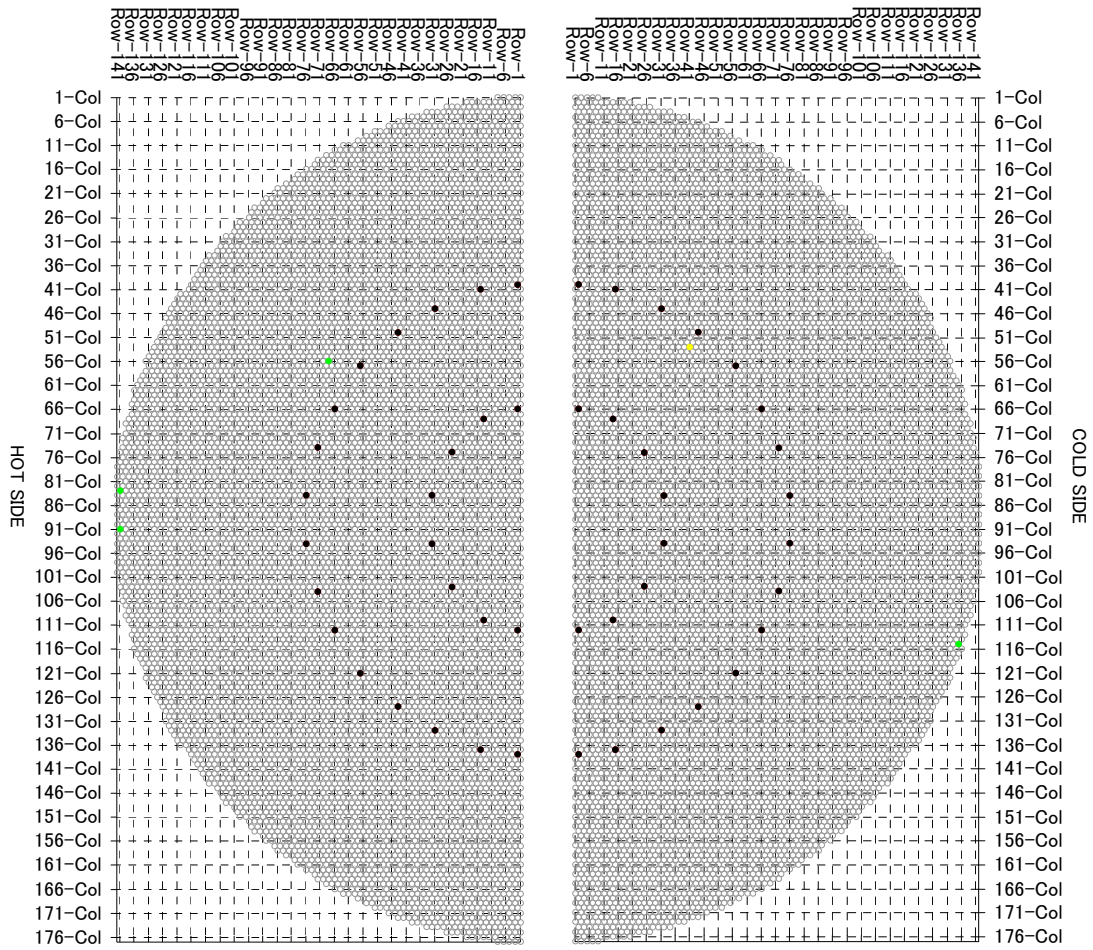
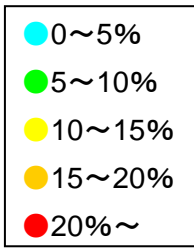
2A_#6TSP



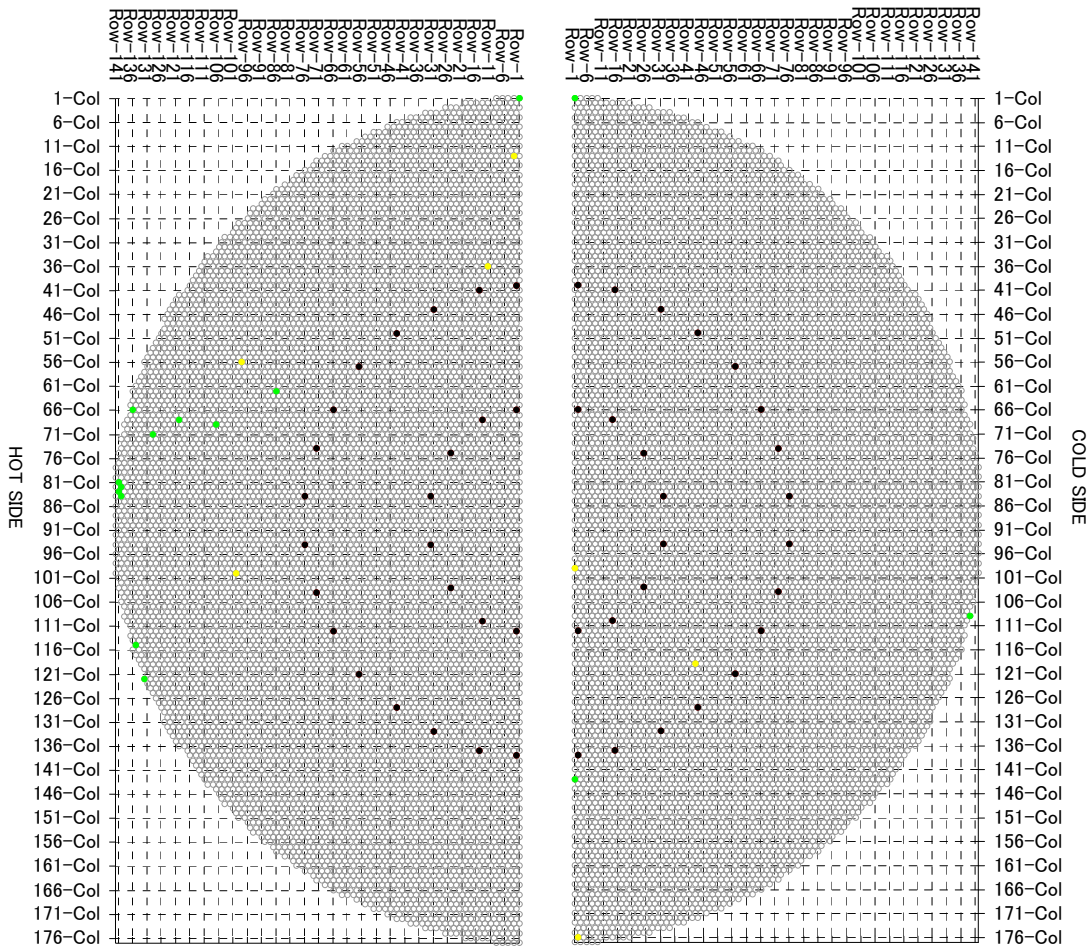
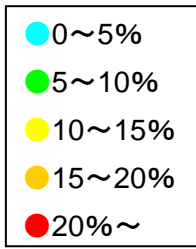
2A_#7TSP



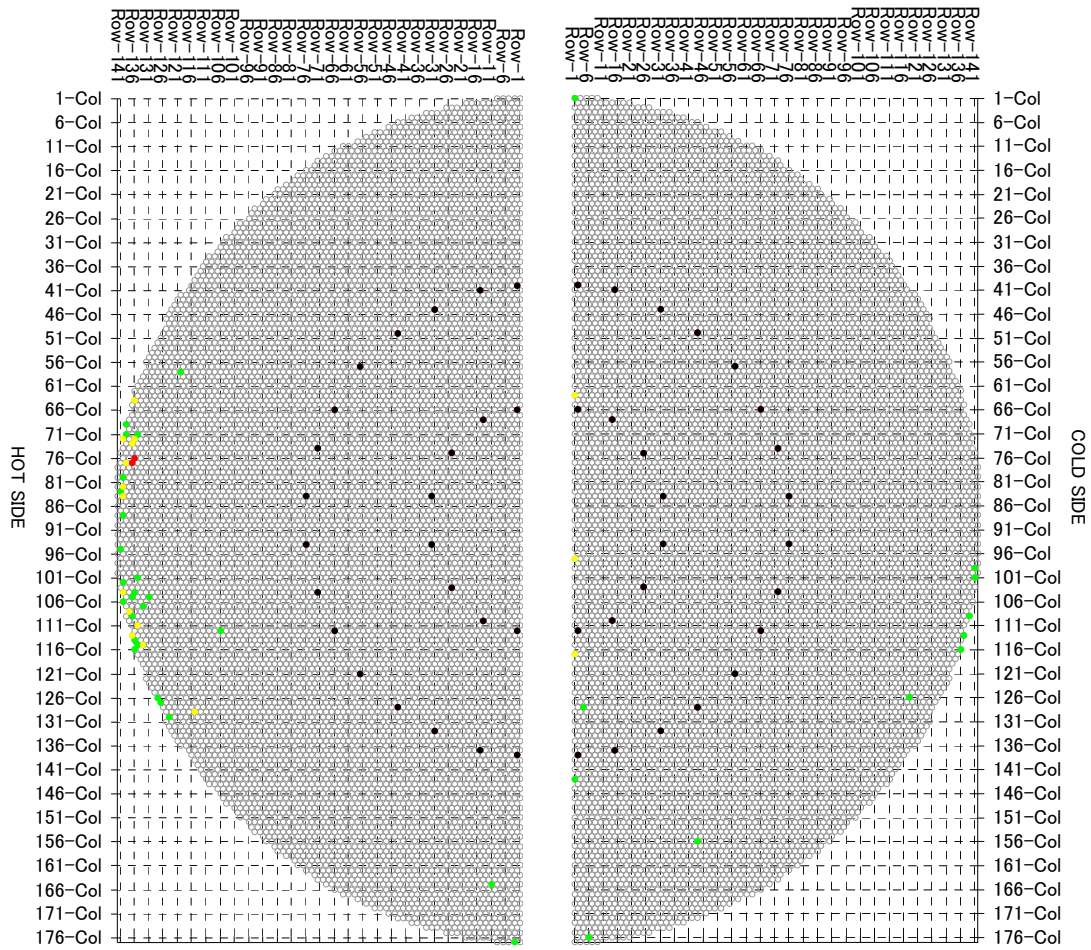
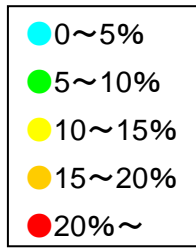
2B_#1TSP



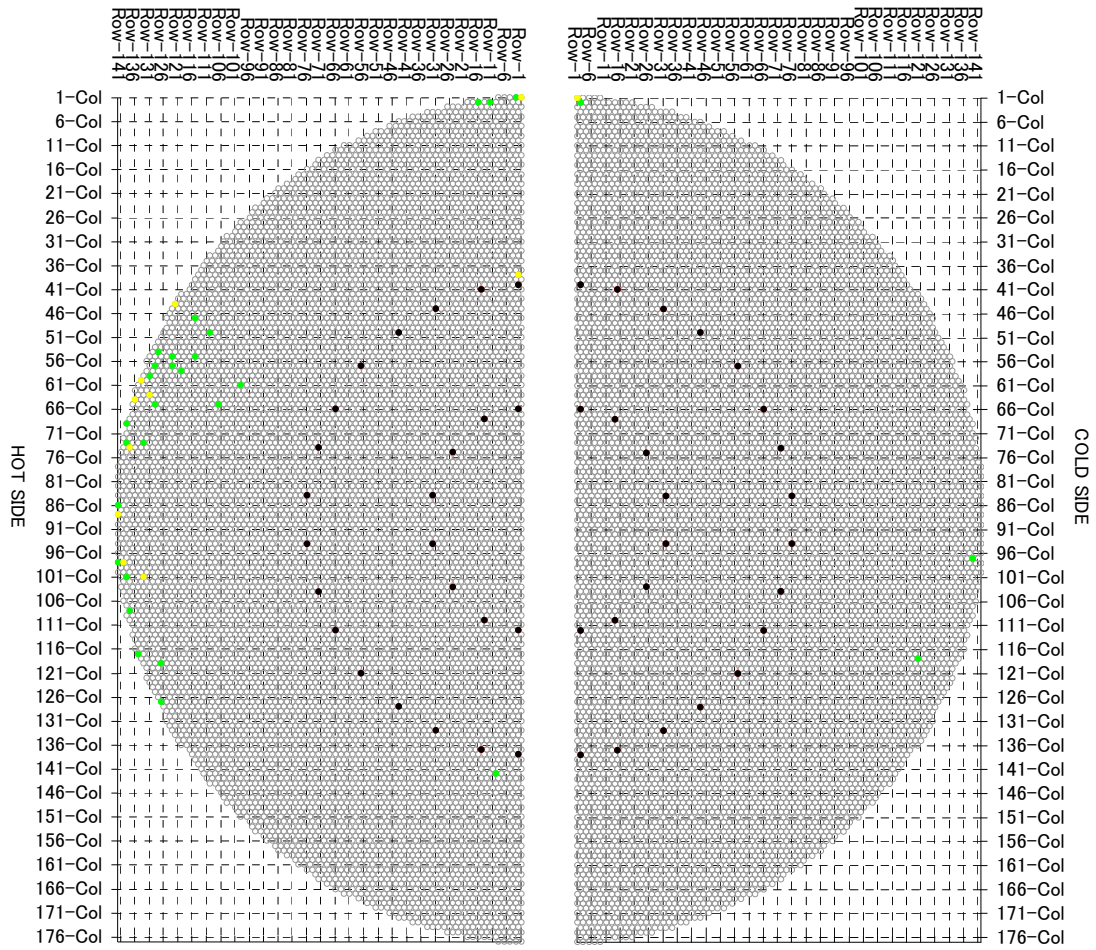
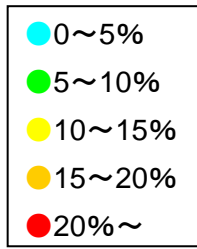
2B_#2TSP



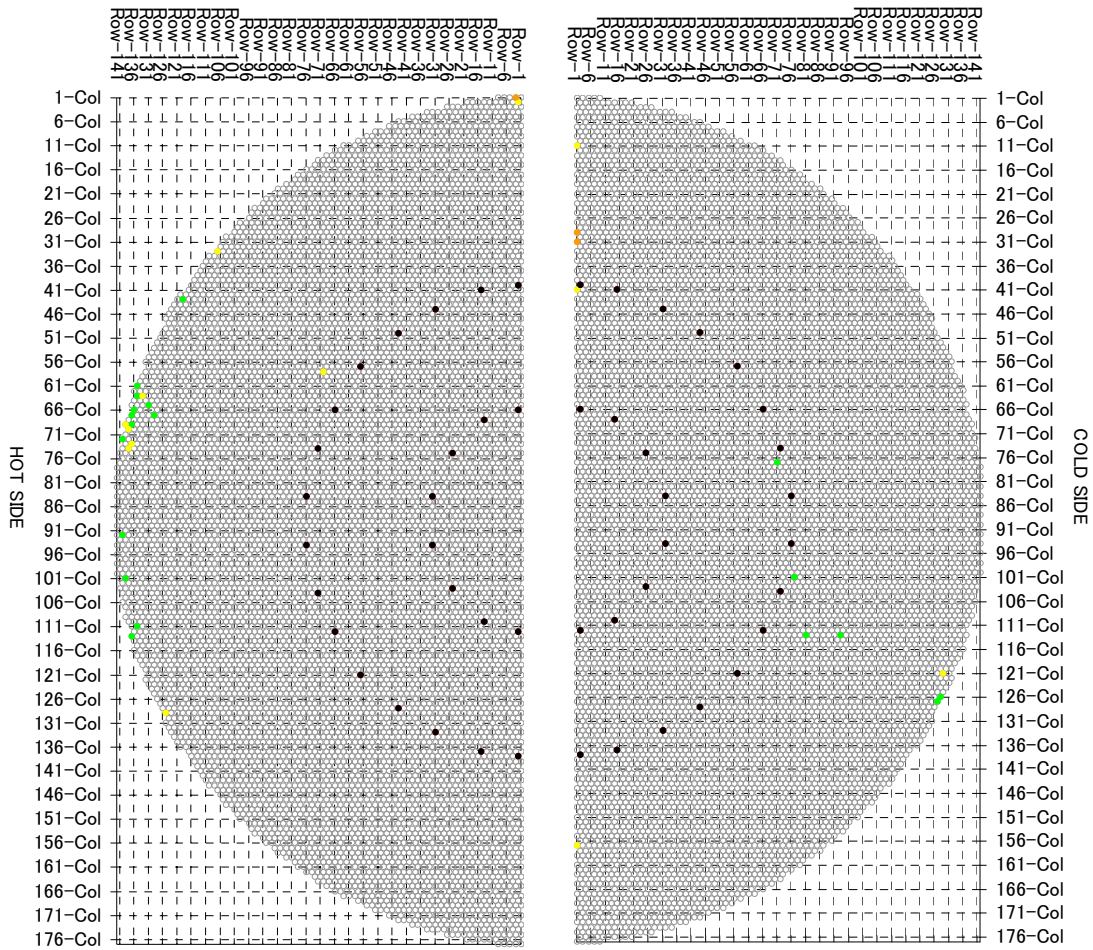
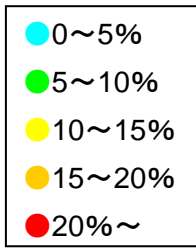
2B_#3TSP



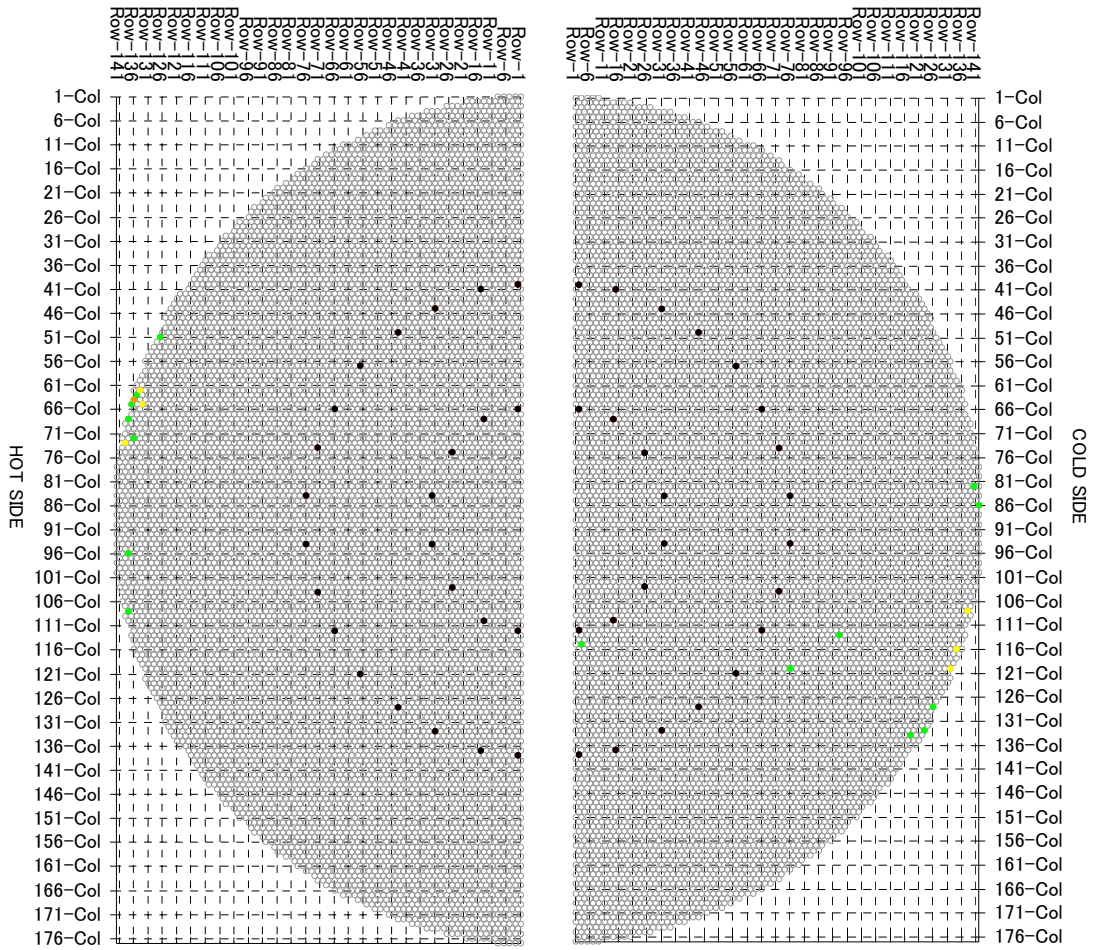
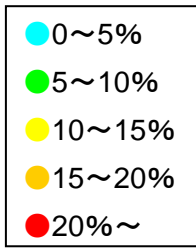
2B_#4TSP



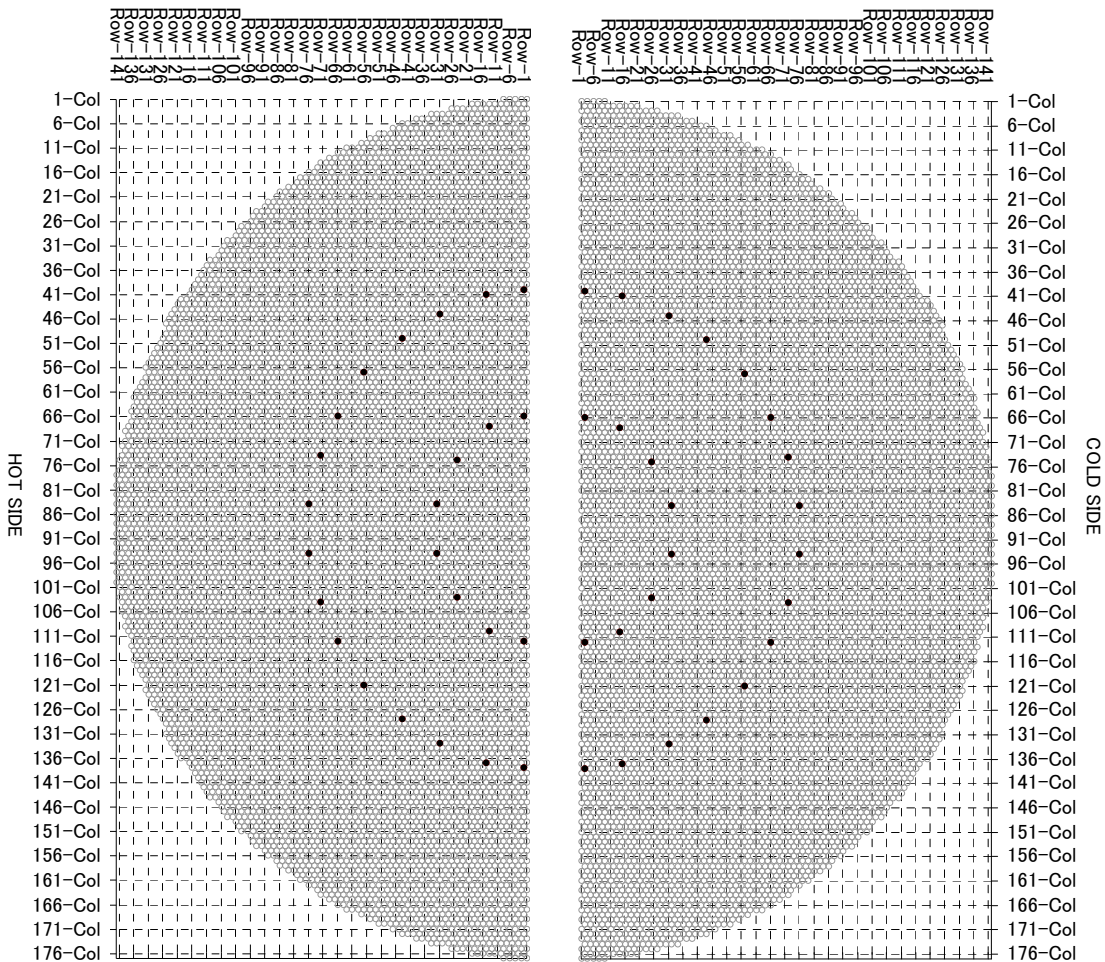
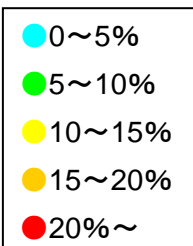
2B_#5TSP



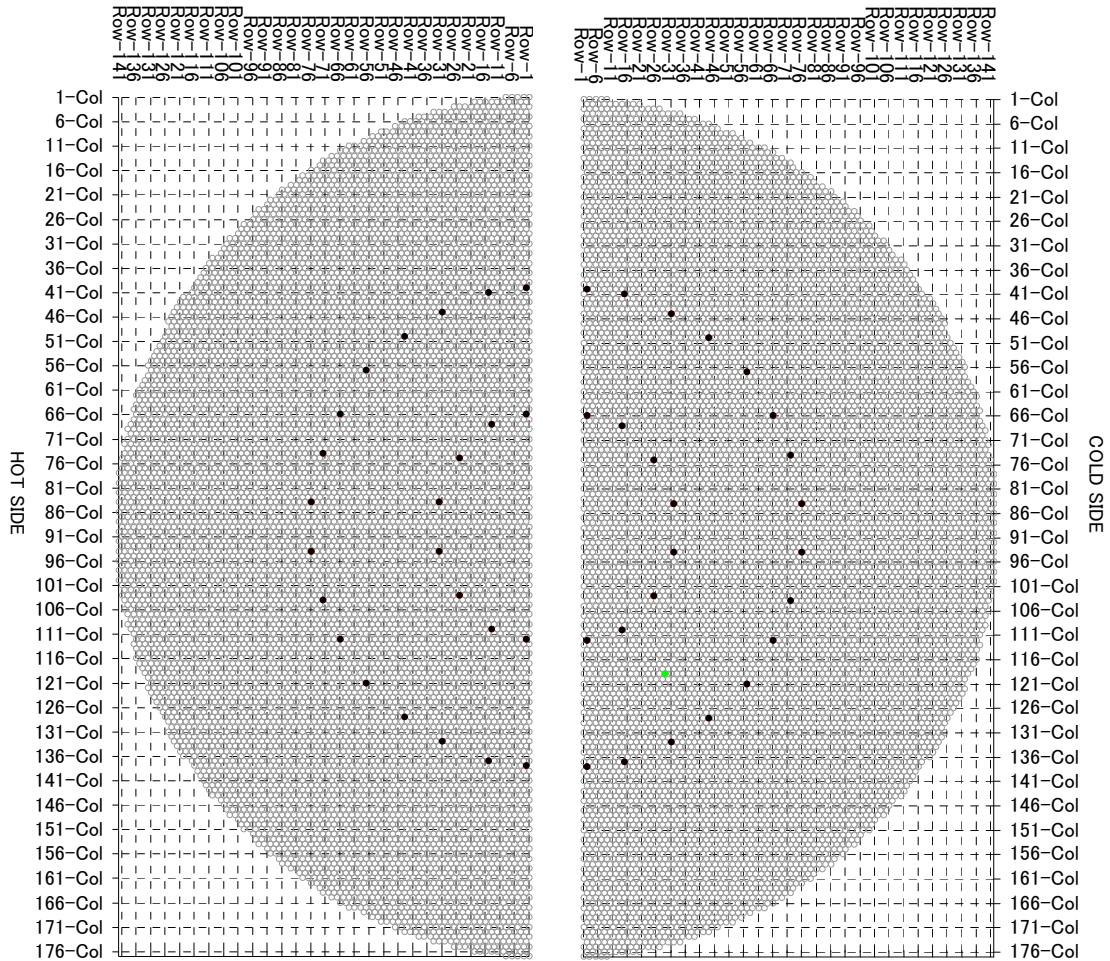
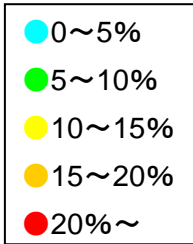
2B_#6TSP



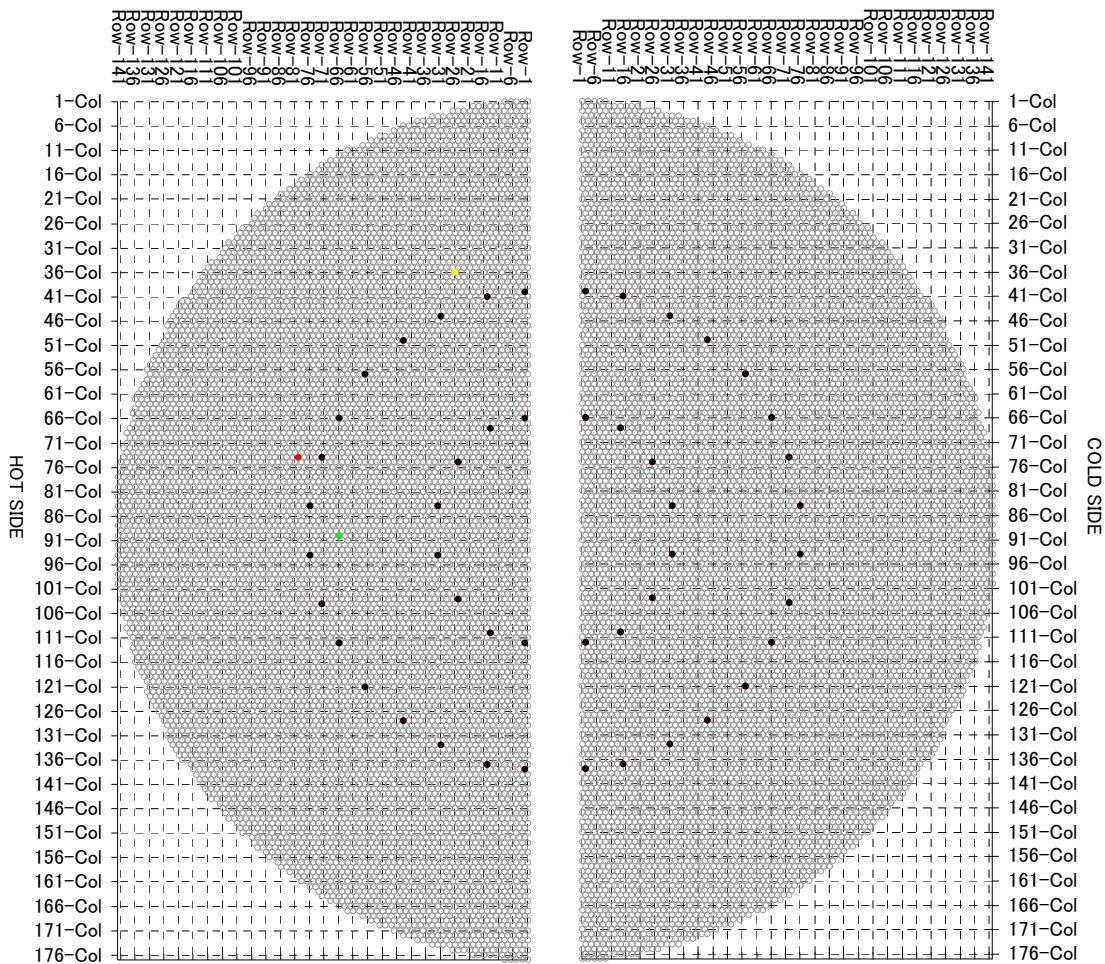
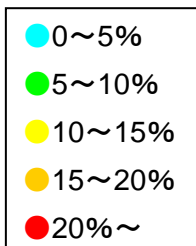
2B_#7TSP



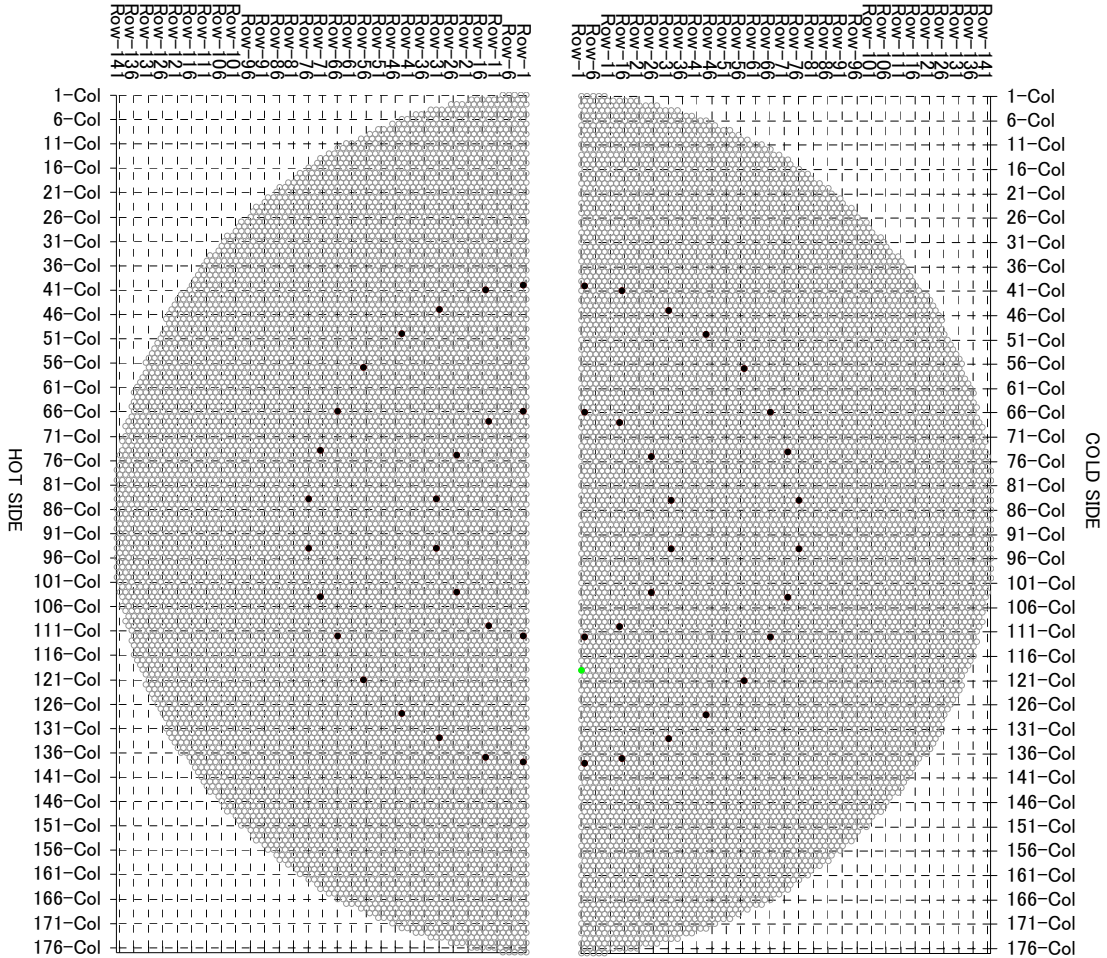
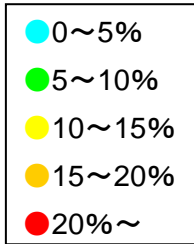
3A_#1TSP



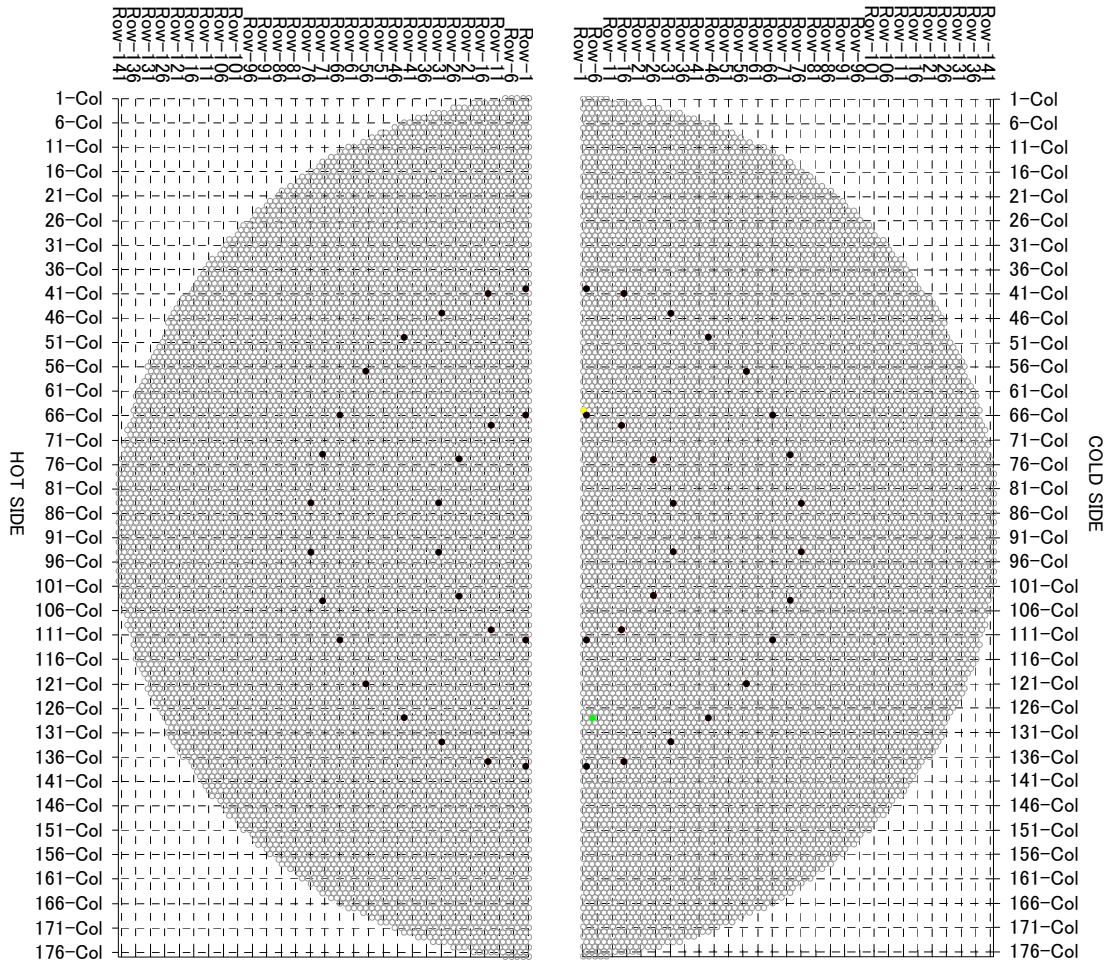
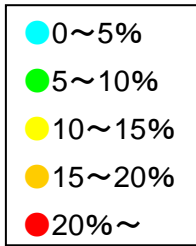
3A_#2TSP



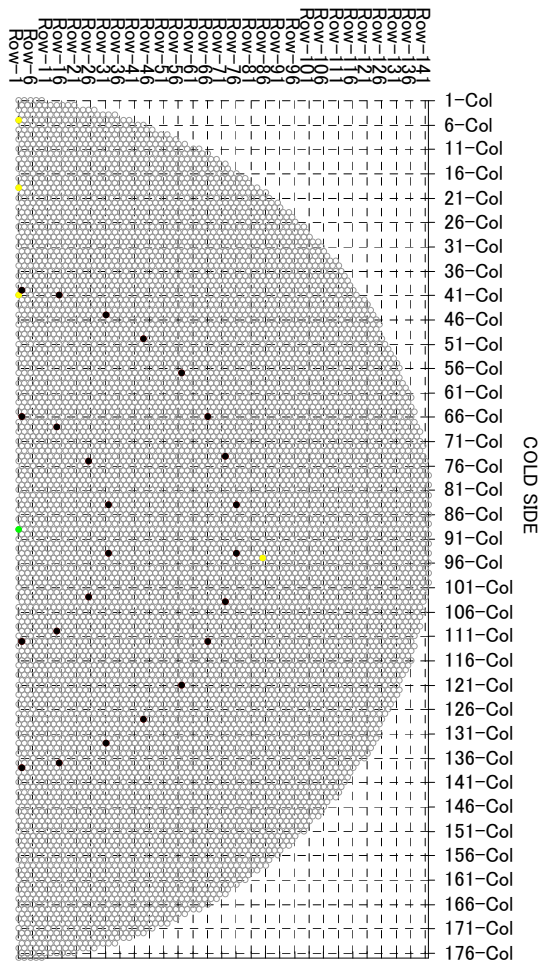
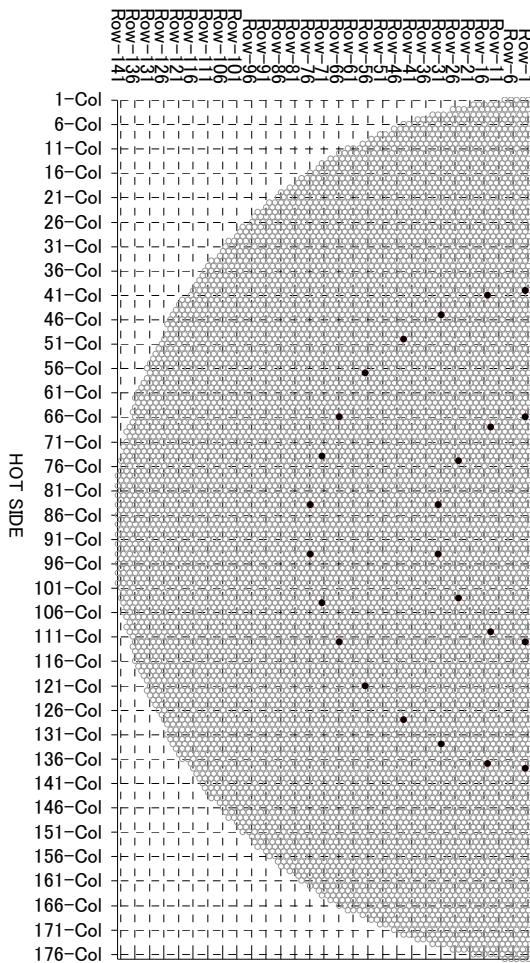
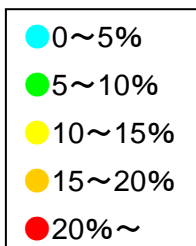
3A_#3TSP



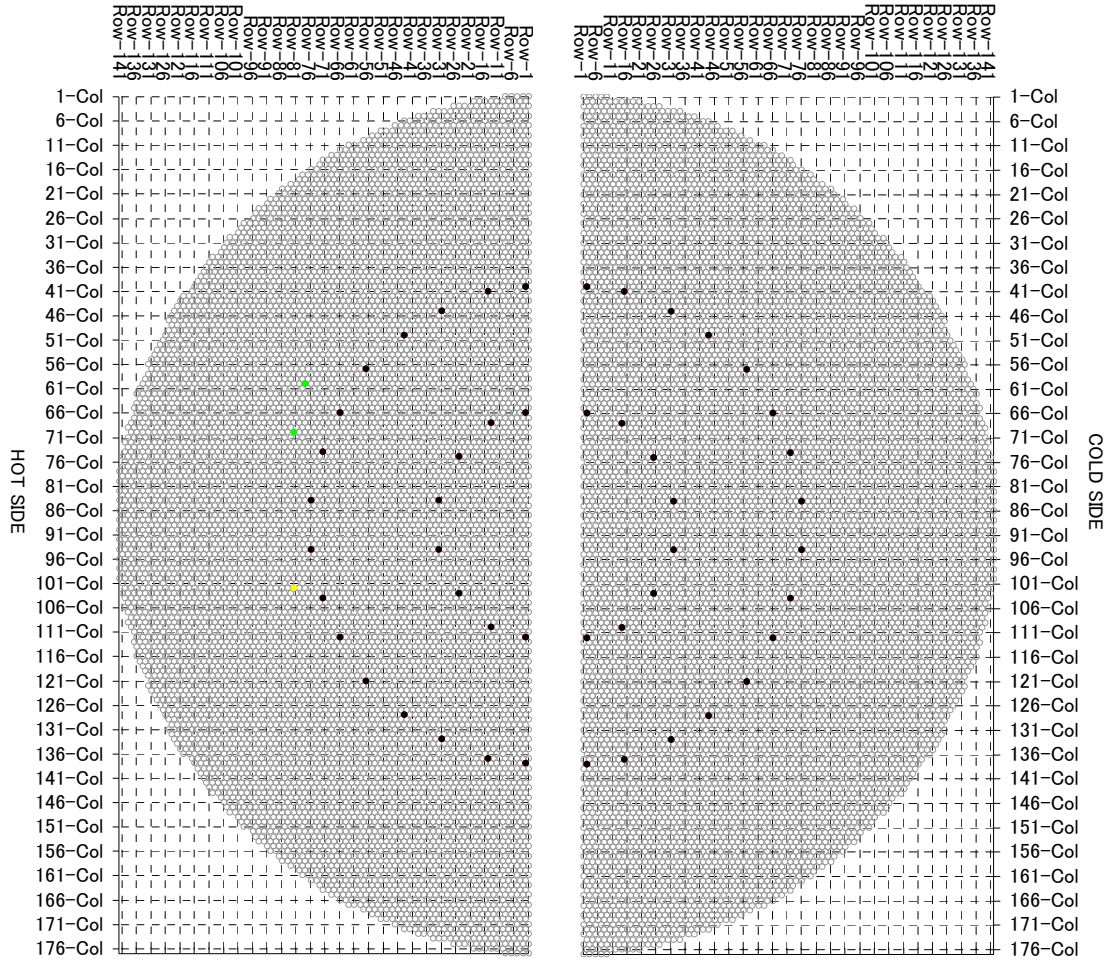
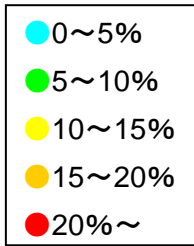
3A_#4TSP



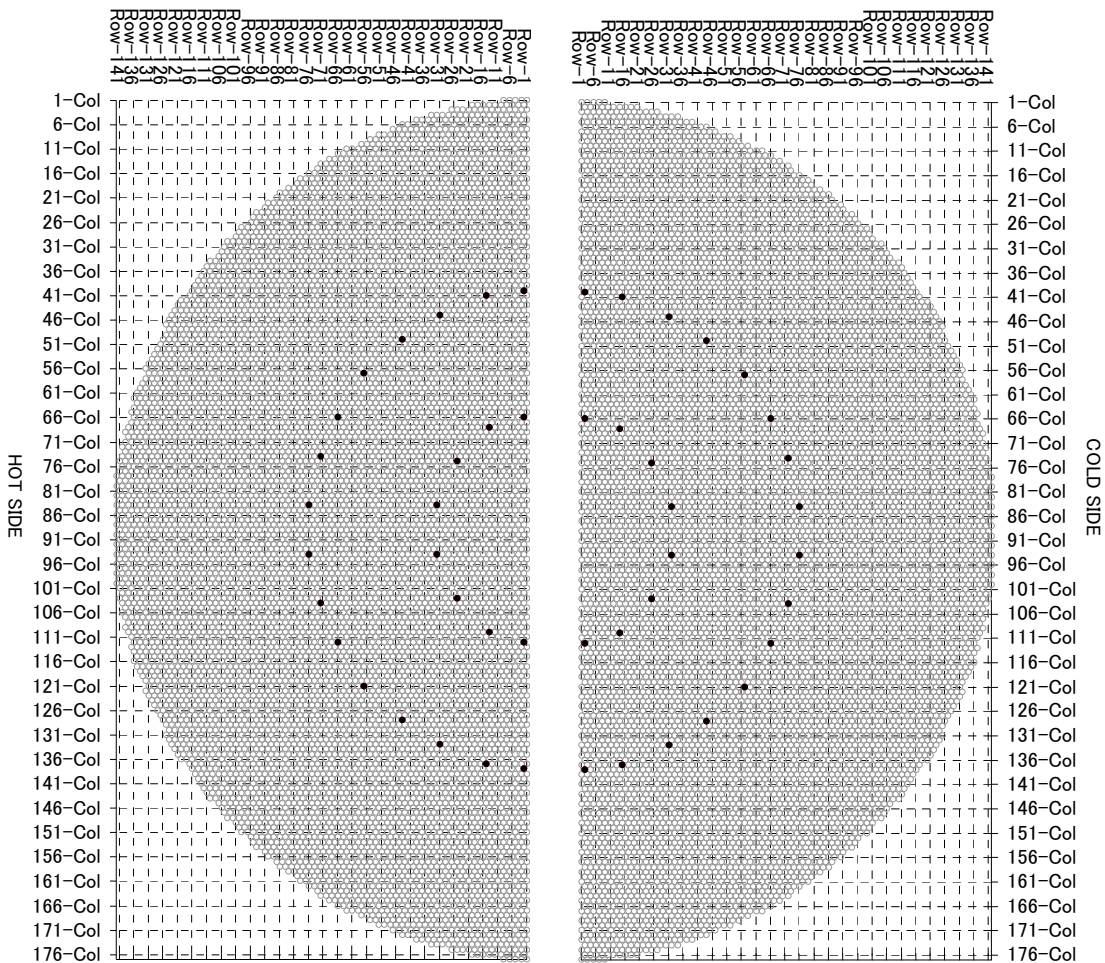
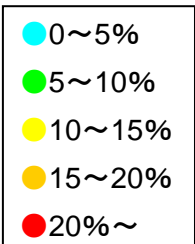
3A_#5TSP



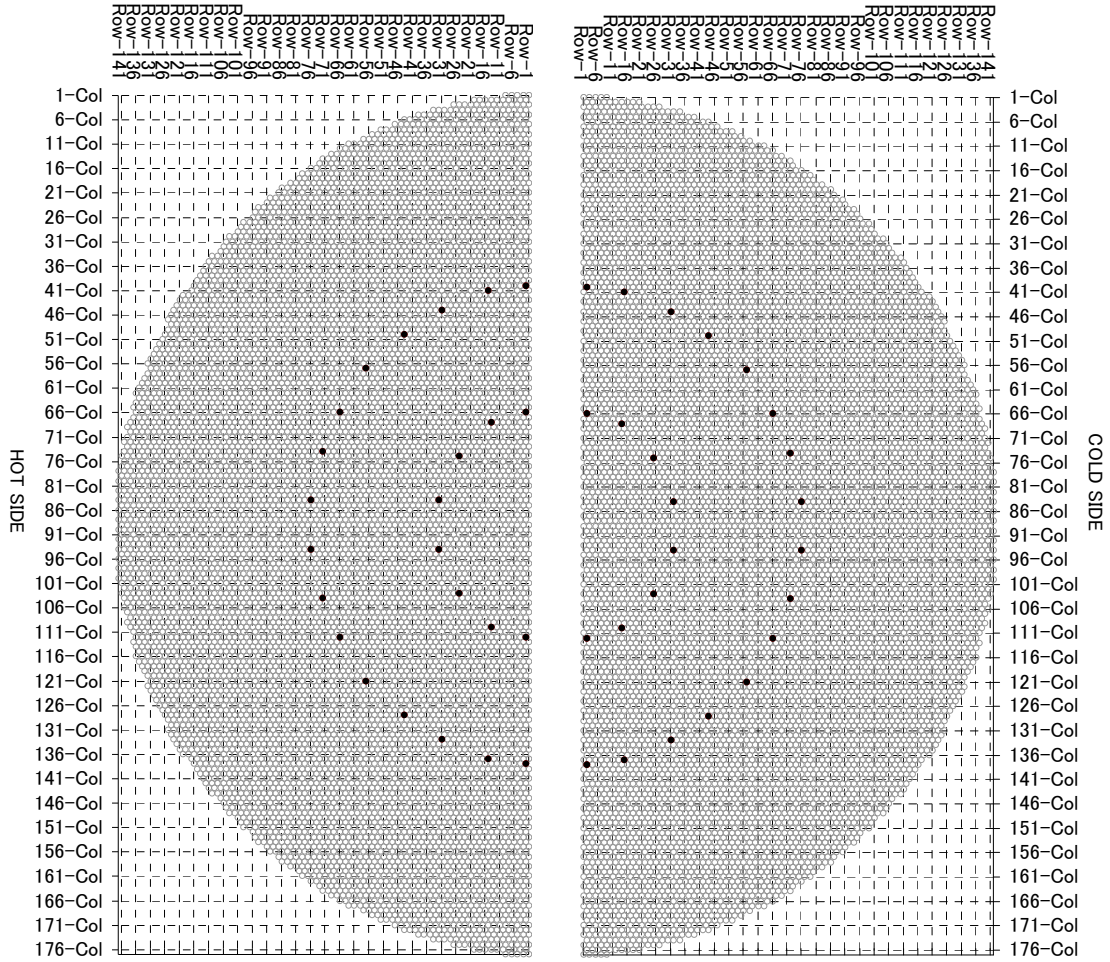
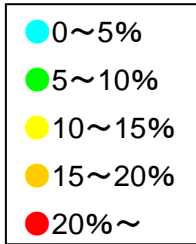
3A_#6TSP



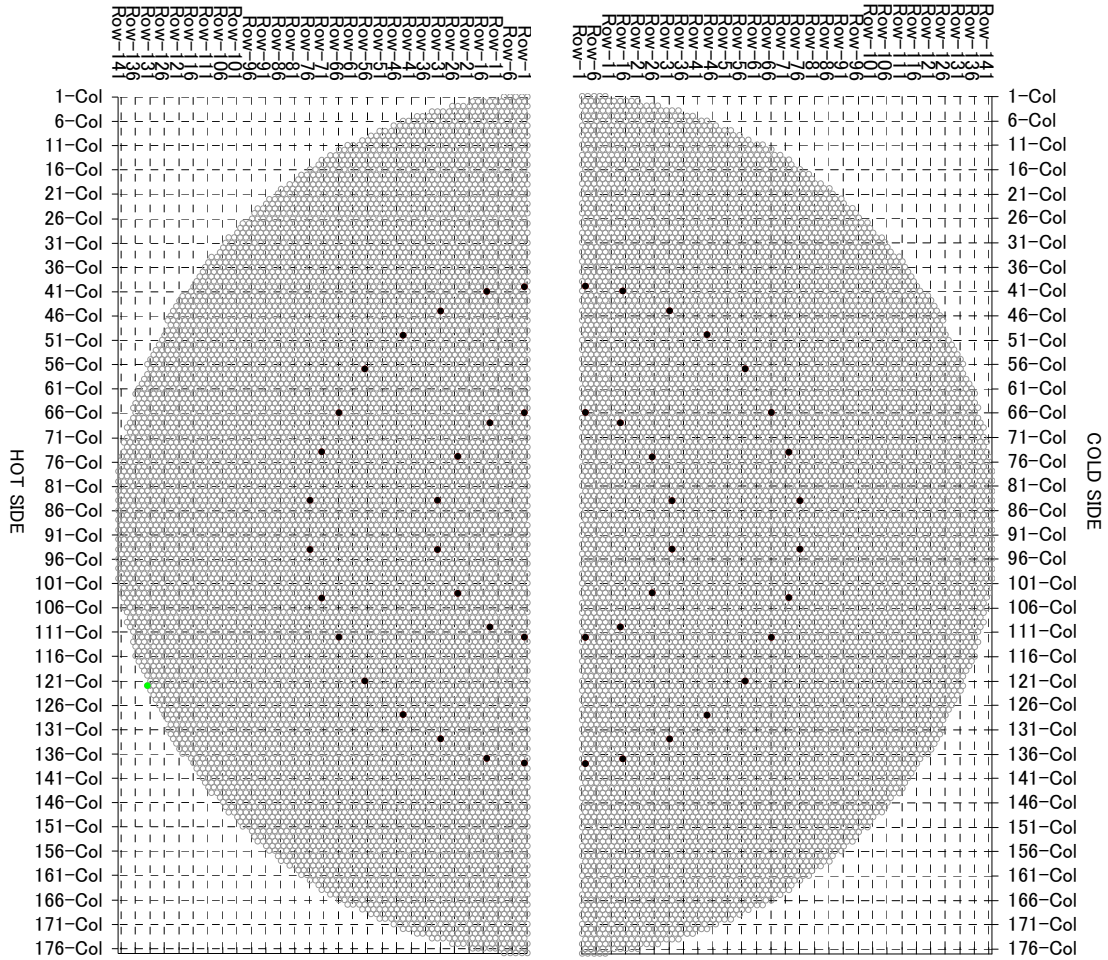
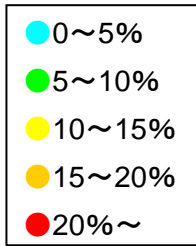
3A_#7TSP



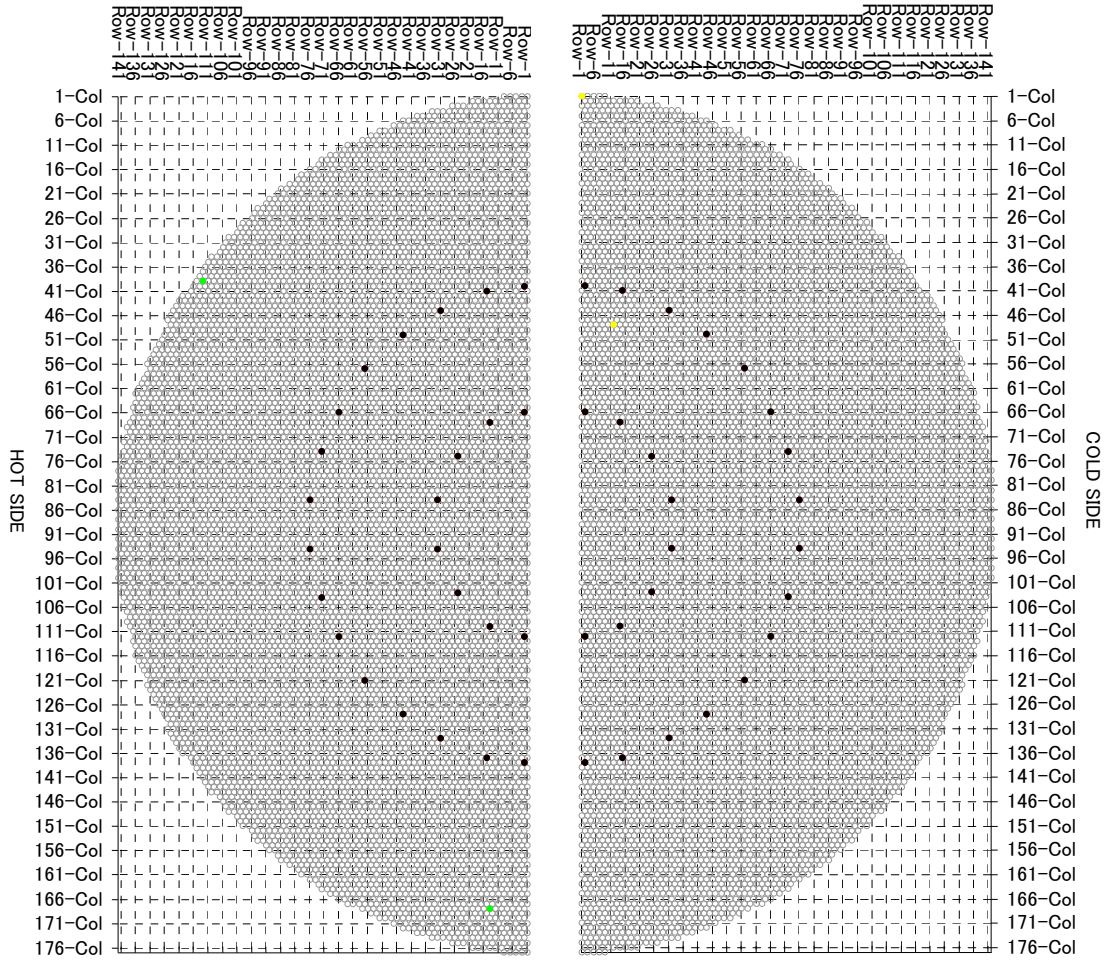
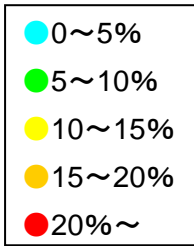
3B_#1TSP



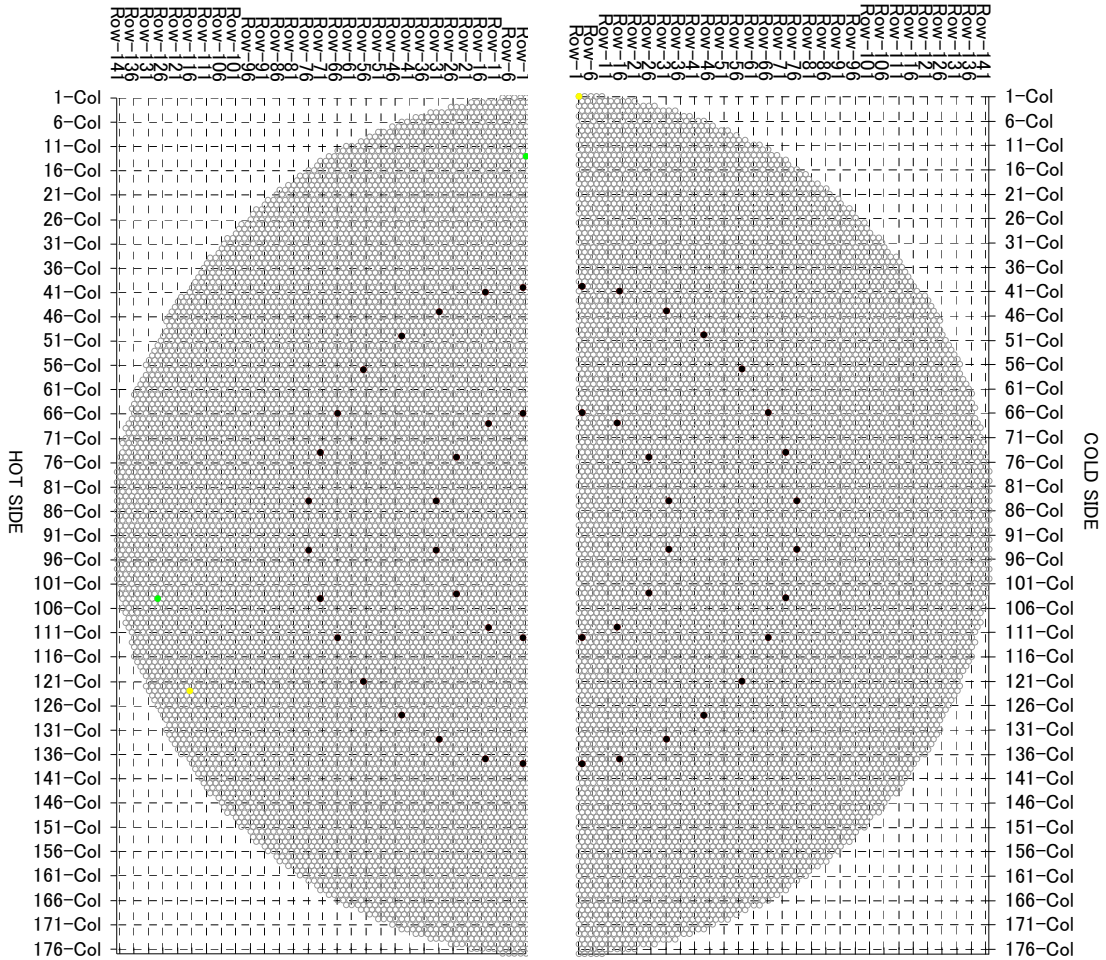
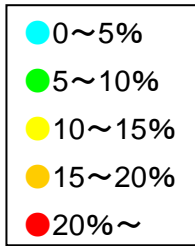
3B_#2TSP



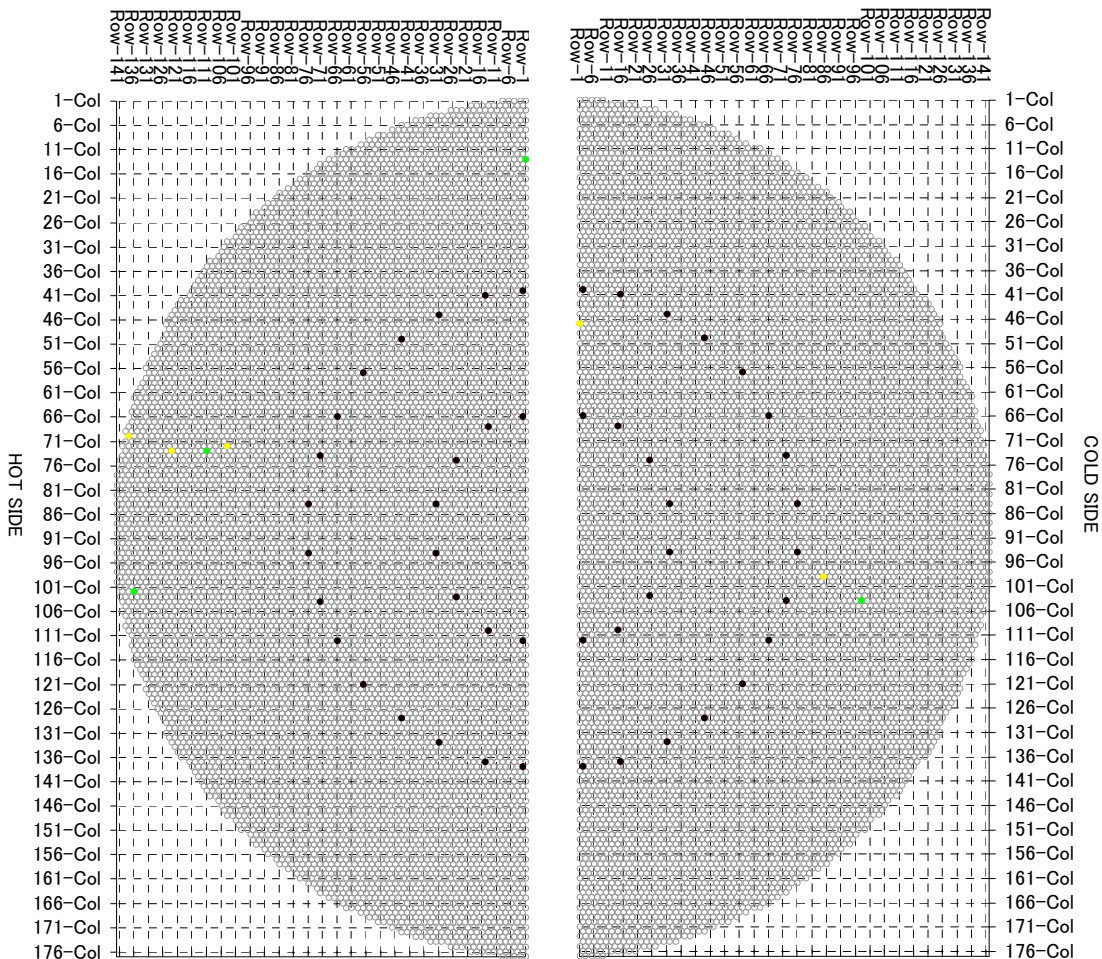
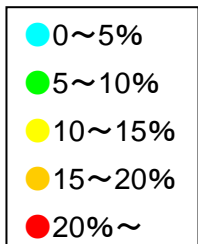
3B_#3TSP



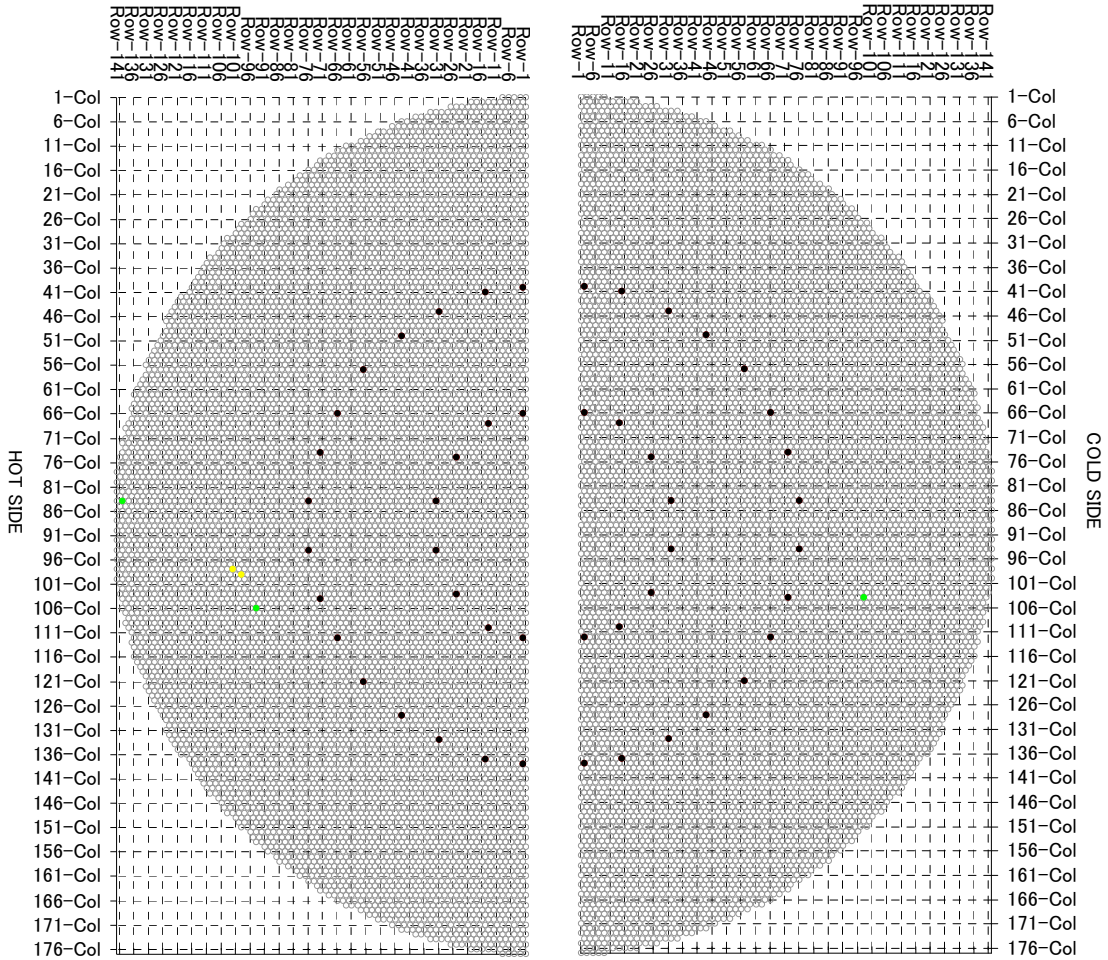
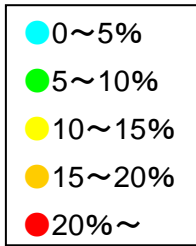
3B_#4TSP



3B_#5TSP



3B_#6TSP



3B_#7TSP



Appendix-2 Attachment-2
Flow velocity data of analysis by ATHOS/SGAP for Unit-2/3



1. Introduction

This attachment provides the data of flow velocity above tube sheet and at each TSPs analyzed by ATHOS/SGAP computer code.

2. Flow velocity data

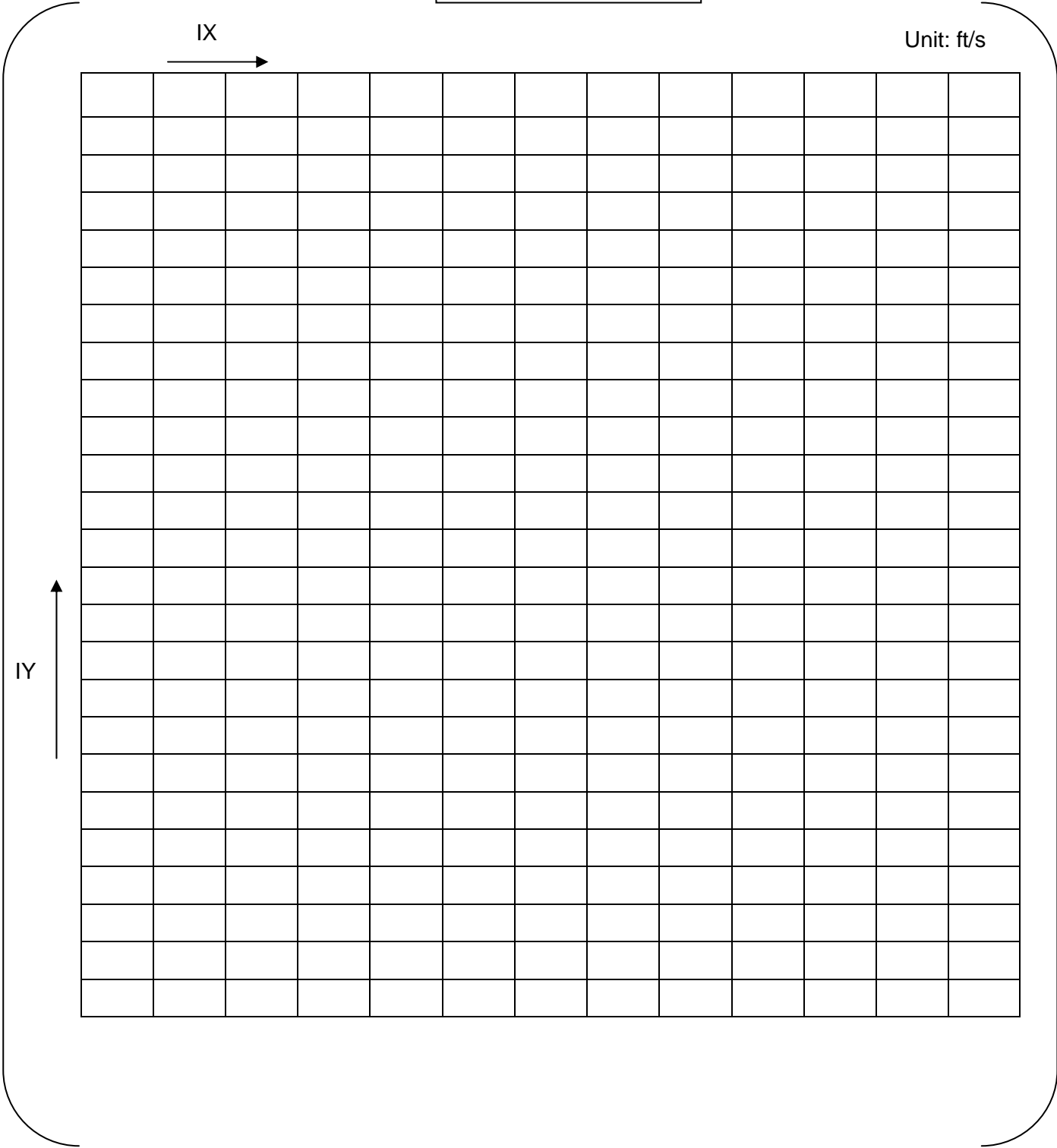
The following tables provide the data of flow velocity above tube sheet and at each TSPs (#1 ~#7TSP). These data indicate superficial velocities in horizontal sections. The directions of these velocities are shown in figs. 5-24~5-31 in Appendix-2. Symbols IX and IY show the position of cells in horizontal sections (shown in following figure).



Position of cells

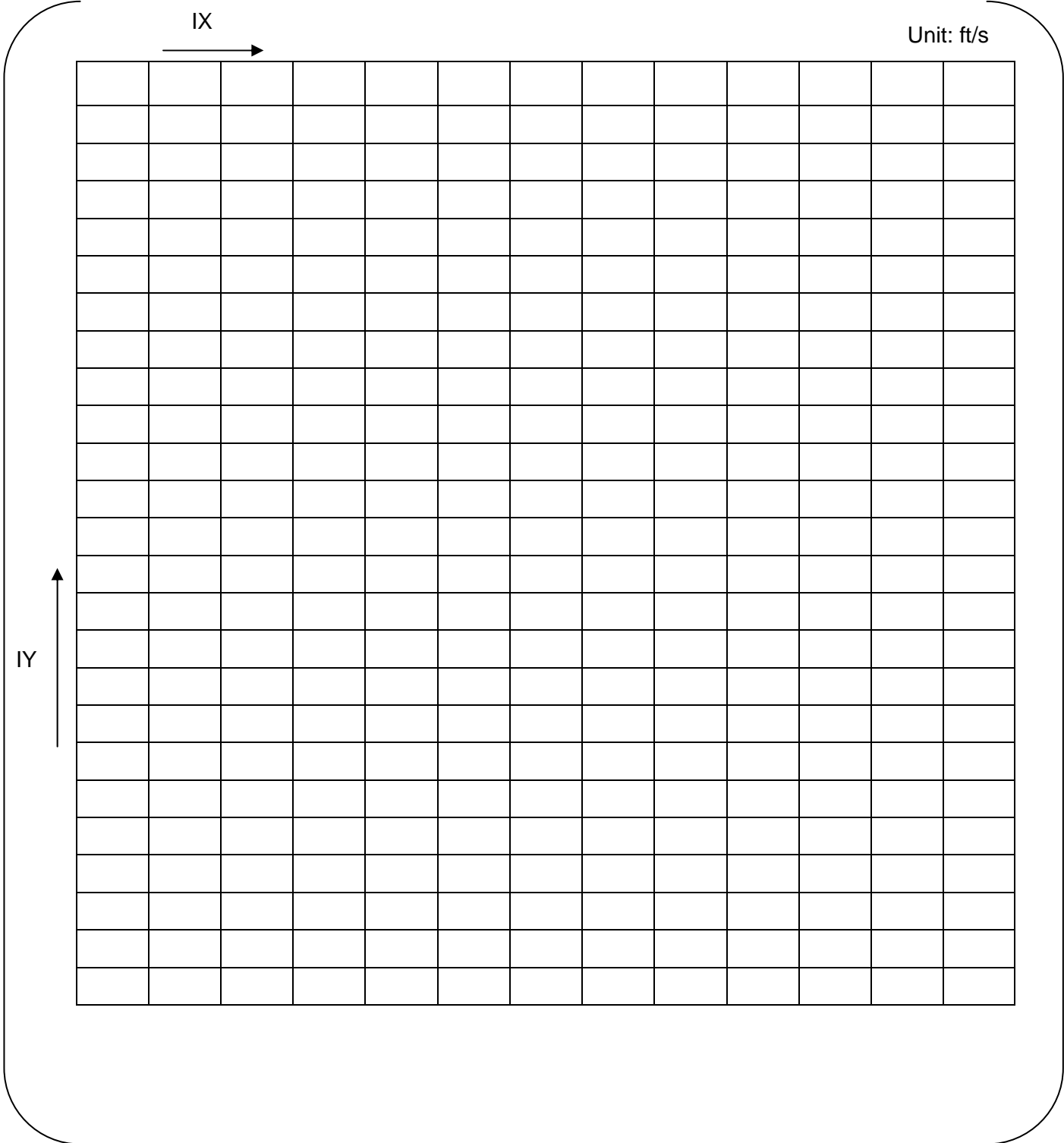


Velocity at #1TSP (1/2)



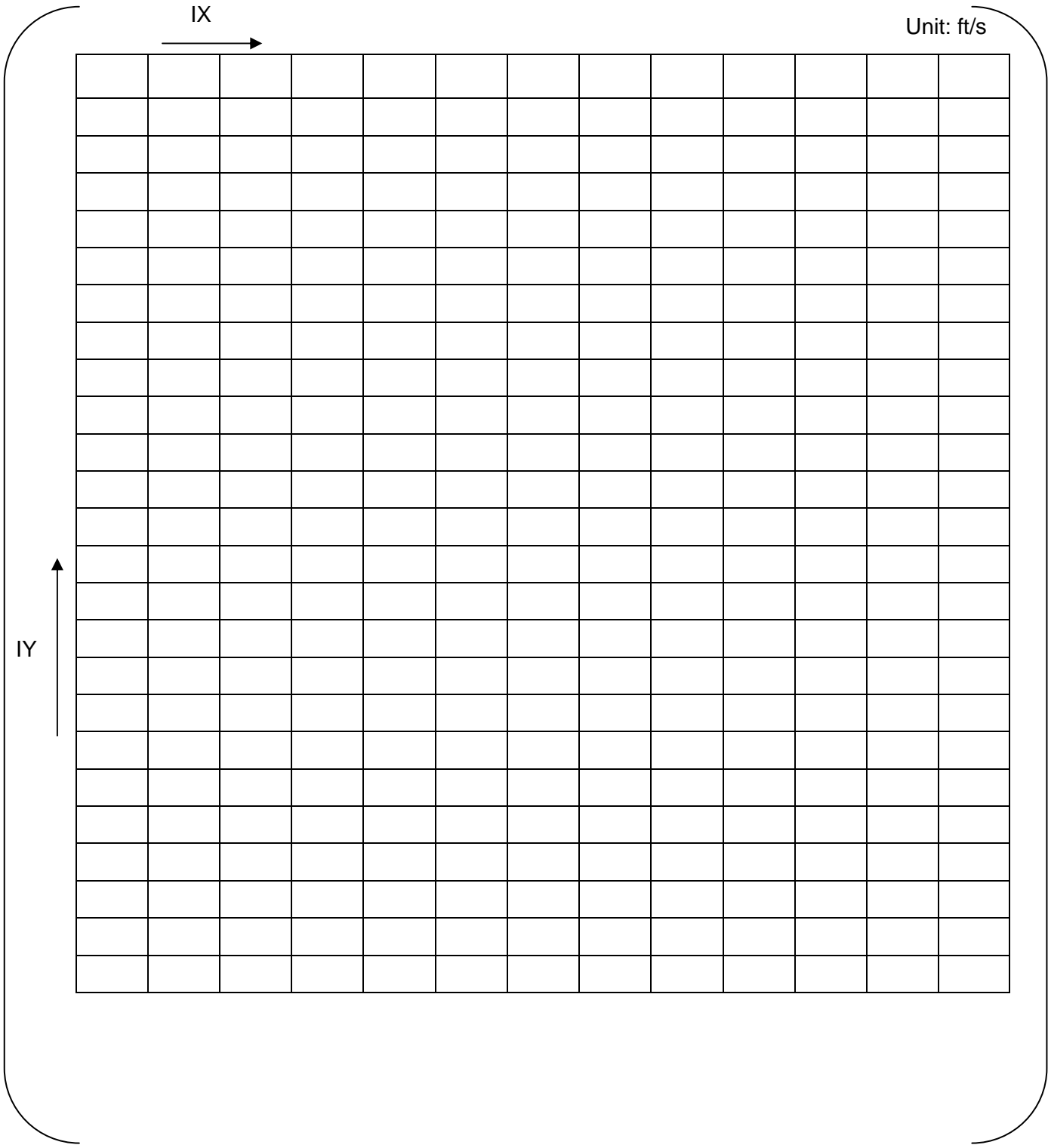


Velocity at #1TSP (2/2)



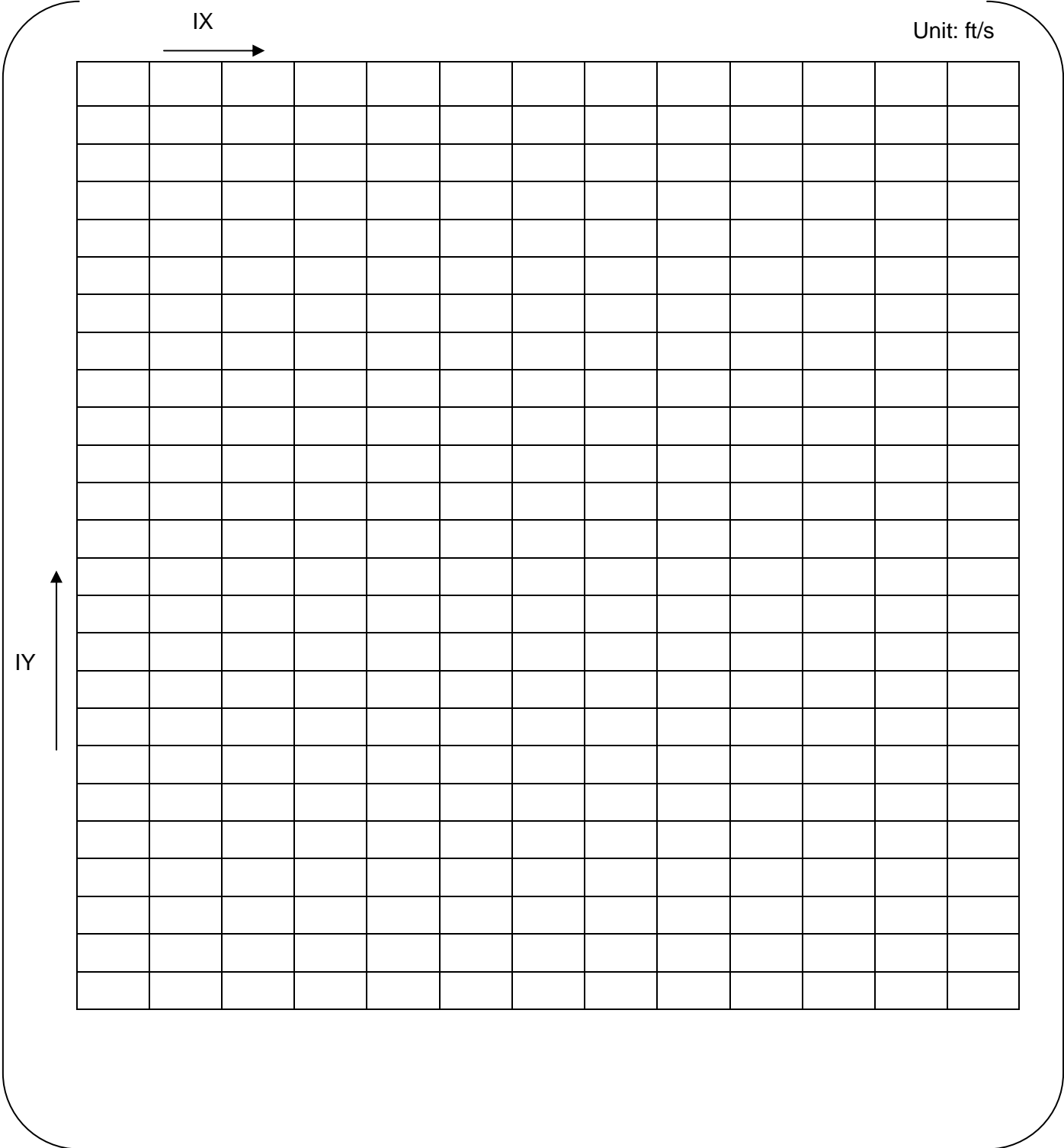


Velocity at #2TSP (1/2)



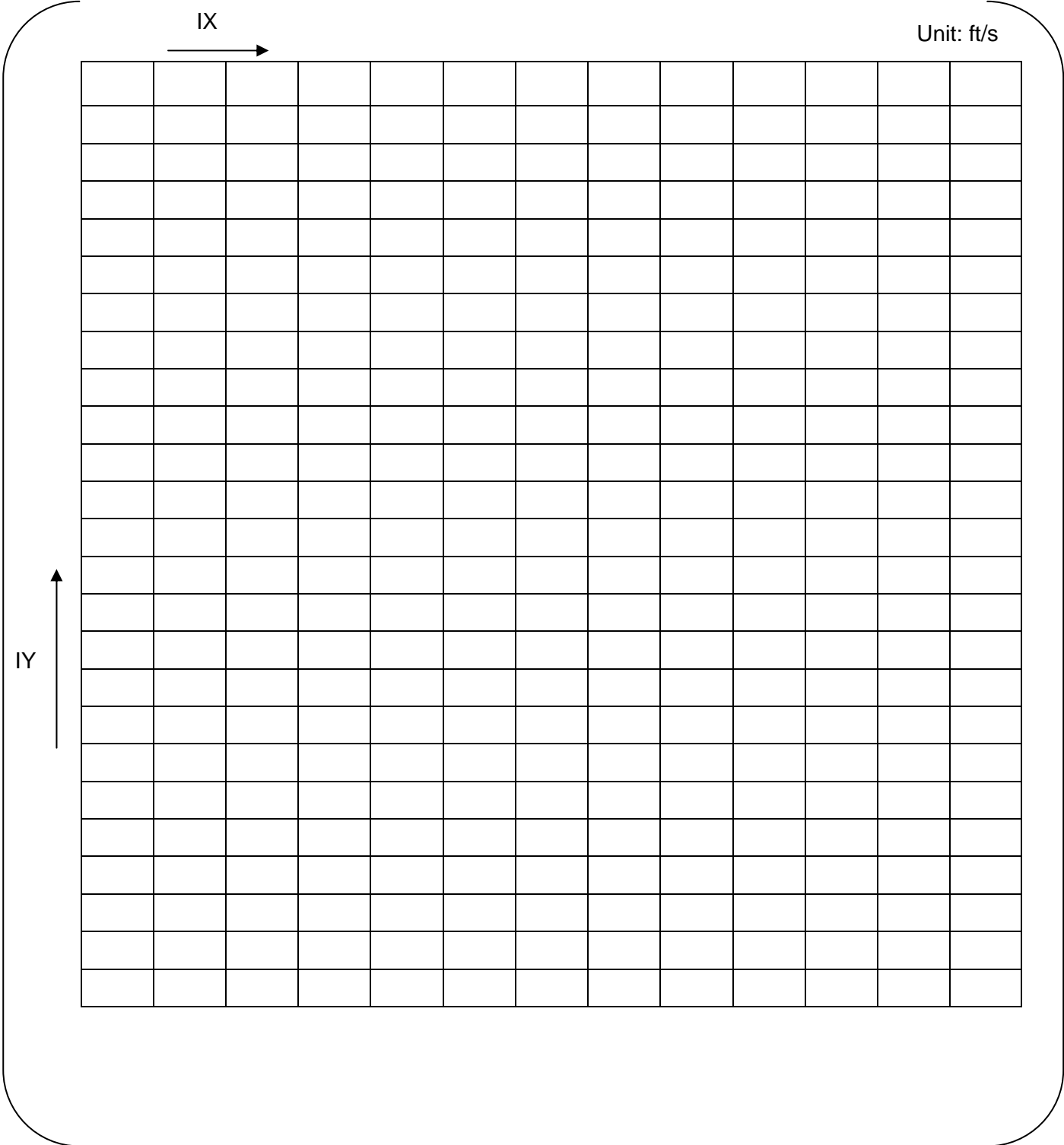


Velocity at #2TSP (2/2)



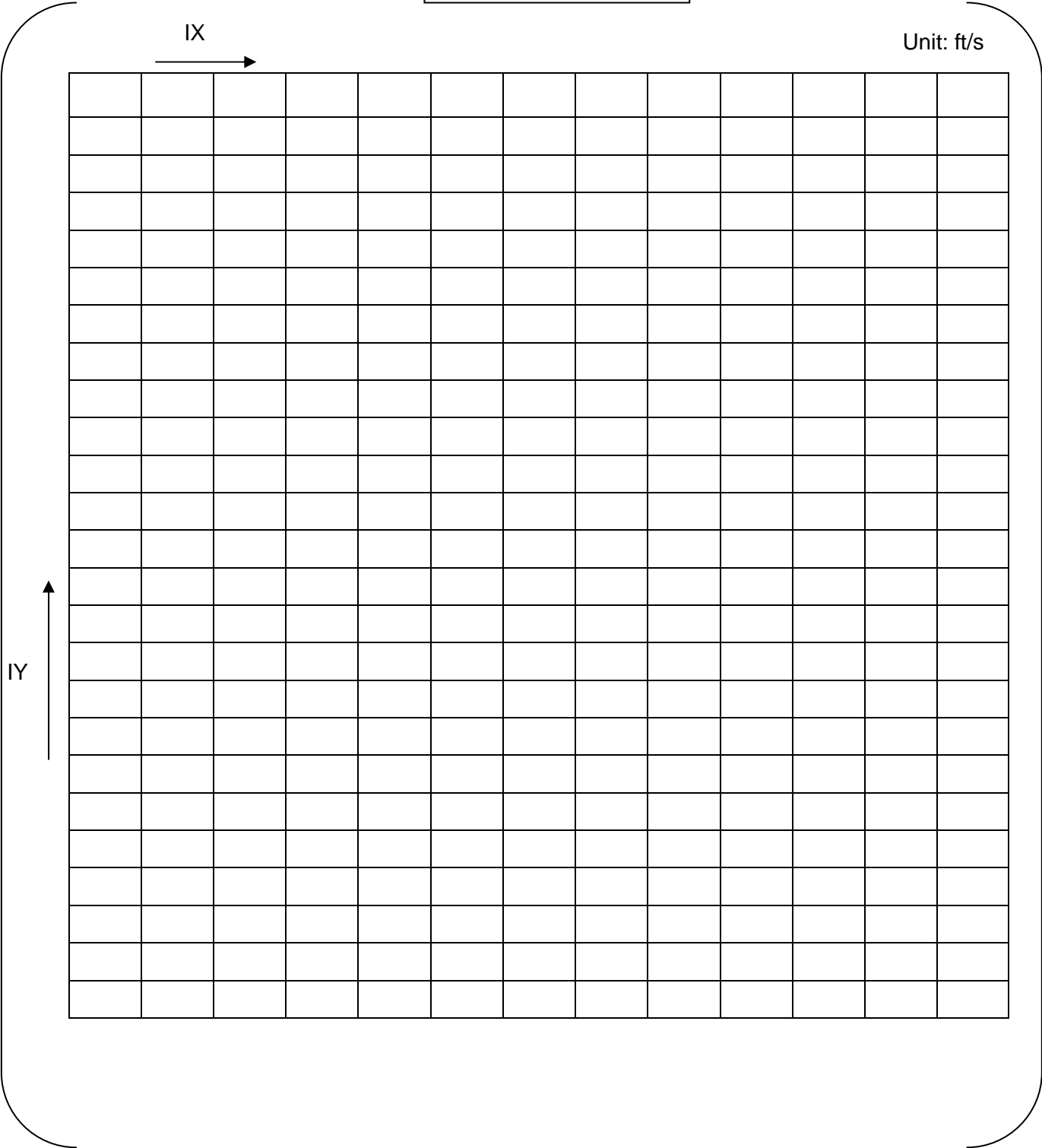


Velocity at #3TSP (1/2)



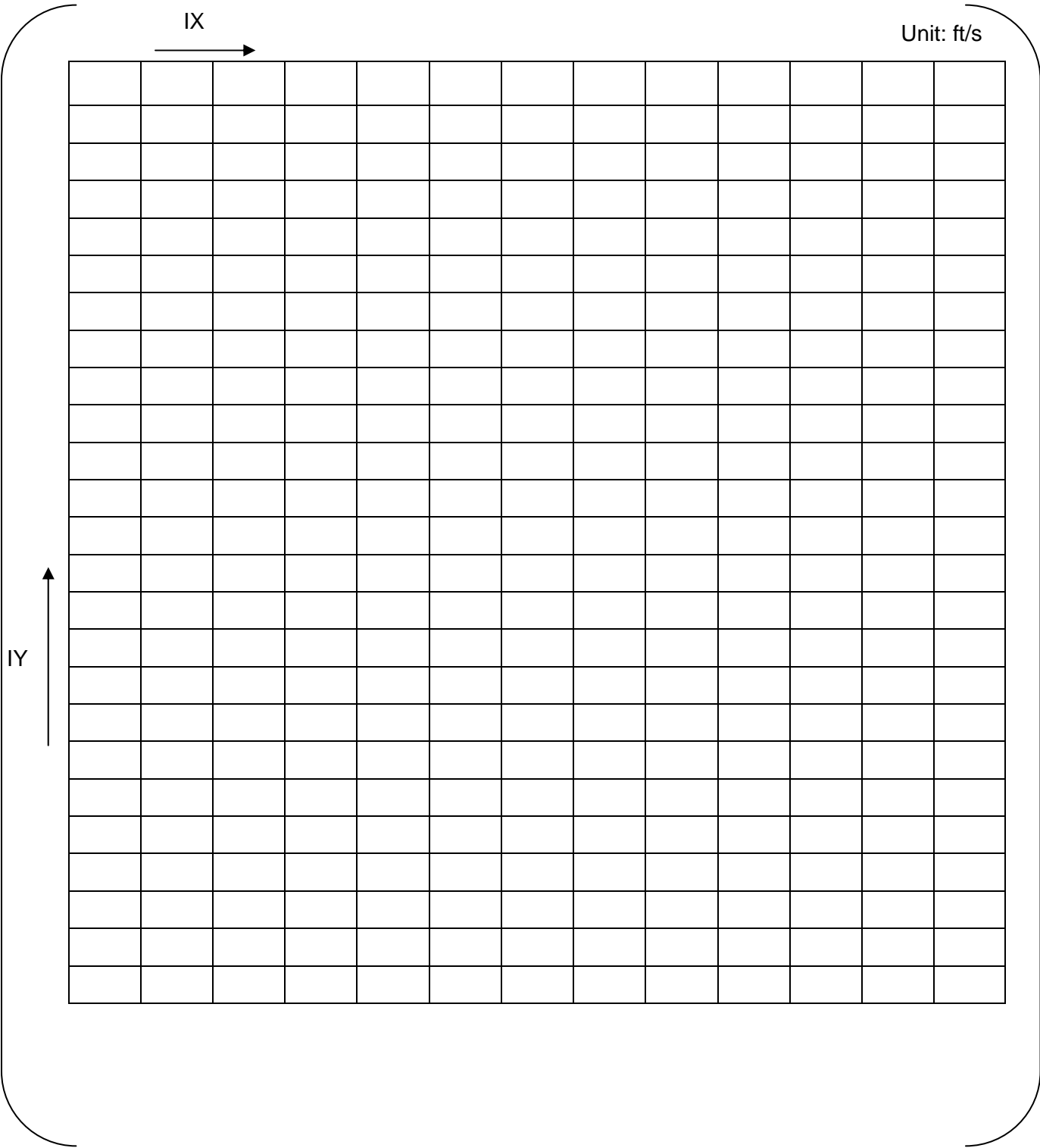


Velocity at #3TSP (2/2)



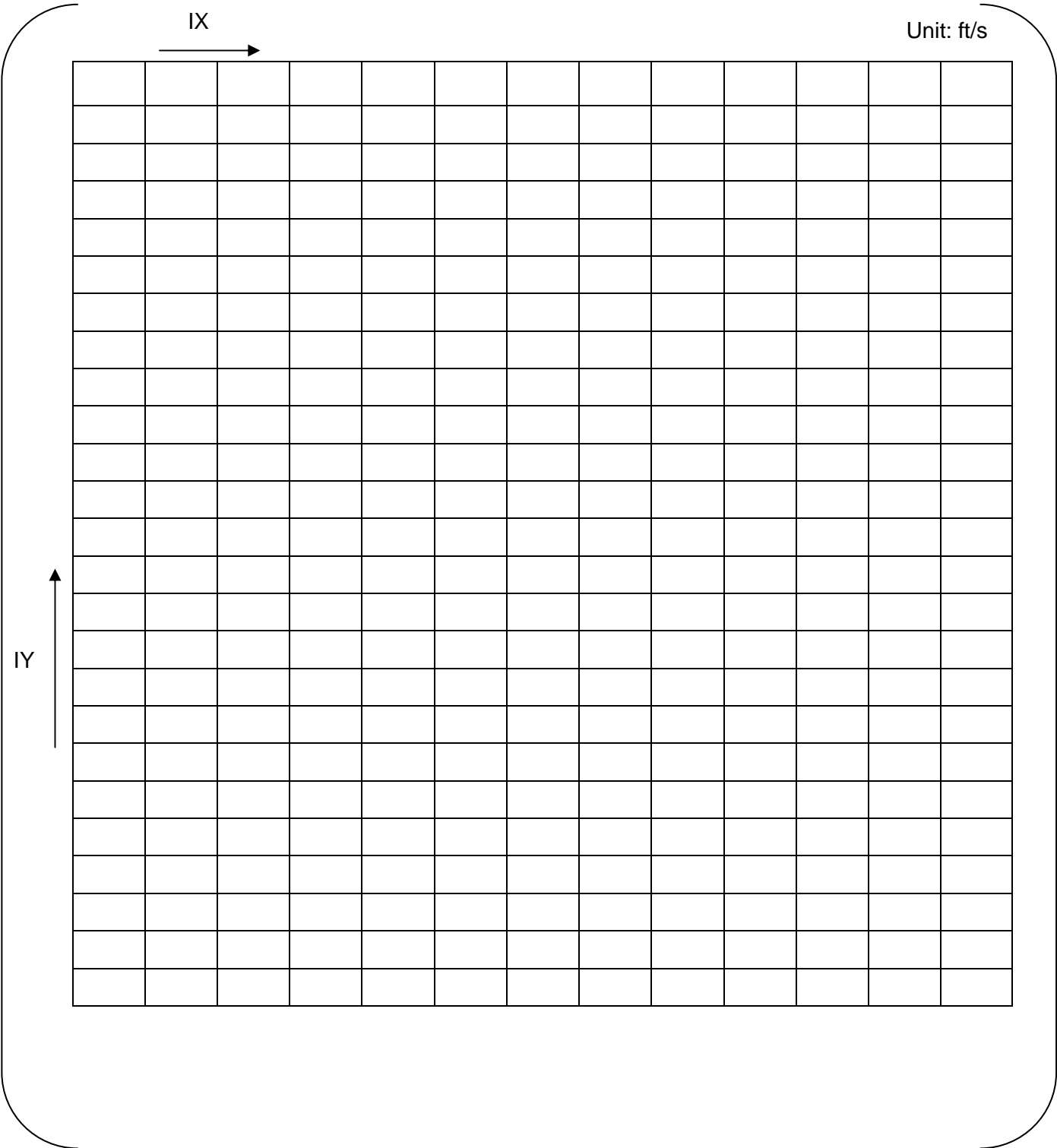


Velocity at #4TSP (1/2)



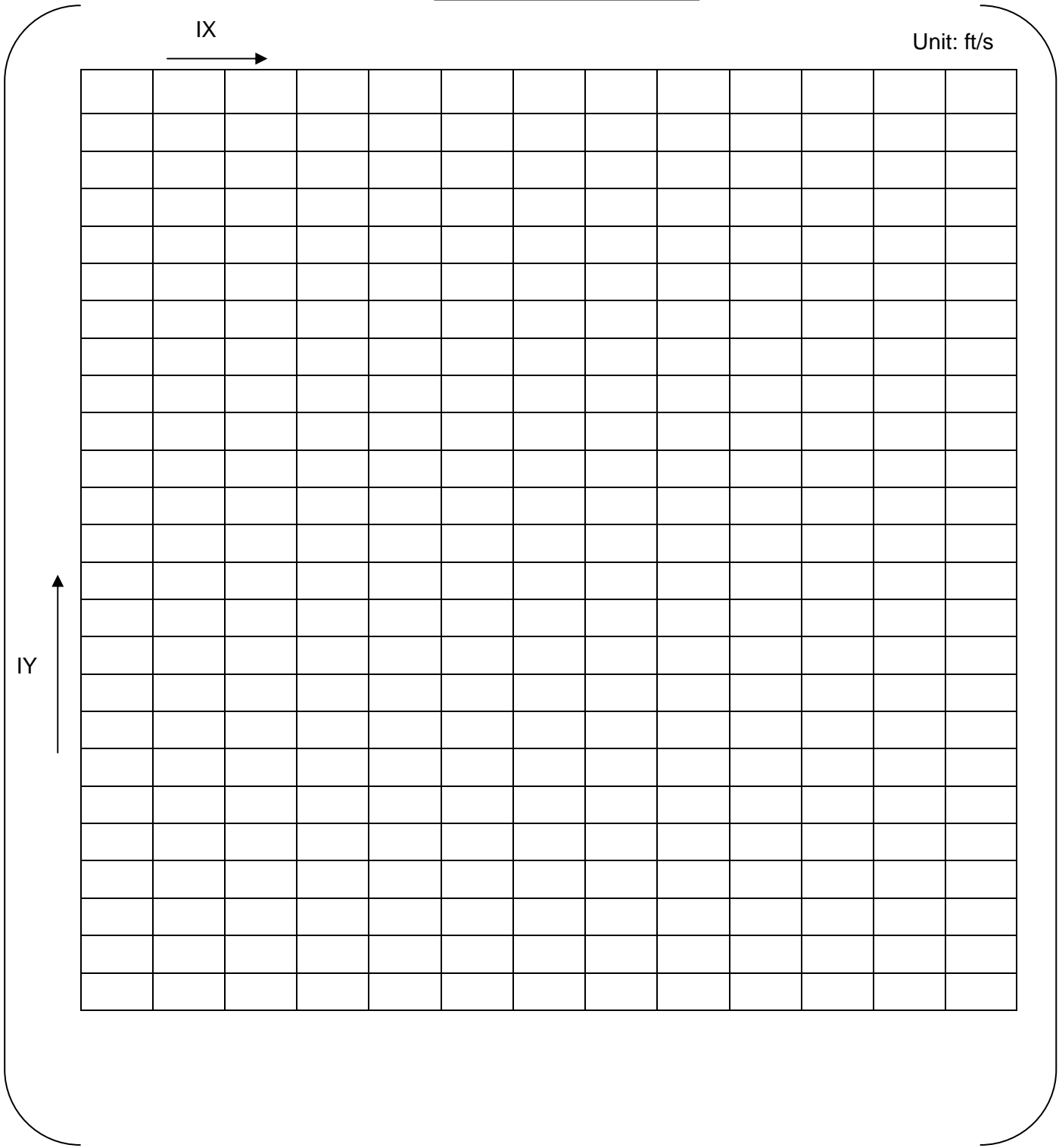


Velocity at #4TSP (2/2)



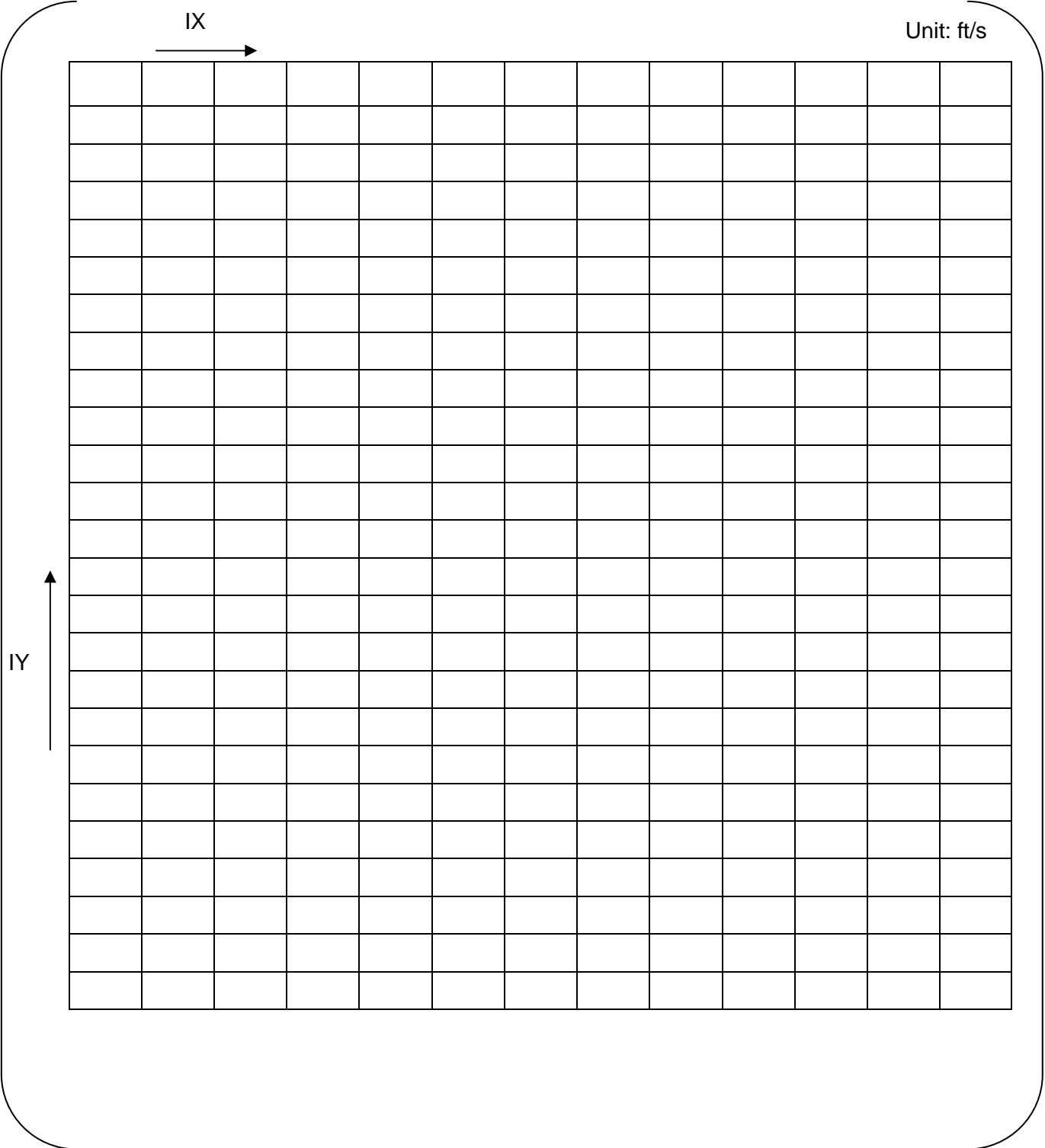


Velocity at #5TSP (1/2)



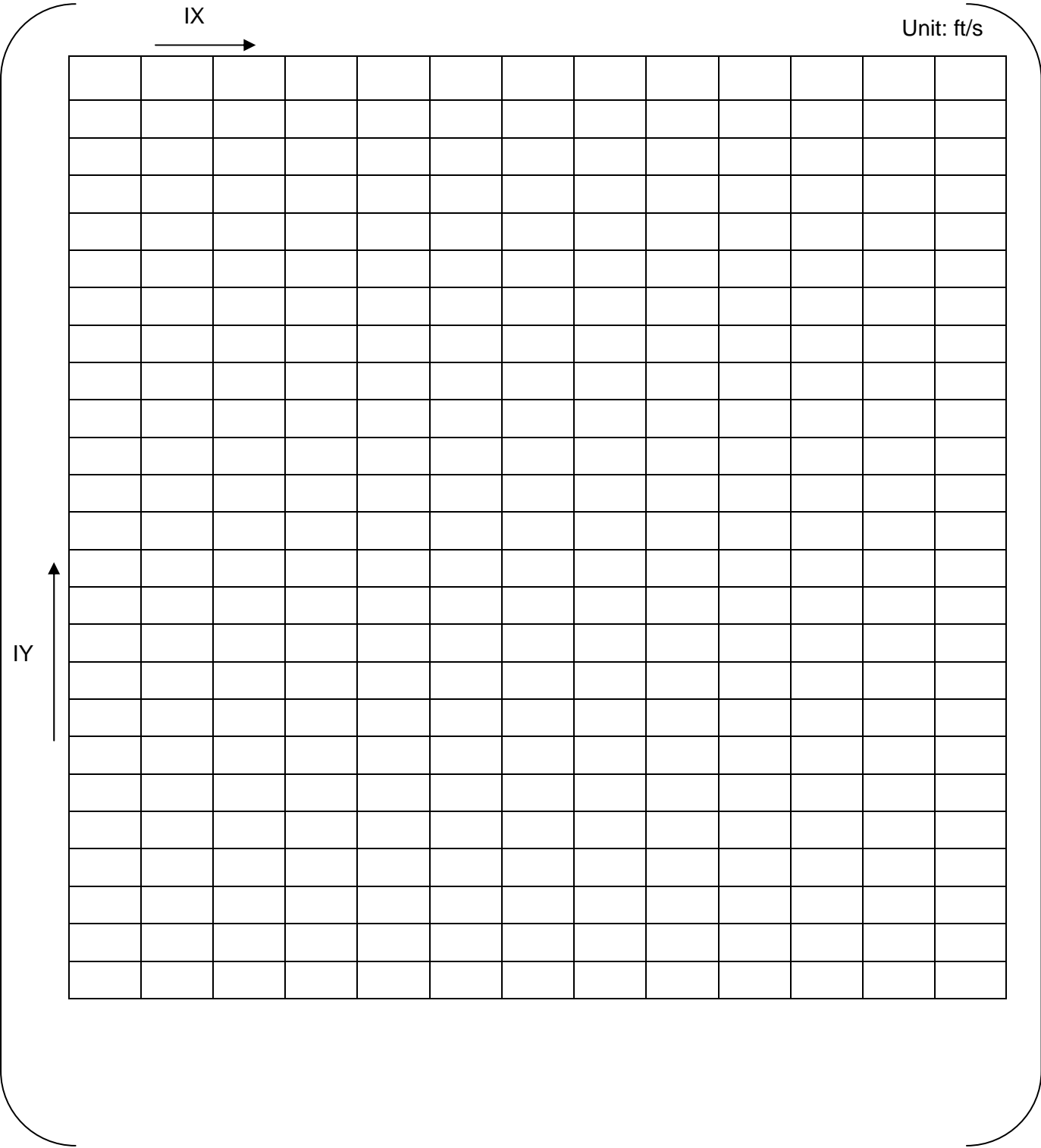


Velocity at #5TSP (2/2)



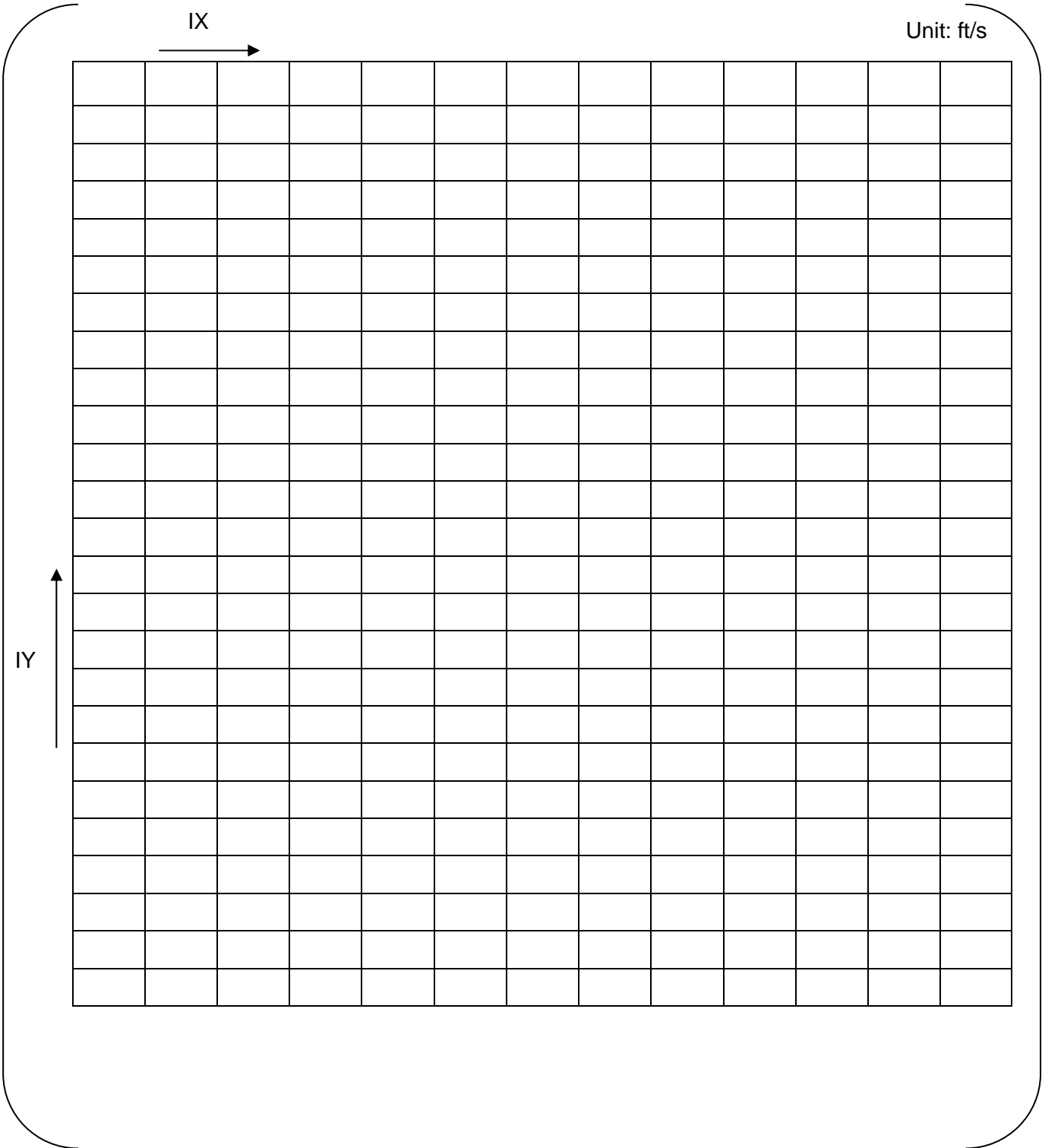


Velocity at #6TSP (1/2)



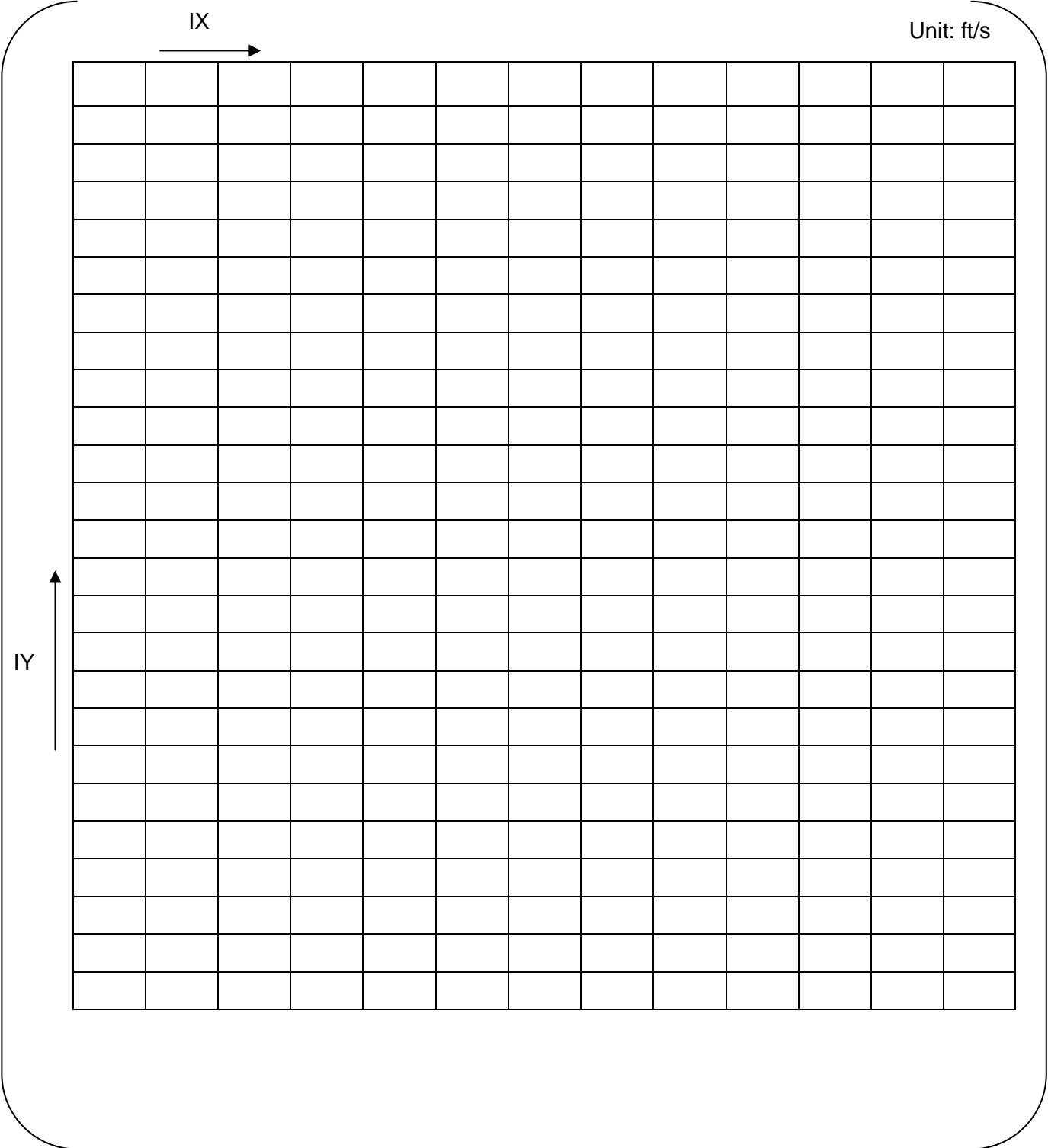


Velocity at #6TSP (2/2)





Velocity at #7TSP (2/2)





Appendix-2A
Random Vibration Evaluation of Tube Straight Portion for Unit-2/3



1. Purpose

Tube-to-tube support plate (TSP) wears at tube straight portions are detected in SONGS-2/3 RSGs. It is possible that the cause of the wears is the random vibration mechanism. The purpose of study provided in appendix-2A is to evaluate the possibility of random vibration of the tube straight portion, through the thermal and hydraulic calculations by ATHOS/SGAP computer code and vibration calculations by IVHET computer code.

2. Conclusion

The tube wear depth for Row1 Column1 tube is calculated with assuming the tube-to-TSP contact force of []. Since contact force due to the thermal expansion is 0.6N which can be variable because of manufacturing tolerances and fluid forces, the contact is a parameter for this case study [].

The nonlinear analysis predicts that the contact force of 1.5N results in tube wear depth of 2 ~ Approx.20%, which is similar to the tube inspection results 0~19%. This parametric study implies that the random vibration mechanism is the probable cause of tube-to-TSP wear and the contact force at the locations where wear indications are detected happened to be larger than the locations where no indication is detected.

Table 2-1 Parameter survey result

Case	Wear depth	Note
Calculation	Approx. 2~20%	Contact force of [] is assumed.
Tube inspection	0~19%	



3. Assumption

The following assumptions are used in the tube vibration calculations.

- 1) The tube vibration is calculated based on the assumption that the cause of tube vibration is the tube cross flow and axial flow.
- 2) Since there are clearances between tubes and tube holes of TSPs, the tube support conditions are uncertain. However, most tube-to-TSP contact points are considered to be effective supports because of the differential thermal expansion of the tubesheet and TSPs (Refer to Assumption of Appendix-2). TSPs supports are generally expected to be in contact with the tubes.

For the tube-to-TSP contact point without tube-to-TSP wear identification, the tube is assumed to be in contact with the TSP (zero touch condition). For the contact point with tube-to-TSP wear indication, the contact force is considered.

- 3) The tube-to-TSP contact force ranging [] is assumed. Since the contact force due to the thermal expansion is [], the contact force [] is considered to be in the realistic range.
- 4) For the conservative evaluation, the large random excitation forces due to the flows are used in the vibration analysis.

4. Acceptance criteria

There is no acceptance criterion because the purpose of the parametric survey is to trace the tube-to-TSP wear depth, which is identified by the tube inspection.



5. Design input

The nominal dimensions are obtained from the design drawings (Ref.3 to 20) and the manufacturing tolerances are not considered.

Flow characteristics are obtained from 3 dimensional thermal and hydraulic analysis (See Appendix-12) .Flow velocity, density, void fraction and hydrodynamic pressure are evaluated for Row 1 Column 1 tube (Fig. 5-1). The reason of selection of the tube is provided in section 6.3.

The velocity, density distribution and volume flow rate quality for tube straight portion are provided in Fig.5-2 and 5-3.

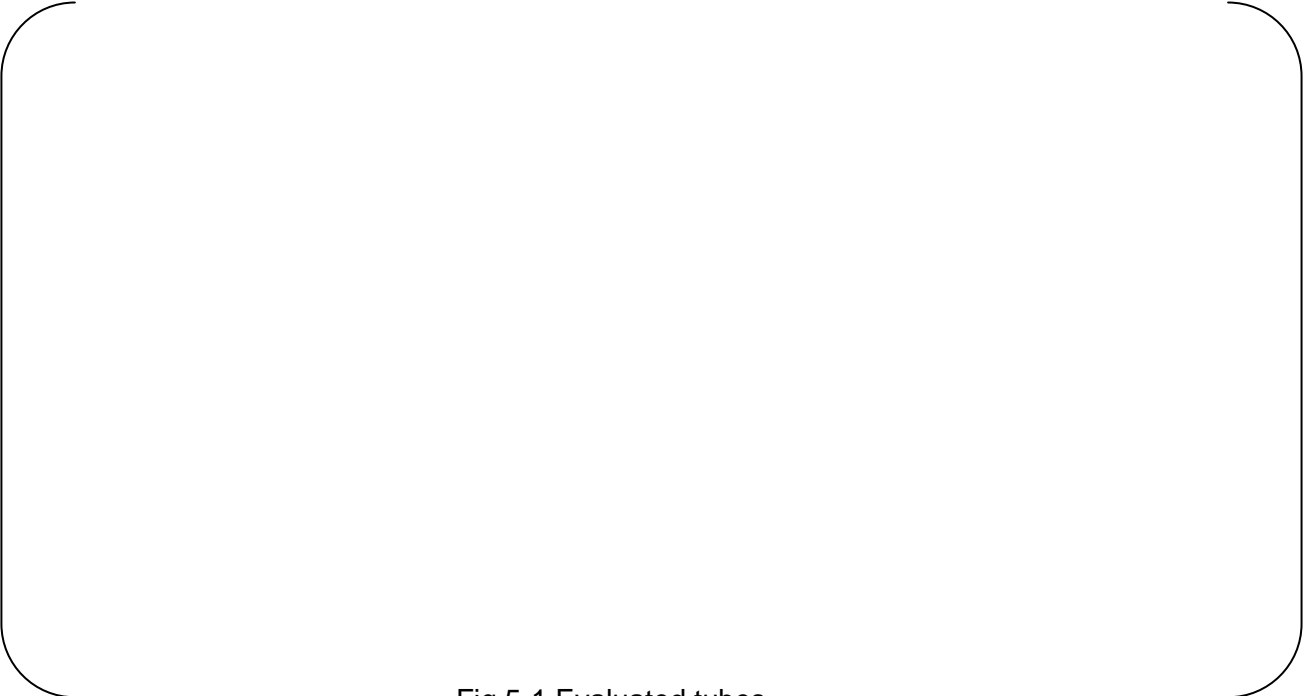


Fig.5-1 Evaluated tubes



Fig 5-2 Flow distribution

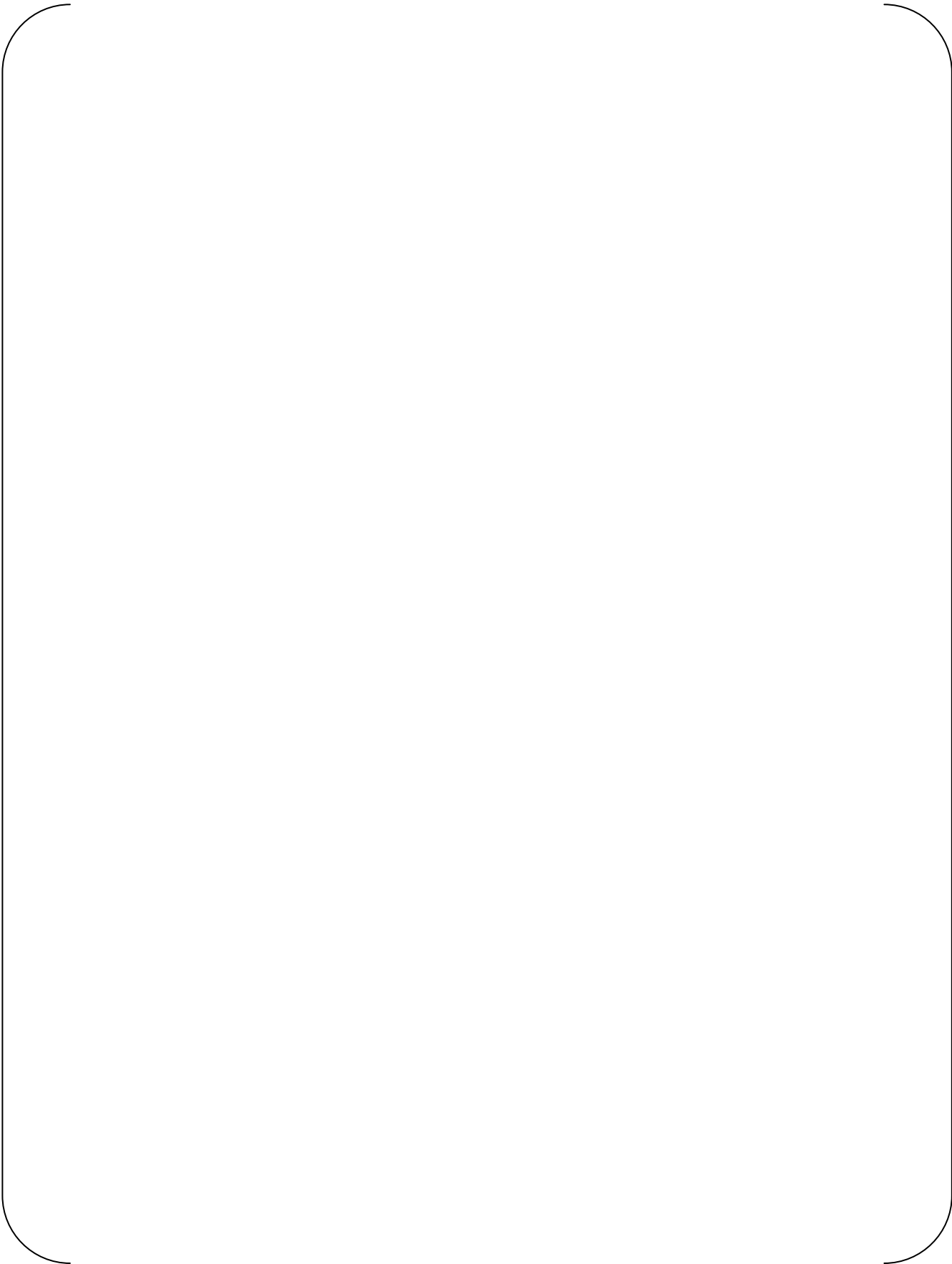


Fig 5-3 density and flow velocity multiplied



6. Methodology

6.1 Outline of analysis

Based on the design input of the operating conditions, the calculation of the circulation ratio is performed by evaluating the pressure loss and the recirculation head with SSPC, which is a 1 dimensional Thermal and Hydraulic parameter calculation code (Ref.21). Using ATHOS/SGAP, the thermal hydraulic analysis is performed to obtain the 3 dimensional flow distribution that includes the flow velocity, the flow density, and the void fraction (See Appendix-12). Then, IVHET is used to evaluate the non-linear tube vibration. The evaluation process is shown in Fig.6-1.

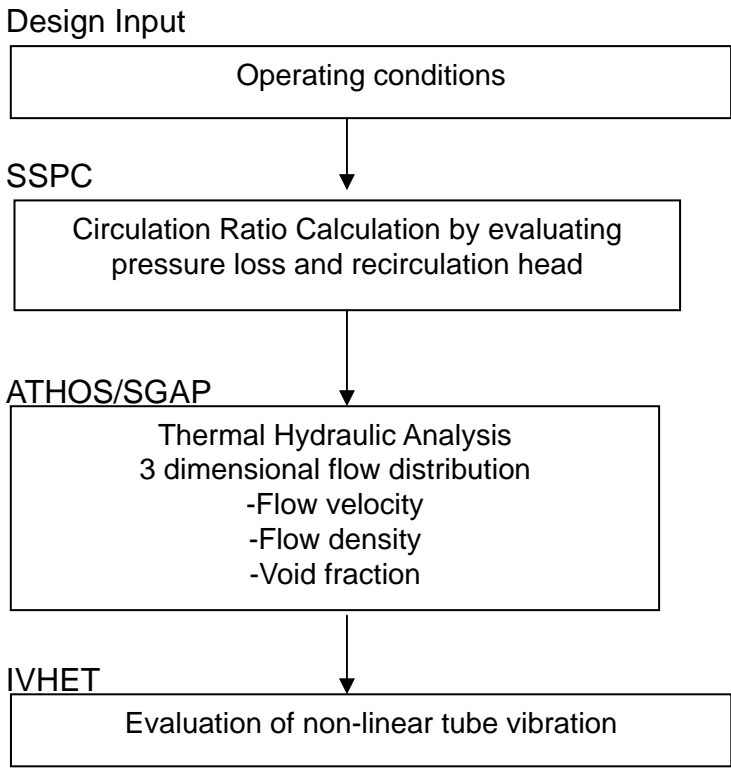


Fig.6-1 Flow of the evaluation



6.2 Evaluation Parameters

In general, larger thermal power is more severe for vibration, because the steam flow rate increases. At constant thermal power, lower steam pressure is more severe for vibration than higher pressure, because ρU^2 increases - (the lower ρ causes the higher U). Basic parameters required for calculations are shown in Table 6-1.

Table 6-1 Basic parameters for calculation

	Condition of Cycle 16
Plugging	()
T_{cold} (°F)	
T_{hot} (Tsg-in) (°F)	
$T_{\text{sg-out}}$ (°F)	
$T_{\text{feedwater}}$ (°F)	
Saturation Steam Pressure (psia)	
Steam Mass Flow (lb/hr)	
Circulation ratio	
Thermal power (MWt/SG)	()

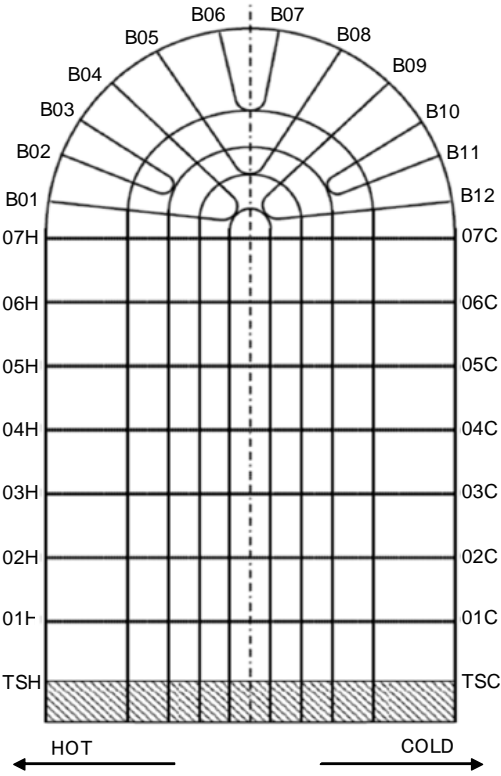


6.3 Selection of tubes to be evaluated

In all SGs, tube-to-TSP wear is present in many Row 1 tubes that border on the tube-free-lane. In this case study, the Row1 Column1 tube is used for the evaluation in order to compare the actual ECT inspection results of R1C1 of 2A-SG and 2B-SG, which are selected as worse cases.

Table 6-2 Tube-to-TSP wear depth of Row1 Column1 of 2B-SG

	Unit (%)													
SG	01H	02H	03H	04H	05H	06H	07H	07C	06C	05C	04C	03C	02C	01C
2A														
2B														





6.4 Random excitation force

The random excitation forces due to the cross flow and axial flow are considered.

(1) Random excitation force due to the cross flow

The random excitation force due to the cross flow is calculated based on Fig.6-2 [22]. Since the “envelop spectrum” in the figure 6-2 is used, the random excitation force is overestimated. The following equation is used for the calculation.

$$\Phi_{cross} = (\rho g D_w D)^2 \cdot \left(\frac{D_w}{U} \right) \cdot \Phi_E$$

$$\Phi_E = \begin{cases} 10 f_r^{-0.5} & ; f_r < 0.06 \\ (2 \times 10^{-3}) f_r^{-3.5} & ; f_r > 0.06 \end{cases}, \quad f_r = \frac{f D_w}{U_{mean}}, \quad D_w = \frac{0.1 D}{\sqrt{1 - \beta_{mean}}}$$

where

Φ_{cross} : Power spectrum density of fluid force per unit length (cross flow)

D : Tube outer diameter

ρ : Density at each element

U : Flow force at each element

U_{mean} : Average flow velocity between each span

β_{mean} : Average volume flow velocity quality between each span

g : Gravity acceleration

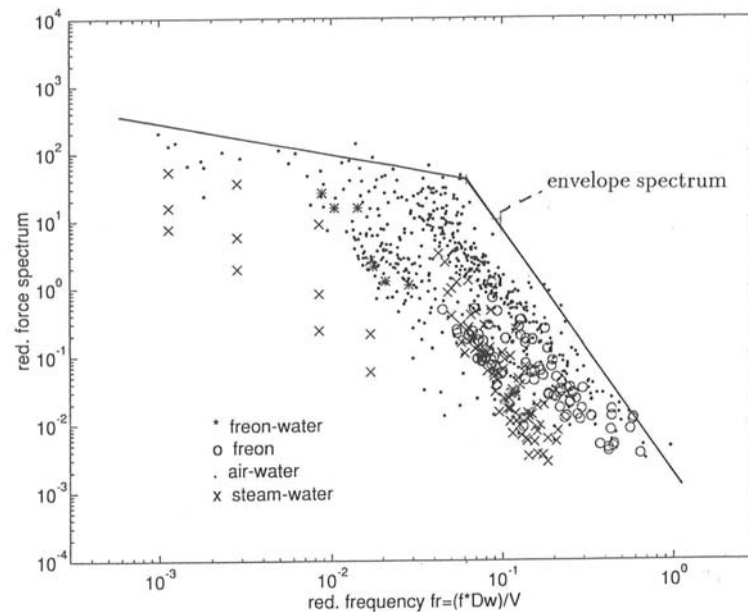


Fig 6-2 Power spectrum density of random excitation force due to the cross flow



(2) Random excitation force due to the axial flow

The random excitation force due to the axial flow is calculated based on Fig.6-3 [23]. Since the design guideline covering most data is used, the random excitation force is overestimated. The following equation is used for the calculation.

$$\Phi_{axial} = (2.0 \times 10^{-7}) \times (\rho U D)^2$$

where

Φ_{axial} : Power spectrum density of fluid force per unit length (axial flow)

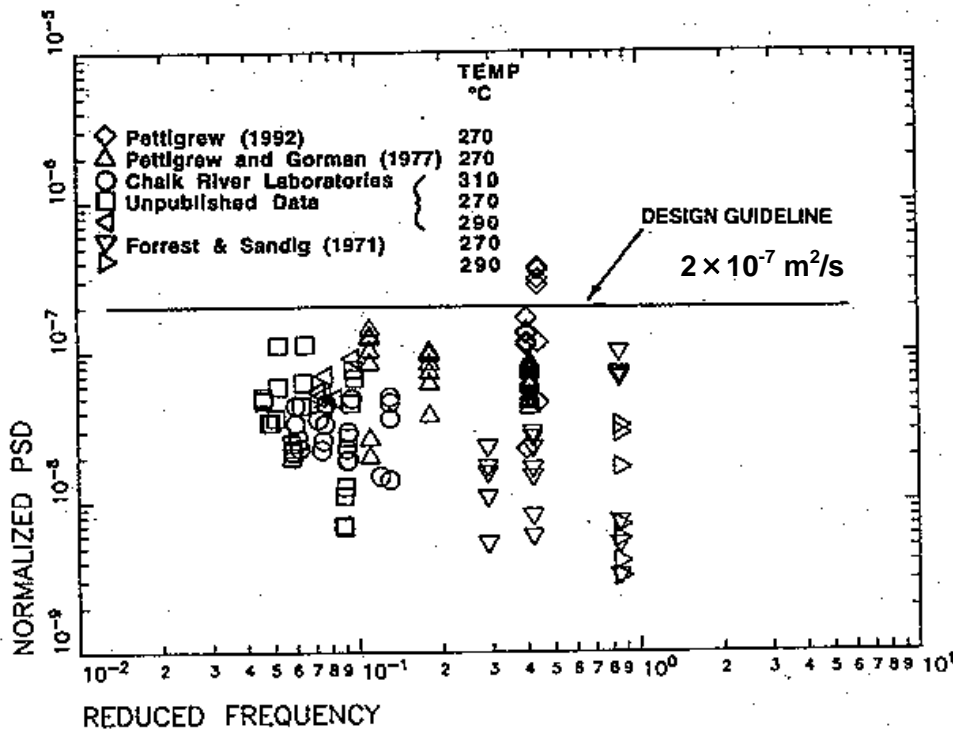


Fig 6-3 Power spectrum density of random excitation force due to the axial flow



7. Results

The vibration analysis results are provided in Fig.7-1. The parametric survey of the contact force shows that the contact force of [] gives the tube wear depth is [], which is similar to the tube inspection results [].

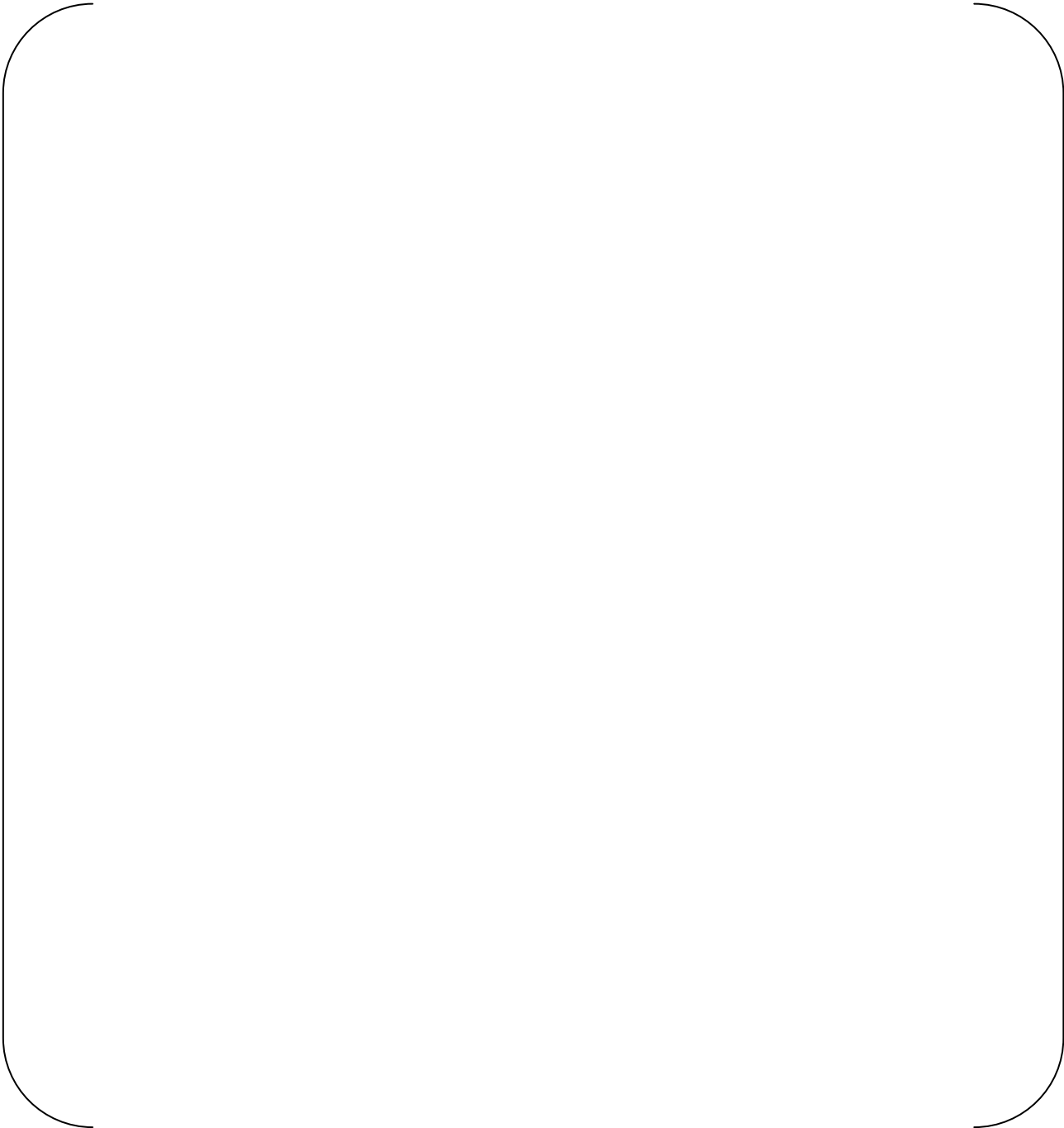


Fig 7-1 Wear depth of analysis result



8. References

- 1) Deleted
- 2) Deleted
- 3) L5-04FU001 the latest revision, Component and Outline Drawing 1/3
- 4) L5-04FU002 the latest revision, Component and Outline Drawing 2/3
- 5) L5-04FU003 the latest revision, Component and Outline Drawing 3/3
- 6) L5-04FU021 the latest revision, Tube Sheet and Extension Ring 1/3
- 7) L5-04FU022 the latest revision, Tube Sheet and Extension Ring 2/3
- 8) L5-04FU023 the latest revision, Tube Sheet and Extension Ring 3/3
- 9) L5-04FU051 the latest revision, Tube Bundle 1/3
- 10) L5-04FU052 the latest revision, Tube Bundle 2/3
- 11) L5-04FU053 the latest revision, Tube Bundle 3/3
- 12) L5-04FU111 the latest revision, AVB assembly 1/9
- 13) L5-04FU112 the latest revision, AVB assembly 2/9
- 14) L5-04FU113 the latest revision, AVB assembly 3/9
- 15) L5-04FU114 the latest revision, AVB assembly 4/9
- 16) L5-04FU115 the latest revision, AVB assembly 5/9
- 17) L5-04FU116 the latest revision, AVB assembly 6/9
- 18) L5-04FU117 the latest revision, AVB assembly 7/9
- 19) L5-04FU118 the latest revision, AVB assembly 8/9
- 20) L5-04FU119 the latest revision, AVB assembly 9/9
- 21) L5-04GA510 the latest revision, Thermal and Hydraulic Parametric Calculations
- 22) "Flow-Induced Vibration", 107-117 P.W. Bearman (Edit)
- 23) "Two-Phase Flow-Induced Vibration : An Overview", Journal of Pressure Vessel Technology 1994 , Vol.116, 233-253 M. J. Pettigrew, C. E. Taylor



Appendix-3
FEI Evaluation of Tube U-bend Portion for Unit-2/3



1. Purpose

The analysis is conducted for 100% reactor power, zero plugged tubes and all AVB supports being active to evaluate design conditions of the RSGs in the first operating period.

The purpose of this appendix is to provide a fluid elastic instability evaluation of out-of-plane direction for the tubes of the San Onofre Units 2 and 3 Replacement Steam Generators (RSGs) in accordance with Section III Appendix N, Article N-1330 based on U-bend flow conditions from the ATHOS/SGAP (EPRI) thermal-hydraulic analysis code instead of the evaluation based on the flow conditions obtained from FIT-III during the RSG design stage (Ref.1).

2. Conclusion

The fluid elastic stability ratios are confirmed to be less than 1.0 at full power and with all AVBs active to satisfy the criteria of ASME Section III Appendix N, Article N-1330. This conclusion applies to all of the steam generator tubes. The results for the most limiting tubes are shown in Table 2-1 and indicate the occurrence of tube out-of-plane FEI is very unlikely when the gap between tube and AVB is very small and the AVB support point is active in the tube out-of-plane direction.



Table 2-1 Fluid Elastic Stability Ratios for the Limiting Tubes

Row	Column	Damping ratio	Critical Factor	Natural frequency f (Hz)	Critical Flow velocity U _c (ft/s)	Effective flow Velocity U _e (ft/s)	Stability ratio
142	88	1.5%*	2.4*				
47	89						
47	7						
26	88						
26	4						
14	88						
14	2						
1	89						
1	1						

Note*: Values recommended by ASME Section III Appendix N, Article N-1331.3



3. Assumption

- (1) Nominal tube thickness and nominal tube length are used in the evaluation model because the effect of the tolerances of these dimensions on the natural frequency is negligible.
- (2) Contact condition between tube and tube support plate is pin-supported. Fixed supported condition at No. 1 TSP is added.
- (3) Contact condition between tube and active support points by the anti-vibration bar (AVB) is pin-supported. And all points are active.
- (4) Modulus of elasticity of tube is interpolated based on the tube average temperature of $\frac{T_{av} + T_s}{2}$ from table of ASME Boiler and Pressure Vessel Code, Sec II, Materials, 1998 Edition, 2000 addenda (Ref.23).

Where,

T_{av} : Primary side average temperature (°F)

T_s : Secondary side temperature (°F)

- (5) Tube has the virtual added mass supposing the fluid-structure interaction (FSI) effect as shown in the following formula (Ref.24).

$$m_v = \frac{\pi D_o^2 \rho_o}{4} \left\{ \frac{(D_e/D_o)^2 + 1}{(D_e/D_o)^2 - 1} \right\} \text{ (lbm/ft)} \dots\dots\dots (1)$$

$$D_e/D_o = \left(1 + \frac{1}{2} P/D_o \right) P/D_o \dots\dots\dots (2)$$

Where,

m_v : Virtual added mass per unit length due to FSI effect;

ρ_o : Average density of water outside the tube;

D_o : Tube outside diameter

P : Tube pitch.



4. Acceptance criteria

The ASME Section III, Appendix N (Ref. 22) methodology and acceptance criteria are used for this analysis. The acceptance criterion is that the effective flow velocity across the tubes be no greater than the Appendix N critical flow velocity. The ratio of these two velocities may not exceed 1.0. The ASME methodology includes conservatisms to account for practical design variability.

5. Design Inputs

The nominal tube dimensions are used in the analysis and are obtained from the design drawings (Ref. 3 to 20). Manufacturing tolerances are not considered.

The basic operating parameters required for the calculations are shown in Table 5-1 (see Appendix-12 for details).

Table 5-1 Basic parameters

Number of tubes plugged	
Thermal power (MWt/SG)	
T _{cold} (°F)	
T _{hot} (Tsg-in) (°F)	
T _{feedwater} (°F)	
Saturation Steam Pressure (psia)	
Steam Mass Flow (lb/hr)	
Circulation ratio	

(Note) The primary inlet temperature range is ()°F. It is conservative for this analysis to use the lower inlet temperature (()°F) because it produces a lower secondary pressure and a higher steam flow velocity.

The tubes selected for evaluation are listed in Table 5-2, which are the same tubes evaluated during the RSG design stage (Ref.1). These tubes have longer support spans, lower damping and higher flow excitation than others.



Table 5-2 Evaluated Tubes

Row	Column
142	88 (Center)
47	89 (Center)
47	7 (Outer-most)
26	88 (Center)
26	4 (Outer-most)
14	88 (Center)
14	2 (Outer-most)
1	89 (Center)
1	1 (Outer-most)

The flow conditions (flow velocity^{*}, flow density and void fraction) applied to these limiting tubes are shown in Fig. 5-1 through 5-5. The ATHOS flow conditions are only applied over the U-bend portion of the tube. The structural model for the U-tubes includes the full tube length including the straight legs, but no cross flow velocities are applied to the straight legs.

Note)

*: Flow velocity shown in Fig. 5-1 through 5-5 indicates the gap velocity in normal direction to tube in-plane.

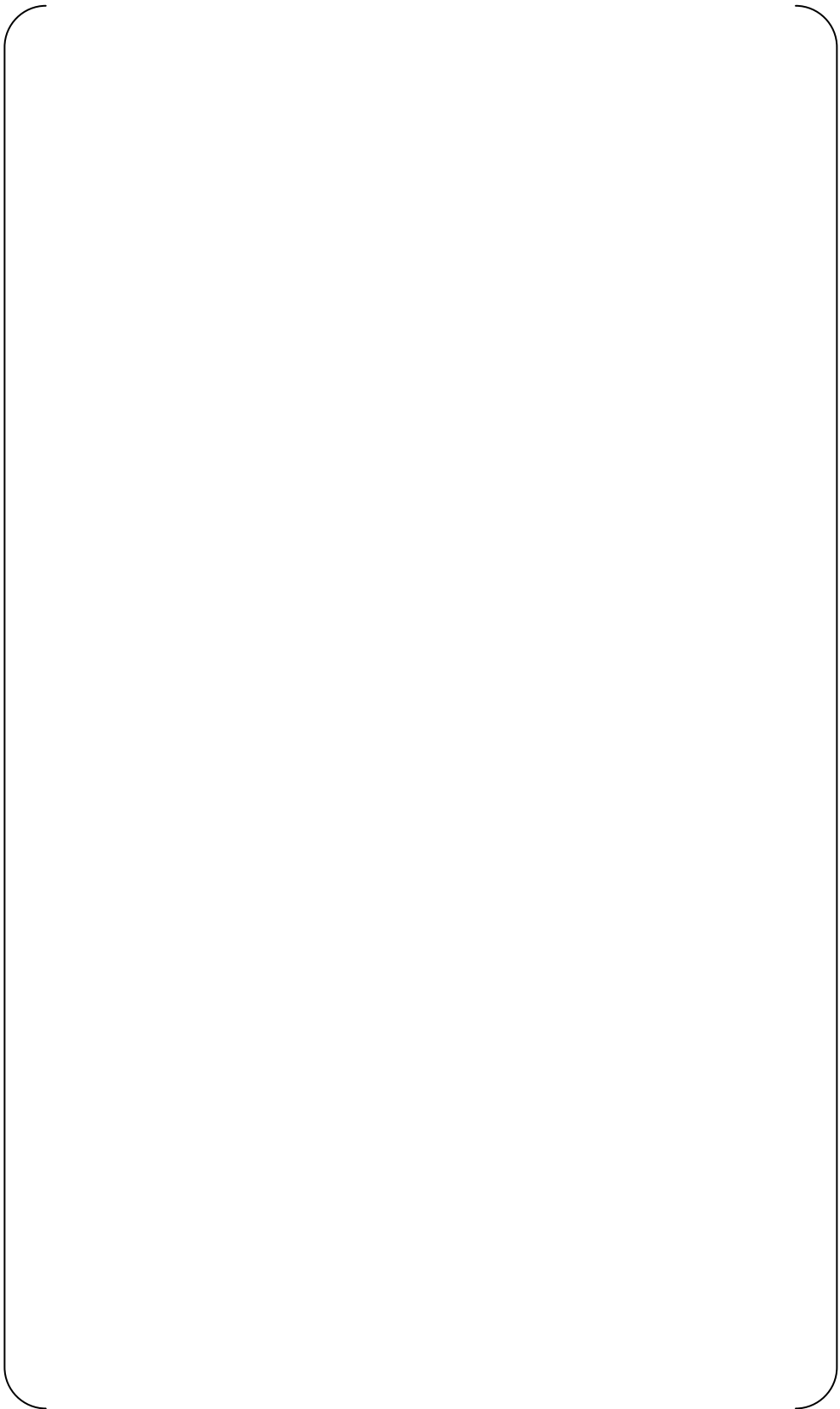


Fig.5-1 Flow distribution of Row 142 Col 88

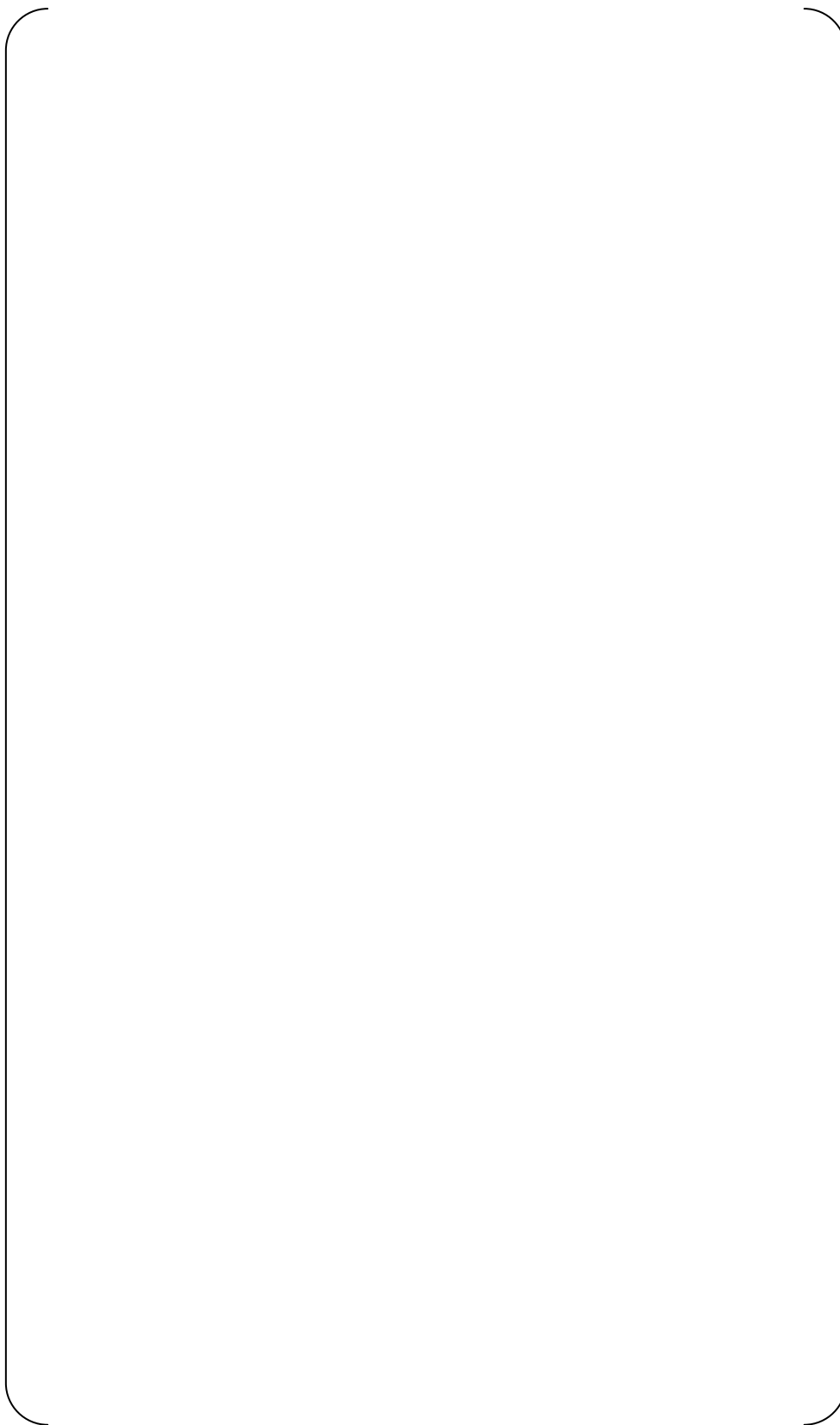


Fig.5-2 Flow distribution of Row 47, Columns 89 and 7

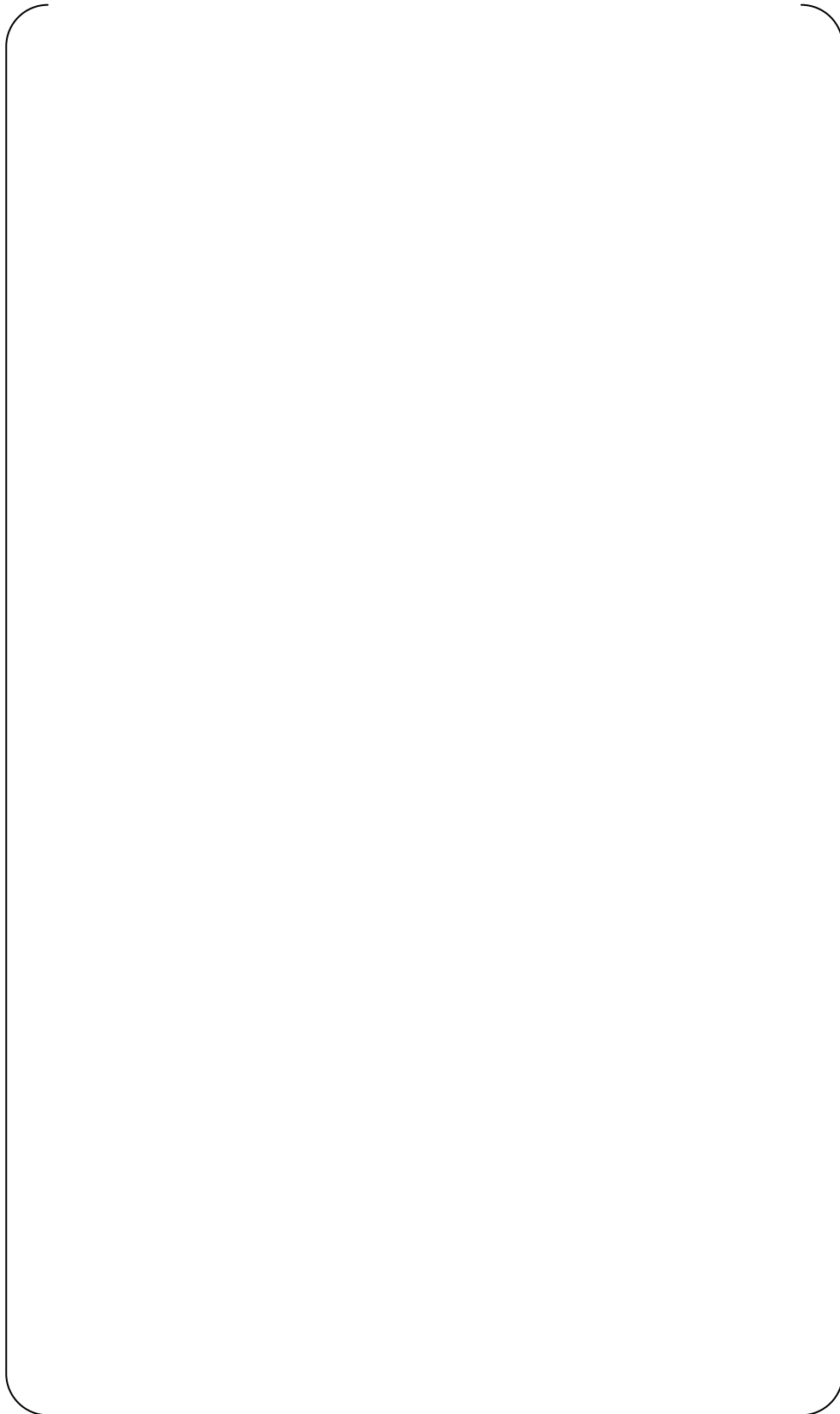


Fig.5-3 Flow distribution of Row 26, Columns 88 and 4

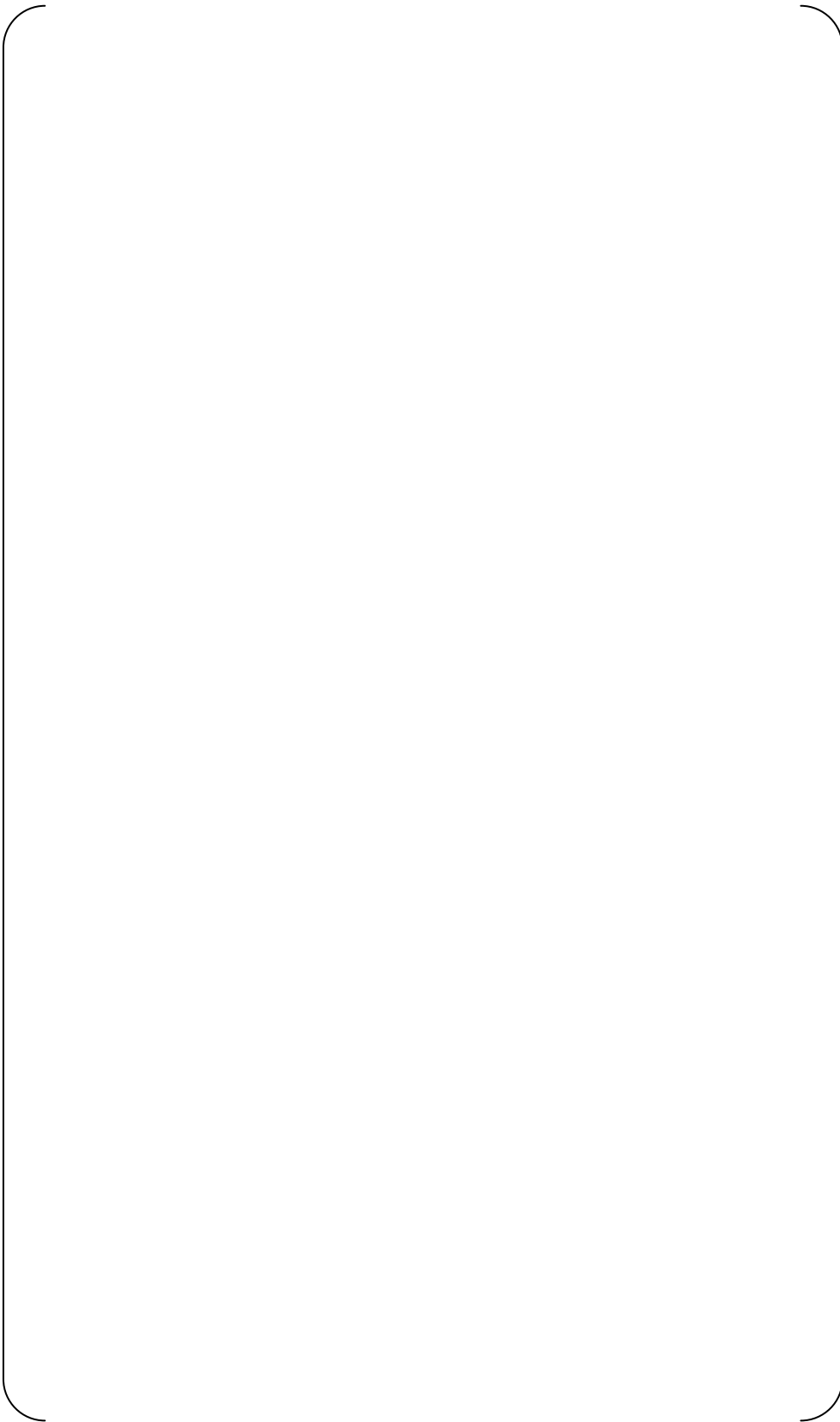


Fig.5-4 Flow distribution of Row 14, Columns 88 and 2



Fig.5-5 Flow distribution of Row 1, Columns 89 and 1



6. Methodology

The term “fluid elastic instability” is generally used to refer to self-excited vibration of tube bundles due to cross flow. In 1969, Connors disclosed the presence of this phenomenon for the first time (Ref.25).

Causes of fluid elastic instability are considered to be the absorption of flow energy due to the interaction of fluid and structure. This phenomenon occurs on tube bundles, and is subjected to effects of tube bundle array. Thus, it is experimentally attempted to determine the criticality of occurrence in various tube bundle arrays.

The critical flow velocity U_c for generating fluid elastic instability is obtained in the following Connors’ formula (Ref.25). This formula is employed in the TEMA (Standards of the Tubular Exchanger Manufactures Association), which is the industrial design standard in the United States.

$$\frac{U_c}{fD_o} = K \left[\frac{m_0 \delta}{\rho_o D_o^2} \right]^{1/2} \dots\dots\dots (3)$$

Where,

- U_c : Critical flow velocity
- f : Tube natural frequency
- D_o : Tube outside diameter
- K : Critical factor
- m_0 : Average tube mass per unit length
- δ : Tube logarithmic decrement(= $2\pi h$)
- h : Damping ratio
- ρ_o : Density of water outside the tube

The critical flow velocity U_c in eq. (3) is evaluated in case of tube vibration of single degree of freedom system with uniform cross flow along the tube axis. In actual tube, however, the vibration of the tube supported by the tube support plate is multi degrees of freedom system with beam type of vibration modes. Therefore, considering the vibration mode and fluid distribution, the effective flow velocity U_{en} is evaluated in the following formula.

$$U_{en} = \left[\frac{\int_0^L \frac{\rho(x)}{\rho_o} \cdot U(x)^2 \cdot \phi_n(x)^2 dx}{\int_0^L \frac{m(x)}{m_o} \cdot \phi_n(x)^2 dx} \right]^{1/2} \dots\dots\dots (4)$$



Where,

- U_{en} : Nth mode effective flow velocity
- $\varphi_n(x)$: Nth vibration mode
- $\rho(x)$: Fluid density distribution of water outside the tube in tube axis direction
- $m(x)$: Tube mass distribution per unit length in tube axis direction
- $U(x)$: Flow velocity distribution orthogonal to tube axis in tube axis direction
- x : Coordinate component along tube axis
- ρ_o : Average density of water outside the tube
- m_o : Average tube mass per unit length
- L : Tube length

The stability ratio is determined as follows in each vibration mode by calculating the ratio of eq. (3) and eq. (4).

$$SR_n = \frac{U_{en}}{U_{cn}} \dots\dots\dots (5)$$

where,

$$\frac{U_{cn}}{f_n \cdot D_o} = K \left[\frac{m_o \delta}{\rho_o D_o^2} \right]^{1/2} \dots\dots\dots (6)$$

This value is called the n-th mode stability ratio SR_n , and if $SR_n > 1$, fluid elastic instability occurs. Generally, the maximum stability ratio in each mode is called the stability ratio of the tube, which is simply expressed as SR.

Evaluation of occurrence of fluid elastic instability in U-tubes is carried out in the following steps :

- ① Using a 1-dimensional Thermal and Hydraulic parameter code (SSPC), determine the tube bundle circulation ratio and other secondary side operating conditions for the normal operating condition (Ref.21).
- ② Using the flow analysis code (ATHOS/SGAP), determine the distributions of flow velocity $U(x)$ and density of the fluid $\rho(x)$ along the tube axis.
- ③ For the damping ratio h and critical factor K , the suggested values based on ASME Sec III Appendix N-1330 are used, and from eqs. (3) ~ (5) stability ratio is evaluated (Ref.24).



The critical factor $K=2.4$ in eq. (3) gives a conservative criteria for avoiding fluid-elastic instabilities of tube arrays. Also, the damping ratio $\eta= 1.5\%$ for wet steam or liquid is used. Natural frequencies, vibration mode and stability ratio are calculated by vibration analysis code FIVATS.

Figure 6-1 describes this process.

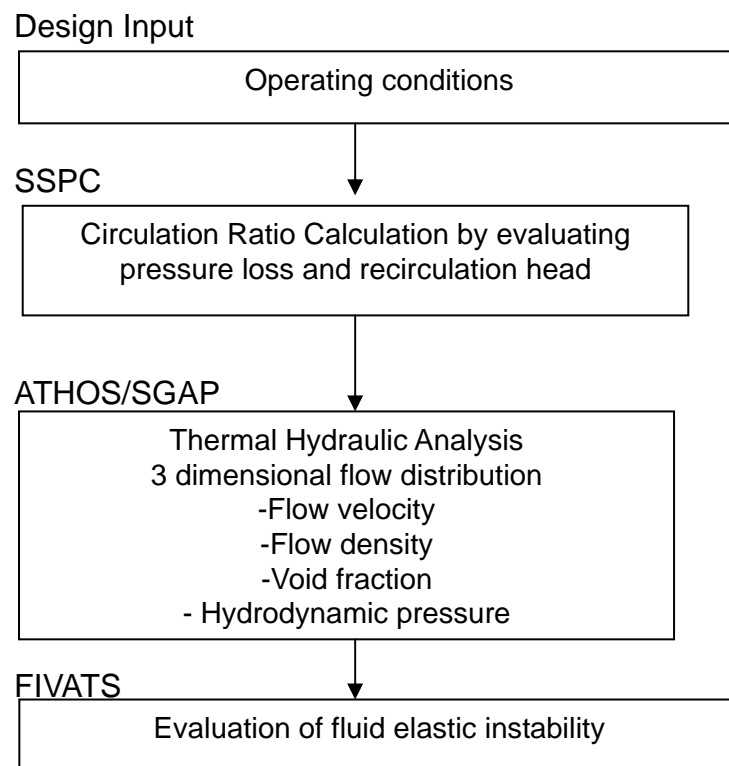


Fig.6-1 Steps in the Analysis Process



7. Results

All of the stability ratios are less than the limiting value of 1.0. The results are summarized in Table 7-1. Figures 7-1 to 7-9 show examples of the tube vibration mode shapes that are associated with the maximum stability ratio for each tube.



Table 7-1 Vibration Analysis Results (1/4)



Table 7-1 Vibration Analysis Results (2/4)



Table 7-1 Vibration Analysis Results (3/4)



Table 7-1 Vibration Analysis Results (4/4)



MODE	FREQ.(HZ)	Uc (ft/s)	Ue(ft/s)	SR
1				
2				
3				
4				
5				
6				
7				
8				
9				
10				
11				
12				
13				
14				
15				
16				
17				
18				
19				
20				
21				
22				
23				
24				
25				
26				
27				
28				
29				
30				

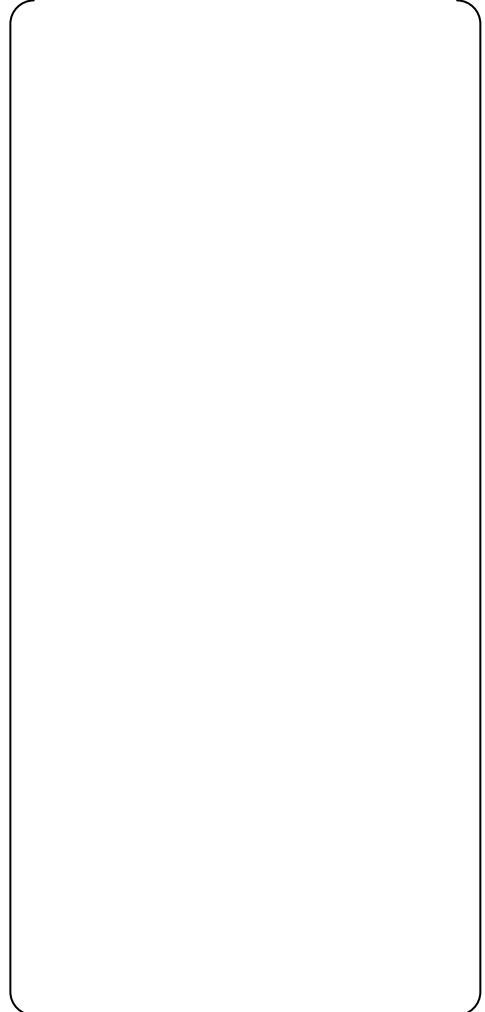


Fig. 7-1 Vibration mode diagram for Row 142 Column 88



MODE	FREQ.(HZ)	Uc (ft/s)	Ue(ft/s)	SR
1				
2				
3				
4				
5				
6				
7				
8				
9				
10				
11				
12				
13				
14				
15				
16				
17				
18				
19				
20				
21				
22				
23				
24				
25				
26				
27				
28				
29				
30				

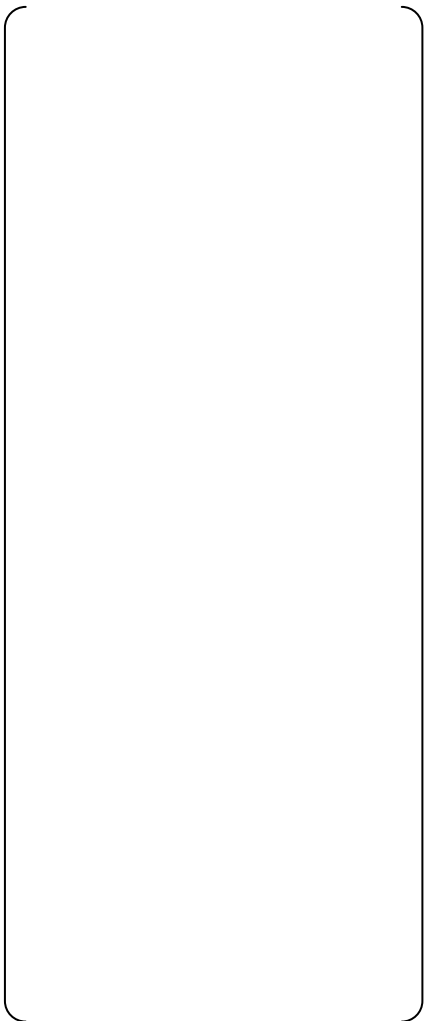


Fig. 7-2 Vibration mode diagram for Row 47 Column 89



MODE	FREQ.(HZ)	Uc (ft/s)	Ue(ft/s)	SR
1				
2				
3				
4				
5				
6				
7				
8				
9				
10				
11				
12				
13				
14				
15				
16				
17				
18				
19				
20				
21				
22				
23				
24				
25				
26				
27				
28				
29				
30				

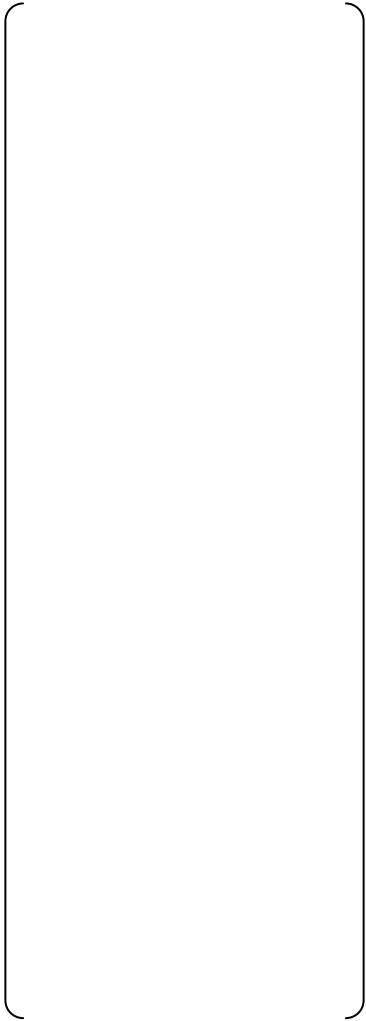


Fig. 7-3 Vibration mode diagram for Row 47 Column 7



MODE	FREQ.(HZ)	Uc (ft/s)	Ue(ft/s)	SR
1				
2				
3				
4				
5				
6				
7				
8				
9				
10				
11				
12				
13				
14				
15				
16				
17				
18				
19				
20				
21				
22				
23				
24				
25				
26				
27				
28				
29				
30				



Fig. 7-4 Vibration mode diagram for Row 26 Column 88



MODE	FREQ.(HZ)	Uc (ft/s)	Ue(ft/s)	SR
1				
2				
3				
4				
5				
6				
7				
8				
9				
10				
11				
12				
13				
14				
15				
16				
17				
18				
19				
20				
21				
22				
23				
24				
25				
26				
27				
28				
29				
30				

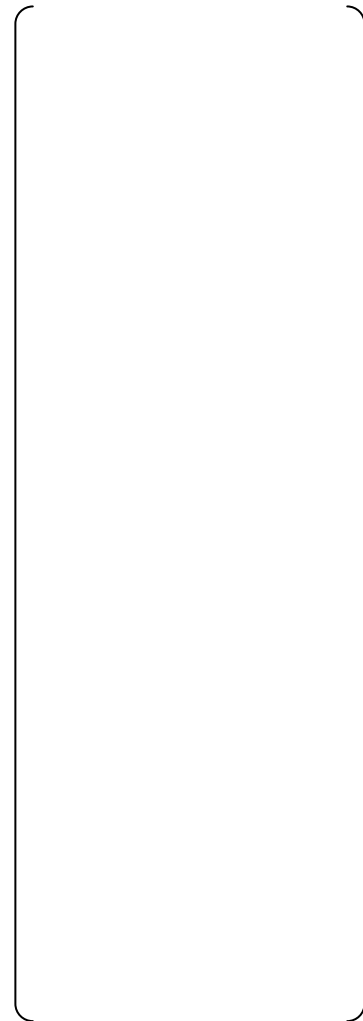


Fig. 7-5 Vibration mode diagram for Row 26 Column 4



MODE	FREQ.(HZ)	Uc (ft/s)	Ue(ft/s)	SR
1				
2				
3				
4				
5				
6				
7				
8				
9				
10				
11				
12				
13				
14				
15				
16				
17				
18				
19				
20				
21				
22				
23				
24				
25				
26				
27				
28				
29				
30				

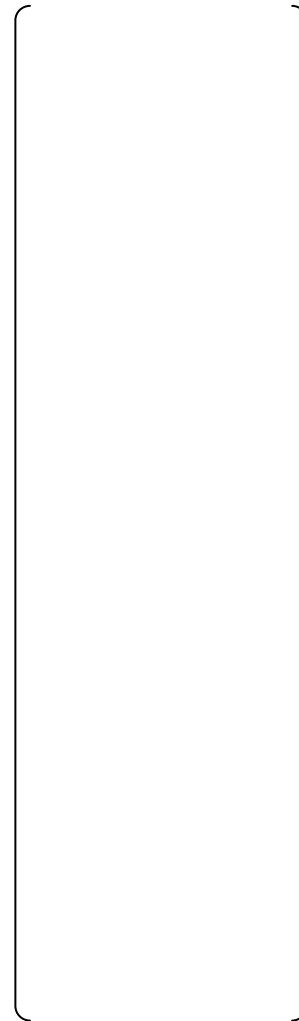


Fig. 7-6 Vibration mode diagram for Row 14 Column 88



MODE	FREQ.(HZ)	Uc (ft/s)	Ue(ft/s)	SR
1				
2				
3				
4				
5				
6				
7				
8				
9				
10				
11				
12				
13				
14				
15				
16				
17				
18				
19				
20				
21				
22				
23				
24				
25				
26				
27				
28				
29				
30				



Fig. 7-7 Vibration mode diagram for Row 14 Column 2



MODE	FREQ.(HZ)	Uc (ft/s)	Ue(ft/s)	SR
1				
2				
3				
4				
5				
6				
7				
8				
9				
10				
11				
12				
13				
14				
15				
16				
17				
18				
19				
20				
21				
22				
23				
24				
25				
26				
27				
28				
29				
30				

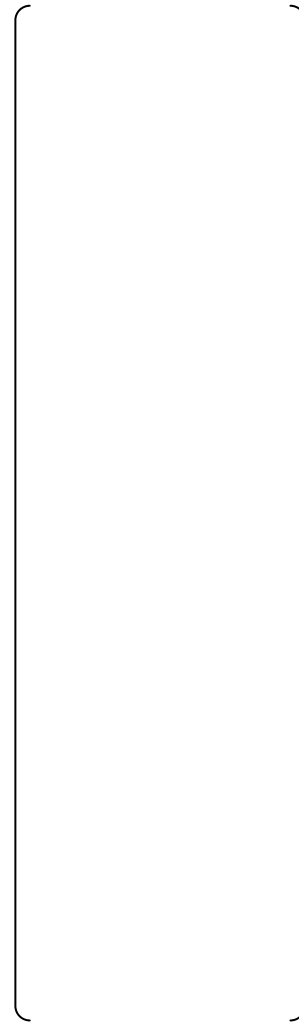


Fig. 7-8 Vibration mode diagram for Row 1 Column 89



MODE	FREQ.(HZ)	Uc (ft/s)	Ue(ft/s)	SR
1				
2				
3				
4				
5				
6				
7				
8				
9				
10				
11				
12				
13				
14				
15				
16				
17				
18				
19				
20				
21				
22				
23				
24				
25				
26				
27				
28				
29				
30				

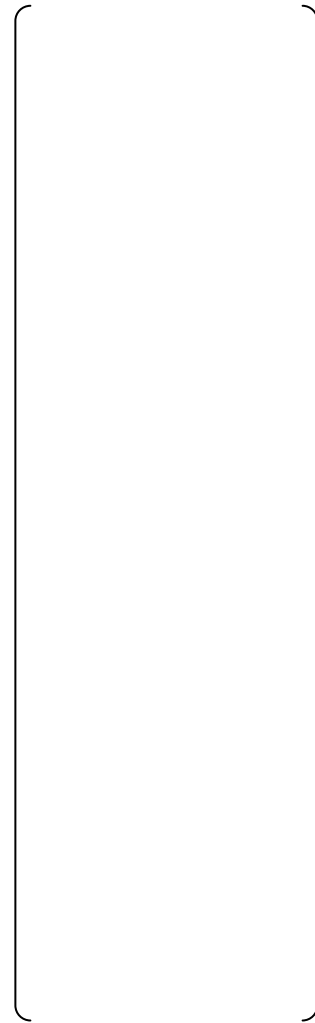


Fig. 7-9 Vibration mode diagram for Row 1 Column 1



8. References

- 1) L5-04GA504 the latest revision, Evaluation of Tube Vibration
- 2) Deleted
- 3) L5-04FU001 the latest revision, Component and Outline Drawing 1/3
- 4) L5-04FU002 the latest revision, Component and Outline Drawing 2/3
- 5) L5-04FU003 the latest revision, Component and Outline Drawing 3/3
- 6) L5-04FU021 the latest revision, Tube Sheet and Extension Ring 1/3
- 7) L5-04FU022 the latest revision, Tube Sheet and Extension Ring 2/3
- 8) L5-04FU023 the latest revision, Tube Sheet and Extension Ring 3/3
- 9) L5-04FU051 the latest revision, Tube Bundle 1/3
- 10) L5-04FU052 the latest revision, Tube Bundle 2/3
- 11) L5-04FU053 the latest revision, Tube Bundle 3/3
- 12) L5-04FU111 the latest revision, AVB assembly 1/9
- 13) L5-04FU112 the latest revision, AVB assembly 2/9
- 14) L5-04FU113 the latest revision, AVB assembly 3/9
- 15) L5-04FU114 the latest revision, AVB assembly 4/9
- 16) L5-04FU115 the latest revision, AVB assembly 5/9
- 17) L5-04FU116 the latest revision, AVB assembly 6/9
- 18) L5-04FU117 the latest revision, AVB assembly 7/9
- 19) L5-04FU118 the latest revision, AVB assembly 8/9
- 20) L5-04FU119 the latest revision, AVB assembly 9/9
- 21) L5-04GA510 the latest revision, Thermal and Hydraulic Parametric Calculations
- 22) ASME Boiler and Pressure Vessel Code, Section III, 1998 edition, 2000 addenda
- 23) ASME Boiler and Pressure Vessel Code, Sec II, Materials, 1998 Edition through 2000 addenda.
- 24) Blevins, R. D., "Flow-induced Vibration", Krieger Publishing Company.
- 25) Connors, H.J., Fluid Elastic Vibration of Tube Arrays Excited by Cross Flow, ASME Annual Meeting, 1970.



Appendix-4
Investigation of Unit-2/3 Manufacturing and Inspection Records



1. Purpose

The purpose of this appendix is to investigate the manufacturing history of the Unit-2 and Unit-3 steam generators to identify differences in dimensions, materials, fabrication processes and inspections that may have a relationship to the differences in U-bend degradation patterns.

2. Conclusion

The major differences between the Unit-2 and Unit-3 steam generators are listed below. The influences of these differences are evaluated in Section 5.2.3 of the main report.

- (1) Number of Rotations due to Divider Plate Repair
- (2) Number of Hydrostatic Tests
- (3) Dimensional Control of Tubes and AVBs



Attachment-1: Difference of fabrication and transportation between Unit-2 and Unit-3 (1/4)

Category		Item	Unit-2	Unit-3	Effect to the final AVB structure assembly and tube bundle (especially tube-to-AVB gap)	
Design		Mechanical property of AVB	All tensile test and hardness test results are within specification for all AVB material for all units.			There is no remarkable difference on any test results.
	Material	Outer diameter of tube (G value)				Standard deviation of G value for Unit-3 RSGs were smaller than that for Unit-2 RSGs. However, difference of the tube dimensions are small between all four SGs, as the tube diameters are within the { } and the standard deviation is within { }
Fabrication & Inspection	Tube insertion	Number of tubing operators Number of manual adjustment of U-bend portion during tubing installation (in case the gap between the tubes are small)				
	AVB assembly	AVB manufacturer, fabrication sequence, and procedure Thickness of AVBs before installation				

Note *) For Unit-3, () N pressing was used for AVB bend nose portion after bending in order to control the twist and flatness of AVB more precisely, while () N pressing was used for Unit-2 as described in Appendix-9.



Attachment-1: Difference of fabrication and transportation between Unit-2 and Unit-3 (2/4)

Category	Item	Unit-2	Unit-3	Effect to the final AVB structure assembly and tube bundle (especially tube-to-AVB gap)
Fabrication & AVB assembly Inspection	Procedure of AVB assembling (Insertion, welding and fixuring the bridge and retainer bar)			The approved procedure(document) was revised up from Unit-2A to Unit-3B. Those for Unit-2A are different from those for the others. However, there is no remarkable difference for Unit-2B and Unit-3 RSGs at the point of the basic manners for AVB assembly.
	Situation and condition of fixturing AVBs at tubes with tie ropes or temporary fixturing equipments			Same manners are applied to all units.
	Size of spacer block used for welding AVBs to retaining bar			Size of spacer for Unit-2A is different from that for the others. Therefore there is no difference for Unit-2B and Unit-3 RSGs.
	AVB assembly rotations			This operation might have led to some difference. AVB assembly rotations for Unit-2A is different from that for the others. Therefore there is no remarkable difference for Unit-2B and Unit-3 RSGs.
	Fillet weld size between retaining bars and end-caps			There is no remarkable difference.
	Increased weld size between AVB and retaining bar			There is no remarkable difference.
	Re-insertion of AVBs			This operation was applied only for Unit-2A. There is no remarkable difference for Unit-2B and Unit-3 RSGs.
	Re-welding retaining bars and end-caps after helium leak tests			This operation was applied only for Unit-2A. There is no remarkable difference for Unit-2B and Unit-3 RSGs.



Attachment-1: Difference of fabrication and transportation between Unit-2 and Unit-3 (3/4)

Category	Item	Unit-2	Unit-3	Effect to the final AVB structure assembly and tube bundle (especially tube-to-AVB gap)
Fabrication & Inspection	Welding position for the bridge and retainer bar assembling			Welding position for Unit-2A is different from that for the others. Therefore there is no difference for Unit-2B and Unit-3 RSGs.
	AVB assembly	Tube-to-AVB Gap measurement results at outermost tubes		These AVB-to-tube gaps were smaller in Unit-3 than in Unit-2.
		Time of tying retaining bar to tube for prevention of pulling AVB out		This difference influenced the number of shell rotations - Unit 2 RSGs were rotated 60 more times than Unit 3 RSGs. Shell rotations are assumed to not impact the tube-to-AVB gap* size.
		Tolerance for pitch of the upper most tube support plate		Same tolerances are applied to all units.
		Time of transition wrapper welding		This difference influenced the number of shell rotations - Unit 2 RSGs were rotated 15 more times than Unit 3 RSGs. Shell rotations are assumed to not impact the tube-to-AVB gap*.
		Helium leak test		This difference influenced the number of shell rotations - Unit 2 RSGs were rotated 20 more times than Unit 3 RSGs. Shell rotations are assumed to not impact the tube-to-AVB gap*.
		Tube expansion		There is no difference.
		Final dryer vane jacking (tightening)		This difference influenced the number of shell rotations - Unit 2 RSGs were rotated 30 more times than Unit 3 RSGs. Shell rotations are assumed to not impact the tube-to-AVB gap*.
		Bundle rotations after completion of AVB assembly (excluding divider plate repair)		No impact is assumed for the point of this difference.

Note) See Appendix-5 for details



Attachment-1: Difference of fabrication and transportation between Unit-2 and Unit-3 (4/4)

Category	Item	Unit-2	Unit-3	Effect to the final AVB structure assembly and tube bundle (especially tube-to-AVB gap)
Fabrication & Inspection	Bundle rotations for divider plate repair	Bundle rotations for divider plate repair		This difference influenced the number of shell rotations - Unit 2 RSGs were rotated 30 more times than Unit 3 RSGs. Shell rotations are assumed to not impact the tube-to-AVB gap.*
	Hydrostatic test	Number of times water was poured into the shell for the hydrostatic test, and number of hydrostatic test		It is confirmed by deformation analysis result no remarkable enlargement of tube-to-AVB gap is caused by this operation.
	Heat treatment after AVB structure assembling	Tubesheet to Channel Head welding & PWHT for divider plate repair		No impact is assumed for the point of this difference.
	Channel head removal from tubesheet	Channel head removal by flame cutting for divider plate repair		No impact is assumed for the point of this difference.
	Tube PSI	Time and situation of tube PSI		Indications of tube PSI results is not changed compared with latest ECT results. Therefore no impact is assumed at the point of this difference.
		Position of the shell during transport		No impact is assumed for the point of this difference.
		Accelerations during transport		There is no remarkable difference.
		Nitrogen recharge system		There is no remarkable difference.
		Ship name		There is no remarkable difference.
		Tugboat company		There is no remarkable difference.
Others		Barge support stand		There is no remarkable difference.
		Off load duration		There is no remarkable difference.
		Transportation time		There is no remarkable difference.
		Platform trailers		There is no remarkable difference.
				There is no remarkable difference.

Note) See Appendix-5 for details



Attachment-2: Difference of fabrication history between Unit-2 and Unit-3 (1/3)

A large, empty rectangular frame with rounded corners, intended for the content of the attachment. The frame is currently blank.

N/R: Number of Rotation, N/L: Number of Loading, SUM: Summation



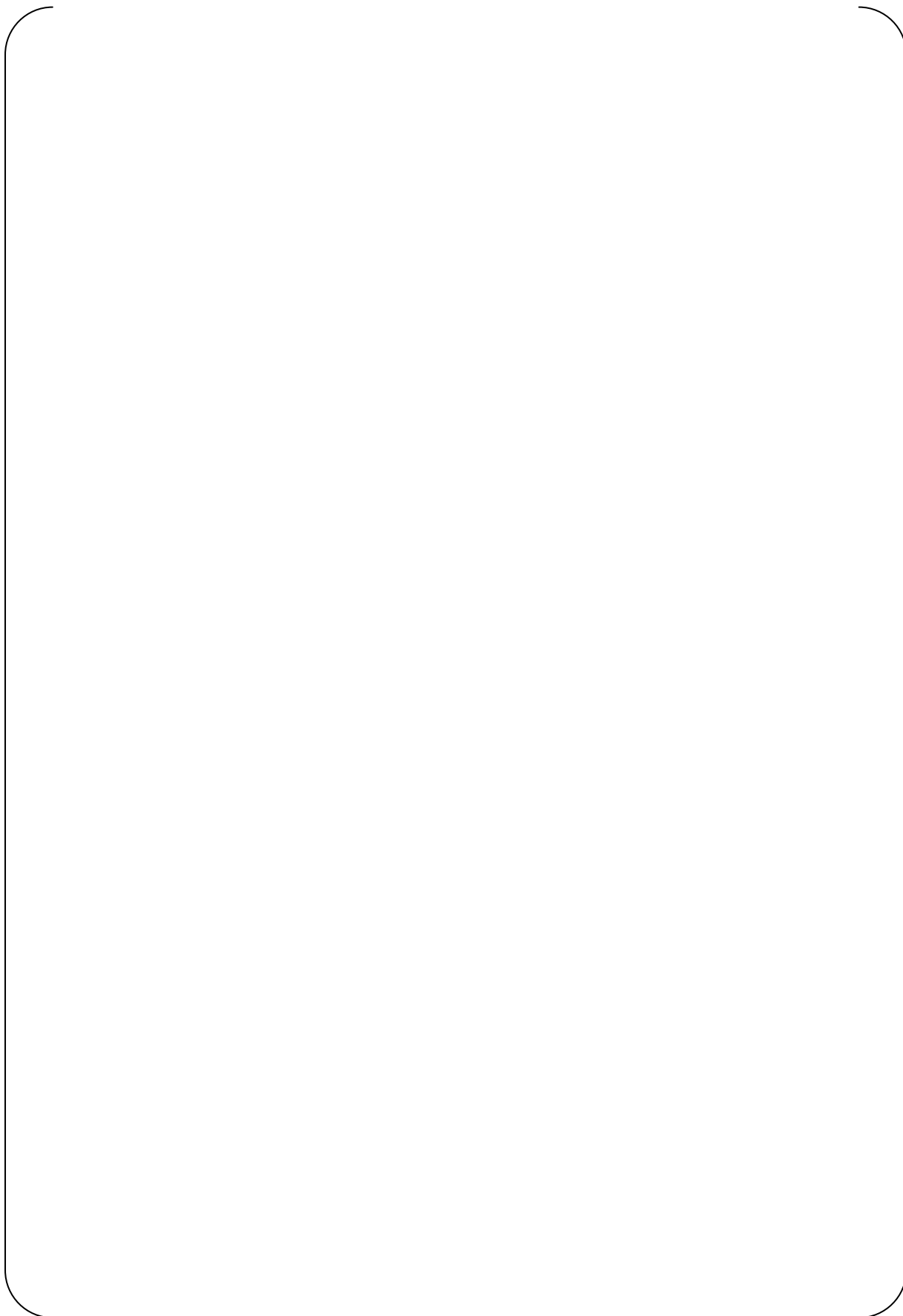
Attachment-2: Difference of fabrication history between Unit-2 and Unit-3 (2/3)

A large, empty rectangular frame with rounded corners, intended for the content of the attachment.

N/R: Number of Rotation, N/L: Number of Loading, SUM: Summation

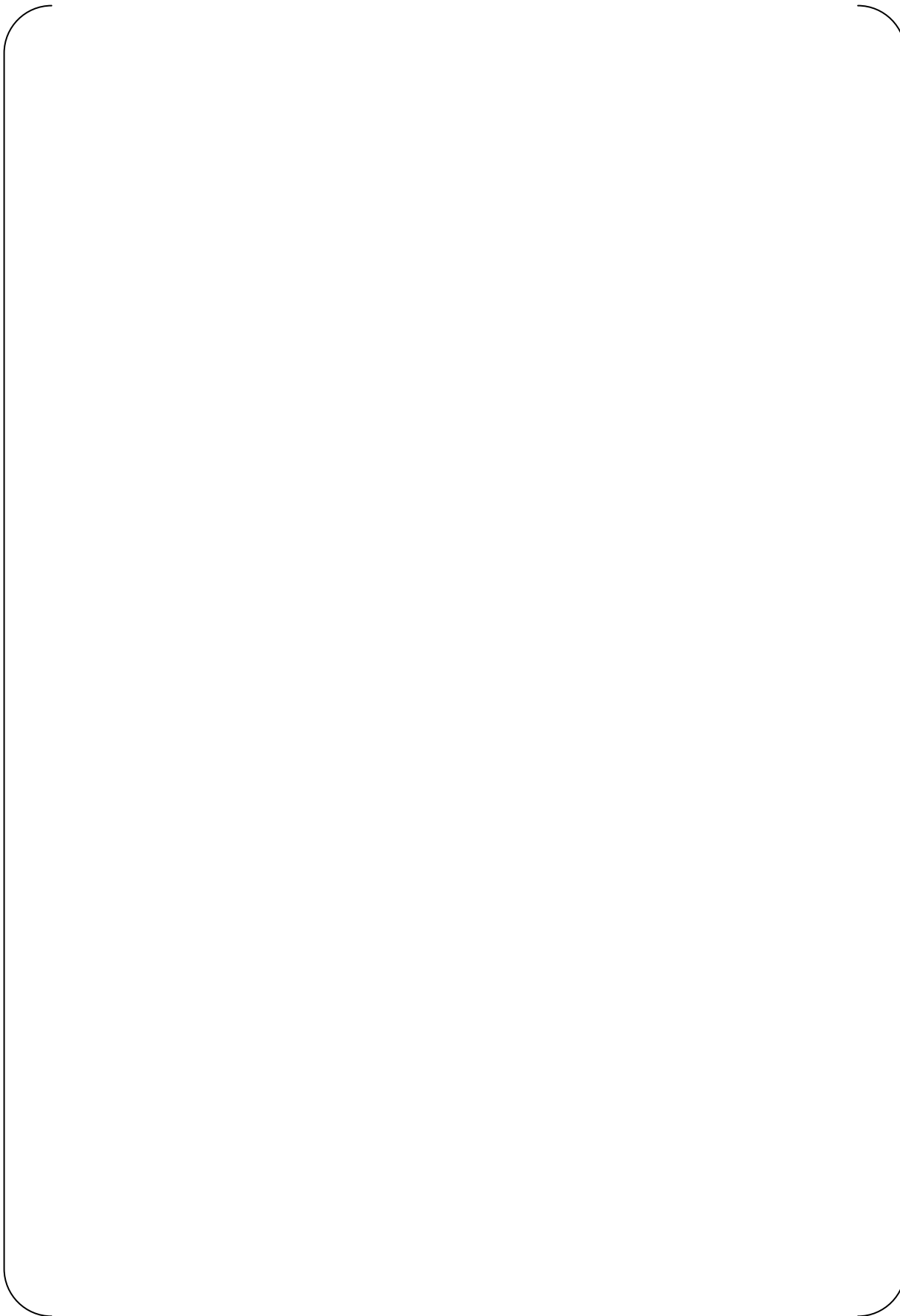


Attachment-2: Difference of fabrication history between Unit-2 and Unit-3 (3/3)





Attachment-3: Detail investigation of AVB assembly





Appendix-5
Analytical Simulation of Tube Bundle Rotation and Hydro Static Test



1. Purpose

The purpose of this evaluation is to analytically simulate the SONGS SG U-bend to evaluate the behavior of the tube-to-AVB gaps during gravitational sagging, shop rotation, and primary hydrotest.

2. Conclusion

2.1 Bundle Rotation

The tube-to-AVB gaps near the center columns increase by [] mm in one rotation. If this gap is postulated to occur at each rotation (which it doesn't), the total gap growth for 300 rotations would be [] mm, which is negligible. In the analyses, small plastic deformation occurred in limited portion, AVB outside the bundle. This small plastic strain level can not cause permanent deformation.

The tube-to-AVB gaps in the outer columns increase by [] in the first rotation; but do not repeat or grow significantly during additional rotations. The difference of the tube-to-AVB gaps between Unit-2 and 3 due to the number of SG rotations is not judged to be significant, even if it is postulated that the increased gaps in the outer columns were redistributed to the center.

The gaps generated by the pressure tests are also determined to be negligible so the difference of the tube-to-AVB gaps between Unit-2 and 3 due to the number of pressure tests is negligible.



3. Assumption

- 1) Nominal dimensions are used for analysis model.
- 2) The initial value of the tube-to-AVB gaps is assumed to be zero.
- 3) The tube pitch is assumed to be the same as the tube hole pitch of the TSP.

4. Acceptance Criteria

The tube-to-AVB gaps are evaluated to determine if they get larger during SG shop rotations or during pressure tests. The results of the analysis are compared to see if there is a significant difference between Unit-2 and Unit-3.

Table 4-1 Difference between Unit-2 and 3 during fabrication

Unit	Number of SG rotations	Number of pressure tests or times the bundle was filled with water
2	[]	2A & 2B: 1
3	[]	3A: 3, 3B: 2

5. Design Inputs

5.1 Geometry

The nominal tube bundle dimensions are obtained from the design drawings



6. Methodology

6.1 Analysis model

The ABAQUS finite element program is used to perform the analysis. The model includes the tubes, AVBs, retaining bars, retainer bars, and bridges. The modeling assumptions are shown in Table 6.1-1 and Figure 6.1-1. The model is shown in Figure 6.1-2. The TSPs are treated as pinned supports. The tubes at the TSP #6 elevation are prevented from displacing in the lateral and axial directions but are free to rotate. The tubes at the TSP #7 elevation are restrained against lateral displacement but are free to displace axially and to rotate. It is appropriate not to simulate initial gaps between TSP and tubes, because all tubes laterally displace just same amount of initial gap in the case of cantilevered U-bend, and the tube pitch is not changed. Modeling the top two TSPs is sufficient to produce a reasonable replication of the cantilevered U-bend.



Table 6.1-1 Condition of analysis models (1/2)

Analysis	Elastic -Plastic	Element					
		Tube	AVB	Retaining bars	Bridges	Retainer bars	Water
(1) Validation of analysis model	{						
(2) Simulation of SG rotation							
(3) Simulation of pressure testing							

Table 6.1-1 Condition of analysis models (2/2)

Analysis	Friction Coefficient (*1)	Boundary condition		
		Contact condition		Fastening condition
		Tubes - AVB	Tubes - Retaining bars	Retainer bars - Tube
(1) Validation of analysis model	{			
(2) Simulation of SG rotation				
(3) Simulation of pressure testing				

Note 1) See Fig. 6.1-1.

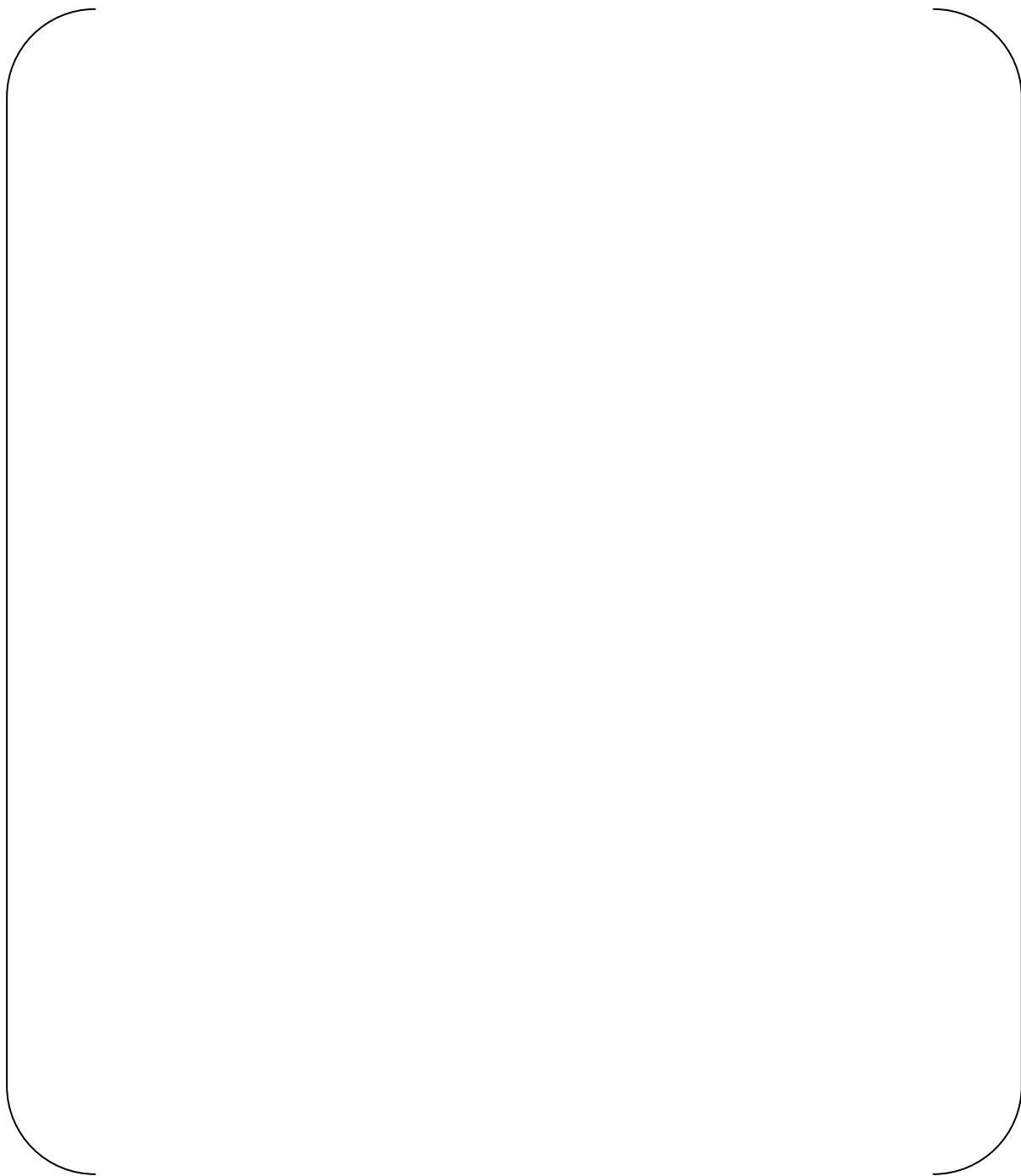


Fig. 6.1-1 Friction coefficient between Inconel 690 and 405 S.S

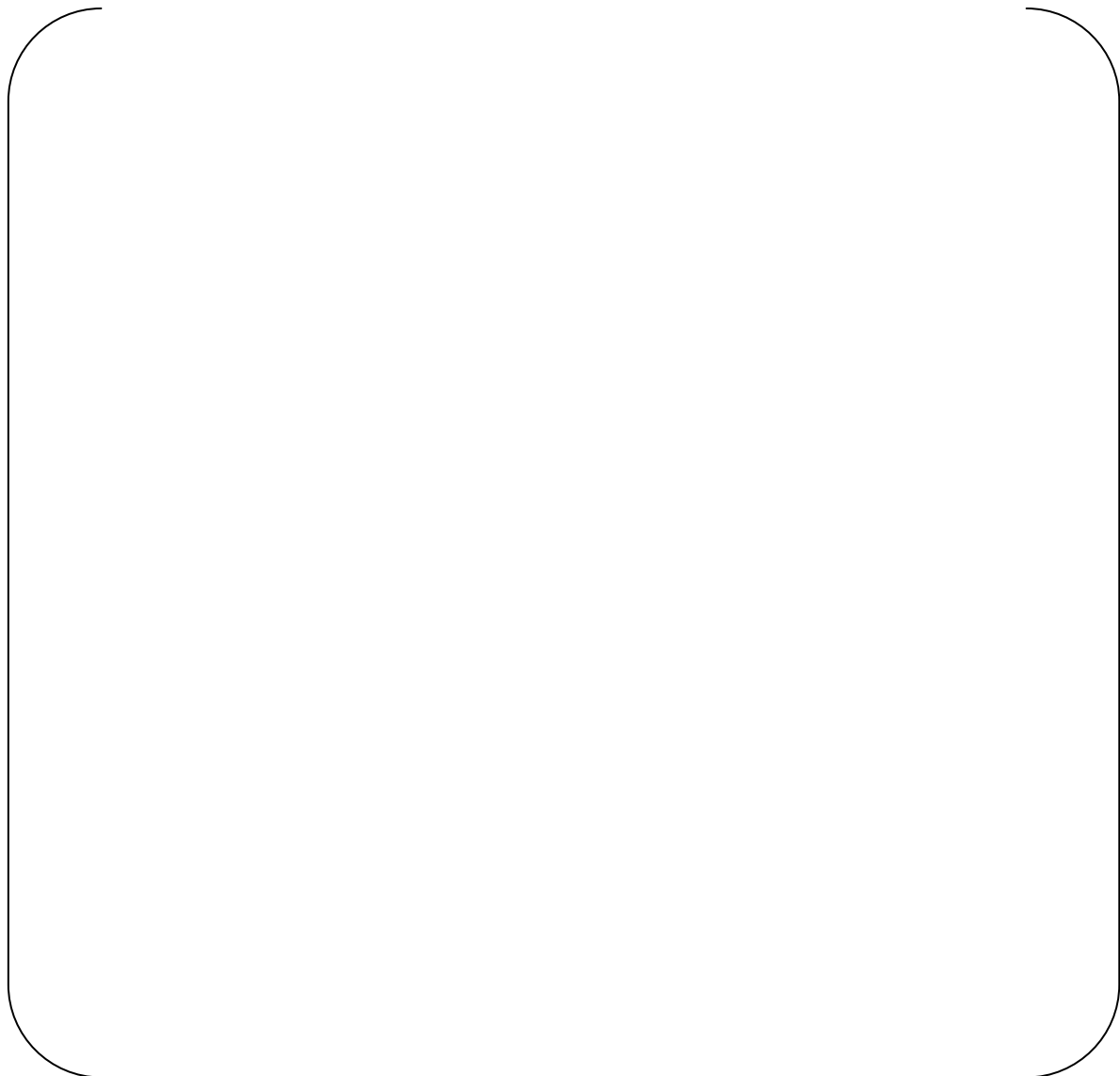


Fig. 6.1-2 Analysis Model



6.2 Evaluation cases

The following three cases were evaluated.

- (i) U-bend Sagging to validate the analytical model
- (ii) Simulation of bundle rotation
- (iii) Simulation of hydrostatic pressure testing

6.2.1 Validation of Analytical Model

A simulation of the U-bend sag due to gravity was performed to compare to measurements made during manufacture to validate the analytical model. Gravity (1G) in the out-of-plane direction (i.e. with the U-tubes in the horizontal plane, perpendicular to the floor) produced sagging that was measured at the tips of AVBs #41 and #69. A one-half model of that shown in Figure 6.1-2 was used taking advantage of symmetry. Since the measurements were taken before the retaining bars, retainer bars, and bridges were installed, those features were excluded from the model.

6.2.2 Simulation of Bundle Rotation

Since the objective of this evaluation is the tube-to-AVB gaps, bundle rotation was simulated by cycling a gravity load from plus to minus with the bundle oriented in the out-of-plane direction. A zero gravity load step was performed between each gravity load reversal. The following diagram describes this load cycle.

0G → +1G → 0G → -1G → 0G → +1G → ...

This model includes the retainer bars, the retaining bars, and the bridges. Figure 6.2.2-1 shows the model and load sequence. Refer to Table 6.1-1 for additional information about this simulation.

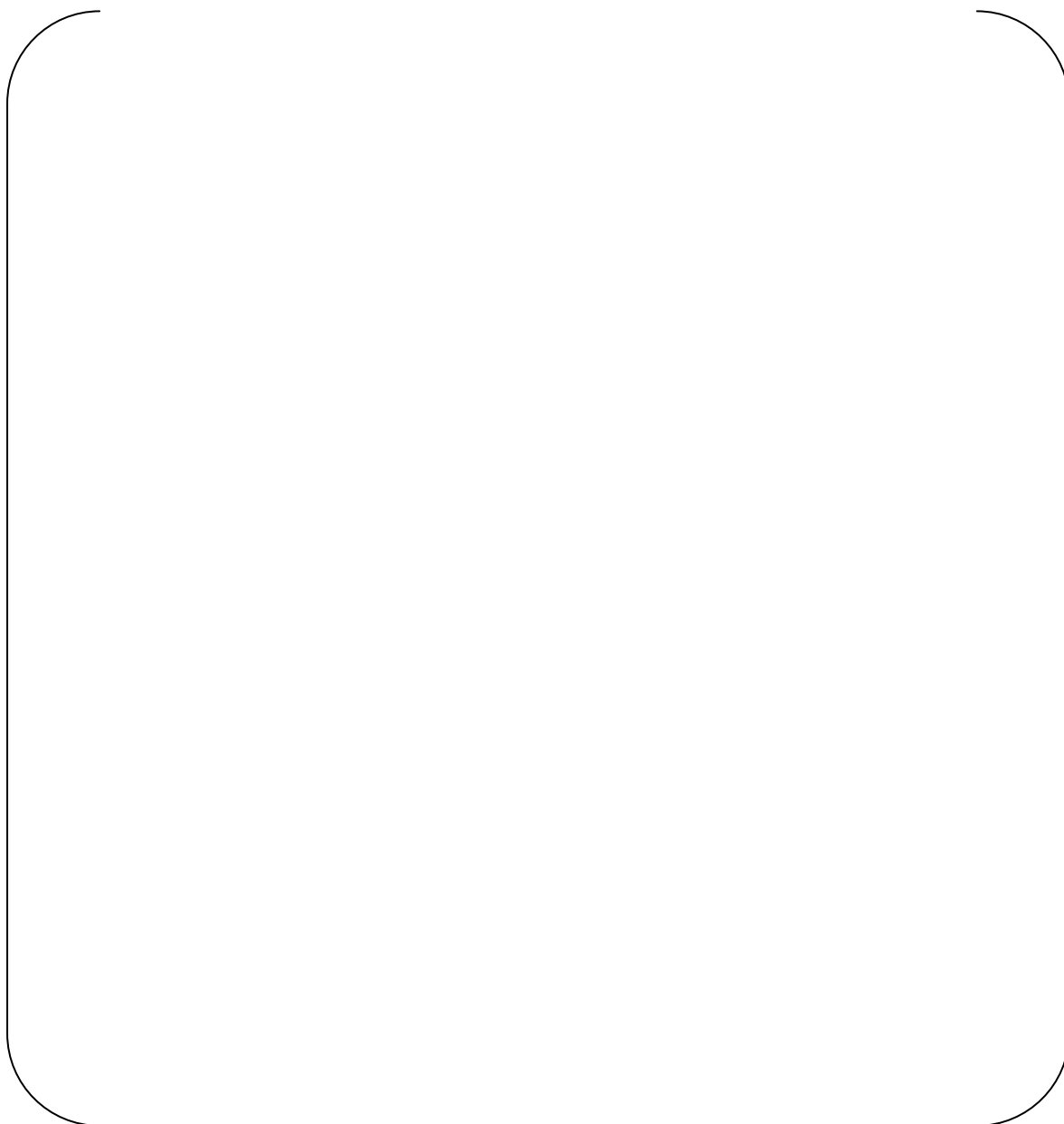


Fig. 6.2.2-1 Load sequence for Shop Rolling



6.2.3 Simulation of Hydrostatic Pressure Testing

To evaluate difference of the tube-to-AVB gaps increment around the center column, where many wears have occurred, between Unit-2 and 3, due to the number of pressure testing, simulation of pressure testing is performed.

The weight of the tube bundle increases by the weight of water inside the tubes during the primary hydrostatic pressure test. The orientation of the tube bundle during pressure testing is with the tube lane inclined at an angle of 45 degrees – but is simulated with tube bundle in the out-of-plane orientation. The test sequence is adding water, pressurization, depressurization, and draining water. The tube mass is increased by a factor of 1.5 to account for the added weight of water. Although gravity is oriented at 45-degree orientation the simulation is run with the bundle in the out-of-plane direction. The out-of-plane equivalent loading for the hydrotest is $+1G/\sqrt{2} \times 1.5 = +1G$. A 0.7G loading is used to represent the draining / depressurization step. The following load sequence is used to model two hydrotests.

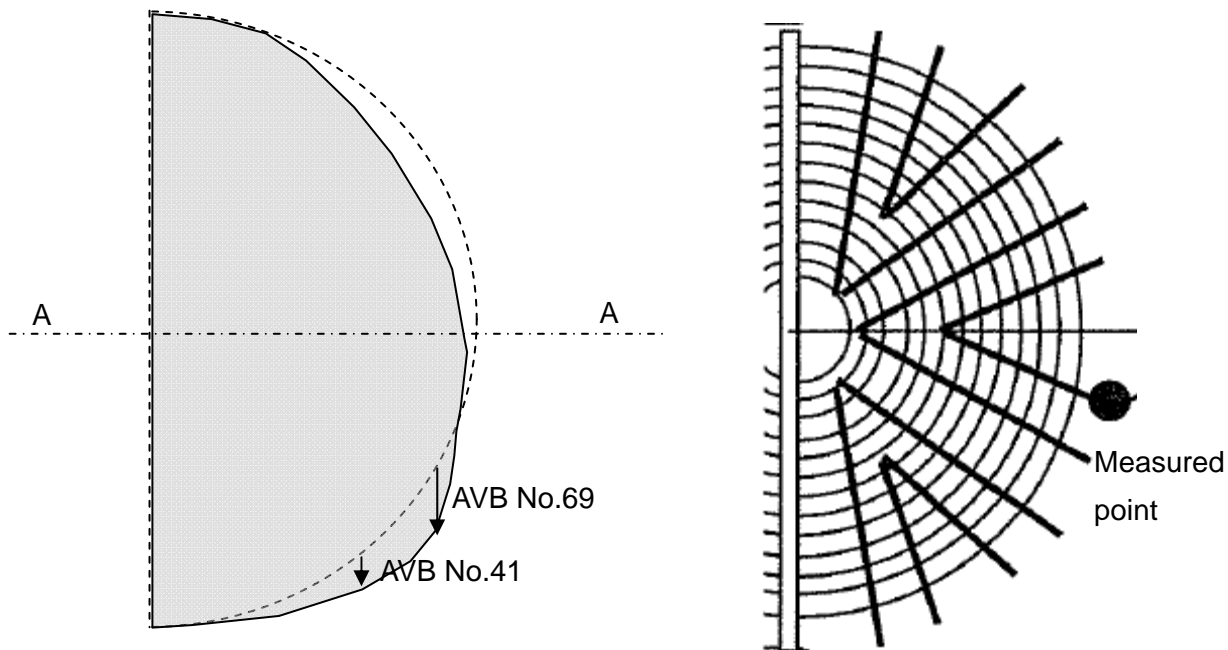
0G → +1G (adding water / pressurization) → +0.7G (draining water) → +1G (adding water / pressurization) → +0.7G (draining water) → 0G



7. Results

7.1 Validation of analysis model

Measurement points of AVB #41 and #69 for sagging during fabrication are shown in Figure 7.1-1. Measurement and analysis results are compared in Table 7.1-1. The calculated sag is slightly less than what was actually measured, but is considered to be close enough to validate the model.



(1) Out-of-Plane Deformation

(2) Section A-A

Fig. 7.1-1 Out-of-Plane Deformation due to Sagging

Table 7.1-1 Comparison Result of Out-of-plane Displacement during Sagging

Case	AVB – Tube	Displacement (mm)	
		AVB No.41	AVB No.69
Analysis	None (Retaining bars are not modeled)	[]	[]
Measurement	Fastened		



7.2 Simulation of SG rotation

7.2.1 Deformation and Gaps during SG rotation

The deformation of tube bundle and the tube-to-AVB gaps during SG rotation are analyzed step by step, as follow.

(1) Step 0: Initial Condition

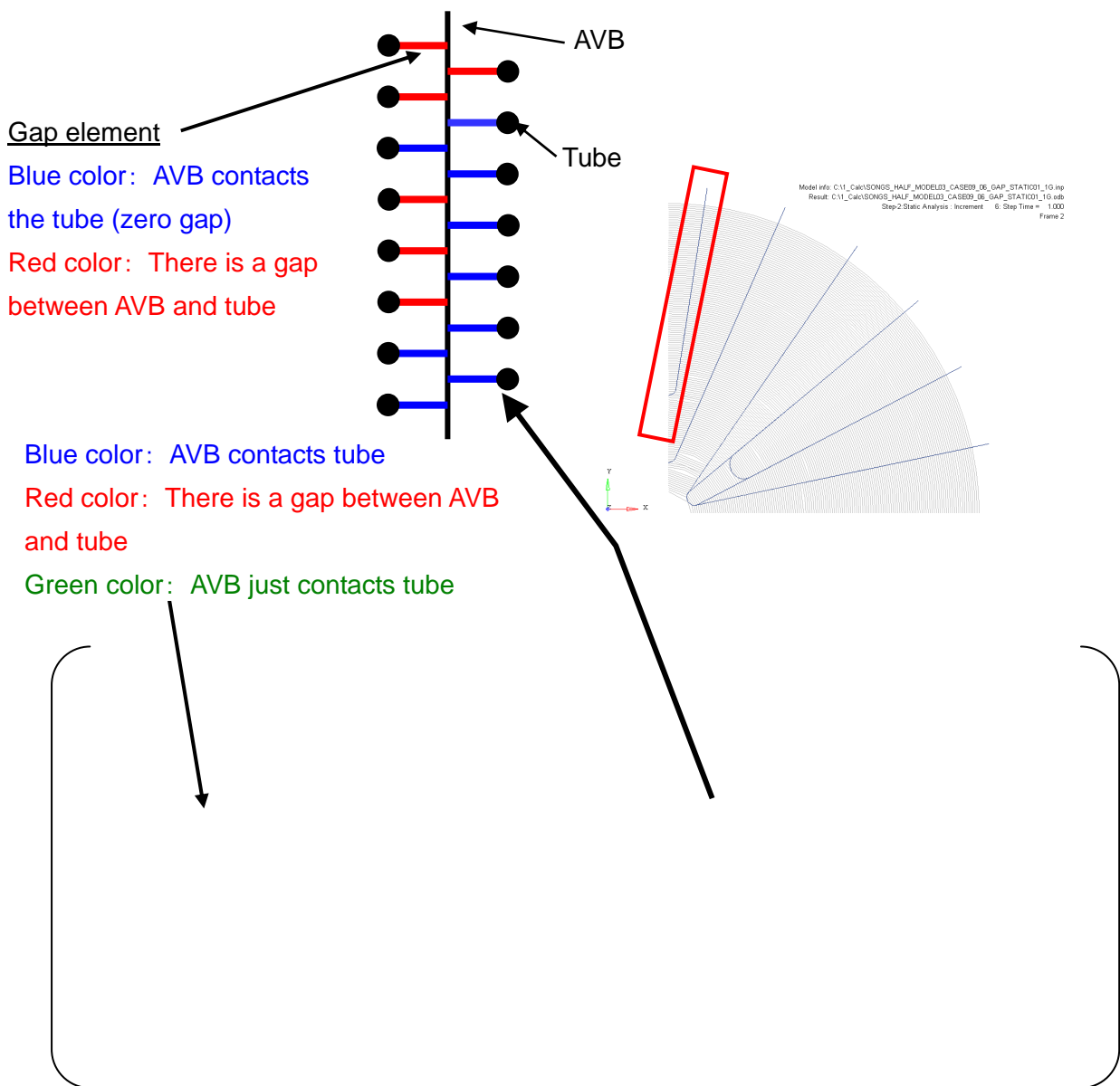
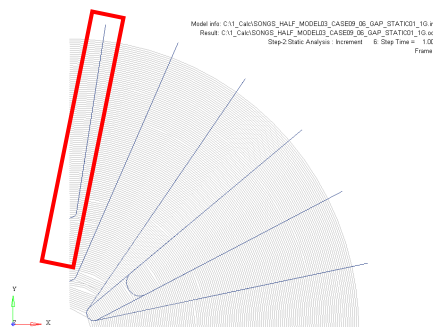


Fig. 7.2.1-1 AVB-Tube Gap contour for initial condition



(2) Step 1: +1G acting (1st turn)



Sagging of retaining bar depends on sagging of tubes in center columns. Retaining bar and AVBs push tubes down, because sagging of retaining bar is larger than gravity deformation of tubes near both ends of retaining bars.

Tubes gravity deformation is different in each column, because gravity deformation is proportional to 4th power of tube radius.

No gap is generated, because retaining bar pull AVBs down

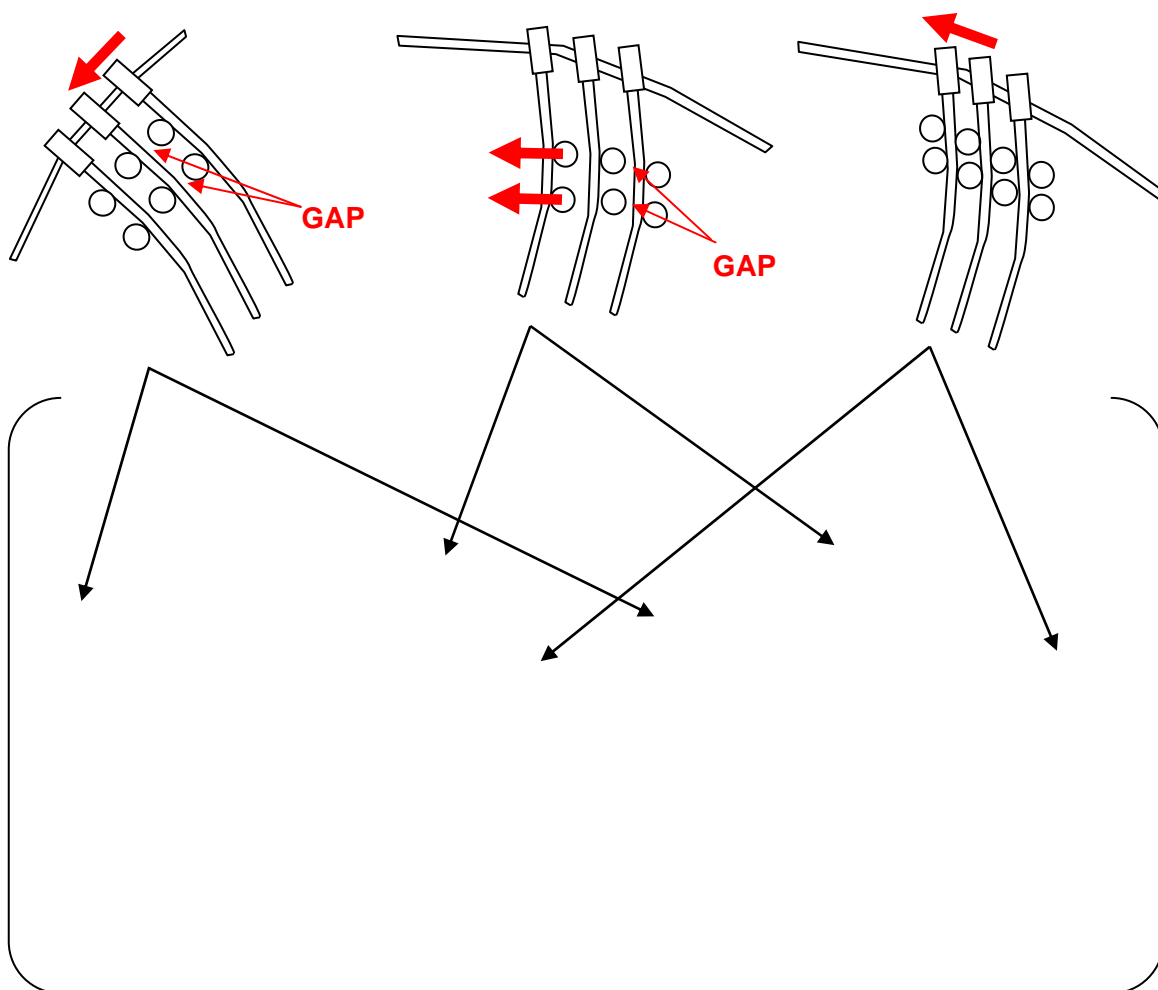
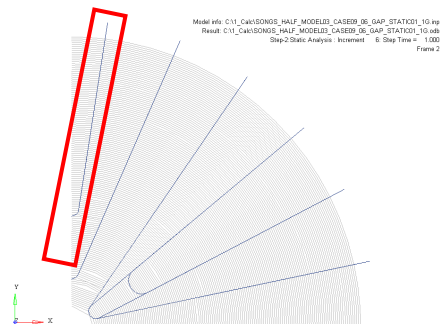


Fig. 7.2.1-2 AVB-Tube Gap contour for +1G condition of first turn



(3) Step 2: 0G condition



It appears that the gaps generated by $\pm 1G$ remain because AVB cannot move into tube bundle due to friction force.

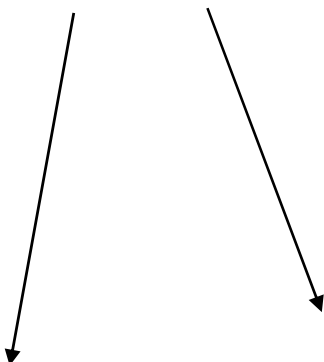
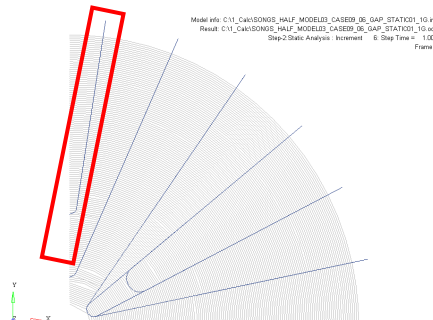


Fig. 7.2.1-3 AVB-Tube Gap contour for 0G condition of first turn



(4) Step 3: -1G acting (1st turn)



The gap is generated at symmetrical position against Step 1.

Retaining bar is deformed in opposite direction of Step 1. AVB near both ends of the retaining bar is dragged by the deformed retaining bar.

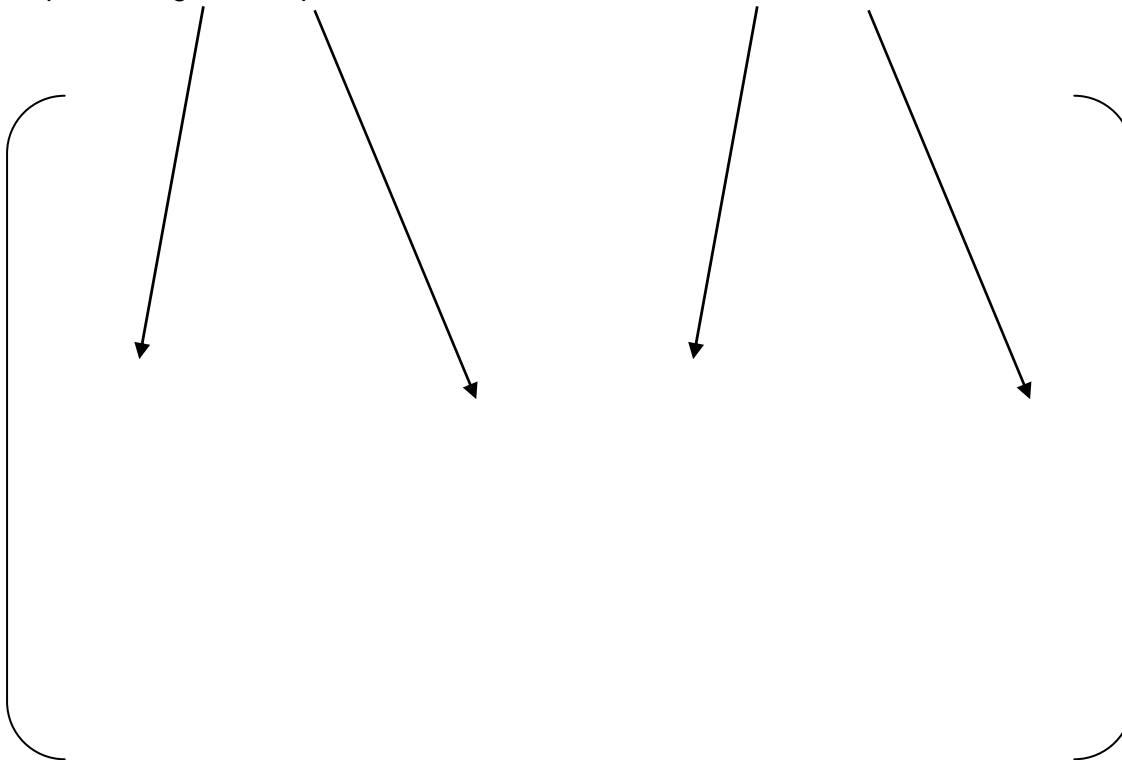
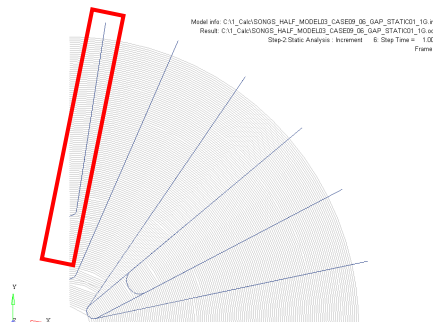


Fig. 7.2.1-4 AVB-Tube Gap contour for -1G condition of first turn



(5) Step 4: Gravity free (After 1st turn)



The gaps generated by the gravity on Step 3 remain.
 The gaps generated by the gravity on Step 1 don't remain.
 (The gaps contour is determined by the last gravity.)

The deformations of the retaining bar and AVB remain. It would appear that the AVB cannot move into the tube bundle due to friction force.

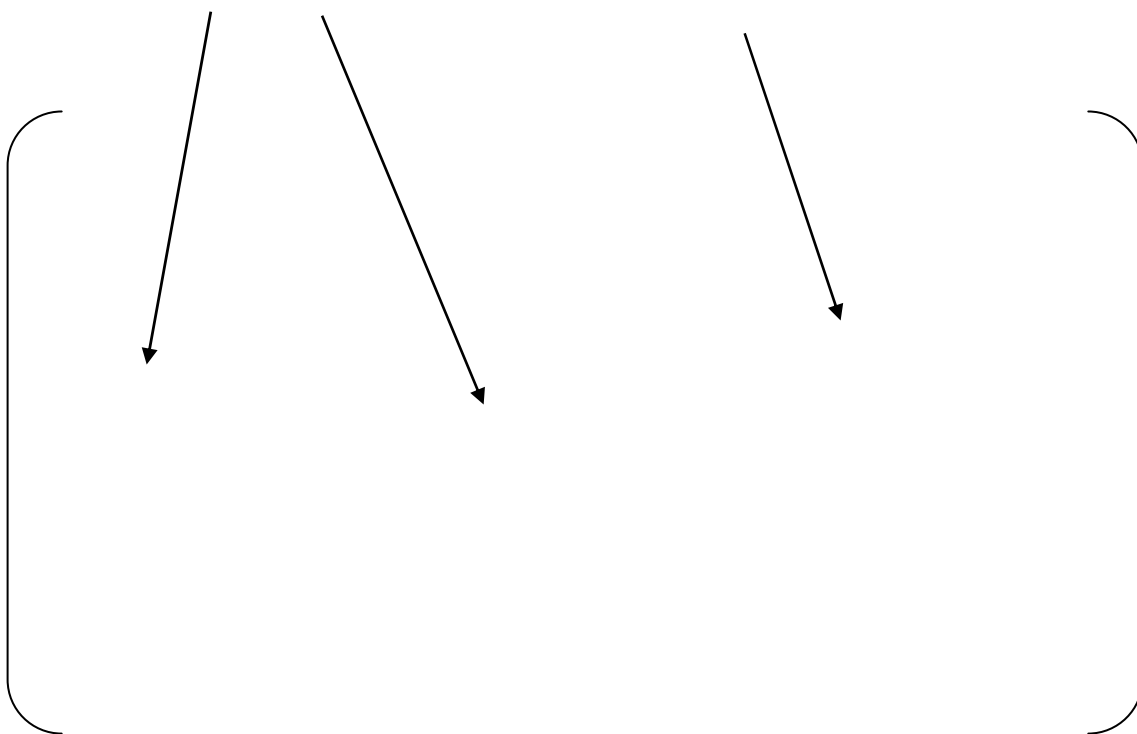


Fig. 7.2.1-5 AVB-Tube Gap contour for 0G condition of first turn



(6) Step 25-28 7th turn

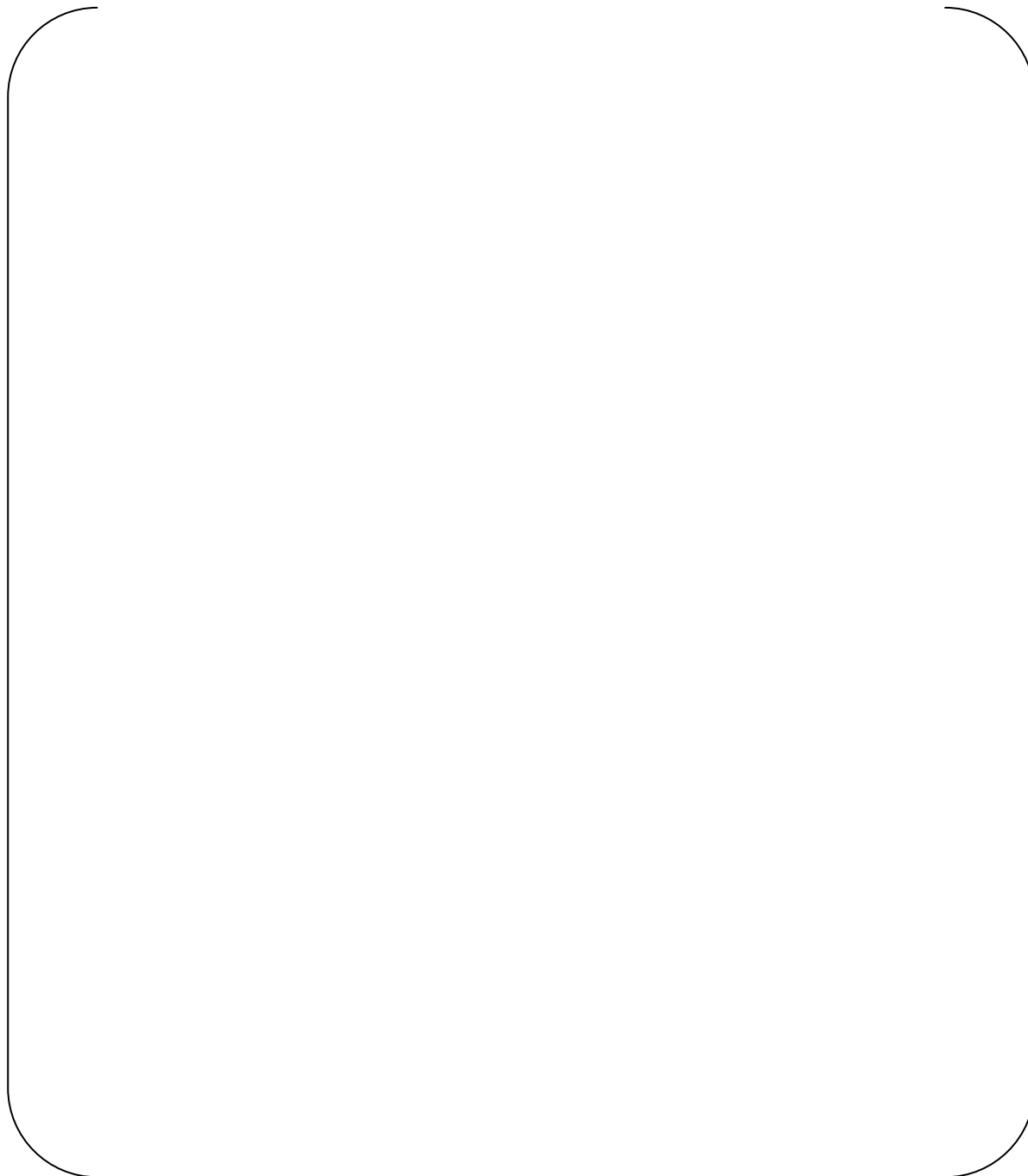
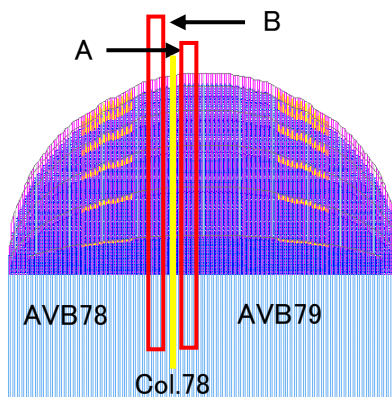


Fig. 7.2.1-6 AVB-Tube Gap contour of 7th turn



(7) Step 28 Gravity free (after 7th turn)

For one surface, there are some unsupported points in one tube. On the other hand, for the opposite surface, the tube contact with the AVB at all points.



These tubes are unsupported by AVBs continuously.

There are consecutive small gaps at AVB support points. However, the increases of gaps are negligibly small.

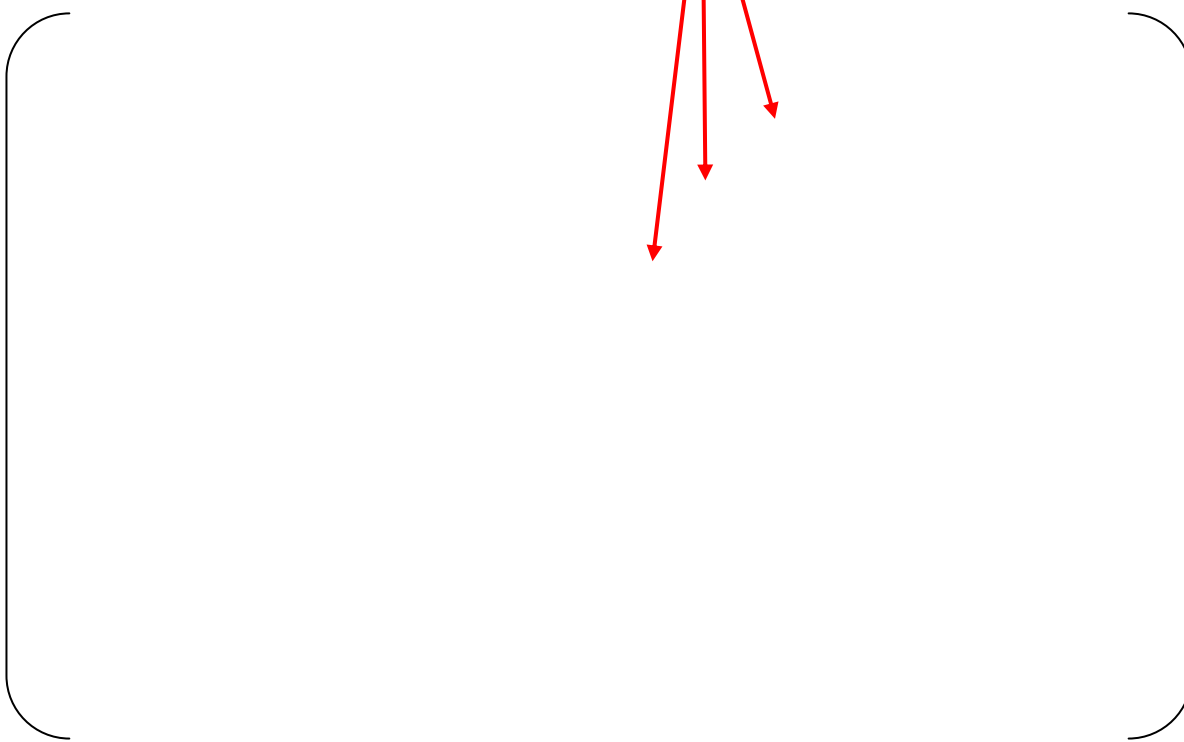


Fig. 7.2.1-7 AVB-Tube gap contour in Column 78



7.2.2 Enlargement of tube bundle width

Enlargement of tube bundle width (cross sections α_1 , α_2 , and α_3) is calculated from 1st to 7th turn at the points shown in Fig. 7.2.2-1.

The width of the tube bundle is not changed after the 3rd turn as shown in Fig. 7.2.2-2. The maximum change of the width is [] mm at cross-section α_3 . The expansion is caused by the AVB-Tube gaps near the edges at the retaining bars. It is theorized that during operation, the fluid hydrodynamic pressure might shift the gaps from the edges to the center. This would equate to a widening of [] near the center column.



Fig. 7.2.2-1 Evaluated points of expansion



Fig. 7.2.2-2 Change per rotation of tube bundle width (first 7 rotations)



7.2.3 Change of the Tube-to-AVB gaps

Changes of the AVB-tube gaps from 1st to 7th turn are investigated. Changes near Col90, 135, and 160 are shown in Fig. 7.2.3-1. Although the small gaps (about [] mm gaps) are generated near Col.90, the large gaps (about [] mm) are generated near the retaining bars. It suggests possibility of the larger gaps (about [] mm) near the center column by redistribution during operation.

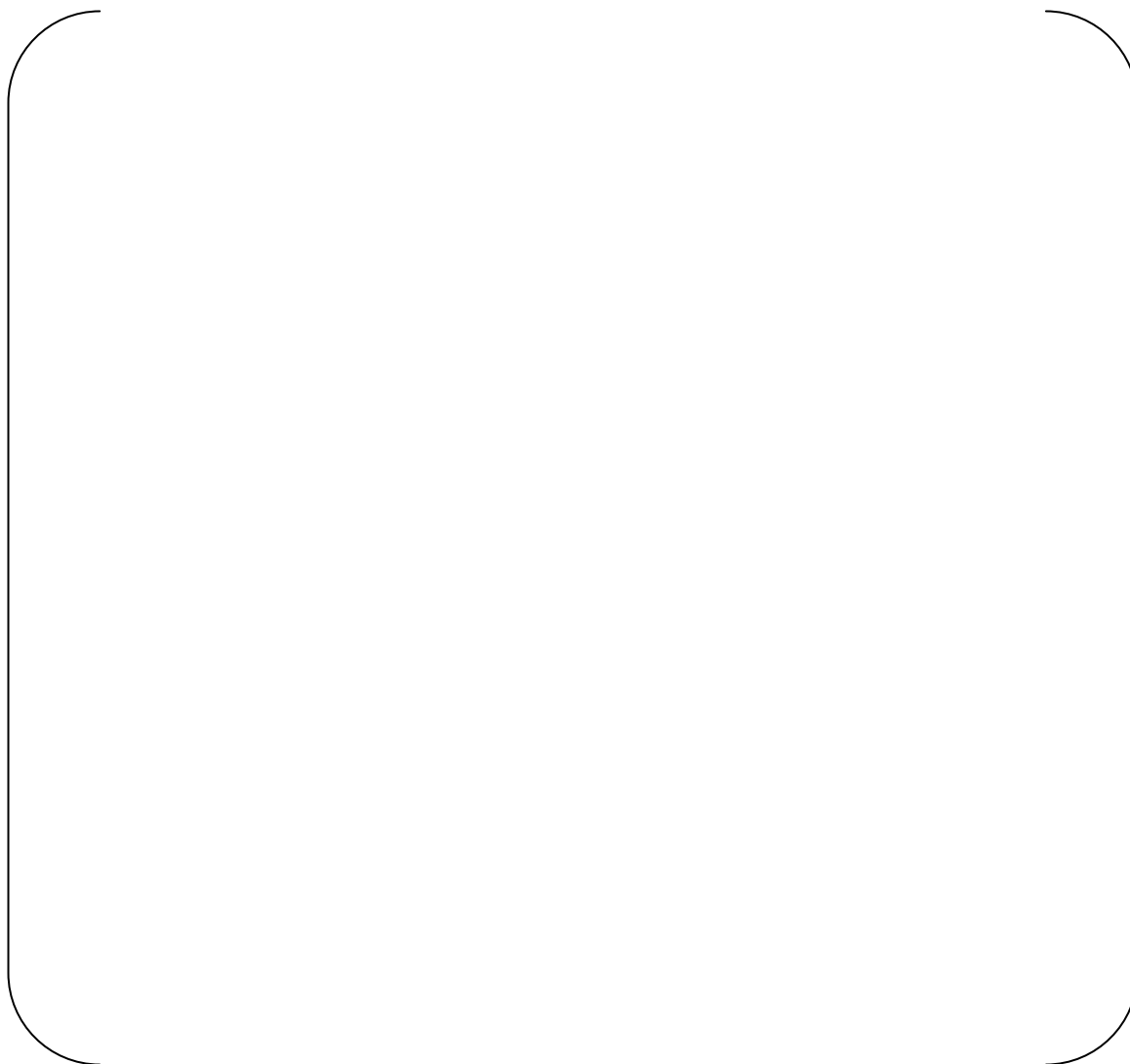


Fig. 7.2.3-1 Change of the AVB-Tube gap between 1st turn through 7th turn



7.3 Simulation of Hydro Test

7.3.1 Deformation and Gaps due to pressure testing

The load direction and deformation during pressure testing is shown in Fig. 7.3.1-1. The tube-to-AVB gaps during pressure testing are shown in Fig. 7.3.1-2 and 7.3.1-3. The tube-to-AVB gaps generated by pressure testing are around [] mm, and are negligibly small.

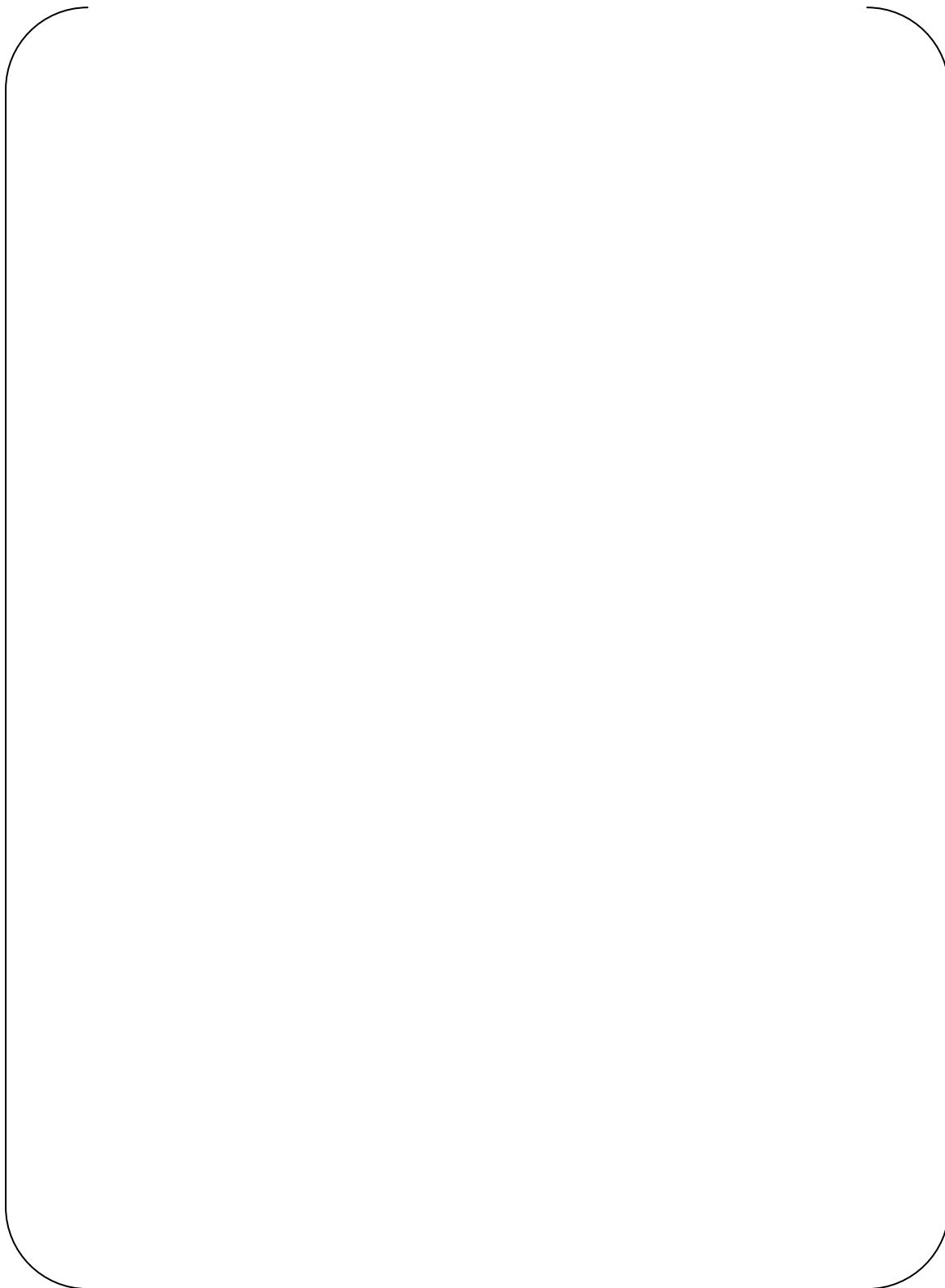


Fig.7.3.1-1 Load direction and deformation during pressure testing

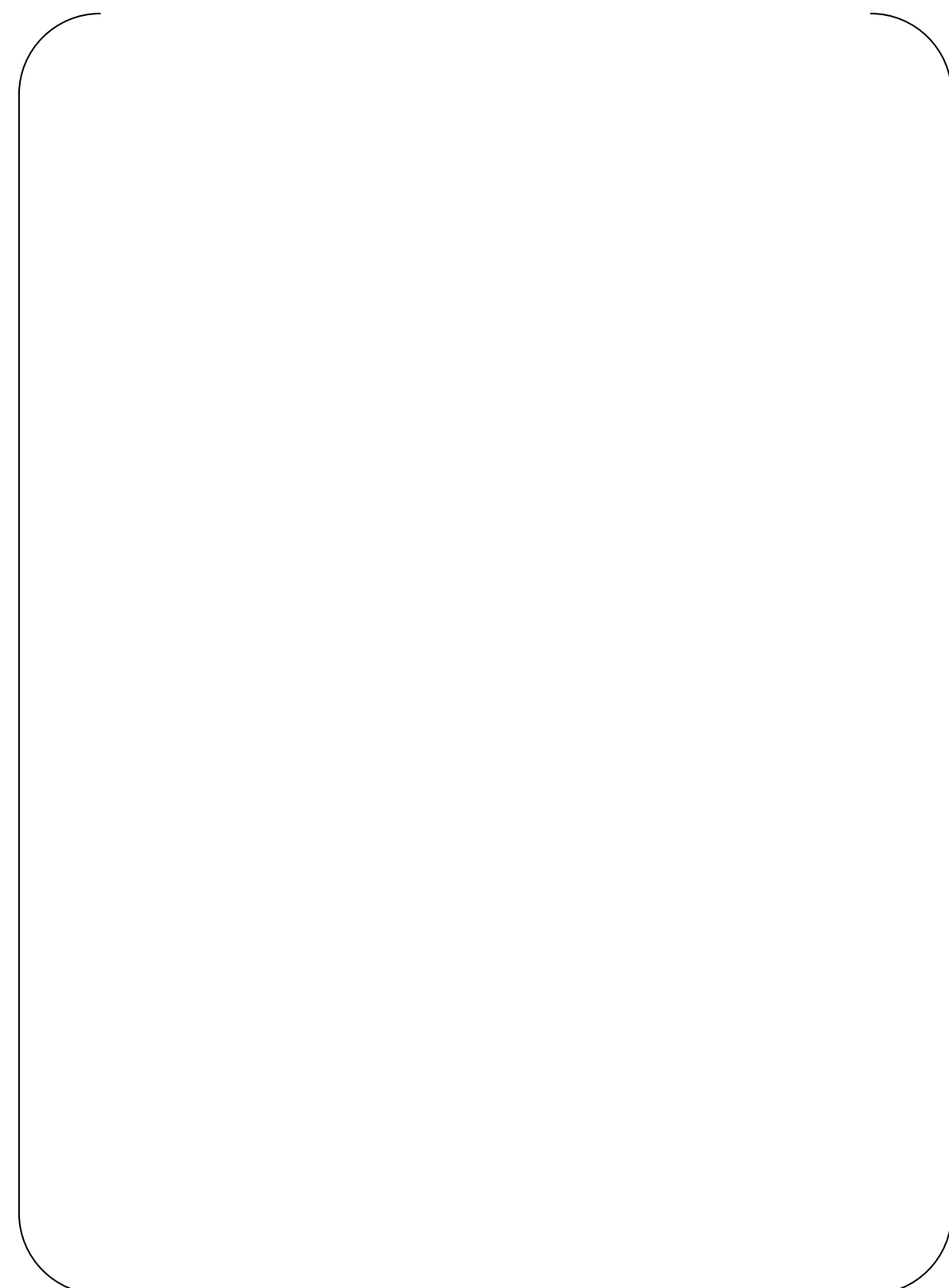


Fig. 7.3.1-2 AVB-Tube Gap Contour in 1st Pressure Testing

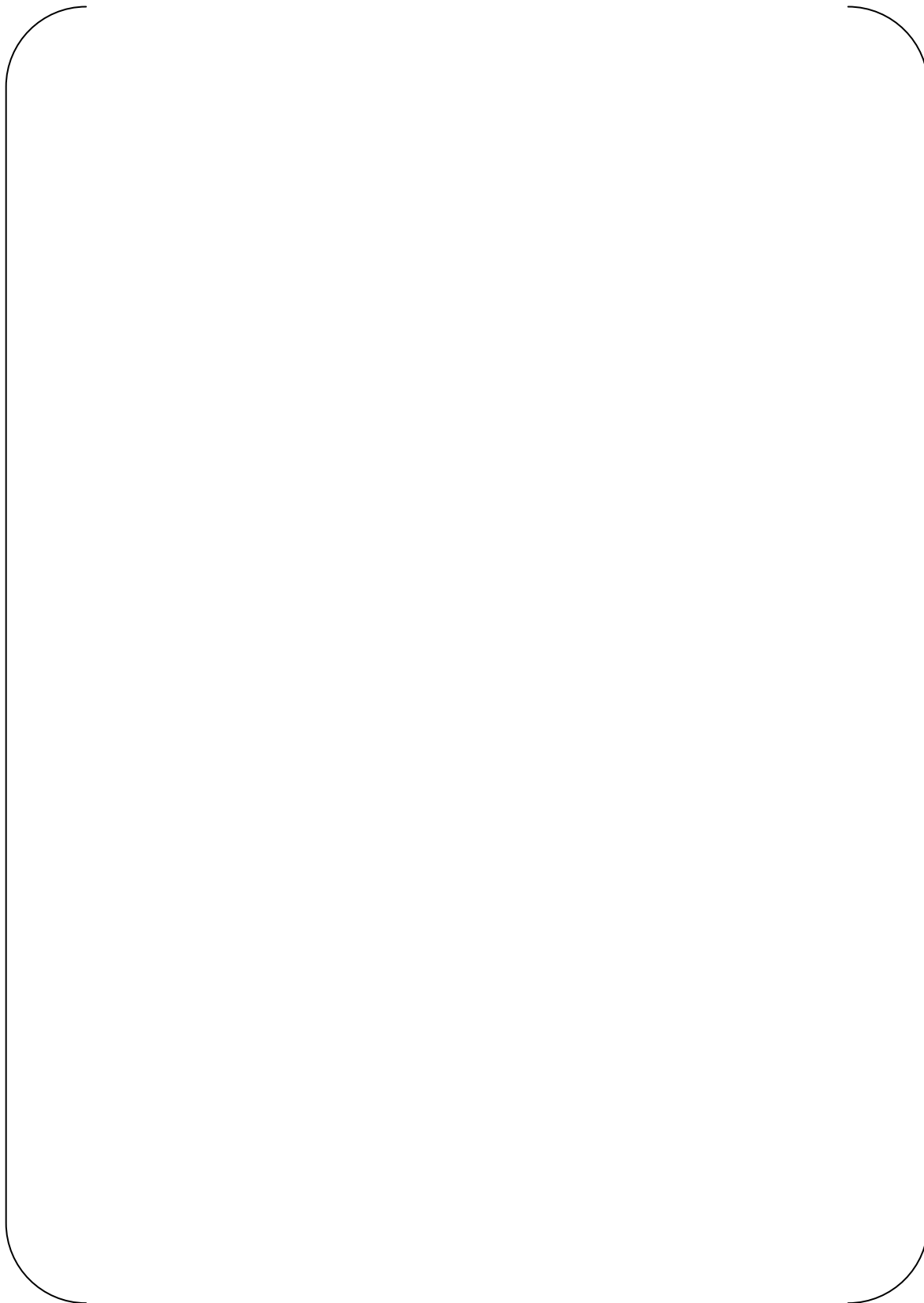


Fig. 7.3.1-3 AVB-Tube Gap Contour in 2nd Pressure Testing



Appendix-6
Investigation of ISI ECT Data for AVB Support Condition for Unit-2/3



1. Tube to AVB gap evaluation

1.1 Introduction

ECT data was used to evaluate the tube-to-AVB gap sizes in the Unit 2 and Unit 3 SGs after 22 months and 11 months of operation, respectively.

Bobbin probe was used for the evaluation.

1.2 Evaluation method

Effort was made to eliminate or minimize sources of error in the ECT data shown in Table 1. Table 2 describes the countermeasures taken in this evaluation.

Table 1 The factors which influence the gap evaluation

	140kHz Abs. Peak-to-peak amplitude		140kHz abs Integral Amplitude	
	X	L	X	L
Thickness reduction or dent of tube	X	L	X	L
Misalignment of AVB	X	L	-	-
Dimensional error on calibration notch	X	M	X	M
Variation of scanning speed of probe	-	-	X	M
Scale on tube outer surface	X	S	X	S
Thickness of tube	X	S	X	S
Width of AVB	X	S	X	S

Note: "L","M" and "S" show the degree of influence on the evaluation.

L: Large, M: Medium, S: Small

Table 2 Significant error factor and countermeasure

Error factor	Correction
Misalignment of AVB	Differential channel is sensitive to the misalignment factor. Absolute channel and the absolute amplitude integral method can reduce the factor. These two methods are adopted. (Attachment 2)
Dimensional error on Calibration notch	Each of Cal std variability is corrected.



1.3 Tube-to-AVB Gap Evaluation

Color maps that show the bobbin absolute AVB signal amplitude for each tube at each AVB in each of the 4 SGs (refer to Attachment 1). Measurements of larger amplitudes are associated with smaller gaps.

The large green areas of the Attachment 1 plots indicate gaps of () or less (approximate). The amplitudes in B01, B12 of SG-3B around Row 50 are slightly smaller than what is present in other SGs in the region, which potentially indicates larger gaps along Row 50.

Figure 1 shows an evaluation of average amplitude at each AVB of the four steam generators. In this figure the ranking of SGs by average amplitude from large to small is 2B, 2A/3B, 3A - where the larger amplitude is associated with smaller tube-to-AVB gaps. This indicates that (slightly) larger average gaps are present in the Unit-3 SGs than in the Unit-2 SGs. It is also noted that Figure 1 shows smaller gaps (larger amplitudes) in the region of the tubes that are closest to the top TSP. This may be related to the uniform tube support plate hole spacing. Figure 2 shows the maximum gap, minimum gap and distribution of ECT amplitude value.

Mock up test results of tube-to-AVB gaps and AVB misalignment are shown in Attachment 2. These results provide insight into the accuracy of the data.

※Remarks for Attachment 1: The white color in 2A and 2B means that ECT data is missing at that location.



Fig.2 Distribution of ECT amplitude value (140kHz-Abs,integral)



4 Conclusion

The results of this evaluation show that the Unit-3 SGs have slightly larger average tube-to-AVB gaps than the Unit-2 SGs, with the largest in SG-3A. This trend indicates the tube-to-AVB contact force of Unit-3 SGs are smaller than that of Unit-2 SGs.

Attachment 1 : Amplitude integral color map of Bobbin probe (Abs)

Attachment 2 : Mock up test result of gap and misalignment evaluation

Non-proprietary Version [

] (P.6-6)
Document No.L5-04GA564(9)



Amplitude integral color map ([}Abs) (1/2)

Non-proprietary Version [

] (P.6-7)
Document No.L5-04GA564(9)



Amplitude integral color map ({ }Abs) (2/2)



Amplitude of Bobbin coil probe v.s. gap and misalignment (Mock-Up)



2. AVB insertion depth evaluation

Evaluation of as-built insertion depth of AVBs was conducted by the bobbin ISI-ECT data for representative columns for 3B-SG.

2.1 Sample tubes and AVBs used for evaluation

See Table-1, 2, 3, 4 and 5.

2.2 Evaluation method

Each AVB location on representative tubes is evaluated by estimating the arch length on tubes by ISI-ECT signal interval from #7 TSP. And these locations are plotted on the drawing for comparison with the design-based locations. (See Table-1, 2, 3, 4 and 5.)

2.3 Result

ECT-based AVB locations are compared with design-based locations as shown in Fig.1, 2, 3, 4 and Fig.5. It is evaluated that AVB insertion depth in actual SG is not changed compared with the design-based location, where the measurement uncertainty of AVB position due to the difference of the scanning speed is considered approximately [].



Table-1 Distance between the center of #7TSP thickness and AVB position (3B-SG)

<Column 9>

Row	B01	B02	B03	B04	B05	B06	B07	B08	B09	B10	B11	B12
1												
3												
5												
7												
9												
11												
13												
15												
19												
23												
27												
29												
31												
33												
35												
37												
41												
43												
47												
49												
51												
53												
55												

(unit ; mm)



Table-2 Distance between the center of #7TSP thickness and AVB position (3B-SG)

<Column 10>

Row	B01	B02	B03	B04	B05	B06	B07	B08	B09	B10	B11	B12
2												
4												
6												
8												
10												
12												
14												
16												
18												
20												
22												
24												
26												
28												
30												
38												
48												
50												
52												
58												

(unit ; mm)



Table-3 Distance between the center of #7TSP thickness and AVB position (3B-SG)

<Column 11>

Row	B01	B02	B03	B04	B05	B06	B07	B08	B09	B10	B11	B12
1												
3												
5												
7												
9												
11												
13												
15												
17												
19												
23												
27												
29												
37												
47												
49												
51												
57												
63												

(unit ; mm)



Table-4 Distance between the center of #7TSP thickness and AVB position (3B-SG)

<Column 77>

ROW	B01	B02	B03	B04	B05	B06	B07	B08	B09	B10	B11	B12
3												
7												
15												
17												
19												
21												
23												
25												
27												
37												
47												
67												
87												
107												
127												
141												

(unit ; mm)



Table-5 Distance between the center of #7TSP thickness and AVB position (3B-SG)

<Column 89>

Row	B01	B02	B03	B04	B05	B06	B07	B08	B09	B10	B11	B12
1												
3												
5												
7												
9												
11												
13												
15												
19												
21												
23												
27												
29												
33												
37												
39												
43												
47												
67												
85												
103												
107												
109												
113												
125												
137												

(unit ; mm)



Fig.1 Column9 AVB Position
(solid line ; design, broken line ; ISI-ECT)



Fig.2 Column10 AVB Position
(solid line ; design, broken line ; ISI-ECT)

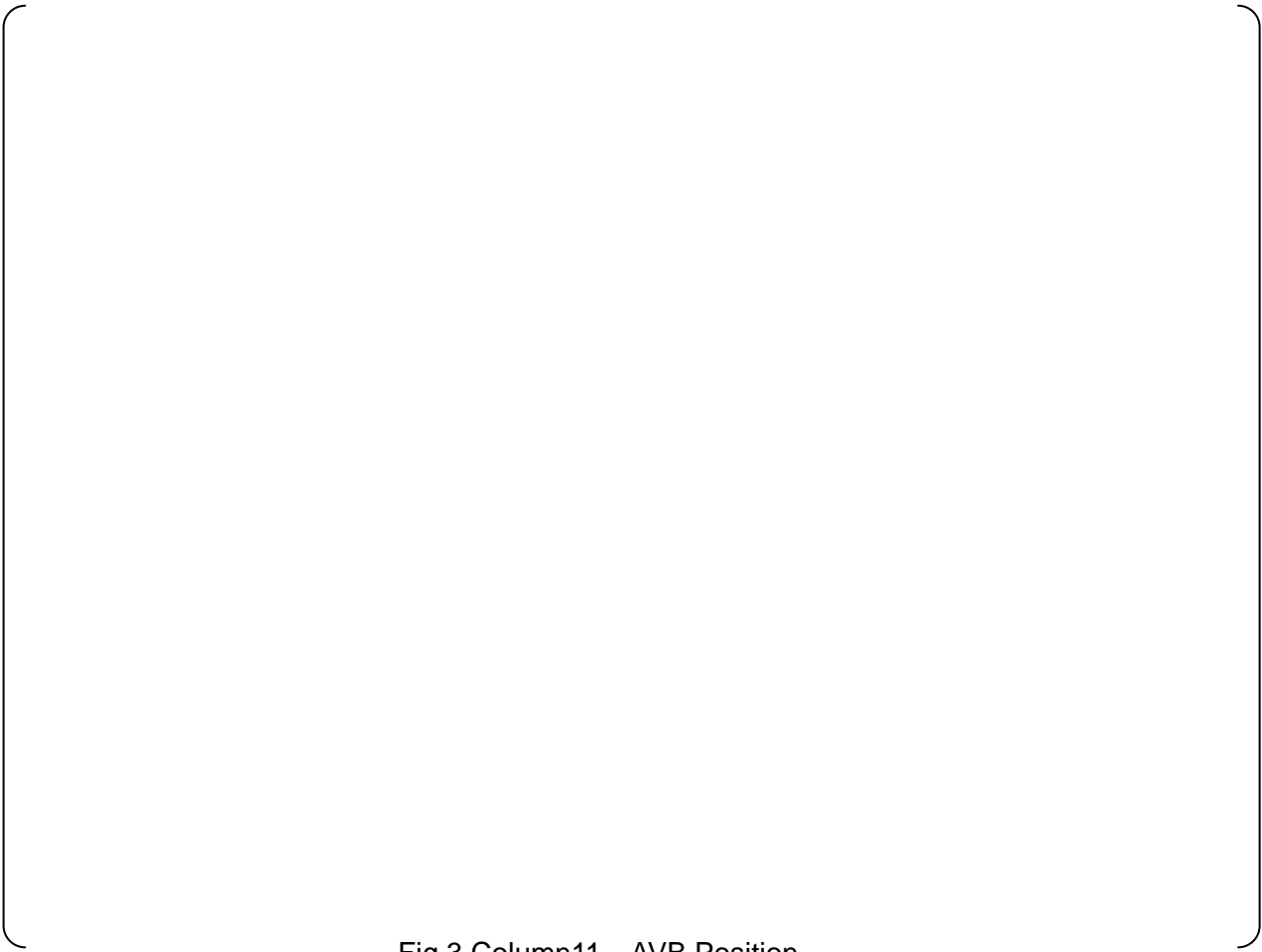


Fig.3 Column11 AVB Position
(solid line ; design, broken line ; ISI-ECT)

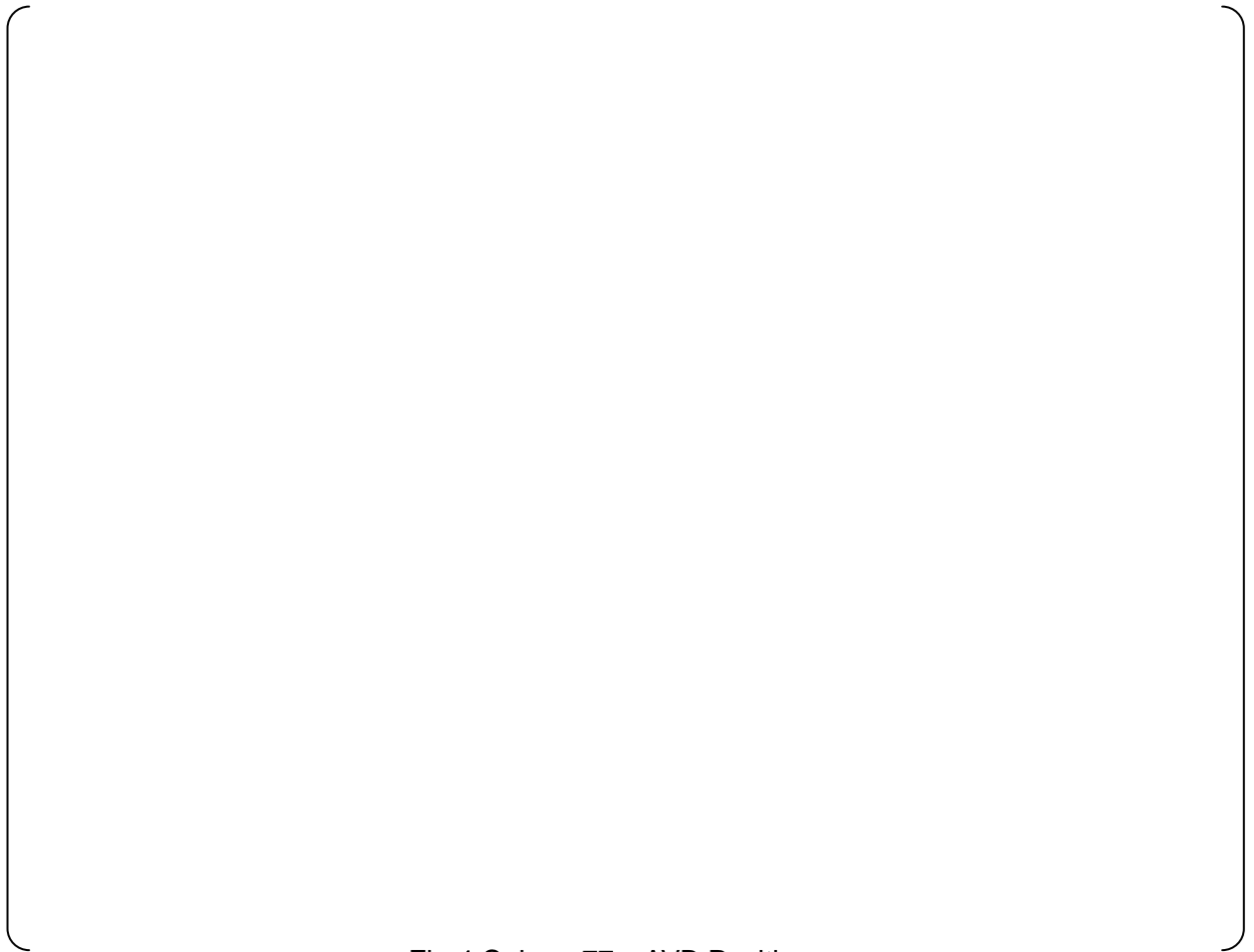


Fig.4 Column77 AVB Position
(solid line ; design, broken line ; ISI-ECT)

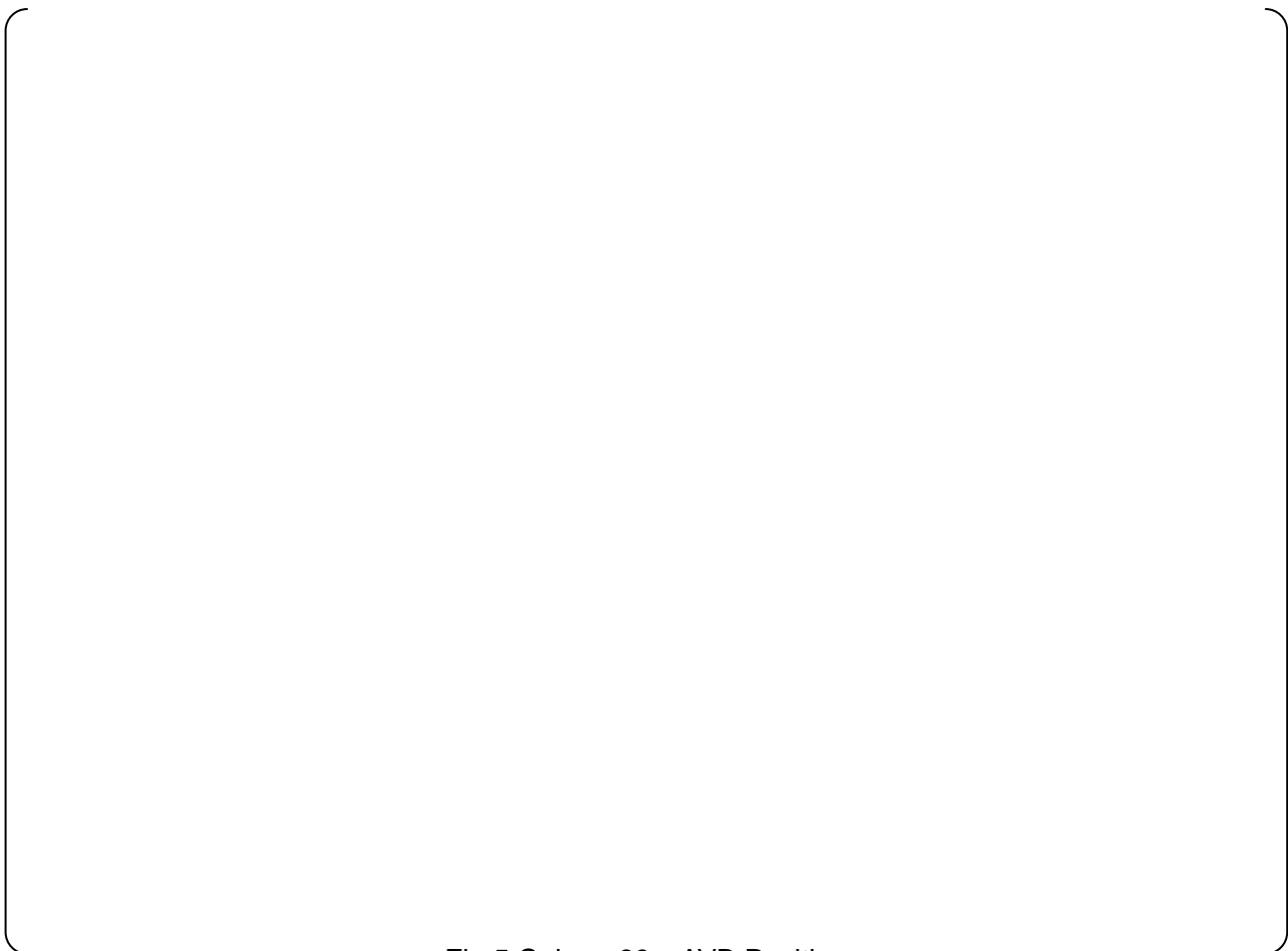


Fig.5 Column89 AVB Position
(solid line ; design, broken line ; ISI-ECT)



Appendix-7
Visual Inspection Results for U-Bend Region for Unit-2/3



1. Purpose

This appendix shows the visual inspection result of the tubes and AVBs in U-bend region of SONGS Unit 2 / Unit-3. These visual inspections were performed using a CCD camera inserted into the U-bend region and recorded on DVD by AREVA.

2. Location Inspected

The locations inspected are shown below.

Unit-3

Unit-3A: AVB 04	Col. 87/86 → 84/83	(4 columns)	
Unit-3A: AVB 09	Col. 86/87 → 80/81	(7 columns)	
Unit-3B: AVB 04	Col. 82/81 → 75/74	(8 columns)	
Unit-3B: AVB 04	Col. 61/60 → 50/49	(12 columns)	Total 31 columns

Unit-2

Unit-2A: AVB 04	Col. 88/87 → 73/72	(16 columns)	
Unit-2B: AVB 04	Col. 87/86 → 76/75	(12 columns)	Total 28 columns

3. Wear Patterns and Characteristics

Two wear patterns were observed at the tube-to-AVB intersections. The wear patterns are described as follows.

3.1 Wear Pattern-1 (Regional Wear on Tube Surface)

Characteristics

- ① Tube wear scar indicates in-plane motion or vibration
- ② Evidence of both parallel and perpendicular movement relative to the AVB

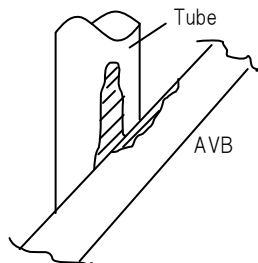


Fig-1 Wear Pattern 1



3.2 Wear Pattern-2 (Local Wear on Tube Surface)

Characteristics

- ① Local wear occurs on the tube but the wear surface is not exposed (cannot be seen)
- ② Unable to determine if wear occurs on tube or AVB or both
- ③ Unable to determine the direction of motion or vibration
- ④ An extreme interpretation is that both tube and AVB are worn into each other.

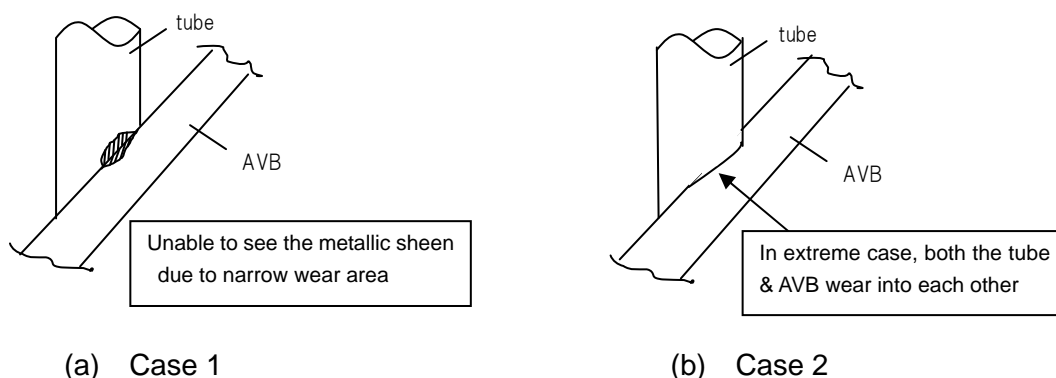


Fig-2 Wear Pattern 2

4. Results of Visual Inspection of Unit-2 / Unit-3

4.1 Common Observations from Unit-2 and Unit-3 (See Photo-1 to Photo-8)

- No large gaps between the AVBs and tubes
- AVBs appeared to be straight, no detectable abnormalities
- No abnormality in the orientation between the AVBs and tubes
- No abnormality in AVB positions or end cap-to-retaining bar welds

4.2 Unit-3

- Pattern-1 wear due to high amplitude in-plane vibration, as shown in Photo-9 and Photo-10, were found in the free span region.
- Pattern-2 wear as shown in Photo-11 and Photo-12 was found near where Pattern-1 occurred.
- There is some Pattern-1 wear identified by visual inspection, for which Bobbin ECT was not able to detect as this type of wear. (See Table-1~Table-4)



2) Unit-2

- As shown in Photo-13, Photo-14, Pattern-2 wear, which was found in Unit-3, was also found in Unit-2. However, no Pattern-1 wear was found.



Photo-3 Visual Inspection Image of Outermost Tube Region [Unit-2B]

Image of Unit-2B Col. 78/79 tubes at AVB 04

Left side is Row 141, right side's far end is Row 142 and right side's closer end is Row 140.

The bottom of the End Cap is seen over the outermost tube.

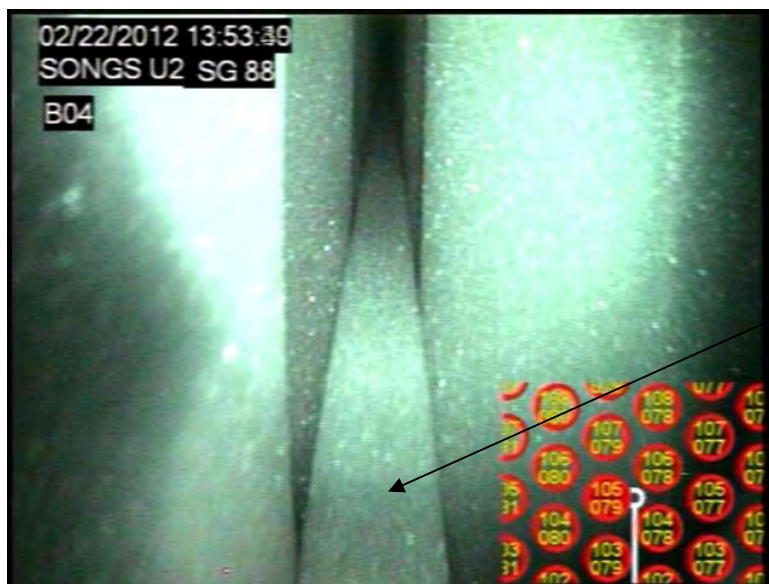


Photo-4 Tube Bundle Visual Inspection Image [Unit-2B]

Image of Unit-2B Col. 78/79 tubes around Row 105 at AVB 04 (Sample).

No gaps between the tube and AVB beyond 0.1mm and no twisting and bending on the AVB are observed.



Photo-5 Visual Inspection Image of Outermost Tube Region [Unit-3A]

Image of Unit-3A Col. 84/83 tubes at AVB 04

Left side's far end is Row 142, right side is Row 141 and left side's closer end is Row 140.

The bottom of the End Cap is seen over the outermost tube.



Photo-6 Tube Bundle Visual Inspection Image [Unit-3A]

Image of Unit-3A Col. 84/83 tubes around Row 125 at AVB 04 (Sample).

No gaps between the tube and AVB beyond 0.1mm and no twisting and bending on the AVB are observed.



Photo-7 Visual Inspection Image of Outermost Tube Region [Unit-3B]

Image of Unit-3B Col. 78/77 tubes at AVB 04

Left side's far end is Row 142, right side is Row 141 and left side's closer end is Row 140.

The bottom of the End Cap is seen over the outermost tube.

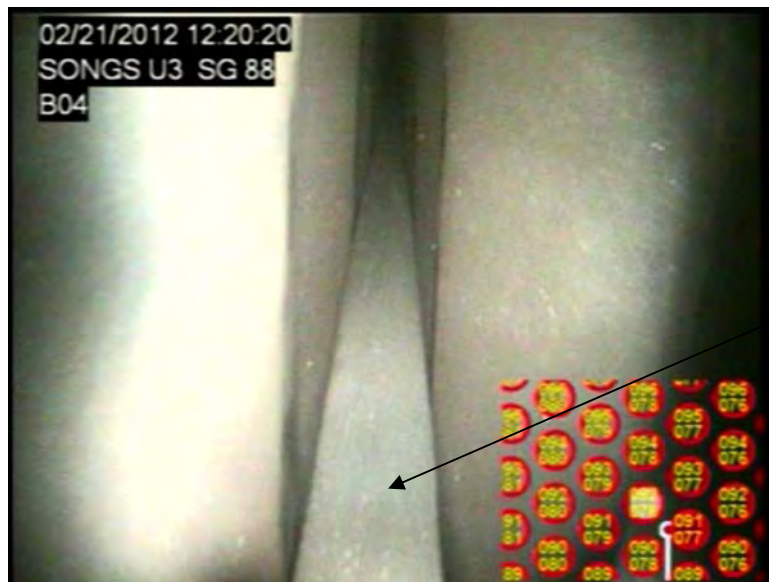


Photo-8 Tube Bundle Visual Inspection Image [Unit-3B]

Image of Unit-3B Col. 78/77 tubes around Row 90 at AVB 04 (Sample).

No gaps between the tube and AVB beyond 0.1mm and no twisting and bending on the AVB are observed.

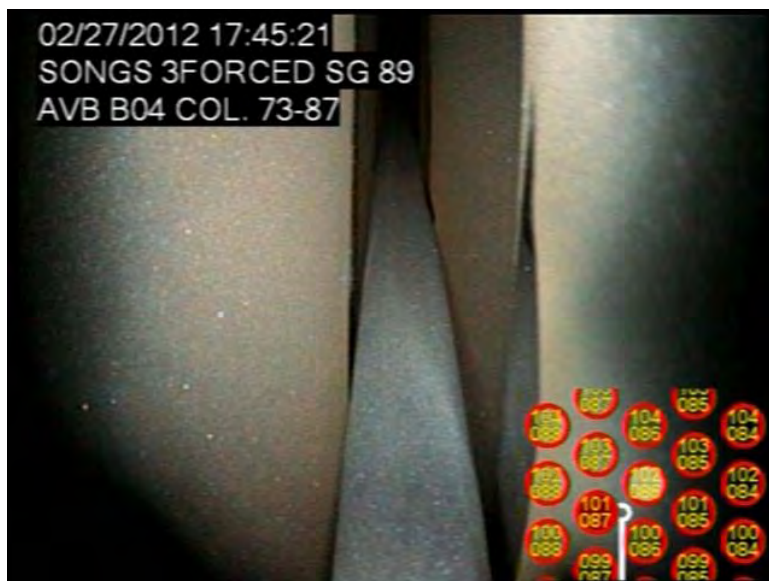


Photo-9 Sample of Pattern-1 [Unit-3A]

Image of Unit-3A Col. 87/86 shows a sample of Pattern-1 wear.

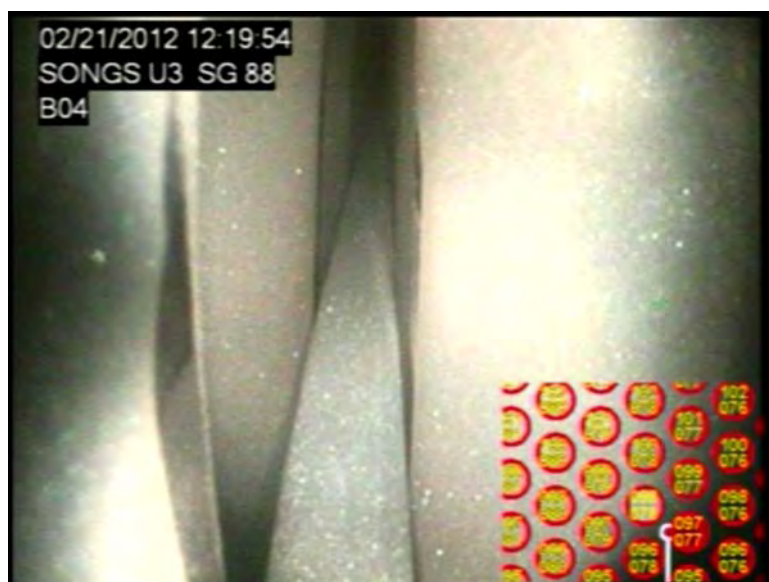


Photo-10 Sample of Pattern-1 [Unit-3B]

Image of Unit-3B Col. 78/77 shows a sample of the Pattern-1 wear.

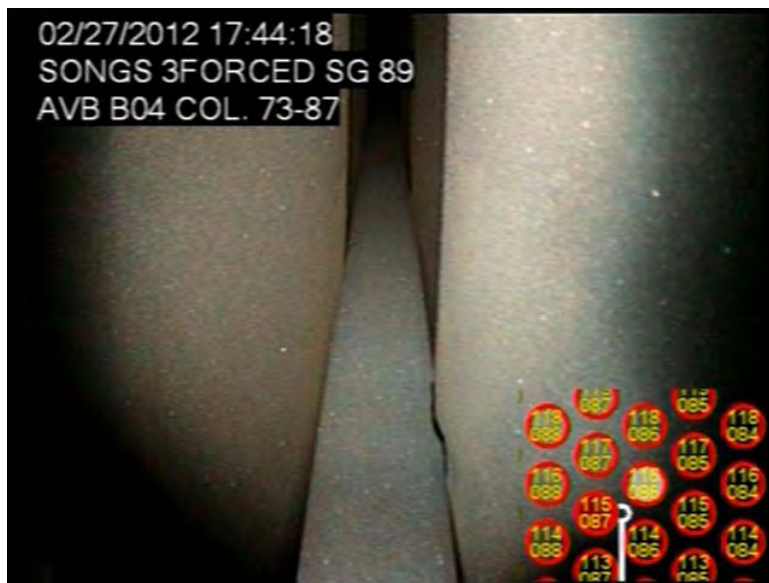


Photo-11 Sample of Pattern-2 [Unit-3A]

Image of Unit-3A Col. 87/86 shows a sample of Pattern-2 wear, where wear between tube and AVB cannot be distinguished.



Photo-12 Sample of Pattern-2 [Unit-3B]

Image of Unit-3B Col. 78/77 shows a sample of the most typical Pattern-2 wear, where wear between the tube and AVB cannot be distinguished.

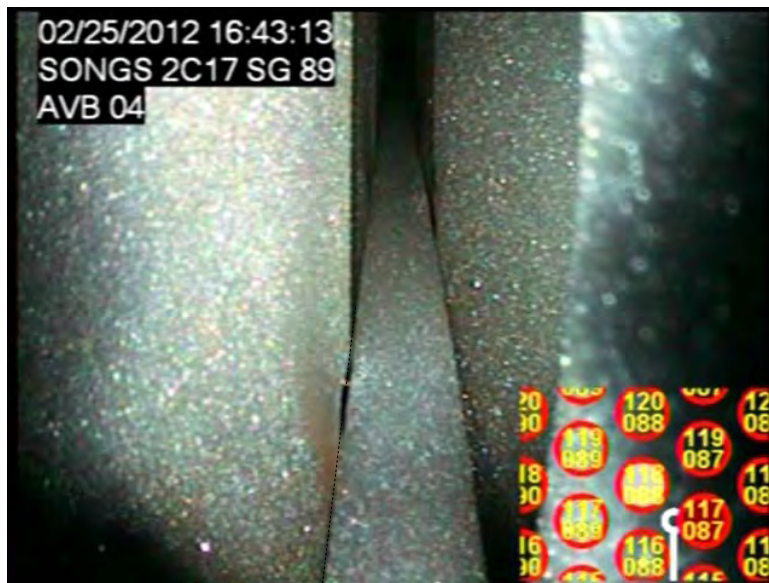


Photo-13 Sample of Pattern-2 [Unit-2A]

Image of Unit-2A Col. 88/87 shows a sample of Pattern-2 wear.

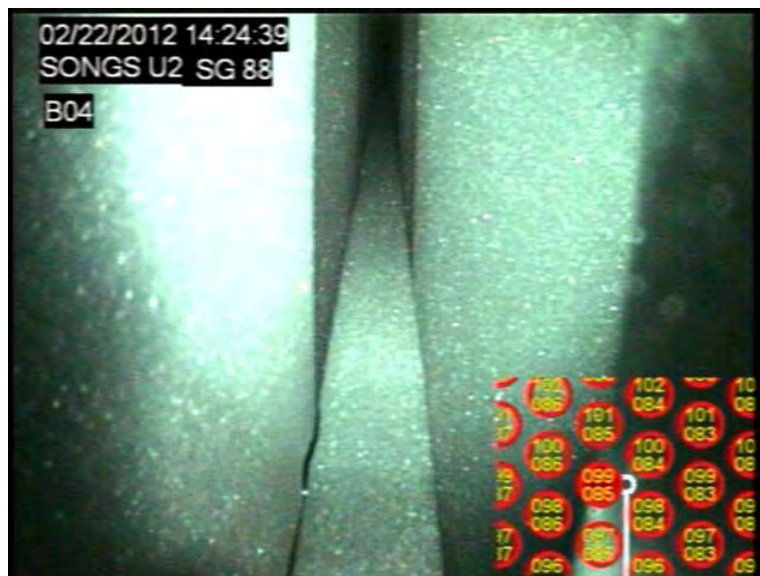


Photo-14 Sample of Pattern 2 [Unit-2B]

Image of Unit-2B Col. 85/84 shows a sample of Pattern-2 wear.



Table-2(1/2) SONGS Unit-3A AVB 09 Visual inspection result

Col.80		Col.80/81		Col.81		Col.81/82		Col.82		Col.82/83		Col.83		Col.83/84		Col.84		
TWD (%)	Row	Col.80	Row	Col.81	TWD (%)	Row	Col.81/82	Col.82	TWD (%)	Row	Col.82	Row	Col.83	TWD (%)	Row	Col.83/84	Col.84	TWD (%)
	142		141			142		142		141		141		141	142			
	140		139			140		140		139		139		139	140			
	138		137			138		P2(minor)		137		137		P2(minor)	138			
	136		135		14	135		P1?		135		135		P2(minor)	136			
	134		133			133				133		133		P2(minor)	134			P2(minor)
	132		131			131		P2(minor)		131		131		P1	132			P1
	130		129		5	129		P2(minor)		129		129		P2(minor)	130			P2(minor)
	128		127			127		P2(minor)	7	127		127		P1	128			P2
7	126		125		8	125				125		125		P2(minor)	126			P2(minor)
	124		123			123				123		123		P2(minor)	124			P2(minor)
	122		121			121		P2(minor)		121		121		P1	122			P2(minor)
	120		119			119			8	120		119		P1	120			P2(minor)
	118		117			117		P2(minor)		118		117		P1	118			P2(minor)
	116		115		11	115				115		115		P1	116			P2(minor)
10	114		113			113		P2(minor)		114		113		P1	114			P2(minor)
	112		111		9	111		P2(minor)		112		111		P2(minor)	112			P2(minor)
15	110		109		11	109				110		109		P2(minor)	110			P2(minor)
17	108		107		12	107		P1	7	108		107		P1	108			P1
17	106		105		10	105		P1		106		105		P2(minor)	106			P1
9	104		103		16	103		P1	21	104		103		P1	104			P1
28	102		101		23	101		P1	20	102		101		P1	102			P1
29	100		99		28	99		P2(minor)	14	100		99		P1	100			P1
41	98		97		15	97		P1	39	98		97		P1	98			P1
29	96		95		15	95		P1	43	96		95		P1	96			P1
30	94		93		15	93		P1	14	94		93		P1	94			P1
	92		91		18	91		P1	34	92		91		P1	92			P1
	90		89		18	89		P1	34	90		89		P1	90			P1
	88		87		11	87		P1?		88		87		P1	88			P1
	86		85		10	85		P2(minor)	7	86		85		P2	86			P1
	84		83		13	83		P2(minor)	10	84		83		P2(minor)	84			P2(minor)
9	82		81			81		P2(minor)		82		81		P2(minor)	82			P2(minor)
	80		79			79		P2(minor)		80		79		P2(minor)	80			P2(minor)
	78		77			77		P2(minor)		78		77		P2(minor)	78			P2(minor)
	76		75		10	75		P2(minor)		76		75		P2(minor)	76			Stav.rod
	74		73		7	73		P2(minor)		74		73		P2(minor)	74			P2(minor)
	72		71			71		P2(minor)		72		71		P2(minor)	72			P2(minor)
	70									70					70			P2(minor)

Free span indication by ECT



Table-2(2/2) SONGS Unit-3A AVB 09 Visual inspection result

Col.84		Col.84/85		Col.85		Col.85/86		Col.86		Col.86/87		Col.87	
TWD (%)	Row	Col.84	Row	Col.85	Row	Col.85	Row	Col.86	Row	Col.86	Row	Col.87	Row
142	141		141		141		142		142		141		141
140	139		139		139		140		140		139		139
138	137		P2(minor)		137		138		138		137		137
136	135		P2(minor)		135		136		136		135		135
134	133		P2(minor)		133		134		134		133		P2(minor)
132	131		P2(minor)		131		132		132		131		P1
130	129			8	129		130		130		129		P2(minor)
128	127			9	127		128		128		127		P1
126	125			7	125		126		126		125		P2(minor)
124	123		P2(minor)	7	123		124		124		123		P2(minor)
122	121		P2(minor)	9	121		122		122		121		P2(minor)
120	119			6	119		120		120		119		P1
118	117		P2(minor)	14	117		118		118		117		P1
116	115		P1	11	115		116		9		115		P1
114	113		P1	18	113		114				113		P1
112	111			11	111		112				111		P1
110	109		P1?		109		110				109		P1
108	107		P2(minor)	24	107		108				107		P2(minor)
106	105		P1	25	105		106		18		105		P2(minor)
104	103		P1	16	103		104		17		103		P1
102	101		P1	6	101		102		11		101		P1
100	99		P1	11	99		100		12		99		P2(minor)
98	97		P1	21	97		98		12		97		P1
96	95		P1	16	95		96		17		95		P1
94	93		P1	9	93		94		9		93		P1
92	91		P1?	16	91		92		33		91		P1?
90	89		P2(minor)	11	89		90		31		89		P1
88	87		P2(minor)	9	87		88		9		87		P1
86	85		P1	8	85		86		7		85		P1
84	83		P1	8	83		84		86		83		P1
82	81		P2(minor)	9	81		82		10		81		P1
80	79		P2(minor)	79	79		80		10		79		P2(minor)
78	77			77	77		78		80		77		P2(minor)
76	75		Stay red	75	75		76		78		75		P2(minor)
74	73		P2(minor)	73	73		74		76		73		P2(minor)
72	71		P2(minor)	71	71		72		74		71		P2(minor)
70	70			70	70		70		72		70		?

Free span indication by ECT





Table-3(1/5) SONGS Unit-3B AVB 04 Visual inspection result

Col. 82		Col. 82		Col. 81		Col. 81		Col. 80		Col. 80		Col. 79		Col. 79		Col. 78		Col. 78	
TWD (%)	Row	Col. 82	Row	Col. 81	Row	Col. 81	TWD (%)	Row	Col. 80	Row	Col. 80	TWD (%)	Row	Col. 79	Row	Col. 79	Row	Col. 78	TWD (%)
	142		141	?	142	?		142		141			141		142		142		
	139		139	?	140	?		140		139			139		140		140		
	138		137	?	138	?		138		137			137		138		138		
	136	P2(minor)	135	6	136	?		136		135			135	P2(minor)	136		136		
	134	?	133	12	134	?		134		133			133	P2	134		134		5
10	132	?	131	13	132	?		132	P2(minor)	131			131	P2(minor)	132		132	P2(minor)	
8	130	P2(minor)	129	?	130	?		130	?	129			129	P2	130		130		9
	128	?	127	12	128	?		128	?	127			127	P2(minor)	128		128		15
	126	P2	125	125	126	?		126	P2(minor)	125			125	P2	126		126	P2(minor)	
22	124	P2	123	14	124	?		124	?	123			123	P2	124		124		19
	122	P2(minor)	121	14	121	?		122	?	121			121	P1?	122		122	P1	18
	120	?	119	27	119	?		120	?	119			119	P1	120		120		17
	118	?	117	12	117	?		118	?	117			117	P1	118		118	P1	18
24	116	?	115	14	115	?		116	?	115			115	P1	116		116	P1	10
15	114	P1	113	27	113	P1		114	?	113			113	P1	114		114	P1?	17
	112	P1	111	14	111	P1		112	P1	111			111	P1	112		112	P1	
9	110	P1	109	18	109	P1		110	?	109			109	P1	110		110	P1?	17
12	108	P1	107	16	107	P1		108	P1	107			107	P1	108		108	P1	10
16	106	P1	105	21	105	P1		106	P1	105			105	P1	106		106	P1	
21	104	P1	103	17	103	P1		104	P1	103			103	P1	104		104	P1	23
16	102	P1	101	25	101	P1		102	P1	101			101	P1	102		102	P1?	13
20	98	P1	99	20	99	P1		100	P1	99			99	P1	100		100	P1?	16
	96	P1	95	19	97	P1		98	P1	97			97	P1	98		98	P1?	
27	94	P1	95	20	95	P1		96	P1?	95			95	P1	96		96	P1?	37
12	92		91	23	93	?		94	P2	93			93	P2	94		94	P2	17
	90		89	15	89	P2		92	P2	91			91	P2	92		92	P2	10
10	88	P2	87	6	87	P2		90	P2	89			89	P2	90		90	P2	11
6	86	P2	85	12	85	P2(minor)		88	P2	87			87	P2	88		88	P2(minor)	7
6	84	P2(minor)	83	8	83	P2(minor)		86	P2	85			85	P2	86		86	P2(minor)	7
12	82	P2(minor)	81	9	81	P2		84	P2	83			83	P2	84		84	P2	17
14	80	P2	79	5	79	P2		82	P2	81			81	P2	82		82	P2(minor)	11
9	78	P2	77	7	77	P2(minor)		80	P2(minor)	79			79	P2	80		80	P2(minor)	21
	76	P2(minor)	75	75	75	P2(minor)		78	P2	77			77	P2	78		78	P2	
	74	P2	73	74	74	P2		76	P2	75			75	P2	76		76	P2	
	72		71	71	71	P2		74	P2	73			73	P2(minor)	74		74	P2	
	70		70	70	70	P2		72	P2	71			71	P2	72		72	P2	

Free span indication by ECT



Table-3(2/5) SONGS Unit-3B AVB 04 Visual inspection result

Col. 78		Col. 78/77		Col. 77		Col. 77/76		Col. 76		Col. 76/75		Col. 75		Col. 75/74		Col. 74	
TWD (%)	Row	Col. 78	Row	Col. 77	TWD (%)	Row	Col. 76	TWD (%)	Row	Col. 76	Row	Col. 75	TWD (%)	Row	Col. 75	Row	Col. 74
	142		141			141			140	?	141			141			
	140		139	?		139			138	?	139			139		140	
	138		137			137			136	?	137			137		138	
	136		135			135			134	?	135			135		136	
5	134	P2(minor)	133			133			132	?	133			133		134	
	132	P2(minor)	131			131			130	?	131			131		132	P2(minor)
9	130	P2	129			129			128	P2?	129			129		130	
15	128	?	127			127			126	P2(minor)	127			127		128	P2(minor)
15	128	P2(minor)	125			125			124	?	125			125		126	P2(minor)
19	124	?	123			123			122	P2	123			123		124	P2(minor)
18	122	P2	121			121			120	P1	121			121		122	
17	120	P1	119			119			118	P1	119			119		120	
18	118	P1	117			117			116	P1	117			117		118	
10	116	P1	115			115			114	P1	115			115		116	
17	114	P1	113			113			112	P1	113			113		114	
11	112	P1	111			111			110	P1	111			111		112	
17	110	P1	109			109			108	P1	109			109		110	P2?
10	108	P1	107			107			106	P1	107			107		108	P1?
106	106	P1	105			105			104	P1	105			105		106	P1
23	104	P1	103			103			102	P1	103			103		104	
13	102	P1	101			101			100	P1?	101			101		102	
16	100	P1	99			99			98	P1	99			99		100	
98	98	P1	97			97			96	P1?	97			97		98	
37	96	P2	95			95			94	P2	95			95		96	
17	94		93			93			92	P2	93			93		94	P2(minor)
10	92		91			91			90	P2(minor)	91			91		92	P2
11	90	P2(minor)	89			89			88	P2(minor)	89			89		90	P2(minor)
7	88	?	87			87			86	P2	87			87		88	
7	86	?	85			85			84	P2	85			85		86	P2(minor)
17	84	?	83			83			82	P2(minor)	83			83		84	P2(minor)
11	82		81			81			80	P2(minor)	81			81		82	P2(minor)
21	80	?	79			79			78	P2(minor)	79			79		80	
78	78	P1?	77			77			76	P2	77			77		78	
76	76	P2(minor)	75			75			74	?	75			75		76	
74	74	P2	73			73			72	?	73			73		74	P1?
72	72	?	71			71			70	?	71			71		72	Stay rod
70	70	P2(minor)	70			70			69	?	70			70		71	

□ : Free span indication by ECT



Table-4 Description of the abbreviations in Table-1 ~ Table-3

Abbreviation	Description
P1	Tube Confirmed with Wear Pattern-1
P1?	Tube Suspected with Wear Pattern-1
P2	Tube Confirmed with Wear Pattern-2
P2 (minor)	Tube Confirmed with Minimal Wear Pattern-2
P2?	Tube Suspected with Wear Pattern-2
? (Unjudgeable)	Tube that cannot be determined due to the inspection rate in the video, etc



Appendix-8
SG Tube Flowering Analysis for Unit-2/3



3. Methodology and Assumptions

1) Analysis model

The ABAQUS finite element program is used to model the U-bend. The tube bundle is symmetric about the central plane perpendicular to the tubelane, so a half-symmetry model is assumed. All of the U-tubes, AVBs, retaining bars, retainer bars, and bridges are modeled using beam elements. The model includes the U-bend and the straight leg of the tubes down to the elevation of the 6th TSP. The model is shown in Figure 3-1. Nominal dimensions are used. Manufacturing tolerances are not considered.

The two TSPs are represented as pinned supports. All tubes at the TSP#6 elevation are prevented from displacing in the lateral and axial directions but are free to rotate. All tubes at the TSP#7 elevation are restrained against lateral displacement but are free to displace axially and to rotate. Modeling the top two TSPs is sufficient to produce a reasonable structural representation of the U-bend portion of the tube bundle.

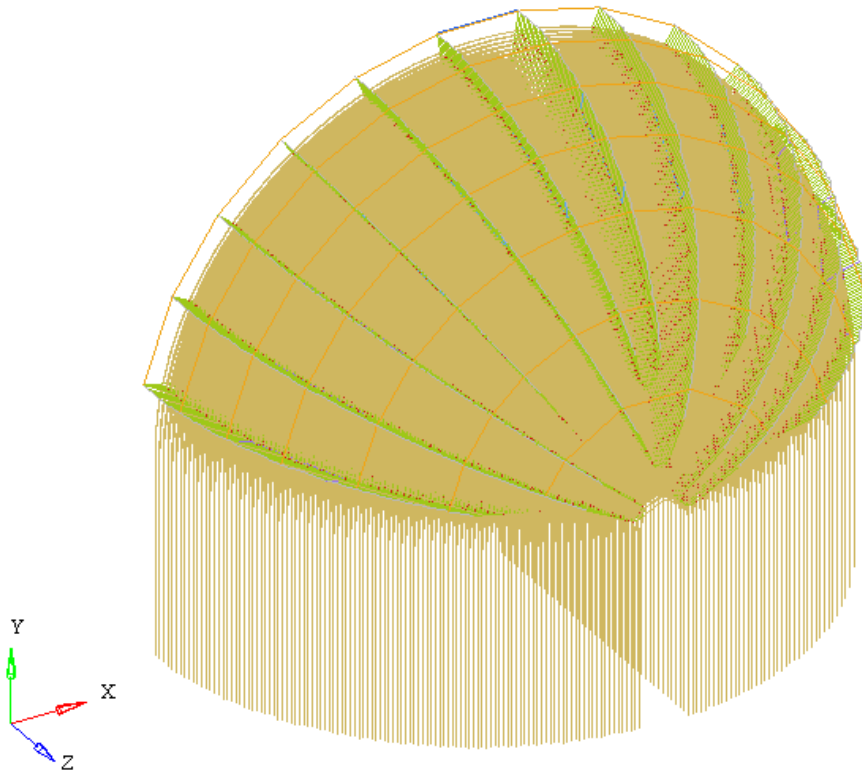
In Case C3A', all tubes at the TSP#6 elevation are able to displace in the lateral within gap range and free to rotate but axially fixed. All tubes at the TSP#7 elevation are restrained against lateral displacement by gap elements but are free to displace axially and to rotate.

Additional modeling details:

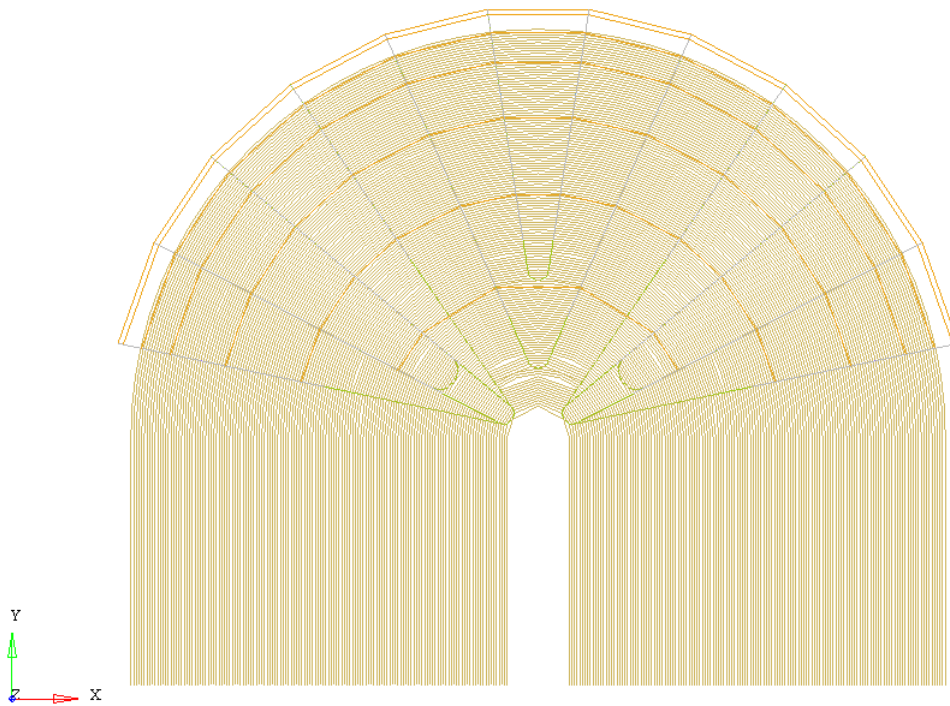
- Water mass inside (and outside) the tubes is simulated by an increase in tube density.
- Contact between tubes and AVBs is simulated by gap elements.
- The tube stiffness in compression is [] which is the spring stiffness of the gap elements under compression when the tube-to-AVB gap is zero.
- The initial tube-to-AVB gaps are set to zero. The gap elements exert a force on the tube when in compression, but displace freely under tension.
- A [] coefficient of friction for lateral movement between tubes and AVB is assumed. Tube can slide along the AVB, if slide force is larger than the force multiplying the compression force by []
- The tube and AVB Modulus of Elasticity is specified based on operating temperature.
- Elastic material behavior is assumed for all parts.

2) Loading conditions

The hydrodynamic pressure across each tube is obtained from the ATHOS thermal hydraulic analysis and is applied to the tubes.



(i) Bird's-eye View of the Model



(ii) Side View of the Model

Fig. 3-1 ABAQUS model



4. Analysis cases

Table 4.1 describes the five cases that were analyzed. Cases C1 and C2 are used to confirm the influence of thermal elongation and hydrodynamic force on the tubes without any AVB supports. In these two cases the AVBs are not included so that the tubes can deform freely and so that the response of each tube can be evaluated independently. Cases C3A and C3B are used to evaluate the tube-to-AVB gap behavior. In Case C3A the hydrodynamic force produced by ATHOS (both in-plane and out-of-plane) is applied to the tubes. In Case C3B, only the hydrodynamic forces in the out-of-plane direction are applied. Case-C3C is a repeat of Case C3A but with much stiffer retaining bars ([]). This case was run to quantify its effectiveness as a countermeasure to prevent further tube wear. In Case C3A', the latest ATOHS output is applied from Appendix-12. Additionally, Case D1 is used to evaluate effects the hydrodynamic force and manufacture dispersion, which is applied from Appendix-9 Case 2-1 analysis condition.

Table 4.1 analyses cases

Analysis Case	Analysis Model				Load		
	Model Region	AVB Assembly		Friction Factor		Method	
C1	Only tubes with water	No AVB (Tubes only)		[]	Elastic Analysis	Temperature distribution	
C2						Dynamic Pressure (in-plane & out)	
C3	AVBs, Retaining bars, Bridges, Retainer bars, and tubes with water	Gap elements for contact between AVBs and tubes (Contact spring : [] [N/mm])	Original Retaining Bar	[]	Elastic Analysis	Dynamic Pressure (in-plane & out)	
			B			Dynamic Pressure (out of plane)	
			C			Retaining Bar stiffness = [] (Twice diameter)	Dynamic Pressure (in-plane & out)
			A'			Gap elements for contact between TSP and tubes (Contact spring : [] [N/mm])	Dynamic Pressure (in-plane & out) From Appendix-12
D1		Manufacturing Dispersion From Appendix-9 Case2-1 for Unit-3			Dynamic Pressure (in-plane & out)		



5. Results of analyses

5.1 Case-C1: Vertical Thermal Expansion Analysis (no AVB contact)

The total and vertical tube deformations of the tube bundle are shown in Figure 5.1-1. The top of the outermost tube grows by [] from the tubesheet surface. The vertical growth and total growth are essentially the same because the difference in the hot and cold side tube temperatures is small. This is because the average tube wall temperature is used, which is mid-way between the primary and secondary side temperatures.

Figure 5.1-2 shows the change in distance between tube rows in column 78 due to thermal expansion. The nominal distance of [] grows [] to a value of []

The change in distance between tubes of the same column, due to tube thermal expansion from room temperature to operating temperature is negligible.

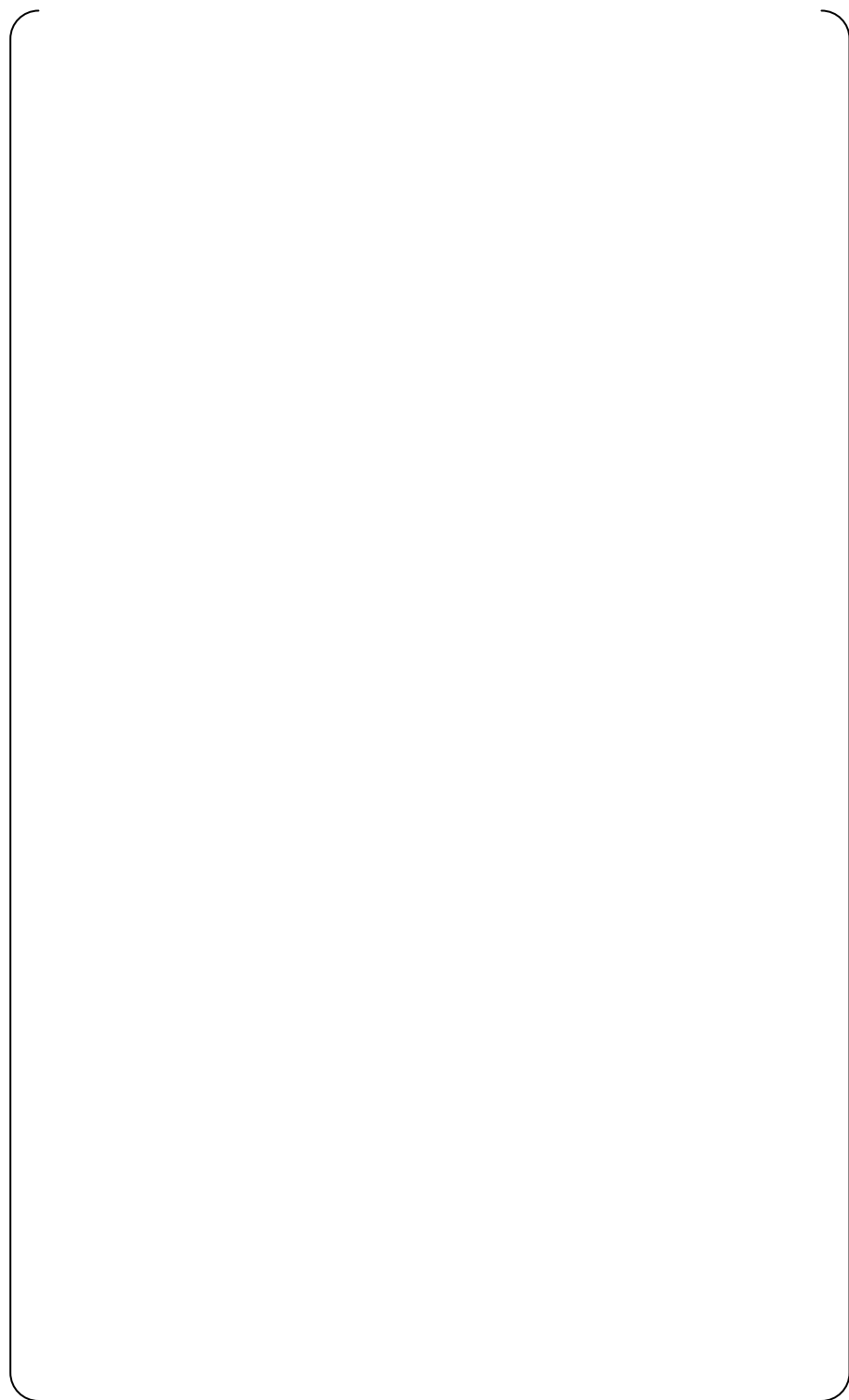


Fig. 5.1-1 Case-C1: Thermal expansion due to tube temperature (ave. wall temp.)



Fig. 5.1-2 Case-C1: Distance between adjacent tubes in Col.78 after thermal elongation



5.2 Case-C2: Tube Deformation from Hydrodynamic Force (no AVB contact)

In the U-bend at operating conditions (without any friction or restraint from the AVBs) the hydrodynamic forces cause the tubes to deform as shown in Figures 5.2-1 and 5.2-2. Figure 5.2-1 shows the overall displacement of the U-bend at operating conditions. The hydrodynamic forces cause the tube columns to spread apart (view i) with the maximum out-of-plane displacement of [] Note that this view of the U-bend does not show the hot and cold sides. This will be important when visualizing the behavior of later load cases.

In the in-plane direction (views ii and iii) the bundle displaces (horizontally) toward the hot side because the hot side hydrodynamic forces are larger than the cold side forces. The outermost, central tube, R142C86, displaces downward by [] at the apex and at about 45° off vertical on the hot side, where the hydrodynamic force is largest, it displaces upward by [] In view ii at this same 45° zone, R142C86 displaces horizontally by []

Figure 5.2-2 displays the change in spacing between adjacent tubes within column 78 in response to the hydrodynamic forces. At the top of the bundle, the tube-to-tube spacing decreases by a maximum of [] as the U-tubes are pulled downward. The tube-to-tube spacing on the hot side (45° off the vertical) has a greater increase in tube spacing than occurs on the cold side. The greater hydrodynamic force on the hot side has a greater effect than that of the cold side. The larger radius tubes have the greatest increases in spacing.

This case (C2) has no AVBs in it and helps understand how the fluid forces push the tubes and how the tubes deform at operating conditions. Case C3A is a repeat of this case, but with the effects of the AVBs, retaining bars, retainer bars, and bridges included.

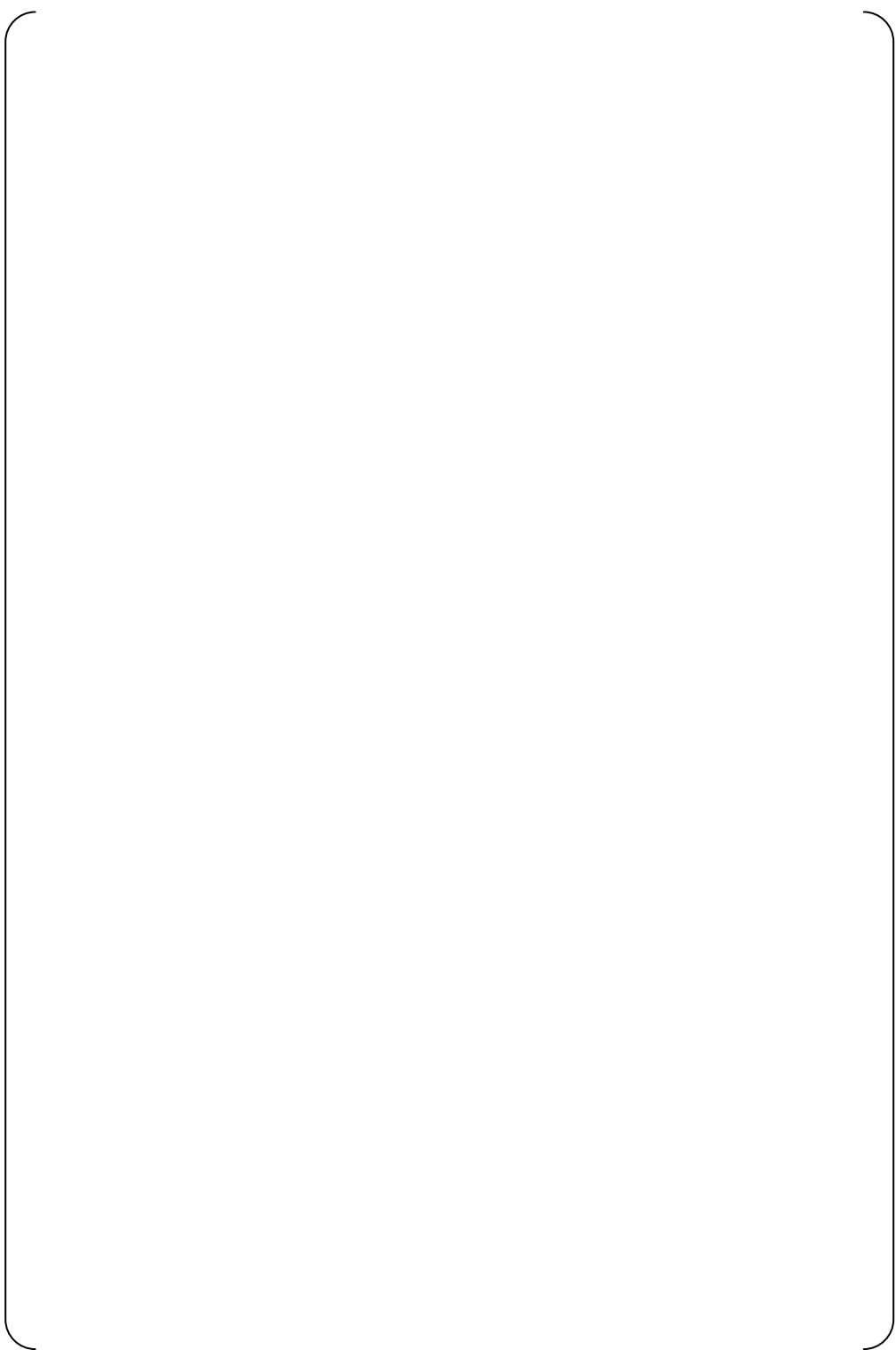


Fig. 5.2-1 Case-C2: Deformation due to dynamic pressure (no AVBs)



Fig. 5.2-2 Case-C2: Distance between adjacent tubes in Col.78 due to dynamic pressure



5.3 Case-C3A: Tube Deformation from Hydrodynamic Force (AVB assembly in)

Figure 5.3-1 (top 3D view) shows a similar overall displacement pattern for Case C3A and Case C2 (i.e. contraction on top and expansion on the hot and cold sides). Figure 5.3-1 (bottom view) shows the “total” tube deformation, which is the combination of the horizontal and vertical displacements. This view was not plotted for Case C2.

Figure 5.3-2 shows how the total deformation relates to the displacement in the vertical direction (top view) and in the horizontal direction (bottom view). The general trend seen in Case C2 where the hydrodynamic forces caused the bundle to displace toward the hot side and for the top of the bundle to move downward is also evident in Case C3A. However, the influence of the AVBs, retaining bars, and retainer bars produces some added effects. Figure 5.3-2 (bottom view) shows that the maximum out-of-plane deformation occurs near Col.10 at the ends of the retaining bars, even though the maximum dynamic pressure is located above Col.30. The maximum out-of-plane deformation is []

Figure 5.3-2 (top view) shows the retaining bar deflection. As the pressure pushes the tubes away from the bundle central plane, they take the AVBs and retainer bars with them – and stretch the retaining bars. This stretching of the retaining bars causes them to flatten out (displace downward) at the top of the bundle (in the center columns). The hot side / cold side hydrodynamic forces also cause the tubes to displace downward (at the top of the bundle). The maximum downward deformation is []

Figure 5.3-3 shows AVB and retaining bar deformation along AVB-B06. The bottom view with 100x magnification shows the downward displacement of the retaining bar at the center columns and shows AVB bending.

Figures 5.3-4 and 5.3-5 show the gap distributions between tubes and AVBs at cross sections along AVBs B06 and B05. The largest gaps are found in the zone bounded by Columns 77 to 81 and Rows 104 to 122. This zone corresponds to the region with the most severe wear in Unit-2 and Unit-3. The largest increase in tube-to-AVB gap in this region is [] for Section B6 and [] for Section B5. Figure 5.3-6 contains another display of the change in tube-to-AVB gaps within Section B5.

Figure 5.3-7 shows the regions along the AVBs in Column 78 where there is tube contact or a gap. On the side of the AVB in the A-direction (view i) there are gaps on the full population of tubes between Row 80 and Row 112. In the B-direction (view ii) there is intermittent contact. Support by an AVB on a single side of the tube is considered to be an



“active” support. Tubes with no AVB contact on either side are considered to be “inactive” supports. Within the Figure 5.3-7 population there are many tubes with consecutive inactive supports. The largest number of consecutive inactive supports in this figure is six. Such an unsupported tube span would have a low natural frequency and would exhibit unstable vibration characteristics under normal operating conditions.

Figure 5.3-8 shows that the distance between Column 78 tubes increases the most on the hot side where the hydrodynamic force is largest. The increase is greatest between the largest radius tubes. Elastic tube bending produces the reduction in spacing on the cold side.

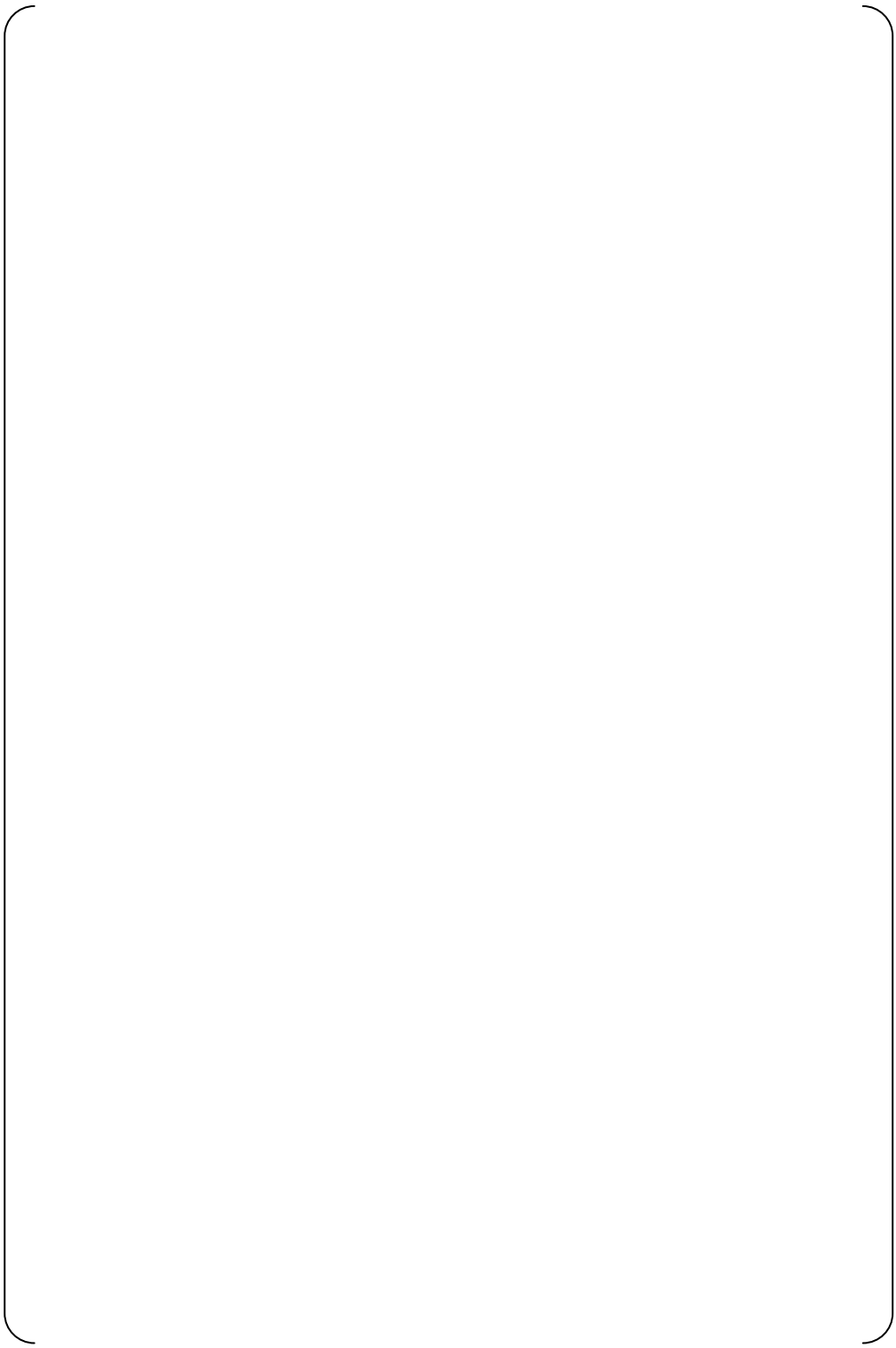


Fig. 5.3-1 Case-C3A: Total deformation due to dynamic pressure (with AVB contact)

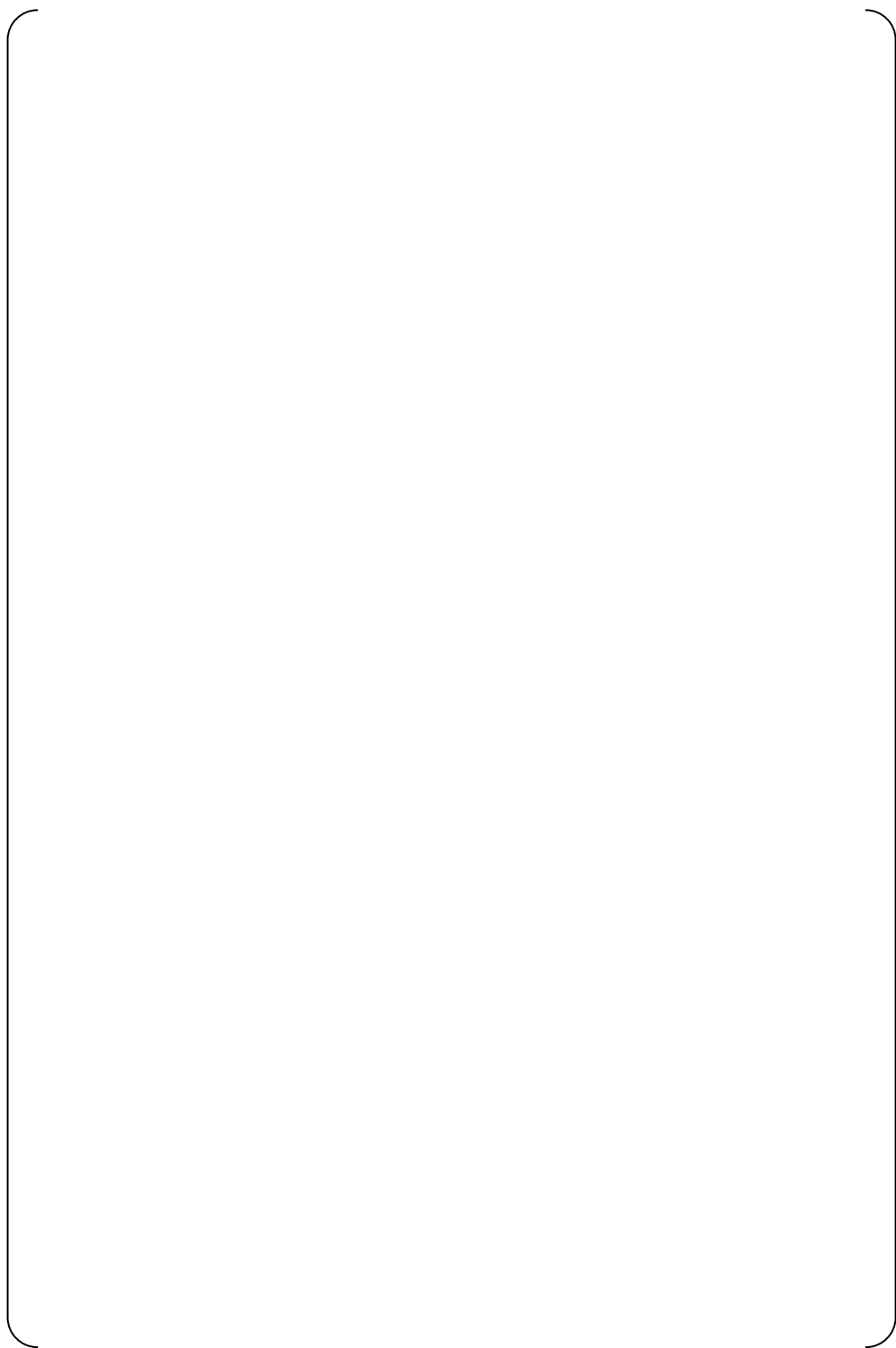


Fig. 5.3-2 Case-C3A: Deformation contour due to dynamic pressure (tubes-AVBs contact)

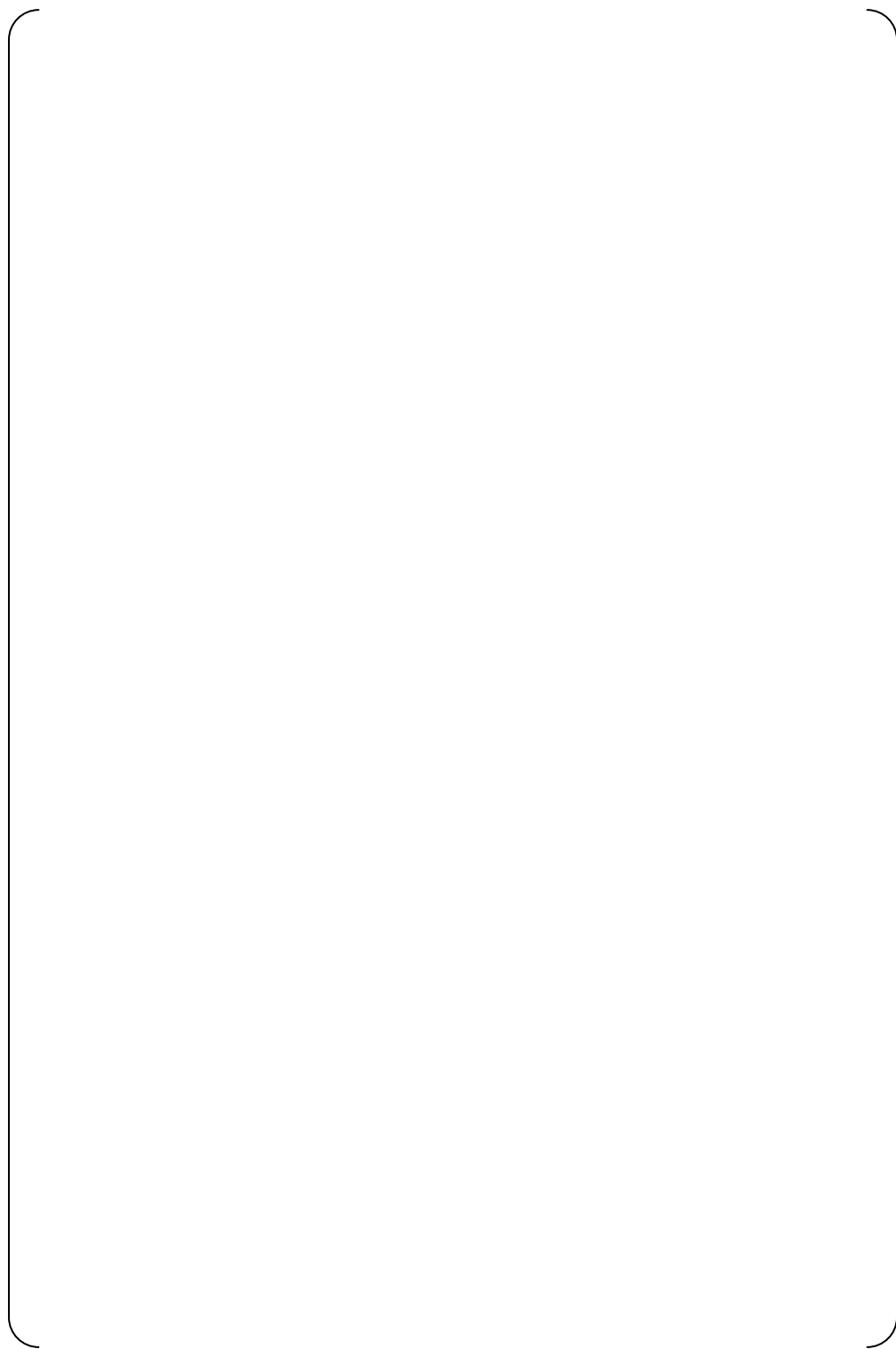


Fig. 5.3-3 Case-C3A: Deformation due to dynamic pressure (tubes-AVBs contact)



Fig. 5.3-4 Case-C3A: Gap distribution between AVBs and tubes in B6 section

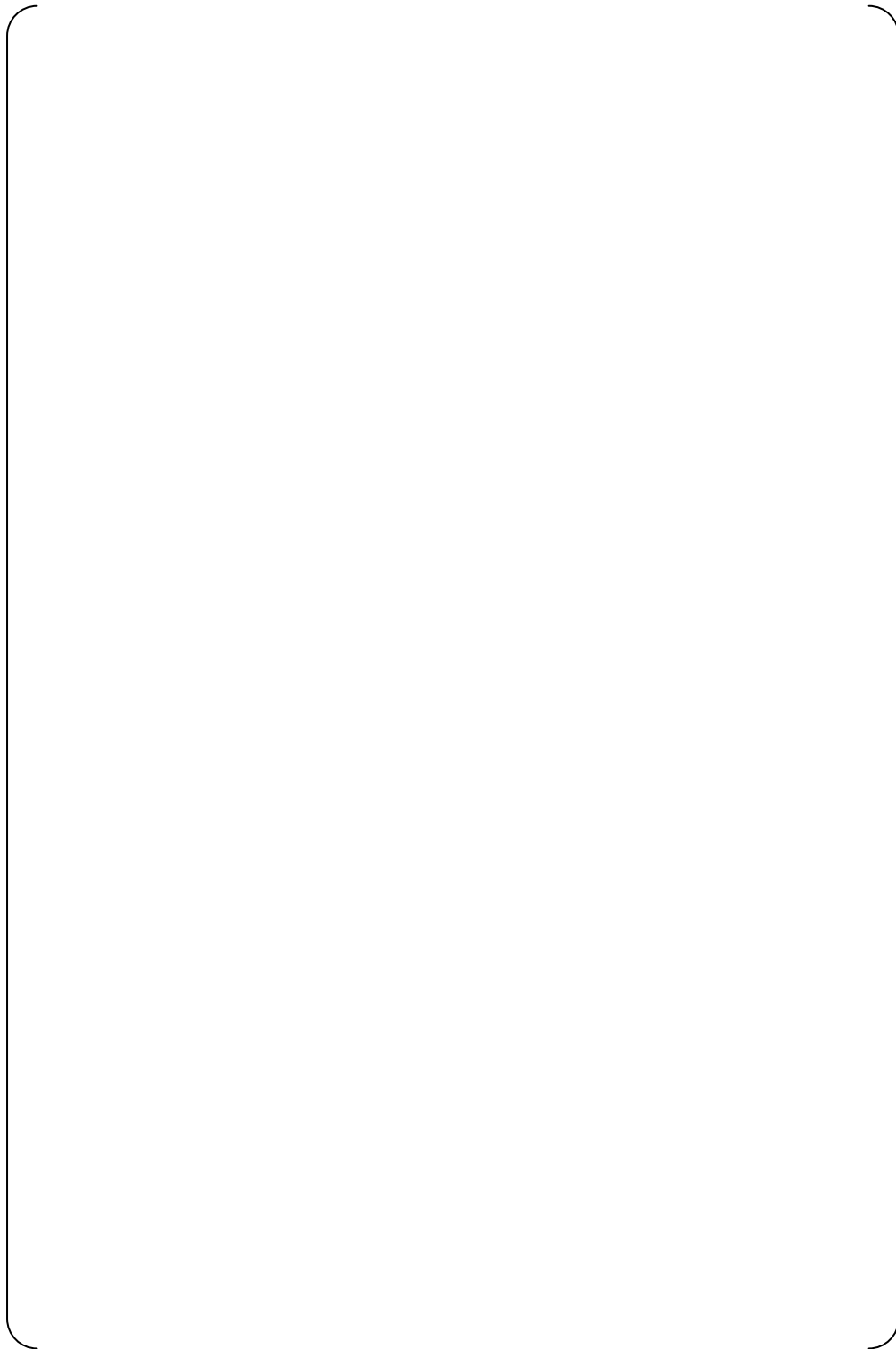


Fig. 5.3-5 Case-C3A: Gap distribution between AVBs and tubes in B5 section

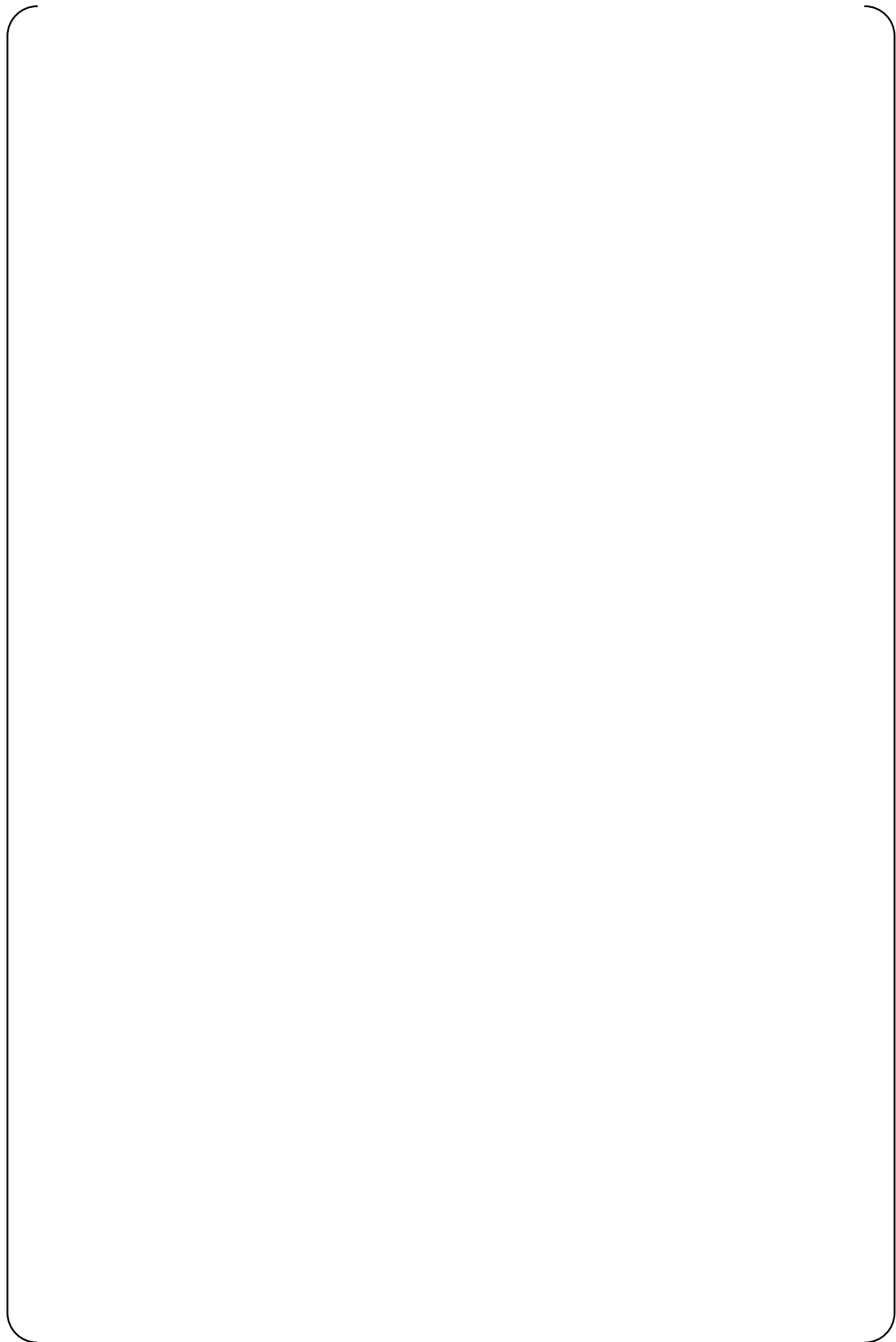


Fig. 5.3-6 Case-C3A: Gaps between AVBs and tubes in each Column in B5 section

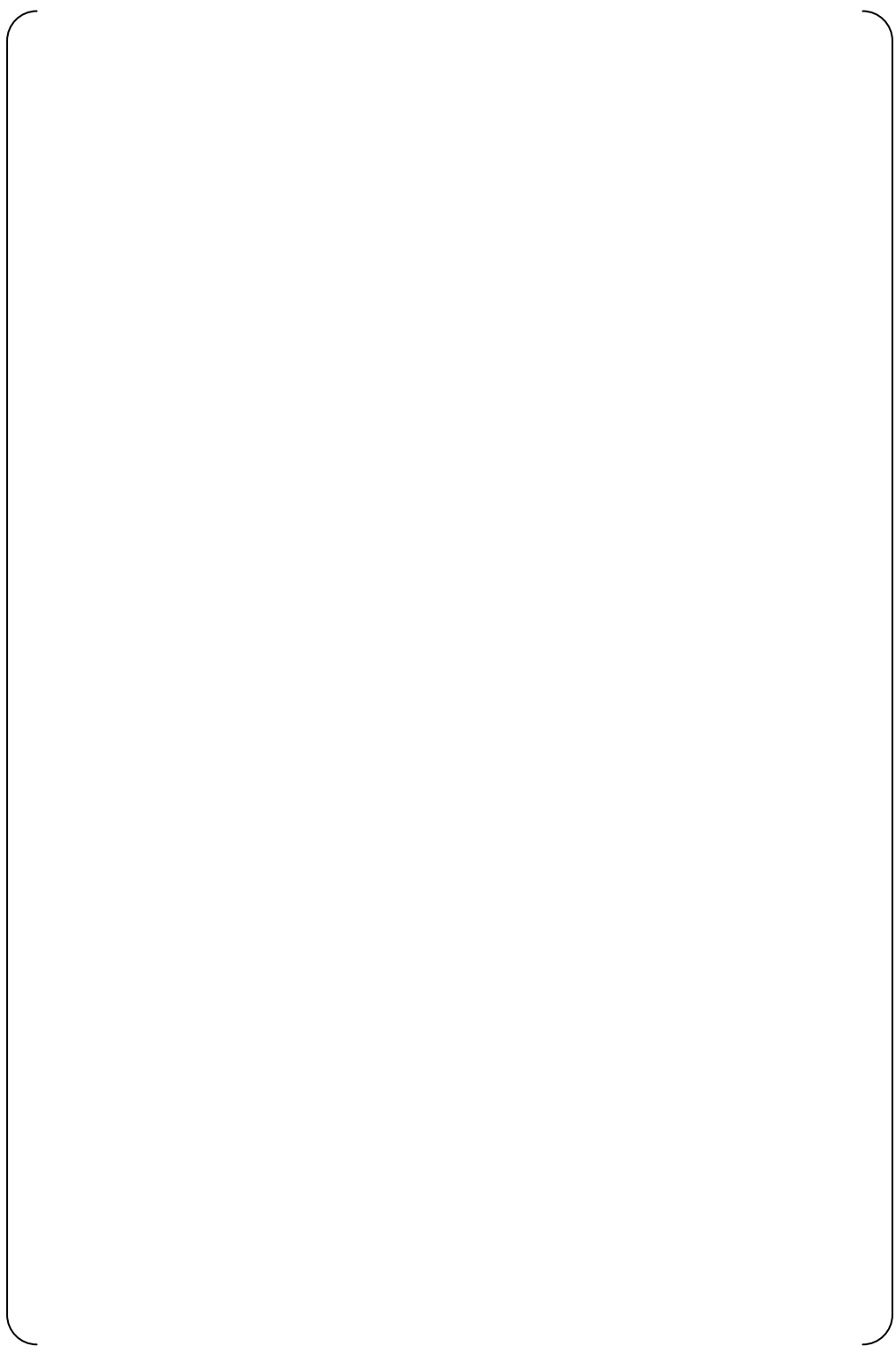


Fig. 5.3-7 Case-C3A: Gaps of tubes in Col.78 to adjacent AVBs

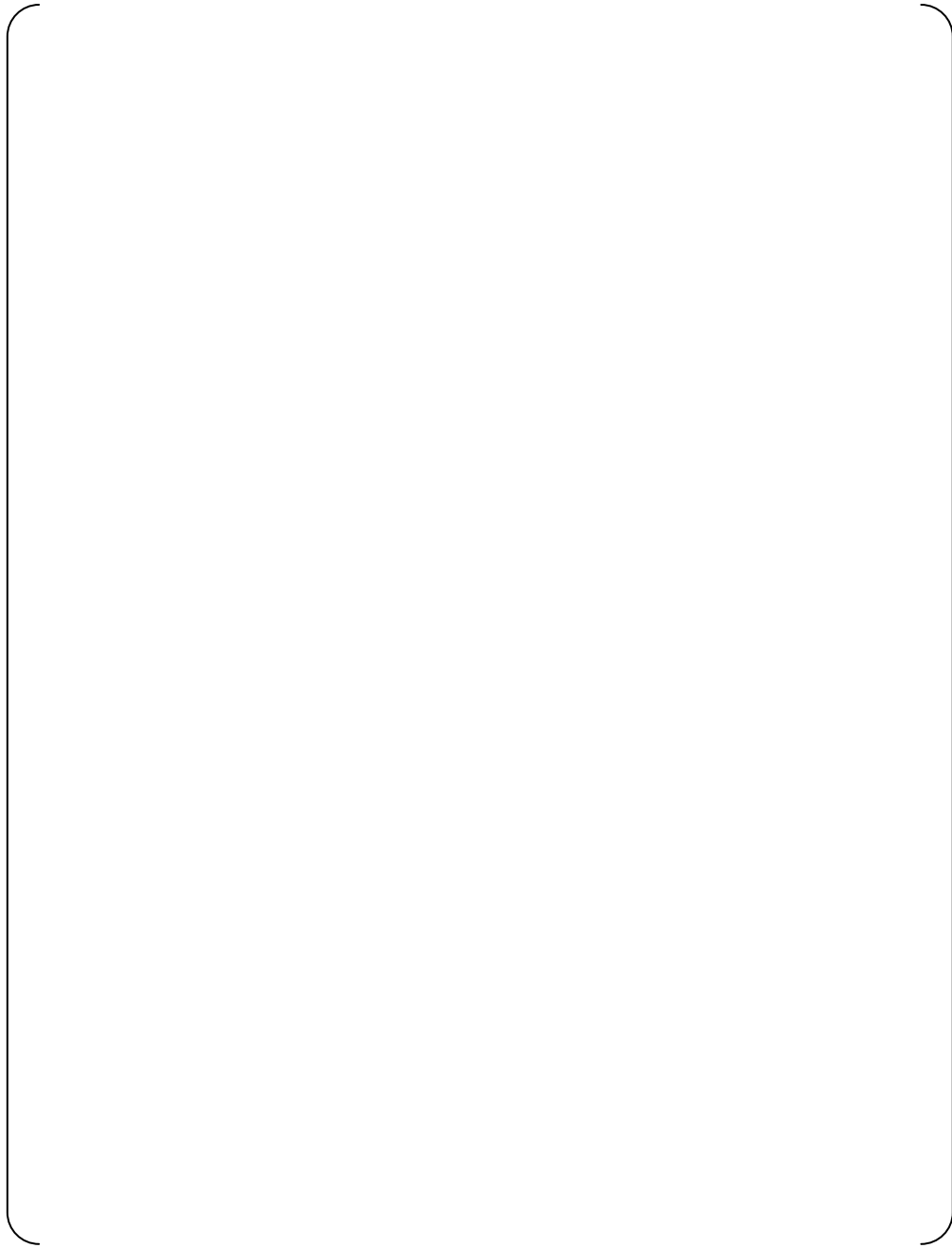


Fig. 5.3-8 Case-C3A: Gap between adjacent tubes in Col.78 under dynamic pressure



5.4 Case-C3B: Tube deformation – Out-of-Plane Hydrodynamic Force Alone

Case-C3B considers only the hydrodynamic pressure effects in the tube out-of-plane direction. Figure 5.4-1 shows a comparison of the horizontal tube displacement from Cases C3A and C3B. The Case C3B out-of-plane maximum displacement is [] [] and for Case C3A the result is [] This indicates that the out-of-plane hydrodynamic pressure without the vertical, in-plane component produces a larger out-of-plane displacement.

Figure 5.4-2 compares the vertical displacements for these two cases. The maximum downward deflection at the top of the tube bundle for Case C3B is [] and for Case C3A it is [] So, the out-of-plane load case has less downward displacement at the top of the bundle.

Figures 5.4-3 and 5.4-4 display the gap distributions between tubes and AVBs in cross sections along AVBs B06 and B05. These results are quite similar for both the C3A and C3B cases.

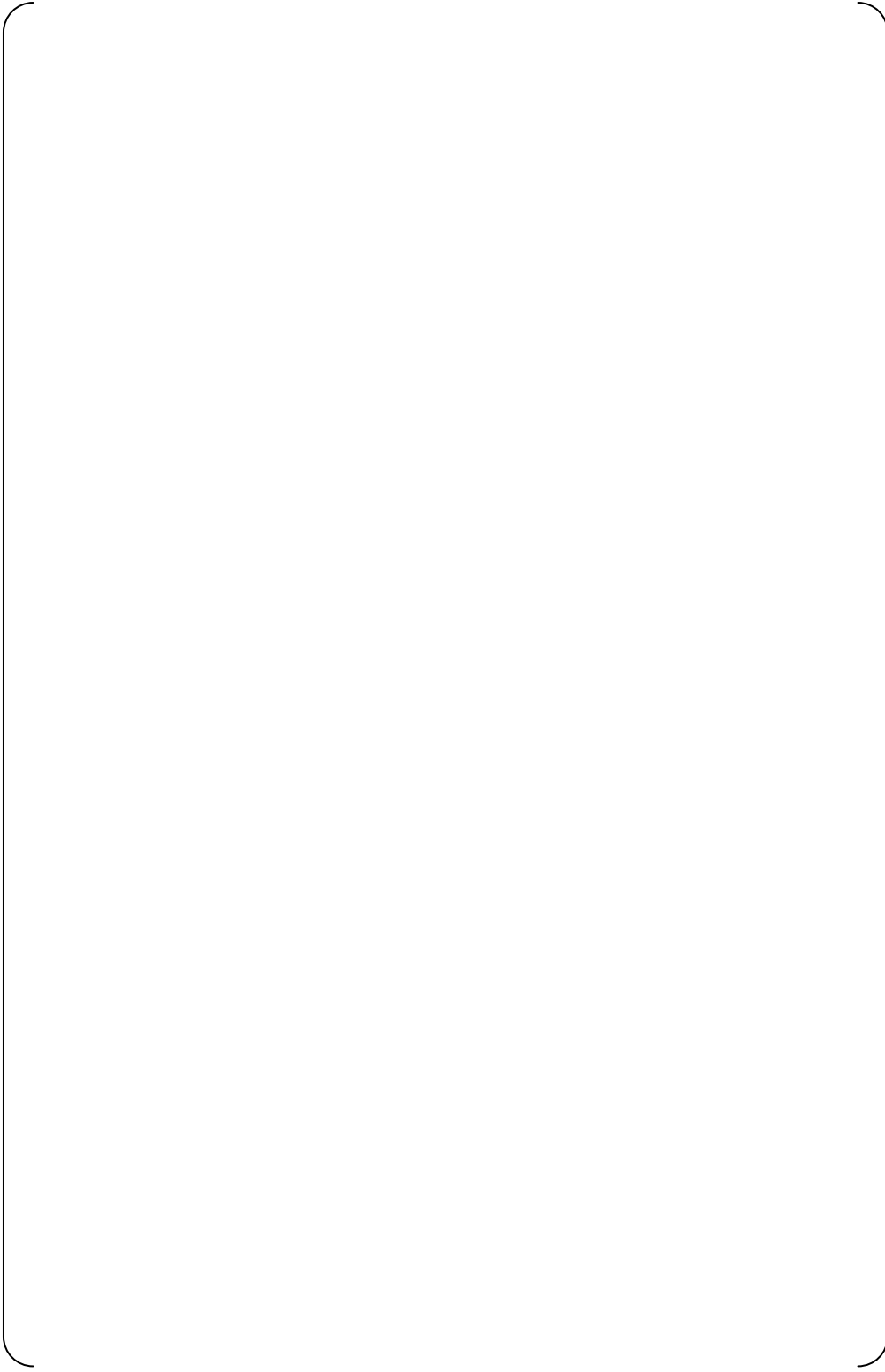


Fig. 5.4-1 Case-C3B: Deformation out of plane contour

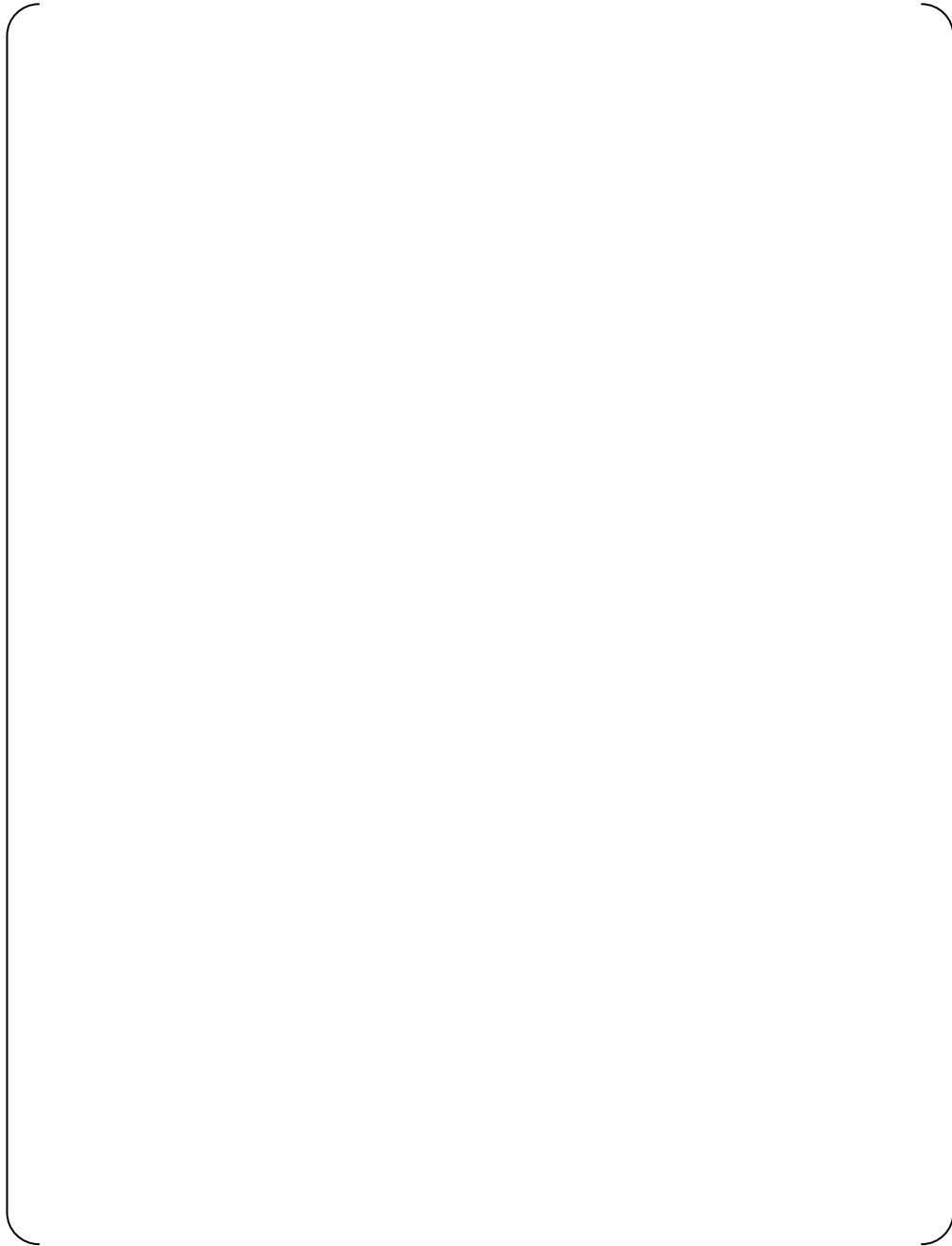


Fig. 5.4-2 Case-C3B: Vertical deformation contour

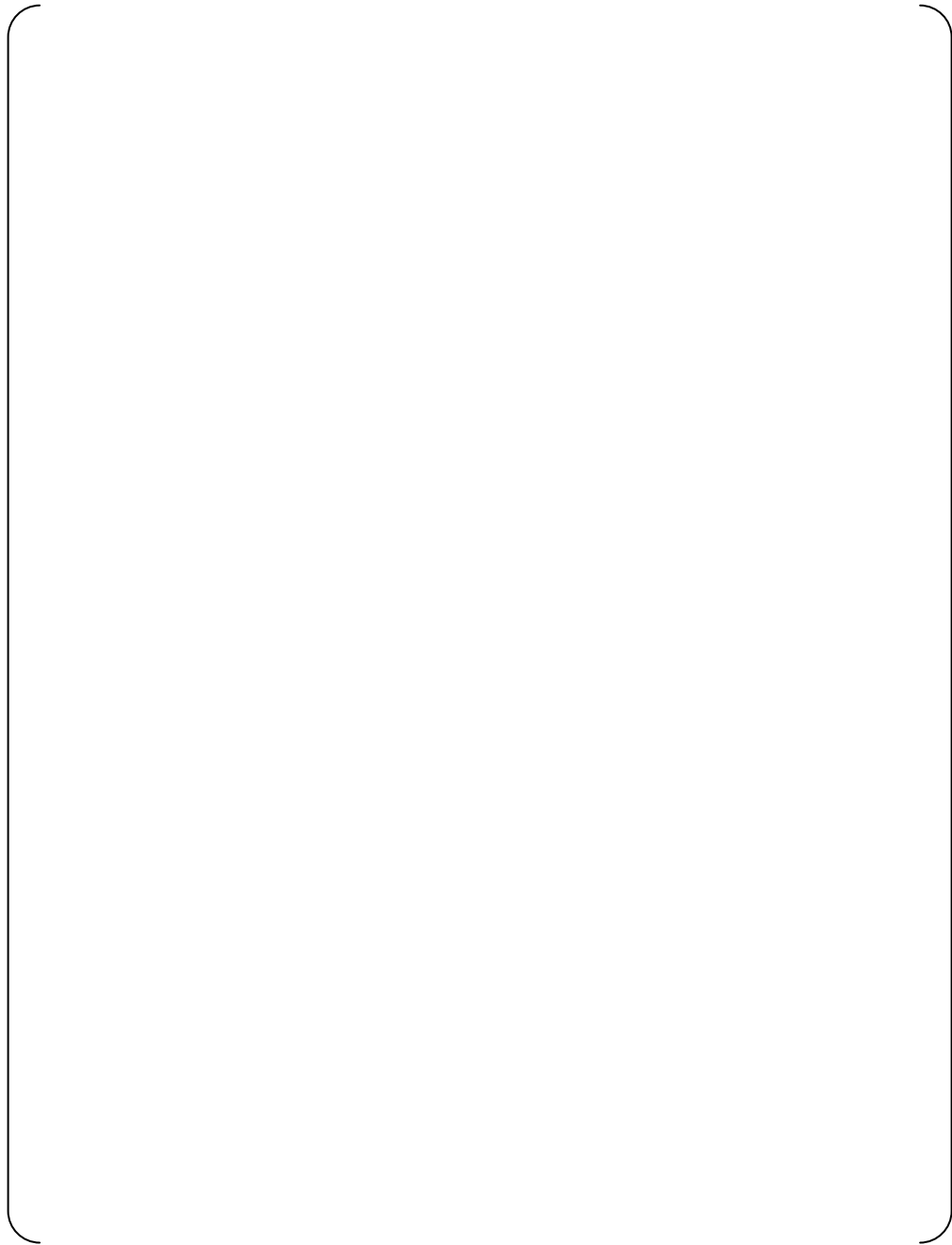


Fig. 5.4-3 Case-C3B: Gap distribution between AVBs and tubes in B6 section

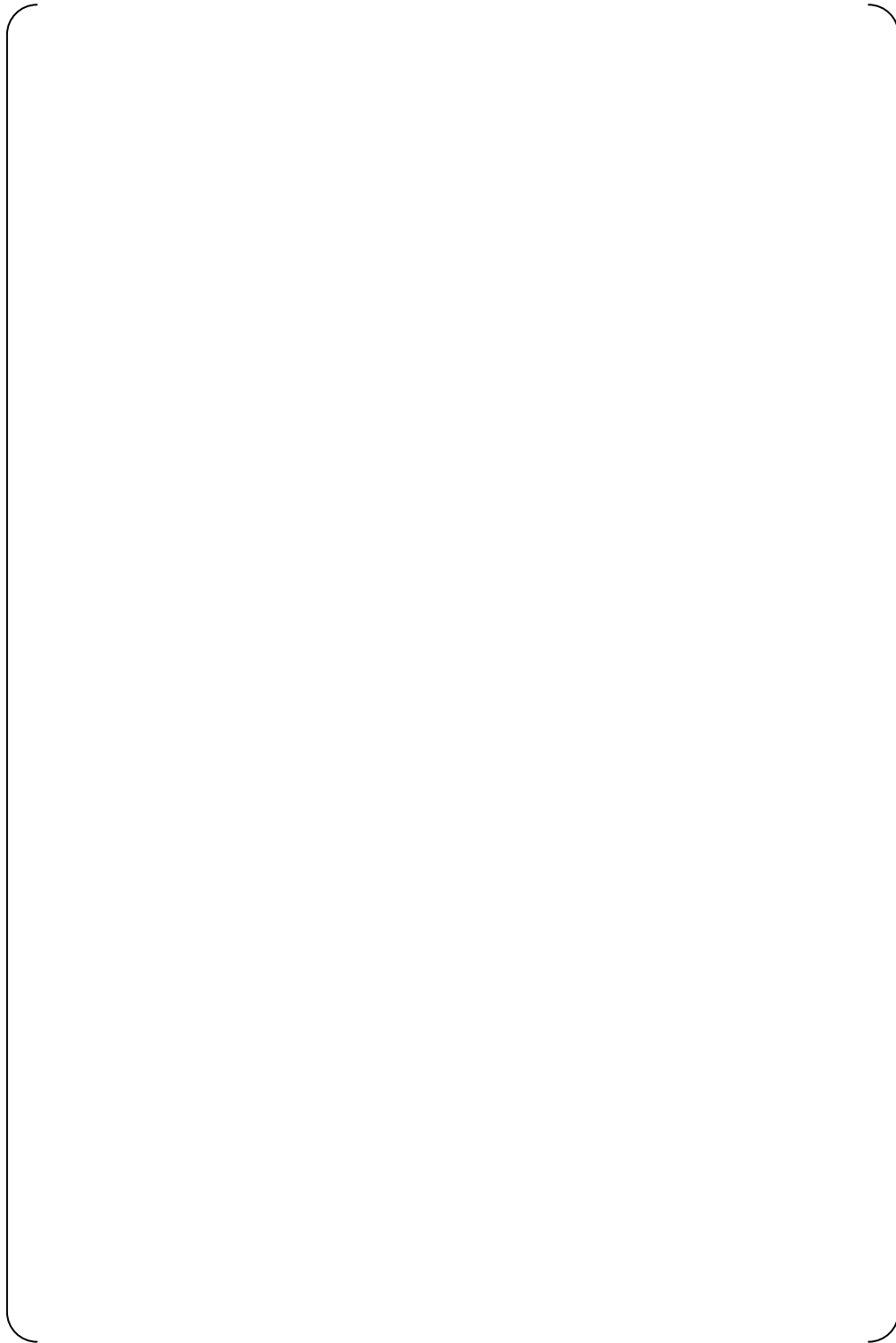


Fig. 5.4-4 Case-C3B: Gap distribution between AVBs and tubes in B5 section



5.5 Case-C3C: Tube deformation with Stiffer Retaining Bars

Case C3C is the same as case C3A, except that it has stiffer retainer bars. The retaining bar stiffness used in case C3C is 16 times larger than that of the actual bar. The factor of 16 results from doubling the retaining bar diameter based on the moment of inertia expressed by $\pi/64 \times d^4$.

Figures 5.5-1 and 5.5-2 show a comparison of the out-of-plane displacement and the vertical displacement for cases C3A and C3C. Stiffening the retainer bar by a factor of 16x produces a 15% reduction in deflection, which is small.

Figure 5.5-3 shows that the retaining bar and AVB deflection shapes are nearly the same. This further demonstrated in Figures 5.5-4 and 5.5-5 show the tube-to-AVB gap distributions at Sections B6 and B5 for cases C3A and C3C. All four cases have a maximum gap change of [] (when rounded off to the nearest mil). If the analytical results are used with their reported number of digits, it might be concluded that there is a 20% reduction in gaps due to the stiffening of the retaining bars.

It is concluded that increasing the retaining bar stiffness is not an effective way to reduce the tube-to-AVB gaps.

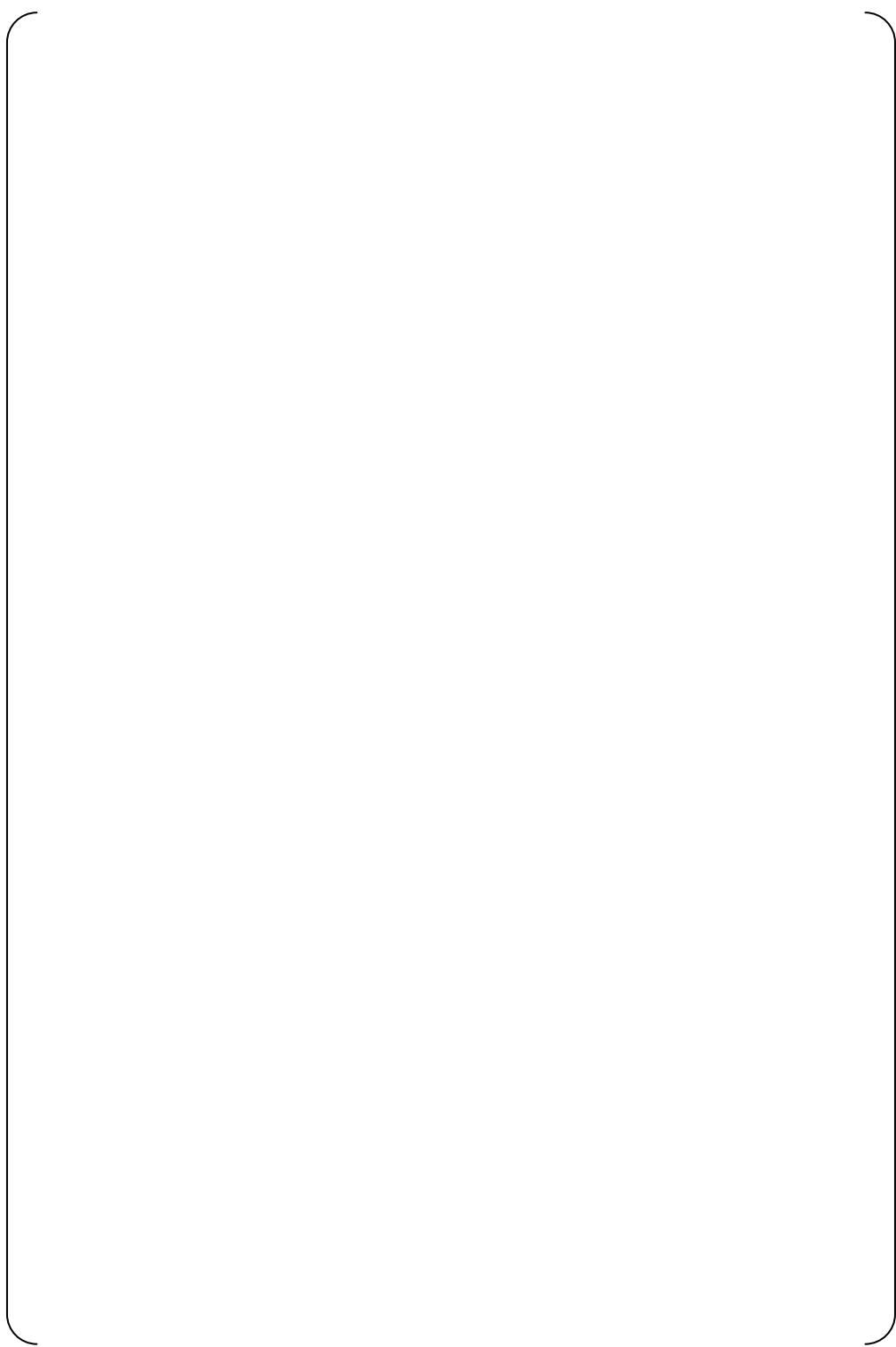


Fig. 5.5-1 Case-C3C: Out-of-Plane Deformation based on Retainer Bar Stiffness

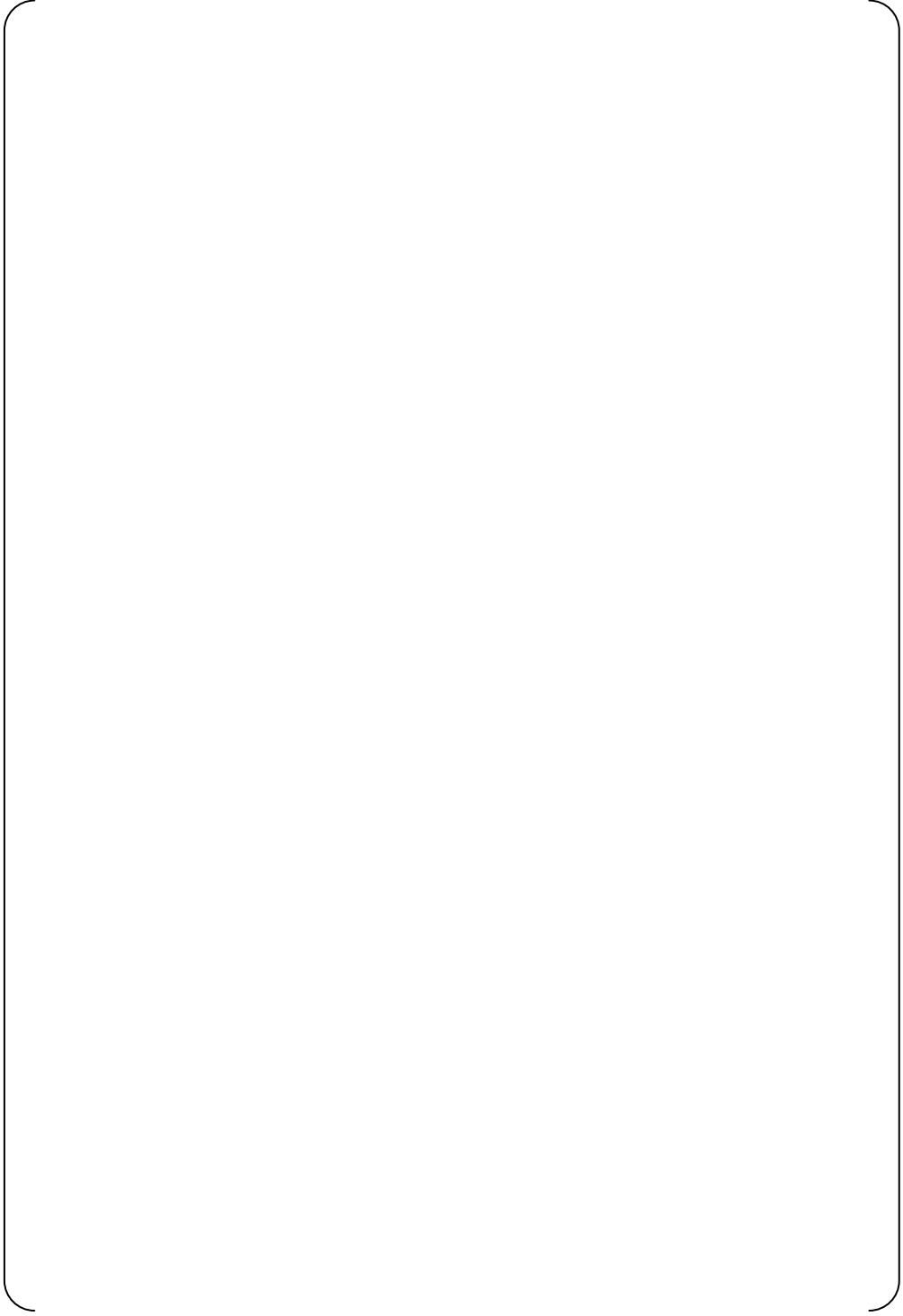


Fig. 5.5-2 Case-C3C: Vertical Displacement based on Retainer Bar Stiffness

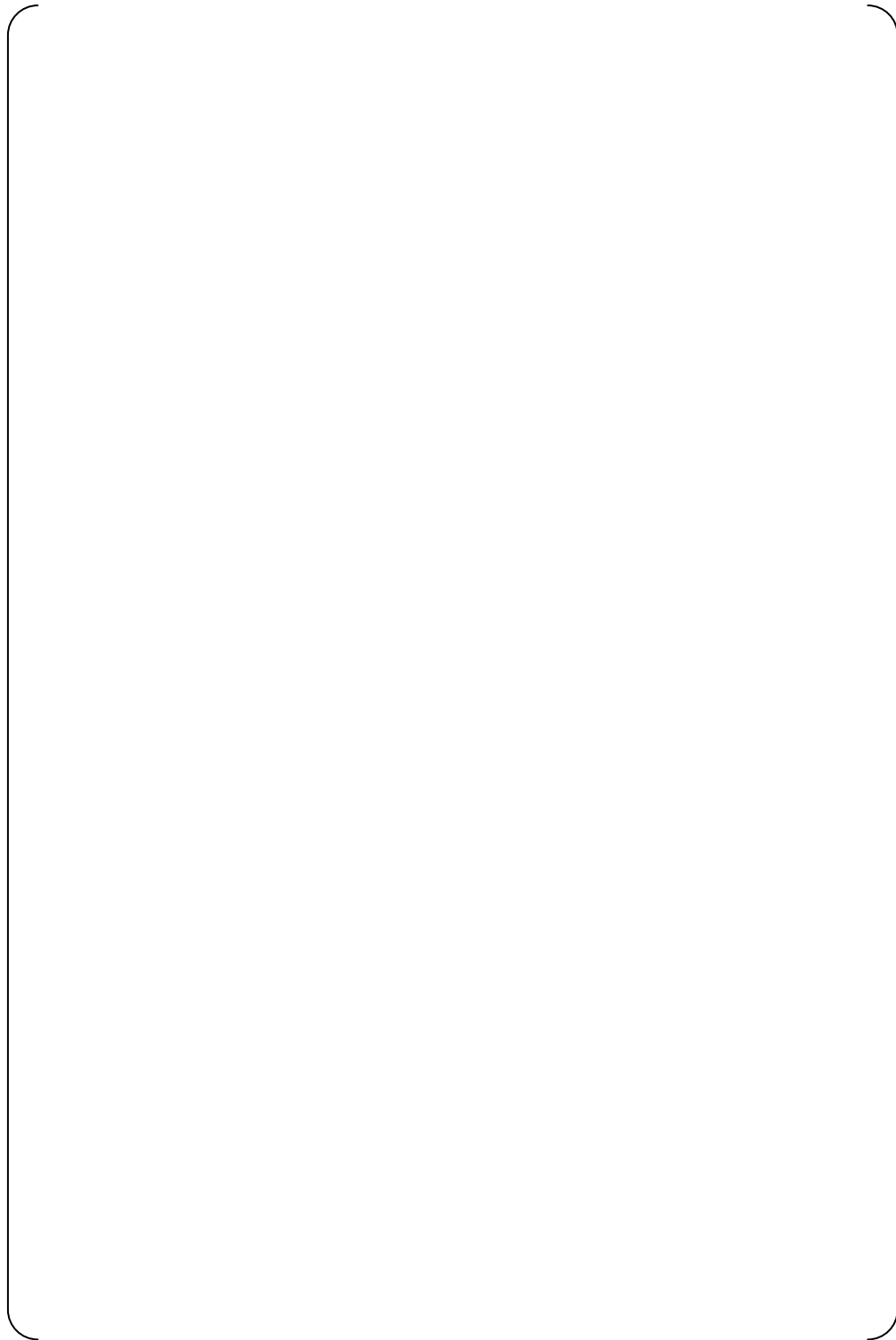


Fig. 5.5-3 Case-C3C: Deformation mode due to dynamic pressure

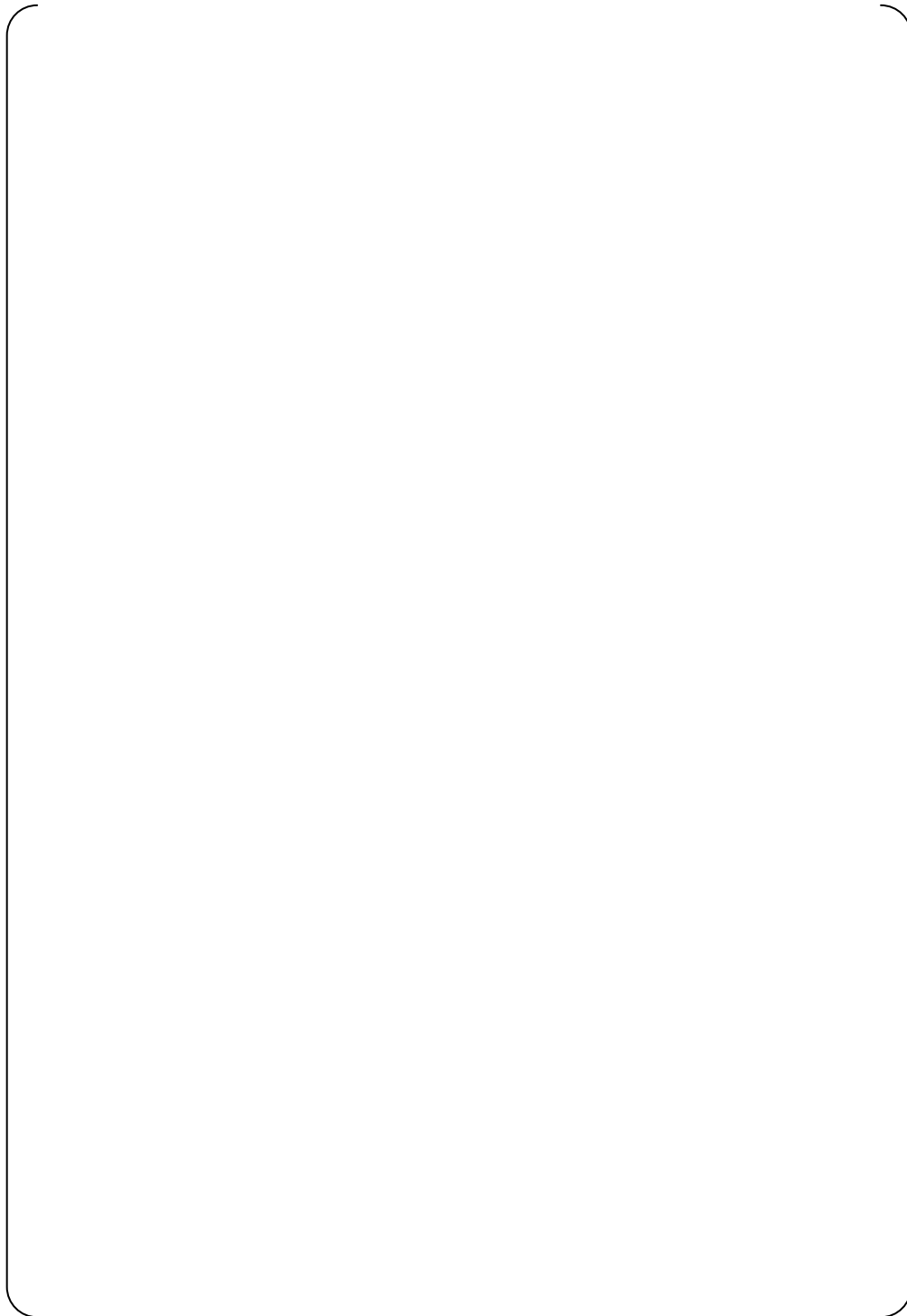


Fig. 5.5-4 Case-C3C: Gap distribution between AVBs and tubes in Section B6

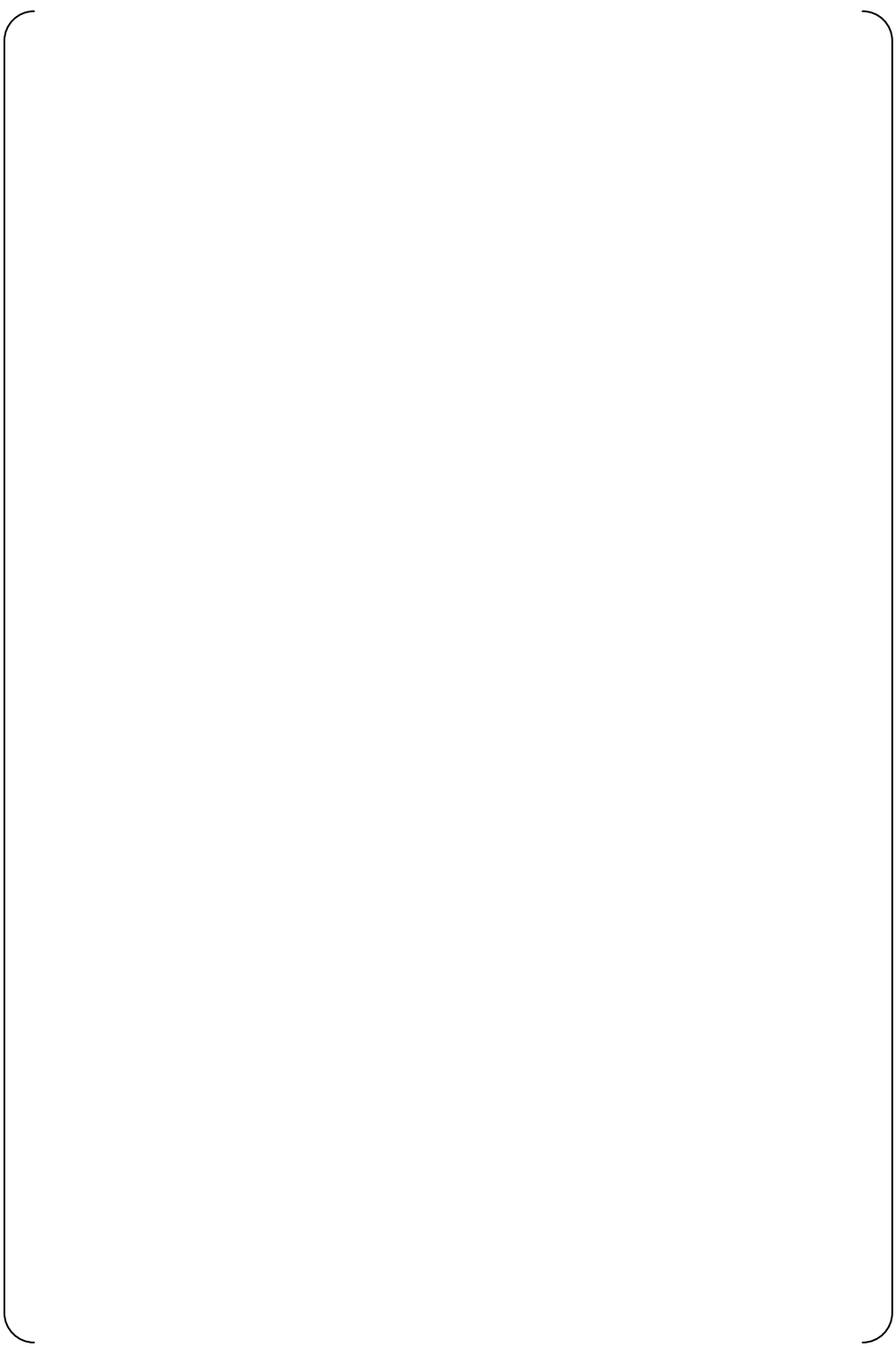


Fig. 5.5-5 Case-C3C: Gap distribution between AVBs and tubes in Section B5



5.6 Case-C3A': Tube Deformation from the latest Hydrodynamic Force (AVB assembly in)

Figure 5.6-1 shows the "total" tube deformation, which is the combination of the horizontal and vertical displacements. Horizontal deformation is dominant to total. The large hydrodynamic force in HOT side makes this horizontal displacement.

Figure 5.6-2 shows how the total deformation relates to the displacement in the vertical direction (top view) and in the horizontal direction (bottom view). The general trend is almost same as Case C3A. The hot side / cold side hydrodynamic forces also cause the tubes to displace downward (at the top of the bundle). The maximum downward deformation is []

Figure 5.6-3 shows AVB and retaining bar deformation along AVB-B06. The deformation trend is same as Case C3A.

Figures 5.6-4 and 5.6-5 show the gap distributions between tubes and AVBs at cross sections along AVBs B06 and B05. The largest gaps are found in the center column and high row zone. This zone corresponds to the region with the most severe wear in Unit-2 and Unit-3. The largest increase in tube-to-AVB gap in this region is [] for Section B6 and B5.

Figure 5.6-6 shows the regions along the AVBs in Column 78 where there is tube contact or a gap. In Case C3A', there are many tubes with consecutive inactive supports as same as Case C3A. Such an unsupported tube span would have a low natural frequency and would exhibit unstable vibration characteristics under normal operating conditions.

Figure 5.6-7 shows the distribution of contact forces between tubes and AVBs. This contour just express compression magnitude, however contact forces can be obtained by multiplying by compression spring stiffness []. In the center column and high Row area, where severe wear occurred, the contact forces are around []. This small force hardly supports and fixes a tube.

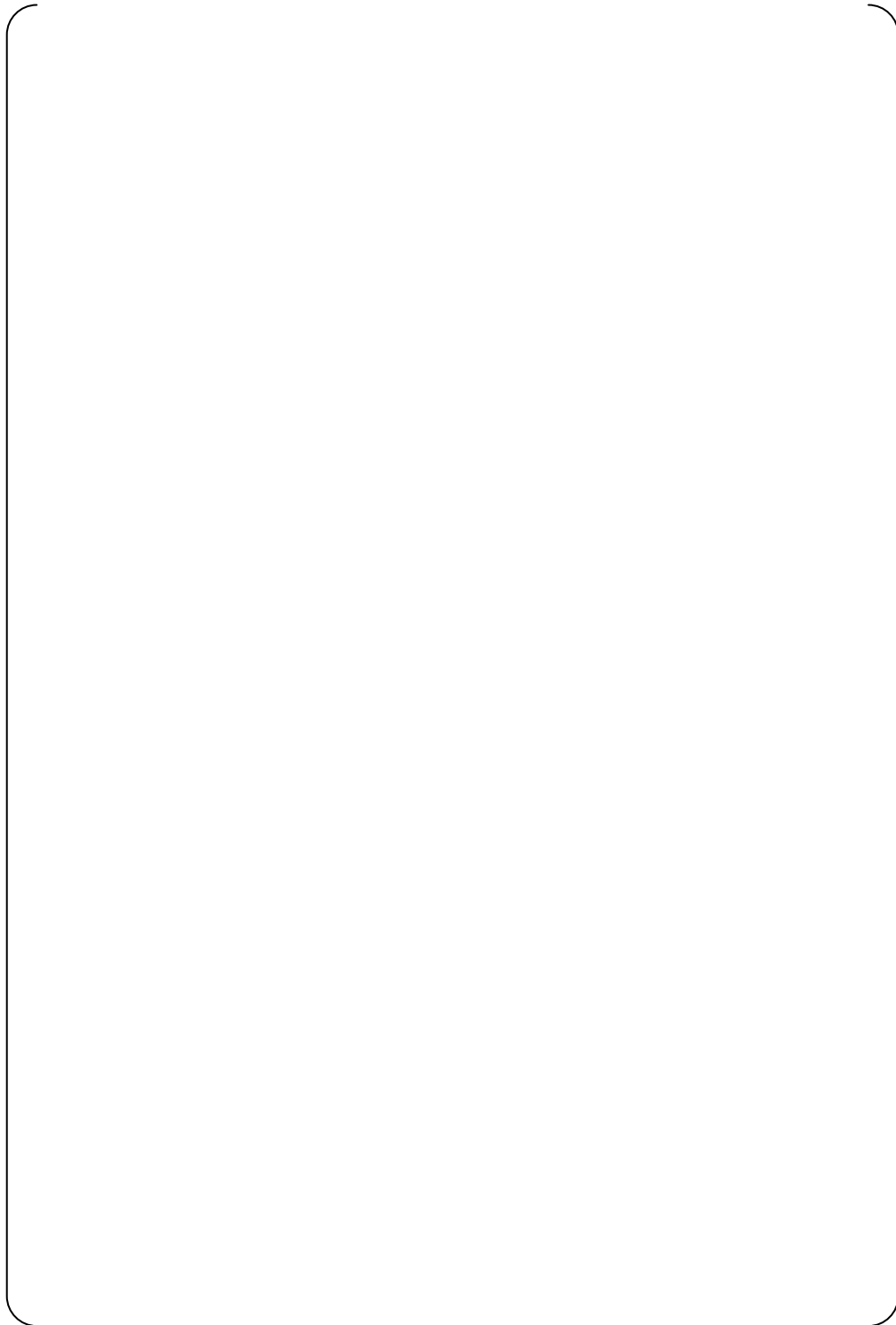


Fig. 5.6-1 Case-C3A': Total deformation due to dynamic pressure (with AVB contact)

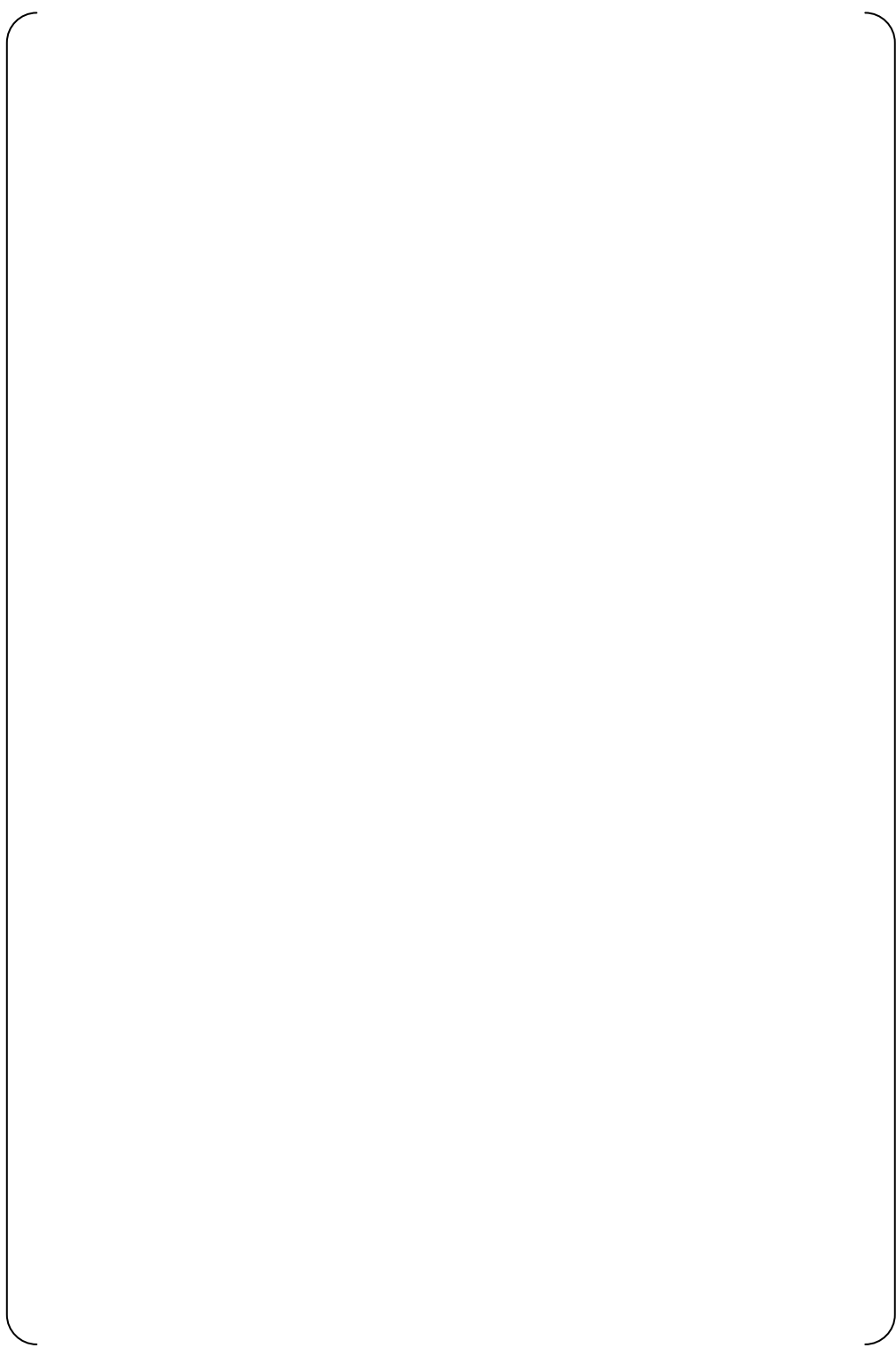


Fig. 5.6-2 Case-C3A': Deformation contour due to dynamic pressure (tubes-AVBs contact)

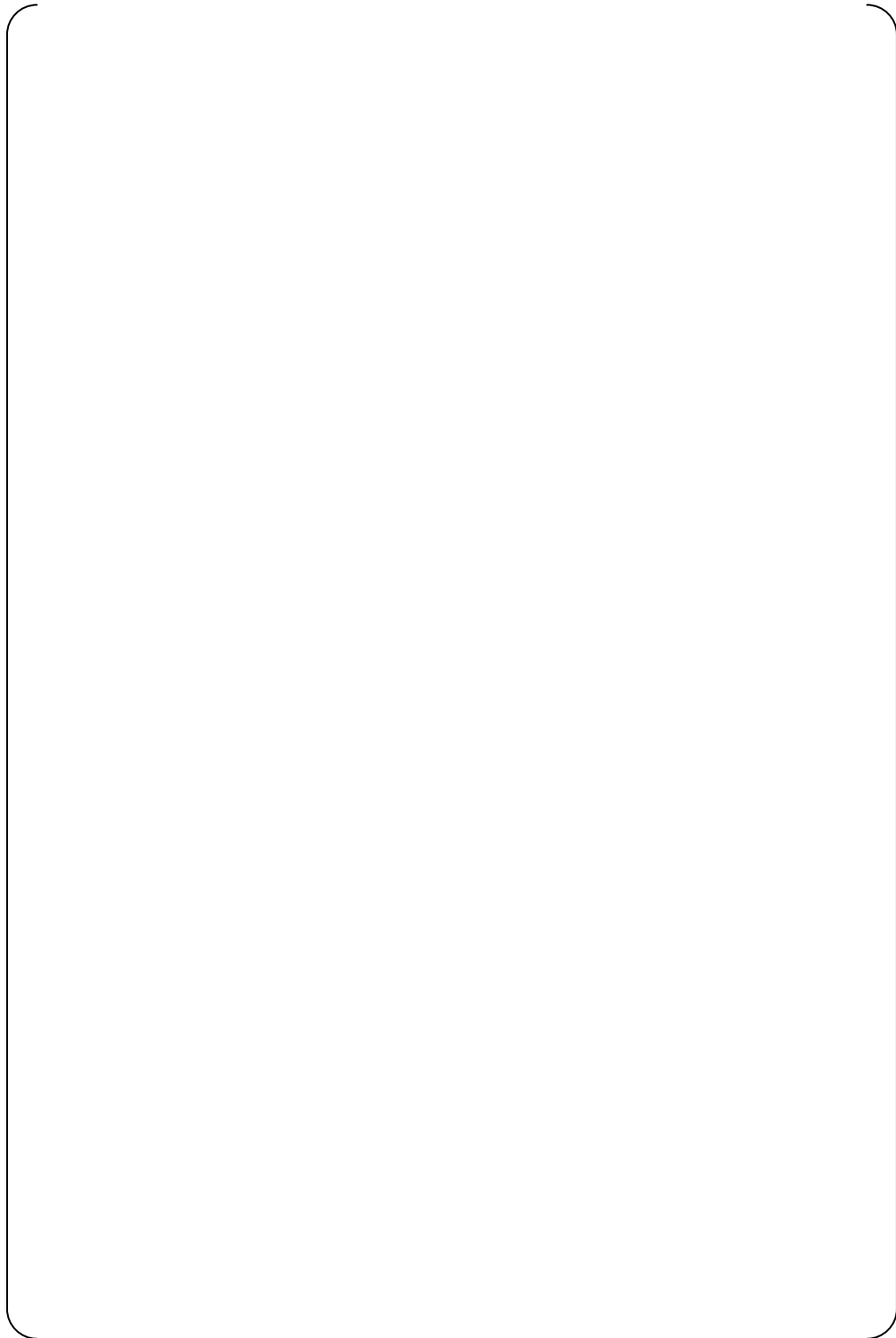


Fig. 5.6-3 Case-C3A': Deformation due to dynamic pressure (tubes-AVBs contact)

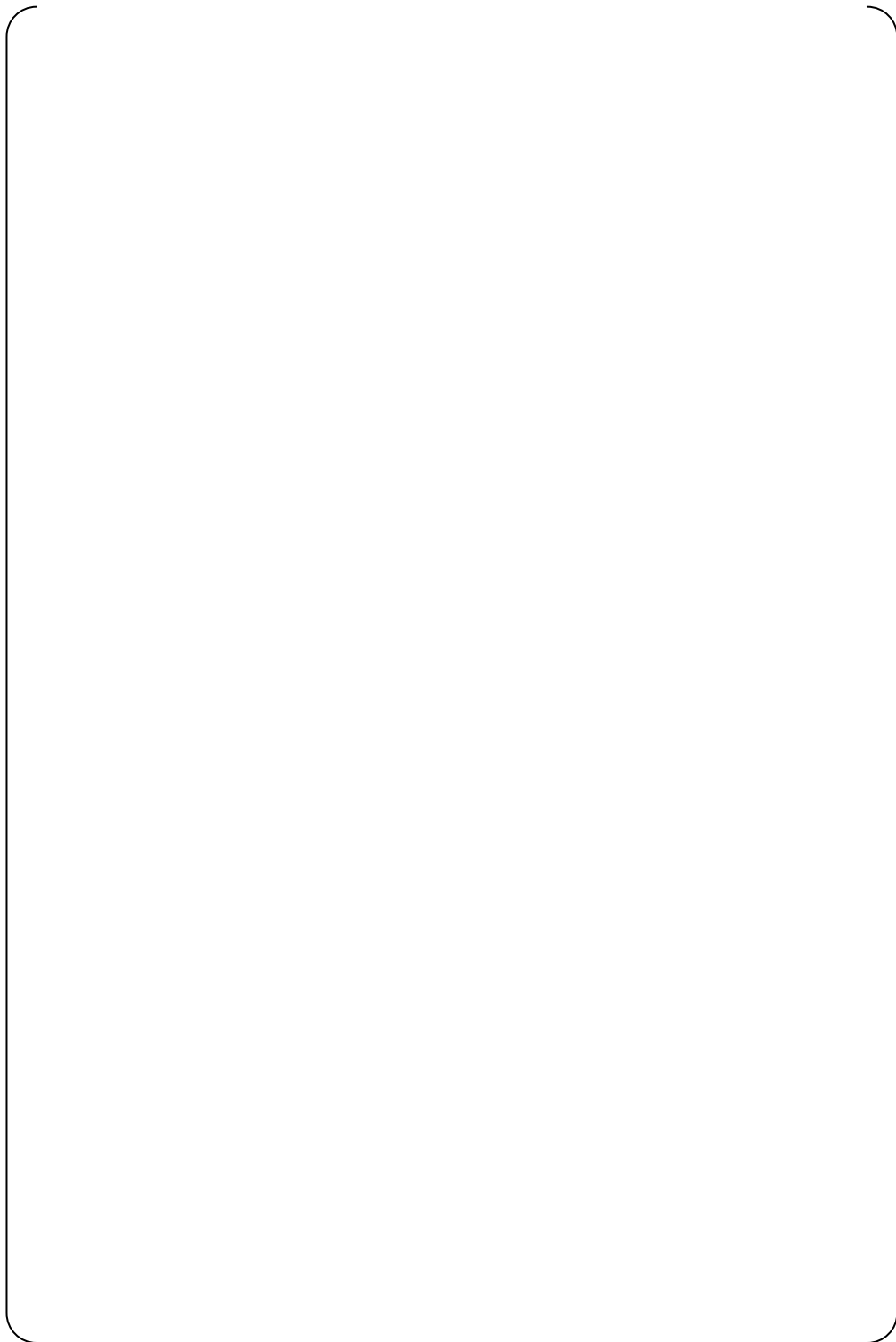


Fig. 5.6-4 Case-C3A': Gap distribution between AVBs and tubes in B6 section

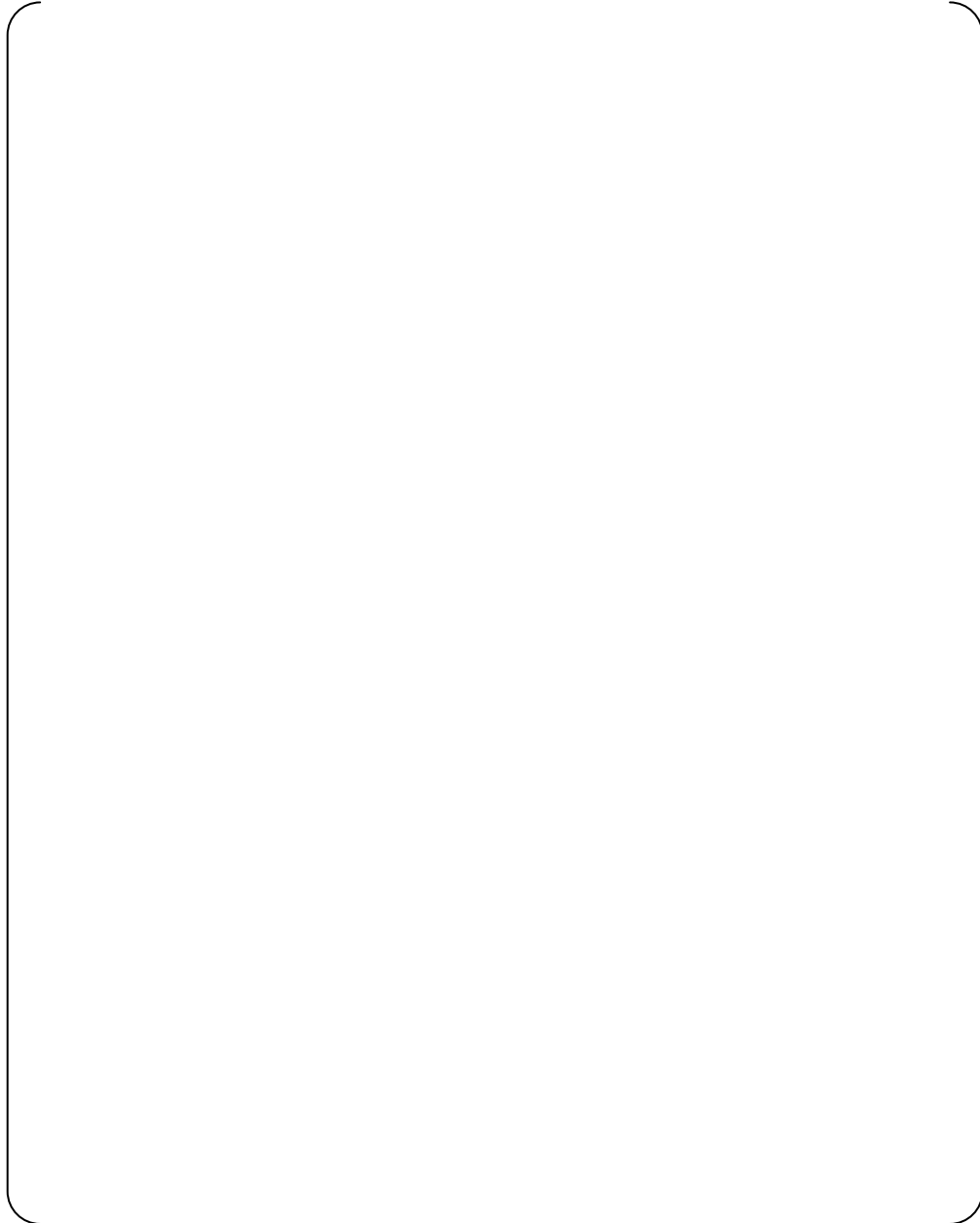


Fig. 5.6-5 Case-C3A': Gap distribution between AVBs and tubes in B5 section

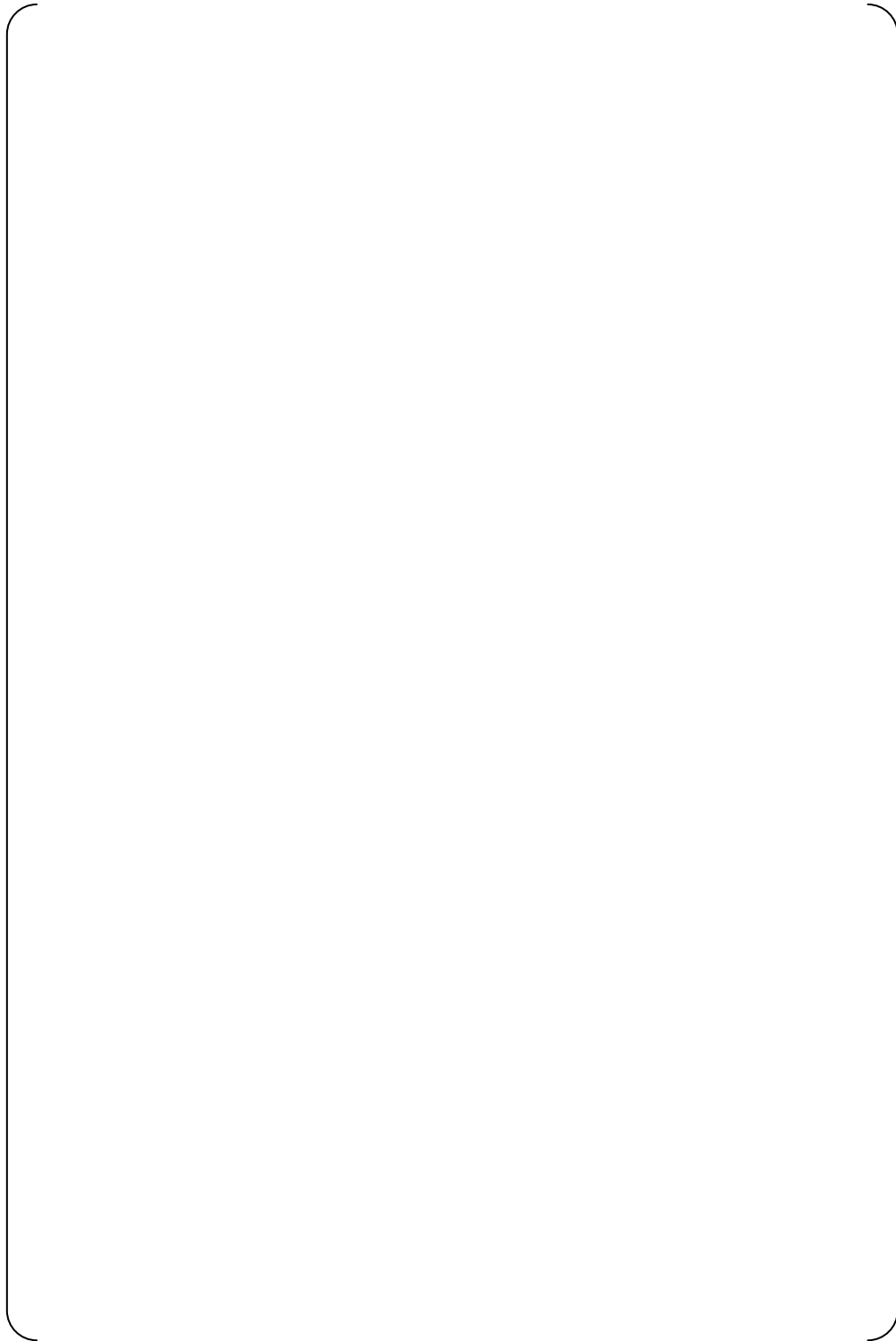


Fig. 5.6-6 Case-C3A': Gaps of tubes in Col.78 to adjacent AVBs

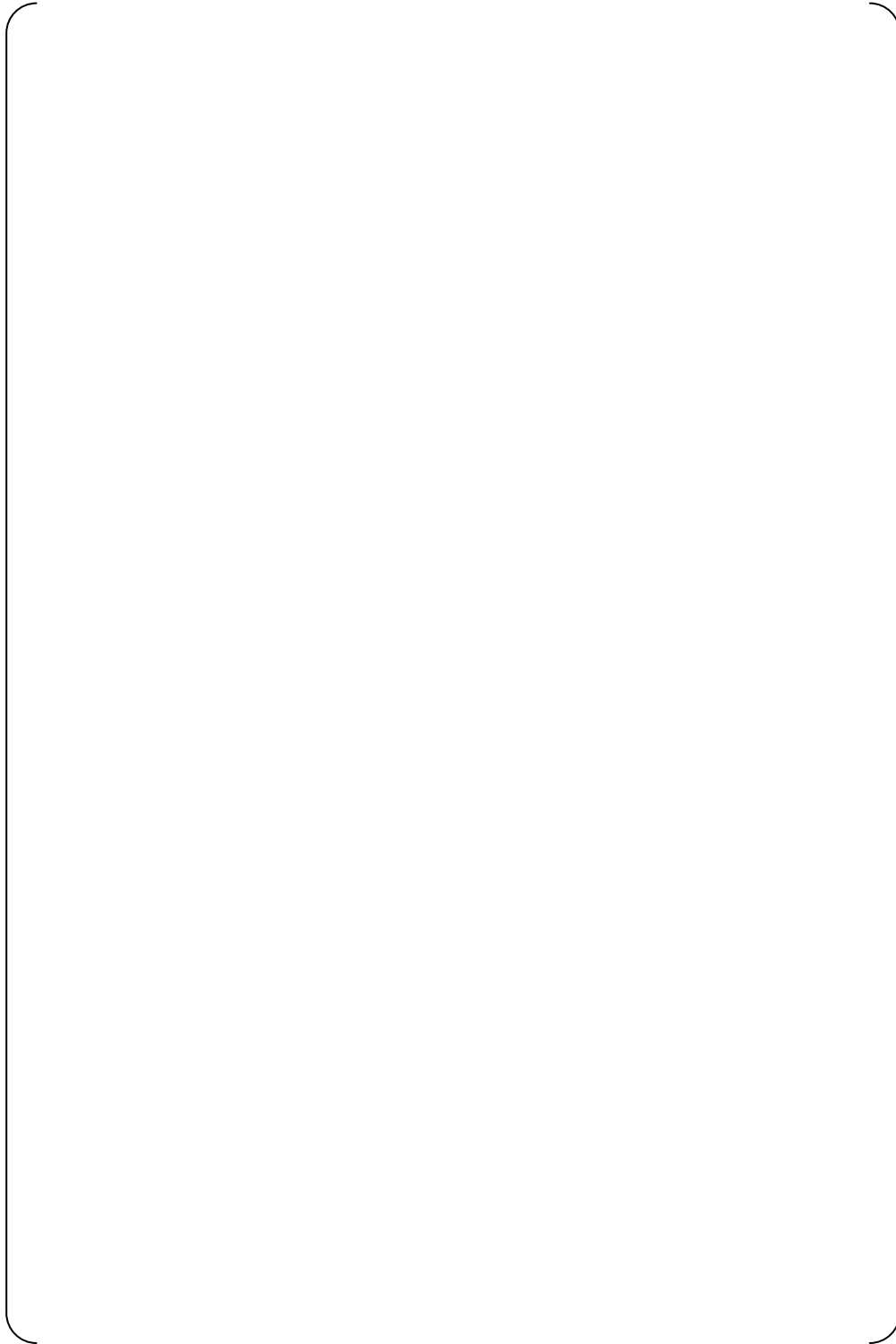


Fig. 5.6-7 Case-C3A': Distribution of contact forces between tubes and AVBs



5.7 Case-D1: Tube Deformation with manufacturing dispersion and the latest Hydrodynamic Force (AVB assembly in)

Figure 5.7-1 shows the “total” tube deformation. Tube bundle expands by manufacturing dispersion. Color counter shows no tendency of hydrodynamic force such as Case C3 series. This indicates that manufacturing dispersion is dominant for tube deformation and prevents hydrodynamic deformation due to large friction force.

In Case C3A', out-of-plane tube displacement pulls AVBs and retainer bars outward. In the center columns, this causes the retaining bars to displace downward. Figure 5.7-2 presents the displacement in vertical direction in Case D1. The center column AVBs in Case D1 seem to be fixed because friction force due to manufacturing dispersion is higher than Case C3A'.

Figure 5.7-3 shows AVB and retaining bar deformation mode along AVB-B06. The deformation mode is different from Case C3 series. The center column AVBs are fixed by high friction force. Outer column AVBs are moved up due to outer column tubes outward displacement.

Figures 5.7-4 shows the gap distributions between tubes and AVBs at cross sections along AVBs B01, B02, and B05. The gaps are scattering by manufacturing dispersion distribution. The color contour in section B1 and B2 includes many blue (compression) plots than section B5. This indicates that reaction forces at B1 and B2 are larger than B5.

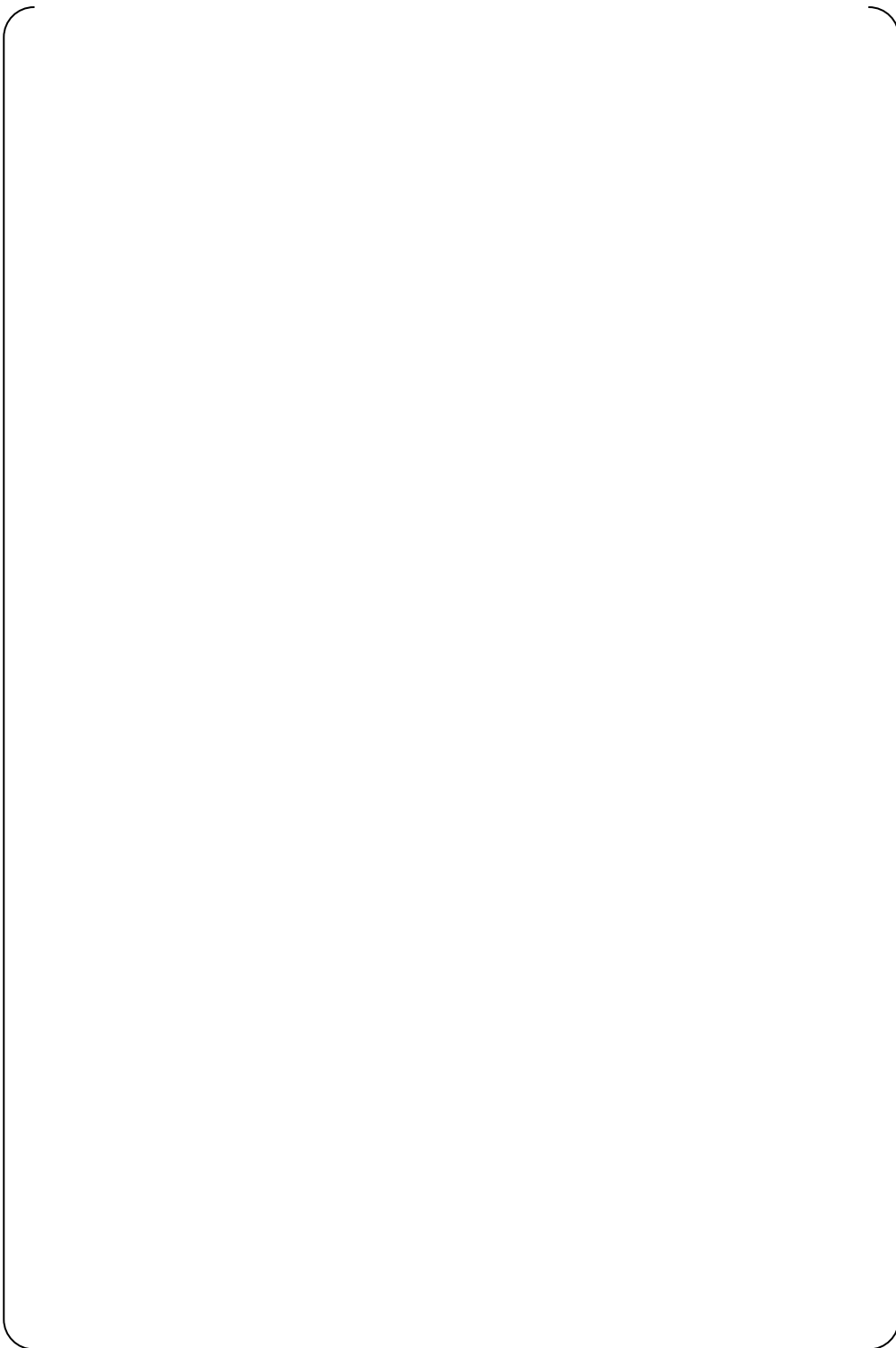


Fig. 5.7-1 Case-D1: Deformations due to dynamic pressure and manufacturing dispersion



Fig. 5.7-2 Case-D1: Vertical deformation contour due to dynamic pressure and manufacturing dispersion



Fig. 5.7-3 Case-D1: Deformation mode due to dynamic pressure and manufacturing dispersion

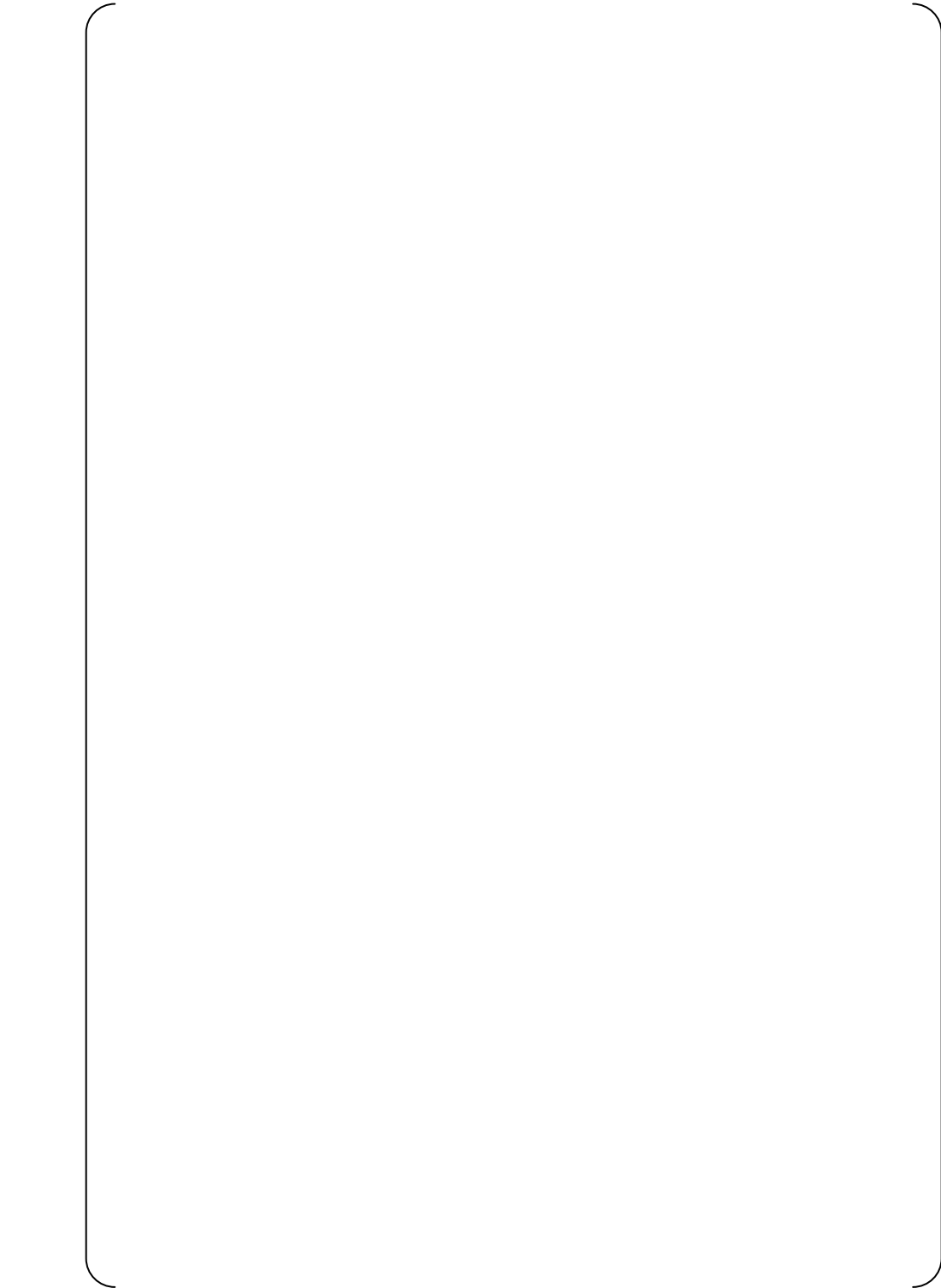


Fig. 5.7-4 Case-D1: Gap distribution between AVBs and tubes in B1, B2, and B5 section



Appendix-9
Simulation of Manufacturing Dispersion for Unit-2/3



1. Purpose

The wear in Unit-3 is more severe than Unit-2. This seems to be caused by difference of AVB-tube contact forces between Unit-2 and Unit-3. The contact force is generated by manufacturing dispersion; tube ovality, tube flatness, tube true position, AVB thickness deviation, AVB flatness, AVB twist. This appendix contains the evaluation of contact forces due to manufacturing dispersion between Unit-2 and Unit-3, and simulation of Ding signals in Unit-2. Fig.2-1 Distribution of contact forces in manufacturing dispersion analysis

2. Conclusion

The analyses results show a consistent with the Ding signal distributions (as shown in Fig.2-1) and trend that contact forces between tube and AVB in Unit-3 are less than half of Unit-2 contact force (as shown in Fig.2-2).



Unit-2

Unit-3

Fig.2-1 Distribution of contact forces in manufacturing dispersion analysis



Unit-2

Unit-3

Fig.2-2 Distribution of contact forces in manufacturing dispersion analysis



3. Assumption

- 1) The manufacturing dispersion of Unit-2 A-SG (E089) represents Unit-2, and Unit-3 A-SG(E089) represents Unit-3.
- 2) Tube G value, tube pitch, tube flatness, AVB thickness and AVB twist deviations are considered as manufacturing dispersion. AVB flatness regards as 0, because AVB flatness means not micro winding beyond each row but macro winding beyond scores rows, and this macro winding makes negligible small contact force due to less stiffness of AVB beyond scores rows. The initial gap between tube and AVB is nominal gap () in cold condition, and this gap is changed according to deviation of above values. Each deviation is randomly given to the gap in the analysis model. The contact force of tube to AVB is generated as reaction force due to accumulation of each deviation.
- 3) The manufacturing deviation is assumed to follow normal distribution, so the standard deviation is adopted in the analysis. The actual standard deviation is used for measured dimensions. AVB twist is deviates based on the actual distribution in the verification test for AVB press load (refer to Attachment 9-1) in this study.
- 4) AVB nose thickness and twist for Unit-3 are assumed to be smaller than Unit-2 as shown in Table 6-1. In a process of AVB making up in shop, AVB nose area is pressed in order to flattening increased inside thickness due to bending. The press load was () [N] for Unit-2 and () [N] for Unit-3. The reason of this change is to improve AVB thickness and twist accuracy. All AVB twists for both Unit-2 and Unit-3 are satisfied with the tolerance specified in the design drawing, however checked by Go/No-go. Before adopting () [N] pressing for Unit-3, a verification testing was performed. Attachment 9-1 shows a summary of the test results and AVB twist in () [N] press is better than () [N].
- 5) ECT ding signals are supposed to indicate elastic ding by reaction force due to manufacturing dispersion. () [N] is a threshold of elastic ding as a result of ding testing. () [N] is necessary to make plastic ding on tube, however such high reaction force is hardly generated in bundle rotation analysis and flowering analysis. Attachment 9-2 presents a result of simple ding testing.



4. Acceptance criteria

There are no acceptance criteria associated with this report since this evaluation is performed to compare the trend of the tube-to-AVB contact force in Unit-2 and Unit-3.

5. Design Inputs

5.1 Geometry

The nominal dimensions are obtained from the design drawings (Ref.1 to 7).

5.2 Manufacturing dispersion and tolerances

Tube G value, tube pitch, tube flatness, AVB thickness deviation, AVB twist, and AVB flatness are considered in manufacturing dispersion analysis. Figure 5.2-1 shows image of each deviation. Table 5.2-1 shows the manufacturing dimensions and tolerances. Table 5.2-2 presents measurement results of the dimensions. AVB thickness in bending portion is measured separately from straight bar, because AVB bending process makes AVB inside thickness increase.

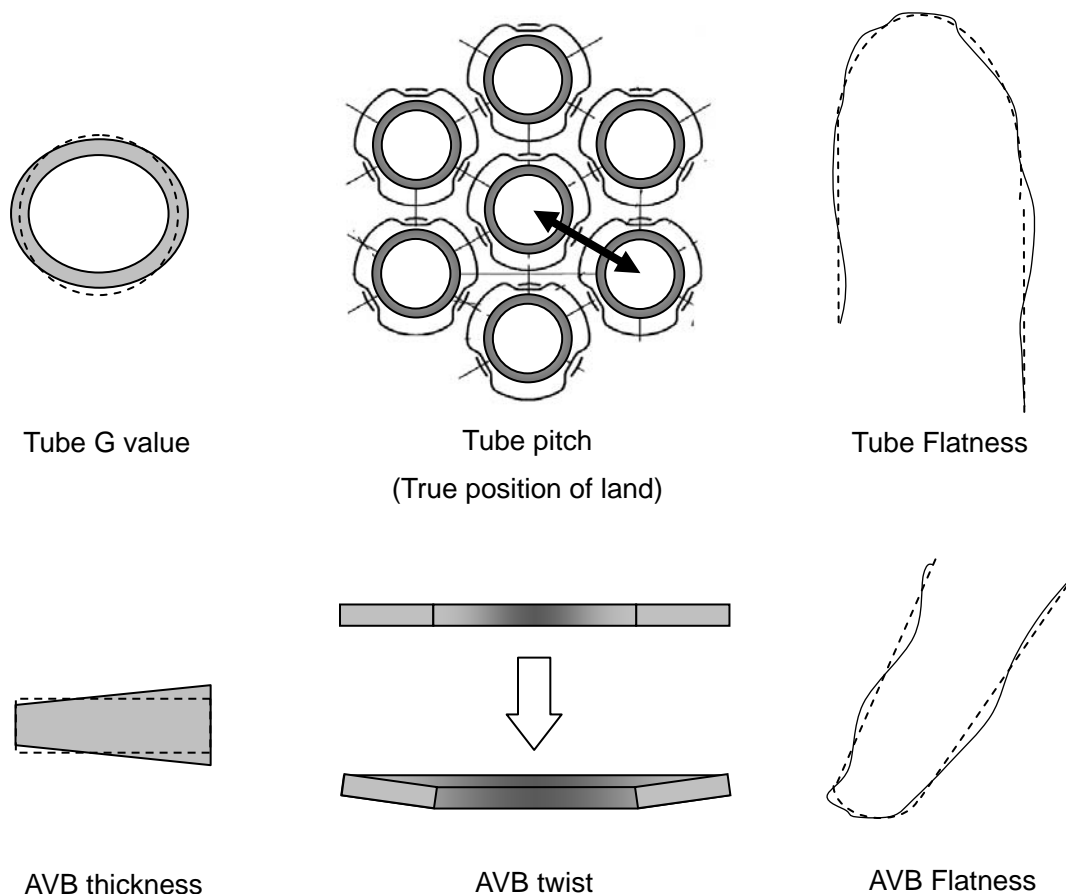


Figure 5.2-1 Image of manufacturing dispersion



Table 5.2-1 Dimensions and tolerances

	AVB			Tube		
	Thickness	Twist	Flatness	G value	Pitch	Flatness
Nominal						
Tolerance						
Note	Measured	Go/No-go checked	Go/No-go checked	Measured	-	Go/No-go checked

Note: The tolerances are specified in the design drawings (Ref.4 and 7) and material specification (Ref.8)

Table 5.2-2 Measurement results of the dimensions

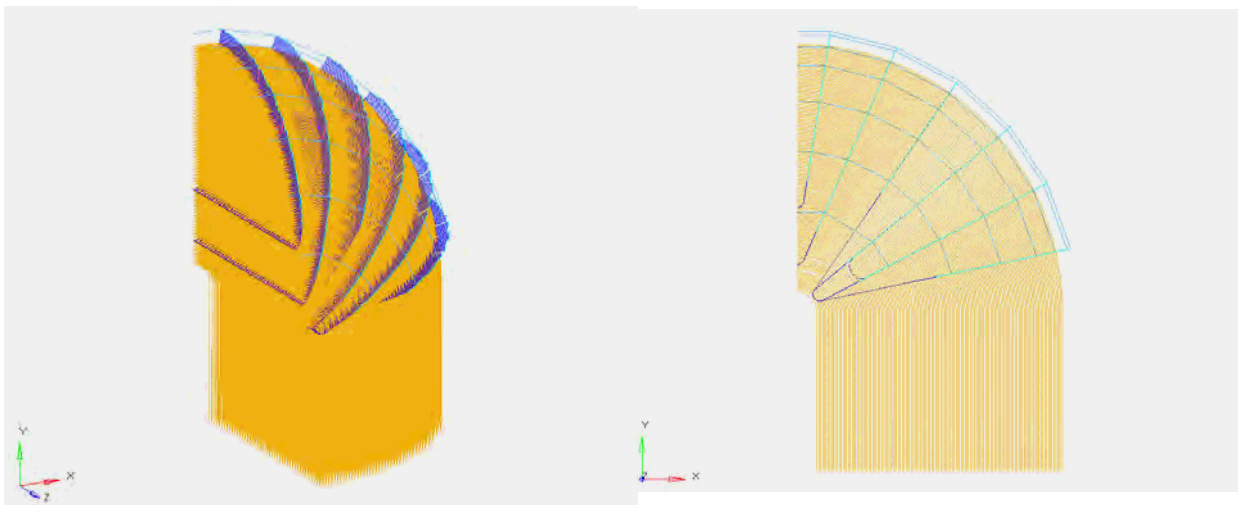
	AVB thickness change from nominal		Tube ovality δ_H	Standard deviation		
	δ_A			AVB thickness change from nominal σ_A		Tube ovality
	Bending portion	Straight Bar		Bending portion	Straight Bar	σ_H
2A						
2B						
Average in Unit-2						
3A						
3B						
Average in Unit-3						



6. Methodology

6.1 Analysis model

All parts of the U-bend assembly above the #6 TSP (Tubes, AVBs, Retaining bars, Retainer bars and Bridges) are modeled as beam elements. Figure 6.1-1 shows overview of the analysis model. The model area is a quarter by taking into account symmetry. The contact points between tube to AVB, and tube to TSP are modeled as gap elements, which show spring property in compression. This model is same as the flowering analysis model in Appendix-6. FEA code used is ABAQUS.



Bird's-eye View of the Model

Front View of the Model

Figure 6.1-1 Analysis model

6.2 Inputs of manufacturing dispersion

6 types of the manufacturing dispersion introduced in Section 5.2 are considered in the analysis model. The deviation is generated according to random number and inputted to the gap elements in the analysis model. The random number dispersion follows normal distribution. Figure 6.2-1 indicates how to input the deviation to gap element in the analysis model. Especially for AVB twist, AVB twist factor in consideration of torsion stiffness is defined as a decrease function of distance from AVB bending peak, because the more contact points leave from AVB nose, the less AVB torsion stiffness is. Figure 6.2.2 shows AVB twist factor. In AVB nose area, the factor is always 1, because increased twist from nose tip and decreased stiffness from nose tip cancel each other. On the other hands, AVB twist is considered to be kept along the straight bar, so the factor decreases according to far from AVB nose. Table 6.2-1 shows inputs used as manufacturing dispersion for the analysis model.



Total deviation = $\delta_0 + (\delta_A \pm 3\sigma_A)/2 + (\delta_H \pm 3\sigma_H)/2 + (\pm 3\sigma_S) + |\pm 3\sigma_{TA}|/2 + (\pm 3\sigma_{BA})/2 + (\pm 3\sigma_B)/2$

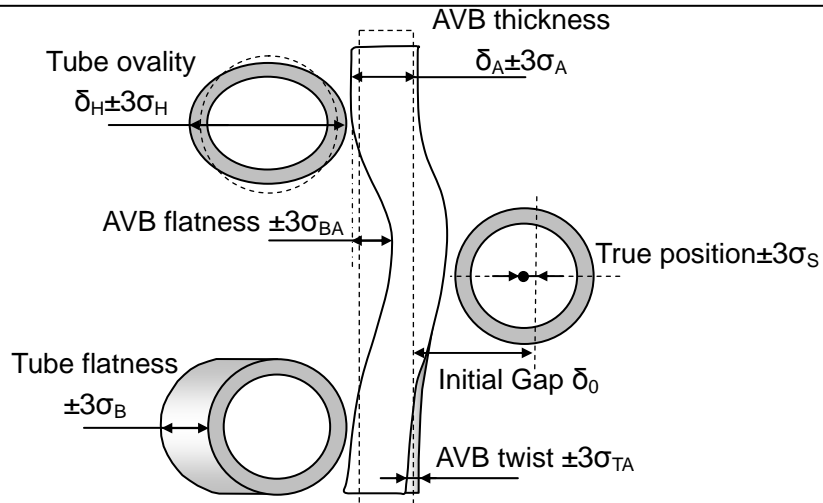


Figure 6.2-1 how to consider manufacturing dispersion

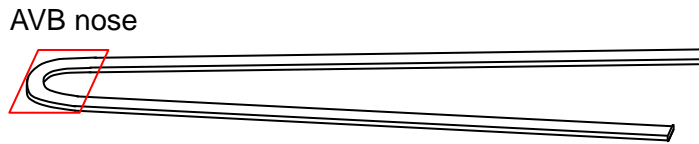


Figure 6.2-2 how to consider manufacturing dispersion

6.3 Analysis cases

The manufacturing dispersion analyses are performed for the cases as shown in Table 6.2-1.



Table 6.2-1 Measurement results of the dimensions

Unit: mm (mils)

Unit	AVB thickness change from nominal δ_A		Tube ovality δ_H	Standard deviation σ						
	Bending portion ^{*1}	Straight Bar		AVB thickness change from nominal σ_A		Tube ovality σ_H	AVB twist ^{*2} σ_{TA}	AVB Flatness ^{*3} σ_{BA}	Tube Flatness σ_B	
				Bending portion	Straight Bar					
Case 1 Unit-2A (U2-E089)										
Case 2 Unit-3A (U3-E089)										
Note	Measured ^{*1}	Measured	Measured	Measured	Measured	Measured	Go/No-go checked	Go/No-go checked	Go/No-go checked	

Note)*1:AVB thickness of bending portion is assumed based on the fact obtained by the AVB pressing test results(See Attachment 9-2 for details), which indicated that AVB nose thicknesses of Unit-2 SGs are larger than Unit-3 SGs due to the difference of AVB pressing load ([] N for Unit-2 SGs and [] N for Unit-3 SGs) and the side wide AVBs of Unit-2 are thinner than other types of AVBs.

*2:AVB twist probability distributions are assumed based on the AVB pressing test results(See Attachment 9-2 for details). The probability distribution multiplied by the factor of each AVB type, shown in this table, is assumed.

*3: AVB Flatness is judged as 0, because AVB flatness is assumed macro distortion.



7. 7. Results

7.1 Simulation of Ding signals

Figure 7.1-1 shows the distribution of contact forces over [] [N], that is threshold of Ding signal, of Case1 and Figure 7.1-2 shows the result of Case2. Case1 simulates Unit-2 and Case2 simulates Unit-3. The results are similar to Fig 1 of Attachment 9-3 of Ding signals distributions on PSI-ECT.

The manufacturing dispersion makes a lot of off-set points between tubes and AVBs. The higher force is generated at stiffer portion of tube and AVB, because the off-set is displacement control type loading. In AVB bending portion, AVB and tube (support span is shorter) are stiffer than straight bar region, so that much higher forces are generated at around Row 15 (Center Wide AVBs nose), around Row 30 (Side Narrow AVBs nose) and around Row 50 (Center narrow AVBs nose). In the manufacturing dispersion analyses, much higher reaction forces are generated at AVB bending portion in Unit-2 than Unit-3, because AVB nose thickness and twist for Unit-2 is larger than those of Unit-3 due to difference of the press loads for flattening. This is assumed to be a mechanism of Ding signals and a cause of Ding signals difference between Unit-2 and Unit-3. Also, the assumptions in this study are supposed to be adequate by showing the similar contact force distributions to Ding signals.

7.2 Contact forces

Figure 7.2-1 and 7.2-2 present the distributions of the average contact forces of each row are shown for both Units and indicate that Unit-3 has smaller contact forces at AVB supports than Unit-2. This difference is one of causes that Unit-3 has more severe wears, because contact forces have a role to restrict tube vibration.

Fig. 7.2-3 presents the displacement tendency of a representative tube (Row 100) in Unit 3 and shows tube bundle expansion at each AVB contact point due to the dimensional variation. The displacements of tubes in outer columns and center AVB support points are larger than those in center columns and side AVB points. This tendency can be explained by Fig. 7.2-4 that shows the image that tubes displacement is restricted by TSP.

This tube displacement means bundle expansion, and the equivalent average gap per each column in each AVB support point is found by dividing the expansion by the number of column. Fig. 7.2-5 shows inverse of the average gap at each AVB support point. The inverse of the gap corresponds with ECT Voltage, because if gap increase, ECT voltage will decrease. Fig. 7.2-5 is similar to the distribution of ECT signals shown in Fig. 1 of Appendix-6.

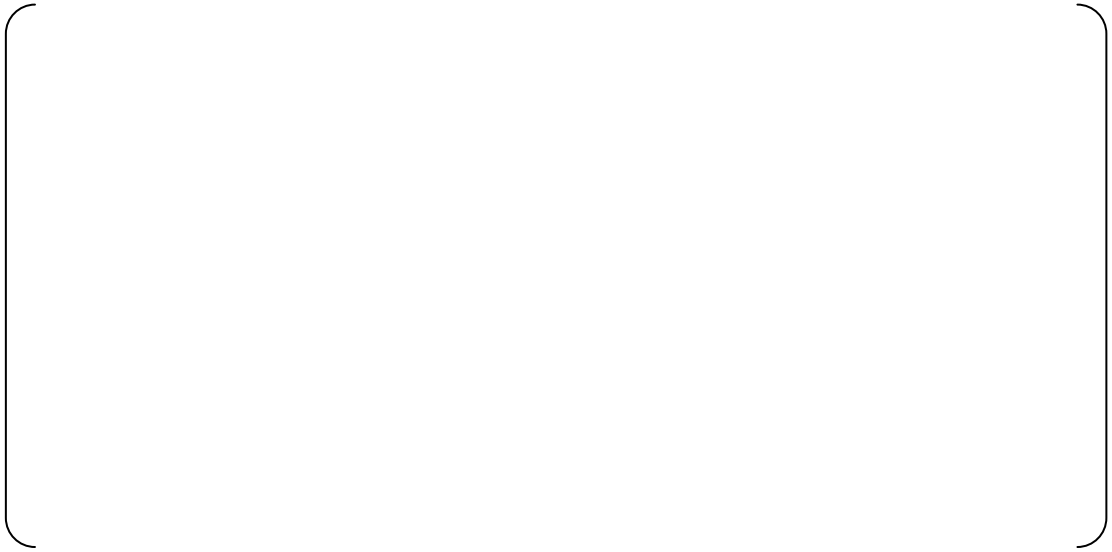


Fig.7.1-1 distribution of contact forces in Case 1 [Unit-2]



Fig.7.1-2 distribution of contact forces in Case 2 [Unit-3]



Fig.7.2-1 Distributions of the average contact forces of each row in Case 1
[Unit-2]



Fig.7.2-2 Distributions of the average contact forces of each row in Case 2
[Unit-3]



Fig.7.2-3 Displacement tendency at each AVB contact point of Row100 tubes in Case 2
[Unit-3]

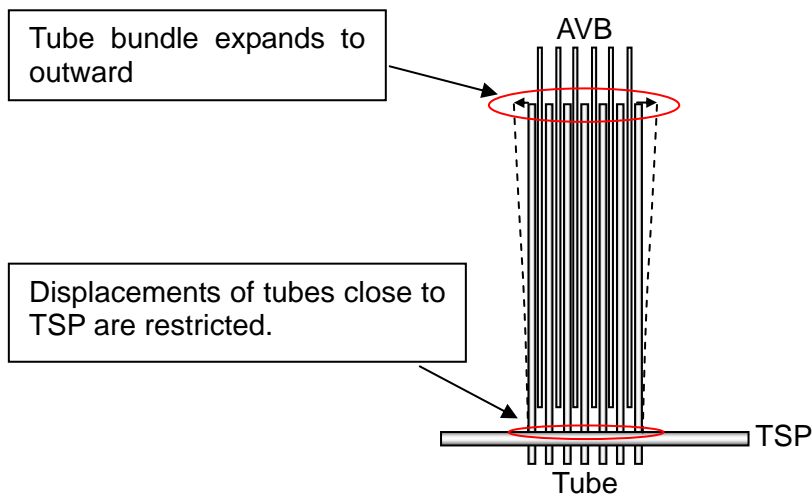


Fig.7.2-4 Interaction of TSP to tube displacement



Fig.7.2-5 Inverse of average gap at each AVB point Row100 tubes in Case 2
[Unit-3]



8. References

- 1) L5-04FU051 Rev.1 Design drawing of Tube Bundle 1/3
- 2) L5-04FU052 Rev.1 Design drawing of Tube Bundle 2/3
- 3) L5-04FU053 Rev.3 Design drawing of Tube Bundle 3/3
- 4) L5-04FU108 Rev.3 Design drawing of Tube Support Plate Assembly 3/3
- 5) L5-04FU111 Rev.2 Design drawing of Anti-Vibration Bar Assembly 1/9
- 6) L5-04FU112 Rev.1 Design drawing of Anti-Vibration Bar Assembly 2/9
- 7) L5-04FU118 Rev.3 Design drawing of Anti-Vibration Bar Assembly 8/9
- 8) L5-04FZ014 Rev.4, Purchase specification of heat transfer tubing

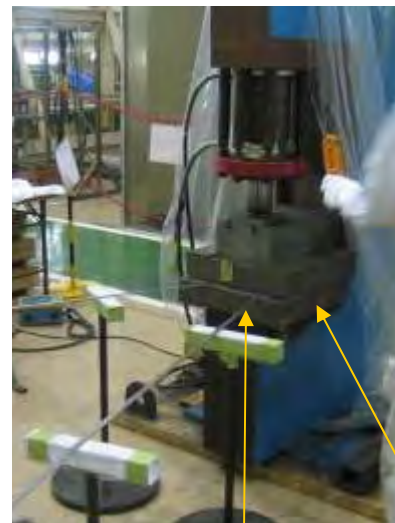
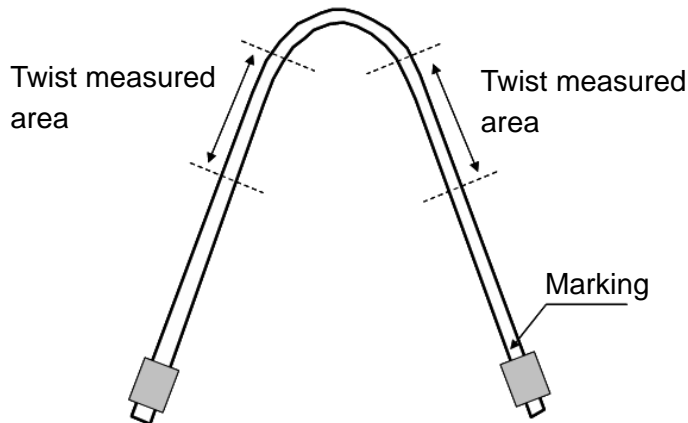


Attachment 9-1 Summary of verification test for AVB press load improvement

There is an AVB bending process in shop for AVB making up. In this process, AVB inside thickness increases due to bending. If as bent, AVB bending portion thickness deviate from the maximum tolerance specified in design drawing, so MHI presses AVB bending portion for flattening. In Unit-2, the press load is [] [N], and it is necessary to touch up AVB bending inside portion after bending, because press load is insufficient to make the thickness within the maximum tolerance. In Unit-3, the press load is changed from [] [N] to [] [N] in order to improve AVB bending portion accuracy.

This attachment introduces the result of verification test for AVB press load change performed at that time.

- press load: [] [N], [] [N], [] [N]
- AVB twist measurement area



- Twist results

➤ Summary

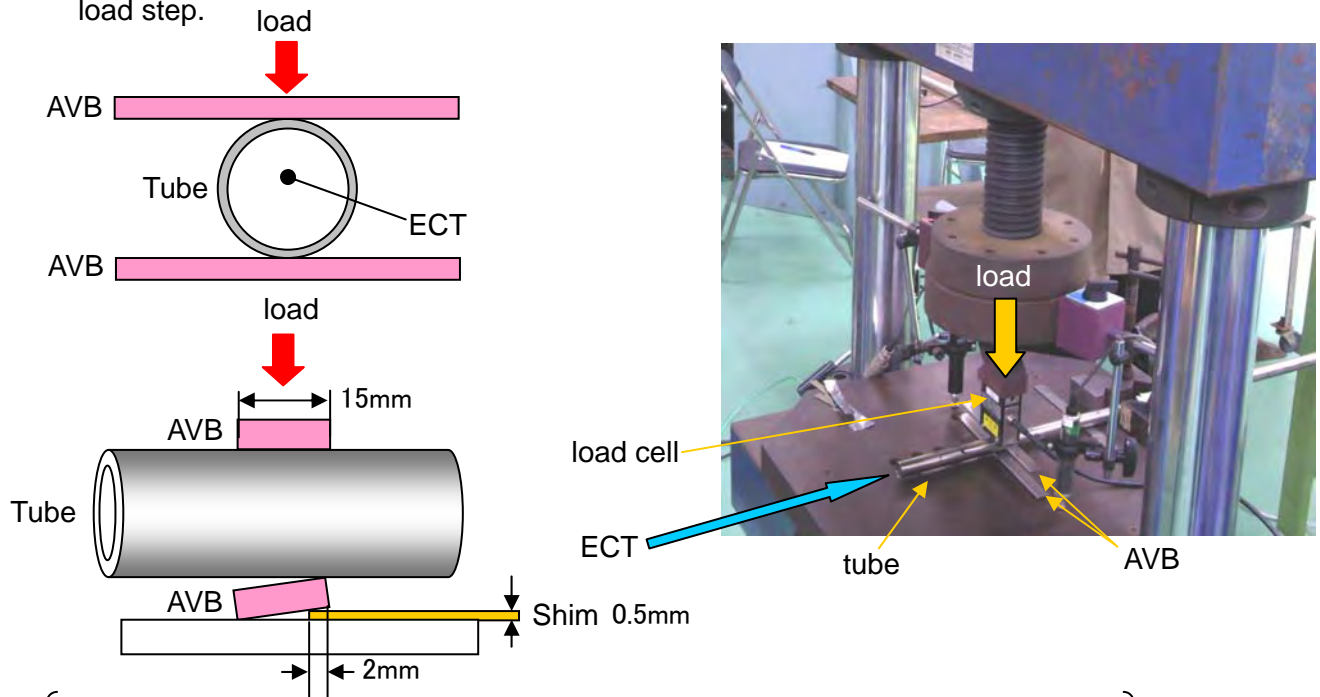
- In Unit-2, AVB which twist deviates from the tolerance is needed to be flattened and touched up by hand, so that AVB twist satisfies the tolerance. In Unit-3, it comes to be not necessary to touch up after the [] [N] press adopted.
- The standard deviation of [] [N] press is supposed to be about a half of [] [N] press.



Attachment 9-2 Confirmation test for Ding load

There are a lot of Ding ECT signals indicated in Unit-2. The distribution trends of Ding signals are quite different between Unit-2 and Unit-3. So, MHI performed a simple mechanical load test in order to confirm that how much load was necessary to make Ding ECT signal ($> []V$). This attachment provides the summary of the confirmation test.

- The correlation between load and ECT Ding signal is achieved by ECT testing at each load step.



➤ Summary

- In the case that $[]V$ Ding signal means elastic ding, the minimum load is $[]N$. If $[]V$ Ding signal means plastic ding, the minimum load $[]N$ will be necessary.



Attachment 9-3 Ding Signals at U-bend Region from PSI

The PSI-ECT inspection was performed with all four SGs in the horizontal position. The Unit-2 SG inspection was performed at the SONGS site and the Unit-3 SG inspection was performed in the MHI shop prior to shipment. Analysis of the PSI data shows a distinct difference between the Unit-2 and Unit-3 SG. In the Unit-2 SGs there were many ding signals at the AVB tips that were not evident in the Unit-3 SGs as shown in Fig.1. The greater number of dings implies more interference between the tubes and AVBs, which correlates with a larger variation in gaps and presumably greater average tube-to-AVB contact force during operation. This is consistent with the finding that the tube-to-AVB gaps in the Unit-3 SG are slightly larger and that the average contact force is smaller in the Unit-3 SGs than in the Unit-2 SGs (refer to Appendix-6).



(a) Unit-2



(b) Unit-3

Fig 4.1.2-3 Ding signals at U-bend region from PSI ECT



Appendix-10
SG Tube Wear Analysis for Unit-2/3



1. Purpose

The purpose of this analysis is to evaluate the tube wear depth at the U-bend region due to fluid elastic instability in order to verify the estimated mechanism of the tube wear observed in both of Unit-2 and Unit-3 as mentioned in Section 6.1 and 6.2 of the main report.

A single tube, R106C78 (that leaked in Unit-3) was selected for analysis. Only the tube support boundary conditions were varied to produce a set of wear depths along the tube that was similar to what was measured by ECT from Unit-2 and Unit-3. The R106C78 tube wear indications (i.e. wear depths reported by ECT at TSPs and AVBs) are replicated analytically.

2. Conclusion

The analysis results indicate followings, which are consistent with the mechanistic causes described in Section 6 of the main report;

- When consecutive AVB support points are inactive and in-plane FEI occurs, the tube vibrates to be in contact with the adjacent tube. The calculated wear depths at the contact point with the adjacent tube, AVBs and the top tube support plates are equivalent to the wear depths measured in Unit-3 SGs.
- When consecutive 6 or 8 AVB support points are inactive and in-plane FEI does not occur, the calculated tube wears at AVB support points due to only the turbulent flow force are equivalent to the wear depths measured in Unit-2 SGs.



3. Assumption

Following assumptions are applied for this analysis.

1) Flow characteristics

The U-bend fluid velocity, density, void fraction, and hydrodynamic pressure distributions are supplied by the ATHOS / SGAP thermal hydraulic analysis program for the normal operating conditions with T-hot = [] as shown in Appendix-12.

2) Damping ratio

The structural damping ratio is assumed to be 0.2%, which is a minimum value based on MHI test results. The relationship between the two-phase damping and void fraction is based on Pettigrew's test results and is described in Section 6.1, paragraph (5).

3) Boundary conditions at tube supports

The support condition at TSPs #1 through #6 is assumed to be pinned. "Pinned" means free to displace parallel to the hole and free to rotate, but prevented from lateral movement by the TSP. The support conditions at TSP #7 and the AVBs are variables in the parametric evaluation.

4) Number of support points

All AVB supports for the Unit-3 free-span simulation are assumed to be inactive with tube support only provided by the TSPs. Number of AVB support points is a parameter for case study of the Unit-2 simulation. All TSP supports are assumed to be active.

5) Contact force at TSP #7 and the gap between TSP and tubes

The tube support condition at TSP #7 (hot and cold sides) is assumed to be a [] compressive contact force based on thermal expansion at operating conditions. The tube-to-TSP diametral clearance is assumed to be [], based on the maximum manufacturing tolerances.



6) Length of tube-to-tube wear

The measured length of the tube-to-tube wear on a typical tube was about []. Since the wear depth is not uniform, the length of tube-to-tube wear (assuming to be uniform over the length) is assumed to be [] to simulate the actual wear depth.

7) Modeling of the adjacent tube for Unit-3 simulation.

The gap elements are used at the impact locations in order to consider sliding and impact vibration of the adjacent tube. Tube to tube gap is assumed to be [] [], since the displacement of the tube which has free span wear indication is assumed to be more than the half of the nominal tube-to-tube gap in-plane ($25.4\text{mm} - 19.05\text{mm} = 6.35\text{ mm}$). This is considered as a parameter of case study and assumed to be [].



4. Acceptance criteria

Acceptance criterion is to simulate the trend of the wear of both of Unit-2 and Unit-3. The tube of Row 106 Column 78 of Unit-3 #B SG and the tube of the same address of Unit-2 #A SG are selected as a representative tubes for this analysis since R106 C78 of 3B SG is the leakage tube and R106 C78 of 2A SG has some wear at AVB locations and since the support condition can be compared without considering the flow characteristics.

Table 4-1 Wear depth of R106 C78 of 2A SG and 3B SG

Location	Wear depth of 2A SG, %	Wear depth of 3B SG, %
#1 to 6 TSP (hot & cold)		
#7TSP at Hot side		
B01		
B02		
B03		
B04		
tube to tube		
B05		
B06		
B07		
B08		
B09		
tube to tube		
B10		
B11		
B12		
#7TSP at Cold side		



5. Design Inputs

5.1 Geometry of tube bundle region

The tube bundle consists of $\frac{3}{4}$ -inch diameter, thermally treated Alloy 690 U-tubes that are arranged in a 1.0-inch equilateral triangular pitch and are supported by the tubesheet, seven tube support plates, and six sets of anti-vibration bars (AVBs). Tube support plates (TSPs) have broached trifoil tube holes. All the contacting support structures above the tubesheet are made of []. The nominal dimension of tube, TSPs and AVBs are listed in Table 5-1.

5.2 Thermal and hydraulic flow of steam generator secondary side

The ATHOS thermal hydraulic analysis program was used to determine the distributions of fluid velocity, fluid density, void fraction, and hydrodynamic pressure (see Appendix 12). Fig 5-1 shows the normal operating, full power, loading conditions that were applied to the tube for the wear analysis.



Table 5-1 Nominal dimensions of tubes, TSPs, and AVBs

Part	Item	Value
Tubes	Material	Thermally treated SB-163 UNS N06690
	Outside diameter	0.75 in
	Thickness	0.043 in
	Number of tubes	9727
	Tube pitch	1.0 in
	Tube arrangement	Triangular
TSPs	Material	
	Thickness	
	Number of TSPs	
	Tube support span (between TSP centers)	
	Tube support span (from tubesheet to TSP-1)	
AVBs	Material	
	Type	
	Thickness	
	Width	

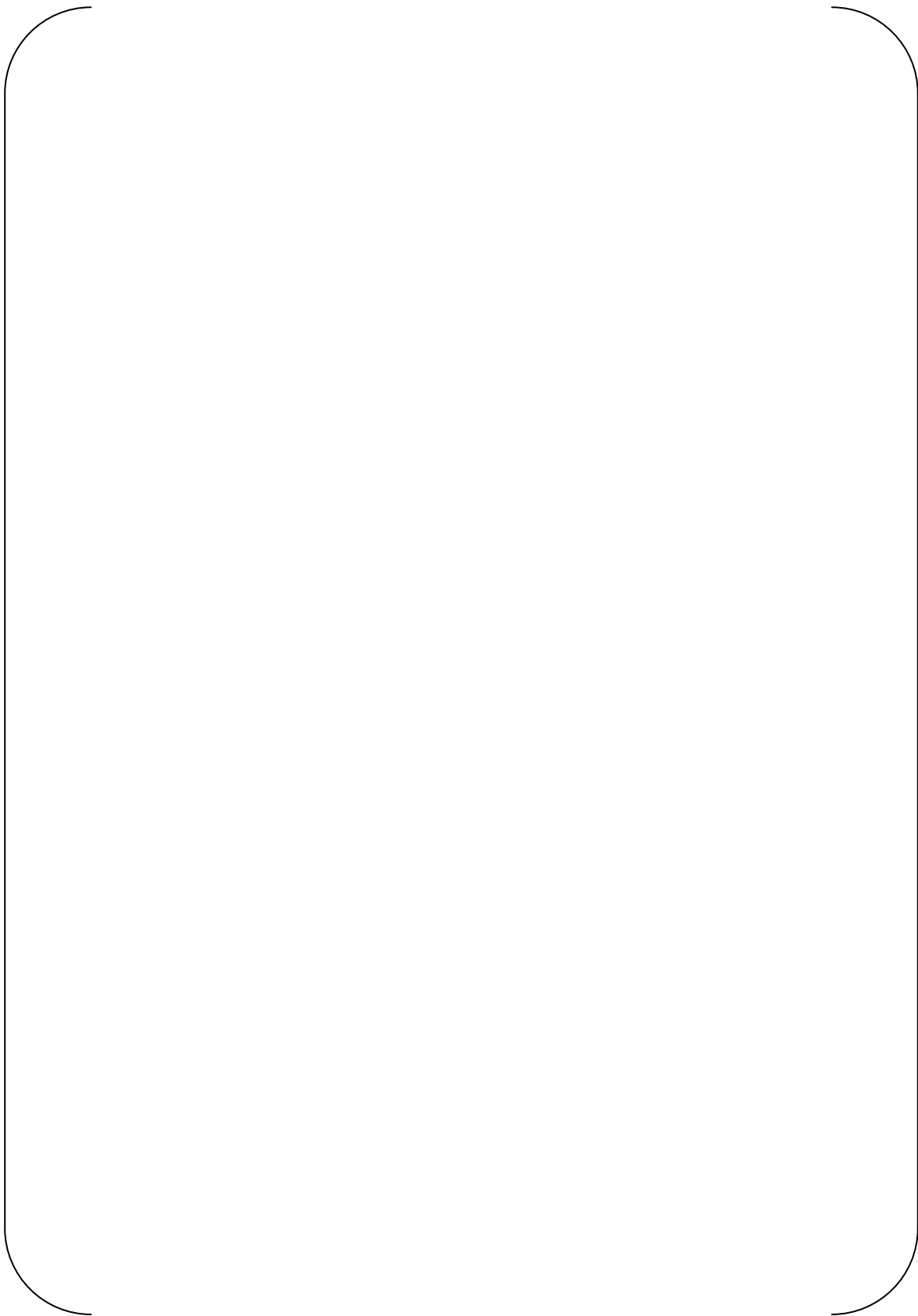


Fig.5-1 Flow distribution of Row 106 Column 78



5.3 Vibration calculation input

The calculation inputs are derived as follows by using the values obtained from the flow analysis code (ATHOS).

Modulus of elasticity of tube E and shear modulus of tube G are interpolated for the tube average temperature of $\frac{T_{av} + T_s}{2}$ from table of ASME Boiler and Pressure Vessel Code, Sec II,

Materials, 1998 Edition, 2000 addenda.

T_{av} : Primary side average temperature (°F)

T_s : Secondary side temperature (°F)

Tube mass distribution per unit length m is calculated according to the following equation.

$$m = \frac{1}{144} (A_i \rho_i + A_t \rho_t + A_e \rho_o) \dots\dots\dots(3)$$

where,

$$A_i = \frac{\pi}{4} D_i^2 \text{ (in}^2\text{)} \dots\dots\dots(4)$$

$$A_t = \frac{\pi}{4} (D_o^2 - D_i^2) \text{ (in}^2\text{)} \dots\dots\dots(5)$$

$$A_e = \frac{\pi D_o^2}{4} \text{ (in}^2\text{)} \dots\dots\dots(6)$$

$$D_e/D_o = \left(1 + \frac{1}{2} P/D_o\right) P/D_o \dots\dots\dots(7)$$

- D_i : tube inside diameter (in)
- D_o : tube outside diameter (in)
- ρ_i : Density of water inside the tube (lbm/ft³)
- ρ_t : Density of tube material (lbm/ft³)
- ρ_o : Density of water outside the tube (lbm/ft³)
- P : Tube pitch (in)



5.4 Wear coefficient

Wear coefficient of AECL data (Alloy800/SS410, which is similar combination to TT690 tube /SS405) at []F is used for this analysis in order to evaluate the effect of the temperature is assumed to be [].

Wear coefficient of tube to tube is 35 times as large as that of 690/SUS405 based on MHI test results (Fig.5-2).

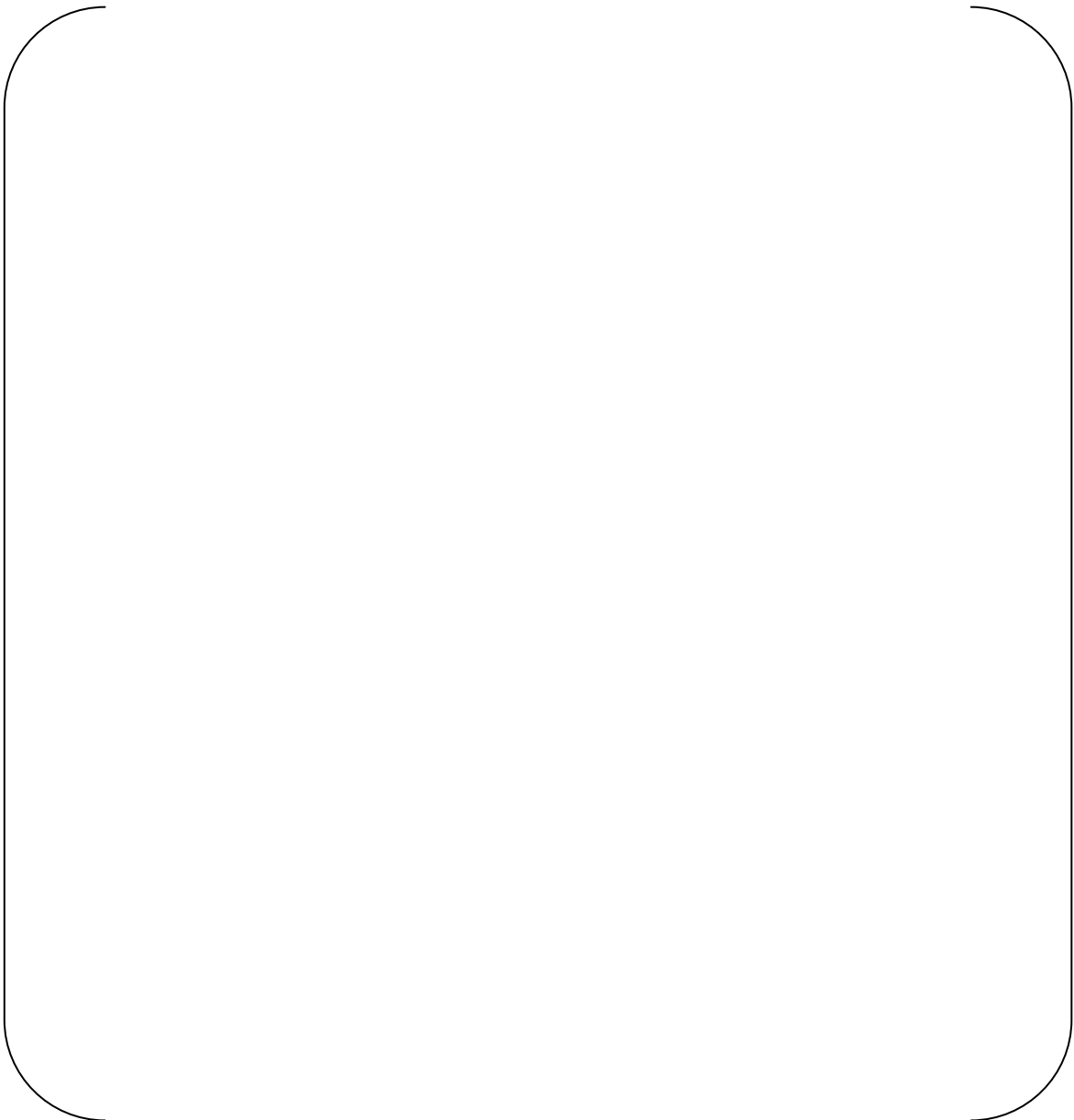


Fig.5-2 Impact Wear Coefficients (MHI internal data)



5.5 Operating duration

Unit 2 completed a cycle of 628 effective full power days (EFPD). Unit 3 shut down after operating 338 EFPD.



6. Methodology

6.1 Evaluation Flow Chart

The leaking tube assuming all inactive AVB supports is evaluated. Wear analysis methodology is described in Figure 6.1

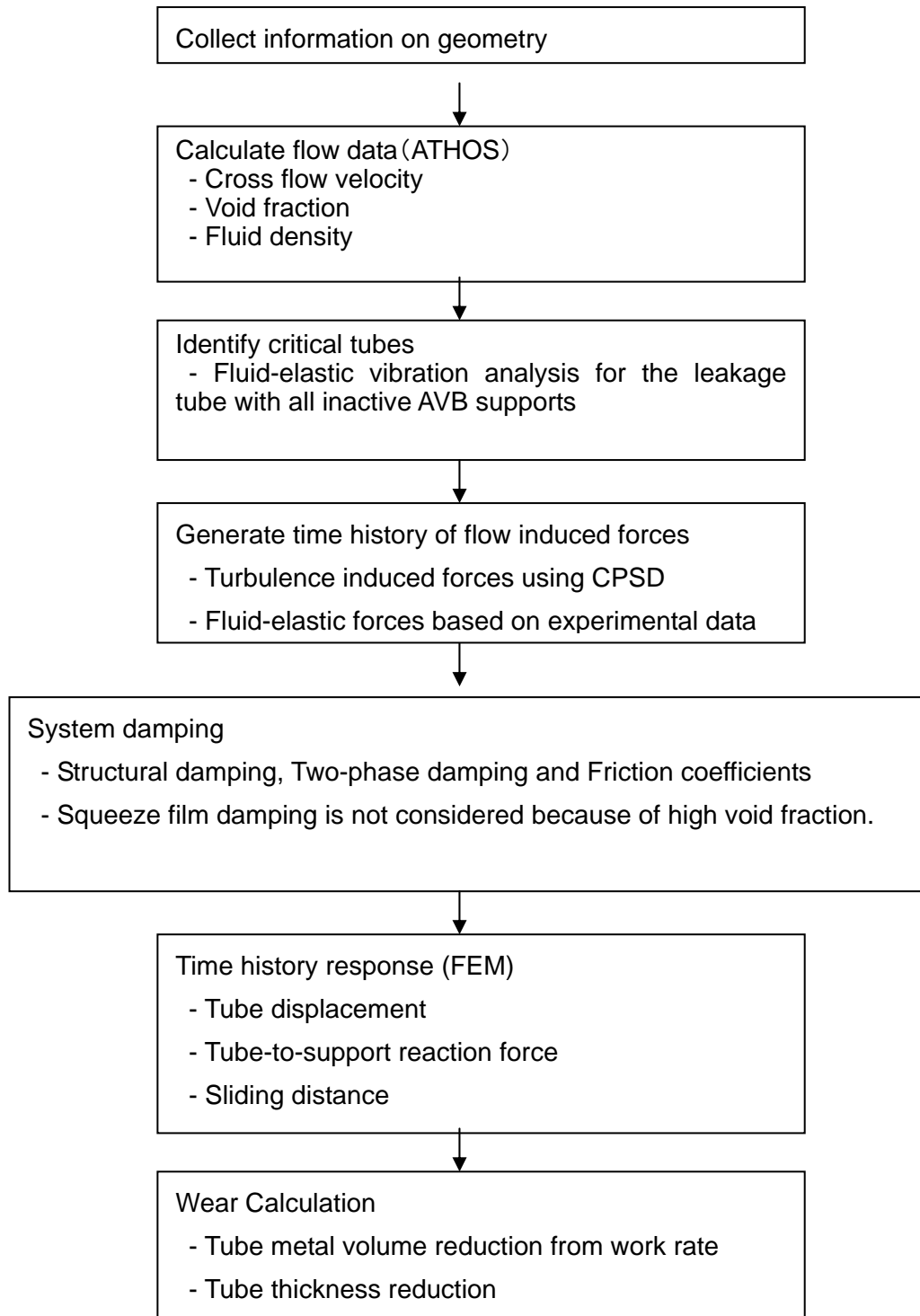


Fig. 6-1 Wear Evaluation Flow Chart



(1) Collect Information on Geometry

Refer to Section 5.1. The gaps between tube and AVBs are a parameter to be evaluated.

(2) Calculate Flow Data

Refer to Section 5.2. The distribution of flow through the steam-generator tube bundle has an influence on the turbulence-induced loads and fluid-elastic instability. The ATHOS thermal and hydraulic analysis code provides the distribution of local cross-flow velocity, fluid density and void fraction. The turbulence-induced loads, fluid-elastic forces, added mass are obtained by analysis.

(3) Identify Critical Tubes

A linear screening analysis is usually used to identify the potential for fluid-elastic instability of the tubes at different locations in the tube bundle and to choose the most unstable tube for wear analysis. However the Unit-3 leaking tube R106C78 is selected for this wear analysis.

(4) Generate Time History of Flow Induced Forces

Turbulence induced forces are obtained by considering spatial correlations of the turbulence forces using the cross-correlated power spectral density (CPSD) functions. The turbulence induced forces in the U-bend portion are determined from the CPSD function from test data. The CPSD (cross power spectral density) is taken from a reference by Axisa, et al (Ref.5).

$$\Phi_{CPSD}(Z_p, Z_q) = (\rho U^2 D/2)^2 \times (U/D) 5 \times 10^{-5} (fD/U)^{-2.7} (U_p U_q)^2 e^{(-|Z_p - Z_q|/\lambda_c)} C_f$$

Where,

Φ_{CPSD} :Cross power spectral density function between elements p and q

U_p :Ratio between tube gap velocity at elements p to U

U_q :Ratio between tube gap velocity at elements q to U

Z_p, Z_q :Separation distance along tube length between centroids of elements p & q

λ_c :Correlation length of turbulence (assumed to be 4D)

C_f :Correlation factor for finite-element approximation



Fluid-elastic forces are those induced on the tubes by a coupling between the tube vibratory motion and the flowing fluid. The fluid-elastic forces are defined by a feedback loop in which the tube forces are calculated from the tube vibratory amplitude through an analytical model based on experimental correlations of fluid-elastic forces in tube bundles.

Fluids-force components were measured as functions of imposed harmonic displacements of a cylinder. These experimental data were reduced by Chen into fluid-damping and fluid stiffness coefficients which were functions of the reduced-flow velocity (U/fD) (Ref.6).

$$\hat{f}_i = -\sum_{j=1}^M \left[(\rho R U \overline{\alpha'_{ij}}) \frac{\partial u_j}{\partial t} + (\rho R U \overline{\sigma'_{ij}}) \frac{\partial v_i}{\partial t} \right] + \rho U^2 \sum_{j=1}^M (\alpha''_{ij} u_j + \sigma''_{ij} v_j)$$

$$\hat{g}_i = -\sum_{j=1}^M \left[(\rho R U \overline{\tau'_{ij}}) \frac{\partial u_j}{\partial t} + (\rho R U \overline{\beta'_{ij}}) \frac{\partial v_i}{\partial t} \right] + \rho U^2 \sum_{j=1}^M (\tau''_{ij} u_j + \beta''_{ij} v_j)$$

These data can be used directly to accurately predict the fluidelastic response in linear cases where the response frequency usually coincides with one of the fundamental frequencies. However, in nonlinear cases where the tube supports have clearances, the tube response can be at a number of frequencies. Such cases require a fluidelastic modeling procedure that accounts for the presence of different frequencies. Transfer function method is used for this purpose.

This approach recognizes that fluidelastic stiffness and fluid damping coefficients are functions of reduced flow velocity and, therefore, functions of frequency. The transfer function method converts these frequency dependent functions into time dependent differential equations.

$$\overline{\alpha'_{ii}} \dot{u}_i \approx a_1 \dot{u}_i + a_3 \frac{d^2 \dot{u}_i}{dt_2} \theta^2$$

$$\overline{\alpha''_{ii}} u_i \approx a_0 u_i + a_2 \ddot{u}_i \theta^2$$

$$\overline{\beta'_{ii}} \dot{v}_i \approx b_1 \dot{v}_i + b_3 \frac{d^2 \dot{v}_i}{dt_2} \theta^2$$

$$\overline{\beta''_{ii}} v_i \approx b_0 v_i + b_2 \ddot{v}_i \theta^2$$

Where,



$$\theta = D/2\pi U$$

$$a_0, a_1, a_2, a_3, b_0, b_1, b_2, b_3 = \text{Constants}$$

f_i, g_i : Forces acting upon the cylinders in the X and Y directions, respectively

ρ : Fluid density

U : Tube gap velocity

R : Radius of tubing

M : Number of tubing

u_j : Displacement in x-direction

v_j : Displacement in y-direction

$\alpha_{ij}, \sigma_{ij}, \tau_{ij}, \beta_{ij}$: Added-mass coefficient

$\alpha'_{ij}, \sigma'_{ij}, \tau'_{ij}, \beta'_{ij}$: Fluid-damping coefficient

$\alpha''_{ij}, \sigma''_{ij}, \tau''_{ij}, \beta''_{ij}$: Fluid-stiffness coefficient

$\bar{\alpha}_{ij}, \bar{\sigma}_{ij}, \bar{\tau}_{ij}, \bar{\beta}_{ij}$: Viscous damping coefficient

The fluid damping and fluid stiffness coefficients are derived for the single flexible tube surrounded by rigid tubes as constraint conditions. Fluid damping and fluid stiffness coefficients measured by MHI experiment are used for this evaluation.



(5) System Damping

Damping ratio consists of structural damping, two-phase damping, viscous damping and squeeze film damping in the crevices between the tube and its support. Although ASME Sec. III Appendix N-1330 suggests that the damping ratio 1.5% as a sum of structural and two-phase damping, more reliable values based on experimental data is used in this evaluation.

For structural damping, MHI test results show 1.0% average (0.2% in minimum) as shown in Figure 6-2 (from Ref.2), therefore 0.2% is assumed for the conservative evaluation.

For two-phase damping, Pettigrew's test result of Figure 6-3, which is the function of superficial void fraction, is used as the effective two-phase damping along the tube length by considering vibration mode (Ref.4).

Since the viscous damping is negligible in high void fraction (Ref.3), it is neglected in this analysis.

Since the void fraction is high and the support condition at AVB is considered to be dry, the squeeze film damping is assumed to be zero.

(6) Time History Response

A finite element model of the tube with support clearances is formulated. The tube vibratory response consists of tube displacements and tube support interaction characteristic of impact and sliding is calculated.

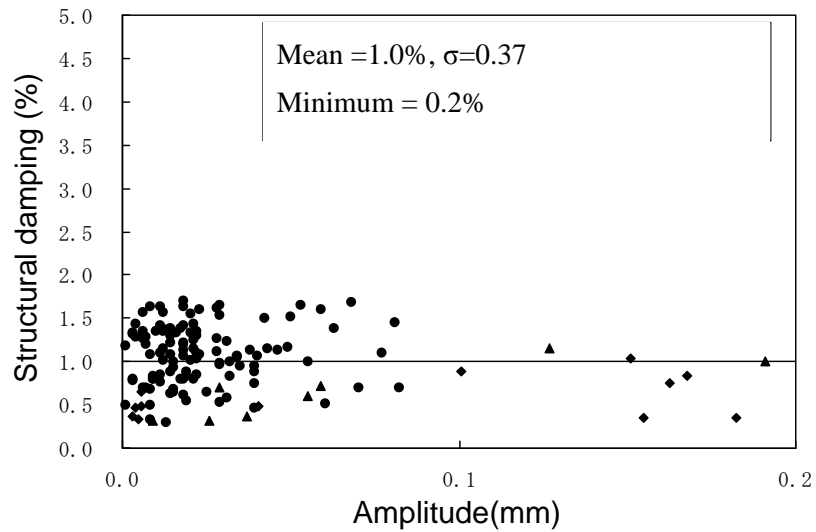
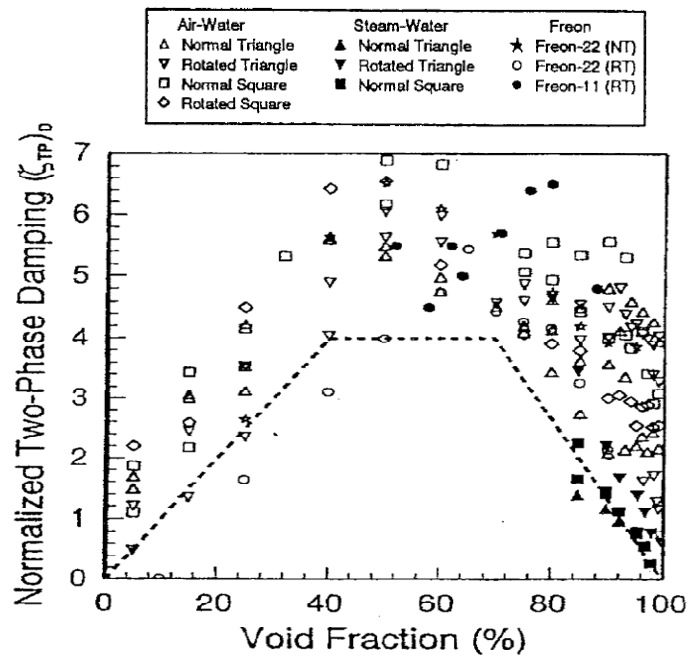


Fig.6-2 Structural damping test data by MHI



$$(\zeta_{TP})_D = \zeta_{TP}(\rho_c D^2/m)^{-1} \{ [1 + (D/D_c)^3] / [1 - (D/D_c)^2]^2 \}^{-1}$$

Fig.6-3 Two phase damping and superficial void fraction



(7) Wear Calculation

Using the time history response of the tube displacements and tube support interactions, a set of wear parameters (work rate parameter, sliding distance, impact forces and contact time) is calculated. The work rate parameter is calculated by integrating the incremental work (the product of support reaction and incremental sliding).

The metal loss is calculated using Archard's wear law.

$$dV/dt = K'W$$

Where,

dV/dt : Volume wear rate

W : Work rate parameter

K' : Specific wear coefficient for tube/AVB material combination

Experimental correlations between the metal loss and the work rate are used to calculate tube metal volume reduction. The relation between wear volume (V) and wear depth (h) is represented as follows.

(a) Tube to AVB wear and Tube-to-Tube wear

The tube thickness reduction is then calculated using the wear properties and work rate parameter as assuming the wear configuration as shown in Fig.6-4.

The wear width of tube to AVB wear is assumed to be the same as the width of AVB.

The measured length of the tube-to-tube wear was about []. Since the wear depth is not uniform, the length of tube to tube wear is assumed to be [] in this calculation to simulate the actual wear depth.

$$V = \frac{1}{2} R^2 (\phi - \sin \phi) \cdot L$$

$$\phi = \cos^{-1} \left(1 - \frac{h}{R} \right) \times 2$$

V: Wear volume

R: Tube radius

h: Wear depth

L: Wear width

ϕ : Wear angle

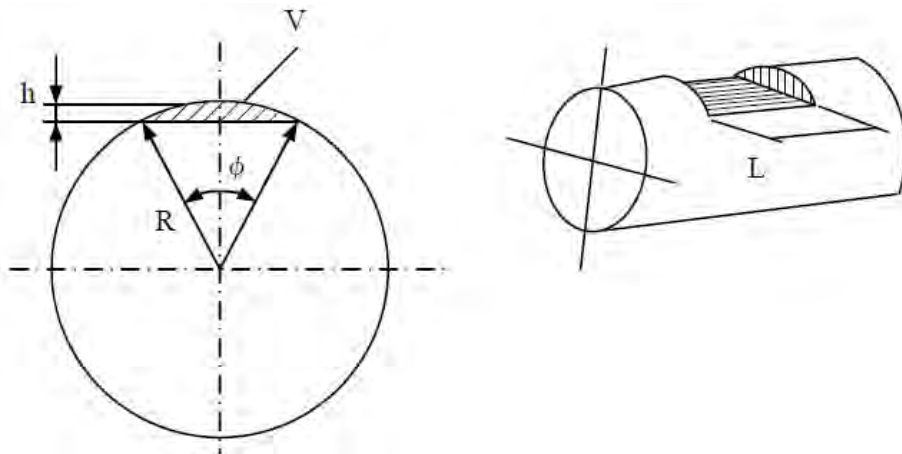


Fig. 6-4 Wear shape of tube at the contact point with AVB

(b) Tube to TSPL contact wear

We use the following equation which shows the relation between wear volume and wear depth. This equation is obtained by 3 dimensional geometry model.

$$V = \left[\frac{2}{3} R h^3 \right]$$

V : Wear volume (mm³)
 h : Wear depth (mm)

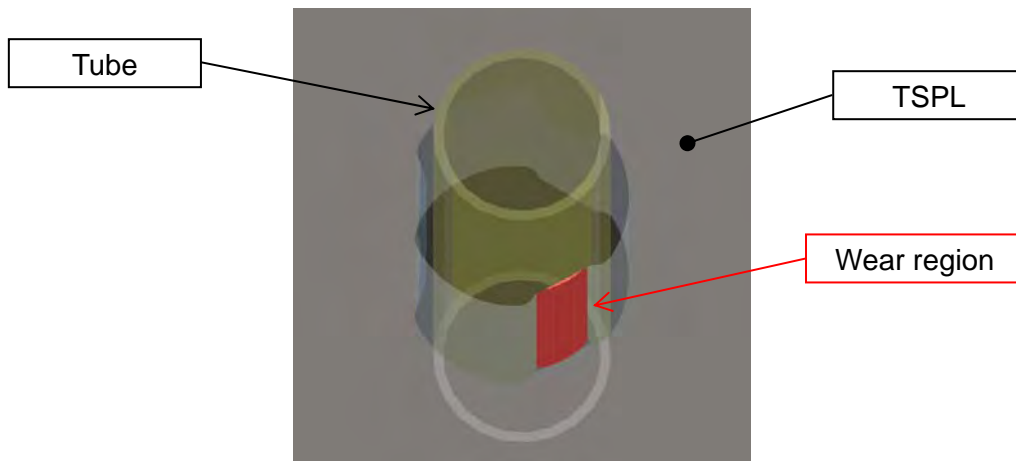


Fig. 6-5 Wear volume evaluation (Wear depth 1.0mm)

The relation between the work rate and wear depth of each unit is calculated based on the equations above, the wear coefficients and the effective full power operating days as shown in Fig.6-6 and Fig.6-7.



Fig.6-6 Relation between Work Rate and Wear Depth of Unit-2 (628 EFPD)



Fig.6-7 Relation between Work Rate and Wear Depth of Unit-3 (338 EFPD)



6.2 Analysis Model

Analysis model is shown in Figure 6-8.

(1) Support Condition with AVB

All AVB support points for Unit-3 are assumed to be inactive (to offer no support of the tube). The 2 - 12 central AVB support points for Unit-2 are assumed to be inactive (For example, the 2 central AVB support points are B06 and B07). Gap elements are used at the inactive support locations in order to produce sliding distance and impact loading information for the wear analysis. The tube-to-AVB clearance is an analysis variable.

(2) Support Condition with TSP

Gap elements are used at the support locations to determine the sliding and impact values at the support locations. The intersection with the top TSP (TSP #7) hot and cold sides is represented by a gap element based on the tube-to-TSP drawing clearance. The initial position of the tube is assumed to be in contact with an assumed contact force against one side of the broached hole.

(3) Impact location with adjacent tube

For the simplicity of the calculation, the wear volume is calculated by using single leaking tube model. The gap elements are used at the impact locations in order to consider sliding and impact vibration adjacent tube. The tube to tube gap is assumed to be []. This means that the tube must travel across that distance before wear can occur.

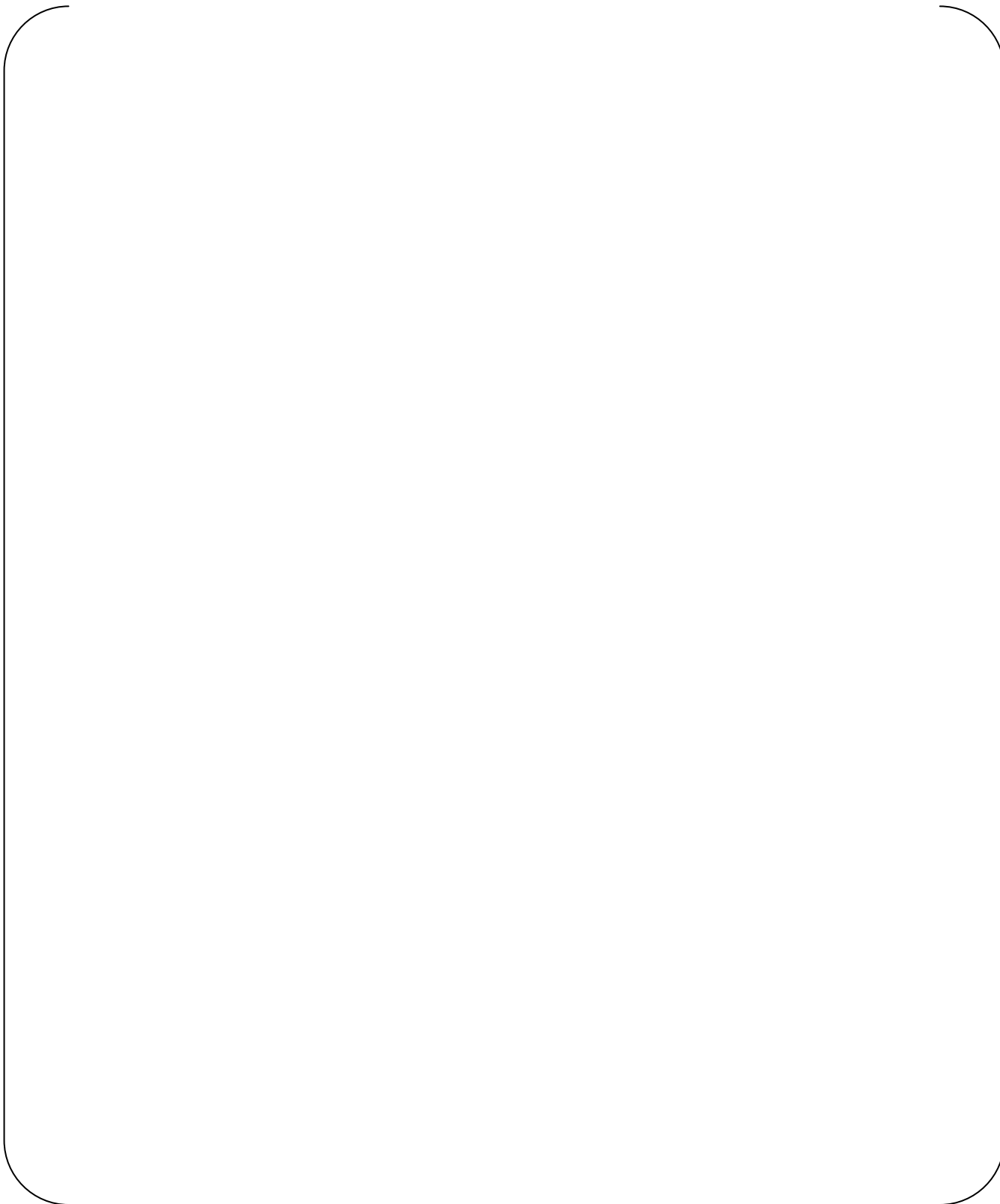


Fig. 6-8 Analysis Model for Tube Wear Evaluation



6.3 Evaluation cases

6.3.1 Simulation of Unit-3 tube wear

To simulate the tube-to-tube wear, tube-to-TSP wear, and tube-to-AVB wear of Unit-3, following cases are evaluated.

(1) Evaluation of gap effect

To evaluate the effect of the tube-to-AVB gap, 3 cases shown in Table 6-1 are analyzed. All AVB supports are assumed to have small gaps as described in Section 4.5 of the main report.

(2) Evaluation of contact force

To confirm the contact force between tube and AVB can prevent the in-plane fluid elastic instability of tube, the case studies shown in Table 6-2 are performed.

(3) Evaluation of distance to the adjacent tube

To evaluate the effect of the distance to the adjacent tube on tube-to-tube wear, the case study with changing the location of the gap element is performed.

In Case 1-3-2, the location of the gap element is changed to [] to evaluate the effect of the distance by comparing Case 1-3-1 in which the distance is [].

(4) Evaluation of random vibration effect

In order to confirm that the energy and frequencies associated with turbulence are not sufficient to produce large displacements necessary for tube-to-tube wear, the case study without fluid elastic instability force is performed.

In Case 1-3-3, the fluid elastic force is not taken into account to evaluate the vibration due to the turbulent flow force by comparing Case 1-3-1 in which both of the fluid elastic force and turbulent flow force are considered.



6.3.2 Simulation of Unit-2 tube wear

(1) Number of active support points

To simulate the Tube-to-AVB wear Unit-2, the case studies shown in Table 6-3 are performed when only the turbulent flow forces are taken into account. The fluid elastic force is not taken into account because MHI concludes the cause of AVB wear is random vibration as described in Section 6.2 of the main report. The number of inactive support points is changed from 2 to 12.

[] of contact load that is sufficient to restrain the tube at these supports are used to simulate the active supports. And the number of active supports is reduced until in-plane instability occurs. The tube is assumed to be the center between the AVBs in order to evaluate the effect of the active support number.

(2) Evaluation of gap effect and contact force

To evaluate the effect of the contact between tube and AVB in one side and contact force, the case studies shown in Table 6-4 are performed.

Table 6-1 Unit-3 Gap Effect Wear Evaluation Cases 1-1 to 1-3

Case	#1-6 TSPs	#7 TSP at hot	B01	B02	B03	B04	B05	B06	B07	B08	B09	B10	B11	B12	#7 TSP at cold
1-1 ***	Gap A**	Pined))
	Gap B**	Pined													
1-2 ***	Gap A**	Pined													
	Gap B**	Pined													
1-3-1 ***	Gap A**	Pined													
1-3-2 ***															
1-3-3 ***	Gap B**	Pined))

*: Contact force

** : The gap is the distance between AVB and tube in each side as shown in the figure below

***: Tube is in contact with the AVBs on one side.

In Case 1-3-2, the location of the gap element is changed from () to () to evaluate the effect of the distance.

In Case 1-3-3, only turbulence flow force is taken into account.

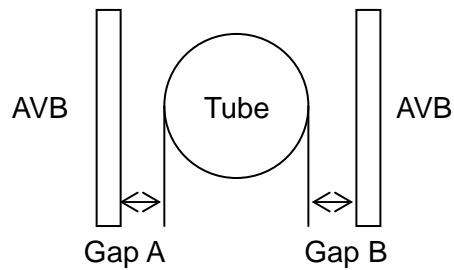


Table 6-2 Unit-3 Contact Force Wear Evaluation Cases 2-1 to 2-3

Case	#1-6 TSPs	#7 TSP at hot	B01	B02	B03	B04	B05	B06	B07	B08	B09	B10	B11	B12	#7 TSP at cold
2-1***	Gap A**	Pined))
	Gap B**	Pined													
2-2***	Gap A**	Pined													
	Gap B**	Pined													
2-3***	Gap A**	Pined))
	Gap B**	Pined													

*: Contact force

** : The gap is the distance between AVB and tube in each side as shown in the figure below

***: Tube is in contact with the AVBs on one side.

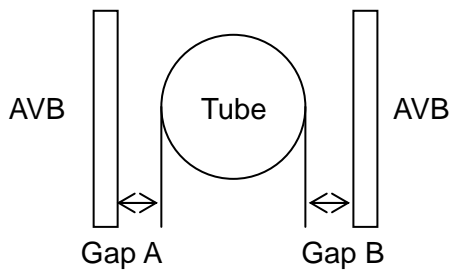




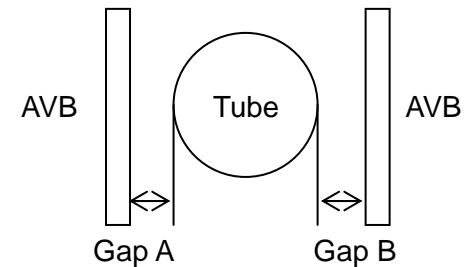
Table 6-3 Unit-2 Wear Evaluation Cases 3-1 to 3-6

Case		#1-6 TSPs	#7 TSP at hot	B01	B02	B03	B04	B05	B06	B07	B08	B09	B10	B11	B12	#7 TSP at cold
3-1	Gap A**	Pined														
	Gap B**	Pined														
3-2	Gap A**	Pined														
	Gap B**	Pined														
3-3	Gap A**	Pined														
	Gap B**	Pined														
3-4	Gap A**	Pined														
	Gap B**	Pined														
3-5	Gap A**	Pined														
	Gap B**	Pined														
3-6	Gap A**	Pined														
	Gap B**	Pined														

*: Contact force

** : The gap is the distance between AVB and tube in each side as shown in the figure below

***: Tube is in contact with the AVBs on one side.





7. Results

The following results supersede the tube wear evaluation performed at the design stage (Ref.8).

7.1 Simulation of tube wear in Unit-3

The analysis model and the natural frequency are shown in Fig.7-1. The analysis results are shown in Fig 7-2, 7-3, Tables 7-1, 7-2 and 7-3. It can be seen from Fig 7-1, that the effect of the tube-to-AVB gap is small when the all support points are inactive in-plane direction. It is consistent with the actual phenomenon of the tube wear at Unit-3. As shown in Fig 7-3, when the tube-to-AVB contact force is large [], the in-plane vibration can be prevented.

Under a condition where small gaps are present in all AVB support points, small contact forces are loaded on each of the inactive support points and all tubes are supported on one side by the top TSP #7 (Case 1-3-1), a free span fluid elastic instability is simulated. The wear depth obtained from the simulation has a consistent trend with the actual measurement results of tube wear in Unit-3.

Case 1-3-2 simulates tube-to-tube wear does not occur when the distance between the tubes in columns is larger than the in-plane amplitude.

The result of Case 1-3-3 indicates the energy and frequencies associated with turbulence are not sufficient to produce large displacements necessary for tube-to-tube wear.

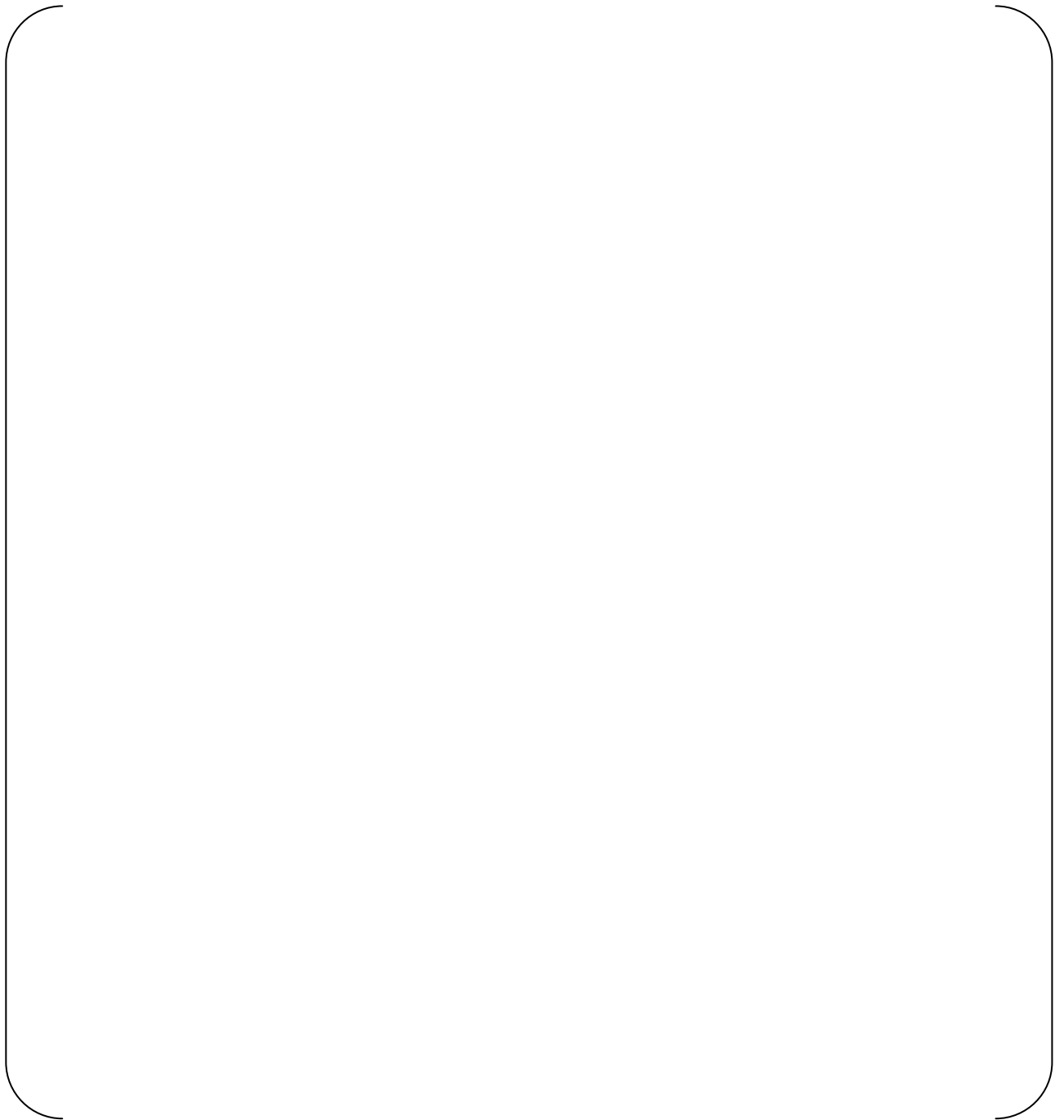


Fig7-1 Verification analysis for Unit-3 free span wear



Fig.7-2 Wear analysis results of Case 1-1 to 1-3-3

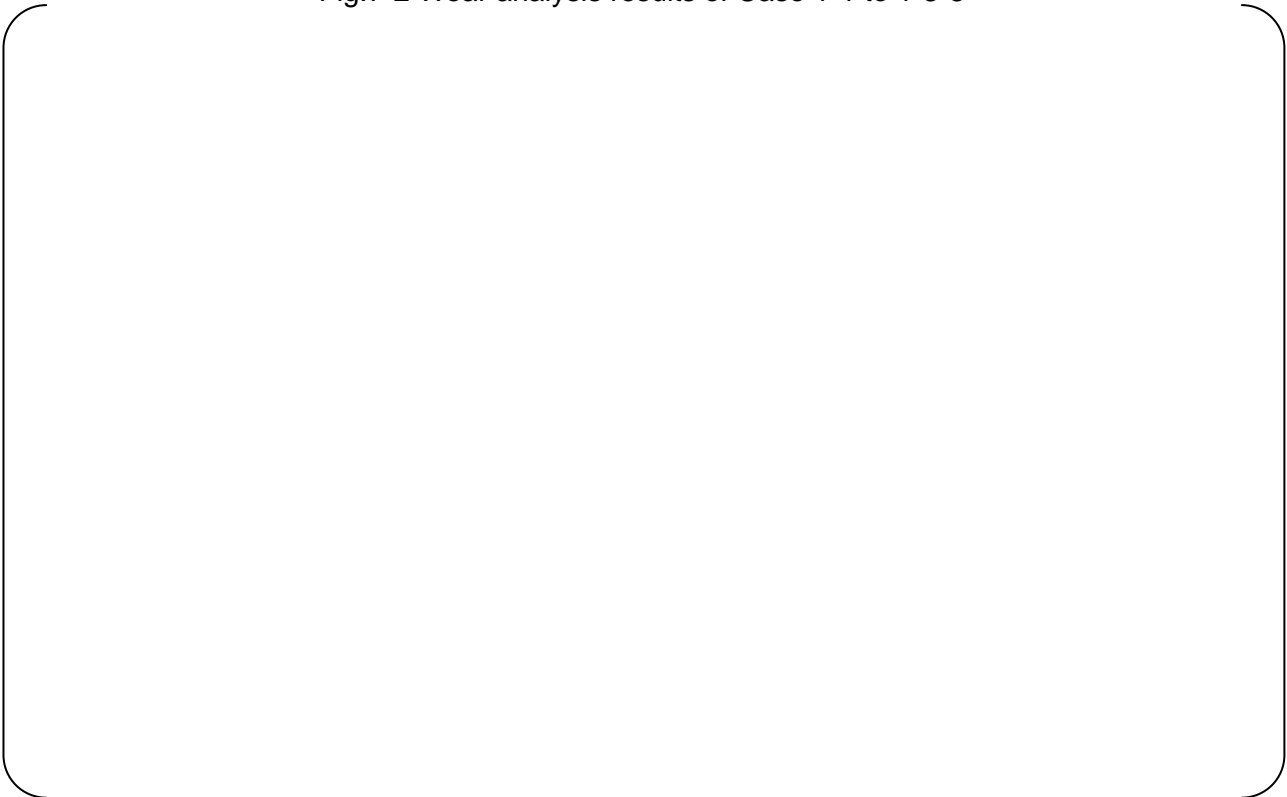


Fig.7-3 Wear analysis results of Case 1-3-1 to 2-3

Table 7-1 Wear analysis results of Case 1-1 to 1-2

Case	#1-6 TSPs	#7 TSP at hot	B01	B02	B03	B04	Tube To Tube	B05	B06	B07	B08	B09	Tube To Tube	B10	B11	B12	#7 TSP at cold
Unit-3 wear																	
1-1	Gap A																
	Gap B																
WR	mW																
Wear depth*	%																
1-2	Gap A																
	Gap B																
WR	mW																
Wear depth	%																

*: Contact force



Table 7-2 Wear analysis results of Case 1-3-1 to 1-3-3

Case	#1-6 TSPs	#7 TSP at hot	B01	B02	B03	B04	Tube To Tube	B05	B06	B07	B08	B09	Tube To Tube	B10	B11	B12	#7 TSP at cold
Unit-3 wear																	
1-3-1	Gap A																
	Gap B																
WR	mW																
Wear depth	%																
1-3-2	Gap A																
	Gap B																
WR	mW																
Wear depth	%																
1-3-3	Gap A																
	Gap B																
WR	mW																
Wear depth	%																

*: Contact force

Table 7-3 Wear analysis results of Case 1-3-1 to 2-3

Case	#1-6 TSPs	#7 TSP at hot	B01	B02	B03	B04	Tube To Tube	B05	B06	B07	B08	B09	Tube To Tube	B10	B11	B12	#7 TSP at cold
Unit-3 wear																	
1-3-1	Gap A																
	Gap B																
WR	mW																
Wear depth*	%																
2-1	Gap A																
	Gap B																
WR	mW																
Wear depth	%																
2-2	Gap A																
	Gap B																
WR	mW																
Wear depth	%																
2-3	Gap A																
	Gap B																
WR	mW																
Wear depth	%																

Non-proprietary Version



Document No. L5-04GA564(9) (P.10-34)



7.2 Simulation of tube wear in Unit-2

The analysis model and the natural frequency are shown in Fig.7-5. The analysis results are shown in Fig 7-6, Tables 7-4 and 7-5. The analysis results of the wear depth due to random vibration, when 6 or 8 consecutive AVB support points are inactive (Case 3-3 and 3-4), show consistent trends with the actual measurement results of tube wear in Unit-2.

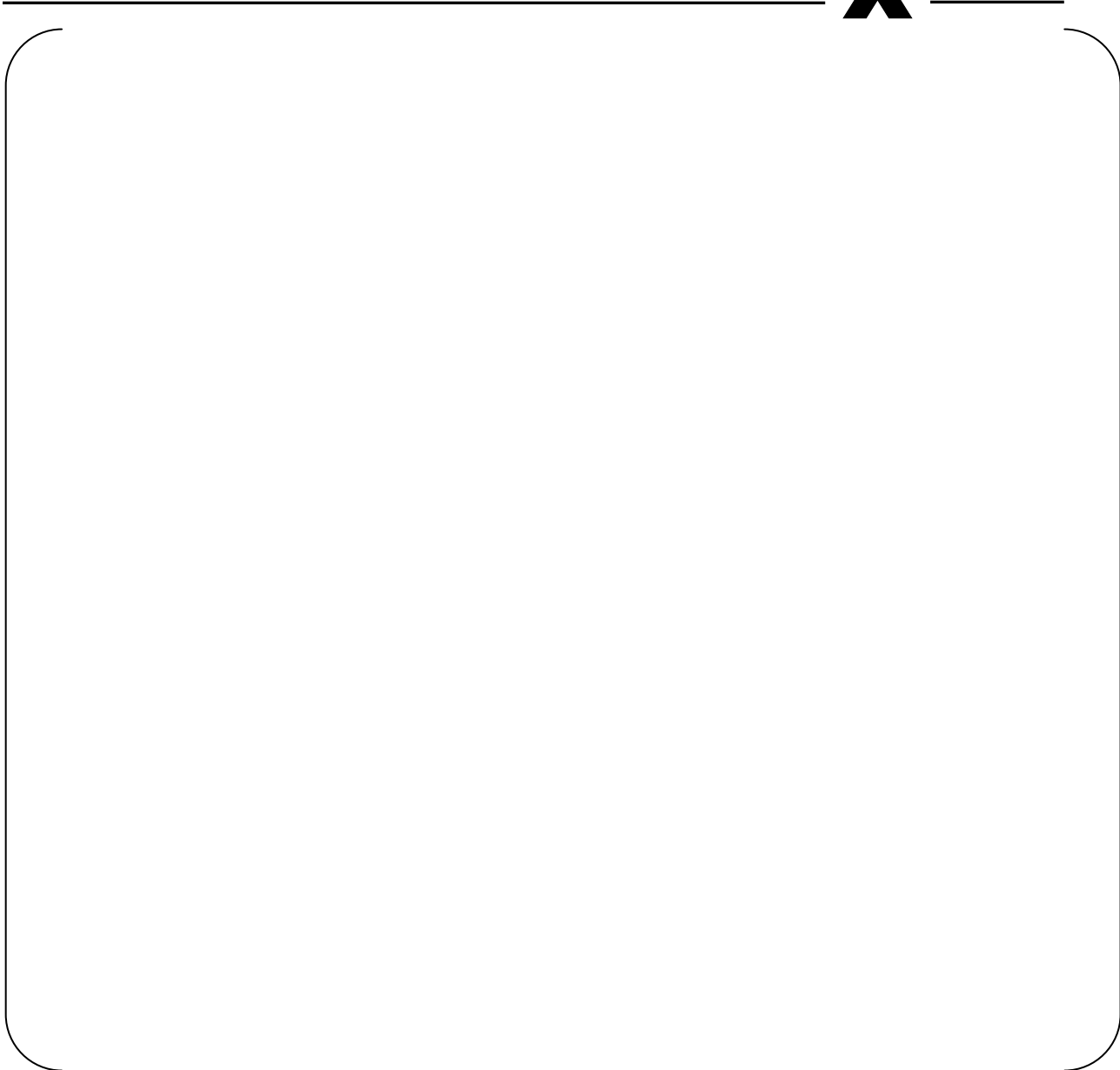


Fig 7-5 Verification analysis for Unit-2 AVB wear

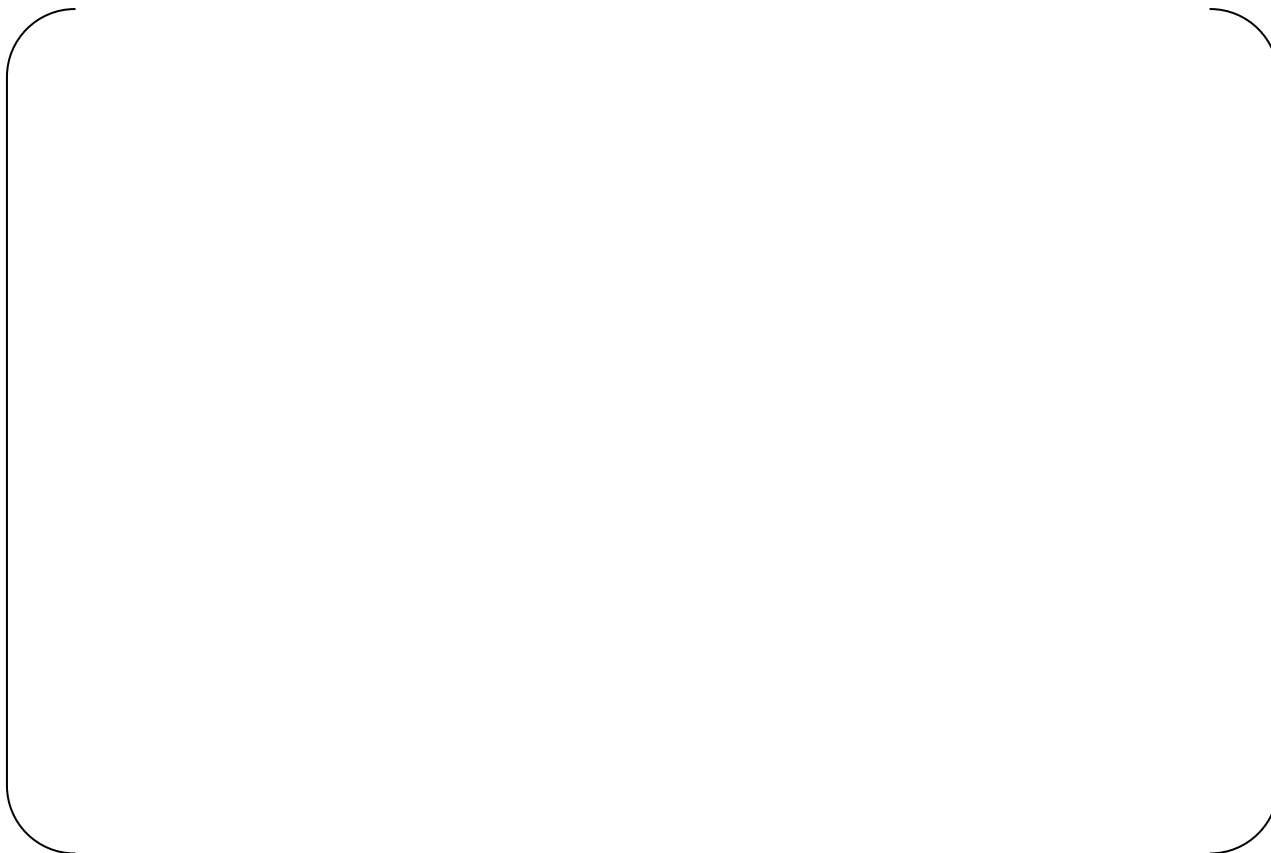


Fig. 7-6 Wear analysis results of Case 3-1 to 3-6

Table 7-4 Wear analysis results of Case 3-1 to 3-3

Case		#1-6 TSPs	#7 TSP at hot	B01	B02	B03	B04	B05	B06	B07	B08	B09	B10	B11	B12	#7 TSP at cold
Unit-2 wear																
3-1	Gap A															
	Gap B															
WR	mW															
Wear depth	%															
3-2	Gap A															
	Gap B															
WR	mW															
Wear depth	%															
3-3	Gap A															
	Gap B															
WR	mW															
Wear depth	%															

*: Contact force



Table 7-5 Wear analysis results of Case 3-4 and 3-6

Case	#1-6 TSPs	#7 TSP at hot	B01	B02	B03	B04	B05	B06	B07	B08	B09	B10	B11	B12	#7 TSP at cold
Unit-2 wear															
3-4	Gap A														
	Gap B														
WR	mW														
Wear depth	%														
3-5	Gap A														
	Gap B														
WR	mW														
Wear depth	%														
3-6	Gap A														
	Gap B														
WR	mW														
Wear depth	%														

*: Contact force





8. References

- 1) (Deleted)
- 2) T. Nakamura, et al., "An advanced method to estimate fluid elastic instability of steam generator U-bend tube bundle.", ASME PVP 2001
- 3) S. M. Fluit and M. J. Pettigrew, "Simplified method for predicting vibration and fretting-wear in nuclear steam generator U-bend tube bundle", ASME PVP 2001
- 4) M.J. Pettigrew, et.al., 2003, "Vibration analysis of shell-and-tube heat exchangers" Journal of Fluids and Structures 18 (2003) 469-483
- 5) F. Axisa, J. Antunes and B. Villard, "Random excitation of heat exchanger tubes by cross-flows", Journal of Fluids and Structures (1990) 4, 321-341
- 6) S. S. Chen, Instability Mechanisms and Stability Criteria of a Group of Circular Cylinders Subjected to Cross-Flow, Part 2: Numerical Results and Discussions, J. of Vibration, Acoustics, Stress, and Reliability in Design, April 1983, Vol. 105, pp. 253-260
- 7) Design of AVB, L5-04GA428 Rev.5



Appendix-11
(Deleted)



Appendix-12
Thermal Hydraulic Evaluation of Area Plugging



1. Purpose

This appendix provides evaluation of flow characteristics of tubes in U-bend region of San Onofre Units 3 Replacement Steam Generators (RSGs) after area plugging. The results of this evaluation are also applicable to the smaller plugging area in the Unit 2 SGs

2. Conclusion

It has been confirmed that the maximum quality and void fraction during reduced power operation are lower than during 100% power operation in Cycle 16. Additionally, the location of the area with high T/H parameters does not change. The results are summarized in Table 2-1 and the contour is shown in Fig. 7-1 and 7-2.

Table 2-1 Summary of quality and void fraction distribution in U-bend region
(3-D contours are shown in Fig. 7-1 and 7-2.)

T/H parameters in U-bend region	Cycle 16	RTS at 70% power
Max. quality		
Max. void fraction		

3. Assumption

- (1) As shown in Table 6-1, the operating condition for Cycle 16 is assumed to be the design condition (Ref.22) and the operating condition for RTS is assumed to be identical to 70% thermal power condition of Unit-3 (Ref.21).

- (2) The void fraction is analyzed utilizing the "ATHOS/SGAP" code (Ref. 1). Therefore, the assumptions used in the ATHOS/SGAP code apply to this document. Two-phase flow is represented by using a drift flux model which is the standard model of two-phase flow analysis. The mathematical models in the ATHOS/SGAP are constituted under the following assumptions: (Ref. 1)

- (3) All dimensions in analysis are assumed in the cold metal condition because the effect of heat expansion of metals on the calculation results is negligible.



4. Acceptance criteria

Void fraction and flow velocity will be lowered by operating the plant upon return to service (RTS) at reduced power.

5. Design Inputs

The nominal dimensions are obtained from the design drawings (Ref.2 to 19) and the manufacturing tolerances are not considered. The geometrical inputs are identical to those used in reference 20 and 21.

6. Methodology

Based on the design input of the operating conditions, the calculation of the circulation ratio is performed by evaluating the pressure loss and the recirculation head with SSPC, which is a 1 dimensional Thermal and Hydraulic parameter calculation code (Ref.22). Using ATHOS/SGAP (Ref.1), the thermal hydraulic analysis is performed to obtain the 3 dimension flow distribution which includes the void fraction.

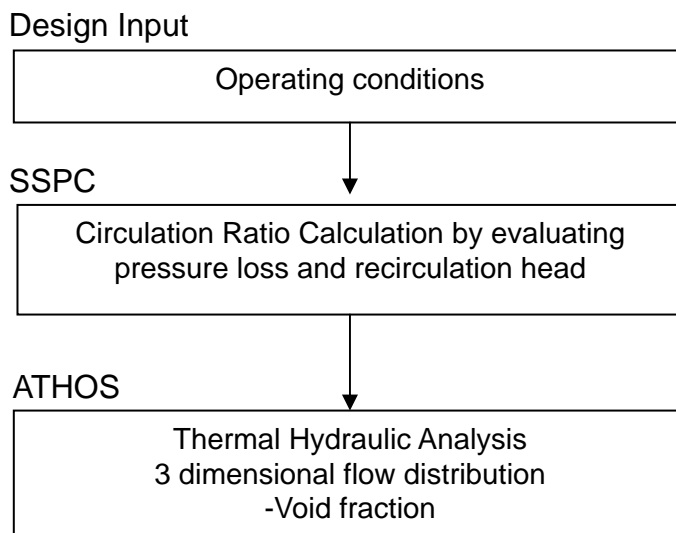


Fig.6-1 Flow of the evaluation



6.1 Thermal and Hydraulic Conditions

The operating parameters used for the calculation are shown in Table 6-1. the primary flow rate when 420 tubes are plugged is calculated by interpolating the flow rate specified in Ref.20 and the operating parameters shown in Table 6-1 are calculated by the steady-state performance calculation code. The overlapping plugged tubes as described in Sec. 6.4 are not taken into account for the calculation of the boundary conditions mentioned above.

Table 6-1 Operating parameters for calculation

	Cycle 16	RTS at 70% power
Thermal power (MWt/SG)		
Plugging		
RCS flow rate(gpm)		
T _{cold} (°F)		
T _{sg-out} (°F)		
T _{hot} (Tsg-in) (°F)		
T _{feedwater} (°F)		
Saturation Steam Pressure (psia)		
Steam Mass Flow (lb/hr)		
Circulation ratio		

6.2 Modeling

The cell structure model is () () cells in vertical and horizontal directions as shown in Fig.6-2(a) and Fig.6-2(b), respectively. The model simulates from the top of tubesheet to the bottom deck plate and this model is symmetrical to the center of tube columns. AVBs are modeled to take into account of the flow resistance. However, the pressure loss due to the resistance of AVB is negligibly smaller than that of the tube bundle. The horizontal tube pitch refers to the average spacing of the sections of tubes that lie horizontally in the U-bend region. Since U-bends of SONGS RSGs start at different elevations for each tube row (U-bend has index), the horizontal pitch is set to a representative average value in the U-bend.



6.3 Boundary conditions

The boundary conditions are shown in Fig. 6-3. 5 Pa of the maximum pressure correction and () of the under relaxation factor are used for the convergence of the solution, which is the same as "Run-5" of L5-04GA565 (Ref.20).

6.4 Tube plugging

Fig.6-4 shows the the address of tubes to be plugged of 3B SGs. Since ATHOS can only created a symmetrical half model of the tube bundle in referece to the center column of the SG, the asymmetrical plugged tubes can not be modeled. Therefore the pluggged tubes are assumed to be overlapped as shown in Fig.6-5.(see Ref.22)

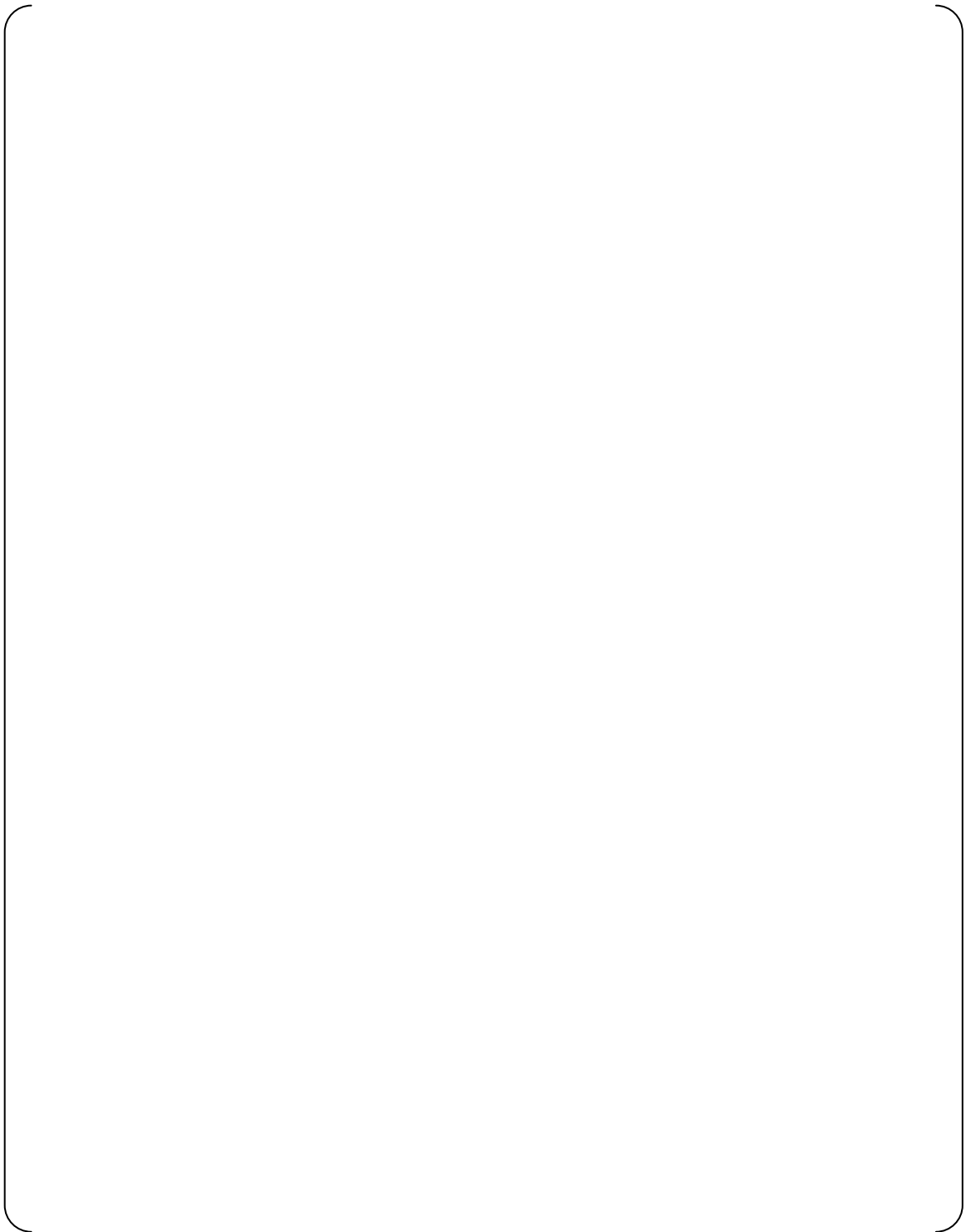


Fig. 6-2 (a) Vertical sectional calculation mesh at center of column



Fig. 6-2 (b) Cross-sectional calculation mesh

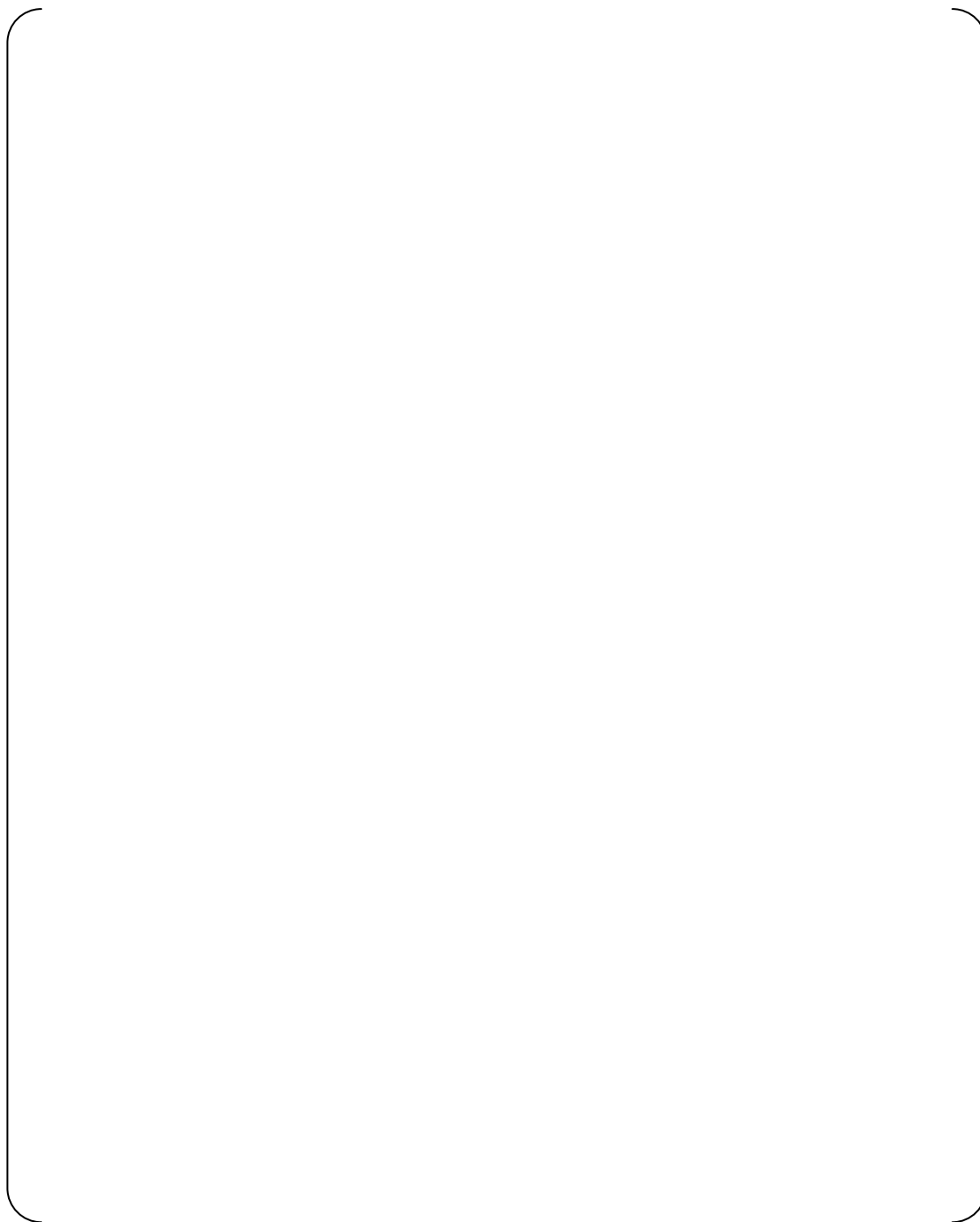


Fig. 6-3 Boundary conditions of ATHOS/SGAP

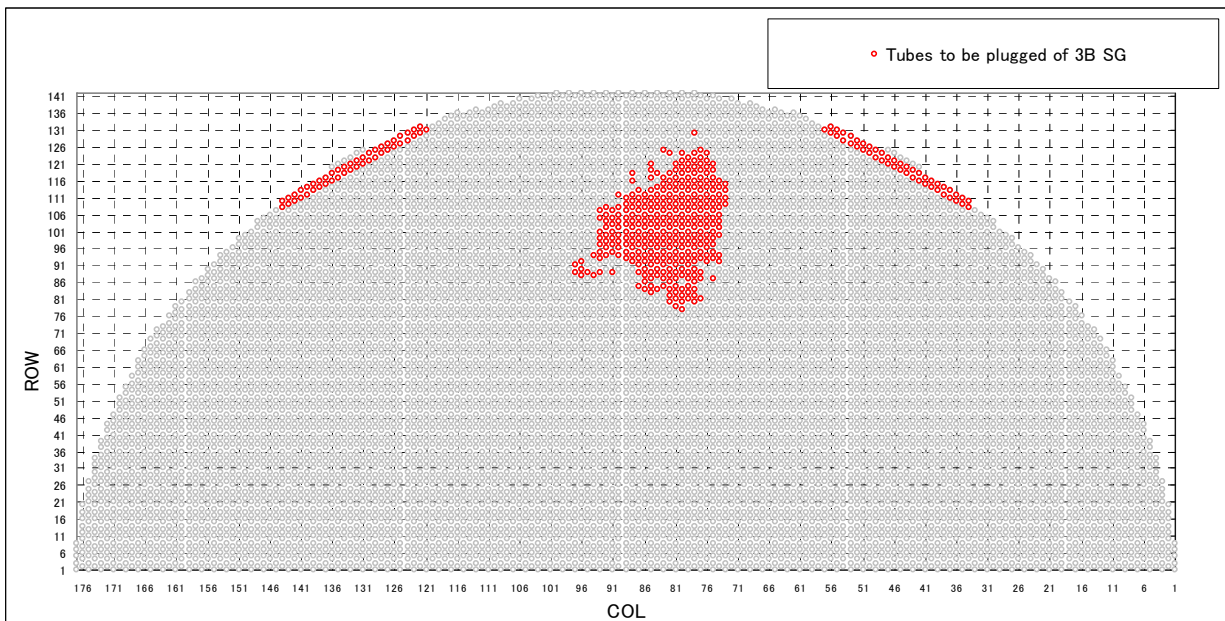


Fig.6-4 Tubes to be plugged of 3B SG



Fig.6-5 Tube plugging model of ATHOS for RTS at 70% power



7. Results

The flow characteristics of U-bend region obtained from the analysis are shown in Fig.7-1 to 7-2. The region where the void fraction is high is concentrated on the region of center columns and the outer rows. Although the trend of 100% power operation is similar to 70% power operation, the maximum void fraction of 70% power operation is lower than that of 100% power operation and the concentrated area is almost identical.

The difference of void fraction between 100% power operation and 70% power operation is described as follows:

The higher saturation steam pressure causes the lower void fraction. Since the thermal power of 70% power operation is lower than that of 100% power operation, the saturation pressure of 70% power operation is higher than that of 100% power operation despite tube plugging condition. For this reason in addition to the lower heat flux, the maximum void fraction of 70% power operation is lower than that of 100% power operation.

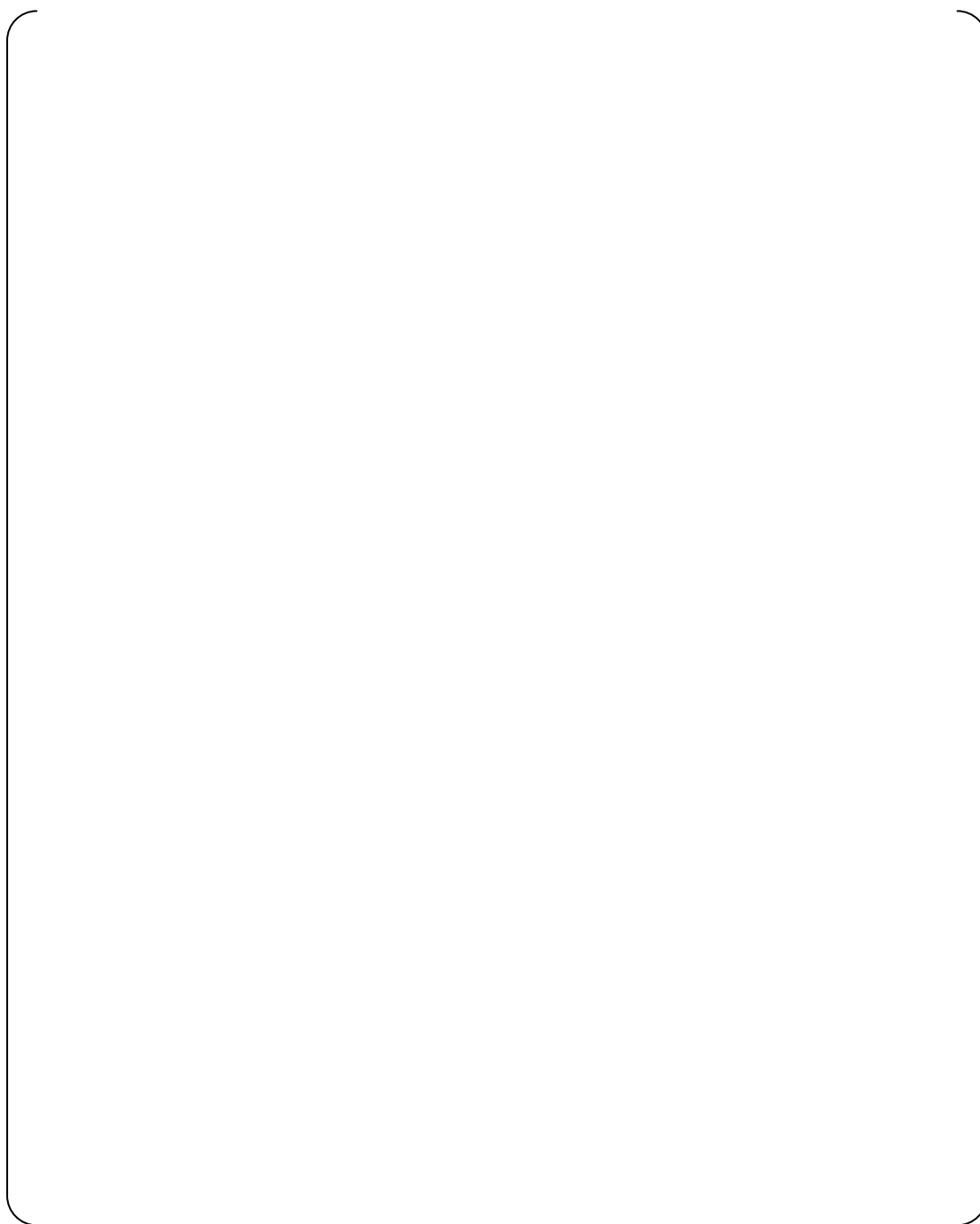


Fig. 7.-1 (a) Contour of vertical sectional quality distribution of Cycle 16

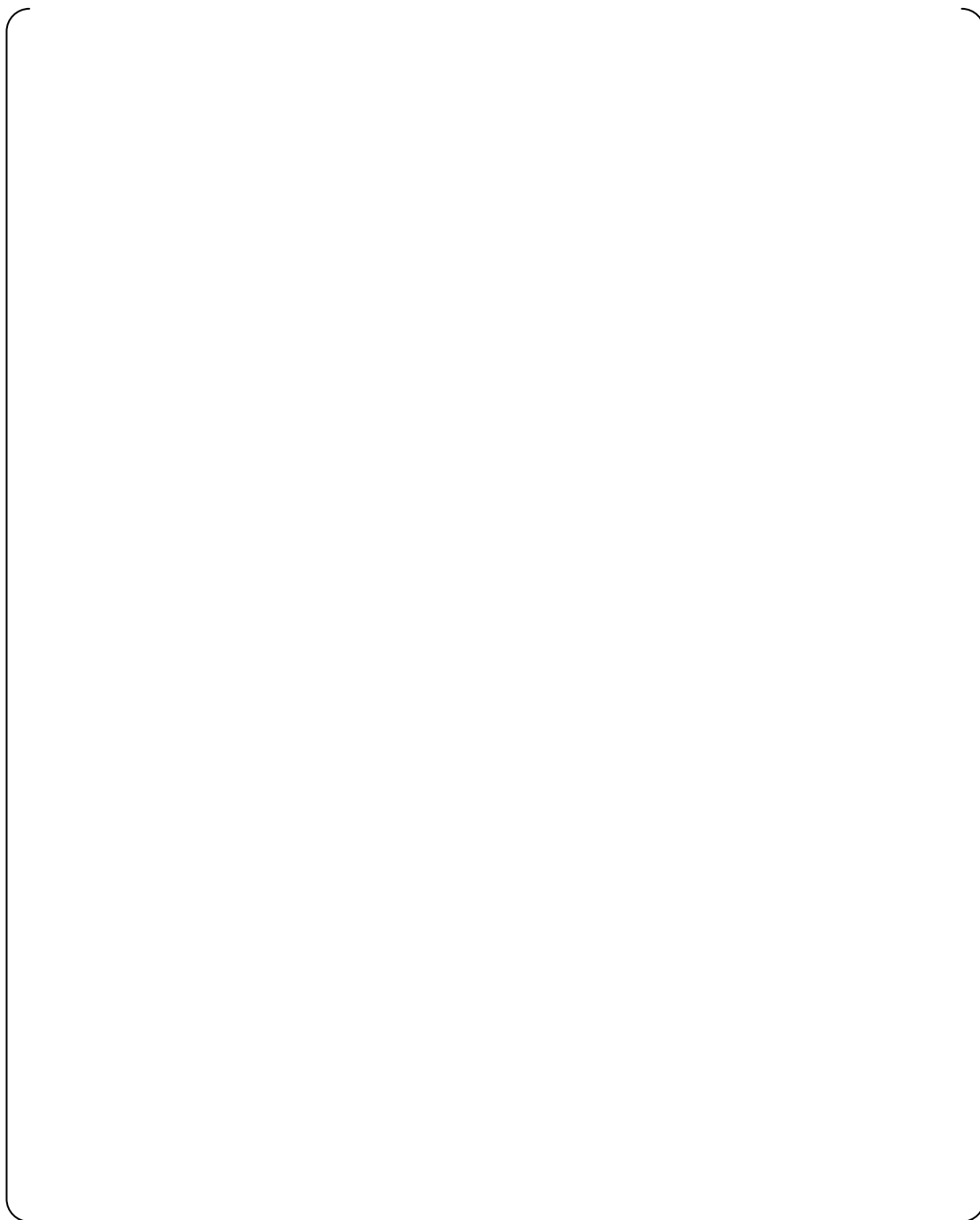


Fig. 7-1 (b) Contour of vertical sectional quality distribution of RTS at 70% power

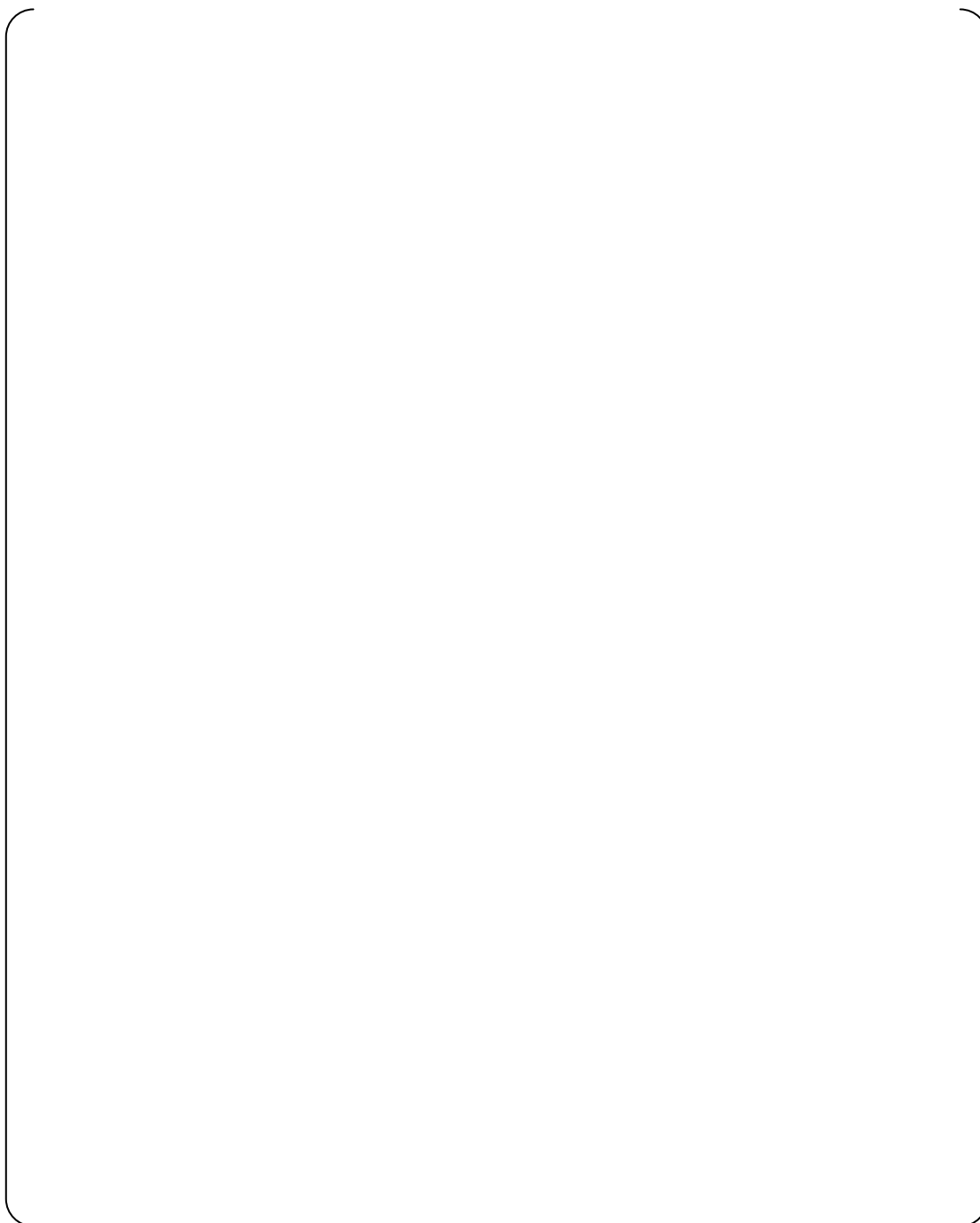


Fig. 7-2 (a) Contour of cross-sectional quality and void fraction distribution at the height of the maximum quality in U-bend region of Cycle 16

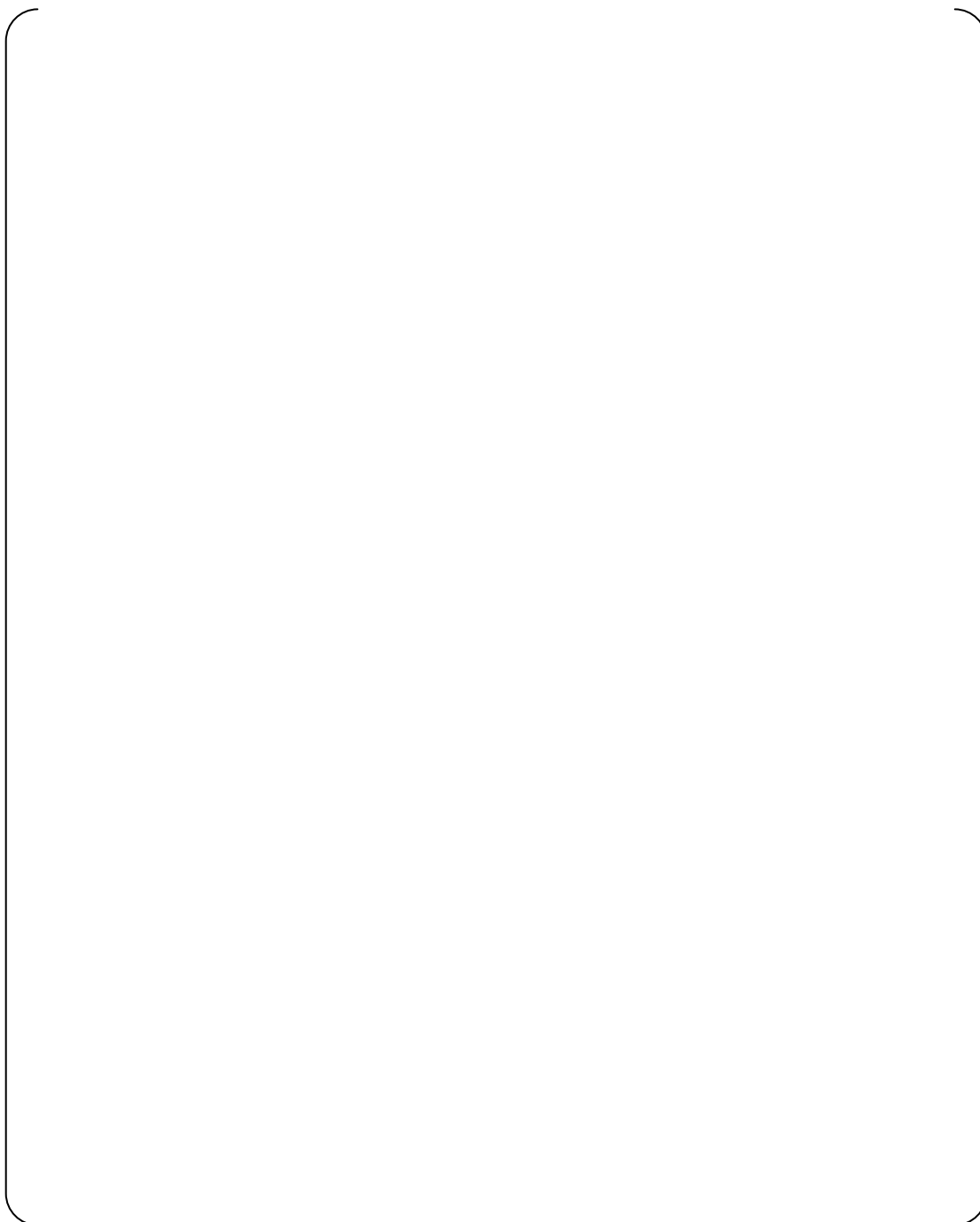


Fig. 7-2 (b) Contour of cross-sectional quality and void fraction distribution at the height of the maximum quality in U-bend region of RTS at 70% power



References

- 1) Analysis of Thermal Hydraulics of Steam Generators/Steam Generator Analysis Package, Ver.3.1, 1016564, EPRI
- 2) L5-04FU001 the latest revision, Component and Outline Drawing 1/3
- 3) L5-04FU002 the latest revision, Component and Outline Drawing 2/3
- 4) L5-04FU003 the latest revision, Component and Outline Drawing 3/3
- 5) L5-04FU021 the latest revision, Tube Sheet and Extension Ring 1/3
- 6) L5-04FU022 the latest revision, Tube Sheet and Extension Ring 2/3
- 7) L5-04FU023 the latest revision, Tube Sheet and Extension Ring 3/3
- 8) L5-04FU051 the latest revision, Tube Bundle 1/3
- 9) L5-04FU052 the latest revision, Tube Bundle 2/3
- 10) L5-04FU053 the latest revision, Tube Bundle 3/3
- 11) L5-04FU111 the latest revision, AVB assembly 1/9
- 12) L5-04FU112 the latest revision, AVB assembly 2/9
- 13) L5-04FU113 the latest revision, AVB assembly 3/9
- 14) L5-04FU114 the latest revision, AVB assembly 4/9
- 15) L5-04FU115 the latest revision, AVB assembly 5/9
- 16) L5-04FU116 the latest revision, AVB assembly 6/9
- 17) L5-04FU117 the latest revision, AVB assembly 7/9
- 18) L5-04FU118 the latest revision, AVB assembly 8/9
- 19) L5-04FU119 the latest revision, AVB assembly 9/9
- 20) L5-04GA565 the latest revision, Selection of Thermal Hydraulic Analysis (ATHOS) Model
- 21) L5-04GA566 the latest revision, Case study of the input parameters and tube plugging impact on internal SG thermal - hydraulics parameters
- 22) L5-04GA510 the latest revision, Thermal and Hydraulic Parametric Calculations



Appendix-13
(Deleted)



Appendix-14
Analytical evaluation of the impact on the Tube Support Plate and Tube
Bundle due to Tubesheet deflection during Divider Plate detachment



1 Purpose



This document demonstrates that even with the SONGS Divider Plate detachment condition at Hydrostatic test, the heat exchanger tube deformation due to tube sheet deformation would not be the cause of the tube wear and thickness reduction since there is no change in the adjacent tubes' gap.



2 Conclusions



For the U-bend portion, the displacements in the X and Y directions are negligible small. As for the Z direction displacement, it is about the same as the Tubesheet towards the upper direction.

As for the neighboring tubes, in comparing the displacement results in all three directions (X, Y & Z), it was found that they are approximately the same and that the gap on the adjacent tubes have no effect.

3 Assumptions and Open Items



Deformation of tubesheet on the secondary side is equivalent to deformation of tubes at the secondary side surface of the tubesheet.

4 Acceptance Criteria

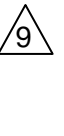


Deformation due to detachment of the divider plate during the hydrostatic test does not have impact on the U-bend portion.

Tube Support Plate (TSP) and Stay Rod do not plastically deform.



5 Design Input



5.1 Geometry

The dimensions are obtained from the design drawings. Major dimensions are shown in Fig 5.1-1 through 5.1-6.

Divider Plate detachment condition: Detachment between Divider Plate and Flat Bottom of Channel Head.

5.2 Loading Conditions



5.2.1 Test Condition

Primary side Hydrostatic test

Pressure: { }

Temperature: { }

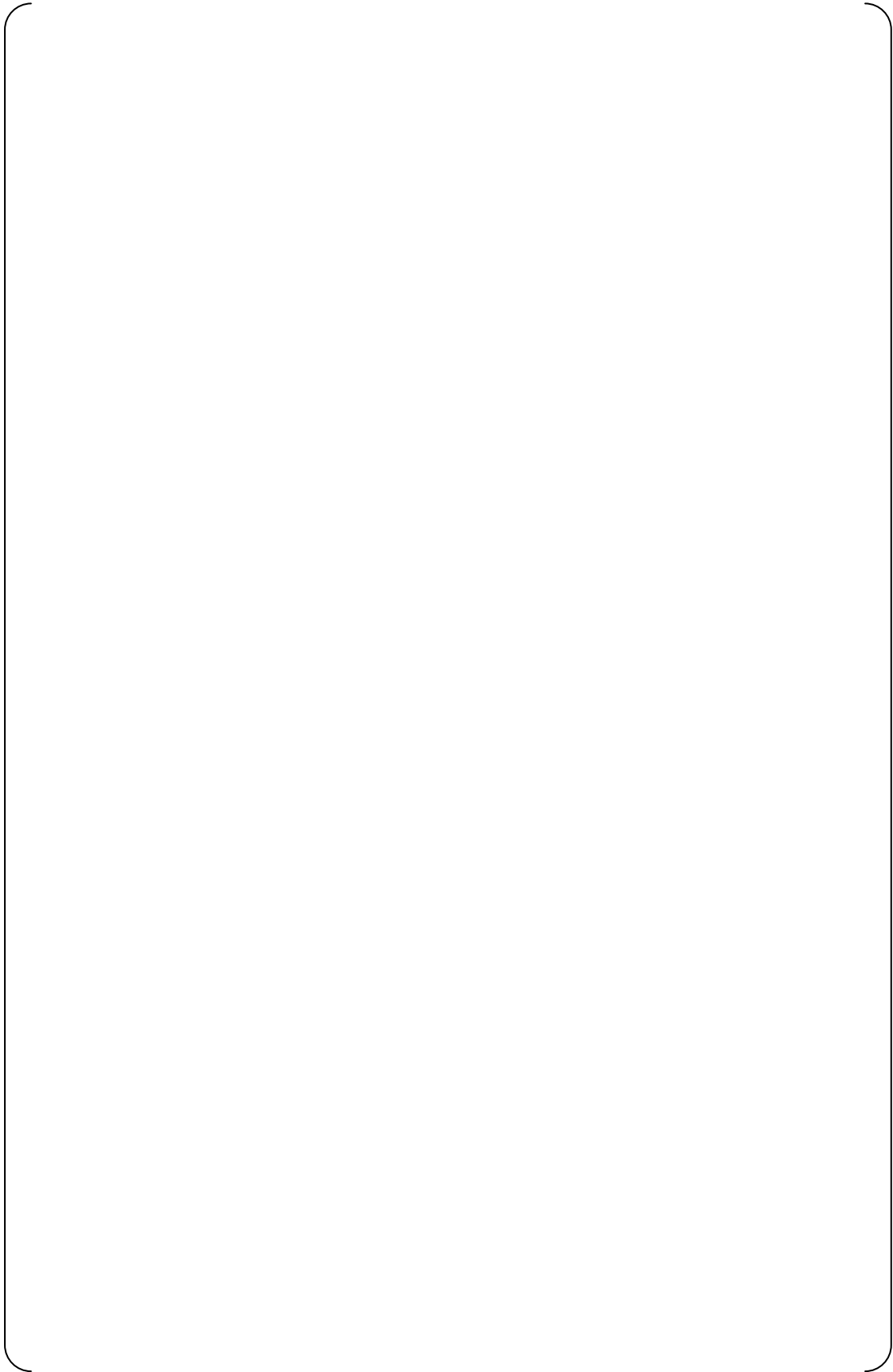


Fig. 5.1-1 Major dimensions of Tubesheet model (1/5)

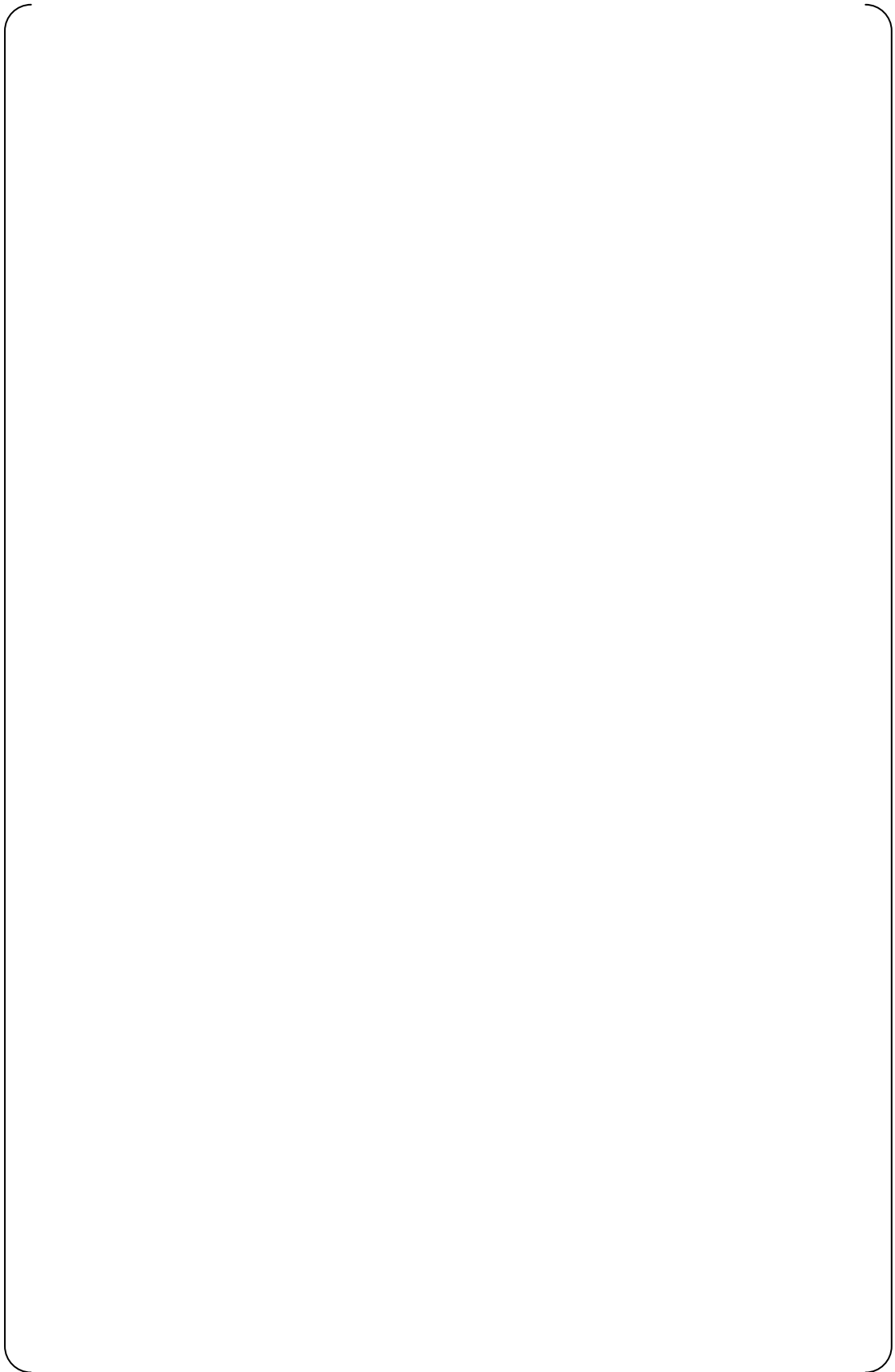


Fig. 5.1-2 Major dimensions of Tubesheet model (2/5)

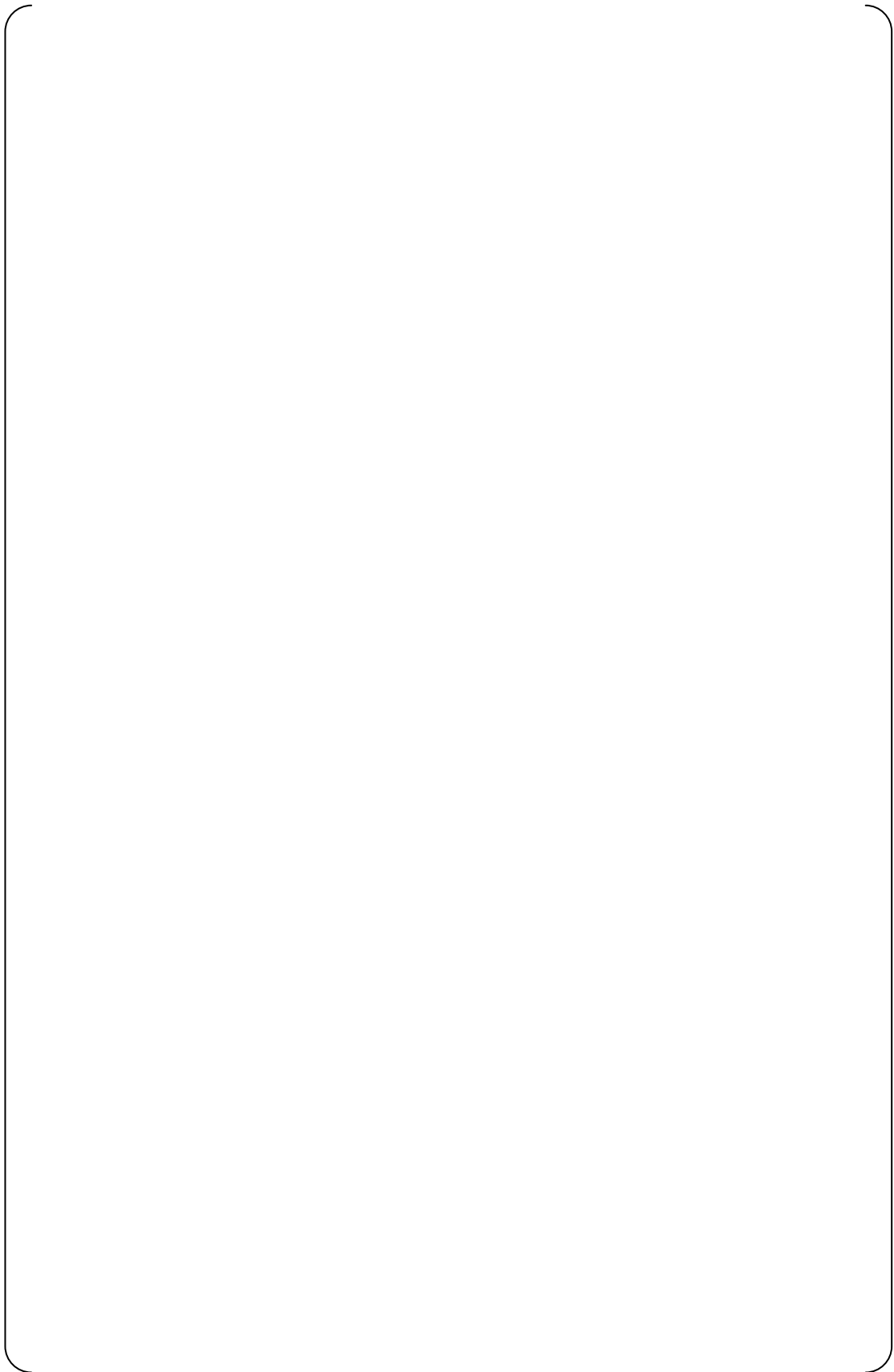


Fig. 5.1-3 Major dimensions of Tubesheet model (3/5)

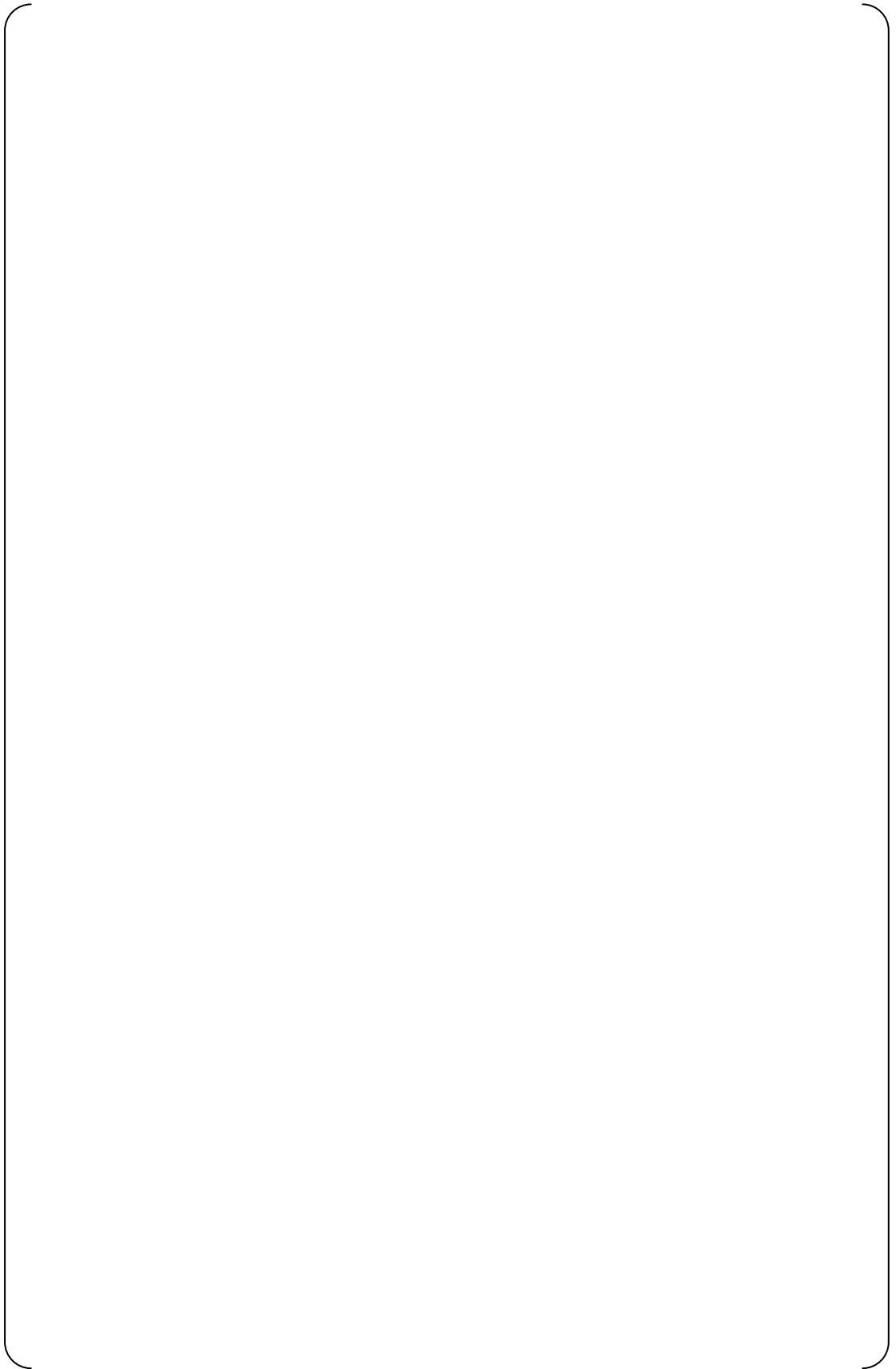


Fig. 5.1-4 Major dimensions of Tubesheet model (4/5)

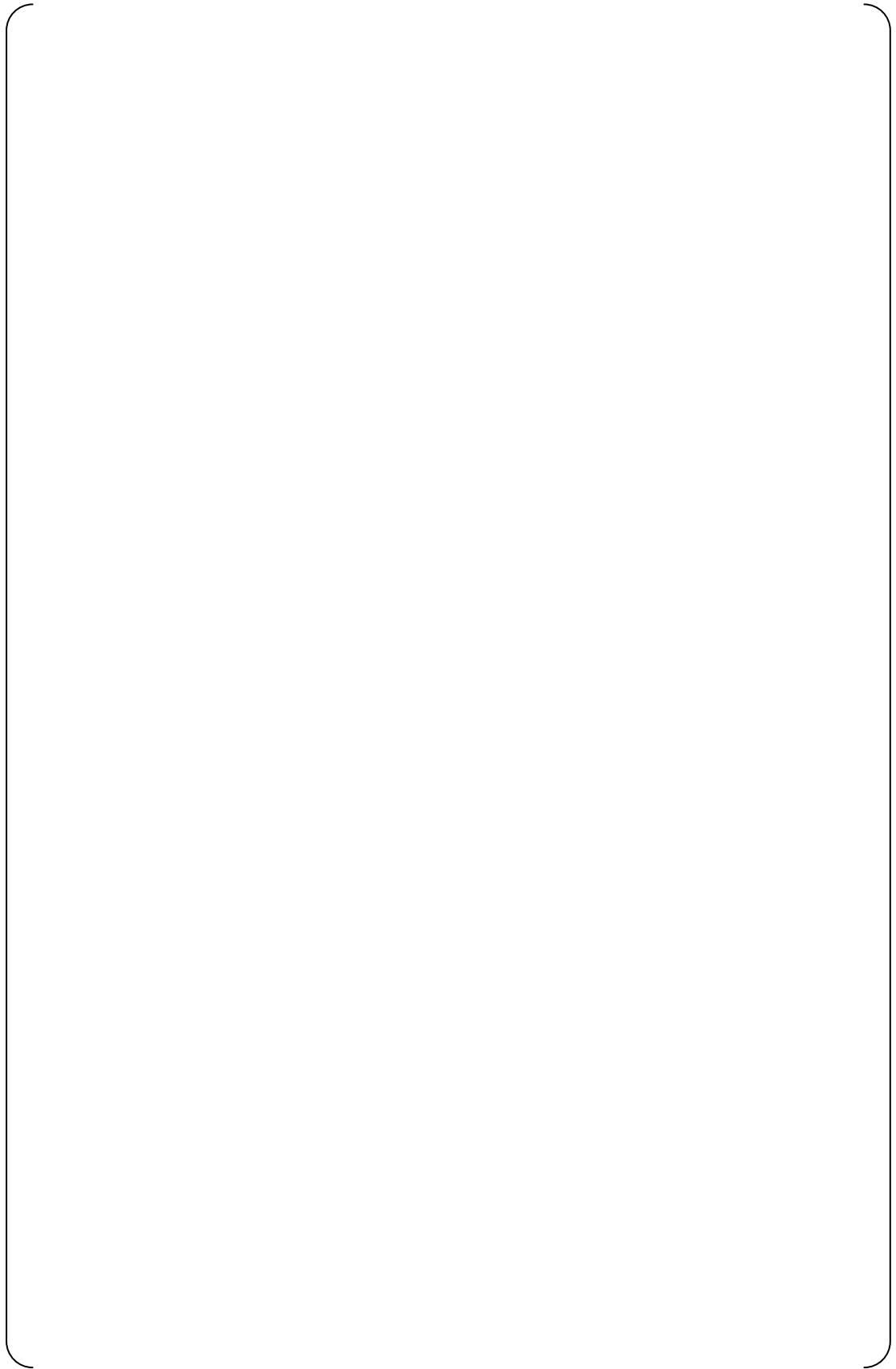


Fig. 5.1-5 Major dimensions of Tubesheet model (5/5)

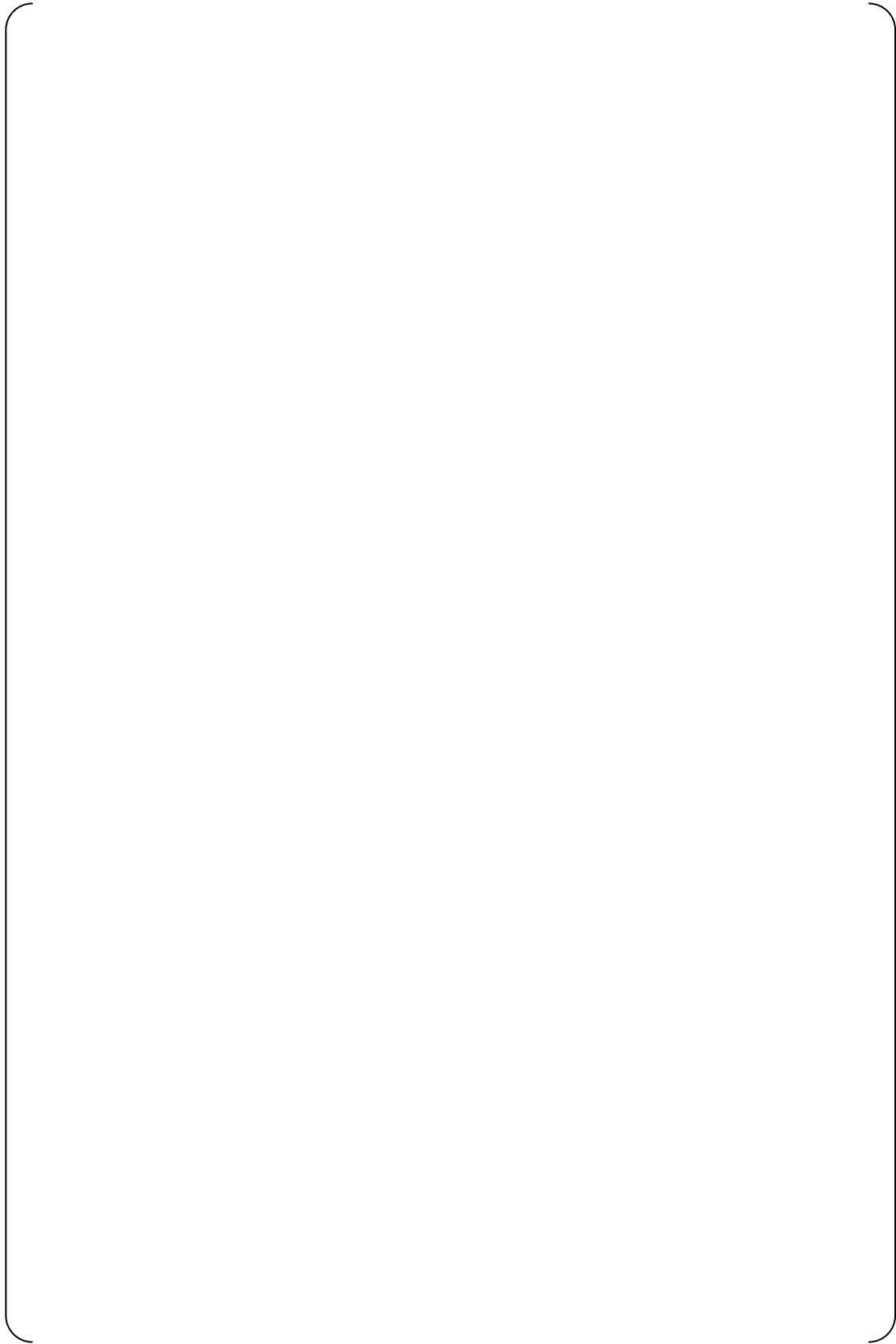


Fig. 5.1-6 Major dimensions of TSP and Stay Rod



5.3 Material Properties



Material properties used in the analysis for each part are shown in Table 5.3-1 through 5.3-6.

Table 5.3-1 Material Properties for []

E (ksi)	ν (-)

Table 5.3-2 Material Properties for [] (Tubesheet perforated area)

E ₁ ^{*1)} (ksi)	ν ₁ ^{*1)} (-)	E ₂ ^{*1)} (ksi)	ν ₂ ^{*1)} (-)

Note 1) E₁^{*} and ν₁^{*} are equivalent properties in radial and hoop directions of the tubesheet, and E₂^{*} and ν₂^{*} are equivalent properties in thickness direction.

Table 5.3-3 Material Properties for [] (Divider Plate)

E (ksi)	ν (-)

Table 5.3-4 Material Properties for [] (TSP)

E (ksi)	ν (-)	E ^{*1)} (ksi)	ν ^{*1)} (-)	Sy (ksi)

Note 1) E^{*} and ν^{*} are equivalent properties in perforated region.

Table 5.3-5 Material Properties for [] (Stay Rod)

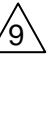
E (ksi)	ν (-)	Sy (ksi)

Table 5.3-6 Material Properties for [] (Tube)

E (ksi)	ν (-)	Sy (ksi)



6 Methodology



6.1 Analytical Model

The following three models used in each analysis are shown in Fig.6.1-1, 6.1-2, and 6.1-3.

- (i) Tubesheet, Channel Head, and Lower Shell
- (ii) Tube Support Plate and Stay Rod
- (iii) Tube

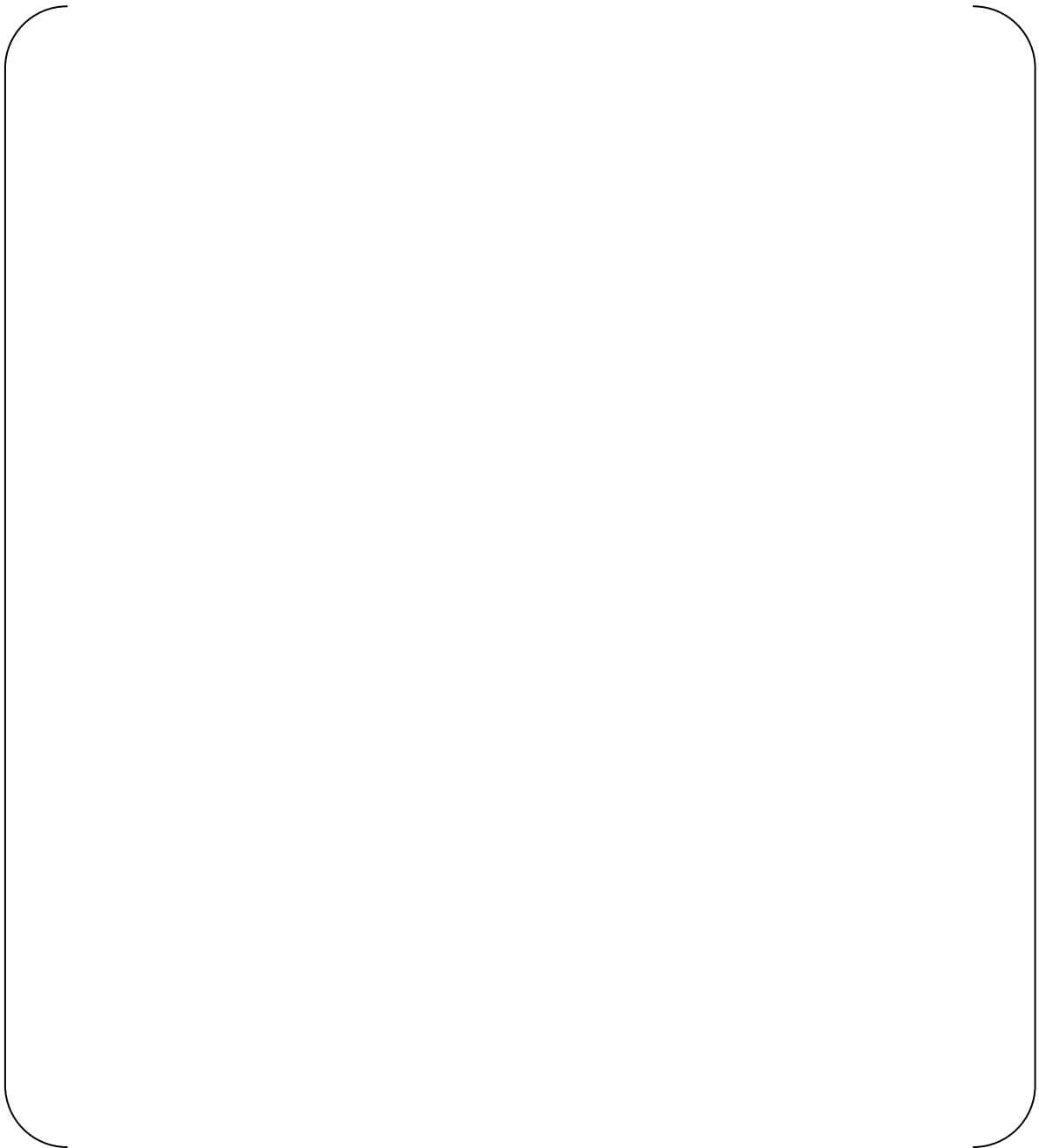
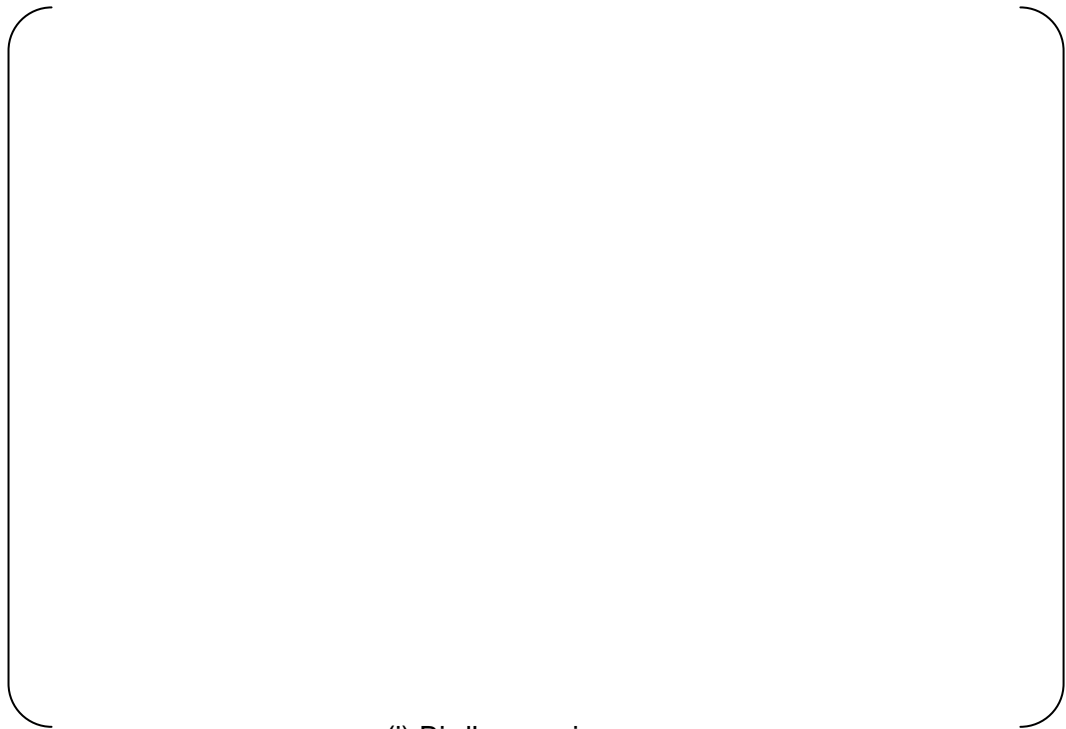


Fig. 6.1-1 Tubesheet model (Tubesheet, Channel Head, and Lower Shell)



(i) Bird's-eye view



(ii) Top view

Fig. 6.1-2 TSP model (Tube Support Plate and Stay Rod)



- Row104 Column78(Neighboring tubes with the leaked tube)
- Row106 Column78(Leaked tube)
- Row140 Column89(Tubes adjacent to the outermost tube)
- Row140 Column89(Outermost tube)

Fig. 6.1-3 Tube model



6.2 Mechanical Boundary Condition



Mechanical boundary condition for each model is shown in Fig.6.2-1 through 6.2-4.

6.3 Method



To simulate the tube deformation due to tubesheet deformation as a result of the hydrostatic test, the following three models are used:

- (i) Tubesheet, Channel Head, and Lower Shell
- (ii) Tube support plate and Stay Rod
- (iii) Tube

At first, the primary side internal pressure is applied on model No. (i) to get the tubesheet deformation. Then the tube sheet deformation results from model No. (i) are input to model No. (ii) to cause the tube support plate deformation. At last, the deformation results from both models No. (i) and (ii) are input to model No. (iii) to analyze the deformation of tubes. The tubes to be analyzed are the following tubes which include the leaked tube and one outermost tube together with the neighboring ones.

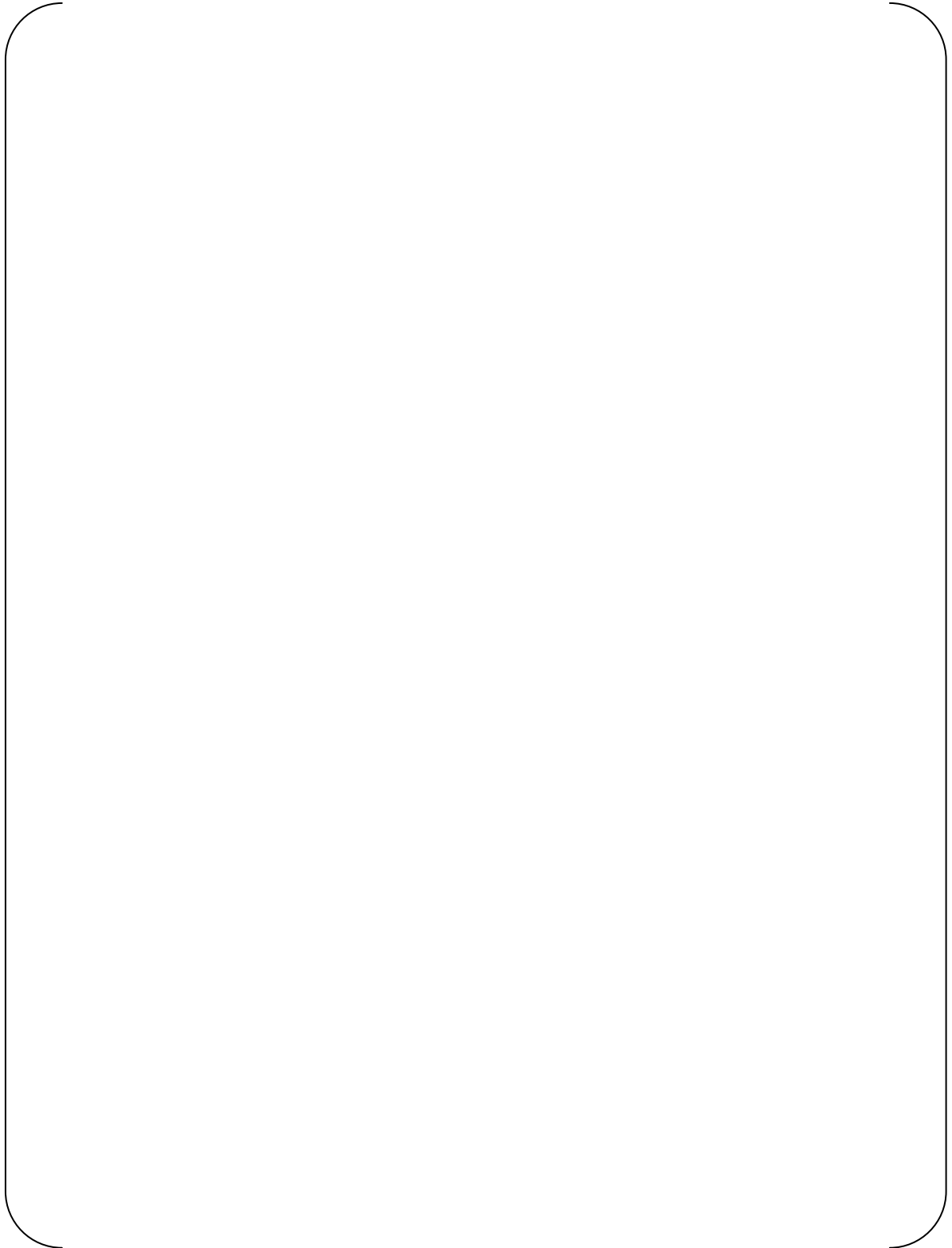


Fig. 6.2-1 Boundary condition for Tubesheet model (1/2)

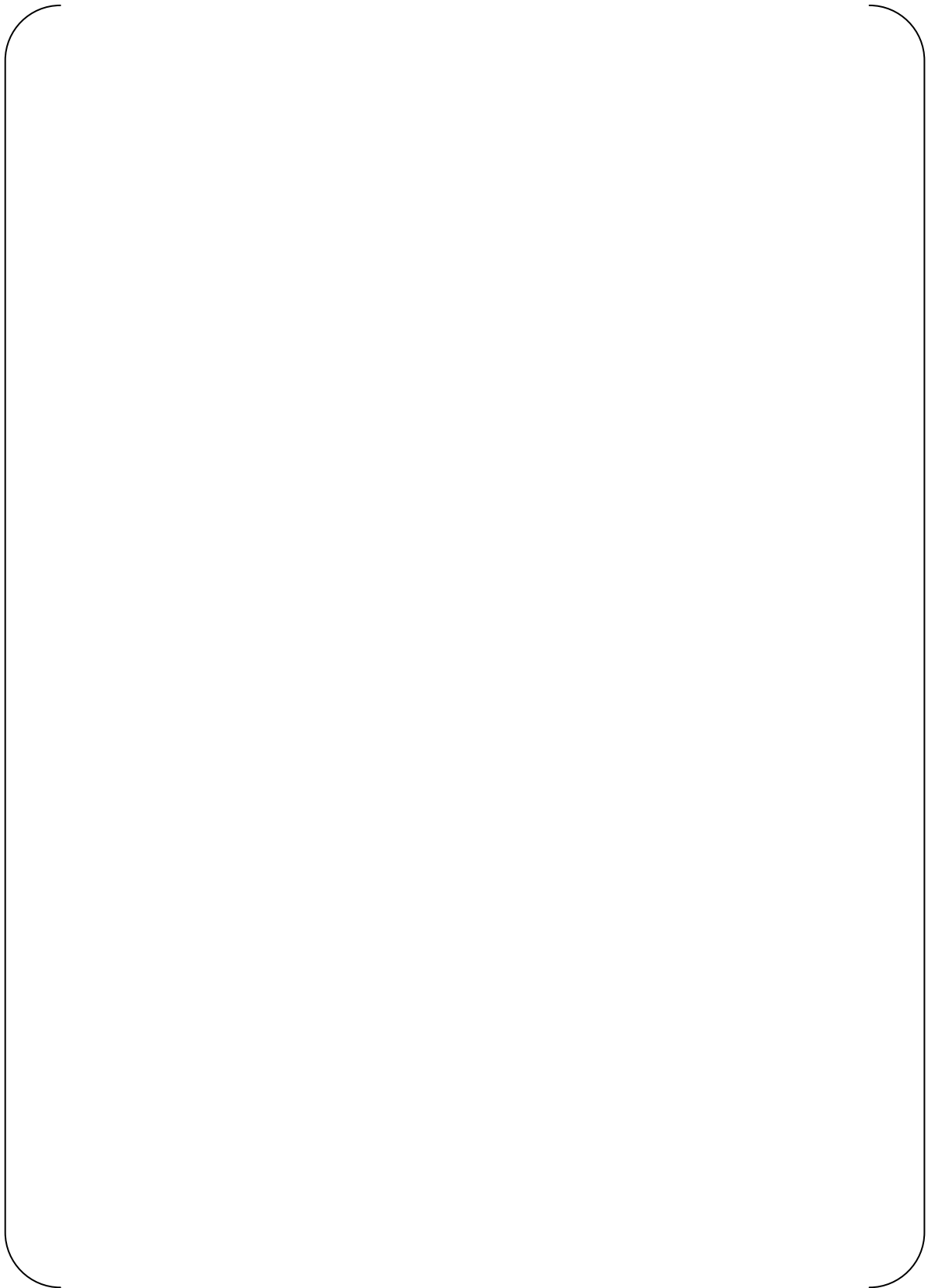


Fig. 6.2-2 Boundary condition for Tubesheet model (2/2)

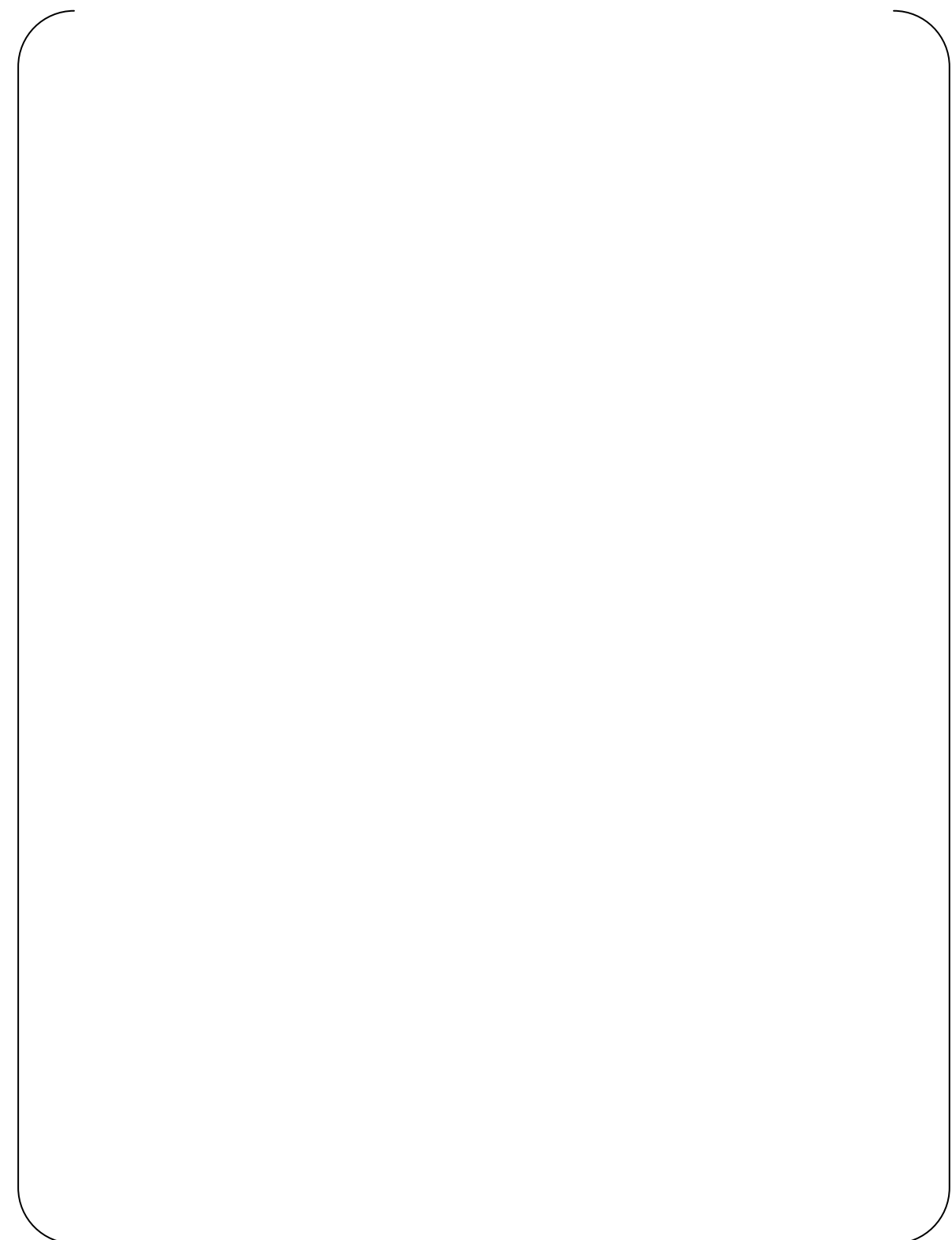


Fig. 6.2-3 Boundary condition for TSP model

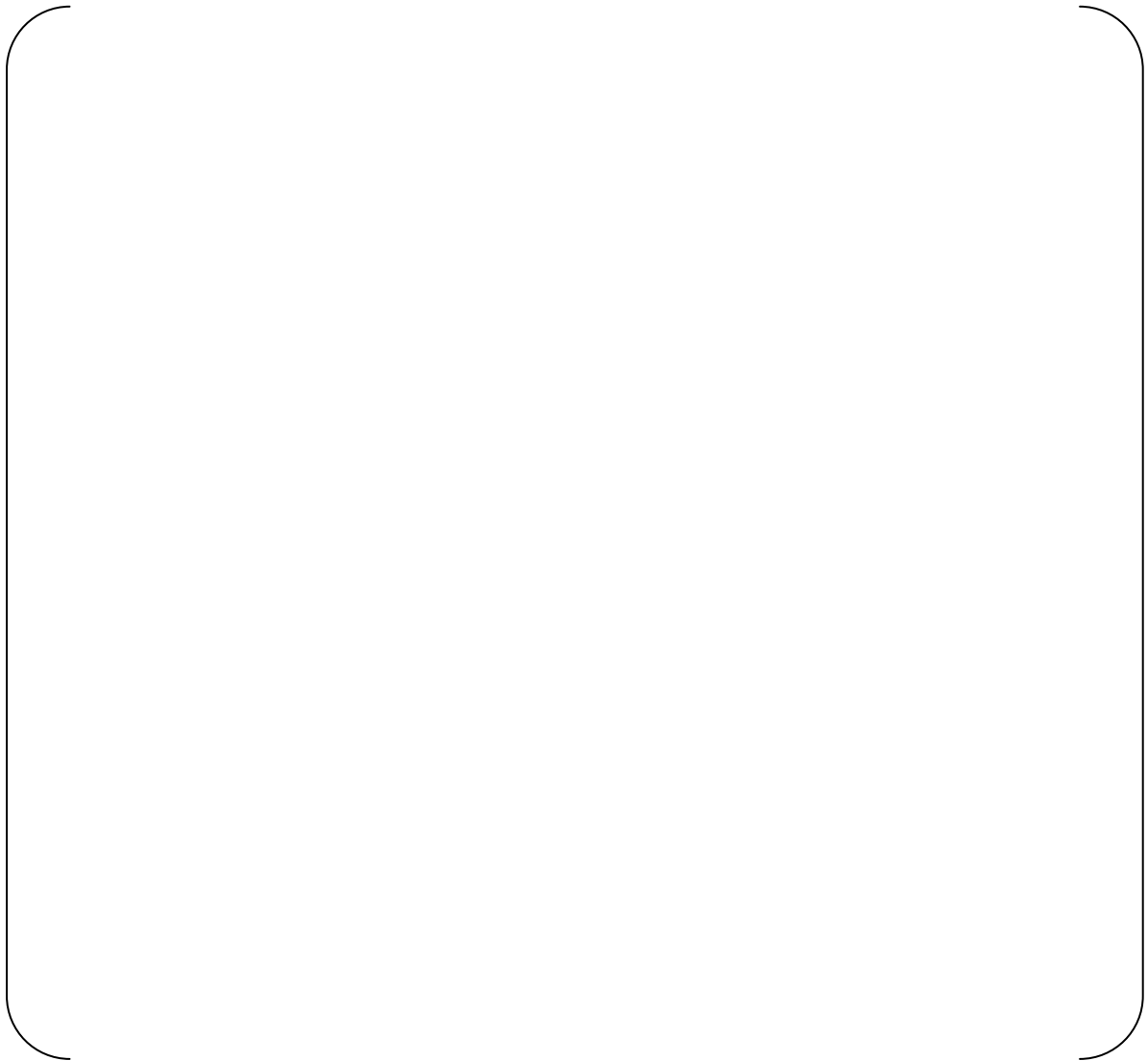


Fig. 6.2-4 Boundary condition for Tube model



7 Computation Results

9

7.1 FE Analysis Results

The tube displacement analysis results for the hydrostatic test effects with divider plate detachment are as follows.

- (1) The tubesheet is swelled out upward with minimal deformation in horizontal direction. Displacements of the stay rod and the tube at the tubesheet on the secondary side surface are shown in Table 7.1-1 and 7.1-2 respectively and related Node No. is shown in Fig. 7.1-1. Displacement of TSP is shown in Table 7.1-3 and 7.1-4.
- (2) Due to this tubesheet deformation, the tubes are displaced a little in horizontal direction at the vicinity of the tubesheet and displaced towards the upper direction over its entire length.

The deformation figures for the tube sheet by the primary side pressure, and the ones for the tube support plate and the tube deformation due to the tubesheet deformation are shown in Figures 7.1-2 through 7.1-7.

From these figures, the following is concluded.

9

- (1) Displacement of the leaked tube

For Row 106 Column78 tube, the maximum displacement along the whole-tube is;

- [] inch in the X direction
- [] inch in the Y direction
- [] inch in the Z direction

Regarding the U-bend portion of this tube, the displacement in the X and Y direction is negligible small. As for the neighboring tubes, in comparing the displacement result in all three directions (X, Y & Z), it was found that they are approximately the same and that the gaps on the adjacent tubes have no effect towards the upper direction. (See Fig. 7.1-8)

9

9

- (2) Comparing two sets of neighboring tubes

9

To look at the tube gap change due to the tube deformation, the following two sets of neighboring tubes are checked.

- I. Leaked tube and the neighboring tube
- II. One outermost tube and the neighboring tube

Fig. 7.1-8 shows that their displacement in all three directions (X, Y & Z) is approximately the same among the sets. Therefore it was found that the gap between the adjacent tubes would not be affected by the hydrostatic test with the divider plate detachment.

9

Contour plots of Tresca stresses for the TSP model are shown in Fig. 7.1-9 and 7.1-10, and calculated stress results of TSP and Stay Rod are shown in Table 7.1-4



Table 7.1-2 Displacement of Tubes at Tubesheet on the secondary side surface

Side	Tube		Displacement				
			Transition (inch)			Rotation (rad)	
	Row	Col.	X	Y	Z	X	Y
Hot	106	78					
	104	78					
	140	89					
	142	89					
Cold	106	78					
	104	78					
	140	89					
	142	89					



Table 7.1-3 Displacement of TSP (Hot side)

Side	Tube		Displacement				
			Transition (inch)			Rotation (rad)	
	Row	Col.	X	Y	Z	X	Y
#1	104	78					
#2							
#3							
#4							
#5							
#6							
#7							
#1	106	78					
#2							
#3							
#4							
#5							
#6							
#7							
#1	140	89					
#2							
#3							
#4							
#5							
#6							
#7							
#1	142	89					
#2							
#3							
#4							
#5							
#6							
#7							

Note: only transitions in X and Y directions are used as input to Tube analysis.



Table 7.1-4 Displacement of TSP (Cold side)

Side	Tube		Displacement				
			Transition (inch)			Rotation (rad)	
	Row	Col.	X	Y	Z	X	Y
#1	104	78					
#2							
#3							
#4							
#5							
#6							
#7							
#1	106	78					
#2							
#3							
#4							
#5							
#6							
#7							
#1	140	89					
#2							
#3							
#4							
#5							
#6							
#7							
#1	142	89					
#2							
#3							
#4							
#5							
#6							
#7							

Note: only transitions in X and Y directions are used as input to Tube analysis.

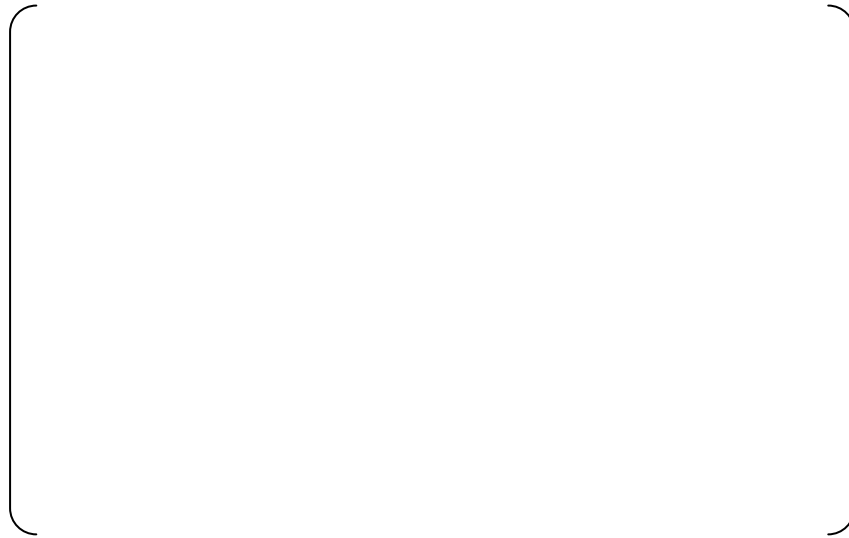


Fig. 7.1-2 Tubesheet deformation (primary side: 1ksi, secondary side 0ksi) (x300)

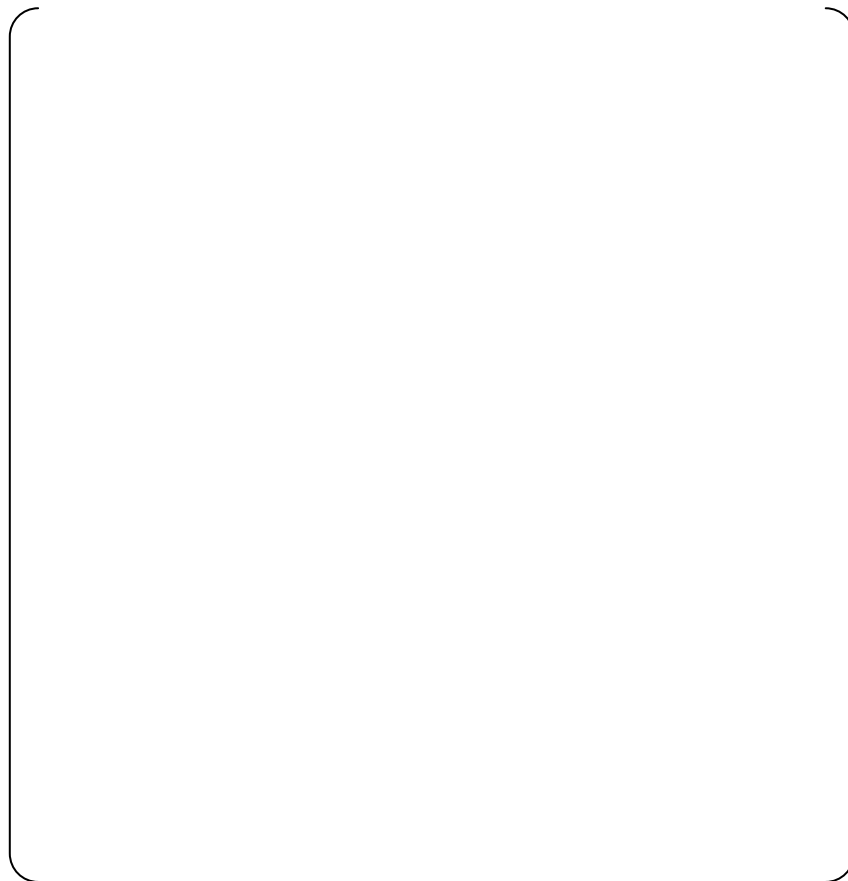


Fig. 7.1-3 TSP Deformation (x10)



Fig. 7.1-4 Tube Deformation Row104(x10)



Fig. 7.1-5 Tube Deformation Row106(x10)

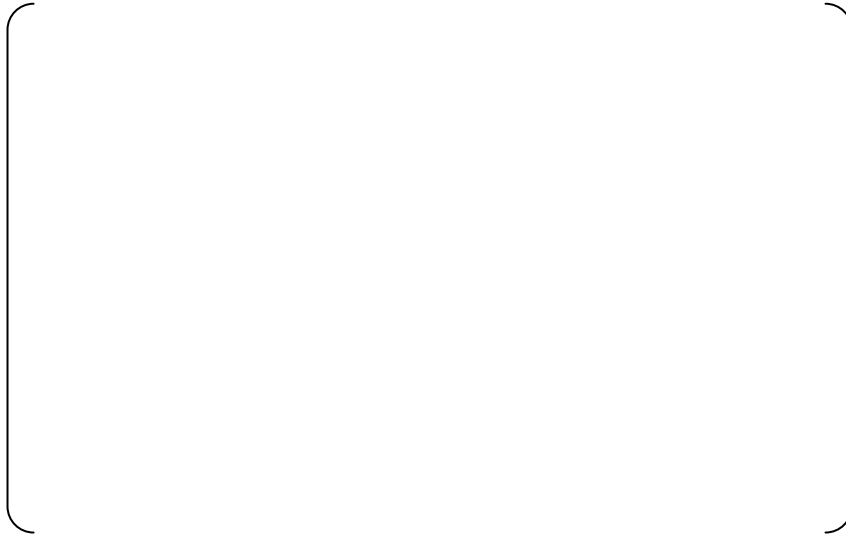


Fig.7.1-6 Tube Deformation Row140(x10)



Fig.7.1-7 Tube Deformation Row142(x10)

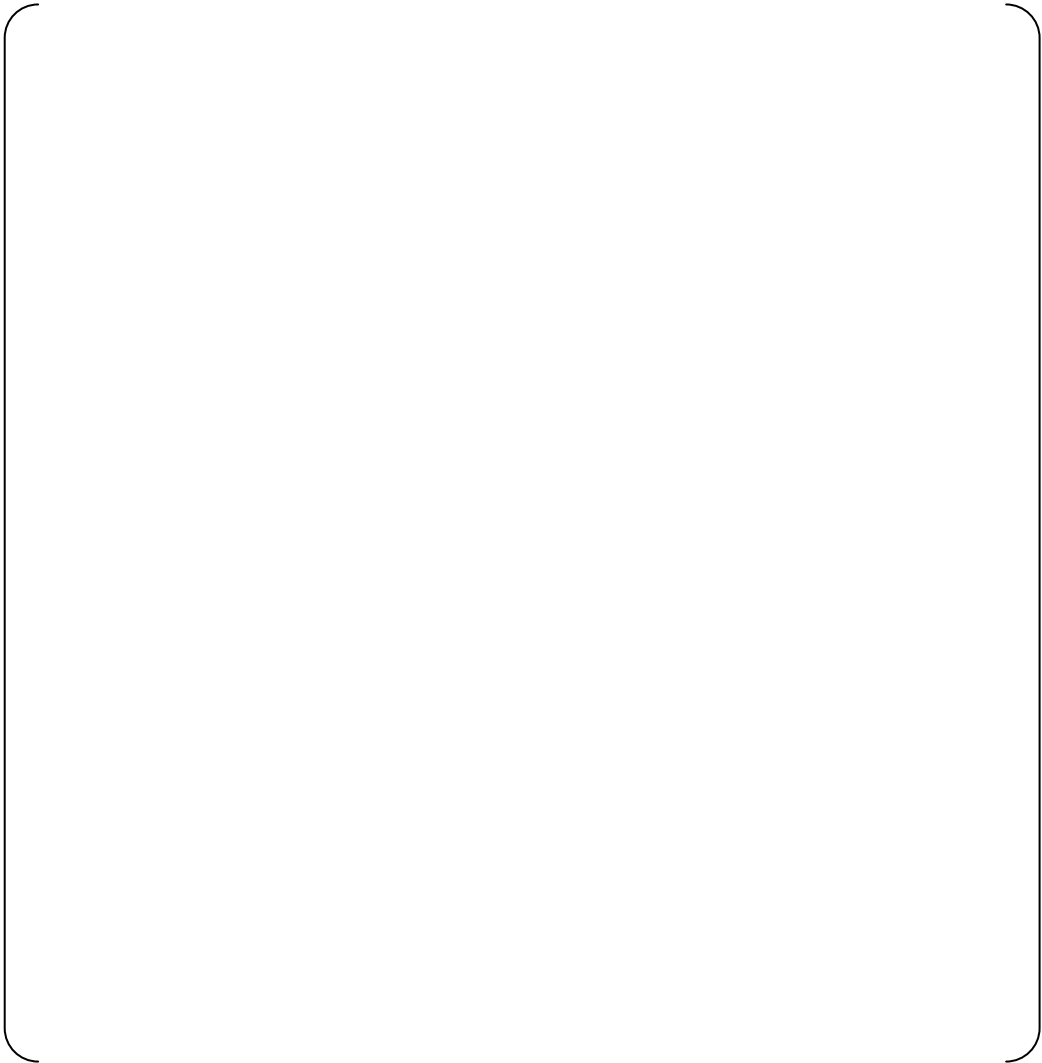
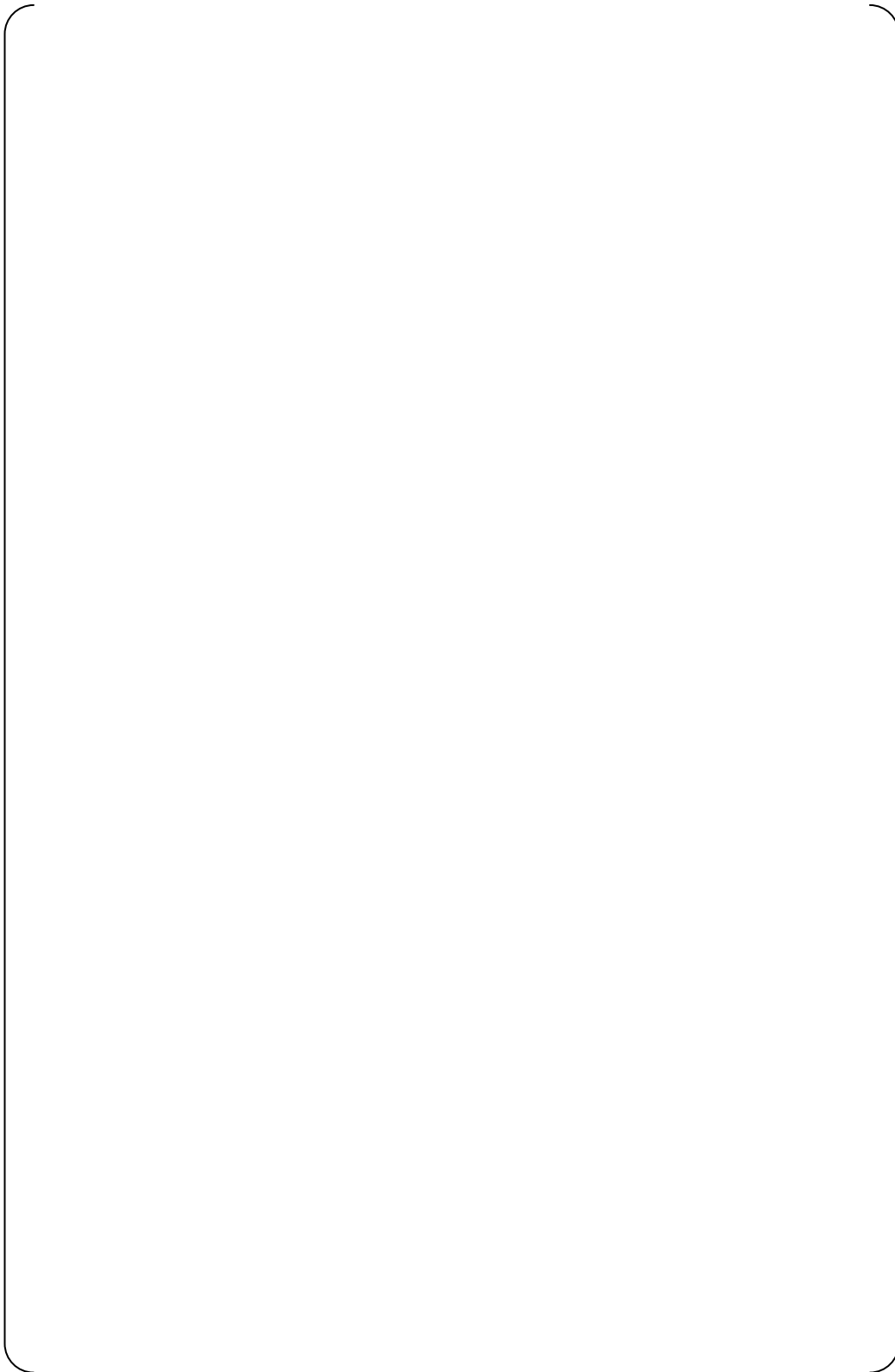


Fig.7.1-8 Tube displacement



Figure 7.1-9 Contour plots of Tresca stresses for TSP model (1/2)



Note) Stress results in regions 1 through 3 in the figure is shown in Table 7.1-5.

Fig.7.1-10 Contour plots of Tresca stresses for TSP model (2/2)



Table 7.1-5 Stress results of TSP and Stay Rod

Region ^(*)	Parts	P/h ²⁾	K ²⁾	Membrane + bending stress (ksi)	Sy (ksi)
1	TSP				
2	TSP(perforated) ²⁾				
3	Stay Rod				

Note 1) See Fig.7.1-8 and 7.1-9.

Note 2) Calculated in accordance with ASME Sec. III App. A-8142.1 using the stress value derived from the FEA results. K=2 is the max value shown in A-8142.1 conservatively.



7.2 Evaluation

9

As long as the tube gaps are uniformly (regularly) spaced, there is no direct relation to the observed thickness reduction wear. In relation to the divider plate's detachment condition at hydrostatic test, the tubes' deformation analysis shows that although there is a slight deformation of the tubes close to the tubesheet in the horizontal direction as a result of the tubesheet deformation and some displacement towards the upper direction due to tubesheet deformation, adjacent tubes displacement value is approximately the same and the gaps remain uniform. Also the U-bend tube displacements in the horizontal directions are minimal and are negligible

The calculated stresses of the Tube Support Plates and the Stay Rods at the hydrostatic test are lower than the yield strength S_y as shown in Table 7.2-1. Therefore plastic deformation does not remain after hydrostatic test and there is no impact on the U-bend portion.

Therefore, the divider plate's detachment at hydrostatic test is considered not related to the observed tube wear phenomenon.

9

Table 7.2-1 Stress results of TSP and Stay Rod

Parts	Membrane + bending Stress (ksi)	S_y (ksi)
TSP		
TSP(perforated)		
Stay Rod		



8 Reference



- [1] MHI document, L5-04GA401 Rev.7, Design Report of the Tubesheet Region (Tubesheet, Extension Ring, Lower Shell, Divider Plate).
- [2] MHI document, L5-04GA411 Rev.7, Design Report of the Tubes Support Plate and Stay Rod.
- [3] MHI document, L5-04GA418 Rev.5, Design Report of the Tube.



Appendix-15
(Deleted)



Appendix-16
Fatigue Evaluation of the Tube due to In-Plane Vibration

9



1. Purpose

The purpose of this document is to show that the stress of the tube in SONGS RSG due to in-plane vibration is under the fatigue limit.

2. Conclusions

The stress on the tube due to in-plane vibration is 4.2ksi and is under fatigue limit (13.6ksi). The tube has structural integrity for the stress due to in-plane vibration from the view point of fatigue evaluation.

3. Assumptions and Open Items

The tube deforms in-plane until contacting with the outer next tube in Row direction due to in-plane vibration.

The stress due to in-plane vibration is high cycle fatigue

4. Acceptance Criteria

The fatigue limit is 13.6ksi according to the following design fatigue curve.

9

Fig. I-9.2.2

1998 SECTION III, DIVISION 1 — APPENDICES

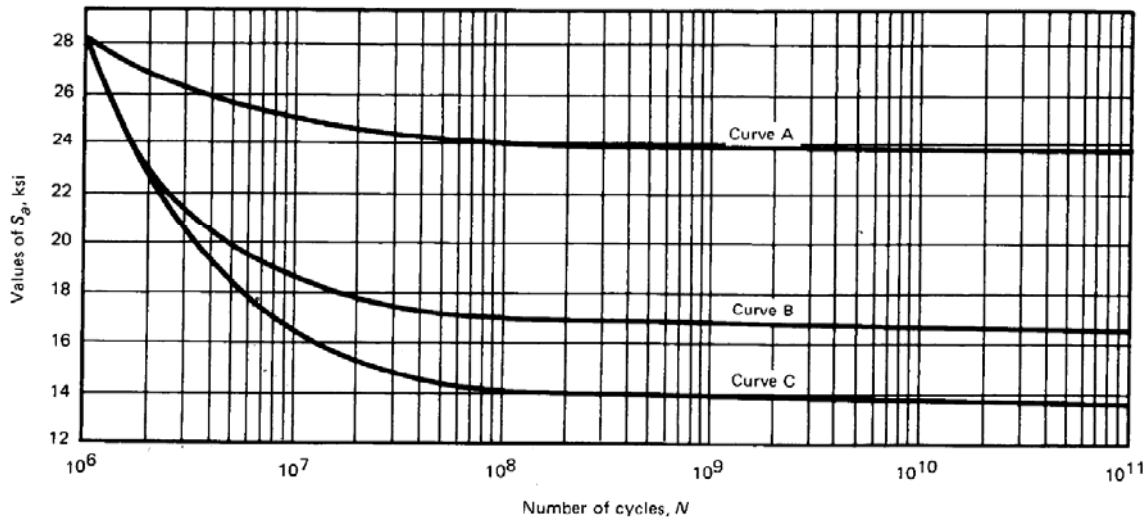


Figure 4-1 Design Fatigue Curve for Tube

5. Design Input

5.1 Geometry

The leaked tube (Row106 Column78) dimensions are used.

5.2 Loading Conditions

5.2.1 Normal Operating Condition

The temperature is as follows.



Thot:[]
Tcold:[]
Tsteam:[]

5.3 Material Properties

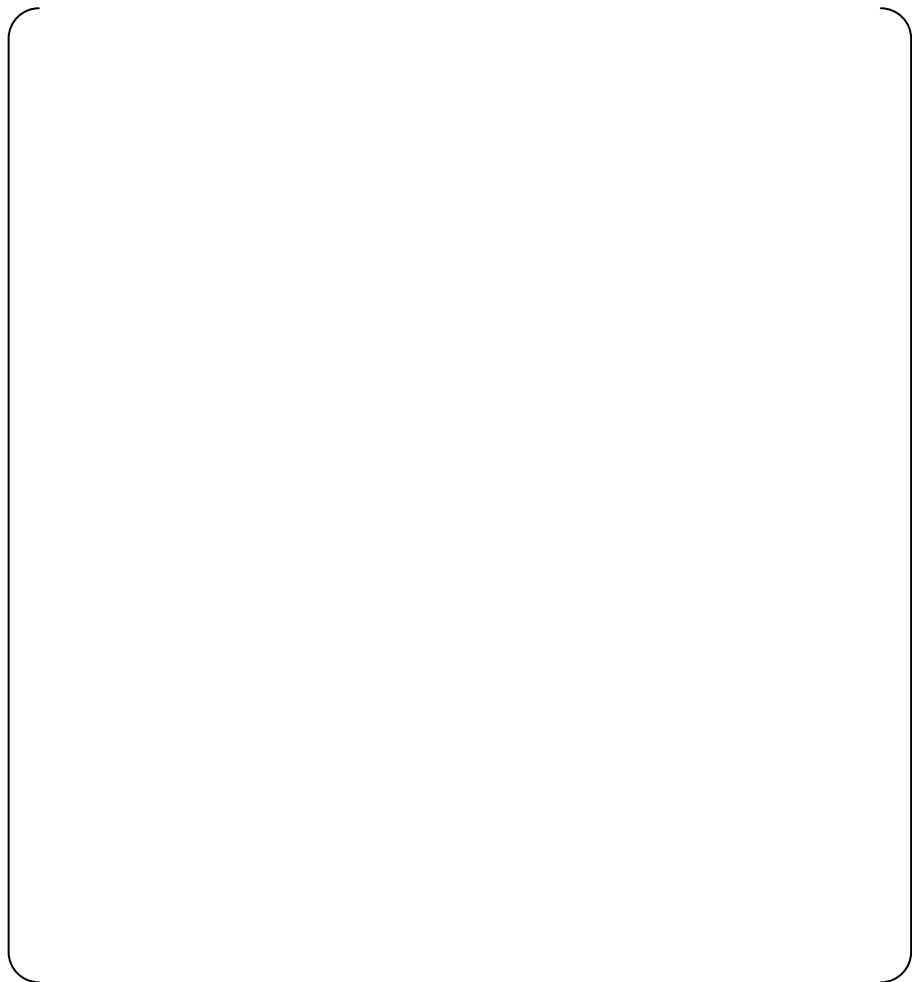
Tube temperature:[] $(=((Thot+Tcold)/2+Ts)/2)$

Young's modulus:[]

6. Methodology

6.1 Analytical Model

The tube of Row106 Column78 is modeled (Figure 6-1).



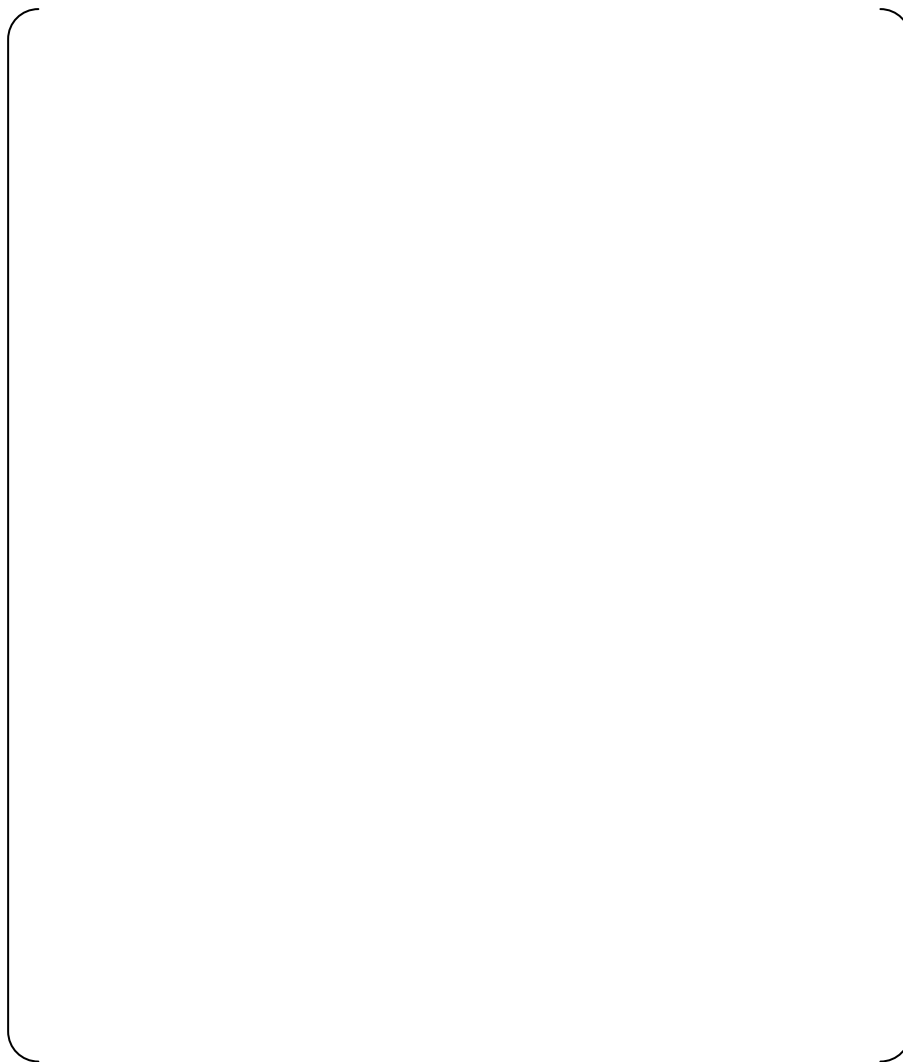
9

Figure 6-1 Analysis Model



6.2 Mechanical Boundary Condition

The tube is fixed on secondary side of the tube sheet and pin supported at each TSP (Figure 6-2).



9

Figure 6-2 Analysis Model



6.3 Method

The stress to contact next tube is calculated and fatigue evaluation is performed with the stress in the following steps.

- (1) A unit force due to gravity 1G is applied on the U-bend tube (Figure 6-3) and the tube deformation (δ_1) (Figure 6-4) and the tube stress (σ_1) at #7TSP are calculated by FE analysis.
- (2) The tube deformation to contact the next tube (δ_2) is calculated using the drawing (Figure 6-4).
- (3) The tube stress to contact next tube is calculated by multiplying σ_1 by the ratio of δ_2/δ_1 .
- (4) The stress obtained in (3) is compared to the fatigue limit and is confirmed under the fatigue limit.

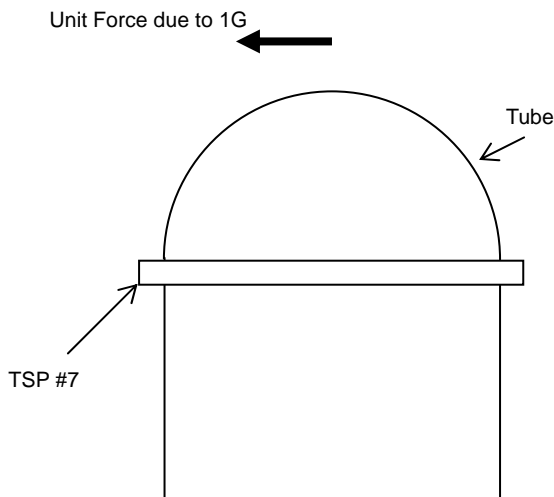


Figure 6-3 Loading Condition

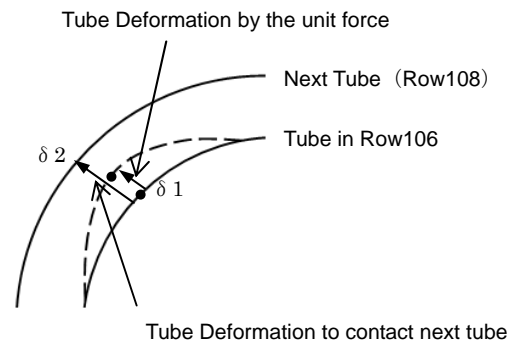


Figure 6-4 Deformation



7. Computation Results

7.1 FE Analysis Results

The deformation of the tube when unit force is applied is shown in Figure 7-1. The deformation by the unit force (δ_1), and the deformation required for the tube to contact the next tube (δ_2), is shown in Table 7-1.

Table 7-1 Location and Deformation of the Tube Contact

Location of the Contact (θ^{*1})	
Deformation by Unit Force (δ_1)	
Deformation required for Tube Contact (δ_2)	
Ratio of δ_2 / δ_1	

Note *1 The definition of θ is shown below

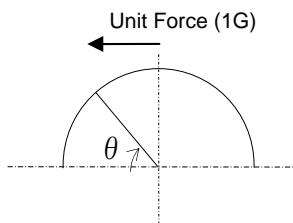


Figure 7-1 Tube Deformation when Unit Force is applied (x100)

9



The tube stress to contact next tube (σ_2) at TSP #7, which is calculated based on σ_1 and the ratio of δ_1 and δ_2 , is shown in Table 7-2. The tube stress due to in-plane vibration is [] and is under the fatigue limit of 13.6ksi.

Table 7-2 Tube stress at TSP #7 due to in-plane vibration

Stress by Unit Force (σ_1)	
Stress to contact next tube	
Fatigue Limit	

Note*1 Calculated as follows

$$\sigma_2 = \sigma_1 \times \delta_2 / \delta_1$$

Where,

- σ_1 : Tube Stress at TSP #7 by Unit Force
- σ_2 : Tube Stress at TSP #7 during In-plane Vibration
- δ_1 : Deformation by the Unit Force
- δ_2 : Deformation Required for Tube Contact

7.2 Evaluation

The stress on the tube due to in-plane vibration is [] and is under fatigue limit (13.6ksi). The structural integrity of the tube is confirmed from the view point of fatigue due to in-plane vibration.



Attachment 1: Fatigue Evaluation of the Wear Tube due to In-Plane Vibration

1. Purpose

The purpose of this attachment is to show that the stress of the wear tube in SONGS RSG due to in-plane vibration is under the fatigue limit.

2. Conclusions

The stress on the tube due to in-plane vibration is [] and is under fatigue limit (13.6ksi). The structural integrity of the tube is confirmed from the view point of fatigue due to in-plane vibration.

3. Assumptions

The tube deforms in-plane until contacting with the outer next tube in Row direction due to in-plane vibration.

The stress due to in-plane vibration is high cycle fatigue.

Thickness of the tube is reduced conservatively with flat surface, which makes the smaller sectional area, at the contact location with the land area of TSP tube hole.

4. Acceptance Criteria

The fatigue limit is 13.6ksi according to the following design fatigue curve.

5. Design Input

5.1 Geometry

Nominal tube dimensions are considered and tube is worn [] in thickness

5.2 Loading Conditions

The member forces from the result of the beam model analysis shown in Figure 7-1 are used.



6. Methodology

6.1 Analytical Model

Part of the tube Row106 Column78 worn [] in thickness at #7TSP is to be evaluated. Modeling methodology of cross section of the tube is shown in Figure A6.1-1. Analysis model is a half sector model considering symmetric configuration and is generated using quadratic solid element as shown in Figure A6.1-2. The thickness of the tube is 0.0429inch for the general part, and the outer diameter is 0.75inch. The height of the model is 1inch.

6.2 Mechanical Boundary Condition

Displacement of the bottom surface of the tube model is constrained in all directions. Boundary condition of the model is shown in Figure A6.2-1.

6.3 Method

Stress of the worn tube is calculated and fatigue evaluation is performed with the stress in the following steps.

- (1) Member forces of the tube at #7TSP due to unit force are derived from the analysis result of the beam model shown in Figure 7-1.
- (2) The member forces are loaded on the top of the model as shown in Figure A6.3-1. The member forces have to be loaded on the node at the center of the tube coupled with the tubes on the same cross section. Tube stresses are influenced locally by this coupling. To avoid the influence, the loading point must be put far away from the evaluated point, therefore tube stresses evaluated on a section at the middle elevation of the model and the member forces are loaded on the top. To evaluate tube stresses on a section at the middle elevation, a counter moment is added to the loading point to cancel the cantilever effect by the shear force, which is loaded above the evaluated point. Pressure stresses are not considered because pressure does not contribute the stresses for the high cycle fatigue due to in-plane vibration.
- (3) Peak stress is calculated by multiplying membrane plus bending stresses derived from FE analysis by a stress concentration factor.
- (4) In addition, the peak stress calculated in (3) is multiplied by the ratio of δ_2/δ_1 (Table 7-1).
- (5) The stress obtained in (4) is compared to the fatigue limit and is confirmed under the fatigue limit.



9

Figure A6.1-1 Modeling Methodology of Tube Cross Section



9

Figure A6.1-2 Analysis model

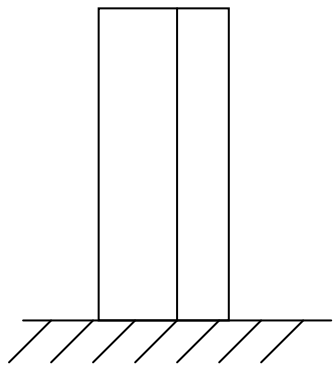


Figure A6.2-1 Mechanical Boundary Condition

9

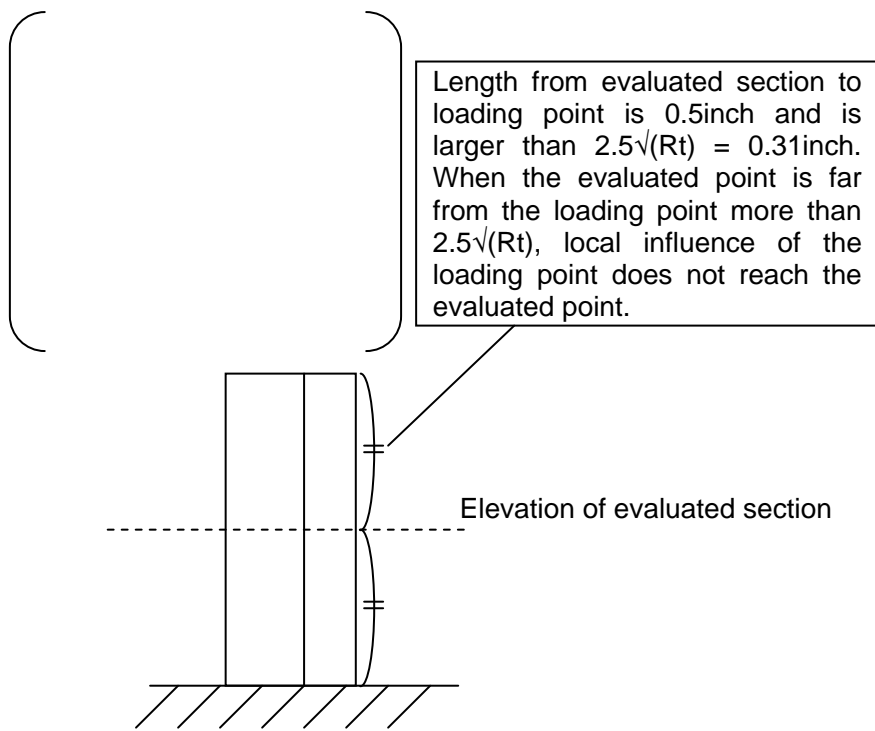


Figure A6.3-1 Loading Condition



7. Computation Results

7.1 FE Analysis Results

Member forces at #7TSP derived from the analysis result of the beam model due to the unit force are provided in Table A7.1-1. Half of each force is loaded on the top of the half model of the worm tube shown in Figure A6.3-1. Deformation of the model is shown in Figure A7.1-1, and contour plot of tresca stress on the evaluated section, which is at middle elevation of the tube model, is shown in Figure A7.1-2. The maximum stress occurred at the worn thickness on the asymmetric boundary.

Stresses on the inner surface resulting from FE analysis is dealt with as membrane plus bending plus peak stress by unit force since there is no discontinuity on the inner surface of the tube. On the outer surface, stress concentration factor shall be applied considering discontinuity of the shape due to the wear. The stresses resulting from FE analysis through the thickness are classified to membrane plus bending stresses, then membrane plus bending plus peak stresses are obtained by multiplying membrane plus bending stresses by a stress concentration factor. Calculated results of the tube stresses at the severest point are provided in Table A7.1-2. The tube stress due to in-plane vibration is [] and is under the fatigue limit of 13.6ksi.

9

7.2 Evaluation

The stress on the tube due to in-plane vibration is [] and is under fatigue limit (13.6ksi). The structural integrity of the tube is confirmed from the view point of fatigue due to in-plane vibration.



Table A7.1-1 Member forces derived from the beam model analysis at #7TSP

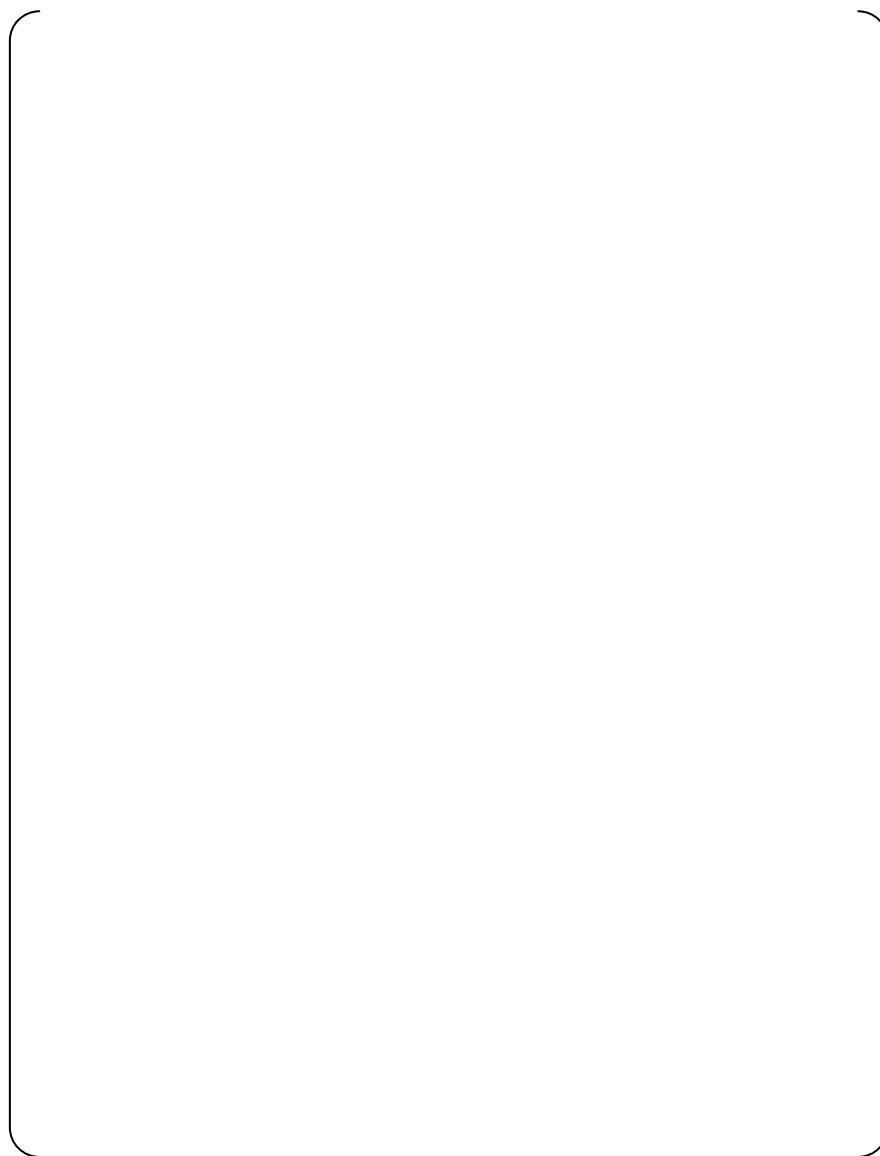
Element	Node	Axial force Fz (kips)	In-plane force Fy (kips)	Bending moment Mx (kips-in.)

Table A7.1-2 Worn tube stress at TSP #7 due to in-plane vibration

Items	Inner surface	Outer surface
Membrane plus bending stresses by unit force		
Stress concentration factor		
Membrane plus bending plus peak stresses by unit force		
Ratio of δ_2 / δ_1		
Membrane plus bending plus peak stresses		
Fatigue limit		

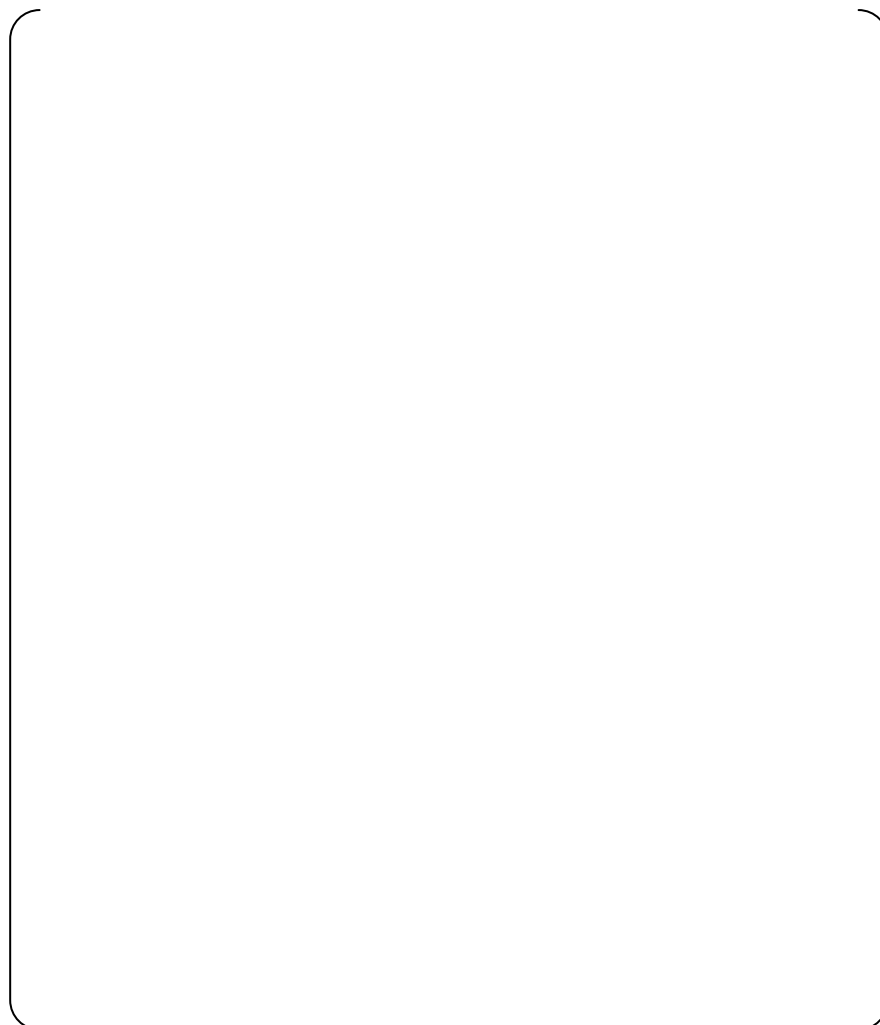
(*1)The stress concentration factor is derived from Chart 3.5 of Ref. [3], which is a chart for a thin tube with fillet. Value t/h (t: thinner thickness, h: thicker thickness) for the tube model is [] Although a curve for t/h = [] is not drawn in the chart, it is obvious that a curve for t/h = [] become lower than the t/h = [] curve in the chart, therefore the t/h = [] curve is used conservatively for evaluation. Parameter t/r is 1.33, where r is fillet radius assuming equal to be t-h = [] therefore stress concentration factor is less than 1.5.

9



9

Figure A7.1-1 Deformation of the worn tube due to the member forces (x500)



9

Figure A7.1-2 Contour plot of tresca stress on the evaluated section



8. Reference

[1] MHI drawing, L5-04FU051 Rev.1, Tube Bundle 1/3.

[2] MHI drawing, L5-04FU108 Rev.3, Tube Support Plate Assembly 3/3.

[3] Walter D. Pilkey, Peterson's Stress Concentration Factors Second Edition, John Wiley & Sons, Inc., 1997.

ATTACHMENT 5

MHI Document L5-04GA571, Screening Criteria for Susceptibility to In-Plane Tube Motion

[Proprietary Information Redacted]



Revision History

No.	Revision	Date	Approved	Checked	Prepared
0	Initial issue	See cover sheet			
1	-Revised in accordance with SCE comment to L5-04GA571 Rev. 0 (RSG-SCE/MHI-12-5690)				
2	-Revised in accordance with SCE comment to L5-04GA571 Rev. 1 (RSG-SCE/MHI-12-5691)				
3	-Revised in accordance with SCE comment to L5-04GA571 Rev. 2 (RSG-SCE/MHI-12-5693)				
4	-Revised in accordance with SCE comment to L5-04GA571 Rev. 3 (RSG-SCE/MHI-12-5702)				
5	-Revised in accordance with SCE comment to L5-04GA571 Rev. 4 (RSG-SCE/MHI-12-5746)				
6	-Revised in accordance with SCE comment to L5-04GA571 Rev. 5 (RSG-SCE/MHI-12-5755)				



Table of Contents

1	Purpose	4
2	Background	4
3	Proposed screening criteria based on Unit 3 results.....	5
4	Screening Level Selection	24
5	Screening results of Unit 2 steam generators	32
6	References	44
	Appendix-1 Screening results for Unit 3 Steam Generators	45
	Appendix-2 Evaluation of Void Fraction Distribution of U-bend Region.....	53
	Appendix-3 Additional details about the number of tube wear indications.....	59





1 Purpose

This document describes steam generator tube screening criteria that can be used as the basis for a return to service strategy. The criteria are designed to identify tubes that are susceptible to in-plane tube motion and freespan wear. Applying the screening criteria to the Unit 2 steam generators will enable Southern California Edison (SCE) to identify tubes that should be preventatively plugged before the steam generators are returned to service.

2 Background

Recent inspections of the San Onofre Nuclear Generating Station (SONGS) Unit 2 steam generators during the first refueling outage following steam generator replacement (SGR) identified the following number of tubes with wear indications (Ref.1):

2A-SG (Steam Generator 2E089): 861 tubes (See Note 1)

2B-SG (Steam Generator 2E088): 734 tubes (See Note 1)

Tubes adjacent to the retainer bars (94 tubes / SG) were plugged in both steam generators. In addition, four tubes in 2B-SG were plugged: two tubes that had wear indications with depths at or above 35% and two tubes that had wear indications with depths at or above 30% and less than 35%.

Inspections of the SONGS Unit 3 steam generators after approximately eleven months of operation following SGR identified more numerous and more severe tube wear indications than Unit 2. In particular, Unit 3 steam generators both experienced tube wear in the U-bend caused by contact with adjacent tubes. This free span tube-to-tube wear (FSW) occurred in 326 tubes (165 tubes in 3A-SG and 161 tubes in 3B-SG) (Ref.1). The consensus from industry experts is that the tube-to-tube contact was caused by in-plane fluid-elastic instability. This caused the tubes to move parallel to the anti-vibration bars (AVBs) and contact one another on the intrados and extrados of the tubes. The conclusion of in-plane tube motion was also confirmed by evidence of wear scars at AVB intersections that are longer than the width of the AVB.

The inspections of SONGS Unit 2 steam generators have identified a single pair of tubes with indications of FSW motions in 2A-SG: Column 81, Rows 111 and 113. The region of Unit 2 tubes affected by AVB wear is similar to the region in the Unit 3 steam generators that experienced AVB wear. MHI has developed empirically-based criteria based on Unit 3 results to identify



tubes that are susceptible to in-plane motion. Since the criteria are developed from Unit 3 wear data, the criteria are directly applicable to Unit 3; however, they may also be conservatively applied to Unit 2 to preventatively plug tubes as a defense-in-depth measure against tube-to-tube wear. This document describes the basis for these screening criteria.

(Note 1)

These values for number of tubes with wear indications are according to the SONGS Unit 2 In-Service Inspection (ISI) records. For the analysis performed in this report, two additional tubes in 2B-SG are included based on MHI's review of the eddy current examination. In addition, tubes that had been previously plugged (6 tubes in 2A-SG and 16 tubes in 2B-SG) are removed from consideration because they are unrelated to FSW and therefore not relevant to the screening criteria. The analysis that follows considers 855 tubes in 2A-SG and 720 tubes in 2B-SG, as shown in Table 13 and 14. For additional detail, see appendix-3.

6

3 Proposed screening criteria based on Unit 3 results

FSW tubes identified in the Unit 3 steam generators are shown in Figures 1 and 2. The FSW tubes are located in a well-defined, contiguous region of the tube bundle from row "X" through row "Y" consecutively for each column. In addition, FSW tubes exhibit specific characteristics in terms of the wear indications in affected tubes. Criteria proposed to select tubes for plugging that are potentially susceptible to FSW (in-plane motion tubes) are based on identifying the specific characteristics in the eddy current inspection data and the steam flow characteristics that could lead to potential susceptibility to the FSW phenomenon.

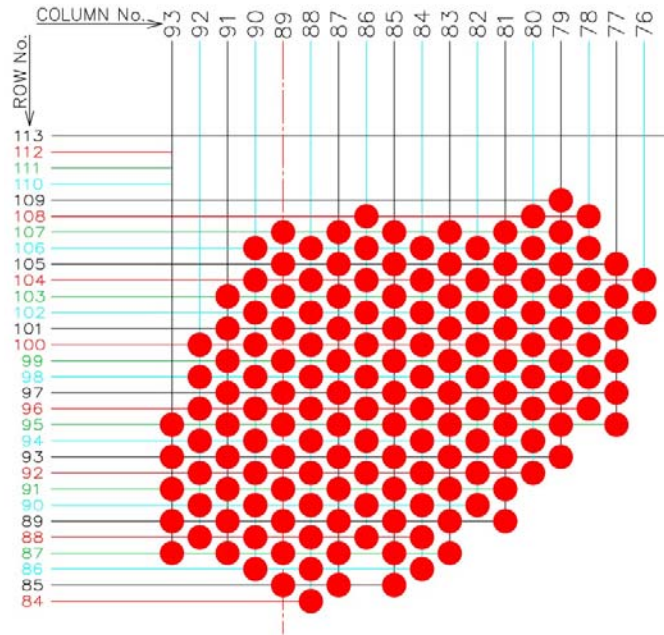


Figure 1 FSW tubes in Unit-3A

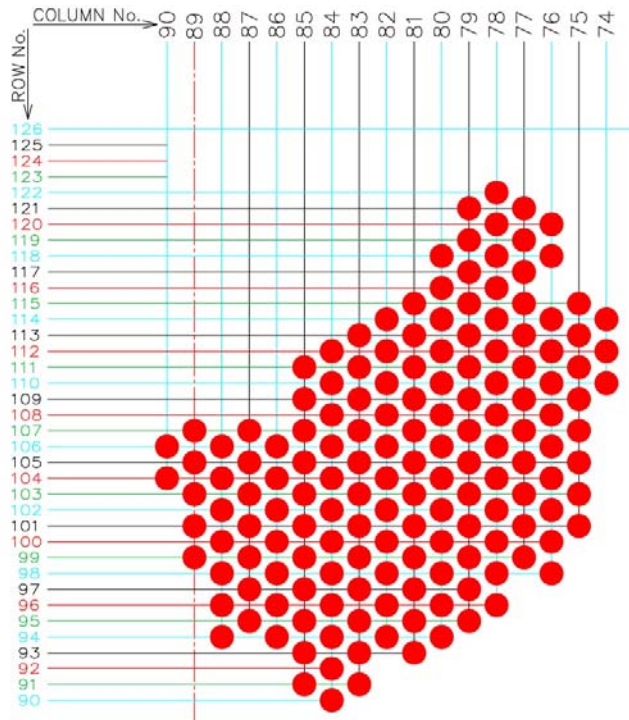


Figure 2 FSW tubes in Unit-3B



MHI developed preventive plugging screening criteria by evaluating the condition necessary to cause the FSW observed in Unit 3. Although the specific causes that resulted in tubes being susceptible to fluid-elastic excitation are not yet completely known, MHI's understanding of fluid-elastic instability and motion of the tubes is sufficient to correlate the observations from the inspections of FSW tubes with the conditions necessary to produce the vibration mechanism. The following conditions are required for, or indicative of, in-plane tube motion in the U-bend of a steam generator:

- Low friction with AVBs – Low friction allows the tube to move freely in the fundamental mode. Lower contact force between a tube and AVB will minimize friction causing high AVB wear rates to develop at these locations.
- Low vibration frequency – The critical velocity determined using Conner's equation is proportional to the vibration frequency of the tube. A low frequency of vibration decreases the velocity threshold for the onset of fluid-elastic instability.
- Low fluid damping – Loss of fluid damping contributes to instability. High steam void fraction reduces squeeze film damping between tubes and the AVBs and increases the potential for fluid-elastic excitation.
- High fluid velocities – The onset of fluid-elastic instability occurs when the steam velocity exceeds the critical velocity. Reducing the steam velocity decreases the potential for fluid-elastic instability and tube in-plane motion.

MHI created nine criteria to identify tubes that have potential for fluid-elastic instability and in-plane tube motion. Each of the nine criteria relates to one of the following characteristics of in-plane fluid-elastic vibration: (1) tube-to-AVB friction, (2) vibration frequency, (3) in-plane tube motion, (4) high void fraction, (5) regional effect, and (6) coupling effect. A screening approach was developed based on assigning a score using steam generator tube inspection data and analytically derived flow conditions. The scoring criteria are based on the FSW probability among all tubes exhibiting wear. A description of each is given below:

Tube-to-AVB friction

Tubes that experience in-plane motion must have low friction with the AVBs, otherwise tubes could not move parallel to the AVBs. Low contact force between tubes and AVBs contributes to in-plane motion leading to FSW. Tubes with wear indications at multiple AVB intersections may have reduced friction. Two criteria are proposed for identifying tubes with low tube-to-AVB



friction. The name of each criterion and a description of how they are calculated are given in Table 1.

Vibration Frequency

Steam generators are designed with multiple AVBs to minimize the span length between successive AVBs. This raises the fundamental frequency of the span between the two support locations, assuming displacements are restrained at the AVBs. The presence of AVB wear indications at the first two AVB intersections above the straight-leg portion and the presence of AVB wear indications at several successive AVB intersections suggests that the tube has limited support over the top of the tube U-bend region. Table 1 provides two criteria used to quantify susceptibility due to low tube vibration frequency.

In-Plane Tube Motion

Inspection data from the Unit 3 steam generators show a strong correlation between tubes with tube-to-tube wear indications and either TSP wear or extended AVB wear length. In FSW tubes, the largest TSP indications occur at the 7th TSP intersections; however, wear depths are similar on the hot and cold leg sides of the steam generator. Extended AVB wear length occurs as a result of differential movement between the tube and AVB. Both of these effects are associated with post-instability behavior, in that the TSP or extended AVB wear develops after the tubes have already experienced in-plane motion. Table 1 provides two criteria proposed to identify tubes that have experienced in-plane tube motion.

6

Void Fraction

The void fraction is equal to the volume of steam in the fluid normalized by the total volume of the steam/water mixture. The tubes in Unit 3 that exhibited FSW pass through a region of the U-bend where the void fraction is relatively high. High void fraction reduces vibration damping and increases a tube's susceptibility to fluid elastic instability. MHI calculated the fluid void fraction in the U-bend during power operation. The results of the analysis are included in Appendix 2. A criterion is proposed to identify tubes that are located where steam void fractions are high in the U-bend thus increasing the potential for in-plane vibration. Table 1 describes this screening factor.

Regional Effect

The majority of tubes with AVB wear indications exist in tubes that are located within a defined region in the center of the steam generator tube bundle. The boundaries of this AVB wear region



vary slightly for each steam generator, which may reflect slight differences in the mechanical configuration of the tube bundle or thermal hydraulic conditions. The FSW tubes exist in an area that is near the center of the AVB wear regions of each steam generator. MHI developed a screening criterion to more heavily weight tubes in the center of the AVB wear region as being more susceptible to in-plane motion and FSW. Table 1 describes the regional effect screening factor.

Coupling Effect

According to laboratory test results, in-plane vibration tends to occur in groups of tubes simultaneously. The Unit 3 FSW phenomenon is also strongly regionalized, to the extent that all FSW tubes are within a contiguous, bounded region. An additional screening criterion is applied to take this coupling effect between adjacent tubes into account when screening FSW tubes. Table 1 describes this screening factor.



Tables 2 through 9 include a column that calculates the ratio of FSW tubes with the screening criterion attribute (that is, the number of true positive results) to the total number of tubes in 3A/3B with the attribute. A point value is assigned, approximately equal to 1 point for each 10 percent of the calculated ratio. Additional tubes are selected by a final weighting factor, COUPLING, added to the point total after summation of the points from the first eight criteria. The point value for COUPLING is assigned based on the number of tubes previously screened in by the point system that are adjacent to the tube in question.

**Table 1** Summary of Steam Generator Tube Screening Criteria

Technical Basis	Criterion	Screening Factor
Tube-to-AVB friction	COUNT	AVB wear trends in the Unit 3 steam generators indicate that FSW tubes tend to have many AVB wear indications (See Figure 3), which indicates low contact forces at these intersections. The value assigned to COUNT is equal to the number of AVB intersections in each tube with a wear indication (See Table 2).
	HOT COUNT	AVB wear trends in the Unit 3 steam generators indicate that FSW tubes tend to have many AVB wear indications on the hot side (See Figure 4). This criterion is calculated similarly to the COUNT criterion described above; only the number of AVBs with wear indications at B01 to B06 are considered (See Table 3).
Vibration frequency	HIGH/LOW	AVB wear trends in the Unit 3 steam generators indicate that many tubes have wear indications at the low (B01/B02) and high (B11/B12) AVB intersections (See Figure 5 and Table 4.).
	CONTINUOUS	AVB wear trends in the Unit 3 steam generators indicate that FSW tubes tend to have a large number of consecutive AVB wear indications (See Figure 6 and Table 5).
In-plane tube motion	TSP	TSP wear trends in the Unit 3 steam generators indicate that most FSW tubes have wear indications at the 5 th through 7 th TSPs (See Figure 7 and Table 6).
	LENGTH	A review of AVB wear trends in the Unit 3 steam generators indicates that FSW tubes tend to have longer wear indications (See Figure 8 and Table 7).
Void fraction	VOID	The tubes with FSW indications in the Unit 3 steam generators are located where the secondary side fluid void fraction is relatively high. Void fraction and fluid damping significantly influence the vibration behavior of steam generator tubes during operation. The value assigned to VOID is the average void fraction in the U-bend (See Figure 9 and Table 8).
Regional effect	REGION	Tubes located close to the center of the AVB wear region in each steam generator tend to be more susceptible to FSW wear. The value assigned to REGION is the distance to the center of the AVB wear region (See Figure 10 and Table 9).
Coupling effect	COUPLING	As shown in Figures 1 and 2, FSW tubes exist in groups (both in row and column directions). Tubes adjacent to a group of susceptible FSW tubes have increased potential for fluid-elastic instability due to fluid coupling with susceptible tubes (See Table 10).

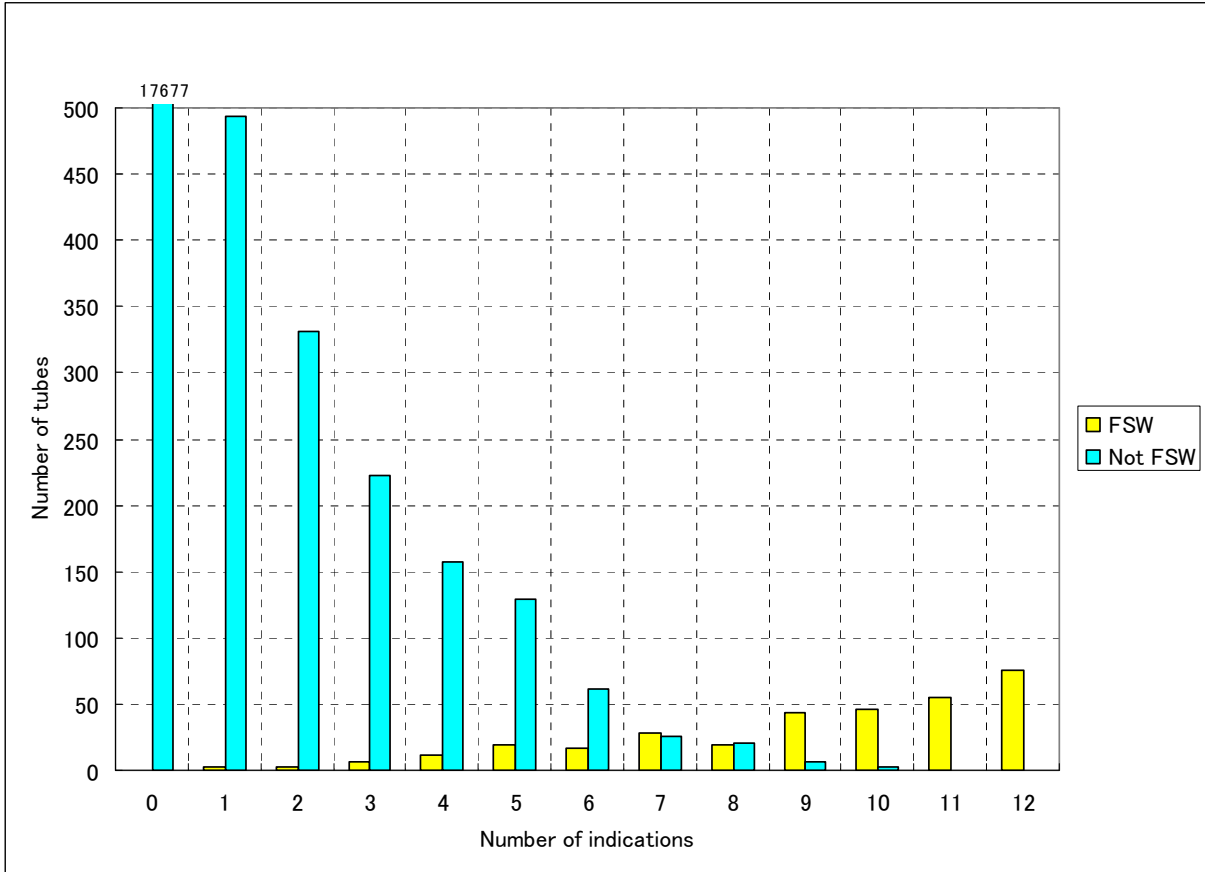


Figure 3 AVB wear indications (COUNT)

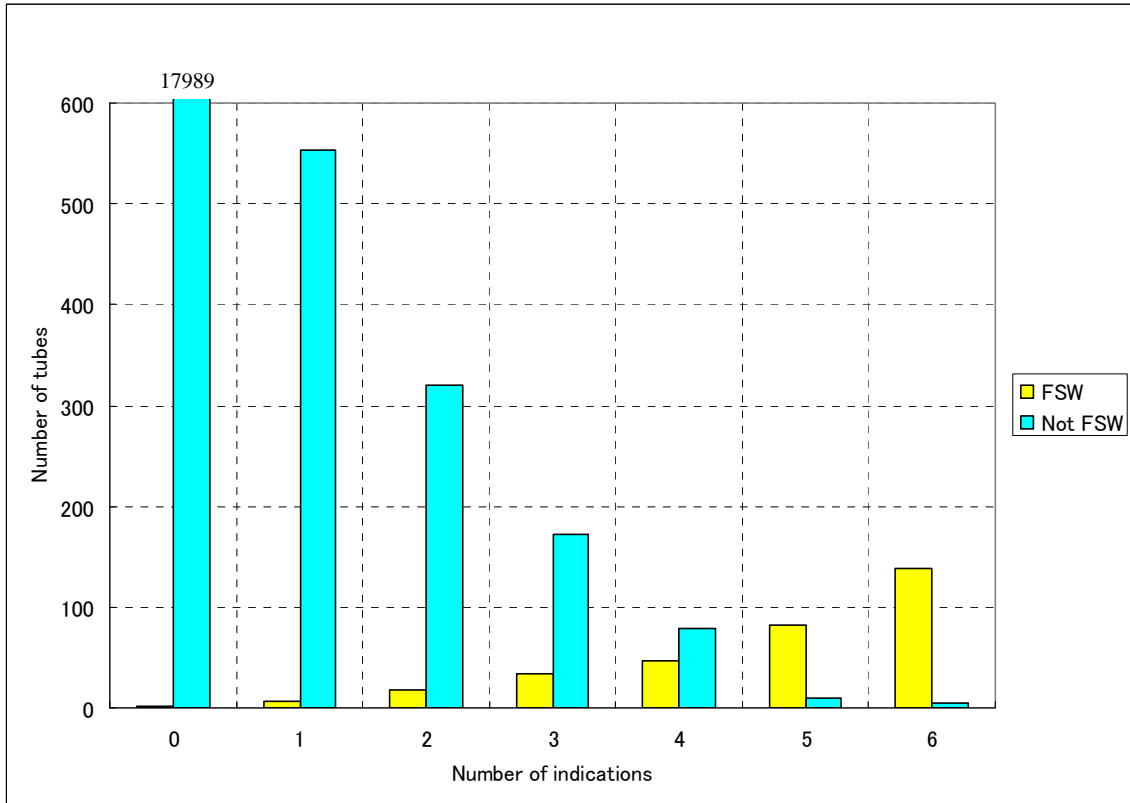


Figure 4 AVB wear indications at hot side (HOT COUNT)

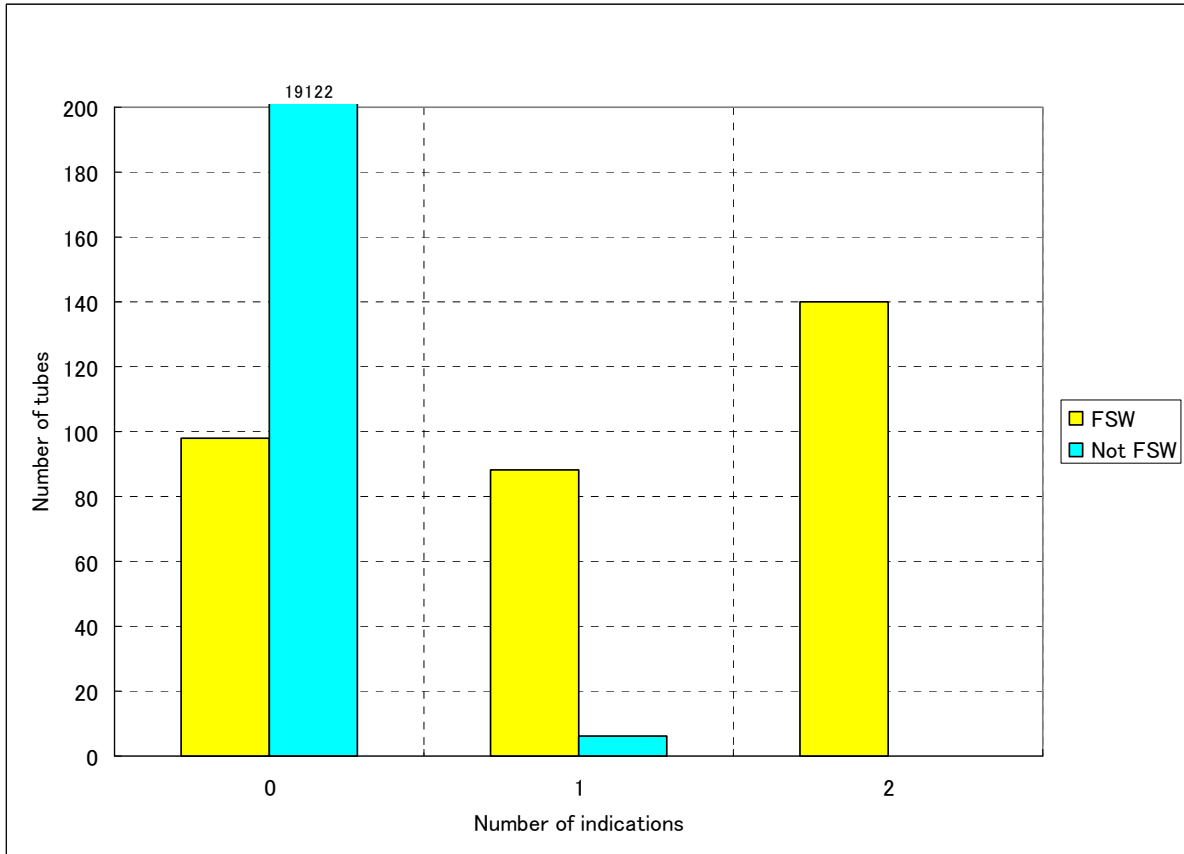


Figure 5 AVB wear indications at B01/B02 or B11/B12 positions (HIGH/LOW)

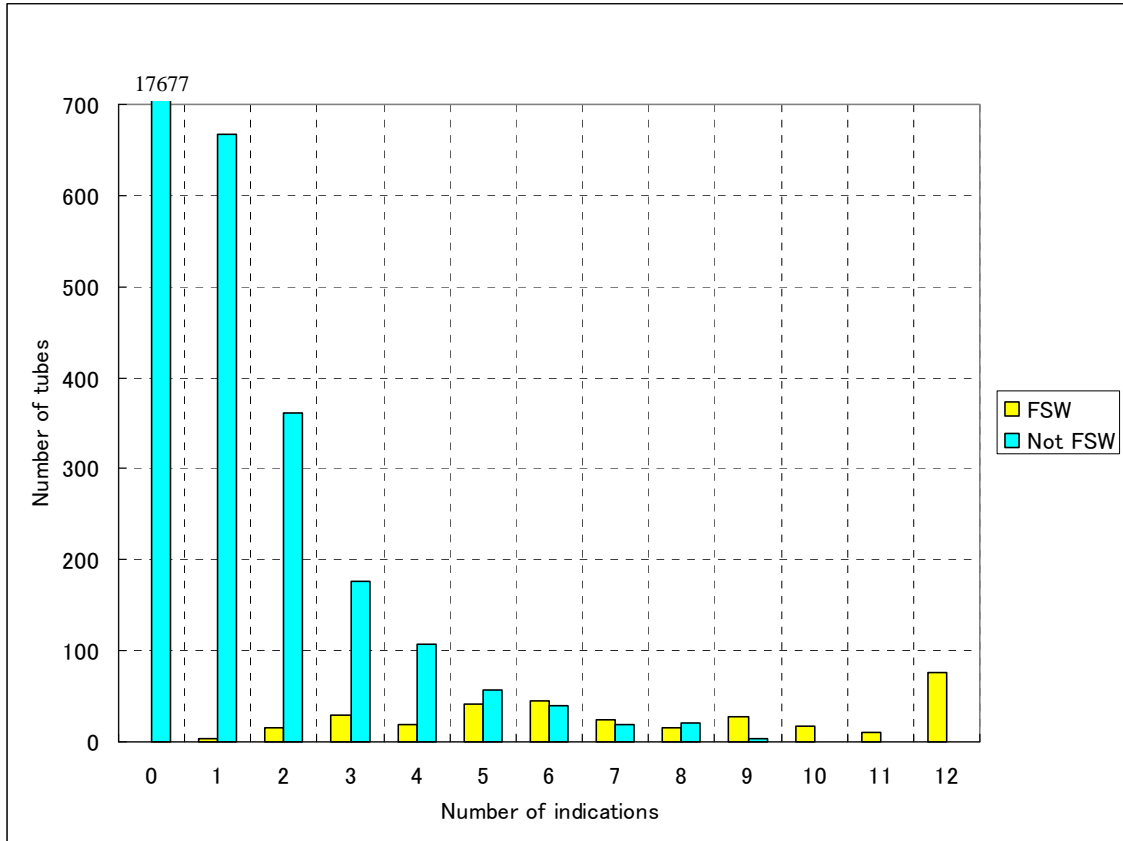


Figure 6 AVB continuous wear indications (CONTINUOUS)

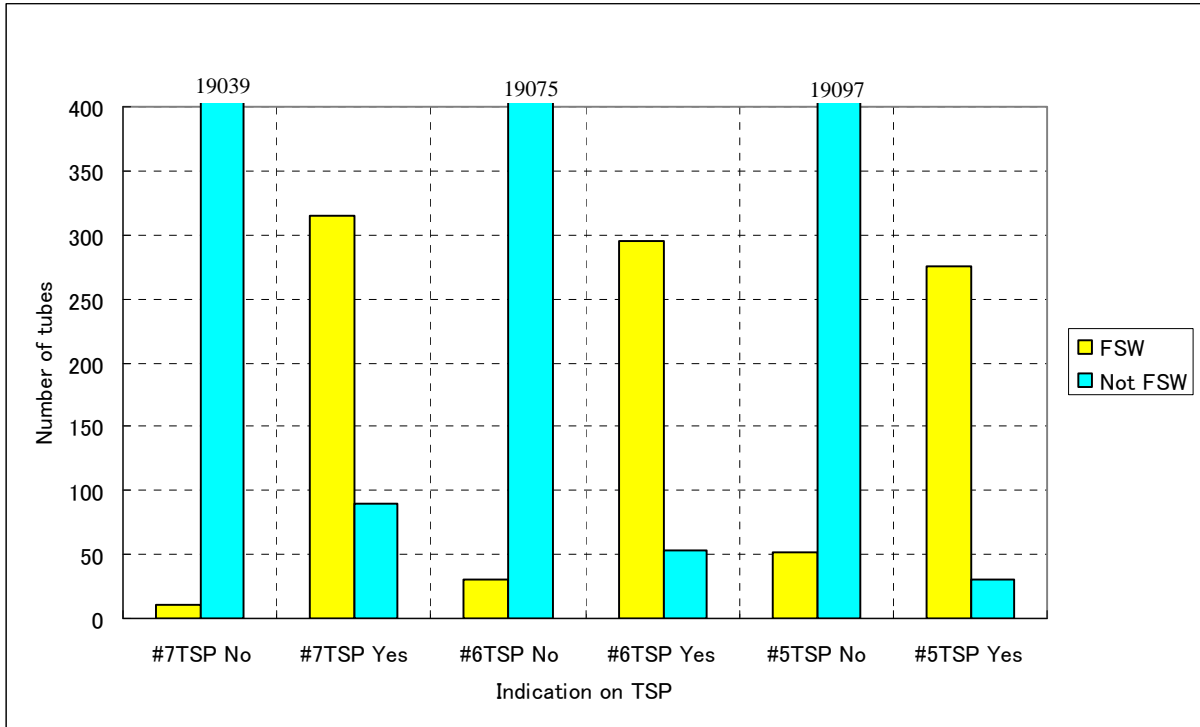


Figure 7 TSP wear (TSP)

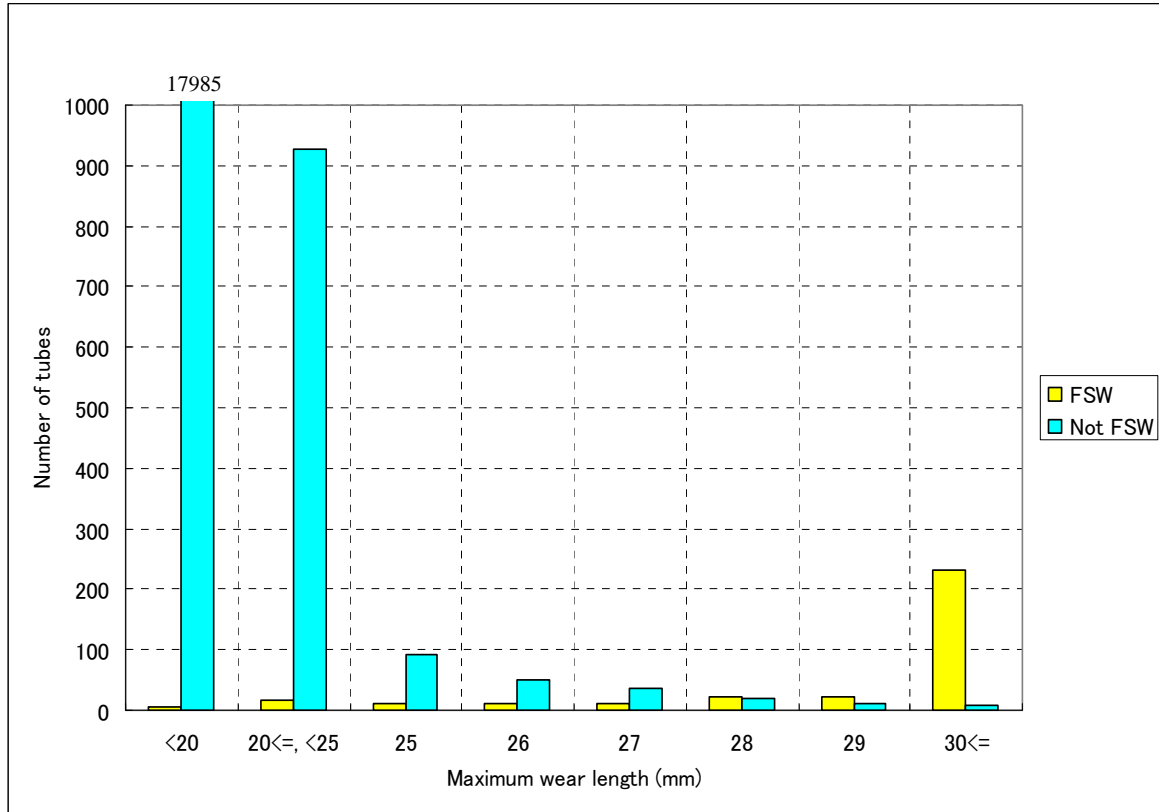


Figure 8 AVB Wear length (LENGTH)



Figure 9 Void fraction (VOID)

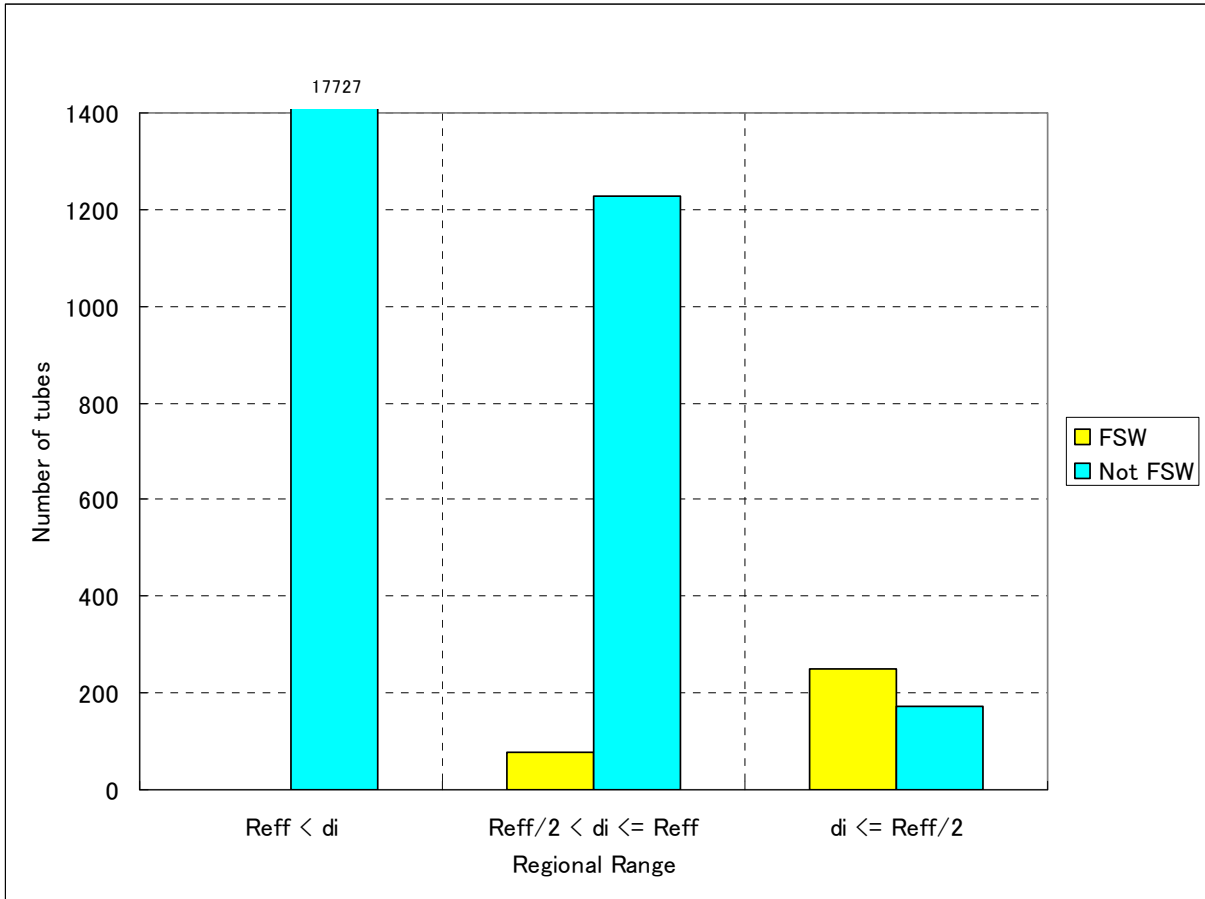


Figure 10 Regional effect (REGION)



Table 2 Number of AVB indications (COUNT)

Number of AVB Indications	Unit 3A/3B Total Tubes [A]	Unit 3A/3B FSW Tubes [B]	[B]/[A] [%]	Points Awarded
0 - 3	18736	11	0	0
4 - 6	395	47	12	1
7 - 9	144	91	63	6
10 - 12	179	177	99	10
Total	19454	326		

Table 3 Number of hot side AVB indications (HOT COUNT)

Number of AVB Indications	Unit 3A/3B Total Tubes [A]	Unit 3A/3B FSW Tubes [B]	[B]/[A] [%]	Points Awarded
0 - 2	18887	25	0	0
3 - 4	331	80	24	3
5 - 6	236	221	94	9
Total	19454	326		



Table 4 AVB wear indications at B01/B02 or B11/B12 positions (HIGH/LOW)

Number of AVB Indications	Unit 3A/3B Total Tubes [A]	Unit 3A/3B FSW Tubes [B]	[B]/[A] [%]	Points Awarded
0	19220	98	1	0
1	94	88	94	9
2	140	140	100	10
Total	19454	326		

Table 5 Number of continuous AVB indications (CONTINUOUS)

Number of AVB Indications	Unit 3A/3B Total Tubes [A]	Unit 3A/3B FSW Tubes [B]	[B]/[A] [%]	Points Awarded
0 – 2	18725	19	0	0
3 – 5	431	91	21	2
6 – 8	163	85	52	5
9 – 12	135	131	97	10
Total	19454	326		



Table 6 TSP wear (TSP)

Indication at #7TSP	Unit 3A/3B Total Tubes [A]	Unit 3A/3B FSW Tubes [B]	[B]/[A] [%]	Points Awarded
No	19050	11	0	0
Yes	404	315	78	8* ¹
Total	19454	326		
Indication at #6TSP	Unit 3A/3B Total Tubes [A]	Unit 3A/3B FSW Tubes [B]	[B]/[A] [%]	Points Awarded
No	19106	31	0	0
Yes	348	295	85	8* ¹
Total	19454	326		
Indication at #5TSP	Unit 3A/3B Total Tubes [A]	Unit 3A/3B FSW Tubes [B]	[B]/[A] [%]	Points Awarded
No	19148	51	0	0
Yes	306	275	90	9* ¹
Total	19454	326		

*1: These points are allocated for "TSP." Only the maximum value of these points is used for screening.

Table 7 Wear length (LENGTH)

Max. AVB Wear Length for Each Tube [mm]	Unit 3A/3B Total Tubes [A]	Unit 3A/3B FSW Tubes [B]	[B]/[A] [%]	Points Awarded
<20	17990	5	0	0
20<=, <25	942	16	2	0
25	103	11	11	1
26	62	11	18	2
27	45	10	22	3
28	41	21	51	5
29	31	21	68	7
30<=	240	231	96	10
Total	19454	326		



Table 8 Void fraction (VOID)

Void Fraction Range [-]	Unit 3A/3B Total Tubes [A]	Unit 3A/3B FSW Tubes [B]	[B]/[A] [%]	Points Awarded

Table 9 Regional effect (REGION)

Regional Range [-]	Unit 3A/3B Total Tubes [A]	Unit 3A/3B FSW Tubes [B]	[B]/[A] [%]	Points Awarded
$d_i \leq \text{Reff}/2$	422	250	59	6
$\text{Reff}/2 < d_i \leq \text{Reff}$	1305	76	6	1
$\text{Reff} < d_i$	17727	0	0	0
Total	19454	326		

UNIT	Reff [inch]
3A-SG	15.46
3B-SG	15.57



Table 10 Coupling effect (COUPLING)

After selection of screening level from the first eight criteria, additional points are added by the following process which accounts for "coupling effect." See Section 4 for details of this process.

0 points	5 points	10 points	
No adjacent tube	One adjacent tube	Two or more adjacent tubes	

: Tube under consideration for coupling effect
 : Screened tubes with more than 16 points



4 Screening Level Selection

The screening effectiveness using the point system for Unit 3 ECT data is checked in the following manner:

- (1) The points for each of the first eight criteria are summed for each tube. Then, the number of tubes and FSW tubes for each point category are counted to give the number of tubes falling in each point range. Table 11 shows the number of tubes with wear, the number of FSW tubes, and the number of tubes without FSW in each point range.
- (2) A screening level is selected, based on the results shown in Table 11, such that a high percentage of tubes exhibiting FSW is above the screening level.
- (3) Additional tubes are selected considering coupling effect.
- (4) A false negative check on the screening level is performed by ensuring that the point total, including coupling effect, for all tubes exhibiting FSW is above the screening level. This conservatively assures that the false negative rate for the final screening level is zero.

A listing of all tubes in the Unit 3 steam generators with tube scores greater than 16 and added tubes for the coupling effect is included in Appendix-1 with the point breakdown. Table 12 shows the non-FSW tubes in 3A-SG and 3B-SG that were screened in. Figure 12 shows that the final screening, including the coupling effect, covers all FSW tubes; that is, the false negative rate for the final screening level is zero.



Table 11 (1/2) False negative / positive check unit 3A

without coupling effect	Total Tubes	Tubes with FSW	Tubes without FSW
25 points +	158	150	8
24 points	2	1	1
23 points	3	1	2
22 points	4	0	4
21 points	4	2	2
20 points	6	1	5
19 points	2	0	2
18 points	4	1	3
17 points	14	2	12
16 points	10	1	9
15 points	9	1	8
14 points	24	2	22
13 points	10	1	9
12 points	9	1	8
11 points	13	1	12
10 points	4	0	4
9 points	43	0	43
8 points	19	0	19
7 points	8	0	8
6 points	39	0	39
5 points	39	0	39
4 points	28	0	28
3 points	215	0	215
2 points	37	0	37
1 points	47	0	47
0 points	143	0	143
Total	894	165	729

Note 1: Tubes with FSW with fewer than 16 points are False Negatives

Total False Negatives = 6

Note 2: Tubes without FSW with 16 points + are False Postivies

Total False Positives = 48

Note 3: Previously plugged tubes related to retainer bar wear (1 tube in 3A-SG) are not included in total tubes.



Table 11 (2/2) False negative / positive check unit 3B

without coupling effect	Total Tubes	Tubes with FSW	Tubes without FSW
25 points +	155	136	19
24 points	7	3	4
23 points	3	2	1
22 points	7	2	5
21 points	4	1	3
20 points	4	0	4
19 points	10	3	7
18 points	12	2	10
17 points	16	4	12
16 points	7	2	5
15 points	9	1	8
14 points	20	1	19
13 points	3	1	2
12 points	17	1	16
11 points	32	2	30
10 points	15	0	15
9 points	45	0	45
8 points	35	0	35
7 points	24	0	24
6 points	19	0	19
5 points	21	0	21
4 points	27	0	27
3 points	192	0	192
2 points	38	0	38
1 points	47	0	47
0 points	149	0	149
Total	918	161	757

Note 1: Tubes with FSW with fewer than 16 points are False Negatives

Total False Negatives = 6

Note 2: Tubes without FSW with 16 points + are False Postivies

Total False Positives = 70

Note 3: Previously plugged tubes related to retainer bar wear (3 tubes in 3B-SG) are not included in total tubes.



Unit 3A

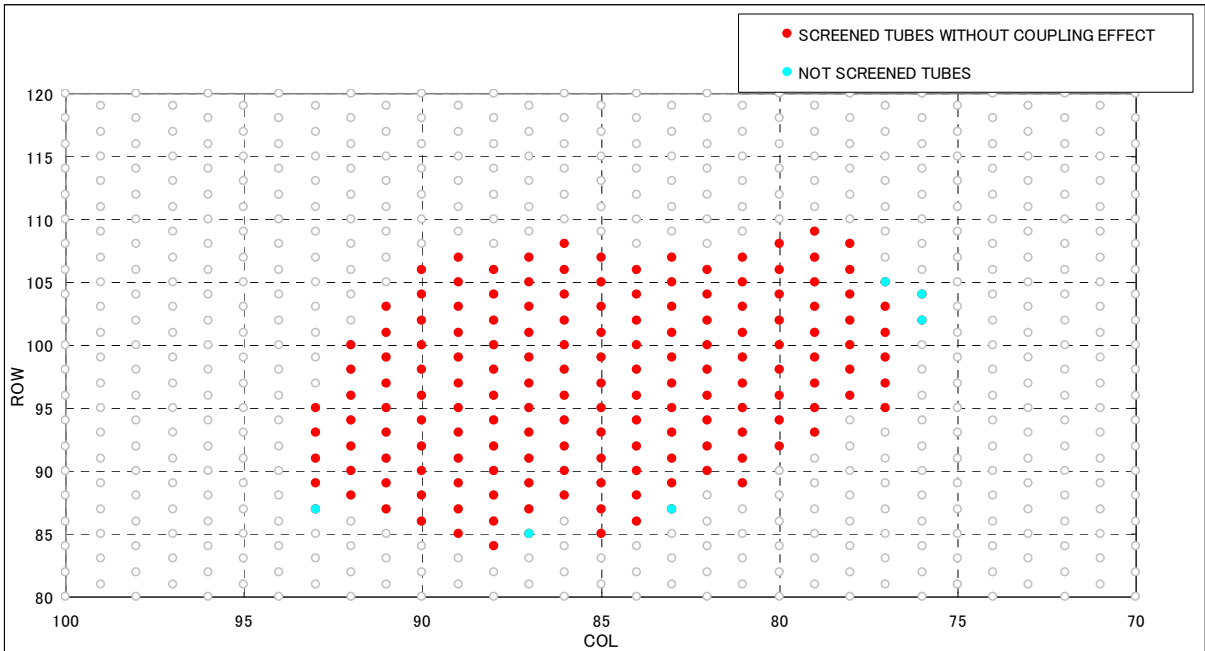
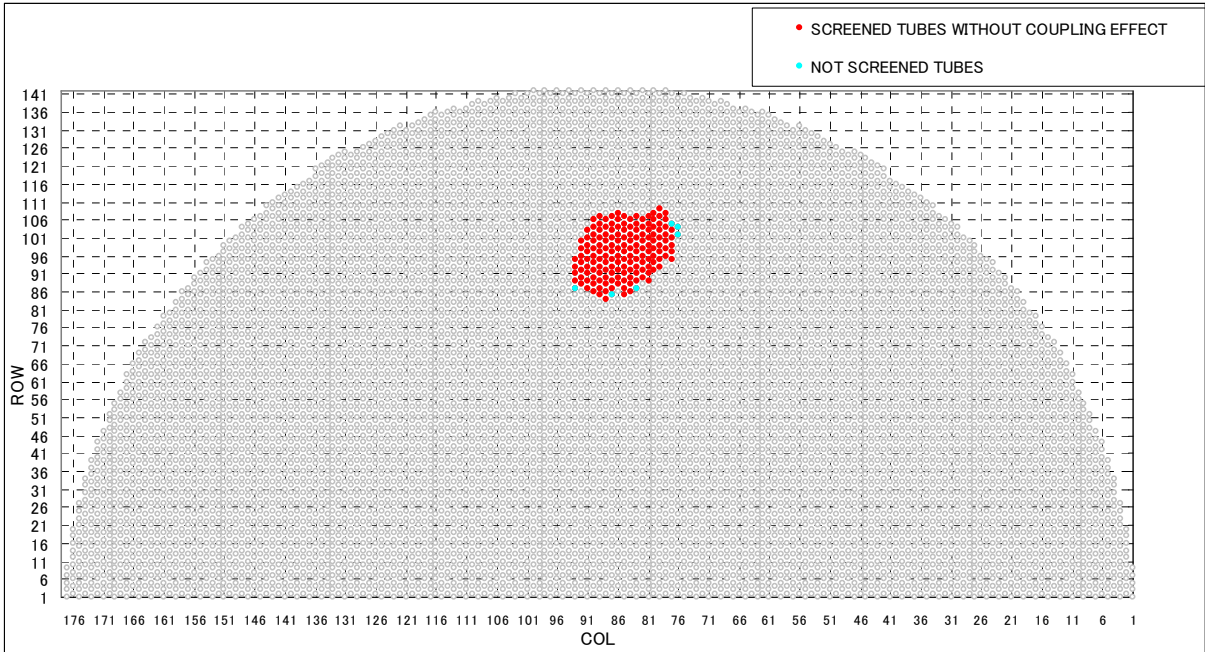


Figure 11 (1/2) False negative check (Unit 3A)



Unit 3B

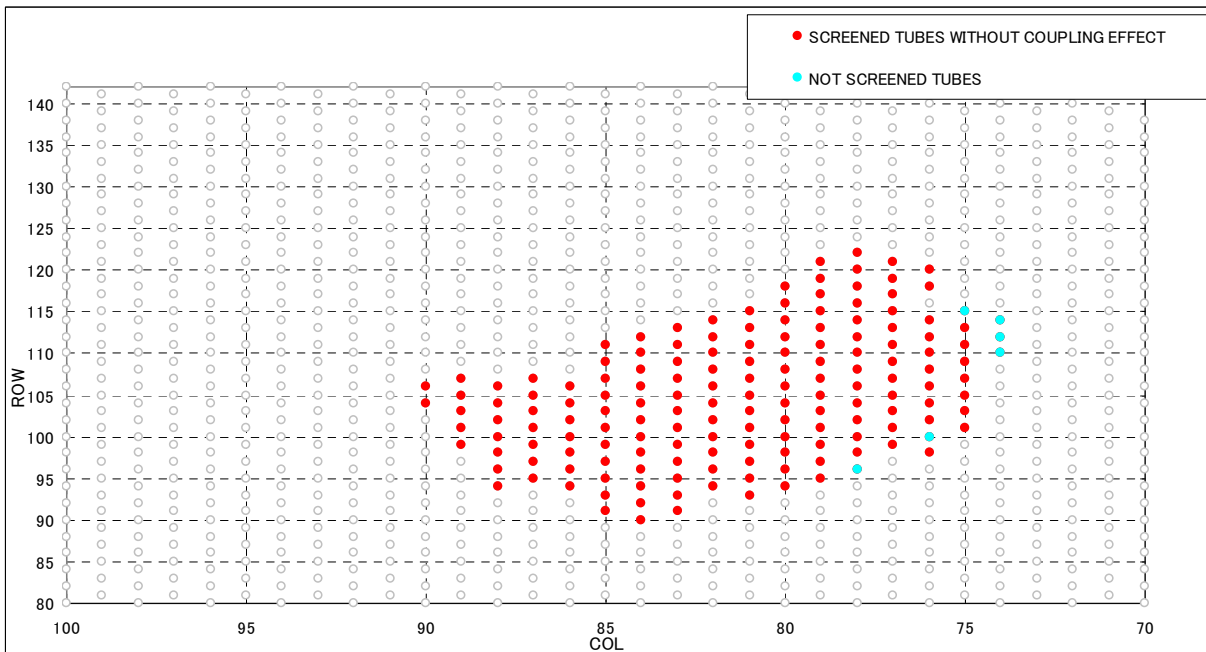
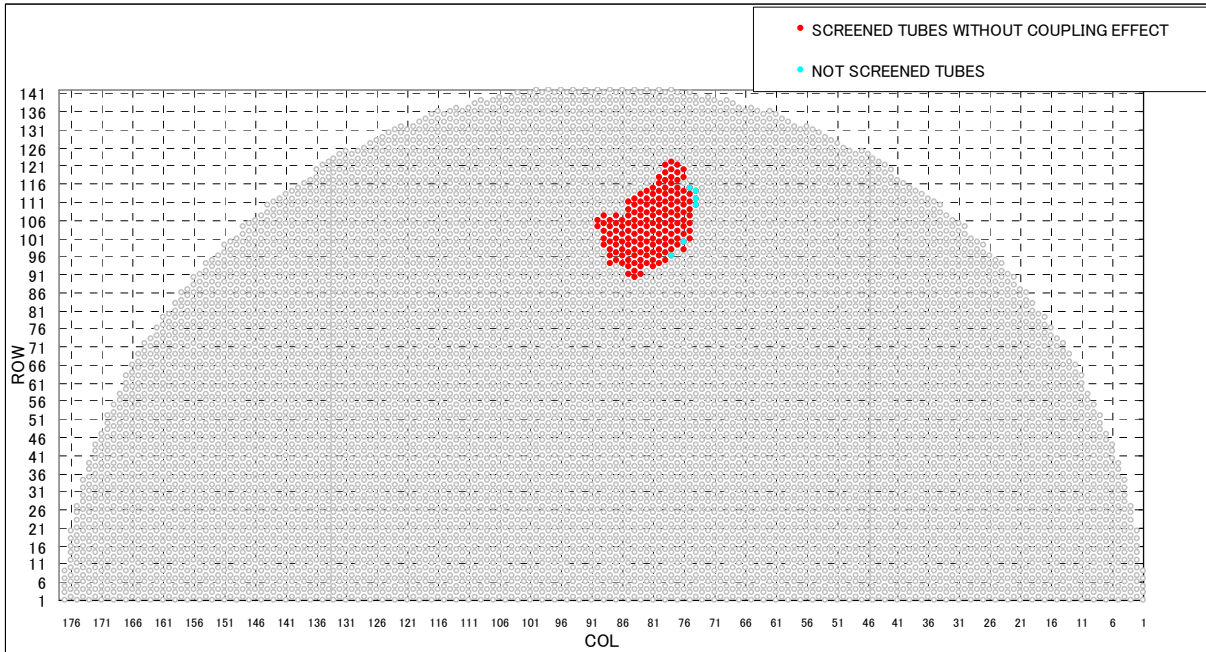


Figure 11 (2/2) False negative check (Unit 3B)



Unit 3A

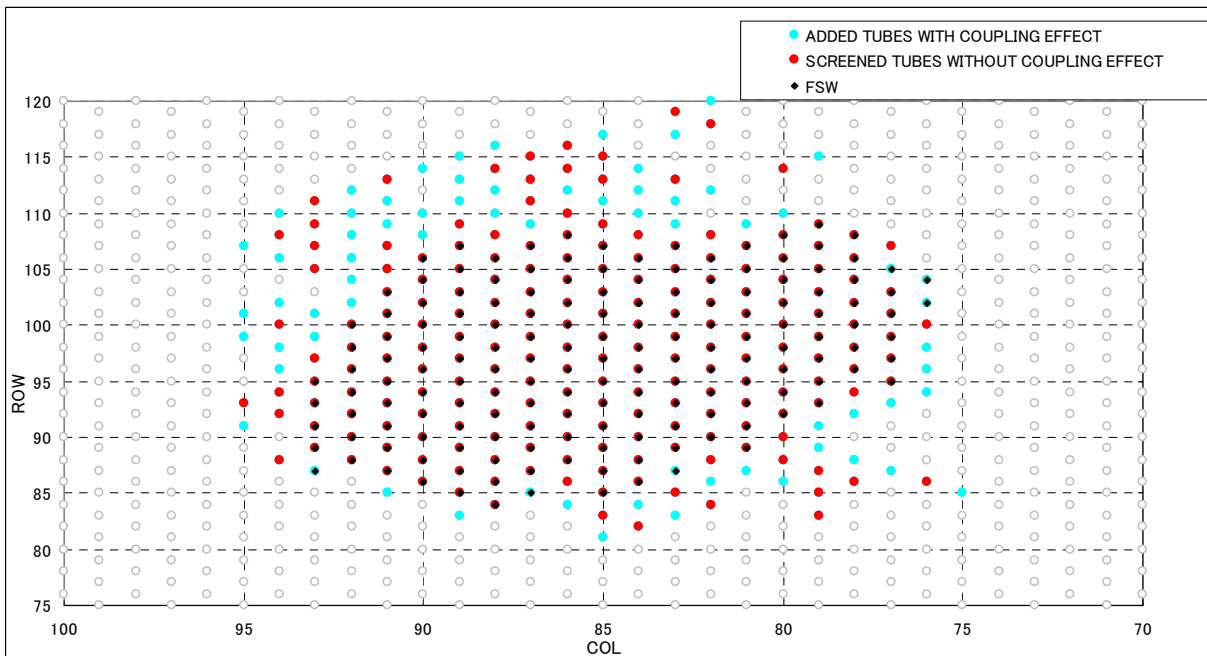
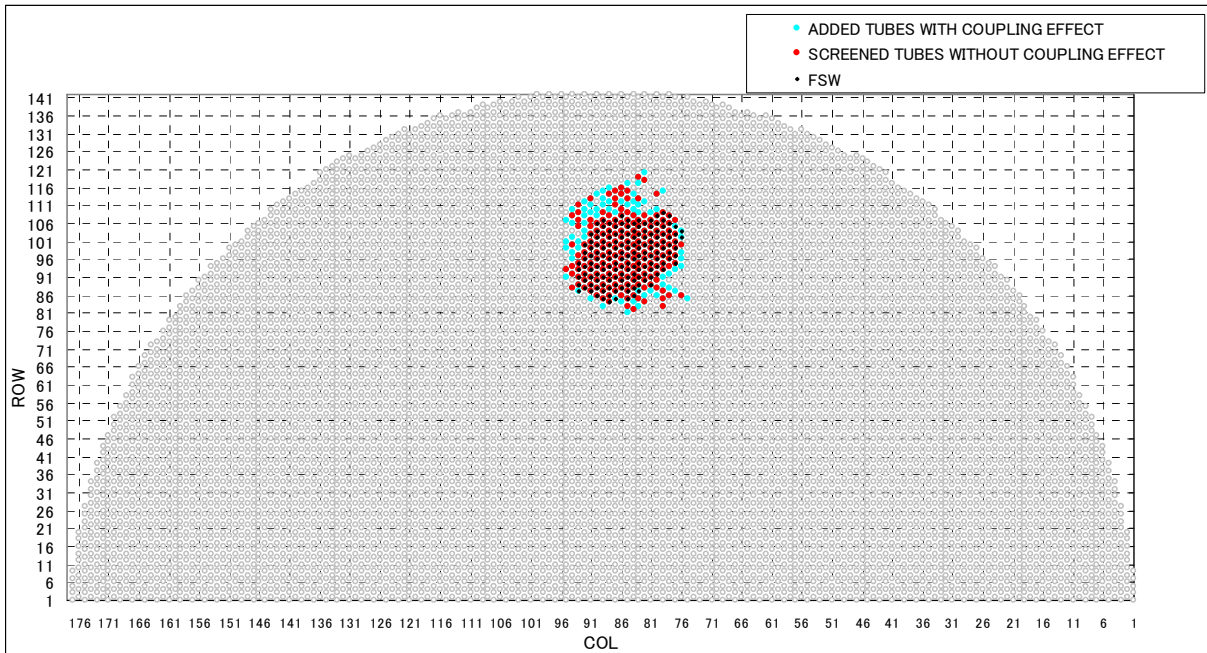


Figure 12 (1/2) False positive check (Unit 3A)



Unit 3B

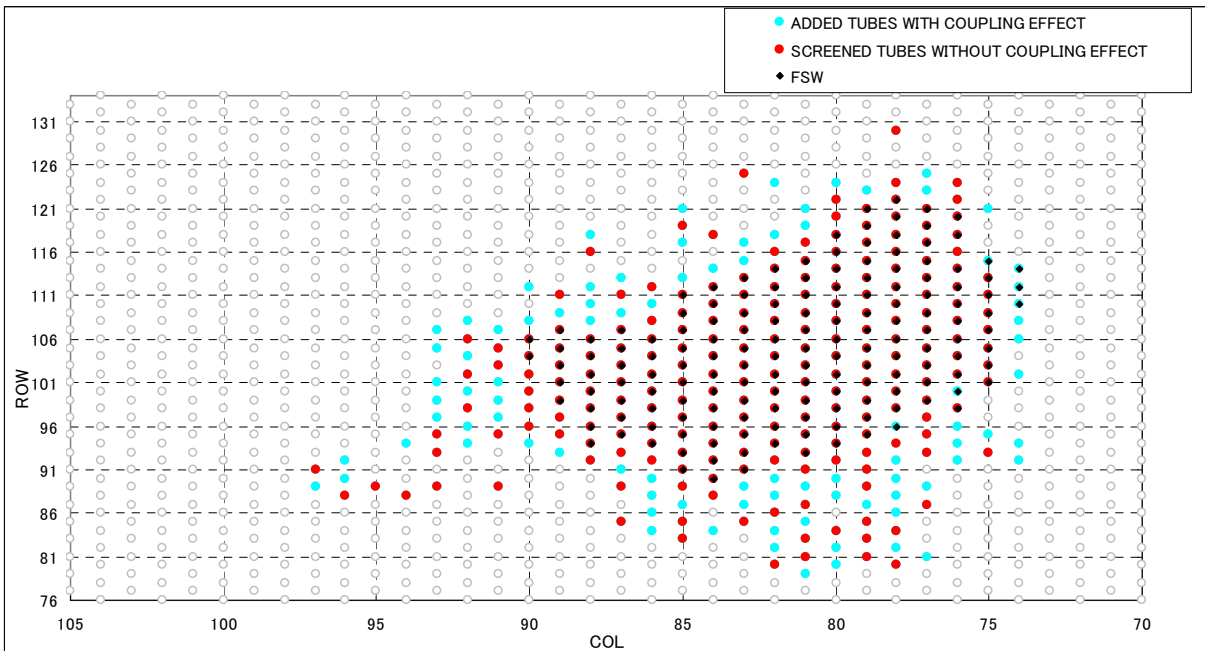
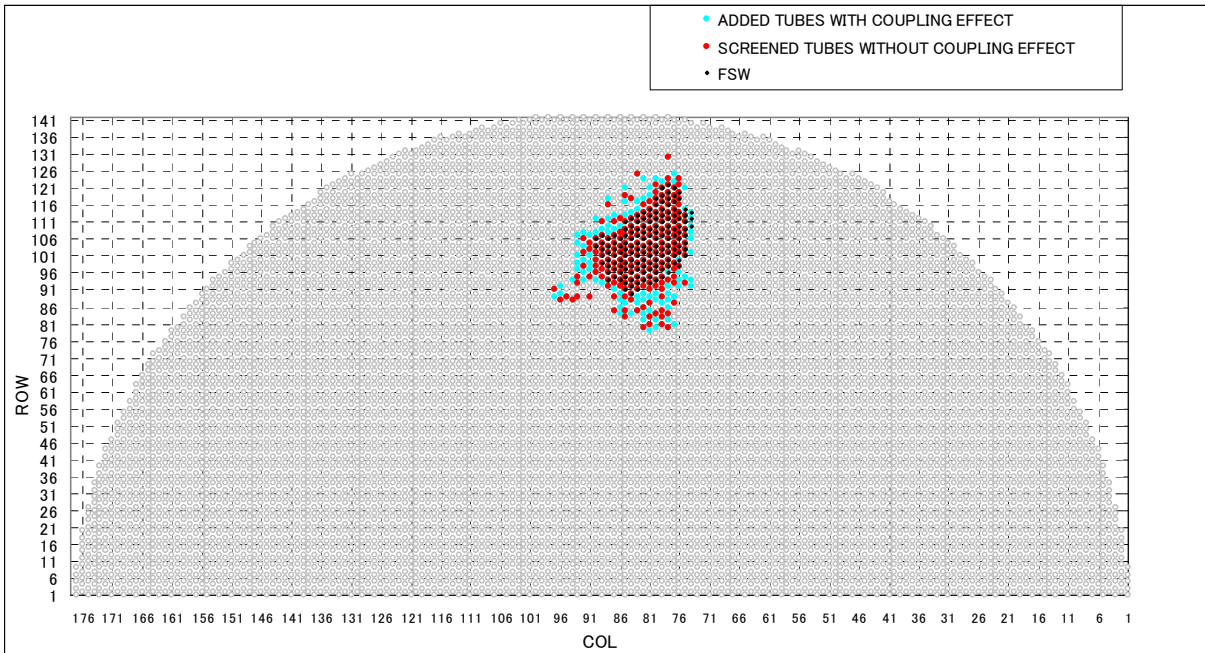


Figure 12 (2/2) False positive check (Unit 3B)



Table 12 (1/2) False positive check (Unit 3A)

	3A					
	Number of tubes (incl. FSW tubes)	Number of FSW tubes		Number of NOT FSW tubes		ratio of FSW/All tubes [B/A] [%]
		Number [A]	Number of FSW [B]	Cumulative ratio [%]	Number of NOT FSW	
Tube point 16 or over	207	159	96	48	7	77
Coupling effect	68	6	4	62	9	9
Total	275 /894	165 /165	100	110 /729	15	60

Table 12 (2/2) False positive check (Unit 3B)

	3B					
	Number of tubes (incl. FSW tubes)	Number of FSW tubes		Number of NOT FSW tubes		ratio of FSW/All tubes [B/A] [%]
		Number [A]	Number of FSW [B]	Cumulative ratio [%]	Number of NOT FSW	
Tube point 16 or over	225	155	96	70	9	69
Coupling effect	88	6	4	82	11	7
Total	313 /918	161 /161	100	152 /757	20	51



5 Screening results of Unit 2 steam generators

MHI selected a value of 16 points to apply as the screening criteria for the Unit 2 steam generators. Table 13 shows the number of tubes that screened-in without the coupling effect. Table 14 shows the number of tubes that screened-in, including tubes added with the coupling effect. A listing of all tubes in the Unit 2 steam generators with tube scores greater than 16 points and tubes added with the coupling effect is included in Tables 15 and 16 with the point break down. The screened tubes are shown in Figure 13.

The number of screened tubes for each point category on each criterion is counted and compared to the number of tubes with wear indications. If a tube has a high number of points the tubes were screened-in (See Tables 17 to 24.)

Table 13 Number of screened tubes of Unit 2 without coupling effect

without coupling effect	2A	2B
	Total Tubes	Total Tubes
16 points +	115	36
15 points	9	8
14 points	31	24
13 points	13	8
12 points	19	14
11 points	28	33
10 points	13	18
9 points	38	67
8 points	33	86
7 points	10	18
6 points	57	37
5 points	36	33
4 points	39	19
3 points	168	157
2 points	56	32
1 points	33	20
0 points	157	110
Total	855	720

Note: Previously plugged tubes related to retainer bar wear (6 tubes in 2A-SG and 12 tubes in 2B-SG) and over 30% AVB wear (4 tubes in 2B-SG) are not included in total tubes in both steam generators.



Table 14 (1/2) Number of screened tubes of Unit 2A with coupling effect

	2A					
	Number of tubes (incl. FSW tubes)	Number of FSW tubes		Number of NOT FSW tubes		ratio of FSW/All tubes [B/A] [%]
		Number [A]	Number of FSW [B]	Cumulative ratio [%]	Number of NOT FSW	
Tube point 16 or over	115	0	0	115	13	0
Coupling effect	88	2	100	86	10	2
Total	203 /855	2 /2	100	201 /853	24	1

Table 14 (2/2) Number of screened tubes of Unit 2B with coupling effect

	2B					
	Number of tubes (incl. FSW tubes)	Number of FSW tubes		Number of NOT FSW tubes		ratio of FSW/All tubes [B/A] [%]
		Number [A]	Number of FSW [B]	Cumulative ratio [%]	Number of NOT FSW	
Tube point 16 or over	36			36	5	
Coupling effect	63			63	9	
Total	99 /720	0 /0		99 /720	14	

Additional tubes in 2A-SG and 2B-SG were selected for preventative plugging even though they were below the screening level of 16 points (see Tables 15 and 16). These tubes were selected for preventative plugging because they had seven or more AVB indications. All other tubes with seven or more AVB indications screened in.



Table 15 Tubes recommended for plugging in Unit 2A

No.	Tube		Tube-to-AVB friction		Vibration frequency		In-plane tube motion		Void fraction	Regional effect	Coupling effect	Total
	Row	Col	COUNT	HOT COUNT	HIGH/LOW	CONTINUOUS	TSP (Max Wear Rate at #5-#7TSP)	MAX LENGTH on AVB WEAR	VOID	REGION	COUPLING	
1	88	86	6	3	0	5	0	0	2	1	0	19
2	90	82	1	0	0	2	0	3	2	1	10	19
3	90	84	1	0	0	2	9	0	2	1	10	25
4	91	81	1	0	0	2	0	2	2	1	10	18
5	91	83	6	3	0	5	0	0	2	1	10	27
6	91	85	6	3	0	5	0	2	2	1	10	29
7	92	80	1	0	0	2	0	2	2	1	10	16
8	92	82	1	3	0	5	8	3	2	1	10	33
9	92	84	6	3	0	5	0	0	2	1	10	27
10	92	86	1	3	0	2	0	0	2	1	10	19
11	93	81	1	0	0	2	8	2	2	1	10	26
12	93	83	1	0	0	2	0	2	2	6	10	23
13	93	85	1	3	0	5	0	3	2	6	10	30
14	93	87	1	0	0	2	8	1	2	6	10	30
15	94	80	6	3	0	5	0	0	2	1	5	22
16	94	82	1	0	0	2	0	7	2	6	10	28
17	94	84	1	3	0	2	0	2	2	6	10	26
18	94	86	6	3	0	5	8	3	2	6	10	43
19	94	88	6	3	0	5	0	0	2	6	10	32
20	95	81	1	0	0	2	0	1	2	6	10	22
21	95	83	1	1	0	2	0	2	2	6	10	23
22	95	85	1	3	0	2	9	3	2	6	10	36
23	95	87	0	0	0	2	8	0	2	6	10	28
24	95	89	6	3	0	5	8	1	2	6	5	36
25	96	80	1	0	0	2	0	0	2	6	5	16
26	96	82	1	3	0	2	0	0	2	6	10	24
27	96	84	1	0	0	2	0	1	2	6	10	22
28	96	86	1	3	0	2	0	0	2	6	10	24
29	96	88	1	3	0	2	0	0	2	6	10	24
30	97	79	1	0	0	2	0	0	2	6	5	16
31	97	81	1	0	0	2	0	0	2	6	10	21
32	97	83	1	0	0	5	0	0	2	6	10	24
33	97	85	6	3	0	5	0	0	2	6	10	32
34	97	87	1	3	0	5	8	0	2	6	10	35
35	97	89	1	3	0	2	0	0	2	6	10	24
36	98	80	1	0	0	2	0	0	2	6	10	21
37	98	82	6	3	0	5	0	0	2	6	10	32
38	98	84	6	3	0	5	0	1	2	6	10	33
39	98	86	6	3	0	5	0	0	2	6	10	32
40	98	88	6	3	0	5	0	0	2	6	10	32
41	98	92	1	3	0	2	9	0	2	1	0	18
42	99	79	1	3	0	5	0	1	2	6	0	18
43	99	81	6	3	0	5	0	2	2	6	10	34
44	99	83	6	3	0	5	0	2	2	6	10	35
45	99	85	6	3	0	5	0	7	2	6	10	39
46	99	87	1	3	0	5	0	2	2	6	10	29
47	99	89	6	3	0	5	0	2	2	6	10	34
48	99	91	1	0	0	2	0	2	2	6	5	18
49	100	78	1	0	0	2	0	0	2	6	10	21
50	100	80	1	0	0	2	0	2	2	6	10	23
51	100	82	1	0	0	5	0	7	2	6	10	31
52	100	84	6	3	0	5	0	3	2	6	10	35
53	100	86	1	3	0	5	0	1	2	6	10	28
54	100	88	6	3	0	5	0	1	2	6	10	33
55	100	90	1	0	0	2	0	1	2	6	10	22
56	101	79	1	0	0	2	0	0	2	6	10	21
57	101	81	1	3	0	5	0	0	2	6	10	27
58	101	83	6	3	0	5	0	3	2	6	10	49
59	101	85	6	3	0	5	0	5	2	6	10	37
60	101	87	1	0	0	2	0	0	2	6	10	21
61	101	89	6	3	0	5	0	0	2	6	10	32
62	102	78	1	0	0	2	0	5	2	6	0	16
63	102	80	1	0	0	2	0	3	2	6	5	19
64	102	82	6	3	0	5	0	3	2	6	10	35
65	102	84	6	3	0	5	0	3	2	6	10	35
66	102	86	6	3	0	5	0	3	2	6	10	35
67	102	88	6	3	0	5	0	1	2	6	10	33
68	102	90	1	0	0	2	0	0	2	6	10	21
69	102	94	1	0	0	2	0	1	2	1	10	17
70	103	77	1	3	0	2	0	0	2	6	5	19
71	103	81	1	0	0	2	0	1	2	6	10	22
72	103	83	1	0	0	5	0	2	2	6	10	29
73	103	85	1	3	0	5	0	5	2	6	10	32
74	103	87	1	3	0	5	0	1	2	6	10	28
75	103	89	1	3	0	5	0	0	2	6	10	27
76	103	93	0	0	0	0	9	0	2	6	0	17
77	103	95	1	3	0	2	8	0	2	1	0	17
78	104	78	1	0	0	2	0	1	2	6	5	17
79	104	82	1	3	0	5	0	1	2	6	10	28
80	104	84	1	3	0	5	0	2	2	6	10	29
81	104	86	6	3	0	5	0	2	2	6	10	34
82	104	88	1	3	0	5	0	1	2	6	10	28
83	104	90	1	3	0	2	0	0	2	6	10	24
84	104	92	1	3	0	2	0	1	2	6	5	20
85	105	81	1	0	0	2	0	3	2	6	10	24
86	105	83	6	3	0	5	0	5	2	6	10	37
87	105	85	6	9	0	5	9	5	2	6	10	52
88	105	87	1	3	0	2	0	3	2	6	10	27
89	105	89	1	3	0	2	0	2	2	6	10	26
90	105	91	0	0	0	2	0	3	2	6	5	18
91	105	95	0	0	0	0	0	3	2	1	10	16
92	106	82	1	3	0	5	0	1	2	6	10	28
93	106	84	6	3	0	5	0	1	2	6	10	33
94	106	86	1	3	0	2	8	0	2	6	10	32
95	106	88	1	0	0	2	0	0	2	6	10	24
96	106	90	1	3	0	2	0	0	2	6	10	24
97	107	81	1	0	0	2	0	3	2	6	10	24
98	107	83	1	0	0	2	0	0	2	6	10	24
99	107	85	6	3	0	5	0	0	2	6	10	32
100	107	87	1	0	0	2	0	7	2	6	10	28
101	107	89	1	3	0	2	0	0	2	6	10	24
102	107	91	1	0	0	2	0	5	2	6	10	26
103	107	95	1	3	0	2	9	0	2	1	0	18
104	108	78	1	0	0	2	0	2	2	6	5	18
105	108	82	6	9	0	5	0	3	2	6	10	41



No.	Tube		Tube-to-AVB friction		Vibration frequency		In-plane tube motion		Void fraction	Regional effect	Coupling effect	Total
	Row	Col	COUNT	HOT COUNT	HIGH/LOW	CONTINUOUS	TSP (Max Wear Rate at #5-#7TSP)	MAX LENGTH on AVB WEAR	VOID	REGION	COUPLING	
106	108	84	1	0	0	2	0	1	2	6	10	22
107	108	86	1	3	0	5	0	0	2	6	10	27
108	108	88	1	3	0	2	0	0	2	6	10	21
109	108	90	1	3	0	5	0	2	2	6	10	29
110	108	92	1	0	0	0	0	0	2	6	10	19
111	109	77	1	0	0	2	0	1	2	6	10	22
112	109	81	1	0	0	2	9	0	2	6	10	30
113	109	83	6	3	0	5	0	1	2	6	10	33
114	109	85	1	0	0	2	8	0	2	6	10	29
115	109	87	1	3	0	2	0	1	2	6	10	25
116	109	89	1	3	0	5	0	0	2	6	10	27
117	109	91	1	3	0	2	1	1	2	6	10	33
118	109	95	0	0	0	0	9	0	2	1	5	17
119	109	97	0	0	0	0	9	0	2	1	5	17
120	110	78	1	0	0	2	9	7	2	6	10	32
121	110	80	1	0	0	2	0	1	2	6	10	22
122	110	82	1	3	0	2	0	3	2	6	10	27
123	110	84	1	3	0	5	0	1	2	6	10	28
124	110	86	1	3	0	2	8	1	2	6	10	33
125	110	88	1	3	0	5	0	2	2	6	10	29
126	110	90	0	0	0	0	0	0	2	6	10	18
127	110	98	1	3	0	2	9	0	2	1	0	18
128	111	77	1	3	0	5	0	1	2	6	5	23
129	111	79	0	0	0	0	0	0	2	6	10	18
130	111	81	1	0	0	2	0	0	2	6	10	21
131	111	83	1	0	0	2	0	0	2	6	10	21
132	111	85	1	0	0	2	0	0	2	6	10	21
133	111	87	0	0	0	2	0	0	2	6	10	20
134	111	89	1	3	0	5	8	0	2	6	10	35
135	112	78	1	0	0	2	0	0	2	6	10	21
136	112	80	0	0	0	0	8	0	2	6	0	16
137	112	82	6	3	0	5	8	1	2	6	10	41
138	112	84	6	3	0	5	8	1	2	6	10	41
139	112	86	1	3	0	2	0	1	2	6	10	25
140	112	88	6	3	0	5	0	1	2	6	10	33
141	112	90	1	3	0	2	0	0	2	6	10	24
142	112	98	0	0	0	0	8	0	2	1	5	16
143	113	81	0	0	0	2	0	0	2	6	10	20
144	113	83	6	3	0	5	0	0	2	6	10	32
145	113	85	6	3	0	5	0	2	2	6	10	34
146	113	87	1	0	0	2	0	0	2	6	10	24
147	113	89	1	3	0	5	0	0	2	6	10	27
148	113	91	0	0	0	0	0	0	2	6	10	18
149	114	80	0	0	0	0	0	0	2	6	10	18
150	114	82	1	3	0	2	0	0	2	6	10	24
151	114	84	6	9	0	5	0	0	2	6	10	38
152	114	86	1	0	0	2	8	0	2	6	10	29
153	114	88	6	0	0	5	8	0	2	6	10	37
154	114	90	1	3	0	5	0	0	2	6	10	27
155	114	92	1	3	0	2	0	0	2	6	5	19
156	114	94	1	3	0	2	8	0	2	1	5	22
157	115	81	6	3	0	5	0	0	2	6	5	27
158	115	83	6	3	0	5	0	0	2	6	10	32
159	115	85	6	9	0	5	0	0	2	6	10	38
160	115	87	1	1	0	2	0	0	2	6	10	27
161	115	89	1	3	0	5	8	0	2	6	10	32
162	115	91	0	0	0	2	9	0	2	6	10	29
163	115	93	1	3	0	2	0	0	2	1	10	19
164	115	95	1	0	0	2	0	0	2	1	10	16
165	116	82	1	3	0	2	8	0	2	6	10	32
166	116	84	6	3	0	5	0	0	2	6	10	32
167	116	86	1	3	0	5	8	0	2	6	10	35
168	116	88	1	3	0	5	0	0	2	6	10	27
169	116	90	1	3	0	5	8	0	2	6	10	35
170	116	92	1	3	0	5	0	0	2	1	5	17
171	116	94	1	3	0	5	8	0	2	1	5	25
172	117	81	1	0	0	2	0	0	2	6	10	24
173	117	83	1	0	0	2	0	0	2	6	10	21
174	117	85	6	3	0	5	0	1	2	6	10	33
175	117	87	1	0	0	2	8	0	2	6	10	29
176	117	89	1	3	0	2	0	0	2	6	10	24
177	117	91	0	0	0	0	0	0	2	6	10	18
178	118	82	1	3	0	5	0	0	2	6	10	27
179	118	84	1	3	0	2	0	0	2	6	10	24
180	118	86	1	3	0	2	0	0	2	6	10	24
181	118	88	1	0	0	2	0	0	2	6	10	21
182	118	90	1	3	0	2	0	1	2	6	5	20
183	119	81	1	3	0	2	0	0	2	6	10	24
184	119	83	1	3	0	2	0	0	2	6	10	24
185	119	85	0	0	0	2	0	0	2	6	10	20
186	119	87	1	0	0	2	0	0	2	6	5	16
187	120	82	1	3	0	5	0	2	2	6	10	29
188	120	84	1	3	0	5	0	0	2	6	0	17
189	121	81	1	0	0	2	0	0	2	1	10	16
190	121	83	1	0	0	0	0	3	2	6	10	22
191	121	85	1	0	0	2	0	0	2	6	5	16
192	122	82	6	3	0	5	0	2	2	1	5	24
193	123	91	6	3	0	5	0	0	2	1	0	17
194	126	84	1	3	0	2	8	0	2	1	0	17
195	127	85	6	3	0	2	0	0	2	1	5	19
196	128	84	1	3	0	5	0	0	2	1	5	17
197	129	87	1	3	0	5	8	0	2	1	5	20
198	130	86	1	0	0	2	9	0	2	1	5	19
199	130	90	1	3	0	2	0	3	2	1	5	17
200	131	89	1	0	0	2	8	1	2	1	5	20
201	132	84	6	0	0	5	8	1	0	1	0	21
202	132	90	6	3	0	5	0	2	0	1	5	22
203	134	90	6	3	0	5	8	0	0	1	5	28
204	122*	86*	6	0	0	5	0	0	2	1	0	14
205	138*	88*	6	3	0	5	0	0	0	0	0	14

* This tube is additionally selected.



Table 16 Tubes recommended for plugging in Unit 2B

No.	Tube		Tube-to-AVB friction		Vibration frequency		In-plane tube motion		Void fraction	Regional effect	Coupling effect	Total
	Row	Col	COUNT	HOT COUNT	HIGH/LOW	CONTINUOUS	TSP (Max Wear Rate at #5-#7TSP)	MAX LENGTH on AVB WEAR	VOID	REGION	COUPLING	
1	94	90	6	3	0	5	0	3	2	1	0	20
2	94	94	6	3	0	5	8	3	2	1	0	25
3	95	89	1	3	0	5	0	0	2	1	5	17
4	95	91	1	3	0	2	0	2	2	1	5	16
5	97	85	6	3	0	5	0	1	2	1	0	18
6	98	86	1	3	0	5	0	0	2	1	5	17
7	98	92	1	0	0	2	0	7	2	1	5	18
8	99	85	1	3	0	5	0	1	2	1	5	18
9	99	93	6	3	0	5	9	7	2	1	0	33
10	100	86	1	3	0	5	0	1	2	1	5	18
11	100	88	1	3	0	2	0	1	2	6	5	20
12	100	90	1	3	0	2	0	1	2	6	5	20
13	100	92	1	0	0	2	0	1	2	1	10	17
14	101	87	1	3	0	5	0	0	2	6	0	17
15	101	89	1	0	0	0	0	0	2	6	10	19
16	101	91	0	0	0	2	0	0	2	6	10	20
17	101	93	1	0	0	5	0	0	2	1	10	19
18	102	86	0	0	0	0	0	0	2	6	10	18
19	102	88	1	3	0	2	0	1	2	6	10	25
20	102	90	1	3	0	2	8	0	2	6	10	32
21	102	92	6	3	0	5	8	2	2	6	5	37
22	103	85	1	0	0	0	0	2	2	6	10	21
23	103	87	0	0	0	2	0	0	2	6	10	20
24	103	89	6	3	0	5	0	1	2	6	10	33
25	103	91	1	3	0	2	0	5	2	6	10	29
26	103	93	1	0	0	0	3	2	2	6	5	19
27	104	84	1	3	0	5	0	0	2	6	10	27
28	104	86	1	3	0	5	0	1	2	6	5	24
29	104	88	1	0	0	2	0	1	2	6	10	22
30	104	90	6	3	0	2	0	1	2	6	10	29
31	104	92	1	0	0	5	0	1	2	6	10	25
32	105	83	0	0	0	0	0	0	2	6	10	18
33	105	85	6	3	0	5	0	0	2	6	10	32
34	105	87	1	3	0	2	0	1	2	6	5	20
35	105	89	1	3	0	5	0	2	2	6	10	29
36	105	91	0	0	0	0	0	1	2	6	10	19
37	106	84	6	3	0	5	0	0	2	6	10	32
38	106	86	1	0	0	0	0	0	2	6	10	19
39	106	88	1	0	0	5	0	1	2	6	5	20
40	106	90	0	0	0	0	0	0	2	6	10	18
41	106	92	1	0	0	2	9	0	2	6	0	20
42	107	83	0	0	0	0	0	0	2	6	5	16
43	107	85	6	3	0	5	0	3	2	6	10	35
44	107	89	1	0	0	2	0	3	2	6	5	19
45	107	91	1	0	0	2	0	2	2	6	5	18
46	107	93	1	0	0	2	0	1	2	6	5	17
47	108	84	1	0	0	2	0	0	2	6	10	21
48	108	86	1	3	0	2	0	0	2	6	5	19
49	108	92	0	0	0	0	0	0	2	6	10	18
50	109	91	1	0	0	2	0	0	2	6	5	16
51	110	88	1	0	0	2	0	0	2	6	10	21
52	110	90	1	0	0	2	0	1	2	6	5	17
53	110	92	1	0	0	0	8	0	2	6	5	22
54	111	87	1	3	0	5	0	1	2	6	0	19
55	111	89	1	3	0	2	0	2	2	6	0	16
56	111	91	1	0	0	2	0	3	2	6	10	24
57	111	93	0	0	0	0	0	1	2	6	10	19
58	112	86	1	3	0	2	0	0	2	6	10	24
59	112	90	1	3	0	2	0	0	2	6	10	24
60	112	92	6	3	0	5	0	1	2	6	10	33
61	113	87	1	0	0	2	0	1	2	6	10	22
62	113	89	1	0	0	2	0	1	2	6	10	22
63	113	91	6	3	0	5	0	1	2	6	10	33
64	114	86	6	3	0	5	0	0	2	6	0	22
65	114	88	1	3	0	2	0	0	2	6	5	19
66	114	90	1	3	0	2	8	0	2	6	10	32
67	114	92	0	0	0	0	0	0	2	6	10	18
68	115	85	1	0	0	2	0	0	2	6	5	16
69	115	87	1	0	0	5	0	0	2	6	5	19
70	115	89	6	3	0	5	0	2	2	6	5	29
71	115	91	1	0	0	2	0	0	2	6	10	21
72	116	86	1	3	0	2	0	0	2	6	5	19
73	116	88	1	0	0	2	0	0	2	6	10	21
74	116	90	1	3	0	2	0	0	2	6	10	24
75	116	92	6	3	0	5	0	0	2	6	5	27
76	117	89	1	0	0	5	0	0	2	6	10	24
77	117	91	1	0	0	2	0	0	2	6	10	21
78	117	93	1	0	0	2	0	0	2	6	10	21
79	118	88	6	3	0	5	0	0	2	6	0	22
80	118	92	6	3	0	5	0	0	2	6	5	27
81	119	89	1	0	0	2	0	0	2	6	5	16
82	120	82	0	0	0	0	8	0	2	1	5	16
83	120	88	0	0	0	2	0	0	2	6	10	20
84	121	81	1	3	0	2	9	0	2	1	0	18
85	121	85	0	0	0	0	0	0	2	6	10	18
86	121	87	1	3	0	2	0	0	2	6	10	24
87	121	89	0	0	0	0	0	0	2	6	10	18
88	122	84	0	0	0	2	9	0	2	6	0	19
89	122	86	1	3	0	5	0	0	2	6	0	17
90	122	88	1	3	0	5	0	0	2	6	5	22
91	123	85	1	3	0	2	0	0	2	6	10	24
92	123	87	0	0	0	0	0	0	2	6	10	18
93	123	89	1	0	0	2	9	0	2	6	5	25
94	124	86	0	0	0	0	0	0	2	6	10	18
95	124	88	0	0	0	0	0	0	2	6	10	18
96	125	87	1	3	0	2	0	0	2	6	5	19
97	126	86	6	3	0	5	0	0	2	1	0	17
98	129	93	1	3	0	5	8	0	2	1	0	20
99	133	85	6	3	0	5	9	0	0	1	0	24
100	127*	89*	6	3	0	2	0	0	2	1	0	14
101	136*	92*	6	3	0	2	0	1	0	1	0	13

* This tube is additionally selected.



Unit 2A

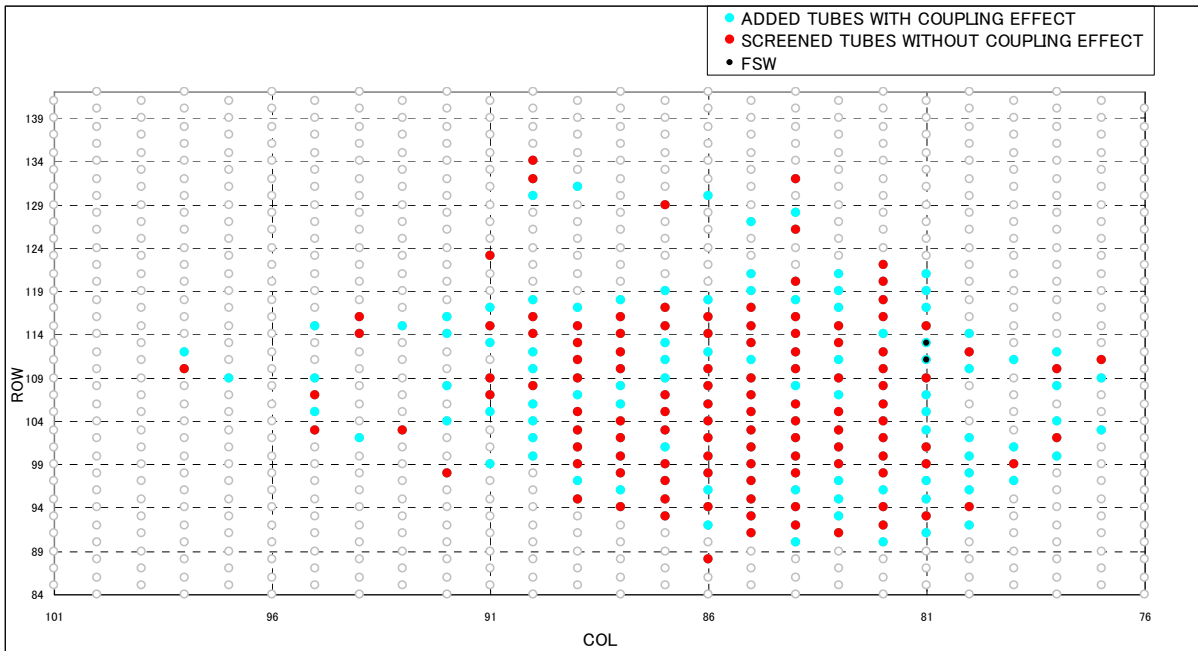
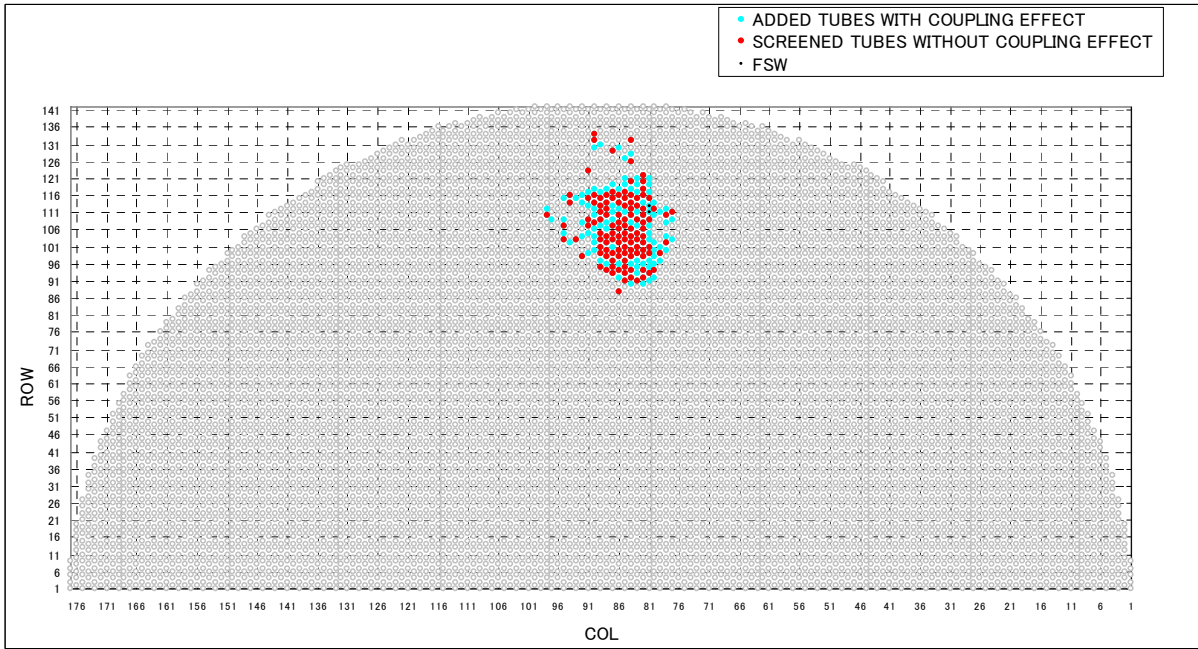


Figure 13 (1/2) Screened tubes (Unit 2A)



Unit 2B

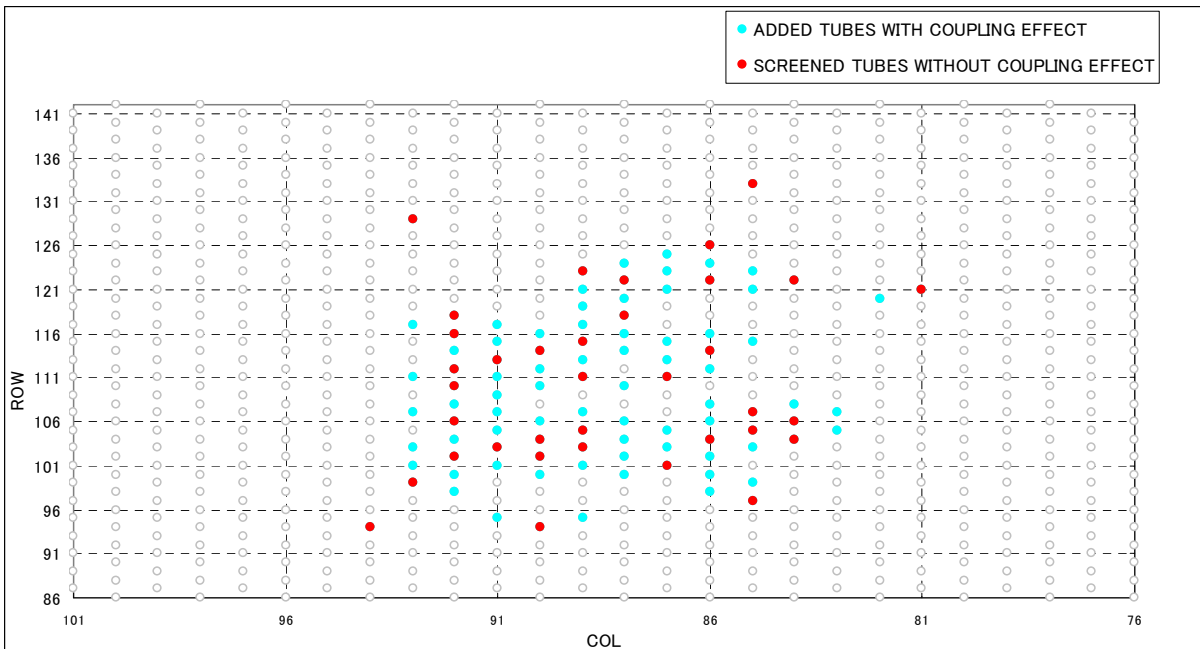
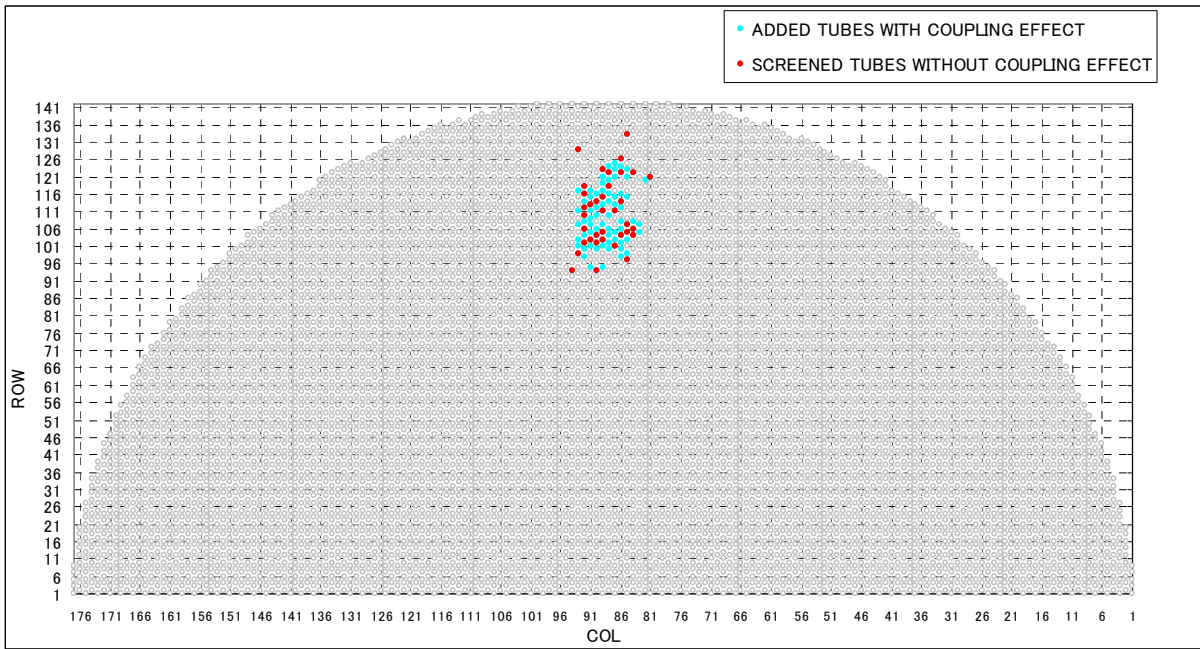


Figure 13 (2/2) Screened tubes (Unit 2B)



Table 17 Number of AVB indications (COUNT)

Number of AVB Indications	2A			2B		
	Number of Tubes [A1]	Break down of screened Tubes [B1]	Rate [B1]/[A1] %	Number of Tubes [A2]	Break down of screened Tubes [B2]	Rate [B2]/[A2] %
0	8923	0	0	9136	0	0
1	207	1	0	176	2	1
2	131	3	2	110	6	5
3	136	13	10	98	10	10
4	127	36	28	75	14	19
5	87	51	59	74	23	31
6	63	48	76	37	25	68
7	32	30	94	17	15	88
8	20	20	100	4	4	100
9	1	1	100	0	0	0
10	0	0	0	0	0	0
11	0	0	0	0	0	0
12	0	0	0	0	0	0
Total	9727	203		9727	99	

Table 18 Number of hot side AVB indications (HOT COUNT)

Number of AVB Indications	2A			2B		
	Number of Tubes [A1]	Break down of screened Tubes [B1]	Rate [B1]/[A1] %	Number of Tubes [A2]	Break down of screened Tubes [B2]	Rate [B2]/[A2] %
0	9103	0	0	9302	5	0
1	285	14	5	200	11	6
2	195	65	33	137	32	23
3	84	68	81	69	41	59
4	55	51	93	19	10	53
5	5	5	100	0	0	0
6	0	0	0	0	0	0
Total	9727	203		9727	99	



Table 19 AVB wear indications at B01/B02 or B11/B12 positions (HIGH/LOW)

Number of AVB Indications	2A			2B		
	Number of Tubes [A1]	Break down of screened Tubes [B1]	Rate [B1]/[A1] %	Number of Tubes [A2]	Break down of screened Tubes [B2]	Rate [B2]/[A2] %
0	9727	203	2	9727	99	1
1	0	0	0	0	0	0
2	0	0	0	0	0	0
Total	9727	203		9727	99	

Table 20 Number of continuous AVB indications (CONTINUOUS)

Number of AVB Indications	2A			2B		
	Number of Tubes [A1]	Break down of screened Tubes [B1]	Rate [B1]/[A1] %	Number of Tubes [A2]	Break down of screened Tubes [B2]	Rate [B2]/[A2] %
0	8923	0	0	9136	0	0
1	260	4	2	226	7	3
2	165	9	5	136	11	8
3	114	25	22	92	18	20
4	101	37	37	51	8	16
5	66	38	58	45	20	44
6	56	48	86	25	19	76
7	25	25	100	13	13	100
8	17	17	100	3	3	100
9	0	0	0	0	0	0
10	0	0	0	0	0	0
11	0	0	0	0	0	0
12	0	0	0	0	0	0
Total	9727	203		9727	99	



Table 21 TSP wear (TSP)

Indication at #7TSP	2A			2B		
	Number of Tubes [A1]	Break down of screened Tubes [B1]	Rate [B1]/[A1] %	Number of Tubes [A2]	Break down of screened Tubes [B2]	Rate [B2]/[A2] %
YES	40	23	58	32	8	25
NO	9687	180	2	9695	91	1
Total	9727	203		9727	99	
Indication at #6TSP	Number of Tubes [A1]	Break down of screened Tubes [B1]	Rate [B1]/[A1] %	Number of Tubes [A2]	Break down of screened Tubes [B2]	Rate [B2]/[A2] %
YES	30	18	60	40	1	3
NO	9697	185	2	9687	98	1
Total	9727	203		9727	99	
Indication at #5TSP	Number of Tubes [A1]	Break down of screened Tubes [B1]	Rate [B1]/[A1] %	Number of Tubes [A2]	Break down of screened Tubes [B2]	Rate [B2]/[A2] %
YES	30	12	40	47	6	13
NO	9697	191	2	9680	93	1
Total	9727	203		9727	99	



Table22 Wear length (LENGTH)

Max. AVB Wear Length for Each Tube [mm]	2A			2B		
	Number of Tubes [A1]	Break down of screened Tubes [B1]	Rate [B1]/[A1] %	Number of Tubes [A2]	Break down of screened Tubes [B2]	Rate [B2]/[A2] %
<25	9576	112	1	9623	61	1
25	73	36	49	59	20	34
26	41	23	56	23	9	39
27	26	21	81	15	6	40
28	6	6	100	4	1	25
29	5	5	100	3	2	67
30 or over	0	0	0	0	0	0
Total	9727	203		9727	99	

Table23 Void fraction (VOID)

Void Fraction Range [-]	2A			2B		
	Number of Tubes [A1]	Break down of screened Tubes [B1]	Rate [B1]/[A1] %	Number of Tubes [A2]	Break down of screened Tubes [B2]	Rate [B2]/[A2] %



Table 24 Regional effect (REGION)

Regional Range [-]	2A			2B		
	Number of Tubes [A1]	Break down of screened Tubes [B1]	Rate [B1]/[A1] %	Number of Tubes [A2]	Break down of screened Tubes [B2]	Rate [B2]/[A2] %
0	8958	0	0	9078	0	0
1	570	39	7	486	17	3
6	199	164	82	163	82	50
Total	9727	203		9727	99	



6 References

1. Letter RSG-SCE/MHI-12-5749, from D. Calhoun (SCE) to T. Kodama (MHI), August 3, 2012, Subject: "Updated ECT Data for Input to Return to Service and Repair Design Documents."
2. Letter RSG-SCE/MHI-12-5688, from D. Calhoun (SCE) to T. Kodama (MHI), March 22, 2012, Subject: "ECT Data for Input to Return to Service and Repair Design Documents."

6



Appendix-1

Screening results for Unit 3 Steam Generators

A listing of all tubes in the Unit 3 steam generators with tube scores greater than 16 and added tubes with the coupling effect is included in Table A-1, A-2 with the point break down.



Appendix-1

Table A-1 Screened tubes for Unit 3A

No.	Tube		Tube-to-AVB friction		Vibration frequency		In-plane tube motion		Void fraction	Regional effect	Coupling effect	Total
	Row	Col	COUNT	HOT COUNT	HIGH/LOW	CONTINUOUS	TSP (Max Wear Rate at #5-#7TSP)	MAX LENGTH on AVB WEAR	VOID	REGION	COUPLING	
1	81	85	1	0	0	2	0	0	2	1	10	16
2	82	84	6	3	0	5	0	0	2	1	5	22
3	83	79	1	3	0	2	8	0	2	1	5	22
4	83	83	1	3	0	2	0	0	2	1	10	19
5	83	85	6	9	0	5	0	0	2	1	10	33
6	83	89	1	3	0	5	0	0	2	1	10	19
7	84	82	1	3	0	5	0	0	2	1	5	25
8	84	84	1	3	0	5	0	0	2	1	10	22
9	84	86	1	0	0	2	9	0	2	1	10	25
10	84	88	1	3	0	2	8	0	2	1	10	27
11	85	75	1	0	0	0	9	0	0	1	5	16
12	85	79	1	3	0	2	9	0	2	1	10	28
13	85	83	6	3	0	5	0	2	2	1	10	29
14	85	85	1	3	0	2	9	0	2	1	10	28
15	85	87	0	0	0	0	9	0	2	1	10	22
16	85	89	1	3	0	2	9	10	2	1	10	38
17	85	91	0	0	0	0	8	0	2	1	10	21
18	86	76	1	3	0	5	9	7	0	1	0	26
19	86	78	1	3	0	2	8	1	2	1	10	28
20	86	80	1	3	0	5	0	1	2	1	10	23
21	86	82	1	3	0	5	0	1	2	1	10	23
22	86	84	6	3	0	5	8	5	2	1	10	40
23	86	86	0	0	0	0	8	5	2	6	10	31
24	86	88	6	3	0	2	9	10	2	6	10	48
25	86	90	1	3	0	2	9	7	2	1	10	35
26	87	77	1	0	0	2	0	0	2	1	10	16
27	87	79	1	3	0	2	8	0	2	1	10	27
28	87	81	1	0	0	2	8	0	2	1	10	24
29	87	83	1	0	0	2	8	0	2	1	10	24
30	87	85	6	9	9	10	9	10	2	6	10	71
31	87	87	6	9	9	10	9	10	2	6	10	71
32	87	89	6	9	9	10	9	5	2	6	10	52
33	87	91	1	3	0	5	10	2	1	1	10	36
34	87	93	0	0	0	0	8	0	2	1	10	21
35	88	78	1	3	0	2	0	0	2	1	10	19
36	88	80	1	3	0	2	8	0	2	1	10	27
37	88	82	1	3	0	2	9	2	2	1	10	30
38	88	84	1	3	0	2	9	3	2	6	10	36
39	88	86	6	9	9	5	9	10	2	6	10	66
40	88	88	10	9	9	5	9	10	2	6	10	70
41	88	90	6	3	9	5	9	10	2	6	10	60
42	88	92	6	3	0	5	9	10	2	1	10	46
43	88	94	0	0	0	0	8	5	2	1	5	21
44	89	79	1	3	0	2	0	2	1	1	10	19
45	89	81	6	3	0	2	8	2	2	1	10	34
46	89	83	1	3	0	9	2	0	2	1	10	42
47	89	85	10	9	9	10	9	0	2	6	10	68
48	89	87	6	9	9	2	9	7	2	6	10	60
49	89	89	10	9	9	10	9	2	2	6	10	67
50	89	91	6	9	9	5	9	5	2	6	10	61
51	89	93	1	3	0	0	9	0	2	1	10	26
52	90	80	6	9	9	5	8	3	2	1	10	53
53	90	82	6	3	0	2	9	0	2	6	10	38
54	90	84	6	9	9	5	9	5	2	6	10	61
55	90	86	10	9	10	10	9	10	2	6	10	76
56	90	88	10	9	10	10	9	10	2	6	10	76
57	90	90	6	9	9	2	9	0	2	6	10	53
58	90	92	1	3	0	9	0	2	2	6	10	33
59	91	79	0	0	0	0	9	0	2	1	10	22
60	91	81	10	9	9	10	9	7	2	1	10	72
61	91	83	6	9	9	10	9	10	2	6	10	71
62	91	85	10	9	9	10	9	10	2	6	10	75
63	91	87	10	9	10	10	9	10	2	6	10	76
64	91	89	10	9	10	5	9	10	2	6	10	71
65	91	91	10	9	10	10	9	10	2	6	10	76
66	91	93	6	9	9	2	9	10	2	6	10	63
67	91	95	1	3	0	2	0	2	2	1	10	21
68	92	78	1	0	0	2	8	1	2	1	10	25
69	92	80	1	3	0	0	9	10	2	6	10	41
70	92	82	10	9	10	10	9	10	2	6	10	76
71	92	84	6	9	9	5	9	10	2	6	10	66
72	92	86	10	9	10	5	9	10	2	6	10	71
73	92	88	6	9	9	10	9	10	2	6	10	71
74	92	90	10	9	9	10	9	10	2	6	10	75
75	92	92	6	9	9	10	9	10	2	6	10	71
76	92	94	0	0	0	0	8	0	2	6	10	26
77	93	77	0	0	0	0	9	0	2	1	10	22
78	93	79	1	9	0	2	9	10	2	1	10	44
79	93	81	10	9	9	10	9	10	2	6	10	75
80	93	83	10	9	9	10	9	10	2	6	10	75
81	93	85	10	9	10	10	9	10	2	6	10	76
82	93	87	10	9	9	10	9	10	2	6	10	75
83	93	89	10	9	10	5	9	10	2	6	10	76
84	93	91	10	9	10	5	9	10	2	6	10	71
85	93	93	10	9	10	9	9	10	2	6	10	75
86	93	95	6	3	0	5	0	0	2	1	10	27
87	94	76	0	0	0	0	9	0	2	1	5	17
88	94	78	1	3	0	2	9	0	2	1	10	28
89	94	80	10	9	9	10	9	10	2	6	10	75
90	94	82	6	9	9	5	9	10	2	6	10	66
91	94	84	6	9	9	2	9	5	2	6	10	58
92	94	86	10	9	10	10	9	10	2	6	10	76
93	94	88	6	9	9	5	9	10	2	6	10	66
94	94	90	10	9	10	10	9	10	2	6	10	76
95	94	92	6	9	9	2	9	10	2	6	10	63
96	94	94	1	0	0	5	0	2	2	6	10	26
97	95	77	0	3	0	5	0	0	2	1	10	27
98	95	79	6	3	0	5	8	0	2	6	10	45
99	95	81	6	3	0	5	9	0	2	6	10	51
100	95	83	10	9	9	10	9	10	2	6	10	75



Appendix-1

No.	Tube		Tube-to-AVB friction		Vibration frequency		In-plane tube motion		Void fraction	Regional effect	Coupling effect	Total
	Row	Col	COUNT	HOT COUNT	HIGH/LOW	CONTINUOUS	TSP (Max Wear Rate at #5-#7TSP)	MAX LENGTH on AVB WEAR	VOID	REGION	COUPLING	
101	95	85	10	9	9	10	9	10	2	6	10	75
102	95	87	10	9	10	10	9	10	2	6	10	76
103	95	89	10	9	10	5	9	10	2	6	10	71
104	95	91	10	9	9	10	9	10	2	6	10	75
105	95	93	6	9	0	5	9	3	2	6	10	50
106	96	76	1	3	0	2	0	0	0	1	10	17
107	96	78	1	3	0	2	9	2	2	1	10	30
108	96	80	1	3	0	2	9	10	2	6	10	43
109	96	82	10	9	9	10	9	7	2	6	10	72
110	96	84	10	9	10	5	9	10	2	6	10	71
111	96	86	10	9	10	10	9	10	2	6	10	76
112	96	88	10	9	10	10	9	10	2	6	10	76
113	96	90	10	9	10	10	9	10	2	6	10	76
114	96	92	6	9	9	10	9	10	2	6	10	71
115	96	94	0	0	0	0	0	0	2	6	10	18
116	97	77	6	3	0	2	9	3	2	1	10	36
117	97	79	6	9	0	5	9	10	2	6	10	57
118	97	81	10	9	10	9	10	10	2	6	10	76
119	97	83	10	9	10	10	9	10	2	6	10	76
120	97	85	10	9	10	10	9	10	2	6	10	76
121	97	87	10	9	10	10	9	10	2	6	10	71
122	97	89	10	9	10	10	9	10	2	6	10	76
123	97	91	10	3	10	5	9	10	2	6	10	65
124	97	93	6	3	0	5	9	10	2	6	10	51
125	98	76	0	0	0	0	0	7	2	1	10	20
126	98	78	10	9	10	10	9	10	2	1	10	71
127	98	80	10	9	9	10	9	5	2	6	10	70
128	98	82	10	9	9	10	9	10	2	6	10	75
129	98	84	10	9	10	2	9	10	2	6	10	68
130	98	86	10	9	10	10	9	10	2	6	10	76
131	98	88	10	9	10	10	9	10	2	6	10	76
132	98	90	10	9	10	10	9	10	2	6	10	76
133	98	92	10	9	10	9	9	10	2	6	10	75
134	98	94	0	3	0	2	0	0	2	6	10	23
135	99	77	6	3	0	2	9	5	2	1	10	38
136	99	79	10	9	9	10	9	10	2	6	10	75
137	99	81	10	3	9	10	9	10	2	6	10	69
138	99	83	10	9	10	5	9	10	2	6	10	71
139	99	85	10	9	9	10	9	10	2	6	10	75
140	99	87	10	9	10	5	9	10	2	6	10	71
141	99	89	10	9	10	10	9	10	2	6	10	76
142	99	91	10	9	9	10	9	10	2	6	10	75
143	99	93	0	0	0	0	0	5	2	6	10	23
144	99	95	1	0	0	2	0	0	2	6	5	19
145	100	76	1	3	0	2	0	10	2	1	10	29
146	100	78	10	9	10	8	9	7	2	1	10	69
147	100	80	6	9	0	10	9	17	2	1	10	57
148	100	82	10	9	9	10	9	10	2	6	10	75
149	100	84	6	9	10	6	9	10	2	6	10	64
150	100	86	10	9	10	10	9	10	2	6	10	76
151	100	88	10	9	10	10	9	10	2	6	10	76
152	100	90	10	9	10	10	9	10	2	6	10	76
153	100	92	6	9	0	5	9	10	2	6	10	57
154	100	94	1	0	0	2	8	1	2	6	0	20
155	101	77	6	3	0	2	9	3	2	1	10	36
156	101	79	6	9	9	2	9	10	2	6	10	63
157	101	81	10	9	9	5	9	7	2	6	10	67
158	101	83	10	9	10	10	9	10	2	6	10	76
159	101	85	10	9	10	10	9	10	2	6	10	76
160	101	87	10	9	10	10	9	10	2	6	10	76
161	101	89	10	9	9	5	9	10	2	6	10	70
162	101	91	6	3	0	2	9	10	2	6	10	51
163	101	93	1	3	0	2	0	0	2	6	10	24
164	101	95	1	0	0	2	0	0	2	6	5	16
165	102	76	1	0	0	0	8	1	2	1	10	23
166	102	78	10	3	9	10	9	10	2	1	10	64
167	102	80	10	9	10	10	9	10	2	6	10	76
168	102	82	6	3	0	5	9	7	2	6	10	48
169	102	84	6	3	9	2	9	10	2	6	10	57
170	102	86	10	9	10	10	9	10	2	6	10	76
171	102	88	10	9	10	10	9	10	2	6	10	76
172	102	90	6	9	9	5	9	10	2	6	10	66
173	102	92	1	3	0	2	0	11	2	6	10	25
174	102	94	1	3	0	2	0	0	2	6	5	19
175	103	77	1	0	9	2	9	10	2	1	10	44
176	103	79	6	9	0	10	9	10	2	6	10	62
177	103	81	10	9	9	2	9	10	2	6	10	67
178	103	83	10	9	10	10	9	10	2	6	10	76
179	103	85	10	9	10	10	9	10	2	6	10	76
180	103	87	10	9	10	5	9	10	2	6	10	71
181	103	89	6	3	0	2	9	10	2	6	10	48
182	103	91	1	0	0	2	8	2	2	6	10	31
183	104	76	1	3	0	2	0	5	2	1	5	19
184	104	78	6	0	0	2	9	10	2	1	10	40
185	104	80	10	9	0	2	9	10	2	6	10	67
186	104	82	6	9	0	5	9	10	2	6	10	52
187	104	84	10	9	10	10	9	10	2	6	10	76
188	104	86	6	9	0	2	9	10	2	6	10	54
189	104	88	6	9	0	5	9	7	2	6	10	54
190	104	90	6	9	9	2	9	1	2	6	10	54
191	104	92	1	3	0	2	0	0	2	6	10	24
192	105	77	1	0	0	2	9	0	2	1	10	25
193	105	79	6	9	9	5	9	10	2	6	10	66
194	105	81	6	3	0	5	9	3	2	6	10	44
195	105	83	10	9	10	10	9	10	2	6	10	76
196	105	85	10	9	10	5	9	5	2	6	10	71
197	105	87	10	9	10	5	9	5	2	6	10	69
198	105	89	1	3	9	0	9	5	2	6	10	44
199	105	91	1	3	0	5	0	0	2	6	10	27
200	105	93	6	3	0	5	0	0	2	6	5	27



Appendix-1

No.	Tube		Tube-to-AVB friction		Vibration frequency		In-plane tube motion		Void fraction	Regional effect	Coupling effect	Total
	Row	Col	COUNT	HOT COUNT	HIGH/LOW	CONTINUOUS	TSP (Max Wear Rate at #5-#7TSP)	MAX LENGTH on AVB WEAR	VOID	REGION	COUPLING	
201	106	78	6	3	0	5	9	5	2	1	10	41
202	106	80	6	9	9	2	9	10	2	6	10	63
203	106	82	6	9	0	10	9	7	2	6	10	59
204	106	84	6	9	0	2	9	0	2	6	10	44
205	106	86	6	9	0	2	9	7	2	6	10	51
206	106	88	6	3	0	5	8	2	2	6	10	42
207	106	90	6	9	9	2	0	3	2	6	10	47
208	106	92	1	3	0	2	0	0	2	6	10	24
209	106	94	1	3	0	2	0	0	2	6	10	24
210	107	77	1	0	0	2	8	10	2	1	10	34
211	107	79	6	9	0	5	9	10	2	6	10	57
212	107	81	10	3	9	10	8	7	2	6	10	65
213	107	83	10	9	10	10	8	10	2	6	10	75
214	107	85	6	9	9	2	8	10	2	6	10	62
215	107	87	10	9	9	10	9	10	2	6	10	75
216	107	89	6	9	0	2	0	10	2	6	10	45
217	107	91	1	3	0	5	0	3	2	6	10	30
218	107	93	1	3	0	2	0	2	2	6	10	26
219	107	95	0	3	0	2	0	0	2	6	5	18
220	108	78	6	3	0	2	8	5	2	1	10	37
221	108	80	1	9	0	2	8	10	2	6	10	48
222	108	82	1	3	0	2	0	7	2	6	10	31
223	108	84	6	9	9	5	0	10	2	6	10	57
224	108	86	6	9	0	5	0	0	2	6	10	38
225	108	88	1	3	0	2	8	0	2	6	10	32
226	108	90	1	3	0	2	0	0	2	6	10	24
227	108	92	1	0	0	2	0	2	2	6	10	23
228	108	94	1	0	0	2	0	5	2	6	10	26
229	109	79	1	3	0	2	9	3	2	1	10	31
230	109	81	1	0	0	0	0	1	0	6	10	21
231	109	83	0	0	0	0	0	0	2	6	10	18
232	109	85	1	3	0	5	9	0	2	6	10	36
233	109	87	0	3	0	2	0	0	2	6	10	23
234	109	89	1	3	0	2	0	2	2	6	10	26
235	109	91	1	0	0	2	0	0	2	6	5	16
236	109	93	1	3	0	5	0	0	2	6	10	27
237	110	80	1	3	0	2	0	0	2	6	10	24
238	110	84	1	3	0	2	0	0	2	6	10	24
239	110	86	0	3	0	2	0	3	2	6	10	26
240	110	88	1	3	0	2	0	0	2	6	10	24
241	110	90	1	3	0	2	0	0	2	6	5	19
242	110	92	1	0	0	0	0	0	2	6	10	19
243	110	94	0	0	0	0	0	0	2	6	10	18
244	111	83	1	3	0	2	0	0	2	6	5	19
245	111	85	1	3	0	2	0	0	2	6	10	24
246	111	87	1	9	0	2	0	0	2	6	10	30
247	111	89	1	3	0	2	0	0	2	6	5	19
248	111	91	1	0	0	5	0	0	2	6	5	19
249	111	93	1	3	0	5	0	0	2	6	5	22
250	112	82	1	3	0	0	0	0	2	6	5	17
251	112	84	1	3	0	2	0	0	2	6	10	24
252	112	86	1	0	0	2	0	0	2	6	10	21
253	112	88	1	3	0	2	0	0	2	6	10	24
254	112	92	1	3	0	2	0	0	2	6	10	24
255	113	83	6	9	0	10	0	0	2	6	0	33
256	113	85	6	9	0	5	0	0	2	6	10	38
257	113	87	6	3	0	5	0	0	2	6	10	32
258	113	89	1	3	0	0	0	0	2	6	5	17
259	113	91	1	3	0	5	0	0	2	6	0	17
260	114	80	6	3	0	5	0	0	2	1	0	17
261	114	84	1	0	0	2	0	2	2	6	10	23
262	114	86	1	3	0	2	0	2	2	6	10	26
263	114	88	1	3	0	2	0	2	2	6	10	26
264	114	90	1	0	0	2	0	0	2	6	5	16
265	115	79	1	3	0	2	0	5	2	1	5	19
266	115	85	1	3	0	2	9	0	2	6	10	33
267	115	87	6	3	0	5	0	0	2	6	10	32
268	115	89	1	3	0	0	0	3	2	6	5	20
269	116	86	6	9	0	10	0	0	2	6	10	43
270	116	88	1	0	0	3	0	0	2	6	10	22
271	117	83	1	3	0	0	0	0	2	1	10	17
272	117	85	1	0	0	2	0	0	2	1	10	16
273	118	82	6	3	0	5	0	0	2	1	5	22
274	119	83	6	3	0	5	0	0	2	1	5	22
275	120	82	1	0	0	2	0	0	2	1	10	16
276	83*	77*	6	3	0	5	0	0	0	1	0	15
277	97*	75*	6	3	0	5	0	0	0	1	0	15

* This tube is additionally selected.



Appendix-1

Table A-2 Screened tubes for Unit 3B

No.	Tube		Tube-to-AVB friction		Vibration frequency		In-plane tube motion		VOID	REGION	COUPLING	Total
	Row	Col	COUNT	HOT COUNT	HIGH/LOW	CONTINUOUS	TSP (Max Wear Rate at #5-#7TSP)	MAX LENGTH on AVB WEAR				
1	79	81	1	3	0	2	0	0	2	1	10	17
2	80	79	6	3	0	5	0	1	0	1	5	21
3	80	80	1	3	0	2	0	0	0	1	10	17
4	80	82	6	3	0	5	0	0	2	1	5	22
5	81	77	6	3	0	5	0	0	0	1	5	20
6	81	79	6	3	0	5	0	2	2	1	10	29
7	81	81	6	3	0	5	0	0	2	1	10	27
8	82	78	1	3	0	2	0	0	2	1	10	19
9	82	80	1	3	0	2	0	0	2	1	10	19
10	82	82	0	3	0	2	0	0	2	1	10	18
11	83	79	6	3	0	5	0	3	2	1	10	30
12	83	81	6	3	0	5	0	7	2	1	10	27
13	83	85	1	3	0	2	0	7	2	1	5	29
14	84	78	6	3	0	5	0	2	2	1	10	29
15	84	80	6	3	0	5	0	1	2	1	10	28
16	84	82	1	3	0	2	0	0	2	1	10	19
17	84	84	1	0	0	5	0	0	2	1	10	19
18	84	86	1	0	0	2	0	3	2	1	10	19
19	85	79	6	3	0	5	0	1	2	1	10	28
20	85	81	1	3	0	0	0	0	2	1	10	17
21	85	83	6	3	0	5	0	2	2	1	5	24
22	85	85	1	3	0	5	8	7	2	1	5	32
23	85	87	1	3	0	2	8	1	2	1	0	18
24	86	78	1	3	0	2	0	0	2	1	10	19
25	86	82	6	3	0	5	0	1	2	1	10	28
26	86	86	1	0	0	2	0	1	2	1	10	17
27	87	77	6	3	0	5	0	1	2	1	0	18
28	87	79	1	3	0	2	0	1	2	1	10	20
29	87	81	6	3	0	5	8	0	2	1	5	30
30	87	83	1	0	0	2	0	0	2	1	10	16
31	87	85	0	0	0	2	0	10	2	1	10	25
32	88	78	1	3	0	2	0	3	2	1	10	22
33	88	80	1	3	0	2	0	3	2	1	10	22
34	88	82	0	3	0	2	0	3	2	1	10	21
35	88	84	6	3	0	5	0	2	2	1	10	29
36	88	86	0	0	0	0	0	3	2	1	10	16
37	88	94	1	0	0	2	8	3	2	1	10	27
38	88	96	0	0	0	0	8	10	2	1	5	26
39	89	77	1	3	0	2	0	5	2	1	5	19
40	89	79	6	3	0	5	0	10	2	1	5	32
41	89	81	1	3	0	2	0	3	2	1	10	19
42	89	83	1	3	0	2	0	3	2	1	10	22
43	89	85	1	0	0	2	8	7	2	6	10	36
44	89	87	6	3	0	5	0	3	2	6	0	25
45	89	91	6	3	0	5	8	5	2	1	0	30
46	89	93	6	3	0	5	0	2	2	1	5	24
47	89	95	1	0	0	0	8	5	2	1	10	27
48	89	97	1	3	0	2	0	3	2	1	10	22
49	90	78	1	0	0	2	0	3	2	1	10	19
50	90	80	1	3	0	5	0	2	2	1	10	24
51	90	82	1	0	0	5	0	2	2	1	10	21
52	90	84	1	3	0	2	0	3	2	6	10	27
53	90	86	0	3	0	2	0	1	2	6	10	24
54	90	96	0	0	0	0	8	0	2	1	10	21
55	91	79	6	3	0	5	8	0	2	1	10	35
56	91	81	10	9	0	10	8	3	2	1	10	53
57	91	83	1	3	0	2	9	1	2	6	10	34
58	91	85	0	0	0	2	8	1	2	6	10	29
59	91	87	1	3	0	2	0	0	2	6	10	24
60	91	97	6	3	0	5	0	0	2	1	0	17
61	92	74	1	3	0	2	8	0	0	1	5	20
62	92	76	1	3	0	2	0	0	2	1	10	19
63	92	78	1	0	0	0	8	0	2	1	10	22
64	92	80	6	3	0	5	0	1	2	1	10	28
65	92	82	1	0	0	5	0	7	2	6	10	27
66	92	84	10	9	0	9	9	7	2	6	10	67
67	92	86	1	0	0	2	0	5	2	6	10	34
68	92	88	6	3	0	5	8	5	2	6	10	45
69	92	96	0	0	0	0	9	0	2	1	5	17
70	93	75	1	3	0	5	8	0	0	1	0	18
71	93	77	1	3	0	2	8	0	2	1	10	27
72	93	79	6	3	0	5	0	5	2	1	10	32
73	93	81	1	3	0	2	8	2	2	6	10	34
74	93	83	6	9	10	2	9	10	2	6	10	64
75	93	85	6	3	9	5	9	10	2	6	10	60
76	93	87	1	3	0	2	9	1	2	6	10	34
77	93	89	1	0	0	0	0	0	2	6	10	19
78	93	93	1	3	0	5	9	0	2	1	5	26
79	94	74	1	3	0	2	8	0	0	1	5	20
80	94	76	1	3	0	2	0	0	2	1	10	19



Appendix-1

No.	Tube		Tube-to-AVB friction		Vibration frequency		In-plane tube motion		Void fraction	Regional effect	Coupling effect	Total
	Row	Col	COUNT	HOT COUNT	HIGH/LOW	CONTINUOUS	TSP (Max Wear Rate at #5-#7TSP)	MAX LENGTH on AVB WEAR	VOID	REGION	COUPLING	
81	94	78	1	3	0	5	8	1	2	1	10	31
82	94	80	6	3	0	2	9	5	2	6	10	43
83	94	82	10	9	10	10	9	10	2	6	10	76
84	94	84	10	3	10	5	9	10	2	6	10	65
85	94	86	6	3	0	5	9	10	2	6	10	51
86	94	88	0	0	0	2	9	0	2	6	10	29
87	94	90	0	0	0	0	0	0	2	6	10	18
88	94	92	0	0	0	0	0	3	2	6	10	21
89	94	94	0	0	0	0	0	1	2	1	10	22
90	95	75	1	3	0	2	8	0	0	1	5	20
91	95	77	6	3	0	5	8	1	2	1	10	34
92	95	79	6	3	0	5	8	10	2	6	10	50
93	95	81	10	9	10	10	9	10	2	6	10	76
94	95	83	6	9	10	2	9	10	2	6	10	64
95	95	85	10	9	10	10	9	10	2	6	10	76
96	95	87	6	3	0	2	9	0	2	6	10	38
97	95	89	0	0	0	0	8	0	2	6	10	26
98	95	91	1	3	0	2	8	0	2	6	5	27
99	95	93	0	0	0	2	8	2	2	6	5	25
100	96	76	1	3	0	2	8	0	0	1	10	25
101	96	78	6	3	0	2	0	0	2	1	10	24
102	96	80	10	9	10	10	9	10	2	6	10	76
103	96	82	10	9	10	10	9	10	2	6	10	76
104	96	84	10	9	10	5	9	10	2	6	10	76
105	96	86	6	3	10	2	9	10	2	6	10	59
106	96	88	10	9	10	5	9	10	2	6	10	71
107	96	90	0	0	0	0	8	0	2	6	10	28
108	96	92	0	0	0	0	0	0	2	6	10	18
109	97	77	1	3	0	2	8	3	2	1	10	30
110	97	79	10	9	9	10	9	10	2	6	10	75
111	97	81	10	9	10	10	9	10	2	6	10	76
112	97	83	10	9	10	10	9	10	2	6	10	76
113	97	85	10	9	10	5	9	10	2	6	10	71
114	97	87	10	9	9	2	9	10	2	6	10	67
115	97	89	1	3	0	2	9	10	2	6	10	43
116	97	91	1	0	0	2	0	0	2	6	10	21
117	97	93	0	0	0	0	0	0	2	6	10	18
118	98	76	1	0	0	2	8	3	2	1	10	27
119	98	78	6	3	9	5	9	10	2	6	10	60
120	98	80	10	9	10	5	9	10	2	6	10	71
121	98	82	10	9	10	2	9	10	2	6	10	68
122	98	84	10	9	10	5	9	10	2	6	10	71
123	98	86	10	9	10	10	9	10	2	6	10	76
124	98	88	6	3	9	5	9	10	2	6	10	60
125	98	90	1	0	0	2	8	3	2	6	10	32
126	98	92	6	0	0	5	8	1	2	6	0	28
127	99	77	1	3	0	2	8	10	2	1	10	37
128	99	79	10	9	9	10	9	10	2	6	10	75
129	99	81	10	9	10	2	9	10	2	6	10	68
130	99	83	10	9	10	10	9	10	2	6	10	76
131	99	85	10	9	10	10	9	10	2	6	10	76
132	99	87	10	9	10	10	9	10	2	6	10	76
133	99	89	1	0	0	2	8	10	2	6	10	39
134	99	91	1	0	0	2	0	0	2	6	10	21
135	99	93	1	0	0	2	0	0	2	6	5	16
136	100	76	1	0	0	2	8	1	2	1	10	25
137	100	78	10	9	9	10	9	10	2	6	10	75
138	100	80	10	9	10	10	9	10	2	6	10	76
139	100	82	10	9	10	10	9	10	2	6	10	76
140	100	84	10	3	10	5	9	10	2	6	10	65
141	100	86	10	9	10	5	9	10	2	6	10	71
142	100	88	10	9	9	10	9	10	2	6	10	75
143	100	90	6	3	0	10	8	7	2	6	10	52
144	100	92	1	0	0	2	0	0	2	6	10	21
145	101	75	0	0	0	2	0	1	2	1	10	27
146	101	77	6	3	0	2	9	10	2	1	10	43
147	101	79	10	9	10	5	9	10	2	6	10	71
148	101	81	10	9	10	10	9	10	2	6	10	76
149	101	83	10	9	10	10	9	10	2	6	10	76
150	101	85	10	9	10	10	9	10	2	6	10	76
151	101	87	10	3	10	5	9	10	2	6	10	65
152	101	89	1	0	0	0	8	5	2	6	10	32
153	101	91	0	0	0	0	0	0	2	6	10	18
154	101	93	1	3	0	2	0	0	2	6	5	19
155	102	74	1	0	0	2	8	0	2	1	10	24
156	102	76	10	3	9	10	9	10	2	1	10	64
157	102	78	10	9	10	10	9	7	2	6	10	73
158	102	80	10	9	10	5	9	10	2	6	10	71
159	102	82	10	9	10	10	9	10	2	6	10	76
160	102	84	10	9	10	2	9	10	2	6	10	68



Appendix-1

No.	Tube		Tube-to-AVB friction		Vibration frequency		In-plane tube motion		VOID	REGION	COUPLING	Total
	Row	Col	COUNT	HOT COUNT	HIGH/LOW	CONTINUOUS	TSP (Max Wear Rate at #5-#7TSP)	MAX LENGTH on AVB WEAR				
161	102	86	10	9	10	10	9	10	2	6	10	76
162	102	88	6	3	9	5	9	10	2	6	10	60
163	102	90	1	3	0	2	8	3	2	6	10	35
164	102	92	0	0	0	0	8	2	2	6	5	23
165	103	75	1	0	9	0	9	1	2	1	10	33
166	103	77	10	9	10	10	9	10	2	1	10	71
167	103	79	10	9	10	10	9	10	2	6	10	76
168	103	81	10	9	10	10	9	10	2	6	10	76
169	103	83	6	9	10	2	9	10	2	6	10	64
170	103	85	10	9	10	10	9	10	2	6	10	76
171	103	87	10	3	10	5	9	10	2	6	10	65
172	103	89	0	0	0	0	0	0	2	6	10	26
173	103	91	0	0	0	0	8	7	2	6	10	33
174	104	76	10	9	10	5	9	7	2	1	10	63
175	104	78	10	9	10	10	9	10	2	6	10	76
176	104	80	10	9	10	10	9	10	2	6	10	76
177	104	82	10	9	10	10	9	10	2	6	10	76
178	104	84	10	9	10	10	9	10	2	6	10	76
179	104	86	10	9	10	5	9	7	2	6	10	68
180	104	88	6	3	9	5	9	10	2	6	10	60
181	104	90	0	0	0	0	9	0	2	6	10	27
182	104	92	0	0	0	0	0	0	2	6	10	18
183	105	75	10	9	10	5	9	10	2	1	10	66
184	105	77	10	9	10	10	9	10	2	1	10	71
185	105	79	10	9	10	10	9	10	2	6	10	76
186	105	81	10	9	10	2	9	10	2	6	10	68
187	105	83	10	9	10	5	9	10	2	6	10	71
188	105	85	10	9	10	5	9	10	2	6	10	71
189	105	87	10	9	9	10	9	10	2	6	10	75
190	105	89	1	3	0	2	8	2	2	6	10	34
191	105	91	0	0	0	0	8	0	2	6	10	26
192	105	93	1	3	0	2	0	0	2	6	5	19
193	106	74	0	0	0	0	8	0	2	1	10	21
194	106	76	10	9	10	10	9	10	2	1	10	71
195	106	78	10	9	10	5	9	10	2	6	10	71
196	106	80	10	9	10	10	9	10	2	6	10	76
197	106	82	10	9	10	10	9	10	2	6	10	76
198	106	84	10	9	10	10	9	10	2	6	10	76
199	106	86	6	9	9	2	9	10	2	6	10	63
200	106	88	6	3	0	5	9	2	2	6	10	43
201	106	90	1	3	0	0	9	1	2	6	10	32
202	106	92	1	0	0	2	8	0	2	6	5	24
203	107	75	6	3	10	2	9	10	2	1	10	53
204	107	77	10	9	10	5	9	10	2	1	10	66
205	107	79	10	9	10	10	9	10	2	6	10	76
206	107	81	10	9	10	10	9	10	2	6	10	76
207	107	83	10	9	10	5	9	10	2	6	10	71
208	107	85	10	9	10	10	9	10	2	6	10	76
209	107	87	1	9	9	5	9	7	2	6	10	58
210	107	89	1	9	0	2	8	10	2	6	10	48
211	107	91	1	0	0	0	0	0	2	6	10	19
212	107	93	1	3	0	0	0	0	2	6	5	17
213	108	74	0	0	0	0	8	0	2	1	10	21
214	108	76	10	9	10	5	9	10	2	1	10	66
215	108	78	10	9	10	10	9	10	2	6	10	76
216	108	80	10	9	10	10	9	10	2	6	10	76
217	108	82	10	9	10	5	9	10	2	6	10	71
218	108	84	10	9	10	5	9	10	2	6	10	71
219	108	86	10	9	9	5	9	2	2	6	10	62
220	108	88	1	3	0	2	0	0	2	6	10	24
221	108	90	1	0	0	2	0	0	2	6	10	21
222	108	92	0	0	0	2	0	2	2	6	5	17
223	109	75	10	3	10	5	9	10	2	1	10	60
224	109	77	10	9	10	5	9	10	2	1	10	66
225	109	79	10	9	10	10	9	10	2	6	10	76
226	109	81	10	9	10	2	9	10	2	6	10	68
227	109	83	10	9	9	10	9	10	2	6	10	75
228	109	85	1	3	0	0	9	10	2	6	10	41
229	109	87	1	0	0	5	0	0	2	6	10	24
230	109	89	1	3	0	2	0	0	2	6	10	24
231	110	74	1	0	0	0	8	1	2	1	10	23
232	110	76	10	3	0	5	9	10	2	1	10	60
233	110	78	10	9	10	10	9	10	2	6	10	76
234	110	80	10	9	10	5	9	10	2	6	10	71
235	110	82	10	9	10	5	9	10	2	6	10	71
236	110	84	1	0	0	2	9	10	2	6	10	40
237	110	86	0	0	0	0	0	0	2	6	10	18
238	110	88	0	0	0	0	0	0	2	6	10	18
239	111	75	1	3	0	2	9	5	2	1	10	33
240	111	77	10	9	10	5	9	10	2	1	10	66



Appendix-1

No.	Tube		Tube-to-AVB friction		Vibration frequency		In-plane tube motion		Void fraction	Regional effect	Coupling effect	Total
	Row	Col	COUNT	HOT COUNT	HIGH/LOW	CONTINUOUS	TSP (Max Wear Rate at #5-#7TSP)	MAX LENGTH on AVB WEAR	VOID	REGION	COUPLING	
241	111	79	10	9	10	10	9	10	2	6	10	76
242	111	81	10	9	10	5	9	10	2	6	10	71
243	111	83	10	9	10	10	9	10	2	6	10	76
244	111	85	1	0	0	2	0	10	2	6	10	31
245	111	87	1	3	0	5	0	0	2	6	5	22
246	111	89	1	3	0	2	8	2	2	6	0	24
247	112	74	0	0	0	0	8	0	2	1	10	21
248	112	76	1	0	9	2	9	5	2	1	10	39
249	112	78	6	3	10	2	9	10	2	1	10	53
250	112	80	10	9	10	2	9	10	2	6	10	68
251	112	82	6	9	10	2	9	10	2	6	10	64
252	112	84	6	9	0	10	9	10	2	6	10	61
253	112	86	6	9	9	5	0	0	2	6	10	47
254	112	88	1	0	0	0	0	0	2	6	10	19
255	112	90	1	0	0	2	0	0	2	6	5	16
256	113	75	0	3	0	0	8	2	2	1	10	26
257	113	77	6	9	0	5	8	7	2	1	10	48
258	113	79	6	3	9	2	9	10	2	6	10	57
259	113	81	10	9	10	2	9	10	2	6	10	68
260	113	83	1	3	0	2	8	5	2	6	10	37
261	113	85	1	3	0	2	0	0	2	6	10	24
262	113	87	1	3	0	2	0	0	2	6	10	24
263	114	74	0	0	0	0	8	0	2	1	5	16
264	114	76	6	3	0	2	8	7	2	1	10	39
265	114	78	6	0	9	5	9	10	2	1	10	52
266	114	80	10	9	10	10	9	10	2	6	10	76
267	114	82	6	9	0	10	0	10	2	6	10	53
268	114	84	1	3	0	0	0	0	2	6	10	22
269	115	75	1	0	0	0	8	0	2	1	10	22
270	115	77	6	9	9	2	8	5	2	1	10	52
271	115	79	10	9	10	10	9	10	2	1	10	71
272	115	81	6	9	0	5	8	10	2	6	10	56
273	115	83	1	3	0	2	0	0	2	6	10	24
274	116	76	1	9	0	2	8	2	2	1	10	35
275	116	78	6	9	9	2	9	10	2	1	10	58
276	116	80	10	9	10	10	9	10	2	1	10	71
277	116	82	1	0	0	2	8	1	2	6	10	30
278	116	88	1	3	0	2	0	0	2	6	0	22
279	117	77	6	9	0	5	9	7	2	1	10	49
280	117	79	10	9	10	10	9	10	2	1	10	71
281	117	81	6	9	9	5	0	2	2	1	10	44
282	117	83	1	3	0	2	0	0	2	6	10	24
283	117	85	1	0	0	2	0	0	2	6	10	21
284	118	76	1	3	0	2	8	1	2	1	10	28
285	118	78	10	9	9	10	9	10	2	1	10	70
286	118	80	10	9	9	10	0	7	2	1	10	58
287	118	82	0	0	0	0	9	1	2	1	10	23
288	118	84	6	9	0	5	0	0	2	6	5	33
289	118	88	1	0	0	2	0	0	2	6	5	16
290	119	77	10	9	9	10	9	10	2	1	10	70
291	119	79	10	9	10	10	9	10	2	1	10	70
292	119	81	1	3	0	2	0	2	2	1	10	21
293	119	85	0	0	0	0	9	1	2	6	5	23
294	120	76	1	3	0	2	8	1	2	1	10	28
295	120	78	10	9	10	10	9	10	2	1	10	71
296	120	80	6	9	0	5	8	2	2	1	10	43
297	121	75	1	3	0	2	0	1	2	1	10	20
298	121	77	1	3	0	2	9	7	2	1	10	35
299	121	79	6	3	0	10	9	5	2	1	10	46
300	121	81	1	3	0	2	0	1	2	1	10	20
301	121	85	1	3	0	2	0	2	2	1	5	16
302	122	76	6	3	0	2	0	3	2	1	10	27
303	122	78	1	3	0	2	8	2	2	1	10	29
304	122	80	6	3	0	5	0	5	2	1	10	32
305	123	77	1	3	0	2	0	0	2	1	10	19
306	123	79	1	3	0	0	0	2	2	1	10	19
307	124	76	1	3	0	2	8	0	2	1	5	22
308	124	78	6	3	0	5	0	2	2	1	5	24
309	124	80	1	3	0	2	0	2	2	1	5	16
310	124	82	1	3	0	5	0	0	2	1	5	17
311	125	77	1	3	0	2	0	0	2	1	10	19
312	125	83	1	3	0	2	8	0	2	1	0	17
313	130	78	6	3	0	5	0	1	2	1	0	18



Appendix-2

Evaluation of Void Fraction Distribution of U-bend Region



1. Purpose

This appendix provides evaluation of void fraction distribution of tubes in U-bend region of San Onofre Units 2 and 3 Replacement Steam Generators (RSGs)

2. Conclusion

The distribution of the void fraction is shown in Fig.6-1.

3. Assumption

- (1) The void fraction is analyzed utilizing the "ATHOS/SGAP" code (Ref. 1). Therefore, the assumptions used in the ATHOS/SGAP code apply to this document. Two-phase flow is represented by using a drift flux model which is the standard model of two-phase flow analysis. The mathematical models in the ATHOS/SGAP are constituted under the following assumptions: (Ref. 1)
- (2) The analysis is performed at the steady state conditions of 100% power (1729MW/SG) and the beginning of life (BOL). That is, the steam pressures are 838 psia for 598 deg.F of the primary inlet temperature.
- (3) All dimensions in analysis are assumed in the cold metal condition because the effect of heat expansion of metals on the calculation results is negligible.



4. Design Inputs

The nominal dimensions are obtained from the design drawings (Ref.2 to 19) and the manufacturing tolerances are not considered. Flow characteristics are obtained from 3 dimensional thermal and hydraulic analysis.

5. Methodology

Based on the design input of the operating conditions, the calculation of the circulation ratio is performed by evaluating the pressure loss and the recirculation head with SSPC, which is a 1 dimensional Thermal and Hydraulic parameter calculation code (Ref.20). Using ATHOS/SGAP (Ref. 1 and 21), the thermal hydraulic analysis is performed to obtain the 3 dimension flow distribution which includes the void fraction.

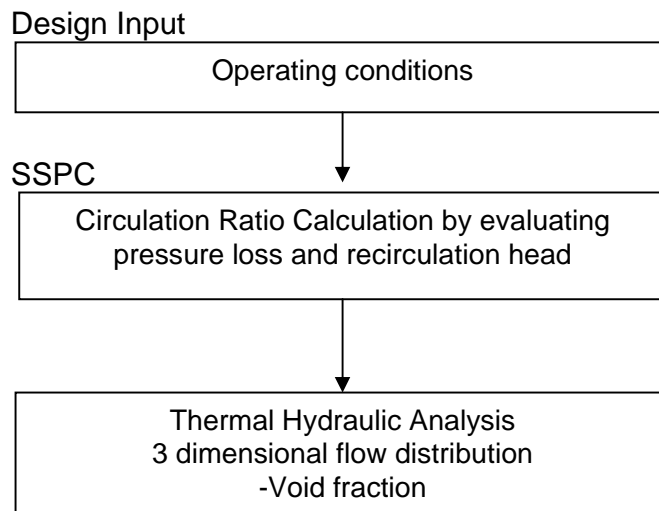


Fig.5-1 Flow of the evaluation



5.1 Evaluation cases

The operating parameters used for the calculation are shown in Table 5-1.

Table 5-1 Basic parameters for calculation

Plugging	
Thermal power (MWt/SG)	
T _{cold} (°F)	
T _{sg-out} (°F)	
T _{hot} (Tsg-in) (°F)	
T _{feedwater} (°F)	
Saturation Steam Pressure (psia)	
Steam Mass Flow (lb/hr)	
Circulation ratio	

6. Results

The average value of the void fraction of U-bend region of each tube is calculated and the distribution is shown in Fig.6-1. The region where the void fraction is high is concentrated on the region of center columns and the outer rows.



Appendix-2

Fig.6-1 Distribution of average void fraction



7. References

- 1) Analysis of Thermal Hydraulics of Steam Generators/Steam Generator Analysis Package, Ver.3.1, 1016564, EPRI
- 2) L5-04FU001 the latest revision, Component and Outline Drawing 1/3
- 3) L5-04FU002 the latest revision, Component and Outline Drawing 2/3
- 4) L5-04FU003 the latest revision, Component and Outline Drawing 3/3
- 5) L5-04FU021 the latest revision, Tube Sheet and Extension Ring 1/3
- 6) L5-04FU022 the latest revision, Tube Sheet and Extension Ring 2/3
- 7) L5-04FU023 the latest revision, Tube Sheet and Extension Ring 3/3
- 8) L5-04FU051 the latest revision, Tube Bundle 1/3
- 9) L5-04FU052 the latest revision, Tube Bundle 2/3
- 10) L5-04FU053 the latest revision, Tube Bundle 3/3
- 11) L5-04FU111 the latest revision, AVB assembly 1/9
- 12) L5-04FU112 the latest revision, AVB assembly 2/9
- 13) L5-04FU113 the latest revision, AVB assembly 3/9
- 14) L5-04FU114 the latest revision, AVB assembly 4/9
- 15) L5-04FU115 the latest revision, AVB assembly 5/9
- 16) L5-04FU116 the latest revision, AVB assembly 6/9
- 17) L5-04FU117 the latest revision, AVB assembly 7/9
- 18) L5-04FU118 the latest revision, AVB assembly 8/9
- 19) L5-04FU119 the latest revision, AVB assembly 9/9
- 20) L5-04GA510 the latest revision, Thermal and Hydraulic Parametric Calculations
- 21) L5-04GA565, the latest revision, Selection of Thermal Hydraulic Analysis (ATHOS) model



Appendix-3
Additional details about the number of tube wear indications



Appendix-3

This appendix explains the number of tube wear indications used in the analysis. In the In-Service Inspection records, SCE included only bobbin ECT data for AVB and TSP indications in Unit-2 and Unit-3 SGs as follows, informed by the project letter (Ref.1).

SCE inclusion method

- AVB Indications: Evaluation only by bobbin ECT
- TSP Indications: Evaluation only by bobbin ECT
- FSW Indications, Retainer Bar (RB) Indications, Foreign Object Indications: Evaluation only by rotated ECT

The numbers of tubes with wear indications counted based on SCE inclusion method mentioned above are summarized in Table (a).

Table (a) Numbers of tubes with wear indication by SCE*

Wear Type	Pick-up manner	SG 2A (2E -089)	SG 2B (2E -088)	SG 3A (3E -089)	SG 3B (3E -088)	Total (Unit-2)	Total (Unit-3)
Type 1 (FSW)	Evaluation only by Rotational ECT	2	0	165	161	2	326
Type 2 (AVB wear)	Evaluation only by Bobbin ECT	802	595	706	735	1397	1441
Type 3 (TSP wear)	Evaluation only by Bobbin ECT	53	135	15	20	188	35
Type 4 (RB wear)	Evaluation only by Rotational ECT	4	2	1	3	6	4
Foreign Object	Evaluation only by Rotational ECT	0	2	0	0	2	0
Total	-	861	734	887	919	1595	1806

*: Each tube is only counted once with the priority given to Type 1 followed by Type 2, Type 3, Type 4 and Foreign Material.

On the other hand, MHI uses both bobbin ECT and rotated ECT data for AVB and TSP indications, because any tubes with wear indications based on only rotated ECT data are not included in the data for AVB and TSP indications. MHI considered that both bobbin ECT and rotated ECT data should be included for more conservative treatment than only bobbin ECT data. The numbers of tubes with wear indications in Unit-2 and Unit-3 SGs are based on the following inclusion method by using both bobbin ECT and rotated ECT data as follows, informed by the project letter (Ref.2).

MHI inclusion method

- AVB Indications: Evaluation by bobbin ECT and rotated ECT, larger one is used
- TSP Indications: Evaluation by bobbin ECT and rotated ECT, larger one is used
- FSW Indications, Retainer Bar (RB) Indications, Foreign Object Indications: Evaluation only by rotated ECT



Appendix-3

The numbers of tubes with wear indications counted based on MHI method mentioned above are summarized in Table (b).

Table (b) Numbers of tubes with wear indication by MHI*

Wear Type	Pick-up manner	SG 2A (2E -089)	SG 2B (2E -088)	SG 3A (3E -089)	SG 3B (3E -088)	Total (Unit-2)	Total (Unit-3)
Type 1 (FSW)	Evaluation only by Rotational ECT	2	0	165	161	2	326
Type 2 (AVB wear)	Evaluation by Bobbin ECT and Rotational ECT, larger one is used	802	595	714	737	1397	1451
Type 3 (TSP wear)	Evaluation by Bobbin ECT and Rotational ECT, larger one is used	53	137	15	20	190	35
Type 4 (RB wear)	Evaluation only by Rotational ECT	4	2	1	3	6	4
Foreign Object	Evaluation only by Rotational ECT	0	2	0	0	2	0
Total	-	861	736	895	921	1597	1816

*: Each tube is only counted once with the priority given to Type 1 followed by Type 2, Type 3, Type 4 and Foreign Material.

In the comparison between Table (a) and (b), the tubes selected by MHI method which are not selected by SCE method are listed below.

(AVB Wear)

○Unit-3A

Row.83 Col.95
 Row.86 Col.94
 Row.95 Col.73
 Row.99 Col.73
 Row.103 Col.73
 Row.105 Col.75
 Row.106 Col.76
 Row.111 Col.77

○Unit-3B

Row.89 Col.89
 Row.110 Col.90

(TSP Wear)

○Unit-2B

Row.118 Col.134
 Row.126 Col.128



Reference

1. Letter RSG-SCE/MHI-12-5749, from D. Calhoun (SCE) to T. Kodama (MHI), August 3, 2012, Subject: "Updated ECT Data for Input to Return to Service and Repair Design Documents."
2. Letter RSG-SCE/MHI-12-5688, from D. Calhoun (SCE) to T. Kodama (MHI), March 22, 2012, Subject: "ECT Data for Input to Return to Service and Repair Design Documents."

ATTACHMENT 6

SONGS U2C17

Steam Generator Operational Assessment

[Proprietary Information Redacted]



SOUTHERN CALIFORNIA
EDISON[®]

An *EDISON INTERNATIONAL*[®] Company

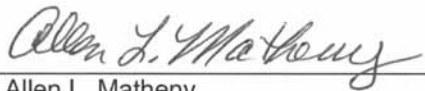
10/3/2012

SOUTHERN CALIFORNIA EDISON
An *EDISON INTERNATIONAL* Company

SONGS U2C17
STEAM GENERATOR OPERATIONAL ASSESSMENT

SONGS U2C17 Steam Generator Operational Assessment

Prepared by:  10/3/12
Richard A. Coe
Steam Generator Recovery Project

Reviewed by:  10/13/12
Allen L. Matheny
Integrity Assessment Program Element Manager
Steam Generator Program

Reviewed by:  10/3/12
Tom Yackle
Steam Generator Recovery Project

Reviewed by:  10/3/2012
Michael P. Short
Steam Generator Recovery Project

Reviewed by:  10/3/2012
David J. Calhoun
Steam Generator Recovery Project


Approved by:  10/3/12
Stephen G. Chun
Manager, Systems Engineer-Mechanical
Steam Generator Program

Table of Contents

	Page
RECORD OF REVISION	3
LIST OF TABLES	5
LIST OF FIGURES	6
LIST OF APPENDICES	7
ABBREVIATIONS AND ACRONYMS.....	8
EXECUTIVE SUMMARY	9
1.0 PURPOSE.....	9
2.0 SONGS STEAM GENERATOR DESIGN FEATURES	9
3.0 OPERATIONAL ASSESSMENT	12
3.1 OA for Degradation Mechanisms Other than TTW	14
3.2 TTW OA Using Tube-to-AVB Support Conditions and Contact Force	15
3.3 “Traditional” Probabilistic OA for TTW.....	16
3.4 Deterministic TTW OA.....	17
3.5 Evaluation of Leakage Integrity	18
3.6 Summary of All OA Conclusions	19
4.0 REFERENCES.....	20

List of Tables

Page

TABLE 3-1: OA APPROACH AND RESULTS COMPARISON	19
---	----

List of Figures

Page

FIGURE 2-1: AVB ARRANGEMENT FOR SONGS STEAM GENERATORS.....	10
FIGURE 2-2: DETAILS OF AVBS, RETAINING BARS, BRIDGES, AND RETAINER BARS	11
FIGURE 3-1: TRADITIONAL OPERATIONAL ASSESSMENT RESULTS.....	17

List of Appendices

Appendix-A: SONGS U2C17 Outage – Steam Generator Operational Assessment*

Appendix-B: SONGS U2C17 Steam Generator Operational Assessment for Tube-to-Tube Wear*

Appendix-C: Operational Assessment for SONGS Unit 2 SG for Upper Bundle Tube-to-Tube Wear
Degradation at End of Cycle 16

Appendix-D: Operational Assessment of Wear Indications in the U-bend Region of San Onofre Unit 2
Replacement Steam Generators

* [Proprietary Information Redacted]

ABBREVIATIONS AND ACRONYMS

2E-089	Unit 2 Steam Generator E-089
AILPC	Accident-Induced Leakage Performance Criteria
ASME	American Society of Mechanical Engineers
ATHOS	Analysis of Thermal-Hydraulics of Steam Generators
AVB	Anti-Vibration Bar
CE	Combustion Engineering
ECT	Eddy Current Testing
EFPY	Effective Full Power Year
EOC	End of Cycle (fuel)
EPRI	Electric Power Research Institute
ETSS	Examination Technique Specification Sheet
FEI	Fluid Elastic Instability
FOSAR	Foreign Object Search and Retrieval
gpd	Gallons Per Day
gpm	Gallons Per Minute
MHI	Mitsubishi Heavy Industries, Ltd.
NEI	Nuclear Energy Institute
NODP	Normal Operating Differential Pressure
NRC	Nuclear Regulatory Commission
OA	Operational Assessment
POB	Probability of Burst
RCS	Reactor Coolant System
SCE	Southern California Edison
SIPC	Structural Integrity Performance Criteria
SG	Steam Generator
SONGS	San Onofre Nuclear Generating Station
SR	Stability Ratio
T/H	Thermal-Hydraulic
TS	Technical Specifications
TSP	Tube Support Plate
TTW	Tube-to-Tube Wear
U2C17	Unit 2 Cycle 17
UNS	Unified Numbering System
WEC	Westinghouse Electric Company

EXECUTIVE SUMMARY

On January 31, 2012, a leak was detected in a Unit 3 Steam generator (SG) at San Onofre Nuclear Generating Station (SONGS). Southern California Edison (SCE) operators promptly shut down the unit in accordance with approved operating procedures. The resulting small radioactive release to the environment was well below the allowable federal limits. Subsequently, on March 27, 2012, the Nuclear Regulatory Commission (NRC) issued a Confirmatory Action Letter [1] to SCE describing actions that the NRC and SCE agreed would be completed prior to returning Units 2 and 3 to service. Since that time, SCE's technical team supplemented by a team of experts in the field of thermal-hydraulics and in SG design, manufacture, operation, and maintenance have performed extensive investigations into the causes of the tube leak and have assisted in the development of compensatory measures and corrective actions that will prevent a loss of SG tube integrity.

As required by the SONGS Technical Specifications (TS) [3], SONGS SG Program [2], and industry guidelines [5], an Operational Assessment (OA) must be performed to ensure that SG tubing will meet established performance criteria for structural and leakage integrity during the operating period prior to the next planned inspection. Because of the unusual and unexpected nature of the SG tube-to-tube wear (TTW) at SONGS, SCE commissioned three independent OAs [Appendices B, C, and D] by experienced vendors applying diverse methodologies. The non-TTW degradation mechanisms have been addressed by a separate OA included in this report [Appendix-A]. Each of these methodologies demonstrates that SCE has implemented compensatory measures and corrective actions to ensure that Unit 2 will operate safely with substantial conservative margin. This report contains the OAs that have been performed to demonstrate that those compensatory measures and corrective actions will prevent a loss of SG tube integrity.

1.0 PURPOSE

In accordance with the SONGS SG Program [2] an OA is performed to ensure that SG tubing meets established performance criteria for structural and leakage integrity during the interval prior to the next planned inspection. The OA projects and evaluates tube degradation mechanisms which have affected the SGs. The performance criteria are defined in plant TS [3] [4] and are based on NEI-97-06 [5].

This summary of the OAs establishes operational limits for Unit 2 and provides reasonable assurance, as required by NRC regulations, that Unit 2 will operate safely.

2.0 SONGS STEAM GENERATOR DESIGN FEATURES

The steam generator is a recirculating, vertical U-tube type heat exchanger converting feedwater into saturated steam. The steam generator vessel pressure boundary is comprised of the channel head, lower shell, middle shell, transition cone, upper shell and upper head. The steam generator internals include the divider plate, tubesheet, tube bundle, feedwater distribution system, moisture separators, steam dryers and integral steam flow limiter installed in the steam nozzle. The channel head is equipped with one reactor coolant inlet nozzle and two outlet nozzles. The upper vessel is equipped with the feedwater nozzle, steam nozzle and blowdown nozzle. In the channel head, there are two 18 inch access manways. In the upper shell, there are two 16 inch access manways. The steam generator is equipped with six (6) handholes and 12 inspection ports providing access for inspection and maintenance. In addition, the steam generators are equipped with several instrumentation and minor nozzles for layup and chemical recirculation intended for chemical cleaning (See Figure 2-1 and Figure 2-2).

Note: The SG design information is provided in References [6] [7] [8] [9] [10] [11] [12].

Figure 2-1: AVB Arrangement for SONGS Steam Generators

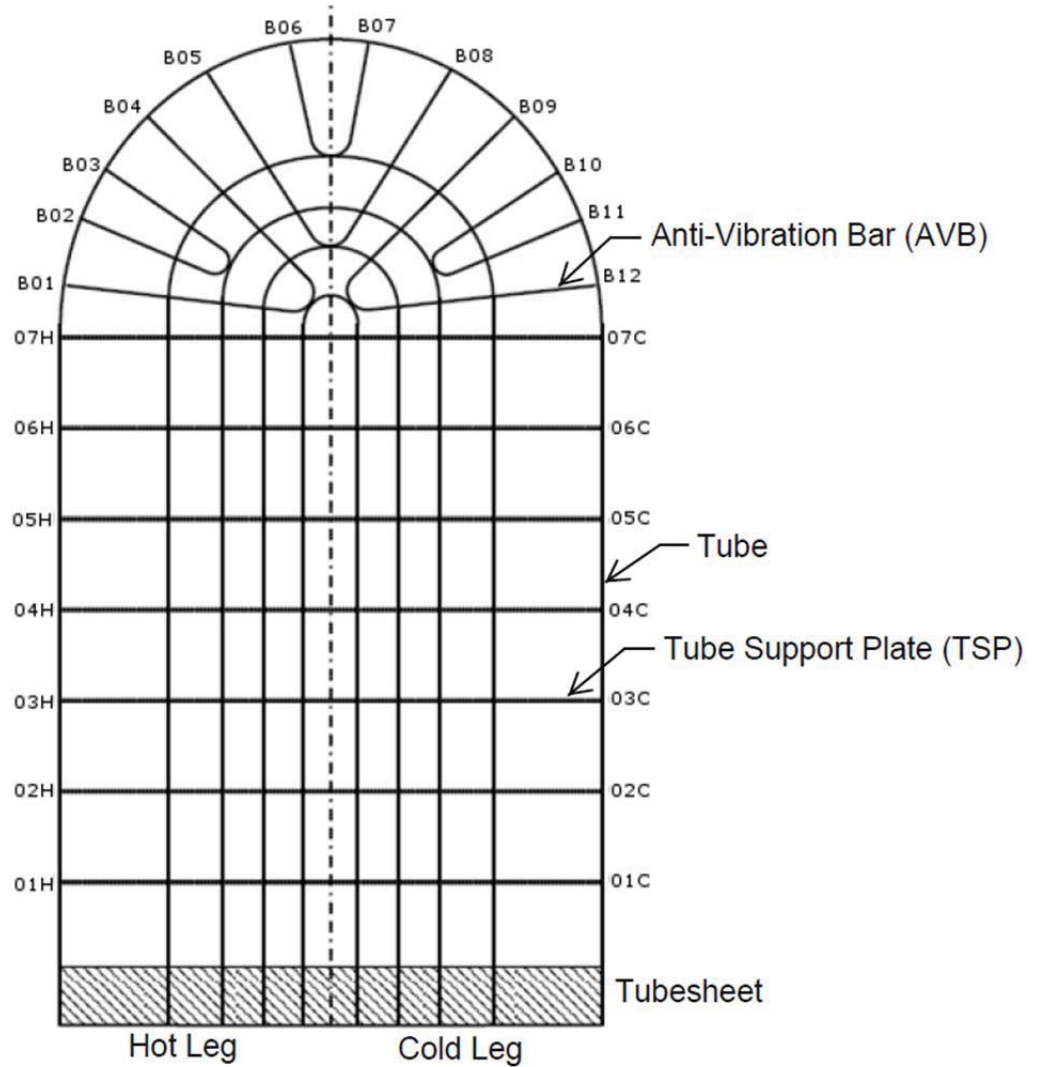


Figure 2-2: Details of AVBs, Retaining Bars, Bridges, and Retainer Bars



3.0 OPERATIONAL ASSESSMENT

As defined in NEI 97-06, the OA is a forward looking evaluation of the SG tube conditions that is used to ensure that the structural integrity and accident leakage performance will not be exceeded during the next inspection interval [5]. The OA projects the condition of SG tubes to the time of the next scheduled inspection outage and determines their acceptability relative to the TS tube integrity performance criteria.

As documented in the “SONGS U2C17 Steam Generator Condition Monitoring Report” [13], the Unit 2 SGs satisfied the three performance criteria specified in the TS for the previous operating period. The SG Program requires an OA to be completed for the next inspection interval within 90 days after initial entry into MODE 4 (MODE is defined in the station TS). This summary of the OAs establishes operational limits for Unit 2 and provides reasonable assurance, as required by NRC regulations, that Unit 2 will operate safely.

The structural integrity performance criteria (SIPC) and accident-induced leakage performance criteria (AILPC) applicable to wear mechanisms are [14]:

Structural Integrity — “All in-service steam generator tubes shall retain structural integrity over the full range of normal operating conditions (including startup, operation in the power range, hot standby, and cool down and all anticipated transients included in the design specification) and design basis accidents. This includes retaining a safety factor of 3.0 against burst under normal steady state full power operation primary-to-secondary pressure differential and a safety factor of 1.4 against burst applied to the design basis accident primary-to-secondary pressure differentials. Apart from the above requirements, additional loading conditions associated with the design basis accidents, or combination of accidents in accordance with the design and licensing basis, shall also be evaluated to determine if the associated loads contribute significantly to burst or collapse. In the assessment of tube integrity, those loads that do significantly affect burst or collapse shall be determined and assessed in combination with the loads due to pressure with a safety factor of 1.2 on the combined primary loads and 1.0 on axial secondary loads.”

Accident-Induced Leakage — “The primary to secondary accident leakage rate for the limiting design basis accident shall not exceed the leakage rate assumed in the accident analysis in terms of total leakage rate for all steam generators and leakage rates for an individual steam generator.”

The acceptance standard for structural integrity is [14]:

The worst-case degraded tube shall meet the SIPC margin requirements with at least a probability of 95% at 50% confidence.

The acceptance standard for accident leakage integrity is [14]:

The probability for satisfying the limit requirements of the AILPC shall be at least 95% at 50% confidence.

The OA may utilize either a deterministic (also known as simplified arithmetic) or a probabilistic methodology.

SCE has assessed all tube wear mechanisms in Unit 2, including TTW. Given the significance of TTW observed in Unit 3, SCE used the experience and expertise of multiple independent companies that routinely perform OAs for the US nuclear industry. AREVA, Westinghouse Electric Company (WEC), and Intertek developed independent OAs to address the TTW found at SONGS. These diverse analyses fulfilled the TS requirement to ensure that SG tube integrity is maintained until the next SG inspection.

SONGS U2C17 Steam Generator Operational Assessment

- Section 3.1 provides a summary of the OA prepared by AREVA evaluating all degradation mechanisms found in Unit 2 SGs with the exception of TTW. This OA demonstrates there is reasonable assurance that the SIPC and AILPC for non-TTW will be satisfied for 18 months at 100% power.
- Section 3.2 provides a summary of the OA prepared by AREVA. This OA deterministically evaluates the potential for TTW for the limiting condition of no in-plane support. The OA also evaluates probabilistically the potential for in-plane Fluid Elastic Instability (FEI) occurring in Unit 2 based on an analysis of the contact forces between tubes and AVBs. The deterministic results demonstrate all tubes are stable (will not experience Thermal-Hydraulic (T/H) conditions that cause FEI) at 70% power for 18 months of operation without relying on the AVBs for in-plane support. Therefore, this OA demonstrates that the SIPC and AILPC for TTW will be satisfied for 18 months at 70% power. The probabilistic results demonstrate a low probability of FEI at 70% power for approximately 8 months of operation even when additional conservatism are introduced.
- Section 3.3 provides a summary of the OA prepared by Intertek following “traditional” industry guidelines for assessing SG tube degradation. This OA evaluates the probability that TTW caused by FEI will not exceed the SG SIPC. This OA demonstrates there is a reasonable assurance that the SIPC and AILPC for TTW will be satisfied for 16 months at 70% power level.
- Section 3.4 provides a summary of the OA prepared by WEC based on an alternate interpretation of the inspection results. This OA determines the TTW in Unit 2 was caused by out-of-plane vibration between two tubes in close proximity. The OA evaluates the potential for in-plane instability and concludes the Unit 2 SG tubes were stable in-plane at 100% power. This OA demonstrates there is reasonable assurance that the SIPC and AILPC for TTW will be satisfied for 18 months at 70% power.

3.1 OA for Degradation Mechanisms Other than TTW

The “SONGS U2C17 Outage – Steam Generator Operational Assessment” report [Appendix-A] addresses all degradation mechanisms found in Unit 2 SGs with the exception of TTW. Due to the relatively large number of AVB and TSP wear indications, identified during the U2C17 outage, a probabilistic approach was used to complete the OA for these mechanisms, which included:

- Tube Wear at AVB Locations
- Tube Wear at TSP Locations
- Tube Wear at Retainer Bar Locations
- Tube Wear as a Result of Foreign Object Wear

The objective of this OA is to ensure that structural and leakage performance criteria will be met over the length of the upcoming inspection interval. The OA tube structural integrity requirement is that the projected worst case degraded tube for each existing degradation mechanism shall meet the limiting structural performance parameter with a 95% probability at 50% confidence [3].

AVB and TSP Wear

Because the tube wear indications are flat and long in the axial direction, the limiting requirement for the inspection interval length is structural integrity (i.e. tube burst at 3x NODP). The projected accident-induced leak rates for tube wear will not be limiting since leakage due to ligament pop-through will not precede burst condition at 3x NODP.

The OA uses a probabilistic method to calculate the growth at End of Cycle (EOC) of each indication by randomly sampling from the growth rate distribution yielding one estimate of the EOC depth for each indication. The burst pressure of the worst case degraded tube is calculated and compared with the value of 3 times NODP. This process is repeated thousands of times in order to develop a probability of burst for the worst case degraded tube. If the probability of burst of the worst case degraded tube is less than 5%, then the plugging criteria and inspection interval are satisfactory.

The projected EOC probabilities of burst for the population of indications in each damage mechanism category were calculated for Unit 2 at 100% power for a full cycle of operation (1.577 Effective Full Power Years, EFPY). The projected EOC probabilities are compared with the 95% probability 50% confidence EPRI guidelines [14] criteria to demonstrate the OA structural integrity criteria for AVB and TSP wear are satisfied for a full fuel cycle of operation at 100% reactor power.

Retainer Bar Wear

Because of the potential for continued retainer bar wear of Unit 2, tubes adjacent to retainer bars have been removed from service. Tubes with retainer bar wear indications were stabilized with U-bend cable stabilizers. The tubes on either side of all retainer bars, at each end of the retainer bars, and at the center of the retainer bars, were also stabilized with U-bend cable stabilizers. These corrective actions provide reasonable assurance that retainer bar wear will not challenge the structural and leakage integrity performance criteria during the remaining life of the SGs. In addition, the stabilization of these tubes provides reasonable assurance that a tube severance event will not occur as a result of retainer bar wear. The SG Program [2] will monitor the tubes adjacent to these plugged tubes during future SG inspections.

SONGS U2C17 Steam Generator Operational Assessment

Foreign Object Wear

All Unit 2 SG tubes were examined full length with Eddy Current Testing (ECT) bobbin coil probes. Two adjacent tubes in SG 2E-089 were identified with foreign object wear indications. The foreign object was identified as weld slag and retrieved from the SG. No other foreign objects were found. The foreign object is not indicative of degradation of secondary side internals.

Because the foreign object has been removed, no potential exists for degradation to progress at these locations. After removal of the object, the affected indications were inspected with ECT. Since the indications are below the SONGS plugging limit and the object was removed, these tubes are left in service.

Based on ECT inspections, secondary side visual examinations, and FOSAR, no foreign objects capable of causing tube degradation remain in the Unit 2 SGs. There is reasonable assurance that foreign objects will not cause the structural or leakage integrity performance criteria to be exceeded prior to the next tube inspection in each SG.

OA for Degradation Mechanisms Other than TTW Conclusion

The OA demonstrates there is reasonable assurance that the SIPC and AILPC for non-TTW will be satisfied for 18 months at 100% power.

3.2 TTW OA Using Tube-to-AVB Support Conditions and Contact Force

The “SONGS U2C17 Steam Generator Operational Assessment for Tube-to-Tube Wear” [Appendix-B] assesses the TTW degradation mechanism deterministically, without taking credit for in-plane support. The OA also implements a probabilistic approach using tube to AVB contact forces for defining an effective tube support. The OA predicts the probability of in-plane FEI and compares this value to the probabilistic SIPC (95% probability at 50% confidence).

The deterministic approach uses Stability Ratios (SRs) as the criterion for susceptibility to FEI. The SR is calculated conservatively using Thermal-Hydraulic (T/H) and tube support conditions on the secondary side of the SG. The T/H conditions are determined using an ATHOS computer model.

The deterministic approach demonstrates in-plane stability (SR less than 1.0) at 70% power with no effective in-plane AVB supports. This demonstrates TTW will not occur and SIPC limits will be met.

As discussed above, a SR of less than 1.0 indicates the SG tubes will be stable. To demonstrate margin, a probabilistic evaluation was performed assuming instability may occur at a calculated SR as low as 0.75. In the probabilistic approach, the number of effective AVB supports for each tube uses a probabilistic contact force distribution and criteria for determining whether a support is effective for a given contact force. A finite element model of tubes, AVBs, tube-to-AVB gaps, and support structures is used to calculate contact forces at AVB locations. Tube wear inputs to the finite element model are determined from actual wear observed in Units 2 and 3. Results from published technical literature, confirmed by benchmarking the FEI probability model to Unit 3 TTW, indicate that effective supports have a contact force that exceeds a specified value.

SRs are determined for each U-bend tube as a function of the number of consecutive ineffective supports and power level. The distributions of contact forces are calculated for each AVB location in the bundle. Tube wear at AVB locations decreases the contact force at those locations. The required contact force for an AVB support to be considered effective is calculated for each AVB location.

SONGS U2C17 Steam Generator Operational Assessment

Using the above as inputs, Monte Carlo trials of a SG are simulated. The probability of instability is the number of trials where the SG contained one or more unstable tubes divided by the total number of trials.

TTW OA Using Tube-to-AVB Support Conditions and Contact Force Assessment Conclusion

The deterministic approach demonstrates FEI will not occur. Using a SR of <1.0 at 70% power, the SIPC and AILPC are satisfied for an 18 month inspection interval. The probabilistic approach also demonstrates that there is safety margin in the planned inspection interval of 150 cumulative days at power. The approach demonstrates that if instability is assumed to initiate at a calculated SR of 0.75, rather than a value of 1.0, the SIPC acceptance standard is satisfied for approximately 8 months at 70% power.

3.3 “Traditional” Probabilistic OA for TTW

The “Operational Assessment for SONGS Unit 2 SG for Upper Bundle Tube-to-Tube Wear Degradation at End of Cycle 16” [Appendix-C] uses established industry methods for assessing degradation mechanisms. This OA uses empirical models for degradation growth and engineering models for determining burst pressure and through-wall leak rates. The non-traditional aspect of this OA is to characterize the presence and severity of TTW degradation indications using wear indices defined by the state of AVB and TSP wear for a specific tube.

Unit 3 wear data establish the initiation and growth of TTW indications in Unit 2 SG. An empirical correlation using a wear index (a measure of the state of wear degradation in each tube) provides the method for comparing the Unit 3 wear to Unit 2. A probabilistic model representing the high-wear region of the tube bundle evaluates TTW for inspection interval. Tube burst and leakage probabilities are calculated by Monte Carlo simulation for initiation and growth of TTW.

Two OA cases are evaluated using the sizing techniques that define the Unit 3 TTW depths. Case 1 evaluates eddy current indication sizing using EPRI ECT Examination Technique Specification Sheet (ETSS) 27902.2 to establish the TTW depth distributions. In Case 2, the TTW depths were determined using a more representative calibration standard.

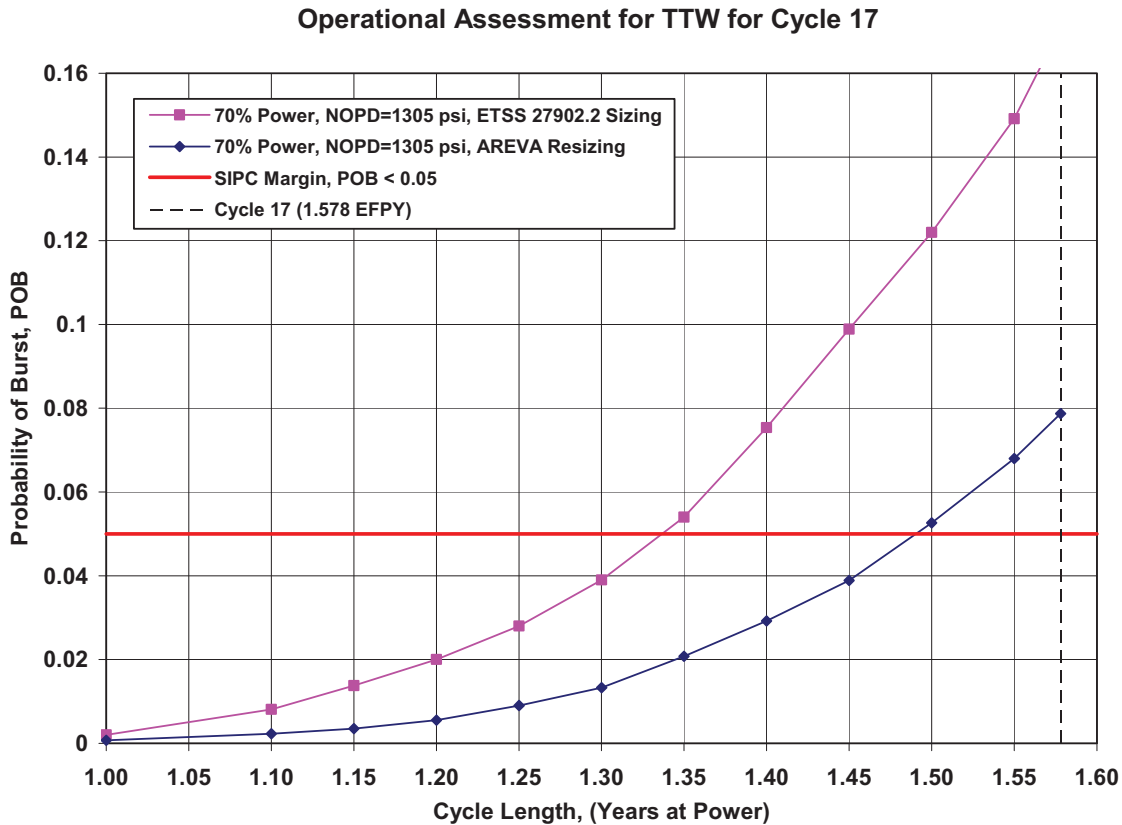
“Traditional” Probabilistic OA for TTW Conclusion

The results for Case 1 indicate that the SIPC margin requirements are satisfied for an inspection interval of 16 months at 70% power. In Case 2, the SIPC margins are met for a cycle length of 17 months at 70% power. The results of this analysis are displayed in Figure 3-1. The figure identifies the probability of burst as a function of operating cycle length (inspection interval) and power.

The SIPC (Tube burst at 3xNOPD) is the limiting requirement for the inspection interval. The AILPC is satisfied since burst margins at 3xNOPD are maintained during the inspection interval.

This OA demonstrates there is a reasonable assurance that the SIPC and AILPC for TTW will be satisfied for 16 months at 70% power level.

Figure 3-1: Traditional Operational Assessment Results



3.4 Deterministic TTW OA

A deterministic TTW OA [Appendix-D] was completed for tube wear at AVBs and TTW. Tube wear projections for in-service tubes confirm the SG performance criteria will be satisfied during the inspection interval. Tube wear projections for plugged tubes confirm that severance will not occur during the inspection interval.

Evaluation of TTW of the two tubes in SG 2E-089 concludes the wear did not result from in-plane vibration of the tubes. ECT data demonstrate the tube wear indications at AVBs did not extend beyond the width of the AVBs in Unit 2. Wear extending beyond the width of AVBs was strongly correlated with Unit 3 tubes with TTW. In-plane SRs indicate that the two Unit 2 tubes with TTW are stable at 100% power. Pre-service inspection data indicates these two tubes were in close proximity prior to SG operation. The OA postulates that during operation out-of-plane vibration and/or turbulence caused the two tubes to wear.

The potential for in-plane vibration leading to TTW in Unit 2 is evaluated by calculating in-plane SRs. The OA methodology predicts in-plane vibration in Unit 3 and confirms the absence of in-plane vibration in Unit 2.

This OA projects the depth of indications to the next inspection using current inspection data. ATHOS results provide the T/H inputs for flow velocity, density, and void fraction along the length of the tube. These conditions are used in the Flow Induced Vibration analysis to generate the SR for out-of-plane and in-plane vibration of the

SONGS U2C17 Steam Generator Operational Assessment

tube for various tube support conditions. The support conditions define whether or not a support location such as an AVB intersection is effective, meaning that the structure provides adequate support with respect to motion of the tube due to vibration. Presence of tube-to-AVB wear indicates an ineffective support.

The vibration analysis results and support conditions are used to make wear projections in the next operating cycle. This calculation is based on empirical test results and involves several input assumptions related to tube-to-AVB gap, the AVB twist, and the wear coefficient between the tube and AVB. The expected ranges of these parameters are known from test results, published data and experience. Wear depth projection is made taking into consideration the inspection results at the current outage. After setting the inputs to match the inspection results for a given indication, the wear calculations are extended to determine the projected wear depth at the next inspection.

Deterministic TTW OA Conclusion

The OA demonstrates there is reasonable assurance that the SIPC and AILPC for TTW will be satisfied for 18 months at 70% power.

3.5 Evaluation of Leakage Integrity

The AREVA non-TTW OA [Appendix-A], Section 6.3, discussed the evaluation of leakage integrity for both in-service and plugged tubes. Since the preparation of the AREVA non-TTW OA, SCE plugged five additional tubes. The five additional tubes resulted in a negligible change to the postulated operational and accident-induced leakage attributed to all of the tube plugs using the methodology from the AREVA non-TTW OA.

The operational leakage performance criterion is met through the plant monitoring program. The accident-induced leakage performance criterion is met by projecting leakage attributed to all degradation mechanisms along with postulated plug leakage and comparing the projected leakage to the allowable accident-induced leak rate limit. For tubes returned to service, the onset of pop-through and leakage for axially oriented indications with limited circumferential extent – the nature of the degradation identified in the Unit 2 SGs – is coincident with burst. None of the identified degradation mechanisms in Unit 2 are projected to exceed the structural performance criteria prior to the next scheduled inspection. The accident-induced leakage is only attributed to postulated plug leakage through out-of-service tubes. There is reasonable assurance the accident-induced leakage performance criteria will not be exceeded prior to the next inspection of the Unit 2 SGs.

SONGS U2C17 Steam Generator Operational Assessment

3.6 Summary of All OA Conclusions

The OA provide reasonable assurance, as required by NRC regulations that Unit 2 will operate safely at 70% power for 150 cumulative days. The OAs (See Table 3-1) summarized in Sections 3.1 and 3.2 conclude the SIPC and AILPC are satisfied. The alternative OA methodologies summarized in Sections 3.3 and 3.4 also confirm the SG tube integrity will be maintained during the inspection interval.

Table 3-1: OA Approach and Results Comparison

OA Description	OA for Degradation Mechanisms Other Than TTW	TTW OA With No Effective AVB Supports	“Traditional” Probabilistic OA Prepared for TTW	Deterministic TTW OA
Reference Appendix	A	B	C	D
Degradation Mechanisms Addressed	All but TTW	TTW	TTW	TTW & AVB Wear
Type	Probabilistic	Deterministic	Probabilistic	Deterministic
Thermal Power Assumption	100%	70%	70%	70%
Resulting Inspection Interval	18 months	18 months	16 months	18 months

As identified in Table 3-1 above, the OAs result in an acceptable inspection interval of at least 16 months at 70% power. These OAs determined that at 70% power, the T/H conditions that cause FEI will be eliminated from the SONGS Unit 2 SGs. As discussed in Section 3.2, an additional probabilistic evaluation, assuming a calculated SR of 0.75, was performed to demonstrate margin. The approach assumes instability initiates at a calculated SR of 0.75 (rather than a SR of 1.0). Using this approach, the SIPC acceptance standard is satisfied for approximately 8 months at 70% power.

Accordingly, the 150 cumulative day inspection interval being implemented by SCE demonstrates substantial conservative margin using any of the OA methodologies.

4.0 REFERENCES

1. Confirmatory Action Letter 4-12-001 – “San Onofre Nuclear Generating Station, Units 2 and 3, Comments to Address Steam Generator Tube Degradation,” March 27, 2012
2. SONGS Steam Generator Program, SO23-SG-1
3. SONGS Technical Specifications Sections 5.5.2.11, “Steam Generator (SG) Program,” Amendment 204
4. SONGS Technical Specifications Section 3.4.12, “RCS Operational Leakage,” Amendment 204
5. NEI 97-06, “SG Program Guidelines,” Rev. 3, January 2011
6. AREVA NP Document 51-9176667-001, “SONGS 2C17 & 3C17 Steam Generator Degradation Assessment.”
7. SCE Drawing SO23-617-1-D116 Rev. 2, “San Onofre Nuclear Generating Station Unit 2 & 3 Replacement Steam Generators – Design Drawing – Tube Bundle 1/3” (MHI Drawing L5-04FU051 Rev. 1)
8. SCE Drawing SO23-617-1-D507 Rev. 5, “San Onofre Nuclear Generating Station Unit 2 & 3 Replacement Steam Generators – Design Drawing – Anti-Vibration Bar Assembly 1/9” (MHI Drawing L5-04FU111 Rev. 2)
9. SCE Drawing SO23-617-1-D542 Rev. 9, “San Onofre Nuclear Generating Station Unit 2 & 3 Replacement Steam Generators – Design Drawing – Anti-Vibration Bar Assembly 7/9” (MHI Drawing L5-04FU117 Rev. 9)
10. SCE Drawing SO23-617-1-D296 Rev. 3, “San Onofre Nuclear Generating Station Unit 2 & 3 Replacement Steam Generators – Design Drawing – Tube Support Plate Assembly 3/3” (MHI Drawing L5-04FU108 Rev. 3)
11. SCE Drawing SO23-617-1-D117 Rev. 2, “San Onofre Nuclear Generating Station Unit 2 & 3 Replacement Steam Generators – Design Drawing – Tube Bundle 2/3” (MHI Drawing L5-04FU052 Rev. 1)
12. SCE Drawing SO23-617-1-D118 Rev. 4, “San Onofre Nuclear Generating Station Unit 2 & 3 Replacement Steam Generators – Design Drawing – Tube Bundle 3/3” (MHI Drawing L5-04FU053 Rev. 3)
13. AREVA NP Document 51-9182368-003, “SONGS 2C17 Steam Generator Condition Monitoring Report”
14. EPRI Report 1019038, “Steam Generator Management Program: Steam Generator Integrity Assessment Guidelines: Revision 3”, November 2009.

ATTACHMENT 6 – Appendix A

SONGS U2C17 Outage – Steam Generator Operational Assessment

[Proprietary Information Redacted]



AREVA NP Inc.

Engineering Information Record

Document No.: 51 - 9182833 - 002

SONGS U2C17 Outage - Steam Generator Operational Assessment

Supplier Status Stamp

VPL No: 1814-AU651-M0157	Rev No: 0	qc: N/A
<input type="checkbox"/> DESIGN DOCUMENT ORDER NO. <u>800918458</u> <input checked="" type="checkbox"/> REFERENCE DOCUMENT - INFORMATION ONLY <input type="checkbox"/> VIRP IOM MANUAL		
MFG MAY PROCEED: <input type="checkbox"/> YES <input type="checkbox"/> NO <input checked="" type="checkbox"/> N/A		
<small>STATUS - A status is required for design documents and is optional for reference documents. Drawings are reviewed and approved for arrangements and conformance to specification only. Approval does not relieve the submitter from the responsibility of adequacy and suitability of design, materials, and/or equipment represented.</small>		
<input type="checkbox"/> 1. APPROVED <input type="checkbox"/> 2. APPROVED EXCEPT AS NOTED - Make changes and resubmit. <input type="checkbox"/> 3. NOT APPROVED - Correct and resubmit for review. NOT for field use.		
APPROVAL: (PRINT / SIGN / DATE)		
RE: <u>E. GRIBBLE</u> <u>10/01/12</u>		
FLS:		
Other:		

SCE DE(123) 5 REV. 3 07/11

REFERENCE: SO123-XXIV-37.8.26



SONGS U2C17 Outage - Steam Generator Operational Assessment

Safety Related? YES NO

Does this document contain assumptions requiring verification? YES NO

Does this document contain Customer Required Format? YES NO

Signature Block

Name and Title/Discipline	Signature	P/LP, R/LR, A/A-CRF, A/A-CRI	Date	Pages/Sections Prepared/Reviewed/ Approved or Comments

Note: P/LP designates Preparer (P), Lead Preparer (LP)
R/LR designates Reviewer (R), Lead Reviewer (LR)
A/A-CRF designates Approver (A), Approver of Customer Requested Format (A-CRF)
A/A-CRI designates Approver (A), Approver - Confirming Reviewer Independence (A-CRI)

Table of Contents

	Page
SIGNATURE BLOCK.....	2
RECORD OF REVISION	3
LIST OF TABLES	5
LIST OF FIGURES	6
1.0 PURPOSE	7
2.0 ABBREVIATIONS AND ACRONYMS	7
3.0 SCOPE	9
4.0 PERFORMANCE CRITERIA.....	9
5.0 BACKGROUND	10
5.1 Steam Generator Design	10
5.2 Tube-to-Tube Wear Finding.....	10
5.3 Condition Monitoring Assessment Summary.....	11
6.0 OPERATIONAL ASSESSMENT.....	15
6.1 Input Parameters	15
6.2 Evaluation of Structural Integrity	18
6.2.1 AVB Wear and TSP Wear.....	18
6.2.2 Retainer Bar Wear	28
6.2.3 Tube-to-Tube Wear	28
6.2.4 Foreign Object Wear.....	29
6.3 Evaluation of Leakage Integrity.....	29
6.4 Secondary Side Internals.....	30
7.0 OPERATIONAL ASSESSMENT CONCLUSION.....	30
8.0 REFERENCES.....	31



List of Tables

Page

TABLE 2-1: ABBREVIATIONS AND ACRONYMS.....	7
TABLE 6-1: UNIT 2 STEAM GENERATOR INPUT VALUES.....	16
TABLE 6-2: EDDY CURRENT ETSS INPUT VALUES [4].....	17
TABLE 6-3: PROJECTED PROBABILITY OF NON-BURST.....	21
TABLE 6-4: U2C17 TUBE-TO-TUBE WEAR INDICATIONS.....	28
TABLE 6-5: POSTULATED PLUG LEAKAGE	30

List of Figures

	Page
FIGURE 5-1: SONGS STEAM GENERATOR SUPPORT STRUCTURE LAYOUT	12
FIGURE 5-2: VIEW FROM ABOVE BUNDLE SHOWING RETAINER BAR LOCATIONS	13
FIGURE 5-3: SKETCH SHOWING RETAINER/RETAINING BAR CONFIGURATION.....	14
FIGURE 6-1: ADJUSTED GROWTH RATE DISTRIBUTION, AVB WEAR >20%TW	22
FIGURE 6-2: ADJUSTED GROWTH RATE DISTRIBUTION, AVB WEAR <20%TW	23
FIGURE 6-3: ADJUSTED GROWTH RATE DISTRIBUTION, TSP WEAR >10%TW	24
FIGURE 6-4: ADJUSTED GROWTH RATE DISTRIBUTION, TSP WEAR <10%TW	25
FIGURE 6-5: AVB WEAR DEPTH HISTOGRAM	26
FIGURE 6-6: TSP WEAR DEPTH HISTOGRAM	27

SONGS U2C17 Outage - Steam Generator Operational Assessment

1.0 PURPOSE

In accordance with the SONGS Steam Generator Program [18] and EPRI Steam Generator Integrity Assessment Guidelines [2], an operational assessment (OA) must be performed to ensure that steam generator (SG) tubing will meet established performance criteria for structural and leakage integrity during the operating period prior to the next planned inspection. The OA evaluates and projects tube degradation mechanisms which have affected the SGs to date. The performance criteria are defined in plant Technical Specifications [13] [14]. The performance criteria are based on NEI 97-06 [1] (see Section 4.0 below).

This report documents the OA performed during the SONGS Unit 2 C17 Refueling Outage. This OA addresses the detected tube degradation OTHER THAN tube-to-tube wear (TTW). TTW will be addressed in a separate OA [15]. This OA concludes that operation at full power for a full cycle of 1.577 Effective Full Power Years (EFPY) is justified based on detected tube degradation other than TTW. The OA for TTW [15] may prescribe operation at reduced power and/or a shorter inspection interval. The more conservative OA shall govern plant operation.

2.0 ABBREVIATIONS AND ACRONYMS

The following table provides a listing of abbreviations and acronyms used throughout this report.

Table 2-1: Abbreviations and Acronyms

Abbreviation or Acronym	Definition
01C to 07C	Tube Support Plate Designations for Cold Leg (7 Locations)
01H to 07H	Tube Support Plate Designations for Hot Leg (7 Locations)
2E-088	Unit 2 Steam Generator 88
2E-089	Unit 2 Steam Generator 89
3E-088	Unit 3 Steam Generator 88
3E-089	Unit 3 Steam Generator 89
3 NOPD	3 Times Normal Operating Pressure Differential
AILPC	Accident Induced Leakage Performance Criterion
ASME	American Society of Mechanical Engineers
AVB	Anti-Vibration Bar
C	Column
CE	Combustion Engineering
CL or C/L	Cold Leg
CM	Condition Monitoring
DA	Degradation Assessment
ECT	Eddy Current Testing
EFPD	Effective Full Power Days
EOC	End of Operating Cycle
EPRI	Electric Power Research Institute

SONGS U2C17 Outage - Steam Generator Operational Assessment

Table 2-1: Abbreviations and Acronyms

Abbreviation or Acronym	Definition
ETSS	Examination Technique Specification Sheet
FOSAR	Foreign Object Search and Retrieval
GPD	Gallons per Day
GPM	Gallons per Minute
HL or H/L	Hot Leg
KSI	Thousand Pounds per Square Inch
MHI	Mitsubishi Heavy Industries
MSLB	Main Steam Line Break
NDE	Non Destructive Examination
NEI	Nuclear Energy Institute
NN	Nuclear Notification
NOPD	Normal Operating Pressure Differential
NRC	Nuclear Regulatory Commission
OA	Operational Assessment
PSI	Pounds per Square Inch
PSIG	Pounds per Square Inch Gage
PWR	Pressurized Water Reactor
QA	Quality Assurance
R	Row
RB	Retainer Bar
RCS	Reactor Coolant System
SCE	Southern California Edison
SG	Steam Generator
SIPC	Structural Integrity Performance Criteria
SLB	Steam Line Break
SONGS	San Onofre Nuclear Generating Station
SSI	Secondary Side Inspection
TEC	Tube End Cold
TEH	Tube End Hot
TSP	Tube Support Plate
TTS	Top of Tubesheet
TTW	Tube to Tube Wear
TW	Through Wall
UB	U-bend

 SONGS U2C17 Outage - Steam Generator Operational Assessment

3.0 SCOPE

This evaluation pertains to the SONGS Unit 2 replacement steam generators which are reactor coolant system components. This report addresses all tube degradation mechanisms except for TTW. The OA for TTW will be addressed separately. In accordance with Reference 10, the OA documented in this report is required to be completed prior to plant entry into Mode 2 during start up from the current outage.

Note that the required SG condition monitoring (CM) assessment is documented in a separate report [11] and is summarized below in Section 5.3.

4.0 PERFORMANCE CRITERIA

The Unit 2 performance criteria, based on NEI 97-06 [1] are shown below. The structural integrity and accident-induced leakage criteria were taken from Section 5.5.2.11 [13] from the Unit 2 Technical Specifications. The operational leakage criterion was taken from Section 3.4.13 [14] of the Unit 2 Technical Specifications.

- Structural Integrity Performance Criterion (SIPC): All in-service steam generator tubes shall retain structural integrity over the full range of normal operating conditions (including startup, operation in the power range, hot standby, and cooldown, and all anticipated transients included in the design specification) and design basis accidents. This includes retaining a safety factor of 3.0 against burst under normal steady state full power operation primary-to-secondary pressure differential and a safety factor of 1.4 against burst applied to the design basis accident primary-to-secondary pressure differentials. Apart from the above requirements, additional loading conditions associated with the design basis accidents, or combination of accidents in accordance with the design and licensing basis, shall also be evaluated to determine if the associated loads contribute significantly to burst or collapse. In the assessment of tube integrity, those loads that do significantly affect burst or collapse shall be determined and assessed in combination with the loads due to pressure with a safety factor of 1.2 on the combined primary loads and 1.0 on axial secondary loads.
- Accident Induced Leakage Performance Criterion (AILPC): The primary to secondary accident induced leakage rate for any design basis accident, other than a SG tube rupture, shall not exceed the leakage rate assumed in the accident analysis in terms of total leakage rate for all SGs and leakage rate for an individual SG. Leakage is not to exceed 0.5 gpm per SG and 1 gpm through both SGs.
- Operational Leakage Performance Criterion (OLPC): RCS operational leakage shall be limited to 150 gallons per day primary to secondary leakage through any one steam generator.”

5.0 BACKGROUND

5.1 Steam Generator Design

SONGS Unit 2 is a two loop Combustion Engineering (CE) Pressurized Water Reactor (PWR) plant which began commercial operation in 1983. The original CE steam generators were replaced in 2009-2010 with new SGs designed and manufactured by Mitsubishi Heavy Industries (MHI). The replacements, referred to by MHI as model 116TT-1, incorporate thermally treated Inconel Alloy 690 (I-690TT) tubing which has demonstrated, through laboratory testing and industry experience, superior resistance to stress corrosion cracking as compared with the I-600 tubing used in the original SGs. Other design features include full tubesheet depth hydraulic tube expansion and seven stainless steel trefoil broached Tube Support Plates (TSPs) which are features chosen primarily to minimize the potential for tube corrosion.

There are 9727 tubes in each SG, in 142 rows and 177 columns, in a triangular pitch arrangement. The tubes in rows 1-13 are thermally stress-relieved to further minimize the potential for in-service stress corrosion cracking in the U-bends. The tube bundle U-bend region is supported by a floating Anti-Vibration Bar (AVB) structure consisting of six V-shaped flat-bar AVBs between each tube column. The AVBs were fabricated from ASME SA-479, Type 405 ferritic stainless steel and are equipped with two Alloy 690 (ASME SB-168 UNS N06690) end caps. Each AVB end cap is welded to an Alloy 690 retaining bar. The retaining bars with AVBs attached are supported by twenty four chrome-plated Alloy 690 retainer bars that anchor the assembly to the tubes. Thirteen Alloy 690 bridges run perpendicular to the retaining bars and retainer bars, and hold the entire assembly together. The AVB structure is not attached to any other steam generator component. Figure 5-1 illustrates the general layout of the tube support structures. Figure 5-2 and Figure 5-3 illustrate the retainer bar and retaining bar arrangement.

5.2 Tube-to-Tube Wear Finding

During the U2C17 outage, SONGS Unit 3 was shut down due to a primary-to-secondary SG tube leak. Eddy current inspections of the Unit 3 steam generators revealed that the cause of the leak was TTW in the U-bend region of the tube bundle. A root cause evaluation has concluded that the tube-to-tube wear in the SONGS steam generators was caused by tube movement caused by fluid-elastic instability (FEI) [16]. No indications of TTW were reported during the initial inspections of the Unit 2 steam generators which included full-length inspections of all tubes with bobbin coil probes. However, to apply the Unit 3 experience to Unit 2 steam generators, supplemental +Point™ inspections of the U-bends were performed in Unit 2. These supplemental inspections included the full-length of the U-bend for a group of tubes in the same tube bundle region which experienced TTW in Unit 3. These supplemental inspections resulted in the finding of two adjacent tubes with shallow (14% TWD as measured with +Point™) tube-to-tube wear in the 2E-089 SG.

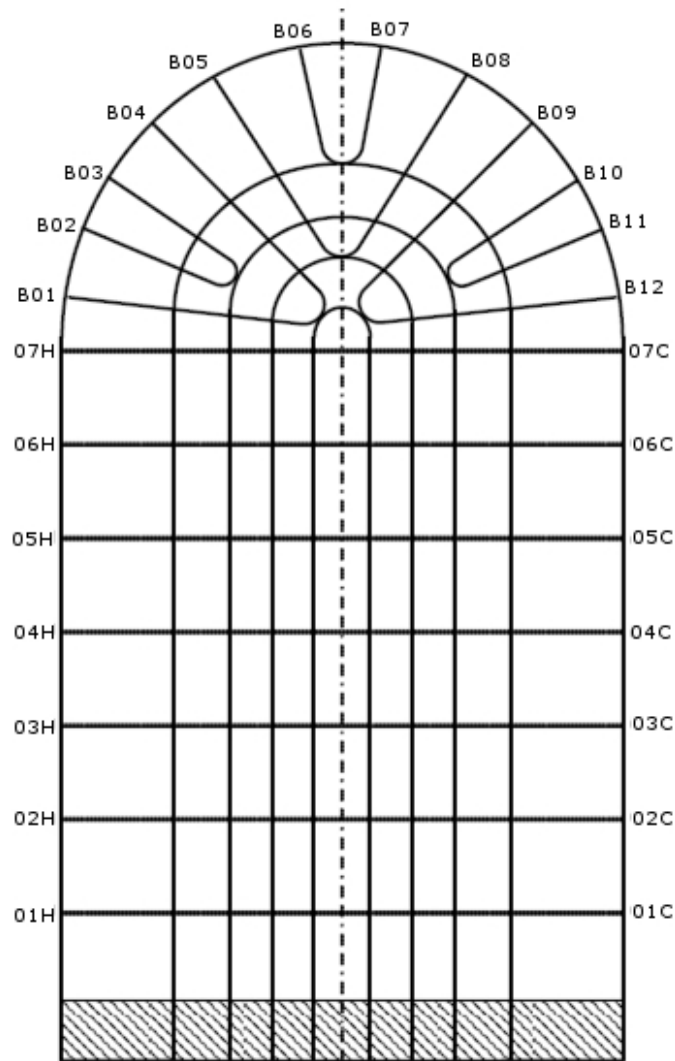
5.3 Condition Monitoring Assessment Summary

A detailed description of the SG scope of work and findings, and the CM assessment of SG tube condition as determined during the U2C17 outage are documented in Reference 11. The U2C17 inspections revealed many indications of wear. Wear indications were reported at anti-vibration bars (AVBs), tube support plates (TSPs), retainer bars (RB), and due to a foreign object. In addition, as discussed above, tube-to-tube wear in the U-bend region was also reported in two adjacent tubes in the 2E-089 SG.

Except for one retainer bar wear indication, all tubes passed CM analytically. The tube with the deep RB wear indication was in-situ pressure tested and successfully met all performance criteria.

The CM assessment evaluated all SG tube degradation detected during the U2C17 outage against the three SONGS technical specification performance criteria in References 13 and 14. Through a combination of eddy current inspection, analytical evaluation, in-situ pressure testing, and operational leakage monitoring, it was determined that all three of the performance criteria were met.

Figure 5-1: SONGS Steam Generator Support Structure Layout



SONGS U2C17 Outage - Steam Generator Operational Assessment

Figure 5-2: View From Above Bundle Showing Retainer Bar Locations

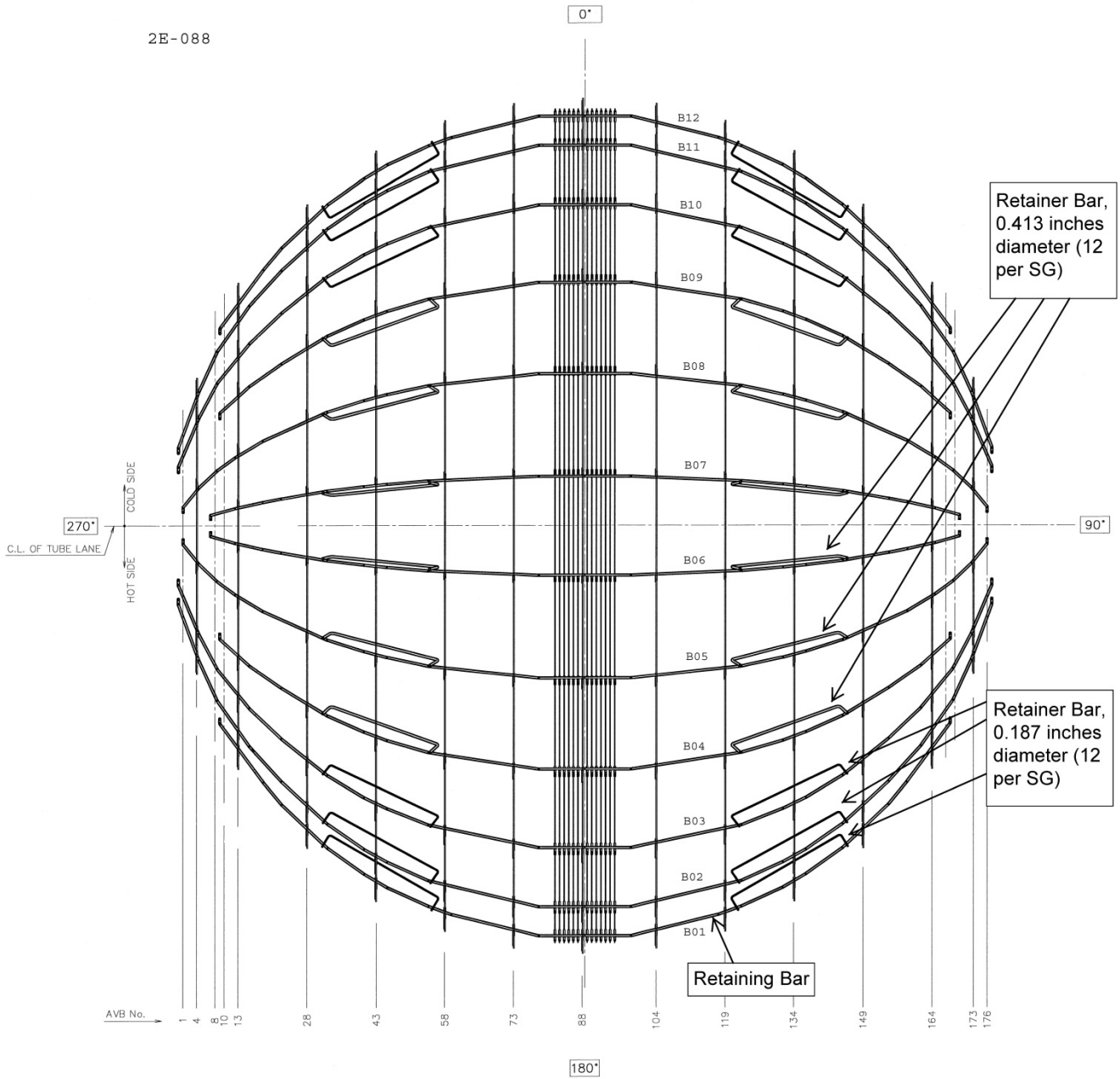
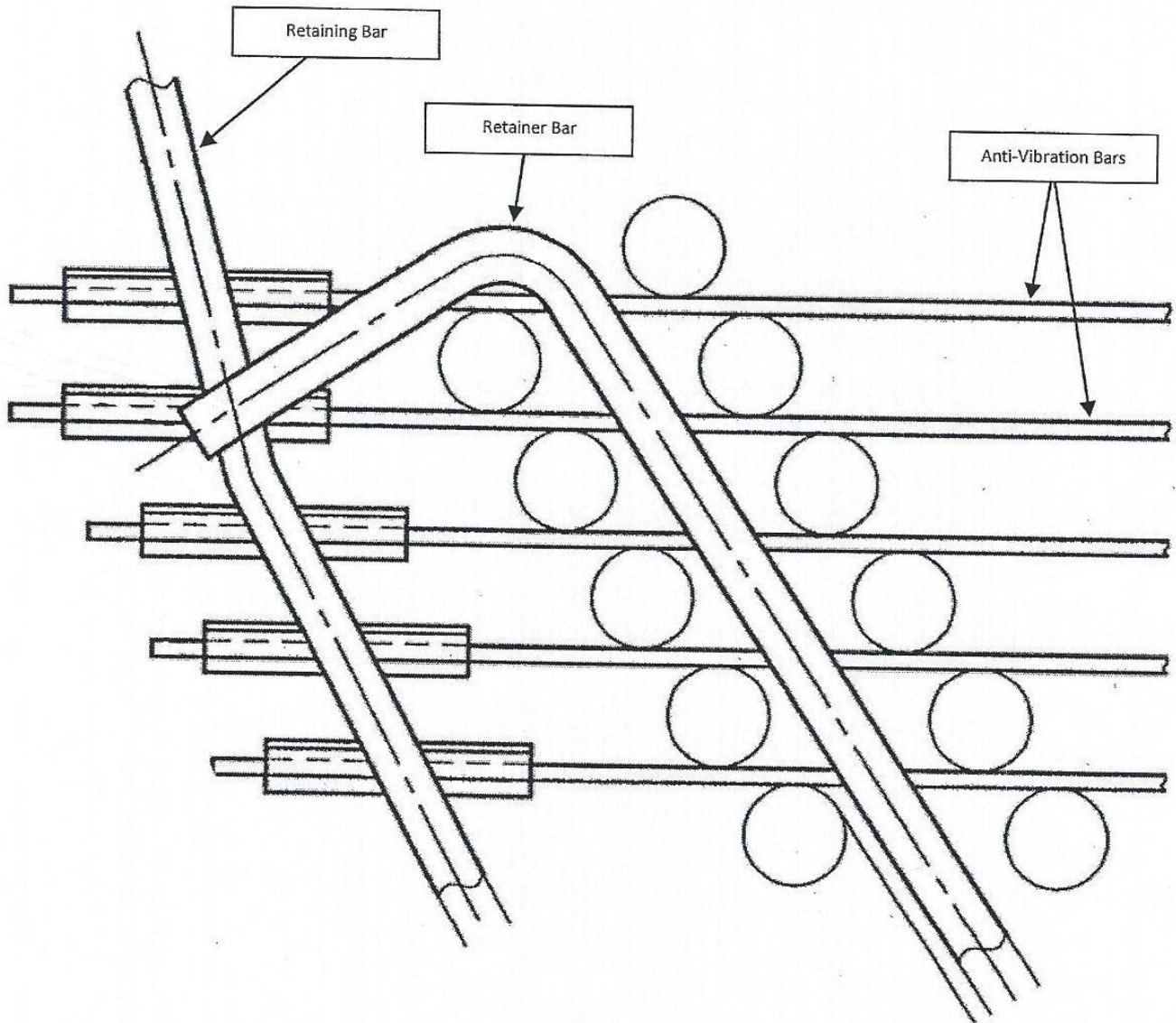


Figure 5-3: Sketch Showing Retainer/Retaining Bar Configuration



6.0 OPERATIONAL ASSESSMENT

The SONGS SG Program requires that a “forward looking” operational assessment (OA) be performed in accordance with Reference 2 to determine if the SG tubing will continue to meet the structural and leakage integrity requirements prior to the next inspection. The OA is based upon an evaluation of the degradation mechanisms observed during the current inspection. As discussed in Reference 11, the following tube degradation mechanisms were identified during the U2C17 outage:

- Anti-vibration bar (AVB) wear
- Tube support plate (TSP) wear
- Retainer bar (RB) wear
- Foreign object wear
- Tube-to-tube wear (TTW)

The degradation mechanisms covered by this operational assessment are being evaluated assuming a full cycle of operation at 100% reactor power. Per Reference 7, the upcoming fuel cycle is planned to be 576 EFPD (Effective Full Power Days). Converting this to EFPY gives a length for Cycle 17 of 1.577 EFPY. As discussed previously, this report addresses all degradation mechanisms except for TTW. The OA for TTW will be documented separately. In the TTW OA, the permissible reactor power level and inspection interval may be reduced from that evaluated in this document. The more conservative OA shall govern plant operation.

6.1 Input Parameters

Table 6-1 and Table 6-2 identify the input parameters used to perform the operational assessment. Consistent with the structural integrity criteria described in Section 4.0, the limiting pressure loading occurs at a value of three times the normal operating pressure differential (NOPD). For Unit 2 at full power, this value is 4290 pounds per square inch differential (psid) and is based on a conservative assessment of Unit 2 secondary side steam pressure during the previous operating cycle. A review of the secondary side steam pressures for the previous operating cycle showed a secondary side steam pressure of about 820 pounds per square inch absolute (psia). With a primary side pressure of 2250 psia, a 3 NOPD value of 4290 psid is obtained. As discussed earlier, it is possible that operation during the next inspection interval will be at reduced power. Operation at reduced power will increase the secondary side steam pressure. Therefore, the 3 NOPD value will be also reduced by operation at reduced power levels and using the 4290 psid value bounds the potential operating conditions for the upcoming operating period.

In addition to pressure loads, the OA must also consider the impact of non-pressure accident loads if they could have a significant effect on the burst pressure of the degraded tubes. The CM assessment [11] provides the basis for concluding that design basis, non-pressure accident loads are not limiting for the tube wear mechanisms identified for the Unit 2 SG tubes. Consequently, the limiting loading scenario for evaluation of structural and leakage integrity is that involving pressure loads evaluated with a safety factor of three (i.e., 3 NOPD).

SONGS U2C17 Outage - Steam Generator Operational Assessment

In order for a degraded tube to be returned to service, the degradation must be measured using a qualified Eddy Current Testing (ECT) sizing technique and the degradation must be evaluated as acceptable for continued operation. The ECT sizing techniques qualified for use at Unit 2 are identified in the degradation assessment [5] and their sizing performance parameters are summarized in Table 6-2. The techniques are identified by their EPRI ETSS (Examination Technique Specification Sheet) numbers. If tube degradation cannot be sized with appropriate sizing confidence, the tube is plugged upon degradation detection. All degradation identified during the current outage was measured with a qualified ECT technique.

Table 6-1: Unit 2 Steam Generator Input Values

<i>Parameter</i>	<i>Value</i>
Desired probability of meeting burst pressure limit	0.95
Tubing wall thickness	0.043 inch, [7]
Tubing outer diameter	0.750 inch, [7]
Mean of the sum of yield and ultimate strengths at temperature	116000 psi, [8]
Standard deviation of the sum of yield and ultimate strengths	2360 psi, [8]
3 Normal Operating Pressure Differential (3 NOPD)	4290 psid, [7]
MSLB Pressure Differential	2560 psid, [9]
EFPD from SG Replacement until U2C17 Refueling Outage	627.11 EFPD, [7]
Operating interval for upcoming fuel cycle as evaluated in this OA*	1.577 EFPY

* This OA only addresses detected degradation mechanism other than TTW. The OA for TTW will be documented separately. The OA for TTW may prescribe operation at lower reactor power and a shorter inspection interval. Whichever OA is more conservative shall govern plant operation.

SONGS U2C17 Outage - Steam Generator Operational Assessment

Table 6-2: Eddy Current ETSS Input Values [4]

Parameter	ETSS 96004.1	ETSS 10908.4	ETSS 27903.1	ETSS 27901.1	ETSS 27902.2	ETSS 96910.1
Probe Type	Bobbin Coil	+Point™	+Point™	+Point™	+Point™	+Point™
NDE depth sizing regression parameters	Slope = 0.98 Intercept = 2.89 %TW	Slope = 1.06 Intercept = 0.13 %TW	Slope = 0.97 Intercept = 2.80 %TW	Slope = 1.05 Intercept = -1.97 %TW	Slope = 1.02 Intercept = 0.94 %TW	Slope = 1.01 Intercept = 4.30 %TW
NDE depth sizing technique uncertainty (standard deviation)	4.19 %TW	3.78 %TW	2.11 %TW	2.30 %TW	2.87 %TW	6.68 %TW
NDE depth sizing analysis uncertainty (standard deviation)	2.10 %TW	1.89 %TW	1.06 %TW	1.15 %TW	1.44 %TW	3.34 %TW
Total NDE (Sizing and Technique) (standard deviation)*	4.69 %TW	4.23 %TW	2.36 %TW	2.60 %TW	3.22 %TW	7.48 %TW

* Total uncertainty is the technique and analysis uncertainties combined via the square root of the sum of the squares.

6.2 Evaluation of Structural Integrity

The fundamental OA structural integrity criteria is that the projected worst case degraded tube for each existing degradation mechanism must meet the limiting structural performance parameter with a 95% probability and 50% confidence [2]. Due to the relatively large number of AVB wear and TSP wear indications identified during the U2C17 outage, a probabilistic approach for analysis of the full bundle is necessary and was used to perform the OA for these mechanisms in accordance with Section 8.3 of Reference 2.

6.2.1 AVB Wear and TSP Wear

With the finding of TTW in Unit 2, over 300 tubes were preventatively plugged in Unit 2 in the region deemed most susceptible to fluid-elastic instability. These tubes contained a significant number of AVB wear indications. Therefore, the number of AVB wear indications returned to service for the next operating interval is significantly less than the number of indications reported during the U2C17 inspection. The quantities of indications detected and returned to service are shown in Table 6-3.

The typical deterministic approach for performing an OA for wear is to identify the worst case flaw during the current outage, apply an upper bound growth rate to reflect growth during operation prior to the next inspection, and compare the resulting depth (i.e., the end-of-cycle (EOC) depth) to the CM limit curve. This is generally appropriate for degradation mechanisms which involve a small number of indications. However, when a large number of indications of a particular mechanism are expected to develop or are left in-service, it is not conservative to perform a deterministic OA evaluation of this type. A probabilistic approach addresses the fact that the presence of a large number of in-service flaws increases the probability that one or more of the flaws will grow to a structurally significant depth by the EOC. Hence, this evaluation approach will yield a lower plugging limit for a SG which has a large population of flaws than would a typical deterministic approach. For the Unit 2 AVB wear and TSP wear, it is prudent to use a probabilistic approach. Consequently, the OA for AVB and TSP wear was performed using AREVA's full tube bundle probabilistic OA tool [6].

AREVA's full-bundle probabilistic OA tool was developed specifically for wear at support structures using the flaw model from Section 5.3.3 of Reference 3 and the Monte Carlo approach from Reference 2. This tool receives as key inputs: 1) the population of wear flaws identified, 2) the growth rate distribution anticipated during the next operating period, 3) Non-Destructive Examination (NDE) Examination Technique Specification Sheet (ETSS) regression and uncertainty parameters, 4) a conservative estimation of the number of flaws present, but not detected, during the U2C17 outage inspection, and 5) newly initiated flaws expected during the next operating period. The tool "grows" each flaw that is left in-service by randomly sampling from the growth rate distribution, yielding one estimate of the EOC depth for each flaw. In addition, the entire population of expected newly initiated flaws is added to the EOC flaw population. From this EOC combined population the burst pressure of the worst case degraded tube is calculated and compared with the value of 3 NOPD. This process is repeated thousands of times (via a Monte Carlo process) in order to develop a probability of survival for the worst case degraded tube. This value must be at least 95% to satisfy the fundamental OA criteria. If the result is less than 95%, a lower plugging limit must be implemented. The calculation also considers uncertainties associated with material strength, ECT sizing, the ratio of maximum flaw depth to structurally significant flaw depth, and the burst equation itself. Within the full bundle OA tool, AVB and TSP wear are evaluated using the EPRI Flaw Handbook [3] degradation model for axial part-throughwall degradation less than 135° in circumferential extent, subjected to pressure loading of 3 NOPD. The basis for the use of this flaw model is discussed in the CM assessment [11].

6.2.1.1 Growth Rates

One of the underlying assumptions implemented within the full bundle OA tool is that growth rates going forward are random with respect to the current wear depth. Because the Unit 2 SGs have operated for only one cycle and have only one in-service inspection, it is not known if or to what extent this behavior will manifest itself in the future. Consequently, AVB wear was evaluated as two separate populations: flaws $>20\%$ Through Wall (TW) in one population, and flaws $\leq 20\%$ TW in the other population. Flaws $>20\%$ TW are assumed to continue to grow at a rate based on their growth during the first operating cycle. In the evaluation, this forces deeper flaws to grow at a higher rate. Likewise, flaws $\leq 20\%$ TW are grown at a rate based on their growth during the first cycle. TSP wear flaws sized $>10\%$ TW were similarly evaluated as a separate population from those sized $\leq 10\%$ TW. Because there are very few TSP flaws sized $>20\%$ TW, a cutoff value of 10% TW was chosen. The selections of the breakpoints at 20% TW for AVB wear and 10% TW for TSP wear were based on AREVA Engineering experience and the numbers of flaws being returned to service in each depth category.

For AVB wear, 2E-088 has the limiting growth distribution. Therefore, the 2E-088 growth distribution was applied to both SGs. Due to the relatively small population of TSP wear indications, the growth rate distribution used in the OA was based on a combined data set from both SGs.

Prior to developing a growth rate distribution, the measured depths of the wear reported must be adjusted to account for the tendency of the EPRI sizing technique in ETSS 96004.1 to undersize flaw depth. This systematic sizing bias need not be considered when growth rate distributions are developed from two consecutive inspections because the sizing bias drops out when calculating depth change. However, because only one inspection result is available this adjustment is necessary. Another way to understand this is to recognize that prior to initial operation of the SGs the *actual* flaw depths were zero. To obtain an unbiased estimate of the growth during the first cycle of operation, the best estimate of *actual* depth during the U2C17 outage is required. Consequently, the through wall depths were adjusted upward by applying the sizing regression for ETSS 96004.1.

In addition, an adjustment was also made to account for the fact that, as the flaw deepens, the wear contact area increases. The volume of tube material removed is proportional to the wear work rate [19]. If the wear work rate is assumed to be constant (i.e., constant volume removal), then the growth rate, as measured in terms of through wall depth, will decrease because more tube material must be removed for a given increase in flaw depth. Based on an evaluation of tube geometry, with constant work rate and a second operating period of the same length as the first period, the growth in depth would be about 60% of the growth in the first cycle. Therefore, based on the assumption of constant volume loss, the first operating period growth rate could be adjusted by a factor of 0.6 to reflect the expectation of constant volume growth rate. For tapered wear such as that observed at the TSPs, this factor would be expected to be even lower since a tapered wear scar would also grow in length with increasing depth. For the OA, full credit for this growth rate reduction was not taken. Instead, a factor of 0.7 was applied to the AVB and TSP wear growth rates. Data from recent replacement steam generators with tube-to-support wear and multiple inspections support the constant volume loss assumption.

Because the upcoming operating period could be at a reduced power level due to TTW, the effect of power level on growth rate of AVB and TSP wear was also evaluated. A reduction in power level will change the velocities and densities on the secondary side of the tube bundle. The growth rate for wear indications is expected to be roughly proportional to the square of the dynamic pressure (where dynamic pressure = ρV^2 ; density times the square of velocity) [19]. As power level is decreased, the density increases. However, the increase in density is more than offset by the decrease in velocity.

Therefore, if there is any noticeable change in growth rate, it is expected to be a decrease in the observed growth rate. For this OA, no adjustment to the growth rate was made to account for any potential change in power level.

The growth rate distributions applicable to AVB wear and TSP wear are provided in Figure 6-1 through Figure 6-4. The AVB wear growth rates are based upon the data for 2E-088 which exhibited a slightly higher growth rate than 2E-089. For TSP wear, the data from the two SGs were combined due to the relatively low number of TSP wear indications.

6.2.1.2 Structural Depths and Lengths

Structural depths and lengths were obtained for 22 AVB wear indications that were line-by-line sized with the +Point™ probe using EPRI ETSS 10908.4. These structurally equivalent dimensions correspond to a rectangular flaw which would burst at the same pressure as the measured flaw; determined using the methods described in Section 5.1.5 of Reference 3. The selection of indications for line-by-line sizing was based on depth of the indication with emphasis placed on the deeper indications. Since the results of the operational assessment are highly dependent on the deepest flaws returned to service, use of the structural lengths and depths from 22 of the deeper indications is justified. The structural depths were compared to the maximum depths for each flaw to obtain a ratio of structural to maximum depth. The ratio of structural depth to maximum depth ranged from a low of 0.76 to a high of 0.94. The average and the standard deviation of this ratio are 0.882 and 0.052, respectively. These values were used as inputs to the full bundle OA tool for the AVB wear evaluations. Using the distribution of structural to maximum depth ratios, the OA tool randomly applies a ratio value, sampled from this normal distribution, to each postulated maximum depth at the EOC. The sampled ratio value is constrained to a minimum and maximum of 0.8 and 1.0, respectively. For TSP wear, a fixed value of 1.0 was conservatively used for the ratio of structural to maximum depth.

For the structural length, a fixed value of 0.7" was used for AVB wear. This is conservative since the width of the AVB is only 0.59". This conservative value was selected based on the observation that some of the AVB wear flaws in Unit 3 extended outside the confines of the AVB intersection. This phenomenon in Unit 3 is believed to be due to the in-plane motion of the affected tubes. No AVB wear indications in Unit 2 were observed to extend outside the AVB intersection. However, based on the Unit 3 observation and the fact that shallow TTW was observed in Unit 2, a conservative length of 0.7" was applied for AVB wear indications in Unit 2.

The structural length for TSP wear was set to a fixed value of 1.6" which is longer than the 1.38" thickness of the TSPs. Again, this conservative value was selected based on the observation that some of the TSP wear flaws in Unit 3 extended outside of the TSP intersection.

6.2.1.3 Initiation and Depth Distribution of New Indications

Based on industry experience with other replacement SGs experiencing relatively large quantities of wear during early operation, it is likely that another operating period of equal length at SONGS would produce fewer new wear flaws than the number reported during the U2C17 inspection. However, for this OA it was assumed that the cumulative number of wear flaws will trend linearly with the cumulative operating EFPY. In addition, it was conservatively assumed that the depth distribution of new indications anticipated after a full fuel cycle of operation will be the same as that observed during the U2C17 outage for the flaw category under evaluation (i.e., AVB wear >20%TW, AVB wear <20%TW, etc.). Again, the OA for AVB and TSP wear is being performed as if a full cycle of operation at 100% power will occur prior to the next inspection. For each category, the flaw population used to model growth was also used to model new flaw size. Figure 6-5 and Figure 6-6 provide histograms illustrating the overall U2C17 depth distribution of each degradation mechanism.

6.2.1.4 Results of Probabilistic OA for AVB Wear and TSP Wear

The fundamental OA structural integrity criterion is that the projected worst case degraded tube for each existing degradation mechanism must meet the limiting structural performance parameter with a 95% probability and 50% confidence. The results of the probabilistic OA for AVB wear and TSP wear are provided in Table 6-3. The values provided in the table represent the projected probability of non-burst for the entire population of flaws in the specified group. These values compare directly with the 95/50 OA criteria. Note that the combined probability of non-burst is simply the product of the probabilities for the different groups evaluated (e.g., $0.9997 \times 0.9921 \times 0.9996 \times 0.9992 = 0.9906$). In all cases, the OA structural integrity criteria for AVB and TSP wear is satisfied for a full cycle of operation at 100% reactor power. The operational assessment for TTW will be documented separately. In the TTW OA, the permissible reactor power level and inspection interval may be reduced from that evaluated in this document. The more conservative OA shall govern plant operation.

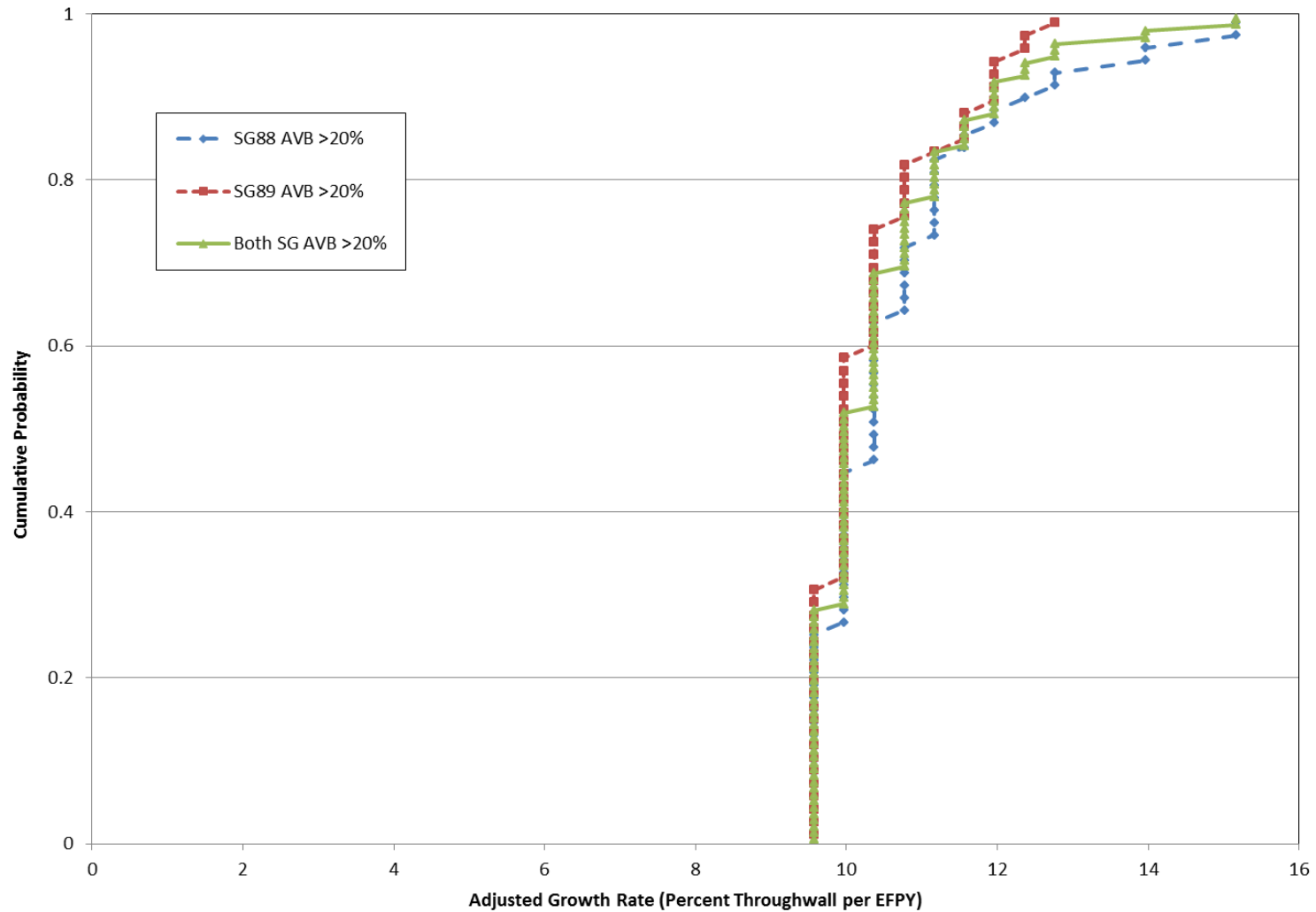
Table 6-3: Projected Probability of Non-Burst

Flaw Category	No. of Indications Detected		No. of Indications Returned to Service		End-of-Cycle Tube Degradation Probability of Non-Burst*	
	2E-088	2E-089	2E-088	2E-089	2E-088	2E-089
AVB Wear >20%	66	64	24	22	0.9997	0.9996
AVB Wear ≤20%	1691	2527	1157	1407	0.9921	0.9902
TSP Wear >10%	77	59	68	31	0.9996	0.9997
TSP Wear ≤10%	148	80	127	49	0.9992	0.9996
AVB & TSP Wear Combined	1982	2730	1376	1509	0.9906	0.9891

* Results shown are for a full cycle of operation (1.577 EFPY) at full power. The operational assessment for TTW will be documented separately. In the TTW OA, the permissible reactor power level and inspection interval may be reduced from that evaluated in this document. The more conservative OA shall govern plant operation.

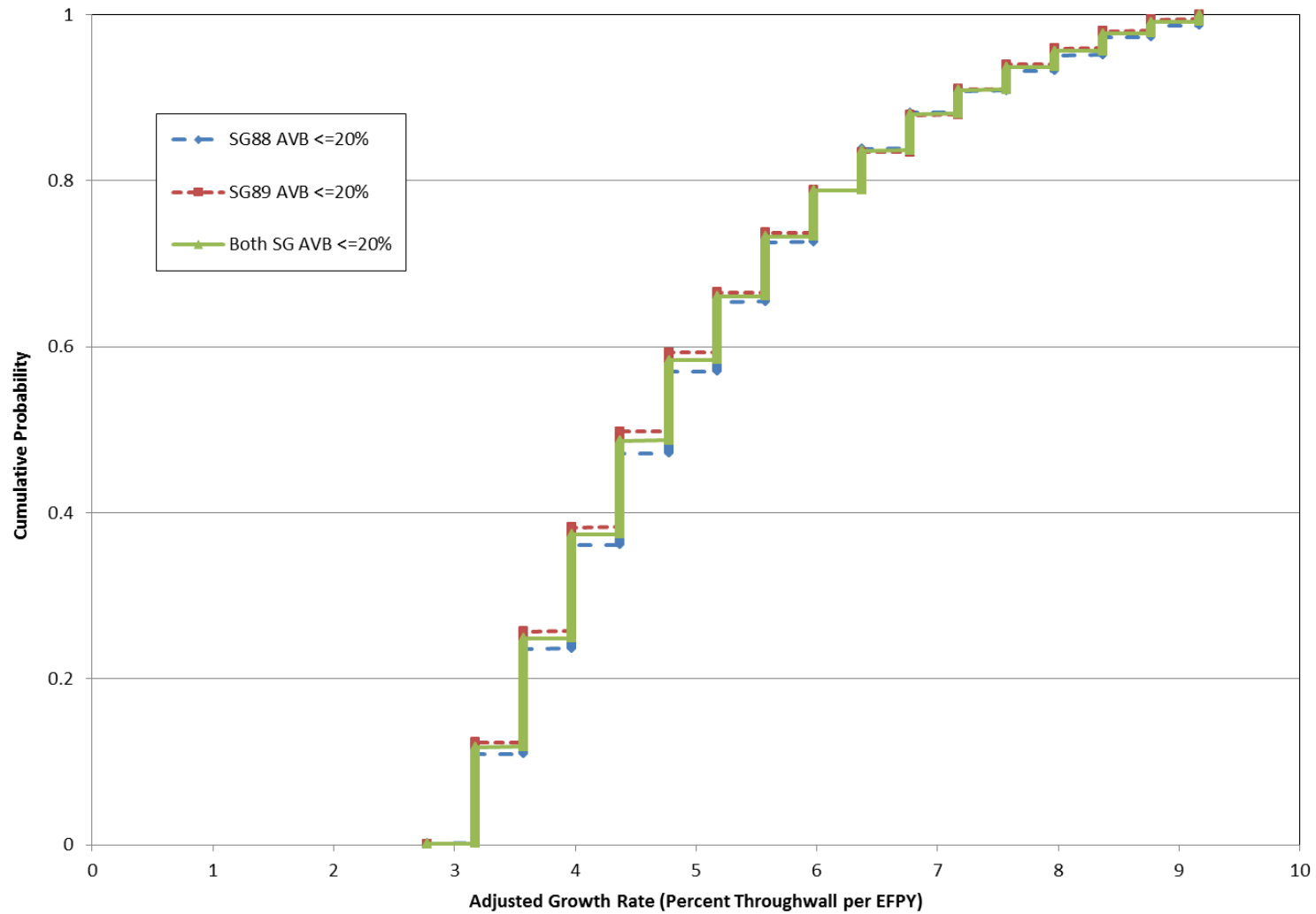
SONGS U2C17 Outage - Steam Generator Operational Assessment

Figure 6-1: Adjusted Growth Rate Distribution, AVB Wear >20%TW



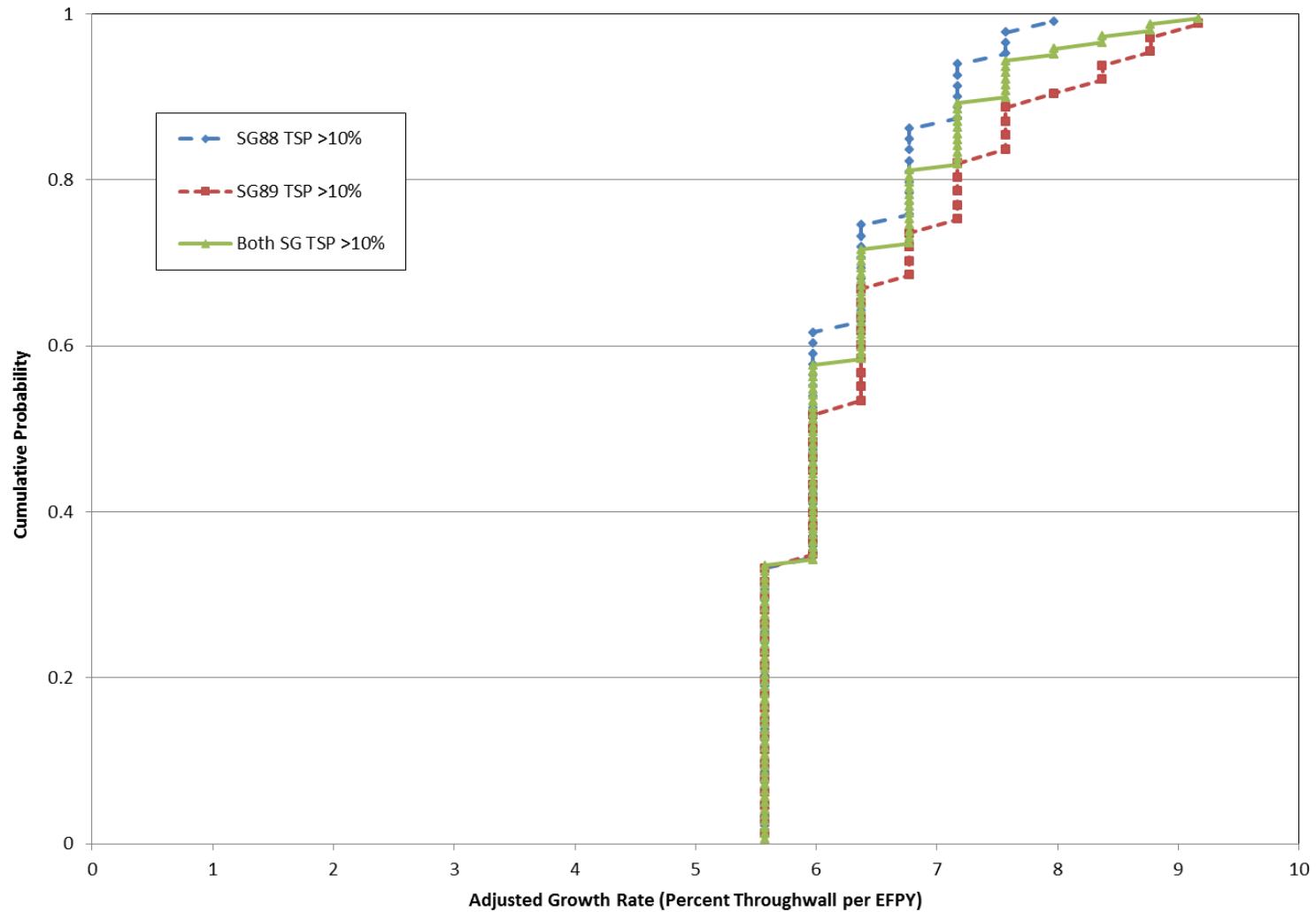
SONGS U2C17 Outage - Steam Generator Operational Assessment

Figure 6-2: Adjusted Growth Rate Distribution, AVB Wear $\leq 20\%$ TW



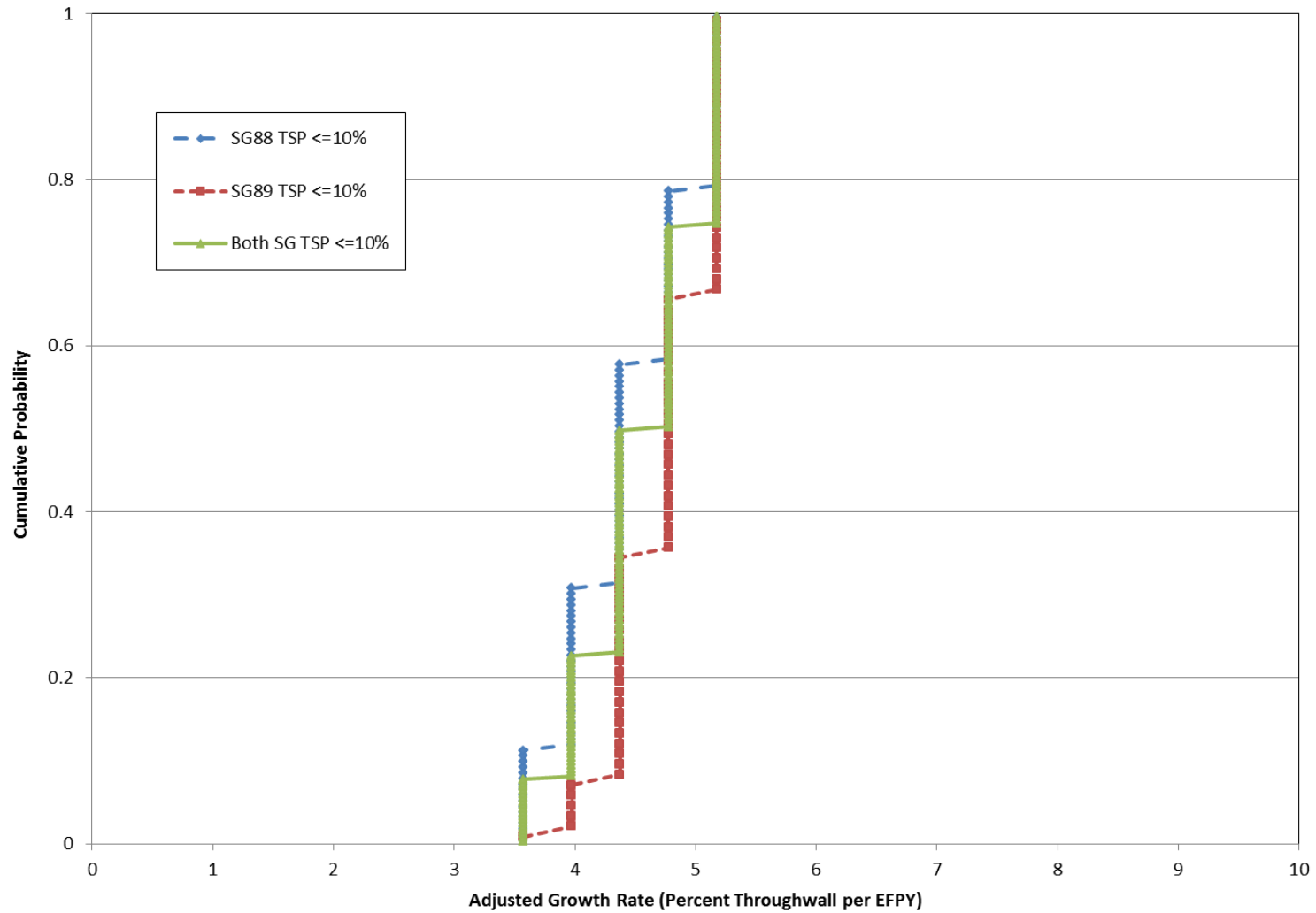
SONGS U2C17 Outage - Steam Generator Operational Assessment

Figure 6-3: Adjusted Growth Rate Distribution, TSP Wear >10%TW



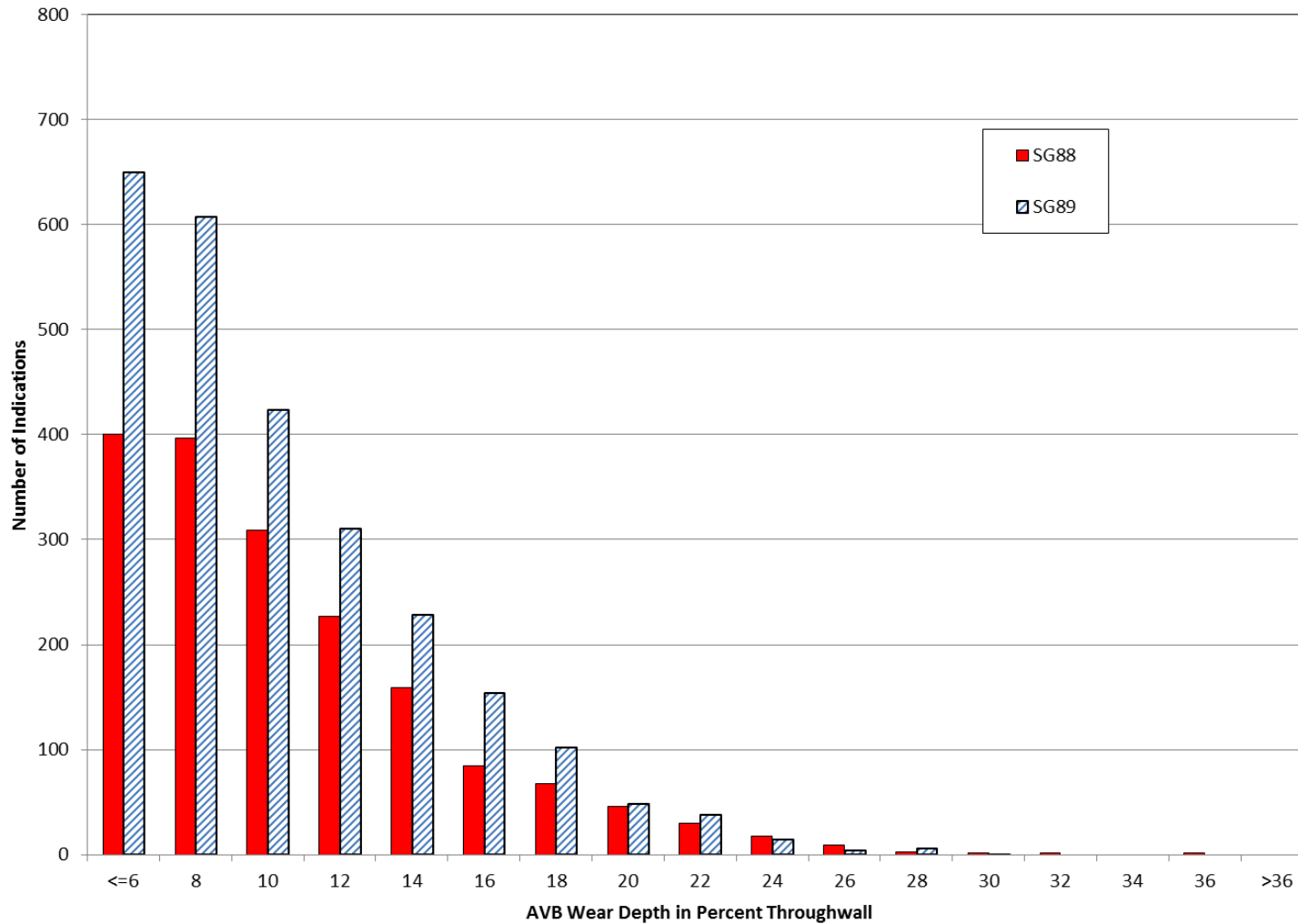
SONGS U2C17 Outage - Steam Generator Operational Assessment

Figure 6-4: Adjusted Growth Rate Distribution, TSP Wear $\leq 10\%$ TW



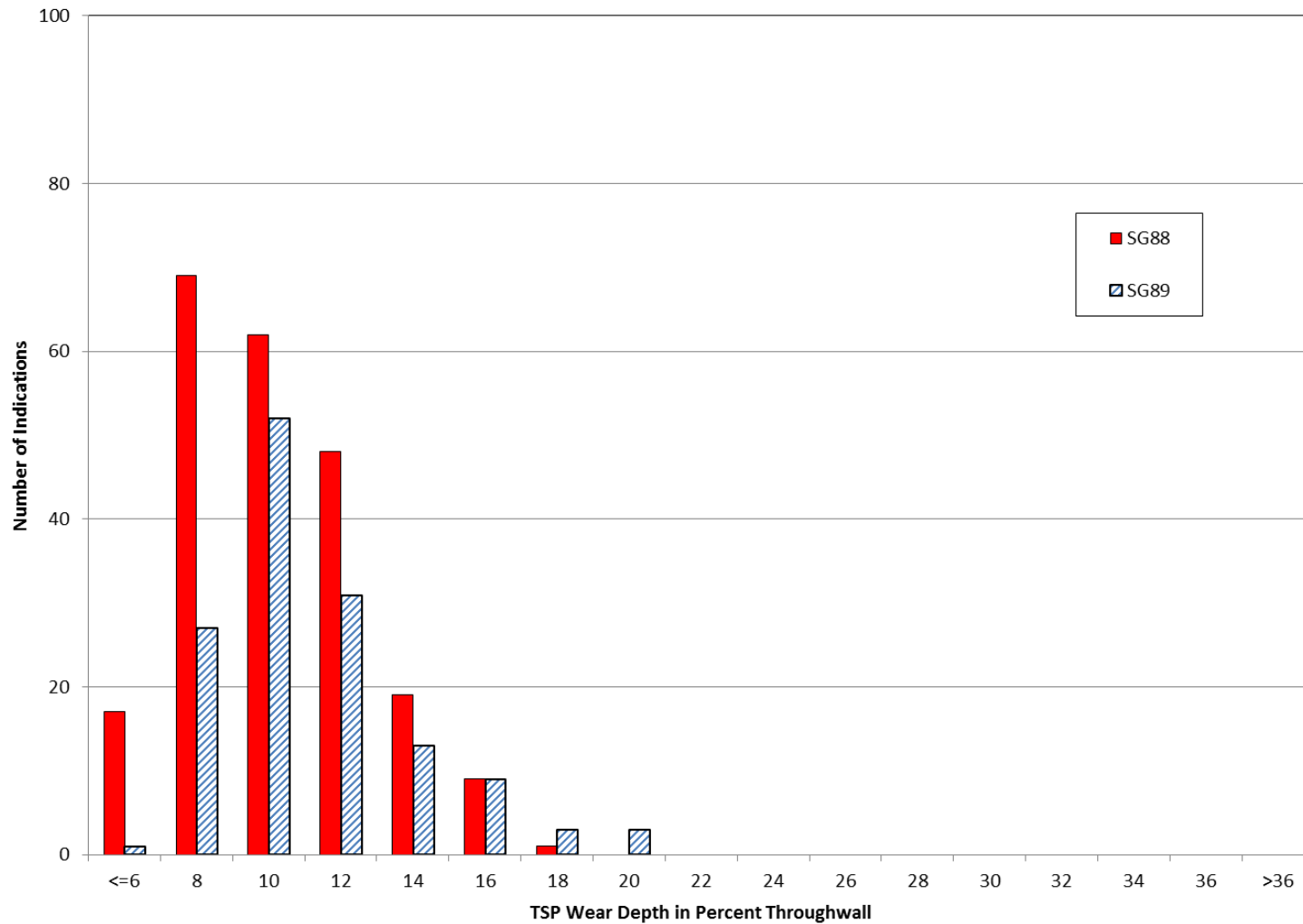
SONGS U2C17 Outage - Steam Generator Operational Assessment

Figure 6-5: AVB Wear Depth Histogram



SONGS U2C17 Outage - Steam Generator Operational Assessment

Figure 6-6: TSP Wear Depth Histogram



6.2.2 Retainer Bar Wear

To eliminate the potential for future RB wear in in-service tubes, all tubes adjacent to the retainer bars have been plugged in both SGs. Prior to plugging, all tubes with RB wear indications were stabilized with U-bend cable stabilizers. The tubes on either side of all retainer bars, at each end of the retainer bars, and at the center of the retainer bars, were also stabilized prior to plugging in both SGs. This augmented stabilization provides additional material volume to resist continued RB wear, and provides added assurance that the retainer bars will not interact with in-service tubes. These corrective actions provide reasonable assurance that retainer bar wear will not challenge the structural and leakage integrity performance criteria during the remaining life of the SGs. In addition, the stabilization of these tubes provides reasonable assurance that a tube severance event will not occur as a result of RB wear during the remaining life of the SGs. Monitoring of the tubes adjacent to these plugged tubes must be performed on a periodic basis during future SG inspections.

6.2.3 Tube-to-Tube Wear

As discussed earlier and in Reference 11, shallow TTW was detected in two tubes in the 2E-089 SG. The inspections that led to the finding of TTW in Unit 2 were performed based on the finding of significant TTW in SONGS Unit 3. Although the numbers and depths of indications between the two units are vastly different, it has been found that Unit 2 was susceptible to TTW. The locations of the indications along with the measured depths and lengths are provided in Table 6-4.

The OA for TTW will be documented separately. In the TTW OA, the permissible reactor power level and inspection interval may be reduced from that evaluated in this document. The more conservative OA shall govern plant operation.

Table 6-4: U2C17 Tube-to-Tube Wear Indications

SG	Row	Col	Location	Maximum Depth (%TW)	Length (in.)	Structural Depth (%TW)	Structural Length (in)
2E-089	111	81	B09 +1.63 to +7.95	15	6.32	14.0	2.28
2E-089	113	81	B09 +2.03 to +8.22	14	6.19	13.7	1.67

6.2.4 Foreign Object Wear

All Unit 2 SG tubes were examined full length with bobbin coil probes. Two tubes in the 2E-088 SG were identified with foreign object and foreign object wear indications. The object which caused the foreign object indication and associated wear was retrieved from the SG. Consequently, there is no possibility for this degradation to progress during future operation. After removal of the object, the affected locations were inspected with a +Point™ technique qualified for depth sizing (with the object not present). Neither indication exceeded the SONGS 35%TW plugging limit. Since the indications were below the SONGS plugging limit and the object was removed, these tubes were left in service. No other foreign objects or foreign object wear flaws were identified during the ECT inspection.

Subsequent analysis by SCE identified the object as weld metal debris. Therefore, the presence of this object was not indicative of degradation of secondary side internals.

The SG work activities performed during this refueling outage included post sludge lancing, secondary side visual inspections of the top-of-tubesheet (TTS) annulus and no-tube lane regions in both SGs, and visual inspections of the upper bundle, including the retainer bars, and the retainer bar-to-retaining bar and AVB end cap-to-retaining bar welds. Other than the object discussed above, these examinations identified no foreign objects, loose parts or conditions which could credibly generate foreign objects or loose parts capable of impacting tube integrity.

In summary, based on extensive ECT inspections augmented by secondary side visual inspections and Foreign Object Search and Retrieval (FOSAR), no foreign objects or loose parts capable of causing tube degradation are known to remain in the Unit 2 SGs. Hence, there is reasonable assurance that foreign objects or loose parts will not cause the structural or leakage integrity performance criteria to be exceeded prior to the next tube inspection.

6.3 Evaluation of Leakage Integrity

All tubes with degradation exceeding the Technical Specification plugging limit have been removed from service by plugging. In addition, many additional tubes were preventatively plugged. For the tubes that were removed from service, primary-to-secondary leakage past the plugs must be considered.

Applying this value to each plug and adjusting the leak rate to the normal operating and accident differential pressures, gives the postulated leak rates provided in Table 6-5. All leak rate values are provided at room temperature conditions because the SONGS leakage performance criteria are specified as volumetric leak rates at room temperature conditions. These values are well below the allowable leak rates as shown in this table.

For the tubes returned to service, per Reference 2, the onset of pop-through and leakage for axially oriented volumetric flaws with limited circumferential extent - the nature of the degradation identified in the Unit 2 SGs - is coincident with burst. Because none of the identified degradation mechanisms are projected to exceed the structural performance criteria prior to the next scheduled inspection in each SG, there is reasonable assurance that neither the operational, nor the accident-induced leakage performance criteria will be exceeded prior to the next inspection of the Unit 2 SGs.

Table 6-5: Postulated Plug Leakage

	2E-088	2E-089
Number of Tubes Plugged	205	305
Total Number of Plugs	410	610
Allowable Accident-Induced Leak Rate (gpm at room temperature)	0.5	0.5

6.4 Secondary Side Internals

No degradation of SG secondary side internals was identified during this outage. No tube support degradation or misplacement was identified during the ECT or secondary side visual inspections.

7.0 OPERATIONAL ASSESSMENT CONCLUSION

This report documents the OA for all detected degradation mechanisms except for TTW. This OA concludes that there is reasonable assurance that the performance criteria for the non-TTW degradation will be met if Unit 2 were to operate for a full fuel cycle of 1.577 EFPY at 100% reactor power.

The TTW OA will be documented separately. Operation at reduced reactor power and a shorter inspection interval may be prescribed in the TTW OA. The more conservative OA shall govern plant operation.

8.0 REFERENCES

1. NEI 97-06, "SG Program Guidelines," Rev. 3, January 2011.
2. EPRI Report 1019038, "SG Integrity Assessment Guidelines: Revision 3", November 2009.
3. EPRI Report 1019037 "Steam Generator Degradation Specific Management Flaw Handbook, Revision 1", December 2009.
4. EPRI, SG Management Project, "sgmp.epri.com".
5. AREVA Document 51-9176667-001, "SONGS 2C17 & 3C17 Steam Generator Degradation Assessment".
6. AREVA Document 32-9104082-002, "MATHCAD Implementation of SG Full Probabilistic Operational Assessment".
7. *Matheny, Southern California Edison, "Numerical Values for the SG OAs, SONGS Units 2 and 3," February 8, 2012.
8. *SONGS Unit 2 Replacement Steam Generator Receipt Inspection QA Document Review Package.
9. *SONGS UFSAR Chapter 5.
10. NRC, "Confirmatory Action Letter – SONGS Units 2 and 3, Commitments to Address SG Tube Degradation," CAL 4-12-001, March 27, 2012.
11. AREVA Document 51-9182368-002, "SONGS 2C17 Steam Generator Condition Monitoring Report".
12. AREVA Document 51-1177797-009, "0.750 Mechanical Rolled Plug Design Verification Report – Alloy 690".
13. *SONGS Technical Specifications Section 5.5.2.11, "Steam Generator (SG) Program", Amendment 204
14. *SONGS Technical Specifications Section 3.4.13, "RCS Operational Leakage", Amendment 204.
15. AREVA Document 51-9187230-000, "SONGS 2C17 Steam Generator Operational Assessment for Tube-to-Tube Wear".
16. *Root Cause Evaluation, San Onofre Nuclear Generating Station, Condition Report: 201836127, "Unit 3 Steam Generator Tube Leak and Tube-to-Tube Wear", Revision 0, 5/7/2012.
17. *Root Cause Evaluation NN 201843216, "Steam Generator Tube Wear, San Onofre Nuclear Generating Station, Unit 2".
18. *SONGS Steam Generator Program, S023-SG-1.

SONGS U2C17 Outage - Steam Generator Operational Assessment

19. Au-Yang, M.K., "Flow-Induced Vibration of Power and Process Plant Components: A Practical Workbook", ASME Press, 2001.
20. *SONGS RGR-U2/3-C17, "SONGS Units 2/3 Cycle 17 Reload Ground Rules", Item X.003, Revision 2.

*Documents are not retrievable from the AREVA document control system, but can be retrieved from the SCE document control system. Therefore, these are acceptable reference per AREVA Administrative Procedure 0402-01, Attachment 8, as authorized by the Project Manager's signature on page 2.

ATTACHMENT 6 – Appendix B

SONGS U2C17

Steam Generator Operational Assessment for Tube-to-Tube Wear

[Proprietary Information Redacted]



AREVA NP Inc.

Engineering Information Record

Document No.: 51 - 9187230 - 000 (NP)

SONGS U2C17 Steam Generator Operational Assessment for Tube-to-Tube Wear

Supplier Status Stamp

VPL No:	1814-AU651-M0160	Rev No:	0	QC:	N/A
<input type="checkbox"/> DESIGN DOCUMENT		ORDER NO.		800918458	
<input checked="" type="checkbox"/> REFERENCE DOCUMENT - INFORMATION ONLY		<input type="checkbox"/> VIRP IOM MANUAL			
MFG MAY PROCEED: <input type="checkbox"/> YES <input type="checkbox"/> NO <input checked="" type="checkbox"/> N/A					
<small>STATUS - A status is required for design documents and is optional for reference documents. Drawings are reviewed and approved for arrangements and conformance to specification only. Approval does not relieve the submitter from the responsibility of adequacy and suitability of design, materials, and/or equipment represented.</small>					
<input type="checkbox"/> 1. APPROVED <input type="checkbox"/> 2. APPROVED EXCEPT AS NOTED - Make changes and resubmit. <input type="checkbox"/> 3. NOT APPROVED - Correct and resubmit for review. NOT for field use.					
APPROVAL: (PRINT / SIGN / DATE)					
RE:	E. GRIBBLE		10/2/12		
FLS:					
Other:					

SCE DE(123) 5 REV. 3 07/11

REFERENCE: SO123-XXIV-37.8.26

SONGS U2C17 Steam Generator Operational Assessment for Tube-to-Tube Wear

Table of Contents

	Page
SIGNATURE BLOCK.....	2
RECORD OF REVISION	3
LIST OF FIGURES	6
LIST OF ABBREVIATIONS	10
1.0 PURPOSE.....	12
2.0 BACKGROUND	12
3.0 INTRODUCTION.....	15
4.0 OPERATIONAL ASSESSMENT STRATEGY.....	16
4.1 Development of TTW	16
4.2 Operational Assessment Strategy.....	20
5.0 STABILITY RATIOS.....	43
6.0 CONTACT FORCES.....	56
6.1 MHI Quarter Bundle Steam Generator Model.....	56
6.2 Contact Force Distributions – Unit 3.....	57
6.3 Contact Force Distributions – Unit 2.....	59
6.4 Dent Evaluation.....	59
6.4.1 Pre-Service Dents.....	59
6.4.2 Non-Classical Dents	60
6.5 Tube-to-AVB Gap Evaluation.....	61
6.5.1 Unit 2 Tube-to-AVB Gaps	62
6.5.2 Effect of Gap Size on Tube-to-AVB Wear.....	62
6.5.3 Unit 3 Tube-to-AVB Gaps	62
6.6 Conclusions – Contact Forces	63
7.0 CRITERIA FOR EFFECTIVE VERSUS INEFFECTIVE SUPPORTS.....	97
7.1 Equal Contact Force at Each AVB	97
7.2 Variable Contact Force at Each AVB	97
7.3 Single AVB Effective (Upper Bound Contact Force).....	98
7.4 Chosen Approach for the OA	98
7.5 Summary – Criteria for Support Effectiveness	99



SONGS U2C17 Steam Generator Operational Assessment for Tube-to-Tube Wear

Table of Contents
(continued)

	Page
8.0 PROBABILITY OF INSTABILITY RESULTS	104
9.0 DEFENSE-IN-DEPTH.....	113
10.0 CONCLUSIONS.....	117
11.0 REFERENCES.....	118
APPENDIX A : ESTIMATES OF FEI-INDUCED TTW RATES.....	A-1

List of Figures

	Page
FIGURE 2-1: AVB ARRANGEMENT FOR SONGS STEAM GENERATORS	13
FIGURE 2-2: VIEW OF TOP OF BUNDLE	14
FIGURE 2-3: ENDS OF AVBS ATTACHED TO RETAINING BARS, BRIDGES AND RETAINER BARS ALSO SHOWN	14
FIGURE 4-1: DEPTH VERSUS AXIAL LENGTH PROFILE FOR THE LEAKING TUBE IN UNIT 3, SG E-088	23
FIGURE 4-2: FIGURE FROM A BOOK BY M. K. AU YANG, "FLOW INDUCED VIBRATION IN POWER AND PROCESS PLANT COMPONENTS", ASME PRESS, 2001	24
FIGURE 4-3: SPIDER DIAGRAM OF THE OPERATIONAL ENVELOPE FOR LARGE U-BEND STEAM GENERATORS	25
FIGURE 4-4: TUBESHEET MAP OF TTW INDICATIONS, UNIT 3, SG E-088	26
FIGURE 4-5: TUBESHEET MAP OF TTW INDICATIONS, UNIT 3, SG E-089	27
FIGURE 4-6: EXPANDED VIEW OF TTW INDICATIONS, UNIT 3, SG E-088	28
FIGURE 4-7: EXPANDED VIEW OF TTW INDICATIONS, UNIT 3, SG E-089	29
FIGURE 4-8: COMBINED VIEW OF TTW INDICATIONS	30
FIGURE 4-9: TTW DEPTH VERSUS ROW AND COLUMN, UNIT 3 SG E-088	31
FIGURE 4-10: TTW DEPTH VERSUS ROW AND COLUMN, UNIT 3 SG E-089	32
FIGURE 4-11: NO ELONGATED AVB WEAR FOUND BEYOND THE REGION OF TTW, UNIT 3 SG E-088	33
FIGURE 4-12: NO ELONGATED AVB WEAR FOUND BEYOND THE REGION OF TTW, UNIT 3 SG E-089	34
FIGURE 4-13: TUBE WEAR LENGTH AT AVBS FOR UNIT 3 SG E-088	35
FIGURE 4-14: TUBE WEAR LENGTH AT AVBS FOR UNIT 3 SG E-089	36
FIGURE 4-15: MODE 1 DISPLACEMENT PATTERN	37
FIGURE 4-16: ELONGATION OF AVB WEAR AT EACH AVB	38
FIGURE 4-17: IMPACT LOCATIONS OF UNSTABLE TUBES	39
FIGURE 4-18: MODE 2 DISPLACEMENT PATTERN	40
FIGURE 4-19: MODE 3 DISPLACEMENT PATTERN	41
FIGURE 4-20: []	42
FIGURE 5-1: SPIDER DIAGRAM OF THE SUCCESSFUL OPERATIONAL ENVELOPE FOR NUCLEAR STEAM GENERATORS WITH LARGE U-BENDS	46
FIGURE 5-2: []	47

List of Figures
(continued)

Page

FIGURE 5-3: STABILITY MAP AT 100% POWER, NO PLUGGING, 95TH PERCENTILE SR, SR ≥ 1 .48

FIGURE 5-4: STABILITY MAP AT 70% POWER WITH PLUGGING AND SPLIT STABILIZERS, 95TH PERCENTILE SR, SR ≥ 1..... 49

FIGURE 5-5: [] 50

FIGURE 5-6: STABILITY MAP AT 100% POWER, 99TH PERCENTILE SR, SR ≥ 1 51

FIGURE 5-7: STABILITY MAP AT 70% POWER WITH PLUGGING AND SPLIT STABILIZERS, 99TH PERCENTILE SR, SR ≥ 1..... 52

FIGURE 5-8: DEPTH OF AVB WEAR INDICATIONS VERSUS AVB NUMBER, UNIT 2, SG E-088 AND SG E-089..... 53

FIGURE 5-9: NUMBER OF AVB WEAR INDICATIONS VERSUS AVB NUMBER..... 54

FIGURE 5-10: STABILITY MAP AT 70% POWER WITH PLUGGING AND SPLIT STABILIZERS, 95TH PERCENTILE SR, SR ≥ 0.75..... 55

FIGURE 6-1: QUARTER MODEL CONTACT FORCE AND GAP LOCATIONS..... 64

FIGURE 6-2: ZONES USED TO DEVELOP CHARACTERISTIC DISTRIBUTIONS OF CONTACT FORCES FOR EACH AVB IN THE ZONE..... 65

FIGURE 6-3: CUMULATIVE CONTACT FORCE DISTRIBUTIONS, ZONE 1, UNIT 3, BOC 16 66

FIGURE 6-4: CUMULATIVE CONTACT FORCE DISTRIBUTIONS, ZONE 3, UNIT 3, BOC 16 67

FIGURE 6-5: CUMULATIVE CONTACT FORCE DISTRIBUTIONS, ZONE 5, UNIT 3, BOC 16 68

FIGURE 6-6: CUMULATIVE CONTACT FORCE DISTRIBUTIONS, ZONE 8, UNIT 3, BOC 16 69

FIGURE 6-7: CUMULATIVE CONTACT FORCE DISTRIBUTIONS, ZONE 29, UNIT 3, BOC 16 70

FIGURE 6-8: CUMULATIVE CONTACT FORCE DISTRIBUTIONS, ZONE 35, UNIT 3, BOC 16 71

FIGURE 6-9: CUMULATIVE CONTACT FORCE DISTRIBUTIONS, ZONE 32, UNIT 3, BOC 16 72

FIGURE 6-10: CUMULATIVE CONTACT FORCE DISTRIBUTIONS, ZONE 56, UNIT 3, BOC 16 73

FIGURE 6-11: CUMULATIVE CONTACT FORCE DISTRIBUTIONS, ZONE 5, UNIT 3, BOC 16 + 3 MONTHS..... 74

FIGURE 6-12: CUMULATIVE CONTACT FORCE DISTRIBUTIONS, ZONE 5, UNIT 3, BOC 16 + 11 MONTHS..... 75

FIGURE 6-13: CUMULATIVE CONTACT FORCE DISTRIBUTIONS, ZONE 1, UNIT 2, BOC 16 76

FIGURE 6-14: CUMULATIVE CONTACT FORCE DISTRIBUTIONS, ZONE 3, UNIT 2, BOC 16 77

FIGURE 6-15: CUMULATIVE CONTACT FORCE DISTRIBUTIONS, ZONE 5, UNIT 2, BOC 16 78

FIGURE 6-16: CUMULATIVE CONTACT FORCE DISTRIBUTIONS, ZONE 8, UNIT 2, BOC 16 79

List of Figures
(continued)

Page

FIGURE 6-17: CUMULATIVE CONTACT FORCE DISTRIBUTIONS, ZONE 5, UNIT 2, EOC 16 (BOC 16 + 22 MONTHS)80

FIGURE 6-18: CUMULATIVE CONTACT FORCE DISTRIBUTIONS, ZONE 5, UNIT 2, BOC 17 + 6 MONTHS..... 81

FIGURE 6-19: TUBESHEET MAP OF DENTS FOUND IN PRE-SERVICE INSPECTION, UNIT 3, SG E-089..... 82

FIGURE 6-20: TUBESHEET MAP OF DENTS FOUND IN PRE-SERVICE INSPECTION, UNIT 2, SG E-089..... 83

FIGURE 6-21: [] 84

FIGURE 6-22: [] 85

FIGURE 6-23: [] 86

FIGURE 6-24: [] 87

FIGURE 6-25: [] 88

FIGURE 6-26: [] 89

FIGURE 6-27: [] 90

FIGURE 6-28: [] 91

FIGURE 6-29: TUBESHEET MAP OF ECT GAP MEASUREMENTS, TOTAL GAP FOR ALL AVB LOCATIONS PER TUBE, UNIT 2, SG E-088, ISI..... 92

FIGURE 6-30: TUBESHEET MAP OF ECT GAP MEASUREMENTS, TOTAL GAP FOR ALL AVB LOCATIONS PER TUBE, UNIT 2, SG E-089, ISI..... 93

FIGURE 6-31: ILLUSTRATIVE SCHEMATIC OF AVB WEAR RATES, HIGH WEAR RATES ARE POSSIBLE FOR VERY SMALL OR LARGE GAPS..... 94

FIGURE 6-32: TUBESHEET MAP OF ECT GAP MEASUREMENTS, TOTAL GAP FOR ALL AVB LOCATIONS PER TUBE, UNIT 3, SG E-088, ISI..... 95

FIGURE 6-33: TUBESHEET MAP OF ECT GAP MEASUREMENTS, TOTAL GAP FOR ALL AVB LOCATIONS PER TUBE, UNIT 3, SG E-089, ISI..... 96

FIGURE 7-1: SCHEMATIC ILLUSTRATION OF A THE AMPLITUDE OF MOTION AS A U-BEND BECOMES UNSTABLE 100

FIGURE 7-2: [] 101

List of Figures
(continued)

	Page
FIGURE 7-3: SCHEMATIC OF A U-BEND WITH AVB LOCATIONS SHOWN	102
FIGURE 7-4: ILLUSTRATIVE EXAMPLE OF A LOG NORMAL DISTRIBUTION OF THE PROBABILITY OF SUPPORT INEFFECTIVENESS	103
FIGURE 8-1: [
]	108
FIGURE 8-2: [
]	109
FIGURE 8-3: [
]	110
FIGURE 8-4: MAP OF CALCULATED FREQUENCY OF OCCURRENCE OF IN-PLANE INSTABILITY, UNIT 3	111
FIGURE 8-5: MAP OF CALCULATED FREQUENCY OF OCCURRENCE OF IN-PLANE INSTABILITY, UNIT 2	112
FIGURE 9-1: TUBES REMOVED FROM SERVICE AS A PREVENTATIVE MEASURE RELATIVE TO IN-PLANE FEI, UNIT 2 SG 2-88	115
FIGURE 9-2: TUBES REMOVED FROM SERVICE AS A PREVENTATIVE MEASURE RELATIVE TO IN-PLANE FEI, UNIT 2 SG 2-89	116

SONGS U2C17 Steam Generator Operational Assessment for Tube-to-Tube Wear

List of Abbreviations

Abbreviation	Definition
01C to 07C	Tube Support Plate Designations for Cold Leg (7 Locations)
01H to 07H	Tube Support Plate Designations for Hot Leg (7 Locations)
2E-088	Unit 2 Steam Generator 88
2E-089	Unit 2 Steam Generator 89
3E-088	Unit 3 Steam Generator 88
3E-089	Unit 3 Steam Generator 89
3 NOPD	3 Times Normal Operating Pressure Differential
ABAQUS	A finite-element structural analysis program sold by Dassault Systemes
AILPC	Accident Induced Leakage Performance Criterion
ASME	American Society of Mechanical Engineers
AVB	Anti-Vibration Bar
BOC	Beginning of Operating Cycle
C	Column
CDF	Cumulative Distribution Function
CE	Combustion Engineering
CL or C/L	Cold Leg
CM	Condition Monitoring
DA	Degradation Assessment
ECT	Eddy Current Testing
EFPD	Effective Full Power Days
EOC	End of Operating Cycle
EPRI	Electric Power Research Institute
ETSS	Examination Technique Specification Sheet
FEA	Finite Element Analysis
FEI	Fluid-elastic Instability
FOSAR	Foreign Object Search and Retrieval
FSM	Fluid-elastic Stability Margin
GPD	Gallons per Day
GPM	Gallons per Minute
HL or H/L	Hot Leg
kHz	kilohertz
KSI	Thousand Pounds per Square Inch
MHI	Mitsubishi Heavy Industries
MSLB	Main Steam Line Break
NDE	Non Destructive Examination
NEI	Nuclear Energy Institute

SONGS U2C17 Steam Generator Operational Assessment for Tube-to-Tube Wear

List of Abbreviations
 (continued)

Abbreviation	Definition
N	Newtons (a measure of force in metric units)
NN	Nuclear Notification
NOPD	Normal Operating Pressure Differential
NRC	Nuclear Regulatory Commission
OA	Operational Assessment
PSI	Pounds per Square Inch
PSI	Pre-service Inspection
PSIA	Pounds per Square Inch Absolute
PSIG	Pounds per Square Inch Gage
PWR	Pressurized Water Reactor
QA	Quality Assurance
R	Row
RB	Retainer Bar
RCS	Reactor Coolant System
RxxxCyyy	Steam Generator tube location, where xxx is the row number and yyy is the column number
SCE	Southern California Edison
SG	Steam Generator
SIPC	Structural Integrity Performance Criteria
SLB	Steam Line Break
SONGS	San Onofre Nuclear Generating Station
SR	Stability Ratio
SSI	Secondary Side Inspection
TEC	Tube End Cold
TEH	Tube End Hot
TSP	Tube Support Plate
TTS	Top of Tubesheet
TTW	Tube-to-tube Wear
TW	Through Wall
U2C17	SONGS Unit 2 End-of-Cycle 17 Outage
UB	U-bend
UT	Ultrasonic Testing

SONGS U2C17 Steam Generator Operational Assessment for Tube-to-Tube Wear

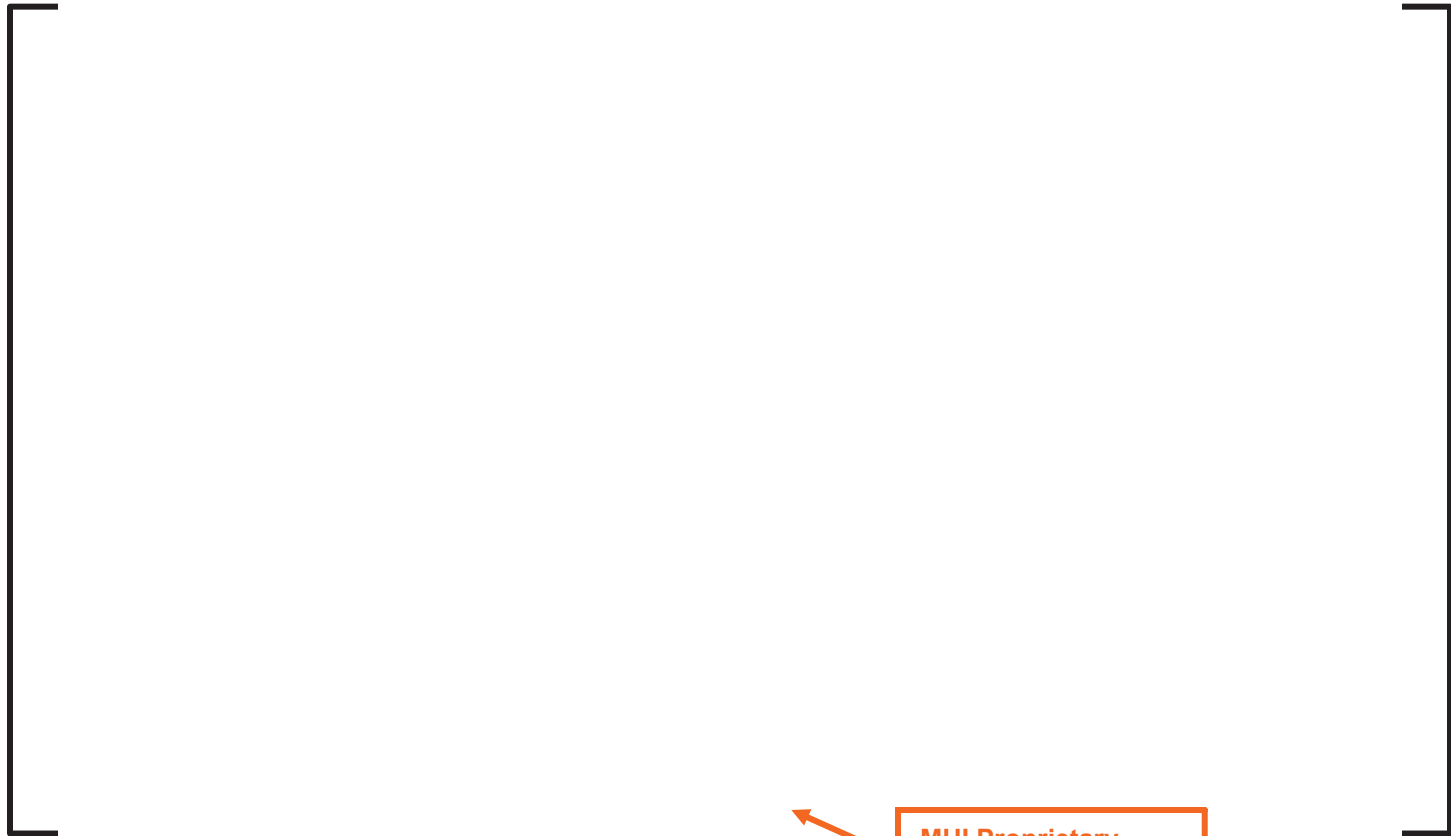
1.0 PURPOSE

In accordance with the SONGS Steam Generator Program [1] and EPRI Steam Generator Integrity Assessment Guidelines [2], an operational assessment (OA) must be performed to ensure that steam generator (SG) tubing will meet established performance criteria for structural and leakage integrity during the operating period prior to the next planned inspection. The OA projects and evaluates tube degradation mechanisms which have affected the SGs to date. The performance criteria are defined in plant technical specifications [3] & [4] and are based on NEI 97-06 [5].

This report documents the OA developed for tube-to-tube wear (TTW) that was discovered during the 2012 SONGS Unit 2 C17 outage. This OA considers the TTW identified in the SONGS-3 steam generators and determines the operating power level and associated inspection interval that provides the required margin relative to the onset of in-plane fluid-elastic instability and thus prevent TTW. This OA only addresses TTW. The OA for all other degradation is documented in a separate report [6].

2.0 BACKGROUND

Note: The steam generator design information in this section is taken from References [7], [8], [9], and [10].



MHI Proprietary

SONGS U2C17 Steam Generator Operational Assessment for Tube-to-Tube Wear

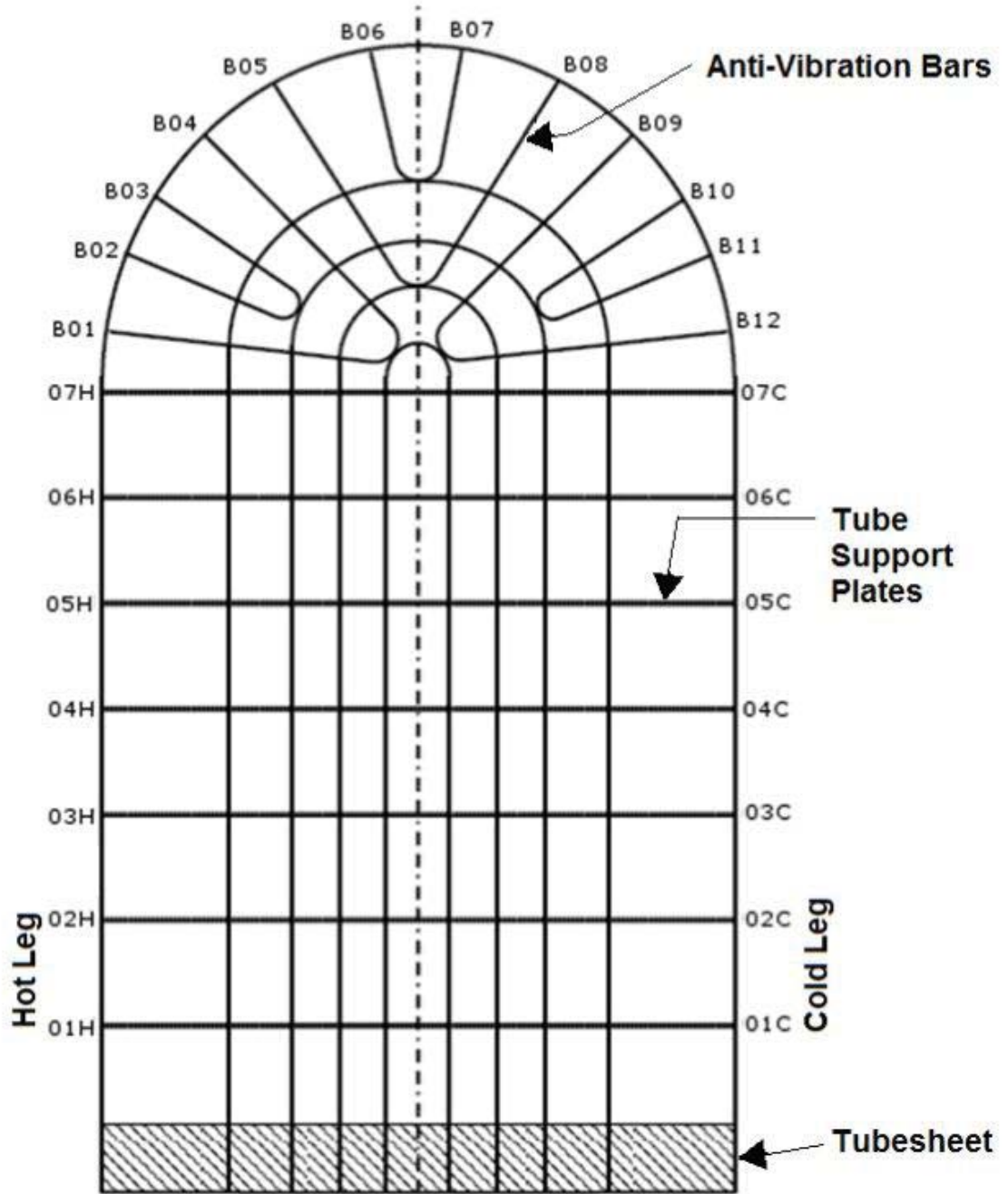


Figure 2-1: AVB Arrangement for SONGS Steam Generators

SONGS U2C17 Steam Generator Operational Assessment for Tube-to-Tube Wear

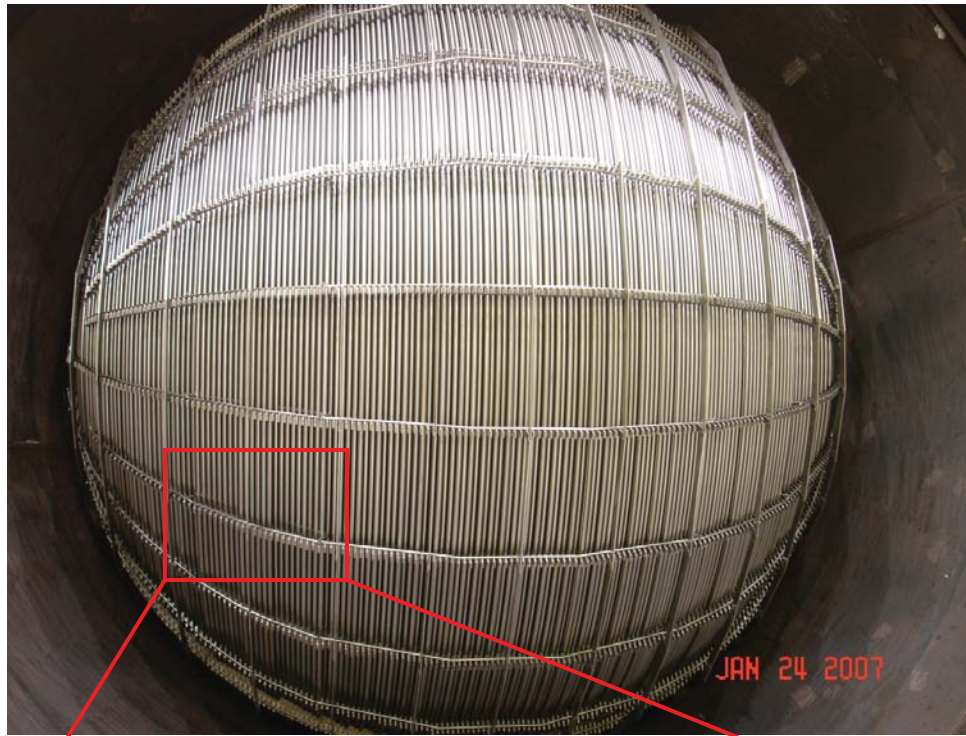
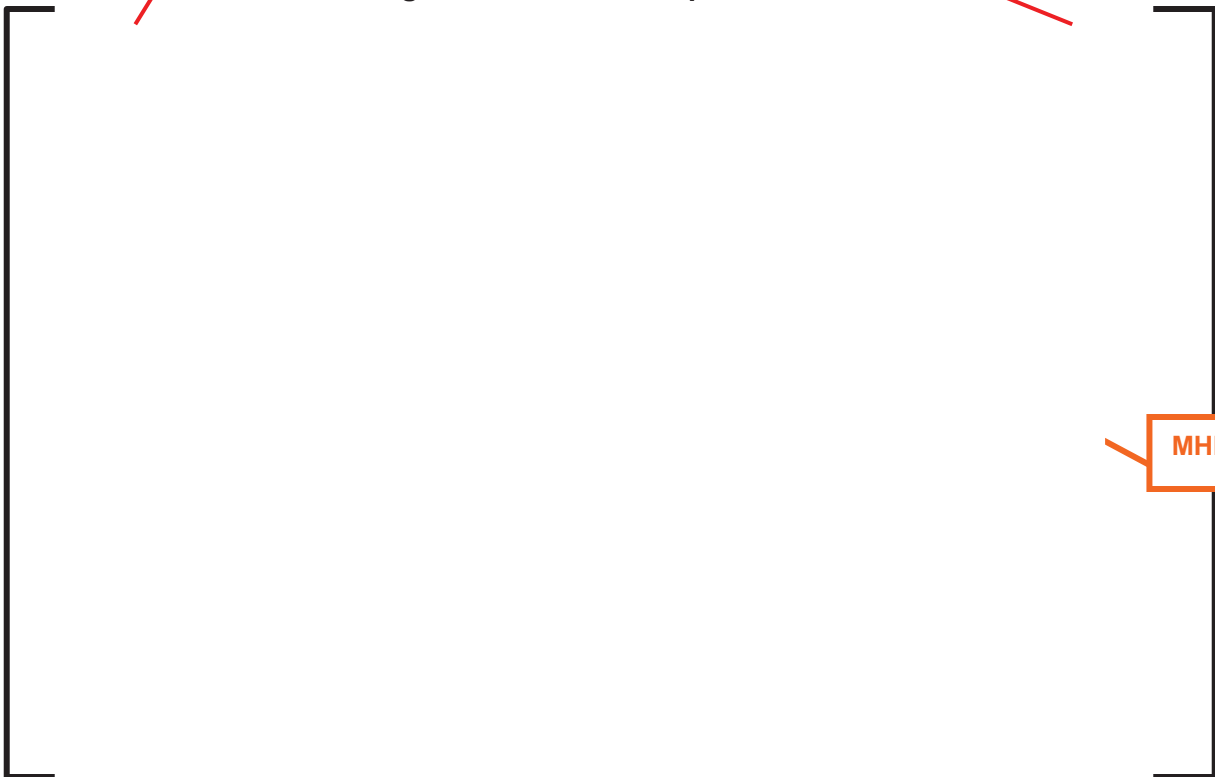


Figure 2-2: View of Top of Bundle



MHI Proprietary

Figure 2-3: Ends of AVBs Attached to Retaining Bars, Bridges and Retainer Bars Also Shown

SONGS U2C17 Steam Generator Operational Assessment for Tube-to-Tube Wear

3.0 INTRODUCTION

During the U2C17 outage, SONGS Unit 3 was shut down due to a primary-to-secondary leak. Eddy current inspections of the Unit 3 steam generators revealed that the cause of the leak was tube-to-tube wear (TTW) in the U-bend region of a cluster of tubes located near the center of the tube bundle. Based on a root cause evaluation performed by SCE [11], the TTW in the SONGS steam generators was caused by in-plane tube movement due to in-plane fluid-elastic instability (FEI).

No indications of TTW were reported during the initial U2C17 inspections of the Unit 2 steam generators, which included full-length eddy current inspections of all tubes with bobbin coil probes. However, since 823 indications of TTW were detected in the SONGS-3 steam generators [12] and the design of the SONGS-3 steam generators is the same as the SONGS-2 steam generators, supplemental +Point™ inspections of the U-bends were performed in SONGS-2. These supplemental inspections included the full-length of the U-bend for a group of tubes in the same region as those with TTW in Unit 3. These supplemental inspections resulted in the finding of two adjacent tubes with shallow TTW in SG E-089 of Unit 2. According to Reference [12], the wear depth was reported to be 14% through-wall (TW) based on EPRI Examination Technique Specification Sheet (ETSS) 27902.2. ETSS 27902.2 was developed for freespan wear caused by loose parts; this technique overestimates the depth of TTW and therefore results in a conservative measurement for purposes of assessing tube integrity. However it is more appropriate to base the engineering assessments in this OA on the best estimate of the wear depth. For this reason the tubes were re-sized using a site-specific ECT calibration standard developed for TTW. The tubes were also re-inspected using an ultrasonic (UT) technique. Both of these techniques resulted in an indicated TTW depth of 7% TW. The assessments in this OA are appropriately based on the 7% TW depth measurement from UT which is considered a more accurate measure of the true depth.

Tube wear at support locations (AVB and TSP) detected in Unit 2 is within previous industry experience and can be evaluated using standard practices as described in the EPRI Tube Integrity Assessment Guidelines [2]. These degradation mechanisms are not threatening in Unit 2, as demonstrated by Reference [6], which justified a full cycle of operation at full reactor power. However, given identical designs, Unit 2 must be judged, a priori, as susceptible to the same TTW degradation mechanism as Unit 3 where 8 tubes failed structural integrity requirements after 11 months of operation [12]. Indeed, the location and orientation of the two shallow TTW indications in Unit 2 are consistent with the behavior observed in Unit 3 and indicates that in-plane fluid-elastic instability in Unit 2 began shortly before the end of cycle 16 operation after 22 months of operation. It should be noted that this statement is contested by a viewpoint that TTW in Unit 2 is simply a consequence of tubes being in very close proximity to one another with self-limiting wear produced by a combination of turbulence and out-of-plane fluid-elastic excitation. This viewpoint has been evaluated completely and is considered to be arguable but not definitive. The argument that incipient in-plane fluid-elastic has developed in Unit 2 is considered a more logical explanation for the observed TTW but again cannot be stated as definitive. It is ultimately a moot point since the observations in Unit 3 make TTW via in-plane fluid-elastic instability a potential degradation mechanism for Unit 2. The severity of potential degradation via this mechanism dictates that it must be evaluated in a thorough manner both as a matter of logic and by the requirements of NEI 97-06 [5] and the EPRI Tube Integrity Assessment Guidelines [2]. Based on the extremely comprehensive evaluation of both Units, supplemented by thermal hydraulic and FIV analysis, assuming, a priori, that TTW via in-plane fluid-elastic instability cannot develop in Unit 2 would be inappropriate.

 SONGS U2C17 Steam Generator Operational Assessment for Tube-to-Tube Wear

4.0 OPERATIONAL ASSESSMENT STRATEGY

Understanding the TTW phenomena observed in Unit 3 is key to developing a rational operational assessment strategy for Unit 2. Extensive analysis has led to a good understanding of how and why TTW developed in both Unit 3 and Unit 2. This is summarized in Section 4.1. The operational assessment strategy is then presented in Section 4.2.

4.1 Development of TTW

Both steam generators in Unit 3 had more than 160 tubes with TTW indications in U-bends. The three most degraded tubes exhibited wear scars that were more than 28 inches long with central regions of essentially uniform wear depths that were greater than 80 %TW. These central regions of uniform wear depth were about 5 inches long. One of these regions contained a pinhole wall penetration that led to a small primary-to-secondary leak, resulting in the shutdown of Unit 3. Figure 4-1 shows the profile of wear depth versus axial length for the leaking tube, R106 C78, in Unit 3 SG E-088.

TTW scars are located on the extrados and intrados locations of U-bends. Wear scars on extrados locations of a given U-bend have matching wear scars on intrados locations of the neighboring row tube in the same column. The matching wear scars have very similar depths of wear [13]. The nominal distance between extrados and intrados locations of neighboring U-bends in the same plane ranges from 0.25 inches to 0.325 inches due to the tube indexing, as mentioned earlier. There are instances where the closest approach distance is less than this value based on field measurements using bobbin coil ECT. The bobbin probe on the 140 kHz absolute channel can detect neighboring U-bends if the separation distance is less than approximately 0.15 inches. Using a proximity signal calibration curve, the separation distance between U-bends was measured for all steam generators. The results of these measurements are reported in Reference [14]. The smallest detected U-bend separation distance is close to contact. There are 36 U-bends in Unit 2 SG E-088 and 34 in SG E-089 with a separation less than or equal to 0.050 inches. The separation of the U-bends in Unit 2 with TTW is 0.190 inches as measured by UT. The U-bends with the smaller separation distances are much better candidates for wear by rubbing yet do not exhibit TTW. In Unit 3, TTW via in-plane fluid-elastic instability is incontrovertible based on evidence presented in the following paragraphs.

An SCE root cause analysis [11] has identified in-plane fluid-elastic instability as the mechanistic cause of TTW in the SONGS steam generators. Out-of-plane fluid-elastic instability has been observed in nuclear steam generators in the past and has led to tube bursts at normal operating conditions. However, the observation of in-plane fluid-elastic instability in steam generators in a nuclear power plant is a true paradigm shift. It is not uncommon for designers of nuclear steam generators to calculate that large U-bends supported only by lateral AVB's are fluid elastically unstable in the in-plane direction under the assumption of no effective in-plane supports. This is textbook knowledge and part of the technical literature.

The caption of Figure 4-2, taken from a book by M. K. Au-Yang that was published in 2001 [15], reads, "In-plane modes that have never been observed to be unstable even though the computed fluid-elastic stability margins are well below 1". The fluid-elastic stability margin, FSM, is the inverse of the stability ratio, SR^1 . An FSM well below 1 means an SR well above 1 and well into the unstable range. As an example of the extensive laboratory

¹ Stability ratio is defined as the ratio of the effective flow velocity to which the tube is subjected to the critical velocity. Critical velocity is the velocity at which the tube, with specific geometry and support conditions, becomes unstable. Stability ratios less than 1.0 represent a stable condition where the actual velocity is less than the critical velocity; stability ratios greater than 1.0 represent an unstable condition where the actual velocity exceeds the critical velocity.

 SONGS U2C17 Steam Generator Operational Assessment for Tube-to-Tube Wear

testing campaigns conducted to detect in-plane fluid-elastic instability, Weaver and Schneider [16], in 1983, examined the flow induced response of heat exchanger U-tubes with flat bar supports. It is worth quoting the first conclusion of their paper:

“The effect of flat bar supports with small clearance is to act as apparent nodal points for flow-induced tube response. They not only prevented the out-of-plane mode as expected but also the in-plane modes. No in-plane instabilities were observed, even when the flow velocity was increased to three times that expected to cause instability in the apparently unsupported first in-plane mode.”

Additionally, in an effort to encourage the development of in-plane instability, Weaver and Schneider [16] substantially increased the clearances between flat bar supports and U-tubes, but no in-plane instability was observed. Other investigators, notably Westinghouse, have deliberately searched for in-plane instability with only support from flat bars and have not detected the phenomena. However in 2005, Janzen, Hagburg, Pettigrew and Taylor [17] reported in-plane instability. The abstract to their paper states, “For the first time in a U-bend tube bundle with liquid or two-phase flow, instability was observed in both the out-of-plane and in-plane direction.” The test setup included tubes with a U-bend radius of 0.646 m (25.4 in.) with flat bar U-bend restraints inserted between columns at the apex of the U-bend. The bundle was subjected to air-water cross-flow directed at the mid-span between the 0° and 90° location (apex) of the bundle. Tube vibration was measured over a range of void fractions and flow rates, and for three tube-to-support diametral clearances: no support, 1.5 mm (59 mil) and 0.75 mm (30 mil). It is noted that these test clearances are significantly larger than the SONGS steam generator design clearance of 2 mils diametral.

Prior to the observations at SONGS Unit 3, no in-plane instability had been observed in any U-bend nuclear steam generator. The service history of U-bends with flat bar supports had been successful up to this point. This includes depending on in-plane effectiveness of flat bar supports to demonstrate relatively low values of stability ratios. Stability depends on both thermal-hydraulic flow conditions and in-plane support effectiveness. Logically either or both of these factors are causing the observed instability in SONGS Unit 3. From an overall engineering perspective it is worth considering an operational envelope that is the set of past design and operational factors that have led to successful performance. One technique for doing so is a spider diagram where many factors for different plants and designs are considered by plotting of relative ranking on axes arranged in a star pattern. Connecting the dots from one axis to another for a given plant creates a periphery that defines the operational parameters for that plant. The outer boundary of all these peripheries of past successful performance is the successful operational envelope.

It should be recognized that the goal of efficient and optimized design leads to expansion of the operational envelope over time and this has occurred in the past. Using data from [18], a spider diagram is presented in Figure 4-3. More parameters are needed to completely define all parameters that have an influence on in-plane FEI, for example some measure of support effectiveness. This could be something as specific as design clearances or as general as the ratio of the total support structure weight to the weight of supported U-bends. The two axes of Figure 4-3 with plotted data are bulk velocity ratio and mean void fraction ratio, which are those parameters that are publically available. High velocities increase susceptibility to instability and a high void fraction indicates lower damping and thus less resistance to instability. At 100% power, the thermal-hydraulic conditions in the u-bend region of the SONGS replacement steam generators exceed the past successful operational envelope for U-bend nuclear steam generators based on presently available data. The operational envelope will be reconsidered in Section 7.0 in the context of a lower power level (see also Figure 5-1). The service performance of SONGS Unit 3 at 100% power shows that there is a boundary to the successful operational envelope.

SONGS U2C17 Steam Generator Operational Assessment for Tube-to-Tube Wear

The following paragraphs discuss inspection results and their consistency with in-plane fluid-elastic instability. This provides the background needed to develop an operational assessment strategy.

Figure 4-4 and Figure 4-5 are tubesheet maps illustrating the U-bends in Unit 3 SG E-088 and SG E-089 that have TTW. The more detailed view of the positions of TTW indications in Figure 4-6, Figure 4-7 and Figure 4-8 are instructive. Note that the positions are contiguous with only one tube not affected. This argues against a random spatial and temporal occurrence of instability. There just aren't enough unaffected tubes to indicate that instability independently initiated at different positions at different times. Three dimensional plots of TTW depth versus column and row in Figure 4-9 and Figure 4-10 reinforce the concept that the development of instability at different positions is a sequence of dependent events and not a sequence of independent events. The plot of wear depths resembles a mound with the largest depths at the top and then sloping to lower values in all directions. This is also illustrated by the color coded depths in Figure 4-4 and Figure 4-5. The two U-bends in Unit 2 SG E-089 with shallow TTW indications are plotted as red points in Figure 4-8 to illustrate their position in the bundle for comparison with Unit 3.

TTW due to in-plane fluid-elastic instability is a unique degradation mechanism because one unstable tube can drive its neighbor to instability through repeated impact events. Repeated impacts move the neighbor tube relative to its AVBs causing accelerated wear and elongated wear. The in-plane effectiveness of the AVBs is degraded and an initially stable neighbor tube eventually becomes unstable. This leads to a growing region of instability and TTW. Impact events lead to the propagation of instability from one tube to another in the same column. Propagation of instability from one column to another must involve fluid coupling since tube-to-tube impact does not occur across columns. Fluid coupling is discussed in Reference [19]. The two basic theories of fluid-elastic instability have been termed fluid stiffness and fluid damping. With fluid damping perturbations/hysteresis effects in flow fields can lead to negative damping and thus lead to instability. Given the large displacements involved with instability and TTW, the fluid coupling argument is undeniably reasonable.

The extent of movement of unstable tubes, as well as tubes being driven to instability by impact from unstable tubes, is revealed by elongated wear scars at some AVB locations. Typically, turbulence induced wear leads to wear scars with a length equal to or less than the width of an AVB.

Figure 4-11 and Figure 4-12 show that the Unit 3 elongated wear scars only occur within the region of unstable tubes with TTW. In these figures elongated wear scars are identified by comparing a bobbin probe evaluation of AVB width with a +Pt™ probe evaluation of wear scar length. More complete results, based only on a bobbin probe evaluation of wear scar lengths, are shown in Figure 4-13 and Figure 4-14. Outside of the region of TTW the length of wear scars at AVB locations returns to normally expected values. It should be noted that because of field spread effects the bobbin probe typically overestimates wear scar lengths. Even though no evidence of elongated wear scars is evident in Unit 2, it doesn't necessarily rule out undetected in-plane instability. Wear scars at AVB locations may be too shallow to evaluate properly and AVB wear scar lengths may be shortened by a contact length that is small because of the presence of AVB twist. The best evidence of in-plane instability is the detection of TTW, not the detection of elongated AVB wear scars. Extensive inspections of the regions of interest with the +Pt™ probe show that possible undetected TTW would be less than 5 %TW. It is unreasonable to expect detectable elongation of AVB wear scars without the detection of TTW. The significance of elongated AVB wear scars is that the amount of elongation reveals the extent of unstable tube motion in-plane.

SONGS U2C17 Steam Generator Operational Assessment for Tube-to-Tube Wear

MHI Proprietary

When the displacement of the unstable tube in a direction perpendicular to the U-bend exceeds the local tube-to-tube spacing, it will impact the neighboring tube. By plotting the radially outward displacement versus angle around the U-bend, the points of impact with a neighboring tube can be determined. For Mode 1 displacements in the tubes of interest, the centers of impact with a neighbor tube are at 48° and 132° as measured from the positive x axis. The numbering sequence used to identify AVBs corresponds to 132° being on the hot leg and 48° being on the cold leg of the U-bends. Depth versus length profiles were determined for 777 separate TTW indications in Unit 3 with almost all containing some central region with an essentially uniform maximum depth. The center of impact was considered to be at the midpoint of this central region of maximum depth. Figure 4-17 shows a plot of impact locations compared to locations consistent with Mode 1, Mode 2 and Mode 3 displacement patterns. The impact points are overwhelmingly consistent with Mode 1 displacements. Parenthetically, the two TTW scars in Unit 2 are at 48°, the Mode 1 impact point. Mode 1 is the lowest natural frequency of in-plane U-bend vibration and thus is the first mode to be excited to instability. Mode 2 and Mode 3 displacements are shown in Figure 4-18 and Figure 4-19, respectively. Note that only one half of the cycle is illustrated in all modal displacement plots. The other half of the cycle produces displacements that are exactly opposite of those shown.

A tube subject to FEI in the in-plane direction can move in different modes, as shown in Figure 4-15, Figure 4-18 and Figure 4-19. Note that some impact points shown in Figure 4-17 are consistent with Mode 2 and Mode 3 displacement patterns. There are three possibilities for the appearance of these locations: excitation of instability in Modes 2 and 3, excitation of other vibration patterns due to initial Mode 1 impact events, or excitation of Mode 2 and Mode 3 vibration due to a momentarily strong interaction of an unstable tube in Mode 1 with an AVB as it passes that AVB. It is likely that some combination of these conditions is operative, but this cannot be conclusively determined by analysis.

The mechanisms and forces involved in fluid-elastic instability in tube bundles are presented later in this section. For the present, it is sufficient to note that the forces at AVB locations needed to prevent the onset of fluid-elastic instability are low. In contrast, after instability develops, the amplitude of in-plane motion continuously increases and the forces needed to prevent in-plane motion at any given AVB location become relatively large. Hence shortly after instability occurs, U-bends begin to swing in Mode 1 and overcome hindrance at any AVB location.

SONGS U2C17 Steam Generator Operational Assessment for Tube-to-Tube Wear

4.2 Operational Assessment Strategy

From the behavior observed in Unit 3 and other non-nuclear heat exchangers, TTW rates driven by fluid-elastic instability are high. Therefore, the fundamental goal of the operational assessment strategy is to adjust the operating power level and inspection interval to reduce the development of in-plane fluid-elastic instability and the resulting occurrence of TTW to an acceptably low probability event. The goal of the power reduction is to place Unit 2 back inside of the successful operational envelope and restore stability.

The strategy of the operational assessment for TTW therefore consists of three elements. These are:

- Identify the plant operating condition and the length of the next operating interval necessary to prevent a loss of SG tube integrity.
- The operating power level and operating interval will be reduced to ensure an acceptably low probability of in-plane FEI. These operating conditions establish a high probability that structural and leakage integrity requirements [2] will be met (operating interval is defined as time at reduced power not calendar time).
- Identify and implement defense in depth (DID) measures relative to TTW that add assurance that structural and leakage integrity requirements will be maintained for the plant operating period.

To ensure U-bend stability, the two tubes in Unit 2 that are now argued to be unstable and exhibiting TTW will be shown to be stable at a lower power level. At sufficiently low flow conditions, no in-plane support is required to maintain stability. At higher flow conditions or, equivalently, to argue that the maximum stability ratio will remain at some low value, say 0.75 for the sake of conservatism, some degree of in-plane support effectiveness needs to be demonstrated. There are no universally established or accepted criteria for support effectiveness. Operating experience and laboratory testing has shown the small gaps between AVBs and U-bends, without any friction force, does provide an effective support condition. Conversely, arguments have been advanced that very small friction forces provide an effective support to preclude in-plane tube motion. For convenience in calculations, support effectiveness is expressed in terms of contact forces at AVB locations. This is a surrogate for more complex tube to support interactions. Lowering the power level is expected to increase support effectiveness by positioning SONGS Unit 2 within the operating window shown to be acceptable for other plants.

Contact forces, as deteriorated by tube wear at support locations over time, will be calculated using advanced computational techniques. This will be combined with calculations of stability ratios to develop the probability of the onset of in-plane fluid-elastic instability, both as a function of operating power level and operating time. The operating power and operating time will be adjusted to provide a probability of occurrence of instability ≤ 0.05 . This probability is based on considerations and requirements described in the EPRI SG Integrity Assessment Guidelines [2]. Without the development of TTW, the Structural Integrity Performance Criteria, SIPC, is automatically satisfied to a probability greater than 0.95.

The defenses in depth measures are as follows:

- After the onset of FEI, TTW would have to progress over some time period to lead to an unacceptable level of wear depth. Estimates of TTW growth rates are provided in this report.
- Tubes with a high risk of developing FEI, based on AVB wear patterns similar to those of Unit 3 unstable tubes, have been plugged and stabilized with wire cables.

 SONGS U2C17 Steam Generator Operational Assessment for Tube-to-Tube Wear

- The onset of FEI is most likely in the high risk region. Since the two tubes with TTW are surrounded by plugged and stabilized tubes, then FEI must progress through a buffer zone of plugged tubes to reach pressurized, in-service tubes.
- Cable stabilizers do not substantially improve U-bend in-plane stability, but will prevent possible generation of large loose parts. []

The three elements of the strategy for the operational assessment of TTW in Unit 2 will provide the needed assurance that structural and leakage integrity requirements will be maintained throughout the next inspection interval.

The parameter that characterizes the state of fluid-elastic stability is termed the stability ratio, SR. Mathematically it represents the ratio of the effective fluid velocity to the critical fluid velocity at instability. At the onset of instability, the SR value is 1.0. If the stability ratio is less than 1.0, the structure of interest is fluid elastically stable. The details of calculating stability ratios are presented in Reference [20]. In general, the factors in the calculation are the geometry of the structure, fluid conditions such as velocity and density, damping sources and the mode of vibration being excited. Calculated stability ratios are benchmarked against laboratory experiments.

The development of in-plane fluid-elastic instability of U-bends depends on four factors. These are:

- Location in the bundle
- Operating power level
- Number of consecutive ineffective supports
- Operating time

Tube location in the bundle determines the thermal-hydraulic environment of a given U-bend. Fluid-elastic excitation depends on the fluid velocity and density. For a U-bend, these factors vary with position around the U-bend from the hot leg to the cold leg. This variation is accounted for in calculations of stability ratio. The operating power level has a dramatic effect on thermal-hydraulic conditions. Reduced power levels substantially lower fluid-elastic excitation. For given thermal-hydraulic conditions and tube geometry, the stability ratio is a direct function of the number of consecutive ineffective AVB supports. If too many consecutive supports are ineffective, the stability ratio will exceed 1.0. The allowable number of consecutive ineffective supports depends on the U-bend location in the bundle and the power level. Tube wear at AVB support locations degrades their effectiveness in terms of providing in-plane support. Thus, tube wear at AVB locations can turn an effective support into an ineffective support. Operating time is important because wear can increase over time. Limiting operating time will in turn limit wear at AVB locations, which then limits degradation of support effectiveness, maximizing stability.

Calculation of the probability of the onset of in-plane fluid-elastic instability requires information in three areas: stability ratios, contact forces at AVB locations and a criteria for deciding whether AVB supports are effective or ineffective in terms of in-plane support. Stability ratios need to be known as a function of position in the bundle, number of consecutive ineffective supports and power level. Contact forces at AVB locations cannot be determined deterministically since the dispersion of gaps between tubes and AVB supports is random, and thus probabilistic in nature. Therefore, contact forces have to be described in a probabilistic manner. At any given

SONGS U2C17 Steam Generator Operational Assessment for Tube-to-Tube Wear

AVB location, the contact force is not known exactly, but it can be demonstrated to be a selection from some known distribution of forces. Whether or not an AVB support is effective or ineffective in terms of in-plane support can be expressed in terms of the contact forces at that location. The derivation of the support effectiveness criterion is explained in Section 7.0.

In principle, the calculation of the probability of instability is straightforward. Stability ratios are available for each U-bend in the bundle as a function of the number of consecutive ineffective supports and power level [20]. Similarly, the distributions of contact forces are available for each AVB location in the bundle. Tube wear at AVB locations decreases the contact force at those locations. The distributions of contact forces as affected by wear have been calculated [26]. The required contact force for any AVB support to be considered effective is defined for each AVB location. With this input, one Monte Carlo trial of a steam generator is constructed in the following manner:



A flow chart of the above process is shown in Figure 4-20.

In principle, the above procedure is followed; in practice, several independent programs use mathematically equivalent algorithms to compute the probability of instability. The goal of the operational assessment is to determine the operating power level and associated inspection interval that provides the needed margin relative to the onset of in-plane fluid-elastic instability and thus precluding TTW.

The following sections describe stability ratios, contact forces at AVB locations and criteria for defining effective versus ineffective supports. This is followed by a more detailed description of probability of instability calculations and results defining the acceptable operating power level and inspection interval.

SONGS U2C17 Steam Generator Operational Assessment for Tube-to-Tube Wear

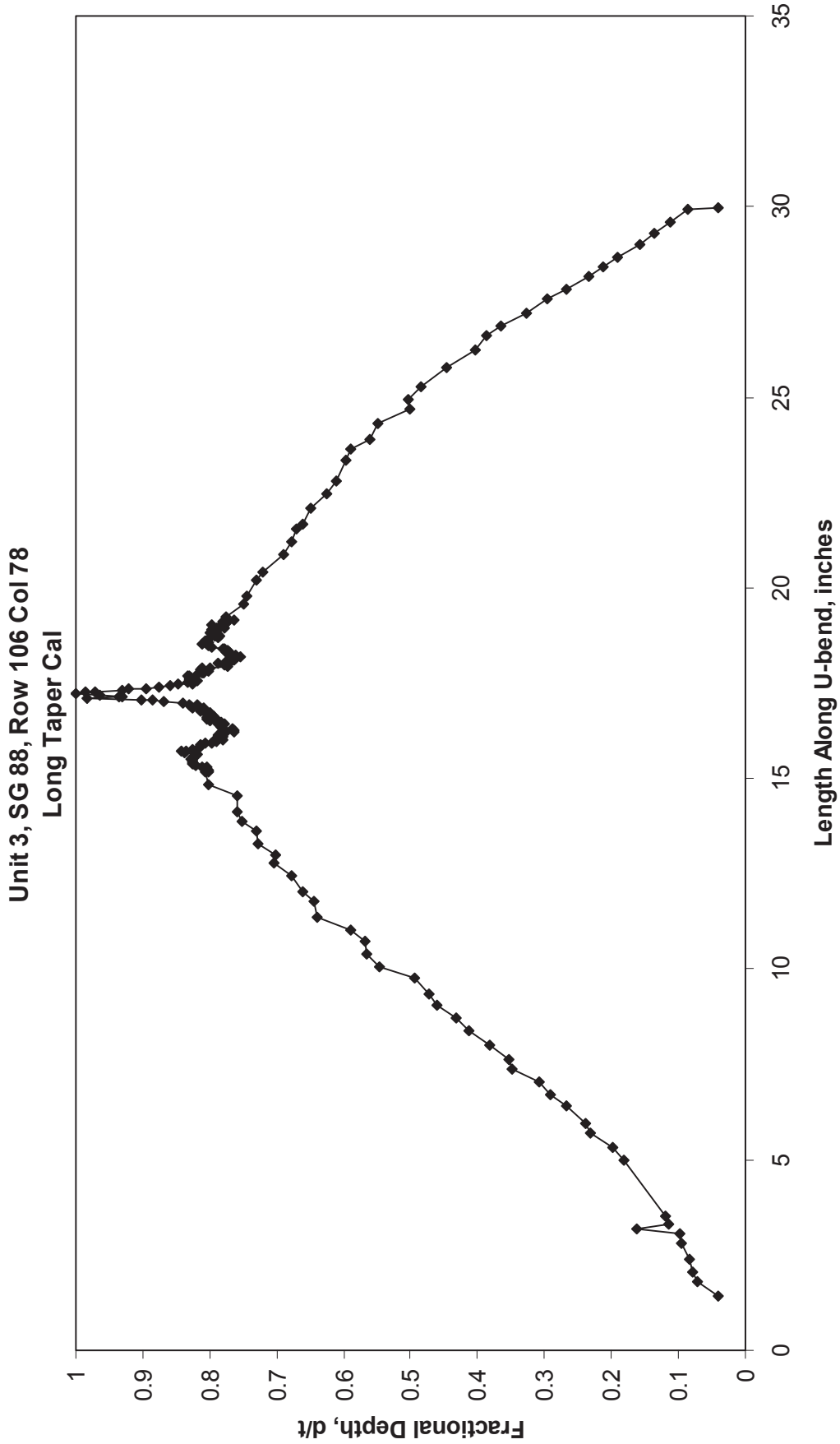
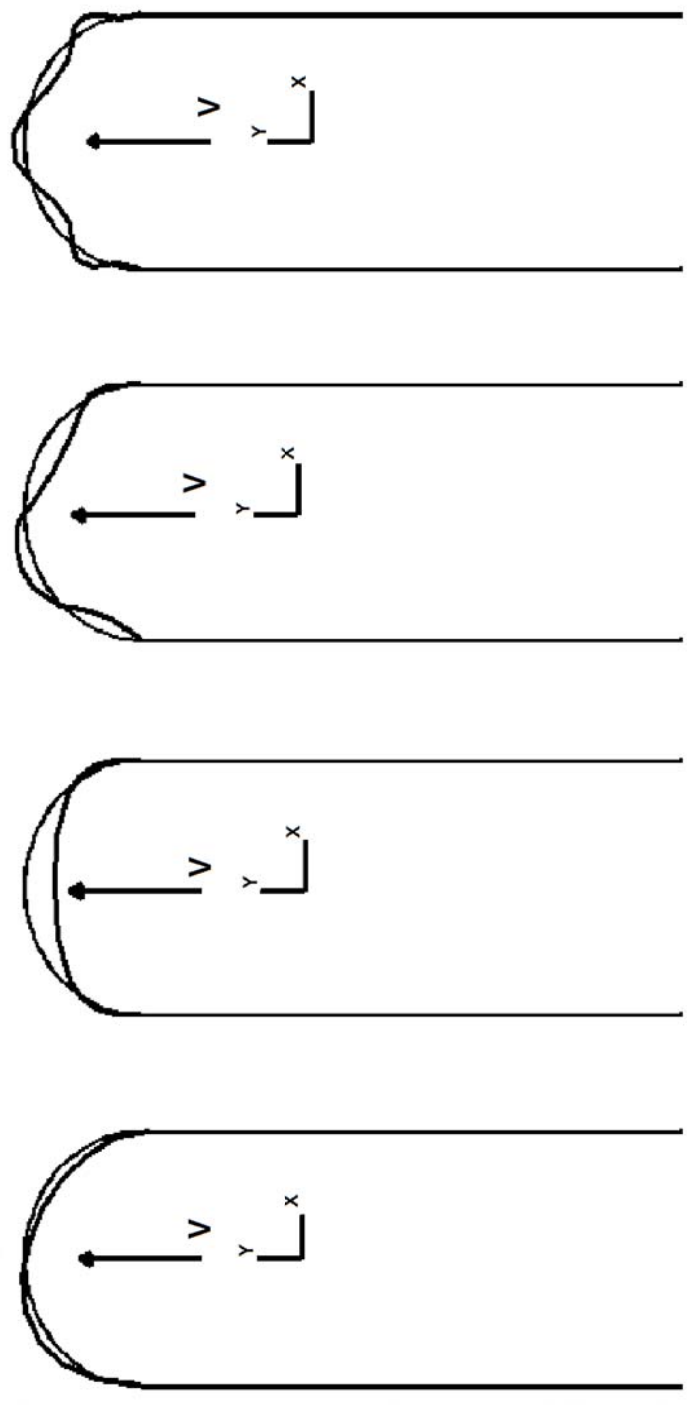


Figure 4-1: Depth versus Axial Length Profile for the Leaking Tube in Unit 3, SG E-088

SONGS U2C17 Steam Generator Operational Assessment for Tube-to-Tube Wear



In-plane modes that have never been observed to be unstable even though the computed fluid-elastic stability margins are well below 1.0. (with $FSM = 1/SR$, $SR \gg 1.0$)

Figure 4-2: Figure from a Book by M. K. Au Yang, "Flow Induced Vibration in Power and Process Plant Components", ASME Press, 2001

SONGS U2C17 Steam Generator Operational Assessment for Tube-to-Tube Wear

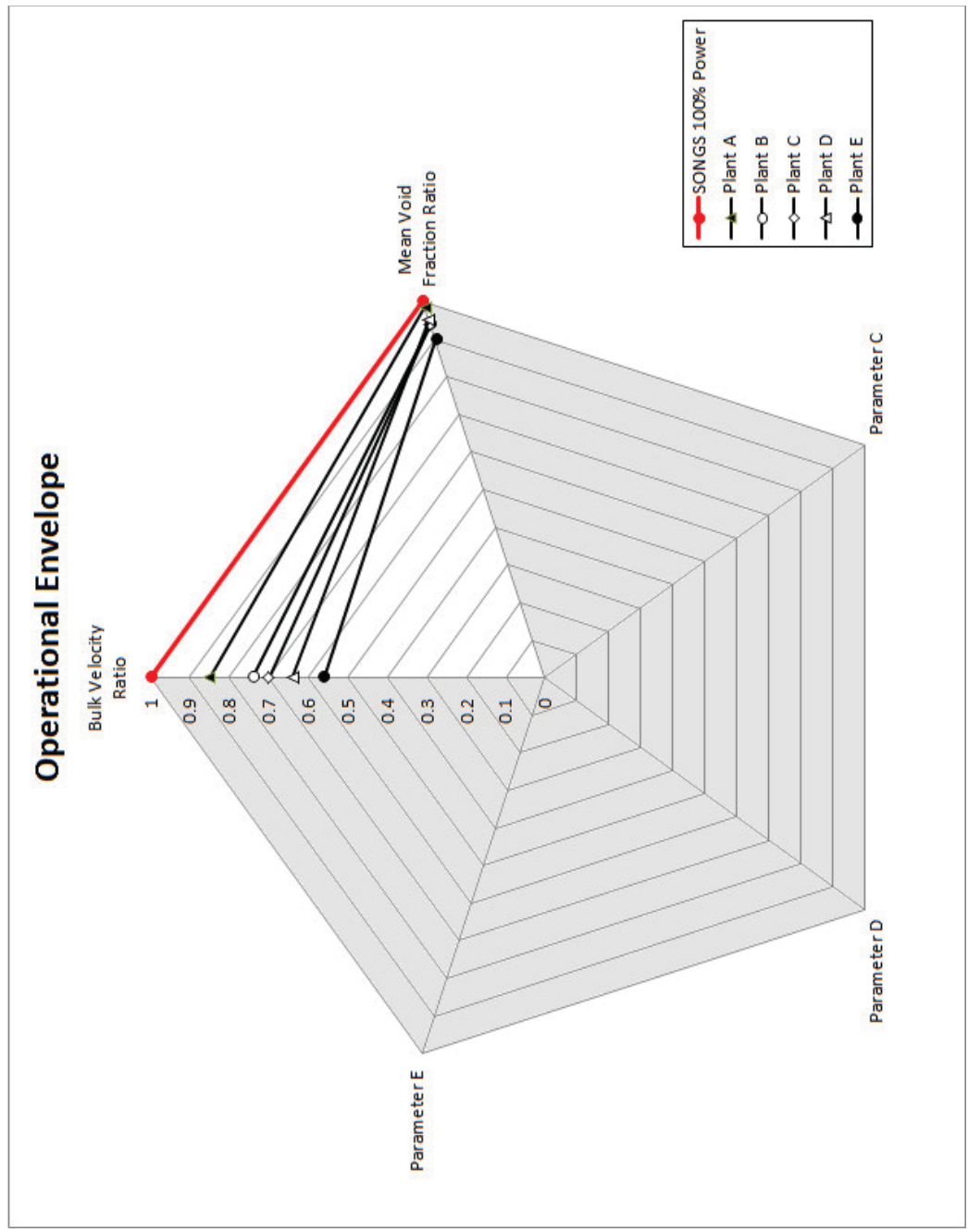


Figure 4-3: Spider Diagram of the Operational Envelope for Large U-bend Steam Generators

SONGS U2C17 Steam Generator Operational Assessment for Tube-to-Tube Wear

<h3>SCE-SONGS Unit 3 - REPL Tube-to-Tube Wear</h3>		<p>GROUP</p> <p>>=50% 25</p> <p>35-49% 74</p> <p>20-34% 52</p> <p><20% 14</p> <p>TUBES</p>
<p>AREVA - FOMI Long寿炉 (Long寿炉) 11.0</p>		<p>SCALE: 0.066571 X</p> <p>Fri May 25 12:12:31 2012</p>
<p>S/G 89 Repl COLD PRIMARY FACE</p>	<p>TOTAL TUBES: 9727</p> <p>SELECTED TUBES: 165</p> <p>OUT OF SERVICE (#): NA</p>	

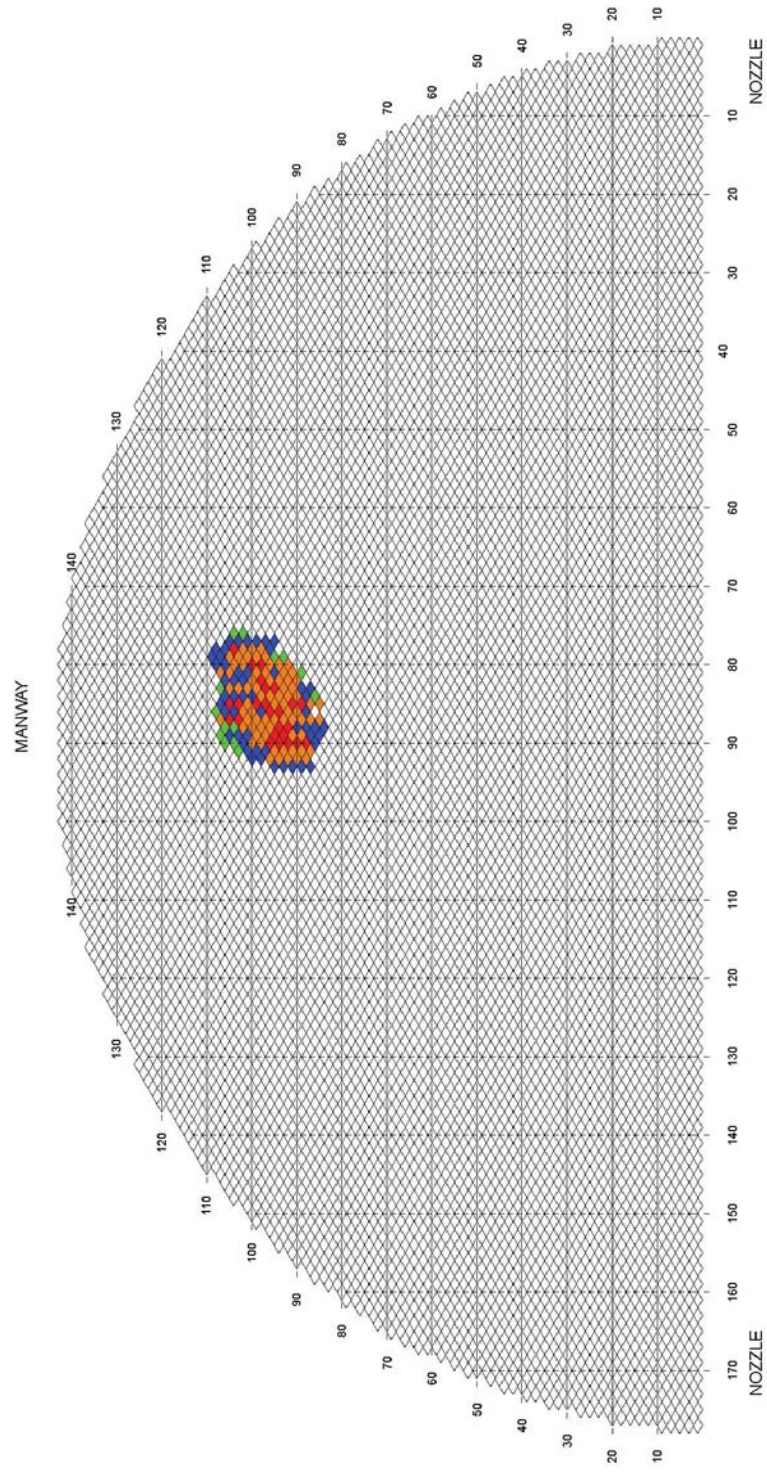


Figure 4-5: Tubesheet Map of TTW Indications, Unit 3, SG E-089

SONGS U2C17 Steam Generator Operational Assessment for Tube-to-Tube Wear

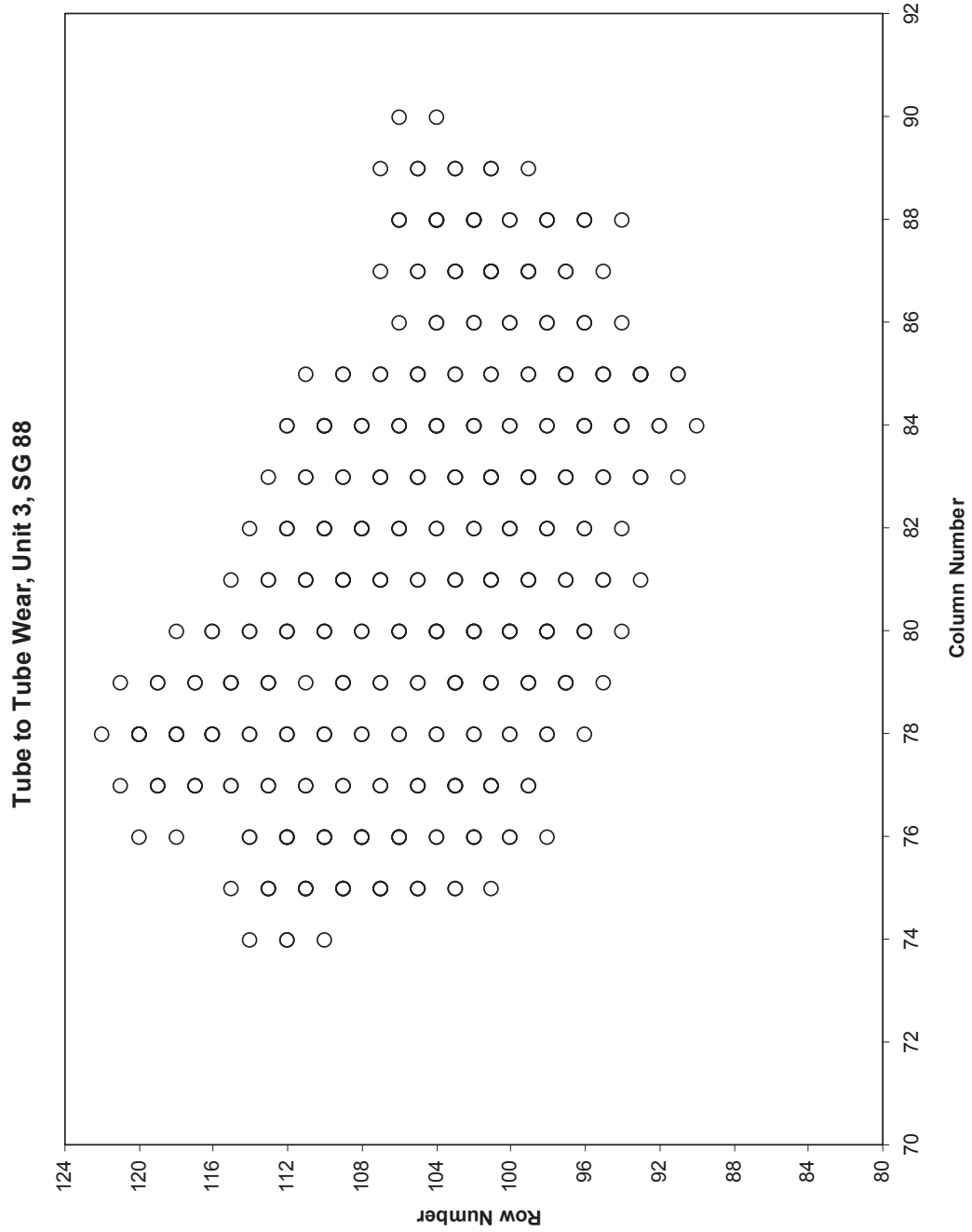


Figure 4-6: Expanded View of TTW Indications, Unit 3, SG E-088

SONGS U2C17 Steam Generator Operational Assessment for Tube-to-Tube Wear

Tube to Tube Wear, Unit 3, SG 89

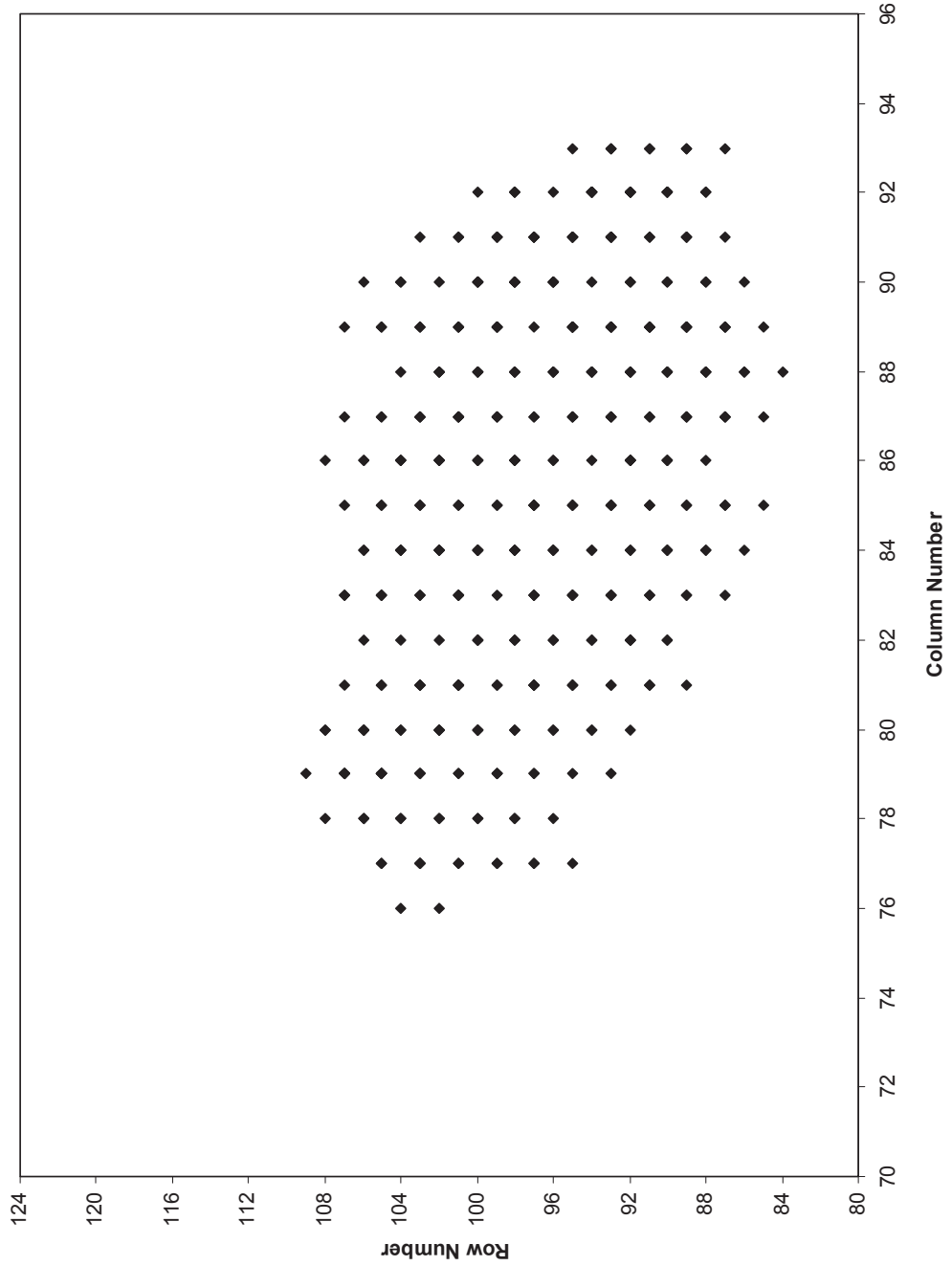


Figure 4-7: Expanded View of TTW Indications, Unit 3, SG E-089

SONGS U2C17 Steam Generator Operational Assessment for Tube-to-Tube Wear

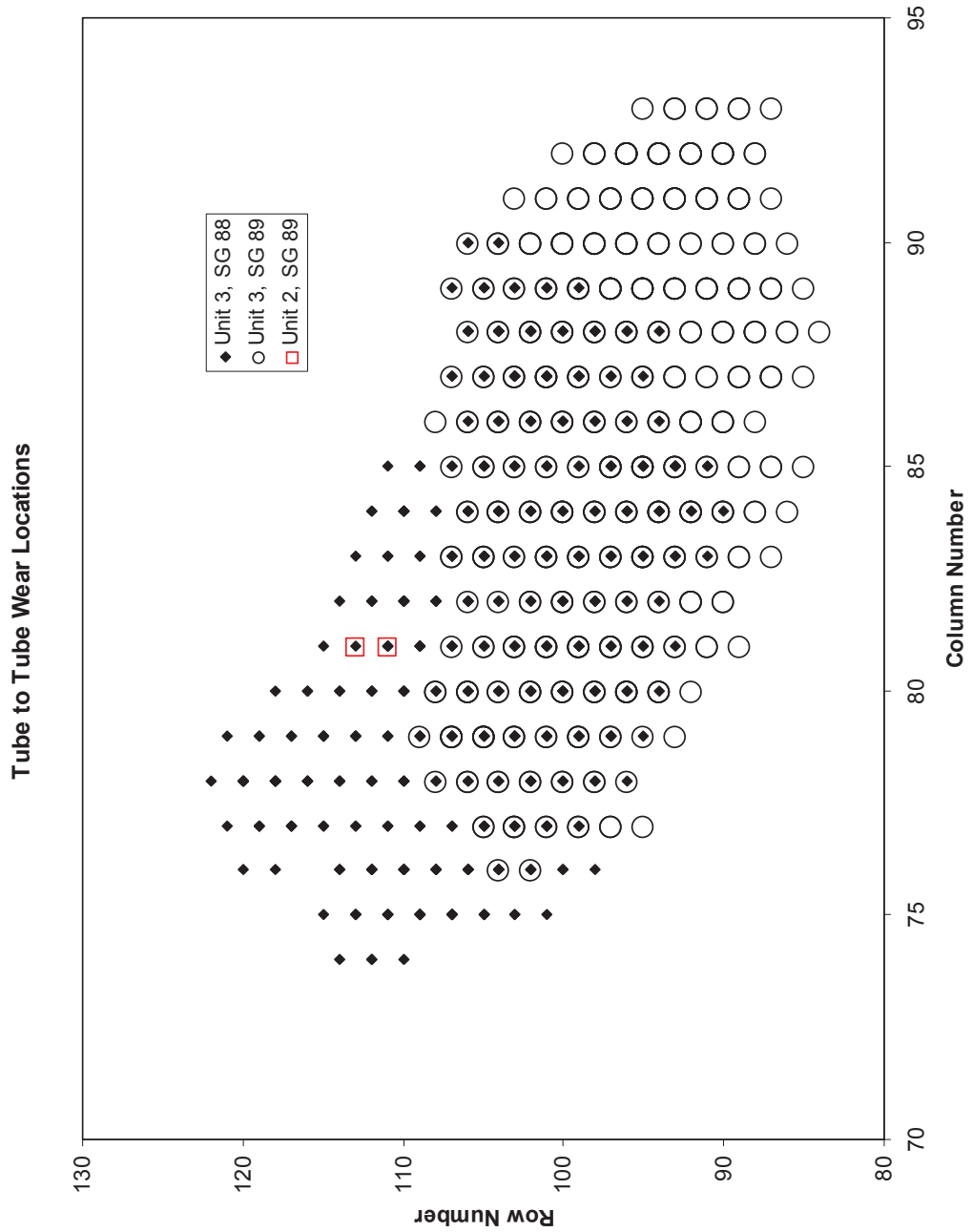


Figure 4-8: Combined View of TTW Indications

SONGS U2C17 Steam Generator Operational Assessment for Tube-to-Tube Wear

The color scheme on this figure is directly related to the %TW Depth (on the vertical axis). ■ is lower %TW and ■ is higher %TW.

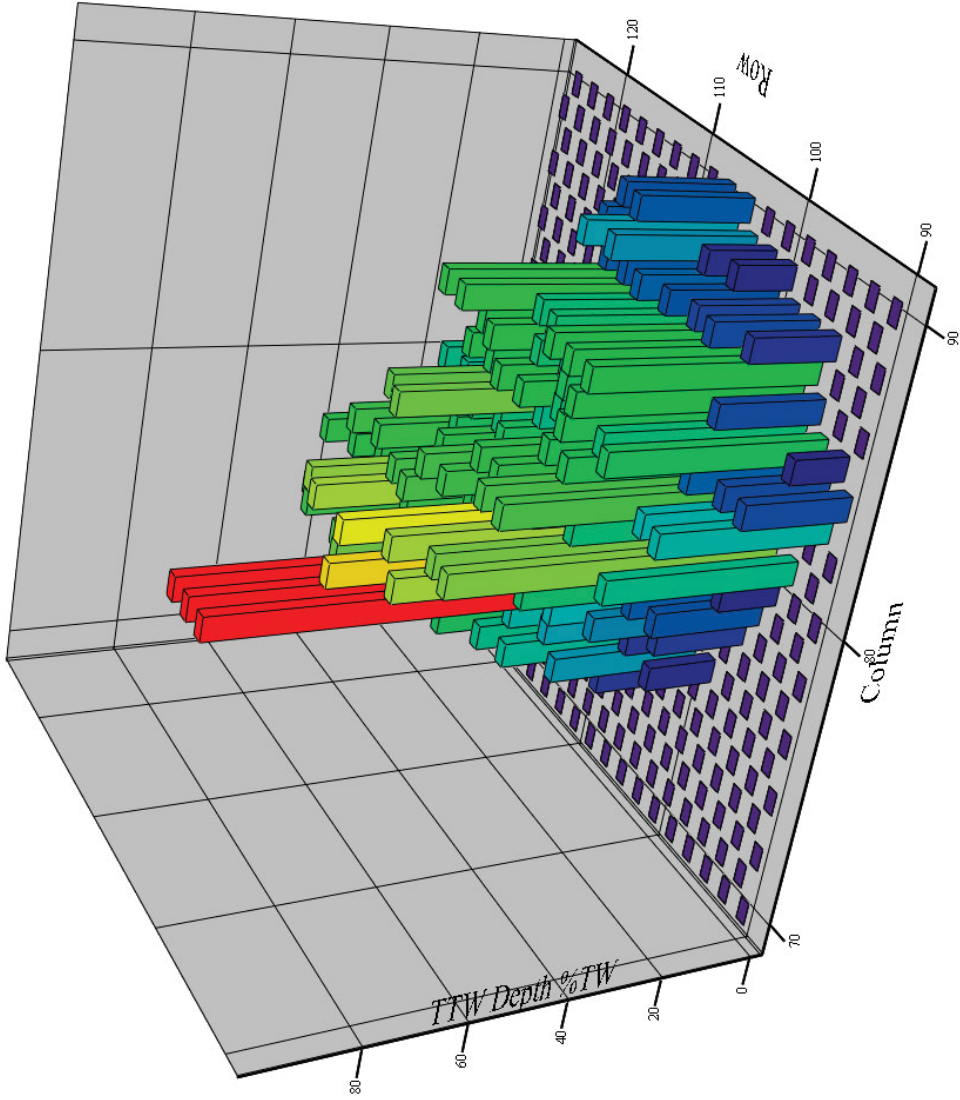


Figure 4-9: TFW Depth versus Row and Column, Unit 3 SG E-088

SONGS U2C17 Steam Generator Operational Assessment for Tube-to-Tube Wear

The color scheme on this figure is directly related to the %TW Depth (on the vertical axis). ■ is lower %TW and ■ is higher %TW.

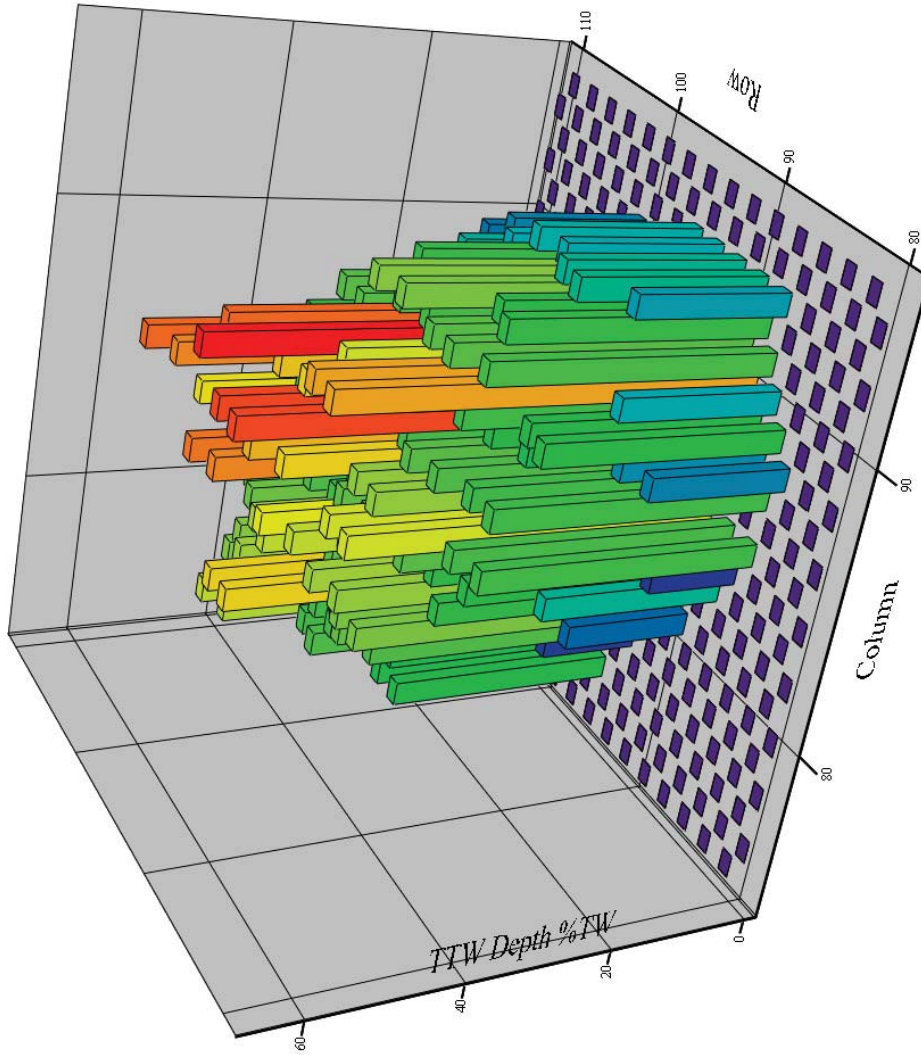
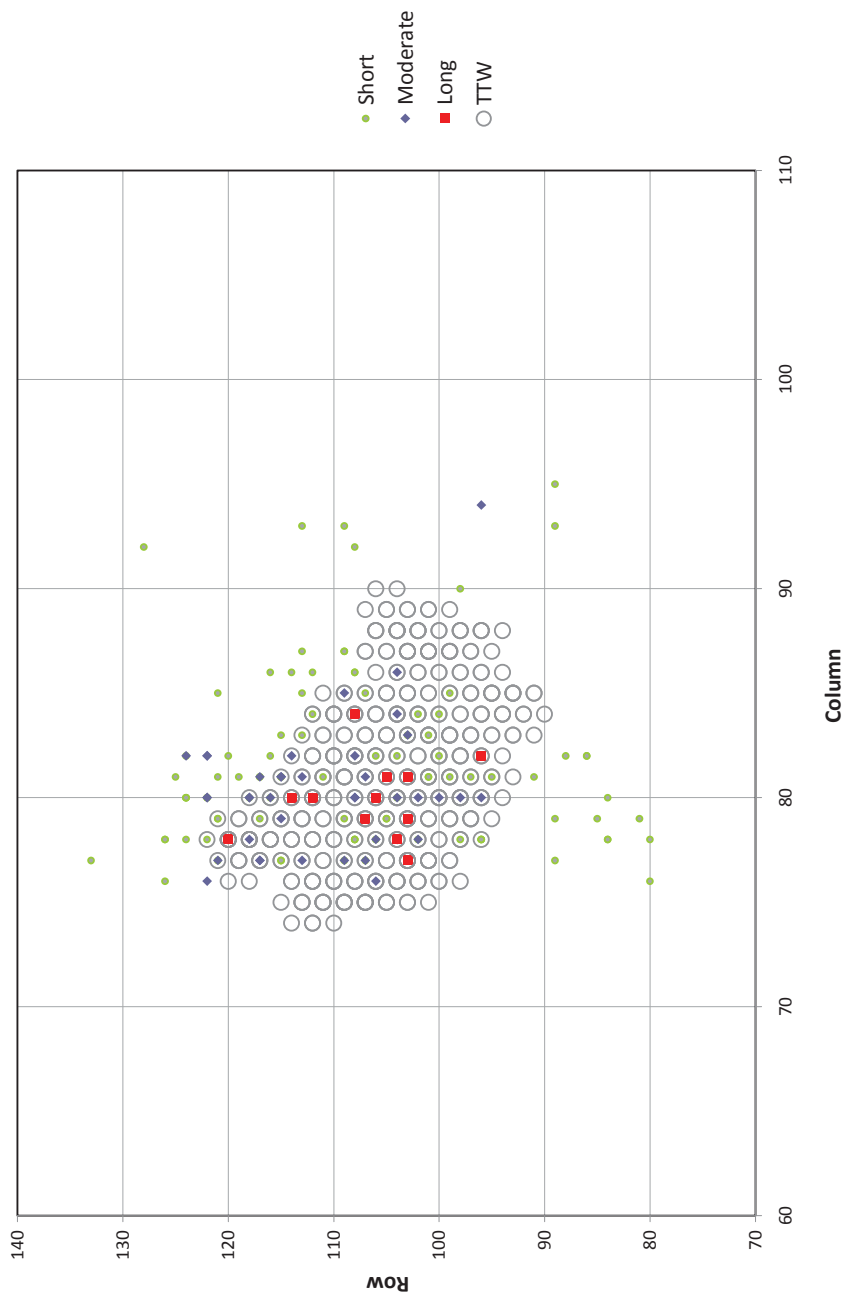


Figure 4-10: TTW Depth versus Row and Column, Unit 3 SG E-089

SONGS U2C17 Steam Generator Operational Assessment for Tube-to-Tube Wear

**AVB Wear Length Review
SONGS-3, SG88**

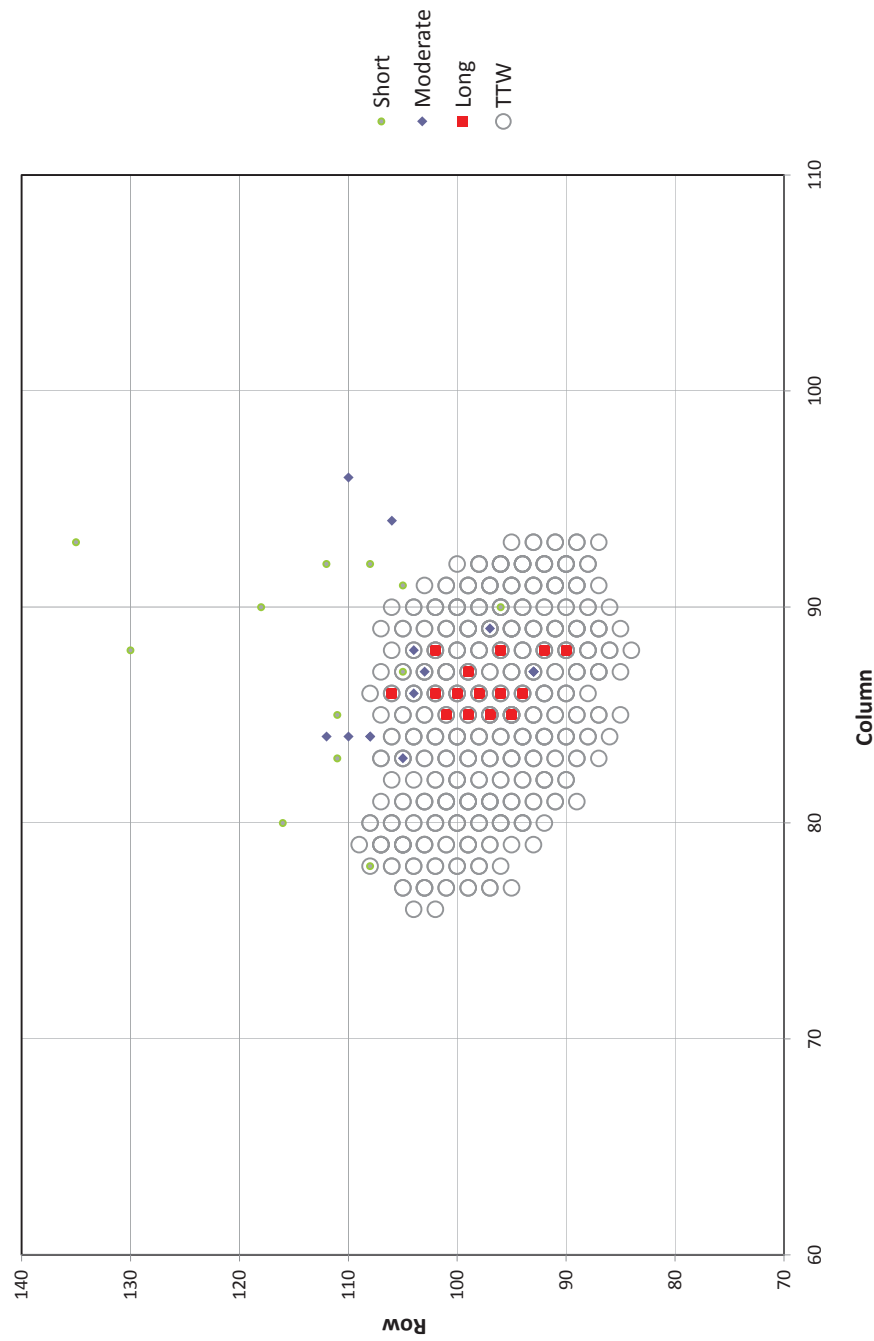


Note: This Figure is based on a +Pt™ probe evaluation of the AVB wear scar length compared to a bobbin probe evaluation of the AVB width.

Figure 4-11: No Elongated AVB Wear Found Beyond the Region of TTW, Unit 3 SG E-088

SONGS U2C17 Steam Generator Operational Assessment for Tube-to-Tube Wear

**AVB Wear Length Review
SONGS-3, SG89**



Note: This Figure is based on a +Pt™ probe evaluation of the AVB wear scar length compared to a bobbin probe evaluation of the AVB width.

Figure 4-12: No Elongated AVB Wear Found Beyond the Region of TTW, Unit 3 SG E-089

Unit 3 Steam Generator 3E088 AVB Indications (LENGTH)

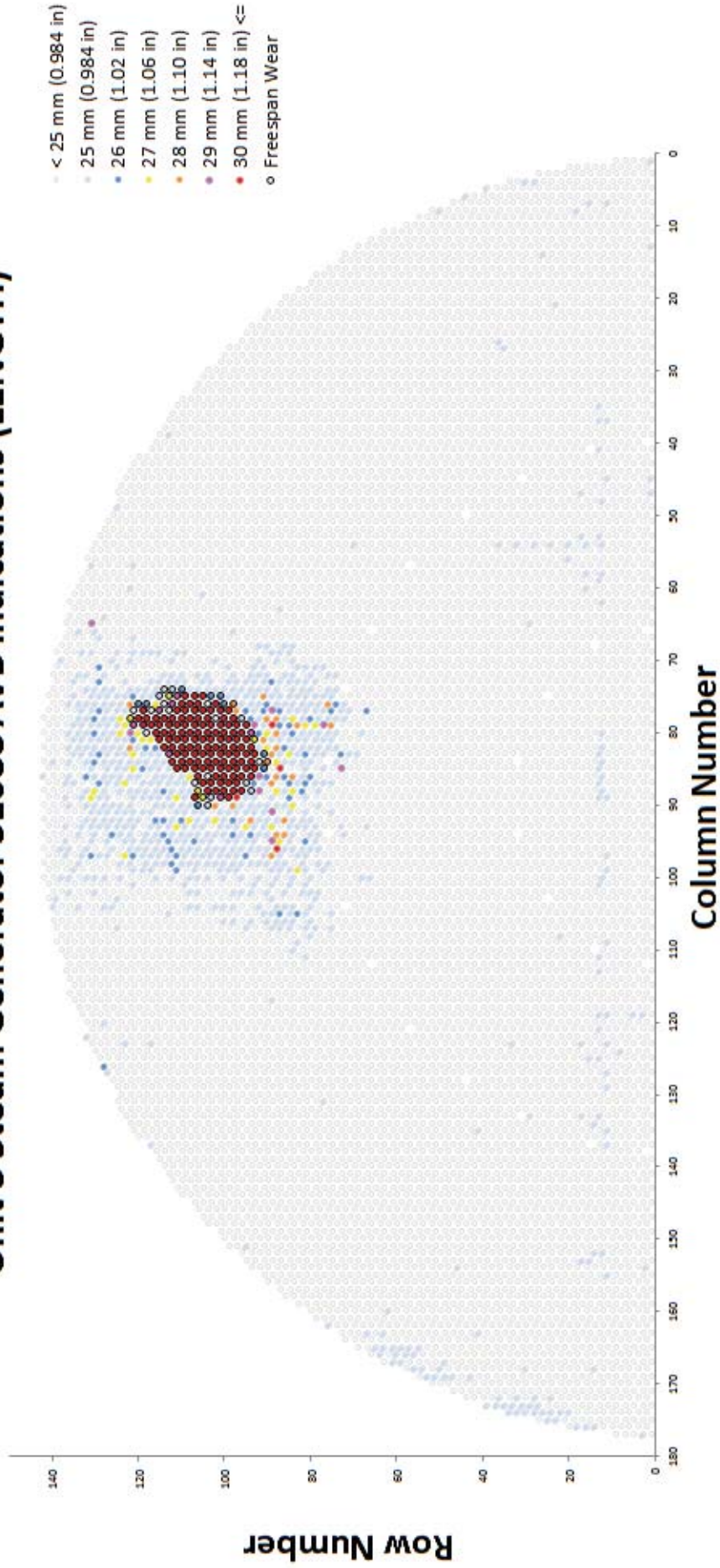


Figure 4-13: Tube Wear Length at AVBs for Unit 3 SG E-088

Unit 3 Steam Generator 3E089 AVB Indications (LENGTH)

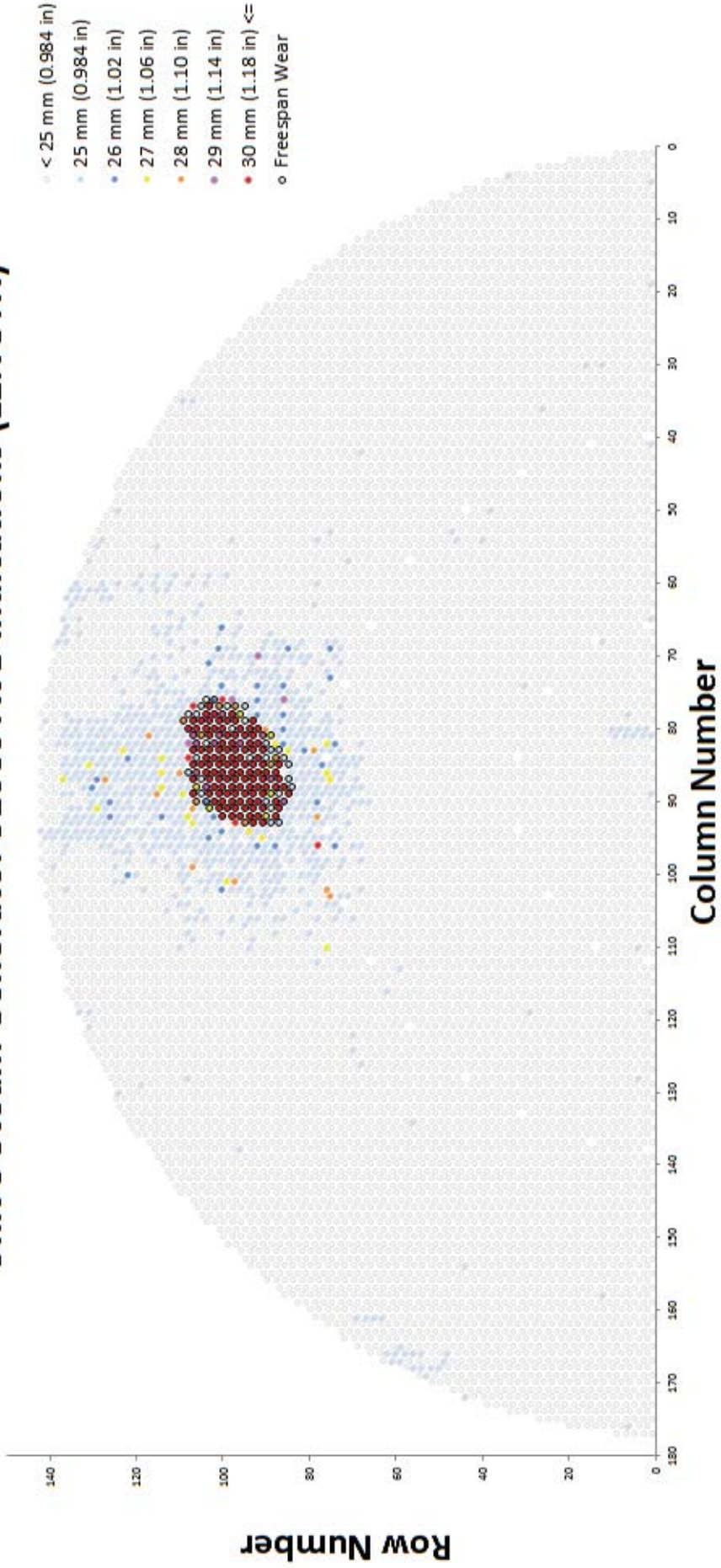


Figure 4-14: Tube Wear Length at AVBs for Unit 3 SG E-089

SONGS U2C17 Steam Generator Operational Assessment for Tube-to-Tube Wear

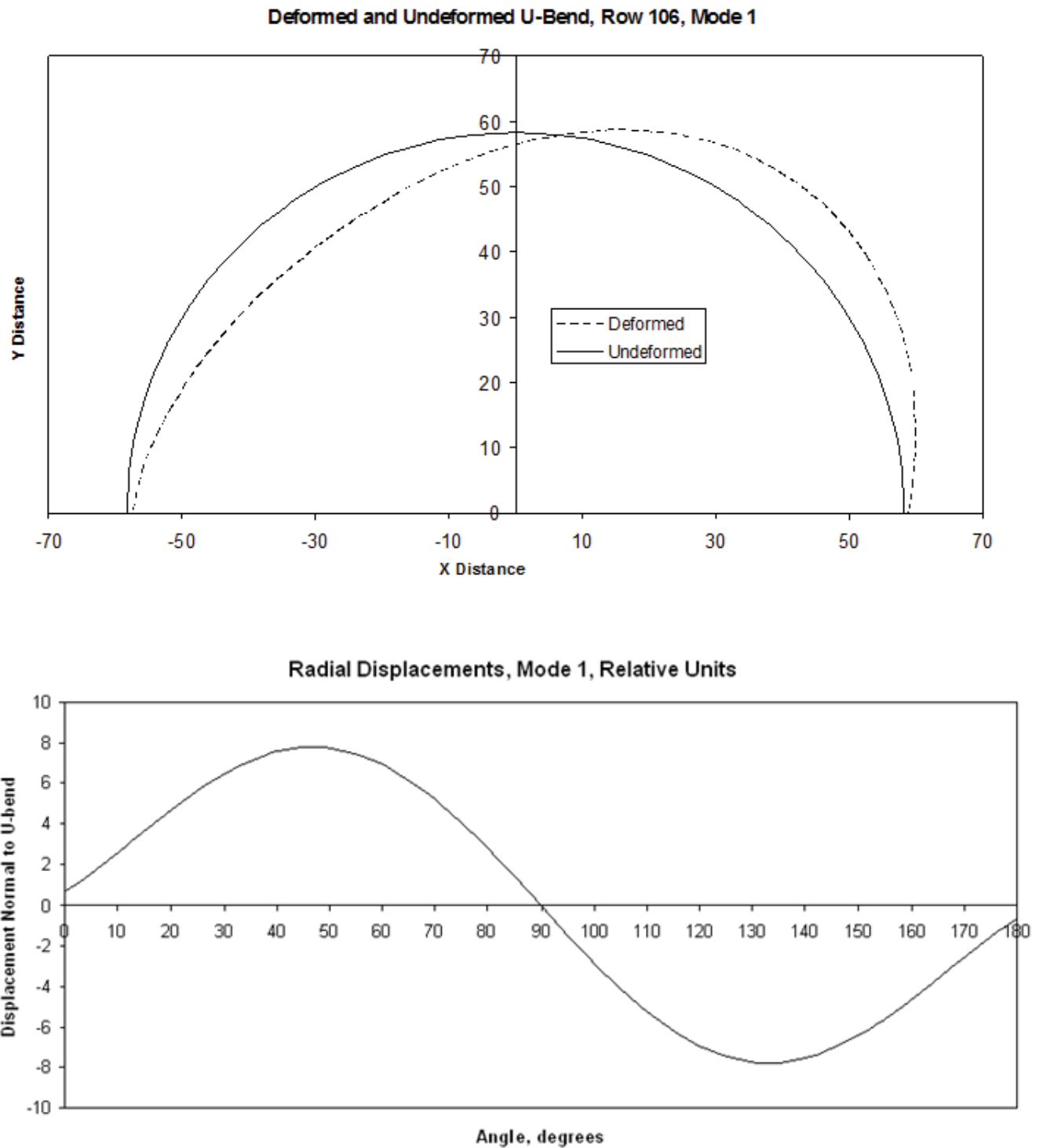


Figure 4-15: Mode 1 Displacement Pattern

SONGS U2C17 Steam Generator Operational Assessment for Tube-to-Tube Wear

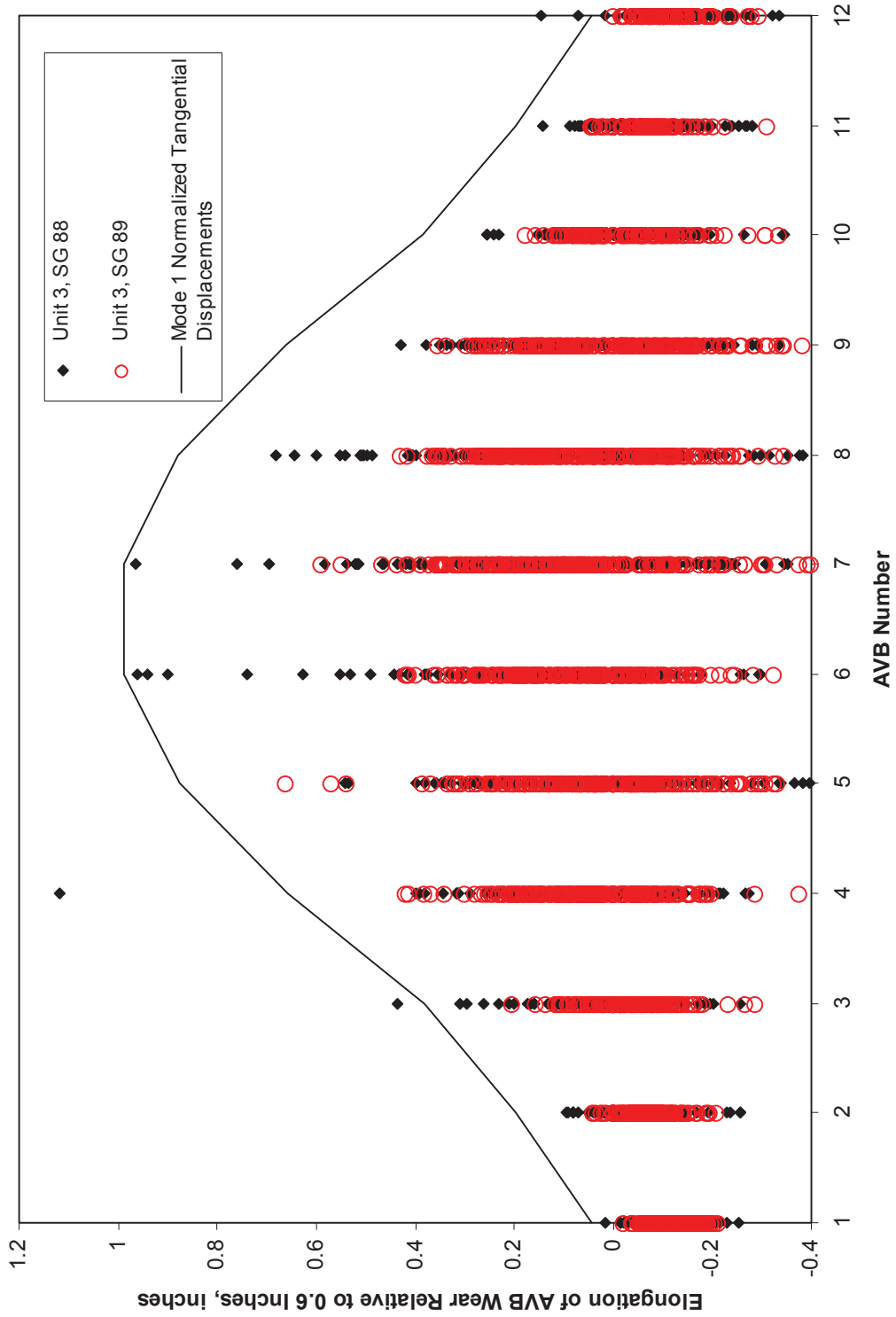


Figure 4-16: Elongation of AVB Wear at Each AVB

SONGS U2C17 Steam Generator Operational Assessment for Tube-to-Tube Wear

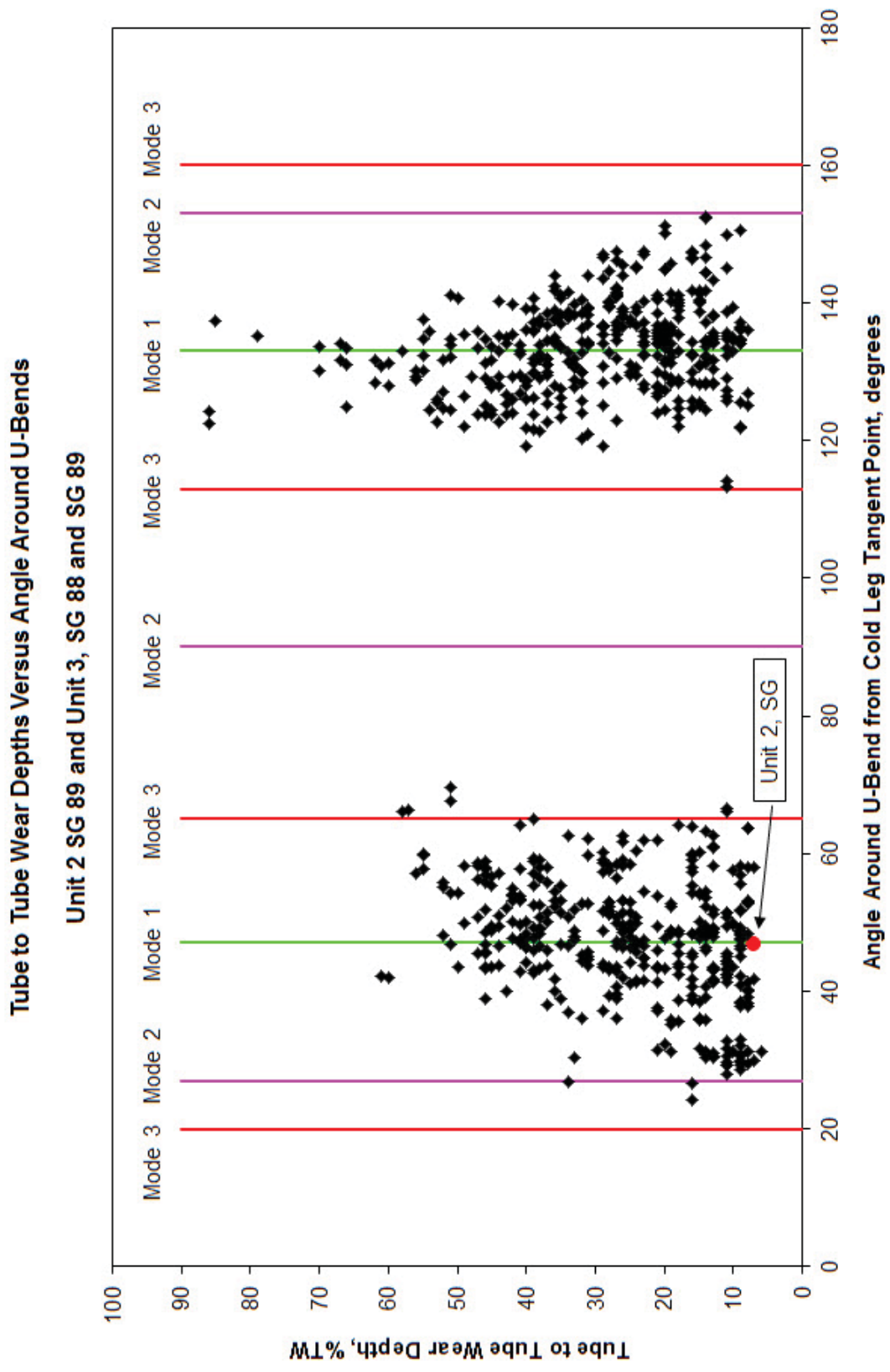


Figure 4-17: Impact Locations of Unstable Tubes

Deformed and Undeformed U-Bend Row 106 Mode 2

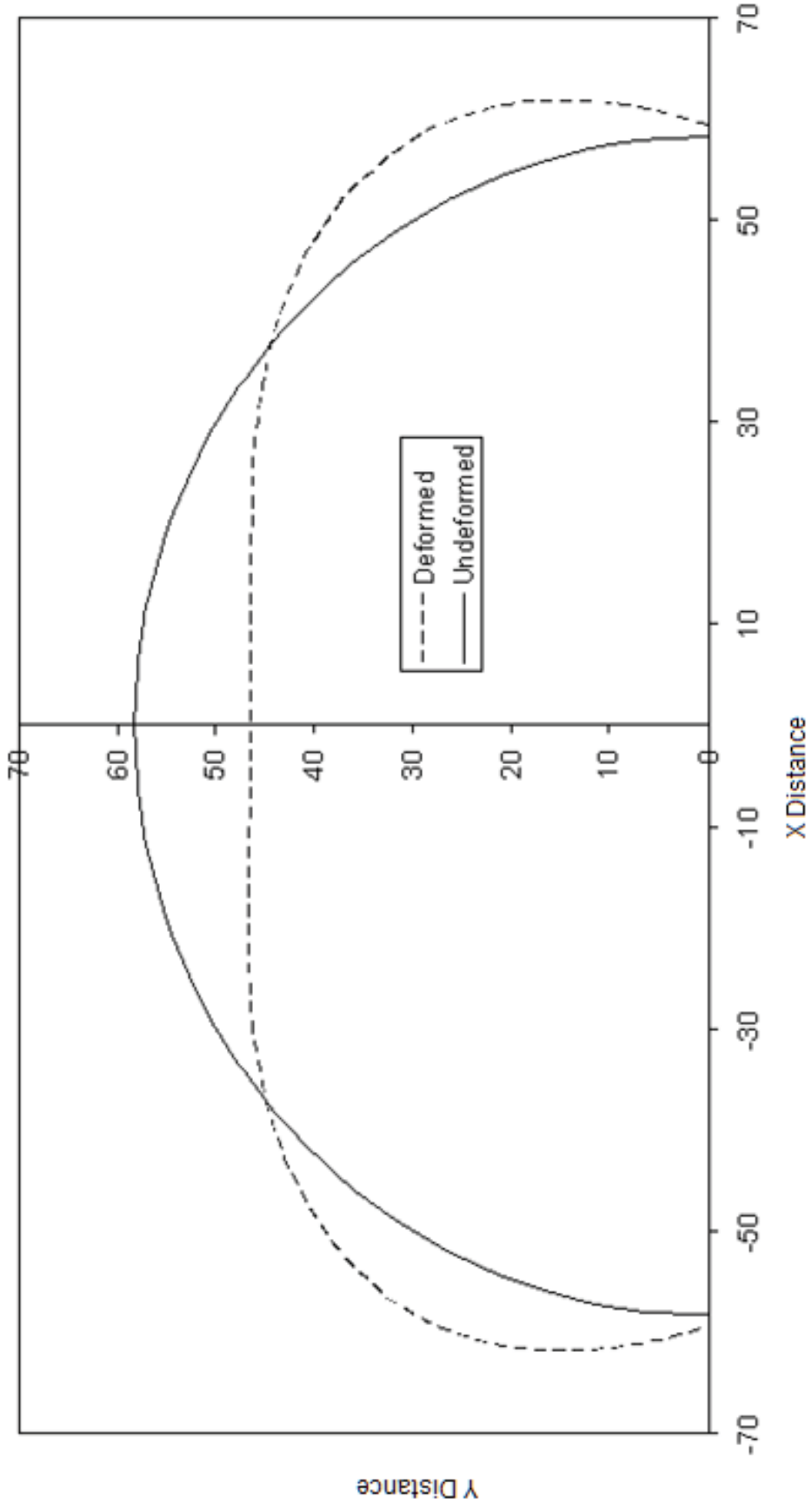


Figure 4-18: Mode 2 Displacement Pattern

SONGS U2C17 Steam Generator Operational Assessment for Tube-to-Tube Wear

Deformed and Undeformed U-Bend, Row 106, Mode 3

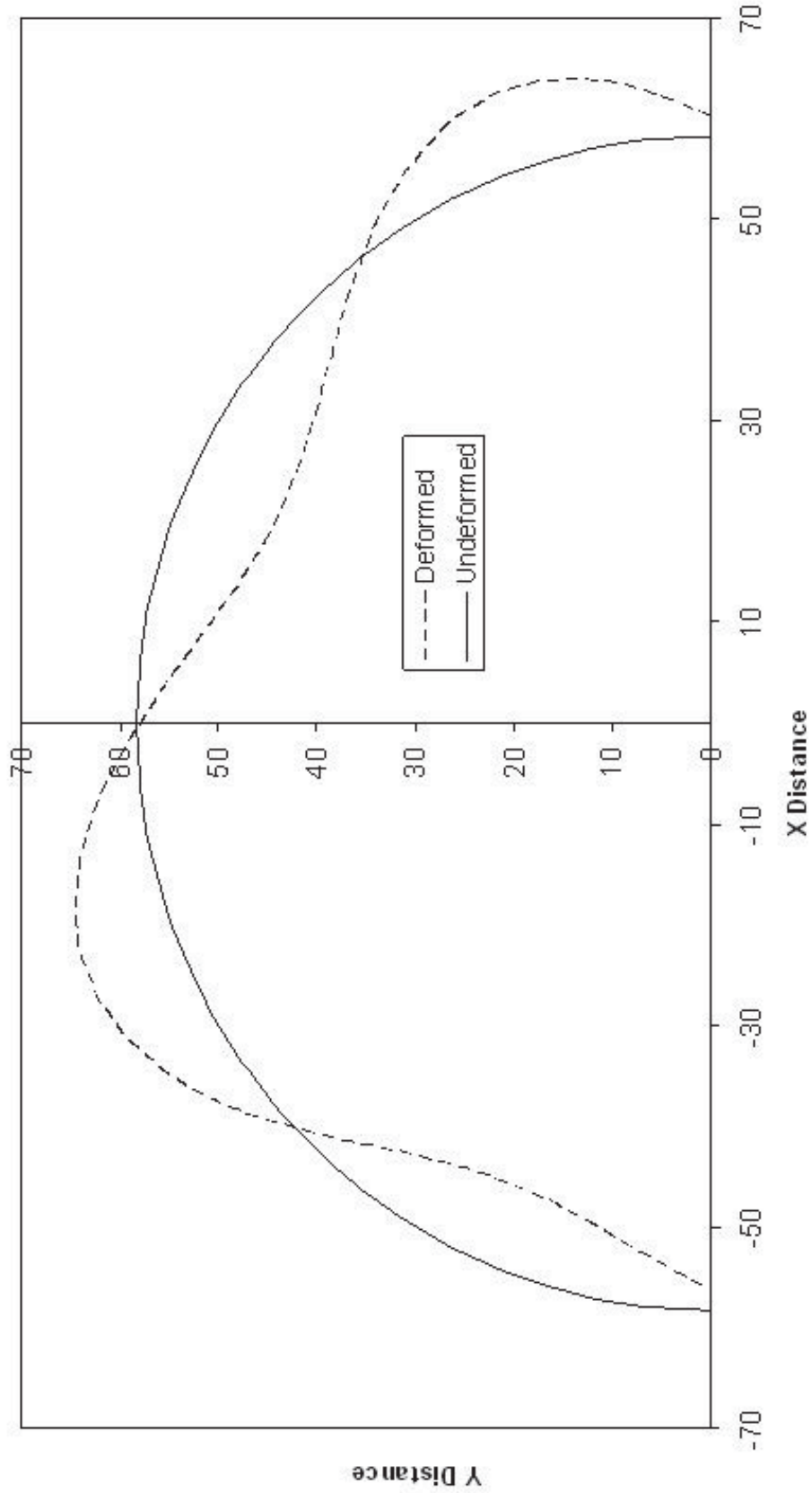


Figure 4-19: Mode 3 Displacement Pattern

SONGS U2C17 Steam Generator Operational Assessment for Tube-to-Tube Wear



SONGS U2C17 Steam Generator Operational Assessment for Tube-to-Tube Wear

5.0 STABILITY RATIOS

An extensive effort was devoted to defining and refining the basis for the calculation of stability ratios. Calculation procedures and results are described in [20]. These results compare very well with independent calculations performed by Westinghouse [21]. It is important to state that stability ratio results are reported for the following conditions:

- 100% Power with an Upper 95th Percentile Stability Ratio
- 70% Power with an Upper 95th Percentile Stability Ratio
- 100% Power with an Upper 99th Percentile Stability Ratio
- 70% Power with an Upper 99th Percentile Stability Ratio

Basic conclusions regarding stability of U-bends at SONGS are based on the 95th percentile stability ratios. The more conservative 99th percentile ratios are presented only to demonstrate margin and degree of conservatism. The same holds true for references to instability developing at a stability ratio of 1 or more in contrast to maintaining a maximum stability ratio of 0.75. Again this later value is discussed in terms of margin and degree of conservatism.

Before beginning the discussion of the effect of power level on in-plane fluid-elastic stability, a more general engineering observation is pertinent. A decrease to 70% power places the SONGS steam generators back inside the operational envelope of demonstrated successful performance relative to in-plane fluid-elastic stability of nuclear steam generators with large U-bends. This is illustrated in Figure 5-1.

A stability ratio is a calculated value which depends on several inputs. A calculation of burst pressure of a degraded tube is exactly analogous. Uncertainties in input values lead to uncertainties in the output calculation. When all inputs are at mean values, a mean value of the output parameter is obtained. [

]

As previously stated, stability ratios depend on U-bend size, thermal-hydraulic conditions along the U-bend and the number of consecutive ineffective in-plane supports. Hence, stability ratios vary with position in the bundle and with the number of consecutive ineffective supports. This information is presented by means of a color coded tubesheet map, which was created by calculating stability ratios at 316 different locations and then interpolating between tube positions to develop a stability ratio for each tube. Figure 5-3 denotes the number of consecutive ineffective supports in-plane by color coding stability ratios equal to or greater than 1 for the SONGS-2 steam generators at 100% power and the no plugging condition at the beginning of life. At low rows, no in-plane supports are needed to maintain tube stability; therefore they have no effect on the probability calculations. In the highest susceptibility regions, instability is predicted if there are 5 consecutive ineffective supports. A decrease to 70% power produces dramatic effects; no in-plane effective supports are needed to maintain a stability ratio less

SONGS U2C17 Steam Generator Operational Assessment for Tube-to-Tube Wear

than 1, and as a result, the tubesheet map for instability is a blank sheet as shown in Figure 5-4. Thus demonstration of stability at 70% power is an appropriate basis for Unit 2 return to service.

There are two additional important considerations included in the 70% power result which are specific to Unit 2. Based on the measured wear at AVB locations, the comparisons with Unit 3 AVB wear patterns and the elevated risk of susceptibility to in-plane fluid-elastic instability, Unit 2 tubes will be plugged. These plugged tubes have an effect on local thermal-hydraulic conditions upon returning the SG to operation and have been included in the stability ratio calculations. [

] R113 C81 is shown because it has slightly higher computed stability ratios than does R111 C81. Stability ratio varies with amplitude as shown. All stability ratios are less than 1.0, assuming zero effective AVBs.

The remaining paragraphs of this section deal with margin, sensitivity and degree of conservatism arguments. These are necessary elements of a complete evaluation of in-plane fluid-elastic stability. [

]



SONGS U2C17 Steam Generator Operational Assessment for Tube-to-Tube Wear



SONGS U2C17 Steam Generator Operational Assessment for Tube-to-Tube Wear

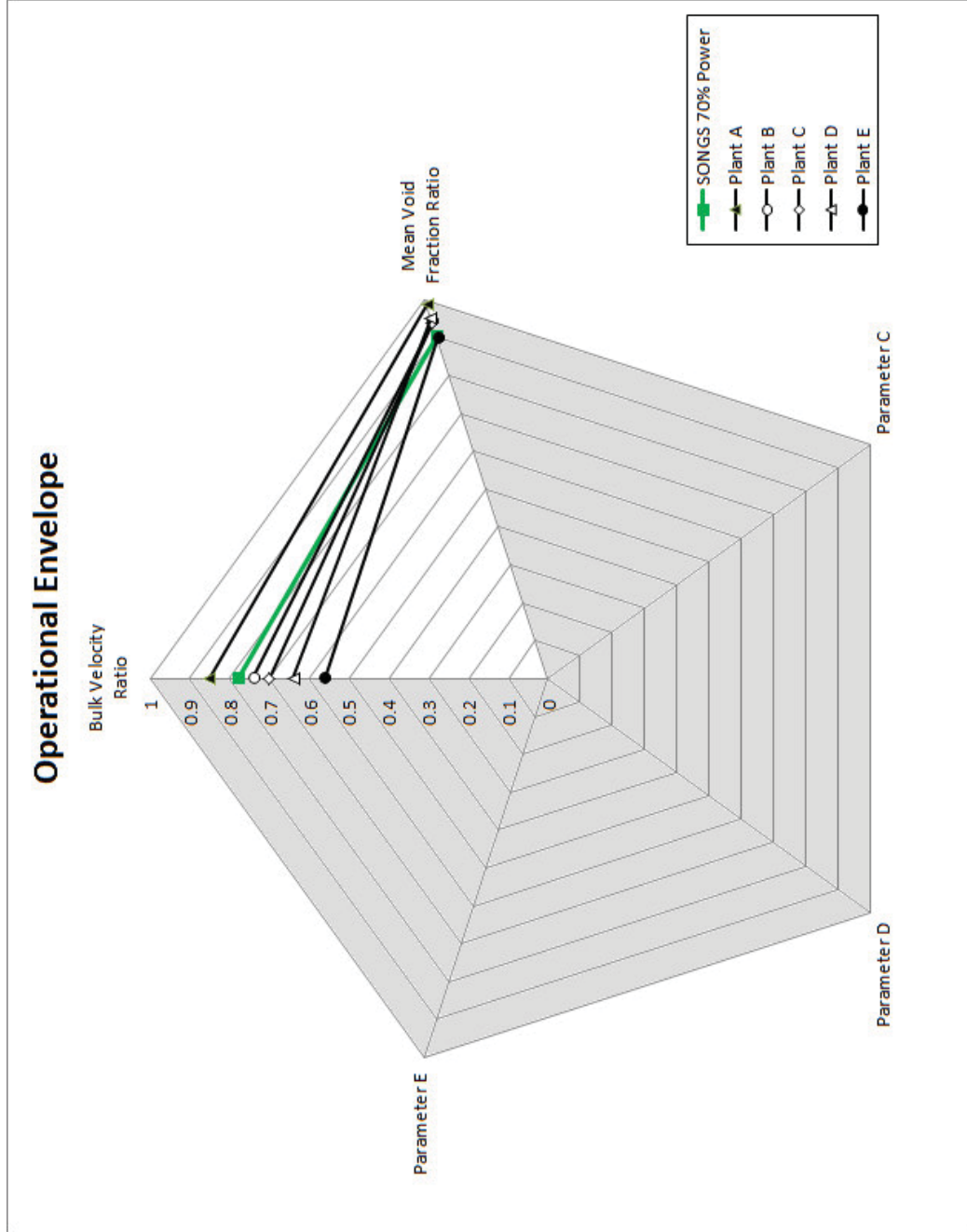


Figure 5-1: Spider Diagram of the Successful Operational Envelope for Nuclear Steam Generators with Large U-bends



SONGS U2C17 Steam Generator Operational Assessment for Tube-to-Tube Wear



SONGS U2C17 Steam Generator Operational Assessment for Tube-to-Tube Wear

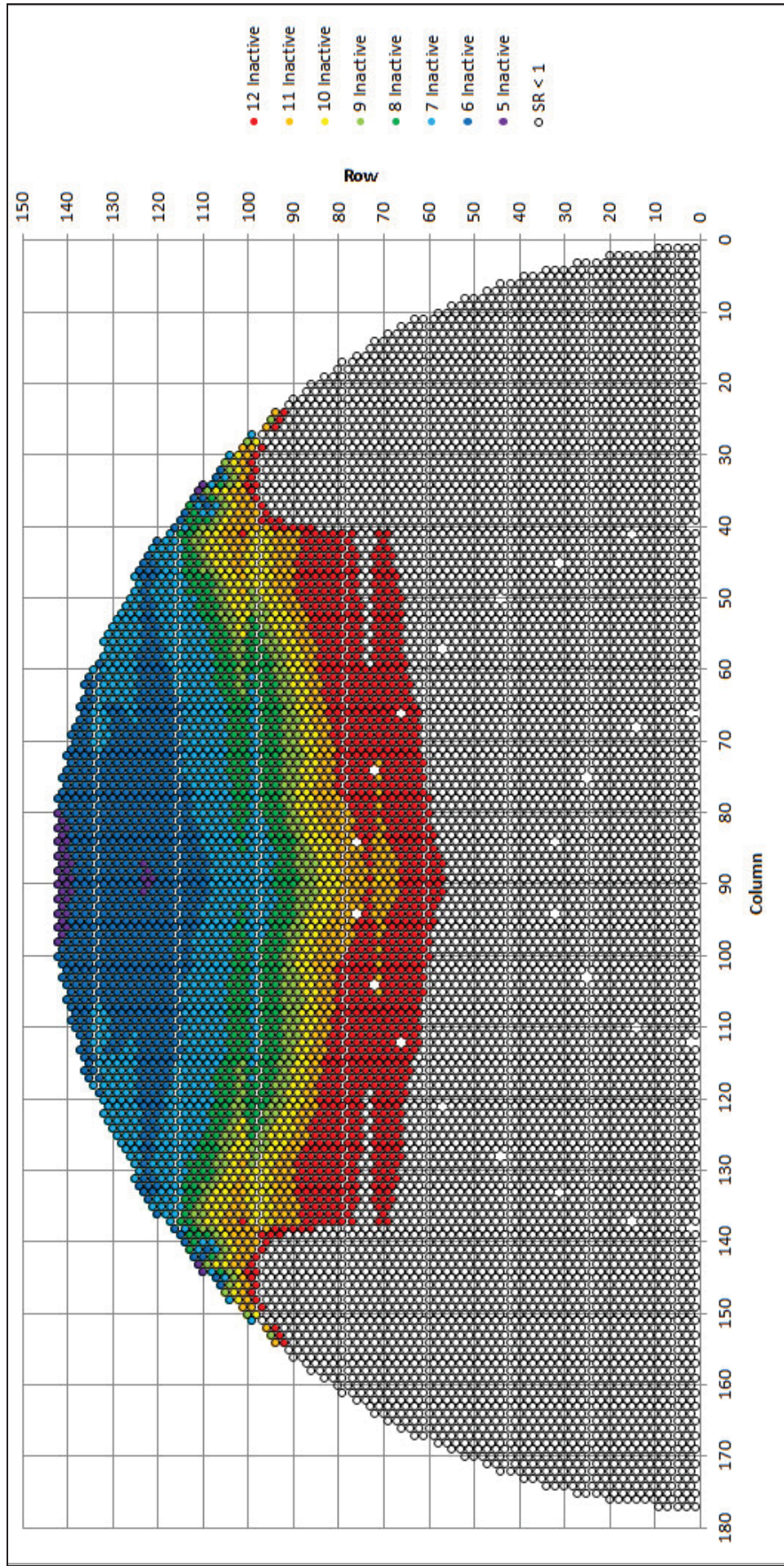
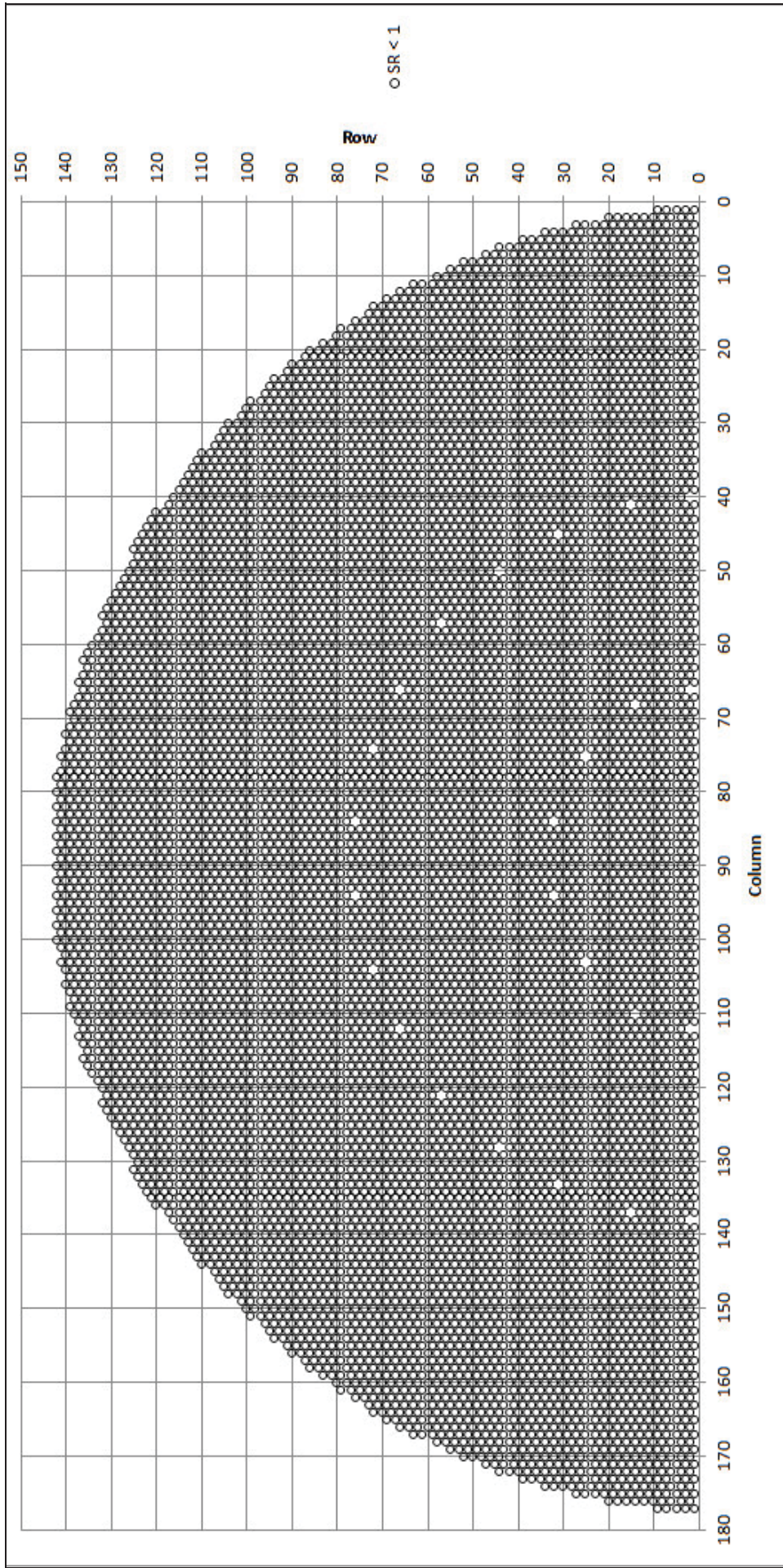


Figure 5-3: Stability Map at 100% Power, No Plugging, 95th Percentile SR, SR ≥ 1

SONGS U2C17 Steam Generator Operational Assessment for Tube-to-Tube Wear



This blank figure is not an error. Even with no effective in-plane supports there are no unstable U-bends at 70% power

Figure 5-4: Stability Map at 70% Power with Plugging and Split Stabilizers, 95th Percentile SR, SR ≥ 1



SONGS U2C17 Steam Generator Operational Assessment for Tube-to-Tube Wear



SONGS U2C17 Steam Generator Operational Assessment for Tube-to-Tube Wear

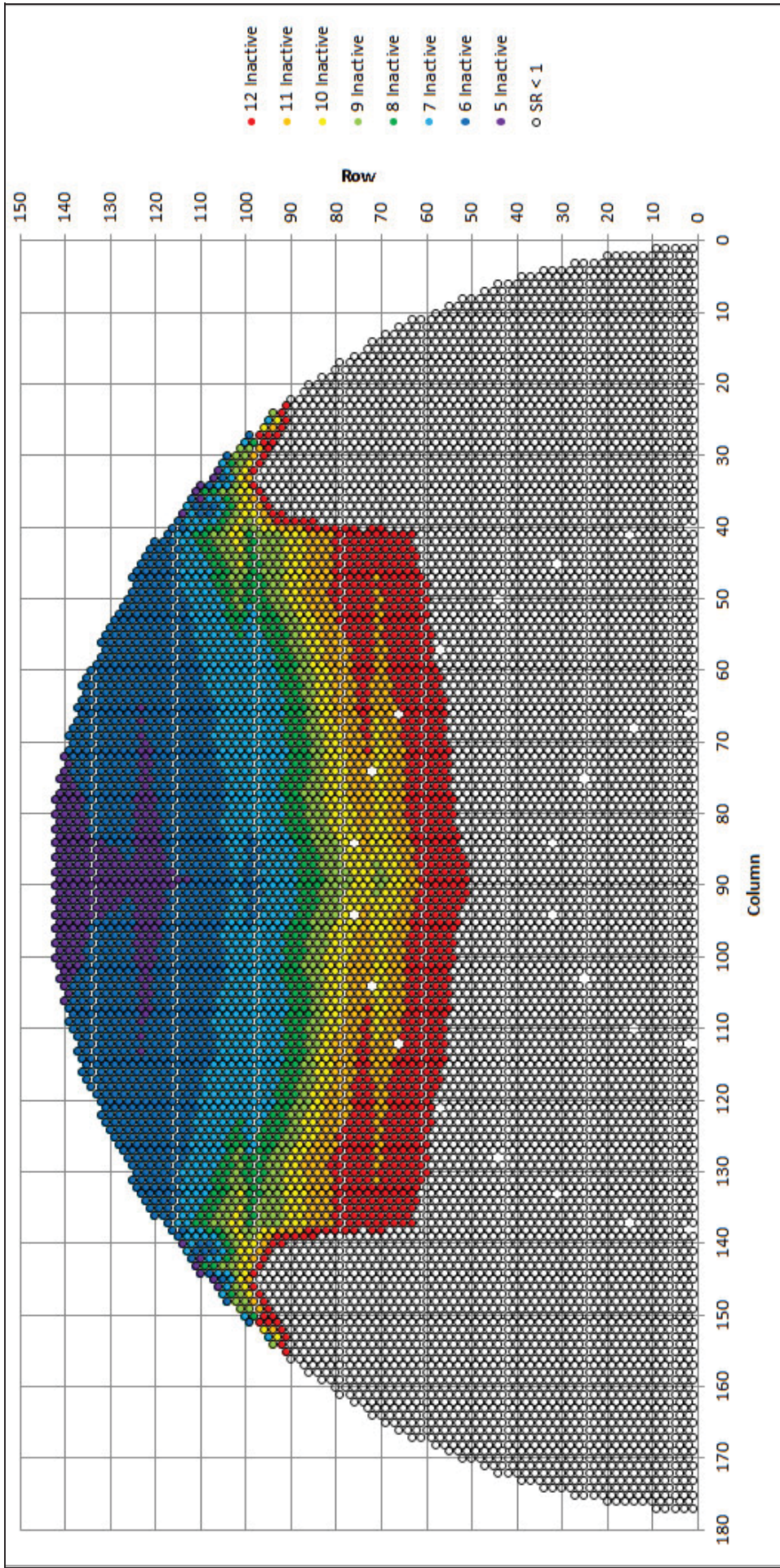


Figure 5-6: Stability Map at 100% Power, 99th Percentile SR, SR ≥ 1

SONGS U2C17 Steam Generator Operational Assessment for Tube-to-Tube Wear

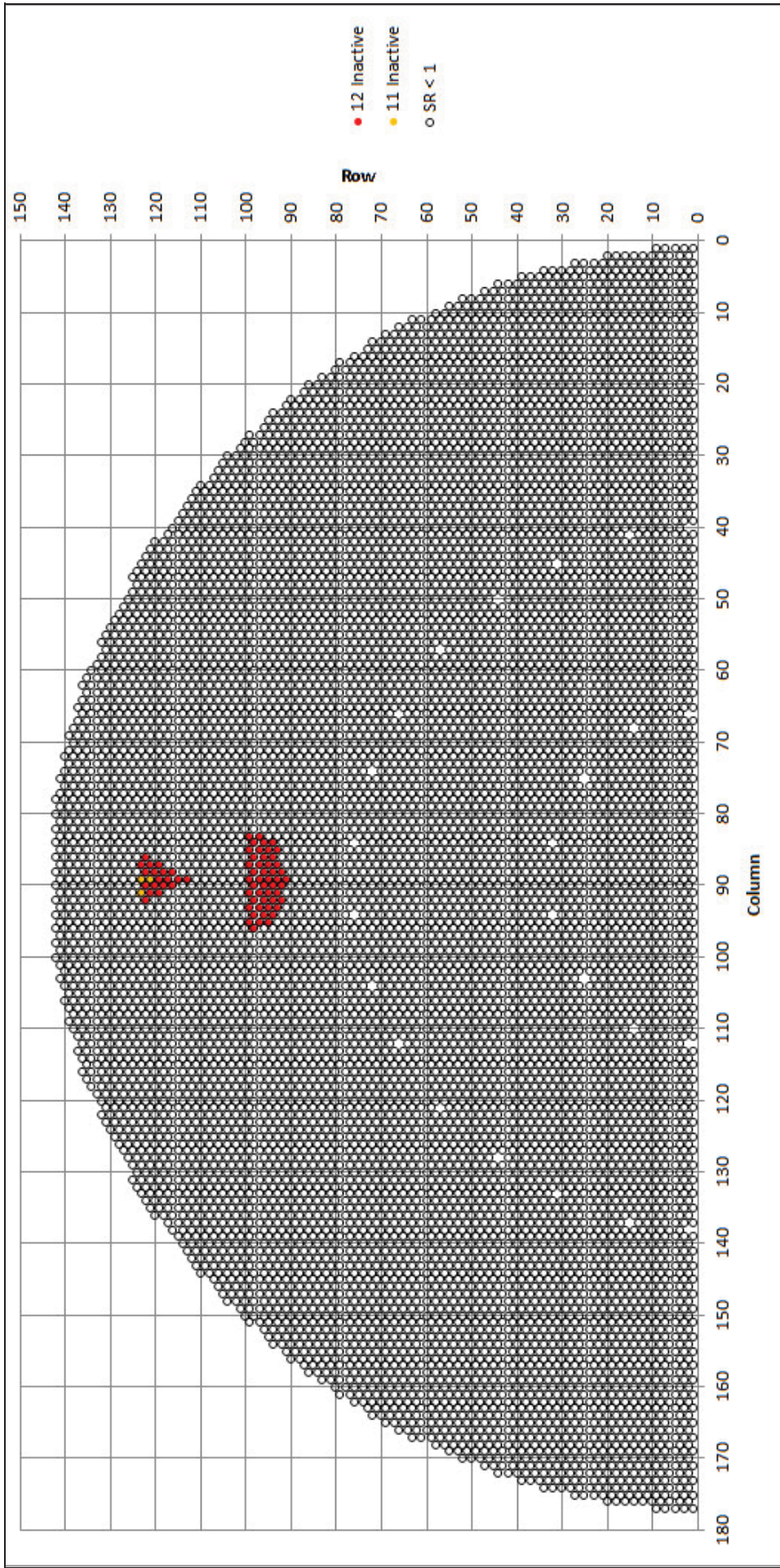


Figure 5-7: Stability Map at 70% Power with Plugging and Split Stabilizers, 99th Percentile SR, SR ≥ 1

SONGS U2C17 Steam Generator Operational Assessment for Tube-to-Tube Wear

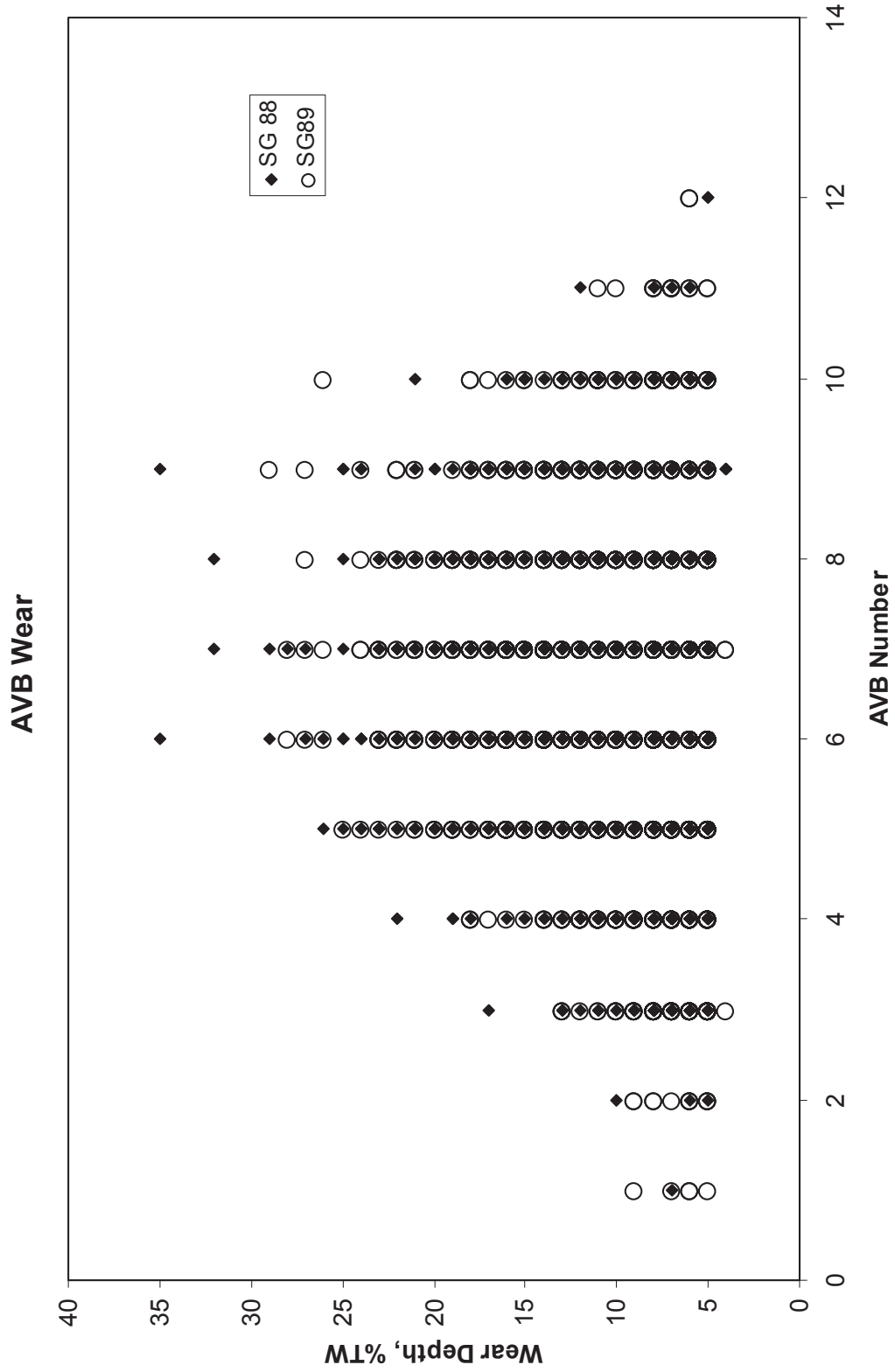


Figure 5-8: Depth of AVB Wear Indications versus AVB Number, Unit 2, SG E-088 and SG E-089

SONGS U2C17 Steam Generator Operational Assessment for Tube-to-Tube Wear

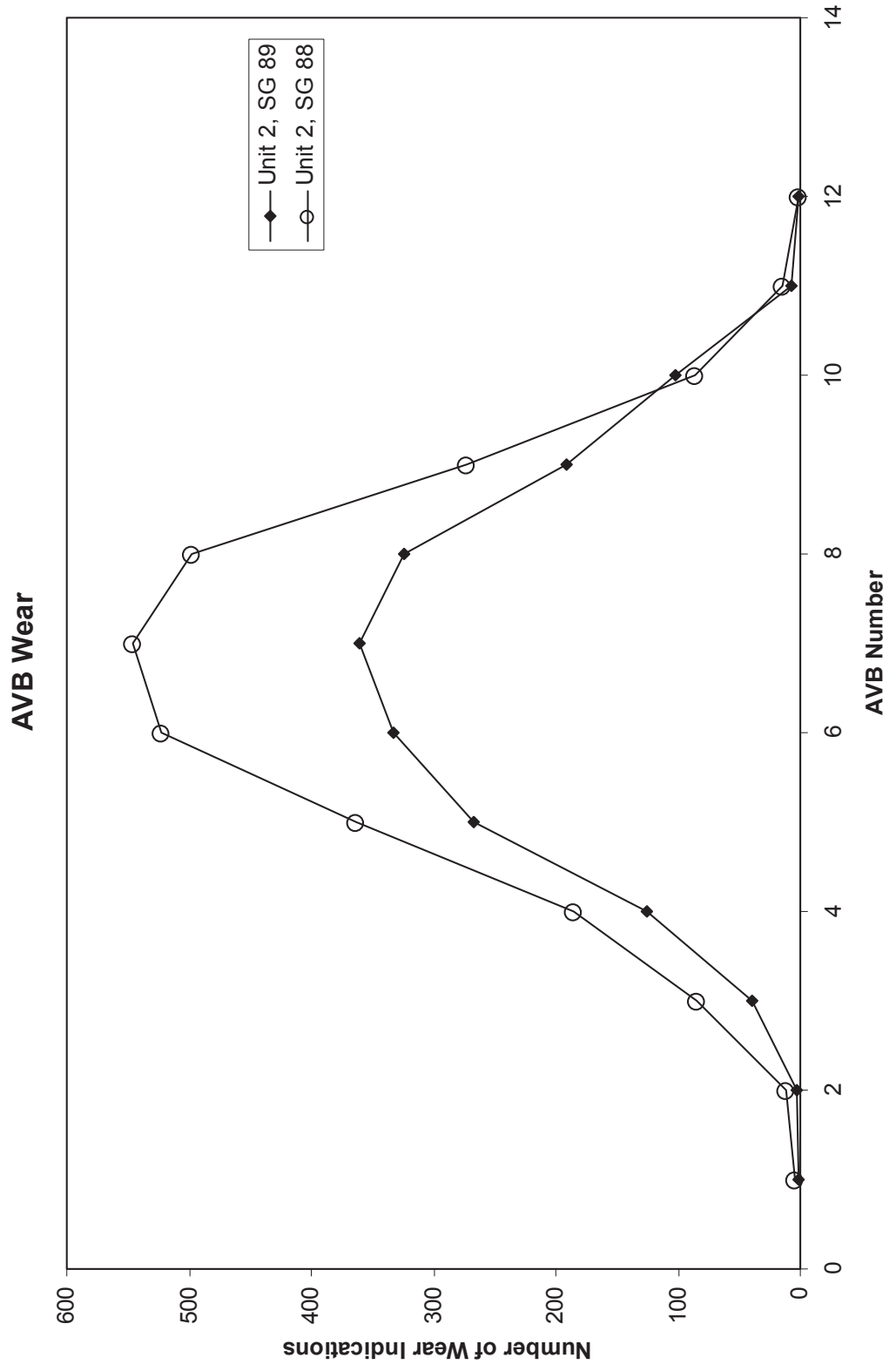


Figure 5-9: Number of AVB Wear Indications versus AVB Number

SONGS U2C17 Steam Generator Operational Assessment for Tube-to-Tube Wear

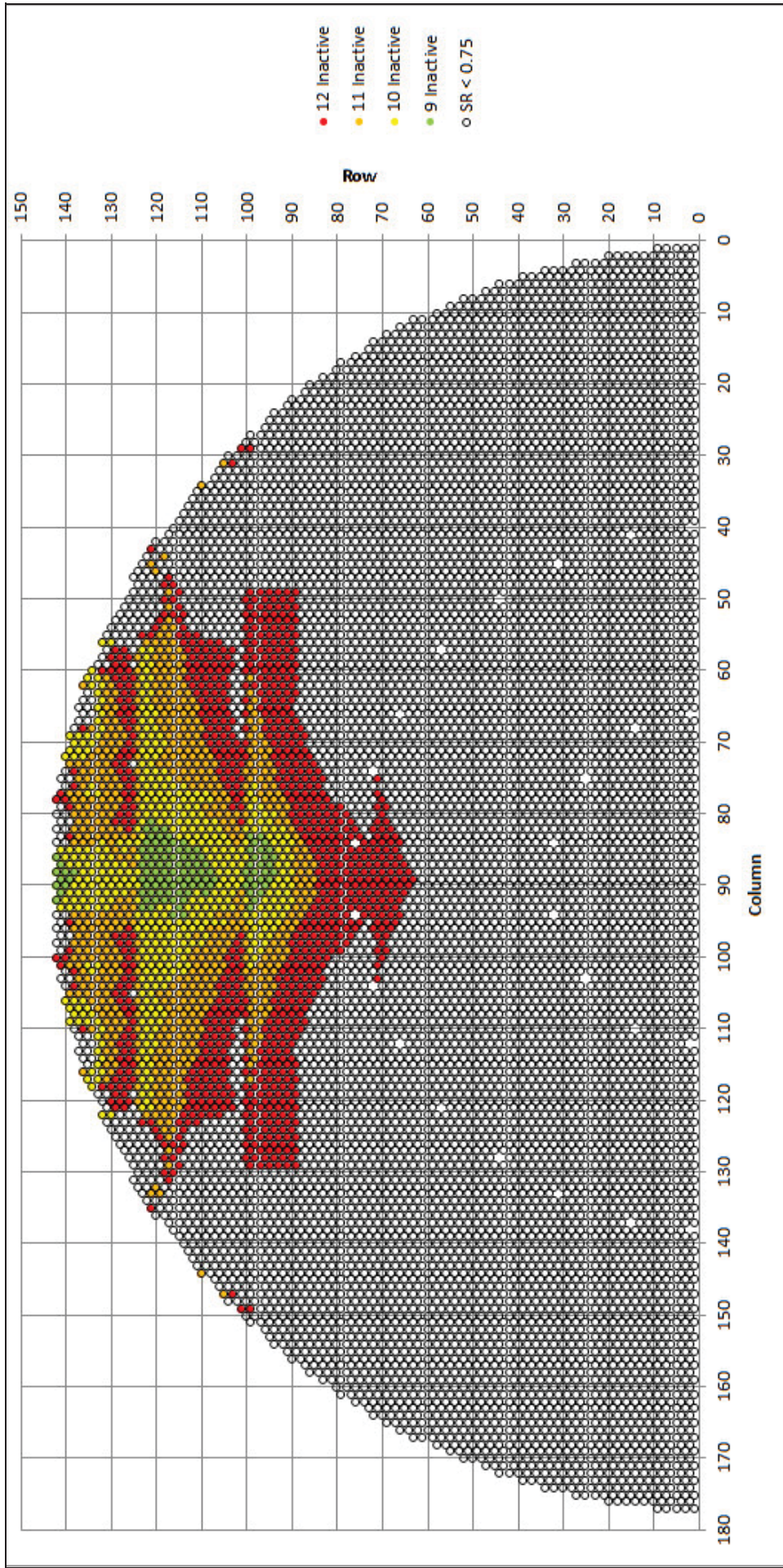


Figure 5-10: Stability Map at 70% Power with Plugging and Split Stabilizers, 95th Percentile SR, SR ≥ 0.75

SONGS U2C17 Steam Generator Operational Assessment for Tube-to-Tube Wear

6.0 CONTACT FORCES

Estimations of tube-to-AVB contact forces are a key component in probability of instability calculations. The contact forces are calculated using a finite element computer model, which is explained in Section 6.1. Contact force distributions output from the model are summarized in Sections 6.2 and 6.3. The calculated gap distributions compare well with observations from PSI and ISI data, as shown in Sections 6.4 and 6.5. Section 6.6 presents a summary of contact force and why the calculated forces are an appropriate basis for demonstrating margins to fluid-elastic instability at 70% power via probability of instability calculations.

6.1 MHI Quarter Bundle Steam Generator Model

[

] A gap distribution provides the input to the contact force problem. The quarter model then computes the interactions between all tubes and AVBs. The contact force on either side of a tube is part of the output along with the resulting balanced gaps which are considerably different from the input gaps. [

]

The contact forces are calculated based on the principle that the sum of the forces in the bundle is equal to zero; the nominal tube bundle geometry; and the random dispersion of the tube bundle component dimensions. Also used as input are the elastic material properties of the tube bundle components. A set of initial gaps is chosen for the model, the bundle geometry constraints are added, and the finite element model is solved to balance all of the forces. The primary source of tube-to-AVB contact forces is the restraint provided by the retaining bars and bridges, reacting against the component dimensional dispersion of the tubes and AVBs. Contact forces are available for both cold and hot conditions. Contact forces significantly increase at normal operating temperature and pressure due to diametric expansion of the tubes and thermal growth of the AVBs.

The initial gaps that are input to the MHI finite element model have a distribution that is approximately normal with a mean of zero. Six factors contribute to the gap distribution:

- Tube diameter
- AVB thickness
- TSP hole mislocation
- AVB twist
- AVB flatness
- Tube flatness

SONGS U2C17 Steam Generator Operational Assessment for Tube-to-Tube Wear



MHI Proprietary

Figure 6-1 shows a 3D plot of the AVB locations in the quarter model. Each run of the quarter model inputs gaps randomly selected from the input distribution. The output of one run is one of many possible states of contact forces and final gaps at each location shown in Figure 6-1. Given lengthy computation times, it is not practical to use an individual run of the quarter bundle model as a single Monte Carlo trial for contact forces. It is necessary to combine runs of the quarter model to define the state of contact forces and gaps in small zones of the bundle. A zone size of ten rows by ten columns was found to be practical. Each zone contains approximately 50 tubes. By combining multiple runs of the quarter model, cumulative distributions of contact forces can be constructed for each AVB in a particular zone. These cumulative distributions are characteristic of the zone and hence Monte Carlo trials for contact forces in the zone can be performed. Four runs of the quarter model are used in constructing cumulative distributions of contact forces for each AVB in the zone.

A wide variety of cases were examined to select the best description of the distributions of the contact forces that best match the NDE data and observations of the Unit 2 and Unit 3 steam generators. The six factors that contribute to the input gap distributions set the scale of the problem but additional guidance is needed. The main benchmark used by MHI is the number and magnitude of classic dent signals found in the pre-service inspections (PSI) of Units 2 and 3. Systematic laboratory testing (Appendix 9 of Reference [22]) correlated both on load and off load dent signal amplitude with applied loads of an AVB pressed at a small angle against a tube. [

] The comparison of dents in the steam generators to the contact forces predicted by the model served as a primary benchmark of contact force calculations.

A post check of the reasonableness of contact force calculations was provided by an extensive program of AVB to tube gap measurements using ultrasonic and newly developed eddy current techniques [14]. While the primary purpose of gap measurements was to determine if there were highly heterogeneous spatial distributions of large gaps that are not included in contact force calculations, the gap measurements were used as a check, albeit subtle, of the reasonableness of contact force calculations and differences between Units 2 and 3. An additional check of differences between Unit 2 and Unit 3 is provided by the use of non-classical dent/contact signals that have been found to be eddy current footprints of contact between tubes and support structures in other steam generators. These checks are discussed after the presentation of contact force results for Units 2 and 3.

6.2 Contact Force Distributions – Unit 3

The zones used to develop characteristic distributions of contact forces for each AVB in the zone are plotted in Figure 6-2. Note that only zones for rows 63 and higher are shown. Contact forces are available for all regions of the steam generator but these are the zones of interest since lower rows have a negligible contribution to probability of instability calculations. Unit 3 is considered first. Figure 6-3 through Figure 6-6 contain plots of the cumulative distributions of contact forces for zones 1, 3, 5 and 8 for Unit 3 at BOC 16. Only AVBs 1 through

 SONGS U2C17 Steam Generator Operational Assessment for Tube-to-Tube Wear

6 are shown since quarter model results are used. By symmetry AVBs 12 to 7 correspond to AVBs 1 through 6 respectively. The tubes included in these zones are as follows:

- Zone 1, Rows 133 to 142, Columns 80 to 89
- Zone 3, Rows 113 to 122, Columns 80 to 89
- Zone 5, Rows 93 to 102, Columns 80 to 89
- Zone 8, Rows 63 to 72, Columns 80 to 89

All of the above zones are adjacent to the center column. Zone 1 is at the periphery and Zone 8 begins at row 63. Figure 6-3 shows that contact forces are relatively high at the periphery. This is a high stiffness region since here the ends of AVBs are welded to the retaining bars which essentially are arranged as longitudinal lines across the hemispherical top of the bundle. At approximately 10 column intervals the retaining bars are welded to bridges which are essentially arranged as latitude lines. See Figure 2-2. Nominal clearances between AVBs and tubes (0.001 inches each side cold) are set by the distances between bridges when the bridges are welded to the retaining bars. Other high stiffness locations are at the noses of AVBs, see Figure 2-1, and the top tube support plate. AVBs 1 and 12 are closest to the top tube support plate.

The cumulative distribution function (CDF) of contact force for a given AVB is read as follows. Select any given contact force and read the value of the cumulative distribution. This is the fraction of all possible contact forces for that AVB in that zone that lie at or below the selected value. If, for example, the selected contact force is identified as the value needed to provide an effective AVB support then the value of the CDF distribution is the probability that the support is ineffective. The rule is simply high CDF plots indicate a higher probability of support ineffectiveness than lower CDF plots. In terms of interpreting CDF plots, a rough figure of merit for effective AVBs is a contact force in the vicinity of 10N. Consider Figure 6-3, all CDF plots at 10N are below a CDF of 0.1. Using the rough figure of merit, the AVBs would be effective more than 90% of time. As one moves away from the high stiffness periphery, contact forces decrease. Note the relatively high CDF plots for Zones 3 and 5 in Figure 6-4 and Figure 6-5. AVBs 4 and 5 exhibit relatively high CDF plots. This is true of AVBs 4 and 5 in almost all zones. These are two of the longest AVBs with a relatively large separation between high stiffness regions at the periphery and the nose of the AVB. Additionally, the longest AVBs have the smallest bend angles at the nose sections. This leads to less distortion and consequently a smaller AVB twist. AVB 1 is as long as AVB 4 but remains relatively close to the top tube support plate. AVBs 1, 2 and 3 usually exhibit the lowest CDF plots. AVB 6 is the shortest AVB and usually exhibits an intermediate CDF plot prior to wear considerations.

As one moves radially outward from Zone 8 toward the periphery, CDF plots lower in Zone 29 and then drop significantly in the periphery in Zone 35. Moving from Zone 8 directly across to lower columns, CDF plots exhibit small changes (see Zone 32 in Figure 6-9 and Zone 56 in Figure 6-10), before decreasing significantly at the periphery in Zone 64 which is comparable to Zone 35.

The introduction of wear at AVB locations produces large changes in contact forces particularly for Unit 3. The wear zone extends approximately from row 70 to row 140 and from the center column out to about column 65. The zones of most interest are 3, 4 and 5. Zone 5 is chosen for illustrative purposes. Comparing Figure 6-5 with Figure 6-11, note the dramatic elevation gain of CDF plots for all AVBs in Zone 5 after 3 months of wear in Unit 3. Note specifically the high fractions of zero contact forces. After 3 months of wear Unit 3 has much fewer effective in-plane supports in Zones 3, 4 and 5. After 11 months of wear, as shown in Figure 6-12, contact forces have been virtually eliminated in Zone 5.

SONGS U2C17 Steam Generator Operational Assessment for Tube-to-Tube Wear

6.3 Contact Force Distributions – Unit 2

Contact force distributions for Unit 2 at the beginning of life are shown in Figure 6-13, Figure 6-14, Figure 6-15 and Figure 6-16 for Zones 1, 3, 5 and 8 respectively. As with Unit 3, CDF plots for Unit 2 are lower near the periphery and increase in elevation for Zones 3 through 5. AVBs 4 and 5 again exhibit the highest CDF plots. The CDF plots are considerably lower for AVB 6 for Unit 2 compared to Unit 3. This is a consequence of increased AVB twist in Unit 2 at the nose of AVBs. Overall, low CDF plots are noted for AVB 1, 2, 3 and 6 for Unit 2.

The contact force distributions developed for Unit 2 are more resistant to the effects of wear. After 22 months of operation the severity of wear in Unit 2 is similar to that experienced by Unit 3 after 11 months of operation. Similar does not mean the same. The worst case steam generator in Unit 2 had about 2600 wear indications at AVBs [23] compared about 3400 wear indications in Unit 3 [12]. There was also significantly less wear in Unit 2 at the four lower AVB locations, 1, 2, 11 and 12.

The effects of wear are now considered in Zone 5 after 22 months of full power operation and then subsequently for 6 months of 70% power after restart. Zone 5 is characteristic of the most significant Zones, 3, 4 and 5. Figure 6-17 shows that wear after 22 months in Unit 2 has grossly altered the contact force distributions for AVB 5 and 6, particularly AVB 6 with very high fractions of zero contact forces. In contrast, AVB 1 and 2 maintain low CDF plots. Wear has moved AVB 3 from a low CDF plot to an intermediate position. Considering all AVB locations, wear has a less dramatic effect on contact force distributions in Unit 2 compared to Unit 3. Comparing Figure 6-17 and Figure 6-18 shows that conservatively projected wear after restart at 70% power produces very little noticeable change in contact force distributions after 6 months of operation at reduced power. This augurs well for demonstration of continuing margin over time at reduced power from probability of instability calculations.

6.4 Dent Evaluation

The following paragraphs describe checks of contact force calculations from observations of PSI dents, ISI contact forces and AVB to tube gap measurements.

6.4.1 Pre-Service Dents

Figure 6-19 and Figure 6-20 present tubesheet maps of dents detected in the pre-service inspections of Unit 3, SG E-089 and Unit 2 SG E-089 respectively. The dent eddy current signal amplitudes vary for 0.5 to 1.5 volts. The larger dents are plotted with enlarged symbol size. In production, minimum reporting levels for dents during eddy current analysis are about 1.0 volts. Dents with lower signal amplitudes are often used as a diagnostic tool. [

] Figure 6-19 shows there are relatively few of these locations in Unit 3 SG E-089 with the same observation being true for SG E-088. In stark contrast, Figure 6-20 shows that there are very many locations of 0.5 volt dents and high loads in Unit 2 SG E-089. These dents occur at the noses of AVBs 6 and 7 near row 48. AVBs 2, 3, 11 and 10 near row 27 have sporadic dents in the vicinity of the noses of AVBs 1, 4, 9 and 12. The larger amount of AVB twist in Unit 2 compared to Unit 3 is illustrated by the presence of these dents. Only classic dents with a magnitude of 0.5 volts and greater were used as a guide to benchmark and optimize MHI contact force calculations. Patterns of dents and associated high contact forces are in good agreement with the final quarter model calculations. Comparisons were naturally made with cold condition quarter model results for Unit 2 and 3 as these are the forces relevant for the pre-service inspection observations.

SONGS U2C17 Steam Generator Operational Assessment for Tube-to-Tube Wear

6.4.2 Non-Classical Dents

Two other sets of observations serve as checks of the reasonableness of contact force calculations. These observations are non-classical dent/contact eddy current signals and AVB to tube gap measurements. They were not used in benchmarking or optimizing calculations. Non-classical dent/contact signals have been found to be eddy current footprints of contact between tubes and support structures in other steam generators. In very broad terms, classic dents are usually reported on the differential mix channel [

]

Non-classical dent/contact signals have been found to be a valuable diagnostic tool in root cause evaluations. They are found by automated analysis of mix residual signals with specified sorting parameters and occasional analyst review. [

] Signals are reported down to a signal amplitude of []. This low reporting threshold is possible in the newer replacement steam generators having tube material with low noise levels. Non-classical dent/contact signals have been found to an eddy current footprint of either past or current contact of tubes with support structures. [

]

Typical amplitude growth of non-classical dent/contact signals from another plant is illustrated in Figure 6-21. [

A three dimensional plot of non-classical dent/contact signals is shown in Figure 6-22 for Unit 2 SG E-088 at the first in-service inspection. [

] The same observations apply to Figure 6-23, a three dimensional plot of non-classical dent/contact signals for Unit 2, SG E-089. [

]

SONGS U2C17 Steam Generator Operational Assessment for Tube-to-Tube Wear

Figure 6-24 and Figure 6-25 illustrate three dimensional plots of non-classical dent/contact signals for Unit 3, SG E-088 and then for Unit 3, SG E-089. [

] More importantly, comparison of the relative numbers of contact signals in the upper bundle for Units 2 and 3 provides a graphic, visual demonstration that contact forces are more significant in Unit 2 than in Unit 3. Unit 2 and 3 are significantly different and different behavior with respect to the development of in-plane FEI is expected.

Calculated contact force distributions are in reasonable agreement with eddy current non-classical dent/contact signals. Significant differences between Unit 2 and Unit 3 are confirmed. Additionally contact signal densities in the upper bundle suggest that calculated contact forces are underestimated somewhat, particularly for AVBs 4 and 5 in Unit 2. This would lead to an overestimated probability of instability for Unit 2. [

] While support effectiveness is not needed in demonstrating a stability ratio less than 1 at 70% power, it is important relative to demonstration of margin by having a high probability of maintaining a maximum stability ratio that is less than 0.75.

6.5 Tube-to-AVB Gap Evaluation

An extensive campaign of gap measurements was undertaken in all steam generators using both eddy current and ultrasonic techniques. The ultrasonic technique is more accurate and can measure smaller gaps but is very time consuming. The eddy current technique is much faster [

] Field inspections are more challenging than laboratory conditions and some degradation of detection thresholds and resolution is expected in field inspections. Figure 6-28 from Reference [14] compares in generator gaps measurements using eddy current and ultrasonic techniques. The overall agreement is very good. In fact, it is quite comparable to the agreement of AVB wear depths using bobbin and +Pt™ eddy current probes when both are setup according to standard EPRI ETSS procedures. For gaps on the order of [] the eddy current gap measurements significantly overestimate the gap size. At larger gap sizes, eddy current measurements are larger than ultrasonic measurements by an average factor of []. Sizing uncertainties increase by about [] from laboratory to in generator conditions. Since the primary purpose of gap measurements was to determine if there were highly heterogeneous spatial distributions of large gaps, eddy current measurements are well suited to this purpose and much more accurate than previous eddy current techniques.

Over 117,000 eddy current gap measurements were performed. Only global findings are reported here. It should be noted that gaps and hence contact forces are significantly affected by wear at AVB locations. Hence it is difficult to make any but the most general inferences about differences in gaps and contact forces between Unit 2 and Unit 3 at the beginning of life. Further, there are plugged tubes in the regions of interest in all steam generators that could not be inspected.

SONGS U2C17 Steam Generator Operational Assessment for Tube-to-Tube Wear

6.5.1 Unit 2 Tube-to-AVB Gaps

Figure 6-29 and Figure 6-30 present tubesheet maps of the total of all measured gaps on a given tube for Unit 2, SG E-088 and Unit 2, SG E-089 [14]. All AVB locations are included in the total reported gap. The distinction noted for wear versus no wear locations indicates that wear was present at one or more AVB locations on a tube. It is important to note that some of the points indicated as “wear influenced” exhibited very low wear signals that are below the reporting level for standard inspections for wear. The presence of wear, particularly standard wear calls, tends to lead to an underestimate of the gap size. Figure 6-29 shows that the spatial distribution of gaps in Unit 2, SG E-088 is unexceptional. Naturally, wear at AVB locations open up gaps. The average 10% depth wear indication represents a material loss of 0.004 inches. In Unit 2, SG E-089 with approximately 800 more wear indications than Unit 2, SG E-088, larger total gaps are observed. See Figure 6-30. Here there is one area where there is some indication of a local spatial heterogeneity in gap sizes. Note the linear sequence of red data points in column 71 centered near row 120. This area was examined in detail. It is the column boundary of AVB wear for the rows in the vicinity of row 120. In this vicinity, column 71 and, to a lesser extent, column 73 have a noticeable row sequence of AVB wear indications. This has created a larger local region of total gap values. The contact force model for Unit 2 is based on wear in SG E-089 with wear locations each discretely modeled based on eddy current inspection results; thus, the contact force model actually includes this local region of heterogeneous gap sizes as part of the calculation of contact forces. Since quarter model results are mirrored to the other side of the steam generator, worst case wear conditions are double counted. With all of the above, the end results are not particularly important for this OA since the lower AVB supports are relatively unaffected and thus there is no challenge from this region to maintaining a maximum stability ratio of 0.75 at 70% power.

6.5.2 Effect of Gap Size on Tube-to-AVB Wear

Before proceeding to a discussion of Unit 3 gap results a consideration of the implication of gap sizes relative to expected wear rates at AVB locations is worthwhile. Figure 6-31 presents a synthesis of viewpoints relative to the relationship between wear rates and tube to support gap sizes. Both seek to explain high wear rates at support locations. One is termed the nil gap hypothesis. The other exclusively favors out-of-plane, gap limited, fluid-elastic excitation. Both have been applied successfully. The nil gap hypothesis maintains that a zero gap condition, perhaps maintained by a small bias force, results in continuously high wear rates from turbulence excitation. For large gaps, out-of plane fluid-elastic excitation is admitted as a consideration but not expressly used. The nil gap hypothesis has been successfully applied and correctly predicts that many individual wear sites will exhibit constant wear rates over multiple cycles of operation. Westinghouse has demonstrated success with the out-of-plane, gap limited, fluid-elastic excitation approach. Figure 6-31 shows high wear rates from turbulence excitation at a nil gap condition and high wear rates at larger gap sizes. Negative gaps imply high contact forces. Conceptually, there is some contact force that hinders motion to the extent that wear effectively ceases. A tube can experience a contact force on one side with a larger gap on the other side. If the contact force is sufficient, out-of-plane gap limited fluid-elastic excitation will not be an important consideration. Hence, a tube with a large one sided gap may or may not exhibit a high wear rate. The support may still be an effective support. Conversely, a tube with a small gap on each side will not exhibit a high wear rate. For small gaps, it will be an effective support.

6.5.3 Unit 3 Tube-to-AVB Gaps

Substantial regions of gap heterogeneity are observed in the Unit 3 steam generators. Part of this heterogeneity is the results of increased wear in Unit 3 compared to Unit 2, particularly at lower AVBs. This is perhaps exacerbated by lower contact forces in Unit 3 and less effective rebalancing of gaps and contact forces as wear was introduced. A very substantial region of large gaps appear under retainer bars in both steam generators from column 40 across to column 50. See Figure 6-32 for Unit 3, SG E-088 and Figure 6-33 for Unit 3, SG E-089 for

SONGS U2C17 Steam Generator Operational Assessment for Tube-to-Tube Wear

gap measurement results. Large gaps are much more pronounced in Unit 3, SG E-089. As advanced by MHI, these gaps are interpreted as a result of downward movement of the entire support structure near the retainer bar locations with a consequent distortion of U-bends and AVBs. This distortion, which can be relatively small in absolute terms, has created substantial gaps. Recall that the upper support structure, to which the AVBs are attached at the periphery, is a floating structure. The weight of the upper support structure is resisted by the friction forces at AVB locations. A downward sagging of the support structures is interpreted as the end result of low initial contact forces further degraded by wear at AVB locations. Unit 3 is indeed different than Unit 2.

6.6 Conclusions – Contact Forces

The primary purpose of gap measurements was to determine if there were highly heterogeneous spatial distributions of large gaps that are not included in contact force calculations. For the purposes of this OA, this is more relevant to Unit 2 rather than Unit 3. In Unit 2 there were no highly heterogeneous spatial distributions of large gaps that challenge contact force calculations. In Unit 3 there are highly heterogeneous spatial distributions of large gaps under the retainer bars from column 40 across to column 50. This region is far enough removed from the region of in-plane fluid-elastic instability and thus probability of instability calculations are not grossly affected. Gap measurements are suggestive that contact forces were smaller in Unit 3 than in Unit 2 at the beginning of life. A far stronger argument is provided by observations regarding classic dent signals and non-classical low level dent/contact signals. Any measurements that could have been made to check contact forces calculations were made. Contact force calculations are appropriately reliable to demonstrate maintenance of adequate margins relatively to in-plane fluid-elastic instability at 70% power.

SONGS U2C17 Steam Generator Operational Assessment for Tube-to-Tube Wear

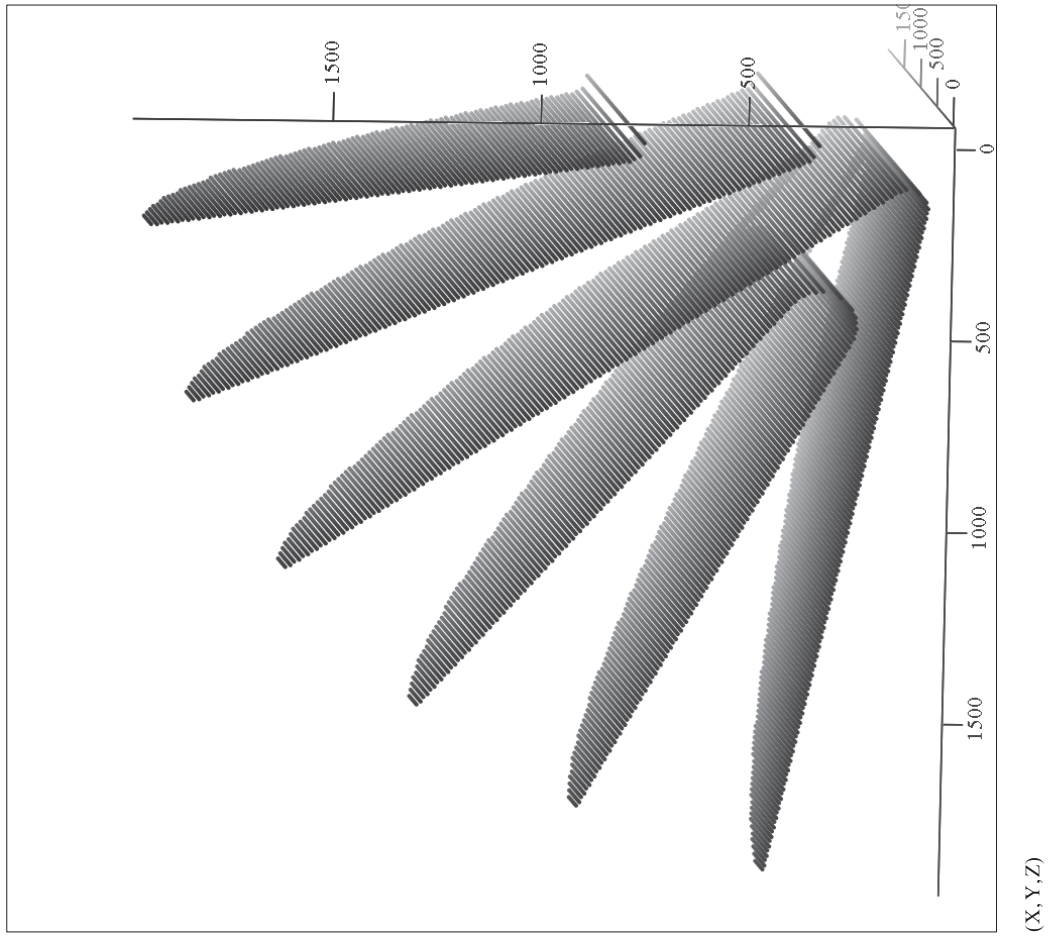


Figure 6-1: Quarter Model Contact Force and Gap Locations

SONGS U2C17 Steam Generator Operational Assessment for Tube-to-Tube Wear

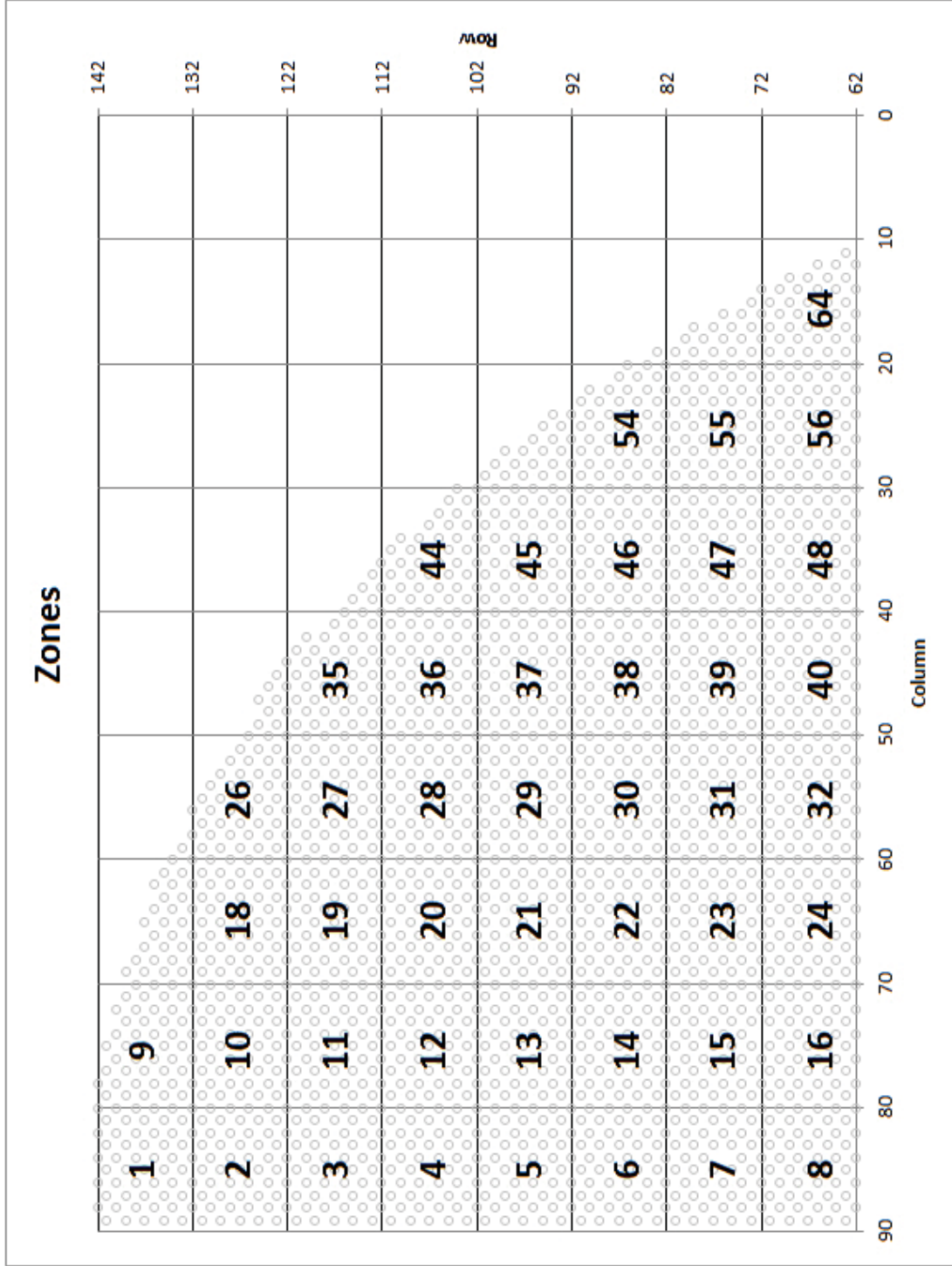


Figure 6-2: Zones Used to Develop Characteristic Distributions of Contact Forces for Each AVB in the Zone

SONGS U2C17 Steam Generator Operational Assessment for Tube-to-Tube Wear

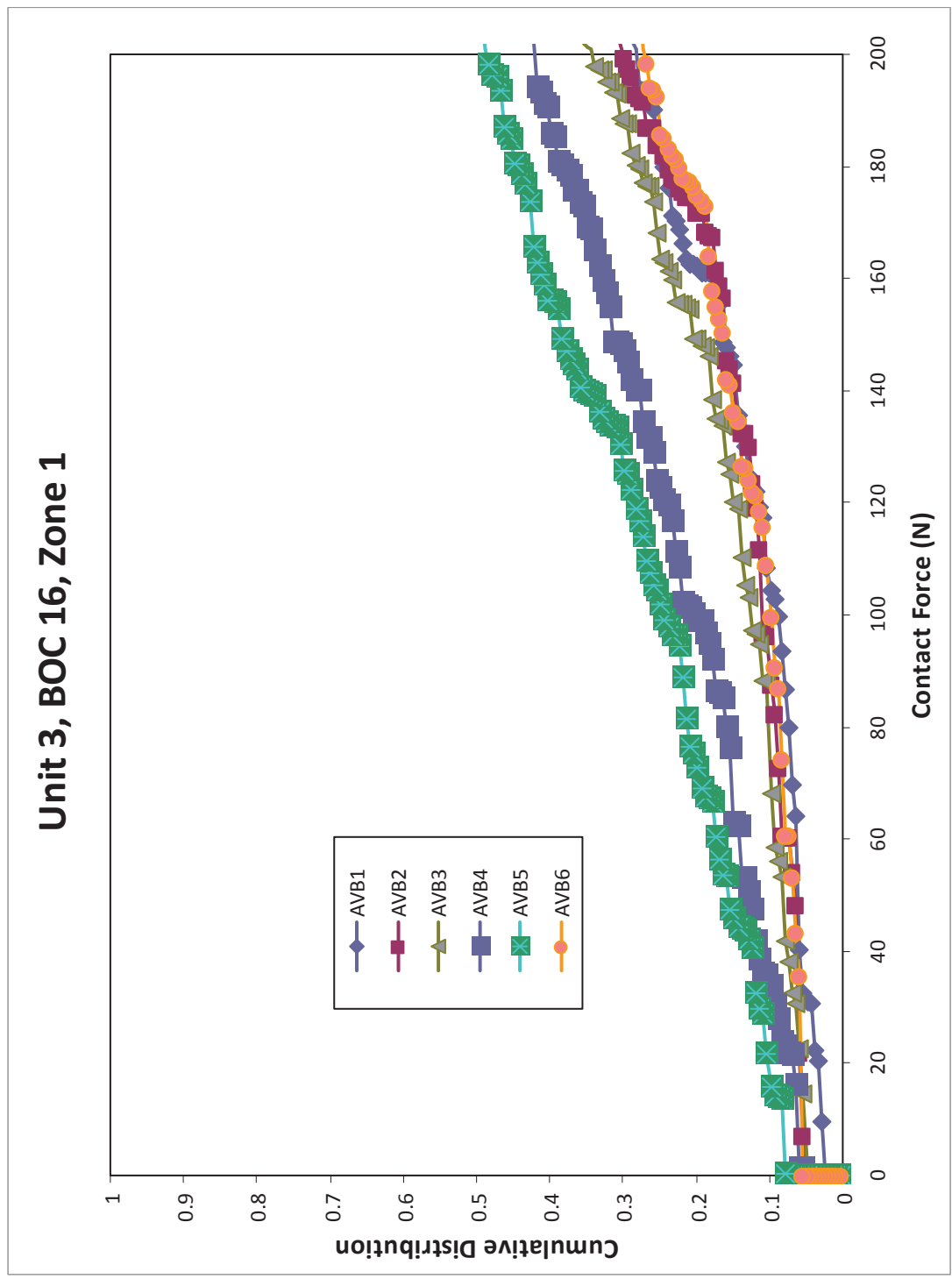


Figure 6-3: Cumulative Contact Force Distributions, Zone 1, Unit 3, BOC 16

SONGS U2C17 Steam Generator Operational Assessment for Tube-to-Tube Wear

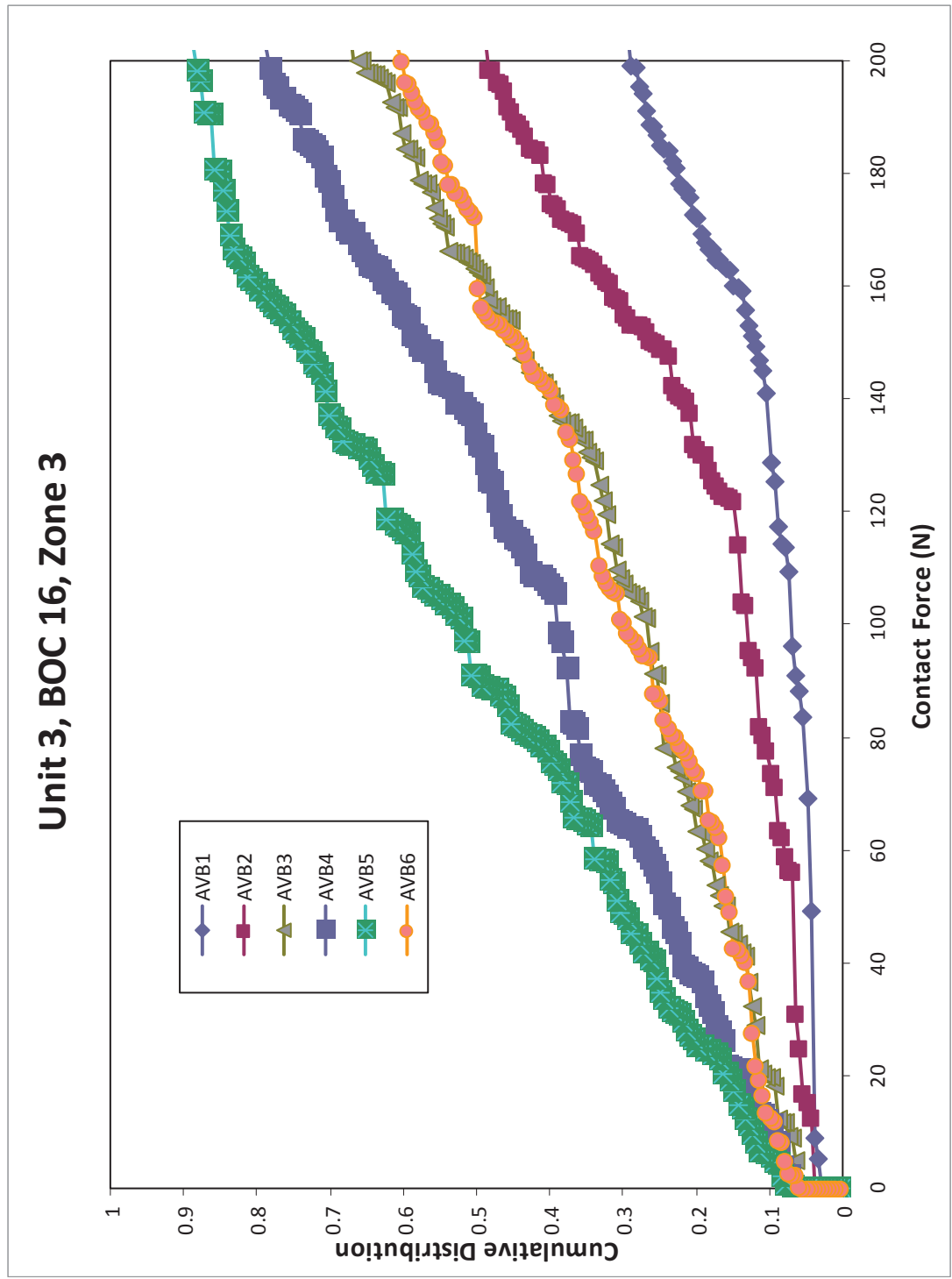


Figure 6-4: Cumulative Contact Force Distributions, Zone 3, Unit 3, BOC 16

SONGS U2C17 Steam Generator Operational Assessment for Tube-to-Tube Wear

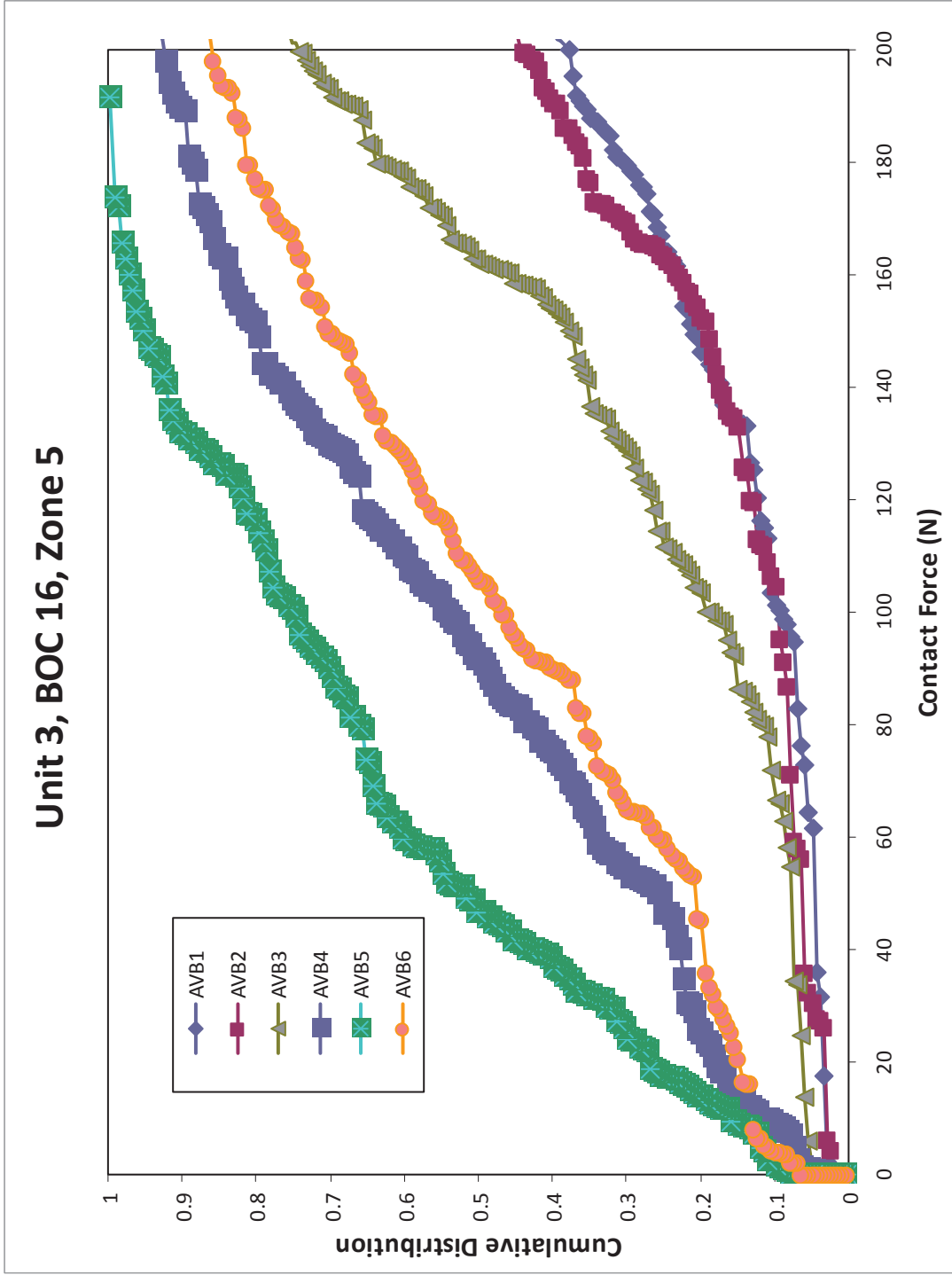


Figure 6-5: Cumulative Contact Force Distributions, Zone 5, Unit 3, BOC 16

SONGS U2C17 Steam Generator Operational Assessment for Tube-to-Tube Wear

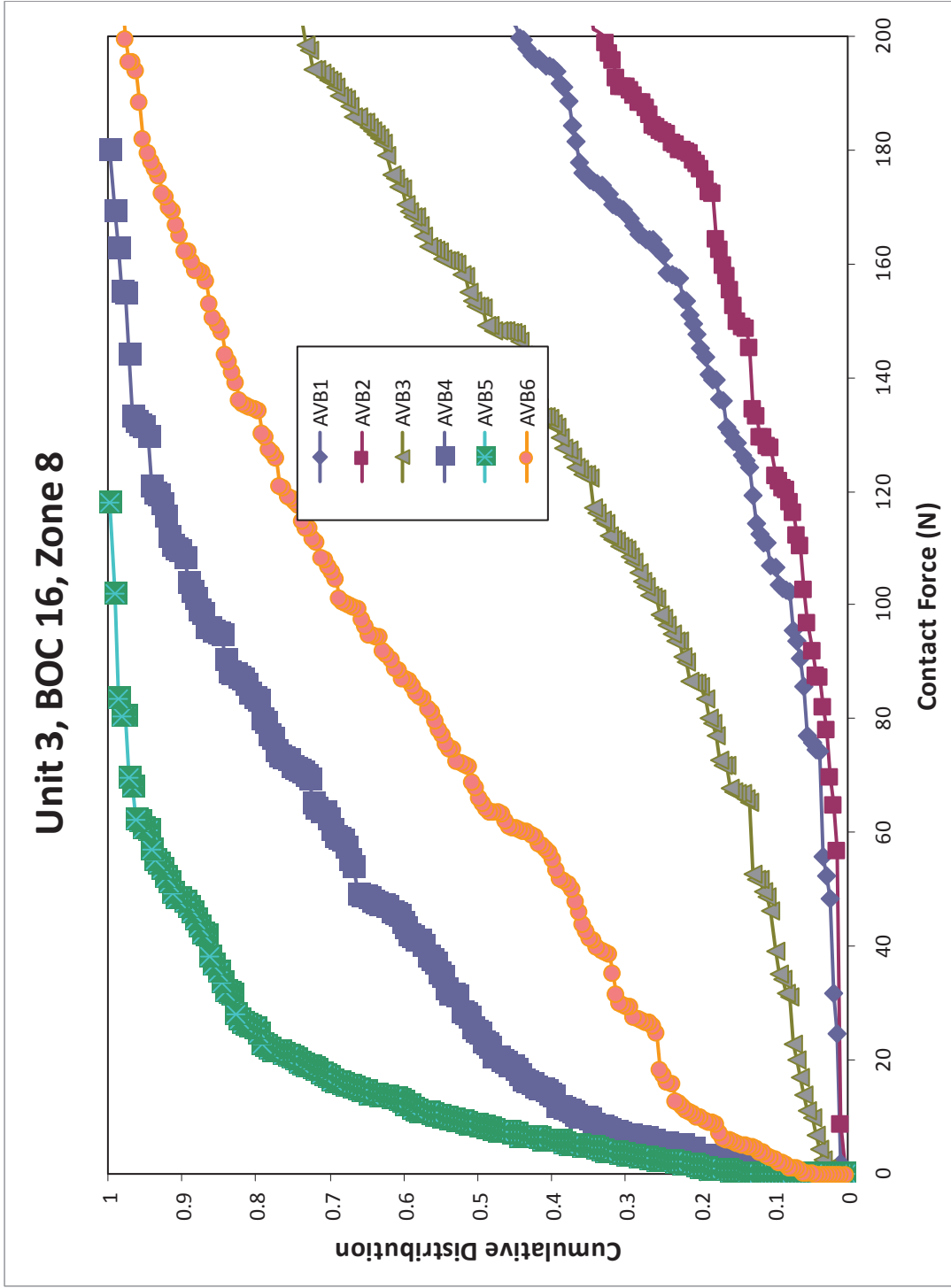


Figure 6-6: Cumulative Contact Force Distributions, Zone 8, Unit 3, BOC 16

SONGS U2C17 Steam Generator Operational Assessment for Tube-to-Tube Wear

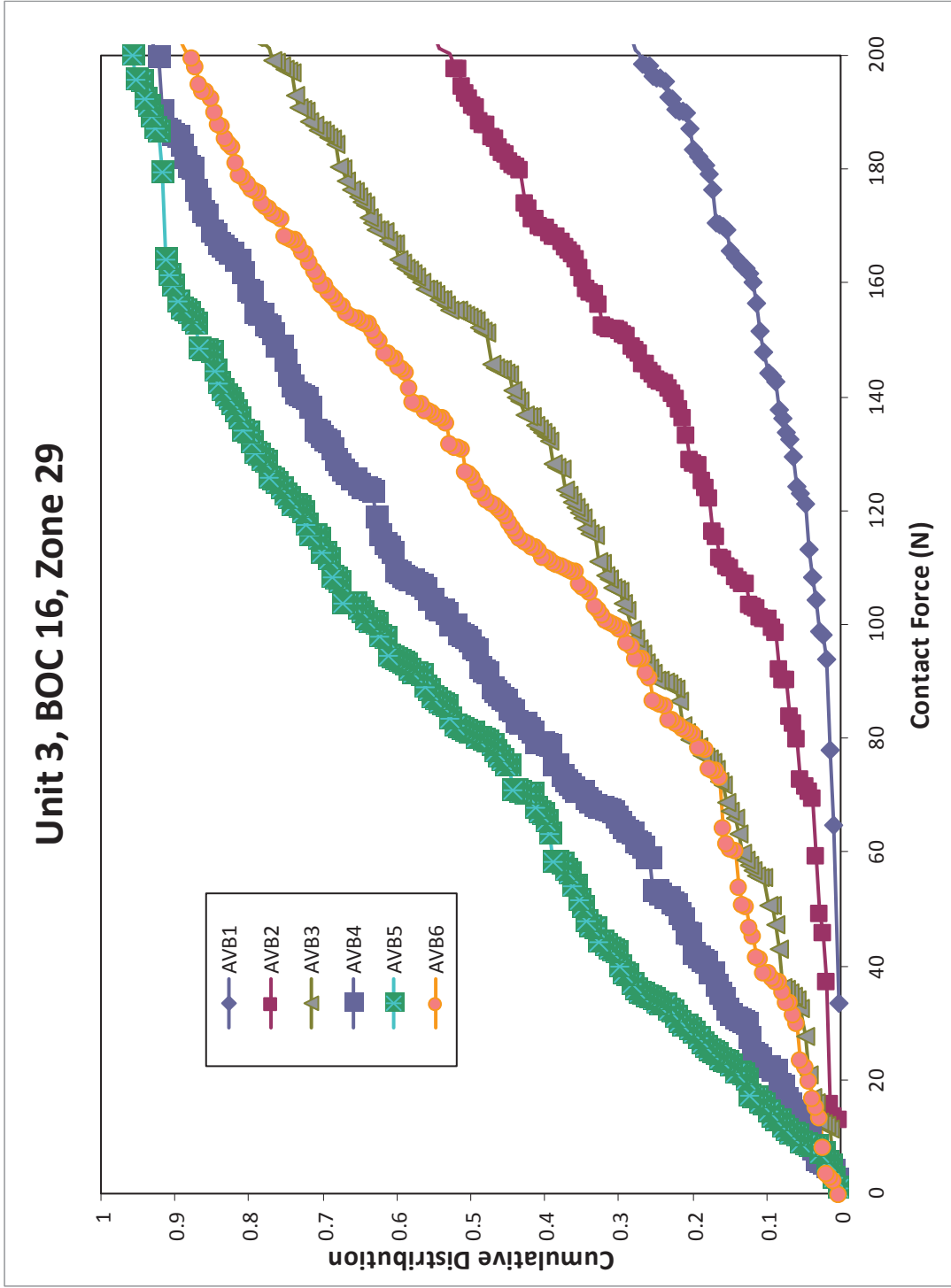


Figure 6-7: Cumulative Contact Force Distributions, Zone 29, Unit 3, BOC 16

SONGS U2C17 Steam Generator Operational Assessment for Tube-to-Tube Wear

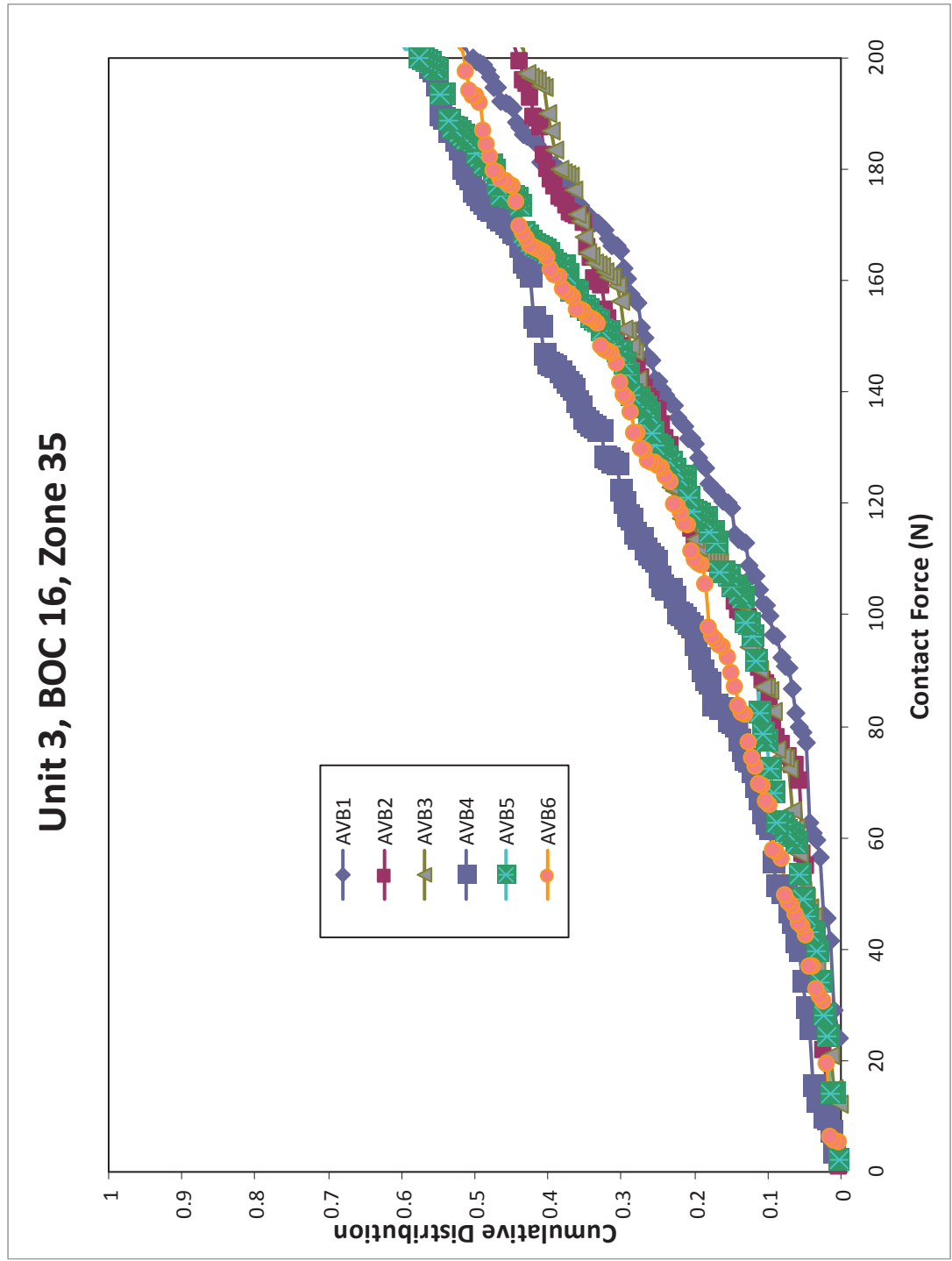


Figure 6-8: Cumulative Contact Force Distributions, Zone 35, Unit 3, BOC 16

SONGS U2C17 Steam Generator Operational Assessment for Tube-to-Tube Wear

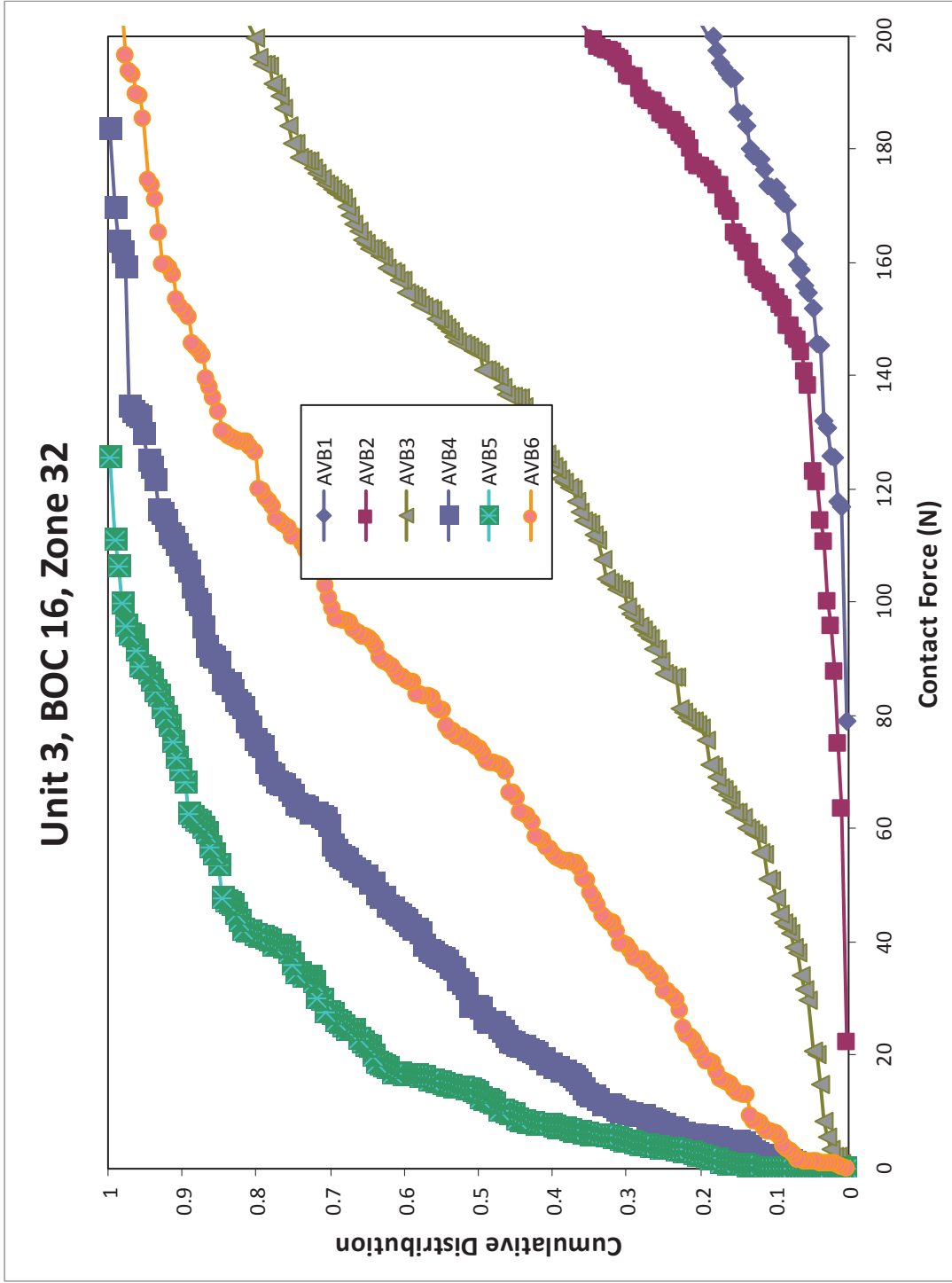


Figure 6-9: Cumulative Contact Force Distributions, Zone 32, Unit 3, BOC 16

SONGS U2C17 Steam Generator Operational Assessment for Tube-to-Tube Wear

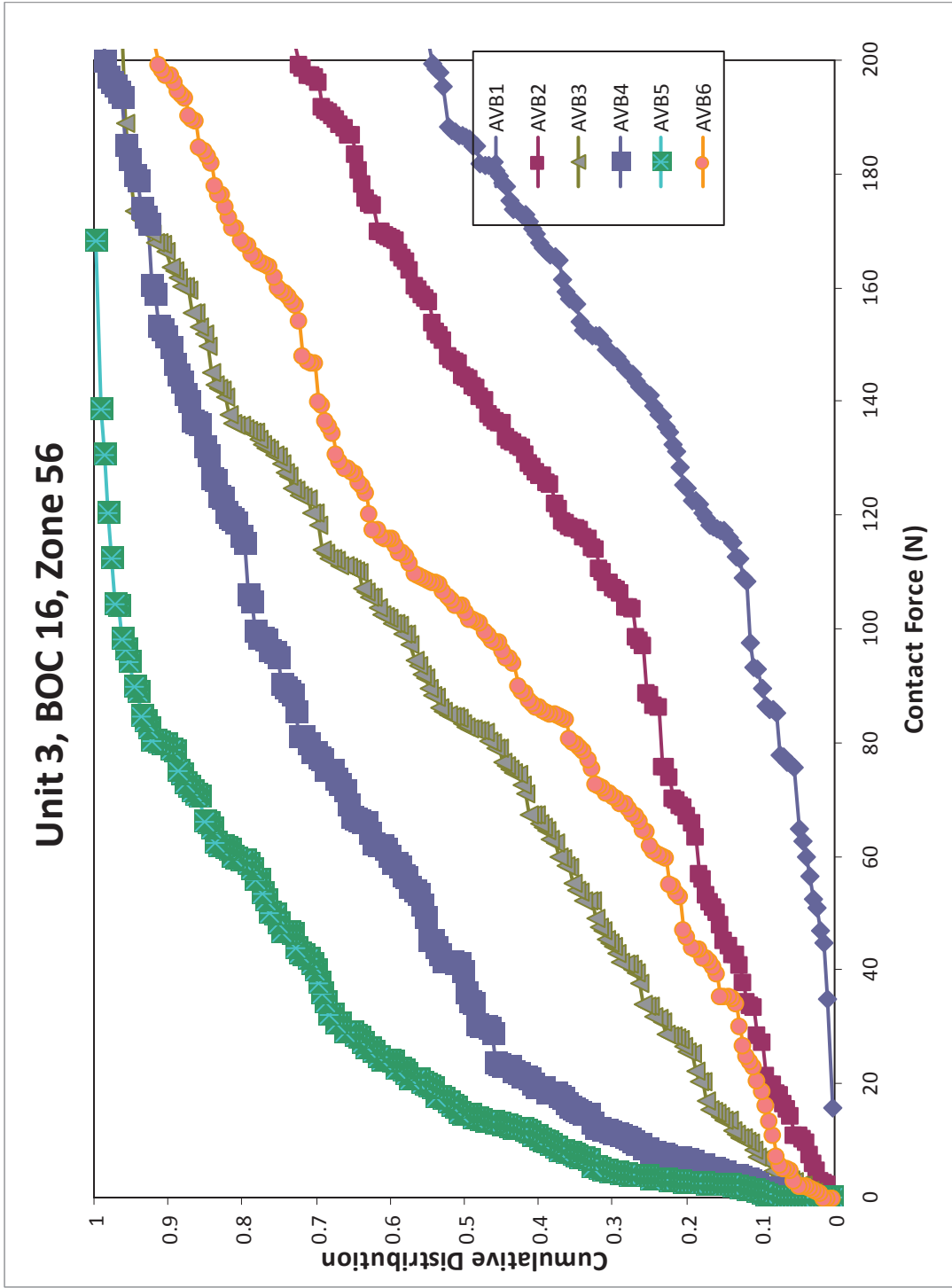


Figure 6-10: Cumulative Contact Force Distributions, Zone 56, Unit 3, BOC 16

SONGS U2C17 Steam Generator Operational Assessment for Tube-to-Tube Wear

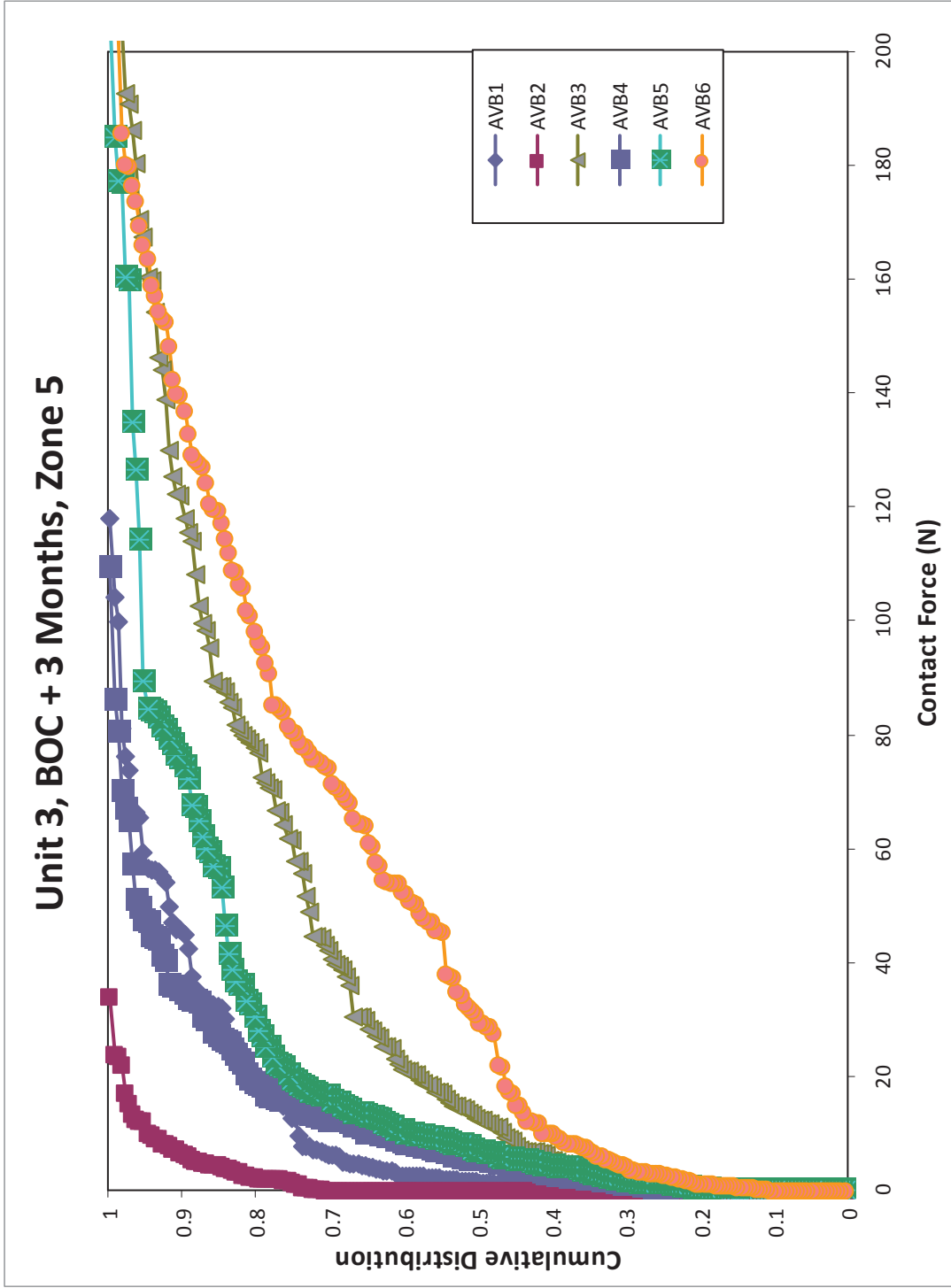


Figure 6-11: Cumulative Contact Force Distributions, Zone 5, Unit 3, BOC 16 + 3 Months

SONGS U2C17 Steam Generator Operational Assessment for Tube-to-Tube Wear

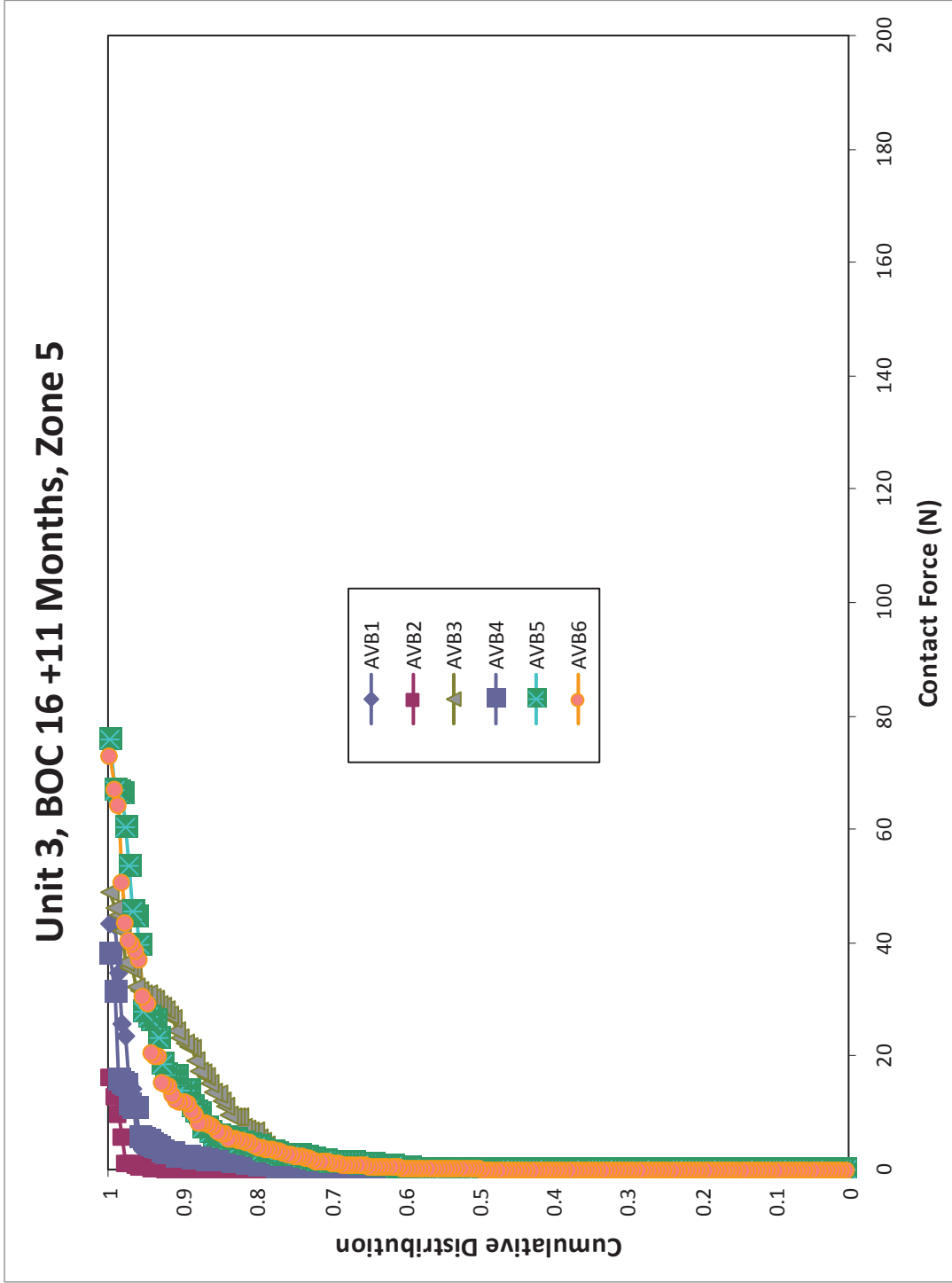


Figure 6-12: Cumulative Contact Force Distributions, Zone 5, Unit 3, BOC 16 + 11 Months

SONGS U2C17 Steam Generator Operational Assessment for Tube-to-Tube Wear

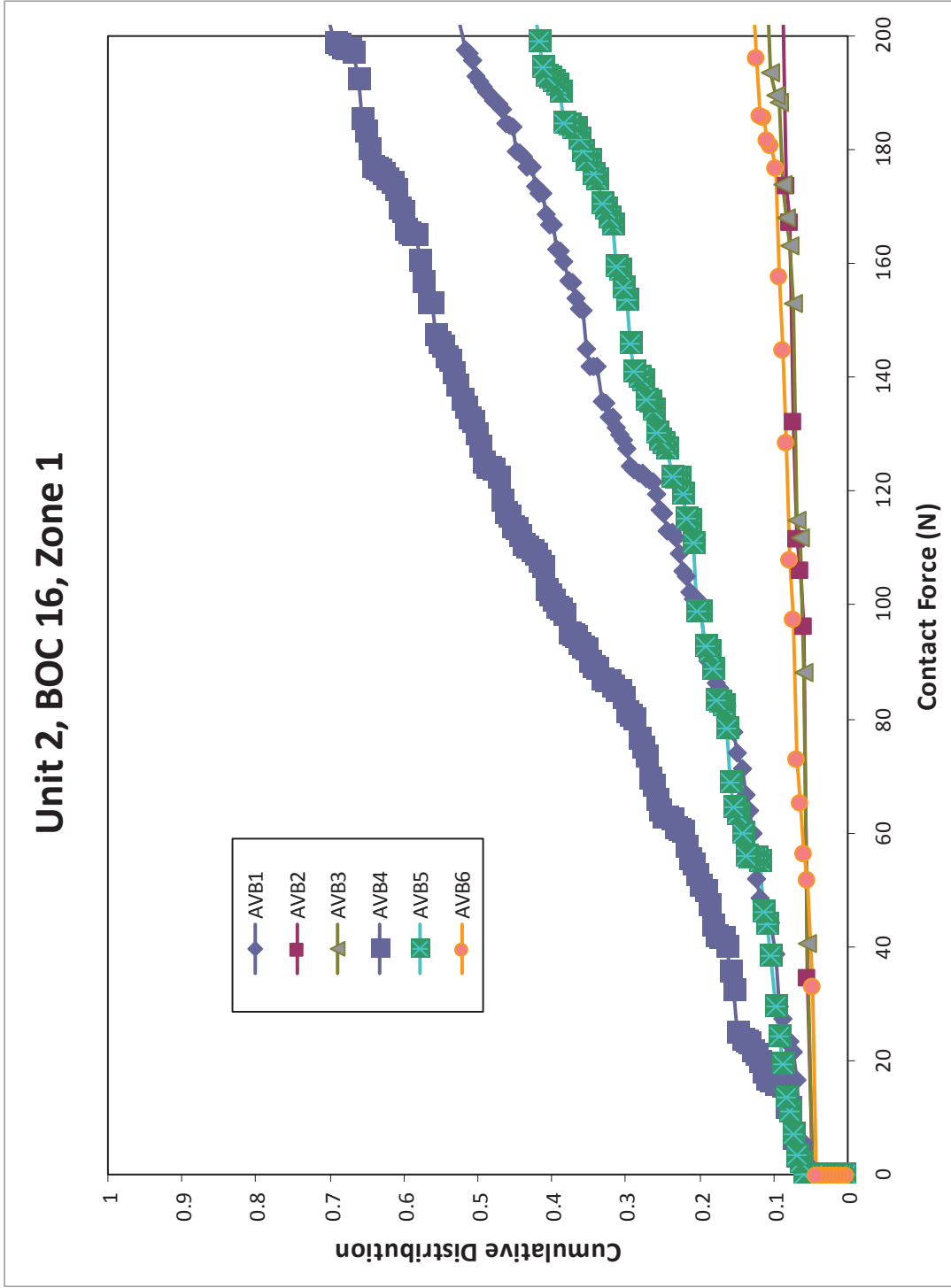


Figure 6-13: Cumulative Contact Force Distributions, Zone 1, Unit 2, BOC 16

SONGS U2C17 Steam Generator Operational Assessment for Tube-to-Tube Wear

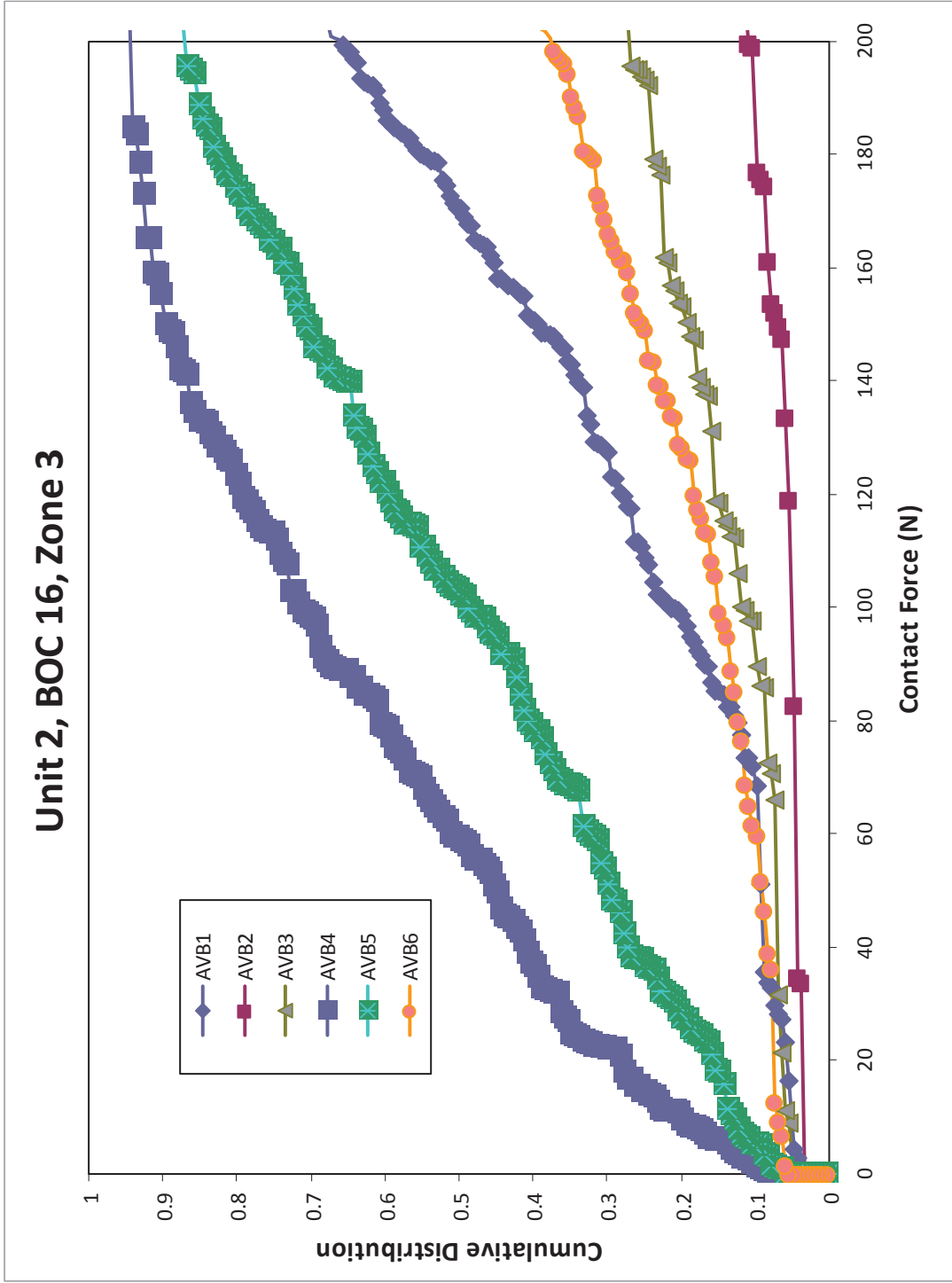


Figure 6-14: Cumulative Contact Force Distributions, Zone 3, Unit 2, BOC 16

SONGS U2C17 Steam Generator Operational Assessment for Tube-to-Tube Wear

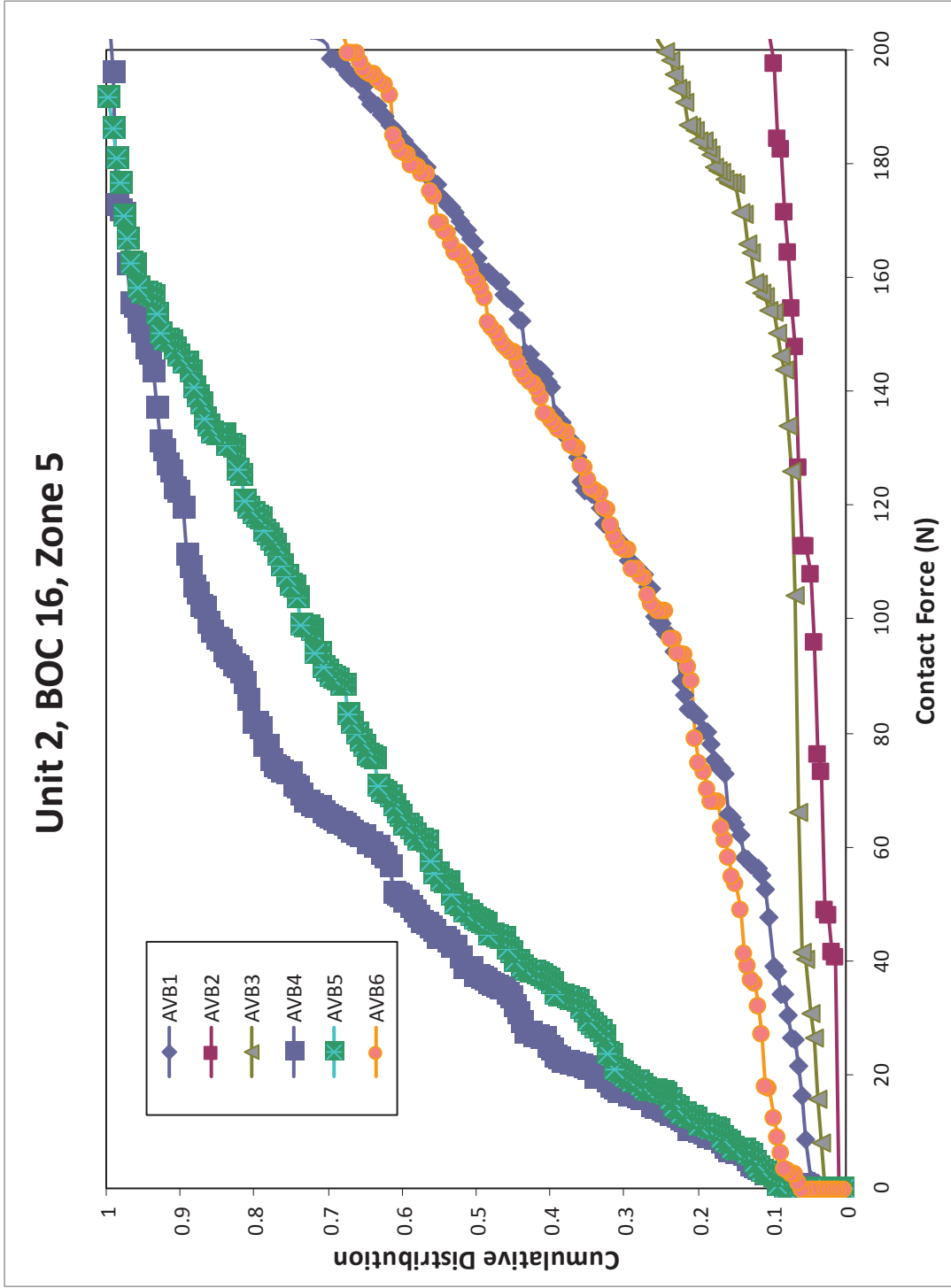


Figure 6-15: Cumulative Contact Force Distributions, Zone 5, Unit 2, BOC 16

SONGS U2C17 Steam Generator Operational Assessment for Tube-to-Tube Wear

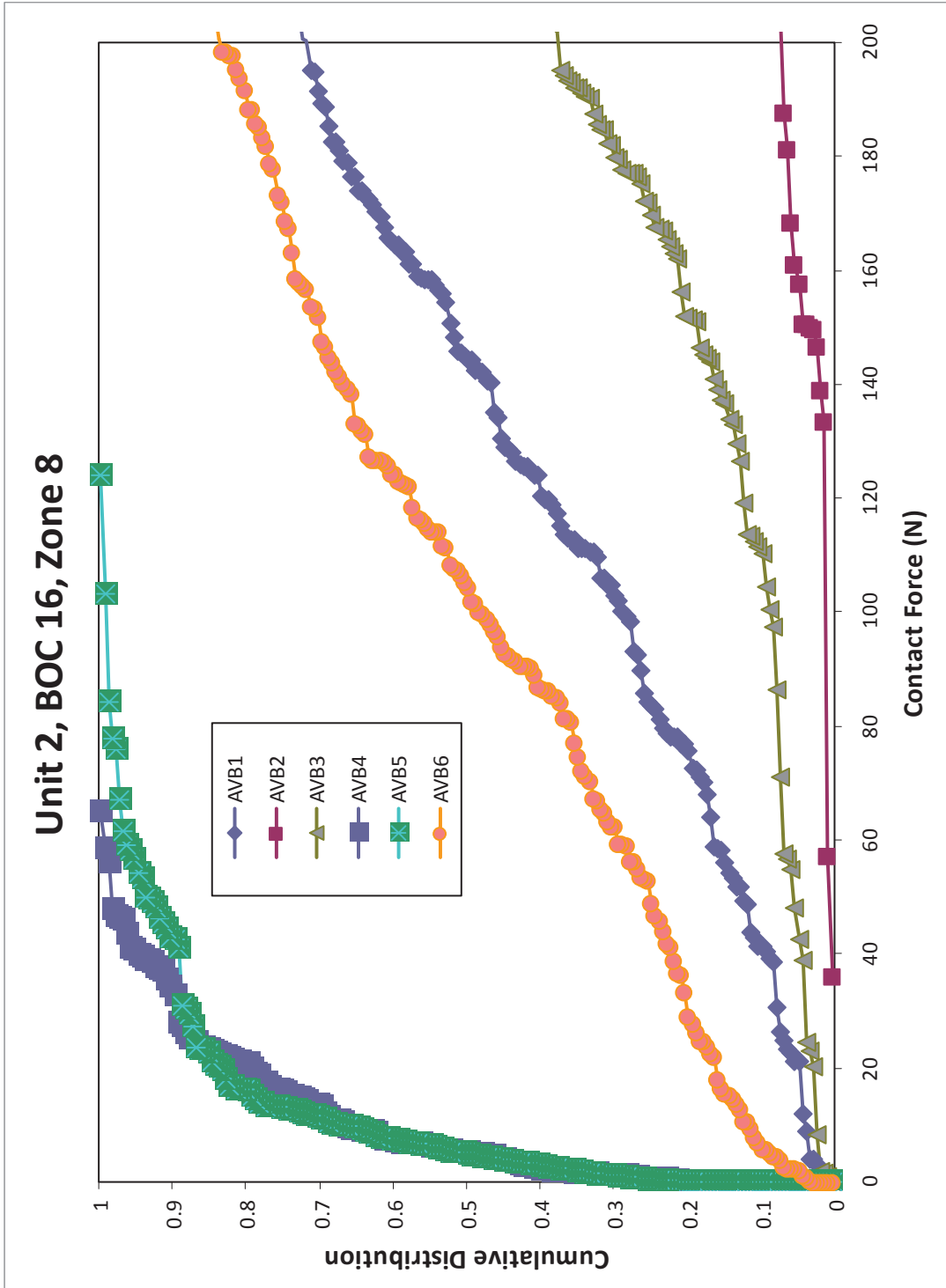


Figure 6-16: Cumulative Contact Force Distributions, Zone 8, Unit 2, BOC 16

SONGS U2C17 Steam Generator Operational Assessment for Tube-to-Tube Wear

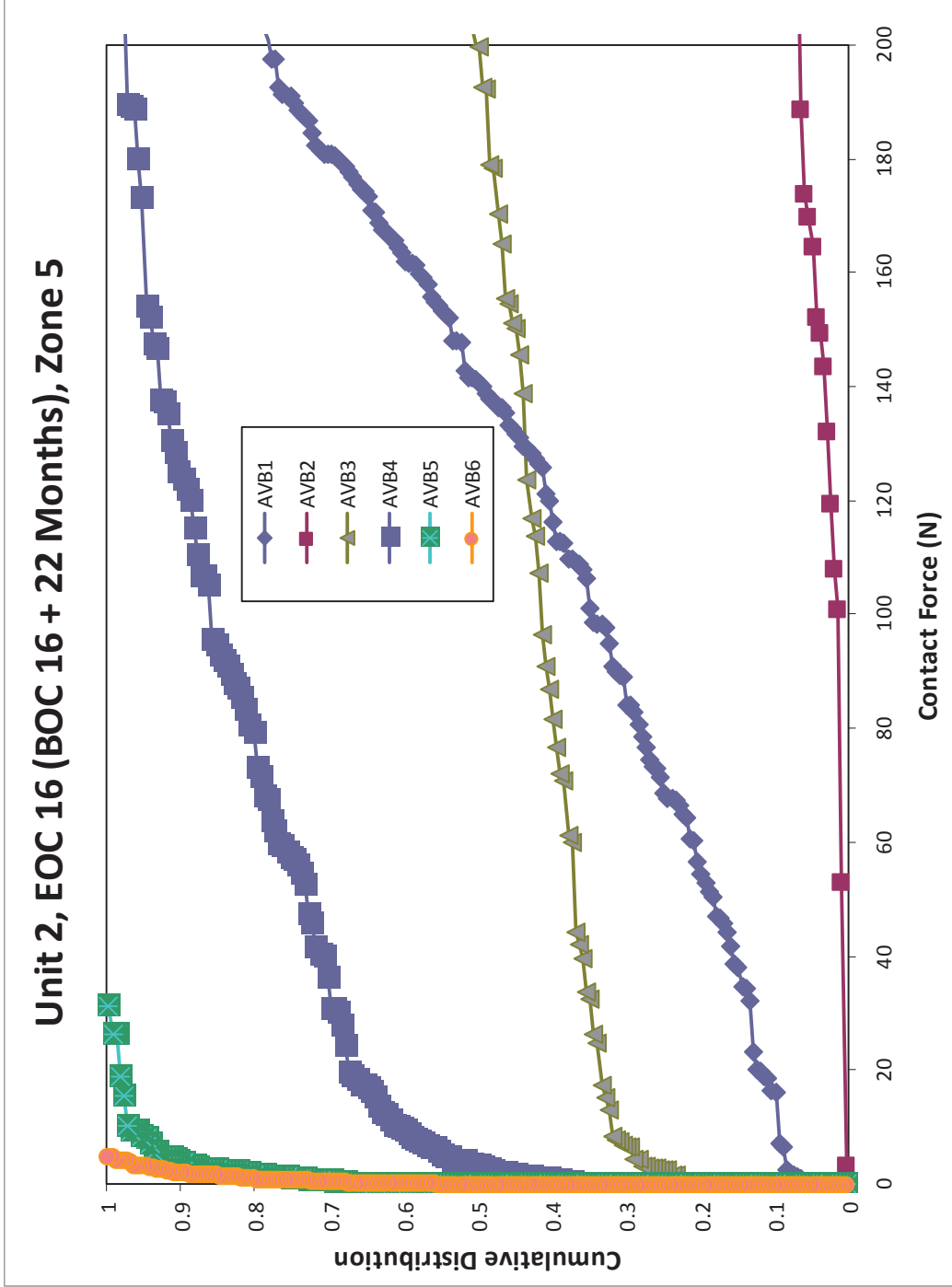


Figure 6-17: Cumulative Contact Force Distributions, Zone 5, Unit 2, EOC 16 (BOC 16 + 22 Months)

SONGS U2C17 Steam Generator Operational Assessment for Tube-to-Tube Wear

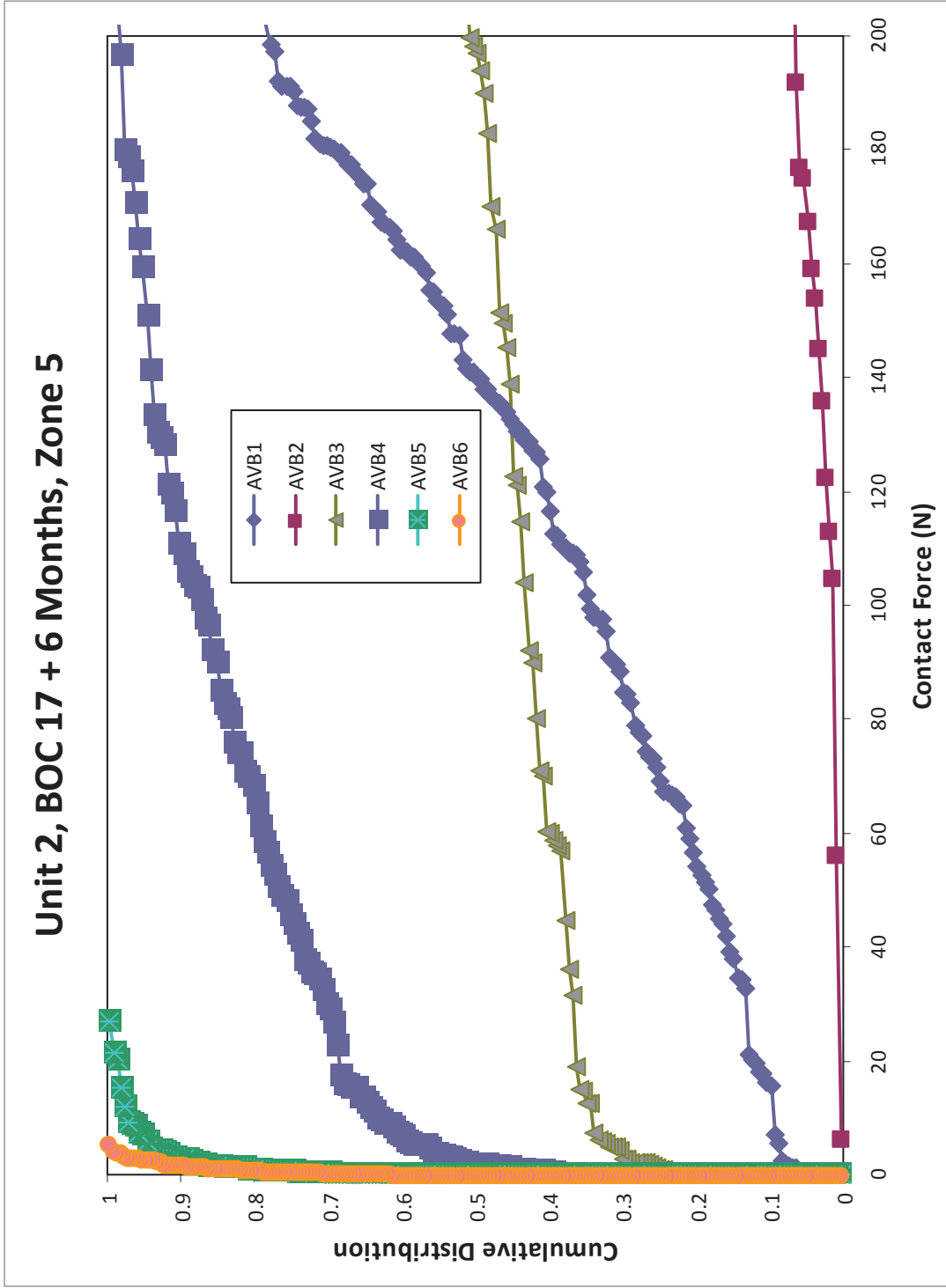


Figure 6-18: Cumulative Contact Force Distributions, Zone 5, Unit 2, BOC 17 + 6 Months

SONGS U2C17 Steam Generator Operational Assessment for Tube-to-Tube Wear

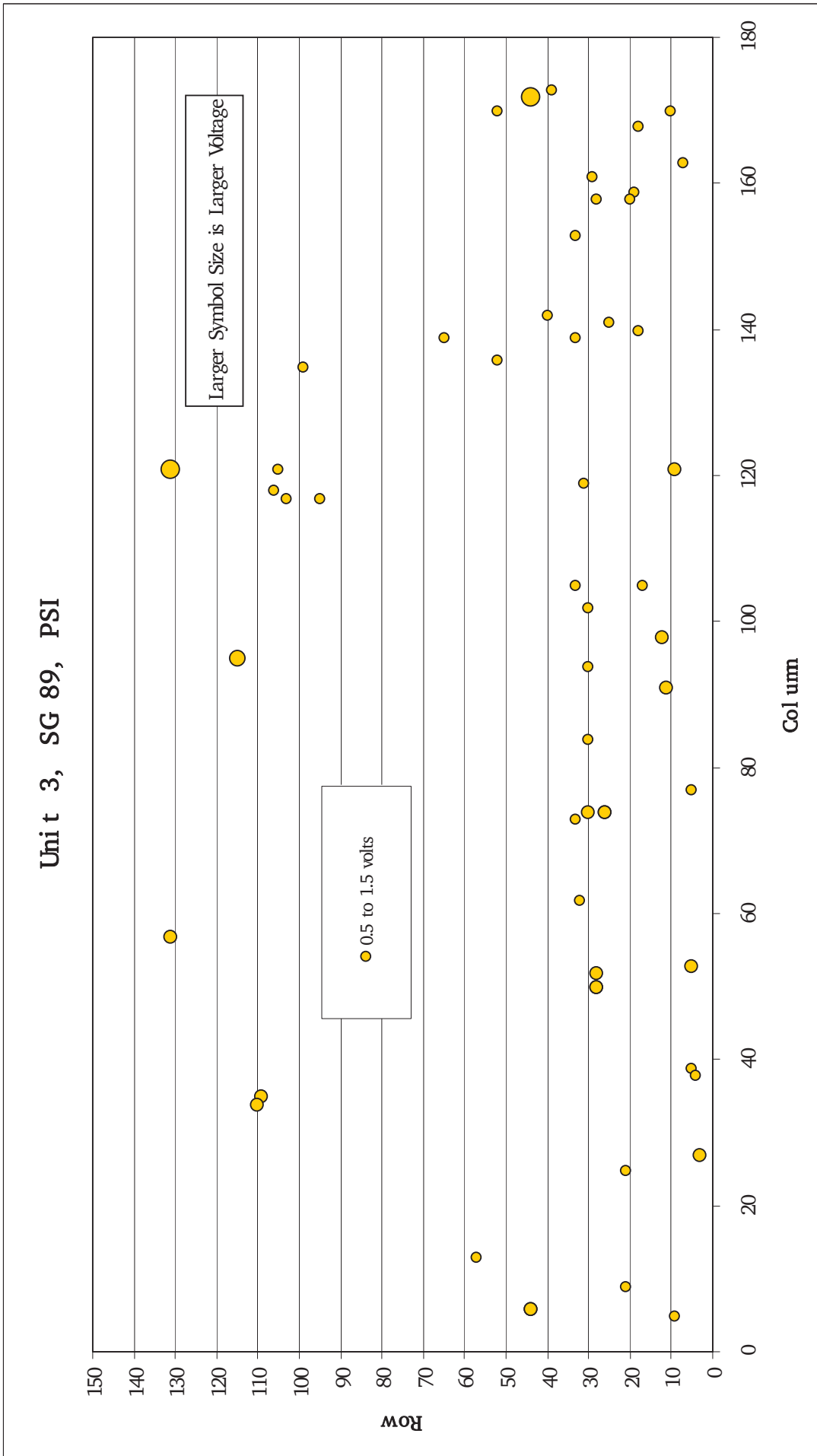


Figure 6-19: Tubesheet Map of Dents Found in Pre-Service Inspection, Unit 3, SG E-089

SONGS U2C17 Steam Generator Operational Assessment for Tube-to-Tube Wear

Unit 2, SG 89, PSI

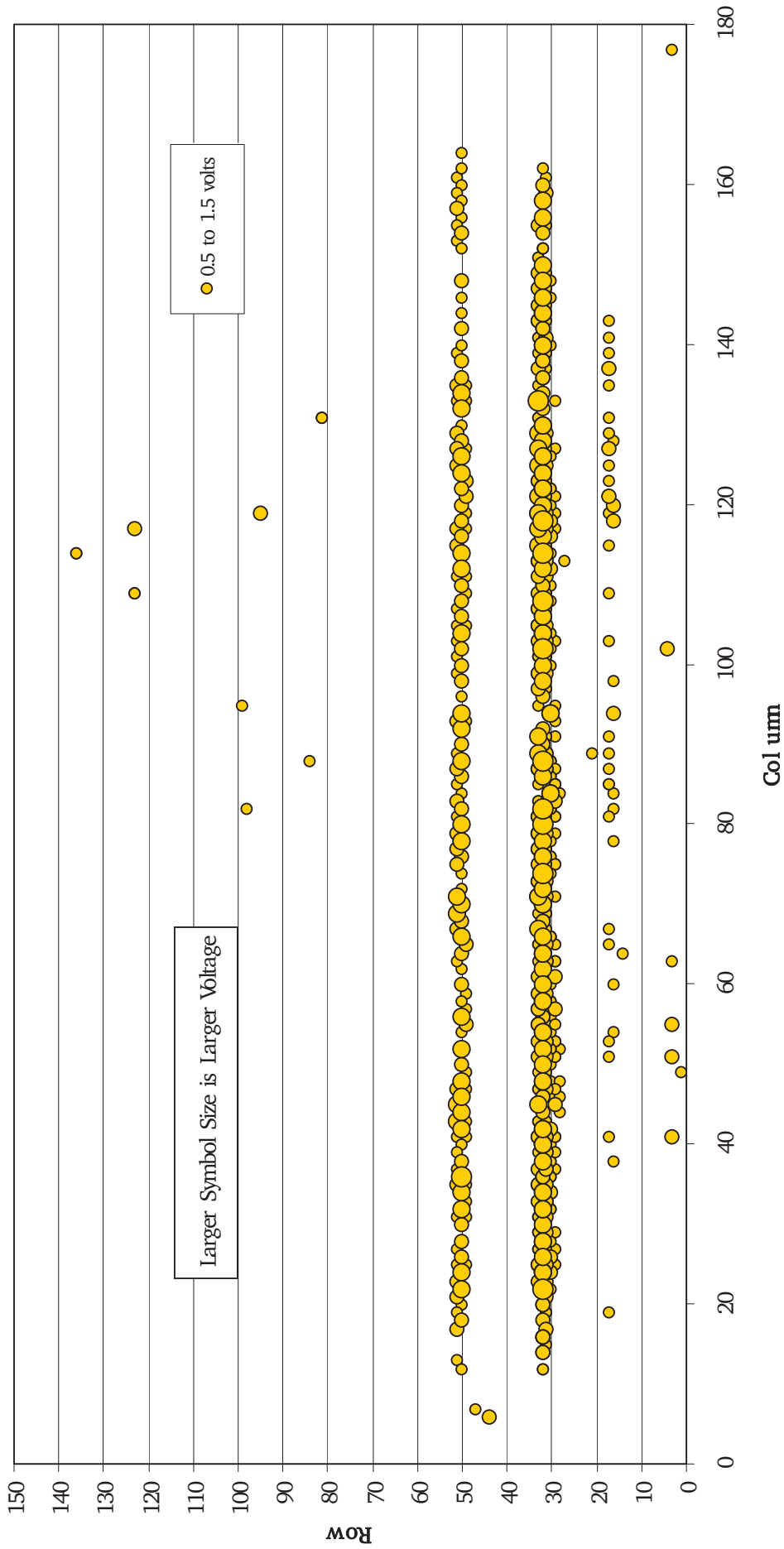
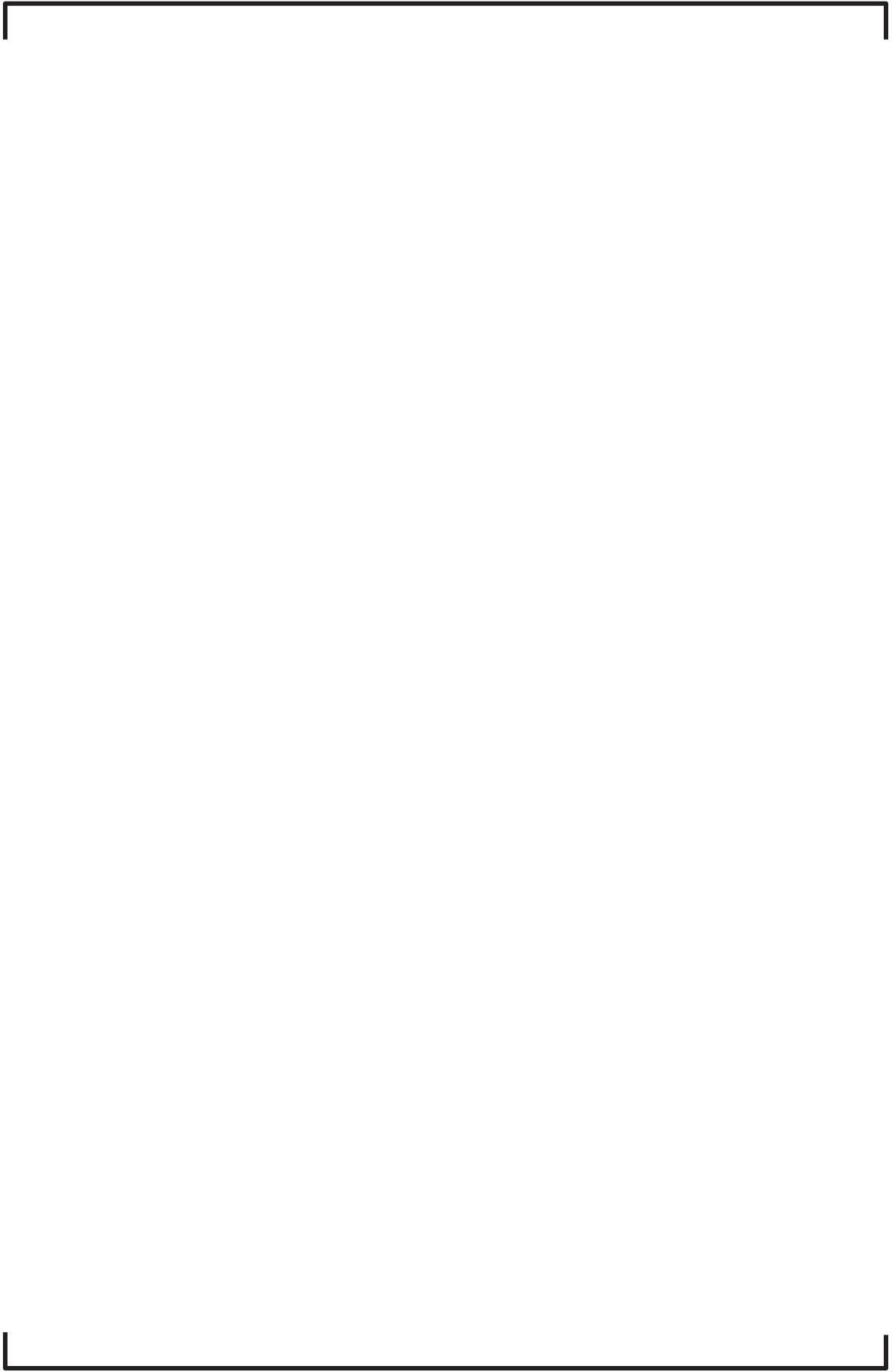


Figure 6-20: Tubesheet Map of Dents Found in Pre-Service Inspection, Unit 2, SG E-089



SONGS U2C17 Steam Generator Operational Assessment for Tube-to-Tube Wear



SONGS U2C17 Steam Generator Operational Assessment for Tube-to-Tube Wear





SONGS U2C17 Steam Generator Operational Assessment for Tube-to-Tube Wear





SONGS U2C17 Steam Generator Operational Assessment for Tube-to-Tube Wear





SONGS U2C17 Steam Generator Operational Assessment for Tube-to-Tube Wear





SONGS U2C17 Steam Generator Operational Assessment for Tube-to-Tube Wear





SONGS U2C17 Steam Generator Operational Assessment for Tube-to-Tube Wear





SONGS U2C17 Steam Generator Operational Assessment for Tube-to-Tube Wear



SONGS U2C17 Steam Generator Operational Assessment for Tube-to-Tube Wear

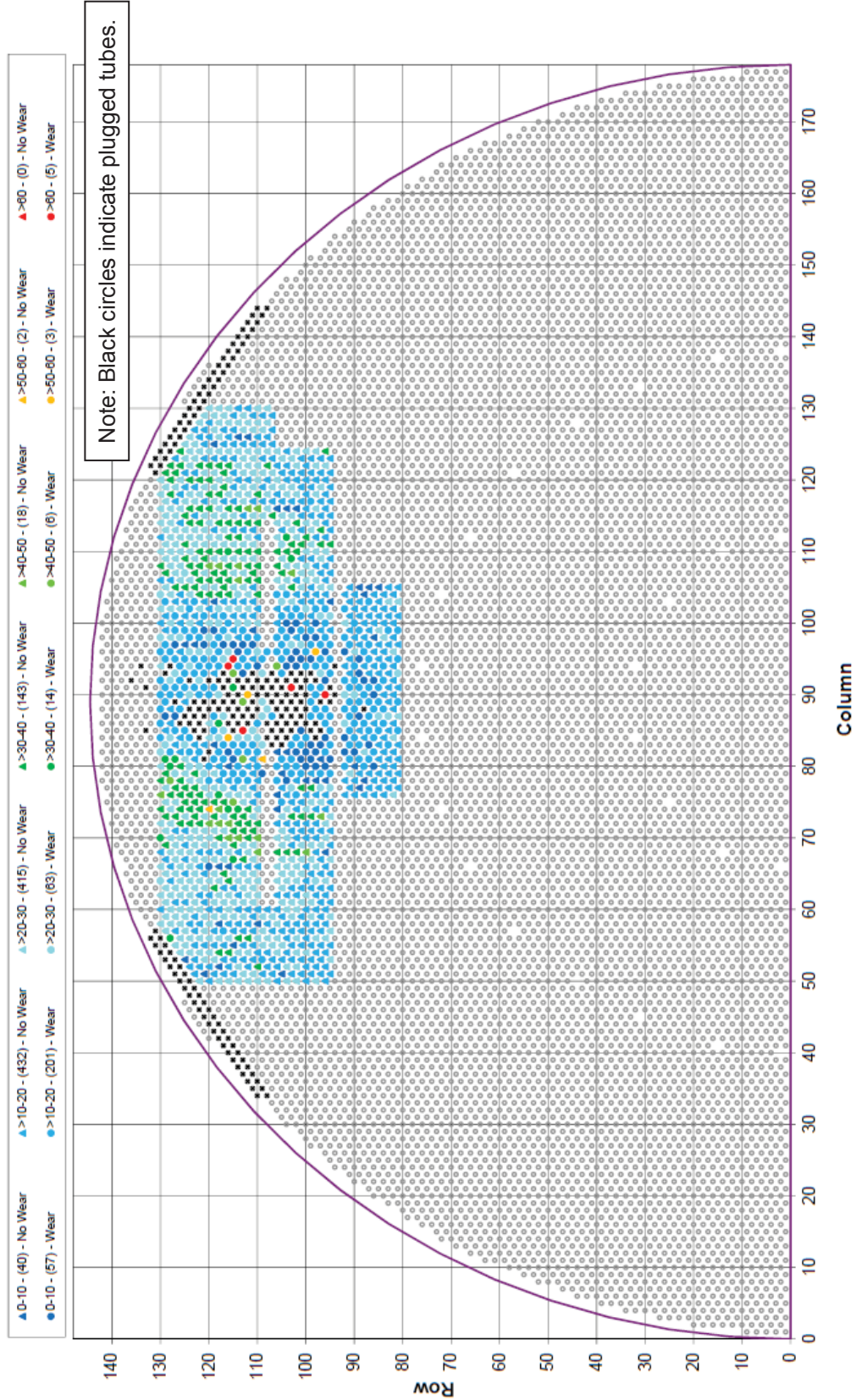


Figure 6-29: Tubesheet Map of ECT Gap Measurements, Total Gap for All AVB Locations per Tube, Unit 2, SG E-088, ISI

SONGS U2C17 Steam Generator Operational Assessment for Tube-to-Tube Wear

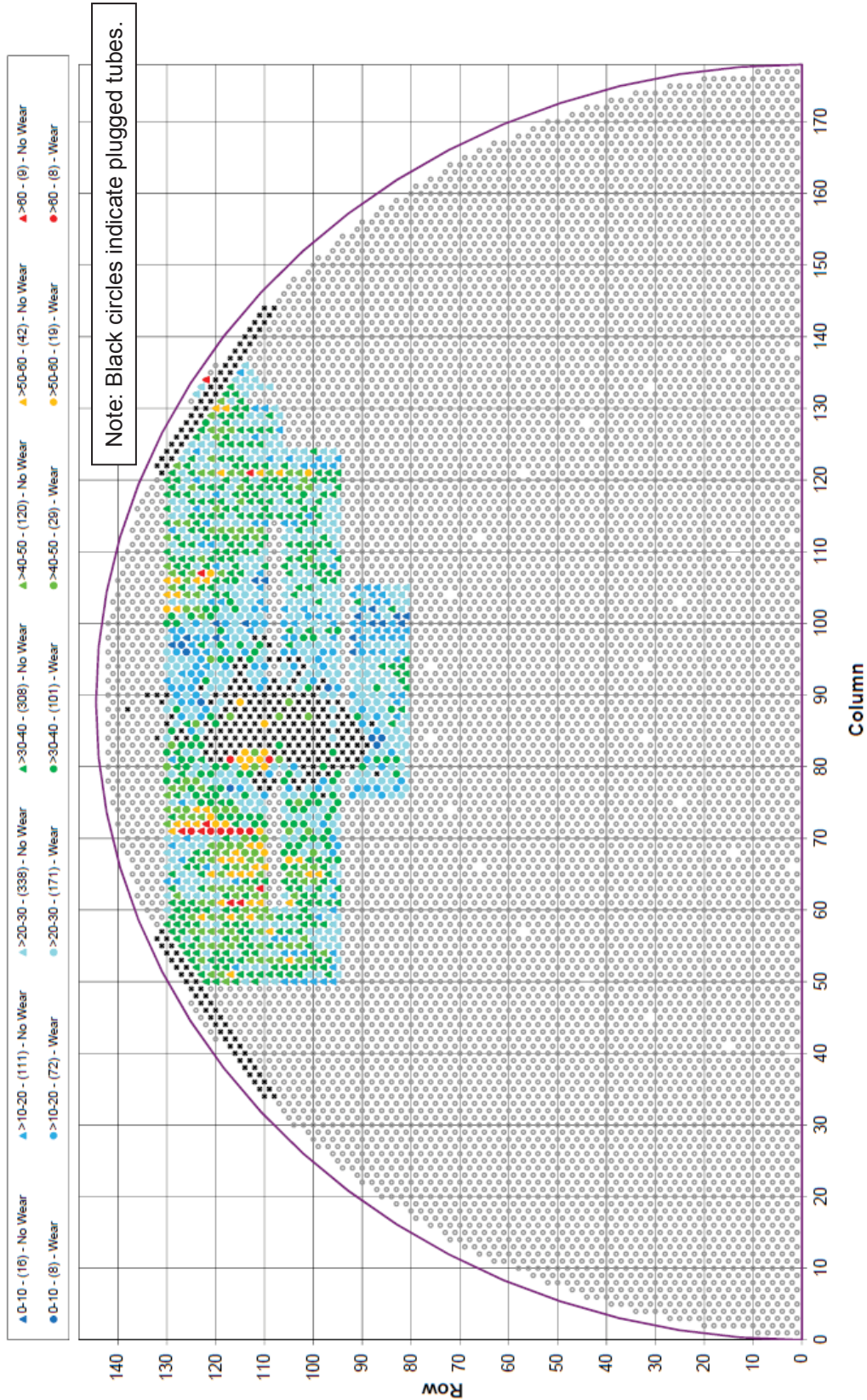


Figure 6-30: Tubesheet Map of ECT Gap Measurements, Total Gap for All AVB Locations per Tube, Unit 2, SG E-089, ISI

SONGS U2C17 Steam Generator Operational Assessment for Tube-to-Tube Wear

Illustrative Schematic, Wear Rate versus Gap Size

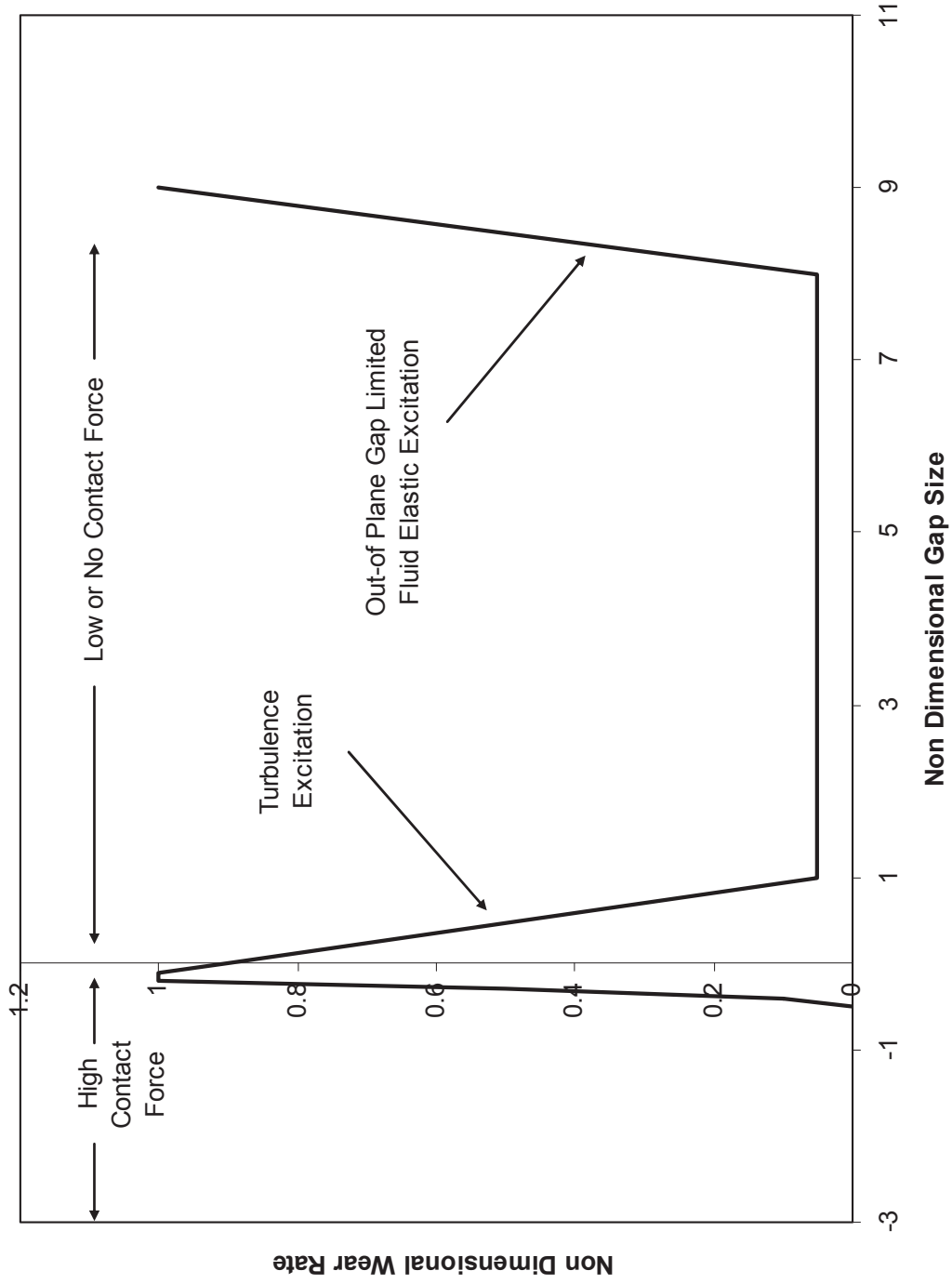


Figure 6-31: Illustrative Schematic of AVB Wear Rates, High Wear Rates are Possible for Very Small or Large Gaps

SONGS U2C17 Steam Generator Operational Assessment for Tube-to-Tube Wear

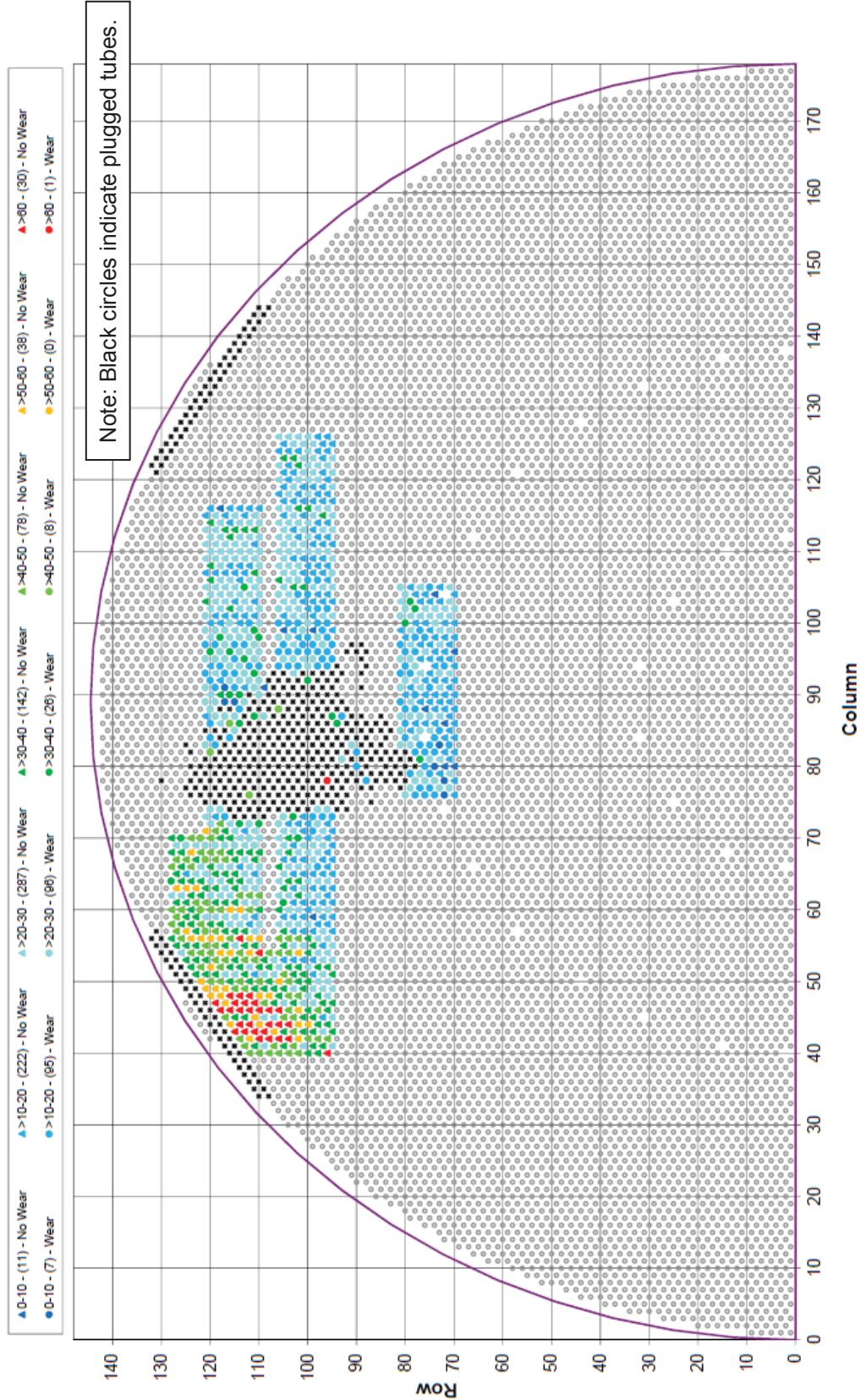


Figure 6-32: Tubesheet Map of ECT Gap Measurements, Total Gap for All AVB Locations per Tube, Unit 3, SG E-088, ISI

SONGS U2C17 Steam Generator Operational Assessment for Tube-to-Tube Wear

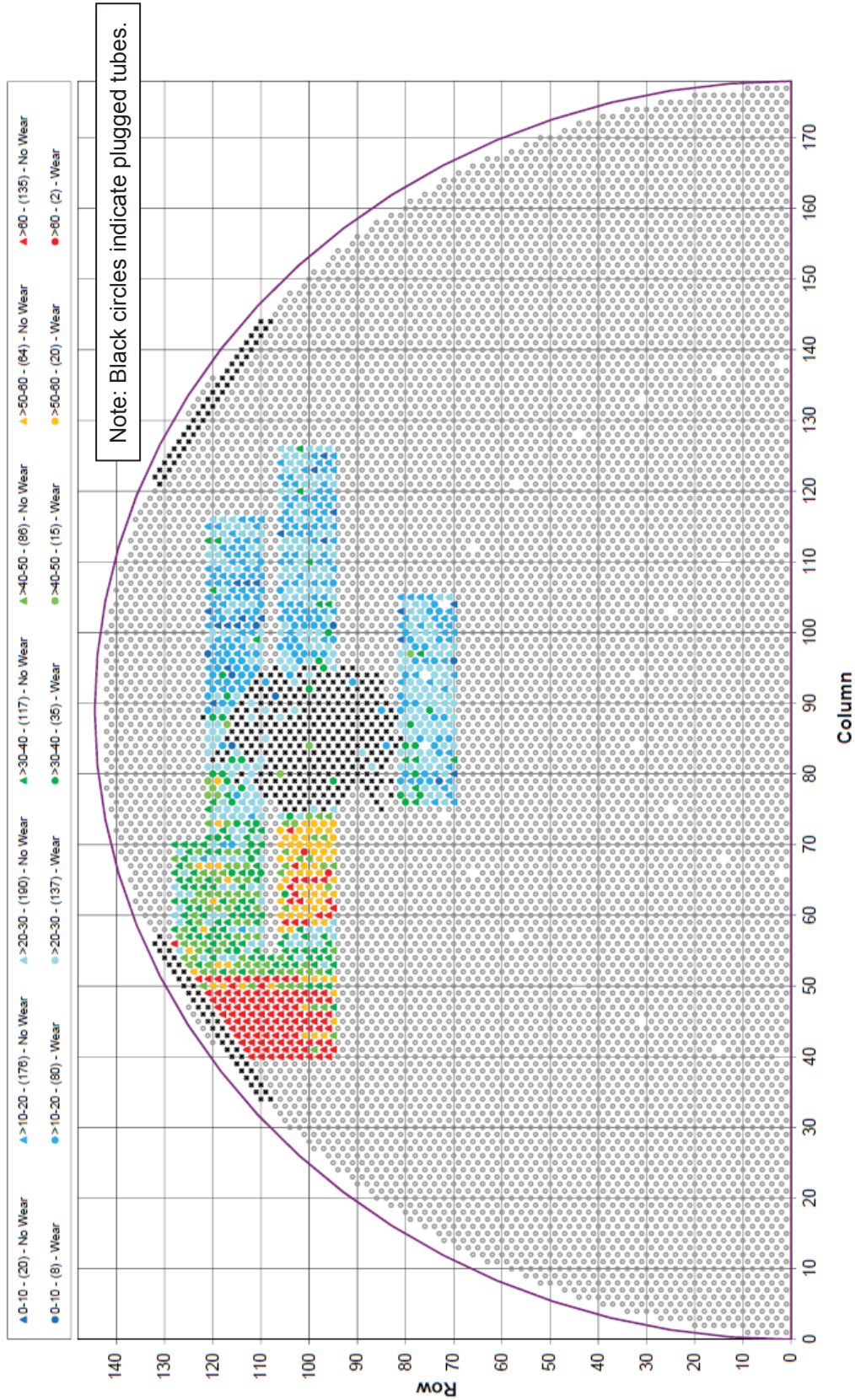


Figure 6-33: Tubesheet Map of ECT Gap Measurements, Total Gap for All AVB Locations per Tube, Unit 3, SG E-089, ISI

7.0 CRITERIA FOR EFFECTIVE VERSUS INEFFECTIVE SUPPORTS

There are no definitive criteria for effectiveness of steam generator tube supports, especially relative to the use of flat bar supports (AVBs) with large radius U-bends and in-plane fluid-elastic instability considerations. As noted in Section 4.0, extensive testing has been performed examining the in-plane support effectiveness of AVBs and large radius U-bends. The general conclusion is that AVBs with small clearances act as apparent nodal points for flow-induced tube response and have been shown by laboratory testing and operating experience to provide effective in-plane support. Westinghouse [21] has stated that no friction force is required for the in-plane effectiveness of AVB supports. In the context of turbulence induced wear the work of Pettigrew and Yetsir [24] suggests a contact force of [] as an effective support condition.

To arrive at a criteria for support effectiveness, three different expressions of force were investigated:

1. The contact force required if an equal force is applied at all 12 AVB locations.
2. Variable contact force at each AVB
3. The contact force required at one AVB if it is the only one that is resisting motion (upper bound contact force).

Each of these is explained in the paragraphs that follow.

7.1 Equal Contact Force at Each AVB

MHI has calculated the response of a large U-bend with AVB supports subjected to turbulence and fluid-elastic excitation forces. Various gap (clearances) conditions were included along with contact forces ranging from 1N to 10N (Appendix 10 of Reference [22]). An equal contact force was applied at all 12 AVB locations. The fluid-elastic excitation function was based on the work of Chen [25]. Given the uncertain nature of fluid-elastic excitation forces, a direct application of the selected excitation function to SONGS at 100% power is problematic. However the scale of the contact force that prevented in-plane vibration is highly useful. A contact force of 1N did not resist in-plane motion but a force of 10N was completely effective. Figure 7-1 is a schematic of movement amplitude versus time for a U-bend becoming fluid elastically unstable. At the instability point the energy added to the U-bend from the fluid just starts to exceed the energy dissipated in movement. From this point onward the energy and thus amplitude of U-bend motion increases continuously over time. The initial forces needed to resist in-plane motion are very low. After instability develops even large friction forces at AVB locations are easily overcome.

7.2 Variable Contact Force at Each AVB

Since support effectiveness is possible with small clearances and no contact/friction forces, expressing support effectiveness in terms of contact forces is an oversimplification of complex support/U-bend interactions. This step is taken as a matter of calculation convenience to evaluate support effectiveness. It is recognized that this purely mechanical analogue is not difficult to overstate. One step in this direction is to consider contact forces which vary from one AVB location to another rather than being equal at each location. Ideally one would wish to consider turbulence and fluid-elastic excitation forces for a very broad range of support conditions and forces. Unfortunately, considering fluid-elastic excitation forces for more than a few cases is intractable. Even if only turbulence forces are considered, the number of possible cases is staggering. Considering only 5 levels of force taken 12 at a time (for 12 AVBs) where the order matters and repeats are possible leads to 244,140,625 cases.

SONGS U2C17 Steam Generator Operational Assessment for Tube-to-Tube Wear

Even after applying engineering judgment and being highly selective this would be a daunting exercise. This is particularly true since it would have marginal utility. Ultimately, the reasonableness of the chosen support effectiveness criteria is how well it corresponds to the observed stability behavior of Units 2 and 3 when combined with contact force and stability ratio calculations to develop probability of instability projections. Another, more practical, tack has been taken; that of examining an upper bound contact force for support effectiveness when no contact forces exist at any other supports.

7.3 Single AVB Effective (Upper Bound Contact Force)

MHI has analyzed the case of a U-bend with a contact force at a single AVB location with the U-bend subjected to turbulence excitation only [26]. The contact force at one AVB needed to resist tube motion was obtained, assuming no contact forces at any other AVB location. This force depends on the AVB location, the power level and the location of the U-bend in the tube bundle. It is considered as the upper bound requirement for support effectiveness when no other contact forces are present on the U-bend. From the analysis of contact forces as described in Section 6.0 this is a very low frequency occurrence. Figure 7-2 contains a plot of upper bound contact force for support effectiveness versus AVB number and power level. These upper bound contact forces vary slightly from one position to another in the bundle. Only the average values are shown. Turbulence excitation produces a spectrum of forces on U-bends. The calculated upper bound contact force prevents motion for 97.7% of this spectrum.

7.4 Chosen Approach for the OA

Figure 7-3 is a schematic of a large U-bend with AVB locations denoted. The contact force needed for support effectiveness at one location may depend on the contact forces at other locations. Note that this is judgment from the purely mechanical analogue viewpoint, which is admittedly simplistic and in some ways conservative since a support can be effective with no contact force. Proceeding with this logic, the contact force for support effectiveness is expressed in a probabilistic fashion. A median contact force is selected (see below) for support effectiveness while the upper bound contact force for support effectiveness is taken from the MHI calculations. From the cumulative distribution of contact forces for each AVB on each tube the probability that the median force will not be met is determined. If the median force is required the support will be ineffective. The same procedure is applied to determine the upper bound probability of support ineffectiveness using the upper bound contact force.

The probability of support ineffectiveness is then estimated as [] The end result is illustrated in Figure 7-4. This is an example distribution of the probability that a given AVB on a given tube will be ineffective. []

]

In Monte Carlo simulations, the probability of support ineffectiveness []

]

SONGS U2C17 Steam Generator Operational Assessment for Tube-to-Tube Wear

[] For all of the complexity of the above discussions it turns out that that same answer for probability of instability is obtained using either the 3N-log normal distribution approach or a single contact force threshold for effectiveness of 3N. Even though the upper and lower tails of the log normal distributions are not symmetric and have a bias toward the upper tail, the end result is controlled by the median value.

7.5 Summary – Criteria for Support Effectiveness

In summary, a single contact threshold of [] was chosen for AVB support effectiveness. This threshold was chosen for two reasons: [

]

The [] threshold is applied [] All AVBs where the contact force exceeds [] are considered effective. Those that fall below 3N are considered ineffective. The total number of consecutive ineffective AVBs determines whether the tube is considered stable or unstable. This process is explained in more detail in Section 8.0.

SONGS U2C17 Steam Generator Operational Assessment for Tube-to-Tube Wear

Schematic of Vibration Amplitude Versus Time
After Onset of Fluid Elastic Instability

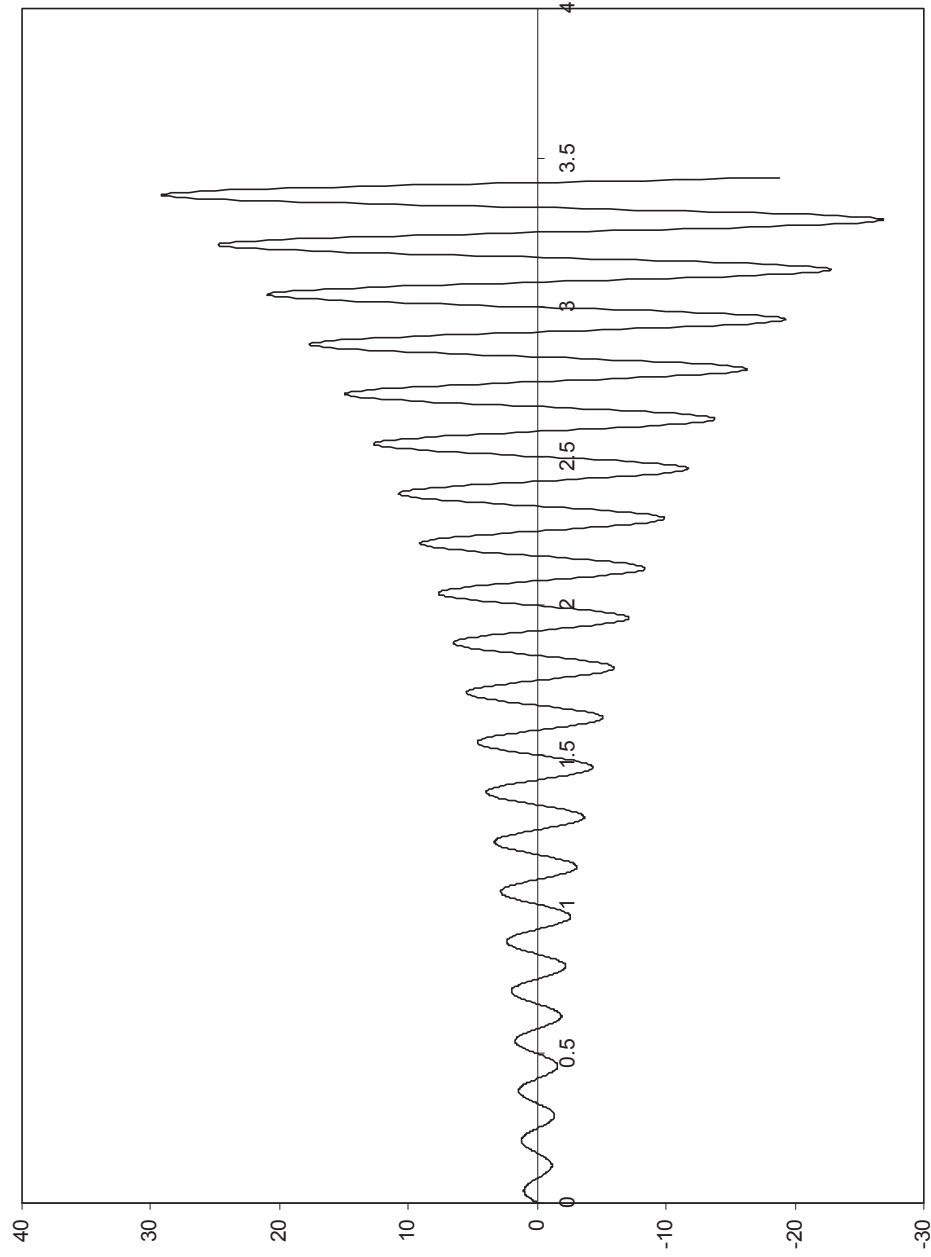


Figure 7-1: Schematic Illustration of a the Amplitude of Motion as a U-bend Becomes Unstable



SONGS U2C17 Steam Generator Operational Assessment for Tube-to-Tube Wear



U-Bend - AVB Location Schematic

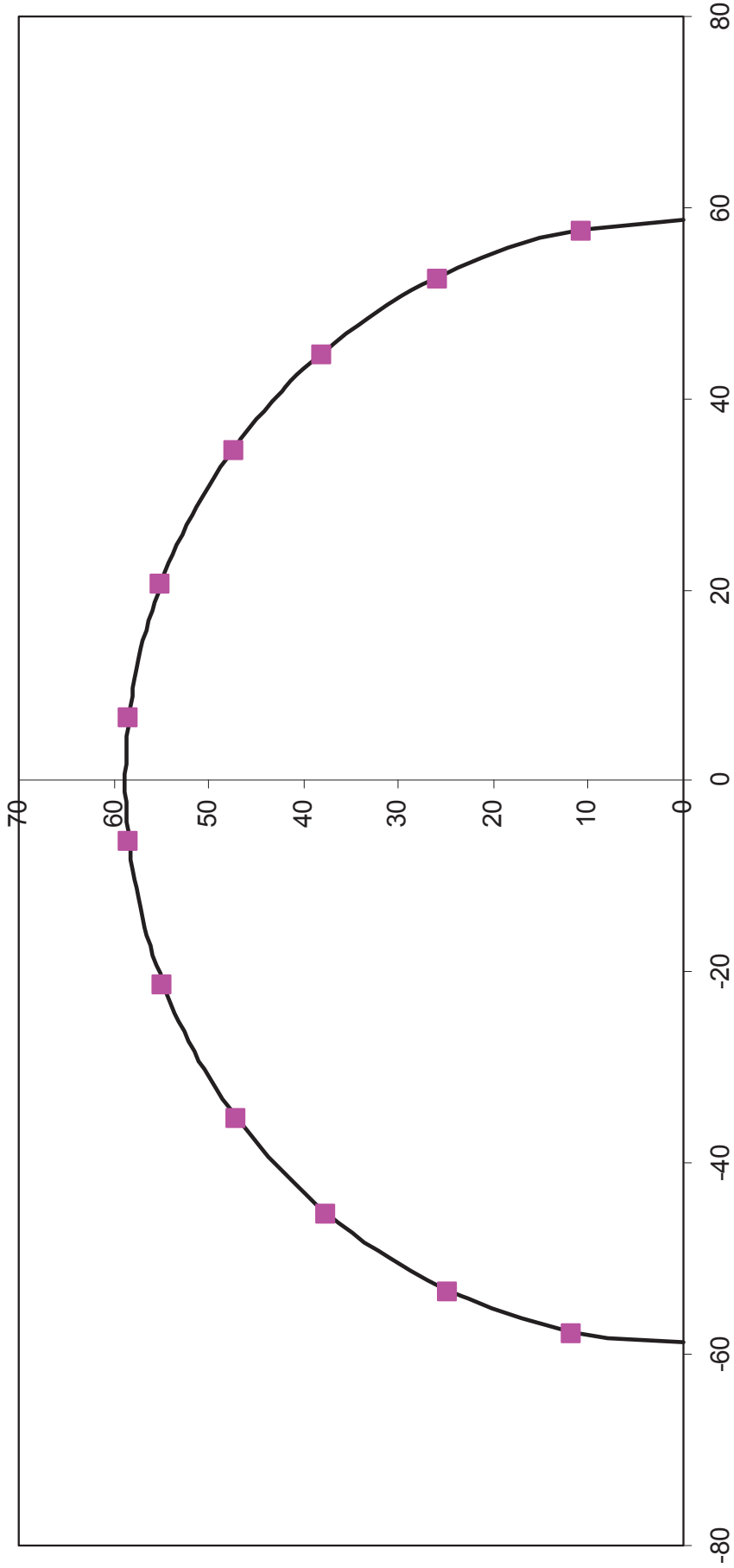


Figure 7-3: Schematic of a U-bend with AVB Locations Shown

SONGS U2C17 Steam Generator Operational Assessment for Tube-to-Tube Wear

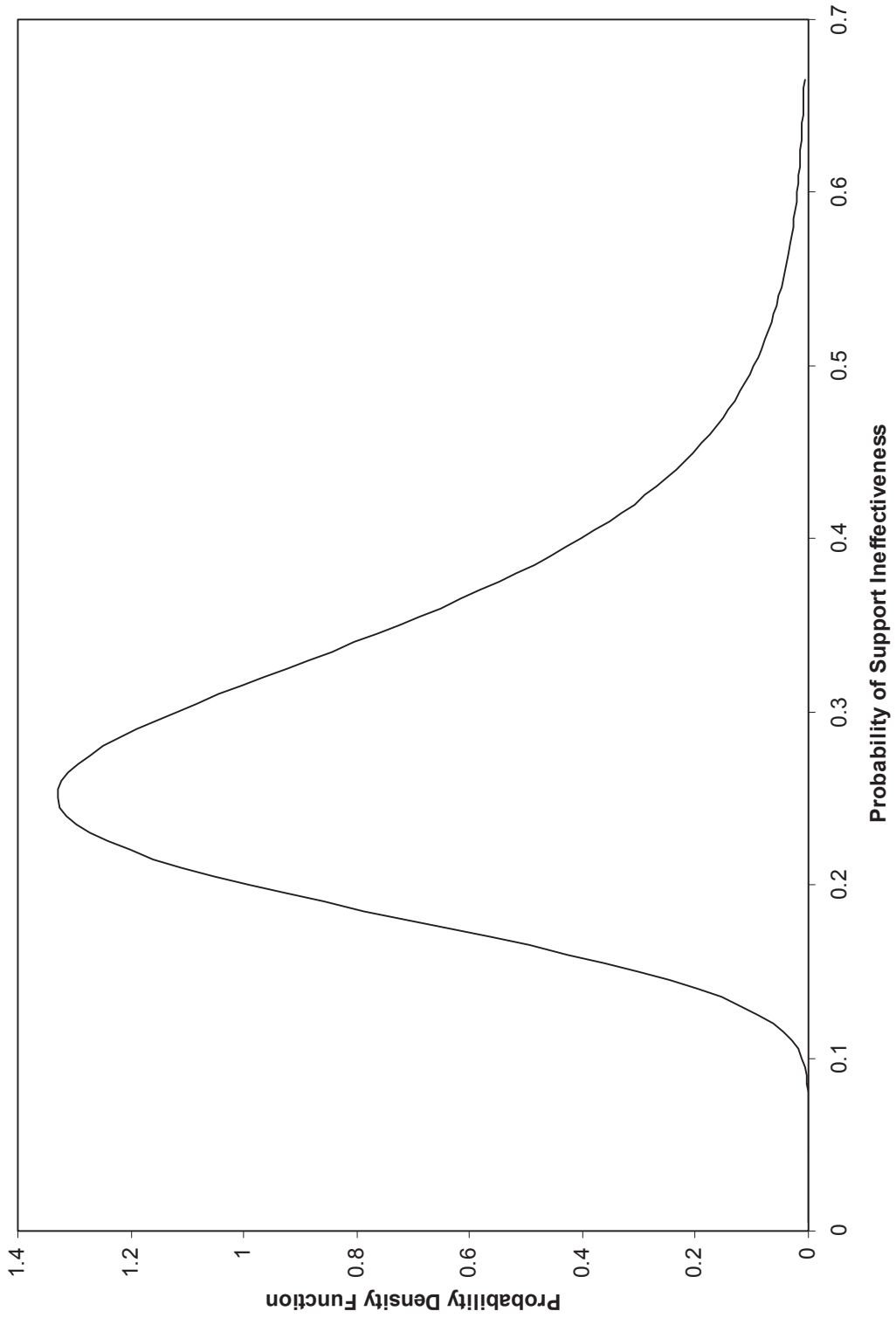


Figure 7-4: Illustrative Example of a Log Normal Distribution of the Probability of Support Ineffectiveness

SONGS U2C17 Steam Generator Operational Assessment for Tube-to-Tube Wear

8.0 PROBABILITY OF INSTABILITY RESULTS

The material presented in Section 5.0 on stability ratios demonstrated that all tubes are stable ($SR < 1$) at 70% power with a probability of 0.95 at 50% confidence without any effective in-plane supports. No TTW will develop and thus the operational assessment goal of meeting structural and leakage integrity requirements with 0.95 probability at 50% confidence is met. Probability of instability calculations are used only to demonstrate margin. The desired margin is a projected maximum stability ratio of 0.75 with 0.95 probability at 50% confidence over the next inspection interval of 5 months. Some effective in-plane supports are needed to maintain a stability ratio of 0.75. In the most limiting case, 4 effective supports are required. This requirement applies to approximately 120 U-bends. See Figure 5-10. Note that all U-bends are considered in probability calculations, including plugged tubes with split stabilizers inserted.

Wear at AVB locations will degrade in-plane support effectiveness over time. The essentially stable behavior of Unit 2, with only two tubes arguably unstable at 100% power at EOC 16, shows that no more than 5 supports were ineffective (Figure 5-6). Immediately after restart at 70% power, stability ratios less than 0.75 are expected. The question of interest is the length of operating time it takes for wear at AVBs to degrade support effectiveness to the point where the probability of a maximum stability ratio of 0.75 is greater than 0.05. The following paragraphs describe the procedure for calculating the probability of instability.

As noted earlier, calculations of the probability of instability is straightforward in principle. The development of in-plane fluid-elastic instability of U-bends depends on four factors. These are:

- Location in the bundle
- Operating power level
- Number of consecutive ineffective supports
- Operating time

These factors affect stability ratios. Support effectiveness in-plane is defined in terms of contact forces at AVB locations. The number of consecutive ineffective supports can change over time as AVB wear reduces contact forces. Descriptions of stability ratios, contact forces at AVB locations and criteria for determining support effectiveness are provided in previous sections. This is the information required to compute the likelihood of encountering in-plane fluid-elastic instability at a given power level as a function of operating time.

The probability of instability is computed using a Monte Carlo approach. One Monte Carlo trial of all tubes in a steam generator is constructed in the following manner:



SONGS U2C17 Steam Generator Operational Assessment for Tube-to-Tube Wear

7. Whether or not the steam generator contains any unstable U-bend in one Monte Carlo trial of the steam generator is recorded.
8. Typically 10,000 Monte Carlo trials of a steam generator are performed. In this case the probability of instability is simply the number of trials where the steam generator contained one or more unstable tubes divided by 10,000.

Several independent programs use mathematically equivalent algorithms to compute the probability of instability. In this case, probability calculations were performed using [] [27]. Independent checks of test cases were performed to verify the methodology using an independent []

Figure 8-1 illustrates the first step in constructing one Monte Carlo trial for a full bundle. The cumulative distribution, CDF, of contact forces for a given AVB location at a given position in the bundle is examined. If a single contact force for support effectiveness is used, for example [], the value of the CDF curve at [] provides the probability that the support will be ineffective. This is true because the value of the CDF curve at [] is the fraction of the total population of contact forces that are equal to or less than 3N. In this case, the support is considered effective if the contact force is any value greater than []. The value of the CDF curve at [] is termed the probability threshold for support ineffectiveness. Support effectiveness for a given AVB on a given tube is determined by selecting a random number from a uniform distribution from 0 to 1. If this value is above the probability threshold for support ineffectiveness the support is effective. If it is equal to or below the threshold, the support is ineffective.

The above is an example of a single parameter criterion for support effectiveness. []

]

The first step is the crucial step in the Monte Carlo trial. It is repeated for all AVB locations in a particular U-bend. []

]

SONGS U2C17 Steam Generator Operational Assessment for Tube-to-Tube Wear

[

]

Before proceeding to probability of instability results for Units 2 and 3, it is worthwhile to examine the actual stability behavior of the two units. There are only 4 data points to consider. With all the caveats attending an extremely small sample size, it is a necessary exercise. Both steam generators in Unit 3 exhibited an advanced state of unstable behavior after 11 months of operation. In contrast, only one steam generator in Unit 2 exhibited “incipient instability” after 22 months of operation. Two out of two observations of instability in Unit 3 at 11 months leads to a 50% confidence estimate of probability of instability of 0.71 ($0.71 \times 0.71 = 0.5$). This would be a minimum expected value since TTW estimates place the onset of instability near the beginning of the operating interval. Thus a probability somewhere near 0.7 early in life is expected. For Unit 2, with one out of two observations of instability at 22 months the 50% confidence estimate of probability of instability is 0.29. This would place the occurrence of no instability in either steam generator as a 50/50 proposition ($(1-0.29) \times (1-0.29) = 0.5$) and the chance of instability occurring in both steam generators at 22 months at a probability of 0.08 ($0.29 \times 0.29 = 0.08$).

The other point regarding the observed stability behavior is the location in the tube bundle where instability first developed. This is taken to be near the maximum observed TTW depths. These observations regarding actual stability behavior provides a means of evaluating the reasonableness of probability of instability calculations. Calculated probabilities should be in reasonable agreement with observed behavior.

Figure 8-3 provides a summary of probability of instability calculations. Figure 8-3 requires careful reading of the notes and legends. It traces the probability of instability versus time for Units 2 and 3. All results are based on 95th percentile stability ratios. First consider results for the probability of instability versus time for 100% power and instability defined as a stability ratio of 1 or more. This serves as a check of results to be reported for a stability ratio of 0.75 which is the main item of interest, that is, demonstrating margin. [

]

Unit 2 has more substantial contact forces and is much more resistant to loss of support effectiveness due to wear at AVB locations. After 22 months, the calculated probability of instability is about 0.85. The intermediate point at 12 months is near 0.3. Both of these values are high and thus conservative. This is judged to be the effect of an underestimation of contact forces. [

]

SONGS U2C17 Steam Generator Operational Assessment for Tube-to-Tube Wear

Before proceeding to a drop in power from 100% to 70%, it is of interest to check the predicted most likely locations of first instability at 100% power. Projections are shown in Figure 8-4 for Unit 3 and in Figure 8-5 for Unit 2. The hotter (yellow and red) colors are the more likely locations of first instability. The U-bends plotted have the largest TTW depths. Overall, calculated locations where first instability will occur agree very well with observations. This re-enforces the reasonableness of the probability of instability calculations and supports the reliability of the probabilistic argument for margin in terms of maintaining a stability ratio less than 0.75.

As noted above, a drop to 70% power makes all U-bends stable, $SR < 1$, with no effective in-plane supports using the 95th percentile stability ratio calculations. Since no effective in-plane supports are required, wear at AVB locations over time is not an issue. Stability will be maintained indefinitely.

The desired margin for stability is a projected maximum stability ratio of 0.75 with 0.95 probability at 50% confidence over the next inspection interval of 5 months. The green line in Figure 8-3 shows that a maximum stability ratio of 0.75 will be maintained with 0.95 probability at 50% confidence for 8 months after restart at 70% power. Note that this is the same as stating the probability of instability for $SR = 0.75$ or greater is less than or equal to 0.05. That is, the green line on Figure 8-3 is below the red line, 0.05 probability, for 8 months. This is a conservative demonstration of margin. The probability of instability at 100% power for $SR \geq 1$ is conservatively high. This means support effectiveness is better than calculated at both 100% power and even then more so at 70% power. Recall the demonstrated stability at 100% power at EOC 16 necessitated that there were no more than 4 consecutive ineffective supports in the worst case region. Hence stability immediately upon restart as 70% power even for stability in terms of $SR \leq 0.75$ is required. The calculated probability of instability at $SR \geq 0.75$ immediately upon restart is 0.012; it is not zero because for an SR threshold of 0.75 there is a population of tubes that require between 1 and 3 effective AVBs to be stable, and the random gap distributions input to the Monte Carlo trials produce this condition for the susceptible population of tubes a small percentage of the time. [

]

With no effective in-plane supports the stability ratio of the two tubes with TTW, R111 C81 and R113 C81 in SG 2-89, is 0.88 at 70% power (Attachment 5 of [20]). It is an open question as to how many supports were effective at 100% power. It is highly likely that there are not 9 consecutive ineffective supports on these tubes under the moderate conditions of 70% power. Substantial margins are demonstrated at 70% power as the probability of maintaining a maximum stability ratio of 0.75 is greater than 0.95 for 8 months with conservative calculations. Other items of conservatism in the analysis are projected wear depth growth rates at AVB locations based on a constant rate of volume loss at levels observed at 100% power and the use of a support effectiveness criteria at 70% power that is effectively the same as at 100% power. In this later context, it is noted that use of the single parameter criteria for support ineffectiveness at [] provides essentially the same probability of instability as use of the log normal distribution of probability of support ineffectiveness with a [] median value and an upper tail based on the upper bound contact force for support ineffectiveness.

One final item is needed for completeness, although the answer is obvious based on the results for a stability ratio threshold of 0.75. Long term stability at 70% power was argued in Section 5.0 even for a 99th percentile stability ratio calculation. With the 99th percentile stability ratios and stability based on $SR \geq 1$, the probability of instability for 12 months after restart is 0.0001. Long term stability will be maintained and large margins are conservatively demonstrated.



SONGS U2C17 Steam Generator Operational Assessment for Tube-to-Tube Wear





SONGS U2C17 Steam Generator Operational Assessment for Tube-to-Tube Wear





SONGS U2C17 Steam Generator Operational Assessment for Tube-to-Tube Wear



SONGS U2C17 Steam Generator Operational Assessment for Tube-to-Tube Wear

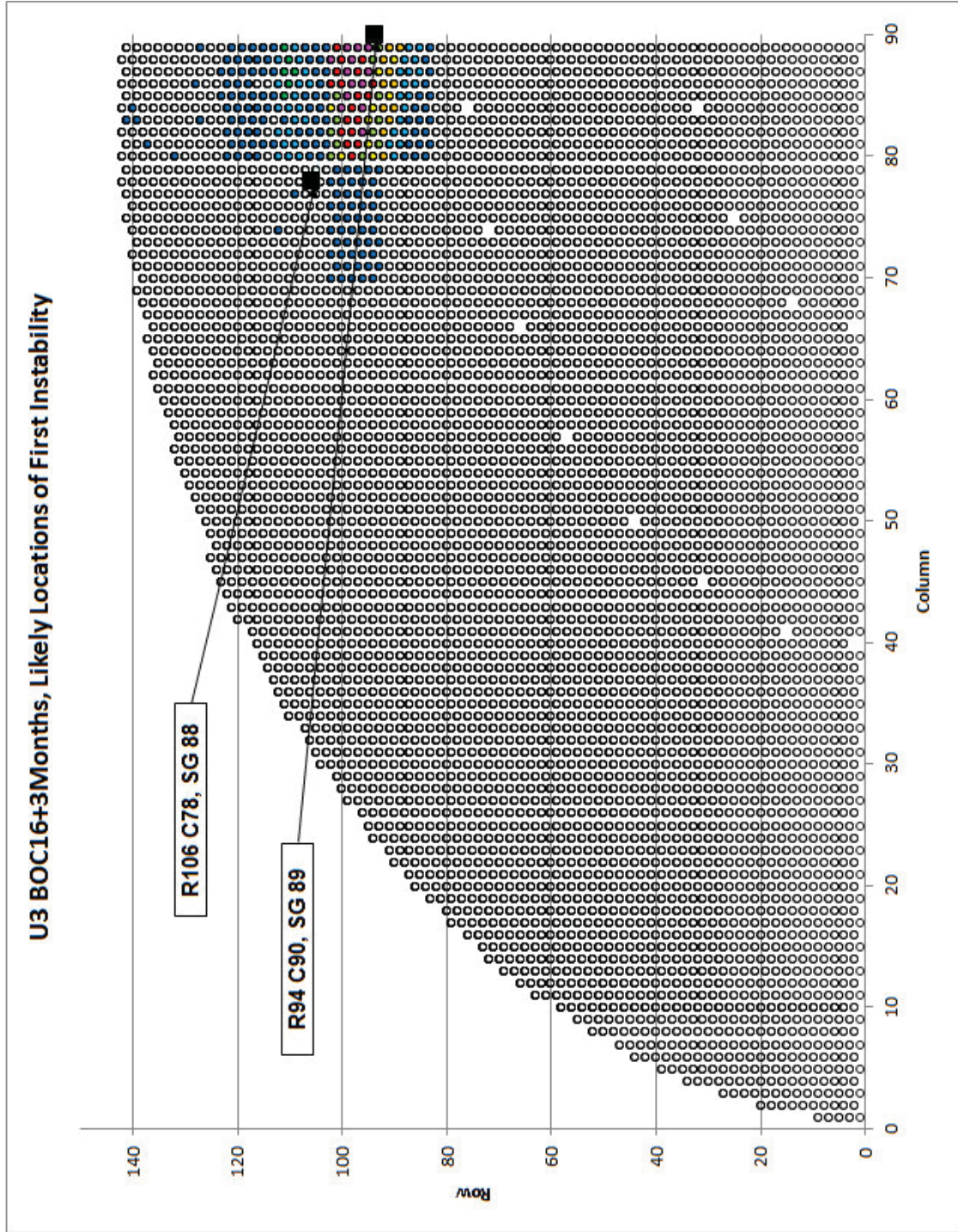


Figure 8-4: Map of Calculated Frequency of Occurrence of In-plane Instability, Unit 3

SONGS U2C17 Steam Generator Operational Assessment for Tube-to-Tube Wear

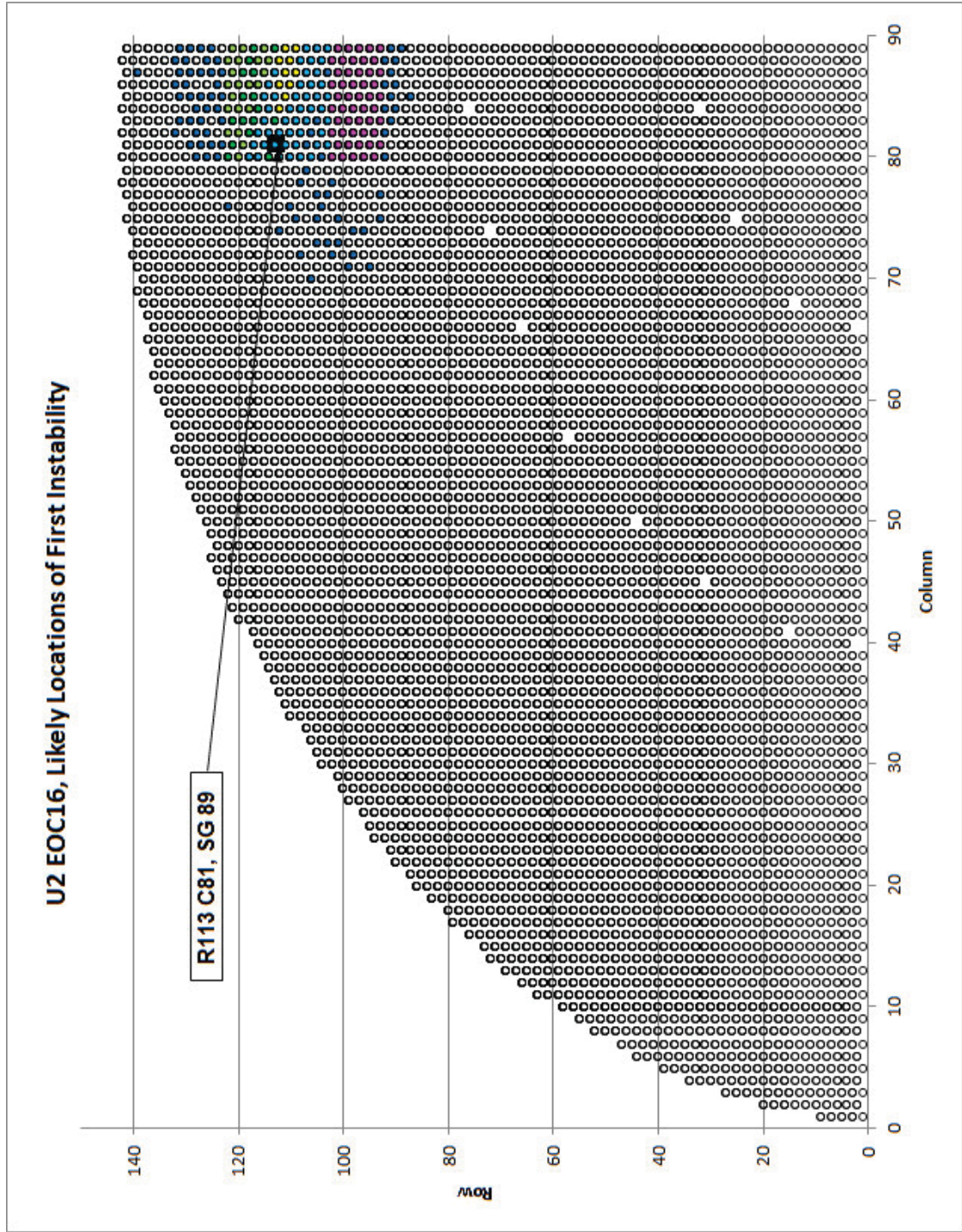


Figure 8-5: Map of Calculated Frequency of Occurrence of In-plane Instability, Unit 2

SONGS U2C17 Steam Generator Operational Assessment for Tube-to-Tube Wear

9.0 DEFENSE-IN-DEPTH

Defense in depth measures relative to TTW in Unit 2 add to the assurance that structural and leakage integrity requirements will be maintained throughout the next inspection interval. These measures go beyond the technical case for restart of Unit 2 at 70% power. A decrease in power to the 70% level returns the steam generators back inside the operational envelop of demonstrated successful performance and assures stability without dependence on any effective in-plane supports. Thus structural and leakage integrity of steam generator tubing is demonstrated. Also, substantial margins have been shown. Still, conservatism demands that the question of the consequences of developing in-plane fluid-elastic instability be addressed. Defense in depth measures are in place to mitigate these consequences if needed in extremis.

Tubes with a high risk of developing FEI, based on AVB wear patterns similar to those of unstable tubes in Unit 3, have been plugged. Wire cable stabilizers have been inserted. Figure 9-1 and Figure 9-2 show tubesheet maps, for Unit 2 SG E-088 and SG E-089 respectively, of tubes preventively plugged for increased susceptibility to in-plane FEI. If FEI occurs, the location will most likely be in the high risk region. Then FEI must progress through a buffer zone of plugged tubes to reach pressurized, in service tubes. From probability calculations this process of instability zone expansion took about 7 months to develop in Unit 3. Only at this point is an in-service pressurized tube driven to instability with consequent development of TTW. Only when instability develops for an in-service tube does structural and leakage integrity begin to be challenged. The preventive plugging patterns shown in Figure 9-1 and Figure 9-2 are based solely on AVB wear patterns in each given tube not a buffer zone concept based on possible instability zone expansion. Therefore there are gaps in the buffer zone. Consequently the time for possible instability zone expansion in Unit 2 at 70% power is reduced to half of the 7 month estimate from Unit 3. It is estimated at 3.5 months.

The function of the wire cable stabilizers is to prevent tube severance in plugged tubes should instability and instability zone expansions develop. Stabilizers provide additional damping for large amplitudes of motion of U-bends and this will mitigate TTW growth rates to some degree. After instability, deep wear scars can develop over time at the 48° U-bend positions on the hot leg and cold leg as well as at the top tube support plate. [

] Stabilizers will prevent the generation of large loose parts if instability and instability zone expansion occurs.

With the assumption of instability and the subsequent instability zone expansion, eventually an in-service pressurized tube will be driven to instability. TTW will occur over time to an extent challenging structural and leakage integrity. For SONGS Unit 2, the SIPC is that the worst case projected wear will not lead to a tube burst at 3 times the normal operating differential pressure, $3\Delta P$. [

] The actual physical wear depth associated with meeting the SIPC is approximately []. For information purposes, the wear depth leading to failure at SLB conditions is [] and a tube burst at NOPD requires degradation that is []. These values are based on very long, uniformly deep wear scars such as is expected from TTW.

Now the question of interest is “After TTW begins how long does it take to reach an unacceptable level of wear depth?”. After 11 months of operation of Unit 3 the TTW depths of 3 tubes, based on ECT results, exceeded 75% TW. Estimates of wear depth growth rate for the tube with the worst case depth, R106 C78 in Unit 3, SG 3-88 were developed using three different approaches:

SONGS U2C17 Steam Generator Operational Assessment for Tube-to-Tube Wear

- Simple estimates
- Dynamic (time domain) modeling of U-bend impact with spring loaded contact areas under turbulence and fluid-elastic excitation.
- Dynamic (time domain) finite element analysis of one U-bend impacting a neighboring U-bend employing a parametric study of forcing function amplitude, conventional damping, and Coulomb (friction) damping during U-bend to U-bend contact.

Results are summarized below. More details are provided in Appendix A for the simple estimates and FEA dynamic analysis of one U-bend impacting its neighboring U-bend. Dynamic modeling of a U-bend impacting spring loaded contact areas is described in Appendix 10 of Reference [20]. All of these analyses assume that the TTW coefficient is the same as determined in wear tests of Alloy 690 wear couples in a secondary side environment under tests conditions (including SONGS SGs) appropriate for turbulence induced wear at AVB locations. It is an open question as to whether or not these wear coefficients are directly applicable to the higher loads and much larger single event sliding distances that are present with tube-to-tube impacts.

Dynamic modeling of a U-bend impacting spring loaded contact areas indicated that work rates and thus volumetric loss rates are consistent with the development of the worst case wear depth in approximately 11 months. This would be consistent with instability beginning in Unit 3 shortly after start-up. Simple estimates of wear rates with consideration of uncertainties in impact forces and wear coefficients set the range of worst case TTW occurring between 2.5 and 11 months. Sophisticated parametric dynamic FEA analysis of one U-bend impacting another show that contact forces and contact lengths vary from one impact event to another and vary even during an impact event. Contact forces were shown to be highly dependent on how tightly a neighbor tube is held in place by its own AVBs as it is impacted by an unstable tube. Further, evaluation of elongated wear scars at AVB locations reveals that the worst case tube, Unit 3 SG E-088 R106 C78, had a substantial amplitude of motion during instability to the point where two outboard neighbors (higher row same column) and two inboard neighbors had to be involved in impact events due to the motion of tube R106 C78. This multiple tube event was not included in any wear estimate. Given these uncertainties the estimated range of wear time for the worst case flaw remains between 2.5 and 11 months after an in-service pressurized tube becomes unstable.

The defense in depth argument then is a combination of time for instability zone expansion (3.5 months) and wear time of an in-service pressurized tube (2.5 months) driven to instability at the boundary of the expansion zone. Under the assumption that instability at 70% power begins immediately upon restart, a highly improbable circumstance, the minimum estimate for time to violate structural and leakage integrity requirements in an unplugged tube is 6 months. This is longer than the planned operating time of 5 months. This is not unreasonable given the extremely conservative assumption of instability occurring immediately upon restart at 70% power.

SONGS U2C17 Steam Generator Operational Assessment for Tube-to-Tube Wear

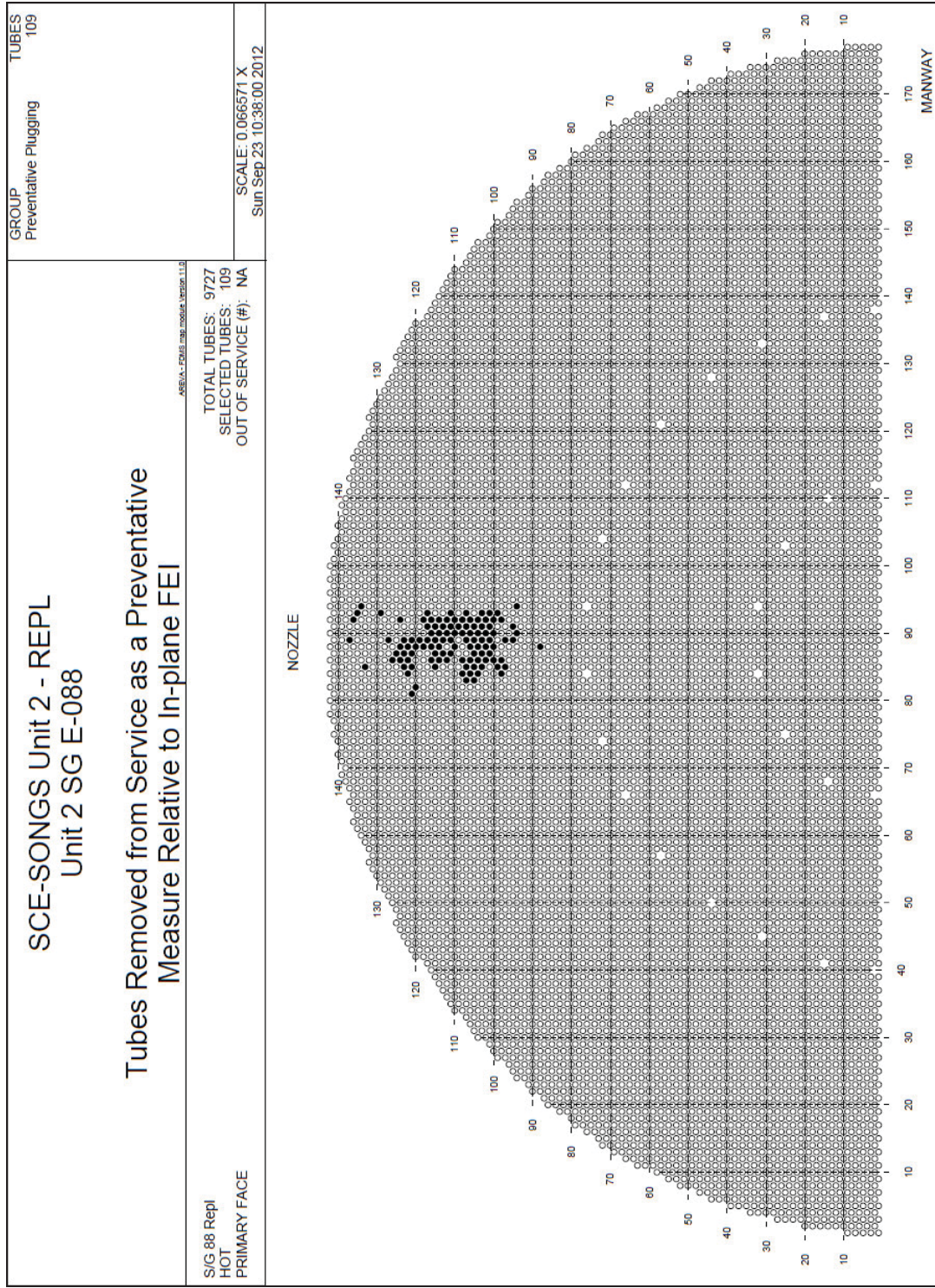


Figure 9-1: Tubes Removed from Service as a Preventative Measure Relative to In-plane FEI, Unit 2 SG 2-88

SONGS U2C17 Steam Generator Operational Assessment for Tube-to-Tube Wear

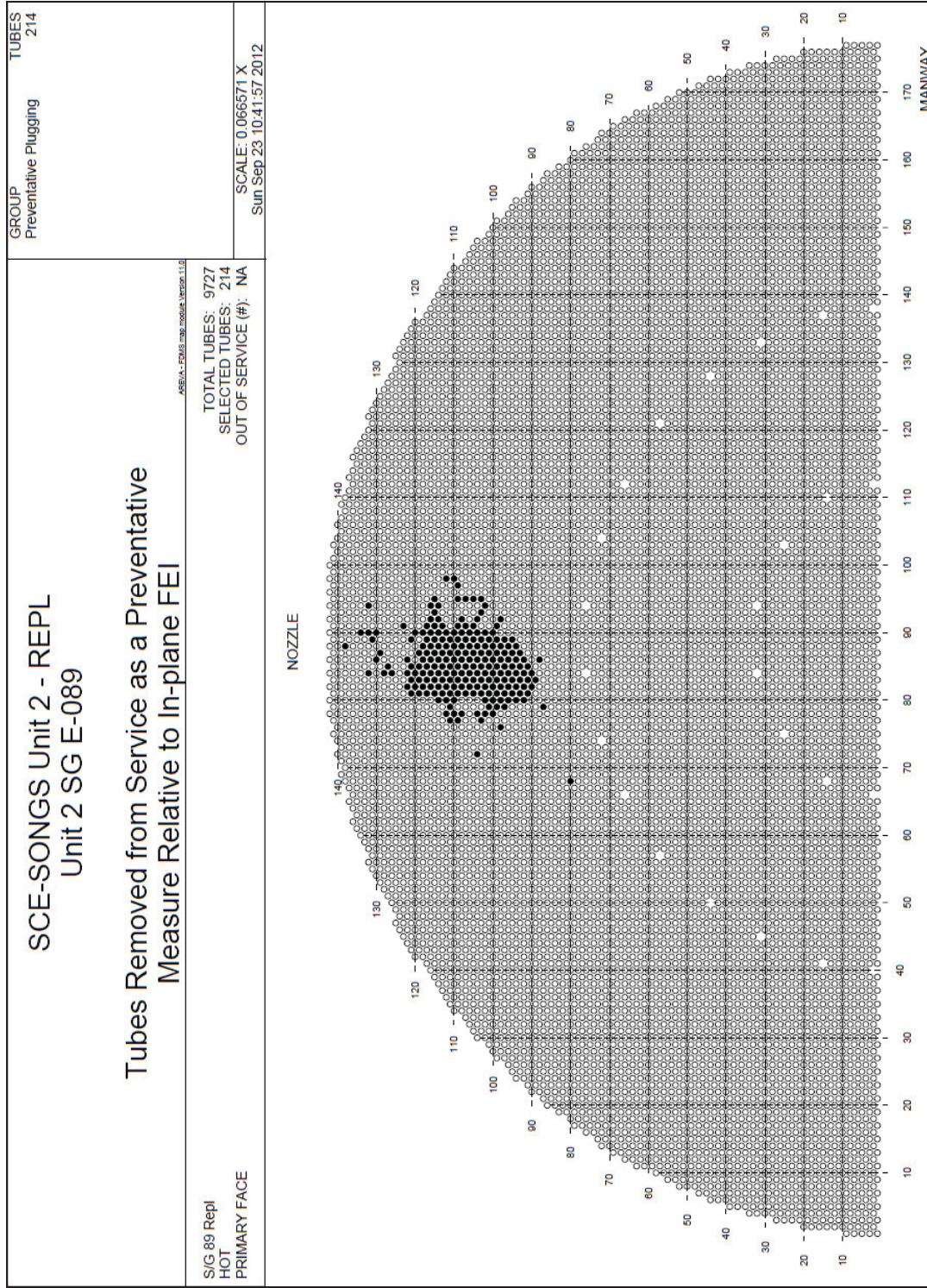


Figure 9-2: Tubes Removed from Service as a Preventative Measure Relative to In-plane FEI, Unit 2 SG 2-89

10.0 CONCLUSIONS

In accordance with the SONGS technical specifications and EPRI Steam Generator Integrity Assessment Guidelines [2], an operational assessment (OA) was performed to ensure that steam generator (SG) tubing will meet established performance criteria for structural and leakage integrity during the operating period prior to the next planned inspection. A conservative approach to prevent the occurrence of TTW ensures that tube integrity requirements will be met with the required probability of 0.95 at 50% confidence. A 70% operating power level returns the Unit 2 steam generators to within the operational envelope of demonstrated successful operation of U-tube nuclear steam generators relative to in-plane fluid-elastic stability. Operation at 70% power assures in-plane stability ($SR < 1$) without dependence on any effective in-plane supports for U-bends. Without the development of in-plane instability no TTW will occur and thus structural and leakage integrity requirements are met.

Since stability at 70% power does not depend on any effective in-plane supports, detailed probabilistic calculations are only relevant to the demonstration of margin and conservatism. A maximum stability ratio of 0.75 will be maintained for 8 months at 70% power with a probability of 0.95 at 50% confidence. A conservative probabilistic analysis demonstrates substantial margin for the planned 5 month operating interval. Additionally, defense in depth measures in terms of preventive tube plugging with wire cable stabilizers in plugged tubes, provides for maintenance of tube integrity under the extreme assumption that instability at 70% power begins immediately upon restart. The minimum estimate for time to violate structural and leakage integrity requirements in an unplugged tube is 6 months based on instability zone expansion from higher risk plugged tubes out to an unplugged tube and then wear of the unplugged tube.

SONGS U2C17 Steam Generator Operational Assessment for Tube-to-Tube Wear

11.0 REFERENCES

1. SONGS Steam Generator Program, S023-SG-1.
2. EPRI Report 1019038, “Steam Generator Management Program: Steam Generator Integrity Assessment Guidelines: Revision 3”, November 2009.
3. SONGS Technical Specifications Sections 5.5.2.11, “Steam Generator (SG) Program,” Amendment 220.
4. SONGS Technical Specifications Section 3.4.13, “RCS Operational Leakage,” Amendment 204.
5. NEI 97-06, “SG Program Guidelines”, Rev. 3, January 2011.
6. AREVA Document 51-9182833-002, “SONGS 2C17 Outage – Steam Generator Operational Assessment” (SONGS Document 1814-AU651-M0144 Rev. 1).
7. AREVA NP Document 51-9176667-001, “SONGS 2C17 & 3C17 Steam Generator Degradation Assessment.”
8. SONGS Drawing SO23-617-1-D116 Rev. 2, “San Onofre Nuclear Generating Station Unit 2 & 3 Replacement Steam Generators – Design Drawing – Tube Bundle 1/3” (MHI Drawing L5-04FU051 Rev. 1).
9. SONGS Drawing SO23-617-1-D507 Rev. 5, “San Onofre Nuclear Generating Station Unit 2 & 3 Replacement Steam Generators – Design Drawing – Anti-Vibration Bar Assembly 1/9” (MHI Drawing L5-04FU111 Rev. 2).
10. SONGS Drawing SO23-617-1-D542 Rev. 9, “San Onofre Nuclear Generating Station Unit 2 & 3 Replacement Steam Generators – Design Drawing – Anti-Vibration Bar Assembly 7/9” (MHI Drawing L5-04FU117 Rev. 9).
11. Root Cause Evaluation, San Onofre Nuclear Generating Station, Condition Report: 201836127, “Unit 3 Steam Generator Tube Leak and Tube-to-Tube Wear”, Revision 0, 5/7/2012.
12. AREVA NP Document 51-9180143-001, “SONGS Unit 3 February 2012 Leaker Outage – Steam Generator Condition Monitoring Report” (SONGS Document 1814-AU651-M0143 Rev. 1).
13. AREVA NP Document 51-9181604-000, “SONGS Unit 2 Cycle-17 and 2012 Return to Service Technical Summary Steam Generator Eddy Current Inspection.”
14. AREVA NP Document 51-9188725-000, “SONGS U2C17 and U3F16B AVB Gap and Tube-to-Tube Proximity Measurement Program” (SONGS Document 1814-AU651-M0151 Rev. 0).
15. Au-Yang, M. K., “Flow Induced Vibration in Power and Process Plant Components”, ASME Press, New York, 2001.
16. Weaver, D.S. and Schneider, W., “The effect of Flat Bar Supports on the Crossflow Induced Response of Heat Exchanger U-Tubes,” *Journal of Engineering for Power*, Vol. 105, October 1983, pp. 775-781.

SONGS U2C17 Steam Generator Operational Assessment for Tube-to-Tube Wear

17. Janzen, V.P., Hagberg, E. G., Pettigrew, M. J., and Taylor, C. E., “Fluidelastic Instability and Work-Rate Measurements of Steam-Generator U-Tubes in Air-Water Cross-Flow,” *Journal of Pressure Vessel Technology*, Vol. 127, February 2005, pp. 84-91.
18. SONGS Document 90200, Rev. 0. Average and Maximum Thermal-Hydraulic Parameter Comparisons between Songs RSGs and Similar Plants.
19. Heat Exchanger Design Handbook, 1st Edition, Kuppan, CRC Press, 2000.
20. SONGS Document SO23-617-1-M1523 Rev. 5, “Replacement Steam Generators, Evaluation of Stability Ratio for Return to Service” (MHI Document L5-04GA567 Rev. 6).
21. SONGS Document 1814-AA086-M0189 Rev. 2, Westinghouse Report LTR-SGDA-12-36 Rev. 0, “Flow-Induced Vibration and Tube Wear Analysis of the San Onofre Nuclear Generating Station Unit 2 Replacement Steam Generators Supporting Restart.”
22. SONGS Document SO23-617-1-M1520 Rev. 6, “Tube Wear of Unit-3 RSG – Technical Evaluation Report” (MHI Document L5-04GA564 Rev. 8).
23. AREVA NP Document 51-9182368-002, “SONGS 2C17 Steam Generator Condition Monitoring Report.”
24. Pettigrew, M. J. and Yetisir, M., “A Simple Approach to Assess Fretting-Wear Damage,” 4th CNS International Steam Generator Conference, Toronto, Ontario, Canada, May 5-8, 2002.
25. Chen, S. S., “Instability Mechanisms and Stability Criteria for a Group of Circular Cylinders Subjected to Cross-Flow, Part 2: Numerical Results and Discussions, *Journal of Vibration, Acoustics, Stress and Reliability in Design*, April, 1983, Vol. 105, pp 253-260.
26. SONGS Document SO23-617-1-M1532 Rev. 2, “Analytical Evaluations for Operational Assessment (MHI Document L5-04GA585 Rev. 2).
27. AREVA NP Document 32-9187024-000, “SONGS Steam Generator Probability of Fluid Elastic Instability Calculation.”

References 1, 3, 4, 8, 9, 10, 11, 18, 20, 21, 22, 24, and 27 are available from Southern California Edison (SCE) and are approved for use as required by AREVA NP procedure 0402-01. See signature page for the Project Manager’s approval signature.

APPENDIX A: ESTIMATES OF FEI-INDUCED TTW RATES

A.1 Simple Estimates of the Maximum TTW Rate

The maximum volume loss as a result of TTW in Unit 3 is 0.123 inches³. This was obtained by integration of the measured wear depth versus length profile with appropriate consideration of the cylindrical tube geometry. A site specific TTW eddy current standard was used to optimize wear depth measurement accuracy. The time to develop a volume loss of 0.123 inches³ can be estimated using Archard’s rule. From Archard’s rule the wear volume is given by the wear coefficient, k, times the work rate times the wear time. Following standard practice the work rate for wear is taken as the product of normal force and sliding distance per unit time.



MHI Proprietary

- Pre-instability formation of the wear scar followed by loss of contact with the tube.
- Post-instability formation or elongation of the wear scar but with a limited AVB width in contact with the tube such as is produced by AVB twist.

Figure A-1 demonstrates that wear elongation at one AVB location can be used to calculate tangential displacements at other locations on the same tube. This calculation provides the sliding distance of interest.

The deepest TTW is observed in Unit 3, SG E-088, tubes R102 C78, R104 C78 and R106 C78. There are no elongated wear scars on tube R102, C78 and R106 C78. These are likely unstable driving tubes. There are elongated wear scars on tubes R100 C78, R104 C78 and R108 C78. These are likely tubes that were initially stable but driven to instability by repeated impacts from neighbor tubes. Tube R108 C78 has elongated wear scars at multiple locations. At AVB 8 the wear length is 1.28 inches, which is the longest wear scar on this tube. Assuming the tube is in contact with the AVB over its full width of 0.6 inches leads to an elongation of 0.68 inches at this location. This is caused by tangential displacements resulting from impacts with tube R106 C78. Half of the elongation of wear at AVB 8 is produced as the tube is forced toward the cold leg with the other half

SONGS U2C17 Steam Generator Operational Assessment for Tube-to-Tube Wear

generated as the tube is forced toward the hot leg. The tangential displacement of a U-bend at AVB 8 is 0.34 inches for a single impact event. The two centers of impact as a tube swings to and fro in Mode 1 are 48° up the semicircular portion of the U-bend from either the hot leg or cold leg. From the mode shape a tangential displacement of 0.34 inches at AVB 8 translates to a tangential displacement of 0.21 inches at the impact location. The sliding distance in TTW is twice the tangential displacement of the driving tube relative to the initial impact point with the neighbor tube to the maximum extent of tangential movement during the impact event. It is twice the value since the driving tube slides to the maximum extent and then back to the point of initial contact. During sliding the normal contact force increases from zero to a maximum and then back to zero. Elongation of wear scars sets the scale for the level of displacements involved. In actuality the driving tube impacts a neighbor with some degree of restriction to movement other than inertia. Both U-bends are deforming and moving. Determination of the actual sliding distance requires a dynamic rather than a static analysis. It is nonetheless useful to consider a static approximation. A sliding distance 0.21 inches is estimated in terms of a tangential displacement relative to a stationary point.

With a sliding distance estimated from eddy current measurements of elongated wear scars all that is needed to calculate a work rate is an estimate of the normal force required to produce the observed displacements. Figure A-2 shows the displacements generated by a radial load applied at the impact location as determined via an FEA model of the U-bend. For convenience in modeling, the U-bend is fixed at the top support plate. Modeling the entire tube with gap elements at the support plates is more appropriate. However, the resulting increase in displacements is not a significant consideration. An applied load of 14.14 lbs. leads to a radial displacement of 0.47 inches. With a Mode 1 displacement pattern and a sliding distance of 0.21 inches the matching radial displacement is 0.39 inches. The estimated radial load in a static analysis that is consistent with a radial displacement of 0.39 inches is then 11.7 lbs. This is an under estimate because at a radial displacement of about 0.2 inches the U-bend comes into contact with a neighbor tube. Thus as an impacted tube is displaced the load increases linearly up to a radial displacement of 0.2 inches then the slope of the radial load versus radial displacement increases since the radial load must then displace two tubes. The final load at a total radial displacement of 0.39 inches is 17.4 lbs. This load does not significantly distort either the driving or impacted tubes since it is actually distributed over a contact length of about 30 inches along the U-bend. From the area under the normal force versus sliding distance curve, the work done in the context of a wear calculation is 3.65 in.lbs. per impact event. The work rate is this value times the frequency or 21.1 in.lbs./sec.

Figure A-3 shows plots of work rate versus time leading to a wear volume of 0.123 inches^3 . The solid curve uses a wear coefficient of 35 times the wear coefficient of an Alloy 690 to Type 405 stainless steel wear couple while the dotted line is for a wear coefficient of 20 times that of an Alloy 690 to Type 405 stainless steel wear couple. The horizontal line is the work rate from a static analysis of the normal force and an essentially measured sliding distance. It leads to a wear time of about 5 months for the larger wear coefficient and 8 months for the smaller wear coefficient. However, the real impact event is dynamic not static. A common approximation of dynamic effects is to multiply the static force by a factor of 2. The upper horizontal line is an estimate of the work rate incorporating a dynamic effect. It leads to estimated wear times from 2.5 to 4.5 months.

In summary, simple estimates of the wear time which led to the deepest TTW in Unit 3 range from about 2.5 to 8 months. The lower wear coefficient from actual Alloy 690 to Alloy 690 wear couple tests is a reasonable choice. This leads to estimated wear times between 4.5 and 8 months. However, variations in wear coefficients dictates conservatism. The minimum estimate for the time interval for the development of worst case wear is 2.5 months.

[] This is about a factor of 4 smaller than the radial displacement that is indicated from measurements of elongation of AVB

SONGS U2C17 Steam Generator Operational Assessment for Tube-to-Tube Wear

wear scars. In order to develop a better understanding of U-bend to U-bend impact events a parametric study of dynamic contact of one U-bend with another was undertaken. These results are described in the next section.

SONGS U2C17 Steam Generator Operational Assessment for Tube-to-Tube Wear

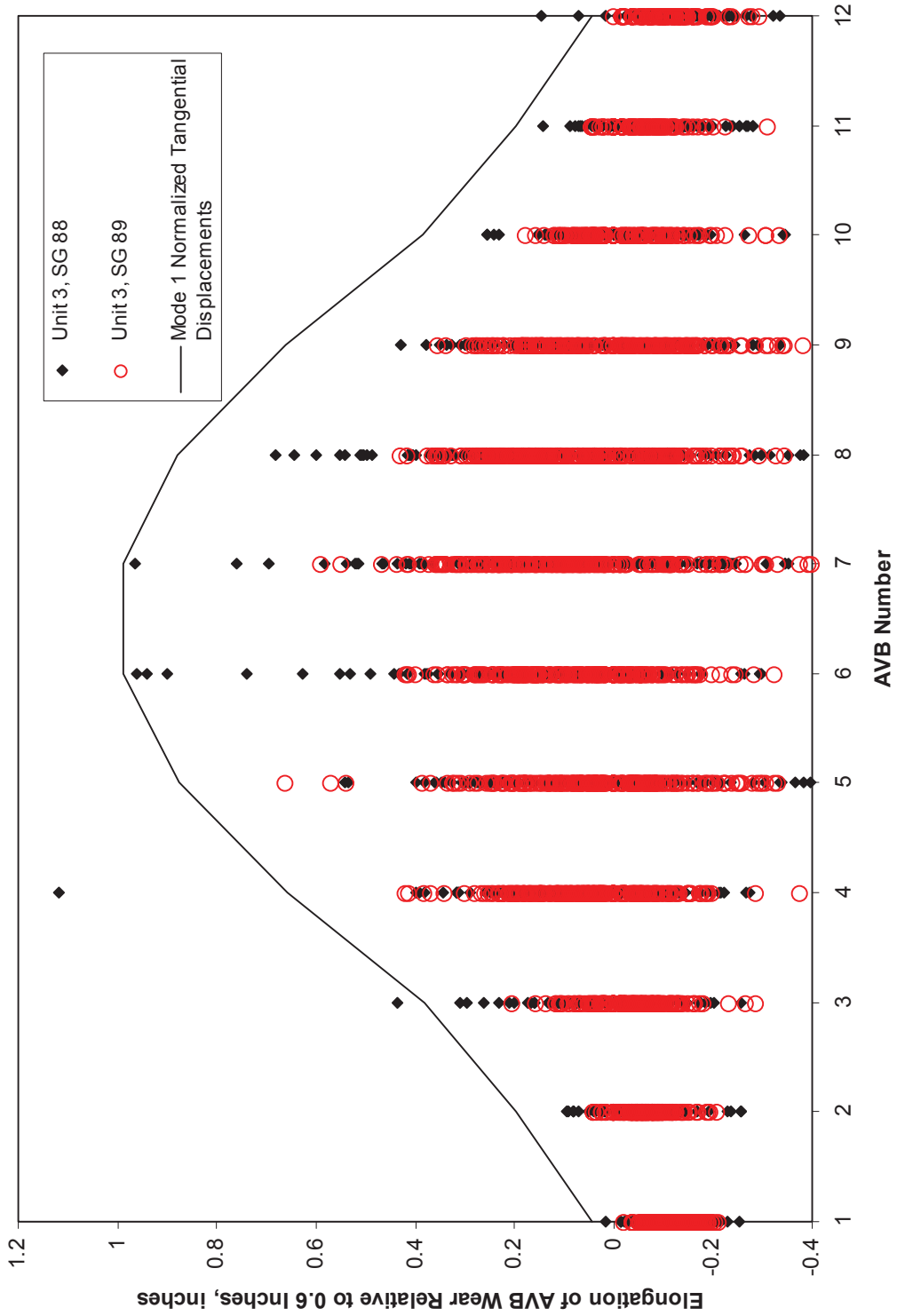


Figure A-1: Elongated Wear at AVBs, Only Observed on Tubes with TTW

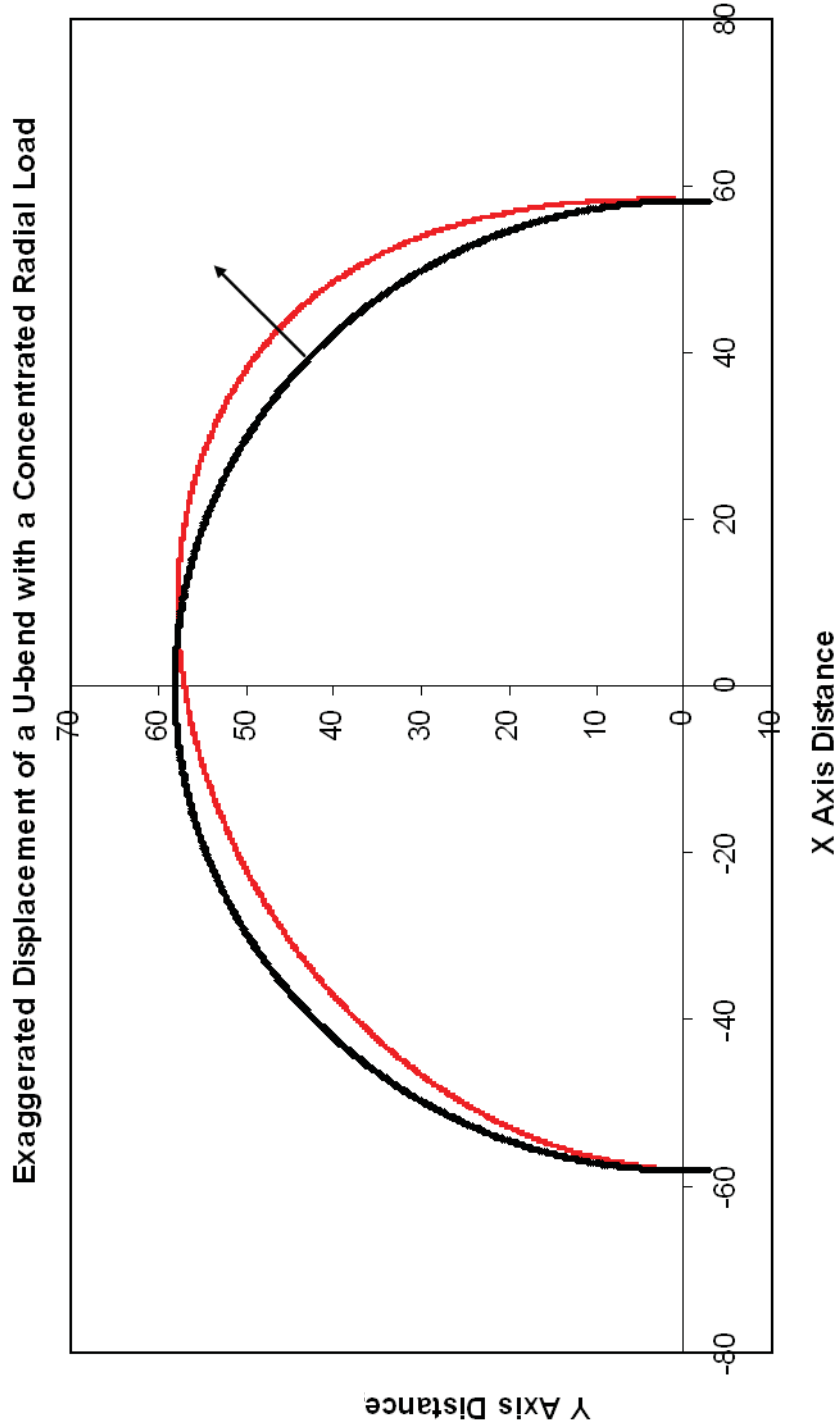


Figure A-2: Radial Load Applied to a U-bend at the Mode I Impact Location, Deformed Shape Greatly Exaggerated

SONGS U2C17 Steam Generator Operational Assessment for Tube-to-Tube Wear

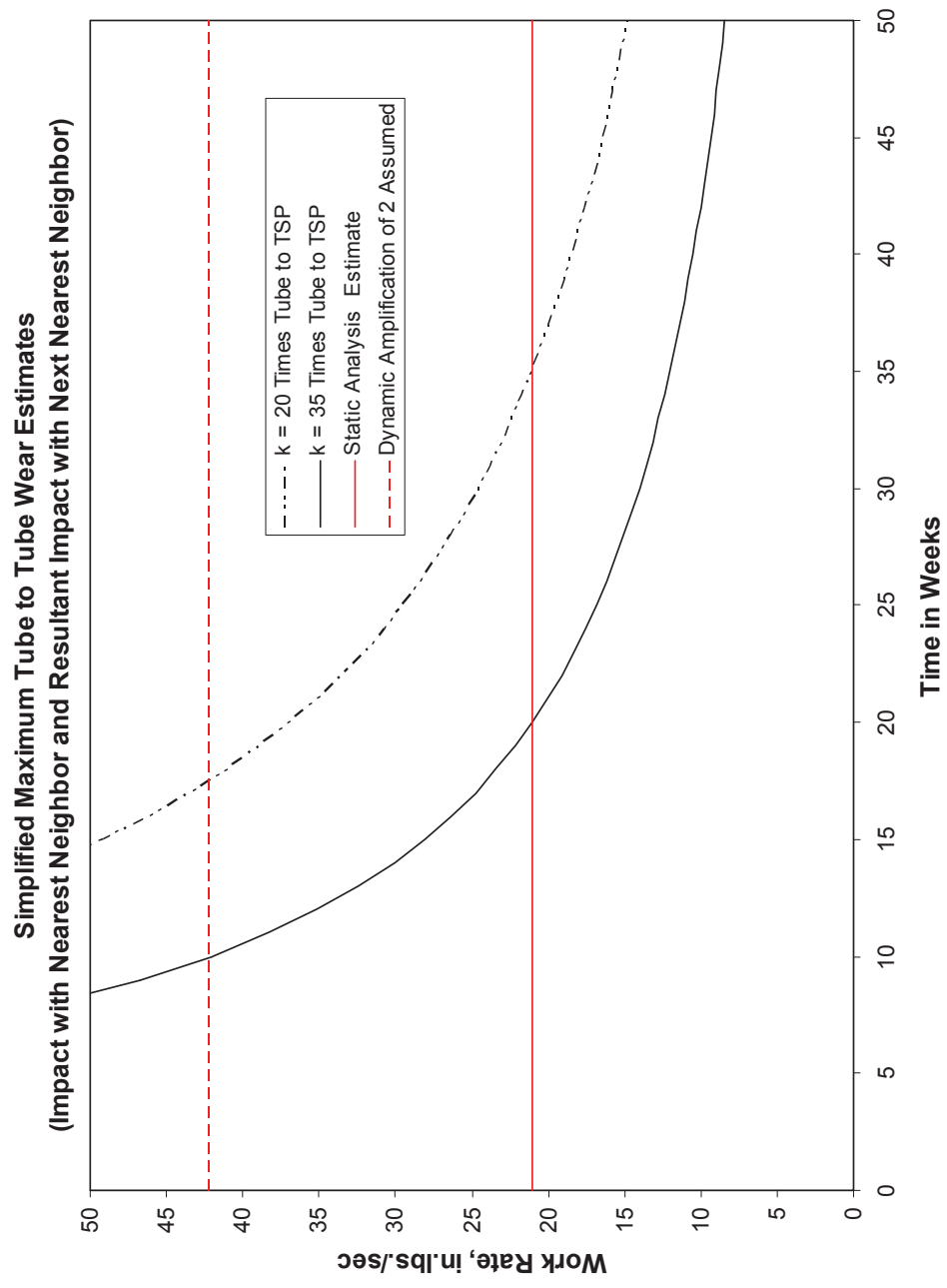


Figure A-3: Estimates of Time Needed to Develop Maximum TTW Volume Loss

A.2 Parametric Time Domain Dynamic Analyses of U-Bend to U-Bend Impact

Dynamic simulations of U-bend to U-bend impact were performed using the ABAQUS Standard finite element program. Computation details can be found in Reference A.3.1. More than 150 simulations were conducted over a broad range of excitation force amplitudes, excitation frequencies, structural damping levels and tube-to-tube friction coefficients. This produced a wide range of contact forces and sliding distances. Only the driving tube and the nearest neighbor tube are modeled. The full length of the tube is included to capture the influence of tube support plates in the straight leg sections. Friction forces at AVB support locations are not included. Instead the overall role of structural damping was established. Friction forces during U-bend to U-bend contact were explicitly treated. It should be noted that the results described in Reference A.3.1 deal with a broad study of U-bend to U-bend impact. Evaluations of the implications of these results to TTW rates are only those of the authors of this report. They are presented in the following paragraphs.

Results are available for one U-bend impacting its outboard nearest neighbor. Possible interaction with the inboard neighbor is ignored. This consideration is mentioned in later paragraphs. The driving U-bend is excited by a cyclic distributed force on the extrados portion on one side of the U-bend above the contact region. The nearest neighbor U-bend is only supported at tube support plate intersections. No AVBs are included. For any given simulation the cyclic excitation force has a constant amplitude. However, a variety of excitation force amplitudes were considered. Several different excitation frequencies were used, bounding the natural frequency. Relative to estimation of TTW rates there are four outstanding features of the results of the Reference A.3.1 studies. These are:

- The normal contact force is highly variable from one impact event to another.
- The length of contact is highly variable from one impact event to another.
- During a single impact event the impact force and length of contact varies with time.
- For a given sliding distance, the maximum contact force is a very strong function of the value of structural damping.

Selected examples of these phenomena are presented below. A much better understanding of the process of U-bend to U-bend impact is obtained by repeated viewing of videos of tube motion.

As the excitation force is applied it takes a few cycles to accelerate to the maximum tube motion. Depending on the damping level the excitation force may result in a final amplitude that is too small to result in tube-to-tube contact. It is a simple matter to increase the excitation force amplitude to overcome damping and develop tube-to-tube contact. When tube-to-tube contact occurs, friction forces develop and are explicitly considered. Figure A-4 plots line contact stress for repeated impact events versus time. The line contact stress is expressed in terms of force per unit length. The total contact force is the product of line stress multiplied by the contact length. Note the variability in the line contact stress for repeated impact events. Also note the variability in the width of the contact spikes. Within a single impact event the contact line stress varies over very short time periods, i.e. it chatters.

Figure A-5 illustrates the variation in maximum contact arc length. This figure does not correspond with Figure A-4. Again notice the substantial variation in contact arc length from one impact event to another. Also, after the first impact event the nearest neighbor tube begins cyclic motion from the impact force. After this point both tubes are in motion and not necessarily in phase. Impact can occur with tubes moving toward each other. The

 SONGS U2C17 Steam Generator Operational Assessment for Tube-to-Tube Wear

substantial temporal variation in line contact stress and contact arc length makes estimation//calculation of work rates a non-trivial exercise. Several additional factors add to the complexity of the problem.

Figure A-6 illustrates the fourth feature of U-bend to U-Bend impact noted above, for a given maximum sliding distance maximum contact force is a very strong function of the value of structural damping. Maximum contact force is plotted versus sliding distance. This force is taken as the product of maximum line contact stress and the maximum contact arc length. For a structural damping value of 2.5 % the impact force at a sliding distance of 0.21 inches is about 16 lbs. Recall that the simple estimates for contact force at this same sliding distance from the preceding section ranged between 11.7 lbs. static and 23.4 lbs. dynamic. The common factor of 2 amplification from a static to a dynamic event is reasonable, even if highly approximate. As damping increases the rate of movement of the impacted tube away from the impact event decreases and the contact force increases at a given sliding distance. At 5% damping the contact force is about 30.5 lbs. and at 10% damping it is about 84 lbs. In broad terms increased damping can be viewed as generally distributed Coulomb friction on the flanks of the U-bend. The flanks of the U-bend are the sides of the tube other than the intrados and the extrados. Hence for a given sliding distance the contact force depends on how tightly the impacted nearest neighbor tube is held in place by friction forces at AVB locations. If the neighbor tube is free to move after impact the contact force is light but if it is held tightly in place the contact force is very much larger.

Motion of tube R106 C78 leads to a measured tangential displacement of 0.21 inches on tube R108 C78 which in turn has an inferred normal displacement of 0.39 inches. Assuming a nominal tube-to-tube gap of 0.20 inches this leads to impact with the next nearest neighbor tube R110 C78. Given the Mode I displacements when contact with an outboard tube (higher row) occurs it must be accompanied by contact with an inboard tube on the opposite side of the U-bend at the same moment in time. Thus when tube R106 C78 impacts tube R108 C78 on the hot leg it impacts tube R104 C78 on the cold leg and drives it into tube R102 C78 on the cold leg. Hence motion of tube R106 C78 involves impact events during one half cycle and 4 impact events on the opposite legs on the other half cycle. The present dynamic analysis only considers impact interactions of two tubes. For the maximum displacement of interest the impact interactions of 5 tubes must be considered. This is another illustration of TTW as a sequence of dependent events and not a sequence of random independent events.

Another observation of interest is the fact that very strong local interactions with one or more AVBs can occur. Substantial stick/slip events can develop and thereby excite other modes of vibrations at other frequencies. This was not included in the analysis. In fact, impact locations consistent with Mode 2 and Mode 3 excitations have been observed. See Section 4.0 and Figure 4-17.

One of the implications of the dynamic parametric study is that the TTW rates should correlate with elongated wear at AVB locations. Elongated wear is indicative of supports with substantial friction hindering the motion of U-bends while being driven to instability by impacts from neighbor tubes. Strongly held tubes will suffer high wear rates from impacting neighbors. Hence a correlation of TTW depths with a tube wear index (summation of AVB wear depths) based only on elongated wear scars is expected. However elongated wear and TTW depths are dependent variables not independent variables. Both are post instability occurrences. While they should be correlated this correlation offers little predictive potential.

A parametric study of the dynamic aspects of U-bend to U-bend impact has led to an improved understanding of the factors involved in these impacts and an appreciation of the complexity of the problem. It underscores the uncertainties involved in estimates of TTW rates and re-enforces the basic premise of this operational assessment. Specifically TTW from in-plane fluid-elastic instability is not a tube degradation mechanism that can be managed in the conventional sense of accepting the fact of ongoing degradation and ensuring tube integrity by limiting the operating time to control the severity of degradation that is likely to develop. Rather actions must be taken to prevent the occurrence of in-plane fluid-elastic instability understood in an engineering sense as an acceptably

SONGS U2C17 Steam Generator Operational Assessment for Tube-to-Tube Wear

low probability of occurrence. This will be accomplished by a decrease to 70% power and an initial inspection interval of 5 months.

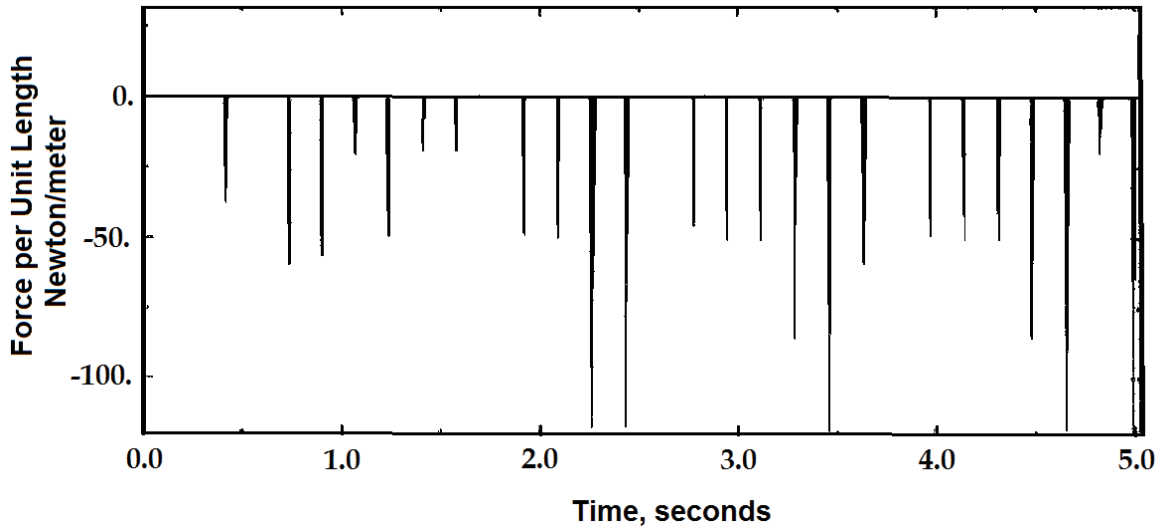


Figure A-4: Line Contact Stress versus Time

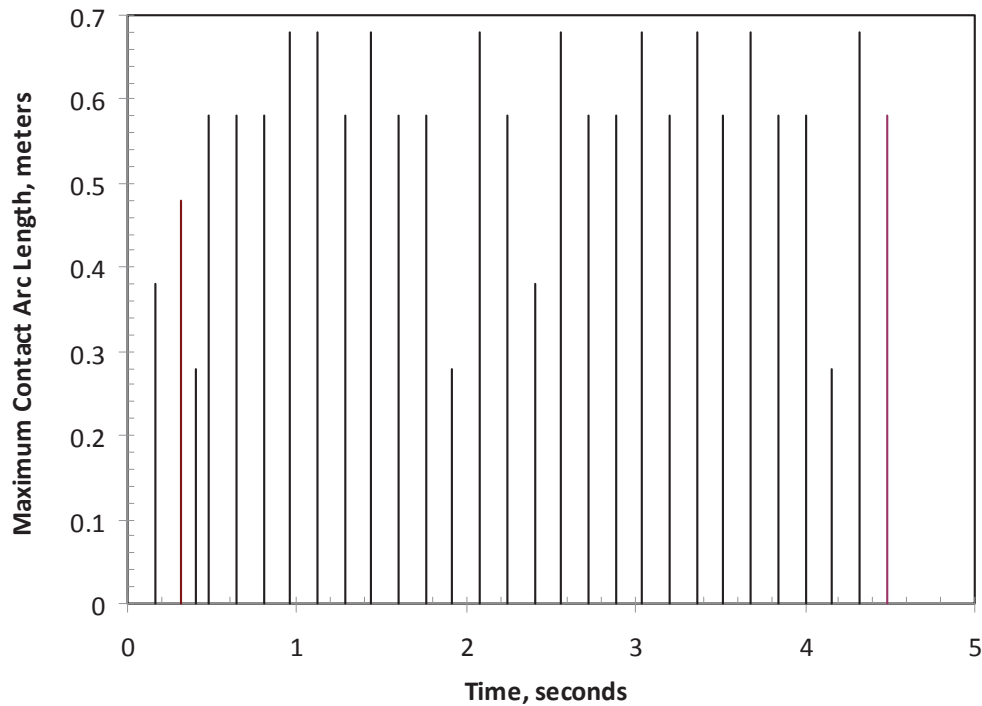


Figure A-5: Maximum Contact Arc Length versus Time

SONGS U2C17 Steam Generator Operational Assessment for Tube-to-Tube Wear

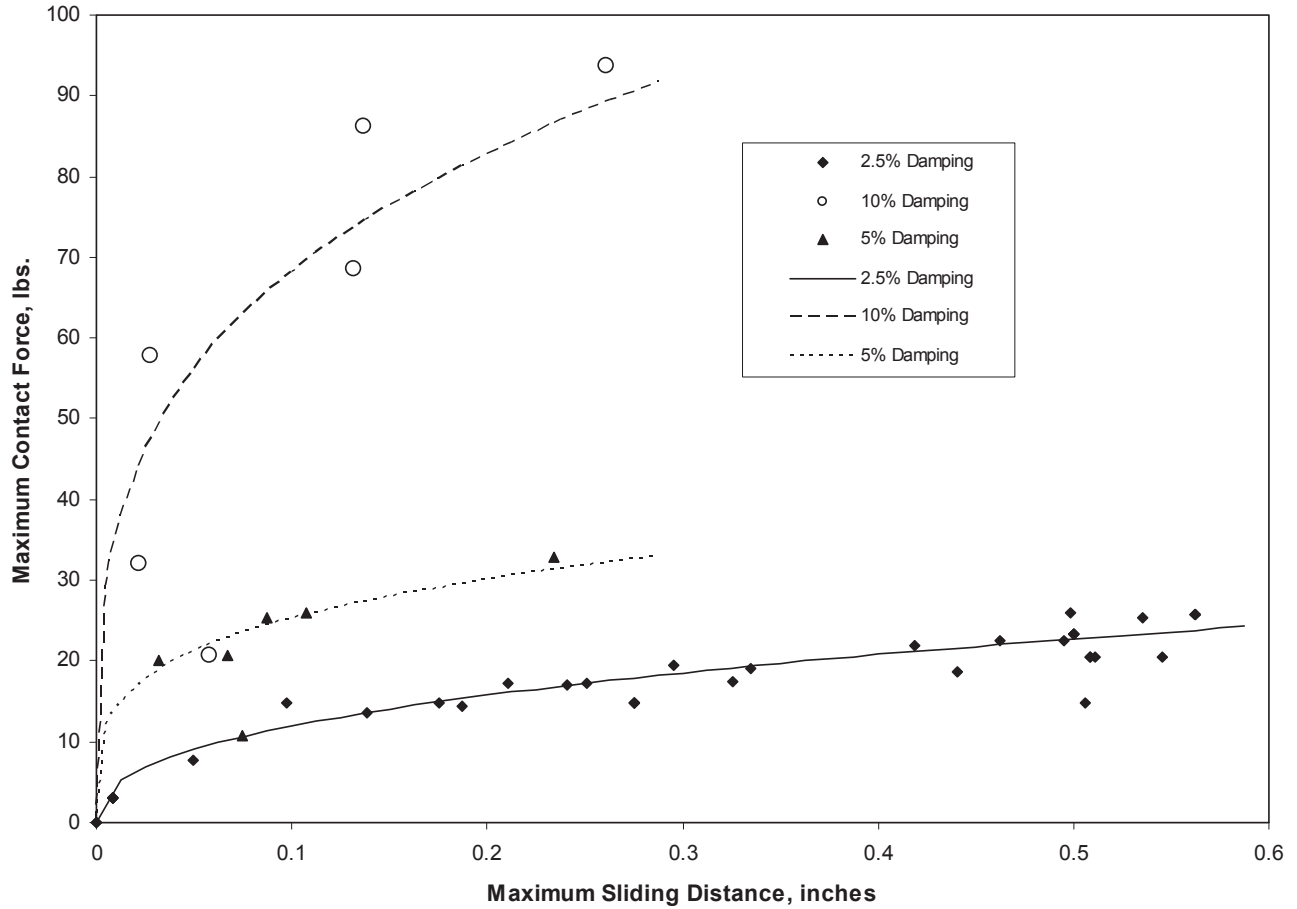


Figure A-6: Maximum Contact Force versus Sliding Distance

A.3 References

A.3.1 [], "Simulation of Tube-to-Tube Impact, Phase 2 Report," June 2012 (AREVA NP Document 38-9191195-000).

ATTACHMENT 6 – Appendix C

Operational Assessment for SONGS Unit 2 SG for Upper Bundle Tube-to-Tube Wear Degradation at End of Cycle 16



AES 12068150-2Q-1
Revision 0
September 2012

Operational Assessment for SONGS Unit 2 Steam Generators for Upper Bundle Tube-to-Tube Wear Degradation at End of Cycle 16

Prepared By

Intertek APTECH
601 West California Avenue
Sunnyvale, California 94086-4831

Prepared For

AREVA, Inc.
3315 Old Forest Road
Lynchburg, VA 24501

Attention: Mr. Jeffrey Fleck

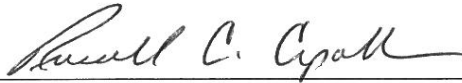
Supplier Status Stamp

VPL No: 1814-AU651-M0145	Rev No: 1	QC: N/A
<input type="checkbox"/> DESIGN DOCUMENT	ORDER NO. 800918458	
<input checked="" type="checkbox"/> REFERENCE DOCUMENT - INFORMATION ONLY	<input type="checkbox"/> VIRP IOM MANUAL	
MFG MAY PROCEED: <input type="checkbox"/> YES <input type="checkbox"/> NO <input checked="" type="checkbox"/> N/A		
<p>STATUS - A status is required for design documents and is optional for reference documents. Drawings are reviewed and approved for arrangements and conformance to specification only. Approval does not relieve the submitter from the responsibility of adequacy and suitability of design, materials, and/or equipment represented.</p> <input checked="" type="checkbox"/> 1. APPROVED <input type="checkbox"/> 2. APPROVED EXCEPT AS NOTED - Make changes and resubmit. <input type="checkbox"/> 3. NOT APPROVED - Correct and resubmit for review. <u>NOT</u> for field use.		
APPROVAL: (PRINT / SIGN / DATE)		
RE:	E. GRIBBLE	10/01/12
FLS:	A. MATHENY	10/01/12
Other:		
SCE DE(123) 5 REV. 3 07/11		REFERENCE: SO123-XXIV-37.8.26


This report was prepared by Intertek APTECH as an account of work sponsored by the organization named herein. Neither Intertek APTECH nor any person acting on behalf of Intertek APTECH: (a) makes any warranty, express or implied, with respect to the use of any information, apparatus, method, or process disclosed in this report or that such use may not infringe privately owned rights; or (b) assumes any liabilities with respect to the use of, or for damages resulting from the use of, any information, apparatus, method, or process disclosed in this report.

CERTIFICATE OF COMPLIANCE/CONFORMANCE

We, the undersigned, certify that the Intertek-APTECH Report AES 12068150-2Q-1, Revision 0, titled "Operational Assessment for SONGS Unit 2 Steam Generators for Tube-to-Tube Wear at End of Cycle 16," which was procured under AREVA NP, Inc. Purchase Order No. 1012045078 dated June 15, 2012, meets the requirements specified in AREVA's purchasing documents, and the quality requirements of the Intertek APTECH Quality Assurance Manual, Revision 7.4.



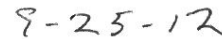
Russell C. Cipolla
Project Manager



Date



David Bosko
Acting Quality Assurance Manager



Date

VERIFICATION RECORD SHEET

Report No.: AES 12068150-2Q-1 Rev.: 0 Date: September 2012
Report Title: "Operational Assessment for SONGS Unit 2 Steam Generators for Upper
Bundle Tube-to-Tube Wear Degradation at End of Cycle 16."

Originated By:	 _____ Project Engineer	<u>9-25-2012</u> Date
Reviewed By:	 _____ Project Engineer	<u>9-25-2012</u> Date
Approved By:	 _____ Project Manager	<u>9-25-2012</u> Date
Verified By:	 _____ Verifier	<u>9-25-2012</u> Date
QA Approved By:	 _____ QA Manager	<u>9-25-2012</u> Date

TABLE OF CONTENTS

<u>Section</u>	<u>Page</u>
Executive Summary	iv
1 Introduction	1-1
2 Structural Requirements	2-1
2.1 Background	2-1
2.2 Structural and Leakage Integrity	2-1
2.3 Tube Burst Model	2-3
2.4 Leak Rate Calculation	2-3
3 Probabilistic Analysis	3-1
3.1 Assessment Overview	3-1
3.2 Analysis Assumptions	3-2
3.3 State of Degradation – Wear Index	3-3
3.4 Probabilistic Model	3-5
3.5 Verification and Validation	3-6
4 Analysis Input Parameters	4-1
4.1 Tubing Properties	4-1
4.2 Operating Parameters	4-2
4.3 Degradation Characterization	4-2
4.4 Probability of Detection	4-4
4.4.1 Inspected Population	4-4
4.4.2 Undetected Population	4-5
4.5 Tube-to-Tube Wear Initiation	4-6
4.6 Degradation Growth Rates	4-10
4.6.1 AVB and TSP Growth Models	4-10
4.6.2 TTW Growth Model	4-11
4.7 Effect of Power Reduction	4-12
4.8 Measurement Uncertainty	4-13
5 Operational Assessment	5-1
5.1 Analysis Cases	5-1
5.2 Simulation Results	5-1
5.3 Structural Margin Evaluation	5-2
5.4 Leakage Evaluation	5-3
6 Summary of Results	6-1
References	R-1
Appendix A – Report Acronyms	A-1

EXECUTIVE SUMMARY

The San Onofre Unit 2 (U2) plant has two new steam generators that replaced the original CE-70 design. The replacement steam generators are MHI Model 116TT1 and began operation in Year 2010. The generators have completed one cycle of operation (Cycle 16) with duration of 1.718 years at power (20.6 months). In the first cycle of operation, the U2 tubing has experienced substantial wear degradation at points of contact with anti-vibration bar (AVB) U-bend supports. There were 4348 indications detected at AVB contact points with a maximum NDE depth of 35%TW during the end-of-cycle (EOC) 16 tube examinations. To a much lesser extent, wear at tube support plates (TSP) was also detected (364 indications) with a maximum NDE depth of 20%TW.

While U2 was in refueling, San Onofre Unit 3 (U3) had a forced outage due to a leak in one of the steam generators after 338 days (0.926 years at power or 11.1 months). The leak was due to tube-to-tube wear (TTW) at freespan locations within the U-bend region. Tube-to-tube wear in U3 was caused by in-plane motion of tubes within a defined region of the bundle. The in-plane motion was due to conditions that created fluid-elastic instability (FEI) of one or more tubes. Subsequent examination of U2 steam generators specifically looking for TTW revealed two indications in 2SG89. Because of the generic designs of both units, and the nature of the FEI, the possibility of having further initiation and progression of TTW in U2 must be addressed in this OA.

This report describes the OA performed for the limiting steam generator (2SG89) in U2 for a simulated population of TTW degradation indications. The OA is a forward-looking process and provides an estimate of the operational period for which the steam generators will maintain tube integrity for both burst strength and through-wall leakage to meet industry margin requirements (Ref. 1). The U2 OA for TTW degradation was performed in a “traditional” manner following established industry assessment guidelines. It is traditional in that the general assessment process follows industry practices for applying current and past NDE inspection data to predict tube integrity at the next inspection. This is performed through empirical models for degradation growth and in combination with engineering models for determining burst pressure and through-

wall leak rates (Ref. 2). The non-traditional aspect of the OA model is the use of pattern recognition based models to characterize the presence and severity of TTW indications based on wear indices defined by the state of AVB and TSP wear for a specific tube. The U3 inspection data from the critical wear area were used to develop predictive models for TTW initiation and growth. The “wear index” defining the state of wear at tube supports in both U2 and U3 steam generators is the method by which initiation and growth of TTW observed at U3 are correlated to U2.

A fully probabilistic model representing the high-wear region of the tube bundle was used to evaluate TTW for Cycle 17. Calculated tube burst and leakage probabilities were obtained by Monte Carlo simulation for initiation and growth of TTW. The results for burst and leakage were compared with the structural and leakage performance margin requirements of NEI 97-06 (Ref. 1). The performance standards for assessing tube integrity to the required margins are delineated in the EPRI Integrity Assessment Guidelines (Ref. 2). This assessment established the probability of burst for the worst-case tube due to TTW predicted for the defined high-wear region.

The U3 wear behavior was used to establish the initiation and growth of TTW indications in U2 steam generators. An empirical correlation based on a wear index parameter (measure of the state of wear degradation in each tube) provided the method for scaling the U3 wear behavior to U2. Two OA analysis cases were evaluated based on the sizing techniques used to define the U3 TTW depths. Case 1 evaluated the situation where voltage based sizing for Eddy Current Testing Examination Sheet ETSS 27902.2 was used to establish the TTW depth distributions and the correlated wear rate with wear index. The results for Case 1 indicate that the SIPC margin requirements are satisfied for a Cycle 17 length of 1.33 years at 70% power level. For Case 2, where the TTW depths were resized by AREVA using a more realistic calibration standard, the SIPC margins will be met for a cycle length of 1.48 years at 70% power level. The plan for U2 is to operate for a short run (about 5 months) at a 70% reduced power level to provide additional margins to the industry requirements for tube integrity.

Tube burst at 3xNOPD is the limiting requirement for cycle length. Therefore, the accident-induced leakage requirements will be satisfied provided that burst margins at 3xNOPD are maintained during the operating cycle.

Section 1

INTRODUCTION

The San Onofre Unit 2 (U2) plant has two new steam generators that replaced the original CE-70 design. The replacement steam generators are MHI Model 116TT1 and began operation in 2010. The generators have completed one cycle of operation (Cycle 16) with duration of 1.718 years at power. In the first cycle of operation, the U2 tubing has experienced substantial wear degradation at anti-vibration bar (AVB) U-bend supports. To a much lesser extent, wear at tube support plates (TSP) was also detected during the end-of-cycle (EOC) 16 tube examinations. A schematic illustration of the tube supports, AVBs labeled B01 through B12 and TSPs labeled 01C through 07C on the cold-leg side and labeled 01H through 07H on the hot-leg side, is shown in Figure 1-1 (Ref. 3).

While U2 was in refueling, U3 had a forced outage due to a leak in one of the steam generators after 338 days (0.926 years at power or 11.1 months). The leak was subsequently determined to be from tube-to-tube wear (TTW) at freespan locations within the U-bend region. Tube-to-tube wear had affected 161 tubes in 3SG88 and 165 tubes in 3SG89. Wear at AVBs and TSPs was also detected which was far more substantial than that observed in the U2 steam generators. Subsequent examination of U2 steam generators specifically looking for TTW revealed two indications involving contact between these tubes in 2SG89.

Tube-to-tube wear in U3 was caused by in-plane motion of tubes within a defined region of the bundle. The in-plane motion was due to conditions that created fluid-elastic instability (FEI). Because of the same design for both units and the nature of the FEI, the possibility of having further initiation and progression of TTW in U2 must be addressed in the OA. The OA is a forward-looking process and provides an estimate of the operational period by which the steam generators will maintain tube integrity for both burst strength and through-wall leakage.

This report describes the OA performed for the limiting steam generator (2SG89) in U2 for TTW degradation. Probabilistic methods have been employed and a Monte Carlo simulation model has been used for establishing the structural and leakage margins for the tubing for this wear

mechanism in a “traditional” manner following industry guidelines. These margins are compared with the structural integrity and leakage performance criteria requirements of Nuclear Energy Institute (NEI) 97-06 (Ref. 1). The performance standards for assessing tube integrity to the required margins are provided in the EPRI Integrity Assessment Guidelines (Ref. 2). This approach established the probability of burst (POB) for the worst-case tube due to TTW predicted for the defined high-wear region as observed in U3.

The scope of this OA is limited to TTW degradation mechanism. The other degradation mechanisms detected during EOC 16 tube examination are addressed in a separate OA performed by AREVA.

The OA was performed by computer analysis using the program TTWEAR_U2. This program is a special-purpose code and has been verified for project use (Ref. 5). A summary of the verification and validation is described in Section 3.5.

A list of acronyms used in this report is given in Appendix A.

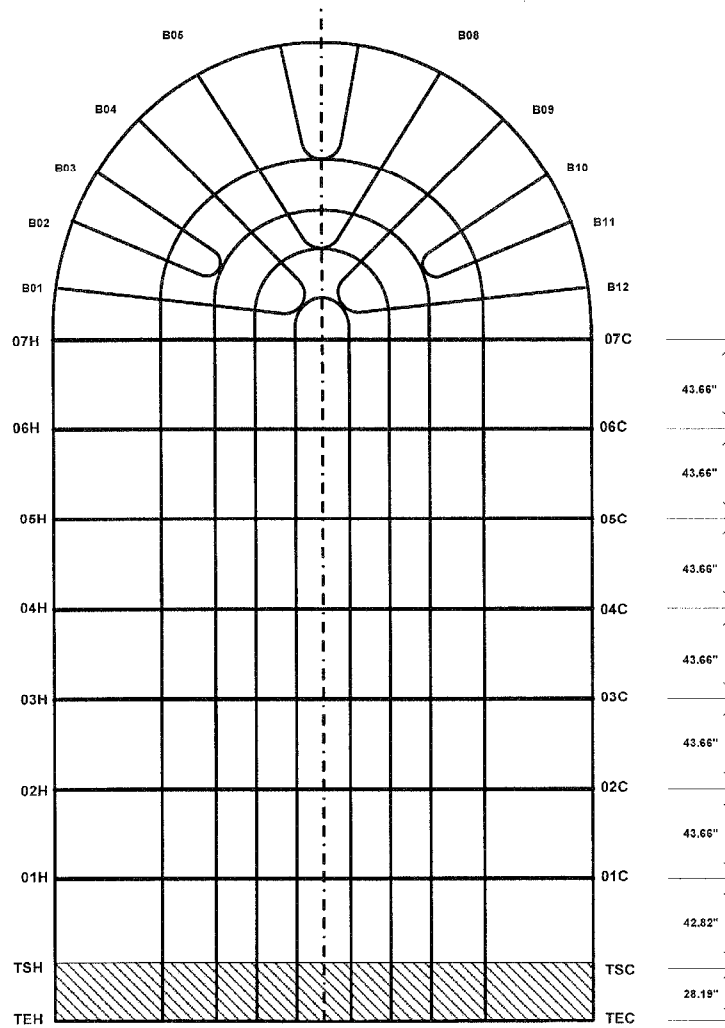


Figure 1-1 SONGS Steam Generator Tube Support Structure Schematic (Ref. 3)

Section 2 STRUCTURAL REQUIREMENTS

2.1 BACKGROUND

In 2006, SONGS adopted the NEI 97-06 "Steam Generator Program Guidelines" (Ref. 1), through a change to the plant Technical Specification, Section 5.5.2.11 Steam Generator Program. The program guidelines specify both condition monitoring (CM) and operational assessment (OA) as a means to manage tube degradation. The preparation of a CM evaluation is a vital element of the NEI guidance and requirements. Condition monitoring provides a comparison between the as-found condition of the steam generators and performance criteria established in Ref. 2. The evaluation of NDE results determines the state of the steam generator tubing for the most recent period of operation relative to structural and leakage integrity performance criteria.

The CM results for U2 at EOC 16 were acceptable for all detected degradation mechanisms including TTW (Ref. 3).

Operational Assessment involves projecting the condition of the steam generator tubes to the time of the next scheduled inspection outage and determining their acceptability relative to the tube integrity performance criteria. All detected degradation mechanisms shall be evaluated, including secondary side inspection results. This OA addresses the TTW degradation mechanism. The required margins for an acceptable OA are discussed in Section 2.2.

2.2 STRUCTURAL AND LEAKAGE INTEGRITY

The structural integrity performance criteria (SIPC) and accident-induced leakage performance criteria (AILPC) applicable to any degradation mechanism including TTW are as follows (Ref. 1):

Structural Integrity — “All in-service steam generator tubes shall retain structural integrity over the full range of normal operating conditions (including startup, operation in the power range, hot standby, and cool down and all anticipated transients included in the design specification) and design basis accidents. This includes retaining a safety factor of 3.0 against burst under normal steady state full power operation primary-to-secondary pressure differential and a safety factor of 1.4 against burst applied to the design basis accident primary-to-secondary pressure differentials. Apart from the above requirements, additional loading conditions associated with the design basis accidents, or combination of accidents in accordance with the design and licensing basis, shall also be evaluated to determine if the associated loads contribute significantly to burst or collapse. In the assessment of tube integrity, those loads that do significantly affect burst or collapse shall be determined and assessed in combination with the loads due to pressure with a safety factor of 1.2 on the combined primary loads and 1.0 on axial secondary loads.”

Accident-Induced Leakage — “The primary to secondary accident leakage rate for the limiting design basis accident shall not exceed the leakage rate assumed in the accident analysis in terms of total leakage rate for all steam generators and leakage rates for an individual steam generator.”

For SONGS, the accident-induced leak rate is 0.5 gallons per minute (gpm) per generator cumulative for all degradation mechanisms.

The acceptance performance standard for structural integrity is (Ref. 2):

The worst-case degraded tube shall meet the SIPC margin requirements with at least a probability of 0.95 at 50% confidence.

The worst-case degraded tube is established from the estimation of lower extreme values of structural performance parameters (e.g., burst pressure) representative of all degraded tubes in the bundle for a specific degradation mechanism.

The acceptance performance standard for accident leakage integrity is (Ref. 2):

The probability for satisfying the limit requirements of the ALLPC shall be at least 0.95 at 50% confidence.

The analysis technique for assessing the above conditions for TTW is a fully probabilistic assessment of all tubes in the at-risk region of the U2 steam generators.

2.3 TUBE BURST MODEL

Tube-to-tube wear indications involve axial volumetric degradation with limited circumferential extent as shown in Figure 2-1. Given the structurally significant length and depth dimensions, the burst pressure for TTW is computed from the burst relationship for axial wear given in Ref. 4:

$$P_b = 0.58(S_y + S_u)(t/R_i) \left[1 - \frac{L(d/t)}{L + 2t} \right] + 291 \text{ psi} + Z\sigma_B \quad (2-1)$$

where P_b is the estimated burst pressure, S_y is the yield strength, S_u is the tensile strength, t is the wall thickness, R_i is the tube inner radius, L is the characteristic degradation length, d is the characteristic wear depth, and d/t is the fractional normalized depth. Relational uncertainty in Eq. 2-1 is represented by the standard normal deviate, Z , ($-\infty \leq Z \leq \infty$), and σ_B , the standard error of regression ($\sigma_B = 282$ psi). The burst equation, when used with the structural significant dimensions (L_{ST} and d_{ST}), produces consistently conservative burst pressure estimates compared with tube burst data.

2.4 LEAK RATE CALCULATION

Leakage predictions for wear-related degradation are subject to large uncertainties. Wear profiles at incipient leakage can vary significantly from simple slits to large holes caused by the blowout of thin membranes. For these situations, absolute leakage rates are not generally

computed. Rather, the probability of through-wall penetration is established from projected maximum depths and ligament rupture calculations. A ligament rupture is where the indication pops-through the remaining wall without causing tube burst. For TTW, leakage at limiting accident conditions (i.e., main steam line break) will not be controlling on cycle length. The requirements for burst at SIPC will be set by the distribution of maximum depths being significantly smaller than those necessary to produce ligament rupture (pop-through) events under accident pressures.

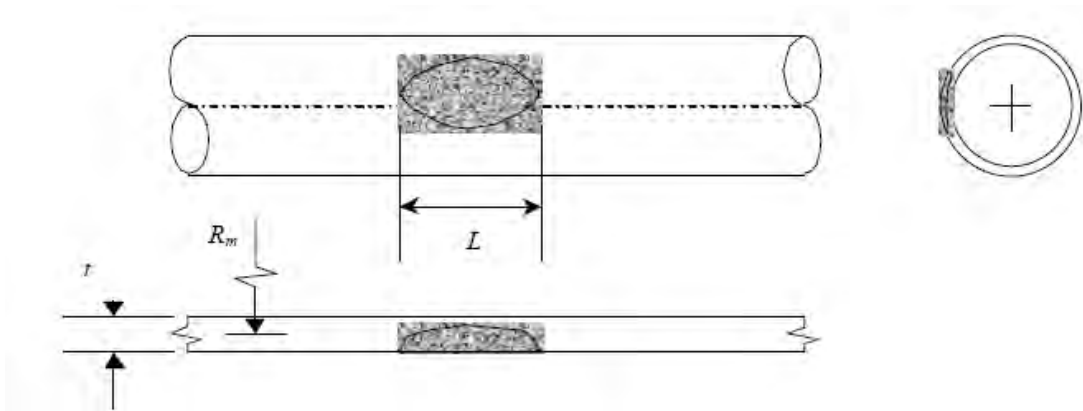


Figure 2-1 — Idealized Wear Profile for Volumetric Degradation with Limited Circumferential Extent (Ref. 4)

Section 3

PROBABILISTIC ANALYSIS

3.1 ASSESSMENT OVERVIEW

A “traditional” operational assessment involves the formal analytical evaluation of inspection data in conjunction with a structural (burst) model for comparing the likelihood of tube burst with the SIPC margin requirements. In the same manner, through-wall leakage probabilities must satisfy the accident-induced leak rate limits. An allowable inspection interval is established by demonstrating the SIPC and AILPC margins will be satisfied for the operating period.

For fully probabilistic OAs for TTW degradation, the probability of detection (POD), the wear rate, and initiation function for creating new wear indications are explicitly treated by statistical distributions for direct input to the structural model. In addition, distributions for tubing strength and relational uncertainties on the tube burst model are addressed in accordance with industry guidelines.

The OA for TTW is performed with a simple single-cycle model applied to a defined region where TTW is assumed active. The models for TTW initiation and the determination and assignment of TTW rates will be the critical input variable to the OA. The overall logic for the OA is shown in Figure 3-1.

3.2 ANALYSIS ASSUMPTIONS

The following are the major assumptions used in OA model development for TTW and input parameters

- 1) Tube-to-tube wear is analyzed as a random process of independent events based on the state of tube support wear degradation of each individual tube in the high wear region at any point in time during the cycle. This philosophy is a consistent approach used in traditional OAs.

- 2) The critical region for evaluation is assumed as a box area defined by Rows 70 to 140 and Columns 60 to 120. This region bounds the high-wear region in the U-bends.
- 3) The state of wear degradation at tube supports for a given tube is assumed to be characterized by the summation of NDE depths at AVBs and TSPs wear locations. This is defined as the “wear index” for a degraded tube. This measure was chosen to capture both the total amount of wear as well as the spatial extent (loss of support from tube-end to tube end), both of which are assumed to be precursors of in-plane tube instability and the on-set of TTW for a given tube. It tracks both the vibratory activity of the tube (indicator of amount of support effectiveness) and the loss of wall thickness which will directly impact the local gaps between tube and supporting structure. Both the existence of TTW and distribution of TTW depths are strongly correlated to the wear index as shown later in Sections 4.5 and 4.6. This TTW behavior observed in U3 supports this modeling assumption.
- 4) The U3 data for TTW is used to define the likelihood of initiating TTW and what will be the TTW growth rate. These data are used to establish the probability of initiation and growth of TTW in U2 through the wear index parameter. Because the TTW degradation is much more extensive in U3 than in U2, use of this approach is conservative.
- 5) Tube-to-tube wear rate is conservatively based on the maximum depths of observed in U3. It is assumed that the TTW in U3 started very early in the cycle so that the growth of TTW occurred over the full cycle. Use of maximum NDE depths to establish TTW rates support this assumption.
- 6) The wear rates for AVB, TSP, and TTW indications are all based on 100% power operation data. This assumption is conservative since operation of U2 for Cycle 17 will be at a reduced power level of 70%.
- 7) The wear rate is based on constant growth on depth rather than constant wear volume basis. This assumption is conservative since wear generally evolves on a constant volume rate basis where the rate of change in depth will decrease as wear progresses.
- 8) It is assumed at the start of Cycle 17, that any tube within the high wear region can initiate TTW including tubes with no detected support wear at the beginning of the cycle. This is a conservative assumption.

- 9) The initiation model of TTW for U2 for operation at 70% power uses the ratio of maximum dynamic pressure to scale the U3 model data. This is supported by vendor analyses on stability ratio and the effect of power reduction on this parameter. This assumption is conservative since it is likely that the potential for tube instability will be significantly reduced to a level where the mechanism will not be active for the planned partial-cycle operation of 5 months.

3.3 STATE OF DEGRADATION – WEAR INDEX

The development of TTW is a complex process. In principle, TTW will initiate when the tube becomes unstable in the in-plane direction under local fluid-elastic conditions. In this assessment for U2, TTW is analyzed as a random process of independent events based on the state of degradation of each individual tube in the high wear region at any point in time during the cycle. It is proposed that the proper measure of the state of wear degradation is the observed wear associated with tube supports (AVBs and TSPs). This measure is taken as a direct indicator of both the likelihood of occurrence and severity of TTW during the operating cycle. This is a key assumption in the probabilistic model and relies on the premise that some significant amount of AVB and TSP wear precedes tube instability and subsequent tube-to-tube contact.

The indication of the state of degradation in the model is called the wear index (WI). The wear index parameter relates the observed AVB and TSP wear states of each tube in the high-wear region to both the initiation and rate of growth of TTW. The wear index captures both the total amount of wear as well as the spatial extent (loss of support), both of which are a precursor to potential in-plane tube instability and the on-set of TTW, as well as the severity (rate) of TTW. Wear depth was selected because it physically represents a change (increase) in the gap between tube and supports and would provide a better physical measure of the onset of tube instability than wear volume. In this capacity, the wear index is used as a means to determine the likelihood of having TTW as well as the rate of growth of TTW.

A model for correlating the observed TTW from the AVB and TSP wear states based on a wear index parameter was developed. The individual contributions from AVB and TSP wear to estimating the existence of TTW was also investigated with the single (combined) model as defined by Eq. 3-1 being used as the correlating parameter. It is clear that a strong correlation

exists for initiation and growth of TTW with the wear index (see Sections 4.5 and 4.6). The wear index model is based the summation of AVB and TSP wear depths in a given tube.

$$\begin{aligned} \text{Wear Index (WI)} &= \text{AVB Wear} + \text{TSP Wear} \\ \text{WI} &= \sum_{i=1}^{12} [\text{AVB depth}]_i + \sum_{j=1}^{14} [\text{TSP depth}]_j \end{aligned} \quad (3-1)$$

where WI is defined in %TW. This measure was chosen to capture both the total amount of wear as well as the spatial extent (loss of support), both of which is assumed to be a precursor to in-plane tube instability and the on-set of TTW for a given tube. It is physically appealing because it tracks both the vibratory activity of the tube (indicator of amount of support effectiveness) and the loss of wall thickness which will directly impact the local gaps between tube and supporting structure.

The observation of significant AVB wear in U2 with only two TTW initiations in 2SG89 and none in 2SG88 suggests that the wear index can be a viable method for comparison of the future performance of U2 for this mechanism compared with U3 past behavior. The TTW indications were small and were sized at 14% TW by ETSS 27902.2. Resizing by AREVA with a different calibration standard suggests these indications could be on the order of 7% TW.

From the magnitude and pattern of tubes having TTW, both initiation and growth of TTW in U2 will be established from the TTW observations in U3 through the wear index parameter. The end of cycle wear degradation states of U2 and U3 is shown in Figure 3-2. There are many more wear indications especially at higher wear index values for U3 compared with U2. The wear index for U3 was as high as 625 (not shown in the graph). The distribution of wear index for U2 was achieved after completion of full cycle of operation (21 months) whereas the U3 wear indices are from about half that operation time. The tubes with TTW in U2 had a maximum wear index value of approximately 82.

The number of affected supports is reflected in the wear index on a tube-by-tube basis. The extent of wear among the tubes supports is shown in Figures 3-3 and 3-4 (Ref. 6). Figure 3-3 shows a comparison of affected AVB supports between U2 and U3. The average number of AVBs that have contacted the tubes is about three per tube in either steam generator of each unit (see Figure 3-3). However, there was a significantly larger number of AVBs associated with tube contact in U3 compared with U2. For U2, there was only one tube having 9 out of the 12

AVB locations with wear contact. For U3, there were about 15 tubes where all 12 AVB locations exhibited tube contact.

Figure 3-4 shows a similar unit comparison for TSP locations with wear. The average number of affected TSPs is one for U2 and six for U3. Many more TSP locations experienced wear for U3 as illustrated in Figure 3-4.

The U2 data shown in Figure 3-3 and 3-4 for the number of affected wear locations was used to define the likelihood for having potential wear locations in those tubes with no detected wear (NDD). All tubes that are NDD within the high wear region are conservatively assumed to have both AVB and TSP wear present at BOC 17. The number of tube intersections with wear is determined by sampling from the cumulative distributions derived from the histograms for U2. The assumed wear depths at these postulated wear locations are based on the POD for the bobbin probe as discussed later in Section 4.4.

3.4 PROBABILISTIC MODEL

A Monte Carlo simulation process was used to solve the probabilistic model for TTW. The simulation process is shown in Figure 3-1, which illustrates one Monte Carlo trial. The probabilistic model includes the processes of initiation, growth, and integrity calculations for the degraded tubes projected to EOC 17. The population contains tubes that are located in the high-wear region. Tubes that have been preventatively plugged based on wear patterns observed in U3 have been removed from the population. This includes Tubes 113-81 and 111-81 in 2SG89 with detected TTW. Therefore, the degraded tubes at BOC 16 include inservice tubes that have detected AVB and TSP wear and tubes that are NDD for any wear within the high-wear region.

The state of degradation of the steam generator tubing is simulated in the model for the total indication population defined in the high wear region of 2SG89. The attributes assigned to each degraded tube are the depth and length of the indications, material properties, and the degradation growth rate. These parameters are treated in a randomized manner and the estimates of burst pressure and leakage are made for each indication of the in the population.

The major steps in the process are:

- 1) Initiation of TTW indications based on the wear degradation state in 2SG89. This is accomplished with the wear index parameter from existing AVB and TSP wear. The initiation of TTW is based on the change in wear index during Cycle 17 as a result of further growth of AVB and TSP wear.
- 2) Define the attributes for each degraded tube for a single trial representing one operating cycle. This includes tube strength properties, the degraded length, and the indication shape factor. This information and the information for the undetected population of wear define the BOC 17 population.
- 3) Growth of the TTW degradation indications for the cycle by sampling from the wear rate distribution dependent on the wear index at the time of initiation. At the end of this step, the EOC 17 degradation indication distribution is defined.
- 4) The set of TTW degradation indications are evaluated for burst pressure and leakage. The degraded tube with the lowest burst pressure is retained for each trial to establish the distribution of worst case values for comparing with the SIPC margin requirements and acceptance standards. Likewise, the leakage probabilities for each trial are retained to determine the 95% probability with 50% confidence (95-50) leak rate for comparison with AILPC.
- 5) In a post-analysis assessment, the POD function can be applied to the degraded tube population at EOC 17 to estimate the number of TTW indications that would be detected at EOC 17.

The simulation process generates a record of the results of all trials performed from which overall burst and leakage probabilities may be inferred and appropriate distributional information obtained.

Discussion and development of the input distributions for the probabilistic model are given in Section 4.

3.5 VERIFICATION AND VALIDATION

A special-purpose computer program called TTWEAR_U2 was developed to perform the Monte Carlo simulation and required calculations as shown in Figure 3-1. The confirmation process of

TTWEAR_U2 followed Intertek APTECH Quality Assurance Procedures for verification and validation of computer software and hardware systems. The main steps followed in the verification process are:

- 1) Line-by-line checking of the coding and logic against the calculation procedure as described in the report.
- 2) Compilation of the program on a different computer using a different compiler by an independent checker. This process verifies hardware compatibility and uncovers code errors and warnings that could be missed in the original code development.
- 3) Checking the program output through statistical methods and selected simulations to establish the output distributions from the analysis subroutines are expected outcomes from the underlying engineering model and statistical input distributions. This is a robust way to verify probabilistic algorithms using the Monte Carlo simulation method.
- 4) Use of a test case for validation the program results against a known outcome. The test case used to validate TTWEAR_U2 was the Cycle 16 operation for U2 and compare program predictions to the actual EOC 17 NDE results regarding wear index distribution and the number of initiated TTW indications.

The documentation of the verification and validation of TTWEAR_U2 is given in Ref. 5.

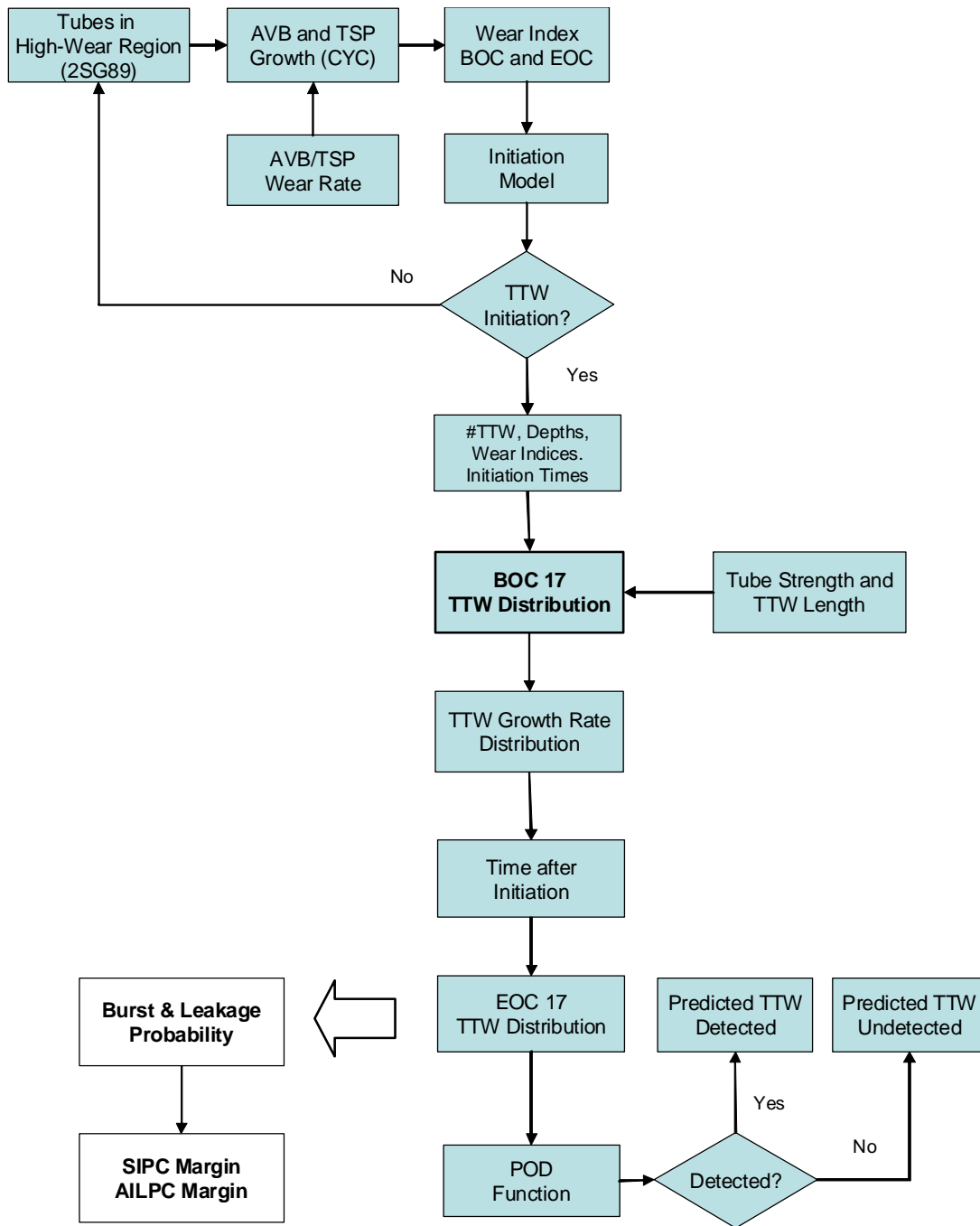


Figure 3-1 — Operational Assessment Logic Flowchart

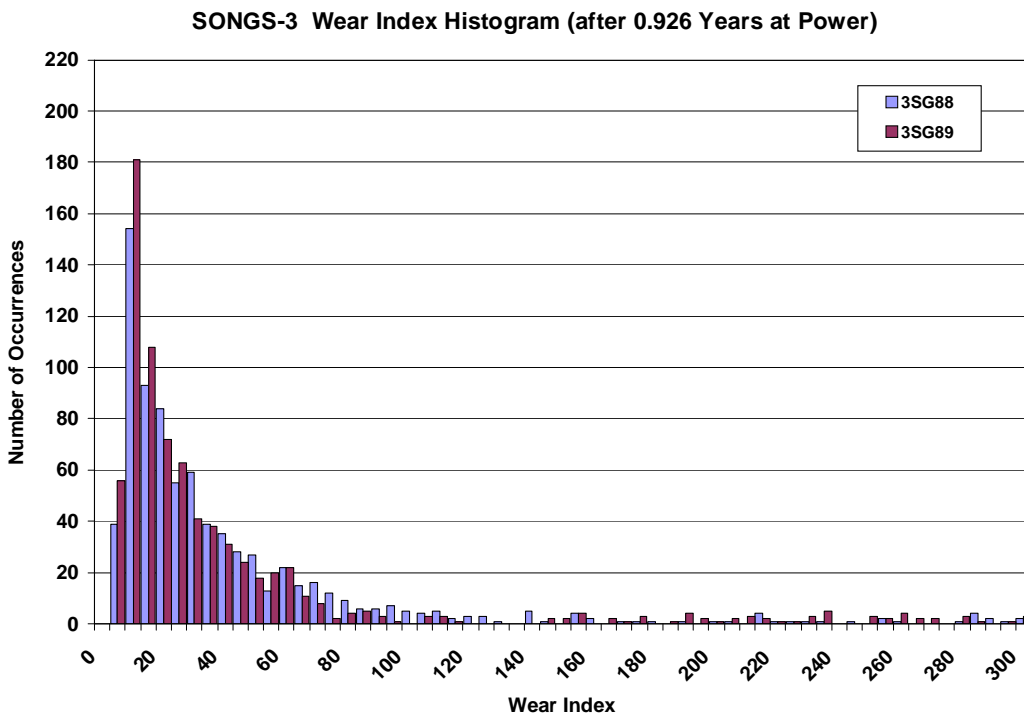
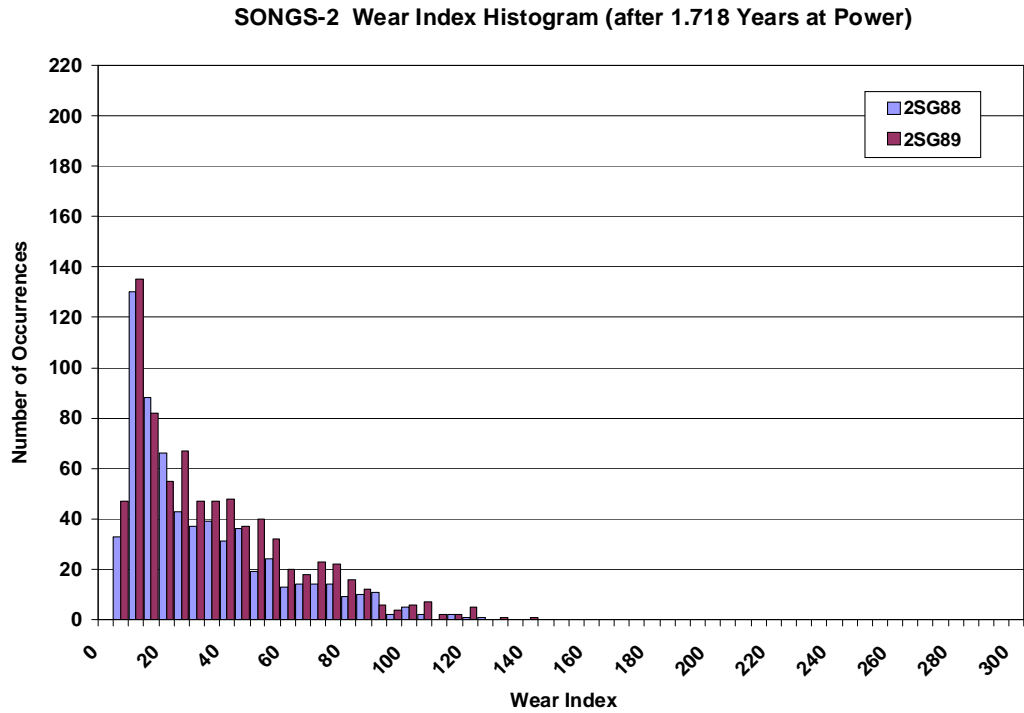
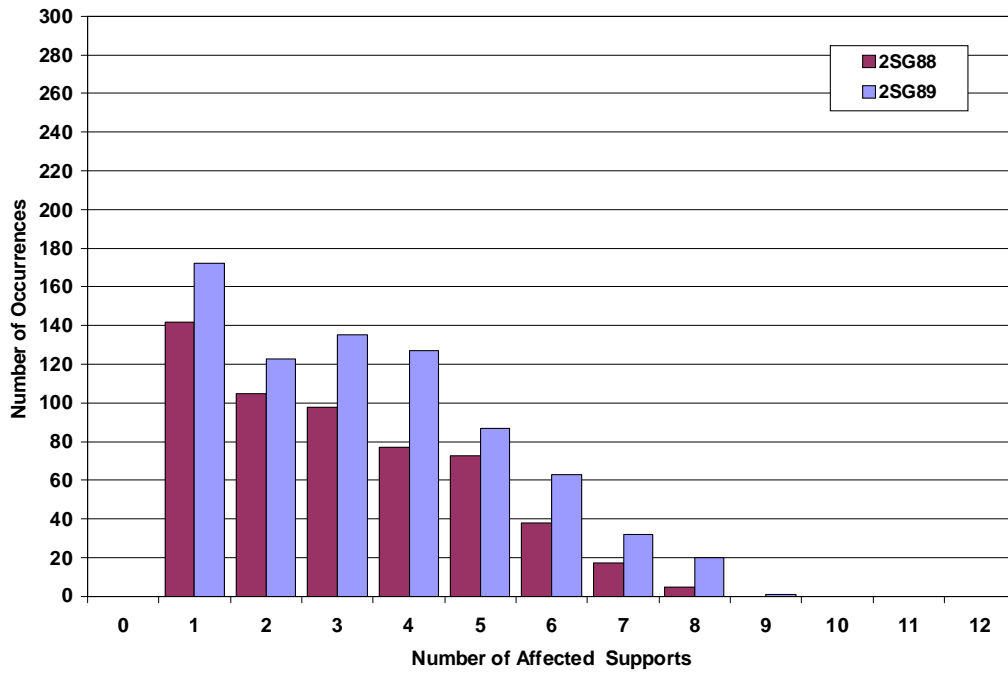


Figure 3-2 — Comparison of Tube Support Wear State for SONGS Units 2 and 3

SONGS-2 Distribution of Wear at AVB Supports



SONGS-3 Distribution of Wear at AVB Supports

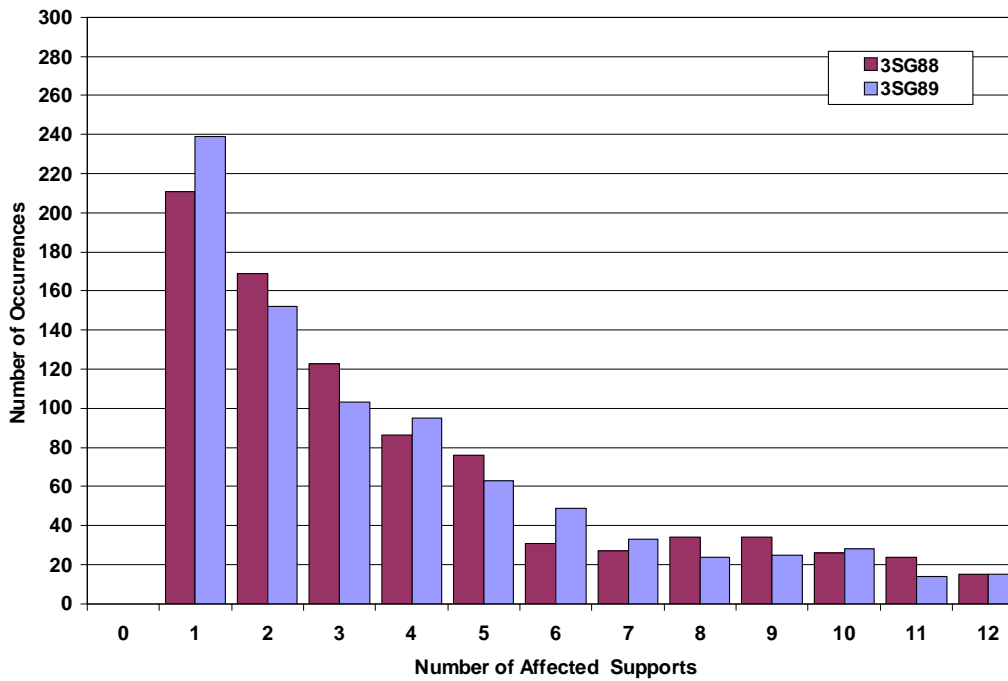
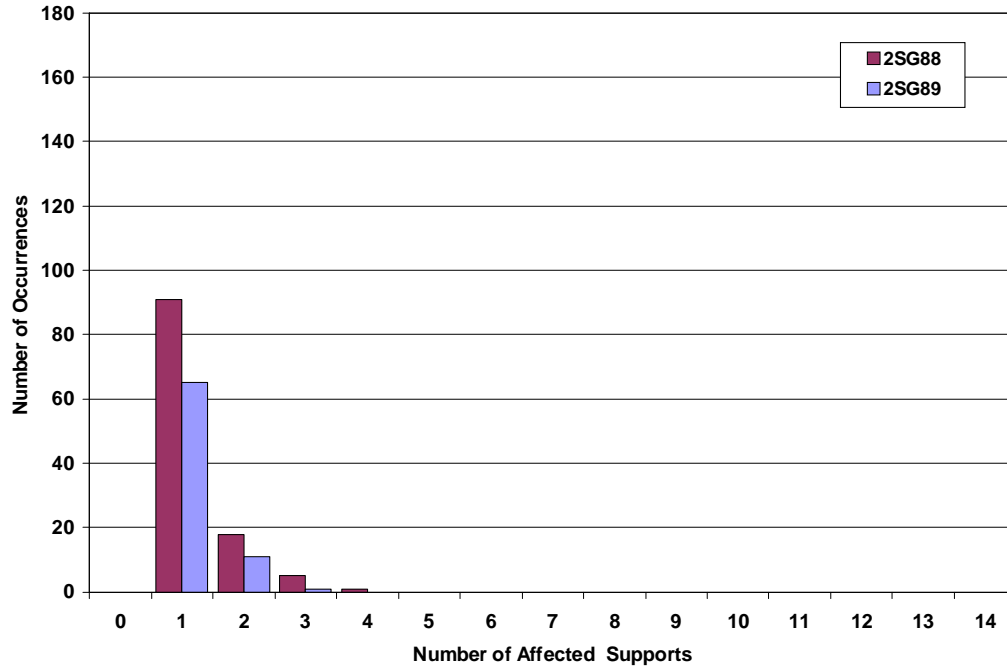


Figure 3-3 — Number of Support Locations per Tube Exhibiting AVB Wear

SONGS-2 Distribution of Wear at TSP Supports



SONGS-3 Distribution of Wear at TSP Supports

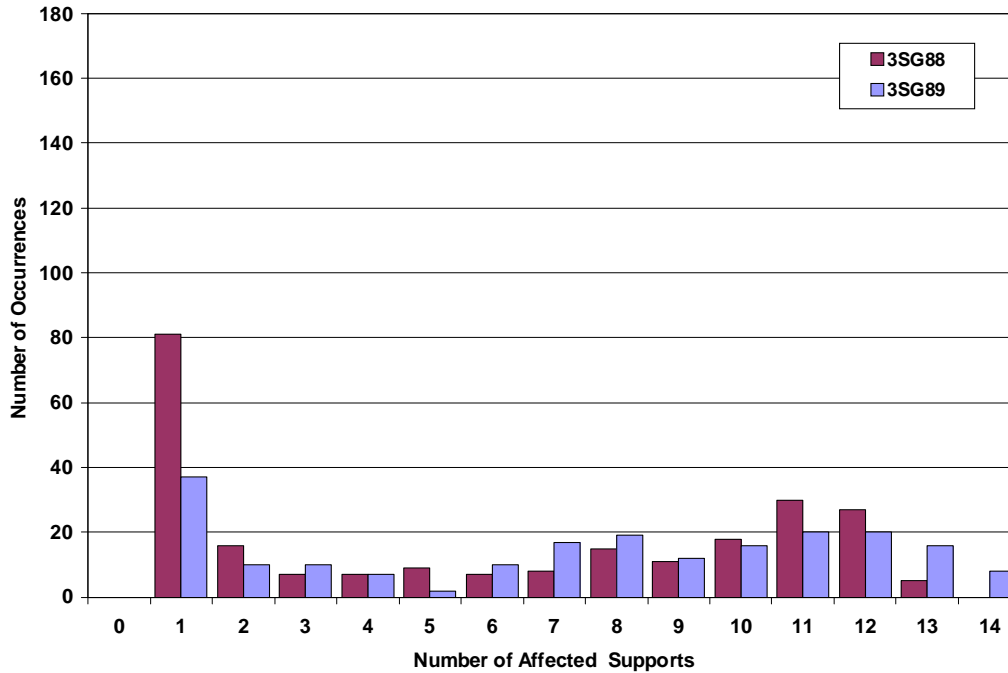


Figure 3-4 — Number of Support Locations per Tube Exhibiting TSP Wear

Section 4

ANALYSIS INPUT PARAMETERS

The input parameters for the OA for TTW by fully probabilistic methods are discussed in this section. These include the mechanical strength, degradation characterization (indication sizes and shapes), the probability of detection function (POD) and most importantly, the initiation and growth rate models for TTW indications projected during Cycle 17.

4.1 TUBING PROPERTIES

The U2 steam generators have 9727 tubes. The steam generator tubing has an outside diameter of 0.75 inch and a nominal wall thickness of 0.043 inch (Ref. 3). The tube material is Alloy 690 thermally treated (A690 TT). The mechanical properties corrected to a temperature of 650°F were provided by AREVA (Ref. 6b) with the following parameters for $S_y + S_u$:

Tubing Yield plus Ultimate Strength Values (psi)

Parameter	S/G 88	S/G 89
$S_y + S_u$ (mean)	115,361	116,633
$S_y + S_u$ (St. Dev)	2,023	2,504
$S_y + S_u$ (min)	108,700	109,900
$S_y + S_u$ (max)	121,600	123,900

These values were obtained from the certified material test report (CMTR) data sheets for the supplied tubing. The value for $S_y + S_u$ for any tube is assumed to be normally distributed with the above parameters for the mean and standard deviation. A plot of the distribution is shown in Figure 4-1.

4.2 OPERATING PARAMETERS

Tube pressure differential under normal operating conditions during Cycle 16 was 1430 psi. Three times normal operating pressure (3xNOPD) is therefore 4290 psi. The operating conditions assumed for Cycle 17 are listed below (Ref. 7 through 9).

Cycle Conditions	Operating Length, (Years at Power)	Steam Pressure, (psi)	NOPD, (psi)
Cycle 16 (actual steam pressures at 100%)	1.718	820	1430
Cycle 17 (w/T _{COLD} implemented at 100% w/3% plugging)	1.578	925	1325
Cycle17 (w/T _{COLD} implemented with reduced power to 70% w/3% plugging)	1.578	945	1305

For accident conditions, maximum steam line break pressure is assumed at 2560 psi (Ref. 3).

4.3 DEGRADATION CHARACTERIZATION

It is beneficial for the OA to focus on the tubes most at-risk to TTW. The numbers of tubes that will be directly affected by TTW are those tubes in the high AVB and TSP wear regions. Wear patterns for AVB and TSP wear encompass the region where TTW was observed and serves as a first cut in defining the size of the at-risk population. A reasonable bound of the TTW region are all tubes within rows 70 to 140, and columns 60 to 120. This at-risk wear region was based on EOC 16 wear patterns for both TTW and AVB wear observed in U3. The table below shows the nature of degradation within the defined high-wear region.

Summary of Degraded Tubes in the U2 Steam Generators High Wear Region

Description	2SG88	2SG89
Total Number of Tubes (High Wear Region)	2121	2121
Tubes Plugged	111	211
Number of TTW Indications	0	2
Number of AVB Indications	1706	2537
Number of TSP Indications	146	90
TSP Indications with No AVB wear	72	11
BOC Tubes with Wear Degradation	516	560
BOC NDD Tubes	1494	1350

It should be noted that five additional tubes in the high-wear region are being preventably plugged: two in 2SG88 and three in 2SG89. This would mean there are actually 113 and 214 tubes removed from service in 2SG88 and 2SG89. The OA contains the three tubes in 2SG89 in the evaluation.

Given the more adverse numbers in 2SG89 and the fact that two TTW indications were detected, 2SG89 is selected as the limiting steam generator for the OA. It will therefore be reasonable to use the NDE data from 2SG89 to establish input distributions for number of degraded tubes and estimated future wear behavior. The number of tubes included in the OA is (Ref. 6 and 10a):

Tubes with existing support wear	560
Tubes with no detected wear	1350
Tubes removed from service	211

Wear at AVB and TSP supports will be randomly assigned to the NDD tubes using the cumulative distributions developed from past observed active wear for 2SG89 shown in Figures 3-3 and 3-4 (Ref. 6). Depths for these wear indications are defined by the POD performance for the bobbin probe (see Section 4.4).

The shapes of the indications were determined by line-by-line +Point™ sizing for U3 tubes exhibiting TTW. The shape factor parameter (F) is defined as the ratio of maximum depth of the indication to the structural average depth of the indication, d_{MAX}/d_{ST} . The shapes were relatively flat ($F=1.0$) with long structural lengths.

The structural lengths (L_{ST}) as determined by the structural-minimum method using the profile data from U3 is shown in Figure 4-2 (Ref. 11). The structural lengths represent the burst-effective lengths from each TTW indication and range between 1 to 8 inches. The cumulative distribution (CDF) of these data is fitted to a lognormal model. This CDF will be sampled in the simulation analysis to define the length of each TTW indication that is calculated to initiate during Cycle 17.

4.4 PROBABILITY OF DETECTION

4.4.1 Inspected Population

The probability of detection performance of the bobbin probe shows that it is capable of reliably detecting AVB wear, TSP wear, and TTW indications in the U-bends. The probability of detection for eddy current test techniques has been established from industry data and made available through published ETSS data. For ETSS 96004.1, Rev. 13 (Ref. 12), the expected POD performance is shown as a log-logistic function in Figure 4-3. For comparison, the expected performance for +Point™ inspection (ETSS 27902.2) is also plotted in Figure 4-3 (Ref. 13). The log-logistic model for POD (Ref. 2) and the parameters for the examination techniques used for support and TTW, are given below:

$$\text{POD}(h) = \left[\frac{1}{1 + \exp[A + B \text{Log}(h)]} \right]$$

Probe	ETSS	Intercept (A)	Slope (B)
Bobbin	96004.1	10.61	-11.20
+Point™	27902.2	14.24	-17.22

where $h = d/t$ and is the degradation depth in % TW. The parameters for ETSS 96004.1 were derived from hit-miss ECT data used to establish the ETSS data statistics. The parameters for ETSS 27902.2 were estimated from the tabular data set in ETSS 27902.2. These data show one missed call at 5% TW depth (0 out of 1 fractional detected) and 100% hit rate (47 out of 47 fractional detected) for depths from 8% to 86% TW. To estimate the POD, a 0.1 fractional detection rate was given to the one missed call at 5% TW and a 0.8 fraction detection rate assigned to 8% TW depth. The log-logistic equation was fit to these two detection levels giving the curve shown in Figure 4-3.

Tubes within the high-wear region that had significant AVB and TSP wear in U2 had received bobbin probe examination. Subsequent to the U3 inspection findings, supplemental +Point™ inspections were performed in U2 to specifically look for TTW with an improved POD. Two TTW indications were found in 2SG89 and none were detected in 2SG88. Therefore, the most

susceptible group of tubes within the high-wear region has been thoroughly examined with a more sensitive inspection with an improved POD.

4.4.2 Undetected Population

It is appropriate to use the POD model to define the undetected indications for the BOC population. A reasonable assumption is to use POD performance for some reasonably conservative level to assign the depth of any undetected indications. This can be used for AVB, TSP, and TTW indications as required for the OA model.

The model addresses three possible scenarios for including additional wear for tubes in the high wear region:

- 1) Tubes with no detected wear (NDD) that may have low level of wear at tube supports (AVB and TSP)
- 2) Tubes that may have support wear but may develop additional wear locations in the during Cycle 17
- 3) Tubes that may have undetected TTW

For the NDD tubes within the high-wear region, degradation sites are assigned by the expected number of AVB and TSP locations that may develop wear during Cycle 17. The depth of degradation is defined by the bobbin probe POD performance for an assumed low POD level.

$$\text{Log}_{10}(h) = \frac{\text{Ln}\left[\frac{1}{\text{RN (POD)}} - 1\right] - A}{B} \quad (4-1)$$

where

h = wear depth equal to (d/t) , (% TW)

POD is the assumed performance level for NDD ($\text{POD} \leq 0.05$)

RN is a randomly selected number between 0 and 1.

A and B are constants (intercept and slope) in the log-logistic function for the bobbin probe POD

The depths are determined by a random process with this equation used for each active wear location (AVB and TSP) in the 1350 NDD tubes. The bobbin probe POD is used in this process.

For the 560 tubes where TTW may have initiated during the prior cycle (Cycle 16), Eq. 4-1 is applied with the +Point™ parameters.

Past operating experience for a similar replacement steam generator provided data on the evolution of tube support wear after two cycles of operation. It has been observed that the number of AVB supports that develop wear in the second cycle of operation can increase dependent on the number of worn AVB locations at the beginning of the second cycle. These data were used in the OA to add AVB locations at the start of Cycle 17 from a statistical representation of these data. It is also observed that number of TSP locations in a given tube do not increase so only AVB wear locations are modeled with increasing affected numbers. When new AVB wear locations are added to a given tube, wear is assumed to start at BOC 17 from an initial zero depth. Wear from all AVB and TSP supports (including the newly added AVB support locations) are used in computing the wear index for the tube.

For undetected TTW, the initiation model for TTW is used to define the situations where there may have been TTW that went undetected at the EOC 16 inspection. When pre-existing TTW is determined, depths are randomly assigned using Eq. 4-1 with the +Point™ POD performance parameters at the lower 5% detection level. Additional discussion on the model prediction of undetected TTW is provided in Section 4.5.

4.5 TUBE-TO-TUBE WEAR INITIATION

This section describes the development of a fundamental empirical model necessary to describe the presence and expected growth rate for TTW on a specific tube, based on the presence and magnitude of existing AVB and TSP support wear on that tube. It relies on the observed TTW at U3 in order to construct the appropriate Cycle 16/17 model for U2.

In principle, TTW will initiate when the tube becomes unstable in the in-plane direction under local fluid-elastic conditions. It is assumed that the existence of TTW in U3 after operating 0.926 years at power can be used to form the basic fundamental model for predicting TTW in U2. This prediction model for TTW will be constructed as a time-to-initiate function based on the likelihood of having TTW for a given wear degradation state. The correlating factor between the two units is the wear index (see Section 3.2). Since the state of wear degradation in U2 is significantly less than that for U3, an adjustment to the distribution describing the existence of TTW in U3 will be required. This is accomplished by benchmarking the model from the U3 data

set of many existing TTW indications, to give approximately the same number of detected TTW indications at EOC 16 for U2, specifically two indications in 2SG89. Because we want the initiation model to account for both detected and undetected indications, the benchmarking process will include the POD model behavior at the appropriate detected depths.

The initiation of TTW was established through an empirical model that relates the probability of initiation (POI) and subsequent growth for TTW based on the wear index parameter. The wear index parameter relates the observed AVB and TSP wear states of each tube in the high-wear region to the POI and rate of growth. The wear index parameter is the calculated sum of all AVB and TSP wear depths in a given tube. Wear depth was selected because it physically represents a change in the gap between tube and supports and would provide a better physical measure to the onset of tube instability than wear volume.

The initiation model was developed using a U3 data base consisting of tubes within a high-wear region of steam generators 3-88 and 3-89 (Ref. 10a). The data base consisted of all records where wear was detected at any of the 26 supports (12 AVB and 14 TSP), and where TTW had occurred or had not occurred. Tube-to-tube wear depths were included where the phenomenon was present. For the correlation work, an AVB index was determined, which was simply a summation of NDE AVB wear depths for a given tube. A TSP index was also computed which was the sum of NDE TSP wear depths. The tube wear index was defined as the sum of the AVB and TSP indices.

The resulting database was partitioned into two groups, one containing TTW indications (initiated) and the other which had no TTW indications (non-initiated). From a data regression point-of-view, this problem is analogous to that of probability of detection. In both situations, the dependent variable is dichotomous (hit/miss). Although a logistic regression is the preferred tool for this particular type of correlation work, a Beta distribution was found to be a better model for representing the U3 data. The Beta distribution has additional fitting parameters that provide more flexibility (degrees of freedom) in fitting both the lower and upper tails of the data distribution.

Two models for correlating TTW presence with wear index are shown in Figure 4-4. The first model distribution, which lies to the left, was developed from the complete data set (both generators) for U3. This model represents the likelihood of having TTW for a given wear index value. The second model is the one developed for U2 based on U3 data set but is

benchmarked to replicate the two detected indications at EOC 16. This benchmarking was necessary because simulations with the more conservative U3 model combined with U2 wear indices resulted in many more initiations of TTW at EOC 16 than were observed in 2SG89 and 2SG88. This alone, provided evidence enough to reject the more conservative model.

This adjusted model was obtained under the following constraints:

- 1) All 2SG89 tubes with wear in the high-wear region at EOC 16 were used as the defined benchmarking population (total of 771 tubes).
- 2) Number of tubes with TTW for benchmarking will be based on POD considerations where only two indications (~7% TW) were detected in the 771 tubes. The lower limit for detection for ETSS 27902.2 is around 5%TW as illustrated in Figure 4-5. For this depth size, the POD is about 0.12.
- 3) Both the base (U3) and adjusted (U2) models should give approximately the same number of existing TTW indications observed in U3 when the U3 wear state is used in the model. This is to ensure that the frequency of TTW for U2 will approach that of U3 in the extreme case of high wear indices.

The two indications found in 2SG89 were sized at 7% TW following review of the NDE results. For the +Point™ POD, the probability of detecting a 7% TW indication is on the order of 50-50 as shown in Figure 4-5. However, the data set for ETSS 27902.2 had limited data in this size range with one flaw at 5% TW being NDD and the next larger flaw at 8% TW being detected. To provide for a conservative model benchmark, the POD for a 5%TW flaw is used which corresponds to a one chance in eight for discovery. Therefore, the model was calibrated to predict about 16 indications on average so that approximately two of them would be detected as was the case for 2SG89.

The benchmarking was done iteratively by progressively changing the U3 model parameters to shift the POI curve to the right while having the two models converging together at the higher wear index values. This was accomplished by filtering some of the initiated (hit) data at the low wear index values. These data points were not removed arbitrarily. A careful examination of the data base revealed a common element among the low index value hits. They were almost all at endpoints of a string of TTW instances. The indices for the remainder (interior) of these

strings were much higher, strongly suggesting that these endpoint tubes were not where the instability initiated but were victims of other initiation events. The simulation results of the benchmarking process are shown in Figure 4-6.

As a final benchmark, the adjusted model was applied to the wear indices for U3. The number of tubes having TTW in both 3SG88 and 3SG89 is 326. The adjusted POI model predicted 290 initiations, which is close to the number of tubes with TTW in U3. When the U3 POI model is used with U3 wear data, 315 tubes with TTW is computed. This serves as confirmation that the U2 initiation model converges to U3 behavior as the state of wear approaches that seen in U3. The final results are shown below:

Average Number of Initiated TTW Model Indications

First Cycle Degradation State	U2 POI Model	U3 POI Model
U2 Wear Index (2SG89)	16	34
U3 Wear Index (Both SGs)	290	315

The U2 initiation model is implemented in a way that both the POI and the time when initiation occurs can be established. Since there is a possibility that TTW may exist undetected in the BOC 17 tube population, the initiation model was adapted to determine under what conditions TTW is pre-existing. Figure 4-7 is an illustrative example on the estimation of the time of initiation for TTW and identifying cases where TTW initiated in Cycle 16 and was undetected. The POI curve is the adjusted model for U2 at 100% Power. For illustrative purposes, the wear index for BOC and EOC for a tube is shown. The condition for initiation of TTW is determined by a random process with the outcome of three different trials shown. The situation for no initiation occurs when the EOC wear index is insufficient to produce TTW for that trial (random sample produces number greater than POI curve).

For cases where initiations are predicted sometime during the cycle but not at or before BOC, the point of initiation is computed from the intersection between the random trial parameter with the POI value for the model function as shown by the middle dashed line. In this situation, initiation is calculated to occur at a wear index between BOC and EOC values. The point in time is determined from the interpolation on the wear index with operating time. The TTW indication is assumed to start growing at the point of initiation with an initial depth of zero and at a wear rate determined from the wear index value at the time of initiation.

The bottom horizontal dashed line shows the situation when initiation occurred during the prior cycle (Cycle 16). For this sample trial, the point in time in Cycle 16 when TTW began can be determined. However, because the tube was NDD at EOC 16, the TTW indication is assumed to begin growing at BOC, with a starting depth determined by a random selection process from the lower 5% tail of the POD curve, and with a wear rate determined from the BOC wear index value. The time of growth is the full cycle length.

When the U2 POI model is applied to a full cycle of operation at 100% power, the model predicts about 50 to 70 TTW initiations by EOC 17. The initiation events are roughly uniformly distributed over the cycle. It is assumed that all tubes in the high-wear region (1910 tubes) have the potential to initiate TTW indications and the indications are subject to growth immediately following initiation.

4.6 DEGRADATION GROWTH RATES

Wear rates for three mechanisms are required for the OA of TTW. The required wear rate distributions are for AVB wear, TSP wear, and TTW. The wear rate is conservatively based on a constant growth in depth.

4.6.1 AVB and TSP Growth Models

The AVB and TSP wear rates are necessary to track the increase in wear index for each tube in the BOC population. The wear rates for AVB degradation were developed from EOC 16 NDE data (Ref. 6). The extent of wear as observed at each of the 12 AVB and 14 TSP tube intersections for U2 is shown in Figure 4-8. It can be seen that there are three distinct groups among the AVB locations where wear rates are substantially different. For Group 1 (B01, B02, B11, and B12), the detected wear depths are less than 15% TW. For Group 2 (B03 and B10), wear depths are elevated and numbers have increased. For Group 3 (B04 through B09), AVBs wear depths are larger and in greater numbers at the middle supports. This suggests the main interactions between tubes and AVBs are in the upper support structure. Wear rates for the three groups are plotted in Figure 4-9 for the two steam generators. As expected, the apparent wear rates for Group 3 are higher on average and in the extremes than Groups 1 and 2. A

similar wear rate determination was performed for TSP wear and a combined generator model for TSP wear rate was developed.

The final wear rate distributions for AVB and TSP wear are shown in Figure 4-10. The AVB wear rate distribution was developed using Group 3 data from both steam generators to provide a conservative growth model for this mechanism. The fitted function uses a lognormal statistical model for sampling in the simulation.

4.6.2 TTW Growth Model

The wear rates for TTW are defined from U3 data. Such rates can be scaled to U2 based on the state of wear using the wear index. Specifically, the extent of both AVB and TSP wear is much less in U2 after 22 months of operation compared with U3 after 11 months of service.

The growth rate model developed from the U3 data base utilized +Point™ data from tubes with freespan wear indications. Such rates are correlated to U2 based on the tube wear index. When all data were examined including tubes which had multiple TTW, large scatter was observed. To address this situation, only the maximum wear depths observed in the tubes were used to define a conservative measure for growth. Since only one TTW indication in a tube is assumed in the assessment, use of the maximum wear depth is appropriate.

The maximum TTW depth has a direct relationship with the observed wear at tube supports over the domain of wear index values. This is shown in Figure 4-11 for depth sizing using ETSS 27902.2 (Ref. 13). A second sizing method was used to explain better the measured sizes with ISPT results. The sizing technique was developed by AREVA using a different calibration standard built by AREVA (Ref. 14). The final sizing technique uses the lower portion of the AREVA sizing curve but fixes the upper part of the curve adjusted to match the 7.54 volt, 100% TW indication in 3SG88. The depth distribution versus wear index for the “AREVA” resizing is also shown in Figure 4-11. The regression fits for both data sets are given below:

$$\text{Depth} = 17.257 + 0.0703 \text{ Wear Index} \quad (\text{ETSS 27902.2 Sizing})$$

$$\text{Depth} = 12.747 + 0.0701 \text{ Wear Index} \quad (\text{AREVA Resized})$$

The scatter in the data at any given wear index shows central tendency so that linear regression error can be statistically defined. The residuals from the regression analysis are well modeled by a normal distribution over the range of interest for wear index. The relational error for both regression models is normally distributed with a mean of zero and a standard deviation of 10.99% TW. The distribution plots of the residuals from the regression analysis are shown Figure 4-12.

The effective TTW growth rates are ultimately computed by dividing the sampled depth from the above relations by the actual cycle length for the first U3 operating period after replacement (0.926 years at power). The TTW growth rates as a function of wear index are shown in Figure 4-13.

4.7 EFFECT OF POWER REDUCTION

It is intended that U2 will begin Cycle 17 operation with power level reduced to 70%. It is expected that the effect of power reduction on dynamic pressure (ρv^2) will have a net beneficial effect on TTW initiation and tube burst probabilities. The maximum dynamic pressure acting on the U-bends decreases significantly with power level. At 100% power, ρv^2 is 4,140 N/m² (Ref. 15). At 70% power, the dynamic pressure reduces to 2,430 N/m². This is a reduction factor (RF) of 0.586. This reduction factor on dynamic pressure is employed in the initiation model for TTW as a direct multiplier on POI where,

$$POI_{70\%} = \frac{\rho v^2|_{70\%}}{\rho v^2|_{100\%}} POI_{100\%} = 0.586 POI_{100\%}$$

The above equation is the assumed behavior for POI model based the uniform population risk reduction using combined probability for 70% power operation. The effect of power reduction will be conservatively assumed to have no lowering effect on AVB, TSP, and TTW wear rates. Consequently, the wear rate distributions for the active wear mechanisms will be based on observed wear at 100% power. The above assumption can be relaxed for future cycle assessments when sufficient data become available to justify attenuation in wear rates at reduced power operation.

As technical basis for using maximum dynamic pressure as a means for reducing the initiation behavior for TTW, the reduction in ρv^2 at 70% power was compared with the in-plane stability ratios computed by MHI (Ref. 7). The evaluation of stability ratio (SR) to mitigate FEI was studied for different power levels (50% to 100%) and for various support configurations (i.e., number of consecutive AVB supports that are no longer effective due to loss of contact force).

For comparing SR with the reduction in ρv^2 , the ratio of stability parameter at reduced power to the same parameter at 100% was used as another measure of improvement on POI. A plot of the evaluated tubes in the MHI assessment is shown in Figure 4-14. As can be seen, the normalized stability ratio decreases monotonically from 100% to 50% power levels for the range of support effectiveness. At 70% power, the normalized SR for the various cases when supports are modeled as inactive falls between 0.528 and 0.652 with an average value of 0.608. The ratio on ρv^2 falls within the scatter for normalized SR and represents a reasonable estimate of the effect of power reduction on initiation. Equation 4-2 is therefore used in the OA to account for the benefit of reduced power operation during Cycle 17.

4.8 MEASUREMENT UNCERTAINTY

Measurement uncertainty for sizing of indications is defined in the ETSSs for estimating actual (true) structural parameters (depth and length) from NDE size data. The OA procedure was constructed so that adjusting for measurement error will not be required. Wear index and any correlations between SONGS units is consistently based on NDE data. Initial depths assigned at BOC are actual values. Growth applied to BOC depths during the cycle are derived from +Point™ depth sizing (ETSS 27902.2) where the systematic error from linear regression is very small. Therefore, sizing uncertainty is not significant for estimating TTW rates.

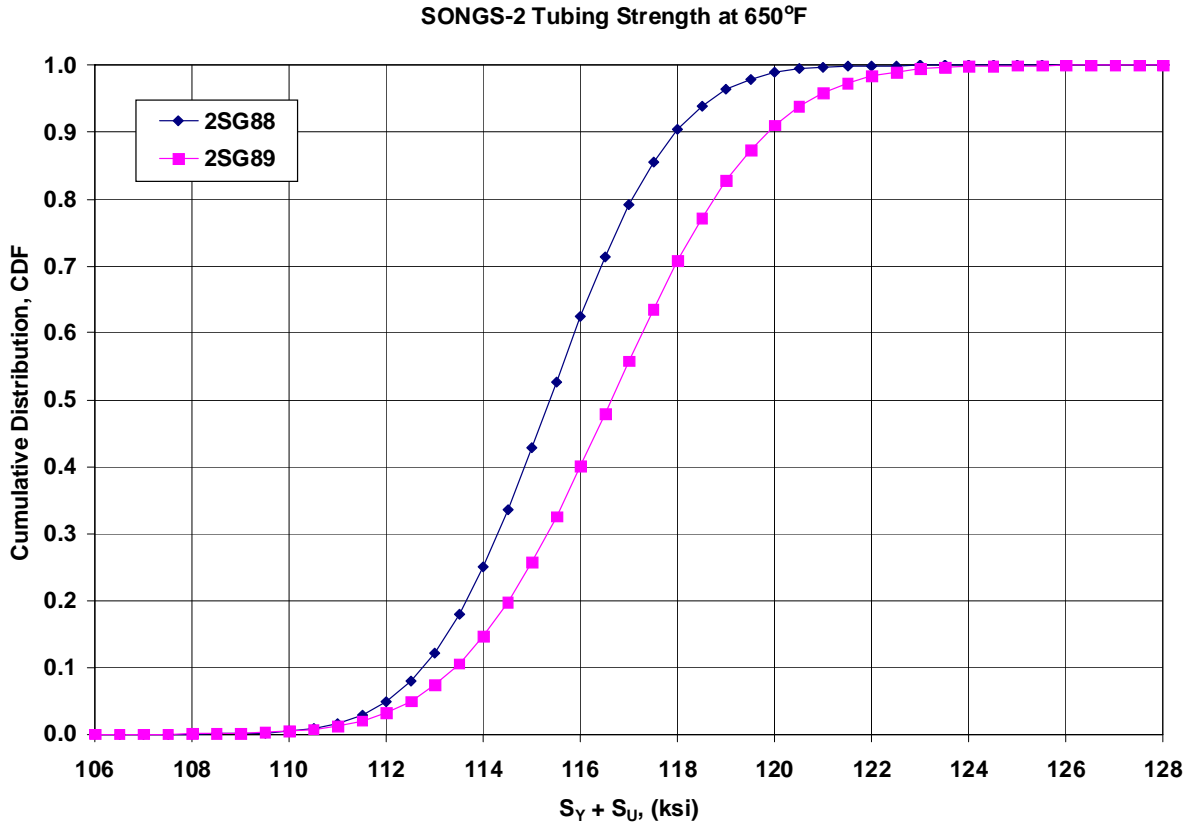


Figure 4-1 — Distribution of Tubing Strength Properties at 650°F

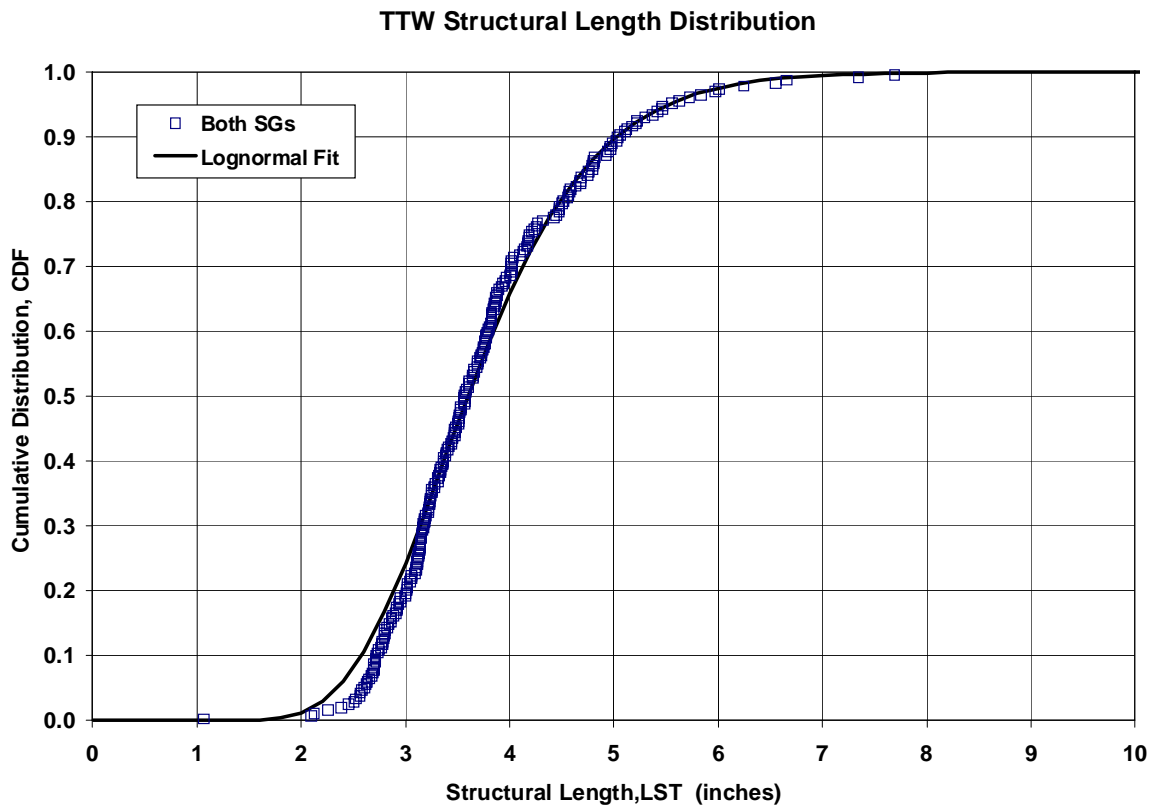


Figure 4-2 — Structural Length Distribution for TTW in U3

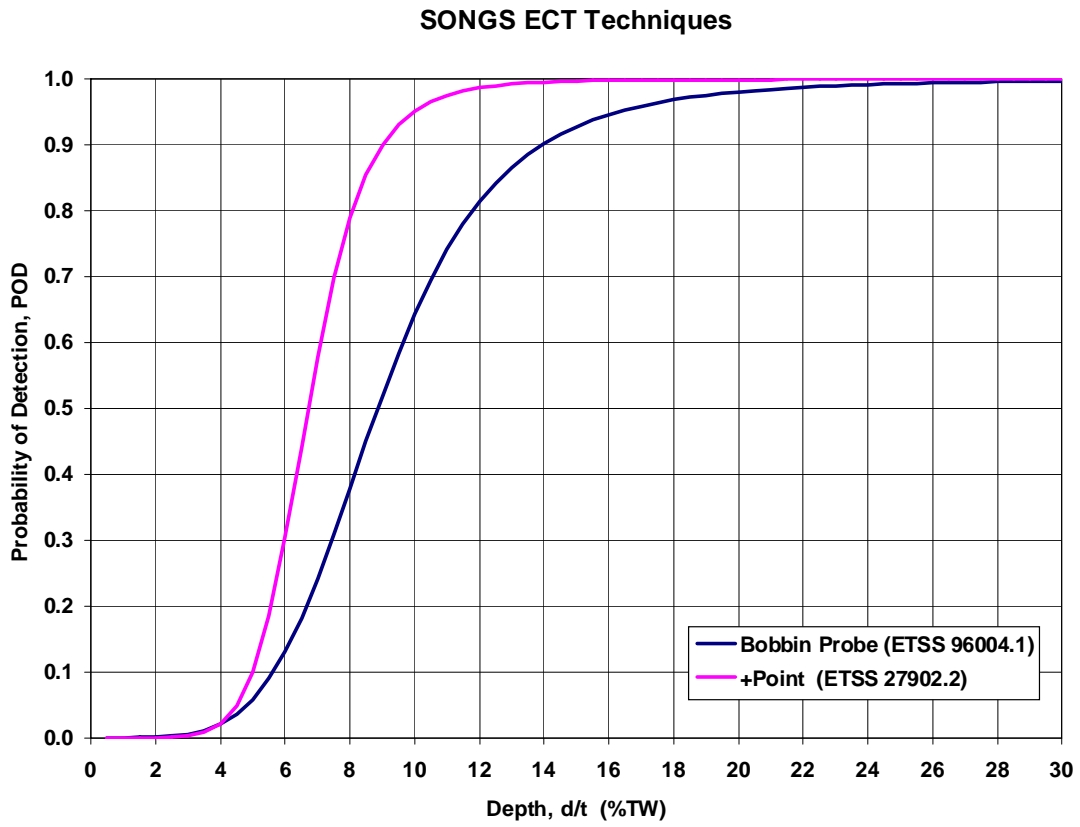


Figure 4-3— Probability of Detection for Tube Wear

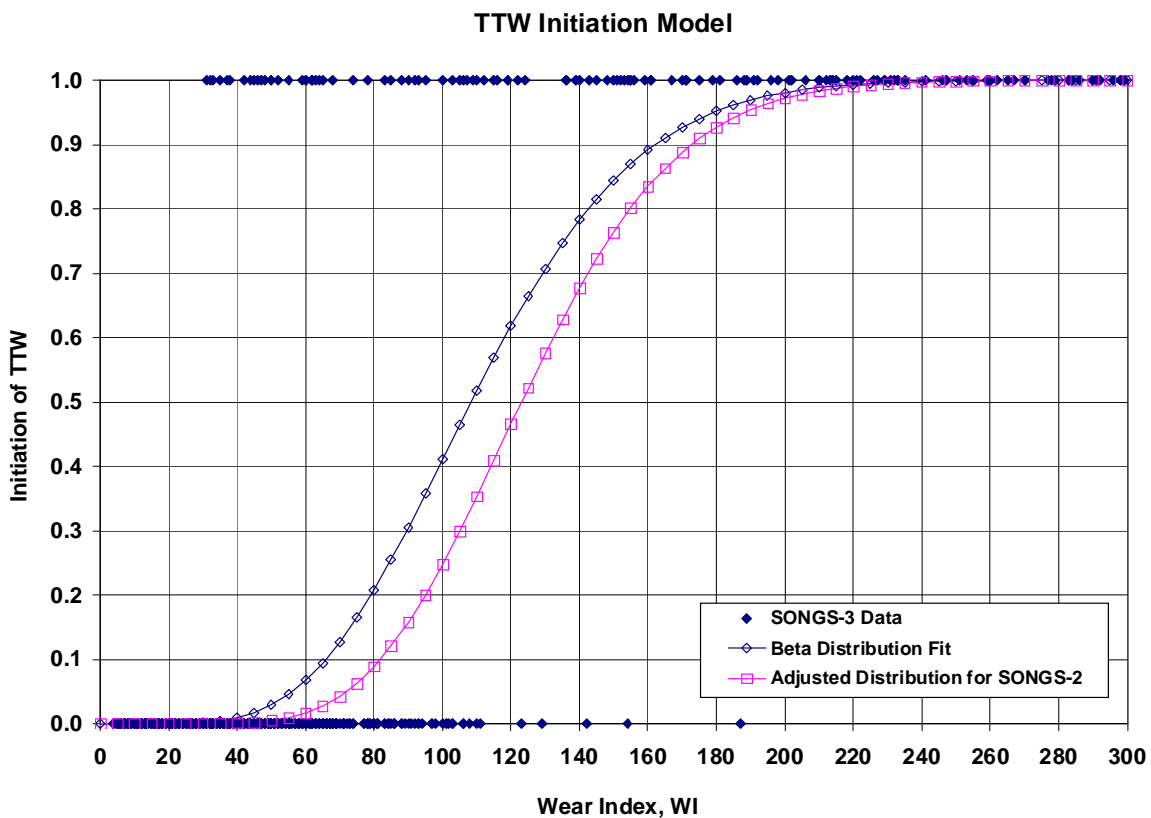


Figure 4-4— Tube-to-Tube Wear Initiation Model Based on Wear Index

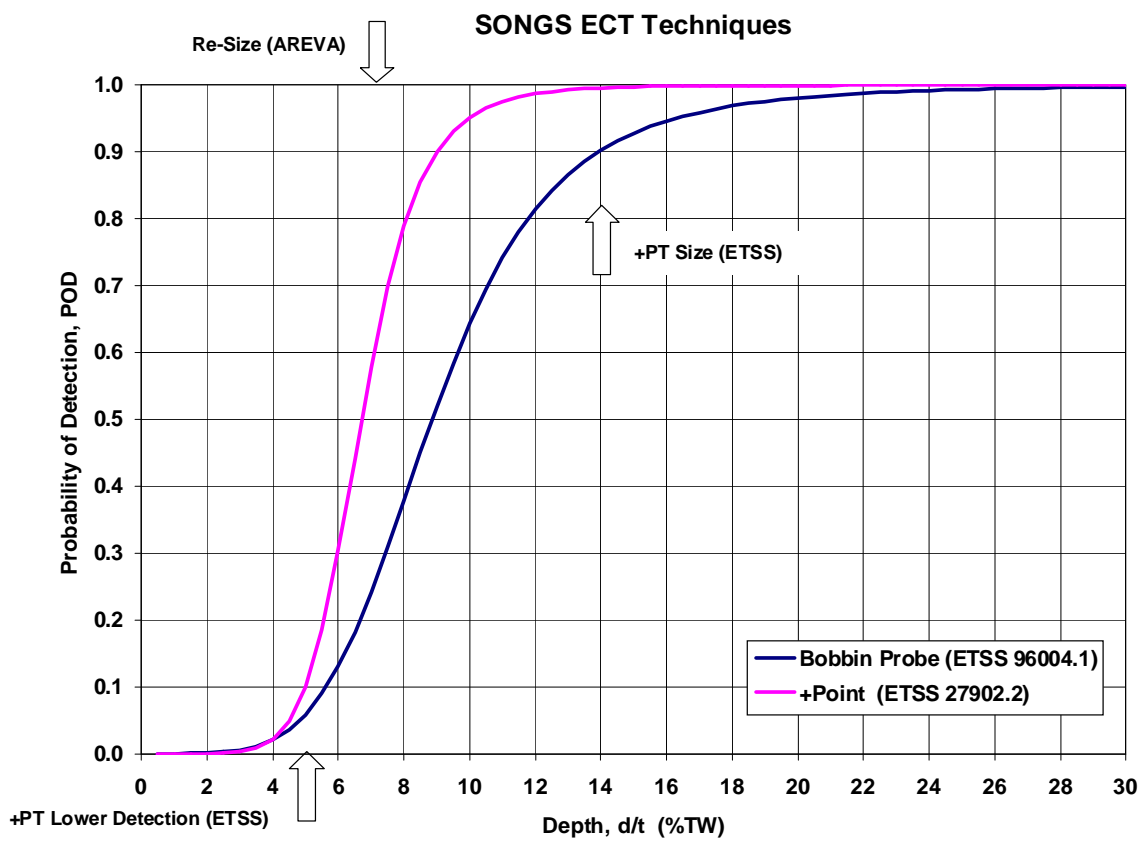
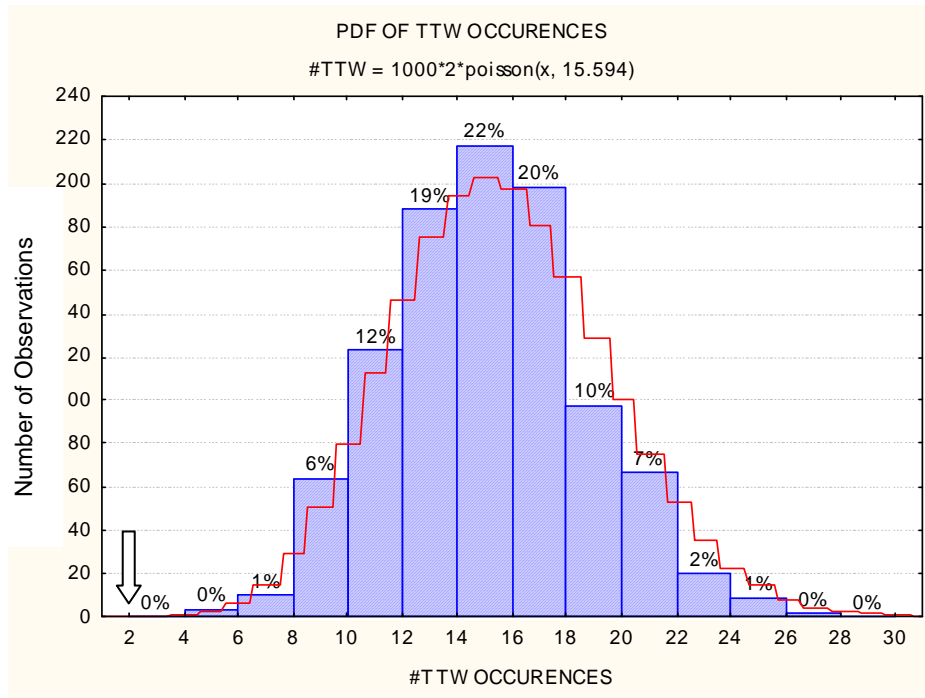
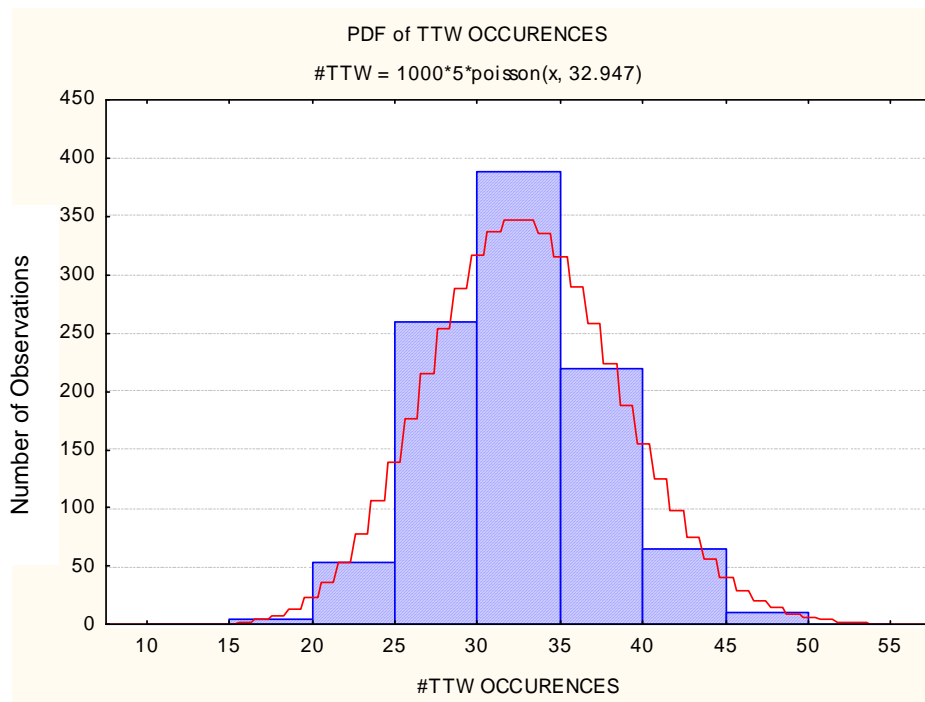


Figure 4-5 — Tube-to-Tube Wear Initiation Model Based on Wear Index



a) U2 Model TTW Occurrences Benchmark Results



b) U3 TTW Occurrences Model Prediction

Figure 4-6 — Initiation Model Adjustment for U2

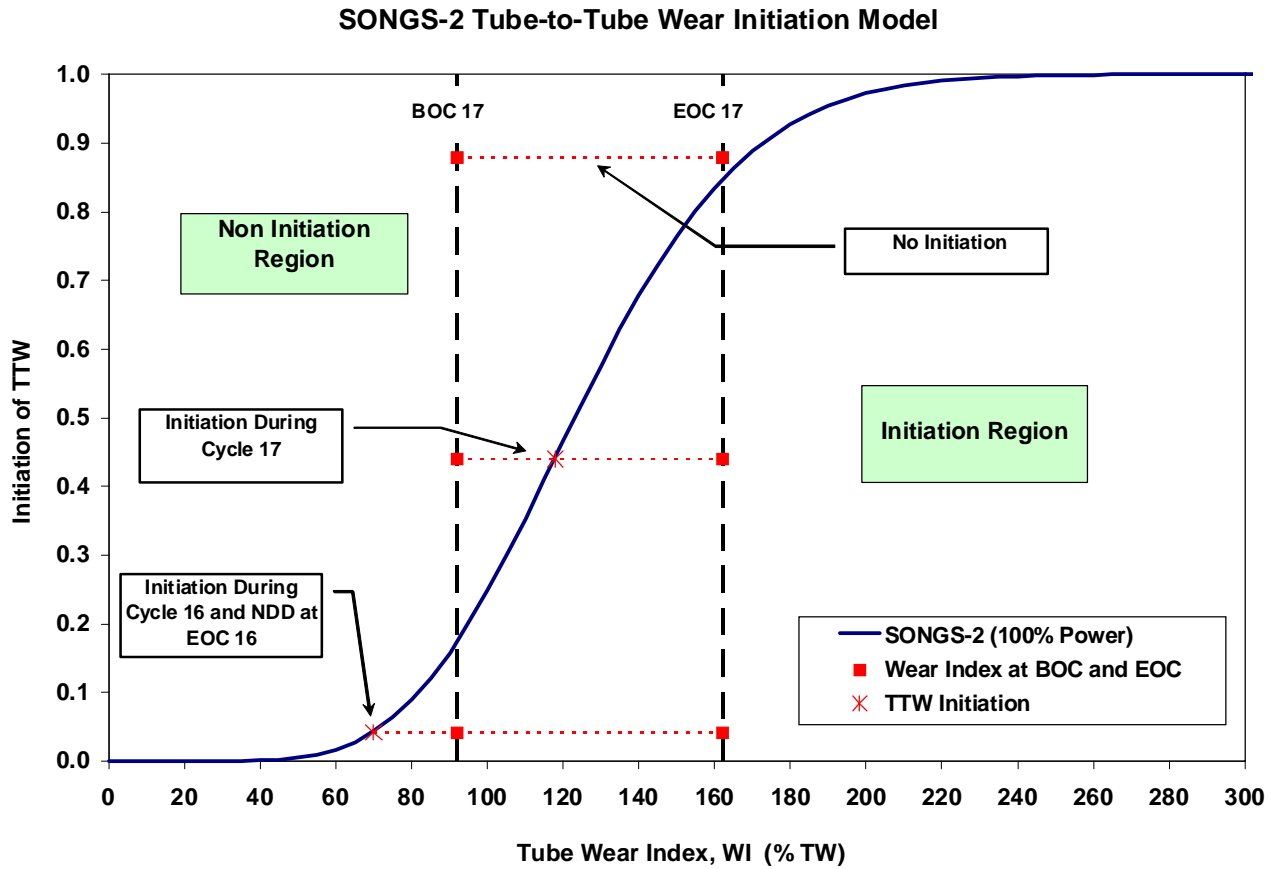


Figure 4-7 — Illustration of TTW Initiation Time Model Estimation

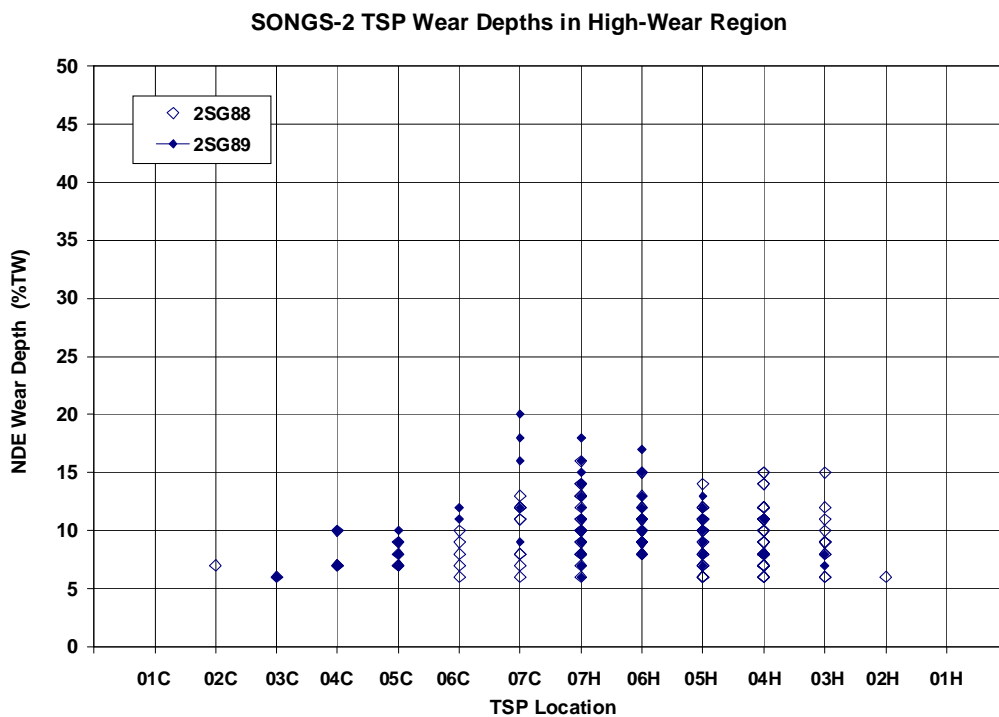
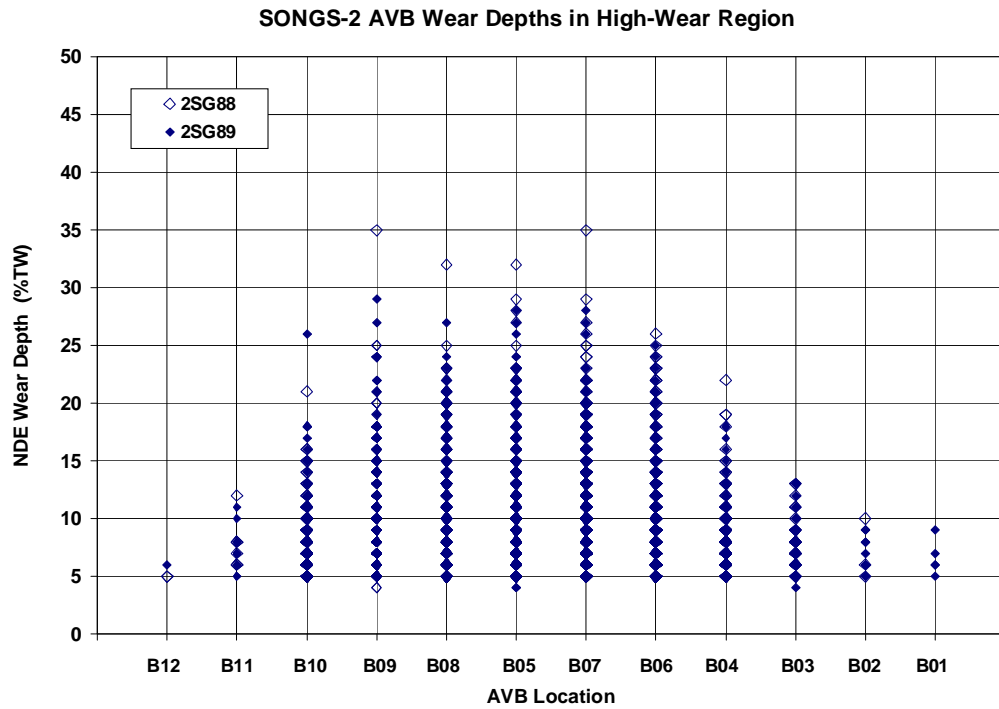


Figure 4-8 — NDE Depth Distributions for AVB and TSP by Support Location

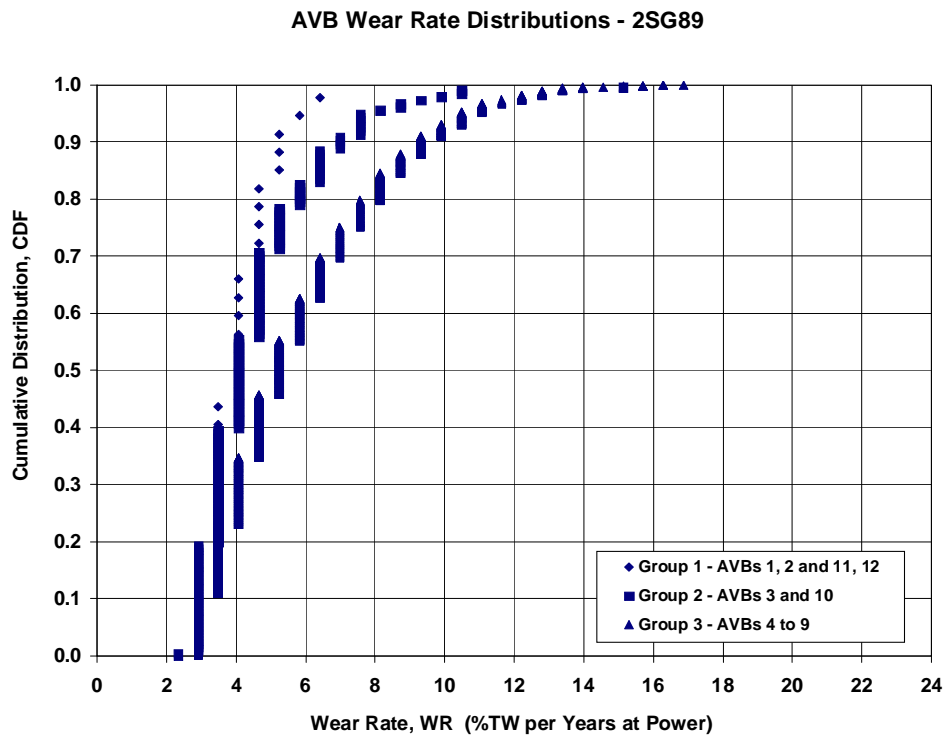
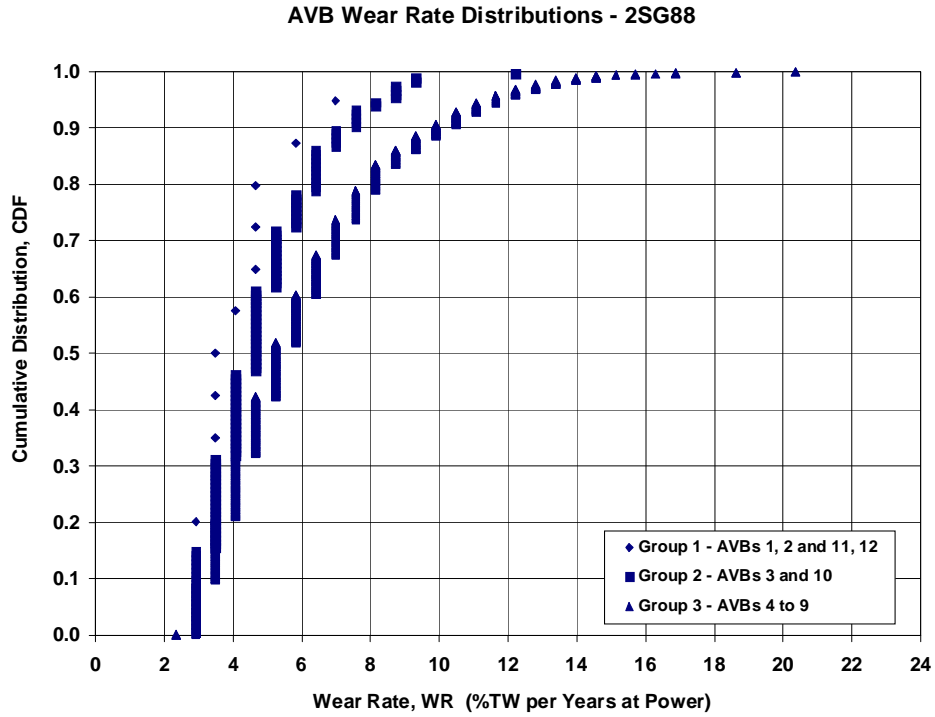


Figure 4-9 — Apparent Wear Rates for AVB Supports

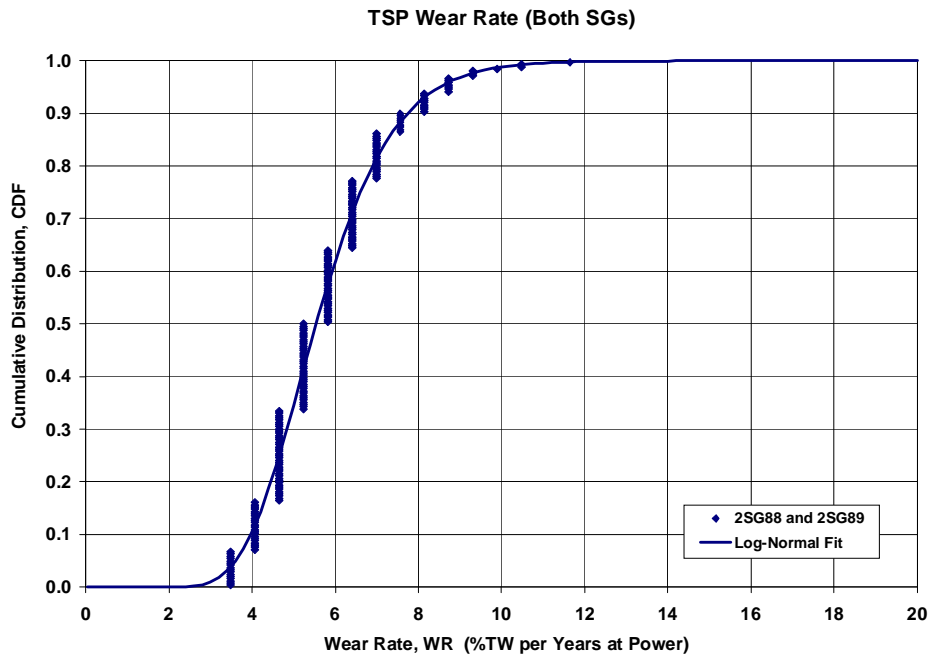
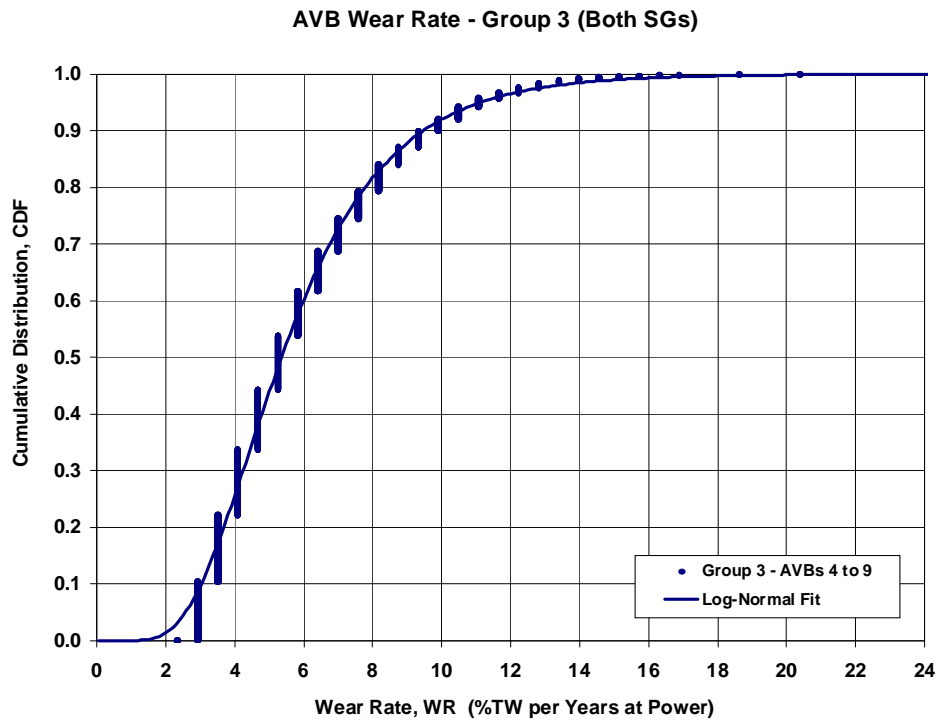
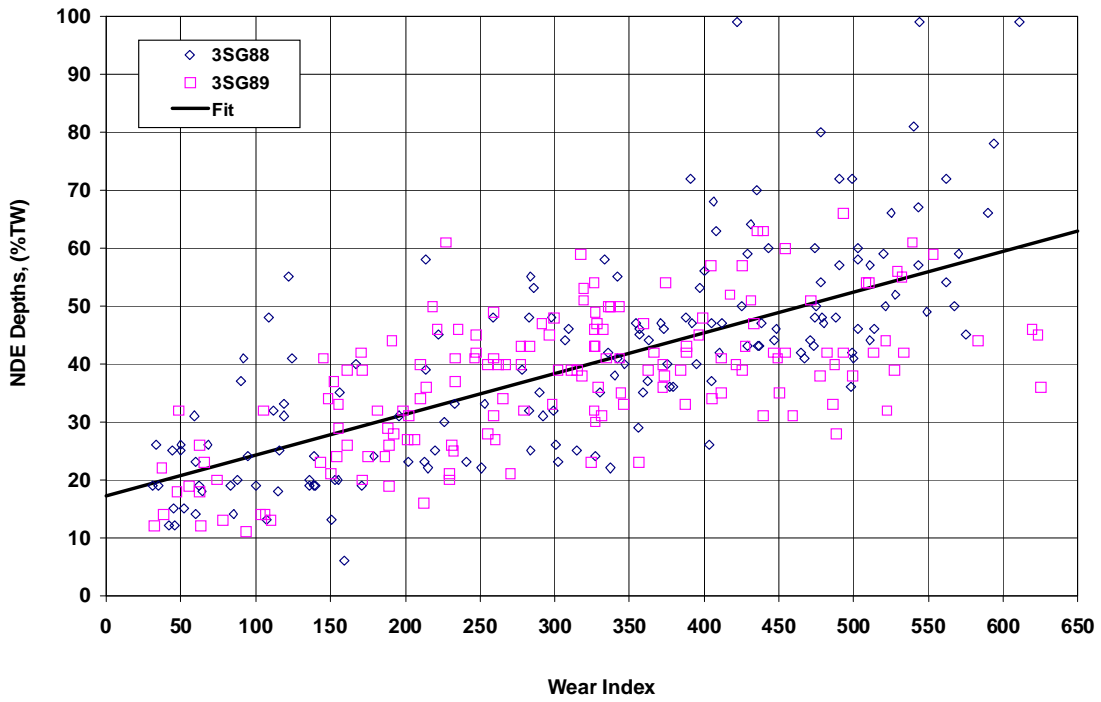


Figure 4-10 — Wear Rate Distributions for AVB and TSP Wear Mechanisms

Tube-to-Tube Wear Depths - Max Data (ETSS 27902.2)



Tube-to-Tube Wear Depths - Max Data (AREVA Resized)

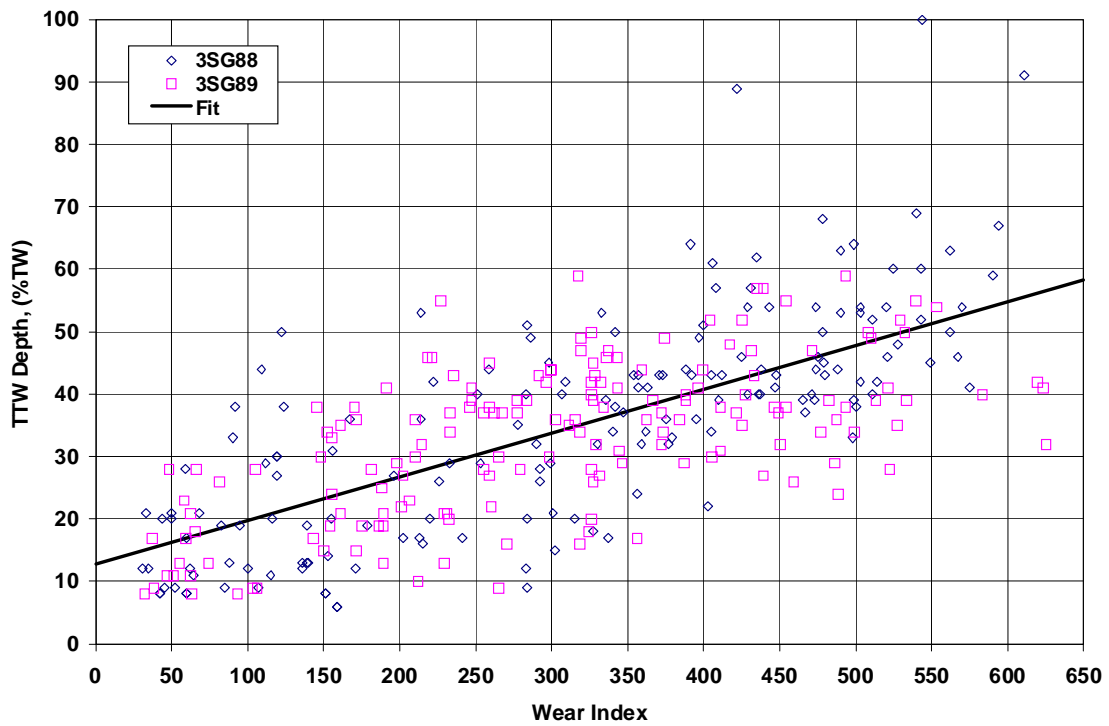


Figure 4-11 — Maximum NDE Depths for TTW

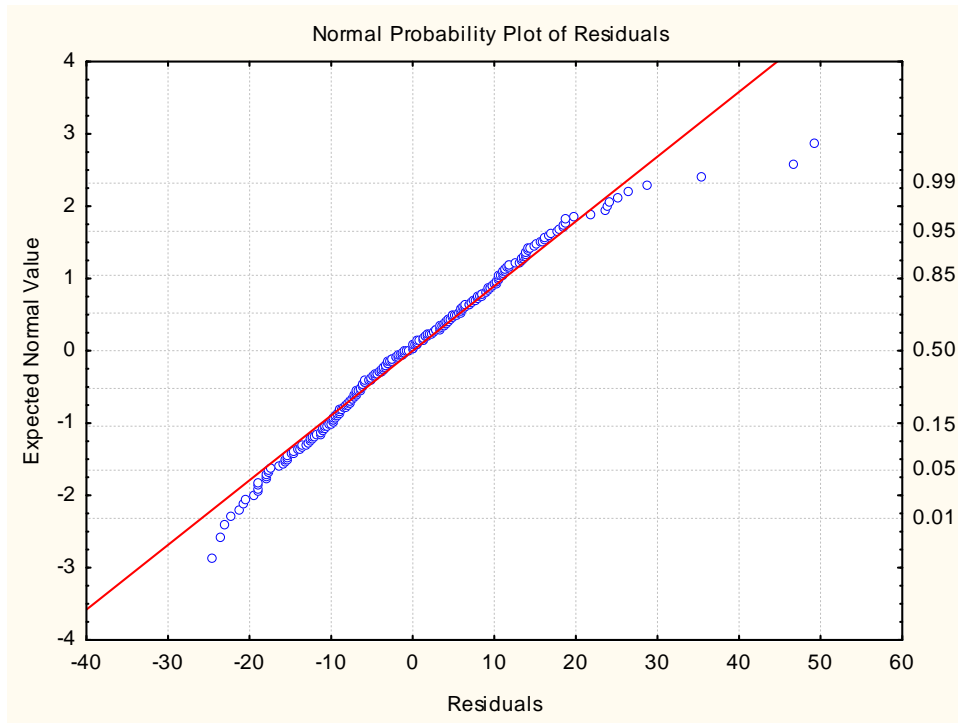
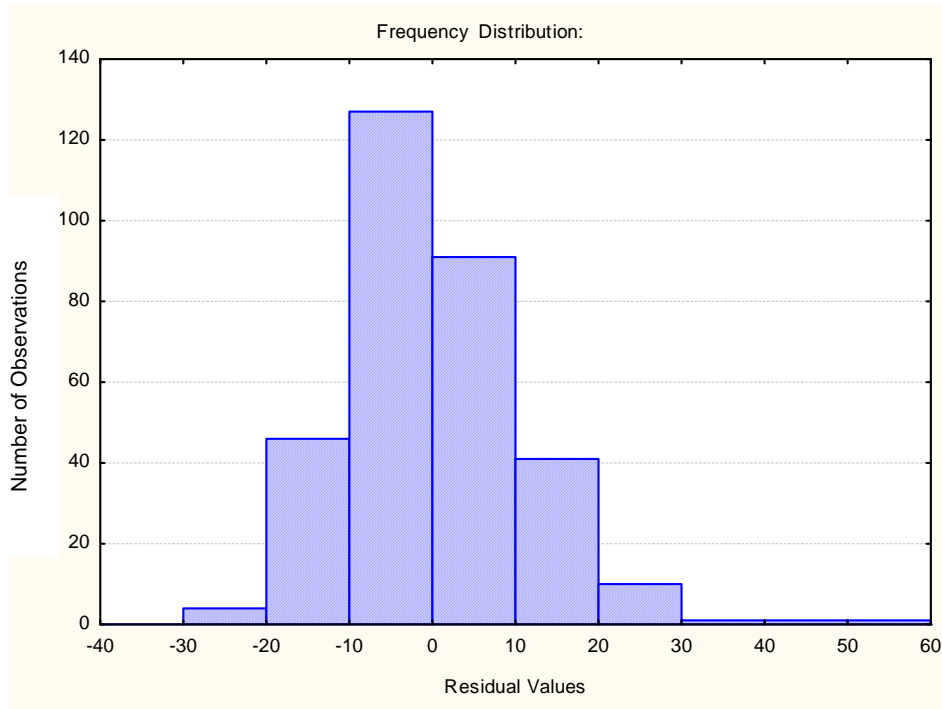
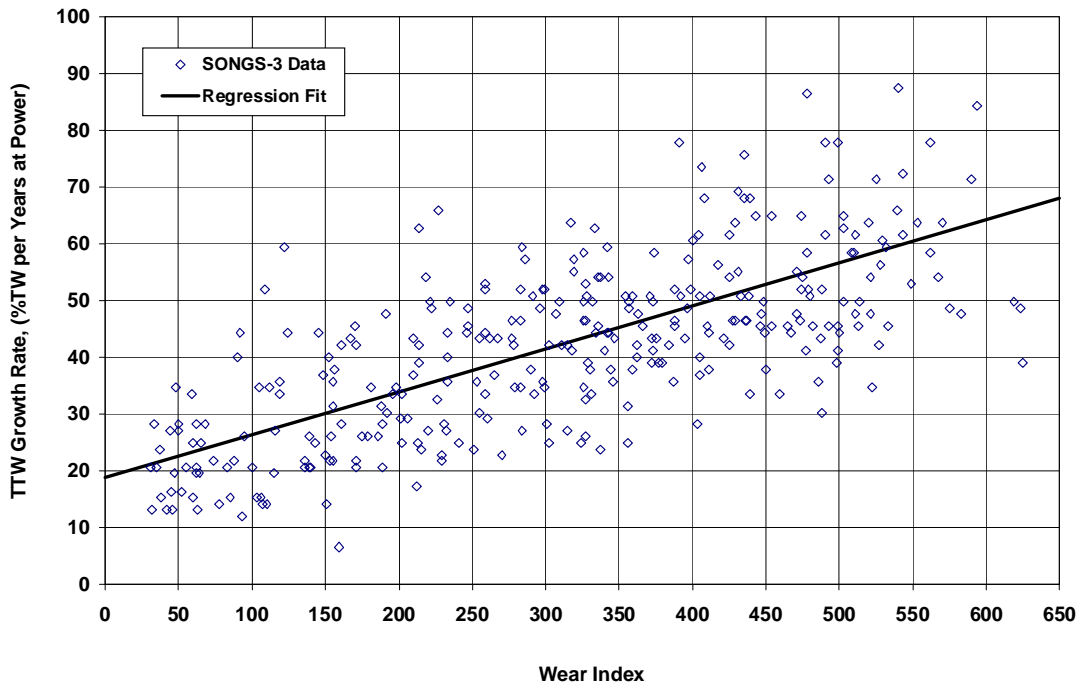


Figure 4-12 — Regression Analysis Results for TTW Depth Data

ETSS 27902.2 Sizing



AREVA Resized

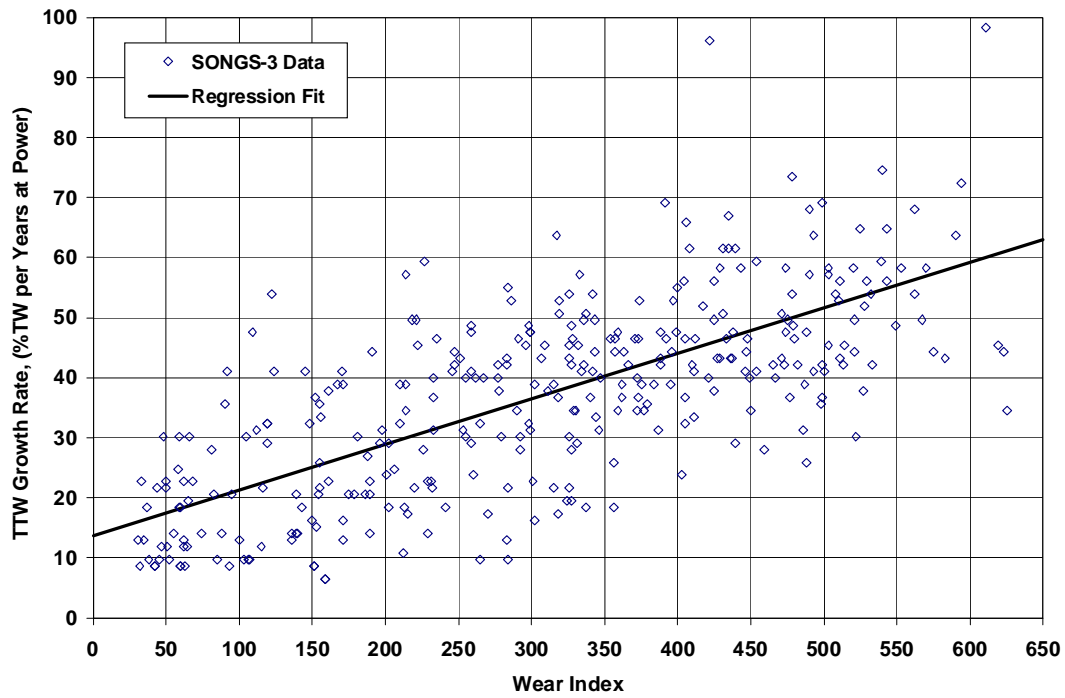


Figure 4-13 — Tube-to-Tube Wear Rate as a Function of Wear Index

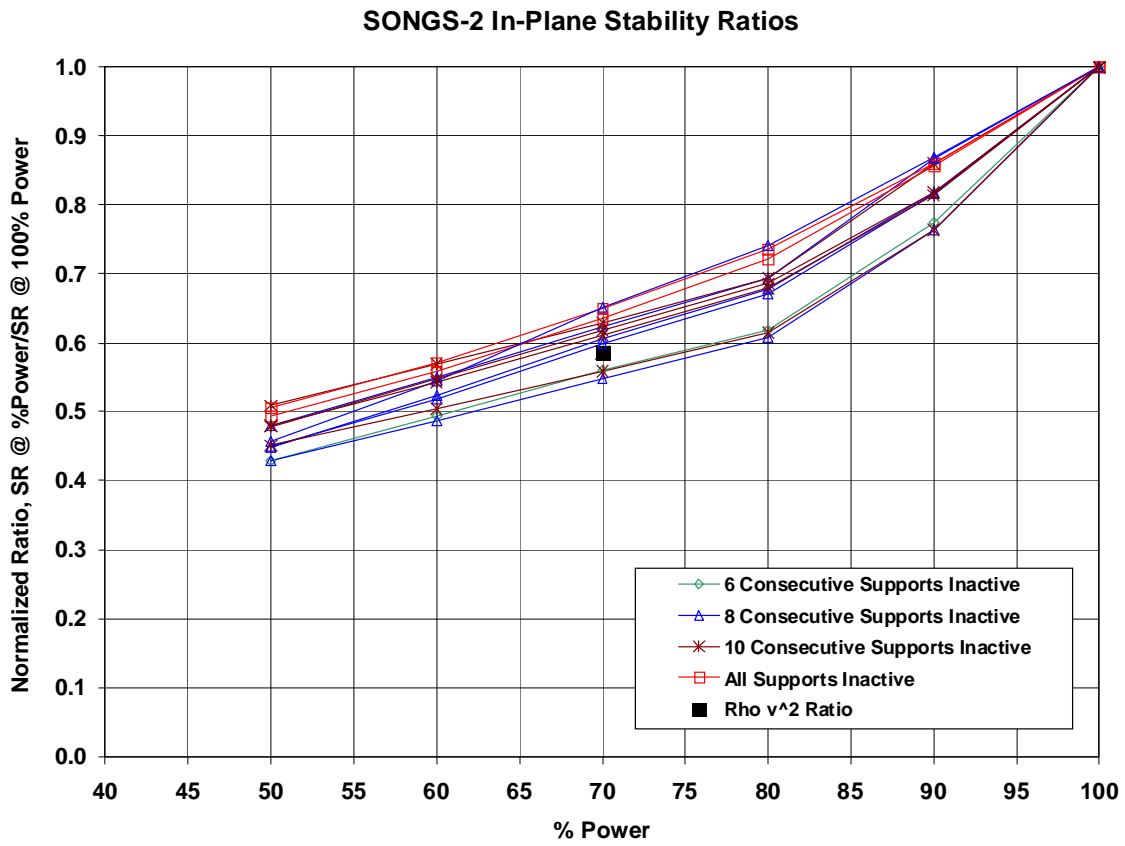


Figure 4-14— Effect of Reduced Power Conditions on Fluid Elastic Instability Ratio for Various Inactive Support Configurations (Ref. 7)

Section 5 OPERATIONAL ASSESSMENT

5.1 ANALYSIS CASES

The OA for TTW degradation was performed by Monte Carlo simulation with 10,000 trials applied to produce the minimum burst pressure and maximum depth distributions at EOC 17. Two basic cases were evaluated that look at the effect of TTW rate models as described below:

Case 1 – Tube-to-tube wear rate based on the U3 wear depths after 0.926 years at power sized with ETSS 27902.2 (Ref. 13)

Case 2 – Tube-to-tube wear rate based on the U3 wear depths after 0.926 years at power sized with AREVA hybrid voltage model (Ref. 14)

Each case was evaluated for 70% reduced power operation. The original schedule length for Cycle 17 is 1.578 years at power and was used as a starting cycle length to evaluate in the OA. The effect of running a shorter cycle was parametrically analyzed. The actual schedule length for Cycle 17 may be as short as 5 months in order to have additional margins for U2 operation.

In the model development, a decrease in NOPD is due to reduced power operation. This effect is included in the assessment for 70% reduced power operation. The effect of the decrease in ρv^2 due to the reduced power is also included in the TTW initiation model as discussed in Section 4.7.

5.2 SIMULATION RESULTS

The structural analysis to establish the margins against tube burst was performed for the two analysis cases. The parameters for the input distributions are given in Table 5-1. Some simulation results are presented to show the evolution of the wear index for Cycle 17 and the effect of sizing assumptions (Cases 1 and 2). For one trial out of 10,000 total trials per simulation, the histogram of BOC and EOC wear index is shown in Figure 5-1. The BOC

distribution begins the cycle with relatively large number of low wear indices that grow over the cycle, 1.578 years at power in this case, to a broader spread of wear index values. For this trial, the largest wear index is about 170% TW projected at EOC 17. In general, the EOC wear index for the worst tube is less than 200% TW.

The EOC wear index is a key indicator on the likelihood that a TTW will initiate sometime during the cycle. The longer the cycle length assumed for Cycle 17, the greater the chance to initiate and grow a TTW flaw to a depth that challenges SIPC margin requirements. The number of initiated TTW flaws for a single trial is shown in Figure 5-2, where the number of initiations is plotted against the time at which initiation is calculated to occur. The total number of TTW initiations in this single trial is 64. Although not shown, the effect of power level has a significant impact on the number of initiations.

As illustrated in Figure 5-2, most TTW flaws are predicted to initiate after half-way through the cycle. A few initiations are calculated to occur early in the cycle. As expected, the increase in TTW flaws increases with operation time. Operating U2 for shorter cycle lengths significantly decreases the chance in having TTW. In most all simulations, the lowest burst pressure tube has initiated TTW at BOC or very early in the cycle. The POB results for the full simulation of TTW degradation mechanism are discussed in Section 5.3.

5.3 STRUCTURAL MARGIN EVALUATION

The structural analysis for tube burst and leakage was completed for a range of operating periods. The POB was determined from the distribution of worst case burst pressures which is compared to the SIPC margin of 3xNOPD. Figure 5-3 illustrates the burst pressure distributions at EOC 17 at 70% power for the two NDE sizing cases. The lower extreme values for the AREVA resized case crosses the $POB \leq 0.05$ line at a burst pressure below the 3xNOPD margin limit. The case using ETSS 27902.2 or the AREVA technique for sizing TTW depths do not satisfy the SIPC margins for the scheduled cycle length of 1.578 years at power.

To determine the effect of cycle length on POB, several simulations were performed for different operating periods. The POB results from this parametric assessment are given in Figure 5-4. Again, it can be seen that full-cycle operation is not achieved at 70% power level for either analysis cases, but the margin requirements can be met at somewhat shorter operating times.

The following allowable cycle lengths have been computed:

Cycle Lengths at POB = 5%

Analysis Case	Years at 70% Power
Case 1 – ETSS 27902.2 Sizing	1.33
Case 2 – AREVA Resized	1.48

The allowable operating cycle times are only 1 to 3 months shorter than the original scheduled operation for U2. The minimum length for Cycle 17 at 70% power is 16 months.

5.4 LEAKAGE EVALUATION

Regarding calculated accident-induced leakage, due to the long and flat nature of TTW degradation, the limiting condition for EOC 17 is tube burst at 3xNOPD as opposed to leakage. This will be the case for all inservice tubes.

Table 5-1
OPERATIONAL ASSESSMENT INPUT PARAMETERS
TTW FOR U2 – EOC 16

Distribution	Type	Parameters	S/G 89 ⁽¹⁾	Basis ⁽²⁾
Probability of Detection	Log-Logistic	Intercept, A Slope, B	10.61 -11.20	ETSS 96004.1 (Ref. 12)
Probability of Detection	Log-Logistic	Intercept, A Slope, B	14.24 -17.22	ETSS 27902.2 (Ref. 13)
AVB Wear Rate (% TW per Years at Power)	Log Normal	Mean Ln(WR) Std Dev Ln(WR) Max Rate	1.68 0.45 20	U2 (Ref. 6b)
TSP Wear Rate (% TW per Years at Power)	Log Normal	Mean Ln(WR) Std Dev Ln(WR) Max Rate	1.71 0.26 20	U2 (Ref. 6b)
TTW Rate (% TW) ⁽³⁾ ETSS 27902.2	Normal	Intercept Slope Std Dev	17.257 0.0703 10.99	U3 (Ref. 13)
TTW Rate (% TW) ⁽³⁾ AREVA Resized	Normal	Intercept Slope Std Dev	12.747 0.0701 10.99	U3 (Ref. 14)
TTW Initiation Model	Beta	Shape 1 Shape 2	9.839 39.138	U3 (Ref.10a & 16))
Structural Length L _{ST} , (in.)	Log Normal	Mean Ln (L _{ST}) Std Dev Ln (L _{ST})	1.28 0.26	U3 (Ref. 11)
Shape Factor, F = d _{MAX} /d _{ST}	Normal	Mean (F) Std Dev (F)	1.00 0.0	U3
Strength, S _y + S _u (psi)	Normal	Mean (S _y + S _u) Std Dev (S _y + S _u) Min (S _y + S _u) Max (S _y + S _u)	116,633 2,504 109,900 123,900	U2 CMTR Data 2SG89 (Ref. 10b)
Normal Operating Pressure Differential, (psi)	Constant	NOPD at 100% NOPD at 70%	1325 1305	U2 (Ref. 7 & 9)
Limiting Accident Pressure Differential, (psi)	Constant	LAPD	2560	U2 (Ref. 3)
Cycle 17 Length (Years at Power)	Constant	τ	1.578	Operating Schedule (Ref. 9)

Notes

- (1) 2SG89 is taken as the limiting steam generator
- (2) Databases for U2 and U3 data are from cited references
- (3) TTW rates computed by dividing depth distribution by 0.926 years at power

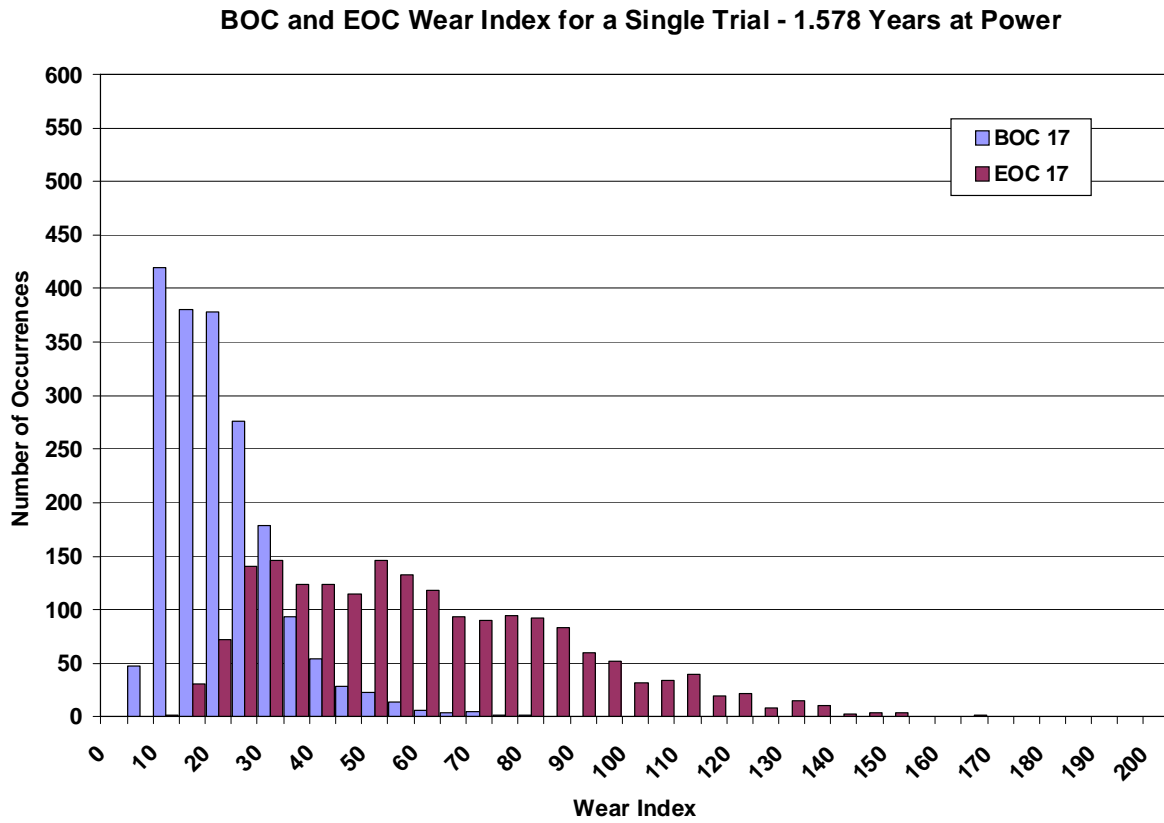


Figure 5-1 — Histogram of BOC and EOC Wear Index for a Single Trial for Cycle 17 (1.578 Years at Power)

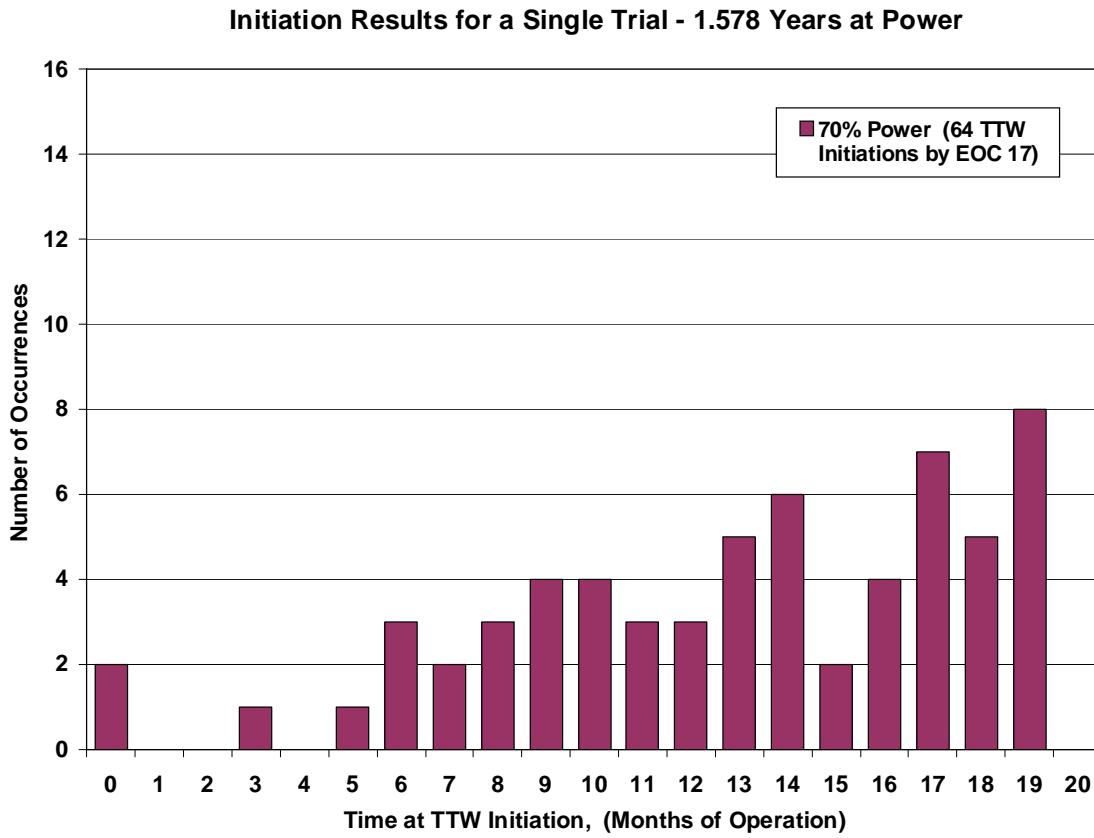


Figure 5-2 — Histogram of TTW Initiations at 70% Power for a Single Trial for Cycle 17 (1.578 Years at Power)

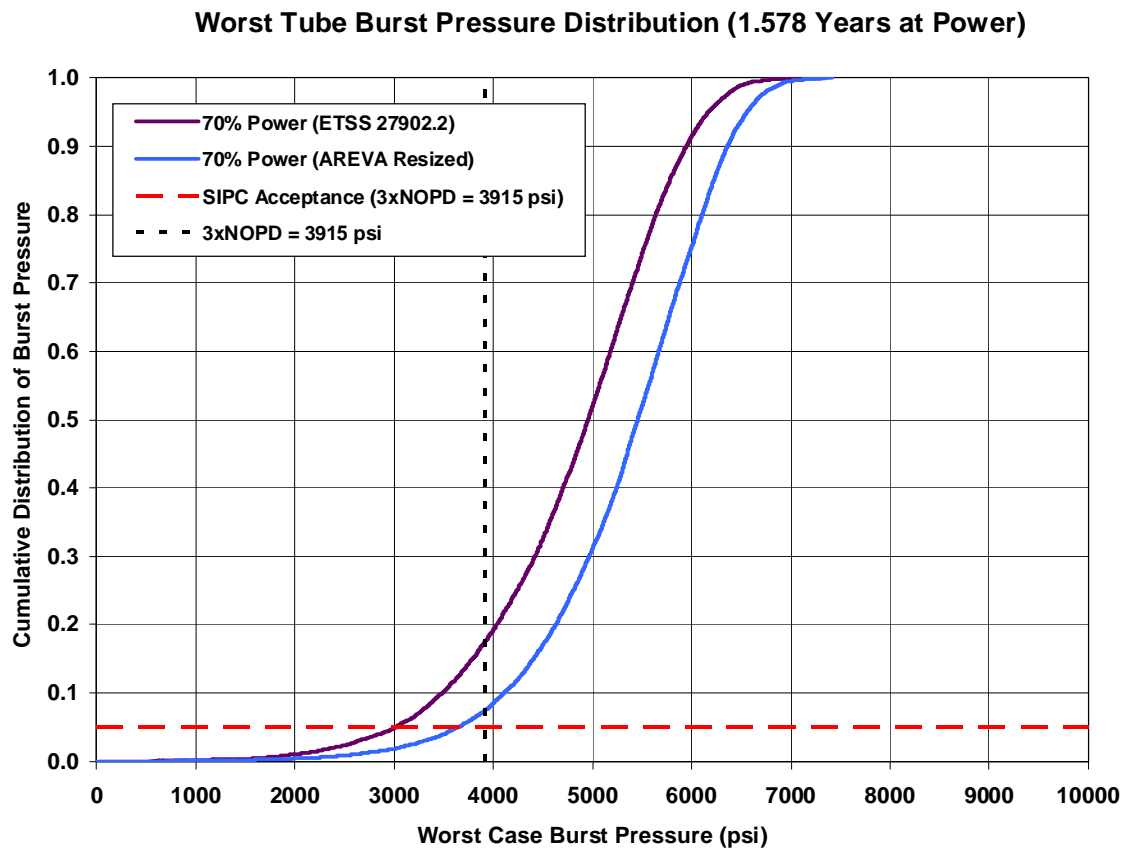


Figure 5-3 — Burst Pressure Distribution for the Worst Tube in the High-Wear Region at EOC 17 after 1.578 Years at 70% Power

Operational Assessment for TTW for Cycle 17

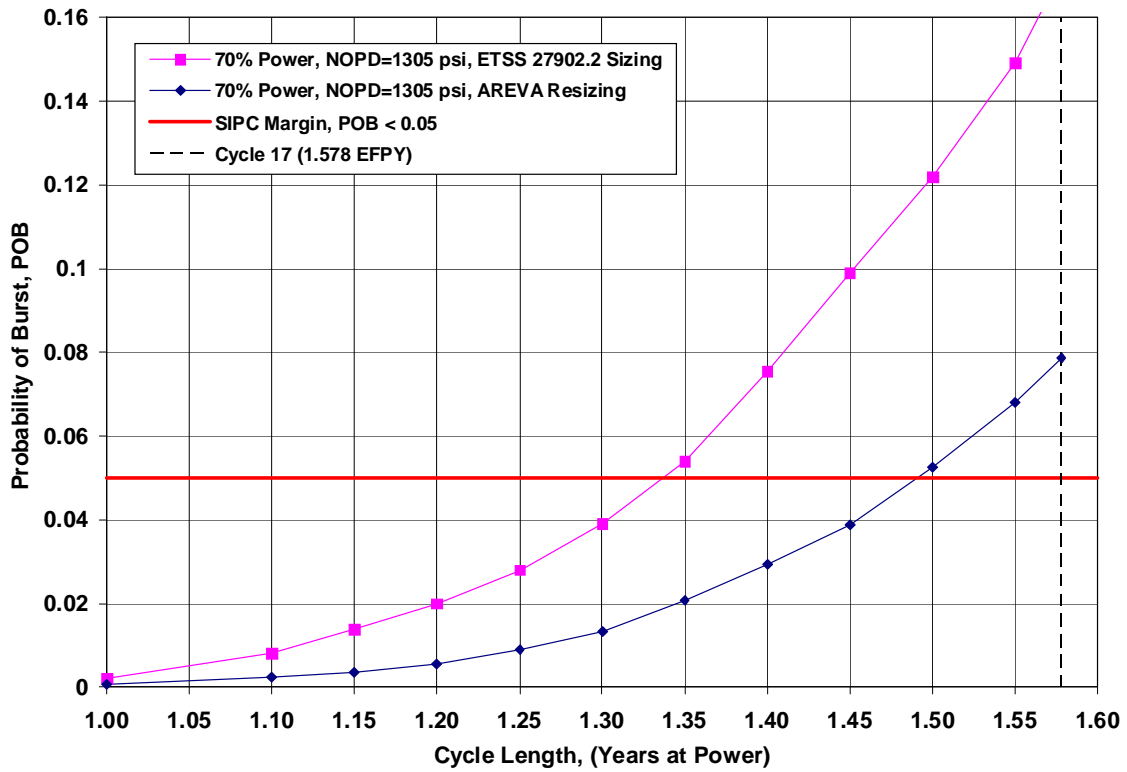


Figure 5-4 — Probability of Burst at 70% Power Level for TTW Growth Rate Models Based on Case 1 - ETSS 27902.2 Sizing (Ref. 13) and Case 2 - AREVA Resizing Models (Ref. 14)

Section 6

SUMMARY OF RESULTS

The steam generator tube examinations for U2 and U3 identified significant wear degradation. The limiting wear mechanism for U3 is freespan TTW in the U-bends where through-wall leakage had occurred after only 0.926 years at power. The cause of this degradation is in-plane tube vibratory motion due to fluid elastic instability under full power operation. The observed wear degradation in U2 is far less than that detected U3. Only minor TTW was detected in U2 steam generator (2SG89), however, both units are basically the same design and Cycle 17 operation for U2 must address TTW degradation mechanism. The U3 wear behavior was used to establish the initiation and growth of TTW indications in U2 steam generators. An empirical correlation based on a wear index parameter (measure of the state of wear degradation in each tube) provided the method of scaling the U3 wear behavior to U2.

Two OA analysis cases were evaluated based on the sizing techniques used to define the U3 TTW depths. Case 1 used ETSS 27902.2 (Ref. 13) for the voltage based sizing and these data were used to establish the TTW growth rate distribution in Figure 4-13. The OA results for Case 1 indicate that the SIPC margin requirements are satisfied for a Cycle 17 length of 1.33 years at the 70% power level. For Case 2, where the wear rates were based on TTW depths as resized by AREVA using a different calibration standard, the SIPC margins will be met for a cycle length of 1.48 years at 70% power level. Therefore, the minimum length for Cycle 17 at 70% power is 16 months based on the more conservative Case 1 results.

Because of the character of TTW indications, being relatively flat and long in the axial direction, tube burst at 3xNOPD is the limiting requirement for cycle length. The projected accident-induced leak rates for TTW will not be limiting since ligament pop-through at limiting accident pressures will not precede burst condition at 3xNOPD. The predicted EOC 17 maximum depths for TTW will not create thin remaining ligaments subject to pop-through conditions. Therefore, the accident-induced leakage requirements will be satisfied provided that burst margins at 3xNOPD are maintained during the operating cycle..

REFERENCES

1. "Steam Generator Program Guidelines," Nuclear Energy Institute NEI 97-06 Rev. 3, (January 2011)
2. "Steam Generator Integrity Assessment Guidelines, Revision 3," Electric Power Research Institute, Steam Generator Management Program, EPRI Report 1019038, (November 2009)
3. "SONGS 2C17 Steam Generator Condition Monitoring Report," Document No. 51-9182368-002, AREVA NP.
4. "Steam Generator Degradation Specific Management Flaw Handbook, Revision 1," 1019037, Electric Power Research Institute, Steam Generator Management Program (December 2009)
5. "Verification of Program TTWEAR_U2 for the Operational Assessment for SONGS Unit 2," Draft Calculation No, AES-C-8150-1, Intertek APTECH, (September 2012)
6. Email from A. Brown (AREVA) to R. Cipolla (Intertek APTECH), "SONGS Tube to-Tube Wear Indications," dated June 09, 2012, Attachments:
 - a) SONGS3 AVB and TSP Wear Depth Distribution.xlsx
 - b) SONGS2 AVB and TSP Wear Depth Distribution.xlsx
7. "Evaluation of Stability Ratio for Return to Service," MHI, L5-04GA567, Rev. 6, (September 11, 2012)
8. Letter from A. Matheny (SCE) to A. Brown (AREVA), "Numerical Values for the Steam Generator Degradation Assessment San Onofre Nuclear Generating Station, Unit 2, Southern California Edison," (January 18, 2012)
9. Letter from A. Matheny (SCE) to A. Brown (AREVA), "Numerical Values for the Steam Generator Operational Assessment San Onofre Nuclear Generating Station, Units 2 and 3," (February 8, 2012)
10. Email from A. Brown (AREVA) to R. Cipolla (Intertek APTECH), "OA Data Request," dated June 14, 2012, Attachments:
 - a) SONGS Wear Table w All Tubes.xlsx
 - b) SONGS2 CMTR.xlsx
11. Email from A. Brown (AREVA) to R. Cipolla (Intertek APTECH), "AVB Wear Info," dated June 16, 2012, Attachments:
 - a) SONGS2 AVB Wear Structural Dimensions.xlsx
 - b) SONGS AVB Wear Length Review.xlsx

12. ETSS 96004.1, Revision 13 (April 2010), Test Application: Wear at tube supports, anti-vibration bars, vertical and diagonal straps,” Source: Electric Power Research Institute, EPRIq.com Performance Database.
13. ETSS 27902.2, Revision 1 (May 2012), Test Application: Detection of Axial Groove Volumetric indications and depth sizing within the freespan area, loose part not present,” Source: Electric Power Research Institute, EPRIq.com Performance Database.
14. Email from A. Brown (AREVA) to R. Cipolla (Intertek APTECH), “OA Data Request,” dated June 14, 2012, Attachments:
 - a) SONGS Sizing Summary.xlsx
 - b) SONGS2 TTW Sizing Comparison.xlsx
15. Email from C. Waskey (AREVA) to R. Cipolla (Intertek APTECH), “Dynamic Pressure Data for Power Reduction,” (June 27, 2012)
16. Emails from A. Brown (AREVA) to R. Cipolla (Intertek APTECH), “SONGS Tube-to-Tube Wear Indications,” Attachment
SONGS TTW Depth Distributions 2012.xlsx, (June 9, 2012)

Appendix A

REPORT ACRONYMS

Acronym	Description
2SG88	Unit 2 Steam Generator 88
2SG89	Unit 2 Steam Generator 89
3SG88	Unit 3 Steam Generator 88
3SG89	Unit 3 Steam Generator 89
3xNOPD	Three times normal operating pressure differential
95-50	95% probability at 50% confidence
AILPC	Accident Induced Leakage performance Criteria
AVB	Anti-vibration bar
BOC	Beginning of operating cycle
CM	Condition monitoring
CYC	Length of cycle
EOC	End of operating cycle
EPRI	Electric Power Research Institute
ETSS	Examination Technique Specification Sheets
GPM	Gallons per minute
NDD	No degradation detected
NDE	Non destructive examination
NEI	Nuclear Energy Institute
OA	Operational assessment
POB	Probability of burst
POD	Probability of detection
POI	Probability of initiation
QA	Quality assurance
RN	Random number
SG	Steam generator

REPORT ACRONYMS (Cont'd)

Acronym	Description
SIPC	Structural Integrity Performance Criteria
SR	Stability ratio
TSP	Tube support plate
TTW	Tube-to-tube wear
TW	Through wall
U2	San Onofre Unit 2 (also SONGS-2)
U3	San Onofre Unit 3 (also SONGS-3)
WI	Wear index
WR	Wear rate

ATTACHMENT 6 – Appendix D

Operational Assessment of Wear Indications In the U-bend Region of San Onofre Unit 2 Replacement Steam Generators

**Operational Assessment of
Wear Indications in the U-bend Region of
San Onofre Nuclear Generating Station Unit 2
Replacement Steam Generators**

**August 2012
(Revision 3: October 2012)**

Prepared by: Electronically Approved*
P. J. Prabhu, Fellow Engineer
Steam Generator Management Programs

Reviewed by: Electronically Approved*
D. J. Ayres, Consultant
Steam Generator Management Programs

Approved by: Electronically Approved*
W. J. Bedont, Manager
Steam Generator Management Programs

** Electronically approved records are authenticated in the electronic document management system.*

©2012 Westinghouse Electric Company LLC
All Rights Reserved

STATUS STAMP ON PAGE 2

Table of Contents

Executive Summary	4
1 Introduction	5
2 Overall Analytical Methodology	6
2.1 Outline of Methodology.....	6
2.2 Thermal-Hydraulic Analysis.....	7
2.2.1 Methods.....	7
2.2.2 Results Summary	9
2.3 Flow-Induced Vibration Analysis	10
2.3.1 Methods.....	10
2.3.2 FIV Results Summary	17
2.4 Determination of Tube Support Effectiveness from Eddy Current Data	17
2.4.1 Out-of-plane Vibration	17
2.4.2 In-plane Vibration	19
2.5 Tube Wear Progression.....	19
2.5.1 Methods.....	19
2.5.2 Application to SONGS Steam Generators	23
2.5.3 Results Summary	24
2.5.4 Wear Projection Uncertainty.....	26
2.6 Evaluation of the Potential for In-Plane Vibration	27
2.6.1 Methodology Benchmarking Using Unit 3 Findings.....	28
3 Operational Assessment.....	82
3.1 Tube Wear at AVBs.....	82
3.1.1 Structural Limits.....	82
3.1.2 Evaluation Method.....	83
3.1.3 Results for Active Tubes	84
3.1.4 Results for Plugged Tubes	84
3.1.5 Evaluation for 18 Months of Operation	85
3.2 Tube-to-Tube Wear in U-bend Free Span.....	85
3.2.1 Eddy Current Inspection Results.....	85
3.2.2 Flow-Induced Vibration Analysis Results	85
3.2.3 Assessment of Tube-to-Tube Wear Mechanism	87
3.3 Potential for In-Plane Vibration	88
3.4 Operational Assessment Conclusion.....	89
4 References	96
5 Nomenclature	98
Appendix A. Tube-to-Tube Wear in Unit 2 U-bend Free Span.....	100

Supplier Status Stamp

VPL No:	1814-AA086-M0190	Rev No:	4	QC:	N/A
<input type="checkbox"/> DESIGN DOCUMENT ORDER NO. 800918458		<input checked="" type="checkbox"/> REFERENCE DOCUMENT - INFORMATION ONLY <input type="checkbox"/> VIRP IOM MANUAL			
MFG MAY PROCEED: <input type="checkbox"/> YES <input type="checkbox"/> NO <input checked="" type="checkbox"/> N/A					
STATUS - A status is required for design documents and is optional for reference documents. Drawings are reviewed and approved for arrangements and conformance to specification only. Approval does not relieve the submitter from the responsibility of adequacy and suitability of design, materials, and/or equipment represented.					
<input checked="" type="checkbox"/> 1. APPROVED <input type="checkbox"/> 2. APPROVED EXCEPT AS NOTED - Make changes and resubmit. <input type="checkbox"/> 3. NOT APPROVED - Correct and resubmit for review. NOT for field use.					
APPROVAL: (PRINT / SIGN / DATE)					
RE:		E. GRIBBLE 10/02/12			
FLS:					
Other:					

SCE DE(123) 5 REV. 3 07/11

REFERENCE: SO123-XXIV-37.8.26

List of Tables & Figures

Table 2-1. ATHOS Model R- θ Finite Difference Grid	31
Table 2-2. ATHOS Model Axial Direction (Z) Finite Difference Grid	32
Table 2-3. SONGS Unit 2 RSG 2E088 Tube Plugging List	33
Table 2-4. SONGS Unit 2 RSG 2E089 Tube Plugging List	34
Table 2-5. Cycle 17 Operating Parameters with 205 Plugged Tubes (SG 2E088).....	35
Table 2-6. Cycle 17 Operating Parameters with 305 Plugged Tubes (SG 2E089).....	36
Table 2-7. Summary of ATHOS Results	37
Table 2-8. Possible AVB Support Cases with Adjacent Ineffective AVBs (Page 1 of 15).....	38
Table 2-9. Wear Projection Results for Limiting Active Tubes and Plugged Tubes.....	53
Table 2-10. In-Plane Stability Ratios for Limiting Tubes	54
Table 2-11. Benchmarking Results for Boundary and Adjacent Tubes (Page 1 of 2)	55
Table 2-12. Benchmarking Results for Interior Tubes (Page 1 of 2).....	57
Table 3-1. Condition Monitoring Limit for Axial Thinning	90
Table 3-2. Wear Projection Results for Active Tubes with Limiting AVB Wear Indications.....	91
Table 3-3. Wear Projection Results for Plugged Tubes with Limiting AVB Wear Indications	92
Table 3-4. Wear Projection Results for Limiting AVB Wear Indications for 18 Months of Operation	93
Figure 2-1. ATHOS Finite Difference Grid in the Horizontal (R- θ) Plane	59
Figure 2-2. ATHOS Finite Difference Grid in the Vertical (R- θ) Plane	60
Figure 2-3. SG 2E089 Tube Row 141/Col. 89: Comparison of Gap Velocities at 50% Power	61
Figure 2-4. SG 2E089 Tube Row 141/Col. 89: Comparison of Gap Velocities at 60% Power	62
Figure 2-5. SG 2E088 Tube Row 141/Col. 89: Comparison of Gap Velocities at 70% Power	63
Figure 2-6. SG 2E089 Tube Row 141/Col. 89: Comparison of Gap Velocities at 70% Power	64
Figure 2-7. SG 2E089 Tube Row 141/Col. 89: Comparison of Gap Velocities at 80% Power	65
Figure 2-8. Representative FASTVIB / FLOVIB Tube Model.....	66
Figure 2-9. Straight Leg Tube Damping in Liquid	67
Figure 2-10. Out-of-Plane Excitation ratio Map – 100% Power – 7 AVBs Ineffective (Case 60)	68
Figure 2-11. In-Plane Stability Ratio Map – 100% Power – 7 AVBs Ineffective (Case 60).....	69
Figure 2-12. Out-of-Plane Excitation Ratio Map – 70% Power – 7 AVBs Ineffective (Case 60).....	70
Figure 2-13. In-Plane Stability Ratio Map – 70% Power – 7 AVBs Ineffective (Case 60).....	71
Figure 2-14. Schematic Illustrations of Triangular Pitch Tube Array Patterns	72
Figure 2-15. Comparison of Analytical Models of FIV Mechanisms.....	73
Figure 2-16. Typical Application of Semi-Empirical Wear Calculation Methodology.....	74
Figure 2-17. Fundamental Characteristic Trends Treated in Semi-Empirical Methodology.....	75
Figure 2-18. Wear Depth vs. Wear Volume (0.75 inch OD Tube, 0.59 inch AVB Width).....	76
Figure 2-19. U-bend OP Mode in Sample Evaluation Showing First Unstable FASTVIB Case and Postulated Initial Positions of AVBs 4 and 5 Relative to Mode Shape	77
Figure 2-20. Significant U-bend OP Modes in Sample Evaluation Showing Two FASTVIB Cases and Postulated Initial Positions of AVBs 3, 4, 5, and 6 Relative to Mode Shape	78
Figure 2-21. Example Illustration of AVB Wear Projection (Tube R121C91 in SG 2E089)	79
Figure 2-22. Logic Applied for Benchmarking the In-Plane Vibration Methodology Using Unit 3	80
Figure 2-23. Location of SG 3E088 Tubes Evaluated for Benchmarking	81
Figure 3-1. Condition Monitoring Limit for Axial Thinning	94
Figure 3-2. Operational Assessment Methodology for the Potential for In-Plane Vibration.....	95

Executive Summary

This report documents the operational assessment (OA) of the tube wear indications in the U-bend region of San Onofre Nuclear Generating Station (SONGS) Unit 2 steam generators (SG) based on inspection results from the 2012 outage (U2C17). This evaluation is a supplement to the OA which uses traditional/probabilistic methods. This evaluation is based on well-established methodology on flow-induced vibration of SG tubes. It utilizes the available test data on in-plane and out-of-plane instability and wear rate resulting from out-of-plane vibration of the tubes against anti-vibration bars (AVB).

Evaluation was performed for three degradation mechanisms: tube wear at AVBs, tube-to-tube wear in the U-bend free span as reported in two tubes in SG 2E089 during U2C17, and the potential for in-plane vibration of the tubes leading to tube-to-tube wear as has been reported in the Unit 3 SGs.

Evaluation of the AVB wear mechanism focused on projecting the flaw depths of AVB wear indications in active tubes (those remaining in service) and in plugged tubes until the next inspection. SCE is planning to perform a Unit 2 mid-cycle inspection after operating for 150 effective days of operation at 70% power. Since the next inspection is planned to be within five months of operation in Cycle 17, projections were carried out at 70% power for an operating duration of six months allowing additional margin. Projected wear depths in the active tubes are compared against allowable depths to satisfy the SG performance criteria. This comparison confirmed that SG performance criteria will be satisfied during the next operating period. The wear projections of plugged tubes confirmed that severance of such tubes will not occur during the next cycle.

An evaluation of the tube-to-tube wear reported in two tubes in SG 2E089 showed that, most likely, the wear did not result from in-plane vibration of the tubes since all available eddy current data clearly support the analytical results that in-plane vibration could not have occurred in these tubes. There is evidence of proximity in these tubes from pre-service inspection results. Hence, the tube-to-tube wear is most likely a result of out-of-plane vibration of the two tubes in close proximity to the level of contact during operation (see Appendix A). The evaluation shows that similar conditions are unlikely in other tubes. An evaluation was performed for an undetected flaw that may be left in service, comparable in size to the detected TTW flaws. This evaluation showed that the SG performance criteria will be satisfied during the next cycle.

Eddy current data (lack of wear scar extension beyond the width of the AVBs in any of the AVB wear indications) clearly suggests that in-plane vibration has not occurred in the Unit 2 SGs during the first operating cycle. The methodology was benchmarked using the Unit 3 results; this indicated that the U-bend free span tube wear in Unit 3 resulted from in-plane vibration of the given tube or in-plane vibration of the neighboring tube with matching wear indication. The active and plugged tubes in the Unit 2 RSGs were evaluated using the same methodology for the potential for in-plane instability. The results show that none of the tubes will be subject to in-plane instability. Therefore, tube-to-tube wear from in-plane vibration will not occur in the next operating cycle and SG performance criteria will be satisfied until the next inspection.

This evaluation concludes that, for the assessed degradations, the SG performance criteria will be satisfied during the planned operating period of five months at 70% power. The evaluations also support the satisfaction of the performance criteria for an operating duration of 18 calendar months at 70% power, for these degradation mechanisms.

1 Introduction

As per the Steam Generator Program Guidelines, NEI 97-06 (Reference 1), a condition monitoring assessment, which evaluates structural and leakage integrity characteristics of the steam generator (SG) at the end of the last operating period, is to be performed following each inspection. This evaluation is “backward looking” and compares the observed SG tube eddy current indication parameters against leakage and structural integrity. Additionally, an operational assessment, or “forward looking” evaluation is used to project the inspection results and trends to confirm that the SG performance criteria will be met during the operating period until the next inspection. This report documents the operational assessment of the indications in the U-bend region of the San Onofre Nuclear Generating Station (SONGS) Unit 2 SGs based on inspection results from the U2C17 refueling outage (2012). It is consistent with the guidelines described in Reference 2.

Southern California Edison (SCE) is preparing an operational assessment for all of the tube degradation mechanisms in the SGs using traditional and probabilistic methods (References 3 and 4). This report documents an evaluation using semi-empirical methodology applicable to tube wear resulting from flow-induced vibration.

The U2C17 inspection was conducted in 2012 which formed the first in-service inspection of these SGs when their accumulated operating life was 1.72 effective full power years (EFPY). SCE is planning to perform a Unit 2 mid-cycle inspection after operating for 150 effective days of operation at 70% power.

2 Overall Analytical Methodology

Most of the evaluation supporting this operational assessment is documented in a detailed technical report (Reference 5). This section provides a summary of the evaluations and results from that report that support the operational assessment.

2.1 Outline of Methodology

This subsection provides an outline of the evaluation methodology. This outline may be useful as a roadmap for the discussions in various sections of this report. The list of references is shown in Section 4 and a list of acronyms used in this report is compiled in Section 5.

A thermal-hydraulic computer code was used to evaluate the secondary side flow conditions in the tube bundle using a three-dimensional analytical model. This evaluation is discussed in Section 2.2. The results of the thermal-hydraulic analysis in the form of secondary side velocity, density and void fraction distributions along the length of individual tubes formed inputs to the flow induced vibration (FIV) analysis. The FIV analysis is discussed in Section 2.3. The results of the FIV analysis included out-of-plane excitation ratios and in-plane stability ratios for various tube support conditions in the U-bend. Various tube support conditions were identified by unique case numbers, each case number describing the specific combinations of AVB locations that are ineffective. The actual tube support conditions of the tube are derived from the eddy current test data collected during the U2C17 outage. The rationale for the use of the eddy current data for this purpose and why an effective support location will remain effective for several cycles are discussed in Section 2.4.

Projection of the depths of tube wear indications at AVB locations is discussed in Section 2.5. In brief, the methodology involves determining the values of several input variables that results in matching the reported wear depths of the indications at U2C17, and using these input values to project the wear depths at the next inspection. The FIV analysis results form an important input to the wear projection evaluation. The projected wear depths are compared to the allowable flaw depths to support the operational assessment discussed in Section 3.1.

The tube-to-tube wear in the U-bend free span reported in two tubes in Unit 2 is determined to be the result of a different mechanism than the tube-to-tube wear reported in the Unit 3 RSGs. One plausible explanation of how the alternate mechanism could manifest is discussed in Appendix A. The operational assessment for this mechanism is treated in Section 3.2.

In-plane vibration has resulted in tube-to-tube wear in the U-bend free span in dozens of tubes in the Unit 3 RSGs. Benchmarking of the Westinghouse evaluation methodology against the Unit 3 findings is discussed in Section 2.6.1. The potential for the occurrence of in-plane vibration in Unit 2 in the next operating cycle is evaluated in Section 2.6. The FIV analysis and the tube support conditions determined from eddy current data formed the inputs for this evaluation. The results of this evaluation are used in Section 3.3 to support the operational assessment for this potential degradation mechanism.

Computer codes used in the evaluations described in this report have been verified and validated as per Westinghouse quality procedures.

2.2 Thermal-Hydraulic Analysis

2.2.1 Methods

Thermal-hydraulic analysis of the SONGS Unit 2 RSGs was performed using the ATHOS (Analysis of the Thermal Hydraulics of Steam Generators) computer code. ATHOS is a three-dimensional computational fluid dynamics (CFD) code for analyzing steam generator (SG) thermal-hydraulic (TH) performance characteristics (Reference 6). ATHOS analysis of a SG involves the execution of a suite of codes consisting of the pre-processors ATHOGPP and PLATES, the ATHOS solver, and the post-processor VGUB. A brief overview of these codes follows.

ATHOGPP

The pre-processor, ATHOGPP, calculates the geometric parameters required for the ATHOS thermal-hydraulic analysis. For each node the code computes: the secondary fluid volume, the flow areas in the R, θ , and Z directions (cylindrical coordinate system), the heat transfer and friction surface areas, the approach to device area ratios required to compute pressure drops through concentrated resistances (flow distribution plate, tube support plates, primary separator, etc.), and the primary fluid flow partitioning factor. The input parameters include: grid distribution in R, θ , and Z directions, shell and shroud (wrapper) dimensions, tube layout and individual tube dimensions as well as the location (row and column numbers) of plugged tubes, inlet (feedwater) and primary separator locations and dimensions, as well as the location of all internal devices (tube support plates, stay-cylinders, etc.). Geometry data processed by ATHOGPP are then transferred via a binary file to the PLATES code for further refinement of the flow areas through the tube support plates. The EPRI version (named ATHOSGPP) of the ATHOGPP pre-processor has been modified by Westinghouse to simulate: anti-vibration bars (AVBs) in the U-bend region and at locations without tubes in the central bundle, and separator openings in the lower deck plate (Reference 7). AVBs are simulated in ATHOGPP by reducing the fluid volume and flow areas of flow cells where the bars are located.

PLATES

The pre-processor, PLATES, calculates the cut-out areas and/or flow holes in the tube lane region of the tube support plates in more detail than ATHOGPP. In ATHOGPP, a tube support plate (TSP) is treated as a homogeneous plate with uniform metal area density which removes all areas attributed to tube holes, flow holes (if any), gaps between the TSP and wrapper, and cut-out areas. In addition, the PLATES code can model the blockage areas associated with tube lane blocking devices if present in the steam generator. The PLATES code reads the binary output file generated by ATHOGPP. The code processes the TSP, tube lane, and central cavity related information and generates a new binary file to be read by the ATHOS thermal-hydraulic solver.

ATHOS

The ATHOS code module solves the governing conservation equations in conjunction with empirical correlations and boundary conditions. For the thermal-hydraulic analysis of a steam generator, boundary conditions include: mass flow rate of primary fluid, initial "guess" for the primary fluid inlet temperature, feedwater flow rate, feedwater temperature, steam pressure, and water level.

VGUB

Post-processor, VGUB, calculates tube gap velocity, density, and void fraction distributions along the steam generator tubes. Local tube gap velocities are calculated from ATHOS cell velocities which are based on the porous media concept. In general, gap velocity components normal to the tube (cross flow) are used in flow-induced vibration and wear analyses since these components produce significantly greater tube vibration than components parallel to the tube (axial flow).

The gap velocities for the SONGS RSG tube bundle were calculated based on the “gap center” method which interpolates velocity components at each gap in the tube array. With this method, VGUB calculates the average and resultant gap velocity for each tube of interest. An alternate method of calculating tube velocities is the simpler “tube center” method which assumes that every tube is fully surrounded by neighboring tubes. The two methods produce similar results within the bundle interior. However, the “tube center” method significantly over-predicts fluid velocities for peripheral tubes. Since the “tube center” method does not accurately capture physical effects around the edge of the tube bundle it was not used in this analysis.

Discussion of Significant Assumptions

1. For ATHOS simulations, each half of the steam generator, Columns 1 through 89 and 89 through 177 are modeled separately to capture the effects of asymmetric tube plugging. The primary and the secondary side operating conditions and properties for both halves are assumed to be the same.
2. Thermal-hydraulic evaluations are performed using the slip flow option. This option is customarily used by Westinghouse as it is more realistic and produces conservative results for two-phase quality, void fraction and velocities.
3. Steam carry under in the recirculating fluid is assumed to be 0.0.

Analysis Inputs

The ATHOS model covers the secondary side flow field inside the steam generator shell from the top surface of the tubesheet to the lower deck plate and from the center of the wrapper to wrapper wall and the downcomer annulus between the wrapper and the shell walls. Design geometry and thermal-hydraulic symmetry is assumed with respect to the diametrical plane perpendicular to the tube lane. Because of this assumption, the analysis model consists of one-half of the steam generator, i.e., an 180°-sector encompassing one half of the hot leg and one half of the cold leg.

The ATHOS finite difference grid in the horizontal plane (radial (R) and circumferential (θ) directions) is listed in Table 2-1 and depicted in Figure 2-1. The grid is selected to optimize the modeling of the wrapper and the tube bundle design. The axial (ZW) locations are selected based on wrapper, shell, tube support, and tube bundle geometry obtained from RSG design documents. The axial grid is presented in Table 2-2 and Figure 2-2. The tube plugging locations in RSGs 2E088 and 2E089 for the evaluations of the next operating cycle are listed in Table 2-3 and Table 2-4; these were not used in the evaluation of the first operating cycle of the RSGs.

ATHOS inputs were prepared for the operating conditions specified in Reference 9. The operating conditions represent 205 out of 9727 plugged tubes in RSG 2E088 and 305 plugged tubes in RSG 2E089. The primary flow rates in RSG 2E088 and 2E089 for the next operating cycle are slightly different: 207,726 gpm in 2E088 versus 206,695 gpm in 2E089 due to different plugging levels. ATHOS analyses for RSG 2E089 were performed at 50%, 60%, 70%, and 80% power levels. For

RSG 2E088, ATHOS analyses were performed only at 70% power level, a likely power level at restart. Based on comparison of the results at 70% power level between two steam generators, it was concluded that flow-induced vibration evaluations are reasonably close and, therefore, do not require ATHOS evaluations for both RSGs at all power levels. As shown in Table 2-3 and Table 2-4, tube plugging locations are asymmetrical between Columns 1-89 and 89-177. The operating conditions for RSG 2E088 and 2E089 utilized for ATHOS analyses are presented in Table 2-5 and Table 2-6. Subsequent to the completion of this analysis, five additional tubes were preventively plugged in the Unit 2 RSGs, two tubes in SG 2E088 and three tubes in SG 2E089. The impact of the additional plugging on the results of the analysis is negligible (see the third paragraph of Section 2.2.2).

2.2.2 Results Summary

Table 2-7 provides an overall summary of the primary and secondary side conditions in the RSGs for ten cases at the part power conditions and the reference case at 100% power (1729 MWt Nuclear Steam Supply System power). Both the calculated and input parameters are included in the table. For the FIV and tube wear evaluations, the TH variables of interest are the gap velocities, densities, and void fraction along the tubes. Table 2-7 includes the maximum quality, void fraction, and velocity in the tube bundle at 50% through 80% power levels, and the reference case at 100% power. There is a significant reduction (improvement) in secondary fluid quality and velocity at the reduced power levels. The void fraction, a fraction of volume occupied by vapor phase in a control volume, shows less reduction than the secondary fluid quality and velocity. This is because of the density difference between the liquid and vapor phases. At the RSG operating conditions, the vapor phase occupies approximately 22 to 25 times more volume per pound of mass than the liquid phase. As a result, the additional liquid inventory at the lower power levels increases the liquid volume by a smaller margin than the decrease in steam volume due to reduced steam mass.

A number of tubes have been plugged in the two RSGs in Unit 2 during the U2C17 outage. As a result, when the RSGs return to service in the next operating cycle, the three-dimensional thermal-hydraulic conditions may be affected as a result of the tube plugging. In addition, since the number of plugged tubes in each half of the SG is different from the other half, the evaluation performed for one half may not be applicable to the other. In order to resolve this difference, separate evaluations were made for the 70% power condition for each half of each SG using four separate models (four different plugging levels corresponding to the actual plugging distribution in the four halves of the two SGs).

At 70% power level, there are no significant differences in thermal-hydraulic characteristics between RSG 2E088 with 205 out of 9727 or 2.1% plugged tubes and 2E089 with 305 or 3.1% plugged tubes. The ATHOS model of RSG 2E089, representing Columns 89 through 177, has slightly higher values for the secondary fluid quality, void fraction and velocities than the other three ATHOS models for the Unit 2 RSGs. Table 2-7 also includes the values for the gap velocity, density and relative dynamic pressure (ρV^2) in the U-bend region of Tube Row 141 / Column 89. These values are provided at the location in the U-bend where the dynamic pressure value is the highest. As expected, these values decrease as the power level decreases. Subsequent to the completion of this analysis, five additional tubes were preventively plugged in the Unit 2 RSGs, two

tubes in SG 2E088 and three tubes in SG 2E089. The impact of the additional plugging on the results of the analysis is negligible.

Local Flow Conditions along Tubes

VGUB (Reference 10) calculates the local flow conditions for all tubes in the bundle for input to the tube vibration and wear analysis to support the operational assessment of the Unit 2 RSGs. Local tube gap velocities are calculated from ATHOS cell velocities based on the cell porosity and the characteristic geometry of the tube array (pitch and diameter).

VGUB-calculated secondary tube gap fluid velocities along the tube Row 141 / Column 89 at part power conditions are compared with the reference case (100% power) in Figure 2-3 through Figure 2-7. This tube has the longest bend radius within the bundle and has relatively high gap velocities in the hot leg side of the U-bend region. Each figure compares the gap velocities at a partial power with 100% power for both ATHOS models representing Columns 1 through 89 (LC) and Columns 89 through 177 (HC) for a given steam generator. Results for RSG 2E089 for power levels of 50%, 60%, 70%, and 80% are shown in Figure 2-3, Figure 2-4, Figure 2-6, and Figure 2-7, respectively. ATHOS analyses were also performed for RSG 2E088 at 70% power for both LC and HC models. The gap velocities for this case are compared in Figure 2-5. For most of the straight leg section of the tube, the gap velocities at lower power levels and at 100% power are similar. As shown in Table 2-7, the recirculating fluid flow rate is relatively constant at all power levels. However, in the U-bend region, the gap velocities are a strong function of power level. The steam flow in the bundle is cumulative and increases as a function of the power level and the bundle height which causes high fluid quality, void fraction, and secondary fluid velocities in the upper bundle. As illustrated in these figures, an asymmetric plugging in the bundle has a small effect on velocities. In RSG 2E089, differences in gap velocities are higher than in RSG 2E088. There are 218 plugged tubes in Columns 1-89 (LC) and 101 plugged tubes in columns 89-177 (HC) in RSG 2E089 compared to 113 plugged tubes in LC model versus 106 plugged tubes in HC model in RSG 2E088. Also, the differences in gap velocities increase with power level. Subsequent to the completion of this analysis, five additional tubes were preventively plugged in the Unit 2 RSGs (R135C93 and R137C89 in SG 2E088 and R80C68, R104C72 and R132C94 in SG 2E089). The impact of the additional plugging on the results of the analysis is negligible.

2.3 Flow-Induced Vibration Analysis

2.3.1 Methods

The flow-induced vibration analysis methods described in this section are covered in References 11 through 22.

Flow-induced vibration (FIV) models of the SONGS replacement steam generators (RSGs) were developed to evaluate the effects of secondary side flow on the tubes. The FIV models included the 7 tube support plates along with the 12 anti-vibration bars (AVBs). Figure 2-8 contains a representative sketch of the model used in the analysis. Table 2-8 contains a listing of the various cases considered with respect to the boundary conditions at the AVB that were imposed on the model. The FIV analysis was performed with the FASTVIB and FLOVIB computer codes using thermal-hydraulic results discussed in Section 2.2. The post-processor that interpolates tube-specific gap velocities from the ATHOS volumetric output recognizes the actual boundary

conditions around the periphery of the bundle; therefore, gap velocities for tubes in Row 142 are not as large as for tubes in Row 141. This effect can be observed in the figures contained in Section 2.3.2 where the outermost tubes have slightly lower excitation ratios than the neighboring in-board tubes. FASTVIB calculates relevant FIV responses for all tubes in a given row, and as can be observed in Section 2.3.2, multiple rows are considered. The result is a 'tubesheet' map of responses that help to identify regions that are more susceptible to FIV for a given support condition.

There are several tasks in the FIV evaluation. The first task was to develop tube stability information for power levels of 100%, 80%, 70%, 60% and 50%. The next task was to provide the input necessary to complete the wear projection evaluations for the tubes of interest discussed in Section 2.5 of this report. In addition to these tasks, there was also a comparative study performed to determine the impact on the FIV response as a result of plugging a tube and whether or not the plugged tube contained a stabilizer. Another comparison was performed to determine the difference between the 2E088 and 2E089 steam generators as well as low column tubes and the high column tubes (symmetry concerns). Tubes that were plugged in the steam generators were not symmetrical about the center column of the tube bundle and the same tubes were not plugged in both steam generators. As a result, potentially different thermal-hydraulic conditions could exist. The purpose of this comparison was to determine the impact that non-uniform plugging has on the FIV evaluation results.

Initially, linear dynamic analyses to characterize the response of the entire tube bundle to flow-induced excitation were performed using FASTVIB. These analyses identify limiting locations for various support conditions and show how the tubes of interest relate to the total bundle response as described in Section 2.3.2. FASTVIB incorporates the analytical approaches that were largely defined by the work of H.J. Connors at the Westinghouse Research Laboratories. Verification and qualification of this methodology for steam generator applications includes not only the analytical comparisons in configuration control files, but also many comparisons with results from tests and operating steam generators. These include comparisons with a 49-tube test model of the inlet region in water flow, a quarter-scale model of the U-bend tested in air, a .01 power scale Model F steam generator (MB-2), cantilever tube air flow tests, and operating Model 51 and Model F steam generators.

FASTVIB uses an assembly of structural elements and lumped masses with up to six degrees of freedom per node in a formulation adapted from FLOVIB, one of the earliest finite element programs applied to FIV analysis. Natural frequencies and mode shapes of the elastic structure are determined by conventional eigenvalue/modal decomposition techniques. Tube response to both flow turbulence and fluidelastic excitation is calculated consistent with the framework and empirical constants originally determined by H.J. Connors that have been applied for decades with confirmatory field experience. Fluid density and gap velocity distributions obtained from VGUB post-processing of ATHOS results are used along with structural properties of the tube and support configuration in these solutions. FASTVIB automates multiple solutions and stores limiting parameters in a format that is very useful for screening and subsequent evaluation (such as inputs to the wear evaluation). Total tube responses to the external flow excitation are obtained during evaluation of the SONGS RSGs, but only the response in the U-bend region of interest has been retained to manage the size of output files.

Velocity components normal to the tube (cross flow) are much more effective in causing tube vibration than components parallel to the tube (axial flow). Therefore, this discussion and subsequent analyses address only the cross flow distribution that results in vibration response that is typically an order of magnitude greater than that for comparable axial flows.

The evaluation of tube wear in the U-bend region focuses on the fluidelastic instability thresholds for various postulated tube/AVB support condition assumptions, but displacements and stresses arising from flow turbulence and the specific excitation applied to each tube of interest are also retained. Separate computer runs are required to obtain out-of-plane (OP) and in-plane (IP) responses.

Fluidelastic Excitation

Fluidelastic tube vibration is potentially more severe than the always present background flow turbulence because it is a self-excited mechanism. That is, relatively large tube amplitudes can feed back proportionally large driving forces if an instability threshold is exceeded as a consequence of fluid-coupled damping or stiffness interaction with tube velocity or displacement. This mechanism is the primary focus of this evaluation because no other flow-induced vibration mechanism is capable of producing the kind of response observed in the highly turbulent, two-phase flow U-bend region of the SONGS steam generators. Tube support spacing incorporated into the design of the tube support system typically provides tube response frequencies such that the instability threshold is not exceeded for anticipated secondary fluid flow conditions. This approach provides margin against initiation of fluidelastic vibration for tubes that are effectively supported as designed for anticipated flow excitation levels.

However, clearances between the tubes and supporting structure introduce the potential that any given tube support location may not be totally effective in restraining tube motion. Initiation of fluidelastic tube response within available support clearances is possible if secondary flow conditions exceed the instability threshold when no support or frictional constraint is assumed at a location with a gap around the tube as a consequence of the longer span initially afforded by the gap. This kind of gap-limited fluidelastic vibration is not as severe as classical instability response between spans that are too long for the existing flow field. This is the result of the constraint of the gap after the tube moves across the available gap when modulation occurs as fluidelastically induced tube/support interaction momentarily increases damping and higher modal frequencies in response to initiation of fluidelastic vibration within the gap. The temporary increase in damping and energy dissipation from the interaction then momentarily reduces or eliminates the fluidelastic component of vibration, which in turn reduces tube/support interaction and some higher frequency response, thereby decreasing damping again.

While the consequential tube/support interaction with intermittent impact/sliding conditions is not as severe as that for classical fluidelastic instability, it is much more severe than interaction induced by flow turbulence alone. This type of motion involves the potential for significant tube wear and fatigue damage and is the mechanism resulting in tube wear at an AVB.

Fluidelastic instability initiates when the fluidelastic stability ratio (FSR) exceeds unity (1.0). FSR is the ratio between the effective velocity (U_e) and the critical velocity (U_c). A more conservative limit can be applied by using a smaller allowable (such as 0.75 in design rather than field evaluation), but the degree of conservatism inherent in the analysis is also directly dependent upon the conservatism of the empirical constants chosen to characterize the instability threshold and overall tube damping. The critical velocity, U_c , at which instability initiates, is calculated in FASTVIB using an equation of the form

$$\frac{U_c}{f_n D} = \beta \left(\frac{m_o \delta_n}{\rho D^2} \right)^{1/2}$$

where f_n is the natural frequency in the n^{th} normal mode, D is the tube diameter, β is the empirical threshold instability constant, and the term in brackets is a damping parameter. U_c is the critical gap velocity for the mode/frequency being considered based on a consistently derived threshold instability constant, β . The damping parameter is a function of the effective or virtual tube mass per unit length, m_o , the damping log decrement in the n^{th} normal mode, $\delta_n = 2\pi\zeta_n$, the outside or secondary fluid density, ρ , and the tube diameter, D . The virtual tube mass per unit length, m_o , includes contributions to effective mass from the fluid inside the tube, the tube itself, and the displaced fluid outside the tube and is calculated by

$$m_o = A_i \rho_i + A_t \rho_t + C_m A_o \rho_o$$

where C_m is an added mass multiplier that is applied to reflect added fluid/structure interaction in closely packed arrays. The added mass multiplier for a single tube in uniform flow is considered to be unity, but it can increase significantly depending upon the confinement effect of the array pattern and spacing and also upon the analytical objective.

There is extensive treatment of inertial coupling and the added mass multiplier in the literature with theoretical derivations, test data and correlations provided as a function of array pattern and pitch spacing. The appropriate value depends somewhat on the immediate objective with lower values recommended when simulating conditions where there is no significant tube coupling (e.g., at low turbulence levels) and higher values where there is significant coupling (e.g., near fluidelastic instability).

The most important input parameter for evaluation of potential for fluidelastic instability is the constant, β that characterizes the threshold of self-excited interaction between the tube motion and the external flow field. There is extensive treatment of this parameter that is a function of the array pattern, the external flow regime, and many other factors in the literature, but most is for straight tubing. Westinghouse uses two different discrete lower bound values for the straight leg and U-bend portions of tubing in recirculating steam generators.

Instability Constant for Straight Leg Region

H.J. Connors first obtained β for the straight leg region from simple tests in both water and air environments for both normal 90° and rotated 45° orientations that simulated Westinghouse steam generators with square arrays and a pitch/diameter ratio of 1.41. Later tests for triangular arrays with similar p/D ratios yielded higher values for the triangular pitch that reflects the reduced tendency for initiation of instability in triangular arrays compared to square arrays. Additional tests and open literature that reference different p/D ratios indicate the trend for significant reduction in instability threshold as p/D decreases, so the value used in FASTVIB for the SONGS evaluation has been reduced to account for the tighter arrangement characterized by $p/D=1.33$. However, focus on the U-bend response for this study means this parameter has no impact on the subsequent discussion.

Instability Constant for U-bend Region

Tests of a 0.214 scale model of a square-pitch U-bend region in the Westinghouse wind tunnel test facility provided lower bound values of 5.23 for tubes without AVBs, and 5.24 for the same tubes with AVBs having gaps so large that tube/AVB interaction did not occur. Later tests on full-size cantilevered straight tubes mounted in the same wind tunnel with different stiffnesses in the lift and drag directions (to simulate relative U-bend tube stiffnesses) resulted in an almost identical value of 5.25. These results are all consistent with instability constants that were derived from testing the MB-2 0.01 power scale model of a Model F steam generator operating in a prototypic steam/water environment without AVBs: individual values ranged from 5.0 to 7.1 with an average of 6.3. In-plane fluidelastic instability could not be induced in the Westinghouse tests with AVBs in place.

A similar range from 5.3 to 9.4 was derived from MB-3 steam/water testing when developing the $\beta = 5.2$ value for U-bend that was used for evaluating a tube without AVB support that involved a tube rupture event. As more supports were added and higher frequencies resulted in the scale model tests, the threshold instability constant tended toward a lower bound of 4.2 for square-pitch arrays. These internally consistent tests with a characteristic downward trend with increasing frequency all indicated that a higher instability threshold existed in the U-bend relative to the straight leg region. These results all refer to initiation of OP instability. IP instability was never observed in any of these square-pitch U-bend tests despite early attempts to force its occurrence without any AVB support for flows up to three times the OP instability threshold.

Subsequent tests of triangular arrays in the same scaled wind tunnel configuration yielded a higher margin against fluidelastic instability in the U-bend region as expected based on prior tests that characterized straight leg response. The same trend of decreasing instability threshold with increasing frequency was observed for configurations with very little support, but continued increases in frequency with more supports being added resulted in a reversing of the downward trend to the point where instability could not be achieved up to the limits of the wind tunnel. The lower bound instability constant over the frequency range had the same relative factor increase over the lower bound for the square array in the U-bend as in the straight leg, but much higher factors for both the very low and very high frequency range. The lower bound value obtained from these tests is typically used for evaluation of the U-bend region of steam generators with triangular array configurations with recognition that actual margin against instability may be much higher depending upon the number of effective supports. This approach is also applied to the SONGS evaluation in this study with the same adjustment factor for p/D ratio that was used for the straight leg region. As was the case for square array patterns, no in-plane (IP) instability was observed in these tests even for U-bend tubes with no supports above the top tube support plate.

When computing the effective velocity that is the numerator of the FSR equation, FASTVIB uses normal mode theory considering span-wise variations in external flow velocity and density. This involves translation of the varying external flow conditions into an effective velocity that can be used to calculate a stability ratio for each normal mode, n , using

$$U_{en}^2 = \frac{\sum_{j=1}^N \frac{\rho_j}{\rho_o} U_j^2 \phi_{jn}^2 \Delta z_j}{\sum_{j=1}^N \frac{m_j}{m_o} \phi_{jn}^2 \Delta z_j}$$

This equation sums contributions from each element having incremental length Δz_j , where U_j , ρ_j , and m_j are the gap velocity, fluid density, and incremental mass at span-wise locations along the tube, and Φ_{jn} is the normalized displacement (mode shape factor) of the j^{th} lumped mass in the n^{th} mode of vibration.

A threshold fluidelastic instability constant (β) of 5.0 was used when evaluating the U-bend region of the SONGS RSGs. This value was derived from tests of triangular-pitch U-bend configurations and scaled down to reflect the smaller pitch/diameter ratio for the SONGS configuration relative to the Westinghouse tested configurations that had a pitch/diameter ratio equal to 1.42. This value of β is applicable to OP instability. A value of $\beta = 7.8$ was conservatively applied for IP instability based on the maximum velocity tested in the same U-bend configuration with all AVBs removed and still without encountering IP instability. For the straight leg sections, based on an evaluation of normalized trends from open literature and Westinghouse tests, a β value of 3.1 was used. This was derived by applying the same scale factor for the tighter pitch in the SONGS design.

Flow Turbulence

This background mechanism is not a primary focus for this evaluation. However, tube displacements from random flow turbulence are calculated in response to a specified spectrum of flow turbulence forces derived from Westinghouse tests using an equation of the form

$$\frac{y_n}{D} = C_1 \left(\frac{\rho_o D^2}{m_o} \right) \left(\frac{U}{f_n D} \right)^{\frac{3+S}{2}} \left(\frac{1}{\delta_n} \right)^{0.5} \left(\frac{D}{L} \right)^{0.5}$$

where y_n is the desired statistically defined root mean square displacement amplitude for mode n , C_1 and S are the empirical constants derived to envelope test data as shown on Figure 2-9, and $\delta_n = 2\pi\xi_n$ is the damping log decrement. The appropriate damping for use in turbulence calculations is a key variable for this and all flow-induced excitation mechanisms of interest. Hence, it is discussed separately at the end of this section with separate explanations appropriate to the straight leg and U-bend regions.

Two different spectra of turbulent cross flow forces are typically used in vibration analyses to reflect different exposure deep inside the tube bundle relative to the inlet region. The higher spectrum, normally used only for evaluation of the straight leg response of tubes located on the bundle periphery and along the tube lane, is conservatively used for all calculations in this evaluation. The bilinear nature of each spectrum assures that calculated responses are either appropriate or conservative regardless of which portion of the curve is used. The statistically defined root mean square (RMS) displacement is a convenient measure for comparison with test or operating plant data. The calculated SRSS (square root of the sum of the squares) of the RMS modal displacements is typically consistent with measured tube response in operating steam generators.

Damping in the Straight Leg Region

Theoretical considerations and correlations from heat exchanger test data cited in open literature are used when evaluating tubes with pinned and open support conditions in the straight leg region of operating steam generators. Analyses typically reference a configured spreadsheet formulation that calculates the constants A and B as a function of specified parameters for the tube, array pattern, and internal and external fluid conditions of interest. This reference equation for the percent of critical damping, ζ , is

$$\zeta = A \left(\frac{1}{f} \right)^{1/2} + \left(\frac{B}{f} \right)$$

where the constant A scales viscous contributions and B scales squeeze-film contributions. The constants A and B are calculated from pertinent properties of the tube and thermal-hydraulic flow field including the tube diameter, the equivalent hydraulic diameter that accounts for array confinement fluid coupling effects, the secondary fluid density, the virtual mass per unit length as defined previously, the kinematic viscosity, the number of spans with significant response, the density of the saturated liquid in the tube/support crevice, the support plate thickness, and a characteristic tube length for the number of spans considered.

Damping in the U-bend Region

A generic two-phase damping model has been developed for the U-bend region using multiple sets of steam-water data at steam generator operating conditions. This generic model has the form

$$\zeta = A + B\alpha + Cf^n$$

where ζ is the percentage of critical damping, α is the two-phase modal effective void fraction calculated using a slip model obtained from ATHOS analyses, f is the tube modal response frequency, and A, B, C, n are empirically derived constants. Multiple-model, multiple-linear-regression fits of all available data were considered to arrive at the final form of the damping equation with three independent terms to address baseline support conditions, void fraction, and frequency effects.

Derived empirical coefficients are consistent with the 10th-15th percentile such that 85-90 percent of the data are less than the resulting calculations. However, there is an added conservatism in that the lowest damping values measured at any response amplitude were chosen when establishing the empirical constant A for each type support condition. The data were insufficient to include response amplitude as an independent variable, so the most conservative data at the smallest amplitudes were used when establishing correlations for six different support configurations.

For any variation of or typical support conditions with the tube “pinned” at the top TSP

$$B = -7.853, C = 7.691, \text{ and } n = -0.5$$

with the constant “A” a function of the degree of interaction between tubes and AVB’s such that “A” is

6.693 for tubes without any AVB support,

6.775 for tubes with preloaded contacts at AVB supports,

7.113 for tubes in contact with AVB’s without preload, and

7.225 for tubes which have gaps at AVB supports.

When calculating damping for any combination of typical support conditions (pinned with preloads, pinned without preloads, pinned at some locations with gaps at others), a minimum value is imposed to reflect mechanical/frictional contributions. The mechanical damping floor is also a function of the tube support configuration and varies with selection of the overall constant A. While it is likely that higher minima actually apply in a steam generator, conservative lower bound values were derived by evaluating results of tests with rounded contacts that provided line contact in an air environment. The lower bound values vary from 0.10 to 0.25 percent for the four itemized support configuration

options. These minima have no practical significance except at locations that have extremely high modal effective void fractions, greater than about 95 percent, depending upon the frequency.

At the other extreme, a ceiling of 3.0 percent is imposed when direct calculations yield higher values. Empirical constants derived from this comprehensive evaluation of available two-phase damping data are considered valid for modal effective void fractions in the 0.8-1.0 range for frequencies between 10 and 100 Hz.

2.3.2 FIV Results Summary

Stability ratio (SR) is the ratio between effective velocity and critical velocity. This term is used in this report in the context of in-plane vibration. For out-of-plane vibration, the presence of the AVBs limits the vibration amplitude and instability in the classical sense cannot occur. Therefore, the term excitation ratio (ER) is used to denote the ratio between effective velocity and critical velocity.

Excitation ratio maps were generated for the various ineffective AVB cases. An excitation ratio map shows the excitation ratios calculated for a given case with specific ineffective AVB(s) for several tube locations displayed in the map. The map uses row and column numbers as abscissa and ordinate respectively, and is populated by excitation ratios for the tubes at corresponding row-column locations. Although all columns from 9 through 89 are displayed (Column 10 is not shown since there are no tubes in the displayed rows), only selected rows are shown in order to fit the map on a page and since the excitation ratios in adjacent rows are comparable in magnitude to those in displayed rows. Further, lower numbered rows have smaller U-bend radii and hence shorter span lengths between supports. Therefore, the excitation ratios for the lower rows tend to be smaller for any support condition and only a few lower rows are selected for display in the stability map.

A typical stability map is shown in Figure 2-10. This example map is for OP excitation ratios at full power (Cycle 16) for Case 60 with seven consecutive ineffective AVBs (specifically, AVB3 through AVB9). The map for IP stability for the same case (60) is shown in Figure 2-11. Note that the IP stability ratio is smaller than the OP excitation ratio for every tube. This is because, for a given support condition, a tube is more stable in the IP mode compared to the OP mode.

At 70% power (Cycle 17), the excitation ratios and stability ratios go down significantly for OP and IP modes, respectively. For Case 60, the excitation ratio and stability ratio plots at 70% power are displayed in Figure 2-12 and Figure 2-13, respectively.

2.4 **Determination of Tube Support Effectiveness from Eddy Current Data**

Application of the Westinghouse methodology for evaluating the tube wear in the SG U-bend involves the use of eddy current results to determine the tube support boundary condition at anti-vibration bars (AVB). Further, the support condition is expected to remain unchanged for several fuel cycles. Hence it is important to describe the rationale and implications associated with this. In the following discussion, out-of-plane (OP) motion due to vibration is treated first followed by in-plane (IP) vibration.

2.4.1 Out-of-plane Vibration

Support at an AVB is considered effective when the gap between the tube and the AVB is small such that the tube motion in the out-of-plane direction is severely limited. However, it does not require a contact force to be present, though a contact force is acceptable. The small gap limits the

amplitude of tube motion at this location. Test data shows that when the AVB gap is small, the limited amplitude of motion reduces the wear rate of the tube due to fretting at that location to be negligibly small. As a result, a tube will not display detectable wear at such a location for several cycles of operation.

If the AVB gap is large, appreciable tube motion becomes possible at the given location. However, the occurrence of tube motion and its amplitude will be determined by fluid forces. Below the onset of fluidelastic excitation, the amplitude of motion will be limited to that resulting from random turbulence. The typical turbulent forces in the U-bend of a SG are not sufficient to cause detectable AVB wear. Occurrence of appreciable AVB wear requires fluidelastic excitation. The discussion of fluidelastic vibration and stability ratio are provided in Section 2.3. Since the tube motion is constrained by the AVB, the stability ratio may be called amplitude-limited fluidelastic excitation ratio (ER).

When ER is below 1, the tube is stable and the amplitude of motion remains near the turbulence level. As the value of ER increases above 1, the increasing level of excitation sets in and the potential for tube wear occurs. The value of ER increases as the span length of tube between effective supports increases (due to adjacent inactive AVB locations in a tube). Under such conditions, the tube moves within the confines of the local geometry and the possible mode shapes that become active. This leads to tube wear at those AVBs with which the tube comes into contact within the unsupported span. For longer unsupported spans, the tube may not contact all AVBs within the span due to geometric constraints, especially at the beginning of operation. Such conditions may lead to an AVB wear pattern in a tube that is not continuous, i.e., one or two AVB location(s) without wear that is possibly nestled between AVB locations with wear. As wear progression occurs at the contacting AVBs, the tube may come into contact with the other AVBs in the unsupported span and wear will initiate at such locations thereby "filling in" the AVB wear pattern.

As described in Section 2.5.1, the rate of progression of wear (volume) at an AVB location is directly proportional to the fluidelastic excitation force. The fluidelastic excitation force, in turn, is directly proportional to the amplitude of vibration which is the gap between the tube and the AVB. When the AVB gap is small, the fluidelastic excitation force and hence, the wear rate will be small. Such locations are defined as effective support locations. Since the wear rate at such locations is small, effective support locations will display no significant tube wear and will remain effective for several fuel cycles of operation. On the other hand, the ineffective support locations have larger gaps and will be subject to higher wear rate (when ER exceeds 1) such that AVB wear will be reported at such sites within one or two fuel cycles of operation at full (100%) power. This is the basis for using the eddy current data to identify whether effective support is present at an AVB location.

An AVB wear indication suggests that the AVB gap at that location is large enough to allow tube wear and hence, is an ineffective support location. It is not the size (depth) of the wear indication, but the mere presence that identifies it as an ineffective AVB. This explains the rationale involved in the use of eddy current data to define U-bend support conditions in a tube.

Note that the amplitude of motion remains small at the AVBs that provide effective support located at both ends of the unsupported span. This is also true for effective AVBs located external to the unsupported span. Hence, no discernible tube wear occurs at such locations. This is a very important point. What this means is that continued wear at unsupported AVBs does not significantly impact effective AVB locations; and thus, the unsupported span remains unaffected. The small impact decreases with increasing unsupported span length. Therefore, the unsupported span length remains stable over time (several fuel cycles).

As described above, occasionally nestled AVB locations without reported wear indications may also be locations of ineffective support. In the case of the SONGS RSGs, since they have operated for only one fuel cycle (at most), wear depths at some of the AVB locations are small and hence, below bobbin probe detection threshold. Westinghouse has reviewed +Point inspection data to identify low level wear at AVBs that was not previously reported in order to identify ineffective support locations. This has resulted in identifying several ineffective support locations.

2.4.2 In-plane Vibration

Test data shows that the onset of IP vibration requires much higher velocities than the onset of OP fluidelastic excitation. Hence, a tube that may vibrate IP would definitely be unstable OP. A small AVB gap that would be considered active in the OP mode would also be active in the IP mode because the small gap will prevent significant in-plane motion due to lack of clearance (gap) for the combined OP and IP motions. Thus, a contact force is not required to prevent significant IP motion.

The above conclusion was demonstrated by a series of tests described in Reference 24. The tests were conducted with U-bends under controlled conditions at different AVB gaps. It was found that “the effect of flat bar supports with small clearance is to act as apparent nodal points for flow-induced tube response. They not only prevented the out-of-plane modes as expected, but also the in-plane modes. No in-plane instabilities were observed, even when the flow velocity was increased to three times that expected to cause instability in the apparently unsupported first in-plane mode.” These tests clearly demonstrated that a contact force is not required to prevent in-plane vibration. A small gap (e.g., 3 mils) is sufficient to prevent in-plane vibration.

Since the eddy current reported AVB wear indications can be used to define the support conditions for OP mode the same support conditions can also be used for the IP mode. This has been demonstrated by benchmarking of the Westinghouse methodology against the Unit 3 data where significant amount of IP motion and tube-tube wear has occurred.

As discussed above, an active AVB location will continue to remain active (at least for several cycles) even though tube wear may occur at other AVB locations in the tube. Hence, a tube that was stable IP during one cycle will remain stable in the next cycle unless the thermal-hydraulic conditions become more severe. The thermal-hydraulic impact can be evaluated analytically.

2.5 Tube Wear Progression

2.5.1 Methods

Tube and support interaction leading to rapid wear in the U-bend region is a complex, highly nonlinear process involving impact dynamics, friction, boundary conditions and forcing functions that change with time during the process. Rather than attempt to calculate and benchmark the nonlinear calculations, Westinghouse performed baseline tests that incorporated the nonlinear interaction for a range of tube and AVB support conditions and measured enveloping workrates that could be scaled to other conditions using forcing functions that are obtained from results of linear vibration analyses. Workrate is the product of the tube/AVB impact force and the sliding distance per unit time during impact. Tube wear is then calculated as a function of time following Archard wear theory using the equation

$$V = K(WR)(t)$$

where V is the calculated wear volume, K is the appropriate tube wear coefficient, WR is the workrate, and t is time. The same equation is used to determine the corresponding AVB wear

volume using an appropriate wear coefficient for the AVB as relative tube and AVB wear volumes are apportioned for conformal interaction. These calculations require three inputs:

1. Specific wear coefficients for the tube and AVB,
2. The normal force/sliding motion workrate, and
3. The depth-volume relationship at the interface.

Each is discussed below in the context of testing, design bases, and application to SONGS operating experience.

The methodology that is applied in this evaluation treats the mechanism that was found to be the cause of moderate wear in the U-bend region of conventional Westinghouse Model 51 and Model F steam generators before the development of advanced tube/AVB support configurations in the mid 1980s. This mechanism has been variously referred to as “fluidelastic vibration in the support inactive mode,” “double-span behavior,” “fluidelastic rattling within loose supports,” and “amplitude or gap limited fluidelastic vibration.” Its characteristics are fundamentally different in many respects from those of random flow turbulence that is always present in steam generators. Given the evolving state of knowledge and analytical capabilities at the time, Westinghouse developed a semi-empirical methodology to use as a design tool in treating the fundamental characteristics observed in testing.

Westinghouse Test Programs

Extensive flow-induced vibration testing and evaluation to support steam generator design were performed using a broad array of consistent methods for much of four decades at the Westinghouse Research Laboratories (now Science and Technology Center). Only those tests pertinent to the methodology applied in evaluation of SONGS flow-induced vibration and wear potential are described in this report.

Figure 2-14 shows the idealized triangular arrangements that were tested first in the same water tunnel that had been used two decades earlier for square pitch configurations. Figure 2-15 provides a context and reference for discussion of tube vibration response characteristics and flow-induced vibration (FIV) mechanisms using sample results that were obtained from one of those tests. The tube response data on Figure 2-15 includes vortex shedding contributions in the idealized water test that may exist around the periphery of the steam generator inlet regions, but they are not a concern in the two-phase, highly turbulent flow in the U-bend region of interest to this evaluation. The narrow band tube response to random flow turbulence typically varies with velocity raised to about the second power¹ and is illustrated by the red line on Figure 2-15. However, there is a critical velocity above which fluidelastic instability initiates and tube response is so extreme that it must be avoided altogether in design. For illustration purposes, the black line on Figure 2-15 varies with velocity to the tenth power, and it envelopes the tube response in the sample shown.

Several overall conclusions from the test programs are important to subsequent discussion:

1. The tests for triangular array configurations are most applicable to the evaluation of the SONGS steam generators. However, the methodology and design bases were originally developed for square pitch configurations based on earlier tests. The amplitude limited fluidelastic vibration mechanism leading to tube/AVB wear affects a larger percentage of tubes in square pitch configurations.

¹ The specific exponent applicable to FIV analyses and to the trend line on this plot using the same correlation is 2.67.

2. Displacements, impact forces, and workrates derived for wear calculations from these laboratory tests are more modulated in steam generators with complex geometry and variations in two-phase flow. This implies they are conservative for the range of tested configurations for the design purposes for which they were intended, but in that sense may overpredict wear in steam generators.
3. Conversely, the range of tube/AVB support conditions tested for design purposes does not cover the apparent range of support conditions implied from the ECT wear indications in the SONGS steam generators. In this sense, the test and design bases may underpredict the extreme wear in the SONGS steam generators prior to benchmarking calculations. In order to overcome this hurdle, the AVB wear depth distribution for each tube was calculated to match the observed wear depths at U2C17 as explained in Section 2.5.2.

Wear Coefficients

Determination of appropriate wear coefficients is based on both extensive testing within Westinghouse and correlation of results from licensees and external sources. Specific wear coefficients for the Alloy 690 tubes (K_t) and 405 Stainless Steel (SS) TSP/AVBs (K_a) were derived from all available impact/sliding wear test data. The median value of the wear coefficient for tubing when interacting with 405 SS from the raw test data was 98 (10^{-12} in²/lb).

The average ratio of AVB material wear coefficient to tubing wear coefficient in the original impact/sliding test data was 2.1. However, this data included much softer AVBs. Relatively harder AVBs that wear slower in the early stages are especially limiting if the AVB is not perfectly aligned with the tube. Therefore, the AVB specific wear coefficient is typically considered to be the same as the tubing for reference calculations, but is varied from 0.01 times (negligible AVB wear) up to two times (more AVB wear than tube wear) in normal design calculations.

Workrates

Workrates are scaled from baseline mechanical shaker test trends using inputs from qualified thermal-hydraulic and FIV analyses such as ATHOS/VGUB and FASTVIB. Evaluating any other geometry, including tube row and AVB location, and any other flow field, requires adjustment of experimentally determined workrates using parameters appropriate to the configuration of interest. In this case, workrates for the SONGS steam generators were determined using scaling factors derived from analyses. This is done using an equation that is a function of tube frequency, secondary fluid density, effective velocity of the fluid for the limiting vibration mode, fluidelastic excitation ratio, effective tube span length, and tube/AVB clearance. The form of this semi-empirical equation for predicting workrates uses an analytical expression of the fluidelastic excitation force,

$$F_n = c_f \rho_o D U_{en}^2 \left(\frac{C_e}{D} \right) \left[1 - \frac{U_{cn}^2}{U_{en}^2} \right] L_{en}$$

that is consistent with measured wind tunnel test results, taken together with experimental trends determined in the baseline U-bend shaker tests. Overall results of the test program were provided in the form of workrate coefficients, W_r , for use in an equation of the form

$$WR = W_r f_n D F_n$$

where F_n is the appropriate fluidelastic force calculated from the previous equation that is a function of cross flow excitation. Values for the parameters are obtained from linear vibration analyses using FASTVIB and the extracted ATHOS properties that have been interpolated using VGUB for the tube.

The semi-empirical formulation was developed to envelope workrates using interactions characterizing the tube/AVB interactions at up to three ineffective supports. Figure 2-16 illustrates the typical logic diagram followed during design analyses. Figure 2-17 shows the basic characteristics of the measured workrate trends from U-bend shaker tests as described more fully in Reference 23. The methodology uses the workrate trend ACDE on Figure 2-17 as the dominant characteristic of the limiting wear from amplitude limited fluidelastic excitation. It therefore captures the effects of increasing flow rates and increasing gaps due to wear on the excitation and impact forces, but it does not explicitly calculate what is happening at the effective support intersections on each end of a long span that would be unstable if the supports with large gaps were actually not present. For nominal tube/AVB gaps, the adjacent effective intersections may indeed have higher initial workrates that could lead to gaps and longer spans as shown on the left side of Figure 2-17. Thus, when performing normal design calculations, a range of potential support conditions must be evaluated separately. However, as wear progresses for any given support configuration, the workrate at the large gap becomes limiting after some point illustrated by D on Figure 2-17. This methodology, therefore, does not explicitly calculate details of modal interactions and detailed physics of the process for the entire tube, but it does follow the dominant trend for the mechanism that can lead to rapid wear in tubes with ineffective supports from large gaps that allow amplitude limited fluidelastic rattling within the clearances. The semi-empirical methodology takes workrates that include all nonlinear interactions present in the shaker tests, scales them to levels appropriate to the design being evaluated using results of thermal-hydraulic and linear FIV analyses, and preserves the mode shape for the unstable frequency as wear progresses.

For fundamental modes resulting from multiple consecutive gaps, wear progresses at the first support with tube/AVB interaction, depending upon the mode shape and the existing gaps, to interaction with successive supports as the tube amplitudes fill the gap as it grows from wear at both the tube and the support. If more ineffective locations with gaps are involved in a configuration being evaluated, the first three to interact depending upon the gaps and relative mode shapes can be evaluated. The total workrate that is available to wear the interacting sites (WR) is determined by scaling the characteristic workrate trend from shaker tests (W_r) using the excitation force (F_n) apportioned to the various intersections to preserve the fundamental mode shape. Sharing among the different intersections depends upon whether one, two, or three intersections are wearing at the same time as illustrated on the right side of Figure 2-17. This process is sensitive to the mode shape and the gaps at the three intersections such that wear begins, pauses or stops at any given location to preserve the dominant mode shape.

One additional factor has a significant effect on the depth of wear at an intersection. If the tube is off-centered more than about ten percent between AVBs, then displacements will be determined by the nearest AVB. While tube displacements are similar for single-sided interaction with one AVB and for double-sided interaction with opposing AVBs, the impact forces are greater for single-sided interaction. This was observed in the U-bend air flow tests, and relative workrates were confirmed during the shaker tests to be about twice as high for single-sided interaction on one side of a tube as for splitting the available energy to wear both sides of the tube at the same intersection. Current coding allows either choice for all sites, but all intersections in the configuration being evaluated must be either single- or double-sided.

Depth-Volume Relationship

Depth-volume relationships are calculated based on tube and matching support geometric relationships. Figure 2-18 illustrates those applicable to 0.750-inch diameter tubing and 0.59-inch wide AVBs for various degrees of twist. Note that there is almost an order of magnitude difference in the depth of the combined tube and AVB wear that results from the volume removed from wear required to reach the dashed line that represents 40% through-wall (TW) for the 0 to 4 degree range illustrated on Figure 2-18. The factor is even higher for smaller wear depths, e.g., about 25 at 10%

TW. The relative factor for the tube alone depends upon the size of the corner radius and the relative tube and AVB wear coefficients in addition to the unknown degree of actual twist.

2.5.2 Application to SONGS Steam Generators

The semi-empirical wear calculation methodology developed for design, and based on testing described, was adapted for characterizing the SONGS tube wear experience. It includes projecting expectations for future operation at different power levels. The only change to the structure of the coding was to allow continued operation from an existing conformal tube/AVB wear geometry developed during an earlier time period with a different excitation level for the new time period. Without this change, the highly nonlinear effects of beginning with a fresh tube and AVB depth-volume relationship as shown on Figure 2-18 would have prevented meaningful extrapolation of continued operation of the existing steam generators.

Normal design practice involves definition of ranges of potential parameter variables and tube/AVB geometry configurations and then demonstrating that the maximum tube wear consequences are less than a design margin. For the SONGS application, the resulting wear distribution after a cycle of operation is known, or can be inferred from existing ECT data, but for any given tube, there are many parameters that resulted in the wear distribution that are unknown. For example, neither the tube nor the AVB wear coefficient is known except over a range of possibilities for the two materials (Alloy 690 TT tubing and 405 SS AVBs). Whether the inferred tube wear distribution has less wear on the AVB, equal wear on the AVB, or more wear on the AVB markedly affects the combination of other parameters that would produce the same tube wear depth distribution. It can be assumed that the tube and AVB surfaces will not have significant run-in effects for the first cycle of operation, but even this assumption involves a potential error of several hundred percent. Most importantly, the tube/AVB geometry is expected to be different than the original design intent, but all that can be inferred with the available information is the minimum length of the dominant tube vibration span. In the largest sense, the answer (wear distribution) is known, but the inputs are unknown.

Calculation of tube/AVB wear for SONGS Unit 2 follows the semi-empirical methodology adapted as described earlier in this section to continue from the end of Cycle 16 interface conditions. The process can be illustrated by an example tube for which ECT indicates wear at intersections with AVB 4 and AVB 5. The first step is to adjust the raw ECT indication to wear depth using the correlation of metallurgical to non-destructive examination (NDE) reported depths for the NDE technique from Reference 25:

$$W_i = 0.98 ECT_i + 2.89$$

where W_i is the wear depth for eddy current indicated depth ECT_i at the tube intersection with AVB_{*i*}. Then FASTVIB solutions for various cases of postulated ineffective AVB supports are reviewed to obtain the case with the lowest number of missing AVBs that is unstable in the OP direction. Values for the reference density, ρ_o , modal effective velocity, U_{en} , excitation ratio, $ER=U_{er}/U_{cn}$, and modal effective length, L_{en} , are then extracted for use in the fluidelastic force scaling equation. These values, along with the corresponding modal frequency for the unstable mode, f_n , are then used in the equation to scale the U-bend shaker test reference workrate, W_r , to obtain the workrate, WR, applicable to the SONGS flow excitation and support configuration being evaluated.

The semi-empirical wear calculation procedure apportions the overall workrate available for the limiting vibration amplitude determined by C_e among the interacting AVBs depending upon the relative clearances at each intersection. Figure 2-19 illustrates this example with a postulated set

of initial clearances that could have produced approximately equal wear at AVBs 4 and 5. Following the observed trends for displacements to fill the available clearance, amplitude limited vibration occurs with the overall workrate applied at the first intersection to interact with the dominant unstable mode. Wear progresses at that AVB until the clearance becomes big enough from combined wear at the tube and the AVB to allow the dominant mode to begin impacting at the second AVB. As shown on Figure 2-19, the workrates and wear volumes at AVBs 4 and 5 will be about equal to half the total amount that is possible for the configuration being evaluated.

If the observed ECT wear indications are not equal, the postulated initial gaps can be changed to make the site with the highest wear closer than the other and wear longer than the second site with all the energy on the first site until impacting at the second site begins. Wear volumes at each site are converted into depths (for both tubes and AVBs) following the selected correlation for different degrees of twist. A manual, iterative “tuning” process then apportions the available energy to produce the relative wear depths observed from ECT. These depths, which have been tuned to match the observations, could have been obtained with many different combinations of wear coefficients, amounts of AVB cross-sectional twist, workrate trends (nominal or maximum to cover individual tests), single- or double-sided interaction choices, and various factors of uncertainty on FIV parameters. After achieving wear at both sites consistent with ECT after Cycle 16, the combination that produced the result can be held constant while evaluating various excitation levels for subsequent operation using FIV scaling parameters from FASTVIB calculations based on appropriate part power ATHOS analyses. This is the approach that has been used to obtain results described in the following section.

When choosing a set of initial conditions for observed wear at AVBs 4 and 5, it is also possible that a different FASTVIB case corresponding to a different span length with more than two AVBs having ineffective supports could exist. Figure 2-20 shows one such possibility with similar clearances that could have existed at AVBs 3, 4, 5, and 6, but the wear during the first cycle did not progress deep enough to lead to interaction at AVBs 3 and 6. An entirely different set of geometric and material parameters could be used with this case to tune the computed wear at AVBs 4 and 5 to match the observed wear. Then, this new combination could also be used to project expectations for future operation at different levels of excitation.

There is no a priori way to know what the correct combination of geometric and material properties is for various tubes in the SONGS steam generators. However, this methodology follows dominant trends of the mechanism considered to be the source of the observed tube/AVB wear in the SONGS Unit 2 steam generators. It takes the available energy arising from constrained amplitude fluidelastic excitation for any support configuration, matches the starting levels of wear for subsequent operation, and allows evaluation of the relative effects of many variables. The methodology benchmarks the calculated wear distribution at each limiting tube to the actual ECT wear depths at U2C17. The overall “work” required to do this (workrate x time) is therefore matched to actual experience for the first operating cycle. Only the level of flow excitation is changed thereafter for projecting future wear. The methodology is therefore appropriate for the gap limited fluidelastic excitation mechanism.

2.5.3 Results Summary

Projection of AVB wear in the limiting active tubes and limiting plugged tubes was performed as described above. Some of the detailed results are explained below using an example.

Tube R121C91 in SG 2E089 is used as the example. This tube had four AVB wear indications with bobbin reported depths of 12%, 15%, 28%, and 23% at AVBs 4 through 7, respectively at U2C17. Wear projection was made for the three deepest indications at AVBs 5 through 7. Projection results

for this tube are shown in Figure 2-21. These values are shown in the small table appearing on the upper left hand corner of the figure as well as on the plots. The bobbin reported wear depths are converted to expected (“true”) wear depths based on the correlation between metallurgical depth and NDE-reported wear depth for the eddy current technique (Reference 25). The resulting “true” wear depths for the three indications are shown in the row below the bobbin reported depths in the small table. The projection of the deepest indication (28%TW by bobbin) is shown plotted in red, the next deepest in green, and the third in blue. The abscissa shows operating duration in months and the ordinate is the maximum wear depth in %TW. It may be noted from the start of the curves that, as per these calculation results, the first location to initiate wear was AVB7. This is because the mode shape allowed contact only at this AVB initially. Once the wear at AVB7 reached approximately 11% after about one month of operation, tube contact with AVB6 was possible and the wear initiated at AVB6. Subsequently, tube wear continued at both of these AVB locations. After five months of operation, the tube started to make contact with AVB5 and wear progression continued at all three locations. After 22 months of operation, wear depths matched the “true” estimated depths at U2C17. The matching of U2C17 values were obtained by manually iterating on relative gaps and other parameters.

A software limitation does not allow calculation of wear progression in more than three AVB intersections in a tube. Hence, the shallowest wear indication was excluded from the calculation. For the deeper indications in a tube with more than three wear scars, for which the wear projection was carried out, the resulting process leads to more conservative results since the workrate is shared by three AVB intersections instead of a higher number of intersections. If the workrate is shared by a higher number of intersections, the projected wear rate at every intersection would be smaller. Therefore, the projected wear depths in such cases are likely to be higher than expected.

The projection in Cycle 17 was performed by maintaining the values of input variables from the iterative calculation. The Cycle 17 projection was performed for different power levels of operation including 100%, 80%, 70%, and 60% for up to 18 months. Taking the deepest indication at AVB6 as an example, its projected depth at the end of 18 additional months of operation at 100% power in Cycle 17 was calculated as 38.5%TW. For the lower power levels of 80%, 70% and 60%, the corresponding calculated wear depth values are 32.5%, 31.6%, and 30.4% respectively. The wear depths at 6 months into Cycle 17 are also listed in the figure for each of the four power levels. At 70% power, the wear depth of the indication at AVB6 is 30.8% after 6 months and 31.6%TW after 18 months.

Similarly, for the indication at AVB7, the projected wear depth at 70% power is 25.7%TW after 6 months and 26.2% after 18 months. For the indication at AVB5, the projected wear depth at 70% power is 18.3% after 6 months and 19.2% after 18 months. This example illustrates the detailed results for one tube.

The calculations were repeated for several limiting active tubes and for several limiting plugged tubes. The results are shown in Table 2-9. In this table, the first column shows the tube number, the second column shows the SG, and the third column shows the tube status. The fourth column lists the bobbin reported wear depth and the fifth column shows the expected or “true” depth based on the correlation between metallurgical and NDE wear depth for the inspection technique (25). Both of these values are in %TW. The next five columns show the baseline calculations. The sixth column shows the FASTVIB case number (see Table 2-8) and the seventh column shows the number of consecutive ineffective AVBs. The next three columns (8 through 10) show the wear depths after six months of operation in Cycle 17 at power levels of 100%, 80%, and 70%, respectively. The 100% power level is labeled as Cycle 1 to denote that the full power conditions corresponding to the Cycle 16 operation were used (T-hot = 598°F). The next five columns (11 through 15) are similar to the base line results, but are based on additional AVBs considered as ineffective and the corresponding FASTVIB case numbers as shown.

The results listed in rows are sorted in the order of active tubes and plugged tubes and within each group in the order of SGs 2E088 and 2E089. Rows showing no tube designation in the first column correspond to the last tube listed in the prior row(s). Reviewing the results for the baseline cases at 70% power, the deepest wear depth projected for active tubes for six months in the next cycle is 31.2%TW (R119C89 in SG 2E089 which had a bobbin reported wear depth of 28% at U2C17) and for plugged tubes is 38.5% (R112C88 in SG 2E088 which had a bobbin reported wear depth of 35% at U2C17). None of the results shown in this table includes accounting of the wear projection technique uncertainty. Impact of uncertainty on the projected wear depth is addressed in Sections 3.1.3 and 3.1.4 and its derivation is described in Section 2.5.4.

2.5.4 Wear Projection Uncertainty

As described in the prior subsections, the wear projection methodology applied here is based on selecting the input variables related to the materials and geometry of the tube-AVB intersections to match the wear depth reported in the 2C17 inspection. The methodology then uses the same values of the input variables for projection of the wear depth in Cycle 17. Since values of several input variables are unknown, this approach involves selecting input values within an expected range based on test results, published data and experience, and using these values to obtain a match for the 2C17 inspection results by trial and error. There will be a number of possible “solutions” (combinations of different values of the given input variables) that satisfy the criteria.

The wear projection process applied here is very time consuming due to the trial and error involved in obtaining a match for the inspection results, often for three different AVB wear indications in a given tube. Therefore, the uncertainty evaluation is based on the following analysis applied to one tube. In this evaluation, the method uncertainty (standard deviation of growth) is determined as a fraction of the mean estimated growth of an AVB wear indication. This allows estimation of the growth uncertainty from the estimated growth by applying this ratio. Tube R121C91 in SG 2E089, which has four AVB indications reported in the 2C17 inspection, was selected since this is one of the tubes that will be returned to service with the deepest wear scar.

First, a solution for the input variables was obtained as described in Section 2.5.3. Then a given input variable was selected and an alternate input value was assigned to it, which is within the variable’s expected range. Values close to the extremes of the range were selected in order to obtain very dissimilar solutions for the input variable combinations. The trial and error process was repeated to obtain another alternate solution that matched the wear depths reported for this tube at each of the three AVB locations with the deepest wear indications reported in 2C17. This process was repeated ten times and a total of eleven different solutions were obtained with different combinations of input values that allowed close match between calculated wear depths and the reported inspection results for this tube.

Using the calculated input values of the variables, the wear projection for Cycle 17 was made for each of the eleven solutions described above. This yielded a set of eleven wear depth projections. For each of the three AVB wear indications (at B5, B6, and B7), wear depths at two different time frames in Cycle 17 were obtained for full power, 80% power, and 70% power operation during the cycle. Thus each indication had six sets (three operating power levels at two time points in Cycle 17) of wear projections each set having eleven projections corresponding to the eleven “solutions.” Hence, there were six sets of eleven separate growth values over the 2C17 inspection results for each of three AVB indications.

Each set consists of eleven separate possible solutions of wear projection for the same tube location, operating power, and Cycle 17 duration (operating length). For each set of growth values, the mean and standard deviation were calculated. The ratio of standard deviation to the mean,

referred to as the normalized standard deviation, was also calculated. The 22 values of the normalized standard deviation ranged from 0.04 to 2.12. The large values of the normalized standard deviations were for the 80% and 70% power cases where the growth values were very small. For the full power cases where the growth values ranged from 1.9% (in 6 months) to 12.4% (in 18 months), the normalized standard deviations ranged from 0.04 to 0.20. Conservatively, the maximum calculated value of 0.20 for the full power cases was selected as the normalized standard deviation for use in this evaluation.

Hence, the standard deviation of growth will be calculated as 0.20 times the estimated growth for an indication. Using this standard deviation, the growth at 95% probability and 50% confidence can be estimated using the normal distribution ($z = 1.645$).

The growth uncertainty will be applied as follows:

- Estimated growth, $g = \text{Projected wear depth in Cycle 17} - \text{Actual wear depth at 2C17}$
- Normalized standard deviation = 0.20
- Standard deviation, $\sigma = 0.20 * g$
- Growth at 95% probability = $g + 1.645 \sigma = g * (1 + 1.645 * 0.20)$

A common sense test of the derived normalized standard deviation was applied as follows. Using the first of the eleven solutions, the growth at 95% probability and 50% confidence was calculated and added to the reported wear depth at 2C17. This was done for each of the three AVB indications at each of the three power levels and two durations of Cycle 17. The number of times the estimated Cycle 17 wear depth in the eleven solutions exceeded the 95% probability 50% confidence values by more than 0.5%² was counted. It was found that, of the 198 projected depths in the eleven solutions, only 4 exceeded the 95 percentile values. Hence, the uncertainty evaluation was validated.

A question may be raised regarding the uncertainties in the supporting evaluations such as thermal-hydraulic evaluation and flow-induced vibration evaluations that formed the inputs to the wear projection. Results of those evaluations were applied consistently for both the Cycle 16 assessments that benchmarked the solutions with the 2C17 inspection results and to the Cycle 17 assessments resulting in the wear projection. Hence the uncertainties in those results, present in both cases, balance out each other and are considered irrelevant.

2.6 Evaluation of the Potential for In-Plane Vibration

An evaluation was performed to assess the potential for in-plane vibration to occur when the Unit 2 SGs are returned to service. This evaluation is discussed in this section. The flow-induced vibration methodology was described in Section 2.3.

The potential for the occurrence of in-plane vibration during the upcoming cycle was performed for limiting tubes. The tubes with the highest potential for in-plane vibration are the tubes having the longest unsupported spans in the U-bend. The unsupported span length increases with the number of ineffective AVB locations, which do not provide adequate support for the tubes against vibration. Since the threshold for instability is much lower for the out-of-plane vibration mode compared to

² For four of the 22 cases, the calculated growth was 0. Hence the estimated uncertainty (standard deviation) was also 0, although the true uncertainty is not. Thus the small 0.5% grace value was used to account for such cases. It is possible to apply a small (0.5% or 1%) grace value as the minimum uncertainty allowance (1.645 times the standard deviation) for growth to overcome this drawback. However, it is judged to be so small and, hence, inconsequential. Thus, the simple approach without any adjustment in the uncertainty value to overcome the calculated growth value of 0 was applied in this evaluation.

the in-plane mode, the unsupported span length required for out-of-plane vibration is shorter than for in-plane vibration. Hence, a tube may exhibit out-of-plane vibration even when in-plane vibration may not be present. There are several such tubes in the Unit 2 SGs. Such tubes have experienced tube-to-AVB wear due to out-of-plane vibration. Therefore, the tubes that have the highest potential for in-plane vibration are those with several AVB wear indications. When a tube vibrates within the constrained geometry of the local AVBs, it is possible that the tube may not contact an AVB due to a large gap such that the tube is restrained by another ineffective AVB within the unsupported span. Therefore, when an AVB location without a wear indication is nestled between AVB wear indications in a tube, such nestled locations are conservatively assumed to be unsupported so as to yield the maximum unsupported span length.

Active tubes in the Unit 2 SGs having several AVB wear indications were identified. Flow-induced vibration results for these tubes for their potential for in-plane vibration were evaluated. This evaluation used a value of 7.8 for the instability constant, β . Westinghouse test data discussed in Section 2.3 suggest that the value of the instability constant may be higher for in-plane vibration. A higher value of instability constant would lead to a lower stability ratio. Hence, the IPSR evaluated using a value of 7.8 for the instability constant is conservative.

The results of the evaluation are shown in Table 2-10. All of the tubes in this table were plugged during U2C17, most of them plugged preventively. The U2C17 eddy current data from all of the tubes in this table were evaluated by Westinghouse for any evidence of in-plane vibration. The eddy current data review clearly showed that the wear indications at AVBs did not extend beyond the width of the AVBs in any of these tubes. This strongly suggests that none of these tubes were subjected to in-plane vibration during Cycle 16. Three of the tubes in the list show IPSR values slightly greater than 1 at full power. Since the tubes were not experiencing IP vibration, it adds support for the statement in the last paragraph that the value of 7.8 for the instability constant is indeed conservative. A value closer to 10 for the instability constant would have resulted in IPSR values of less than 1 at full power for all of these tubes, which is more realistic and supported by the eddy current test results.

It may be noted from Table 2-10 that all of the limiting tubes have predicted in-plane stability ratios of less than 1 at 70% power. Since these are the limiting tubes (tubes with largest number of ineffective AVB supports) in the Unit 2 RSGs, all of the other tubes will have even smaller stability ratios. Therefore, all tubes in the Unit 2 SGs will be stable against in-plane vibration in the next operating cycle.

The methodology used for the assessment of the potential for in-plane vibration in the Unit 2 RSGs was benchmarked against the tube-to-tube wear reported in dozens of tubes in the Unit 3 RSGs. This is discussed in more detail below.

2.6.1 Methodology Benchmarking Using Unit 3 Findings

In summary, a sample of 86 tubes from Unit 3, each having tube-to-tube wear in the U-bend free span, was evaluated. The logic used in the benchmarking evaluation is displayed in Figure 2-22. It was demonstrated in each case that the free span wear resulted either from in-plane vibration of the given tube or from in-plane vibration of the neighboring tube, which also had a matching wear scar at the same axial location as the given tube.

More severe tube/AVB wear occurred in Unit 3 than in Unit 2. Unit 3 also experienced significant tube-to-tube wear and more extensive tube/TSP wear than in Unit 2. Therefore, the Unit 3 tube wear experience was reviewed to correlate the Unit 3 results in order to apply the same methodology to Unit 2. A large (86) sample of tubes from SG 3E088 that had experienced tube-to-tube wear was selected for this evaluation. There was a focus on 16 tubes that had tube-to-tube

wear with only a few bobbin-reported indications of tube/AVB wear because these tubes would be the most difficult to explain the tube-to-tube wear using the methodology. It is not likely just a coincidence that these tubes happened to be around the boundary of the region with the most severe tube-to-tube wear as shown on Figure 2-23³. These “boundary tubes” reflect the transition from severe free span wear experienced by the “interior tubes” in Figure 2-23. While developing criteria to correlate these two extremes of tube-to-tube wear experience, 15 additional “adjacent tubes” were added to the evaluation.

The 86 tubes from SG 3E088, comprising 55 interior tubes, 16 boundary tubes, and 15 adjacent tubes, were subjected to an in-depth, independent evaluation of RPC results contained in the digital ECT files provided by SCE. Both the original reported wear indications from bobbin data and the new RPC results were used to define a range of potential ineffective AVB locations. This range of potential support conditions was evaluated using various FASTVIB cases using the methods described in Section 2.3. Then, all calculations and ECT observations were reviewed to establish the most likely physical explanation for the tube-to-tube wear that occurred in the Unit 3 RSGs. Table 2-11 and Table 2-12 provide a summary of the pertinent results.

Table 2-11 addresses the more difficult to explain boundary tubes along with the adjacent tubes that are required to explain the occurrence of free span (FS) tube-to-tube wear in some instances. Notes explaining legends used in the evaluation follow at the bottom of the second page. The first tube in the table, R114C74, is a boundary tube that has an indicated FS wear depth of 26 %TW on the hot leg side between AVBs B3 and B4, but the only indications of tube/AVB wear are at AVBs B3 and B4 from the bobbin data plus an indication of very small wear (too small for the bobbin detection threshold) at B2 from the RPC evaluation. The support conditions evaluated for the implied support configuration Cases 15 and 25 (see Table 2-8), that simulated ineffective supports at the AVBs with wear, show that OP gap limited fluidelastic excitation could produce wear at those AVBs. The same support configuration Cases 15 and 25 are also clearly insufficient to have the possibility of IP fluidelastic instability as the explanation for the FS wear because the calculated stability ratio is only about half the required threshold using a value of $\beta_{IP} = 7.8$ for the instability constant. Furthermore, the wear scars that were present showed no extensions beyond the AVB intersections, so there had been no apparent significant in-plane motion of this tube.

The next tube in the Column R112C74 (nearest inside neighbor in the same column) was already in the list as a boundary tube because it had only one wear call at B5, so it was also reviewed to determine if it could be the source of the FS wear that had been found on R114C74. Table 2-11 shows how this is considered to be a possible explanation since it showed indications of in-plane motion as the wear scar extended outside the AVB at B8, and the IP stability ratio would have exceeded the threshold if the nestled AVBs B2, B6, and B7 had been ineffective in providing support in-plane in addition to the seven other locations with small wear observed only with detailed RPC inspection. Since the Unit 3 RSGs operated for only half of a fuel cycle, it is not surprising that the wear depth resulting from out-of-plane vibration at some of the ineffective AVB locations were too small to be detectable by the bobbin probe, and in some cases by the +Point RPC probe. The wear depths on these two boundary tubes were similar (26% and 25 %TW) to support this conclusion.

The inside neighbor adjacent Tube R110C74 had 4 bobbin indications and 4 more low level RPC indications, and it also required 3 additional nestled AVBs to be ineffective at preventing in-plane motion in order to have potential IP instability. It also had reasonably similar FS wear between B3

³ Note that the tubes later called “boundary tubes” due to their location on the map were originally selected by sorting ECT data results and choosing ones that appeared not to have many tube wear indications at the AVBs. The adjacent tubes were added later. The original terminology was retained for the evaluation and the map labels.

and B4 (19%TW). These three tubes illustrate tubes that are most challenging to identify by observation of FS wear on the tube or an adjacent neighbor that interacts with it.

The next two tubes are similar in that one (R101C75) has FS wear on the cold leg between AVBs B9 and B10, but there is no analytical basis to explain it. However, the adjacent Tube R103C75 is potentially unstable in the IP direction using support conditions evident from both bobbin and RPC test results. The FS wear scars also match at 19% and 18%TW, and there is clear evidence of in-plane motion demonstrated by wear scar extensions.

The remaining tubes in Table 2-11 with FS wear that were selected as being the most difficult to explain all have adjacent neighbors that appear to be the sources of IP motions that cause wear at the interface of both tubes. Some are obvious after reviewing the additional RPC indications while others require reasonable, but not obvious, assumptions that are consistent with physical observations and analytical predictions of potential for IP instability. However, the main conclusion of the evaluation is that tubes with FS wear can all be explained as either having that potential, or by interacting with neighbors that have the potential to be unstable in-plane.

The results of the evaluation of the interior tubes in the 86-tube sample are shown in Table 2-12. Here, due to the large number of ineffective AVBs identified by the eddy current inspection results, it is easy to conclude that vibration resulting from in-plane instability led to the free span tube wear in the sample tubes. The long unsupported spans lead to higher SR values for these tubes compared to those in Table 2-11.

A second major conclusion relates to the observed levels of TSP wear that characterize the results shown for most of the interior tubes in Table 2-12 and for several of the adjacent tubes in Table 2-11. Tubes with significant TSP wear correspond to the calculated OP gap limited stability ratios from about 7 to 9 and IP stability ratios greater than about 1.5. As such, they correspond to tubes having very long unsupported spans with obvious potential for IP instability based on the FASTVIB cases considered most representative of the available observations.

The benchmarking evaluation showed that the methodology is capable of accurately predicting the potential for the occurrence of in-plane vibration. It was demonstrated in each case that the free span wear resulted either from in-plane vibration of the given tube or from in-plane vibration of the neighboring tube, which also had a matching wear scar at the same axial location as the given tube.

Table 2-1. ATHOS Model R- θ Finite Difference Grid

IX	Circumferential Grid (XU) (Degrees)	IY	Radial Grid (YV) at Tubesheet (inches)	Radial Grid (YV) at Lower Deck (inches)
1	6.00	1	7.023	9.371
2	12.00	2	12.077	16.113
3	18.00	3	17.130	22.855
4	24.00	4	21.070	28.112
5	30.00	5	26.123	34.854
6	36.00	6	31.177	41.596
7	42.00	7	36.230	48.338
8	48.00	8	40.170	53.595
9	54.00	9	45.223	60.337
10	60.00	10	50.277	67.079
11	66.00	11	55.330	73.821
12	72.00	12	59.270	79.078
13	78.00	13	64.323	85.820
14	84.00	14	69.377	92.563
15	90.00	15	74.430	99.305
16	96.00	16	77.400	103.267
17	102.00	17	79.980	106.710
18	108.00			
19	114.0			
20	120.0			
21	126.0			
22	132.0			
23	138.0			
24	144.0			
25	150.0			
26	156.0			
27	162.0			
28	168.0			
29	174.0			
30	180.0			

Table 2-2. ATHOS Model Axial Direction (Z) Finite Difference Grid

IZ	ZW(in)	Comment		
1	3.75			
2	7.50			
3	11.25			
4	15.00	DC Opening		
5	21.95			
6	28.91			
7	35.86			
8	42.81	TSP #1		
9	53.73			
10	64.65			
11	75.56			
12	86.48	TSP #2		
13	97.39			
14	108.31			
15	119.22			
16	130.14	TSP #3		
17	141.05			
18	151.97			
19	162.88			
20	173.80	TSP #4		
21	184.71			
22	195.63			
23	206.55			
24	217.46	TSP #5		
25	228.38			
26	239.29			
27	250.21			
28	261.12	TSP #6		
29	268.06			
30	274.99			
31	281.92			
32	288.86			
33	295.79	Start of Shell Exp.		
34	300.29			
35	304.78	TSP #7		
36	317.41	Start of Wrapper Exp.		
37	325.13			
38	332.84			
39	340.56			
40	348.28			
41	353.42			
42	358.57			
43	363.71	End of Wrapper Exp.		
44	371.39	Top of Shell Cone		
45	377.01			
46	382.63			
47	388.25	Above the U-Bend Region		
48	394.11			
49	399.98			
50	405.84	Bottom of Moisture Sep. Barrel		

Table 2-3. SONGS Unit 2 RSG 2E088 Tube Plugging List

Row	Column																			Col ≤ 89	Col ≥ 89
88	88																			1	0
94	90	94																		0	2
95	89	91																		1	2
97	85	89																		2	1
98	84	86	92																	2	1
99	85	93																		1	1
100	86	88	90	92																2	2
101	87	89	91	93																2	3
102	86	88	90	92																2	2
103	85	87	89	91	93															3	3
104	84	86	88	90	92															3	2
105	83	85	87	89	91															4	2
106	84	86	88	90	92															3	2
107	83	85	89	91	93															3	3
108	34	84	86	90	92	144														3	3
109	35	91	143																	1	2
110	34	36	88	90	92	142	144													3	4
111	35	37	87	89	91	93	141	143												4	5
112	36	38	86	88	90	92	140	142												4	4
113	37	39	87	89	91	139	141													4	4
114	38	40	86	88	90	92	138	140												4	4
115	39	41	85	87	89	91	137	139												5	4
116	40	42	86	88	90	92	136	138												4	4
117	41	43	89	91	93	135	137													3	5
118	42	44	88	92	134	136														3	3
119	43	45	89	133	135															3	3
120	44	46	82	88	92	132	134													4	3
121	45	47	81	85	87	89	131	133												6	3
122	46	48	84	86	88	130	132													5	2
123	47	49	85	87	89	129	131													5	3
124	48	50	86	88	92	128	130													4	3
125	49	51	87	127	129															3	2
126	50	52	86	126	128															3	2
127	51	53	89	125	127															3	3
128	52	54	94	124	126															2	3
129	53	55	93	123	125															2	3
130	54	56	122	124																2	2
131	55	57	121	123																2	2
132	56	122																		1	1
133	85	91																		1	1
134	94																			0	1
136	92																			0	1
																			Total:	113	106

Note: Tubes R135C93 and R137C89 in this SG were plugged subsequent to this analysis.

Table 2-5. Cycle 17 Operating Parameters with 205 Plugged Tubes (SG 2E088)

Case	50%	60%	70 %	80 %	90 %	100 %	100 % with no plugging
Plugging ⁶	205	205	205	205	205	205	0
Thermal power (MWt)	869.5 (50%)	1041.4 (60%)	1213.3 (70%)	1385.2 (80%)	1557.1 (90%)	1729 (100%)	1729
RCS flow rate (gpm) ¹¹	207,726	207,726	207,726	207,726	207,726	207,726	209,880
T _{hot} (Tsg-in) (°F)	576.9	583.0	589.1	595.0	600.7	606.3	597.7
T _{eg-out} (°F) ¹²	547.2	547.7	548.3 ¹⁴	548.8 ¹⁴	549.3	549.7	541.0
T _{cold} (°F) ¹²	547.5	548.0	548.6 ¹⁴	549.1 ¹⁴	549.6	550.0	541.3
Saturation Steam Pressure (psia)	956	951	946	940	935	928	864
Fouling Factor (ft ² hr°F /Btu)	0	0	0	0	0	0	0
T _{feedwater} (°F)	375.2	390.9	406.5 ¹⁵	419.6 ¹⁵	430.5	443	443
Circulation Ratio	7.5	6.2	5.2	4.4	3.8	3.3	3.3
Steam Mass Flow (lb/hr)	3,494,000	4,274,500	5,087,100	5,914,000	6,750,600	7,630,800	7,611,000
Feed Water Mass Flow (lb/hr) ¹³	3,598,000	4,378,800	5,191,600	6,018,800	6,855,600	7,736,000	7,716,900
Blowdown flow rate (gpm)	270	270	270	270	270	270	270

Note: Two additional tubes were plugged in this SG after the completion of this analysis.

Table 2-6. Cycle 17 Operating Parameters with 305 Plugged Tubes (SG 2E089)

Case	50%	60%	70 %	80 %	90 %	100 %	100 % with no plugging
Plugging ⁶	305	305	305	305	305	305	0
Thermal power (MWt)	869.5 (50%)	1041.4 (60%)	1213.3 (70%)	1385.2 (80%)	1557.1 (90%)	1729 (100%)	1729
RCS flow rate (gpm) ¹¹	206,695	206,695	206,695	206,695	206,695	206,695	209,880
T _{hot} (Tsg-in) (°F)	577.0	583.1	589.2	595.2	601.0	606.6	597.7
T _{eg-out} (°F) ¹²	547.2	547.7	548.3 ¹⁴	548.8 ¹⁴	549.3	549.7	541.0
T _{cold} (°F) ¹²	547.5	548.0	548.6 ¹⁴	549.1 ¹⁴	549.6	550.0	541.3
Saturation Steam Pressure (psia)	955	950	945	939	933	926	864
Fouling Factor (ft ² hr°F /Btu)	0	0	0	0	0	0	0
T _{feedwater} (°F)	375.2	390.9	406.5 ¹⁵	419.6 ¹⁵	430.5	443	443
Circulation Ratio	7.5	6.2	5.2	4.4	3.8	3.3	3.3
Steam Mass Flow (lb/hr)	3,493,900	4,274,300	5,086,800	5,913,700	6,750,200	7,630,300	7,611,000
Feed Water Mass Flow (lb/hr) ¹³	3,597,900	4,378,600	5,191,400	6,018,500	6,855,200	7,735,500	7,716,900
Blowdown flow rate (gpm)	270	270	270	270	270	270	270

Note: Three additional tubes were plugged in this SG after the completion of this analysis.

Table 2-7. Summary of ATHOS Results

Parameter	Summary of ATHOS Results											
	Reference	1-a	1-b	2-a	2-b	3-a	3-b	3-c	3-d	4-a	4-b	
Power Level (%)	100	50	60	70	80	80	80	80	80	80	80	
Steam Generator	Units 2 and 3	2E89	2E89	2E89	2E89	2E88	2E89	2E89	2E89	2E89	2E89	
Number of Plugged Tubes	0	305	305	305	305	205	305	305	305	305	305	
Tube Columns	All	1-89	89-177	1-89	89-177	1-89	89-177	1-89	89-177	1-89	89-177	
Tube Bundle Model	N/A	2E89LC	2E89HC	2E89LC	2E89HC	2E88LC	2E89HC	2E89LC	2E89HC	2E89LC	2E89HC	
Number of Plugged Tubes ⁽¹⁾	0	218	101	218	101	113	108	218	101	218	101	
Operating Conditions and ATHOS Calculated Thermal-Hydraulic Characteristics												
NSSS Power ⁽²⁾ , per SG MCM	1729	870.6	870.6	1042.6	1042.6	1214.6	1214.6	1214.6	1214.6	1386.6	1386.6	
Primary Flow Rate, Mlbm/hr	79,779	77,926	77,926	77,873	77,873	78,198	78,198	77,810	77,810	77,757	77,757	
Primary Pressure, psia	2250	2250	2250	2250	2250	2250	2250	2250	2250	2250	2250	
Primary Inlet Temperature ⁽²⁾ , °F	598.02	579.48	579.13	586.76	586.35	591.59	591.57	592.06	591.61	598.06	597.55	
Primary Outlet Temperature ⁽²⁾ , °F	541.35	549.64	549.29	550.32	549.91	550.75	550.72	550.99	550.53	551.54	551.04	
Feedwater/Steam Flow 1375 ⁽²⁾ , Mlbm/hr	7,903	3,5147	3,5147	4,293	4,293	5,104	5,104	5,104	5,104	5,929	5,929	
Feedwater Temperature, °F	442.0	375.2	375.2	380.9	380.9	406.5	406.5	406.5	406.5	419.6	419.6	
Steam Pressure in the Dome, psia	837.6	955.0	955.0	950.0	950.0	945.0	946.0	945.0	945.0	939.0	939.0	
Circulation Ratio ⁽²⁾	3.26	6.93	6.92	5.75	5.75	4.87	4.87	4.87	4.87	4.20	4.20	
Downcomer Flow Hot Side ⁽²⁾ , Mlbm/hr	12,454	12,207	12,208	12,395	12,393	12,481	12,481	12,480	12,481	12,492	12,493	
Downcomer Flow Cold Side ⁽²⁾ , Mlbm/hr	12,297	12,108	12,059	12,287	12,283	12,362	12,362	12,363	12,361	12,367	12,364	
Maximum Quality ⁽²⁾	0.8665	0.1639	0.1948	0.2636	0.2632	0.3586	0.3593	0.3597	0.3673	0.5113	0.6250	
Maximum Void Fraction ⁽²⁾	0.9655	0.8405	0.8413	0.8876	0.8874	0.9254	0.9256	0.9253	0.9251	0.9724	0.9739	
Maximum Velocity ⁽²⁾ , ft/s	25.12	9.66	9.95	11.34	11.93	12.55	12.58	12.37	12.65	14.07	14.06	
Thermal-Hydraulic Parameters at the Maximum p² Location in the U-bend Section of Row 14f / Column 89												
Gap Velocity, ft/sec	16.83	8.62	9.95	9.99	10.29	11.51	11.54	11.29	11.59	12.65	13.03	
Secondary Fluid Density, lbm/ft ³	7.04	16.11	15.22	13.92	14.03	12.06	12.05	11.98	12.03	10.22	10.24	
Relative p ²	1.00	0.60	0.65	0.70	0.74	0.80	0.80	0.77	0.81	0.82	0.87	

Notes:

- (1) There are 14 plugged tubes in Column 89 in both steam generators. Column 89 is a common column for each half of ATHOS tube bundle mode.
- (2) ATHOS calculated values. These values may be different than SG parameters in Reference 3-4.

Table 2-8. Possible AVB Support Cases with Adjacent Ineffective AVBs (Page 1 of 15)

FASTVIB - FLOVIB Case Descriptions																
Case	AVB	Status	Group	Rows	AVB Number											
					1	2	3	4	5	6	7	8	9	10	11	12
Case 0	0	All Supported	Group 1	Rows 48 to 142	1	2	3	4	5	6	7	8	9	10	11	12
			Group 2	Rows 27 to 47	1	2	3	4	5	n.a	n.a	8	9	10	11	12
			Group 3	Rows 15 to 26	1	n.a	n.a	4	5	n.a	n.a	8	9	n.a	n.a	12
			Group 4	Rows 1 to 14	1	n.a	n.a	4	n.a	n.a	n.a	n.a	9	n.a	n.a	12
Case 1	1	AVB 1 Missing	Group 1	Rows 48 to 142	X	2	3	4	5	6	7	8	9	10	11	12
			Group 2	Rows 27 to 47	X	2	3	4	5	n.a	n.a	8	9	10	11	12
			Group 3	Rows 15 to 26	X	n.a	n.a	4	5	n.a	n.a	8	9	n.a	n.a	12
			Group 4	Rows 1 to 14	X	n.a	n.a	4	n.a	n.a	n.a	n.a	9	n.a	n.a	12
Case 2	1	AVB 2 Missing	Group 1	Rows 48 to 142	1	X	3	4	5	6	7	8	9	10	11	12
			Group 2	Rows 27 to 47	1	X	3	4	5	n.a	n.a	8	9	10	11	12
			Group 3	Rows 15 to 26	1	n.a	n.a	4	5	n.a	n.a	8	9	n.a	n.a	12
			Group 4	Rows 1 to 14	1	n.a	n.a	4	n.a	n.a	n.a	n.a	9	n.a	n.a	12
Case 3	1	AVB 3 Missing	Group 1	Rows 48 to 142	1	2	X	4	5	6	7	8	9	10	11	12
			Group 2	Rows 27 to 47	1	2	X	4	5	n.a	n.a	8	9	10	11	12
			Group 3	Rows 15 to 26	1	n.a	n.a	4	5	n.a	n.a	8	9	n.a	n.a	12
			Group 4	Rows 1 to 14	1	n.a	n.a	4	n.a	n.a	n.a	n.a	9	n.a	n.a	12
Case 4	1	AVB 4 Missing	Group 1	Rows 48 to 142	1	2	3	X	5	6	7	8	9	10	11	12
			Group 2	Rows 27 to 47	1	2	3	X	5	n.a	n.a	8	9	10	11	12
			Group 3	Rows 15 to 26	1	n.a	n.a	X	5	n.a	n.a	8	9	n.a	n.a	12
			Group 4	Rows 1 to 14	1	n.a	n.a	X	n.a	n.a	n.a	n.a	9	n.a	n.a	12
Case 5	1	AVB 5 Missing	Group 1	Rows 48 to 142	1	2	3	4	X	6	7	8	9	10	11	12
			Group 2	Rows 27 to 47	1	2	3	4	X	n.a	n.a	8	9	10	11	12
			Group 3	Rows 15 to 26	1	n.a	n.a	4	X	n.a	n.a	8	9	n.a	n.a	12
			Group 4	Rows 1 to 14	1	n.a	n.a	4	n.a	n.a	n.a	n.a	9	n.a	n.a	12

Table 2-8. Possible AVB Support Cases with Adjacent Ineffective AVBs (Page 2 of 15)

Case 6	1	AVB 6 Missing	Group 1	Rows 48 to 142	1	2	3	4	5	X	7	8	9	10	11	12
			Group 2	Rows 27 to 47	1	2	3	4	5	n.a	n.a	8	9	10	11	12
			Group 3	Rows 15 to 26	1	n.a	n.a	4	5	n.a	n.a	8	9	n.a	n.a	12
			Group 4	Rows 1 to 14	1	n.a	n.a	4	n.a	n.a	n.a	n.a	9	n.a	n.a	12
Case 7	1	AVB 7 Missing	Group 1	Rows 48 to 142	1	2	3	4	5	6	X	8	9	10	11	12
			Group 2	Rows 27 to 47	1	2	3	4	5	n.a	n.a	8	9	10	11	12
			Group 3	Rows 15 to 26	1	n.a	n.a	4	5	n.a	n.a	8	9	n.a	n.a	12
			Group 4	Rows 1 to 14	1	n.a	n.a	4	n.a	n.a	n.a	n.a	9	n.a	n.a	12
Case 8	1	AVB 8 Missing	Group 1	Rows 48 to 142	1	2	3	4	5	6	7	X	9	10	11	12
			Group 2	Rows 27 to 47	1	2	3	4	5	n.a	n.a	X	9	10	11	12
			Group 3	Rows 15 to 26	1	n.a	n.a	4	5	n.a	n.a	X	9	n.a	n.a	12
			Group 4	Rows 1 to 14	1	n.a	n.a	4	n.a	n.a	n.a	n.a	9	n.a	n.a	12
Case 9	1	AVB 9 Missing	Group 1	Rows 48 to 142	1	2	3	4	5	6	7	8	X	10	11	12
			Group 2	Rows 27 to 47	1	2	3	4	5	n.a	n.a	8	X	10	11	12
			Group 3	Rows 15 to 26	1	n.a	n.a	4	5	n.a	n.a	8	X	n.a	n.a	12
			Group 4	Rows 1 to 14	1	n.a	n.a	4	n.a	n.a	n.a	n.a	X	n.a	n.a	12
Case 10	1	AVB 10 Missing	Group 1	Rows 48 to 142	1	2	3	4	5	6	7	8	9	X	11	12
			Group 2	Rows 27 to 47	1	2	3	4	5	n.a	n.a	8	9	X	11	12
			Group 3	Rows 15 to 26	1	n.a	n.a	4	5	n.a	n.a	8	9	n.a	n.a	12
			Group 4	Rows 1 to 14	1	n.a	n.a	4	n.a	n.a	n.a	n.a	9	n.a	n.a	12
Case 11	1	AVB 11 Missing	Group 1	Rows 48 to 142	1	2	3	4	5	6	7	8	9	10	X	12
			Group 2	Rows 27 to 47	1	2	3	4	5	n.a	n.a	8	9	10	X	12
			Group 3	Rows 15 to 26	1	n.a	n.a	4	5	n.a	n.a	8	9	n.a	n.a	12
			Group 4	Rows 1 to 14	1	n.a	n.a	4	n.a	n.a	n.a	n.a	9	n.a	n.a	12

Table 2-8. Possible AVB Support Cases with Adjacent Ineffective AVBs (Page 3 of 15)

Case 12	1	AVB 12 Missing	Group 1	Rows 48 to 142	1	2	3	4	5	6	7	8	9	10	11	X
			Group 2	Rows 27 to 47	1	2	3	4	5	n.a	n.a	8	9	10	11	X
			Group 3	Rows 15 to 26	1	n.a	n.a	4	5	n.a	n.a	8	9	n.a	n.a	X
			Group 4	Rows 1 to 14	1	n.a	n.a	4	n.a	n.a	n.a	n.a	9	n.a	n.a	X
Case 13	2	AVB 1, 2 Missing	Group 1	Rows 48 to 142	X	X	3	4	5	6	7	8	9	10	11	12
			Group 2	Rows 27 to 47	X	X	3	4	5	n.a	n.a	8	9	10	11	12
			Group 3	Rows 15 to 26	X	n.a	n.a	4	5	n.a	n.a	8	9	n.a	n.a	12
			Group 4	Rows 1 to 14	X	n.a	n.a	4	n.a	n.a	n.a	n.a	9	n.a	n.a	12
Case 14	2	AVB 2, 3 Missing	Group 1	Rows 48 to 142	1	X	X	4	5	6	7	8	9	10	11	12
			Group 2	Rows 27 to 47	1	X	X	4	5	n.a	n.a	8	9	10	11	12
			Group 3	Rows 15 to 26	1	n.a	n.a	4	5	n.a	n.a	8	9	n.a	n.a	12
			Group 4	Rows 1 to 14	1	n.a	n.a	4	n.a	n.a	n.a	n.a	9	n.a	n.a	12
Case 15	2	AVB 3, 4 Missing	Group 1	Rows 48 to 142	1	2	X	X	5	6	7	8	9	10	11	12
			Group 2	Rows 27 to 47	1	2	X	X	5	n.a	n.a	8	9	10	11	12
			Group 3	Rows 15 to 26	1	n.a	n.a	X	5	n.a	n.a	8	9	n.a	n.a	12
			Group 4	Rows 1 to 14	1	n.a	n.a	X	n.a	n.a	n.a	n.a	9	n.a	n.a	12
Case 16	2	AVB 4,5 Missing	Group 1	Rows 48 to 142	1	2	3	X	X	6	7	8	9	10	11	12
			Group 2	Rows 27 to 47	1	2	3	X	X	n.a	n.a	8	9	10	11	12
			Group 3	Rows 15 to 26	1	n.a	n.a	X	X	n.a	n.a	8	9	n.a	n.a	12
			Group 4	Rows 1 to 14	1	n.a	n.a	X	n.a	n.a	n.a	n.a	9	n.a	n.a	12
Case 17	2	AVB 5, 6 Missing	Group 1	Rows 48 to 142	1	2	3	4	X	X	7	8	9	10	11	12
			Group 2	Rows 27 to 47	1	2	3	4	X	n.a	n.a	8	9	10	11	12
			Group 3	Rows 15 to 26	1	n.a	n.a	4	X	n.a	n.a	8	9	n.a	n.a	12
			Group 4	Rows 1 to 14	1	n.a	n.a	4	n.a	n.a	n.a	n.a	9	n.a	n.a	12

Table 2-8. Possible AVB Support Cases with Adjacent Ineffective AVBs (Page 4 of 15)

Case 18	2	AVB 6, 7 Missing	Group 1	Rows 48 to 142	1	2	3	4	5	X	X	8	9	10	11	12
			Group 2	Rows 27 to 47	1	2	3	4	5	n.a	n.a.	8	9	10	11	12
			Group 3	Rows 15 to 26	1	n.a	n.a	4	5	n.a	n.a.	8	9	n.a	n.a.	12
			Group 4	Rows 1 to 14	1	n.a	n.a	4	n.a	n.a	n.a.	n.a	9	n.a	n.a.	12
Case 19	2	AVB 7, 8 Missing	Group 1	Rows 48 to 142	1	2	3	4	5	6	X	X	9	10	11	12
			Group 2	Rows 27 to 47	1	2	3	4	5	n.a	n.a.	X	9	10	11	12
			Group 3	Rows 15 to 26	1	n.a	n.a	4	5	n.a	n.a.	X	9	n.a	n.a.	12
			Group 4	Rows 1 to 14	1	n.a	n.a	4	n.a	n.a	n.a.	n.a	9	n.a	n.a.	12
Case 20	2	AVB 8, 9 Missing	Group 1	Rows 48 to 142	1	2	3	4	5	6	7	X	X	10	11	12
			Group 2	Rows 27 to 47	1	2	3	4	5	n.a	n.a.	X	X	10	11	12
			Group 3	Rows 15 to 26	1	n.a	n.a	4	5	n.a	n.a.	X	X	n.a	n.a.	12
			Group 4	Rows 1 to 14	1	n.a	n.a	4	n.a	n.a	n.a.	n.a	X	n.a	n.a.	12
Case 21	2	AVB 9, 10 Missing	Group 1	Rows 48 to 142	1	2	3	4	5	6	7	8	X	X	11	12
			Group 2	Rows 27 to 47	1	2	3	4	5	n.a	n.a.	8	X	X	11	12
			Group 3	Rows 15 to 26	1	n.a	n.a	4	5	n.a	n.a.	8	X	n.a	n.a.	12
			Group 4	Rows 1 to 14	1	n.a	n.a	4	n.a	n.a	n.a.	n.a	X	n.a	n.a.	12
Case 22	2	AVB 10, 11 Missing	Group 1	Rows 48 to 142	1	2	3	4	5	6	7	8	9	X	X	12
			Group 2	Rows 27 to 47	1	2	3	4	5	n.a	n.a.	8	9	X	X	12
			Group 3	Rows 15 to 26	1	n.a	n.a	4	5	n.a	n.a.	8	9	n.a	n.a.	12
			Group 4	Rows 1 to 14	1	n.a	n.a	4	n.a	n.a	n.a.	n.a	9	n.a	n.a.	12
Case 23	2	AVB 11, 12 Missing	Group 1	Rows 48 to 142	1	2	3	4	5	6	7	8	9	10	X	X
			Group 2	Rows 27 to 47	1	2	3	4	5	n.a	n.a.	8	9	10	X	X
			Group 3	Rows 15 to 26	1	n.a	n.a	4	5	n.a	n.a.	8	9	n.a	n.a.	X
			Group 4	Rows 1 to 14	1	n.a	n.a	4	n.a	n.a	n.a.	n.a	9	n.a	n.a.	X

Table 2-8. Possible AVB Support Cases with Adjacent Ineffective AVBs (Page 5 of 15)

Case 24	3	AVB 1, 2, 3 Missing	Group 1	Rows 48 to 142	X	X	X	4	5	6	7	8	9	10	11	12
			Group 2	Rows 27 to 47	X	X	X	4	5	n.a	n.a	8	9	10	11	12
			Group 3	Rows 15 to 26	X	n.a	n.a	4	5	n.a	n.a	8	9	n.a	n.a	12
			Group 4	Rows 1 to 14	X	n.a	n.a	4	n.a	n.a	n.a	n.a	9	n.a	n.a	12
Case 25	3	AVB 2, 3, 4 Missing	Group 1	Rows 48 to 142	1	X	X	X	5	6	7	8	9	10	11	12
			Group 2	Rows 27 to 47	1	X	X	X	5	n.a	n.a	8	9	10	11	12
			Group 3	Rows 15 to 26	1	n.a	n.a	X	5	n.a	n.a	8	9	n.a	n.a	12
			Group 4	Rows 1 to 14	1	n.a	n.a	X	n.a	n.a	n.a	n.a	9	n.a	n.a	12
Case 26	3	AVB 3, 4, 5 Missing	Group 1	Rows 48 to 142	1	2	X	X	X	6	7	8	9	10	11	12
			Group 2	Rows 27 to 47	1	2	X	X	X	n.a	n.a	8	9	10	11	12
			Group 3	Rows 15 to 26	1	n.a	n.a	X	X	n.a	n.a	8	9	n.a	n.a	12
			Group 4	Rows 1 to 14	1	n.a	n.a	X	n.a	n.a	n.a	n.a	9	n.a	n.a	12
Case 27	3	AVB 4, 5, 6 Missing	Group 1	Rows 48 to 142	1	2	3	X	X	X	7	8	9	10	11	12
			Group 2	Rows 27 to 47	1	2	3	X	X	n.a	n.a	8	9	10	11	12
			Group 3	Rows 15 to 26	1	n.a	n.a	X	X	n.a	n.a	8	9	n.a	n.a	12
			Group 4	Rows 1 to 14	1	n.a	n.a	X	n.a	n.a	n.a	n.a	9	n.a	n.a	12
Case 28	3	AVB 5, 6, 7 Missing	Group 1	Rows 48 to 142	1	2	3	4	X	X	X	8	9	10	11	12
			Group 2	Rows 27 to 47	1	2	3	4	X	n.a	n.a	8	9	10	11	12
			Group 3	Rows 15 to 26	1	n.a	n.a	4	X	n.a	n.a	8	9	n.a	n.a	12
			Group 4	Rows 1 to 14	1	n.a	n.a	4	n.a	n.a	n.a	n.a	9	n.a	n.a	12
Case 29	3	AVB 6, 7, 8 Missing	Group 1	Rows 48 to 142	1	2	3	4	5	X	X	X	9	10	11	12
			Group 2	Rows 27 to 47	1	2	3	4	5	n.a	n.a	X	9	10	11	12
			Group 3	Rows 15 to 26	1	n.a	n.a	4	5	n.a	n.a	X	9	n.a	n.a	12
			Group 4	Rows 1 to 14	1	n.a	n.a	4	n.a	n.a	n.a	n.a	9	n.a	n.a	12

Table 2-8. Possible AVB Support Cases with Adjacent Ineffective AVBs (Page 6 of 15)

Case 30	3	AVB 7, 8, 9 Missing	Group 1	Rows 48 to 142	1	2	3	4	5	6	X	X	X	10	11	12
			Group 2	Rows 27 to 47	1	2	3	4	5	n.a	n.a	X	X	10	11	12
			Group 3	Rows 15 to 26	1	n.a	n.a	4	5	n.a	n.a	X	X	n.a	n.a	12
			Group 4	Rows 1 to 14	1	n.a	n.a	4	n.a	n.a	n.a	n.a	X	n.a	n.a	12
Case 31	3	AVB 8, 9, 10 Missing	Group 1	Rows 48 to 142	1	2	3	4	5	6	7	X	X	X	11	12
			Group 2	Rows 27 to 47	1	2	3	4	5	n.a	n.a	X	X	X	11	12
			Group 3	Rows 15 to 26	1	n.a	n.a	4	5	n.a	n.a	X	X	n.a	n.a	12
			Group 4	Rows 1 to 14	1	n.a	n.a	4	n.a	n.a	n.a	n.a	X	n.a	n.a	12
Case 32	3	AVB 9, 10, 11 Missing	Group 1	Rows 48 to 142	1	2	3	4	5	6	7	8	X	X	X	12
			Group 2	Rows 27 to 47	1	2	3	4	5	n.a	n.a	8	X	X	X	12
			Group 3	Rows 15 to 26	1	n.a	n.a	4	5	n.a	n.a	8	X	n.a	n.a	12
			Group 4	Rows 1 to 14	1	n.a	n.a	4	n.a	n.a	n.a	n.a	X	n.a	n.a	12
Case 33	3	AVB 10, 11, 12 Missing	Group 1	Rows 48 to 142	1	2	3	4	5	6	7	8	9	X	X	X
			Group 2	Rows 27 to 47	1	2	3	4	5	n.a	n.a	8	9	X	X	X
			Group 3	Rows 15 to 26	1	n.a	n.a	4	5	n.a	n.a	8	9	n.a	n.a	X
			Group 4	Rows 1 to 14	1	n.a	n.a	4	n.a	n.a	n.a	n.a	9	n.a	n.a	X
Case 34	4	AVB 1, 2, 3, 4 Missing	Group 1	Rows 48 to 142	X	X	X	X	5	6	7	8	9	10	11	12
			Group 2	Rows 27 to 47	X	X	X	X	5	n.a	n.a	8	9	10	11	12
			Group 3	Rows 15 to 26	X	n.a	n.a	X	5	n.a	n.a	8	9	n.a	n.a	12
			Group 4	Rows 1 to 14	X	n.a	n.a	X	n.a	n.a	n.a	n.a	9	n.a	n.a	12
Case 35	4	AVB 2, 3, 4, 5 Missing	Group 1	Rows 48 to 142	1	X	X	X	X	6	7	8	9	10	11	12
			Group 2	Rows 27 to 47	1	X	X	X	X	n.a	n.a	8	9	10	11	12
			Group 3	Rows 15 to 26	1	n.a	n.a	X	X	n.a	n.a	8	9	n.a	n.a	12
			Group 4	Rows 1 to 14	1	n.a	n.a	X	n.a	n.a	n.a	n.a	9	n.a	n.a	12

Table 2-8. Possible AVB Support Cases with Adjacent Ineffective AVBs (Page 7 of 15)

Case 36	4	AVB 3, 4, 5, 6 Missing	Group 1	Rows 48 to 142	1	2	X	X	X	X	7	8	9	10	11	12
			Group 2	Rows 27 to 47	1	2	X	X	X	n.a	n.a	8	9	10	11	12
			Group 3	Rows 15 to 26	1	n.a	n.a	X	X	n.a	n.a	8	9	n.a	n.a	12
			Group 4	Rows 1 to 14	1	n.a	n.a	X	n.a	n.a	n.a	n.a	9	n.a	n.a	12
Case 37	4	AVB 4, 5, 6, 7 Missing	Group 1	Rows 48 to 142	1	2	3	X	X	X	X	8	9	10	11	12
			Group 2	Rows 27 to 47	1	2	3	X	X	n.a	n.a	8	9	10	11	12
			Group 3	Rows 15 to 26	1	n.a	n.a	X	X	n.a	n.a	8	9	n.a	n.a	12
			Group 4	Rows 1 to 14	1	n.a	n.a	X	n.a	n.a	n.a	n.a	9	n.a	n.a	12
Case 38	4	AVB 5, 6, 7, 8 Missing	Group 1	Rows 48 to 142	1	2	3	4	X	X	X	X	9	10	11	12
			Group 2	Rows 27 to 47	1	2	3	4	X	n.a	n.a	X	9	10	11	12
			Group 3	Rows 15 to 26	1	n.a	n.a	4	X	n.a	n.a	X	9	n.a	n.a	12
			Group 4	Rows 1 to 14	1	n.a	n.a	4	n.a	n.a	n.a	n.a	9	n.a	n.a	12
Case 39	4	AVB 6, 7, 8, 9 Missing	Group 1	Rows 48 to 142	1	2	3	4	5	X	X	X	X	10	11	12
			Group 2	Rows 27 to 47	1	2	3	4	5	n.a	n.a	X	X	10	11	12
			Group 3	Rows 15 to 26	1	n.a	n.a	4	5	n.a	n.a	X	X	n.a	n.a	12
			Group 4	Rows 1 to 14	1	n.a	n.a	4	n.a	n.a	n.a	n.a	X	n.a	n.a	12
Case 40	4	AVB 7, 8, 9, 10 Missing	Group 1	Rows 48 to 142	1	2	3	4	5	6	X	X	X	X	11	12
			Group 2	Rows 27 to 47	1	2	3	4	5	n.a	n.a	X	X	X	11	12
			Group 3	Rows 15 to 26	1	n.a	n.a	4	5	n.a	n.a	X	X	n.a	n.a	12
			Group 4	Rows 1 to 14	1	n.a	n.a	4	n.a	n.a	n.a	n.a	X	n.a	n.a	12
Case 41	4	AVB 8, 9, 10, 11 Missing	Group 1	Rows 48 to 142	1	2	3	4	5	6	7	X	X	X	X	12
			Group 2	Rows 27 to 47	1	2	3	4	5	n.a	n.a	X	X	X	X	12
			Group 3	Rows 15 to 26	1	n.a	n.a	4	5	n.a	n.a	X	X	n.a	n.a	12
			Group 4	Rows 1 to 14	1	n.a	n.a	4	n.a	n.a	n.a	n.a	X	n.a	n.a	12

Table 2-8. Possible AVB Support Cases with Adjacent Ineffective AVBs (Page 8 of 15)

Case 42	4	AVB 9, 10, 11, 12 Missing	Group 1	Rows 48 to 142	1	2	3	4	5	6	7	8	X	X	X	X
			Group 2	Rows 27 to 47	1	2	3	4	5	n.a	n.a	8	X	X	X	X
			Group 3	Rows 15 to 26	1	n.a	n.a	4	5	n.a	n.a	8	X	n.a	n.a	X
			Group 4	Rows 1 to 14	1	n.a	n.a	4	n.a	n.a	n.a	n.a	X	n.a	n.a	X
Case 43	5	AVB 1, 2, 3, 4, 5 Missing	Group 1	Rows 48 to 142	X	X	X	X	X	6	7	8	9	10	11	12
			Group 2	Rows 27 to 47	X	X	X	X	X	n.a	n.a	8	9	10	11	12
			Group 3	Rows 15 to 26	X	n.a	n.a	X	X	n.a	n.a	8	9	n.a	n.a	12
			Group 4	Rows 1 to 14	X	n.a	n.a	X	n.a	n.a	n.a	n.a	9	n.a	n.a	12
Case 44	5	AVB 2, 3, 4, 5, 6 Missing	Group 1	Rows 48 to 142	1	X	X	X	X	X	7	8	9	10	11	12
			Group 2	Rows 27 to 47	1	X	X	X	X	n.a	n.a	8	9	10	11	12
			Group 3	Rows 15 to 26	1	n.a	n.a	X	X	n.a	n.a	8	9	n.a	n.a	12
			Group 4	Rows 1 to 14	1	n.a	n.a	X	n.a	n.a	n.a	n.a	9	n.a	n.a	12
Case 45	5	AVB 3, 4, 5, 6, 7 Missing	Group 1	Rows 48 to 142	1	2	X	X	X	X	X	8	9	10	11	12
			Group 2	Rows 27 to 47	1	2	X	X	X	n.a	n.a	8	9	10	11	12
			Group 3	Rows 15 to 26	1	n.a	n.a	X	X	n.a	n.a	8	9	n.a	n.a	12
			Group 4	Rows 1 to 14	1	n.a	n.a	X	n.a	n.a	n.a	n.a	9	n.a	n.a	12
Case 46	5	AVB 4, 5, 6, 7, 8 Missing	Group 1	Rows 48 to 142	1	2	3	X	X	X	X	X	9	10	11	12
			Group 2	Rows 27 to 47	1	2	3	X	X	n.a	n.a	X	9	10	11	12
			Group 3	Rows 15 to 26	1	n.a	n.a	X	X	n.a	n.a	X	9	n.a	n.a	12
			Group 4	Rows 1 to 14	1	n.a	n.a	X	n.a	n.a	n.a	n.a	9	n.a	n.a	12
Case 47	5	AVB 5, 6, 7, 8, 9 Missing	Group 1	Rows 48 to 142	1	2	3	4	X	X	X	X	X	10	11	12
			Group 2	Rows 27 to 47	1	2	3	4	X	n.a	n.a	X	X	10	11	12
			Group 3	Rows 15 to 26	1	n.a	n.a	4	X	n.a	n.a	X	X	n.a	n.a	12
			Group 4	Rows 1 to 14	1	n.a	n.a	4	n.a	n.a	n.a	n.a	X	n.a	n.a	12

Table 2-8. Possible AVB Support Cases with Adjacent Ineffective AVBs (Page 9 of 15)

Case 48	5	AVB 6, 7, 8, 9, 10 Missing	Group 1	Rows 48 to 142	1	2	3	4	5	X	X	X	X	X	11	12
			Group 2	Rows 27 to 47	1	2	3	4	5	n.a	n.a.	X	X	X	11	12
			Group 3	Rows 15 to 26	1	n.a	n.a	4	5	n.a	n.a.	X	X	n.a	n.a.	12
			Group 4	Rows 1 to 14	1	n.a	n.a	4	n.a	n.a	n.a.	n.a	X	n.a	n.a.	12
Case 49	5	AVB 7, 8, 9, 10, 11 Missing	Group 1	Rows 48 to 142	1	2	3	4	5	6	X	X	X	X	X	12
			Group 2	Rows 27 to 47	1	2	3	4	5	n.a	n.a.	X	X	X	X	12
			Group 3	Rows 15 to 26	1	n.a	n.a	4	5	n.a	n.a.	X	X	n.a	n.a.	12
			Group 4	Rows 1 to 14	1	n.a	n.a	4	n.a	n.a	n.a.	n.a	X	n.a	n.a.	12
Case 50	5	AVB 8, 9, 10, 11, 12 Missing	Group 1	Rows 48 to 142	1	2	3	4	5	6	7	X	X	X	X	X
			Group 2	Rows 27 to 47	1	2	3	4	5	n.a	n.a.	X	X	X	X	X
			Group 3	Rows 15 to 26	1	n.a	n.a	4	5	n.a	n.a.	X	X	n.a	n.a.	X
			Group 4	Rows 1 to 14	1	n.a	n.a	4	n.a	n.a	n.a.	n.a	X	n.a	n.a.	X
Case 51	6	AVB 1, 2, 3, 4, 5, 6 Missing	Group 1	Rows 48 to 142	X	X	X	X	X	X	7	8	9	10	11	12
			Group 2	Rows 27 to 47	X	X	X	X	X	n.a	n.a.	8	9	10	11	12
			Group 3	Rows 15 to 26	X	n.a	n.a	X	X	n.a	n.a.	8	9	n.a	n.a.	12
			Group 4	Rows 1 to 14	X	n.a	n.a	X	n.a	n.a	n.a.	n.a	9	n.a	n.a.	12
Case 52	6	AVB 2, 3, 4, 5, 6, 7 Missing	Group 1	Rows 48 to 142	1	X	X	X	X	X	X	8	9	10	11	12
			Group 2	Rows 27 to 47	1	X	X	X	X	n.a	n.a.	8	9	10	11	12
			Group 3	Rows 15 to 26	1	n.a	n.a	X	X	n.a	n.a.	8	9	n.a	n.a.	12
			Group 4	Rows 1 to 14	1	n.a	n.a	X	n.a	n.a	n.a.	n.a	9	n.a	n.a.	12

Table 2-8. Possible AVB Support Cases with Adjacent Ineffective AVBs (Page 10 of 15)

Case 53	6	AVB 3, 4, 5, 6, 7, 8 Missing	Group 1	Rows 48 to 142	1	2	X	X	X	X	X	X	9	10	11	12
			Group 2	Rows 27 to 47	1	2	X	X	X	n.a.	n.a.	X	9	10	11	12
			Group 3	Rows 15 to 26	1	n.a.	n.a.	X	X	n.a.	n.a.	X	9	n.a.	n.a.	12
			Group 4	Rows 1 to 14	1	n.a.	n.a.	X	n.a.	n.a.	n.a.	n.a.	9	n.a.	n.a.	12
Case 54	6	AVB 4, 5, 6, 7, 8, 9 Missing	Group 1	Rows 48 to 142	1	2	3	X	X	X	X	X	X	10	11	12
			Group 2	Rows 27 to 47	1	2	3	X	X	n.a.	n.a.	X	X	10	11	12
			Group 3	Rows 15 to 26	1	n.a.	n.a.	X	X	n.a.	n.a.	X	X	n.a.	n.a.	12
			Group 4	Rows 1 to 14	1	n.a.	n.a.	X	n.a.	n.a.	n.a.	n.a.	X	n.a.	n.a.	12
Case 55	6	AVB 5, 6, 7, 8, 9, 10 Missing	Group 1	Rows 48 to 142	1	2	3	4	X	X	X	X	X	X	11	12
			Group 2	Rows 27 to 47	1	2	3	4	X	n.a.	n.a.	X	X	X	11	12
			Group 3	Rows 15 to 26	1	n.a.	n.a.	4	X	n.a.	n.a.	X	X	n.a.	n.a.	12
			Group 4	Rows 1 to 14	1	n.a.	n.a.	4	n.a.	n.a.	n.a.	n.a.	X	n.a.	n.a.	12
Case 56	6	AVB 6, 7, 8, 9, 10, 11 Missing	Group 1	Rows 48 to 142	1	2	3	4	5	X	X	X	X	X	X	12
			Group 2	Rows 27 to 47	1	2	3	4	5	n.a.	n.a.	X	X	X	X	12
			Group 3	Rows 15 to 26	1	n.a.	n.a.	4	5	n.a.	n.a.	X	X	n.a.	n.a.	12
			Group 4	Rows 1 to 14	1	n.a.	n.a.	4	n.a.	n.a.	n.a.	n.a.	X	n.a.	n.a.	12
Case 57	6	AVB 7, 8, 9, 10, 11, 12 Missing	Group 1	Rows 48 to 142	1	2	3	4	5	6	X	X	X	X	X	X
			Group 2	Rows 27 to 47	1	2	3	4	5	n.a.	n.a.	X	X	X	X	X
			Group 3	Rows 15 to 26	1	n.a.	n.a.	4	5	n.a.	n.a.	X	X	n.a.	n.a.	X
			Group 4	Rows 1 to 14	1	n.a.	n.a.	4	n.a.	n.a.	n.a.	n.a.	X	n.a.	n.a.	X

Table 2-8. Possible AVB Support Cases with Adjacent Ineffective AVBs (Page 11 of 15)

Case 58	7	AVB 1, 2, 3, 4, 5, 6, 7 Missing	Group 1	Rows 48 to 142	X	X	X	X	X	X	X	8	9	10	11	12
			Group 2	Rows 27 to 47	X	X	X	X	X	n.a	n.a	8	9	10	11	12
			Group 3	Rows 15 to 26	X	n.a	n.a	X	X	n.a	n.a	8	9	n.a	n.a	12
			Group 4	Rows 1 to 14	X	n.a	n.a	X	n.a	n.a	n.a	n.a	9	n.a	n.a	12
Case 59	7	AVB 2, 3, 4, 5, 6, 7, 8 Missing	Group 1	Rows 48 to 142	1	X	X	X	X	X	X	X	9	10	11	12
			Group 2	Rows 27 to 47	1	X	X	X	X	n.a	n.a	X	9	10	11	12
			Group 3	Rows 15 to 26	1	n.a	n.a	X	X	n.a	n.a	X	9	n.a	n.a	12
			Group 4	Rows 1 to 14	1	n.a	n.a	X	n.a	n.a	n.a	n.a	9	n.a	n.a	12
Case 60	7	AVB 3, 4, 5, 6, 7, 8, 9 Missing	Group 1	Rows 48 to 142	1	2	X	X	X	X	X	X	X	10	11	12
			Group 2	Rows 27 to 47	1	2	X	X	X	n.a	n.a	X	X	10	11	12
			Group 3	Rows 15 to 26	1	n.a	n.a	X	X	n.a	n.a	X	X	n.a	n.a	12
			Group 4	Rows 1 to 14	1	n.a	n.a	X	n.a	n.a	n.a	n.a	X	n.a	n.a	12
Case 61	7	AVB 4, 5, 6, 7, 8, 9, 10 Missing	Group 1	Rows 48 to 142	1	2	3	X	X	X	X	X	X	X	11	12
			Group 2	Rows 27 to 47	1	2	3	X	X	n.a	n.a	X	X	X	11	12
			Group 3	Rows 15 to 26	1	n.a	n.a	X	X	n.a	n.a	X	X	n.a	n.a	12
			Group 4	Rows 1 to 14	1	n.a	n.a	X	n.a	n.a	n.a	n.a	X	n.a	n.a	12
Case 62	7	AVB 5, 6, 7, 8, 9, 10, 11 Missing	Group 1	Rows 48 to 142	1	2	3	4	X	X	X	X	X	X	X	12
			Group 2	Rows 27 to 47	1	2	3	4	X	n.a	n.a	X	X	X	X	12
			Group 3	Rows 15 to 26	1	n.a	n.a	4	X	n.a	n.a	X	X	n.a	n.a	12
			Group 4	Rows 1 to 14	1	n.a	n.a	4	n.a	n.a	n.a	n.a	X	n.a	n.a	12

Table 2-8. Possible AVB Support Cases with Adjacent Ineffective AVBs (Page 12 of 15)

Case 63	7	AVB 6, 7, 8, 9, 10, 11, 12 Missing	Group 1	Rows 48 to 142	1	2	3	4	5	X	X	X	X	X	X	X
			Group 2	Rows 27 to 47	1	2	3	4	5	n.a	n.a.	X	X	X	X	X
			Group 3	Rows 15 to 26	1	n.a	n.a	4	5	n.a	n.a.	X	X	n.a	n.a.	X
			Group 4	Rows 1 to 14	1	n.a	n.a	4	n.a	n.a	n.a.	n.a	X	n.a	n.a.	X
Case 64	8	AVB 1, 2, 3, 4, 5, 6, 7, 8 Missing	Group 1	Rows 48 to 142	X	X	X	X	X	X	X	X	9	10	11	12
			Group 2	Rows 27 to 47	X	X	X	X	X	n.a	n.a.	X	9	10	11	12
			Group 3	Rows 15 to 26	X	n.a	n.a	X	X	n.a	n.a.	X	9	n.a	n.a.	12
			Group 4	Rows 1 to 14	X	n.a	n.a	X	n.a	n.a	n.a.	n.a	9	n.a	n.a.	12
Case 65	8	AVB 2, 3, 4, 5, 6, 7, 8, 9 Missing	Group 1	Rows 48 to 142	1	X	X	X	X	X	X	X	X	10	11	12
			Group 2	Rows 27 to 47	1	X	X	X	X	n.a	n.a.	X	X	10	11	12
			Group 3	Rows 15 to 26	1	n.a	n.a	X	X	n.a	n.a.	X	X	n.a	n.a.	12
			Group 4	Rows 1 to 14	1	n.a	n.a	X	n.a	n.a	n.a.	n.a	X	n.a	n.a.	12
Case 66	8	AVB 3, 4, 5, 6, 7, 8, 9, 10 Missing	Group 1	Rows 48 to 142	1	2	X	X	X	X	X	X	X	X	11	12
			Group 2	Rows 27 to 47	1	2	X	X	X	n.a	n.a.	X	X	X	11	12
			Group 3	Rows 15 to 26	1	n.a	n.a	X	X	n.a	n.a.	X	X	n.a	n.a.	12
			Group 4	Rows 1 to 14	1	n.a	n.a	X	n.a	n.a	n.a.	n.a	X	n.a	n.a.	12
Case 67	8	AVB 4, 5, 6, 7, 8, 9, 10, 11 Missing	Group 1	Rows 48 to 142	1	2	3	X	X	X	X	X	X	X	X	12
			Group 2	Rows 27 to 47	1	2	3	X	X	n.a	n.a.	X	X	X	X	12
			Group 3	Rows 15 to 26	1	n.a	n.a	X	X	n.a	n.a.	X	X	n.a	n.a.	12
			Group 4	Rows 1 to 14	1	n.a	n.a	X	n.a	n.a	n.a.	n.a	X	n.a	n.a.	12

Table 2-8. Possible AVB Support Cases with Adjacent Ineffective AVBs (Page 13 of 15)

Case 68	8	AVB 5, 6, 7, 8, 9, 10, 11, 12 Missing	Group 1	Rows 48 to 142	1	2	3	4	X	X	X	X	X	X	X	X	X
			Group 2	Rows 27 to 47	1	2	3	4	X	n.a	n.a.	X	X	X	X	X	X
			Group 3	Rows 15 to 26	1	n.a	n.a	4	X	n.a	n.a.	X	X	n.a	n.a.	X	X
			Group 4	Rows 1 to 14	1	n.a	n.a	4	n.a	n.a	n.a.	n.a	X	n.a	n.a.	X	X
Case 69	9	AVB 1, 2, 3, 4, 5, 6, 7, 8, 9 Missing	Group 1	Rows 48 to 142	X	X	X	X	X	X	X	X	X	X	10	11	12
			Group 2	Rows 27 to 47	X	X	X	X	X	n.a	n.a.	X	X	X	10	11	12
			Group 3	Rows 15 to 26	X	n.a	n.a	X	X	n.a	n.a.	X	X	n.a	n.a.	X	X
			Group 4	Rows 1 to 14	X	n.a	n.a	X	n.a	n.a	n.a.	n.a	X	n.a	n.a.	X	X
Case 70	9	AVB 2, 3, 4, 5, 6, 7, 8, 9, 10 Missing	Group 1	Rows 48 to 142	1	X	X	X	X	X	X	X	X	X	X	X	X
			Group 2	Rows 27 to 47	1	X	X	X	X	n.a	n.a.	X	X	X	11	12	X
			Group 3	Rows 15 to 26	1	n.a	n.a	X	X	n.a	n.a.	X	X	n.a	n.a.	X	X
			Group 4	Rows 1 to 14	1	n.a	n.a	X	n.a	n.a	n.a.	n.a	X	n.a	n.a.	X	X
Case 71	9	AVB 3, 4, 5, 6, 7, 8, 9, 10, 11 Missing	Group 1	Rows 48 to 142	1	2	X	X	X	X	X	X	X	X	X	X	X
			Group 2	Rows 27 to 47	1	2	X	X	X	n.a	n.a.	X	X	X	X	X	X
			Group 3	Rows 15 to 26	1	n.a	n.a	X	X	n.a	n.a.	X	X	n.a	n.a.	X	X
			Group 4	Rows 1 to 14	1	n.a	n.a	X	n.a	n.a	n.a.	n.a	X	n.a	n.a.	X	X
Case 72	9	AVB 4, 5, 6, 7, 8, 9, 10, 11, 12 Missing	Group 1	Rows 48 to 142	1	2	3	X	X	X	X	X	X	X	X	X	X
			Group 2	Rows 27 to 47	1	2	3	X	X	n.a	n.a.	X	X	X	X	X	X
			Group 3	Rows 15 to 26	1	n.a	n.a	X	X	n.a	n.a.	X	X	n.a	n.a.	X	X
			Group 4	Rows 1 to 14	1	n.a	n.a	X	n.a	n.a	n.a.	n.a	X	n.a	n.a.	X	X

Table 2-8. Possible AVB Support Cases with Adjacent Ineffective AVBs (Page 14 of 15)

Case 73	10	AVB 1, 2, 3, 4, 5, 6, 7, 8, 9, 10 Missing	Group 1	Rows 48 to 142	X	X	X	X	X	X	X	X	X	X	11	12
			Group 2	Rows 27 to 47	X	X	X	X	X	n.a	n.a	X	X	X	11	12
			Group 3	Rows 15 to 26	X	n.a	n.a	X	X	n.a	n.a	X	X	n.a	n.a	12
			Group 4	Rows 1 to 14	X	n.a	n.a	X	n.a	n.a	n.a	n.a	X	n.a	n.a	12
Case 74	10	AVB 2, 3, 4, 5, 6, 7, 8, 9, 10, 11 Missing	Group 1	Rows 48 to 142	1	X	X	X	X	X	X	X	X	X	X	12
			Group 2	Rows 27 to 47	1	X	X	X	X	n.a	n.a	X	X	X	X	12
			Group 3	Rows 15 to 26	1	n.a	n.a	X	X	n.a	n.a	X	X	n.a	n.a	12
			Group 4	Rows 1 to 14	1	n.a	n.a	X	n.a	n.a	n.a	n.a	X	n.a	n.a	12
Case 75	10	AVB 3, 4, 5, 6, 7, 8, 9, 10, 11, 12 Missing	Group 1	Rows 48 to 142	1	2	X	X	X	X	X	X	X	X	X	X
			Group 2	Rows 27 to 47	1	2	X	X	X	n.a	n.a	X	X	X	X	X
			Group 3	Rows 15 to 26	1	n.a	n.a	X	X	n.a	n.a	X	X	n.a	n.a	X
			Group 4	Rows 1 to 14	1	n.a	n.a	X	n.a	n.a	n.a	n.a	X	n.a	n.a	X
Case 76	11	AVB 1, 2, 3, 4, 5, 6, 7, 8, 9, 10, 11 Missing	Group 1	Rows 48 to 142	X	X	X	X	X	X	X	X	X	X	X	12
			Group 2	Rows 27 to 47	X	X	X	X	X	n.a	n.a	X	X	X	X	12
			Group 3	Rows 15 to 26	X	n.a	n.a	X	X	n.a	n.a	X	X	n.a	n.a	12
			Group 4	Rows 1 to 14	X	n.a	n.a	X	n.a	n.a	n.a	n.a	X	n.a	n.a	12
Case 77	11	AVB 2, 3, 4, 5, 6, 7, 8, 9, 10, 11, 12 Missing	Group 1	Rows 48 to 142	1	X	X	X	X	X	X	X	X	X	X	X
			Group 2	Rows 27 to 47	1	X	X	X	X	n.a	n.a	X	X	X	X	X
			Group 3	Rows 15 to 26	1	n.a	n.a	X	X	n.a	n.a	X	X	n.a	n.a	X
			Group 4	Rows 1 to 14	1	n.a	n.a	X	n.a	n.a	n.a	n.a	X	n.a	n.a	X

Table 2-8. Possible AVB Support Cases with Adjacent Ineffective AVBs (Page 15 of 15)

Case 78	12	AVB 1 ALL - Missing	Group 1	Rows 48 to 142	X	X	X	X	X	X	X	X	X	X	X	X
			Group 2	Rows 27 to 47	X	X	X	X	X	n.a	n.a.	X	X	X	X	X
			Group 3	Rows 15 to 26	X	n.a	n.a	X	X	n.a	n.a.	X	X	n.a	n.a.	X
			Group 4	Rows 1 to 14	X	n.a	n.a	X	n.a	n.a	n.a.	n.a	X	n.a	n.a.	X

Table 2-9. Wear Projection Results for Limiting Active Tubes and Plugged Tubes

Tube	SG No	Tube Status	Max Wear Depth, %		Baseline Calculations @ 6 Months in Cycle 17				Additional Missing AVB Check - @ 6 Months					
			ECT Reported	Expected Value	FASTVIB Case	No Seq AVBs	Far Depth @ Power Cycle 1	80%	70%	FASTVIB Case	No Seq AVBs	Depth @ Power Cycle 1	80%	70%
R97C87	88	Active	25	27.4	38	4	29.9	27.4	27.4	46	5	29.6	27.8	27.4
R119C89	89	Active	28	30.3	46	5	32.8	31.3	31.2	54	6	32.9	31.8	31.7
R121C91	89	Active	28	30.3	37	4	33.3	31.2	31	45	5	32.6	31.0	30.9
			x	30.3	x	x	x	x	x	46	5	33.2	31.6	31.3
			x	30.3	x	x	x	x	x	53	6	33.1	31.5	31.4
R131C91	89	Active	21	23.5	17	2	25.4	23.5	23.5	38	4	25.9	24.2	23.8
R129C93	89	Active	22	24.5	29	3	-	-	-	47	5	26.8	25.9	25.8
R126C90	89	Active	21	23.5	45	5	24.7	24.1	24.0	60	7	25.6	24.7	24.6
R112C88	88	Plugged	35	37.2	47	5	38.7	38.1	37.9	x	x	x	x	x
R133C91	88	Plugged	35	37.2	38	4	40.7	38.4	38.1	45	5	41.8	39.7	39.4
R114C90	88	Plugged	22	24.5	48	5	26.7	25.7	25.4	60	7	26.6	25.7	25.6
R111C91	88	Plugged	26	28.4	38	4	29.9	28.4	28.4	x	x	x	x	x
R116C86	88	Plugged	29	31.3	46	5	34.4	32.7	32.4	61	7	34.0	33.1	32.9
R117C93	88	Plugged	27	29.4	47	5	31.9	30.7	30.4	x	x	x	x	x
R115C85	88	Plugged	27	29.4	48	5	32.0	30.8	30.6	61	5	31.9	31.2	31.0
R114C86	88	Plugged	21	23.5	53	6	25.7	24.6	24.5	66	8	25.5	24.7	24.6
R112C88	88	Plugged	35	37.2	55	6	39.7	38.7	38.5	x	x	x	x	x
R128C94	88	Plugged	32	34.3	60	7	37.3	36.1	35.7	x	x	x	x	x
R120C92	88	Plugged	32	34.3	66	8	37.4	36.4	36.2	x	x	x	x	x
R121C83	89	Plugged	24	26.4	16	2	29.0	26.4	26.4	46	4	29.3	27.6	27.4
R117C89	89	Plugged	26	28.4	46	5	30.6	29.4	29.2	x	x	30.6	x	x
R108C90	89	Plugged	27	29.4	53	6	32.2	30.9	30.7	x	x	32.1	x	x
R117C81	89	Plugged	29	31.3	55	6	33.4	32.8	32.7	x	x	33.4	x	x
R134C90	89	Plugged	26	28.4	56	6	31.6	30.8	30.6	67	8	31.6	30.7	30.6
R114C88	89	Plugged	24	26.4	56	6	30.4	29.3	28.9	67	8	29.2	28.5	28.3
R117C85	89	Plugged	24	26.4	62	7	28.9	28.2	28.1	74	10	29.4	28.3	28
R122C82	89	Plugged	27	29.4	66	8	32.3	31.2	31.0	x	x	32.3	x	x
R112C84	89	Plugged	27	29.4	67	8	32.1	31.4	31.2	x	x	32.1	x	x
R111C81	89	Plugged	18	20.5	38	4	22.0	20.6	20.6	55	6	22.5	21.9	21.7
			x	20.5	x	x	x	x	x	67 (1st)	8	22.4	21.8	21.7
			x	16.6	x	x	x	x	x	67 (2nd)	8	18.5	17.2	16.8

Table 2-10. In-Plane Stability Ratios for Limiting Tubes

Tube	SG	Case	No Missing AVBs	IP SR 100% power	IP SR 70% power	
R133C91	2e88	45	5	0.763	0.40	Note1
R112C88	2e88	55	6	0.590	0.36	
R120C92	2e88	66	8	1.071	0.71	
R97C85	2e88	66	8	0.827	0.56	
R99C93	2e88	67	8	0.718	0.48	
R117C81	2e89	55	6	0.583	0.38	
R122C82	2e89	66	8	1.083	0.72	
R106C84,	2e89	66	8	0.929	0.62	
R105C83	2e89	66	8	0.929	0.62	
R104C86	2e89	66	8	0.929	0.60	
R98C86	2e89	66	8	0.865	0.56	
R123C91	2e89	66	8	1.096	0.72	
R98C88	2e89	66	8	0.853	0.55	
R112C84	2e89	67	8	0.821	0.58	
R100C84	2e89	67	8	0.718	0.49	

Note 1: AVB5 assumed to be ineffective even though no wear was reported at this location

Table 2-12. Benchmarking Results for Interior Tubes (Page 1 of 2)

TubeID		Selected Tubes with > 7 AVB Indications (Bobbin)													Cases					SR for $\beta=5.0$					SR for $\beta=7.8$						
SG	Row	Col	B01	B02	B03	F _{5h}	B04	B05	B06	B07	B08	B09	F _{5c}	B10	B11	B12	1	2	3	4	5	OP1	OP2	OP3	OP4	OP5	IP1	IP2	IP3	IP4	IP5
106076	SG88	106	76	13	14	11	40	21	5	15	13	16	46	17	10	15	78						7.56				1.68				
103077	SG88	103	77	13	18	23	37	14	6	8	12	7	19	8	7	22	78						7.30				1.60				
107077	SG88	107	77	15	21	28	80	20	X	8	9	14	16	48	16	13	78						7.80				1.70				
109077	SG88	109	77	21	19	25	39	14	X	6	7	11	13	48	11	8	78						8.10				1.74				
113077	SG88	113	77		9	14	11	21	6	9	6	5	31	15	12		52	78					8.50				0.75	1.85			
115077	SG88	115	77	25	22	9	10	11	14		5	12	20	16	13		43	76	78			2.70	7.25	8.70		0.78	1.62	1.90			
117077	SG88	117	77		17	7	58	12	8	22	27	12	7	12	13		52	74	78			2.70	5.70	8.90		0.80	1.41	1.93			
102078	SG88	102	78	10	21	18	99	13	15	16	17	7	14	24	14	14	78						7.30				1.60				
104078	SG88	104	78	25	13	24	99	23	14	10	14	13	23	18	25	20	78						7.60				1.65				
106078	SG88	106	78	19	13	15	99	X	6	9	12	16	46	18	23	24	78						8.00				1.69				
108078	SG88	108	78	22	14	17	66	10	6	17	9	11	13	49	15	27	78						7.80				1.71				
118078	SG88	118	78	8	24	17	18	12	11	10	10	15	12	22	5	6	78						9.00				1.97				
103079	SG88	103	79	19	17	18	39	20	11	9	6	13	23	45	14	11	78						7.50				1.60				
105079	SG88	105	79	13	9	15	50	20	10	9	13	11	17	38	13	23	78						7.72				1.67				
107079	SG88	107	79	11	11	13	57	14	7	13	8	13	20	43	17	19	78						8.00				1.71				
109079	SG88	109	79	10	18	18	39	16	17	10	12	16	10	41	13	25	78						8.10				1.75				
115079	SG88	115	79	10	18	15	24	10	8	9	11	7	14	35	21	14	78						8.80				1.90				
117079	SG88	117	79	17	11	18	50	10	16	8	11	11	10	38	13	10	78						9.00				1.98				
121079	SG88	121	79		21	22	17	27	13	13	13	13	13	12	7		71	77					4.40	7.30		1.22	1.68				
96080	SG88	96	80	7	16	10	15	15	31	9	9	10	13	32	13	8	78						6.75				1.50				
98080	SG88	98	80	11	16	18	72	26	16	X	8	7	8	31	12	17	78						7.00				1.54				
100080	SG88	100	80	19	22	18	81	11	18	7	10	12	9	19	15	16	78						7.24				1.56				
102080	SG88	102	80	20	16	14	57	19	7	X	6	9	10	14	11	16	78						7.40				1.60				
104080	SG88	104	80	13	22	17	59	23	7	12	5	9	14	30	17	18	78						7.50				1.64				
106080	SG88	106	80	31	24	11	11	12	7	5	8	9	19	57	15	23	78						7.75				1.68				
108080	SG88	108	80	17	22	18	22	22	13	14	6	9	16	51	17	14	78						8.00				1.72				
112080	SG88	112	80	10	18	20	33	21	9	X	X	8	9	53	9	12	78						8.50				1.82				
114080	SG88	114	80	6	15	17	35	22	5	13	11	7	8	47	6	9	78						8.60				1.88				
116080	SG88	116	80	22	24	12	31	17	7	9	8	7	12	6	7		76	78					7.58	8.98		1.66	1.93				
118080	SG88	118	80	7	25	19	19	19	18	20	10	13	10	10	11		76	78					7.70	9.15		1.69	1.98				

Table 2-12. Benchmarking Results for Interior Tubes (Page 2 of 2)

Selected Tubes with > 7 AVB Indications (Bobbin)		Cases					SR for β=5.0					SR for β=7.8																				
TubeID	SG	Row	Col	B01	B02	B03	FS _H	B04	B05	B06	B07	B08	B09	FS _C	B10	B11	B12	1	2	3	4	5	OP1	OP2	OP3	OP4	OP5	IP1	IP2	IP3	IP4	IP5
95081	SG88	95	81	22	9	18	68	16	12	8	11	11	10	41	12	5	19	78					6.63					1.49				
97081	SG88	97	81	18	16	18	67	16	16	7	12	9	5	45	6	8	21	78					6.75					1.51				
99081	SG88	99	81	17	12	15	72	20	13		6	5		44	12	10	18	43	63	78		2.25	1.95	7.10			0.69	0.42	1.55			
101081	SG88	101	81	20	15	18	78	25	15	7	6	5	8	27	6	10	18	78					7.30					1.59				
103081	SG88	103	81	13	15	20	50	16	6	12	6	7	11	41	9	10	17	78					7.50					1.63				
105081	SG88	105	81	22	19	23	60	13	X	9	7	11	10	38	X	13	17	78					7.69					1.66				
107081	SG88	107	81	10	19	22	59	15	6	8	5	8	9	35	11	9	14	78					8.00					1.70				
111081	SG88	111	81	7	12	17	56	14	5		6	8	6	13	10	10	23	57	43	78		1.86	2.56	8.32			0.39	0.75	1.78			
113081	SG88	113	81	9	10	18	58	23	10		9	9			9	11	5	43	57	78		2.65	1.90	8.50			0.77	0.42	1.85			
115081	SG88	115	81	X	26	21	14	15	22	18	X	8	8	6	25	10		76	78			7.40	8.80				1.60	1.90				
96082	SG88	96	82	9	8	13	43	22	22	7	6	9	8	30	9	11	18	78					6.75				1.41					
100082	SG88	100	82	13	7	14	42	14	10	6	10	8	10	39	11	7	21	78					7.20				1.57					
104082	SG88	104	82	15	10	11	59	18	15	6	12	8	13	48	16	11	20	78					7.50				1.64					
106082	SG88	106	82	20	8	15	52	13	17	14	16	10	8	51	9	15	19	78					7.75				1.70					
108082	SG88	108	82	13	12	13	46	12		7	8	15	14	22	16	20	19	63	78			2.20	8.00				0.47	1.75				
114082	SG88	114	82	12	12	12	18	15	7	19	27	8	6		9	X	X	77	78			6.60	8.50				1.60	1.85				
101083	SG88	101	83	9	8	15	31	15	13	10	6	10	9	54	9	17	23	78					7.30				1.60					
103083	SG88	103	83	12	12	16	42	16	9	X	X	10	X	46	8	21	25	78					7.50				1.64					
100084	SG88	100	84	17	17		38	7	25	X	8	11	8		7	6	13	72	78			3.31	7.17				0.80	1.56				
102084	SG88	102	84	15	23	11	41	X	18	12	10	10	11	36	12	10	17	51	50	78		2.70	1.25	7.40			0.79	0.29	1.60			
104084	SG88	104	84	11	21	17	32	17	11	11	5	11	12	66	19	8	18	78					7.70				1.65					
108084	SG88	108	84	10	20	22	37	9	X	16	13	7	9	10	11	7	17	78					8.10				1.74					
112084	SG88	112	84	11	8	14	6	6	5	6	9	6	23	14	10			70	73	76		4.30	6.00	7.20			1.20	1.40	1.84			
99085	SG88	99	85	13	21	12	37	14	8	6	9	12	10	44	11	6	15	78					7.10				1.53					
104086	SG88	104	86	14	20	9	50	6	9	12		11	9	44	8	9	15	51	50	78		2.80	1.30	7.70			0.80	0.29	1.63			

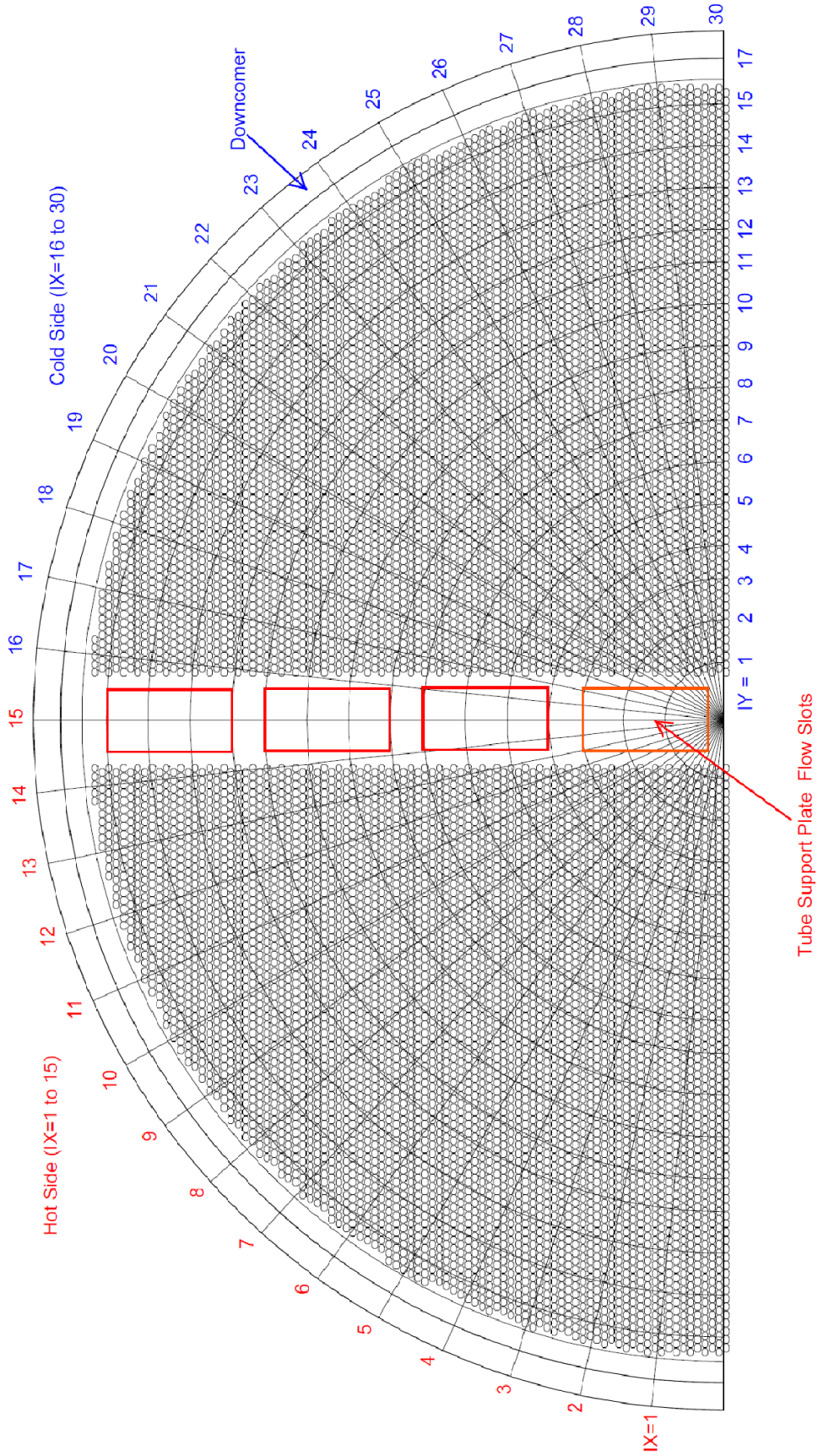


Figure 2-1. ATHOS Finite Difference Grid in the Horizontal (R-θ) Plane

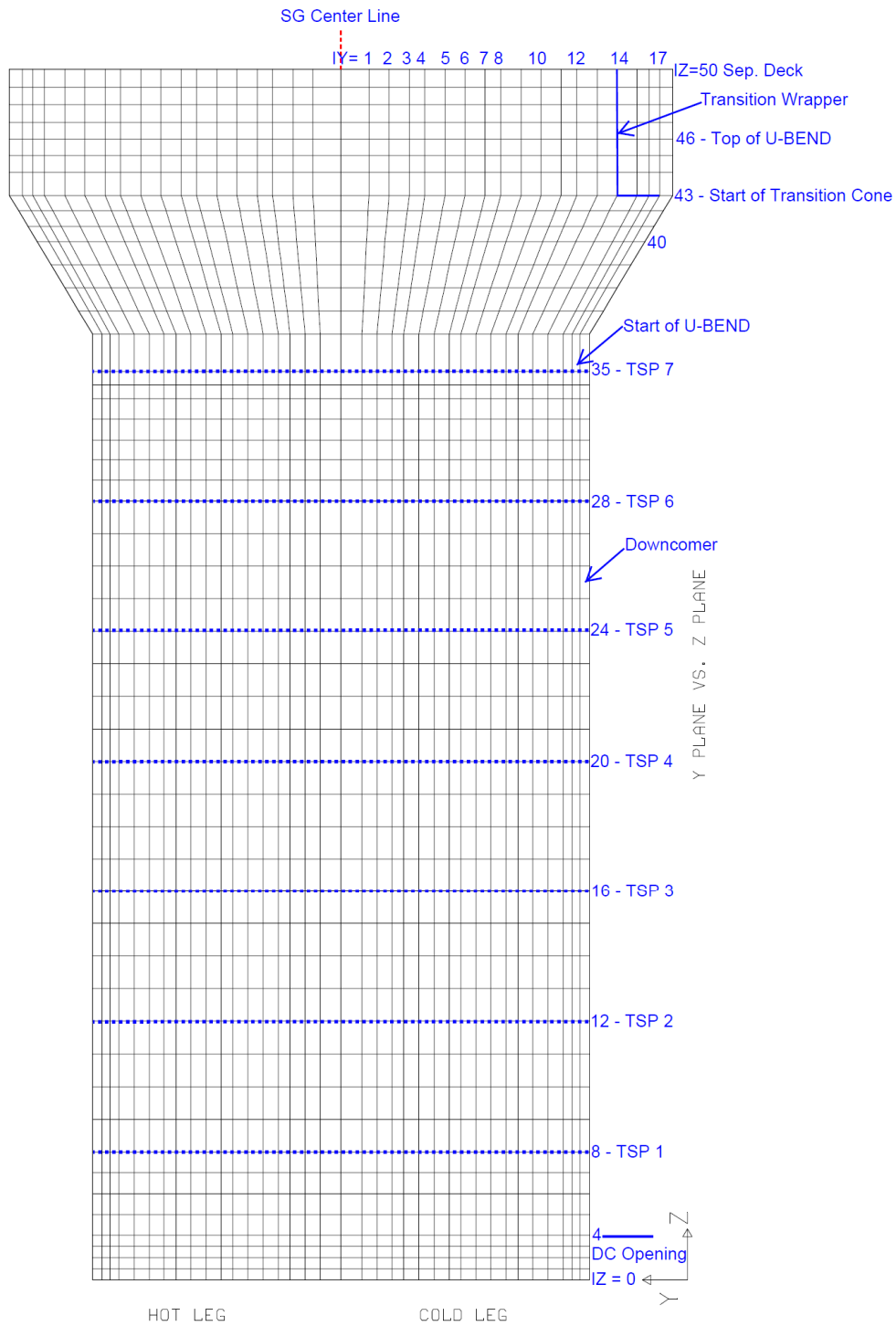


Figure 2-2. ATHOS Finite Difference Grid in the Vertical (R-θ) Plane

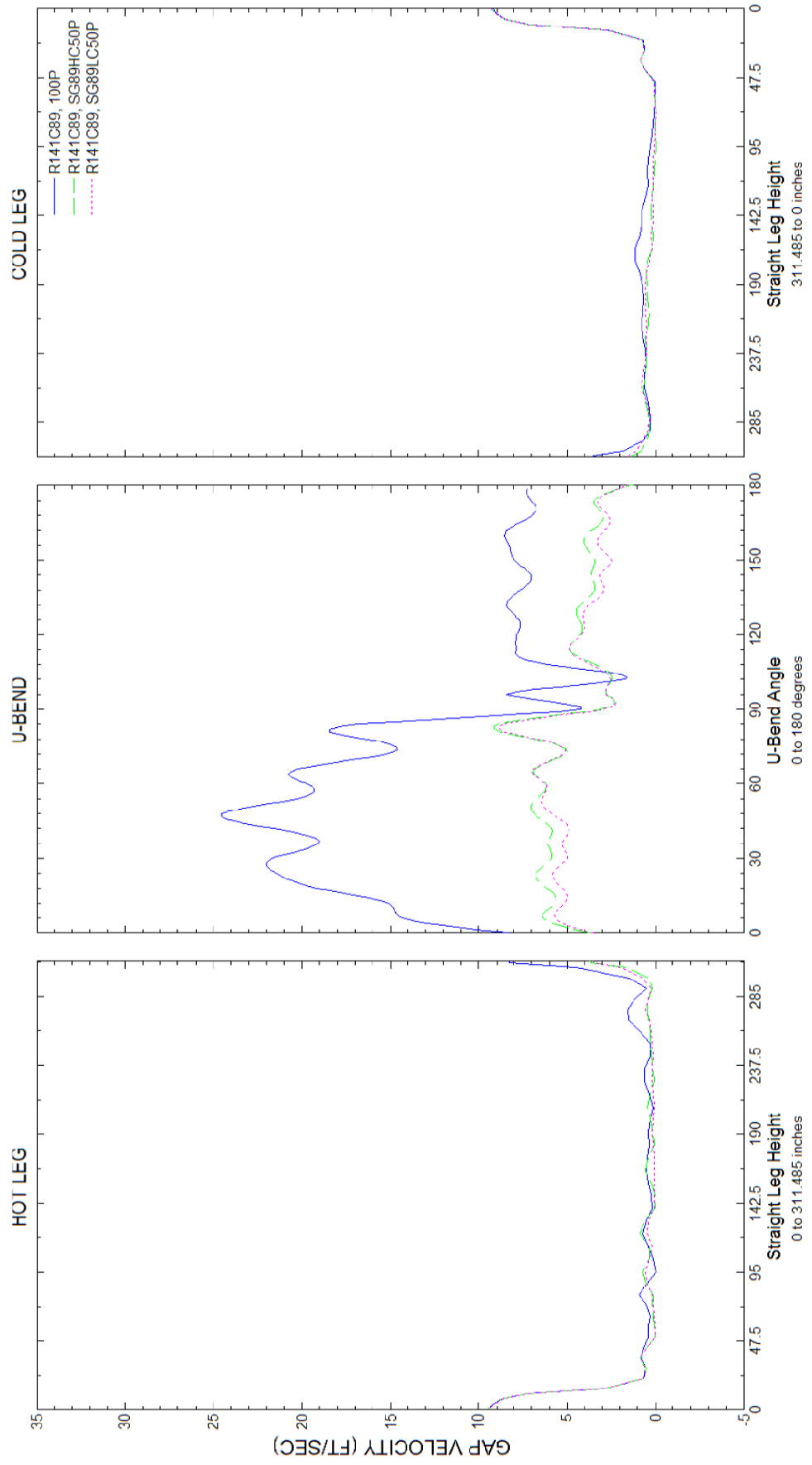


Figure 2-3. SG 2E089 Tube Row 141/Col. 89: Comparison of Gap Velocities at 50% Power

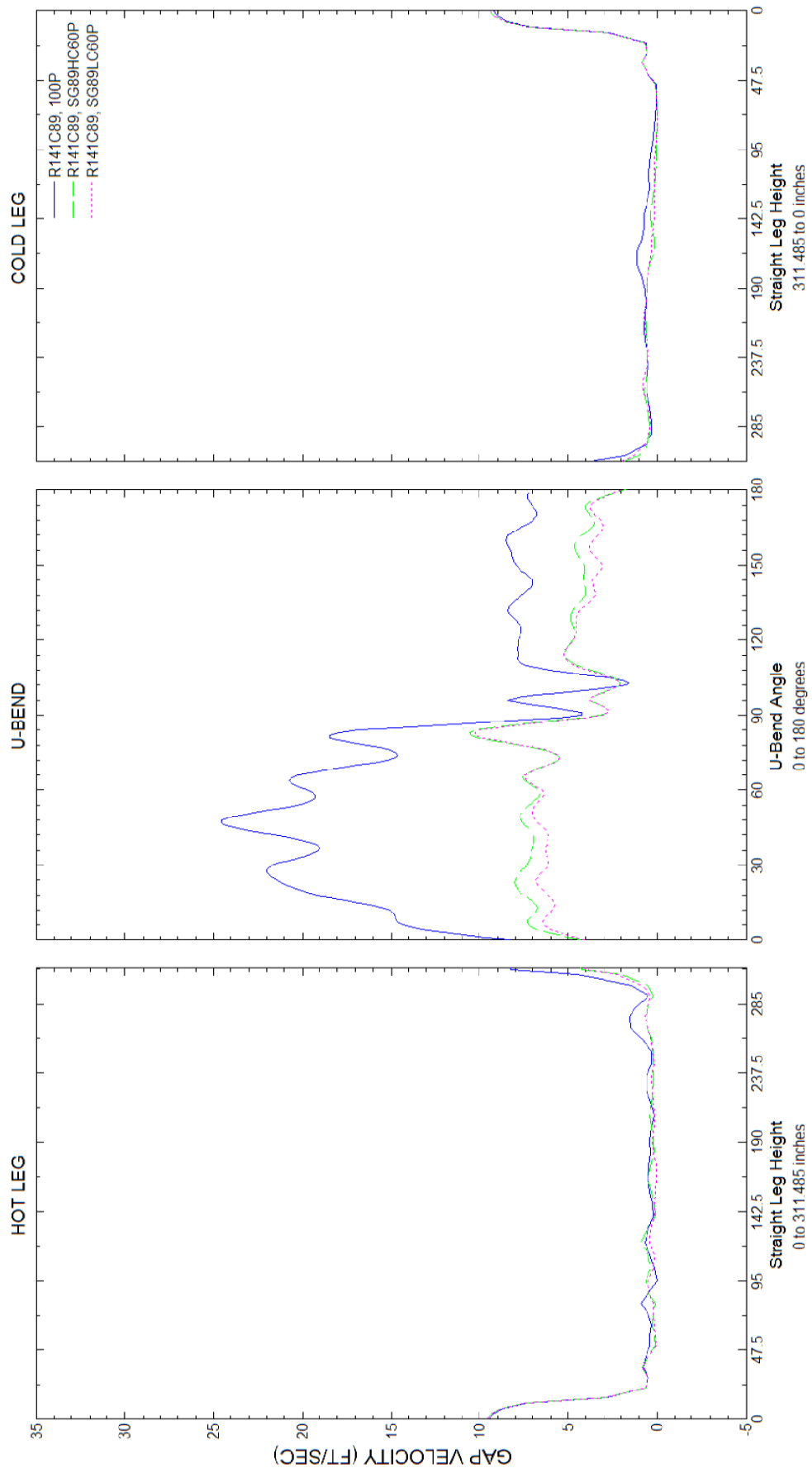


Figure 2-4. SG 2E089 Tube Row 141/Col. 89: Comparison of Gap Velocities at 60% Power

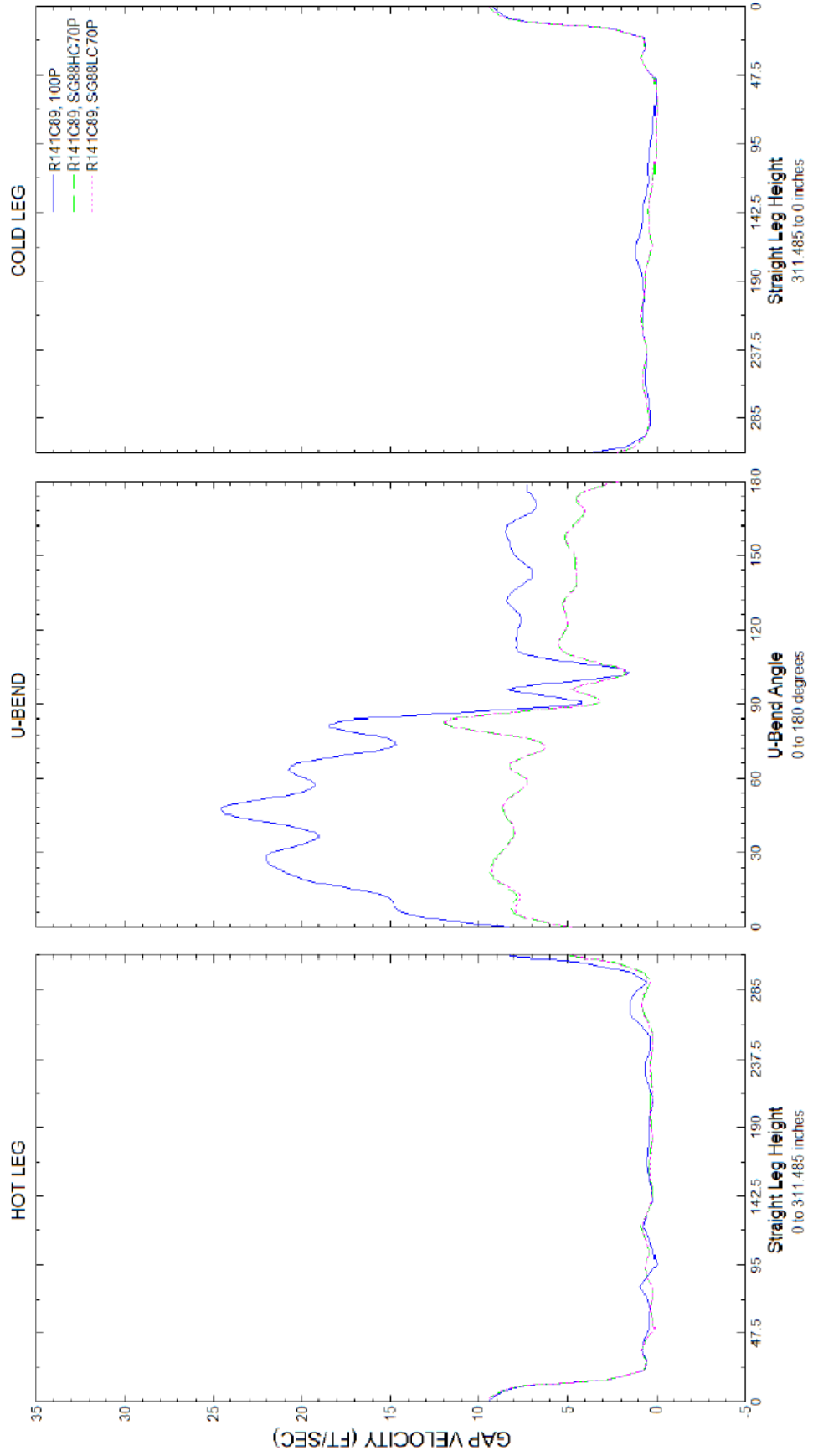


Figure 2-5. SG 2E088 Tube Row 141/Col. 89: Comparison of Gap Velocities at 70% Power

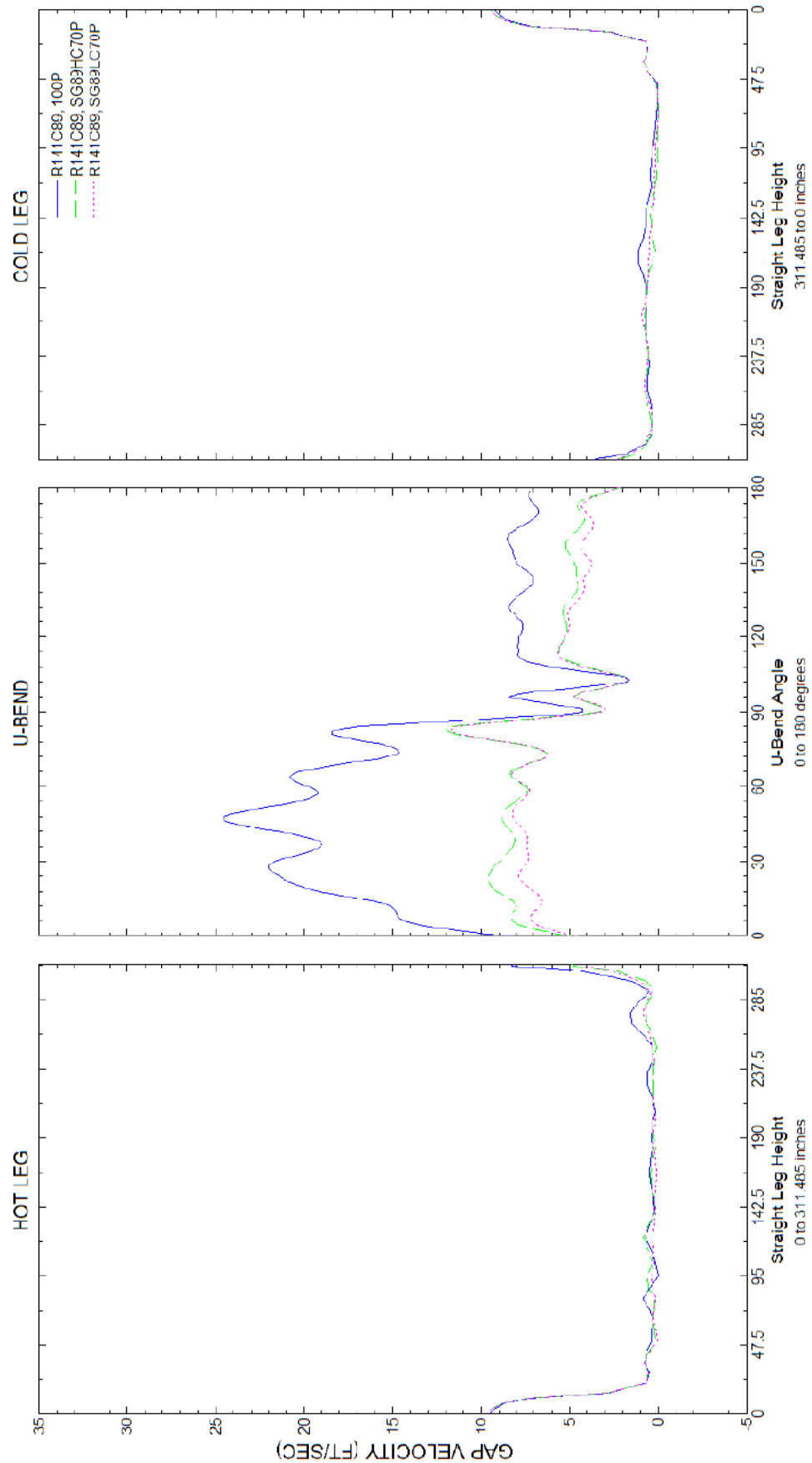


Figure 2-6. SG 2E089 Tube Row 141/Col. 89: Comparison of Gap Velocities at 70% Power

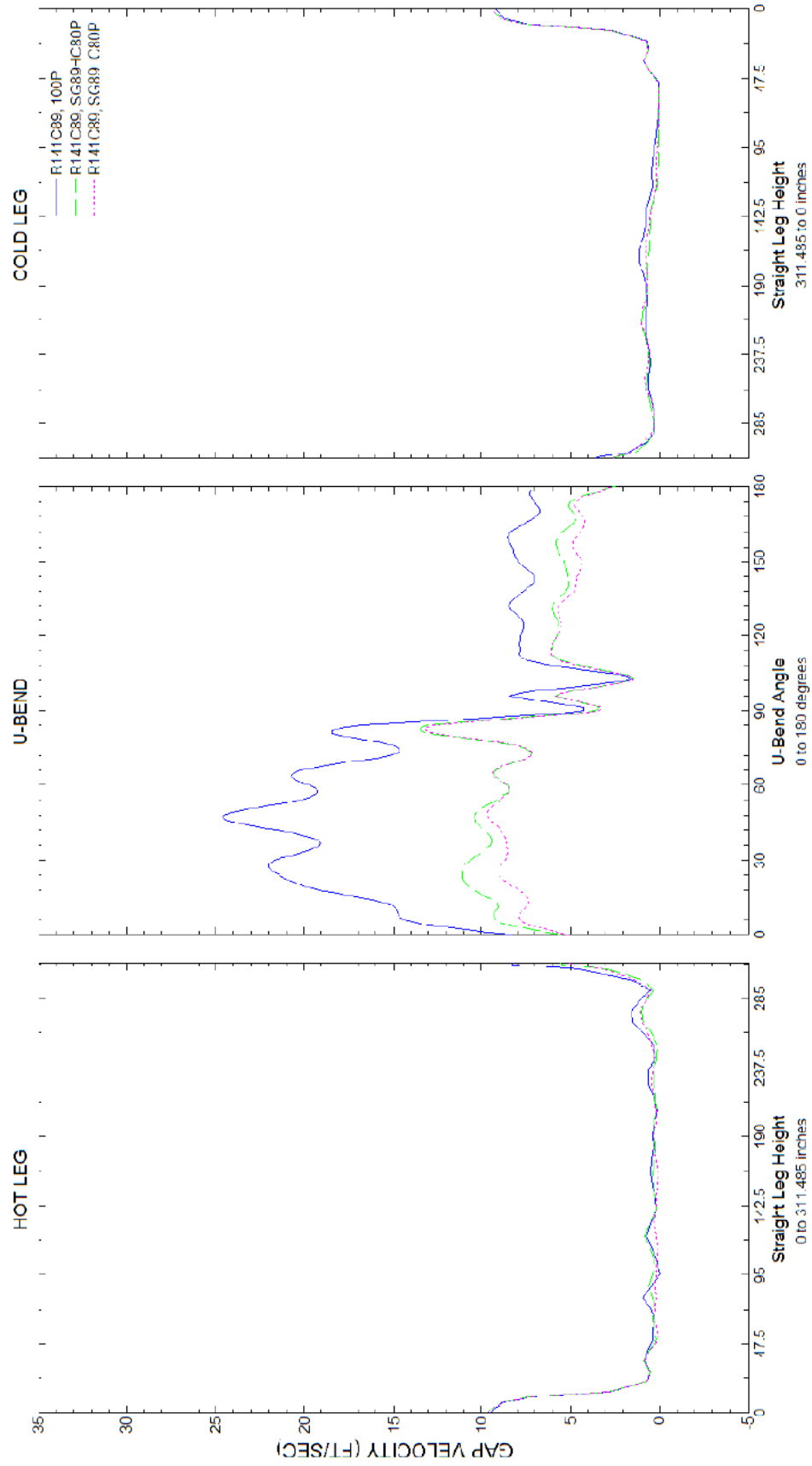


Figure 2-7. SG 2E089 Tube Row 141/Col. 89: Comparison of Gap Velocities at 80% Power

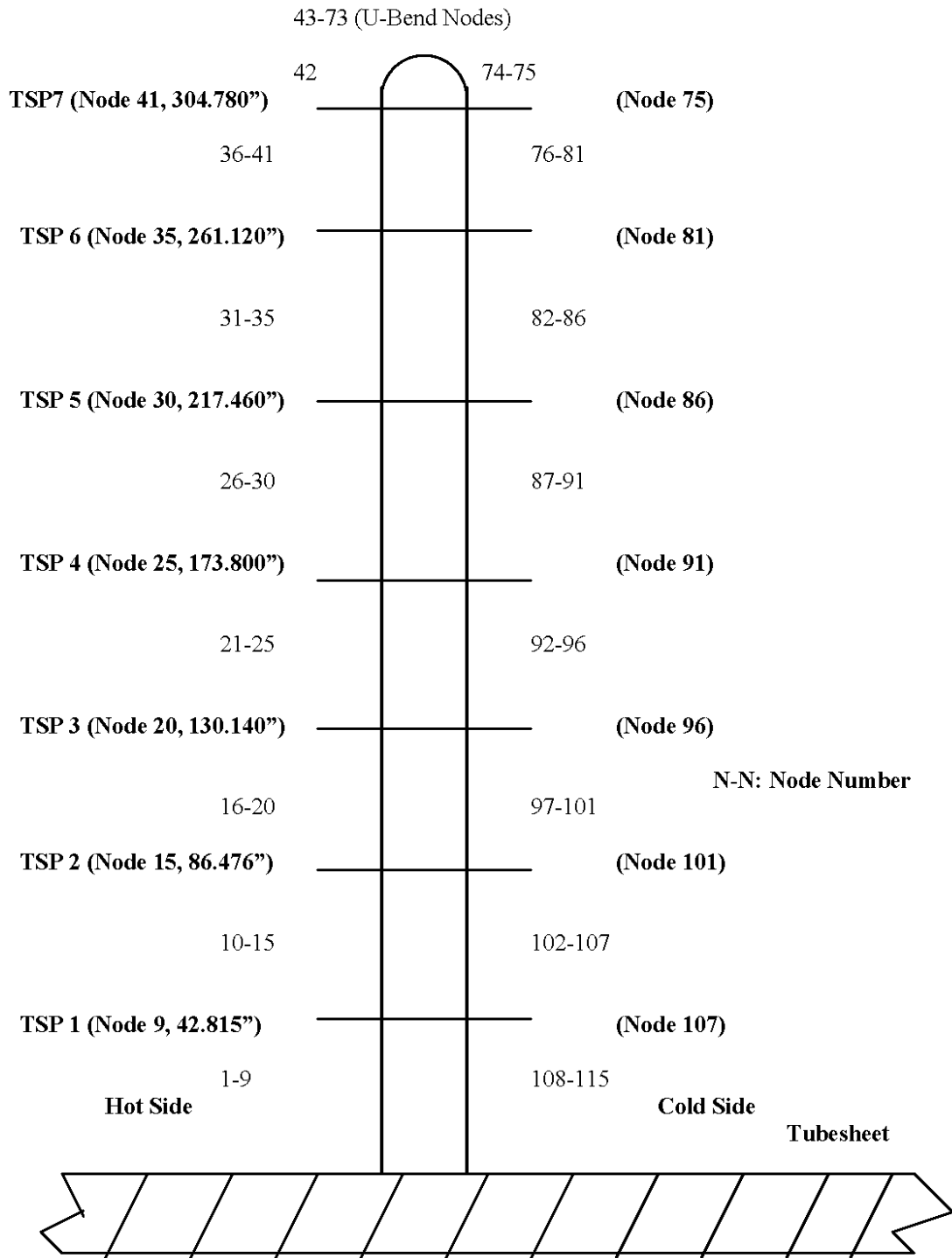


Figure 2-8. Representative FASTVIB / FLOVIB Tube Model

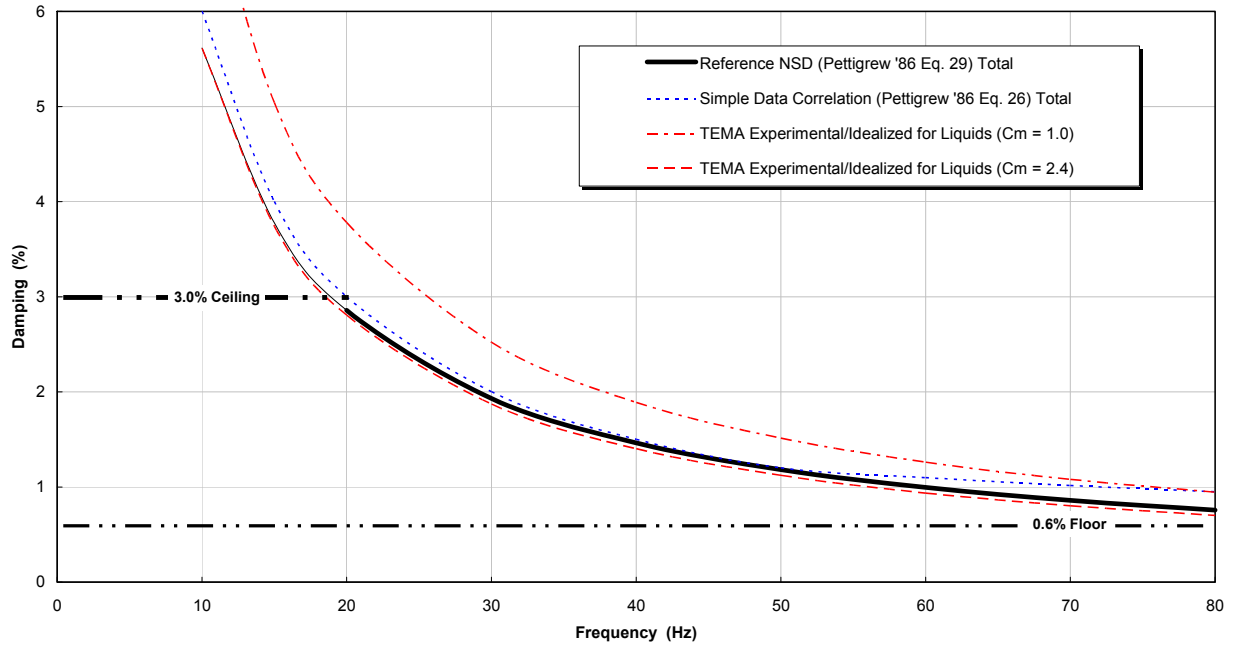


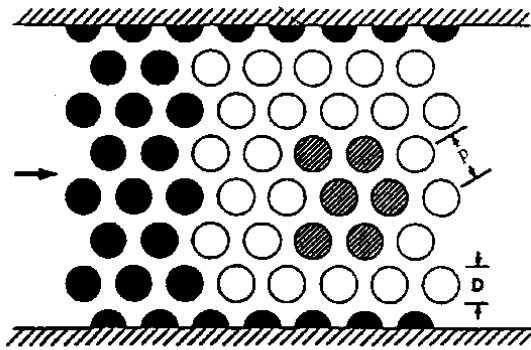
Figure 2-9. Straight Leg Tube Damping in Liquid

COL	49	60	74	80	85	90	94	95	100	105	110	111	120	122	124	125	127	130	135	137	138	139	140	141	142	
9	0.82																									
11	0.77																									
12		1.00																								
13	0.76																									
14		0.98																								
15	0.76																									
16		0.99	1.13																							
17	0.77																									
18		1.00	1.31	1.28																						
19	0.77																									
20		0.98	1.31	1.43																						
21	0.78				1.68																					
22		0.98	1.27	1.43		1.35																				
23	0.77				1.59																					
24		0.98	1.29	1.43		1.75	1.44																			
25	0.78				1.55			1.68																		
26		0.98	1.28	1.41		1.65	1.84																			
27	0.79				1.53			1.86																		
28		0.97	1.30	1.42		1.60	1.76		1.77																	
29	0.78				1.53			1.77																		
30		1.01	1.31	1.42		1.61	1.73		2.02																	
31	0.79				1.53			1.75		1.92																
32		1.00	1.31	1.43		1.63	1.72		1.92																	
33	0.79				1.54			1.74		2.22																
34		0.97	1.30	1.41		1.61	1.70		1.87		1.77															
35	0.77				1.53			1.74		2.05		2.04														
36		0.97	1.30	1.39		1.64	1.72		1.85		2.33															
37	0.74				1.53			1.75		2.02		2.35														
38		1.00	1.29	1.41		1.65	1.73		1.85		2.26															
39	0.75				1.54			1.75		1.99		2.30														
40		1.01	1.30	1.42		1.66	1.74		1.84		2.24															
41	0.79				1.55			1.73		1.95		2.25														
42		1.02	1.30	1.41		1.61	1.68		1.77		2.13		1.93													
43	0.80				1.55			1.70		1.92		2.11														
44		1.01	1.33	1.44		1.62	1.68		1.78		2.08		2.56	2.25												
45	0.80				1.55			1.71		1.90		2.07														
46		1.01	1.33	1.47		1.62	1.70		1.81		2.03		2.54	2.69	2.40											
47	0.81				1.55			1.73		1.92		2.06														
48		0.98	1.30	1.45		1.64	1.72		1.84		2.04		2.55	2.70	2.83											
49	0.79				1.55			1.74		1.95		2.12														
50		0.99	1.32	1.43		1.62	1.71		1.82		2.14		2.59	2.71	2.84											
51	0.79				1.55			1.72		1.97		2.19														
52		1.04	1.34	1.45		1.64	1.70		1.82		2.15		2.54	2.66	2.82											
53	0.79				1.57			1.74		1.99		2.17														
54		1.04	1.35	1.50		1.64	1.72		1.84		2.14		2.48	2.56	2.64											2.63
55	0.77				1.56			1.76		2.00		2.17														
56		1.03	1.33	1.47		1.65	1.75		1.87		2.15		2.49	2.58	2.67											3.05
57	0.78				1.57			1.78		2.02		2.17														
58		1.03	1.34	1.44		1.65	1.77		1.89		2.14		2.45	2.52	2.60											3.01
59	0.79				1.54			1.81		2.02		2.19														
60		1.03	1.31	1.41		1.65	1.80		1.92		2.17		2.44	2.51	2.60											2.96
61	0.78				1.55			1.82		2.07		2.19														2.87
62		1.03	1.33	1.47		1.71	1.80		1.96		2.15		2.47	2.53	2.60											2.90
63	0.77				1.61			1.84		2.09		2.21														3.36
64		1.01	1.35	1.49		1.72	1.83		1.97		2.24		2.48	2.56	2.63											2.89
65	0.77				1.62			1.86		2.11		2.30														3.31
66		1.03	1.38	1.51		1.73	1.84		1.99		2.28		2.55	2.60	2.65											2.88
67	0.84				1.64			1.88		2.13		2.33														3.32
68		1.06	1.38	1.49		1.74	1.87		2.01		2.33		2.57	2.62	2.67											2.85
69	0.83				1.64			1.94		2.22		2.38														3.15
70		1.07	1.40	1.52		1.83	1.92		2.09		2.38		2.59	2.65	2.71											2.87
71	0.84				1.72			2.00		2.26		2.41														3.17
72		1.07	1.40	1.55		1.85	1.99		2.16		2.41		2.57	2.62	2.69											2.87
73	0.85				1.72			2.04		2.26		2.39														3.16
74		1.07	1.45	1.60		1.88	2.02		2.14		2.34		2.59	2.63	2.69											2.92
75	0.89				1.78			2.02		2.24		2.35														3.16
76		1.09	1.48	1.63		1.86	1.95		2.10		2.39		2.69	2.74	2.79											2.95
77	0.86				1.76			2.01		2.30		2.45														3.39
78		1.12	1.49	1.62		1.92	2.04		2.22		2.46		2.78	2.84	2.89											3.27
79	0.81				1.75			2.12		2.38		2.54														3.08
80		1.18	1.53	1.68		1.93	2.10		2.27		2.54		2.76	2.82	2.89											3.29
81	0.86				1.80			2.09		2.39		2.54														3.01
82		1.18	1.49	1.68		1.92	2.06		2.28		2.50		2.75	2.80	2.86											3.26
83	0.95				1.87			2.12		2.38		2.54														3.02
84		1.15	1.57	1.78		2.01	2.11		2.28		2.56		2.84	2.90	2.97											3.43
85	0.91				1.93			2.20		2.47		2.58														3.15
86		1.21	1.63	1.80		2.09	2.17		2.28		2.53		2.78	2.86	2.92											3.46
87	0.96				1.92			2.15		2.44		2.55														3.10
88		1.15	1.56	1.69		2.00	2.10		2.22		2.50		2.77	2.84	2.90											3.44
89	0.84				1.80			2.07		2.37		2.48														3.06
COL	49	60	74	80	85	90	94	95	100	105	110	111	120	122	124	125	127	130	135	137	138	139	140	141	142	

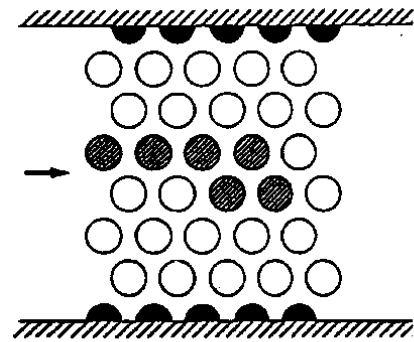
Figure 2-10. Out-of-Plane Excitation ratio Map – 100% Power – 7 AVBs Ineffective (Case 60)

COL	49	60	74	80	85	90	94	95	100	105	110	111	120	122	124	125	127	130	135	137	138	139	140	141	142		
9	0.23																										
11	0.21																										
12		0.29																									
13	0.21																										
14		0.28																									
15	0.21																										
16		0.28	0.33																								
17	0.21																										
18		0.28	0.38	0.37																							
19	0.21																										
20		0.28	0.38	0.43																							
21	0.21				0.49																						
22		0.28	0.37	0.42		0.39																					
23	0.22				0.47																						
24		0.28	0.37	0.43		0.51	0.41																				
25	0.22				0.46			0.47																			
26		0.28	0.37	0.42		0.49	0.53																				
27	0.22				0.46			0.55																			
28		0.28	0.38	0.42		0.49	0.53		0.51																		
29	0.22				0.47			0.55																			
30		0.28	0.38	0.43		0.51	0.54		0.60																		
31	0.22				0.48			0.55		0.56																	
32		0.28	0.39	0.44		0.51	0.54		0.59																		
33	0.22				0.49			0.55		0.66																	
34		0.27	0.39	0.43		0.50	0.53		0.58		0.52																
35	0.21				0.47			0.54		0.62		0.60															
36		0.27	0.39	0.43		0.50	0.54		0.58		0.69																
37	0.21				0.47			0.55		0.62		0.69															
38		0.29	0.39	0.43		0.51	0.54		0.58		0.68																
39	0.21				0.47			0.55		0.62		0.70															
40		0.29	0.39	0.44		0.52	0.55		0.58		0.69																
41	0.21				0.48			0.55		0.62		0.70															
42		0.29	0.38	0.43		0.51	0.54		0.57		0.69		0.57														
43	0.21				0.48			0.54		0.63		0.69															
44		0.29	0.39	0.44		0.51	0.53		0.57		0.69		0.77	0.66													
45	0.21				0.48			0.54		0.62		0.67															
46		0.29	0.40	0.45		0.51	0.54		0.59		0.66		0.77	0.80	0.70												
47	0.22				0.48			0.56		0.63		0.67				0.53											
48		0.28	0.38	0.44		0.52	0.56		0.60		0.67		0.78	0.82	0.84												
49	0.21				0.48			0.57		0.64		0.69				0.72											
50		0.28	0.39	0.43		0.51	0.55		0.60		0.69		0.80	0.83	0.85												
51	0.21				0.48			0.55		0.64		0.70				0.86	0.74										
52		0.29	0.40	0.44		0.52	0.55		0.59		0.70		0.79	0.81	0.85												
53	0.21				0.49			0.56		0.64		0.70				0.84	0.88										
54		0.29	0.41	0.46		0.52	0.55		0.60		0.69		0.77	0.79	0.81			0.76									
55	0.21				0.49			0.57		0.64		0.69				0.83	0.86										
56		0.28	0.40	0.46		0.52	0.56		0.61		0.68		0.77	0.79	0.82			0.90									
57	0.21				0.49			0.58		0.65		0.70				0.83	0.85										
58		0.28	0.40	0.44		0.53	0.57		0.61		0.70		0.77	0.78	0.80			0.89									
59	0.21				0.48			0.58		0.66		0.71				0.81	0.83										
60		0.29	0.39	0.43		0.52	0.57		0.61		0.70		0.77	0.78	0.80			0.88									
61	0.21				0.48			0.57		0.67		0.71				0.81	0.83		0.82								
62		0.30	0.40	0.45		0.52	0.56		0.62		0.70		0.78	0.79	0.80			0.86									
63	0.21				0.49			0.58		0.66		0.71				0.81	0.83		0.96								
64		0.28	0.41	0.45		0.53	0.57		0.62		0.71		0.78	0.79	0.81			0.86									
65	0.21				0.50			0.58		0.66		0.73				0.81	0.83		0.94	0.61							
66		0.28	0.41	0.46		0.54	0.58		0.62		0.72		0.79	0.80	0.81			0.86									
67	0.22				0.51			0.59		0.67		0.72				0.82	0.83		0.94	0.81							
68		0.29	0.40	0.46		0.54	0.59		0.63		0.71		0.80	0.81	0.82			0.86			0.84						
69	0.22				0.51			0.61		0.67		0.73				0.83	0.84		0.91	0.95			0.64				
70		0.30	0.41	0.45		0.56	0.59		0.63		0.72		0.80	0.81	0.83			0.87			0.97						
71	0.22				0.52			0.61		0.68		0.73				0.84	0.85		0.92	0.95			0.84				
72		0.31	0.41	0.46		0.57	0.61		0.65		0.73		0.80	0.81	0.83			0.88			0.97		0.64				
73	0.23				0.52			0.62		0.68		0.74				0.85	0.86		0.92	0.95			1.00				
74		0.30	0.42	0.47		0.56	0.62		0.66		0.73		0.81	0.82	0.84			0.89			0.97		0.84				
75	0.24				0.53			0.62		0.69		0.74				0.85	0.87		0.92	0.95			0.98		0.64		
76		0.30	0.43	0.48		0.57	0.61		0.66		0.74		0.82	0.83	0.84			0.89			0.96		1.00				
77	0.23				0.53			0.62		0.71		0.75				0.85	0.87		0.93	0.95			0.98		0.85		
78		0.31	0.44	0.48		0.58	0.62		0.67		0.75		0.83	0.84	0.85			0.90			0.96		1.00		0.65		
79	0.23				0.52			0.64		0.72		0.77				0.87	0.87		0.94	0.96			0.98		1.01		
80		0.32	0.45	0.50		0.57	0.63		0.67		0.76		0.83	0.84	0.87			0.90			0.97		1.00		0.65		
81	0.24				0.55			0.65		0.72		0.78				0.87	0.88		0.95	0.97			0.99		1.02		
82		0.34	0.45	0.52		0.59	0.63		0.68		0.78		0.84	0.85	0.86			0.91			0.99		1.01		0.66		
83	0.26				0.56			0.64		0.73		0.78				0.88	0.89		0.97	0.99			1.01		1.03		
84		0.35	0.46	0.53		0.61	0.64		0.69		0.78		0.86	0.87	0.88			0.92			1.00		1.03		0.67		
85	0.26				0.57			0.66		0.74		0.79				0.88	0.90		0.98	1.00			1.02		1.05		
86		0.36	0.47	0.53		0.61	0.64		0.68		0.78		0.85	0.87	0.87			0.92			1.01		1.03		0.67		
87	0.27				0.57			0.64																			

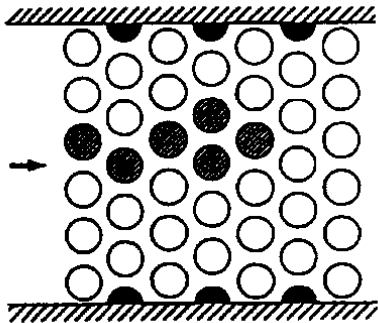
COL	49	60	74	80	85	90	94	95	100	105	110	111	120	122	124	125	127	130	135	137	138	139	140	141	142	
9	0.17																									
11	0.15																									
12		0.22																								
13	0.15																									
14		0.20																								
15	0.15																									
16		0.20	0.26																							
17	0.14																									
18		0.20	0.30	0.30																						
19	0.14																									
20		0.20	0.29	0.34																						
21	0.14				0.40																					
22		0.20	0.28	0.33		0.33																				
23	0.15				0.38																					
24		0.20	0.28	0.33		0.42	0.36																			
25	0.15				0.36			0.40																		
26		0.20	0.27	0.31		0.38	0.43																			
27	0.15				0.34			0.43																		
28		0.20	0.28	0.31		0.37	0.41		0.41																	
29	0.15				0.34			0.42																		
30		0.20	0.28	0.31		0.37	0.41		0.47																	
31	0.15				0.34			0.41		0.44																
32		0.20	0.28	0.31		0.37	0.40		0.45																	
33	0.15				0.34			0.40		0.51																
34		0.20	0.27	0.30		0.36	0.39		0.42	0.42																
35	0.15				0.33			0.40		0.47	0.46															
36		0.20	0.27	0.30		0.36	0.39		0.42	0.53																
37	0.15				0.33			0.39		0.46	0.53															
38		0.20	0.27	0.31		0.37	0.39		0.42	0.51																
39	0.15				0.34			0.39		0.45	0.52															
40		0.21	0.28	0.31		0.37	0.39		0.42	0.50																
41	0.15				0.34			0.39		0.44	0.51															
42		0.21	0.27	0.31		0.36	0.38		0.41	0.49	0.43															
43	0.15				0.34			0.39		0.45	0.49															
44		0.20	0.28	0.31		0.36	0.38		0.41	0.48	0.49															
45	0.15				0.34			0.38		0.44	0.48															
46		0.20	0.28	0.32		0.36	0.38		0.41	0.47	0.55	0.58	0.51													
47	0.15				0.34			0.39		0.44	0.47			0.39												
48		0.20	0.27	0.31		0.37	0.39		0.42	0.47	0.54	0.57	0.59													
49	0.15				0.34			0.40		0.44	0.48			0.50												
50		0.20	0.28	0.30		0.36	0.39		0.41	0.48	0.55	0.57	0.59													
51	0.15				0.34			0.39		0.44	0.48			0.60	0.52											
52		0.21	0.28	0.31		0.36	0.38		0.41	0.48	0.54	0.56	0.58													
53	0.15				0.34			0.39		0.44	0.47			0.58	0.61											
54		0.20	0.28	0.32		0.36	0.38		0.41	0.47	0.52	0.54	0.55			0.52										
55	0.15				0.34			0.39		0.44	0.47			0.56	0.58											
56		0.20	0.27	0.31		0.36	0.39		0.41	0.46	0.52	0.54	0.55			0.61										
57	0.15				0.34			0.39		0.44	0.47			0.56	0.58											
58		0.20	0.27	0.30		0.36	0.39		0.41	0.47	0.52	0.53	0.54			0.60										
59	0.15				0.33			0.39		0.44	0.47			0.54	0.56											
60		0.20	0.27	0.30		0.35	0.38		0.41	0.47	0.52	0.53	0.54			0.59										
61	0.15				0.33			0.39		0.45	0.47			0.54	0.56		0.55									
62		0.21	0.27	0.31		0.36	0.38		0.41	0.47	0.52	0.53	0.54			0.58										
63	0.15				0.34			0.39		0.44	0.47			0.55	0.56		0.63									
64		0.20	0.28	0.31		0.36	0.38		0.41	0.48	0.52	0.53	0.54			0.58										
65	0.15				0.34			0.39		0.44	0.48			0.55	0.56		0.62	0.40								
66		0.20	0.27	0.31		0.36	0.38		0.41	0.48	0.53	0.54	0.55			0.58										
67	0.15				0.34			0.39		0.44	0.48			0.55	0.56		0.63	0.54								
68		0.20	0.27	0.31		0.36	0.39		0.41	0.47	0.53	0.54	0.55			0.57										
69	0.15				0.34			0.40		0.44	0.48			0.55	0.56		0.61	0.63								
70		0.20	0.28	0.30		0.37	0.39		0.42	0.48	0.53	0.54	0.55			0.58										
71	0.15				0.34			0.40		0.45	0.48			0.56	0.57		0.62	0.63								
72		0.21	0.27	0.30		0.37	0.40		0.43	0.48	0.52	0.54	0.55			0.59										
73	0.16				0.34			0.41		0.45	0.48			0.56	0.57		0.62	0.63								
74		0.20	0.28	0.31		0.37	0.40		0.43	0.48	0.53	0.54	0.55			0.59										
75	0.16				0.35			0.41		0.45	0.48			0.56	0.58		0.61	0.62								
76		0.20	0.28	0.31		0.37	0.39		0.42	0.48	0.53	0.54	0.55			0.59										
77	0.16				0.34			0.40		0.46	0.48			0.55	0.57		0.61	0.62								
78		0.20	0.28	0.31		0.37	0.40		0.43	0.48	0.53	0.54	0.55			0.59										
79	0.15				0.34			0.41		0.46	0.49			0.55	0.56		0.61	0.61								
80		0.21	0.29	0.32		0.37	0.40		0.43	0.49	0.53	0.53	0.55			0.58										
81	0.15				0.35			0.41		0.46	0.49			0.55	0.56		0.60	0.61								
82		0.22	0.29	0.33		0.38	0.40		0.43	0.49	0.53	0.53	0.54			0.57										
83	0.17				0.36			0.41		0.46	0.49			0.55	0.56		0.61	0.61								
84		0.22	0.29	0.34		0.39	0.41		0.43	0.49	0.53	0.54	0.55			0.58										
85	0.17				0.36			0.42		0.47	0.49			0.55	0.56		0.61	0.61								
86		0.22	0.30	0.34		0.39	0.41		0.43	0.49	0.53	0.54	0.54			0.57										
87	0.17				0.36			0.41		0.46	0.49			0.55	0.56		0.61	0.62								
88		0.21	0.29	0.32		0.38	0.40		0.42	0.48	0.53	0.53	0.54			0.57										
89	0.15				0.35			0.40		0.46	0.48			0.54	0.55		0.61	0.61								
COL	49	60	74	80	85	90	94	95																		



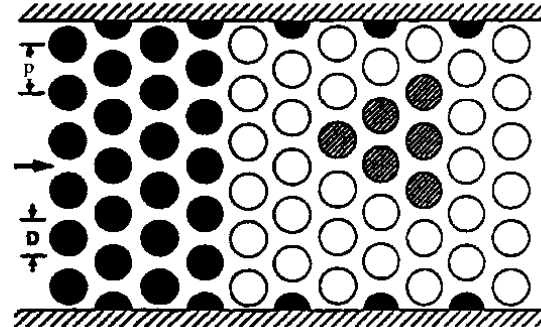
Test 1



Test 2



Test 3



Test 4

- Rigid Tube
- Flexible Tube
- ◐ Flexible Instrumented Tube

Figure 2-14. Schematic Illustrations of Triangular Pitch Tube Array Patterns Tested in the Water Tunnel with Pitch/Diameter Equal to 1.42

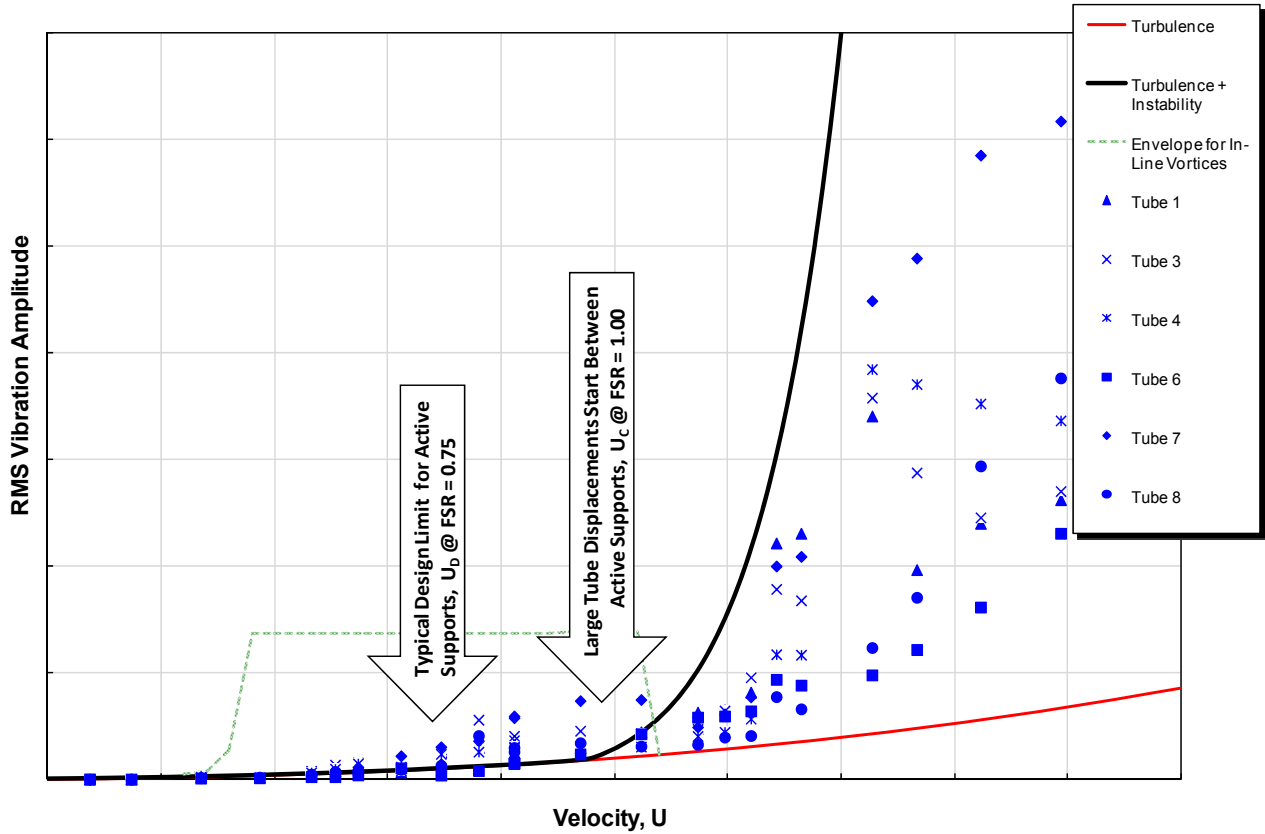


Figure 2-15. Comparison of Analytical Models of FIV Mechanisms with RMS Tube Displacements for Sample Vibration Test Data

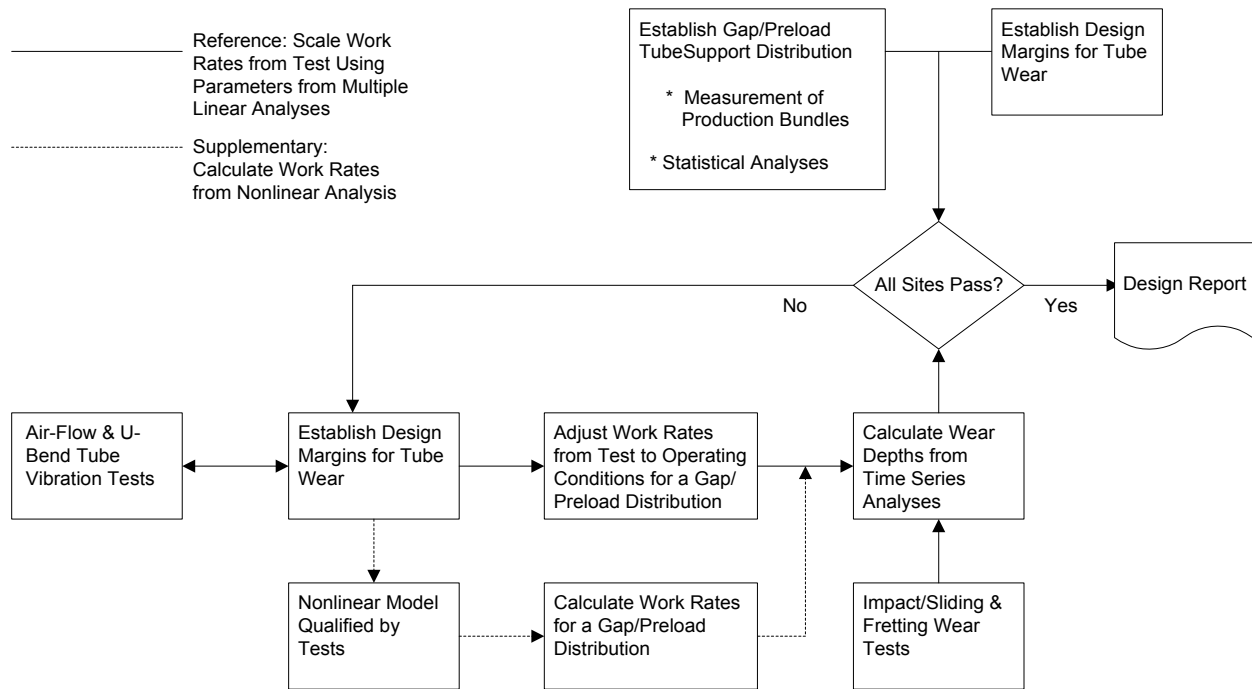


Figure 2-16. Typical Application of Semi-Empirical Wear Calculation Methodology for Amplitude Limited Fluidelastic Excitation in Steam Generator Design

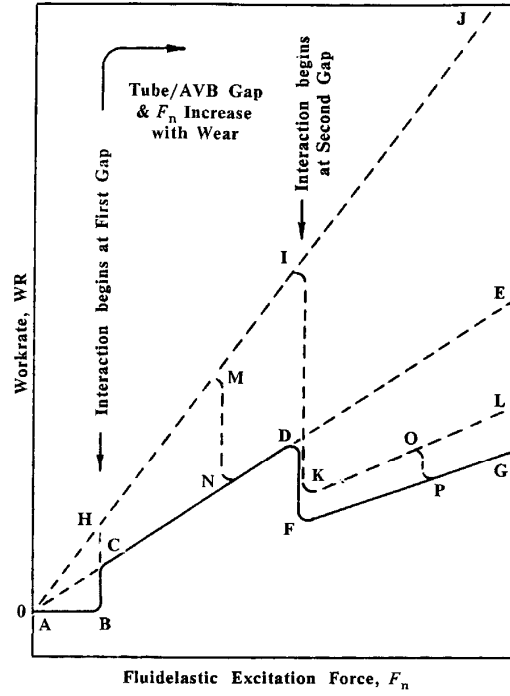
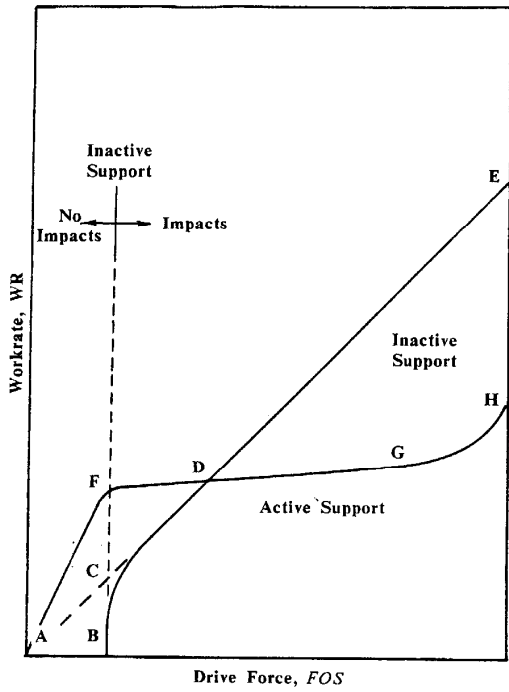


Figure 2-17. Fundamental Characteristic Trends Treated in Semi-Empirical Methodology

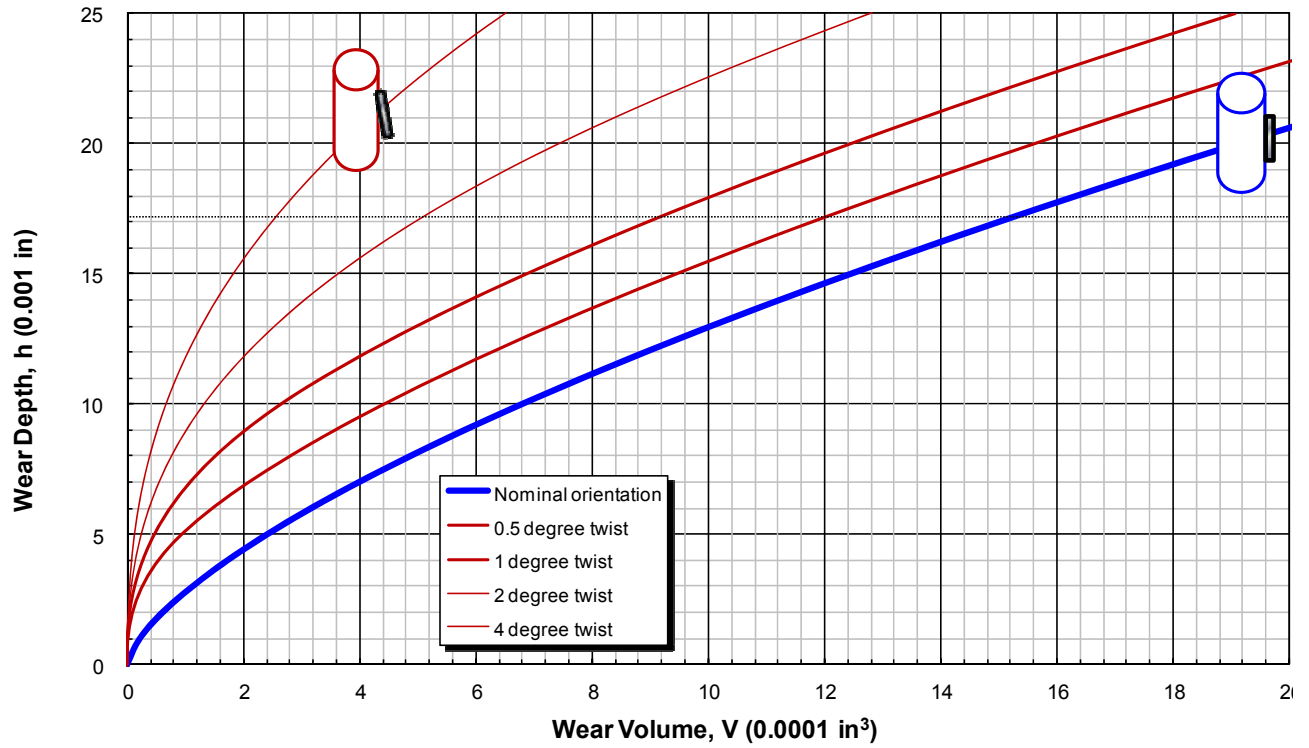


Figure 2-18. Wear Depth vs. Wear Volume (0.75 inch OD Tube, 0.59 inch AVB Width)

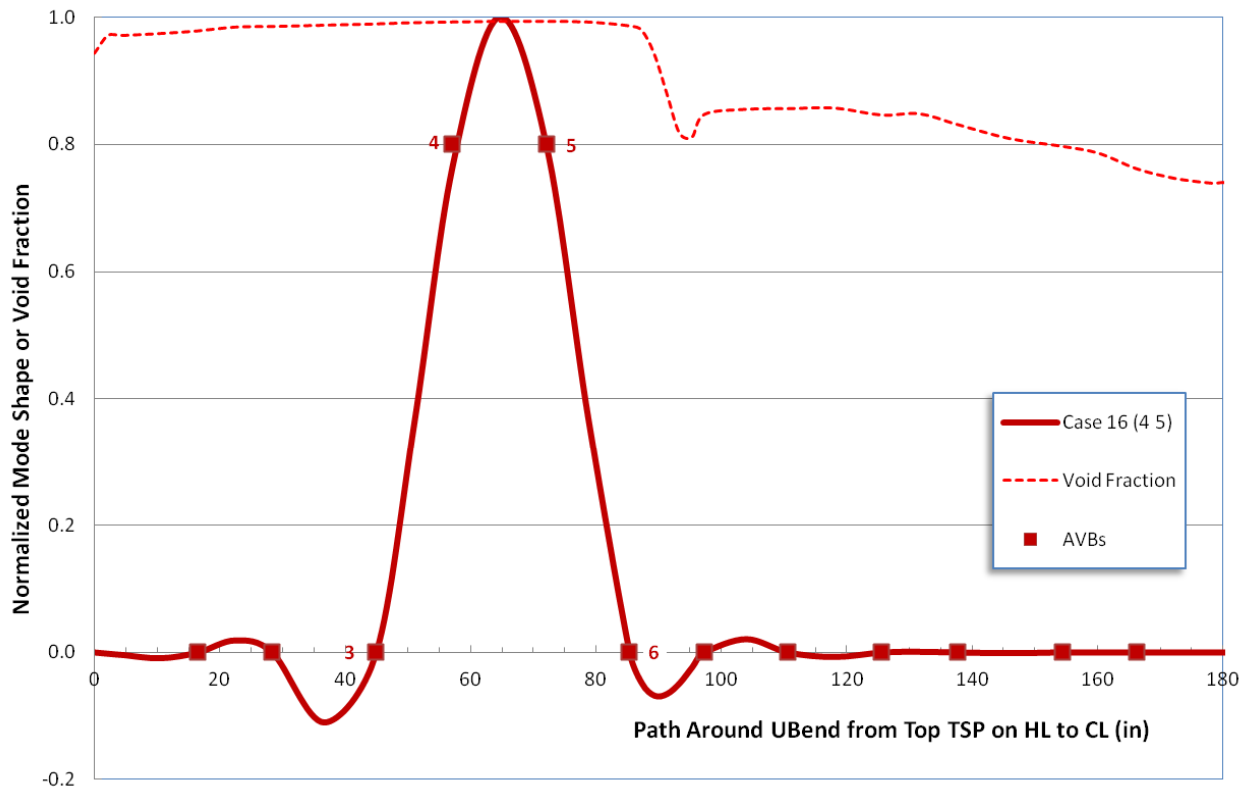


Figure 2-19. U-bend OP Mode in Sample Evaluation Showing First Unstable FASTVIB Case and Postulated Initial Positions of AVBs 4 and 5 Relative to Mode Shape

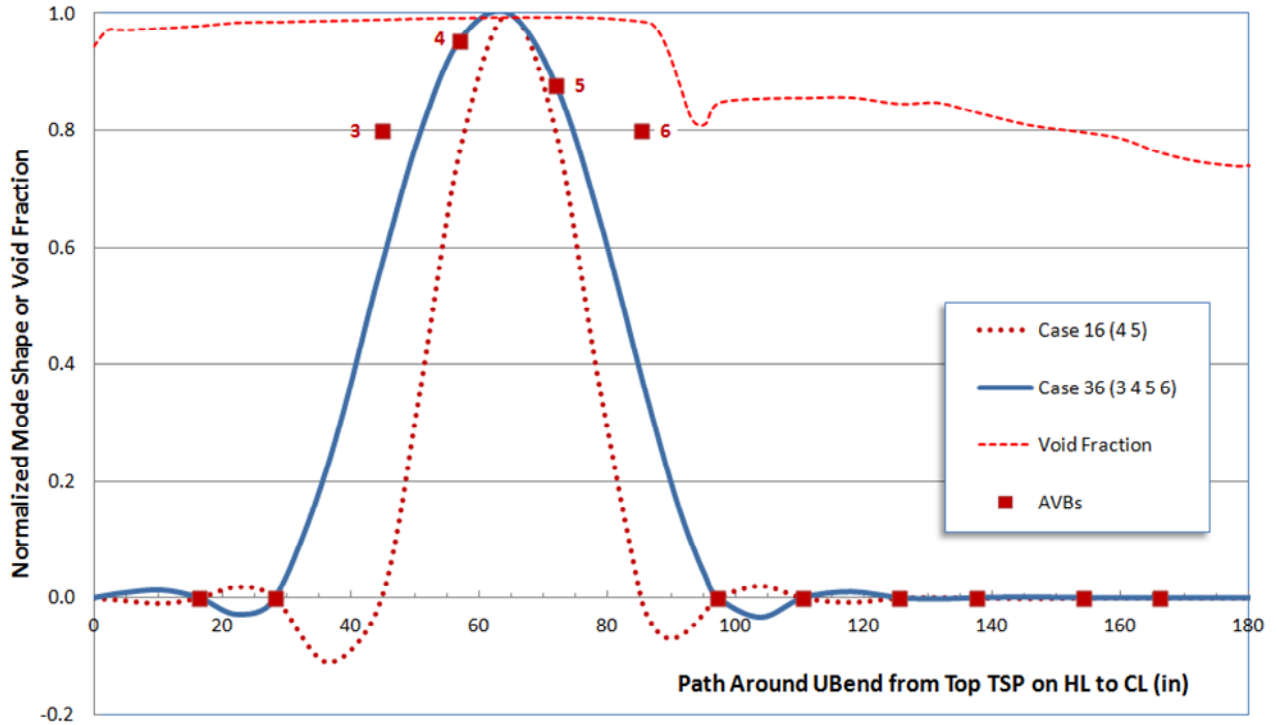


Figure 2-20. Significant U-bend OP Modes in Sample Evaluation Showing Two FASTVIB Cases and Postulated Initial Positions of AVBs 3, 4, 5, and 6 Relative to Mode Shape

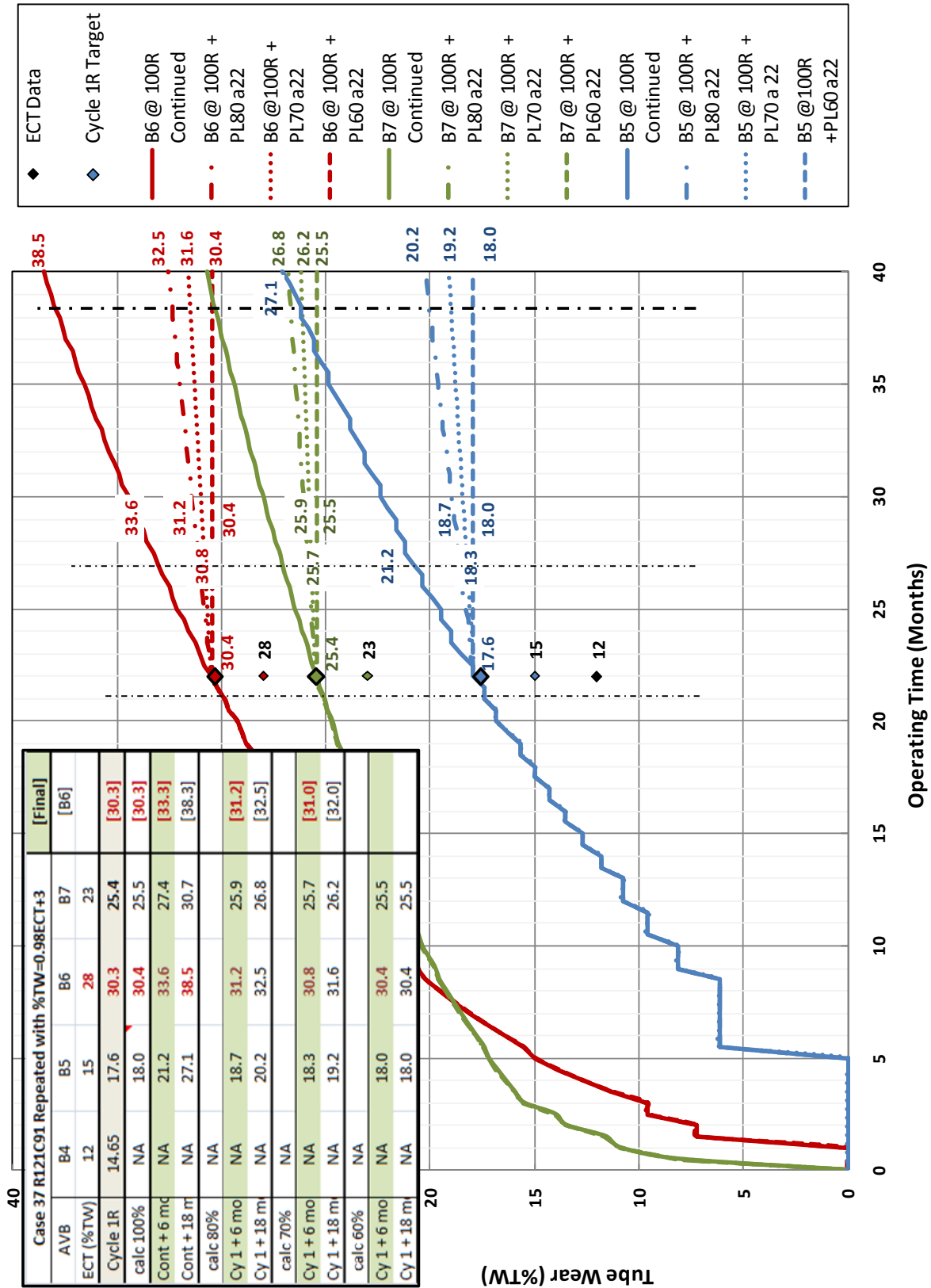
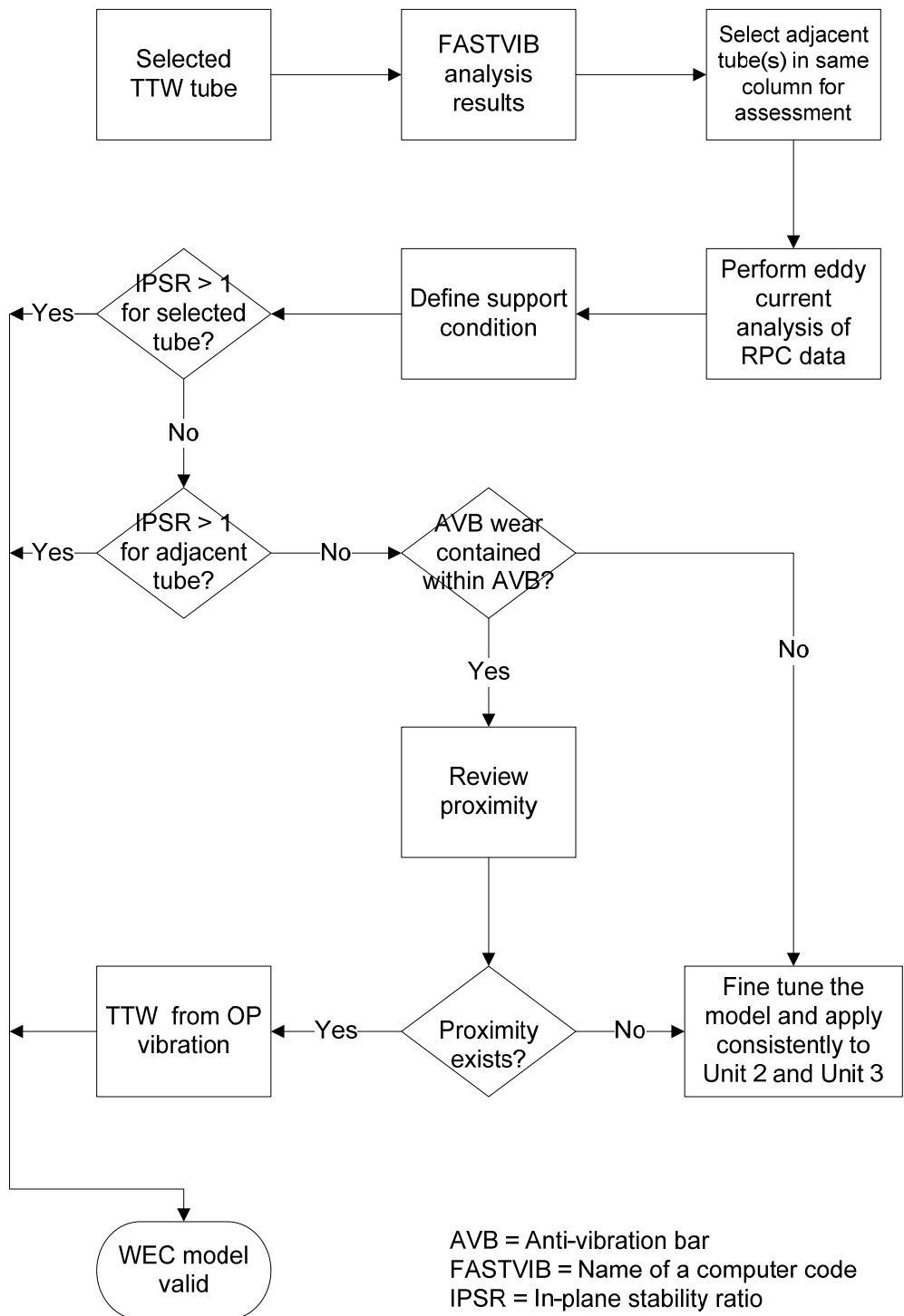


Figure 2-21. Example Illustration of AVB Wear Projection (Tube R121C91 in SG 2E089)



AVB = Anti-vibration bar
 FASTVIB = Name of a computer code
 IPSR = In-plane stability ratio
 OP = Out-of-plane
 RPC = Rotating pancake coil probe
 TTW = Tube-to-tube wear (in U-bend free span)

Figure 2-22. Logic Applied for Benchmarking the In-Plane Vibration Methodology Using Unit 3

- 16 Boundary Tubes
 - Have FS wear but only a few bobbin ECT indications at AVBs
- ⦿ 15 Adjacent Tubes
 - Investigated as potential sources of TtT interaction
- 55 Interior Tubes
 - All have clear evidence of multiple ineffective AVB supports based on bobbin ECT indications

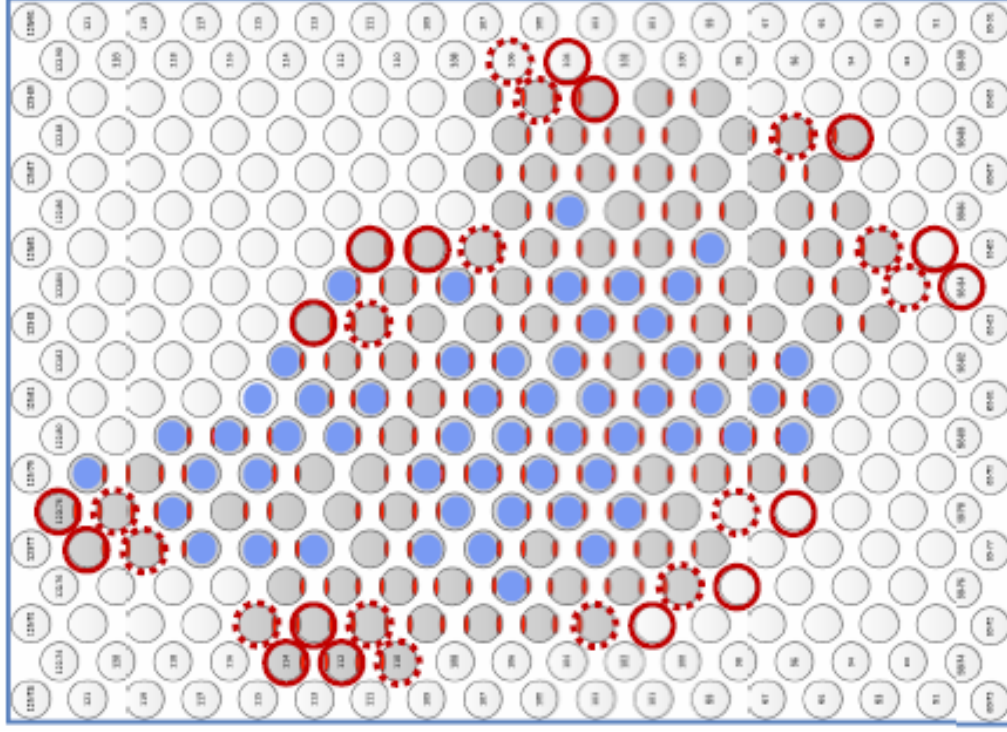


Figure 2-23. Location of SG 3E088 Tubes Evaluated for Benchmarking

3 Operational Assessment

The operational assessment is the forward-looking evaluation to assess if the steam generators will meet the structural, operating leakage, and accident condition leakage performance criteria until the next scheduled inspection.

This operational assessment covers three tube degradation mechanisms, namely, tube wear at AVBs, tube-to-tube wear in the U-bend free span, and the potential for in-plane vibration that can lead to tube-to-tube wear as has been observed in the Unit 3 SGs. These mechanisms are covered in the following subsections.

3.1 Tube Wear at AVBs

3.1.1 Structural Limits

This operational assessment deals with the tube wear indications reported in the U-bend region of the SONGS Unit 2 SGs. Tube degradation in the U-bend has resulted from wear at the AVB locations and wear from the interaction of two adjacent tubes in the same column. The structural limits for AVB wear are discussed in this sub-section.

Material properties of the tubes in the SONGS Unit 2 and Unit 3 SGs were provided by SCE (Reference 8). The parameters (mean and standard deviation) of the sum of yield and ultimate stress at temperature (650°F) were very close between the Unit 2 and Unit 3 tube populations. Hence, these parameters were determined for the combined population of both units and used in the current calculation. The mean value was found to be 116.22 ksi and the standard deviation was 2.42 ksi.

Operating conditions during the next cycle were provided by SCE for both full power and several part power conditions (Reference 9). Although SCE is planning to operate Unit 2 at part power until the next inspection, in the current calculation, the more conservative steam pressure at full power was used to determine the primary-to-secondary pressure differential. The full power steam pressure in the next cycle would be 926 psia. Since the primary side pressure is 2250 psia, the primary-to-secondary pressure differential for full power steam pressure in the next cycle would be 1324 psi.

The AVBs in the SONGS RSGs have a width of 0.59 inch and a thickness 0.114 inch. In the Unit 2 RSGs, the wear indications at the AVBs do not extend beyond the width of the AVBs. Hence, an axial length of 0.6 inch is used as the flaw length in this assessment.

Inspection results based on bobbin probe inspection are used in the current evaluation. For the detection and sizing of tube wear at an AVB location, SCE has applied the inspection technique described by Examination Technique Specification Sheet (ETSS) 96004.1 (Reference 25). It is anticipated that the same technique will be applied at the next inspection of the SGs. The actual-to-reported wear depth correlation, and its uncertainty associated with this ETSS, was used in the current calculation to determine the condition monitoring limits that would be applicable at the next inspection.

Tube wear at AVB locations can be either single-sided wear resulting from the interaction of the tube with an adjacent AVB or double-sided wear resulting from the interaction of the tube with both of the adjacent AVBs at the given location. A one-sided AVB flaw will become through-wall at a circumferential extent of 56 degrees. The total circumferential extent of a two-sided AVB flaw that becomes through-wall is 112 degrees or less. Since this is below the applicable threshold value of 135 degrees, the axial thinning correlation can be used to evaluate the burst pressure for

AVB wear indications. For flaws of circumferential extent greater than 135 degrees, the uniform thinning correlation would be applicable. Hence, the structural and condition monitoring limits for such flaws can be calculated based on the correlation for axial thinning provided in the Electric Power Research Institute (EPRI) Flaw Handbook (Reference 26).

The limiting performance criterion for burst is that the tube must meet three times the normal full power pressure differential ($3\Delta P_{\text{NOP}}$) between the primary side and the secondary side. In the next fuel cycle, assuming full power steam pressure, the $3\Delta P_{\text{NOP}}$ will be 3972 psi. The structural limit for axial thinning for a 0.6 inch long flaw is 66% through-wall (TW). Applying the uncertainties for burst relation, material properties, and inspection technique (including eddy current analysis), the condition monitoring (CM) limit at 95% probability at 50% confidence is calculated as 54% for the bobbin inspection results. The condition monitoring limits as a function of axial length of the flaw are shown in Table 3-1 and are plotted in Figure 3-1. The table and the figure show the CM limit based on bobbin inspection, which is the inspection of record for this degradation mechanism.

As noted above, the CM limit is 54% (maximum) depth from bobbin inspection. The actual maximum depth of such a flaw is expected to be below 60% (at 95% probability). Hence, a flaw of this size will not result in leakage either at normal operating conditions or at limiting accident conditions. Thus an indication satisfying the performance criterion for burst will also satisfy the performance criteria for leakage at normal operating and accident conditions.

3.1.2 Evaluation Method

As discussed in more detail in Section 2, the analytical methodology involves projection of the flaw size (depth) of indications reported at the current inspection to the next inspection. This evaluation is performed for the most limiting tubes on an individual basis. ATHOS results provide the thermal-hydraulic boundary conditions – flow velocity, density, and void fraction along the length of the tube. These are used in the FIV analysis to generate the excitation ratios for out-of-plane and in-plane vibration of the tube for various tube support conditions. The support conditions define whether or not a support location such as an AVB intersection is effective, meaning that the structure provides adequate support with respect to motion of the tube due to vibration. The actual tube support boundary conditions for a tube are deduced from U2C17 inspection results based on the presence or absence of a wear indication at the support location. Presence of a wear indication suggests the absence of adequate support; and hence, such locations are treated as ineffective support locations for that tube. The absence of a wear indication at a given structure is generally treated as a supported location. However, there are exceptions to this, such as an AVB location without wear indication nestled between wear indications in adjacent AVB locations in the same tube. In addition, evaluations have been performed to demonstrate that raising the number of unsupported locations does not significantly affect the projected wear depths at the next inspection (Reference 3).

The vibration analysis results and support conditions are used to make wear projection in the next operating cycle. This calculation is based on empirical test results and involves several input assumptions related to tube-to-AVB gap, wear coefficient for the tube and the AVB, the AVB twist, etc. The expected ranges of these parameters are known from test data and experience. Wear depth projection is made taking into consideration the inspection results at the current outage (U2C17). After setting the inputs to match the U2C17 inspection results for a given flaw, the wear calculations are extended to determine the projected wear depth at the next inspection.

Thus, the depth of an AVB wear indication is projected at the next inspection. In order to meet the performance criteria (operational assessment), the projected wear depth must remain below the condition monitoring limit.

3.1.3 Results for Active Tubes

The tubes left in service with the deepest wear indications in the U-bend are shown in Table 3-2. The fourth column in this table lists the bobbin reported wear depth and the fifth column shows the expected or “true” depth based on the correlation between metallurgical and NDE wear depth for the inspection technique (Reference 25). Both of these values are in %TW. The penultimate column of the table shows the projected wear depth at six months of operation in the next cycle, without accounting for method uncertainty. As shown in Section 2.5.4, the uncertainty associated with the wear projection method may be expressed using the normalized standard deviation of 0.20 in the estimated growth rate. This uncertainty was applied to the projected wear depth to calculate the wear depth with uncertainty as shown in the last column of Table 3-2.

The deepest AVB indication returned to service in the Unit 2 SGs has a reported wear depth of 28% TW by bobbin probe, in Tubes R119C89 and R121C91 in SG 2E089. Applying the methodology described in Section 2, these flaws are calculated to grow to a maximum wear depth of 32% at the next planned mid-cycle inspection based on the 70% power operating condition in Cycle 17. The projected flaw depth is well below the condition monitoring limit of 54% TW. There is considerable margin from the CM limit. Hence, these tubes are predicted to satisfy the SG performance criteria during the next operating period. The projected flaw depths of all of the remaining flaws in the active tubes are smaller than 30% TW; and hence, they also will satisfy the performance criteria. Operating experience with SGs indicate that wear at indications below the detection threshold or in tubes not exhibiting AVB wear will not develop large AVB wear scars that could threaten tube integrity within a five-month operating period. SCE is planning to perform a Unit 2 mid-cycle inspection after operating for 150 effective days of operation at 70% power.

3.1.4 Results for Plugged Tubes

Tube wear projection evaluation was carried out for flaws in the limiting plugged tubes. Stainless steel rope stabilizers were installed in many of the plugged tubes prior to plugging. Testing performed by Mitsubishi Heavy Industries (MHI) indicated that the stabilizers would not improve tube damping in the in-plane mode. Although stabilizers are expected to provide a benefit for the out-of-plane mode of vibration, since the quantification of the impact was not available, no beneficial impact from stabilizers was applied in the current evaluation.

The results of the evaluation for the limiting plugged tubes (tubes with the largest wear indications) are shown in Table 3-3. This table is quite similar to Table 3-2, including the calculation of projected wear depth with uncertainty. It may be noted that the increase in wear depth during the first 6 months of Cycle 17 is small. The projected maximum wear depth for the AVB wear indications is 39% TW. Unlike the active tubes, the acceptance criteria for plugged tubes are much broader. Plugged tubes do not need to meet the condition monitoring limits applicable to active tubes. A conservative criterion for plugged tubes may be that the projected wear depth should remain below 100% through-wall. As can be noted from Table 3-3, none of the indications in the plugged tubes approach the 100% TW depth, the maximum projected wear depth being 39%. Hence, the plugged tubes meet the acceptance criteria for the next operating cycle.

3.1.5 Evaluation for 18 Months of Operation

The results discussed in Sections 3.1.3 and 3.1.4 were for six months of operation in the next fuel cycle (17). Even though SCE is planning to perform a mid-cycle inspection of the Unit 2 RSGs after five months of operation in the next cycle, the wear projection was carried out for an operating duration of 18 months in the next cycle. The results for both active tubes and plugged tubes are shown in Table 3-4. It may be noted that the maximum projected wear depth with uncertainty for active tubes is 34% TW which is well below the CM limit of 54%. Similarly, the maximum projected wear depth for plugged tubes is 43% TW which is well below the criterion value of 100% TW. These wear depths satisfy the acceptance criteria established in Section 3.1.1. Therefore, it is acceptable to operate the SGs for 18 months in the next cycle with this degradation mechanism (tube wear at AVBs).

3.2 **Tube-to-Tube Wear in U-bend Free Span**

3.2.1 Eddy Current Inspection Results

Free span wear in the U-bend was reported (from +Point inspection) in two tubes during the U2C17 outage. They were in Tubes R111C81 and R113C81 in SG 2E089. These are adjacent tubes in the same column. In both tubes, the wear is located between AVB9 and AVB10 in the cold leg. The matching wear locations confirm that the wear resulted from contact between the two tubes. The wear depths in both tubes were shallow at 14% TW and the axial extents were six inches by eddy current inspection. An ultrasonic inspection (UT) was also performed on these tubes. The UT results indicated flaw depths of 7% TW.

Bobbin inspection identified AVB wear at five locations in Tube R111C81 (at AVBs 5, 6, 7, 8, and 10) and at three locations in Tube R113C81 (at AVBs 5, 6, and 7). Subsequent review of +Point data at all AVB intersections in these tubes confirmed the bobbin reported indications and in addition revealed low level wear indications from AVB4 through AVB10. There were no low level wear indications at the other AVBs. Therefore, both of these tubes had ineffective support at seven continuous AVB locations from AVB4 through AVB10.

None of the AVB wear scars extended beyond the width of the AVBs. In-plane motion of a tube against an AVB results in the wear scar extending beyond the width of the AVB (this was observed extensively in the Unit 3 RSGs). Since the AVB wear scars on two of the Unit 2 tubes with TTW were contained within the width of the AVBs, it indicates that the tube motion was not in-plane in either tube. This observation and conclusion were true for not only these two tubes but all tubes in the Unit 2 SGs. Thus the eddy current inspection data suggests that the AVB wear indications in Unit 2 did not result from in-plane vibration of the tubes.

A reanalysis of the pre-service inspection (PSI) data performed by Westinghouse in 2012 revealed proximity signals in these two tubes suggesting that the tubes were close to one another during the PSI. The PSI inspection was performed with the SGs in horizontal condition. No proximity signal was reported during the U2C17 inspection.

3.2.2 Flow-Induced Vibration Analysis Results

The flow-induced vibration analysis was performed considering many postulated boundary conditions regarding how AVBs can support the SG tubes in SONGS Unit 2. A detailed discussion of the FIV analysis is provided in Section 2.3. For the two tubes with free span wear, as discussed above, there are seven continuous ineffective AVB support locations (from 4

through 10). The support conditions for these two tubes, derived from the eddy current inspection results, are depicted in the following chart.

SG	Row	Col	07C	B12	B11	B10	FS _c	B09	B08	B07	B06	B05	B04	FS _s	B03	B02	B01	07H
SG89	113	81				X	14	X	X	5	5	16	X					
SG89	111	81				7	14	X	18	13	8	14	X					

X - Low level wear observed on +pt data from WEC review

This condition is covered by Case 61 (see Table 2-8). The out-of-plane excitation ratio (ER) for this case at 100% power is 2.12 showing that these tubes were unstable in the out-of-plane mode during Cycle 16. The ER for other FASTVIB cases with different numbers of ineffective AVB support locations is shown in the following table. As a point of clarification, no benefit from stabilization was included in the calculation of the results shown in the last two columns.

Out-of-Plane Excitation Ratio

Case Number	Number of Ineffective AVBs	100% Power Excitation Ratio	80% Power Excitation Ratio	70% Power Excitation Ratio
38	4	0.99	0.75	0.69
55	6	1.60	1.40	1.35
61	7	2.12	1.83	1.77
67	8	2.72	2.41	2.32
71	9	3.88	3.27	3.15

The in-plane stability ratio (IPSR) for Case 61 is 0.72 at 100% power in Cycle 16. The value of less than 1 indicates that the tubes were stable against in-plane vibration. The following table shows the IPSR for other support conditions and power levels. No benefit from stabilization was included in the calculation. It may be noted that these tubes will be stable in-plane at full power even with eight ineffective AVB supports. The IPSR calculation is based on a value of 7.8 for the instability constant (β). This is considered to be conservative in that the value of β is expected to be higher such that the true IPSR values may indeed be lower since the higher the value of β , the smaller the stability ratio.

In-Plane Stability Ratio

Case Number	Number of Ineffective AVBs	100% Power Stability Ratio	80% Power Stability Ratio	70% Power Stability Ratio
38	4	0.33	0.16	0.20
55	6	0.53	0.39	0.35
61	7	0.72	0.52	0.47
67	8	0.81	0.60	0.54
71	9	1.15	0.83	< 0.83

Thus, the vibration analysis indicates that the two tubes with free span wear were stable against in-plane vibration during Cycle 16. This further corroborates the evidence from eddy current test data showing no evidence of in-plane vibration in these tubes.

This paragraph provides a plausible explanation about how the tube-to-tube contact and wear may have occurred in the two tubes. The PSI data showing proximity of these tubes offers an insight. When one considers the proximity of the tubes and the fact that the tubes were vibrating out-of-plane, one can draw the conclusion that it is this combination that led to tube-to-tube wear in these tubes. The explanation is that the tubes were in contact as a result of tube expansion from heat up and pressurization during plant operation and that as a result of the out-of-plane vibration of these tubes due to fluidelastic excitation and turbulence, the free span wear occurred with the tubes fretting against each other at the contact location. Appendix A provides additional information that supports this plausible explanation.

3.2.3 Assessment of Tube-to-Tube Wear Mechanism

As discussed in the previous paragraphs, all available data suggest that the tube-to-tube wear in the U-bend free span did not result from in-plane vibration of the tubes. There is strong indication that it resulted from out-of-plane vibration of the two tubes in close proximity to the level of actual contact during operation.

It is expected that if the two tubes continue to wear, they may lose close proximity (i.e., contact during plant operation). It is not clear whether the loss of contact has already occurred or how much longer they will maintain contact and wear against each other. When loss of contact occurs, the wear arrest will result. The two tubes have been stabilized and plugged. The stabilizer will reduce the potential for, and the severity of, out-of-plane vibration. Stabilization will also tend to reduce the wear rate, if they remain in contact. Since the tubes are plugged, they can neither burst nor lead to primary-to-secondary leakage and hence, cannot challenge SG performance criteria.

Tube-to-tube wear in the free span was reported only in the two tubes. It is understandable that this is the case since close proximity of the tubes to the level of contact during operation as well as out-of-plane vibration of the tubes is required for this wear mechanism to occur. If there are other tubes with similar conditions, they would have exhibited tube-to-tube wear. If indeed there are a few other tubes with similar conditions, the lack of reported wear suggests that the wear progression has remained below the detection threshold. Hence, wear rates in such potential cases were even smaller. SCE is planning to perform a Unit 2 mid-cycle inspection after operating for 150 effective days of operation at 70% power. Since the reported free span wear was 14% by eddy current inspection and 7% by UT inspection after one full cycle of operation, a lower wear rate for only five months of operation at reduced power will result in only very small wear depths until the next inspection. As discussed in the last paragraph, when the wear depth increases, the tubes will lose contact and the wear will arrest itself.

Thus, it is extremely unlikely that other tubes in these SGs will exhibit free span wear similar to those reported in two tubes during U2C17. If there are a few remaining tubes with similar conditions, the wear rates and wear depths in such tubes will be even smaller than in the reported cases. An evaluation was conducted as described below.

An evaluation was carried out for a hypothetical undetected flaw left in service. The evaluation projected its size at the next inspection and compared it to the condition monitoring (allowable) limit for burst. The size of the undetected flaw at the beginning of cycle (BOC) was assumed to be the same as the size of the detected TTW flaws in SG 2E089. These flaws had a depth of 14% TW and an axial length of 6 inches (Reference 27) from +Point inspection using

ETSS 27902.2. These dimensions were conservatively used as the BOC conditions for the undetected flaw. The growth rate of these TTW flaws were calculated based on the operating length of 22 calendar months for Cycle 16. Using a conservative 6-month operation until the next inspection, a depth growth of 14% times 6/22 or 4% TW was calculated. Similarly, a growth value of 6 inches times 6/22 or 2 inches was calculated for axial length. These values were rounded up, conservatively. Please note that the next cycle of operation will be at 70% power; however, no credit was taken for the potentially lower growth rate resulting from the reduction in power level. The size of the undetected flaw at the next inspection was determined by adding the growth values to the BOC conditions. This yielded the projected flaw size as 18% TW and 8 inches in axial length.

The allowable depth for an 8-inch long flaw was determined based on the $3\Delta P_{NOP}$ value of 3972 psi (see Section 3.1.1). The EPRI Flaw Handbook (Reference 26) methodology for axial thinning was used in conjunction with the material properties of tubes in the SONGS RSGs and the NDE uncertainties for the ETSS 27902.2 (Reference 28). The calculation yielded an allowable limit of 48% TW. Since the projected wear depth of 18% TW is lower than the allowable limit, the burst performance criterion will be satisfied. The projected flaw depth is far below 100% TW and hence, no leakage will occur either during normal operation or during a postulated accident condition.

The evaluation was extended for an operating length of 18 months in Cycle 17. The projected dimensions of the undetected flaw for this operating length are 26% TW and 11 inch axial length. The condition monitoring limit for an 11 inch long flaw is 48% TW. Since the projected flaw depth is less than the allowable limit, and well below 100% TW, the burst and leakage criteria will be satisfied for an operating length of 18 months as well.

Therefore, the SG performance criteria will be satisfied for this degradation mechanism until the next inspection.

3.3 Potential for In-Plane Vibration

As discussed in Section 3.2, all available information indicates that in-plane vibration has not occurred in the Unit 2 SGs during their first cycle of operation. This section addresses the potential for in-plane vibration to occur during operation until the next inspection. Figure 3-2 shows a simplified diagram of the operational assessment methodology for this degradation mechanism.

Justification for the use of eddy current data to determine the support conditions in the U-bend is discussed in Section 2.4. It was also shown that an effective support at an AVB location will remain effective for several fuel cycles because the tube wear rate from out-of-plane vibration at such an AVB location will be negligible. Section 2.4.2 also shows that a contact force is not required to prevent in-plane vibration, but a small AVB gap is sufficient to provide effective support. Benchmarking of the methodology against Unit 3 findings is discussed in Section 2.6.1. By applying the methodology, it showed that the TTW indications in Unit 3 resulted from in-plane vibration of the given tube or from in-plane vibration of the neighboring tube. The same methodology was applied to the evaluation of Unit 2 RSGs.

All tubes in the Unit 2 SGs that will be returned to service were evaluated for the potential for in-plane vibration to occur in the next cycle. This flow-induced vibration evaluation was discussed in Section 2.6. It showed that there are no tubes in the Unit 2 SGs that are likely to become unstable in the in-plane vibration mode during the upcoming operating cycle. This is not surprising because the operation in the first cycle was at full power when no tubes were subjected to in-plane vibration. The next cycle of operation will be at 70% power. The vibration potential in the U-

bend decreases significantly as the power is reduced. Since the tubes were stable in-plane at 100% power, they will be stable in-plane at 70% power with additional margin. Evaluation of the most limiting tubes in the Unit 2 RSGs was discussed in Section 2.6. The results for the limiting tubes are shown in Table 2-10. Please note that all of these limiting tubes have already been stabilized and plugged, most of them preventively. The evaluation showed that the in-plane stability ratios of all tubes in Unit 2 are less than 1 at 70% power. Hence, in-plane vibration will not occur in the Unit 2 SGs during the upcoming operating cycle at power levels up to 70%.

Since all active tubes will be stable against in-plane vibration in the next cycle, tube-to-tube wear due to in-plane vibration in the U-bend free span, as has been observed in Unit 3, will not occur in Unit 2 during the next cycle of operation. SG performance criteria will be satisfied for this degradation mechanism until the next inspection.

3.4 Operational Assessment Conclusion

Three degradation mechanisms were evaluated as described in the prior subsections. They are tube wear at AVBs, tube-to-tube wear in the U-bend free span observed in two tubes in the Unit 2 SGs during the current refueling outage, and the potential for in-plane vibration that can lead to tube-to-tube wear in the U-bend free span as has been reported in the Unit 3 SGs. SCE is planning to perform a Unit 2 mid-cycle inspection after operating for 150 effective days of operation at 70% power. The operational assessment was performed in conformance with the EPRI Guidelines. It clearly demonstrates that for a 5-month operating period at 70% power the SGs will meet the performance criteria established in the Steam Generator Program Guidelines, NEI 97-06 (Reference 1), for both burst strength and for primary-to-secondary leakage during normal operation and accident conditions.

The evaluations also show that, for these degradation mechanisms, the SG performance criteria will be satisfied for the duration of 18 months and hence, it is acceptable to operate the Unit 2 SGs for a period of 18 months in the next fuel cycle at 70% power.

Table 3-1. Condition Monitoring Limit for Axial Thinning

Axial Thinning	
Length (inch)	CM Limit Depth (Bobbin ETSS 96004.1)
0.3	62.6%
0.4	58.5%
0.5	56.1%
0.6	54.5%
0.7	53.5%
0.8	52.6%
0.9	51.9%
1	51.3%
1.125	50.8%
1.2	50.5%
1.5	49.7%
2	48.9%
2.5	48.5%
3	48.2%

Table 3-2. Wear Projection Results for Active Tubes with Limiting AVB Wear Indications

Tube	SG No	Tube Status	Max Wear Depth, %		Max Depth @ at 70% Power After 6 Months			
			ECT Reported	Expected Value	FASTVIB Case	No Seq AVBs	Without Uncertainty	With Uncertainty
R97C87	88	Active	25	27.4	38	4	27.4	27.4
R119C89	89	Active	28	30.3	46	5	31.2	31.5
R121C91	89	Active	28	30.3	37	4	31.0	31.2
R131C91	89	Active	21	23.5	17	2	23.5	23.5
R129C93	89	Active	22	24.5	47 *	5	25.8	26.2
R126C90	89	Active	21	23.5	45	5	24.0	24.2

* Baseline Case 29 being stable, Case 47 was used for wear projection

Table 3-3. Wear Projection Results for Plugged Tubes with Limiting AVB Wear Indications

Tube	SG	Tube Status	Max Wear Depth, %		Max Depth @ at 70% Power After 6 Months			
			ECT Reported	Expected Value	FASTVIB Case	No Seq AVBs	Without Uncertainty	With Uncertainty
R112C88	88	Plugged	35	37.2	47	5	37.9	38.1
R133C91	88	Plugged	35	37.2	38	4	38.1	38.4
R114C90	88	Plugged	22	24.5	48	5	25.4	25.7
R111C91	88	Plugged	26	28.4	38	4	28.4	28.4
R116C86	88	Plugged	29	31.3	46	5	32.4	32.8
R117C93	88	Plugged	27	29.4	47	5	30.4	30.7
R115C85	88	Plugged	27	29.4	48	5	30.6	31.0
R114C86	88	Plugged	21	23.5	53	6	24.5	24.8
R112C88	88	Plugged	35	37.2	55	6	38.5	38.9
R128C94	88	Plugged	32	34.3	60	7	35.7	36.2
R120C92	88	Plugged	32	34.3	66	8	36.2	36.8
R121C83	89	Plugged	24	26.4	16	2	26.4	26.4
R117C89	89	Plugged	26	28.4	46	5	29.2	29.5
R108C90	89	Plugged	27	29.4	53	6	30.7	31.1
R117C81	89	Plugged	29	31.3	55	6	32.7	33.2
R134C90	89	Plugged	26	28.4	56	6	30.6	31.3
R114C88	89	Plugged	24	26.4	56	6	28.9	29.7
R117C85	89	Plugged	24	26.4	62	7	28.1	28.7
R122C82	89	Plugged	27	29.4	66	8	31.0	31.5
R112C84	89	Plugged	27	29.4	67	8	31.2	31.8
R111C81	89	Plugged	18	20.5	38	4	20.6	20.6

Table 3-4. Wear Projection Results for Limiting AVB Wear Indications for 18 Months of Operation

Tube	SG No	Tube Status	Max Wear Depth, %		Max Depth @ at 70% Power After 18 Months			
			ECT Reported	Expected Value	FASTVIB Case	No Seq AVBs	Without Uncertainty	With Uncertainty
R97C87	88	Active	25	27.4	38	4	27.4	27.4
R119C89	89	Active	28	30.3	46	5	32.8	33.6
R121C91	89	Active	28	30.3	37	4	32.0	32.5
R131C91	89	Active	21	23.5	17	2	23.5	23.5
R129C93	89	Active	22	24.5	47 *	5	28.0	29.2
R126C90	89	Active	21	23.5	45	5	24.9	25.4
R112C88	88	Plugged	35	37.2	47	5	38.5	38.9
R133C91	88	Plugged	35	37.2	38	4	39.8	40.7
R114C90	88	Plugged	22	24.5	48	5	27.2	28.1
R111C91	88	Plugged	26	28.4	38	4	28.4	28.4
R116C86	88	Plugged	29	31.3	46	5	34.7	35.8
R117C93	88	Plugged	27	29.4	47	5	32.4	33.4
R115C85	88	Plugged	27	29.4	48	5	32.8	33.9
R114C86	88	Plugged	21	23.5	53	6	26.3	27.2
R112C88	88	Plugged	35	37.2	55	6	41.5	42.9
R128C94	88	Plugged	32	34.3	60	7	39.0	40.6
R120C92	88	Plugged	32	34.3	66	8	39.5	41.2
R121C83	89	Plugged	24	26.4	16	2	26.4	26.4
R117C89	89	Plugged	26	28.4	46	5	30.7	31.5
R108C90	89	Plugged	27	29.4	53	6	33.2	34.5
R117C81	89	Plugged	29	31.3	55	6	35.2	36.5
R134C90	89	Plugged	26	28.4	56	6	34.4	36.4
R114C88	89	Plugged	24	26.4	56	6	33.2	35.4
R117C85	89	Plugged	24	26.4	62	7	31.0	32.5
R122C82	89	Plugged	27	29.4	66	8	33.8	35.3
R112C84	89	Plugged	27	29.4	67	8	34.4	36.1
R111C81	89	Plugged	18	20.5	38	4	20.6	20.6

* Baseline Case 29 being stable, Case 47 was used for wear projection

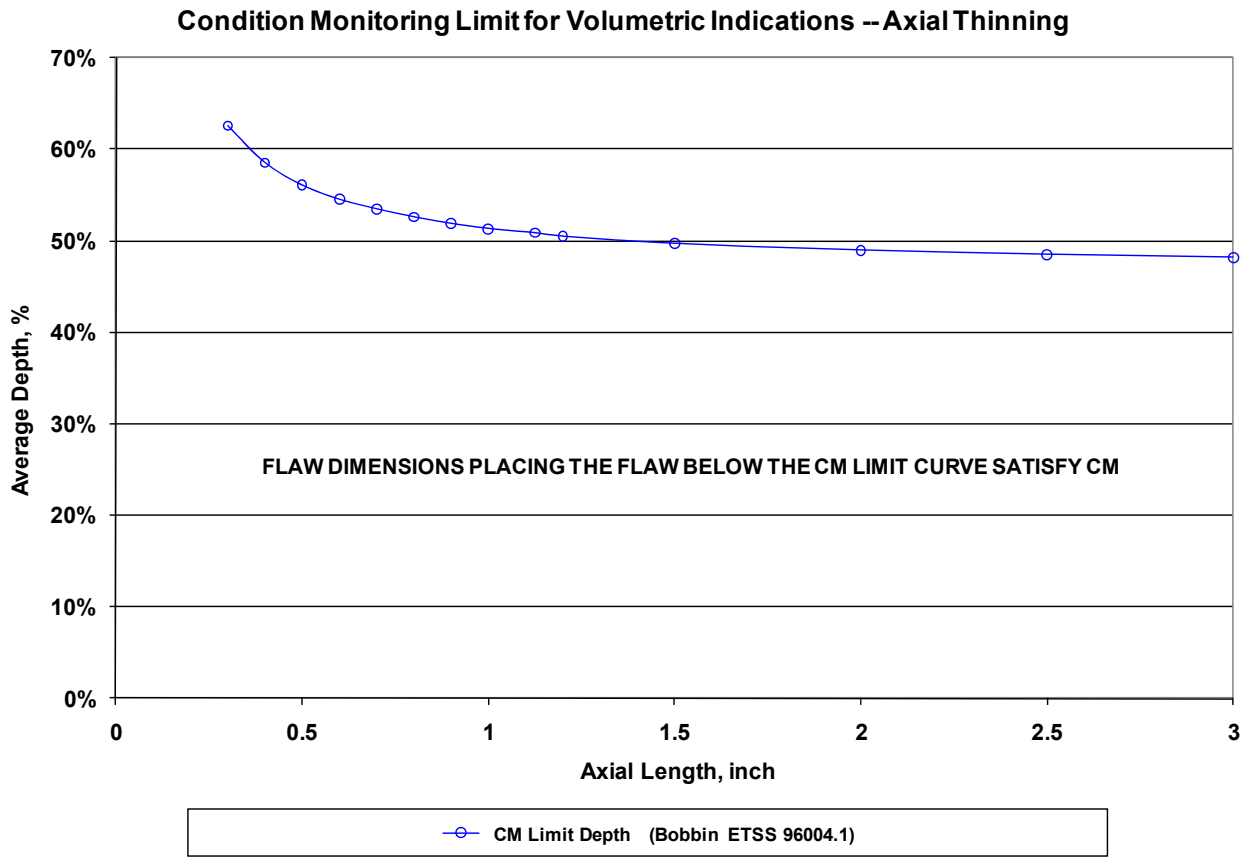
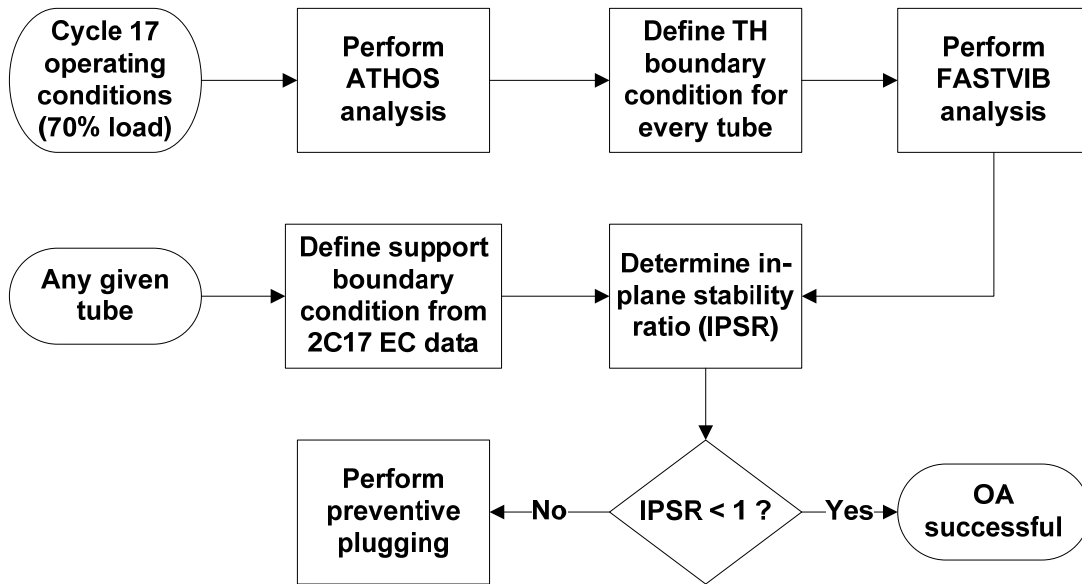


Figure 3-1. Condition Monitoring Limit for Axial Thinning



In concept, this analysis is repeated for every tube; in practice, for every limiting tube
Figure 3-2. Operational Assessment Methodology for the Potential for In-Plane Vibration

4 References

1. "Steam Generator Program Guidelines," NEI 97-06 Revision 3, January 2011.
2. "Steam Generator Integrity Assessment Guidelines Revision 3", EPRI Report 1019038, October 2008.
3. "Operational Assessment for SONGS Unit 2 Steam Generators for Upper Bundle Tube-to-Tube Wear Degradation at End of Cycle 16," APTECH Report, AES 12068150-2Q-1, September 2012.
4. "SONGS 2C17 Steam Generator Operational Assessment for Tube-to-Tube Wear," AREVA Report, 51-9187230, September 2012.
5. "Flow-Induced Vibration and Tube Wear Analysis of the San Onofre Nuclear Generating Station Unit 2 Replacement Steam Generators Supporting Restart," Westinghouse Report LTR-SGDA-12-36, Revision 1, September 13, 2012.
6. "ATHOS3: A Computer Program for the Thermal-Hydraulic Analysis of Steam Generators," EPRI-NP-4604-CMM, July 1986.
7. "Software Release Letter for Modules of the ATHOS Family of Codes and Executable Scripts: GPP60 Version 4.0, RUN_ATHOGPP Version 1.4, PLATES60 Version 3.0, and RUN_PLATES Version 1.4," Westinghouse letter LTR-SGDA-08-148, June 13, 2008.
8. "SONGS Material Properties," E-mail transmittal with Excel files "SONGS2 CMTR.xlsx" and "SONGS3 CMTR.xlsx" from Mr. David Calhoun of SCE to Vince Merritt of Westinghouse, June 22, 2012.
9. "San Onofre Nuclear Generating Station Units 2 and 3 Replacement Steam Generators Evaluation of Stability Ratio for Return to Service," Mitsubishi Heavy Industries Ltd., L5-04GA567, Revision 4, July 21, 2012.
10. "User's Manual for the Version 4.0 of PLTATHOS and VGUB to Read SG Model Data at Execution Time," Westinghouse document LTR-NCE-04-105, February 11, 2005.
11. M. J. Pettigrew, C. E. Taylor, and B. S. Kim, "Vibration of Tube Bundles in Two-Phase Cross-Flow: Part I—Hydrodynamic Mass and Damping," Transactions of the ASME Vol. 111, Nov. 1989, pp. 466-477.
12. F. Axisa, M. Wullschleger, B. Villard, and C. E. Taylor, "Two-Phase Cross-Flow Damping," ASME Publication PVP Vol. 133, Damping—1988, ASME PVP Conference, Pittsburgh, Pa., June 1988.
13. Standards of Tubular Exchanger Manufacturers Association, Tubular Exchanger Manufacturers Association, Inc., 7th Edition, New York, NY.
14. M. J. Pettigrew, R. J. Rogers, and F. Axisa, "Damping of Multispan Heat Exchanger Tubes: Part 2 In Liquids," ASME PVP Publication PVP Vol. 104, Chicago, IL, July 20-24, 1986, pp. 89-98.
15. M. J. Pettigrew and C. E. Taylor, "Damping of Heat Exchanger Tubes in Two-Phase Flow," ASME 4th International Symposium on Fluid-Structure Interactions, Aeroelasticity, Flow-Induced Vibration and Noise AD Vol. 53-2, Nov. 16-21, 1997, Dallas, TX pp. 407-418.
16. H. J. Connors, "Flow-Induced Vibration and Wear of Steam Generator Tubes," Nuclear Technology Vol. 55, Nov. 1981, pp.311-331.
17. H. J. Connors, "Fluidelastic Vibration of Tube Arrays Excited by Nonuniform Cross Flow,"

Flow-Induced Vibration of Power Plant Components –PVP-41 edited by M. K. Au-Yang, The American Society of Mechanical Engineers, New York, pp. 93-107, 1988.

18. "N-1331 Instability of Tube Arrays in Cross Flow," Nonmandatory Appendix N, ASME Boiler and Pressure Vessel Code Section III, "Rules for Construction of Nuclear Power Plant Components," 1998 Edition, The American Society of Mechanical Engineers, New York.
19. D. R. Polak and D. S. Weaver, "Vortex Shedding in Normal Triangular Tube Arrays," Flow-Induced Vibration 1994, The 1994 Pressure Vessels and Piping Conference, Minneapolis, Minnesota, ASME Pressure Vessels and Piping Division Report PVP-Vol. 273, pp. 145-156, June 19-23, 1994.
20. A. Zukauskas and V. Katinas, "Flow Induced Vibration in Heat Exchanger Tube Banks," Proceedings of the IUTAM-IAHR Symposium on Practical Experiences with Flow-Induced Vibrations, Karlsruhe, Editors E. Naudascher and D. Rockwell, Springer-Verlag, Berlin, pp.188-196, 1980.
21. D. S. Weaver, J. A. Fitzpatrick, and M. El-Kashlan, "Strouhal Numbers for Heat Exchanger Tube Arrays in Cross Flow," ASME Journal of Pressure Vessel Technology, Vol. 109, pp 219-223.
22. H. J. Connors, "Vortex Shedding Excitation and Vibration of Circular Cylinders," paper presented at the ASME Pressure Vessels and Piping Technology Conference, PVP-52, San Francisco, CA, Aug. 14, 1980, pp. 47-73.
23. P. J. Langford and H. J. Connors, "Calculation of Tube/AVB Wear from U-Bend Shaker Test Data," Fifth International Conference on Flow-Induced Vibrations, Paper C416/040, IMechE, Brighton, U. K., May, 1991, pp. 45-55.
24. D. S. Weaver and W. Schneider, "The Effect of Flat Bar Supports on the Crossflow Induced Response of Heat Exchanger U-tubes," Journal of Engineering for Power, October 1983, pp. 775-781.
25. "Examination Technique Specification Sheet 96004.1," Revision 13, EPRI, April 2010.
26. "Steam Generator Degradation Specific Management Flaw Handbook, Revision 1," EPRI Report 1019037, December 2009.
27. "SONGS Unit 2 Tube-to-tube Wear Indication Data" Westinghouse letter LTR-SGMP-12-80, October 2, 2012.
28. "Examination Technique Specification Sheet 27902.2," Revision 1, EPRI, May 2012.

5 Nomenclature

A	area
A_i	tube inside area
A_s	stabilizer area
A, B, C	empirical constants in damping correlations
ASME	American Society of Mechanical Engineers
ATHOS	Analysis of the Thermal-Hydraulics of Steam Generators
ATHOGPP	Westinghouse's version of the pre-processor program to ATHOS
ATHOSGPP	EPRI's version of the pre-processor program to ATHOS
AVB	anti-vibration bar
C_1	empirical turbulence constant (magnitude)
C_L	lift coefficient
C_m	added mass coefficient
C_R	random excitation coefficient
CCQR	pressure loss factors for AVBs in the U-bend region
CE	Combustion Engineering
CFD	computational fluid dynamics
CL	cold leg
CLCOLD	pressure loss factors for the downcomer on cold leg
CLEGGC	pressure loss factors for the tube support plates
CLHOT	pressure loss factors for the downcomer on hot leg
CLSEP	pressure loss factors for the primary separators
d, D	tube diameter
D_e	equivalent hydraulic diameter
Ditube	tube inner diameter
E	modulus of elasticity
ECT	eddy current test
EFPM	effective full power months
EPRI	Electric Power Research Institute
ER	Excitation Ratio, used in the context of OP vibration
f_n	vibration frequency in n^{th} mode (Hz)
F	force
FASTVIB	computer code for FIV analysis
FLOVIB	computer code for FIV analysis
FIV	flow-induced vibration
FSR	fluidelastic instability ratio = U_e/U_c
FW	feedwater
HL	hot leg
HTRESF	fouling factor value input to ATHOS
ID	inside diameter
IP	in-plane
ISI	in-service inspection
IX, IY, IZ	index directions, x, y, and z in ATHOS model
K	appropriate tube wear coefficient

L	length
m	mass per unit length
MHI	Mitsubishi Heavy Industries
Ms, m _s	stabilizer weight per length
N	number
NDD	no detectable degradation
NSSS	nuclear steam supply system
OD	outer diameter
OP	out-of-plane
p	tube pitch
PDRUM	pressure in the steam dome
Peff_Air	stabilizer effective density with air surrounding
Peff_Water	stabilizer effective density with water surrounding
PLATES	pre-processor program to ATHOS
Ps, p _s	stainless steel density
Pw, p _w	water density
R	radius, radial direction
RMS	root mean square
RPC	rotating pancake coil
RSG	replacement steam generator
RxCy	row x column y tube location
S	empirical turbulence constant (slope)
SCE	Southern California Edison
SG	steam generator
SONGS	San Onofre Nuclear Generating Station
SR	stability ratio (same as FSR), used in the context of IP vibration
SS	stainless steel
SVI	single volumetric indication
t	time
TAPE7, TAPE20	binary files to the PLATES program
Tod	tube outer diameter
TW	throughwall
TEMA	Tubular Exchanger Manufacturers Association
TH	thermal-hydraulic
TSP	tube support plate
TTW	tube-to-tube wear
U	velocity
U _c , U _{cn}	critical velocity
U _e , U _{en}	effective velocity
V	calculated wear volume
VGUB	post-processor program from ATHOS
W _r	workrate coefficient
WR	workrate
ZW	axial locations in ATHOS model

Appendix A. Tube-to-Tube Wear in Unit 2 U-bend Free Span

This appendix provides a reasonable explanation of how the two tubes in SG 2E089 could have come in contact during plant operation so as to produce the free span wear found on R111C81 and R113C81. It is recognized that there may be other explanations regarding how this wear was produced; however, the following provides a basis for the observations found during both the PSI and the recent ISI inspections. Based on a reanalysis of the pre-service inspection data performed by Westinghouse, it was determined that a proximity condition existed for these two tubes (R111/113C81). These indications are likely to be associated with conditions that developed during SG manufacture. How proximity and increased AVB gap could result from fabrication is discussed in Section A.1. Evaluation of the eddy current inspection results and its conclusions are discussed in Section A.2. Evaluation of the impact of plant operation and shut down on the gap between the two tubes is discussed in Section A.3. The overall gap closure considerations are summarized in Section A.4.

A.1 Manufacturing Considerations

There are several potential manufacturing considerations associated with review of the design drawings based on Westinghouse experience. The first two are related to increased proximity potential that is likely associated with the ECT evidence for proximity that is described in Section A-2. Two others are associated with the AVB configuration and the additional orthogonal support structure that can interact with the first two during manufacturing. Another relates to AVB fabrication tolerances. These potential issues include:

1. The smaller nominal in-plane spacing between large radius U-bend tubes than comparable Westinghouse experience.
2. The much larger relative shrinkage of two sides (cold leg and hot leg) of each tube that can occur within the tubesheet drilling tolerances. Differences in axial shrinkage of tube legs can change the shape of the U-bends and reduce in-plane clearances between tubes from what was installed prior to hydraulic expansion.
3. The potential for the ends of the lateral sets of AVBs (designated as side narrow and side wide on the Design Anti-Vibration Bar Assembly Drawing (LU-04FU116, Rev. 2) that are attached to the AVB support structure on the sides of the tube bundle to become displaced from their intended positions during lower shell assembly rotation.
4. The potential for the 13 orthogonal bridge structure segments that are welded to the ends of AVB end cap extensions to produce reactions inside the bundle due to weld shrinkage and added weight during bundle rotation.
5. Control of AVB fabrication tolerances sufficient to avoid undesirable interactions within the bundle. If AVBs are not flat with no twist in the unrestrained state they can tend to spread tube columns and introduce unexpected gaps greater than nominal inside the bundle away from the fixed weld spacing.

The weight of the additional support structure after installation could accentuate any of the above potential issues. There is insufficient evidence to conclude that any of the listed potential issues are directly responsible for the unexpected tube wear, but these issues could all lead to unexpected tube/AVB fit-up conditions that would support the amplitude limited fluidelastic

vibration mechanism described in Section 2.3. None were extensively treated in the SCE root cause evaluation.

A.1.1 Nominal In-Plane Tube Spacing

Table A-1 shows that the nominal tube spacing between the apex of successive tubes in the same column is 0.400 inch for the largest radius tubes and only 0.344 inch for the tubes in Rows 101 through 124 that have much of the observed tube wear. This nominal value at the apex is misleading in the sense that it is the maximum clearance if all tube fabrication tolerances are precisely maintained including the length of the straight legs which positions the U-bend relative to the primary face of the tubesheet. The distance between tubes on the sides at the intersection with the top TSP is 0.250 inch plus or minus the small broached hole tolerances. The actual shape of the U-bend has a profile tolerance that is not provided in the referenced drawings, but Westinghouse experience is that it may be between 0.040 and 0.120 inch (1-3 mm) for similar size tubing. The only check during tube bundle assembly is the ability to pass a 0.12 to 0.14 inch pin gauge between successive tubes⁴. Any tube that fits between the adjacent tubes in a given column during fabrication will satisfy this check. However, any variations in leg length or form tolerances will lead to tubes that are much closer than the nominal spacing, and most deviations will lead to tubes being closer on one side, for example near AVB3 and AVB4 and farther from AVB9 and AVB10, or vice versa. Westinghouse nominal spacing in this region is typically about 50 percent greater with a required simultaneous (rather than a sweep gauge) check of 0.18 inch clearance all around in the unrestrained as-installed condition, and it is not rare to require the use of spare tubes or trimming of tube ends to meet this requirement. Therefore, it is expected that it would have been difficult to maintain uniform spacing in the U-bend given the smaller incremental spacing on the SONGS manufacturing drawings. The root cause evaluation notes that between 132 and 390 tubes required adjustment of tube bending radius for each of the steam generators. This process is inherently difficult to control in a manufacturing environment.

A.1.2 Tube Leg Shrinkage During Hydraulic Expansion (HX)

The entire tube bundle is assembled before hydraulic expansion is performed with no ability to see the consequences of variations in leg shrinkage inside the bundle. Expansion is a process that involves plastic deformation of the portion of tubing that is inside the tubesheet, and plastic deformation is a constant volume process that necessitates shortening the length of the straight portions of tubing to account for the increase in diameter because wall thinning is small for the pressures involved. Figure A-1 shows expectations for the range of relative shrinkage for Plant B and for the SONGS steam generators using drawing tolerances shown on Table A-1. For most of the holes, both applications would have a maximum variation of about 0.10 inch between different sides of the same tube. However, the SONGS drawing allows up to one percent of the holes to be so large that a difference twice that large is possible for about 100 tubes in each RSG. When combined with the small clearances that are possible after installation, the superimposed HX shrinkage could lead to the level of proximity indications observed as discussed in Section A.2. When installed and then heated and pressurized, it is possible that tube-to-tube contact may occur, and in the extreme, there could be interference leading to tubes pushing against each other and then against adjacent AVBs tending to increase the column spacing. Any such conditions would tend to make the next two issues more problematic during fabrication.

⁴ Westinghouse does not have access to the assembly procedures. The 0.12 to 0.14 dimensions are anecdotal without verification.

A.1.3 Lateral AVB Nose Movement During Shop Rotation

The side-wide and side-narrow AVBs that are cantilevered from the sides of the bundle must be held in place by attachments to the retaining bars, and these bars must in turn be held in position by the orthogonal support bridge structure. For this design, gravity and friction tend to interact with the cantilevered AVBs whenever the horizontal SG is rotated during fabrication in an asymmetric way that could potentially move the noses of the AVBs and deform the straight portions leading to bending or twisting that could expand the column spacing in some regions and leave some regions of tubing with larger than nominal clearances. During shop rotation the overhanging portion of the tube bundle (about 83 inches or almost 7 feet for SONGS) bends downward several inches when the tube U-bends are horizontal, less when they become vertical, and then several inches in the opposite direction at 180 degrees from the starting position. This rotation occurs several hundred times during welding operations for not only the channel head but also the closing weld after AVB assembly. The ends of each leg of each AVB are deflected the same amount for AVBs that have their bends along the bundle centerline, but each rotation of the cantilevered AVBs deflects the leg that is nearest the center more than the one that is nearest the TSP. If the noses do not return to the original position they had when installed during the tube column and AVB layering process, the tube column spacing could be adversely impacted from consequential bending or twisting of the AVB legs. If there were any extreme proximity conditions from a combination of the first two potential issues that tended to push one tube locally against its neighbor, there could be a tendency to push the AVB legs apart locally and make it more difficult for all AVBs to maintain their original positions after rotation.

A.1.4 Orthogonal Bridge Structure Impact on Bundle During Fabrication

The segments of the orthogonal bridges are welded to the ends of longer than normal AVB end caps at 13 columns spaced evenly around each retaining ring. Weld shrinkage at these attachments could possibly impose forces on the ends of those AVBs that must be reacted inside the bundle. The added weight of the structure would also tend to amplify gravitational effects during shop rotations.

A.1.5 Control of AVB Fabrication Tolerances

Large radius U-bend tubing has very little flexural rigidity out-of-plane of the U-bend even when pressurized during SG operation. The tops of the straight leg portions are held in place by the TSP broached hole spacing, and the AVB end cap-to-retaining bar welds maintain spacing around the periphery, more at the bundle center, but less so around the bundle because the bars are also flexible. However, there is no structural component to keep the interior of the bundle at the intended nominal spacing in the region of most wear in the SONGS steam generators, especially along a line between the bottoms of the locations where the weight of the structure is reacted by retainer bars that can tend to push the columns apart near the Row 111 tube radius. Therefore, it is even more critical for the SONGS steam generators to maintain flatness and twist tolerances on AVBs so they will not have any tendency to separate the tube columns anywhere between the end caps and the bends deep inside the bundle. If acceptance criteria for AVB tolerances did not include inspections for flatness and twist in the unrestrained condition⁵, the AVBs could contribute to the apparent off-nominal spacing in the SONGS steam generators.

⁵ Westinghouse does not have access to final manufacturing or inspection details, but anecdotal input indicates that six-pound weights were allowed and used during AVB inspection for consistency with AVB drawing tolerances.

A.1.6 Additional Considerations from Unit 3

Except as noted, the discussion included in Section A.1.6 is related to the Unit 3 RSGs. It is included to here to point out the manufacturing considerations. Extensive review of ECT data available for the Unit 3 RSGs was conducted to benchmark the Westinghouse methodology against Unit 3 findings of tube-to-tube wear. Figures A-2 through A-6 identify various findings of tube proximity, AVB symmetry variance on opposite sides of the same intersection, and tapered wear scars associated with twisted AVB legs that are inconsistent with assuming tube/AVB interactions based on Gaussian distributions about nominal design conditions. Figure A-2 is an overview of all the noted variables. There is a line of proximity indications in Rows 121 and 122 that is not random, but there is insufficient information to know if it is associated with the weight of the AVB structure imparted here through the retainer bar supports or if it could be that the next incremental tube index does not occur until Row 124. The distribution of significant symmetry variances and tapered wear scar locations also does not appear random. The boundary between tubes with mostly double-sided wear scars inside the affected region (the region of the bundle with tube-to-tube wear indications) and single-sided wear scars above and below is not shown here, but the boundary is consistent and markedly not random.

Figure A-3 shows both the spatial and quantitative distribution of AVB symmetry variance in this region. The maximum symmetry variance of 0.78 inches occurs at AVB 6 on Row 87 in Column 85, and it decreases both going outward at larger radii going towards the tube/AVB weld and inward going towards the bend region. It is not likely that the middle of an AVB can be displaced this much in-plane without introducing significant bending and twist beyond design expectations. The ECT review noted that more tubes in Unit 2 had symmetry variances than in Unit 3, but they were more scattered with a smaller maximum (about 0.5 inch). Figure A-4 shows that locations with twist are present in the vicinity with the largest taper distribution from about 5 to 35%TW shown on Figure A-5.

A.2 **Eddy Current Review**

The FIV analysis performed by Westinghouse concludes that tube locations R111 C81 and R113 C81 in SG 2E089 remain stable in the in-plane direction at both 100% and 70% power levels. The review of AVB wear scar characteristics indicates that there was no extension of the wear scars beyond the width of the AVBs, thus supporting the analysis results that these tubes, as well as all other tubes in SGs 2E088 and 2E089 which had a review of their ECT data performed, remained stable in the in-plane direction.

Westinghouse was requested to provide an explanation as to how freespan wear could be observed on R111C81 and R113C81 without in-plane vibration of the tubes. The following discussion presents an explanation of how this could occur.

A.2.1 Industry Freespan Wear Experience Without In-Plane Instability

In recirculating SGs, there are numerous examples of tube-to-tube wear without in-plane instability; these examples are exclusive to the original Combustion-Engineering (C-E) SGs, in the upper bundle square bend region. The tube OD and triangular pitch array in the original C-E style is identical to the SONGS RSGs. In the original C-E SG design, variances in the tube horizontal run dimension, square bend control, and eggcrate tube support positioning can create a reduced tube-to-tube gap condition. Tube wear patterns at the vertical strap assembly often showed tapered wear scars on both of the vertical strips, and sometimes at both edges of the

vertical strips. This would indicate that the tube was experiencing out-of-plane displacement, with an oscillatory pattern. It is then entirely plausible that tube-to-tube wear could be experienced at reduced tube-to-tube gap conditions just below the square bend region.

At one plant, tube-to-tube wear was experienced in the horizontal run region, just outside of the square bend. In this instance, variance in the tube vertical straight leg dimension created a reduced tube-to-tube gap at this location.

At another plant in 2004, tube-to-tube wear was reported on a tube in the vertical straight leg region, just below the square bend. The elevation of the indication was actually within the bounds of the diagonal bar, but clearly rotated 90 degrees from the diagonal bar on the +Point terrain plot. One of the adjacent tubes in the same column was degradation free; the other tube was plugged several outages prior and no RPC data was available for this tube at the time of plugging. It should be noted that this indication would have remained in service if the RPC testing had not been performed. This SG has mill annealed tubing and one of the special interest RPC programs implemented was a sampling of historic bobbin signals at tube support structures to confirm the degradation morphology. Due to the tubing material, axial ODSCC was a potential degradation mechanism thus the RPC sampling program intended to confirm the morphology of the historic bobbin signals. Scrutiny of the bobbin data could not identify presence of tube-to-tube proximity below the indication. In the square bend region, it was judged that the inherent interference associated with the square bend geometry limited the detection of proximity using the bobbin coil. Figure A-7 presents the 0.115 pancake coil terrain plot showing the proximity signal and the tube-to-tube wear signal. The cursor (small white arrow) is located at the upper edge of the wear signal.

A.2.2 Causative Mechanism for Freespan Wear Without Wear Extension from AVBs

A reanalysis of the pre-service inspection (PSI) data performed by Westinghouse in 2012 for SG 2E089 indicates that numerous proximity signals were present on the Row 95 to 123 tubes in Column 81. Based on the bobbin coil proximity amplitude on R111C81, the estimated gap with R113C81 is 0.11 to 0.12 inch. The signal amplitude on R113C81 could estimate the gap at 0.02 to 0.03 inch, however, a proximity signal with R115C81 is also present. Since RPC data was not collected at the PSI, the true contribution to the signal observed on R113C81 cannot be determined. Therefore, the gap condition has to apply the most conservative value of 0.11 to 0.12 inch.

The proximity review shows that between the PSI and ISI inspections, proximity signals can remain unaffected, could no longer be observable, could be created, or could shift from one leg to the other on the same tube. With that said, the proximal condition at any point in time during the first operating cycle could be indeterminate.

The PSI proximity condition suggests that the U-bend shape could be non-uniform. This non-uniform condition will create residual stresses within the U-bend. Contact forces between tubes and AVBs could be such that tubes could be held in position for some operating period until such time that these forces are reduced or relaxed, thereby allowing the tube to return to its equilibrium condition.

An evaluation of tube motions due to thermal, pressure, and turbulence effects indicate that relative displacements of these tubes to each other can close a proximal gap of 0.03 inch but not quite sufficient to close a gap of 0.11 to 0.12 inch.

The ISI bobbin data could not identify a proximity condition on these (R111/R113 C81) tubes. Similarly, a proximity condition was not observed on R115C81 in the ISI data. UT examination

performed by AREVA suggests a tube-to-tube proximity condition between R111C81 and R113C81 of approximately 0.19 inch in the area of the tube-to-tube wear, while at the same elevation, the tube-to-tube gap between R113C81 and R115C81 was approximately 0.31 inch, or near the design nominal condition. Thus, the UT data suggests that the proximity condition between R111, R113, and R115 could imply that if these tubes returned to an equilibrium condition during the first operating cycle, the gap between R113 and R115 is near nominal, whereas the gap between R111 and R113 could suggest that the R111 U-bend length is longer than design nominal. Alternatively, this condition could be attributed to a longer than by design vertical straight leg dimension for R111, which would only increase the potential for tube-to-tube wear due to out-of-plane vibration. The UT data for R111C81 also indicates that the dimensions to R112C80 and R112C82 are much smaller than nominal, while the dimensions to R110C80 and R110C82 are larger than nominal. These observations also support the judgment that either the R111C81 U-bend is not near normal, or the vertical straight leg length of R111C81 is longer than nominal.

Still the question which must be answered is how the current gaps could be justified. An extensive review of the wear scars on the Column 81 tubes was performed. A pattern quickly emerged, which was that oddly shaped wear scars were observed at AVB 5. The profile of these wear scars has a differing depth profile that is not uniformly deep (flat wear) and not a single tapered indication. Instead, these wear scars exhibited a “saw-tooth” profile, clearly formed by two distinct wear scars. This pattern can be explained by a sudden shift in the tube position relative to the AVB, in other words, the tube “skipped” relative to the AVB. The proximity review concludes that changing proximity condition is common within these SGs. To rule out displacement of the AVB, the bobbin data of the PSI and ISI examinations was reviewed. Since no RPC data is available for the PSI, bobbin data must be used. The bobbin low frequency differential channel was used to establish that the overall length of the bobbin signal response (from a null-to-null condition) was essentially identical between the PSI and ISI exams. If one of the AVBs on either side of the tubes in Column 81 had moved, then the relative position of the two AVBs with respect to each other would change. This would also change the combined AVB width as observed by the bobbin probe along the axial length of the tubes in Column 81. Since the lengths of the AVB signals (combined AVB width) in the PSI and ISI were identical, it is concluded that the AVBs did not change position.

These characteristic wear scars were observed on R113C81, R115C81, R117C81, R119C81, R121C81 and R123C81, all at the AVB 5 location. An example of such wear scars is shown on Figure A-8, Figure A-9, and Figure A-10. Figure A-10 presents the +Point terrain plot of R113C81 at the AVB 5 location. Each figure includes the +Point 300/100 mix channel (for flaw detection) and the 35 kHz channel response, for identification of the edges of the AVBs. If the wear bounded by the AVB edges represents the most recent wear (prior to shutdown), and the wear is tapered, the distance from the edge of the original wear to the edge of the AVB can be used to estimate the amount of tube displacement. This dimension has been estimated to range from 0.12 to 0.40 inches, for those tubes which show this characteristic. Note also that this same characteristic was observed on R129C91, at AVB 5. This tube was reported with a proximity call on the cold leg in the PSI data and on the hot leg in the ISI data.

Another characteristic of the wear at AVB 5 on these tubes was that shallow depth, short length wear scars were sometimes observed on the opposite AVB. These wear scars were clearly of much shallower depth than the wear scars which exhibited the odd shape. The only way that a wear scar could be observed in the middle of the AVB (not extending to any AVB edge) is if the tube shifted relative to the AVB at some point in time during operation.

These atypical indications are associated with significant observations of AVB symmetry variance. The term symmetry variance is used to describe the relative position (axial distance) of

the two AVBs on either side of a tube along the tube axis. In SG 2E089, the largest AVB symmetry variance is observed at AVB 6, and for Column 81; AVB 7 also has significant AVB symmetry variance. If the AVB symmetry variance is associated with AVB twist, and the amount of twist is correlated with symmetry variance, then the largest contact forces would be observed for AVB 6 and AVB 7. As the larger contact forces would reduce the potential for wear, once sufficient wear has occurred at other AVBs to reduce the overall contact force thus permitting the tube to return to its equilibrium condition, the tube would then skip to its current condition. For AVBs 5, 6, 7, and 8, the 95th percentile AVB wear depths are essentially equal, but the wear indications at AVB 5 are deeper for Column 81. For R113C81, the deepest AVB wear is observed at AVB 5 (based on +Point results).

The deepest AVB wear indication (from +Point analysis) in SG 2E089 was reported on R121C83 at AVB 5. The indication appears to be uniformly deep and does not show signs of tube displacement relative to the AVB. The wear is single sided; the opposite AVB has not caused degradation of the tube. The +Point 35 kHz residual data suggest no AVB twist on either AVB, however the residual responses for the AVB without wear are modestly less than for the AVB with wear. The deepest indication in SG 2E089 reported by bobbin coil analysis was reported on R117C81 at AVB 9; this indication also appears to have a uniformly deep profile. The deepest wear from bobbin coil analysis in SG 2E088 was reported on R133C91 at AVB 6. The +Point terrain plot for this location showed that the indication is stepped. The opposite AVB does not contain wear. The +Point 35 kHz residual voltages are essentially equal for this AVB, indicating no twist. The 35 kHz +Point residual voltages on the AVB with wear show a large variance, suggesting significant AVB twist (estimated to be about 2 degrees).

A.2.3 Detection Condition Associated with Wear Extension from AVBs

The detection condition associated with wear extension from AVBs was investigated. To perform this assessment, the +Point 300/100 mix channel noise was compared for the middle of the AVB region and the freespan region just outside of the AVB. The vertical maximum noise condition outside of the AVB was exceptionally small; on the order of 0.02 to 0.04 volt. The noise condition within the AVB was typically 50% larger than just outside of the AVB. Therefore, if tapered wear is experienced, and the shallower edge of the wear has a distinct character (i.e., the tapered wear extends for the full length of the AVB width) and no wear is observed outside of the AVB, it can be concluded that no wear is present outside of the AVB as the length along the tube axis from the edge of the wear to just outside of the AVB is short, and not of sufficient length to allow the wear to runout to the tube OD. Since the noise condition within the AVB is greater than just outside of the AVB, the detection of wear within the AVB would then imply a detectable condition and the wear extension outside the AVB would be detected if present.

A.3 Temperature, Pressure and FIV Effects

A tube-to-tube gap of approximately 0.19 inch between the R111C81 and R113C81 tubes near the tube-to-tube wear region was measured by ultrasonic testing (UT) after the first cycle of operation. The gaps between AVBs 3 and 4 were also measured for these tubes. The gap between R111C81 and R113C81 was not measurable at this location, but a gap of 0.18 inch was measured between R109C81 and R111C81. The gaps between AVBs 3 and 4 and AVBs 9 and 10 between R113C81 and R115C81 were measured around 0.30 to 0.31 inch which is close to the nominal gap of 0.31 inch for this location in the U-bend. The maximum design spacing is 0.344 inch at the top of the U-bend for these tubes. The design spacing of the tubes is shown in Figure A-11. In the UT data there is no reference point to determine if any of the tubes are in the

design shape so an assumption needs to be made for the geometry of these tubes. It appears that the R111C81 tube is deformed relative to the other tubes so it will be assumed that the R113C81 tube is nominal in shape and the R111C81 tube is deformed in a way that follows the gap measurements (see discussion in Section A-2). A sketch of this geometry is shown in Figure A-12.

A.3.1 Tube Thermal Expansion

One way to postulate a closure in the tube spacing to occur is for the two tubes with tube-to-tube wear to move within the tube support plate holes as they expand due to operating temperature and pressure.

Using the tube support plate drawing (Reference A-1), the maximum geometrical tolerances for the tube support plate holes were considered. Using the maximum tube support plate dimensions and the minimum tube size, it was determined that the tube can move 0.033 inch within the tube support plate before it comes to rest on the opposite side of the broached hole. The maximum dimensions of the tube support plate broaching are shown in Figure A-13. The maximum tube movement within the tube hole is also shown in Figure A-13. The scenario that would cause the maximum movement between the tube support plate is when R111C81 is resting on the left side of the broach at the hot leg and cold leg side. When the tube is brought up to the normal operating temperature and pressure, the tube will expand outward which will cause the tube to move to the outside positions in the tube support plate holes. The R113C81 tube is assumed to be in the exact opposite configuration where the tube is pushed to the right side of the tube support plate holes. A schematic of this effect is shown in Figure A-14.

This tube model was simulated using the ANSYS finite element program using Solid186 three-dimensional structural solid elements and Solid90 thermal elements. These elements are a 20 node brick element. A plot of the meshed model in the U-bend region is shown in Figure A-15. The temperature solution was obtained from the FASTVIB output for the 100% power case for the R111C81 tube. The temperature profile for the R113C81 tube was almost identical to the R111C81 tube so the same temperature profile was applied to both tubes. The temperature distribution was applied to the tube by fixing the temperature at the tube support plate locations and then solving for the steady state temperature solution. The temperature change around the tube is fairly gradual such that the steady state solution from ANSYS matches the ATHOS data fairly closely.

The tubes were fixed at the tubesheet end of the model and nodes were pinned in the X and Z directions at the tube support plate locations. The AVB supports were neglected in the model. The AVB supports are assumed to be sufficiently loose such that they do not provide support in the in-plane direction.

A.3.2 Tube Movement at AVB 5

It has been found from the shape of the wear scar in the eddy current data that at AVB 5 for Tube R113C81 there appears to be a shift in the tube position. There are two sawtooth shapes on the wear scar on one side of the tube which indicates that the AVB is twisted and wore a mark that twice moved slightly and resumed wear in a different spot. In the opposite side of the tube, the AVB also appears to be twisted but the wear scar is near the center of the AVB position at the cold leg. This is an indication that the tube has shifted in position relative to AVB 5. The postulation that R111C81 and R113C81 were initially much closer than suggested by the current gap measurement states that they moved farther apart when this shift in tube position occurred. The finite element model works backwards from this scenario by assuming the inspection

geometry of the tubes and then applying a displacement to determine how close the tubes were prior to the displacement. The eddy current wear scars indicate that the tube moved approximately 0.12 inch to 0.18 inch.

The deformed shape model from Section A.2 was used and the tube was displaced towards the cold leg side in the X direction 0.12 inch then 0.18 inch. The displacement was applied to the model at the centerline where AVB 5 would cross Tube R113C81. A local coordinate system was then used to determine the amount of displacement of Tube R111C81 relative to Tube R113C81.

The results of the displacement models are shown in Figure A-16 and Figure A-17 for the 0.12 inch and 0.18 inch displacement, respectively. It is shown that for a displacement of 0.12 inch or 0.18 inch, the close up in the gap is approximately one for one. The difference in displacement versus gap closure is only 1 mil.

A.3.3 Impact of In-Plane Turbulence

In addition to the finite element models used to show that the tube gap closes, there can also be in-plane motion due to flow turbulence. This in-plane turbulence motion is displacement limited and should not be considered a similar effect as in-plane stability. The purpose of this section is to evaluate the magnitude of turbulent displacement to be used to support the explanation that the tubes with tube-to-tube contact are not unstable in-plane. It is known that these tubes have closer than nominal proximity at the cold condition so the tube-to-tube contact is being explained as extreme tube-to-tube proximity with a combination of in-plane turbulent motion and out-of-plane fluidelastic motion.

A FASTVIB evaluation was performed for the tubes that had tube-to-tube contact in Steam Generator 2E089. These tubes are R111C81 and R113C81. The turbulent constants C1 and S applicable to the SONGS steam generators are shown in Table A-2. There are two sets of constants based on the flow characteristics around the tube. Two FASTVIB runs for each case are evaluated based on each set of constants. The FASTVIB evaluation was condensed to only include the tubes in Row 111 and Row 113. The two tubes, R111C81 and R113C81, have a defined missing AVB Case 61.

The results of the FASTVIB runs show that the root mean square (RMS) turbulent displacement is approximately 0.003 inch for each tube using either set of turbulence constants. Using Reference A-2, the RMS turbulent displacement can be converted to a peak displacement using a factor of 3.5. Assuming both tubes are vibrating, the maximum distance the tubes can be apart and still come into contact due to turbulent displacement is $2 \times 3.5 \times 0.003 = 0.021$ inch.

A.4 Summary

From the review of the eddy current data and the analysis of the tubes response due to pressure temperature and FIV effects, it appears that the two tubes were very close or were in contact at the start of operation following replacement. The tubes would not have necessarily been in contact before operation, but could have contacted due to peak displacements as a result of in-plane turbulence. Note that displacements associated with the fluidelastic mechanism are not similar to turbulence induced displacements, as the turbulence mechanism is self limiting.

UT measurements performed during the recent outage indicates that the tubes could be as close as 0.19 inch. As with all measurements of this type, there are measurement uncertainties that are present in the signals. The uncertainty associated with the UT measurements could range from an estimated low of 4 mils to ~20 mils. This means that the actual low end of the gap could range from 170 mils to 186 mils. This is the range of gap sizes that could have developed after

the tubes have shifted to the current location. Figure A-18 describes how the tubes could have initially worn due to proximity, and then moved or shifted during operation coupled with temperature and pressure effects to result in the currently observed condition.

In summary, it appears as if the tubes were initially very close, or actually contacting prior to operation, where FIV induced turbulence vibration could have produced the observed wear. Then after operation for a period of time, the tubes moved, or skipped to a new location, similar to the skip found in other tubes in the region (up to 0.4 inches). Figures A-19 and A-20 provide a visual indication of how these tubes could have moved. Additional movement of the tubes is possible due to pressure and temperature effects that would then result in the currently observed condition.

A.5 References

- A-1. San Onofre Nuclear Generating Station Units 2 and 3 Replacement Steam Generators MHI Design Drawings:
- A. L5-04FU001, Rev. 6, "Component and Outline Drawing 1/3".
 - B. L5-04FU051, Rev. 1, "Tube Bundle 1/3".
 - C. L5-04FU052, Rev. 1, "Tube Bundle 2/3".
 - D. L5-04FU053, Rev. 3, "Tube Bundle 3/3".
 - E. L5-04FU101, Rev. 5, "Wrapper Assembly 1/5"
 - F. L5-04FU107, Rev. 3, "Tube Support Plate Assembly 2/3".
 - G. L5-04FU108, Rev. 3, "Tube Support Plate Assembly 3/3".
 - H. L5-04FU112, Rev. 1, "Anti-Vibration Bar Assembly 2/9".
 - I. L5-04FU118, Rev. 3, "Anti-Vibration Bar Assembly 8/9".
 - J. L5-04FU134, Rev. 6, "Moisture Separator Assembly 4/6".
 - K. L5-04FU135, Rev. 5, "Moisture Separator Assembly 5/6".
- A-2. B. Brenneman and J. Q. Talley, "RMS Fatigue Curves for Random Vibrations," Transactions of the ASME, Volume 108, November 1986.

Table A-1. Feature Comparison of SONGS and Plant B Steam Generators

Feature	SONGS	Plant B
Number of Tubes	9727	10637
Tube Material	Alloy 690 TT	Alloy 690 TT
Tube Dimensions (in)	0.750 OD x 0.043 t	0.688 OD x 0.040 t
Triangular Pitch (in)	1.00	0.95
Pitch/Diameter	1.33	1.38
Largest Radius, R _{max} (in)	76.27	74.025
Number of TSPs	7	8
TSP Material	405 SS	405 SS
Trifoil Broach Radius (in)	0.381-0.384	0.349-0.353
Radial Tube Clearance (in)	0.006-0.009	0.005-0.009
TSP Thickness (in)	1.38 (0.2-1.07 land height)	1.125 (0.94-1.08 land height)
TSP CL Spacing (in)	42.82 first, 43.66 typical	34.67 first, 35.23 typical
Number of AVB Sets	6 (2 Each Side, 2 Centered)	5 Centered + Staggered
AVB Material	405 SS	405 SS
AVB Dimensions (in)	0.590 W x 0.114 t	0.480 W x 0.133 t
Nominal* Diametrical Gaps (in)	0.0020	0.0017
Average U-bend Span @ R _{max}	13 @ ~ 19.4 in	11 @ ~ 23.9 in
U-bend Overhang (in)	83	89
IP Tube Spacing** at Apex (in)	0.298, 0.344, 0.400	0.442, 0.502, 0.562
Alloy 690 Retainer Bars (in)	24 Round (12 ea @ 0.19, 0.41)	20 @ 0.63 W x 0.125 t
Alloy 690 Retaining Rings (in)	0.38 Round	0.38 Square
Alloy 690 End Caps (in)	0.38 t x 1.00 W x 1.97 L	0.451 t x 0.860 W x 2.00 L
End Cap to Ring Welds (in)	0.12 leg	0.19 leg x 0.38-0.63 long
Orthogonal Structure	13 Segmented Bridges	None
SG Power Level (MWt)	1729	1522
Maximum Steam Quality	0.89	0.75
Maximum Void Fraction	0.9955	0.9851
Operating Time @ Last ISI	Cycle 16 (1.7 EFPY)	Cycle 6 (8.1 EFPY)
Tubesheet Thickness (in)	27.95	31.56
Hole Tolerances (in)	0.756-0.762 (0.769 for 1%)	0.696-0.701
Diametrical Expansion (in)	0.006-0.012 (0.019 for 1%)	0.008-0.013

*Assuming AVBs are welding at the nominal TSP hole pitch spacing.

**For larger tubes in radial zones ~41-55, 56-67, and 68-maximum.

Table A-2. Turbulence Constants

Parameter	Straight Leg Region	U-bend Region
Turbulence ($fD/U > 0.13$)		
C_1	1×10^{-3}	1×10^{-3}
S	2.34	2.34
Turbulence ($fD/U < 0.13$)		
C_1	7.8×10^{-3}	7.8×10^{-3}
S	0.304	0.304

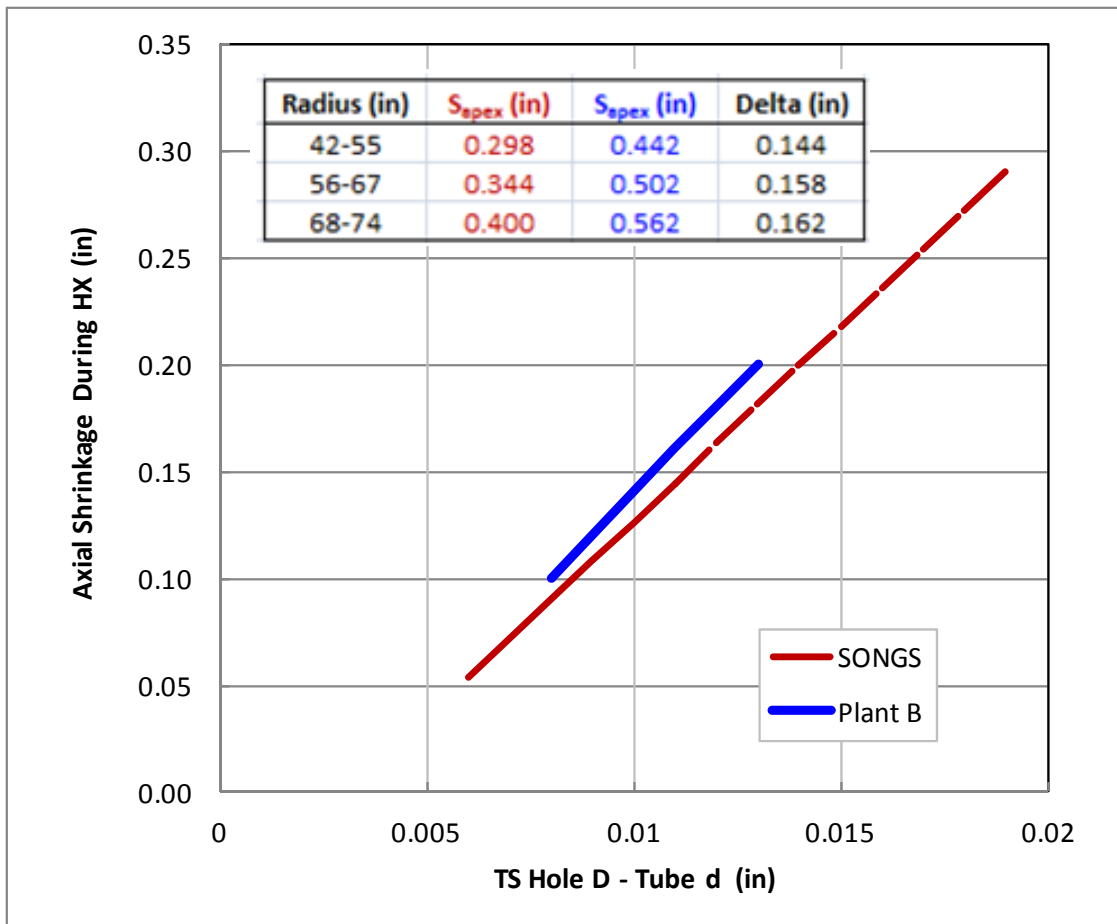


Figure A-1. Potential Range of Axial Shrinkage for Plant B and SONGS Steam Generators Using Drawing Tolerances for TS Drilled Hole Diameter

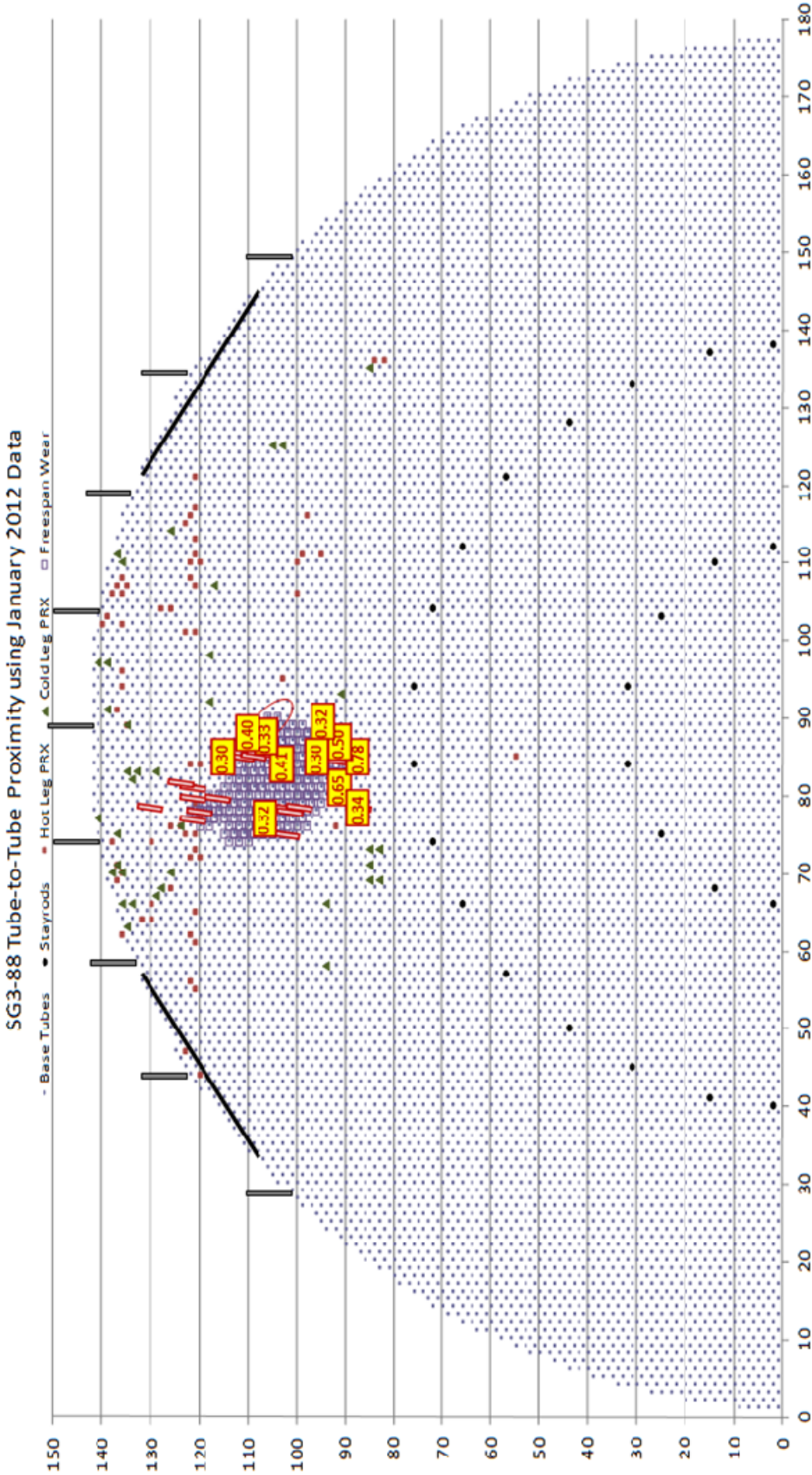


Figure A-2. Overview of ECT Results from SG 3E088 Using ISI Proximity Results Map with AVB Support Structure (Boxes with numbers are locations of AVB symmetry variance; smaller rectangles are locations with twist)

AVB Symmetry Variances Near SVI Region in SG 3E088

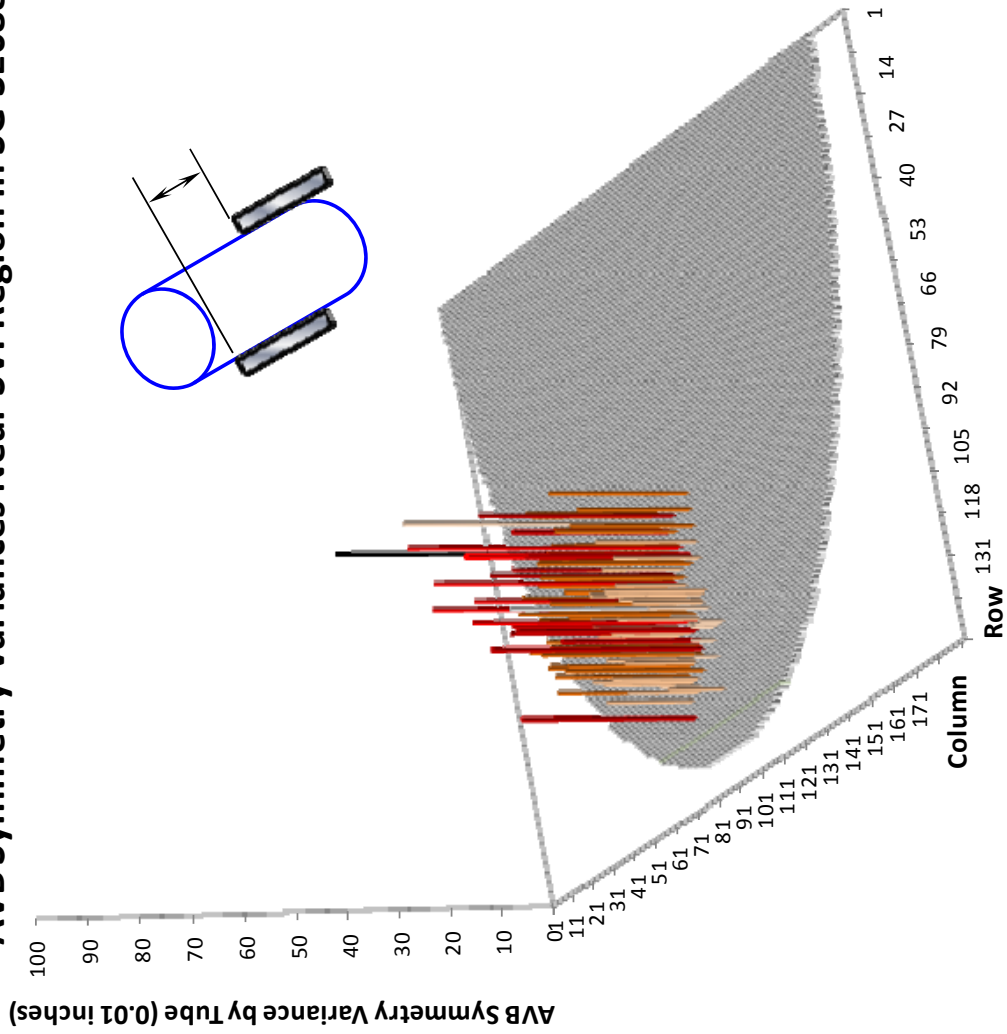


Figure A-3. Locations and Magnitudes of AVB Symmetry Variances Near TTW Region of SG 3E088 (SVI Region = TTW Region)

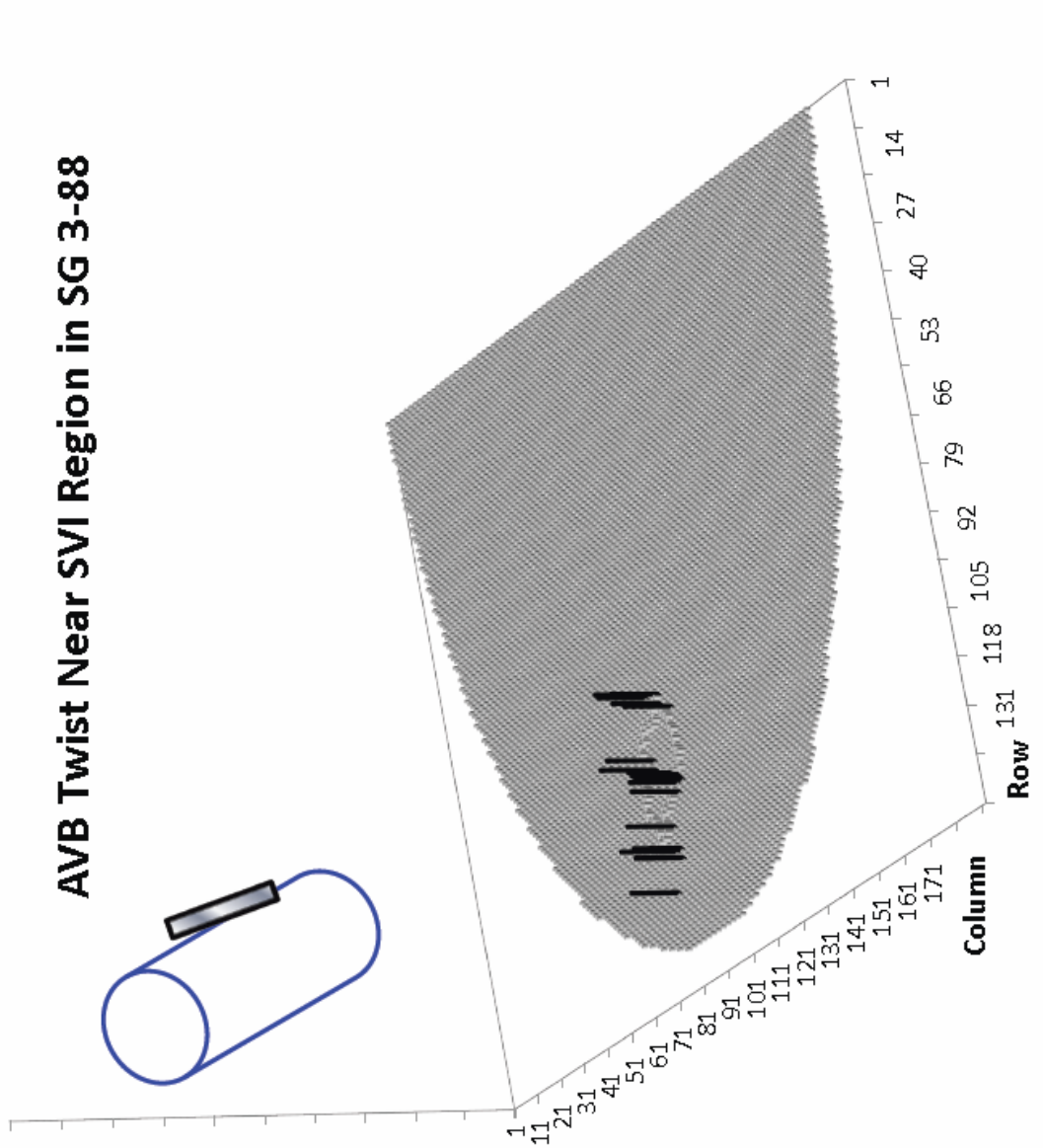


Figure A-4. Distribution of AVB Locations with Tapered Wear Scars Indicating AVB Twist (SVI Region = TTW Region)

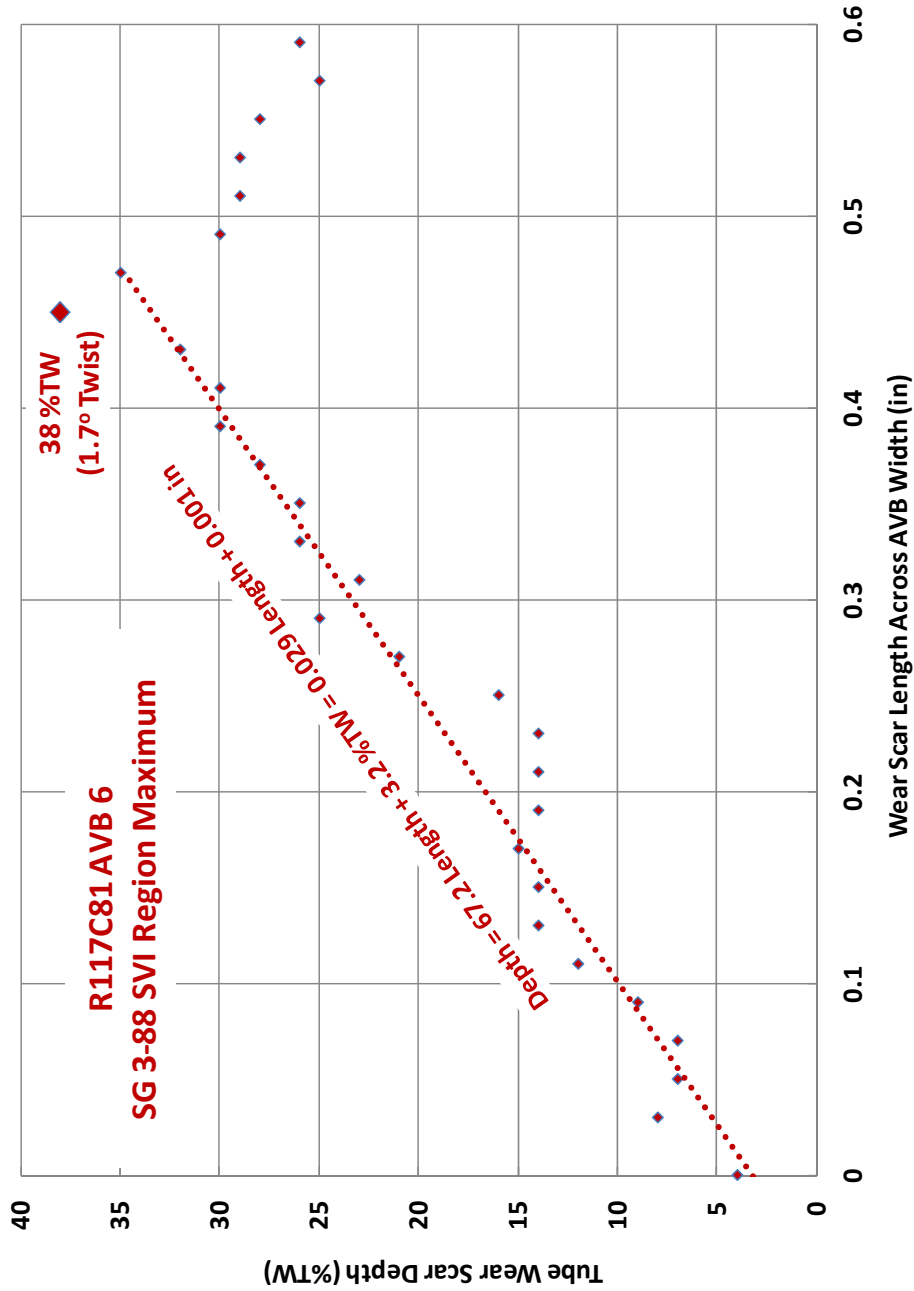


Figure A-5. Largest Implied Twist from Preliminary Tapered Wear Scar Review Near TTTW Region of SG 3E088 (SVI Region = TTTW Region)

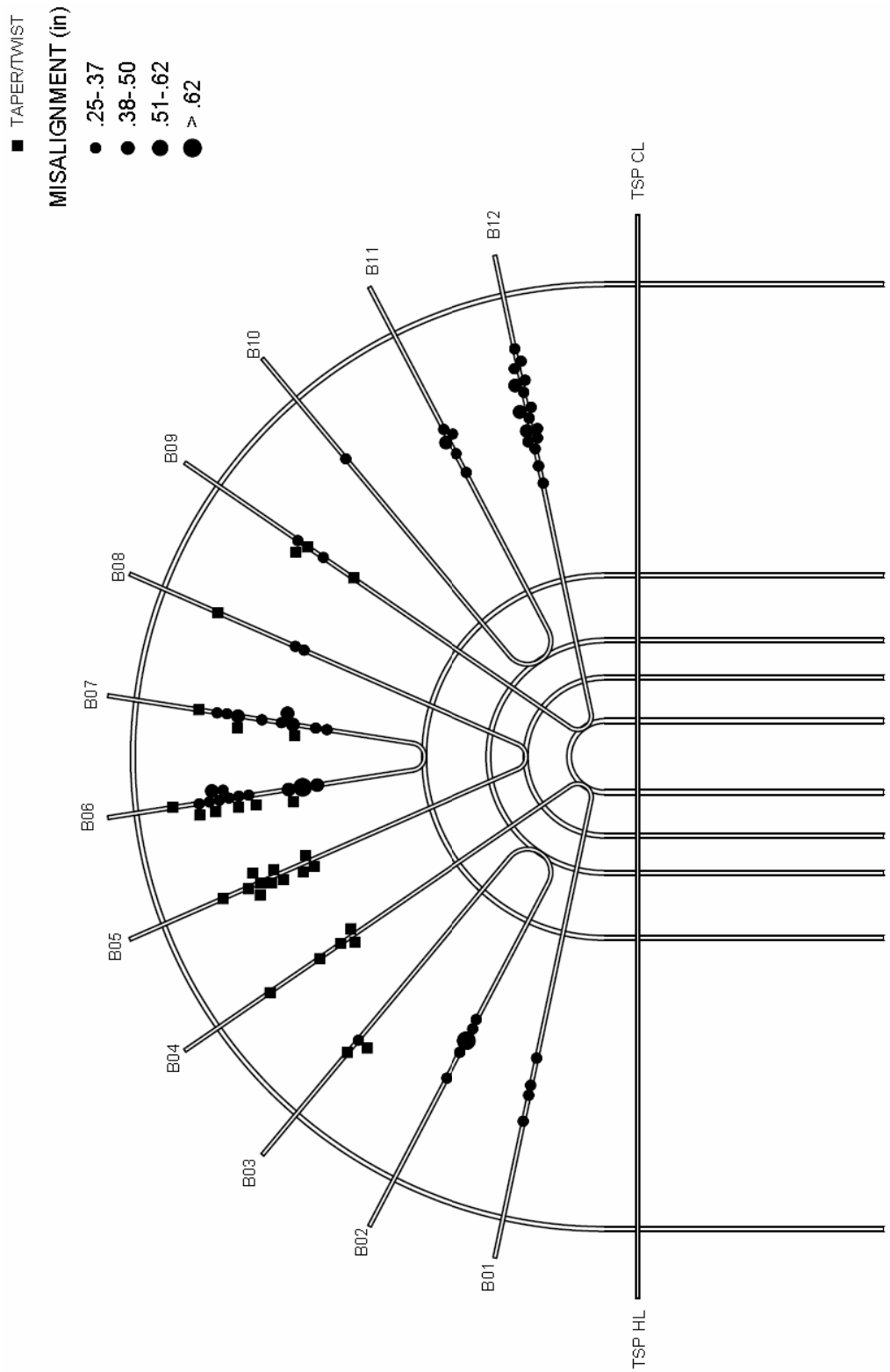


Figure A-6. Elevation View of Locations of AVB Misalignment and Tapered Wear Scars Obtained During ECT Review of the SG 3E088 TTW Region

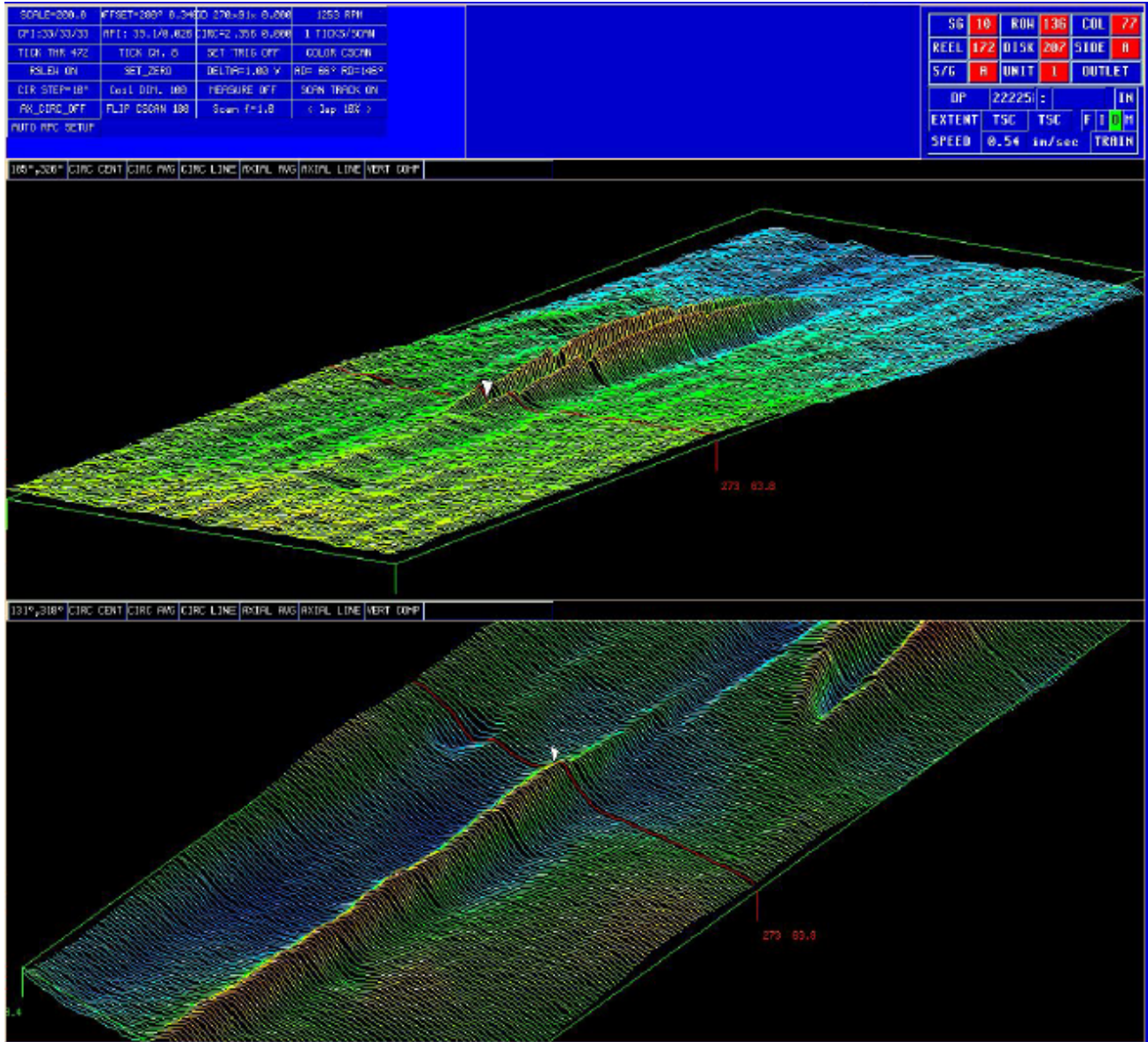


Figure A-7. Other Plant Experience Showing Relation of Tube-to-Tube Wear and Proximity at Shutdown Condition

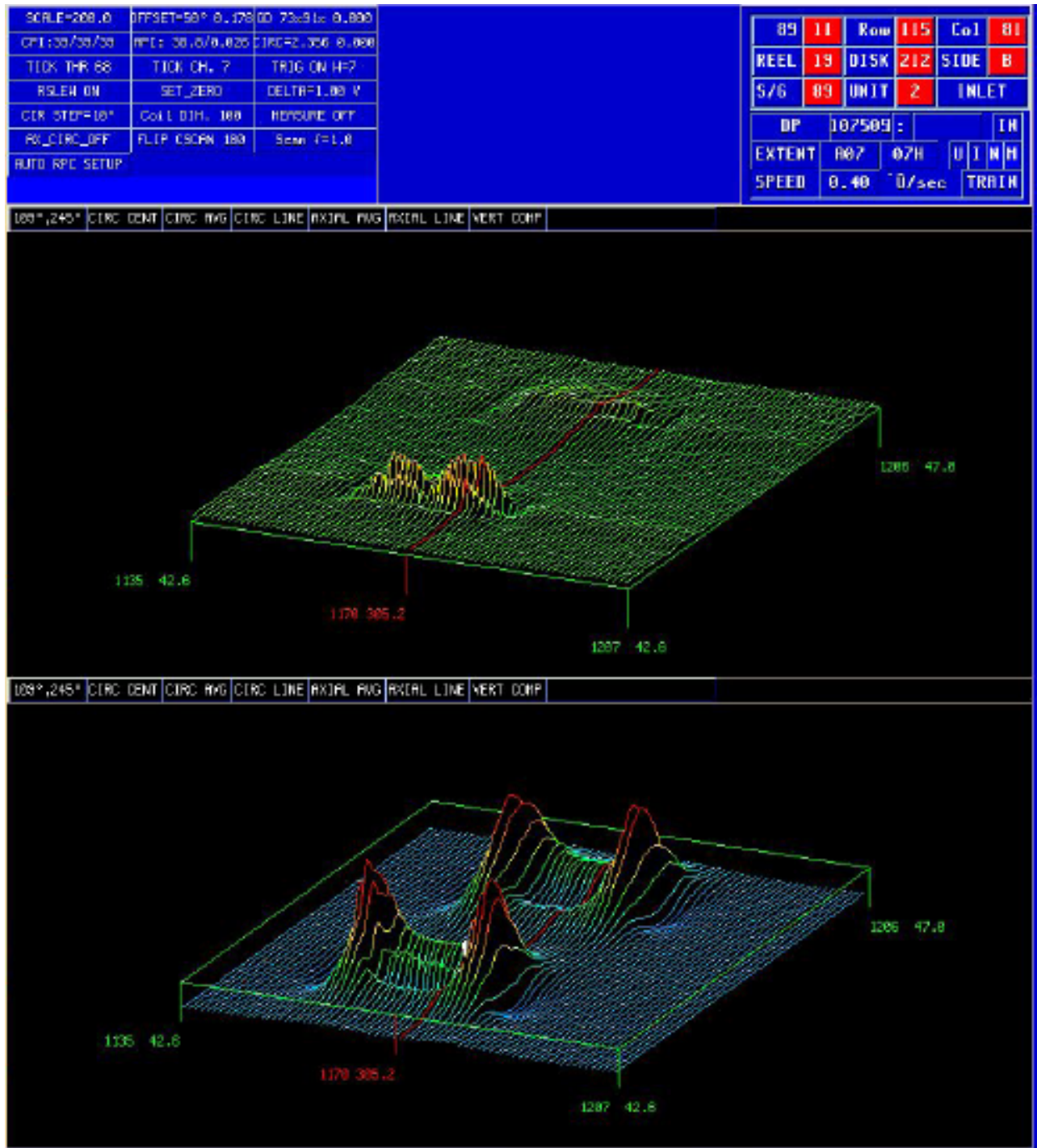


Figure A-8. SONGS SG 2E089 Stepped Indication at AVB 5 on R115C81

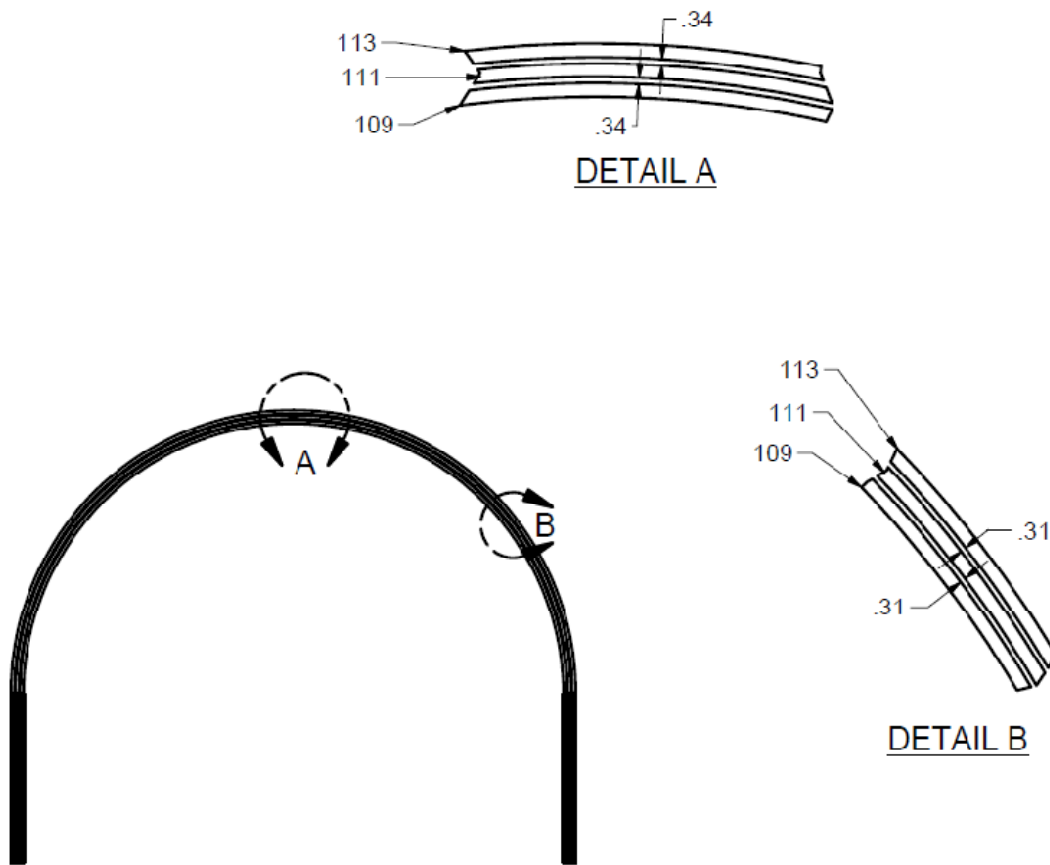


Figure A-11. Shape of R111C81 and R113C81 Tubes Based on Nominal Dimensions

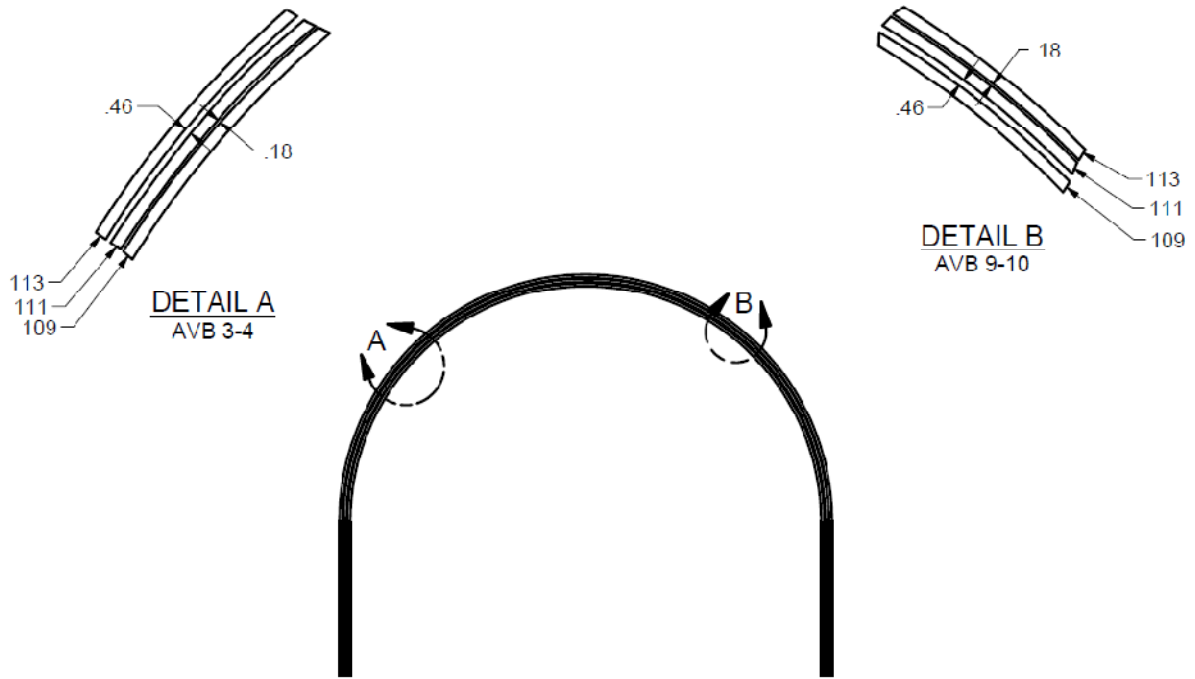
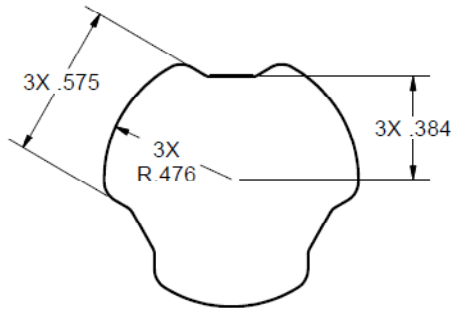
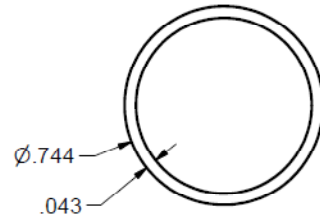


Figure A-12. Shape of R111C81 and R113C81 Tubes Based on Measured Gaps



MAX BROACH SIZE
REF DWG: L5-04FU108



MIN TUBE DIA
REF DWG: L5-04FU051

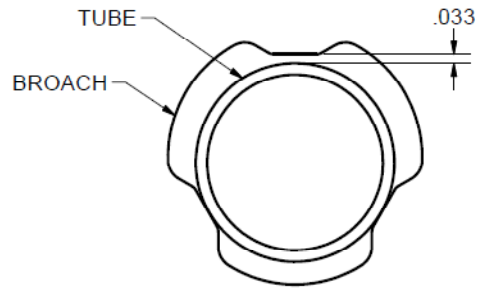
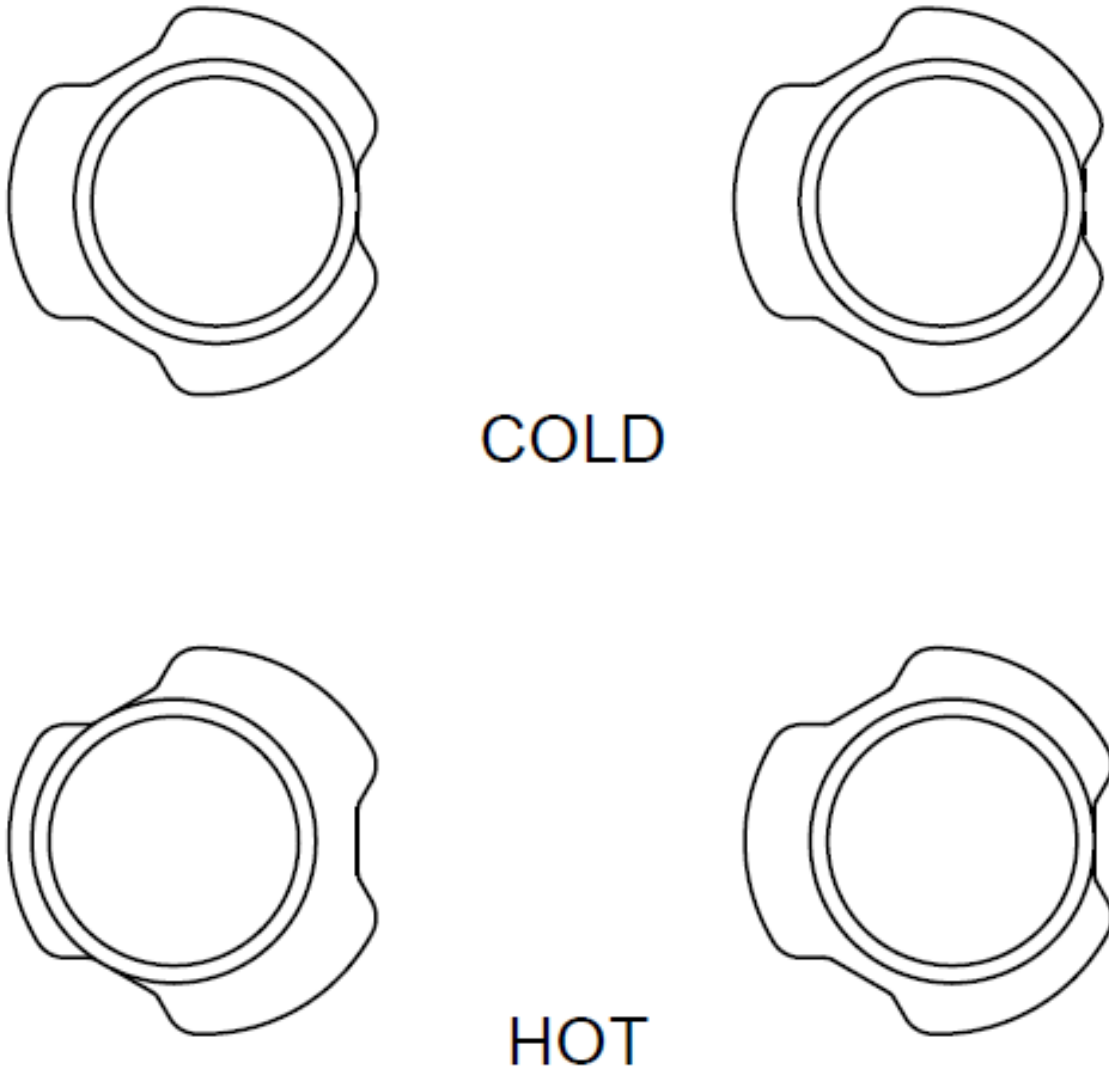


Figure A-13. Tube Support Plate Maximum Dimensions



*TUBE NOT TO SCALE TO SHOW EXAGGERATED MOVEMENT.

Figure A-14. Tube Support Plate Hole – Tube Movement

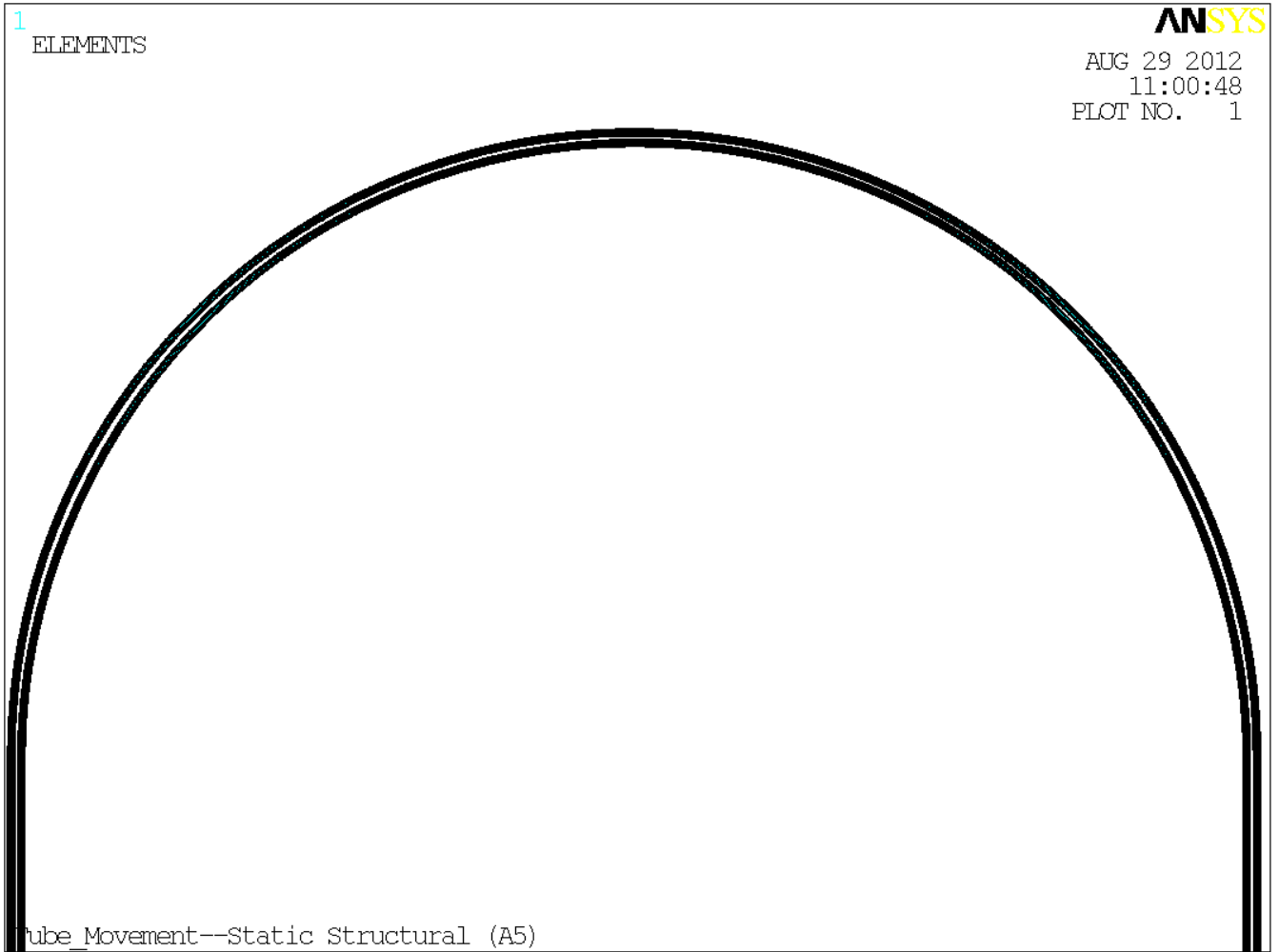


Figure A-15. Meshed Tube Model

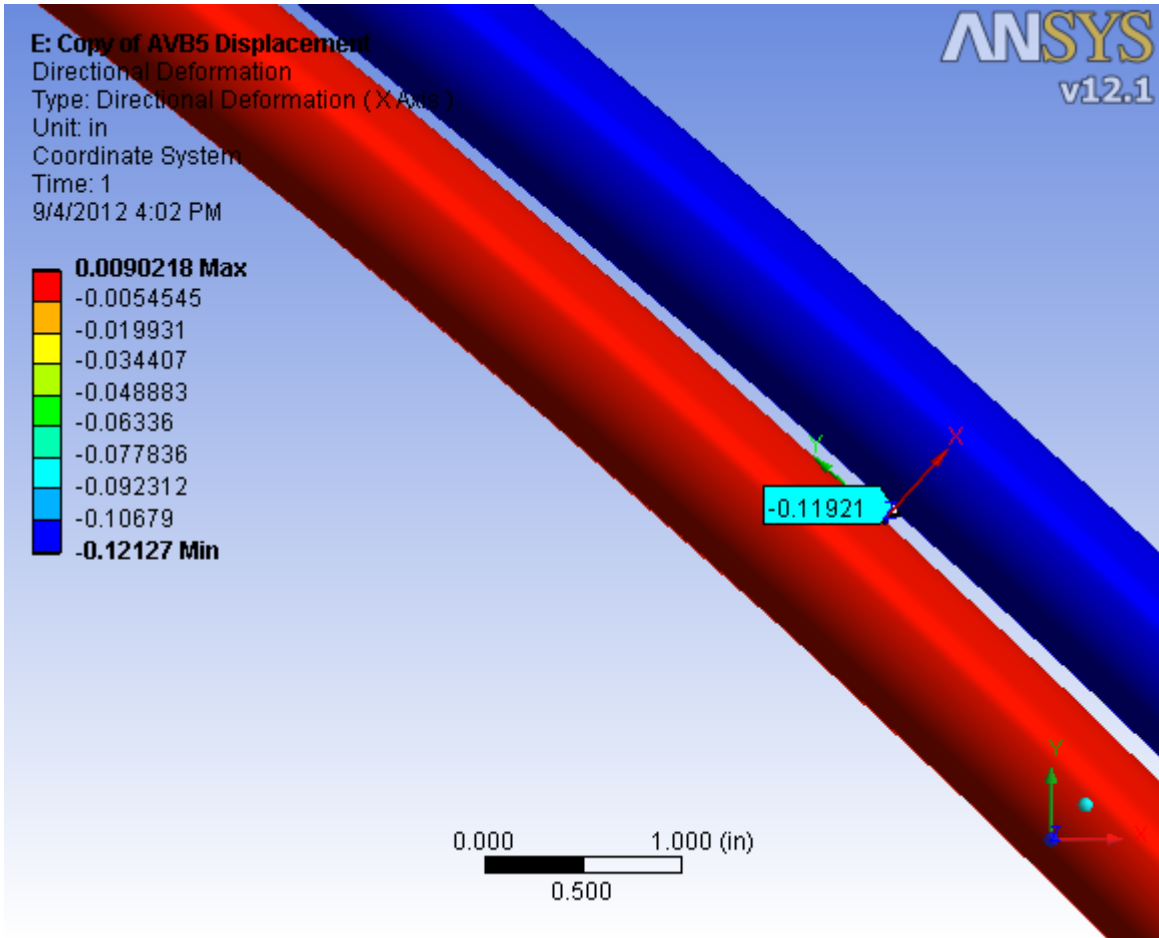


Figure A-16. 0.12 Inch Displacement at AVB 5 Results (inches)

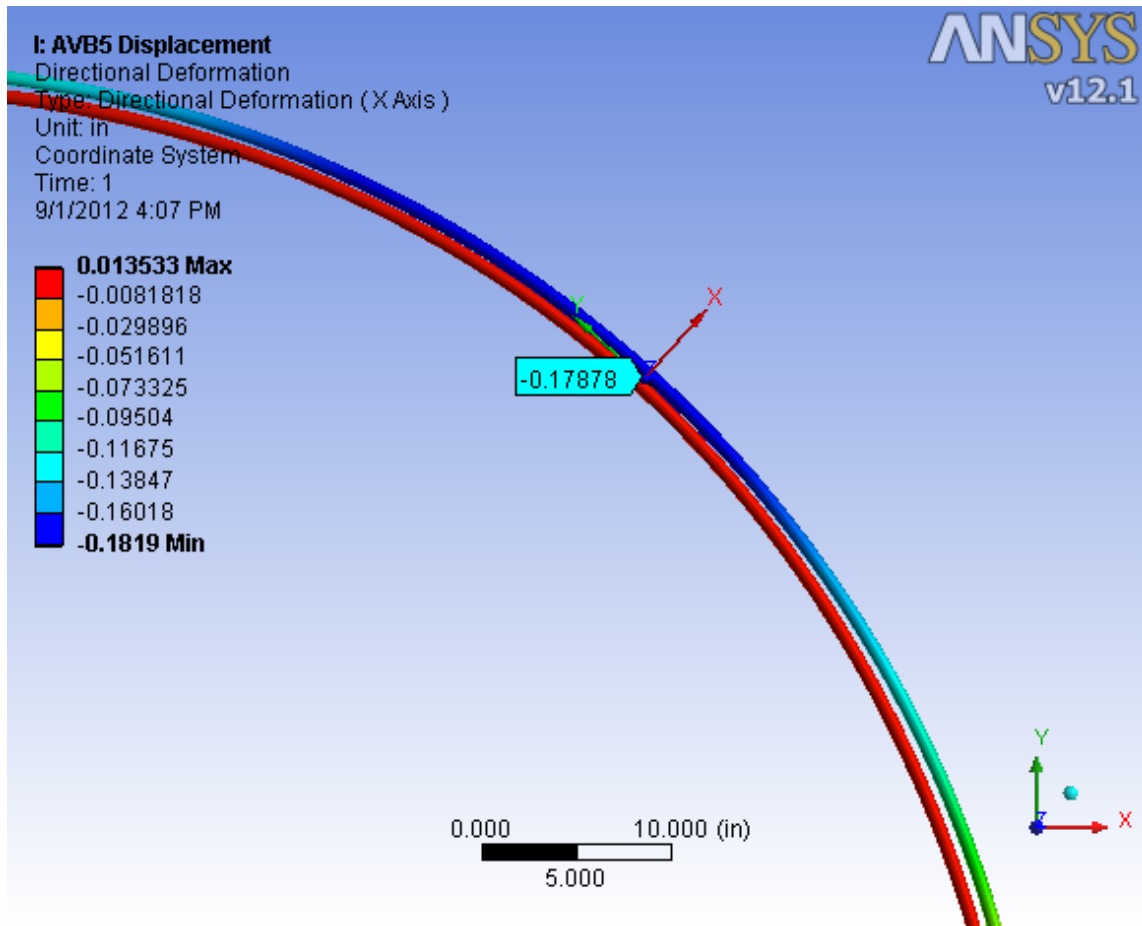


Figure A-17. 0.18 Inch Displacement at AVB 5 Results (inches)

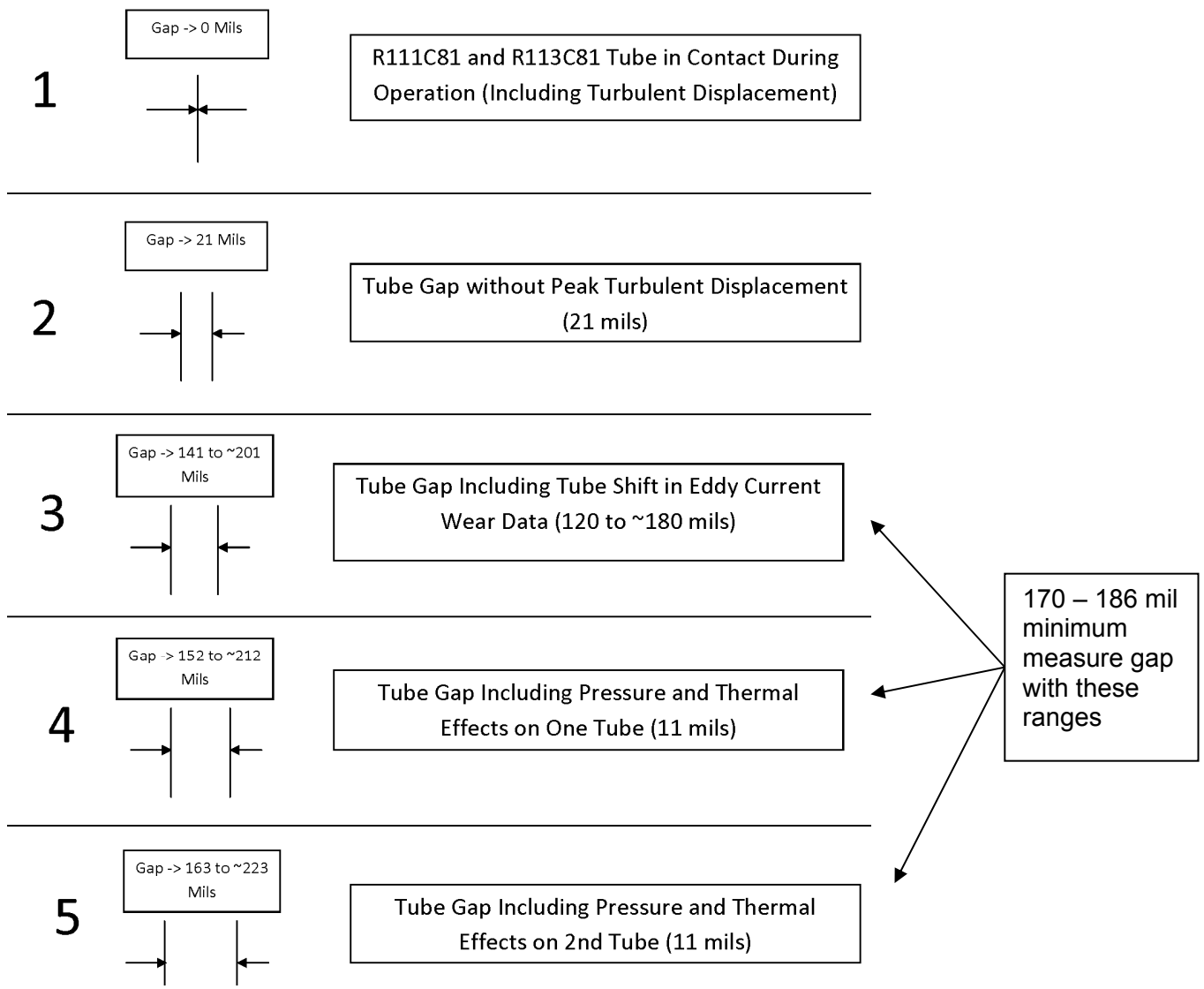


Figure A-18. Tube Gap Development

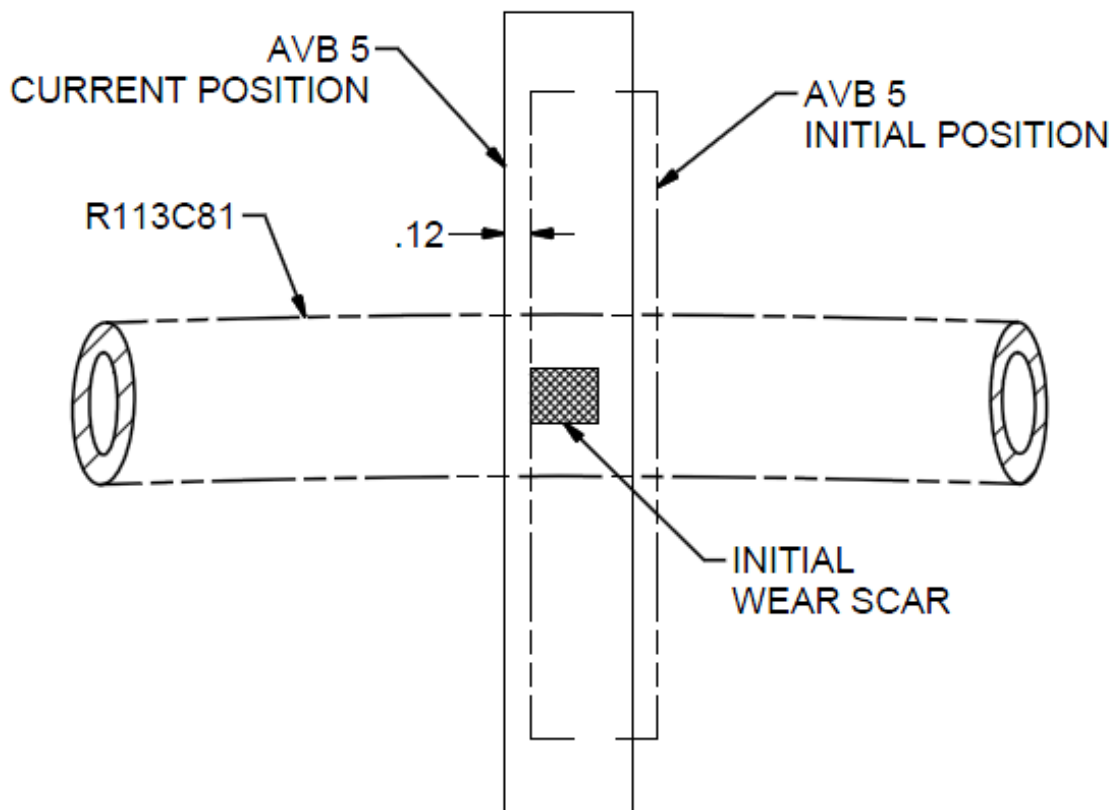


Figure A-19. R113C81 AVB "A" Eddy Current Wear Profile

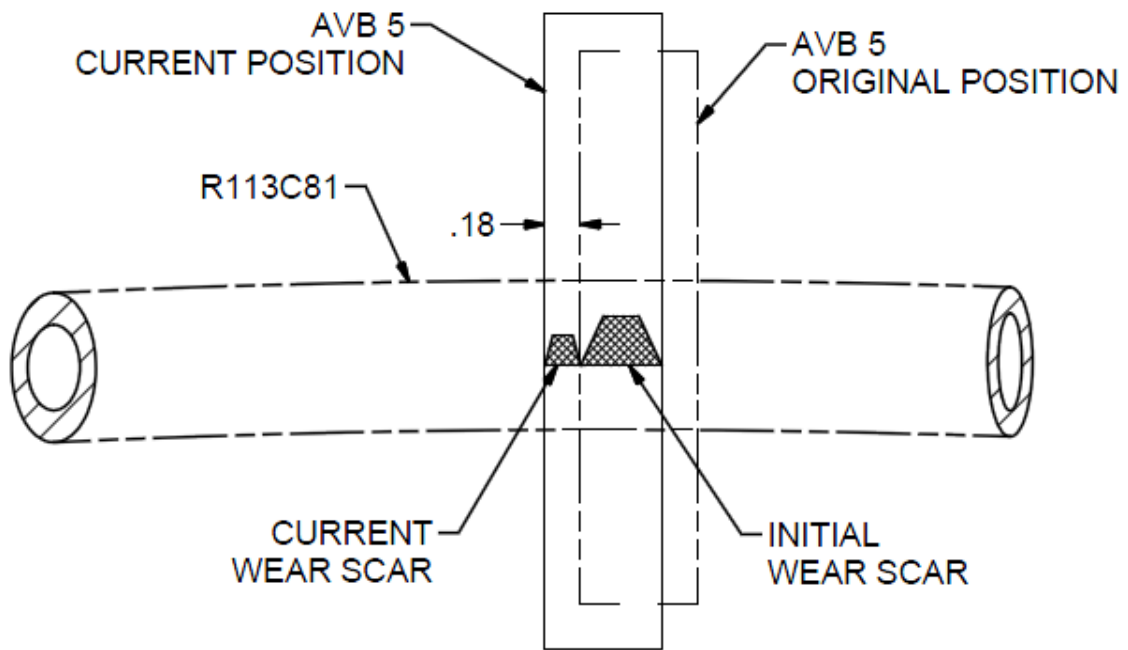


Figure A-20. R113C81 AVB "B" Eddy Current Wear Profile